

# ATMOSPHERIC OZONE 1985

## ASSESSMENT OF OUR UNDERSTANDING OF THE PROCESSES CONTROLLING ITS PRESENT DISTRIBUTION AND CHANGE

(NASA-TM-89237) ATMOSPHERIC OZONE 1985.  
ASSESSMENT OF OUR UNDERSTANDING OF THE  
PROCESSES CONTROLLING ITS PRESENT  
DISTRIBUTION AND CHANGE, VOLUME 1 Global  
Ozone Research and (National Aeronautics and

N87-10612  
THRU  
N87-10618  
Unclas  
44057

VOLUME I



ORIGINAL CONTAINS  
COLOR ILLUSTRATIONS

NATIONAL AERONAUTICS AND SPACE ADMINISTRATION  
FEDERAL AVIATION ADMINISTRATION • NATIONAL OCEANIC AND ATMOSPHERIC ADMINISTRATION  
UNITED NATIONS ENVIRONMENT PROGRAM • WORLD METEOROLOGICAL ORGANIZATION  
COMMISSION OF THE EUROPEAN COMMUNITIES • BUNDESMINISTERIUM FÜR FORSCHUNG UND TECHNOLOGIE

Copies of this report are available from:

**Europe**

World Meteorological Organization  
Case Postale No. 5  
CH 1211 Geneva 20, Switzerland

Commission of the European Communities  
Directorate-General for Science Research and Development  
Rue de la Loi 200  
1049 Brussels, Belgium

Gesellschaft für Strahlen und Umweltforschung  
MBH Munchen  
Bereich Projekttragerschaften  
Josephspitalstr. 15  
8000 Munchen 2, Federal Republic of Germany

**Africa**

United Nations Environment Program  
P.O. Box 30552  
Nairobi, Kenya

**United States**

National Aeronautics and Space Administration  
Earth Science and Applications Division, Code EE  
Washington, D.C. 20546, U.S.A.

National Aeronautics and Space Administration  
Laboratory for Atmospheres, Code 610  
Goddard Space Flight Center  
Greenbelt, Maryland 20771, U.S.A.

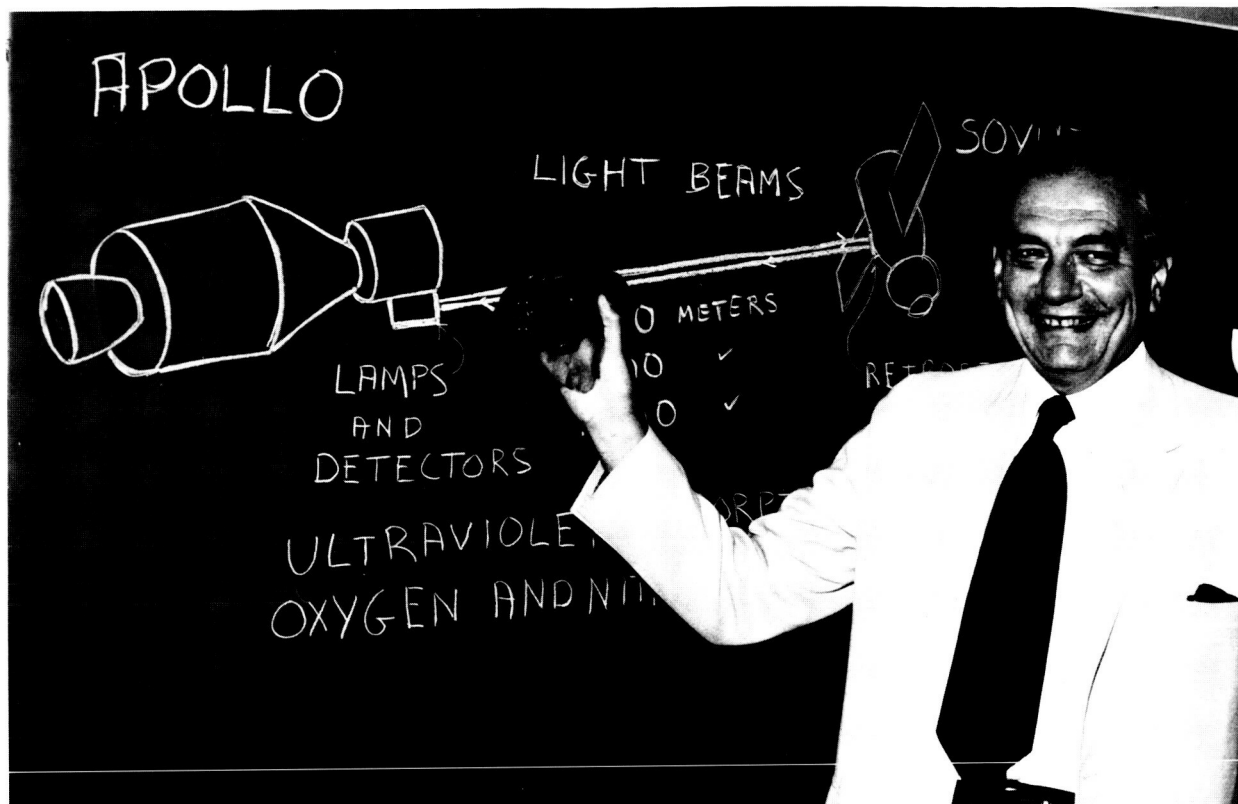
WORLD METEOROLOGICAL ORGANIZATION  
GLOBAL OZONE RESEARCH AND MONITORING PROJECT  
REPORT NO. 16

# **ATMOSPHERIC OZONE 1985**

**ASSESSMENT OF OUR UNDERSTANDING OF THE PROCESSES  
CONTROLLING ITS PRESENT DISTRIBUTION AND CHANGE**

NATIONAL AERONAUTICS AND SPACE ADMINISTRATION  
FEDERAL AVIATION ADMINISTRATION  
NATIONAL OCEANIC AND ATMOSPHERIC ADMINISTRATION  
UNITED NATIONS ENVIRONMENT PROGRAM  
WORLD METEOROLOGICAL ORGANIZATION  
COMMISSION OF THE EUROPEAN COMMUNITIES  
BUNDESMINISTERIUM FÜR FORSCHUNG UND TECHNOLOGIE

Dedicated to the memory of  
FRED KAUFMAN



*“He was a scholar, and a ripe and good one;  
Exceeding wise, fair-spoken, and persuading.”  
From Henry VIII (Griffith in Act IV, Sc. ii,  
lines 58–59)*

This report is dedicated to the memory of Fred Kaufman. It is the last and most ambitious of many studies to which he made major contributions for advisory committees of the National Academy of Sciences, National Aeronautics and Space Administration, Air Force Office of Scientific Research, National Science Foundation, National Research Council, and other institutions. Fred's service was so often sought, out of respect for his leadership in research and his judgment, vision, and luminous integrity. That he so often accepted these arduous tasks and devoted such effort to them exemplified his commitment to vital scientific development.

Frederick Kaufman stood among us as an intellectual and ethical leader for more than three decades. He established a taste for superb quality and originality in atmospheric chemistry through his field of gas phase radical kinetics. Born in Vienna, Austria in 1919, his early avocation was music; standing room only on Saturdays at the back of the upper balcony of the Opera House and practicing the piano under parental tutelage, he was to become a concert pianist. Fred acquired a vast knowledge of the musical literature and would gladly whistle any of the Mahler symphonies and many other pieces from memory; often quietly during boring scientific presentations.

Forced to leave Austria with his family in the late '30s, Fred's professional music career ended with an accident which seriously injured his hands and brought him from the family's temporary haven in Panama to Johns Hopkins School of Medicine as a patient. In 1941, his family emigrated to the United States and Fred returned to Hopkins as a student, moving from a beginning undergraduate to a Ph.D. in chemistry in just six years. The year was 1948. While his thesis dealt with organic solution kinetics, he turned to far more fundamental studies following his Ph.D. At the Ballistic Research Labs, then a leading research center in combustion chemistry and gas phase kinetics, Fred began his studies of gas phase free radicals. A Rockefeller Award took him to Cambridge, England where he simultaneously acquired control of free radical sources, an essential step in modern gas phase chemical kinetics, and brought discharge flow techniques into the forefront of atom-radical kinetics. It was from this point forward that Fred's immense power as an intellect, raconteur, and educator emerged in the fields of chemical kinetics and atmospheric physical chemistry.

Those privileged to work with Fred relished the opportunity. His zest and ardor in pursuit of science and his integrity and dedication were made all the more compelling by his intense interest in his colleagues. Fred was a natural teacher and leader. He drove toward intellectual excitement and provoked active involvement. He brought also boyish enthusiasm, eagerness, and exuberant humor, which somehow meshed naturally with great resources of charm, poise, and dignity. In the course of a typical encounter at a working dinner, a conversation with Fred would be likely to include a trenchant assessment of recent work in chemical kinetics as well as current political crises, a new art exhibit or concert, and the inside story of a favorite sports team.

Fred became the chemical conscience of the Space Research Coordination Center at the University of Pittsburgh in 1964 which was the foremost group of chemical physicists and aeronomers of that day. For the next twenty years, Fred and his research group concentrated on energy transfer processes, radical-molecule kinetics, excited state chemistry and spectroscopy and ion-molecule reactions.

The explosive development of the field of atmospheric chemistry following the realization that homogeneous gas phase chemical catalysis could distort the global distribution of ozone in the stratosphere revealed a new dimension in Fred Kaufman. In addition to innovation, strict standards of intellectual quality and scientific taste, he became the moral heart of an entire scientific community which was buffeted by new pressures from industry, government and the media. He steered our ship with wisdom, compassion and warmth.

James G. Anderson and Dudley R. Herschbach

## TABLE OF CONTENTS

### VOLUME I

Page

<b>CHAPTER 1 INTRODUCTION AND SCIENCE SUMMARY</b> .....	1
---	---

### **CHAPTER 2 STRATOSPHERIC CHEMISTRY**

2.0 INTRODUCTION .....	27
2.1 CURRENT STATUS OF KINETICS AND PHOTOCHEMICAL DATA BASE FOR TRACE GAS FAMILIES INVOLVED IN OZONE CHEMISTRY .....	29
2.2 SPECIAL ISSUES IN STRATOSPHERIC CHEMISTRY .....	43
2.3 SUMMARY AND CONCLUSIONS .....	54

### **CHAPTER 3 TROPOSPHERIC TRACE GASES: SOURCES, DISTRIBUTIONS AND TRENDS**

3.0 INTRODUCTION .....	57
3.1 HALOCARBONS .....	58
3.2 NITROUS OXIDE (N <sub>2</sub> O) .....	77
3.3 OXIDES OF NITROGEN (NO <sub>x</sub> ) .....	85
3.4 METHANE (CH <sub>4</sub> ) .....	88
3.5 CARBON MONOXIDE (CO) .....	100
3.6 CARBON DIOXIDE (CO <sub>2</sub> ) .....	106
3.7 SOURCE GASES FOR STRATOSPHERIC SULFATE AEROSOLS (OCS, CS <sub>2</sub> ) .....	112
3.8 VOLCANIC INJECTIONS OF CHLORINE INTO THE STRATOSPHERE .....	114
3.9 SECULAR TRENDS OF TRACE GASES FROM POLAR ICE CORES .....	115
3.10 SUMMARY AND RESEARCH RECOMMENDATIONS .....	115

**TABLE OF CONTENTS (Continued)**

**VOLUME I (Continued)**

*Page*

**CHAPTER 4 TROPOSPHERIC CHEMISTRY: PROCESSES CONTROLLING  
OZONE AND HYDROXYL RADICAL**

4.0 INTRODUCTION .....	117
4.1 PHOTOCHEMISTRY OF THE BACKGROUND TROPOSPHERE .....	117
4.2 CHEMISTRY OF OZONE FORMATION IN THE POLLUTED TROPOSPHERE .....	126
4.3 HETEROGENEOUS CHEMISTRY .....	132
4.4 SURFACE EXCHANGE AND VERTICAL REDISTRIBUTION .....	141
4.5 RESEARCH NEEDS .....	147

**CHAPTER 5 STRATOSPHERE-TROPOSPHERE EXCHANGE**

5.0 INTRODUCTION .....	151
5.1 EXCHANGE IN THE TROPICS .....	152
5.2 EXTRATROPICAL EXCHANGE .....	174
5.3 LARGE SCALE NUMERICAL MODELLING OF STRATOSPHERE- TROPOSPHERE EXCHANGE .....	230
5.4 ASSESSMENT OF STRATOSPHERE-TROPOSPHERE EXCHANGE .....	235

**CHAPTER 6 DYNAMICAL PROCESSES**

6.0 INTRODUCTION .....	241
6.1 CLIMATOLOGICAL MEANS AND VARIABILITY OF THE MIDDLE ATMOSPHERE .....	243
6.2 THEORY OF THE CIRCULATION OF THE MIDDLE ATMOSPHERE .....	278
6.3 MIDDLE ATMOSPHERE GENERAL CIRCULATION MODELS .....	297
6.4 OBSERVATIONS OF TRANSPORT PROCESSES .....	311
6.5 THEORY OF TRANSPORT PROCESSES .....	318

## TABLE OF CONTENTS (Continued)

<b>VOLUME I (Continued)</b>	<i>Page</i>
6.6 FUTURE NEEDS .....	337
6.7 SUMMARY .....	343
 <b>CHAPTER 7 RADIATIVE PROCESSES: SOLAR AND TERRESTRIAL</b>	
7.0 INTRODUCTION .....	349
7.1 SOLAR RADIATION AND ITS ABSORPTION IN THE STRATOSPHERE AND MESOSPHERE .....	349
7.2 TERRESTRIAL RADIATION .....	378
7.3 CONCLUSIONS AND FUTURE RESEARCH NEEDS .....	391
 <b>REFERENCES</b>	
 <b>VOLUME II</b>	
<b>SPECIAL INTRODUCTION FOR CHAPTERS 8, 9, 10 AND 11 OXYGEN, HYDROGEN, NITROGEN, AND HALOGENATED SPECIES: OBSERVATIONS AND INTERPRETATIONS .....</b>	
	393
 <b>CHAPTER 8 OXYGEN SPECIES: OBSERVATIONS AND INTERPRETATION</b>	
8.0 INTRODUCTION .....	401
8.1 OZONE REFERENCE PROFILES .....	403
8.2 COMPARISON OF CALCULATED AND OBSERVED OZONE PROFILES .....	420
8.3 OZONE AND TEMPERATURE CORRELATIONS .....	429
8.4 OZONE AND SOLAR VARIABILITY .....	433
8.5 OZONE AND SOLAR PROTON EVENTS .....	437
8.6 OZONE VARIATIONS ASSOCIATED WITH EL CHICHON/EL NINO .....	438
8.7 SUMMARY AND SUGGESTIONS FOR FUTURE RESEARCH .....	439

**TABLE OF CONTENTS (Continued)**

**VOLUME II (Continued)**

*Page*

**CHAPTER 9 HYDROGEN SPECIES: OBSERVATIONS AND INTERPRETATION**

9.0 INTRODUCTION .....	441
9.1 HYDROXYL (OH) MEASUREMENTS .....	441
9.2 HYDROPEROXYL (HO <sub>2</sub> ) MEASUREMENTS.....	450
9.3 HYDROGEN PEROXIDE (H <sub>2</sub> O <sub>2</sub> ) MEASUREMENTS .....	454
9.4 WATER (H <sub>2</sub> O) MEASUREMENTS .....	456
9.5 METHANE (CH <sub>4</sub> ) MEASUREMENTS .....	476
9.6 CONCLUSIONS .....	494
9.7 FUTURE RESEARCH NEEDS.....	495

**CHAPTER 10 NITROGEN SPECIES: OBSERVATIONS AND INTERPRETATION**

10.0 INTRODUCTION .....	497
10.1 NON-SATELLITE DATA .....	499
10.2 SATELLITE DATA .....	529
10.3 ODD NITROGEN MODELLING .....	576
10.4 CONCLUSIONS .....	601
10.5 FUTURE RESEARCH .....	603

**CHAPTER 11 HALOGENATED SPECIES: OBSERVATIONS  
AND INTERPRETATION**

11.0 INTRODUCTION .....	605
11.1 CHLORINE MONOXIDE (ClO).....	605
11.2 ATOMIC CHLORINE (Cl) .....	616
11.3 CHLORINE NITRATE (ClONO <sub>2</sub> ) .....	616
11.4 HYDROGEN CHLORIDE AND HYDROGEN FLUORIDE (HCl, HF) .....	618

## TABLE OF CONTENTS (Continued)

<b>VOLUME II (Continued)</b>	<i>Page</i>
11.5 STRATOSPHERIC DISTRIBUTION OF HALOCARBONS .....	632
11.6 TOTAL CHLORINE .....	646
11.7 CONCLUSIONS .....	647
11.8 FUTURE RESEARCH NEEDS.....	648

### REFERENCES

## VOLUME III

### CHAPTER 12 ASSESSMENT MODELS

12.0 INTRODUCTION .....	649
12.1 ON THE COMPARISON OF MODELS AND DATA.....	649
12.2 1-D MODELS: FORMULATION AND INTERPRETATION—RECENT DEVELOPMENTS .....	654
12.3 1-D MODELS: INTERCOMPARISON OF NO <sub>y</sub> DIFFERENCES .....	658
12.4 TWO-DIMENSIONAL MODELS—SOME THEORETICAL IDEAS .....	662
12.5 CURRENT MODELS.....	670
12.6 A COMPARISON OF TWO-DIMENSIONAL MODELS .....	681
12.7 CHEMISTRY IN THREE-DIMENSIONAL MODELS .....	711
12.8 ON THE USE OF MODELS FOR ASSESSMENT STUDIES .....	714
12.9 CONCLUSIONS .....	719

### CHAPTER 13 MODEL PREDICTIONS OF OZONE CHANGES

13.0 INTRODUCTION .....	721
13.1 RESULTS OF MODEL CALCULATIONS.....	722
13.2 DISCUSSION OF CURRENT MODEL PREDICTIONS AND ASSESSMENT OF RECOGNIZED UNCERTAINTIES .....	771
13.3 SUMMARY AND CONCLUSIONS .....	786

**TABLE OF CONTENTS (Continued)**

**VOLUME III (Continued)**

*Page*

**CHAPTER 14 OZONE AND TEMPERATURE TRENDS**

14.0 INTRODUCTION .....	789
14.1 OZONE TRENDS .....	789
14.2 TEMPERATURE TRENDS .....	808
14.3 SUMMARY .....	819

**CHAPTER 15 TRACE GAS EFFECTS ON CLIMATE**

15.0 INTRODUCTION .....	821
15.1 NATURE OF RADIATIVE FORCING .....	829
15.2 THEORY AND MODELS .....	845
15.3 EFFECTS ON ATMOSPHERIC AND SURFACE TEMPERATURES .....	854
15.4 TRANSIENT CLIMATIC EFFECTS OF INCREASING ATMOSPHERIC CO <sub>2</sub> .....	866
15.5 TRACE GAS EFFECTS ON OBSERVED AND FUTURE CLIMATE TRENDS .....	871
15.6 SCIENTIFIC CHALLENGES FOR THE FUTURE .....	885

**APPENDIX A KINETICS AND PHOTOCHEMICAL DATA BASE .....** 895

**APPENDIX B SPECTROSCOPIC DATABASE: INFRARED TO MICROWAVE**

B-0 INTRODUCTION .....	911
B-1 OVERVIEW OF ATMOSPHERIC SPECTROSCOPY .....	911
B-2 QUANTITATIVE HIGH-RESOLUTION ATMOSPHERIC SPECTROSCOPY .....	912
B-3 LABORATORY SPECTROSCOPY BY SPECTRAL ANALYSIS AND PREDICTIONS .....	923
B-4 USE OF SPECTROSCOPIC DATA TO DERIVE ATMOSPHERIC COMPOSITION .....	926

**TABLE OF CONTENTS (Continued)**

**VOLUME III (Continued)**

*Page*

B-5 EXAMPLES OF SPECTROSCOPIC DATA REQUIREMENTS FOR SPACE-BASED REMOTE SENSING OF THE ATMOSPHERE ..... 929

B-6 DATABASE ASSESSMENT ..... 935

B-7 CONCLUSIONS AND RECOMMENDATIONS ..... 938

**APPENDIX C INSTRUMENT INTERCOMPARISONS AND ASSESSMENTS**

C-0 INTRODUCTION ..... 951

C-1 OZONE (O<sub>3</sub>) ..... 953

C-2 WATER VAPOR (H<sub>2</sub>O) ..... 963

C-3 OTHER SPECIES ..... 968

C-4 CONCLUSIONS ..... 975

C-5 FUTURE RESEARCH NEEDS ..... 977

**APPENDIX D MONTHLY MEAN DISTRIBUTION OF OZONE AND TEMPERATURE**

D-0 INTRODUCTION ..... 981

D-1 DATA ..... 981

D-2 REGULAR COMPONENTS: ANNUAL, SEMI-ANNUAL AND QUASI-BIENNIAL WAVES ..... 983

D-3 INTERANNUAL VARIABILITY ..... 998

D-4 MONTHLY MEAN CHARTS OF TOTAL OZONE, AND OF OZONE MIXING RATIOS AND TEMPERATURES AT SELECTED PRESSURE LEVELS ..... 1007

**APPENDIX E LIST OF CONTRIBUTORS** ..... 1033

**APPENDIX F LIST OF FIGURES** ..... 1043

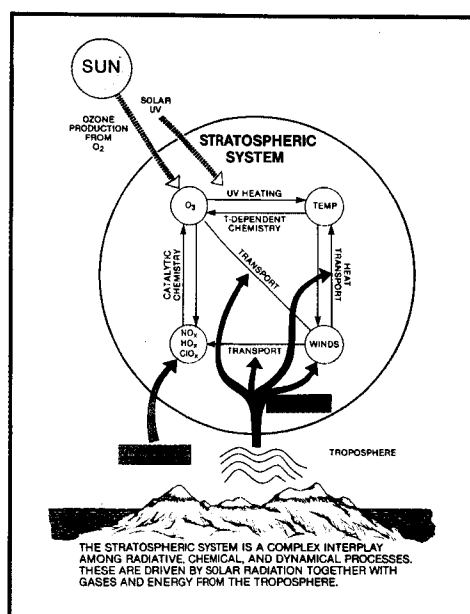
**APPENDIX G LIST OF TABLES** ..... 1077

**TABLE OF CONTENTS (Continued)**

<b>VOLUME III (Continued)</b>	<i>Page</i>
<b>APPENDIX H MAJOR ACRONYMS</b> .....	1083
<b>APPENDIX I CHEMICAL FORMULAE AND NOMENCLATURE</b> .....	1091
<b>APPENDIX J PRESSURE-ALTITUDE CONVERSION CHART</b> .....	1095
<b>REFERENCES</b>	

# **VOLUME I**

# INTRODUCTION AND SCIENCE SUMMARY



## Panel Members

R.T. Watson

R.A. Cox  
S.C. Wofsy  
V.A. Mohnen  
A.F. Tuck  
R.A. Plumb  
J. Frederick  
C. Leovy

G. Brasseur  
H.I. Schiff  
J.E. Harries  
M.J. Molina  
J.A. Pyle  
H.S. Johnston  
A.J. Miller

K. Labitzke  
V. Ramanathan  
W.B. DeMore  
N. Husson  
D.L. Albritton  
R. Stolarski  
M. Geller

## CHAPTER 1: INTRODUCTION AND SCIENCE SUMMARY

For several decades scientists have sought to understand the complex interplay between the chemical, radiative, and dynamical processes that govern the structure of the Earth's atmosphere. During the last decade or so there has been particular interest in studying the processes which control atmospheric ozone since it has been predicted that man-made pollutants might cause harmful effects to the environment by modifying the total column content and vertical distribution of atmospheric ozone. Until recently most of the emphasis was directed towards understanding the stratosphere where greater than 90% of the ozone resides. However, during the last few years there has been an increasing interest in studying those factors which control ozone in the troposphere.

Changes in the total column content of atmospheric ozone would modify the amount of biologically harmful ultraviolet radiation penetrating to the Earth's surface with potential adverse effects on human health (skin cancer) and on the aquatic and terrestrial ecosystems. Changes in the vertical distribution of atmospheric ozone, along with changes in the atmospheric concentrations of other infrared active gases, could contribute to a change in climate on a regional and global scale by modifying the atmospheric temperature structure.

The ozone issue has evolved from one of the effect of individual pollutants to consideration of a multiplicity of possible pollutants the effects of which must be considered together. The man-made and natural chemicals of interest include the nitrogen oxides ( $\text{NO}_x$ ) from subsonic and supersonic aircraft, nitrous oxide ( $\text{N}_2\text{O}$ ) from agricultural and combustion practices, chlorofluorocarbons (CFC's) used as aerosol propellants, foam blowing agents, and refrigerants, brominated compounds used as fire retardants, carbon monoxide ( $\text{CO}$ ) and carbon dioxide ( $\text{CO}_2$ ) from combustion processes, and methane ( $\text{CH}_4$ ) from a variety of sources including natural and agricultural wetlands, tundra, biomass burning, and enteric fermentation in ruminants. It is now clear that these same gases are also important in the climate issue.

It should be noted that there are two distinct aspects of the issue that need to be considered, i.e. understanding those processes that control the atmospheric distribution of ozone today, and those processes that need to be understood in order to be able to predict the atmospheric distribution of ozone in the future. If changes are observed in the distribution of ozone we must be able to understand how periodic and episodic natural phenomena such as solar activity and volcanic eruptions cause ozone to vary in space and time in order to isolate the impact of the changing atmospheric concentrations of gases such as the CFC's,  $\text{CO}_2$ ,  $\text{CH}_4$ , and  $\text{N}_2\text{O}$ .

Since the scientific community first attempted to understand the chemical, radiative, and dynamical processes which control the temporal and spatial distribution of atmospheric ozone today, and to predict the distribution of ozone in the future, our recognition of the breadth of the issue has steadily increased. Originally the research emphasis was focused on understanding the physical and chemical processes occurring within the stratosphere. Now, however, we recognize that in order to be able to predict the distribution of ozone in the future we cannot be confined to simply understanding stratospheric chemistry, radiation, and dynamics but we also need to understand the processes controlling the chemical composition of the troposphere, the exchange mechanisms for energy, mass and chemical constituents across the tropopause, and the role of biospheric processes in controlling the emissions of gases into the atmosphere. This has made the ozone issue an example of how one problem requires us to bring knowledge from a variety of sources to bear on its solution and how understanding this problem contributes back to other fields such as the trace gas-climate problem and the global cycling of nitrogen and carbon.

## INTRODUCTION

Thus to really understand the processes which control atmospheric ozone and to predict perturbations we are drawn into a study of the complete Earth system. This requires us to study the Earth as a single coupled system which involves chemical, physical, and biological processes occurring in the atmosphere, on land, and in the oceans. This is exactly the same situation which exists if we want to understand and have some predictive capability for the climate system. This report mirrors these increasing perceptions of the coupled nature of the system and, while focusing on the stratosphere, gives more consideration to the other aspects of the issue than previous reports on the ozone issue.

In particular the scientific community recognizes, and this report discusses, that:

- (a) There is strong coupling in the stratosphere between the chemistry, radiation, and dynamics. This is because atmospheric ozone is a strong absorber of solar radiation, thus strongly influencing the temperature structure and circulation of the stratosphere, which in turn controls the distribution of atmospheric ozone and the trace gases which control ozone.
- (b) Since 1930, when Chapman first proposed a simple photochemical scheme involving only odd oxygen species to explain the atmospheric concentration of ozone, our understanding of the photochemistry of the atmosphere has evolved significantly. Scientists have refined this simple scheme by invoking the importance of trace concentrations (ppbv) of  $\text{HO}_x$ ,  $\text{NO}_x$ ,  $\text{ClO}_x$ , and to a lesser extent  $\text{BrO}_x$  species in catalytically controlling atmospheric ozone. In addition, we also recognize that the atmospheric concentrations of a number of carbon compounds including  $\text{CO}$ ,  $\text{CO}_2$ , and  $\text{CH}_4$  play a vital role in the photochemistry of ozone. In particular, we recognize that there is strong coupling between the individual members of each chemical family, and that while each of these families individually is important in controlling odd oxygen, there is strong chemical coupling between the different chemical families, thereby modifying their individual roles in controlling ozone.
- (c) At different times during the last decade or so scientists have suggested that the atmospheric concentrations of one or more of the source gases of the hydrogen, carbon, nitrogen, chlorine, or bromine chemical families may be changing due to human activities, and in each case have attempted to predict the response of the ozone layer to such individual changes. We now have reliable experimental evidence that the atmospheric concentrations of several of the source gases, i.e.  $\text{CH}_4$ ,  $\text{N}_2\text{O}$ , and the chlorofluorocarbons, are all currently changing at a significant rate and that their impact on atmospheric ozone must be considered collectively and not in isolation.
- (d) We need to understand the role of the biosphere in regulating the emissions of gases such as  $\text{CH}_4$ ,  $\text{CO}_2$ ,  $\text{N}_2\text{O}$ , and  $\text{CH}_3\text{Cl}$  to the atmosphere, and we need to know the most probable future industrial release rates of gases such as the CFC's,  $\text{N}_2\text{O}$ ,  $\text{CO}$ , and  $\text{CO}_2$  which depend upon economic, social, and political factors.
- (e) Because of the fact that neither the chemical composition nor the interplay between meteorology and chemistry can be duplicated exactly in the laboratory, heavy reliance must be placed on theoretical models to describe the present and future behavior of the atmosphere. As a consequence it is necessary to define a careful strategy of investigation involving the proper balance between laboratory studies of fundamental processes, field measurements, and theoretical studies.

- (f) While one-dimensional photochemical models have been, and will continue to be, extensively used for assessment purposes we must place more emphasis in the future on the development of two-dimensional and three-dimensional interactive photochemical models. Such multidimensional models allow us to explore the seasonal, latitudinal, and longitudinal behavior of ozone. Also, given that they more realistically represent the real world, they are more amenable to validation using field measurements of atmospheric composition.
- (g) The climate problem has broadened in scope from the CO<sub>2</sub>-climate problem to the trace gas-climate problem. Changes in the atmospheric concentrations of ozone as well as H<sub>2</sub>O, CH<sub>4</sub>, N<sub>2</sub>O, the CFC's, and other gases will all modify the thermal structure of the atmosphere.
- (h) We need to improve our understanding of tropospheric chemistry because of its vital role in controlling the atmospheric lifetimes of many of the source gases such as CH<sub>4</sub> and CH<sub>3</sub>Cl, which influence atmospheric ozone and the radiative balance of the atmosphere. We also recognize that changes in tropospheric ozone will influence the climate system and will affect our interpretation of trends in the total ozone column.
- (i) A vital component of any atmospheric research program is the acquisition of well calibrated long-term (multiyear) measurements of atmospheric parameters in order to monitor the state of the atmosphere and to differentiate between the different scales of temporal variability.
- (j) Global data sets obtained from satellites are essential to complement data obtained using ground, aircraft, balloon, and rocket based instrumentation. Such data sets are essential to more fully understand the interplay on a global scale between chemical, radiative and dynamical processes, and to validate aspects of the multidimensional models. In addition, such data are needed to check the geographical representativeness of local measurements of large scale phenomena.

Unlike some other more localized environmental issues, e.g. acid deposition, ozone layer modification is a global phenomenon which affects the well-being of every country in the world. Many nations around the world have actively demonstrated their commitment to understand the processes which control atmospheric ozone, and its susceptibility to change because of human activities, by funding research which should reduce the uncertainties that currently exist concerning the magnitude of predicted ozone modification for different atmospheric concentrations of pollutants. In order to achieve this required greater level of understanding, national and international scientific agencies have implemented long range research programs aimed at developing an organized, reliable body of knowledge of upper atmospheric processes while providing, in the near term, assessments of potential effects of human activities on the atmosphere.

Many governments around the world have recognized that the use of chlorofluorocarbons constitutes a potential threat to the stability of the ozone layer, and have taken a series of individual actions to regulate the use of these substances. However, there has been no coordinated international approach to safeguard the ozone layer. It was recognized by several nations that effective protection of the ozone layer requires a coordinated international approach to regulating substances that are thought to modify atmospheric ozone. Consequently, the United Nations Environment Program (UNEP) Governing Council, at its ninth session in 1981, decided to initiate work aimed at the elaboration of a global framework convention for the protection of the ozone layer. It was decided to establish an Ad Hoc Working Group of Legal and Technical Experts nominated by interested governments and intergovernmental organizations. Representatives from about twenty different countries met in Stockholm, Sweden in January 1982 to initiate formal discussions on the desirability of a global framework ozone convention which would (a) harmonize regulatory control

## INTRODUCTION

actions on ozone modifying substances at the international level, (b) increase coordination of ozone related research, and (c) increase the exchange of information on all scientific, economic, technical, and legal issues relevant to the ozone issue. After a series of meetings of the Ad Hoc Working Group of Legal and Technical Experts, a Convention for the Protection of the Ozone Layer was adopted by twenty-one nations at a Diplomatic Conference held in Vienna, Austria, in March 1985. Since that time four more nations have signed the convention. At the thirteenth UNEP Governing Council meeting held in May, 1985, a schedule was adopted for the possible completion of a protocol to regulate chlorofluorocarbons. Since the convention specifically states that all measures taken under this convention should be based on relevant scientific and technical considerations, and that nations should collaborate on scientific assessments, the need for a comprehensive evaluation by the international scientific community of all facets of the ozone issue is clear.

Therefore, in order to provide governments around the world with the best scientific information currently available on whether human activities represent a substantial threat to the ozone layer, several scientific agencies agreed to co-sponsor a peer reviewed international assessment of our current state of knowledge. This assessment is much more comprehensive than any previous assessment. It discusses, among other topics, the physical, chemical, and radiative processes which control the spatial and temporal distribution of ozone in the troposphere and stratosphere; the magnitude of natural and industrial sources of substances capable of modifying atmospheric ozone; observations of the composition and structure of the stratosphere; the predicted magnitude of ozone perturbations for a variety of emission scenarios involving a number of substances changing both individually and together; the predicted climate change for similar trace gas scenarios employed to predict ozone perturbations; and the ozone and temperature data used to detect the presence or absence of a long-term trend. Previous assessments have tended to be narrower both in scope and in the degree of international participation.

There has been an increasing level of cooperation and coordination at the international level over the last decade for ozone assessment activities. This is demonstrated by the international participation in this report and the previous World Meteorological Organization (WMO)/National Aeronautics and Space Administration (NASA)/National Oceanic and Atmospheric Administration (NOAA)/Federal Aviation Administration (FAA) report in 1982. There have been at least three types of assessment report relating to the ozone issue produced over the last decade, i.e.

- (a) comprehensive national assessment reports such as the series produced biennially by the National Academy of Sciences in the USA, the latest of which is "Causes and Effects of Changes in Stratospheric Ozone: Update 1983," and those issued by the Department of the Environment, United Kingdom, the latest of which is "Chlorofluorocarbons and Their Effect on Stratospheric Ozone (second report)" - Pollution Paper #15, 1979.
- (b) international summary reports written by a small select group of scientists at a one-week meeting such as the yearly series issued by the UNEP Coordinating Committee on the Ozone Layer (CCOL), the latest of which is "Environmental Assessment of Ozone Layer Depletion and its Impact as of October 1984," and the one issued in 1981 by the Commission of the European Communities, (CEC), "Evaluation of the Effects of Chlorofluorocarbons on Atmospheric Ozone: Present Status of Research."
- (c) comprehensive international reports such as that issued by the WMO in 1982 which had over 100 participants from the international scientific community, "The Stratosphere 1981: Theory and Measurements" WMO Global Ozone Research and Monitoring Project Report #11.

## INTRODUCTION

This scientific assessment is being co-sponsored by three US agencies, i.e. the National Aeronautics and Space Administration (NASA), the Federal Aviation Administration (FAA), and the National Oceanic and Atmospheric Administration (NOAA); three international agencies, i.e. the World Meteorological Organization (WMO), the United Nations Environment Program (UNEP), and the Commission of the European Communities (CEC), and Bundesministerium für Forschung und Technologie (BMFT) of the Federal Republic of Germany.

Approximately 150 scientists from Australia, Belgium, Brazil, Canada, the Federal Republic of Germany, France, Italy, Japan, Norway, the United Kingdom, and the United States of America contributed towards this assessment, which was coordinated by NASA.

This assessment builds upon previous national and international assessments, in particular the most recent comprehensive report, "The Stratosphere 1981: Theory and Measurements" WMO Global Ozone Research and Monitoring Project Report #11 which was prepared in 1981 (issued in 1982) and was co-sponsored by the same three U.S. scientific agencies, (NASA, FAA, and NOAA) and by one international scientific agency, WMO. The rationale for the scope of the present assessment report was based on information gained at a scientific workshop, entitled "Current Issues in Our Understanding of the Stratosphere and the Future of the Ozone Layer" which was held in Feldafing, Federal Republic of Germany in June 1984 with international participation, co-sponsored by NASA, FAA, WMO, and BMFT. The assessment activities officially began in the fall of 1984 when leading scientists were selected as chairpersons, and each charged with the responsibility to produce a specific chapter in the assessment report. At a meeting held in November, 1984, the timetable for the assessment was established and key atmospheric scientists who could make valuable contributions were identified and invited to participate in chapter working groups. The participants were chosen for their expertise and represented a cross section of the international scientific community. The assessment was developed through a series of small focused workshops, chapter by chapter, each addressing a specific scientific issue. Considerable care was taken to ensure that those aspects of the issue which involved more than one chapter were carefully coordinated. Over 30 small working meetings were held between November, 1984, and May, 1985, to prepare draft chapters which were then critically peer reviewed at a workshop held at Les Diablerets, Switzerland July 7-14, 1985. The 32 participants who attended the meeting included 19 chapter chairpersons, 8 senior reviewers from the atmospheric scientific community, and 5 sponsoring agency representatives. Based on the reviews, the chapters were then finalized and sent to the printers in November/December 1985.

The following section of the Introduction describes the contents, and major conclusions and recommendations for future research of each chapter of the assessment report.

## CHAPTER 2: STRATOSPHERIC CHEMISTRY

This Chapter deals with the elementary chemical and photochemical processes involving atmospheric trace gases and is written in two parts. The first part discusses the recent improvements in the data base for the reactions currently identified to be important in describing the chemistry of the major chemical families of trace gases in the stratosphere or unpolluted troposphere, i.e. oxygen, hydrogen, nitrogen, chlorine, bromine, sulfur, halocarbons and hydrocarbons. The second part discusses a number of special issues relating to stratospheric chemistry including:

- (a) The importance of ion chemistry; sodium chemistry; heterogeneous chemistry; and reactions between long-lived reservoir species in controlling ozone;

## INTRODUCTION

- (b) The ability of current reaction rate theory to describe reactions with complex pressure and temperature dependence functions;
- (c) Errors and uncertainties in current kinetic and photochemical data, and the prospects for improvement;
- (d) Prospects for developing a systematic approach for identifying gaps in the chemical description of the atmosphere.

## Major Conclusions and Recommendations

- (1) There has been continued steady improvement in the data base for the reaction rate coefficients, product distributions, absorption cross sections, and photodissociation quantum yields of the elementary processes;
- (2) No significant new catalytic cycles, or radical or reservoir species have been identified since WMO (1982);
- (3) Changes or re-evaluations in accepted rate coefficients for several important reactions, e.g.  $O + ClO$ ,  $OH + HCl$ ,  $OH + HNO_3$ , and  $HO_2 + NO_2 + M$  have led to refinements in predictions of ozone depletion, and have in general improved agreement between measured and computed vertical profiles for trace gases.
- (4) Further laboratory studies of the rates, branching ratios and photodissociation channels of reactions involved in the production of  $NO_x$  from  $N_2O$  in the stratosphere, are required to reduce the uncertainties in this source term.
- (5) Several key reactions involving  $HO_x$  species proceed through long lived intermediates, resulting in complex pressure and temperature behavior, e.g.  $OH + CO$ ,  $HO_2 + O_3$ ,  $HO_2 + OH$ , etc. These reactions need further study to provide better characterization over the full range of atmospheric conditions.
- (6) Uncertainties in the data base for  $BrO_x$  and coupled  $BrO_x-ClO_x$  catalyzed ozone destruction need to be reduced.
- (7) A continued effort is required to identify possible missing chemistry or species of significance in the stratosphere, making use of all state-of-the-art experimental and computational techniques.

## CHAPTER 3: TROPOSPHERIC TRACE GASES: SOURCES, DISTRIBUTION AND TRENDS

This Chapter discusses the important source gases (CFC's,  $CH_4$ ,  $CO$ ,  $CO_2$ ,  $N_2O$ , and  $NO_x$ ) which are emitted at the Earth's surface. For each of these gases, measurements of their current atmospheric concentrations and trends are discussed, as well as information about their sources and their possible future course.

## Major Conclusions and Recommendations

- (1) There is now compelling evidence that the composition of the atmosphere is changing on a global scale reflecting in part the metabolism of the biosphere and in part a broad range of human activities. These source gases play important direct and indirect roles in both atmospheric chemistry and climate.
- (2) Halocarbons
  - The halocarbons are generally of industrial origin except for  $\text{CH}_3\text{Cl}$ .
  - The atmospheric concentrations of CFC-11, CFC-12,  $\text{CH}_3\text{CCl}_3$ , and  $\text{CCl}_4$  as of late 1985 were about 230 pptv, 400 pptv, 130 pptv and 125 pptv and are observed to be increasing at annual rates of about 5% for CFC's 11 and 12, 7% for  $\text{CH}_3\text{CCl}_3$  and 1% for  $\text{CCl}_4$ .
  - The Atmospheric Lifetime Experiment (ALE) measurements indicate an increase in the atmospheric concentration of CFC-11 consistent with the Chemical Manufacturers Association (CMA) release estimates, but to explain the observed increase in the atmospheric concentration of CFC-12 requires a substantial additional source. Insufficient information is available about possible releases from the USSR and Eastern Europe. There is consistency between the sources and inventory for  $\text{CCl}_4$  and  $\text{CH}_3\text{CCl}_3$ .
  - Based on ALE data the atmospheric residence times for CFC-11, CFC-12,  $\text{CCl}_4$ , and  $\text{CH}_3\text{CCl}_3$  are calculated to be approximately 75, 110, 50 and 6.5 years, respectively.
  - Only a few atmospheric measurements exist, and there is limited information on emission strengths, for the numerous other halocarbons.
- (3) Methane ( $\text{CH}_4$ ), Carbon Monoxide (CO) and Carbon Dioxide ( $\text{CO}_2$ )
  - The world-wide average atmospheric concentration of methane as of late 1985 was 1.65 ppmv, and for the last decade or so has been increasing at an annual rate of about 1%. In addition ice-core data indicate that the atmospheric concentration of  $\text{CH}_4$  may have steadily increased over the last several hundred years from a value of approximately 0.7 ppmv.
  - The important sources of methane include anaerobic environments such as: natural and agricultural wetlands, termites, enteric fermentation in ruminants, and biomass burning.
  - The atmospheric concentration of CO is significantly greater in the Northern Hemisphere than the Southern Hemisphere, and there are indications of an annual rate of increase of 1-2%.
  - Projections of concentrations of atmospheric methane and carbon monoxide into the future are difficult because the origins of the current increase of  $\text{CH}_4$  are unknown, i.e. what fraction of the increase can be attributed to increased source strengths versus decreased atmospheric removal rates.
  - The global mean concentration of  $\text{CO}_2$  is currently about 344 ppmv and there is clear evidence of an annual rate of increase of about 0.5% predominantly because of the combustion of fossil fuels.
  - The atmospheric concentrations of each of the carbon species exhibit seasonal variability which is largest at high latitudes in the Northern Hemisphere and smallest in the Southern Hemisphere. The seasonal variability in CO reaches 50%,  $\text{CO}_2$  ranges from 0.5 to 5%, and  $\text{CH}_4$  ranges from 2 to 4%.
- (4) Nitrous Oxide ( $\text{N}_2\text{O}$ )
  - The atmospheric concentration of nitrous oxide as of late 1985 was about 304 ppbv and is increasing at an annual rate of about 0.25%. Because of its long atmospheric lifetime, i.e. ~ 150 years, this implies that the current strength of the sources is 30% greater than that of the sinks.

## INTRODUCTION

Consequently, if the emissions of  $N_2O$  continue at their present rates the atmospheric abundance of  $N_2O$  would increase to about 400 ppbv. In addition, there is reason to believe that the strengths of the combustion and intensive agricultural sources of  $N_2O$  will continue to increase.

- (5) Odd Nitrogen ( $NO_x$ )
  - There are still many disputes over the magnitude of the lightning source of  $NO_x$ .
  - It is likely that global emission rates of  $NO_x$  are increasing and little doubt that concentrations are now higher than preindustrial values. It is not clear to what extent industrial emissions of  $NO_x$  affect the remote atmosphere.
- (6) Continued development of baseline measurements for  $CO$ ,  $CH_4$ ,  $N_2O$ ,  $CO_2$  and the halocarbons are vital.
- (7) Flux measurements of biogenic gases from representative ecosystems, especially for  $CO_2$ ,  $CH_4$ ,  $N_2O$ , and  $NO$ , are needed in conjunction with studies of the underlying biological and geochemical processes which regulate the observed fluxes. In the case of  $CH_4$ , isotopic studies promise to elucidate the relative importance of various ecosystems in producing  $CH_4$ .
- (8) Studies of trace gases in ice cores should elucidate the historical atmospheric concentrations of these gases.
- (9) It is essential that the world-wide industrial production figures of all halocarbons be available.

## CHAPTER 4: TROPOSPHERIC CHEMISTRY

This Chapter discusses various aspects of the chemistry of the troposphere. Significant emphasis is placed on discussing factors which control the abundance and distribution of  $OH$  and  $O_3$ . In addition the roles of these species are discussed in some detail, e.g. the role of  $OH$  in controlling the atmospheric abundances (lifetimes) of many trace gases which can affect the chemical composition or the radiative balance of the stratosphere and troposphere. The problems of the chemical description of the unpolluted or non-urban troposphere are considered separately from the polluted troposphere and the problem of transport from polluted to relatively unpolluted regions is discussed. Heterogeneous chemistry is highlighted as a poorly understood area which is likely to be important in the troposphere. Finally, there is a discussion of the problems of surface exchange and vertical redistribution.

### Major Conclusions and Recommendations

- (1) It is encouraging that the values of globally averaged  $OH$  calculated in models of the unpolluted troposphere now seem consistent with  $CH_3CCl_3$  lifetime estimates. However, it should be noted that the lack of reliable atmospheric measurements of  $NO_x$  and  $CO$  contributes significantly to uncertainties in  $O_3$  and  $OH$  photochemistry in the unpolluted troposphere.
- (2) Many industrial compounds reach the unpolluted troposphere only after residence in the polluted troposphere - e.g.,  $NO_x$ ,  $CO$ , and non-methane hydrocarbons.
- (3) One major difference between the chemistry of the troposphere and stratosphere is the recognized importance of heterogeneous reactions. However, our present understanding of heterogeneous

reactions is rudimentary. Consequently, theoretical models currently have to use simple parameterizations of processes not yet understood. Calculations indicate that in regions of high aerosol loading, scavenging by the aerosol could represent a significant sink for  $\text{HNO}_3$ ,  $\text{NO}_3$ ,  $\text{H}_2\text{O}_2$  and possibly  $\text{HO}_2$ .

- (4) Large temporal and spatial variations in the hydrological cycle can lead to large temporal and spatial variations in rainout removal rates and concentrations of species like odd nitrogen.
- (5) Vertical redistribution in the troposphere is mainly accomplished by highly intermittent cloud processes that cannot be adequately described in a diffusive model.
- (6) Surface deposition is dependent on a combination of the turbulent exchange rate near the surface and the interaction of the particular species with the surface.
- (7) To understand the basic chemical cycles in the troposphere, and to predict the tropospheric response to perturbations requires:
  - An evaluation of biological sources of chemical substances in the troposphere.
  - Determination of the the global distribution of tropospheric trace gases and aerosol particles and assessment of relevant physical properties.
  - Testing of photochemical theory through field and laboratory investigations of photochemically driven transformation processes.
  - Investigations of wet and dry removal processes for trace gases and aerosol particles.
- (8) Methods are now becoming available to measure surface fluxes of chemical species.
- (9) Further laboratory studies are needed to determine the kinetics and mechanisms of the oxidation of methyl and other organic radical species under the 'low  $\text{NO}_x$ ' conditions pertaining in the background troposphere.

## CHAPTER 5: STRATOSPHERE-TROPOSPHERE EXCHANGE

This Chapter discusses the transport of mass and trace species between the stratosphere and troposphere. Meteorological processes in the tropics which are believed to affect exchange are reviewed; a special section is devoted to cumulonimbus clouds. Detailed aircraft case studies are described, and discussed in the context of the stratospheric water vapor budget. Exchange in the extratropics is considered from the meteorological point of view, and is largely concerned with tropopause folding during upper level frontogenesis. A theoretical outline is briefly presented, followed by a global scale isentropic diagnosis using First GARP Global Experiment (FGGE) data. Past work is reviewed, and recent aircraft studies are considered in some detail. Information about ozone exchange from ground based and satellite studies is also discussed. Results from general circulation models are considered, and analyses from an operational numerical weather prediction model are compared with aircraft data.

### Major Conclusions and Recommendations

- (1) While considerable progress has been made in aircraft-based studies, both of tropical cumulonimbus and extratropical exchange near polar front jet streams, there remains the need to incorporate

## INTRODUCTION

our understanding of these individual cloud-mass and synoptic-scale events into a global framework. In particular, synthesis of the global scale morphology of the cross-tropopause flux of specific molecules will require considerable thought and work, on case studies, satellite data, and global meteorological analyses.

- (2) Case studies of exchange processes at subtropical jet streams, particularly above their cores, are required.
- (3) Studies of exchange processes at polar front jet streams, particularly where the flow is split, are required, to investigate both the extent of mixing and the possibility of return flow to the stratosphere.
- (4) Exchange in cut-off lows needs to be studied further, to establish how much of it is reversible.
- (5) Studies near tropopause level should be made in cut-off anticyclones, with a view to establishing the tropopause behavior on radiative time scales.
- (6) Investigation of exchange processes in connection with the largest (highest reaching) cumulonimbus storms is required, to establish whether or not they are consistent with the height of the hygropause.
- (7) The sources of the water vapor between the tropopause and the hygropause needs to be established, especially in middle and high latitudes. This will afford valuable insight into the role of large scale, quasi-horizontal processes in cross-tropopause fluxes.

## CHAPTER 6: DYNAMICAL PROCESSES

The Chapter begins with a description of the structure and circulation of the middle atmosphere and a discussion of the observational techniques on which this picture is based. Our current theoretical understanding of the circulation is presented; particular emphasis is given to the crucial role of eddy motions in the maintenance of the circulation. The present status of general circulation modeling of the region is discussed and the shortcomings of model climatologies are discussed in the light of theoretical knowledge.

The advent of satellite observations of middle atmosphere constituent distributions is having a major impact on our knowledge of these distributions and our understanding of the processes which control them. These new observations are described and our theoretical understanding of global transport processes and their representation in zonally-averaged transport models is discussed.

### Major Conclusions and Recommendations

- (1) Much of our information on the middle atmosphere circulation is based on satellite observation of temperature alone. Wind and higher-order derived quantities such as potential vorticity are derived from these measurements, together with lower boundary conditions from conventional analyses, using mathematical manipulations such as spatial differentiation which can degrade the signal-to-noise ratio. The availability of direct wind observations from UARS will greatly improve this situation.
- (2) The major advantage of satellite measurements is their global coverage and uniformity. One further attribute which needs greater emphasis than it has received in the past is continuity of measure-

ment. This is highly desirable for the establishment of climatologies and absolutely vital for the detection of trends. It is therefore urged that further remote sensing missions be planned to succeed UARS following 1989 and that more emphasis be given to the intercalibration of successive satellite measurements.

- (3) Ground-based techniques (radars and lidars) have proven to be very useful for dynamical studies, especially for important small-scale motions such as gravity waves. It is desirable that these facilities operate on a more continuous basis and that observations from different sites be coordinated. Equatorial measurements are needed and networks would be very valuable. Lidars and radars should be co-located.
- (4) While general circulation modeling of the middle atmosphere is increasingly proving to be a useful tool in studies of the region, such models continue to have major deficiencies. The most serious of these is their pathology in generating winter high-latitude temperatures far below those observed. Theory suggests that this must be due to an underestimate of eddy transport processes; this could be a result of an inadequate representation of planetary wave activity or of the inability of the models to resolve gravity waves. The role of gravity waves in the actual stratospheric momentum budget requires further study.
- (5) Our conceptual picture of stratospheric transport processes has changed dramatically in recent years and the theoretical basis of the parameterization of transport in zonally-averaged models has been made more secure. At the same time, however, the limitations of such models are becoming more apparent. Some of these limitations are obvious, given the highly three-dimensional nature of the wintertime flow (especially during active periods in the Northern Hemisphere). Others, such as the inability of zonally-averaged models to be truly interactive in the sense of predicting climate changes, are perhaps less obvious but equally important. Given the present problems of general circulation modeling and the expense of running such models with chemistry included, however, it is not envisaged that fully three-dimensional assessments will be forthcoming in the near future. Three-dimensional transport modeling may depend on a simplified approach; a new theoretical framework is needed to make this a reality.

## CHAPTER 7: RADIATIVE PROCESSES; SOLAR AND TERRESTRIAL

There are two distinct parts to this Chapter. The first deals with solar radiation and its absorption in the stratosphere and mesosphere, and the second deals with terrestrial, or long-wave radiation. The discussion of the solar spectrum is broken up into irradiance from wavelengths shorter than 175 nm which affects the mesosphere and above, and the irradiance for wavelengths longer than this that affects the stratosphere. Tables are given for a reference solar spectrum, and variations of the solar spectral irradiance over the 27-day solar rotation period and the 11-year cycle. Other topics in the solar part of this chapter concern Rayleigh scatter, absorption by molecular oxygen, and ozone. The portion of this chapter dealing with terrestrial radiations deals with the adequacy of spectroscopic data to check our radiation calculations. It also deals with concepts of radiative damping, long-wave radiation in the stratosphere and mesosphere, as well as the distribution of net radiative heating through the atmosphere.

### Major Conclusions and Recommendations

- (1) Solar spectral irradiance is known to an accuracy of  $\pm 10-15\%$  between 175-210 nm,  $\pm 10\%$  or better between 210 and 330 nm, and to  $\pm 5\%$  or better at longer wavelengths.

## INTRODUCTION

- (2) The variability in solar irradiance is well determined for the 27-day solar rotation period but not for the 11-year solar cycle.
- (3) The accepted values for the molecular oxygen absorption cross-sections at wavelengths relevant to the stratosphere and mesosphere are significantly smaller than those used a few years ago.
- (4) An improved determination of cross sections in the Huggins bands would be valuable, especially for ground-based atmospheric ozone measurements.
- (5) Improved determination of line shapes, line widths, and their temperature dependencies are needed to better calculate terrestrial heating rates. Present line-by-line calculations are based on idealized values that have not been verified in many cases.
- (6) Other uncertainties in calculating terrestrial radiation include the influence of clouds and volcanic aerosols.
- (7) The radiative role of trace gases such as  $N_2O$  and the CFC's merits further study.
- (8) The continued analysis of satellite data sets for ozone, temperature, solar irradiance, and the outgoing terrestrial emission is essential for developing a complete understanding of radiative processes in the Earth's stratosphere and mesosphere.
- (9) A drift-free record of the ultraviolet solar irradiance covering at least the wavelength range 175-400 nm is needed over one or more entire solar cycles.

### CHAPTERS 8, 9, 10, AND 11: OXYGEN, HYDROGEN, NITROGEN AND HALOGENATED SPECIES: OBSERVATIONS AND INTERPRETATION

These Chapters review, and compare to both one-dimensional and two-dimensional model descriptions of the present-day stratosphere, the stratospheric measurements of oxygen, hydrogen, nitrogen, and halogen containing species obtained from ground, aircraft, balloon, rocket, shuttle, and satellite based instruments. There is a brief discussion of each of the *in situ* and remote sensing techniques currently being used to determine the chemical composition of the atmosphere, and a brief discussion of the accuracy and precision of the experimental data. The types of data described include vertical distributions and column contents as a function of season both at a limited number of geographic locations and globally, diurnal variabilities, and long term (multiyear) trends in the column contents. The species described include the source gases of the trace constituents ( $H_2O$ ,  $N_2O$ ,  $CH_4$ , and the halocarbons), and the active and inactive inorganic species from the oxygen ( $O(^3P)$ ,  $O(^1D)$ , and  $O_3$ ), hydrogen ( $H$ ,  $OH$ ,  $HO_2$ , and  $H_2O_2$ ), nitrogen ( $N$ ,  $NO$ ,  $NO_2$ ,  $NO_3$ ,  $N_2O_5$ ,  $ClONO_2$ ,  $HNO_3$ , and  $HNO_4$ ), chlorine ( $Cl$ ,  $ClO$ ,  $HCl$ ,  $HOCl$ , and  $ClONO_2$ ), and fluorine ( $HF$ ) families.

Major emphasis is placed on describing the satellite data sets which have been analyzed, validated, released, and partially interpreted during the last four years. This includes data obtained by the Limb Infrared Monitor of the Stratosphere (LIMS), the Stratospheric and Mesospheric Sounder (SAMS), and the Solar Backscatter Ultraviolet/Total Ozone Monitoring System (SBUV/TOMS) instruments flown on the Nimbus 7 satellite, the Stratospheric Aerosol and Gas Experiment (SAGE) flown on the Applications Explorer II satellite, and the visible and infrared spectrometers flown on the Solar Mesospheric Explorer satellite.

## Major Conclusions and Recommendations

Before discussing specific conclusions which may involve only one particular family of species there are seven conclusions of a more general character.

- (1) The most significant recent development in our knowledge of  $O_x$ ,  $HO_x$ , and  $NO_x$  in the stratosphere has been the release of several large satellite data sets. They have greatly improved our knowledge of the spatial and temporal distributions of  $O_3$ ,  $H_2O$ ,  $CH_4$ ,  $N_2O$ ,  $NO_2$ , and  $HNO_3$  on a global scale.
- (2) There are now some measurements of most key species, including the temporary reservoir species  $ClONO_2$ ,  $N_2O_5$  and  $HO_2NO_2$  predicted to be important in the photochemistry of stratospheric ozone. However, the data base is rather limited in some instances, and while the observed abundances are generally consistent with current theory to within a factor of two or so, the measurements are not adequate for critically testing the photochemical models.
- (3) Ground, aircraft, balloon, and rocket-based instrumentation have continued to provide an invaluable data base for vital but limited tests of photochemical theory.
- (4) While there has recently been a significant advance in our understanding of the accuracy and precision of atmospheric composition data it is vital to continue the intercomparison of data obtained from different measurement techniques, especially for  $ClO$ ,  $OH$ ,  $HO_2$ ,  $NO$  and  $NO_2$ .
- (5) Several new experimental techniques have recently been developed and demonstrated which will enable us to obtain the type of data needed to test the photochemical models.
- (6) We are still data limited, the accuracy and precision of many of the measurements need to be improved, and an improved measurement strategy needs to be formulated in order to more stringently test the photochemical models.
- (7) Long term data sets of the vertical distributions of  $O_x$ ,  $HO_x$ ,  $NO_x$  and  $ClO_x$  species are needed both at discrete geographic locations and globally to determine changes in the composition of the stratosphere.

We will now discuss the specific major conclusions in the following order, i.e., oxygen, hydrogen, nitrogen, and halogen species.

## CHAPTER 8: OXYGEN SPECIES

- (1) Comparison of three distinct satellite measurements (SBUV, LIMS and SAGE), suggests that we can determine ozone in an absolute sense to about 15% (one standard deviation) from 25-30 km and about 6% from 30-55 km.
- (2) Comparison of ozone satellite and balloonsonde data suggests that the balloonsondes are systematically lower than SBUV above about 32 km. The cause of this is not currently recognized.
- (3) Utilizing SBUV as the basic data source for four year zonal average profiles, the random uncertainties appear to be about 4% (one standard deviation) in mid- and high-latitude winter and about 2% elsewhere.

## INTRODUCTION

- (4) The observed O<sub>3</sub> abundance above 35 km is underestimated, typically by 30 to 50%, by both one-dimensional and two-dimensional photochemical model calculations. The reason for this discrepancy is not yet clear but could be due to an underestimation of the calculated odd oxygen production rate, an overestimation of the calculated loss rate by HO<sub>x</sub> in the mesosphere and/or NO<sub>x</sub> in the stratosphere or to missing chemistry.
- (5) This significant ozone imbalance in the photochemically controlled region of the middle atmosphere limits the confidence that can be attached to model predictions of future ozone changes in response to long-term increases in the atmospheric concentrations of source gases (e.g. chlorofluorocarbons, nitrous oxide, methane).
- (6) Precise determinations of the [O]/[O<sub>3</sub>] ratio and of the diurnal variation of O<sub>3</sub> in the upper stratosphere and in the mesosphere are needed.
- (7) Stratospheric measurements relating the O<sub>2</sub> cross section determinations by high resolution measurements of the solar irradiance from 180 to 250 nm are required, as are additional laboratory studies of the O<sub>2</sub> absorption cross sections (Schumann-Runge bands and Herzberg continuum) and of the photodissociation rate of O<sub>3</sub> producing O(<sup>1</sup>D).

## CHAPTER 9: HYDROGEN SPECIES

- (1) There has been no major expansion of the profile data base for HO<sub>x</sub> (OH, HO<sub>2</sub>, and H<sub>2</sub>O<sub>2</sub>) species since the last assessment.
- (2) The only new profile data for OH since the last assessment is lower than most of the earlier data and current model predictions and, while not in serious conflict with model predictions, is insufficient to provide a critical test of theory.
- (3) There are over seven years of quasi-continuous column measurements of OH which show a long-term trend, seasonal, diurnal, and spatial variability, and response to volcanic eruptions and a solar eclipse. A large fraction of the OH signal is due to OH in the mesosphere. This data awaits a theoretical interpretation.
- (4) HO<sub>2</sub> measurements between 16 and 34 km, and 35 and 60 km have been obtained by *in situ* and ground-based techniques, respectively. The *in situ* HO<sub>2</sub> data between 16 and 34 km is significantly higher than predicted, and suggests a problem with either the measurements or our understanding of HO<sub>x</sub> photochemistry.
- (5) There has not yet been a single definitive observation of H<sub>2</sub>O<sub>2</sub>.
- (6) From balloon *in situ* data there is clear evidence of a hygropause, a region of minimum H<sub>2</sub>O mixing ratios a few km above the tropopause, and small scale vertical structure at northern mid-latitudes.
- (7) The LIMS and SAMS H<sub>2</sub>O and CH<sub>4</sub> data have clearly demonstrated that air is transported upward and poleward from the tropics, consistent with the Brewer-Dobson hypothesis, and that the total hydrogen budget of the stratosphere, principally H<sub>2</sub>O + 2 × CH<sub>4</sub>, is relatively constant with values ranging from 6 to 7 ppmv.

- (8) LIMS data has been used to derive global OH fields; (a) using the  $\text{HNO}_3/\text{NO}_2$  ratio, and (b) by calculating its production and loss with temperature,  $\text{H}_2\text{O}$ ,  $\text{O}_3$ , and  $\text{HNO}_3$  data.
- (9) Simultaneous measurements of odd hydrogen containing species are required over a full diurnal cycle to provide a more critical test of the photochemical models (OH,  $\text{HO}_2$ ,  $\text{H}_2\text{O}_2$ ,  $\text{H}_2\text{O}$ , in conjunction with temperature, solar flux, O,  $\text{O}_3$ , and  $\text{NO}_x$  determinations).

### CHAPTER 10: NITROGEN SPECIES

- (1) While we have a reasonable understanding of the diurnal variability of  $\text{NO}_2$ , a more rigorous test of theory requires more accurate experimental data.
- (2) The observations of  $\text{HNO}_3$  at high latitudes in winter, and above 30 km at all latitudes are not in agreement with the theoretical predictions.
- (3) The global morphology and variability of  $\text{N}_2\text{O}$  has been measured from satellite, and can be adequately simulated with a two-dimensional photochemical model if the influences of the semiannual oscillation on the zonal mean cross-sections are taken into account.
- (4) Using LIMS data the magnitude of the thermospheric source of total odd nitrogen to the stratosphere has been shown to be significant on a local, but not global, scale.
- (5) Total budgets for odd nitrogen have been derived from satellite measurements (LIMS) of  $\text{HNO}_3$  and nighttime  $\text{NO}_2$ . These are generally consistent with those derived from balloon observations, and predicted by two-dimensional photochemical models near 40 km. However, there are serious discrepancies between observations and two-dimensional photochemical models at lower altitudes.
- (6) We now have a basic understanding of the dynamical and photochemical processes responsible for regional phenomenon such as the  $\text{NO}_2$  Noxon Cliff.
- (7) Global OH fields have been derived using LIMS  $\text{NO}_2$  and  $\text{HNO}_3$  data. However, given that we do not fully understand the quality of LIMS  $\text{HNO}_3$  data above 35 km, and the  $\text{HNO}_3$  profile above 30 km is not understood, care must be exercised in using the derived OH fields.
- (8)  $\text{N}_2\text{O}_5$ ,  $\text{HNO}_4$ , and  $\text{ClONO}_2$  have been positively identified from ATMOS spectra.
- (9) Simultaneous measurements of nitrogen containing species over a full diurnal cycle are required to critically test the photochemical models. These ratio measurements should be taken in conjunction with appropriate measurements of  $\text{O}_x$ ,  $\text{HO}_x$ , and  $\text{ClO}_x$  species.

### CHAPTER 11: HALOGENATED SPECIES

- (1) While there has not been a significant expansion of the ClO profile data base the measured and model predicted ClO profiles now agree to within a factor of 2 between 28 and 38 km.
- (2) The observed diurnal variation of ClO is in reasonable agreement with model predictions, but does show a somewhat slower morning rise than expected.

## INTRODUCTION

- (3) The existing data base is inadequate to establish seasonal and latitudinal variations, or long-term increases in ClO predicted by theoretical models.
- (4) Evidence of the presence of ClONO<sub>2</sub> has improved, with balloon-based observations being made in a second spectral region. In addition, ClONO<sub>2</sub> has been observed in the ATMOS spectra.
- (5) The expected increase with time in stratospheric HCl has not been observed. It has presumably been masked by significant short-term variability in both tropospheric and stratospheric HCl.
- (6) The measured and predicted increase with time in stratospheric HF are compatible.
- (7) There is now general agreement between calculated and observed vertical profiles for the halogen source species.
- (8) Simultaneous measurements of chlorine-containing species are required to provide a satisfactory test of the photochemical models (Cl, HCl, ClO, and ClONO<sub>2</sub>, preferably coupled to temperature, solar flux, O<sub>3</sub>, H<sub>2</sub>O, CH<sub>4</sub> and NO<sub>x</sub> determinations).

## CHAPTER 12: ASSESSMENT MODELS

This Chapter considers the various types of models of the stratosphere which have been used to make predictions concerning the stratospheric composition and possible response to perturbations. One-dimensional models, although limited in many respects, have been our traditional tools. Recent important advances in the treatment of two-dimensional transport have opened the way for a new generation of assessment models with all the photochemical detail of the one-dimensional models but with a more physically-based transport.

### Major Conclusions and Recommendations

#### (1) One-Dimensional Models

- One-dimensional models will continue to play a major role in assessment activities, particularly in the development of new photochemical schemes.
- A comparison of one-dimensional models shows a large range of calculated odd-nitrogen in the middle and upper stratosphere ranging from 13-20 ppbv. An important source of these differences is the treatment of radiation penetration in the Schumann-Runge bands, and more work appears necessary here. However, models with similar radiation schemes still show significant differences in odd nitrogen, and other causes are evidently also important.

#### (2) Two-Dimensional Models

- There have been significant theoretical advances in the treatment of transport in two-dimensional models.
- There is a good understanding of the cancellation between mean and eddy transport. A net transport circulation can be defined which is closely related to the residual and diabatic circulations.

- The limitations of the treatment of eddy transport in terms of K-theory, and the physical basis for this approach, are better understood.
- Important estimates of the size of the eddy coefficients have come from theoretical, GCM and data studies. These studies suggest the use of somewhat smaller k coefficients than hitherto, in combination with the transport circulation. However, more work is urgently needed in this area, bearing in mind, for example, the known limitations of GCM's and the problem of unresolved scales of motion in satellite data analyses.
- There has been important work on the dependence of the k coefficients (in one-dimensional as well as two-dimensional models) on photochemical lifetimes.
- Two-dimensional models can include some of the important photochemical-radiative-dynamical feedbacks.
- The goal of a completely self-consistent two-dimensional model is denied by our inability to model the eddies in a completely interactive fashion.

### (3) Two-Dimensional Model Results

- With the above advances there are now two major classifications of two-dimensional models.
  - (1) Traditional Eulerian (with generally large eddy coefficients)
  - (2) Models with modified Eulerian — residual or diabatic — circulations (and generally smaller eddy coefficients).
- Whichever approach is employed, the eddies remain important. It is the establishment of the correct balance between mean and eddy transport which is crucial. The residual circulation models with small diffusion, in general, predict greater latitudinal structure than the other models. However, equally large differences are sometimes found between models of similar types as between modified and traditional Eulerian models.
- As with one-dimensional models, significant differences in the predicted odd-nitrogen values are found. Tropospheric removal and transport in the equatorial lower stratosphere are believed to play major roles in producing these differences. The equatorial lower stratosphere, where the radiative balance is the small difference of small terms, is identified as an extremely important area for future study.
- As with one-dimensional models, two-dimensional models generally underestimate ozone in the upper stratosphere.

### (4) Three-Dimensional Models

- There have been some significant efforts to incorporate detailed chemistry schemes into three-dimensional models.

## INTRODUCTION

### (5) Models for Assessment

- There is no indication at present that results from two-dimensional models should invalidate in a gross sense assessment studies with one-dimensional models.
- Two-dimensional models provide a much broader predictive capability than one-dimensional models. They can predict important latitudinal and seasonal effects which the one-dimensional models generally cannot. Two-dimensional models thus add significantly to our assessment capability.
- The inability of one-dimensional and two-dimensional models to reproduce upper stratospheric ozone and the significant differences sometimes found between models, for example in calculated odd-nitrogen, undermines our confidence in long term assessment. Priority must be given to resolving these problems.

### (6) Testing Models

- Our confidence in models (especially for assessment purposes) depends on satisfactorily 'validating' these models against available data. This is too often an extremely subjective exercise.
- A hierarchy of tests for comparison of models and data could include:
  - (a) Identification of predicted species
  - (b) Comparison of altitude profiles, latitudinal and seasonal variations.
  - (c) Isolation of processes (e.g. chemistry from dynamics by ratio measurements, diurnal variations, correlations).
  - (d) Study of natural perturbations (Volcanic eruptions, solar proton events, sudden warmings, etc.)
  - (e) Study of chemistry along air parcel trajectories.

## CHAPTER 13: MODEL PREDICTIONS

This Chapter presents a series of model calculations detailing the present best estimates of the response of atmospheric composition to a variety of potential perturbations. The computations emphasize the coupled nature of the perturbations. The choice of scenarios involving changes in concentrations of CFC's, N<sub>2</sub>O, CH<sub>4</sub> and CO<sub>2</sub> reflect the findings that all of their concentrations are currently increasing and that the perturbations are strongly coupled.

### Major Conclusions and Recommendations

- (1) Continued release of chlorofluorocarbons 11 and 12 at the 1980 rate would reduce the ozone vertical column by about 5-8% according to one-dimensional photochemical models and by a global average of about 9% according to two-dimensional models, with reductions of ~4% in the tropics, ~9% in temperate zones and ~14% in polar regions.
- (2) A major finding of recent years is that two-dimensional models predict large seasonal and latitudinal variations in chlorine-induced ozone column reductions.
- (3) All models with all scenarios predict that continued release of CFC's 11 and 12 at the 1980 rate will reduce local ozone at 40 km by ~40% or more.

## INTRODUCTION

- (4) One dimensional models predict that the magnitude and even the sign of the ozone column changes due to increasing CFC's depend on the future trends of CO<sub>2</sub>, CH<sub>4</sub>, and N<sub>2</sub>O. For example, at about 80% of the present CFC release rate, coupled with a doubling of CH<sub>4</sub> and an increase in N<sub>2</sub>O by a factor of 1.2, one-dimensional models predict an ozone decrease of about 3% at steady state while two-dimensional models predict an ozone decrease of 4%. If a simultaneous doubling of CO<sub>2</sub> is also considered, one-dimensional models predict ozone column changes between +0.1 and -3.5%.
- (5) If the release rate of CFC's should become twice the present level or if stratospheric Cl<sub>x</sub> reaches 15 ppbv, the one-dimensional models predict that there will be a 3% to 12% reduction of the ozone column, assuming that the annual rates of increase in the atmospheric concentrations of CO<sub>2</sub>, N<sub>2</sub>O, and CH<sub>4</sub> continue at their present rate.
- (6) One-dimensional models predict that the total ozone column is increased by CO, CO<sub>2</sub>, and CH<sub>4</sub>, and decreased by CFC's, N<sub>2</sub>O and stratospheric aircraft. These individual perturbations do not have an additive effect on ozone.
- (7) Time dependent scenarios were performed using one-dimensional models assuming CO<sub>2</sub>, CH<sub>4</sub>, and N<sub>2</sub>O annual growth rates of 0.5%, 1% and 0.25%, respectively, in conjunction with CFC growth rates of 0%, 1.5% and 3% per year. The ozone column effects are relatively small (<3% over the next 70 years) for CFC increases of ≤1.5% per year, but with a CFC growth rate of 3% per year the predicted ozone depletion is 10% after 70 years and still rapidly increasing.
- (8) Over the range 1 to 15 ppbv of stratospheric chlorine, one-dimensional models are strongly non-linear in terms of ozone-column change as a function of added Cl<sub>x</sub>, in contrast to the two-dimensional models which are nearly linear over this range of Cl<sub>x</sub>. The onset of the nonlinearity occurs in the regime where the Cl<sub>x</sub> and NO<sub>y</sub> mixing ratios become comparable.
- (9) Monte Carlo calculations over the full range of the assessed uncertainties of photochemical parameters were performed with two one-dimensional models. One calculation considered only CFC perturbations. For the release of CFC's at the 1980 rate an ozone column depletion of  $-(5.7 \pm 5.4)\%$  was calculated ( $1\sigma$  uncertainty range). In the second calculation an ozone column depletion of  $-(7.7 \pm 5.8)\%$  was calculated for an increase of 14 ppbv of Cl<sub>x</sub> in conjunction with a doubling of CH<sub>4</sub> and a 20% increase in N<sub>2</sub>O. In each case the ozone depletion distribution was unsymmetrical with a long tail toward large perturbations.
- (10) The past and future changes of the trace species, CH<sub>4</sub>, N<sub>2</sub>O, and CO<sub>2</sub>, involve the biosphere and its great complexity. As the stratospheric models mature, the largest uncertainty in making future predictions of ozone concentrations will probably be the uncertainty in formulating the scenarios for future changes in CH<sub>4</sub>, N<sub>2</sub>O, and CO<sub>2</sub>.
- (11) It is vital to continue the development of two-dimensional models for assessment purposes. These must include the effects of temperature feedback.
- (12) The new Monte Carlo method that screens the results against atmospheric observations should be emphasized.

## INTRODUCTION

### CHAPTER 14: OZONE AND TEMPERATURE TRENDS

This Chapter contains a discussion of the evidence for statistically significant trends in ozone and temperature. In particular, the evidence for a trend in the total ozone and in ozone profiles is examined. Temperature data in the troposphere and in the lower stratosphere are also examined from the viewpoint of looking for trends.

#### Major Conclusions and Recommendations

- (1) Global trend estimates of total ozone determined from the Dobson spectrophotometer network indicate little overall support for a statistically significant trend during the 14-year period 1970-1983.
- (2) Recent evidence has been presented that indicates a considerable decrease in Antarctic total ozone during the spring period since about 1968. This is presently the subject of further analysis.
- (3) Trend estimates from 13 ozone balloonsondes indicate statistically significant positive trends in the lower troposphere and negative trends in the lower stratosphere. The interpretation of these results, however, is clouded by uncertainties in instrument behavior and lack of a global station network.
- (4) Ozone trend estimates from 13 Umkehr stations indicate statistically significant negative trends from 1970 to 1980 in the middle stratosphere that are in substantive agreement with results from one-dimensional numerical models. The observational results are sensitive to the inclusion of a term to account for stratospheric aerosol impact on the measurements and the spatial distribution of the sites, but do not appear sensitive to the inclusion of a 10.7 cm flux variation (an indicator for solar flux variation).
- (5) Examination of the NOAA SBUV-2 satellite measurement program indicates that if the system operates as designed, it is capable of global ozone trend detection in the middle to upper stratosphere, as well as total ozone, to within about 1.5% over a period of one decade at the 95% confidence level.
- (6) As with other long-term measurement programs however, it is necessary to examine continually the SBUV-2 instrument performance and satellite measurements and compare them with independent data.
- (7) We note, moreover, that the SBUV-2 data are inherently total ozone and ozone profiles between 25 and 55 km. If ozone trends can be determined unambiguously from the Earth's surface to the overlap region with the SBUV-2 profiles, a high-quality measurement program would exist.
- (8) Two independent analyses of lower stratospheric temperatures during the period 1965-1979 are suggestive of a downward temperature trend. Inconsistencies between the two analyses, however, preclude firm conclusions.
- (9) The large cooling in rocketsonde temperatures reported for the early 1970's appears now to be due to a change in the rocketsonde temperature measurement system. Taking this into account, statistically significant negative trends are observed in June rocketsonde data at 40-45 km from 1973-1983 that are in substantive agreement with results from one-dimensional numerical models. These preliminary results will have to be examined further with a more complete data set.

## INTRODUCTION

- (10) Examination of the NOAA TOVS stratospheric satellite temperature measurement program indicates that it is essential that the instrument-to-instrument consistency be verified by a high quality, independent data system. Such a system does not exist.
- (11) Resolve the causes of the ozone measurement biases between SBUV, LIMS and SAGE and thereby, reduce the absolute error estimates.
- (12) Determine the impact of implementation of the Bass and Paur (1984) ozone absorption coefficients on the ground-based measurements and compare the results with the satellite observations.
- (13) Continue development of the ground-based ozone profile measurement program with particular emphasis on the following:
  - (a) determination of the aerosol impact on Umkehr measurements from El Chichon.
  - (b) development of the high altitude ( $\approx 40$  km) balloon sampling system with specific attention to the adjustment procedure to match the Dobson total ozone measurements.
  - (c) development of a lidar system capable of routine ozone measurements in the troposphere and stratosphere, especially above 40 km.
- (14) Develop a long-term satellite and ground-based temperature measurement program sufficient to measure a mid-stratospheric temperature trend to a 95% confidence level of 1.5K/decade.
- (15) Update the accuracy (as opposed to precision) estimates of the meteorological rocketsondes and satellite observations.
- (16) Determine the satellite ozone and temperature temporal and spatial sampling requirements with estimates of resolution, accuracy and precision necessary to verify chemical, dynamical and radiation theory.

## CHAPTER 15: TRACE GAS EFFECTS ON CLIMATE

This Chapter examines our understanding of how increasing concentrations of radiatively active trace gases might lead to changes in the Earth's climate. The nature of the radiative forcing of the climate system from changes in trace gas concentration is discussed. The roles of the various types of climate models are discussed, and the predictions of resulting climate perturbations resulting from individual increases in atmospheric trace gas concentrations are presented from such models. The role of the oceans in delaying these climate changes is discussed. Finally, the effects of simultaneous increases in trace gas concentrations on the climate are estimated.

### Major Conclusions and Recommendations

- (1) The problem concerning the greenhouse effects of human activities has broadened in scope from the CO<sub>2</sub>-climate problem to the trace gas-climate problem.
- (2) Non-CO<sub>2</sub> greenhouse gases in the atmosphere are now adding to the greenhouse effect by an amount comparable to the effect of CO<sub>2</sub>. This is a fundamental change from the situation during the period of 1850-1960.

## INTRODUCTION

- (3) The rate of increase of the total greenhouse forcing is now 3-10 times greater than the mean rate for the period 1850-1960.
- (4) The cumulative effect of the increase in all trace gases for the period from 1850-1980 is a predicted equilibrium warming in the range of 0.7 to 2 K. The three-fold range in the estimated equilibrium warming arises from the currently perceived uncertainty in the sensitivity of climate models. The contribution of the non-CO<sub>2</sub> trace gases to the cumulative equilibrium surface warming is about 30%. Time dependent calculations with a simplified one dimensional diffusive ocean model suggest that a surface warming of about 0.4-0.8 K (of the 0.7 to 2 K) should have occurred during 1850 to 1980. The estimated surface warming is not inconsistent with the value of 0.5 to 0.6 K that can be inferred from observed surface-air temperature records.
- (5) If the growth rates of trace gas concentrations (or their emission rates) that were observed during the decade of the 1970's continue unabated for the next several decades, non-CO<sub>2</sub> trace gases can have as much impact as CO<sub>2</sub> on future trends of surface and atmospheric temperatures. For the various trace gas scenarios considered in this study, the equilibrium surface warming for the period 1980 to 2030 range from 0.8 to 4.1 K. This wide range in the projected warming is due to the range in the assumed scenarios as well as due to the earlier mentioned uncertainty in climate sensitivity of current models.
- (6) Thus for the 180 year period from 1850 to 2030, our assessment suggests a trace gas induced cumulative equilibrium surface warming in the range of 1.5 to 6.1 K. Because of the huge thermal inertia of the world oceans, only about 40 to 50% of the above equilibrium warming will be realized by the year 2030. Consequently, if the current rate of increase in trace gas concentrations continue unabated for the next several decades, the climate system would be increasingly in a state of disequilibrium with the radiative forcing by the trace gases.
- (7) The important non-CO<sub>2</sub> greenhouse gases are CFC<sub>13</sub>, CFC<sub>12</sub>, CH<sub>4</sub>, N<sub>2</sub>O, O<sub>3</sub> and stratospheric H<sub>2</sub>O. On time scales longer than a century, radiatively active gases with lifetimes of the order of 100-500 years (e.g., CFC<sub>11</sub>, CFC<sub>12</sub>, CFC<sub>113</sub>, CFC<sub>114</sub>, CFC<sub>115</sub>, CFC<sub>120</sub>, CFC<sub>121</sub>, CFC<sub>122</sub>, CFC<sub>123</sub>, CFC<sub>124</sub>, CFC<sub>125</sub>, CFC<sub>126</sub>, CFC<sub>127</sub>, CFC<sub>128</sub>, CFC<sub>129</sub>, CFC<sub>130</sub>, CFC<sub>131</sub>, CFC<sub>132</sub>, CFC<sub>133</sub>, CFC<sub>134</sub>, CFC<sub>135</sub>, CFC<sub>136</sub>, CFC<sub>137</sub>, CFC<sub>138</sub>, CFC<sub>139</sub>, CFC<sub>140</sub>, CFC<sub>141</sub>, CFC<sub>142</sub>, CFC<sub>143</sub>, CFC<sub>144</sub>, CFC<sub>145</sub>, CFC<sub>146</sub>, CFC<sub>147</sub>, CFC<sub>148</sub>, CFC<sub>149</sub>, CFC<sub>150</sub>, CFC<sub>151</sub>, CFC<sub>152</sub>, CFC<sub>153</sub>, CFC<sub>154</sub>, CFC<sub>155</sub>, CFC<sub>156</sub>, CFC<sub>157</sub>, CFC<sub>158</sub>, CFC<sub>159</sub>, CFC<sub>160</sub>, CFC<sub>161</sub>, CFC<sub>162</sub>, CFC<sub>163</sub>, CFC<sub>164</sub>, CFC<sub>165</sub>, CFC<sub>166</sub>, CFC<sub>167</sub>, CFC<sub>168</sub>, CFC<sub>169</sub>, CFC<sub>170</sub>, CFC<sub>171</sub>, CFC<sub>172</sub>, CFC<sub>173</sub>, CFC<sub>174</sub>, CFC<sub>175</sub>, CFC<sub>176</sub>, CFC<sub>177</sub>, CFC<sub>178</sub>, CFC<sub>179</sub>, CFC<sub>180</sub>, CFC<sub>181</sub>, CFC<sub>182</sub>, CFC<sub>183</sub>, CFC<sub>184</sub>, CFC<sub>185</sub>, CFC<sub>186</sub>, CFC<sub>187</sub>, CFC<sub>188</sub>, CFC<sub>189</sub>, CFC<sub>190</sub>, CFC<sub>191</sub>, CFC<sub>192</sub>, CFC<sub>193</sub>, CFC<sub>194</sub>, CFC<sub>195</sub>, CFC<sub>196</sub>, CFC<sub>197</sub>, CFC<sub>198</sub>, CFC<sub>199</sub>, CFC<sub>200</sub>, CFC<sub>201</sub>, CFC<sub>202</sub>, CFC<sub>203</sub>, CFC<sub>204</sub>, CFC<sub>205</sub>, CFC<sub>206</sub>, CFC<sub>207</sub>, CFC<sub>208</sub>, CFC<sub>209</sub>, CFC<sub>210</sub>, CFC<sub>211</sub>, CFC<sub>212</sub>, CFC<sub>213</sub>, CFC<sub>214</sub>, CFC<sub>215</sub>, CFC<sub>216</sub>, CFC<sub>217</sub>, CFC<sub>218</sub>, CFC<sub>219</sub>, CFC<sub>220</sub>, CFC<sub>221</sub>, CFC<sub>222</sub>, CFC<sub>223</sub>, CFC<sub>224</sub>, CFC<sub>225</sub>, CFC<sub>226</sub>, CFC<sub>227</sub>, CFC<sub>228</sub>, CFC<sub>229</sub>, CFC<sub>230</sub>, CFC<sub>231</sub>, CFC<sub>232</sub>, CFC<sub>233</sub>, CFC<sub>234</sub>, CFC<sub>235</sub>, CFC<sub>236</sub>, CFC<sub>237</sub>, CFC<sub>238</sub>, CFC<sub>239</sub>, CFC<sub>240</sub>, CFC<sub>241</sub>, CFC<sub>242</sub>, CFC<sub>243</sub>, CFC<sub>244</sub>, CFC<sub>245</sub>, CFC<sub>246</sub>, CFC<sub>247</sub>, CFC<sub>248</sub>, CFC<sub>249</sub>, CFC<sub>250</sub>, CFC<sub>251</sub>, CFC<sub>252</sub>, CFC<sub>253</sub>, CFC<sub>254</sub>, CFC<sub>255</sub>, CFC<sub>256</sub>, CFC<sub>257</sub>, CFC<sub>258</sub>, CFC<sub>259</sub>, CFC<sub>260</sub>, CFC<sub>261</sub>, CFC<sub>262</sub>, CFC<sub>263</sub>, CFC<sub>264</sub>, CFC<sub>265</sub>, CFC<sub>266</sub>, CFC<sub>267</sub>, CFC<sub>268</sub>, CFC<sub>269</sub>, CFC<sub>270</sub>, CFC<sub>271</sub>, CFC<sub>272</sub>, CFC<sub>273</sub>, CFC<sub>274</sub>, CFC<sub>275</sub>, CFC<sub>276</sub>, CFC<sub>277</sub>, CFC<sub>278</sub>, CFC<sub>279</sub>, CFC<sub>280</sub>, CFC<sub>281</sub>, CFC<sub>282</sub>, CFC<sub>283</sub>, CFC<sub>284</sub>, CFC<sub>285</sub>, CFC<sub>286</sub>, CFC<sub>287</sub>, CFC<sub>288</sub>, CFC<sub>289</sub>, CFC<sub>290</sub>, CFC<sub>291</sub>, CFC<sub>292</sub>, CFC<sub>293</sub>, CFC<sub>294</sub>, CFC<sub>295</sub>, CFC<sub>296</sub>, CFC<sub>297</sub>, CFC<sub>298</sub>, CFC<sub>299</sub>, CFC<sub>300</sub>, CFC<sub>301</sub>, CFC<sub>302</sub>, CFC<sub>303</sub>, CFC<sub>304</sub>, CFC<sub>305</sub>, CFC<sub>306</sub>, CFC<sub>307</sub>, CFC<sub>308</sub>, CFC<sub>309</sub>, CFC<sub>310</sub>, CFC<sub>311</sub>, CFC<sub>312</sub>, CFC<sub>313</sub>, CFC<sub>314</sub>, CFC<sub>315</sub>, CFC<sub>316</sub>, CFC<sub>317</sub>, CFC<sub>318</sub>, CFC<sub>319</sub>, CFC<sub>320</sub>, CFC<sub>321</sub>, CFC<sub>322</sub>, CFC<sub>323</sub>, CFC<sub>324</sub>, CFC<sub>325</sub>, CFC<sub>326</sub>, CFC<sub>327</sub>, CFC<sub>328</sub>, CFC<sub>329</sub>, CFC<sub>330</sub>, CFC<sub>331</sub>, CFC<sub>332</sub>, CFC<sub>333</sub>, CFC<sub>334</sub>, CFC<sub>335</sub>, CFC<sub>336</sub>, CFC<sub>337</sub>, CFC<sub>338</sub>, CFC<sub>339</sub>, CFC<sub>340</sub>, CFC<sub>341</sub>, CFC<sub>342</sub>, CFC<sub>343</sub>, CFC<sub>344</sub>, CFC<sub>345</sub>, CFC<sub>346</sub>, CFC<sub>347</sub>, CFC<sub>348</sub>, CFC<sub>349</sub>, CFC<sub>350</sub>, CFC<sub>351</sub>, CFC<sub>352</sub>, CFC<sub>353</sub>, CFC<sub>354</sub>, CFC<sub>355</sub>, CFC<sub>356</sub>, CFC<sub>357</sub>, CFC<sub>358</sub>, CFC<sub>359</sub>, CFC<sub>360</sub>, CFC<sub>361</sub>, CFC<sub>362</sub>, CFC<sub>363</sub>, CFC<sub>364</sub>, CFC<sub>365</sub>, CFC<sub>366</sub>, CFC<sub>367</sub>, CFC<sub>368</sub>, CFC<sub>369</sub>, CFC<sub>370</sub>, CFC<sub>371</sub>, CFC<sub>372</sub>, CFC<sub>373</sub>, CFC<sub>374</sub>, CFC<sub>375</sub>, CFC<sub>376</sub>, CFC<sub>377</sub>, CFC<sub>378</sub>, CFC<sub>379</sub>, CFC<sub>380</sub>, CFC<sub>381</sub>, CFC<sub>382</sub>, CFC<sub>383</sub>, CFC<sub>384</sub>, CFC<sub>385</sub>, CFC<sub>386</sub>, CFC<sub>387</sub>, CFC<sub>388</sub>, CFC<sub>389</sub>, CFC<sub>390</sub>, CFC<sub>391</sub>, CFC<sub>392</sub>, CFC<sub>393</sub>, CFC<sub>394</sub>, CFC<sub>395</sub>, CFC<sub>396</sub>, CFC<sub>397</sub>, CFC<sub>398</sub>, CFC<sub>399</sub>, CFC<sub>400</sub>, CFC<sub>401</sub>, CFC<sub>402</sub>, CFC<sub>403</sub>, CFC<sub>404</sub>, CFC<sub>405</sub>, CFC<sub>406</sub>, CFC<sub>407</sub>, CFC<sub>408</sub>, CFC<sub>409</sub>, CFC<sub>410</sub>, CFC<sub>411</sub>, CFC<sub>412</sub>, CFC<sub>413</sub>, CFC<sub>414</sub>, CFC<sub>415</sub>, CFC<sub>416</sub>, CFC<sub>417</sub>, CFC<sub>418</sub>, CFC<sub>419</sub>, CFC<sub>420</sub>, CFC<sub>421</sub>, CFC<sub>422</sub>, CFC<sub>423</sub>, CFC<sub>424</sub>, CFC<sub>425</sub>, CFC<sub>426</sub>, CFC<sub>427</sub>, CFC<sub>428</sub>, CFC<sub>429</sub>, CFC<sub>430</sub>, CFC<sub>431</sub>, CFC<sub>432</sub>, CFC<sub>433</sub>, CFC<sub>434</sub>, CFC<sub>435</sub>, CFC<sub>436</sub>, CFC<sub>437</sub>, CFC<sub>438</sub>, CFC<sub>439</sub>, CFC<sub>440</sub>, CFC<sub>441</sub>, CFC<sub>442</sub>, CFC<sub>443</sub>, CFC<sub>444</sub>, CFC<sub>445</sub>, CFC<sub>446</sub>, CFC<sub>447</sub>, CFC<sub>448</sub>, CFC<sub>449</sub>, CFC<sub>450</sub>, CFC<sub>451</sub>, CFC<sub>452</sub>, CFC<sub>453</sub>, CFC<sub>454</sub>, CFC<sub>455</sub>, CFC<sub>456</sub>, CFC<sub>457</sub>, CFC<sub>458</sub>, CFC<sub>459</sub>, CFC<sub>460</sub>, CFC<sub>461</sub>, CFC<sub>462</sub>, CFC<sub>463</sub>, CFC<sub>464</sub>, CFC<sub>465</sub>, CFC<sub>466</sub>, CFC<sub>467</sub>, CFC<sub>468</sub>, CFC<sub>469</sub>, CFC<sub>470</sub>, CFC<sub>471</sub>, CFC<sub>472</sub>, CFC<sub>473</sub>, CFC<sub>474</sub>, CFC<sub>475</sub>, CFC<sub>476</sub>, CFC<sub>477</sub>, CFC<sub>478</sub>, CFC<sub>479</sub>, CFC<sub>480</sub>, CFC<sub>481</sub>, CFC<sub>482</sub>, CFC<sub>483</sub>, CFC<sub>484</sub>, CFC<sub>485</sub>, CFC<sub>486</sub>, CFC<sub>487</sub>, CFC<sub>488</sub>, CFC<sub>489</sub>, CFC<sub>490</sub>, CFC<sub>491</sub>, CFC<sub>492</sub>, CFC<sub>493</sub>, CFC<sub>494</sub>, CFC<sub>495</sub>, CFC<sub>496</sub>, CFC<sub>497</sub>, CFC<sub>498</sub>, CFC<sub>499</sub>, CFC<sub>500</sub>, CFC<sub>501</sub>, CFC<sub>502</sub>, CFC<sub>503</sub>, CFC<sub>504</sub>, CFC<sub>505</sub>, CFC<sub>506</sub>, CFC<sub>507</sub>, CFC<sub>508</sub>, CFC<sub>509</sub>, CFC<sub>510</sub>, CFC<sub>511</sub>, CFC<sub>512</sub>, CFC<sub>513</sub>, CFC<sub>514</sub>, CFC<sub>515</sub>, CFC<sub>516</sub>, CFC<sub>517</sub>, CFC<sub>518</sub>, CFC<sub>519</sub>, CFC<sub>520</sub>, CFC<sub>521</sub>, CFC<sub>522</sub>, CFC<sub>523</sub>, CFC<sub>524</sub>, CFC<sub>525</sub>, CFC<sub>526</sub>, CFC<sub>527</sub>, CFC<sub>528</sub>, CFC<sub>529</sub>, CFC<sub>530</sub>, CFC<sub>531</sub>, CFC<sub>532</sub>, CFC<sub>533</sub>, CFC<sub>534</sub>, CFC<sub>535</sub>, CFC<sub>536</sub>, CFC<sub>537</sub>, CFC<sub>538</sub>, CFC<sub>539</sub>, CFC<sub>540</sub>, CFC<sub>541</sub>, CFC<sub>542</sub>, CFC<sub>543</sub>, CFC<sub>544</sub>, CFC<sub>545</sub>, CFC<sub>546</sub>, CFC<sub>547</sub>, CFC<sub>548</sub>, CFC<sub>549</sub>, CFC<sub>550</sub>, CFC<sub>551</sub>, CFC<sub>552</sub>, CFC<sub>553</sub>, CFC<sub>554</sub>, CFC<sub>555</sub>, CFC<sub>556</sub>, CFC<sub>557</sub>, CFC<sub>558</sub>, CFC<sub>559</sub>, CFC<sub>560</sub>, CFC<sub>561</sub>, CFC<sub>562</sub>, CFC<sub>563</sub>, CFC<sub>564</sub>, CFC<sub>565</sub>, CFC<sub>566</sub>, CFC<sub>567</sub>, CFC<sub>568</sub>, CFC<sub>569</sub>, CFC<sub>570</sub>, CFC<sub>571</sub>, CFC<sub>572</sub>, CFC<sub>573</sub>, CFC<sub>574</sub>, CFC<sub>575</sub>, CFC<sub>576</sub>, CFC<sub>577</sub>, CFC<sub>578</sub>, CFC<sub>579</sub>, CFC<sub>580</sub>, CFC<sub>581</sub>, CFC<sub>582</sub>, CFC<sub>583</sub>, CFC<sub>584</sub>, CFC<sub>585</sub>, CFC<sub>586</sub>, CFC<sub>587</sub>, CFC<sub>588</sub>, CFC<sub>589</sub>, CFC<sub>590</sub>, CFC<sub>591</sub>, CFC<sub>592</sub>, CFC<sub>593</sub>, CFC<sub>594</sub>, CFC<sub>595</sub>, CFC<sub>596</sub>, CFC<sub>597</sub>, CFC<sub>598</sub>, CFC<sub>599</sub>, CFC<sub>600</sub>, CFC<sub>601</sub>, CFC<sub>602</sub>, CFC<sub>603</sub>, CFC<sub>604</sub>, CFC<sub>605</sub>, CFC<sub>606</sub>, CFC<sub>607</sub>, CFC<sub>608</sub>, CFC<sub>609</sub>, CFC<sub>610</sub>, CFC<sub>611</sub>, CFC<sub>612</sub>, CFC<sub>613</sub>, CFC<sub>614</sub>, CFC<sub>615</sub>, CFC<sub>616</sub>, CFC<sub>617</sub>, CFC<sub>618</sub>, CFC<sub>619</sub>, CFC<sub>620</sub>, CFC<sub>621</sub>, CFC<sub>622</sub>, CFC<sub>623</sub>, CFC<sub>624</sub>, CFC<sub>625</sub>, CFC<sub>626</sub>, CFC<sub>627</sub>, CFC<sub>628</sub>, CFC<sub>629</sub>, CFC<sub>630</sub>, CFC<sub>631</sub>, CFC<sub>632</sub>, CFC<sub>633</sub>, CFC<sub>634</sub>, CFC<sub>635</sub>, CFC<sub>636</sub>, CFC<sub>637</sub>, CFC<sub>638</sub>, CFC<sub>639</sub>, CFC<sub>640</sub>, CFC<sub>641</sub>, CFC<sub>642</sub>, CFC<sub>643</sub>, CFC<sub>644</sub>, CFC<sub>645</sub>, CFC<sub>646</sub>, CFC<sub>647</sub>, CFC<sub>648</sub>, CFC<sub>649</sub>, CFC<sub>650</sub>, CFC<sub>651</sub>, CFC<sub>652</sub>, CFC<sub>653</sub>, CFC<sub>654</sub>, CFC<sub>655</sub>, CFC<sub>656</sub>, CFC<sub>657</sub>, CFC<sub>658</sub>, CFC<sub>659</sub>, CFC<sub>660</sub>, CFC<sub>661</sub>, CFC<sub>662</sub>, CFC<sub>663</sub>, CFC<sub>664</sub>, CFC<sub>665</sub>, CFC<sub>666</sub>, CFC<sub>667</sub>, CFC<sub>668</sub>, CFC<sub>669</sub>, CFC<sub>670</sub>, CFC<sub>671</sub>, CFC<sub>672</sub>, CFC<sub>673</sub>, CFC<sub>674</sub>, CFC<sub>675</sub>, CFC<sub>676</sub>, CFC<sub>677</sub>, CFC<sub>678</sub>, CFC<sub>679</sub>, CFC<sub>680</sub>, CFC<sub>681</sub>, CFC<sub>682</sub>, CFC<sub>683</sub>, CFC<sub>684</sub>, CFC<sub>685</sub>, CFC<sub>686</sub>, CFC<sub>687</sub>, CFC<sub>688</sub>, CFC<sub>689</sub>, CFC<sub>690</sub>, CFC<sub>691</sub>, CFC<sub>692</sub>, CFC<sub>693</sub>, CFC<sub>694</sub>, CFC<sub>695</sub>, CFC<sub>696</sub>, CFC<sub>697</sub>, CFC<sub>698</sub>, CFC<sub>699</sub>, CFC<sub>700</sub>, CFC<sub>701</sub>, CFC<sub>702</sub>, CFC<sub>703</sub>, CFC<sub>704</sub>, CFC<sub>705</sub>, CFC<sub>706</sub>, CFC<sub>707</sub>, CFC<sub>708</sub>, CFC<sub>709</sub>, CFC<sub>710</sub>, CFC<sub>711</sub>, CFC<sub>712</sub>, CFC<sub>713</sub>, CFC<sub>714</sub>, CFC<sub>715</sub>, CFC<sub>716</sub>, CFC<sub>717</sub>, CFC<sub>718</sub>, CFC<sub>719</sub>, CFC<sub>720</sub>, CFC<sub>721</sub>, CFC<sub>722</sub>, CFC<sub>723</sub>, CFC<sub>724</sub>, CFC<sub>725</sub>, CFC<sub>726</sub>, CFC<sub>727</sub>, CFC<sub>728</sub>, CFC<sub>729</sub>, CFC<sub>730</sub>, CFC<sub>731</sub>, CFC<sub>732</sub>, CFC<sub>733</sub>, CFC<sub>734</sub>, CFC<sub>735</sub>, CFC<sub>736</sub>, CFC<sub>737</sub>, CFC<sub>738</sub>, CFC<sub>739</sub>, CFC<sub>740</sub>, CFC<sub>741</sub>, CFC<sub>742</sub>, CFC<sub>743</sub>, CFC<sub>744</sub>, CFC<sub>745</sub>, CFC<sub>746</sub>, CFC<sub>747</sub>, CFC<sub>748</sub>, CFC<sub>749</sub>, CFC<sub>750</sub>, CFC<sub>751</sub>, CFC<sub>752</sub>, CFC<sub>753</sub>, CFC<sub>754</sub>, CFC<sub>755</sub>, CFC<sub>756</sub>, CFC<sub>757</sub>, CFC<sub>758</sub>, CFC<sub>759</sub>, CFC<sub>760</sub>, CFC<sub>761</sub>, CFC<sub>762</sub>, CFC<sub>763</sub>, CFC<sub>764</sub>, CFC<sub>765</sub>, CFC<sub>766</sub>, CFC<sub>767</sub>, CFC<sub>768</sub>, CFC<sub>769</sub>, CFC<sub>770</sub>, CFC<sub>771</sub>, CFC<sub>772</sub>, CFC<sub>773</sub>, CFC<sub>774</sub>, CFC<sub>775</sub>, CFC<sub>776</sub>, CFC<sub>777</sub>, CFC<sub>778</sub>, CFC<sub>779</sub>, CFC<sub>780</sub>, CFC<sub>781</sub>, CFC<sub>782</sub>, CFC<sub>783</sub>, CFC<sub>784</sub>, CFC<sub>785</sub>, CFC<sub>786</sub>, CFC<sub>787</sub>, CFC<sub>788</sub>, CFC<sub>789</sub>, CFC<sub>790</sub>, CFC<sub>791</sub>, CFC<sub>792</sub>, CFC<sub>793</sub>, CFC<sub>794</sub>, CFC<sub>795</sub>, CFC<sub>796</sub>, CFC<sub>797</sub>, CFC<sub>798</sub>, CFC<sub>799</sub>, CFC<sub>800</sub>, CFC<sub>801</sub>, CFC<sub>802</sub>, CFC<sub>803</sub>, CFC<sub>804</sub>, CFC<sub>805</sub>, CFC<sub>806</sub>, CFC<sub>807</sub>, CFC<sub>808</sub>, CFC<sub>809</sub>, CFC<sub>810</sub>, CFC<sub>811</sub>, CFC<sub>812</sub>, CFC<sub>813</sub>, CFC<sub>814</sub>, CFC<sub>815</sub>, CFC<sub>816</sub>, CFC<sub>817</sub>, CFC<sub>818</sub>, CFC<sub>819</sub>, CFC<sub>820</sub>, CFC<sub>821</sub>, CFC<sub>822</sub>, CFC<sub>823</sub>, CFC<sub>824</sub>, CFC<sub>825</sub>, CFC<sub>826</sub>, CFC<sub>827</sub>, CFC<sub>828</sub>, CFC<sub>829</sub>, CFC<sub>830</sub>, CFC<sub>831</sub>, CFC<sub>832</sub>, CFC<sub>833</sub>, CFC<sub>834</sub>, CFC<sub>835</sub>, CFC<sub>836</sub>, CFC<sub>837</sub>, CFC<sub>838</sub>, CFC<sub>839</sub>, CFC<sub>840</sub>, CFC<sub>841</sub>, CFC<sub>842</sub>, CFC<sub>843</sub>, CFC<sub>844</sub>, CFC<sub>845</sub>, CFC<sub>846</sub>, CFC<sub>847</sub>, CFC<sub>848</sub>, CFC<sub>849</sub>, CFC<sub>850</sub>, CFC<sub>851</sub>, CFC<sub>852</sub>, CFC<sub>853</sub>, CFC<sub>854</sub>, CFC<sub>855</sub>, CFC<sub>856</sub>, CFC<sub>857</sub>, CFC<sub>858</sub>, CFC<sub>859</sub>, CFC<sub>860</sub>, CFC<sub>861</sub>, CFC<sub>862</sub>, CFC<sub>863</sub>, CFC<sub>864</sub>, CFC<sub>865</sub>, CFC<sub>866</sub>, CFC<sub>867</sub>, CFC<sub>868</sub>, CFC<sub>869</sub>, CFC<sub>870</sub>, CFC<sub>871</sub>, CFC<sub>872</sub>, CFC<sub>873</sub>, CFC<sub>874</sub>, CFC<sub>875</sub>, CFC<sub>876</sub>, CFC<sub>877</sub>, CFC<sub>878</sub>, CFC<sub>879</sub>, CFC<sub>880</sub>, CFC<sub>881</sub>, CFC<sub>882</sub>, CFC<sub>883</sub>, CFC<sub>884</sub>, CFC<sub>885</sub>, CFC<sub>886</sub>, CFC<sub>887</sub>, CFC<sub>888</sub>, CFC<sub>889</sub>, CFC<sub>890</sub>, CFC<sub>891</sub>, CFC<sub>892</sub>, CFC<sub>893</sub>, CFC<sub>894</sub>, CFC<sub>895</sub>, CFC<sub>896</sub>, CFC<sub>897</sub>, CFC<sub>898</sub>, CFC<sub>899</sub>, CFC<sub>900</sub>, CFC<sub>901</sub>, CFC<sub>902</sub>, CFC<sub>903</sub>, CFC<sub>904</sub>, CFC<sub>905</sub>, CFC<sub>906</sub>, CFC<sub>907</sub>, CFC<sub>908</sub>, CFC<sub>909</sub>, CFC<sub>910</sub>, CFC<sub>911</sub>, CFC<sub>912</sub>, CFC<sub>913</sub>, CFC<sub>914</sub>, CFC<sub>915</sub>, CFC<sub>916</sub>, CFC<sub>917</sub>, CFC<sub>918</sub>, CFC<sub>919</sub>, CFC<sub>920</sub>, CFC<sub>921</sub>, CFC<sub>922</sub>, CFC<sub>923</sub>, CFC<sub>924</sub>, CFC<sub>925</sub>, CFC<sub>926</sub>, CFC<sub>927</sub>, CFC<sub>928</sub>, CFC<sub>929</sub>, CFC<sub>930</sub>, CFC<sub>931</sub>, CFC<sub>932</sub>, CFC<sub>933</sub>, CFC<sub>934</sub>, CFC<sub>935</sub>, CFC<sub>936</sub>, CFC<sub>937</sub>, CFC<sub>938</sub>, CFC<sub>939</sub>, CFC<sub>940</sub>, CFC<sub>941</sub>, CFC<sub>942</sub>, CFC<sub>943</sub>, CFC<sub>944</sub>, CFC<sub>945</sub>, CFC<sub>946</sub>, CFC<sub>947</sub>, CFC<sub>948</sub>, CFC<sub>949</sub>, CFC<sub>950</sub>, CFC<sub>951</sub>, CFC<sub>952</sub>, CFC<sub>953</sub>, CFC<sub>954</sub>, CFC<sub>955</sub>, CFC<sub>956</sub>, CFC<sub>957</sub>, CFC<sub>958</sub>, CFC<sub>959</sub>, CFC<sub>960</sub>, CFC<sub>961</sub>, CFC<sub>962</sub>, CFC<sub>963</sub>, CFC<sub>964</sub>, CFC<sub>965</sub>, CFC<sub>966</sub>, CFC<sub>967</sub>, CFC<sub>968</sub>, CFC<sub>969</sub>, CFC<sub>970</sub>, CFC<sub>971</sub>, CFC<sub>972</sub>, CFC<sub>973</sub>, CFC<sub>974</sub>, CFC<sub>975</sub>, CFC<sub>976</sub>, CFC<sub>977</sub>, CFC<sub>978</sub>, CFC<sub>979</sub>, CFC<sub>980</sub>, CFC<sub>981</sub>, CFC<sub>982</sub>, CFC<sub>983</sub>, CFC<sub>984</sub>, CFC<sub>985</sub>, CFC<sub>986</sub>, CFC<sub>987</sub>, CFC<sub>988</sub>, CFC<sub>989</sub>, CFC<sub>990</sub>, CFC<sub>991</sub>, CFC<sub>992</sub>, CFC<sub>993</sub>, CFC<sub>994</sub>, CFC<sub>995</sub>, CFC<sub>996</sub>, CFC<sub>997</sub>, CFC<sub>998</sub>, CFC<sub>999</sub>, CFC<sub>1000</sub>), may also become important in determining climate change if their growth rates continue to increase indefinitely.
- (8) CFC's, through their indirect chemical effects on O<sub>3</sub>, have a potentially large stratospheric cooling effect, as large as that due to CO<sub>2</sub> increase. For a given scenario for increase in trace gases (including CO<sub>2</sub>), the computed stratospheric cooling is significantly larger (by factors ranging from 2 to 10 depending on the altitude) than the computed surface warming.
- (9) In addition to the direct radiative effect, many of the trace gases have indirect effects on climate. For example, addition of gases such as CH<sub>4</sub>, CO and NO<sub>x</sub> can alter tropospheric O<sub>3</sub>, which is a radiatively active gas. Within the troposphere, the indirect climate effects can be as large as the direct effects. On the other hand, within the stratosphere, temperature changes are largely determined by indirect effects of CFC's. Stratospheric H<sub>2</sub>O will increase due to the oxidation of the increasing concentrations of CH<sub>4</sub>, and can be influenced by the trace gases through their effect on tropical tropopause temperatures. Furthermore, increases in tropospheric H<sub>2</sub>O, through the temperature-H<sub>2</sub>O feedback, can perturb tropospheric chemistry and alter the concentration of CH<sub>4</sub> and O<sub>3</sub>.

- (10) The fundamental issue that needs to be addressed within the context of the trace gas-climate problem is the relative importance of transport, chemistry and the indirect effects of trace gases in governing the long-term trends of tropospheric and stratospheric O<sub>3</sub>, CH<sub>4</sub> and stratospheric H<sub>2</sub>O. A credible and successful attack on this problem must include model as well as *in situ* observational studies. The specifics of such studies are identified in this assessment.
- (11) Cloud feedback continues to be the major source of uncertainty in the surface temperature sensitivity of climate models. At present, even the sign of this feedback is not known.
- (12) The next crucial issue concerns accurate determination of decadal trends in radiative forcings, trace gases, planetary albedo (to determine effects of aerosols and cloud feedback) and surface-troposphere-stratosphere temperatures. The observational challenges are formidable and must be overcome for a scientifically credible interpretation of the human impacts on climate.

### APPENDIX A: CHEMICAL KINETICS DATA BASE

This Appendix contains tables of evaluated data for chemical rate constants and equilibrium constants. The first table gives rate constants for second order reactions. The reactions are grouped into the classes: O, O(<sup>1</sup>D), HO<sub>x</sub>, NO<sub>x</sub>, hydrocarbon reactions, ClO<sub>x</sub>, BrO<sub>x</sub>, FO<sub>x</sub>, SO<sub>x</sub>, and metal reactions. The second table gives rate constants for three-body reactions in the form of values for the low pressure limit and for the high pressure limit. There is also a table of equilibrium constants for those systems in which unstable products may be formed in association reactions. The values given are those recommended by the NASA Panel for Data Evaluation in the Panel's complete report which was published by the Jet Propulsion Laboratory, Pasadena, CA as JPL Publication 85-37.

### APPENDIX B: SPECTROSCOPIC DATABASE: INFRARED TO MICROWAVE

Accurate modeling of radiative transfer in the atmosphere is very dependent on the accuracy to which the spectroscopic parameters of the optically active atmospheric gases are known. The primary objective of this Appendix is to review the status of the presently available database of spectroscopic parameters (line positions, intensities, pressure-broadened halfwidths, etc.) in the infrared to microwave spectral region for molecules of interest for remote sensing and climate studies in the terrestrial atmosphere. In addition, this review contains detailed discussions of quantitative high-resolution atmospheric spectroscopy, laboratory spectroscopy (including reviews of current capabilities and efforts in progress), and spectroscopic data accuracy requirements for space-based remote sensing of the atmosphere.

#### Major Conclusions and Recommendations

- (1) The three major computer-accessible compilations of spectroscopic line parameters (AFGL, GEISA, and JPL) contain among them data on over 400,000 transitions for 42 molecular species, covering the spectral range from 0 cm<sup>-1</sup> to 18,000 cm<sup>-1</sup>. For the parameters presently contained in the compilations approximately 80% of the line positions, 50% of the intensities, and only 5% of the air-broadened halfwidths may be considered to be of sufficient accuracy for most atmospheric remote sensing applications. In addition, spectroscopic parameters are totally missing from the compilations for a number of species of atmospheric interest (e.g. N<sub>2</sub>O<sub>5</sub> and HNO<sub>4</sub>).

## INTRODUCTION

- (2) With the present capabilities for laboratory spectroscopy and analysis, line positions can be routinely determined with high absolute accuracy. However, absolute line or band intensities and pressure-broadened halfwidths can be measured with accuracies no better than 5%. This level of accuracy is insufficient to meet some of the requirements for future space-based atmospheric sensors.
- (3) The two major requirements for further work in laboratory spectroscopy for atmospheric measurements and climate modeling are:
  - (a) Line Positions and Intensities: Spectral parameters are needed for several infrared bands of major and trace constituents where data are either totally missing from the present compilations or are of very poor quality. These problems are generally more severe at wavelengths shorter than 3  $\mu\text{m}$ , although improvements are needed for certain species in all spectral regions.
  - (b) Line Widths: Improved knowledge of air-broadened halfwidths and their temperature dependence is needed for nearly all of the optically active atmospheric species. Self-broadened and nitrogen-broadened halfwidths are also needed for special applications such as gas correlation radiometry.
- (4) Other requirements, in order of their relative importance, include laboratory and theoretical studies of deviations from the Lorentz line shape, accurate integrated intensities and band model representations for unresolved bands, more accurate absorption coefficients for the important pressure induced bands of oxygen and nitrogen, improved models for the temperature and pressure dependence of the water vapor continuum, improved parameters for transitions involved in non-LTE radiative transfer in the upper atmosphere, and quantification of other effects such as pressure induced line shifts which are presently considered to be insignificant for atmospheric spectroscopy.

## APPENDIX C: INSTRUMENT INTERCOMPARISONS AND ASSESSMENTS

This Appendix summarizes what has been learned regarding the reliability with which the concentrations of stratospheric trace species can be measured with current techniques and instruments. During the last several years, there have been a number of field campaigns that have focused on the assessment of this reliability by direct intercomparison of results for a given species obtained by a variety of different methods applied simultaneously under representative atmospheric conditions. These formal and rigorous intercomparisons have revealed both strengths and shortcomings.

### Major Conclusions and Recommendations

- (1) Stratospheric ozone can likely be measured with a  $\pm 4\%$  relative uncertainty at altitudes up to about 40 km with state-of-the-art balloon-borne *in situ* UV absorption photometers.
- (2) The monitoring-type electrochemical ozonesondes appear to have, on the average, an overall uncertainty of  $\pm 10\%$  and a precision of 5% at stratospheric altitudes below 25-30 km, given consistent preparation of the sondes.
- (3) The data from the frostpoint and fluorescence water vapor instruments have a systematic difference of about 0.75 ppmv (20%), the origin of which remains unknown.
- (4) Such intercomparisons are vital to real progress in assessing the reliability of stratospheric observations and must be a component of experimental research in this field.

- (5) There are numerous unresolved differences among the results of balloon-borne long path techniques for several species, e.g.  $\text{NO}_2$ .

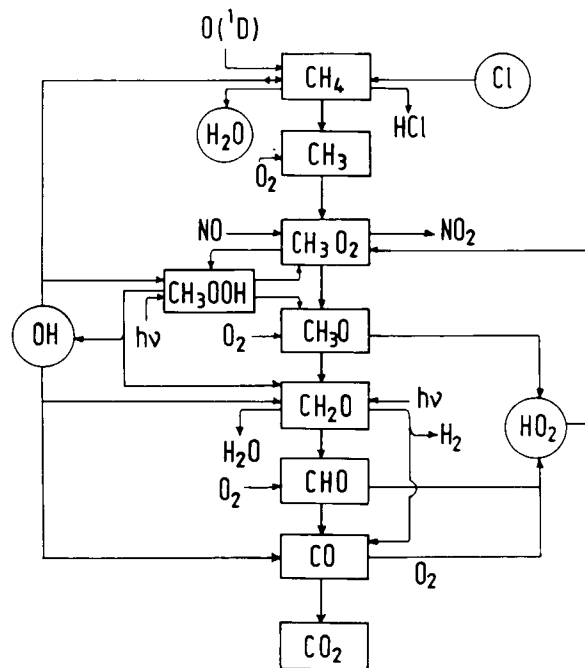
### **APPENDIX D: OZONE AND TEMPERATURE MONTHLY MEANS**

This Appendix is provided because global monthly mean charts of ozone and temperature have become available, covering for the first time the height range 30 to 0.1-mbar, (approximately 24 to 64 km).

For both hemispheres these charts are given for the four mid-season months, and for the pressure levels 30, 10, 1, and 0.1 mbar, (0.4 mbar for ozone). Charts with total ozone are provided separately. This set of charts shows clearly the very close coupling between the temperatures and the ozone distribution and demonstrates the influence of the large-scale planetary waves, giving rise to very large longitudinal variations.

A discussion on the regular and interannual variability of temperature and ozone is followed by a description of the mean state.

# STRATOSPHERIC CHEMISTRY



## Panel Members

R.A. Cox, Chairman

W.B. DeMore

S.P. Sander

E.E. Ferguson

N.D. Sze

R. Lesclaux

R. Zellner

A.R. Ravishankara

## CHAPTER 2

### STRATOSPHERIC CHEMISTRY

#### TABLE OF CONTENTS

2.0 INTRODUCTION .....	27
2.1 CURRENT STATUS OF KINETICS AND PHOTOCHEMICAL DATA BASE FOR TRACE GAS FAMILIES INVOLVED IN OZONE CHEMISTRY.....	29
2.1.1 O <sub>x</sub> Chemistry .....	29
2.1.2 HO <sub>x</sub> Chemistry .....	30
2.1.3 NO <sub>x</sub> Chemistry .....	32
2.1.4 ClO <sub>x</sub> Chemistry .....	35
2.1.5 BrO <sub>x</sub> Chemistry .....	38
2.1.6 Sulfur Chemistry .....	40
2.1.7 Hydrocarbon Oxidation Chemistry .....	40
2.1.8 Halocarbon Oxidation Chemistry .....	42
2.2 SPECIAL ISSUES IN STRATOSPHERIC CHEMISTRY .....	43
2.2.1 Role of Reactions Involving Sodium Species .....	43
2.2.2 Ion Chemistry .....	44
2.2.3 Homogeneous Reactions Between Temporary Reservoir Species .....	45
2.2.4 Heterogeneous Reactions .....	46
2.2.5 Reactions With Complex Temperature and Pressure Functions .....	48
2.2.6 General Comments on Photodissociation Processes .....	50
2.2.7 Errors and Uncertainties in Kinetic and Photochemical Data .....	51
2.2.8 Identification of Gaps in the Chemical Description of the Atmosphere .....	53
2.3 SUMMARY AND CONCLUSIONS .....	54

## 2.0 INTRODUCTION

Ozone is present in the earth's atmosphere at all altitudes from the surface up to at least 100 km. The bulk of the ozone resides in the *stratosphere* with a maximum ozone concentration of  $5 \times 10^{12}$  molecule  $\text{cm}^{-3}$  at about 25 km. In the *mesosphere* ( $> 60$  km)  $\text{O}_3$  densities are quite low and are not discussed in the present report. Although  $\text{O}_3$  concentrations in the *troposphere* are also less than in the stratosphere, ozone plays a vital role in the atmospheric chemistry in this region and also affects the thermal radiation balance in the lower atmosphere.

Atmospheric ozone is formed by combination of atomic and molecular oxygen.



where M is a third body required to carry away the energy released in the combination reaction. At altitudes above approximately 20 km production of O atoms results almost exclusively from photodissociation of molecular  $\text{O}_2$  by short wavelength ultraviolet radiation ( $\lambda < 243$  nm):



At lower altitudes and particularly in the troposphere, O atom formation from the photodissociation of nitrogen dioxide by long wavelength ultraviolet radiation is more important:



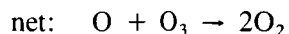
Ozone itself is photodissociated by both UV and visible light:



but this reaction together with the combination reaction (1) only serves to partition the 'odd oxygen' species between O and  $\text{O}_3$ . The production processes (2) and (3) are balanced by chemical and physical loss processes. Until the 1950s, chemical loss of odd oxygen was attributed only to the reaction:



originally proposed by S. Chapman (1930). It is now known that ozone in the stratosphere is removed predominantly by catalytic cycles involving homogeneous gas phase reactions of active free radical species in the  $\text{HO}_x$ ,  $\text{NO}_x$ ,  $\text{ClO}_x$  and  $\text{BrO}_x$  families:



where the catalyst  $\text{X} = \text{H}, \text{OH}, \text{NO}, \text{Cl}$  and  $\text{Br}$ . Thus these species can, with varying degrees of efficiency, control the abundance and distribution of ozone in the stratosphere. Assignment of the relative importance and the prediction of the future impact of these catalytic species is dependent on a detailed understanding of the chemical reactions which form, remove and interconvert the active components of each family.

## STRATOSPHERIC CHEMISTRY

This in turn requires knowledge of the atmospheric life cycles of the hydrogen, nitrogen and halogen-containing precursor and sink molecules, which control the overall abundance of  $\text{HO}_x$ ,  $\text{NO}_x$  and  $\text{ClO}_x$  species.

Physical loss of ozone from the stratosphere is mainly by dynamical transport to the troposphere where further photochemically driven sources and sinks modify the ozone concentration field. Ozone is destroyed at the surface of the earth and so there is an overall downward flux in the lower part of the atmosphere. Physical removal of ozone and other trace gaseous components can also occur in the precipitation elements and on the surface of atmospheric aerosols. Since most of the precursor and sink molecules for the species catalytically active in ozone removal in the stratosphere are derived from or removed in the troposphere, global tropospheric chemistry is a significant feature of overall atmospheric ozone behavior.

Numerical simulation techniques are used to describe and investigate the behavior of the complex chemical system controlling atmospheric composition, the models having elements of chemistry, radiation and transport. The chemistry in such models may include some 150 elementary chemical reactions and photochemical processes involving some 50 different species. Laboratory measurements of the rates of these reactions have progressed rapidly over the past decade and have given us a basic understanding of the kinetics of these elementary processes and the way they act in controlling ozone. This applies particularly in the upper stratosphere where local chemical composition is predominantly photochemically controlled.

It has proved more difficult to describe adequately both the chemistry and the dynamics in the lower stratosphere. Here the chemistry is complicated by the involvement of temporary reservoir species such as  $\text{HOCl}$ ,  $\text{H}_2\text{O}_2$ ,  $\text{HNO}_3$ ,  $\text{HCl}$ ,  $\text{HNO}_4$ ,  $\text{N}_2\text{O}_5$  and  $\text{ClONO}_2$  which 'store' active radicals and which strongly couple the  $\text{HO}_x$ ,  $\text{NO}_x$  and  $\text{ClO}_x$  families. The long photochemical and thermal lifetimes of ozone and the reservoir species in this region give rise to strong interaction between chemistry and dynamics (transport) in the control of the distribution of ozone and other trace gases. Moreover, seasonal variability and natural perturbations due to volcanic injections of gases and aerosol particles add further to complicate the description and interpretation of atmospheric behavior in this region. Most of the changes in the predicted effects of chlorofluoromethanes and other pollutants on ozone column density have resulted from changes in our view of the chemistry in the lower stratosphere. A great deal of importance must therefore be attached to achieving an understanding of the key factors in ozone chemistry in this region of the atmosphere.

Description of atmospheric chemistry in the troposphere is similarly complicated by dynamical influence and additionally by involvement of the precipitation elements (i.e. cloud, rain and snow) in the chemical pathways. The homogeneous chemistry of the troposphere is centered round the role of the hydroxyl radical in promoting oxidation and scavenging of trace gases released from surface terrestrial sources. Tropospheric OH is an important issue for stratospheric ozone since it controls the flux of source gases such as  $\text{CH}_4$ , halogenated hydrocarbons, and sulfur compounds to the stratosphere. Although the mechanisms are more complex due to the involvement of larger and more varied entities, the overall pattern of relatively rapid photochemical cycles involving a coupled carbon/hydrogen/nitrogen and oxygen chemistry is similar to that in the stratosphere. The photochemical cycles influence both the odd hydrogen budget and also, through coupling of the hydrocarbon oxidation with  $\text{NO}_2$  photochemistry, the *in situ* production and removal of tropospheric ozone. The concentration and distribution of tropospheric ozone is important in respect of its significant contribution to the total ozone column, and its radiative properties in the atmospheric heat balance. A detailed description of tropospheric chemistry is given in Chapter 4.

The numerical models employed to investigate atmospheric behavior require the best available input data. Provision of an evaluated photochemical and kinetics data base for modelling atmospheric chemistry

and ozone perturbations, has been recognized as an important feature of atmospheric programmes for some years now. With the rapid growth in the amount of information and expertise available in recent years this has become even more important. The evaluated data base produced by the NASA panel for Data Evaluation, updated in February 1985 (NASA, 1985) is provided in Appendix A of this assessment. An updated evaluation, containing more detailed presentation of the available data, has been published by the CODATA Task Group for Chemical Kinetics (Baulch *et al.*, 1984). These ongoing evaluation activities ensure that atmospheric models can benefit promptly from new laboratory data and improvements in the data base.

There have been a number of detailed descriptions of the basic chemical and photochemical processes which occur in the atmosphere and which control ozone and other trace gas budgets (NAS, 1976; NASA, 1979; Brasseur and Solomon, 1984; Wayne, 1985). The present discussion focusses mainly on the current key issues in chemistry relating to atmospheric ozone in the stratosphere and on changes that have occurred in the data base and perception of the problem since the last international report (WMO, 1982). An evaluation of the prospects for improvement in the knowledge in the near future is also given for some key areas. The present discussion does not attempt to assess the state of knowledge of chemistry related to ozone formation in the atmospheric boundary layer.

The first part of the assessment deals with the recent improvements in the data base for the currently identified reactions describing the chemistry of the major families of trace gas species,  $\text{HO}_x$ ,  $\text{NO}_x$ ,  $\text{ClO}_x$ , hydrocarbons, etc. The important coupling reactions between the families are introduced progressively in the subsections e.g., new data for the reactions which lead to net removal of  $\text{HO}_x$  but involve  $\text{NO}_x$  species are considered in the  $\text{NO}_x$  subsection. Discussion of the chemistry of sulphur and organic species (hydrocarbons and halocarbons) is restricted to those aspects impacting on the stratosphere and the unpolluted troposphere. The fluorine released in the breakdown of fluorocarbons in the stratosphere is converted ultimately to hydrogen fluoride, HF. As a result of the very high stability of HF, it is the predominant form of fluorine at all altitudes. The amounts of other  $\text{FO}_x$  species, which could become involved in catalytic cycles are too small to have a significant effect on stratospheric ozone. Kinetic data for  $\text{FO}_x$  species which may be formed in the breakdown of fluorocarbons are included in the evaluation given in Appendix I. The rate data are considerably more uncertain than those for the corresponding Cl and Br reactions, reflecting the fewer experimental measurements available for  $\text{FO}_x$  reactions.

The second part of the assessment considers a number of special issues relating to stratospheric chemistry. This includes a discussion of chemical aspects such as heterogeneous reactions and reactions of sodium species, the importance of which have not yet been completely established. Recent attempts to reconcile some of the more unexpected kinetic behavior which has emerged from the extensive experimental studies of key reactions with current reaction rate theory are also examined. Finally, a discussion of the uncertainties in the current kinetic and photochemical data base is given. An attempt is made to assess the prospects for improvement of the data for known reactions of atmospheric importance as well as for the identification of gaps in the chemical description of the atmosphere.

## 2.1 CURRENT STATUS OF DATA BASE FOR TRACE GAS FAMILIES INVOLVED IN OZONE CHEMISTRY

### 2.1.1 $\text{O}_x$ Chemistry

The kinetic data base related to the reactions of O,  $\text{O}_2$  and  $\text{O}_3$  species appears to be well established. There remains some concern about the possible role of the excited singlet states of molecular oxygen in

## STRATOSPHERIC CHEMISTRY

particular  $O_2(^1\Delta)$  which is present at high concentrations in the stratosphere. Possible reactions with free radicals such as H or ClO are of concern and discussed in the following sections. There is also a possible role of  $O_2(^1\Delta)$  in providing an additional source of odd oxygen if the photodissociation reaction:



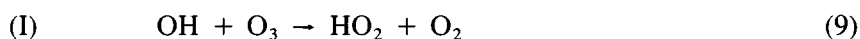
occurred at a comparable rate to the photodissociation of ground state  $O_2$ . A significant effect would require an absorption cross section for  $O_2(^1\Delta)$  in the 200 nm region of the order of  $10^{-19} \text{cm}^2 \text{molecule}^{-1}$ . However, there is no definite evidence to date that  $O_2$  singlet states have any important effects on the chemistry of the stratosphere.

The quantum yield of  $O(^1D)$  atoms in the photolysis of ozone still needs to be considered carefully. Quantum yields in the 'fall-off' region ( $\lambda > 300 \text{ nm}$ ) have been measured relative to the yields for shorter wavelengths where a value of 0.9 has been selected in the NASA evaluation for  $\Phi(O^1D)$ . Additional measurements are required to confirm this value and to better establish the temperature dependence of the quantum yields in the 280-330 nm region.

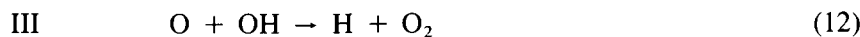
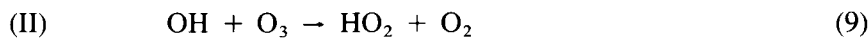
Observed ozone abundance in the upper stratosphere and lower mesosphere is larger than predicted by model calculations (Solomon *et al.*, 1983a, Ko and Sze, 1983). Possible reasons for this discrepancy which are related to  $O_x$  chemistry are discussed in the chapter on  $O_x$  measurements.

### 2.1.2 $HO_x$ Chemistry

There have been relatively few changes recently in the kinetics data base for  $HO_x$ . The principal catalytic cycle for odd-oxygen destruction within the  $HO_x$  family is:

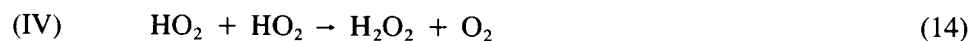


Depending on altitude the following cycles may also become important:



Most of the reactions involved in these cycles are now reasonably well characterized. An exception is reaction (11) which is the rate controlling step in cycle (II). Previous revisions in the measured temperature dependence of  $k_{11}$  have had a significant effect on calculated ozone depletion. There has been only one direct temperature dependence study of reaction (11), the results of which indicate an A-factor for the rate coefficient which is surprisingly low. The temperature dependence of reactions (10) and (12) are also in need of additional study in view of the sensitivity of the upper stratospheric ozone profile to these rate coefficients.

Recent changes in the data base for  $\text{HO}_x$  reactions have also affected processes involved in the destruction of odd hydrogen. An example is the catalytic cycle which result in the recombination of OH and  $\text{HO}_2$  through  $\text{H}_2\text{O}_2$ :



The complex dependence of the rate coefficient for reaction (14) on pressure, temperature and water vapor has now been examined in detail, and this behavior has been incorporated into atmospheric models. The rate coefficient for reaction (15) is also now reasonably well known.

The direct reaction between OH and  $\text{HO}_2$ ,



has received considerable attention recently. DeMore (1982) has shown that the rate coefficient for this reaction increases from a low-pressure limiting value of  $7.0 \times 10^{-11} \text{cm}^3 \text{molecule}^{-1} \text{s}^{-1}$  at 298 K to about  $1.1 \times 10^{-10} \text{cm}^3 \text{molecule}^{-1} \text{s}^{-1}$  at a total pressure of 1 atm.  $\text{N}_2$ . Sridharan *et al.* (1984) recently carried out the first temperature dependence study of this reaction, obtaining a value for E/R of  $-(416 \pm 86)$  K. While this reaction is now reasonably well characterized, additional temperature and pressure dependence studies would be desirable in view of the important role of this reaction in  $\text{HO}_x$  destruction.

The branching ratios for the reaction



have recently been measured by Keyser (1985 private communication) with the values  $k_{17a}/k_{17} = (0.91 \pm 0.08)$ ,  $k_{17b}/k_{17} = (0.09 \pm 0.04)$  and  $k_{17c}/k_{17} < 0.1$  being obtained at 298 K. These results are in reasonably good agreement with the study by Sridharan *et al.* (1982). In the only measurement of the temperature dependence, Keyser (1985) reports a value for  $k_{17}$  independent of temperature between 245 and 300 K. The temperature dependences of the individual reaction channels has not yet been determined.

The potential role of  $\text{HO}_x$ -chemistry arising from species in low lying electronically excited states such as  $\text{O}_2(^1\Delta_g)$  and  $\text{HO}_2(\tilde{\text{A}}^2\text{A}')$  has been a subject of much speculation in the past. Recent laboratory

## STRATOSPHERIC CHEMISTRY

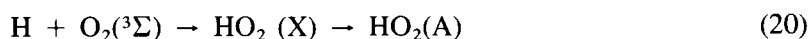
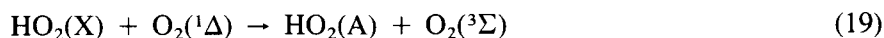
work, however, suggests that neither source nor sink reactions of  $\text{HO}_x$  are likely to be influenced by these electronically excited states.

For example, the reaction



is too slow ( $k_{18} = 1.8 \times 10^{-13} \exp(-1560/T) \text{ cm}^3 \text{ molecule}^{-1} \text{ s}^{-1}$ ; Hack, Kurzke, 1985) to be relevant in either  $\text{HO}_x$  or  $\text{O}_x$  chemistry in the stratosphere.

The importance of  $\text{HO}_2(\text{A}^2\text{A}')$  can be assessed by estimating its steady state concentration relative to the ground state. Using the rate coefficients for the excitation processes (Hack, Kurzke, 1984; Holstein *et al.*, 1983).



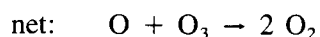
and for de-excitation,



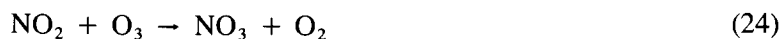
the fraction of  $\text{HO}_2(\text{A})$  relative to ground state  $\text{HO}_2(\text{X})$  is below  $2 \times 10^{-6}$  throughout the stratosphere. Since this factor is unlikely to be compensated for by an enhanced reactivity of  $\text{HO}_2(\text{A})$ , no influence on stratospheric  $\text{HO}_2$  chemistry can be expected.

### 2.1.3 $\text{NO}_x$ Chemistry

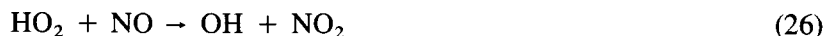
Odd nitrogen species are important in the stratosphere because they are involved in catalytic cycles which directly destroy  $\text{O}_3$ ,



and



The first of these two cycles is much more important than the second. Even though all the above reactions have been studied in the laboratory, there exist some uncertainties in the values for the rate coefficient for reaction (22) at stratospheric temperatures and the quantum yield for NO in NO<sub>3</sub> photolysis. In addition to their involvement in direct O<sub>3</sub> destruction, NO<sub>x</sub> species play crucial roles in the partitioning of odd hydrogen and odd chlorine into various forms. The rates of conversion of HO<sub>2</sub> to OH and ClO to Cl are determined by the reactions involving NO,



and those involving O(<sup>3</sup>P), i.e., O + HO<sub>2</sub> → OH + O<sub>2</sub> and O + ClO → Cl + O<sub>2</sub>. Thus, these reactions in conjunction with reactions of OH and Cl with O<sub>3</sub>, control the ratios [HO<sub>2</sub>]/[OH] and [ClO]/[Cl]. Both reactions 26 and 27 are well characterized. NO<sub>x</sub> species are also involved in sequestering HO<sub>x</sub> species in temporary reservoirs e.g.:



The above processes have been thoroughly investigated and their rate coefficients are quite well established. The photolysis of NO<sub>2</sub>, reaction (3), serves as the major source of odd oxygen in the troposphere. The absorption cross section for NO<sub>2</sub> and the quantum yield for O atom production are still somewhat uncertain, as are their temperature dependences.

In addition to the above mentioned reactions, the majority of reactions involving NO<sub>x</sub> that are important in understanding stratospheric chemistry are well characterized. In the following section, we will discuss only the problem areas and areas where significant new data have been recently reported.

N<sub>2</sub>O is the major source of NO<sub>x</sub> in the stratosphere. The predominant path for N<sub>2</sub>O destruction is photolysis. Its reaction with O(<sup>1</sup>D) contributes only 2% to N<sub>2</sub>O destruction but is currently assumed to be the main NO<sub>x</sub> production mechanism. Therefore, the possibility of N<sub>2</sub>O photolysis to give NO + N needs to be very carefully assessed. Even if such a pathway constitutes only 1% of the total N<sub>2</sub>O photolysis rate, it could be equal to the O(<sup>1</sup>D) + N<sub>2</sub>O source [for each N<sub>2</sub>O photolyzed to give NO + N, one more molecule of NO is produced due to the reaction of N with O<sub>2</sub> or O<sub>3</sub>].

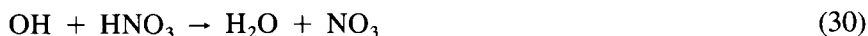
The majority of O(<sup>1</sup>D) produced by O<sub>3</sub> is physically deactivated to O(<sup>3</sup>P). The thermal rate coefficients for the reaction/deactivation of O(<sup>1</sup>D) by atmospheric gases N<sub>2</sub>, O<sub>2</sub>, O<sub>3</sub>, CO<sub>2</sub>, Ar, N<sub>2</sub>O, H<sub>2</sub>O and CH<sub>4</sub> are well defined (NASA evaluation). However, the yield of NO due to the O(<sup>1</sup>D) + N<sub>2</sub>O reaction in the stratosphere is uncertain by as much as 30%. This uncertainty is partly due to the combined errors in the measured values of all the rate coefficients for O(<sup>1</sup>D) removal reactions, and is partly due to the possibility that the branching ratio of O(<sup>1</sup>D) + N<sub>2</sub>O reaction to yield NO (as opposed to N<sub>2</sub> and O<sub>2</sub>) changes with the kinetic energy of O(<sup>1</sup>D). Since O(<sup>1</sup>D) produced by ozone photolysis is translationally hot, and since the O(<sup>1</sup>D) + N<sub>2</sub> and O(<sup>1</sup>D) + O<sub>2</sub> quenching rates are temperature dependent, the uncertainty of the atmospheric rate of O(<sup>1</sup>D) + N<sub>2</sub>O → 2NO reaction branch is further enhanced if translationally hot O(<sup>1</sup>D) reacts differently than thermal O(<sup>1</sup>D). Therefore, experiments designed to measure NO production under stratospheric conditions which do not rely on the accuracy of the individual reaction rates need to be carried out.

## STRATOSPHERIC CHEMISTRY

Currently, all stratospheric  $N_2O$  is assumed to be produced at the ground level and transported into the stratosphere. However, local production of  $N_2O$  due to reactions such as  $N_2(A^3\Sigma) + O_2$  and  $OH(A^2\Pi) + N_2$  cannot be ruled out (Zipf, Prasad 1982). If such reactions occur in the mesosphere they could influence the stratospheric  $NO_x$  budget by downward transport of  $N_2O$ .

The main known process which removes  $NO_x$  from the stratosphere is transport of long lived species such as  $HNO_3$ , but a small amount of  $NO_x$  loss occurs through the  $N+NO$  and  $N+NO_2$  reactions in the upper stratosphere. The latter reaction may produce  $N_2O$  as a major product. Kinetic data for reaction of  $N$  with  $NO$  are reasonably well established, but the rate constant for reaction with  $NO_2$  is only reliable to within a factor of 3 at room temperature and its temperature dependence has not been established.

Removal of odd-hydrogen in the lower stratosphere occurs mainly by the reaction of  $OH$  with nitric acid and peroxyntic acid:



Changes in the recommended rate coefficients for these reactions have previously resulted in significant revisions of the calculated ozone column. The existence of a negative temperature dependence for the  $OH + HNO_3$  reaction is now well established and confirmation of the small pressure dependence may help explain some of the divergence between results of the kinetics studies in different laboratory systems (NASA, 1985). The equally important  $OH + HO_2NO_2$  reaction is not as well characterized, either with regard to the temperature dependence or the reaction products. New data have been reported recently for the temperature and pressure dependence of the  $HO_2NO_2$  formation reaction (Sander and Peterson, 1984):



The rate constant for stratospheric conditions is about 40% lower than previously recommended. The products and temperature dependence of the photodissociation of  $HO_2NO_2$  are still not established and the equilibrium constant for  $HO_2NO_2$  formation is not reliably known. These gaps in the data base lead to some uncertainty in the description of peroxyntic acid behavior in the lower stratosphere and the troposphere.

The possibility of formation of an isomer of nitric acid in the recombination reaction of  $OH$  with  $NO_2$  reaction (28) has also been considered. Such an isomer, if more reactive than  $HONO_2$ , would serve to reduce the effective rate of nitric acid formation. To date no firm evidence has been found for a complication of this kind in the kinetics of the  $OH + NO_2$  reaction.

Recently, direct determinations of the rate constants for some key  $NO_3$  reactions including those with  $NO_2$  and  $NO$  have been made. The reliability of the data base for these reactions is now greatly improved.



The equilibrium constant for the formation in the latter reaction of the important temporary reservoir species  $N_2O_5$  has also been measured directly in several studies, but there remains some uncertainty in this quantity.

Reaction of  $\text{NO}_3$  with the stable stratospheric species  $\text{CO}$ ,  $\text{CH}_4$  and  $\text{H}_2\text{O}_2$  has been found to be too slow to be important; reaction with  $\text{HCl}$  has not been investigated. The recent suggestion (Johnston *et al.*, 1985) that  $\text{NO}_3$  can thermally decompose to give  $\text{NO} + \text{O}_2$  needs to be carefully examined. If this reaction is fast (i.e.,  $10^{-5}$ – $10^{-4}\text{s}^{-1}$  under stratospheric conditions) it could have significant effects on  $\text{NO}_x$  chemistry. The temporal behavior, the observed absolute concentration and the seasonal variations of atmospheric  $\text{NO}_3$  are still unexplained. These field observations point to an incomplete understanding of the atmospheric chemistry of  $\text{NO}_3$ .

The absorption cross sections of  $\text{NO}_2$ ,  $\text{NO}_3$ ,  $\text{N}_2\text{O}_5$ ,  $\text{HNO}_3$  and  $\text{HO}_2\text{NO}_2$  have been measured at 298 K. The temperature dependence of the cross sections have been investigated only in the cases of  $\text{NO}_2$  and  $\text{N}_2\text{O}_5$  (see NASA, 1985 evaluation). Since photolysis can be the major stratospheric removal channel for many of these species, it is imperative that the absorption cross sections of species such as  $\text{HNO}_3$  and  $\text{HO}_2\text{NO}_2$  be measured over the temperature range of 220–298 K. It is unlikely that the discrepancies in the absorption cross sections of  $\text{NO}_3$  or its temperature dependence will have any effect on stratospheric chemistry. However, they do affect the accuracy of the field measurement data obtained using long path visible absorption methods. The identity and quantum yield of products in the photolysis of  $\text{NO}_2$  and  $\text{HNO}_3$  are reasonably well known but not their temperature dependencies. There is still some controversy regarding the quantum yields for various products (i.e.,  $\text{O}(^3\text{P})$ ,  $\text{NO}$ ,  $\text{NO}_2$  and  $\text{NO}_3$ ) in the photolysis of  $\text{N}_2\text{O}_5$  (Swanson *et al.*, 1984 and Ravishankara *et al.*, 1985). Since  $\text{NO}$ ,  $\text{NO}_2$  and  $\text{NO}_3$  are rapidly interconverted, the nature of their photochemical pathways has minimal effect on stratospheric chemistry. All indications to date suggest that  $\text{NO}_3$  and  $\text{NO}_2$  are the major products. The photochemistry of  $\text{NO}_3$  is not well understood. The quantum yields for the two channels —  $\text{NO} + \text{O}_2$  and  $\text{NO}_2 + \text{O}(^3\text{P})$  — are not accurately measured even at 298 K. The dissociation threshold for the second channel has been established to be 620 nm (Nelson *et al.*, 1983, Ishiwata *et al.*, 1983, and A. Torabi, 1985). The quantum yields for  $\text{NO}$  and  $\text{NO}_2$  production could also be pressure and temperature dependent.

#### 2.1.4 $\text{ClO}_x$ Chemistry

The principal odd oxygen destruction cycle involving  $\text{ClO}_x$  is:



However, in large parts of the stratosphere, the conversion of  $\text{ClO}$  to  $\text{Cl}$  occurs mainly by coupling with  $\text{NO}_x$ :



In this case the sequence: reaction (34) followed by reaction (27) does not destroy odd oxygen, because  $\text{NO}_2$  is rapidly photolyzed, reaction (3).

The main sink of active chlorine species is the reaction



## STRATOSPHERIC CHEMISTRY

from which Cl-atoms are recycled by



$\text{ClO}_x$  species also form temporary reservoir species in the following reactions:



Of these, the latter is of less importance. The recycling of  $\text{ClO}_x$  from both reservoirs is by photolysis.

Most of these processes are now well understood, including the issue of formation of isomers of chlorine nitrate in reaction (38). There have been minor changes in the kinetics data base which are discussed in the following paragraphs. In addition remaining problem areas such as the formation of HCl in the reaction of OH with ClO, and the potential role of higher oxides of chlorine is considered.

The four new studies of the O + ClO reaction by Margitan (1984a), Leu (1984), Schwab *et al.* (1984) and Ongstad and Birks (1984) together average about 20% less than previous determinations of the 298 K rate constant. The temperature dependences, which were reported in the recent studies, are consistent with an E/R value of  $(50 \pm 100)$  K. Ozone depletion calculations are particularly sensitive to this rate constant since the O + ClO reaction is the rate-limiting step in the chlorine-catalyzed destruction of odd oxygen in the upper stratosphere. However, it is unlikely that additional studies of this reaction using techniques thus far employed will significantly reduce the uncertainty in the rate constant.

A number of early studies of the reaction:



by direct methods had suggested a consensus value of  $6.5 \times 10^{-13} \text{ cm}^3 \text{ molecule}^{-1} \text{ s}^{-1}$  for  $k_{37}$  at 298 K. However, measurements by Molina *et al.* (1984) and Keyser (1984) resulted in values of  $(7.9 \pm 1.2)$  and  $(8.5 \pm 0.4) \times 10^{-13} \text{ cm}^3 \text{ molecule}^{-1} \text{ s}^{-1}$ , respectively. These studies are considered more reliable than the earlier determinations because of their more careful measurement techniques for HCl. In view of the sensitivity of model calculations of ozone depletion to this rate constant, the increase of 25% implied by the two recent measurements is significant.

There have been no significant changes recently in other reactions of odd-chlorine radicals including Cl + O<sub>3</sub>, HO<sub>2</sub>, HCHO, and ClO + HO<sub>2</sub>, NO<sub>2</sub> and NO. The suggestion by Chang *et al.* (1979) and Molina *et al.* (1980) that the nascent product of the reaction

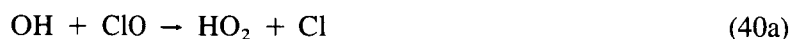


is an isomer of chlorine nitrate is now considered incorrect. This possibility was based on the observation that the value of  $k_{38}$  determined from direct studies was several times larger than the value inferred from the equilibrium constant and measurements of the chlorine nitrate thermal decomposition rate. If, as had been assumed, the isomer were to photolyze rapidly in the stratosphere, the effective rate of ClONO<sub>2</sub> formation would be 2-4 times slower than the rate suggested by direct studies. Recent work by Margitan

(1983), however, showed that the isomer, if formed, photodecomposes in a manner identical to that of ClONO<sub>2</sub>. In addition, neither Cox *et al.* (1984) nor Burrows *et al.* (1984) were able to detect an isomer by direct spectroscopic methods.

Relatively little attention has been paid to the kinetics and photochemistry of HOCl in the last few years. Despite the current uncertainties in reaction rates, photolysis pathways and cross-sections, the role of HOCl in stratospheric chemistry appears to be well understood. The HO<sub>2</sub> + ClO reaction is the only known stratospheric HOCl source, and photolysis is sufficiently rapid that HOCl cannot act as a significant reservoir of odd chlorine. Although the reactions of HOCl with other stratospheric radicals such as O, Cl and OH have not been fully investigated, these processes cannot compete with photolysis for HOCl removal.

Because of the possibility of HCl formation as a minor channel, the OH + ClO reaction,



has received considerable attention recently. Determination of branching ratio  $k_{40b}/k_{40a}$  is complicated experimentally by the Cl + HO<sub>2</sub> back-reaction which primarily forms HCl + O<sub>2</sub>. Two recent studies by Hills and Howard (1984) and Burrows *et al.* (1984) agree as to the room-temperature branching ratio for HO<sub>2</sub> formation, obtaining  $(0.86 \pm 0.14)$  and  $(0.85 \pm 0.07)$ , respectively. On the other hand Poul *et al.* (1985) report a branching ratio of  $(0.98 \pm 0.07)$ . Due to the complexity of the methods involved, the HCl yield for this reaction cannot be considered established. The three studies are in fair agreement as to the overall rate constant. However, Hills and Howard report a temperature dependence of  $(235 \pm 46)/T$ , and Burrows *et al.*, report no temperature dependence over the range 243 - 298 K. The currently accepted overall rate constant (NASA, 1985) is about 30% larger than the previously accepted values. Additional work focussing on the HCl product channel as a function of temperature is required.

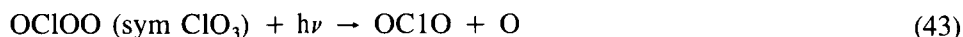
It is generally assumed that Cl and ClO are the only active chlorine species in the stratosphere. The potential importance of higher chlorine oxides, however, also needs some consideration. Prasad (1980) suggested the formation of asymmetric chlorine trioxide by the interaction of ClO with O<sub>2</sub>:



this species has not been observed in the laboratory, however its existence in the stratosphere cannot be ruled out *a priori*. The corresponding reaction of ClO with O<sub>2</sub> (<sup>1</sup>Δ) would energetically also allow the formulation of symmetric ClO<sub>3</sub>:



If these reactions proceeded at sufficient rate and extent, and if the resulting trioxides were photolyzed to yield oxygen atoms:



## STRATOSPHERIC CHEMISTRY

a chain mechanism could be set up in which  $O_2$  molecules were catalytically photodissociated. Therefore, instead of ClO destroying odd oxygen in the normal  $ClO_x$ -catalyzed  $O_3$  destruction chain it could provide a net odd oxygen source.

Moreover, the rates of radical-radical reactions involving ClO (i.e., reactions  $NO + ClO$ ,  $O + ClO$ ,  $OH + ClO$ ), to which the calculated  $O_3$  perturbation due to  $ClO_x$  is highly sensitive, could be affected if ClO were complexed with  $O_2$  under stratospheric conditions. None of these reactions has so far been studied under conditions of high  $O_2$  concentration.

Evidence from recent laboratory kinetic studies (Fritz and Zellner 1984; Handwerk and Zellner 1984) suggests the reactions forming the trioxides  $OCIOO$  and sym  $ClO_3$  are very slow:  $k_{41} < 10^{-19} \text{cm}^3 \text{molecule}^{-1} \text{s}^{-1}$  and  $k_{42} < 3 \times 10^{-15} \text{cm}^3 \text{molecule}^{-1} \text{s}^{-1}$ , both at 298 K. These studies also allowed an estimate of the equilibrium constant for  $OCIOO$  formation  $K_{41}^* < 10^{-20} \text{cm}^3 \text{molecule}^{-1}$  at 298 K.

The low value of  $k_{42}$  precludes an important role for reaction with  $O_2(^1\Delta)$ . However the upper limit for  $k_{41}$  implies competitive rates with other ClO reactions in the lower stratosphere. Furthermore at the low temperatures prevalent in this region, the equilibrium constant  $K_{41}^*$  may be considerably higher than the upper limit value obtained at room temperature leading to significant amounts of active  $ClO_x$  present as  $OCIOO$ . Further studies to establish the magnitude of  $K_{41}^*$  at low temperatures are needed.

The mutual interaction of two ClO radicals also needs consideration in the situation of a highly  $Cl_x$  perturbed stratosphere:



Whereas reaction (45) would not affect the concentration of active  $ClO_x$  since Cl atoms are readily regenerated via the photolysis of  $Cl_2$ , the formation of  $Cl_2O_2$  in reaction (46) may serve as a temporary  $ClO_x$  reservoir. The available kinetic data base (Cox *et al.*, 1979; Cox, Derwent, 1979; Basco, Hunt, 1979; Watson, 1977) suggests that for stratospheric pressures and temperatures reaction (46) is dominant over reaction (45). The subsequent chemistry of  $Cl_2O_2$ , however, is not well defined. Its likely fate is photolysis and reaction with Cl, O, or OH. Mutual reactions between ClO are expected to become important at  $ClO_x$  levels exceeding 10 ppb.

### 2.1.5 $BrO_x$ Chemistry

Although stratospheric Br and BrO destroy odd hydrogen in an analogous manner to  $ClO_x$  species, bromine chemistry differs from chlorine chemistry in several important respects. Because the H-Br bond strength is about  $16 \text{ kcal mol}^{-1}$  less than the H-Cl bond strength, hydrogen abstractions tend to be much more rapid for chlorine than for bromine. Indeed, reactions such as  $X + CH_4$  and  $X + H_2$  are important for  $X = Cl$  but are endothermic and can be neglected for  $X = Br$ . For the corresponding XO radicals, the Cl-O bond strength is about  $8 \text{ kcal mole}^{-1}$  stronger than the Br-O bond strength with the result that the  $ClO + ClO$  reaction is much slower than the  $BrO + BrO$  reaction. For this reason, and because BrO is expected to be the dominant form of  $BrO_x$  in the stratosphere (Yung *et al.*, 1980), the  $BrO + BrO$  reaction takes on particular importance in the stratosphere despite the relatively low  $BrO_x$  mixing ratio.

Since the review and modelling study of Yung *et al.* (1980), relatively few changes have occurred in the kinetics data base for BrO reactions. Most of the work on BrO<sub>x</sub> has focused on the hydrogen abstraction reactions of Br including Br + HO<sub>2</sub> and Br + H<sub>2</sub>CO, and on the OH + HBr reaction. Two recent studies seem to indicate that the reaction



is much slower than previously thought. While initial estimates based on the Cl + HO<sub>2</sub> reaction (Yung *et al.*, 1980) placed  $k_{47}$  at  $2 \times 10^{-11} \text{ cm}^3 \text{ molecule}^{-1} \text{ s}^{-1}$ , studies by Posey *et al.* (1981) and Poulet *et al.* (1984) resulted in values of 2.2 and  $7.6 \times 10^{-13} \text{ cm}^3 \text{ molecule}^{-1} \text{ s}^{-1}$ , respectively. Additional work on this reaction is needed. The data base for the reaction



is somewhat more consistent, with a value for  $k_{48}$  near  $1 \times 10^{-12} \text{ cm}^3 \text{ molecule}^{-1} \text{ s}^{-1}$  at 298 K being obtained by both Nava *et al.* (1981) and Poulet *et al.* (1981).

Recent work on the reaction



has yielded somewhat inconsistent results with values of  $k_{49}$  ranging from 6.0 to  $11.7 \times 10^{-12} \text{ cm}^3 \text{ molecule}^{-1} \text{ s}^{-1}$  at 298 K being obtained. While some of the variation may be due to imprecise measurement of the excess reagent, HBr, as in the case of the OH + HCl reaction, most of the recent studies seem to lie near the high end of the range. While the results of recent work on reactions 47 - 49 have been at odds with estimates made in early modelling studies, the impact on predictions of ozone depletion has been minor.

The status of the data base for reactions of BrO with O, NO, NO<sub>2</sub>, BrO and ClO remains essentially the same with kinetic data still lacking on the BrO + HO<sub>2</sub> and BrO + OH reactions. Of this group, the reactions



are still key steps in the odd-oxygen catalytic destruction cycle involving bromine in the lower stratosphere. This is the case despite recent changes in model predictions which have significantly lowered the ClO mixing ratio below 35 km in better agreement with observations. The temperature dependences of the rate coefficient and product distributions for this reaction are still highly uncertain and require additional work. In addition, because the catalytic cycle involving reaction (50) has diminished in importance, the reactions



and



## STRATOSPHERIC CHEMISTRY

have assumed a more significant role in the cycling of BrO to Br and should therefore be given added scrutiny. The possible role of a Br<sub>2</sub>O<sub>2</sub> adduct in the BrO + BrO reactions at lower stratospheric temperature should also be investigated.

### 2.1.6 Sulfur Chemistry

Our current understanding of sulfur chemistry suggests that the only sulfur compound that is not completely degraded in the troposphere and hence can be transported into the stratosphere is COS. In addition various sulfur compounds (including SO<sub>2</sub>) can be directly injected into the stratosphere during volcanic eruptions. The current data base suggests that the main fate of sulfur in the stratosphere is the conversion to sulfuric acid aerosols. There are possible catalytic cycles involving the HS radical which could affect the ozone concentration (Friedl *et al.*, 1985). However, our overall understanding of HS and HSO chemistry is limited and, in addition, there are no proven sources of significance for HS in the stratosphere.

Details of the oxidation of SO<sub>2</sub> to H<sub>2</sub>SO<sub>4</sub> in the homogeneous gas phase are not completely understood. However, recent work by Stockwell and Calvert (1983), Margitan (1984b) and Bando and Howard (1985 private communication) have shown that the reaction of OH with SO<sub>2</sub> followed by the reaction of the adduct with O<sub>2</sub> leads to the formation of SO<sub>3</sub> at 298 K. The possibility of HSO<sub>3</sub> adding to O<sub>2</sub> at low temperatures needs to be assessed. SO<sub>3</sub> is believed to react very rapidly with H<sub>2</sub>O to form H<sub>2</sub>OSO<sub>3</sub> which in turn isomerizes to H<sub>2</sub>SO<sub>4</sub> (Hoffman-Sievert and Castleman (1984)). The rate of SO<sub>3</sub> reaction with H<sub>2</sub>O to form H<sub>2</sub>SO<sub>4</sub> under stratospheric conditions of temperature, pressure, and H<sub>2</sub>O concentrations must be firmly established. If the rate of this gas to particle conversion reaction is too slow under those conditions, the possibility of SO<sub>3</sub> uptake by existing aerosols and the photochemistry of SO<sub>3</sub> need to be studied.

The main fate of COS in the stratosphere is photolysis and reaction with O(<sup>3</sup>P), and the rates of these processes are reasonably well known. Recent laboratory studies have shown that CS<sub>2</sub> will be oxidized in the troposphere leading to COS (Jones *et al.* (1982)), Barnes *et al.* (1983), Wine and Ravinshankara (1982) and Wine *et al.* (1985).

Currently, there is a large research effort underway to understand tropospheric sulfur chemistry. This effort will, undoubtedly, provide a great deal more information on stratospheric sulfur chemistry.

### 2.1.7 Hydrocarbon Oxidation Chemistry

Hydrocarbon oxidation represents a particular sub-set of atmospheric chemistry, which is closely coupled to all other reactive trace gas species (O<sub>x</sub>, HO<sub>x</sub>, NO<sub>x</sub>, ClO<sub>x</sub>) and hence to O<sub>3</sub> photochemistry. CH<sub>4</sub> is the dominant hydrocarbon in the stratosphere and its primary role is the production of H<sub>2</sub>O from its oxidation and the conversion of active ClO<sub>x</sub> to inactive HCl via reaction (36). The role of higher hydrocarbons, i.e., C<sub>2</sub>H<sub>6</sub>, C<sub>3</sub>H<sub>8</sub>, C<sub>2</sub>H<sub>4</sub>, C<sub>2</sub>H<sub>2</sub> etc., in the stratosphere is mainly as an additional sink for active chlorine. They can also be used as tracers to test the transport and chemistry used in current atmospheric models. Our present knowledge of CH<sub>4</sub> oxidation chemistry is illustrated in Figure 2-1. The dominant sink for CH<sub>4</sub> is reaction with OH



The CH<sub>3</sub> radical product is further oxidized to CO<sub>2</sub> through the intermediate products; CH<sub>3</sub>O<sub>2</sub>, CH<sub>3</sub>O, HCHO and CO.

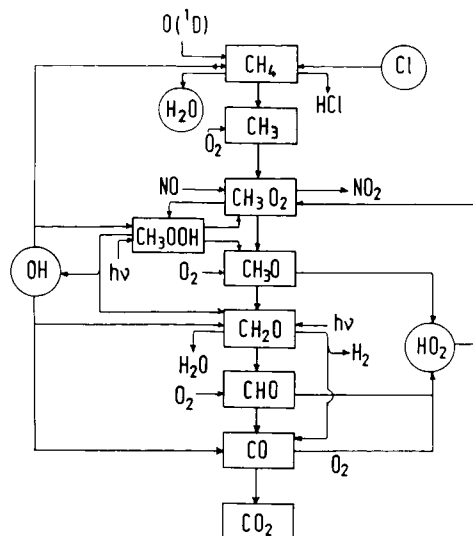
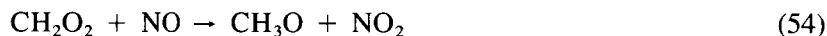
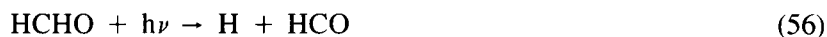


Figure 2-1. Atmospheric Methane Oxidation Scheme

For the stratosphere below 35 km the oxidation scheme is simplified by the presence of sufficient NO for complete conversion of the peroxy radicals by reaction with NO. This makes  $\text{CH}_4$  oxidation a net source of  $\text{O}_x$  through the reactions:



This scheme is also a source of  $\text{HO}_x$  through the photolysis of formaldehyde formed by oxidation of  $\text{CH}_3\text{O}$ :



The rate data for these reactions are all reasonably well established, the remaining uncertainties being in the rates of (55) (56) and (57). For the stratosphere the contributions of this source to the total  $\text{O}_3$  budget is minor.

The final reaction of the methane oxidation chain,  $\text{OH} + \text{CO} \rightarrow \text{CO}_2 + \text{H}$ , is known to show a complex dependence on pressure and temperature. In view of the importance of this reaction at all altitudes further studies, particularly of the temperature dependence at high and low pressures, are needed.

The higher hydrocarbons are removed by reaction with OH and Cl. The rate coefficients are well established for the saturated hydrocarbons, but are more uncertain for the unsaturated species, due to the

## STRATOSPHERIC CHEMISTRY

complexities of the reactions. No significant effect, however, is to be expected from such uncertainties for stratospheric ozone perturbations. The mechanism of non-methane hydrocarbon oxidation is discussed in detail in Chapter 4.

CH<sub>3</sub>CN and HCN have been observed in the atmosphere up to 50 km (Arijs *et al.*, 1982). If they are oxidized instead of being physically removed, these molecules could be minor sources of NO<sub>x</sub> (Cicerone and Zellner, 1983). Details of the oxidation pathways are not well known and studies aimed at elucidating the chemistry of these species in the stratosphere are needed.

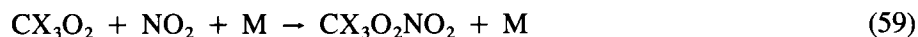
### 2.1.8 Halocarbon Oxidation Chemistry

Halocarbons are oxidized in the stratosphere in a sequence of radical reactions initiated by the photolysis of the molecule or by its reaction with O(<sup>1</sup>D) atoms. The oxidation mechanism of chlorofluoromethanes has been established by laboratory photooxidation studies and was described in detail in the review by Simonaitis (1980). The kinetics of the elementary reactions involved in the oxidation mechanism were not known until recently and it has been generally assumed in model calculations that all the chlorine atoms of the molecule were released simultaneously in the atmosphere with a negligible delay following the initial photolysis or O(<sup>1</sup>D) attack. The new data provide further information on the reaction mechanism prevailing in the stratosphere and reveal the possibility of the formation of reservoir species.

The chlorofluoromethyl radical initially produced by the photolysis of CFMs or by their reactions with O(<sup>1</sup>D) atoms, combines rapidly with oxygen to form the peroxy radical CX<sub>3</sub>O<sub>2</sub> (X = F or Cl). Under stratospheric conditions this radical reacts principally with NO in the fast reaction (Dognon *et al.*, 1985):



However, in contrast to the CH<sub>3</sub>O<sub>2</sub> radical, the combination of the CX<sub>3</sub>O<sub>2</sub> radical with NO<sub>2</sub>



is fast enough at the low stratospheric temperatures and pressures (Lesclaux and Caralp, 1984) to form the peroxyxynitrate to a significant extent. Unlike CH<sub>3</sub>O<sub>2</sub>NO<sub>2</sub>, the halogenated peroxyxynitrates may act as a temporary reservoir for ClO<sub>x</sub> and NO<sub>x</sub> in the lower stratosphere.

The peroxyxynitrates are thermally stable in the stratosphere (Simonaitis 1980). Therefore, the photolysis rate is the principal factor which determines their lifetime. Morel *et al.* (1980) have measured the absorption spectra of CCl<sub>3</sub>O<sub>2</sub>NO<sub>2</sub> and CFCI<sub>2</sub>O<sub>2</sub>NO<sub>2</sub> which have similar features to those of HO<sub>2</sub>NO<sub>2</sub> and CH<sub>3</sub>O<sub>2</sub>NO<sub>2</sub>. However the cross section values at the longest wavelength of measurements (270-280 nm) seem significantly lower for the halogenated compounds. Therefore, the photolysis rates may be low enough to make it possible to consider these compounds as potential reservoirs for ClO<sub>x</sub> and NO<sub>x</sub> particularly in winter and at high latitudes. An approximate calculation indicates that the ClO<sub>x</sub> concentration should not be affected by more than a few percent. However, more accurate cross section measurements are needed in the critical wavelength region 290-320 nm and the temperature dependence of the reaction rate for CX<sub>3</sub>O<sub>2</sub> + NO<sub>2</sub> + M should be determined.

The chlorofluoromethoxy radicals CX<sub>2</sub>ClO are thought to decompose rapidly into CX<sub>2</sub>O + Cl, even at the low stratospheric temperature (Rayez *et al.*, 1983). However, an experimental confirmation is necessary.

The remaining chlorine atoms are released by photolysis of the intermediate products, CFCIO and CCl<sub>2</sub>O (phosgene) or their reaction with O(<sup>1</sup>D). These compounds have fairly low absorption cross sections resulting in low photolysis rates and this should be taken into account in stratospheric modelling. Preliminary calculations have shown that the stratospheric ClO<sub>x</sub> concentration is a few percent lower than when the simplified treatment is applied. Moreover, a possible gas phase reaction of phosgene with water may be envisaged since this compound undergoes hydrolysis in the presence of liquid water.

Halogenated hydrocarbons such as CH<sub>3</sub>Cl, CH<sub>3</sub>CCl<sub>3</sub>, etc. can be oxidized in the troposphere by reaction with OH. However, this reaction is relatively slow for most of these compounds and consequently, their input in the stratosphere is important. The oxidation of CH<sub>3</sub>Cl, initiated by reaction with OH, results in the formation of CHClO (Sanhueza and Heicklen 1975). The photolysis and the reactions of this compound should be taken into account.

The industrial production of methyl chloroform and CF<sub>3</sub>Br is increasing. The oxidation chemistry of these species is not well understood and further studies are required.

## 2.2 SPECIAL ISSUES IN STRATOSPHERIC CHEMISTRY

### 2.2.1 Role of Reactions Involving Sodium Species

Meteors are the source of several metallic elements in the upper atmosphere, by far the most important being sodium. The concentration profile of free sodium, which resides mainly in the mesosphere, has been measured. (Megie, Blamont, 1977). However, very little is known about the stratospheric chemistry of sodium. Recent investigations have shown that sodium and sodium compounds are very reactive. Oxides of sodium, unlike many other atmospheric metallic oxides, regenerate atomic sodium and react with many stratospheric constituents. Therefore, the possibility exists for sodium to have a role in chemistry controlling ozone. The current data base is not sufficient to carry out a complete modelling study of the homogeneous gas phase photochemistry of sodium in the stratosphere. However, the total concentration of free sodium in the stratosphere is extremely small. Therefore, it is unlikely that free sodium catalyzed ozone destruction can contribute significantly to the total ozone destruction rate.

One possible role that sodium compounds may play in the stratosphere is to release Cl from HCl augmenting the OH + HCl reaction. Many compounds of sodium (NaOH, NaO<sub>2</sub>, and NaO) react rapidly with HCl to form NaCl. (Silver *et al.*, 1984a, 1984b). If NaCl is rapidly photolyzed, a catalytic chain for the conversion of HCl to Cl may be possible. e.g.



The photolysis of NaCl is expected to be rapid in the upper stratosphere but there is some uncertainty in the photolysis rate at longer UV wavelengths, which would be necessary for release of the active species

## STRATOSPHERIC CHEMISTRY

and completion of the catalytic cycle at lower altitudes (Rowland and Rogers, 1982). Further uncertainty arises from the lack of knowledge of the rate of gas to particle conversion of gaseous sodium compounds in the stratosphere.

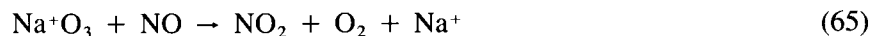
Clusters containing sodium compounds such as NaOH, NaO<sub>2</sub>, and NaO can scavenge stratospheric acids and oxides such as HNO<sub>3</sub>, HCl, NO<sub>2</sub>, and N<sub>2</sub>O<sub>5</sub>. However, the estimated amount of sodium compounds in the stratosphere is too small for scavenging to be important.

### 2.2.2 Ion Chemistry

Over the last few decades, considerable effort has been expended in the understanding of mechanisms by which ions can affect the stratospheric ozone budget. As a result it is clear that ion chemistry is not important for the ozone budget. However recent work has shown that useful measurements of neutral species can be made through their interaction with atmospheric ions. With the exception of the rare solar proton events, the ion production rate in the upper stratosphere is relatively small, ranging from 10-50 ion pairs/cm<sup>3</sup>/s at 100 km to 0.1 ion pairs/cm<sup>3</sup>/s at 50 km. With this small ion input, and the relatively rapid ion recombination rates only the most efficient catalytic processes would be expected to be important. No such catalytic processes involving ions have been identified to date.

Direct ionization processes are now known to produce hydrated ion clusters which are relatively stable. Nascent positive ions, primarily N<sub>2</sub><sup>+</sup> and O<sub>2</sub><sup>+</sup> rapidly form proton hydrates H<sub>3</sub>O<sup>+</sup> (H<sub>2</sub>O)<sub>n</sub>, with a net input of two odd hydrogen molecules per ion. Similarly, electrons resulting from ionization events form hydrates of the nitrate ion, NO<sub>3</sub><sup>-</sup> eventually resulting in nitric acid clusters. Both positive and negative ion clusters are stable towards reaction with most neutral species. However, such clustering processes form a sensitive basis for the stratospheric measurement of species such as NH<sub>3</sub>, CH<sub>3</sub>OH, HNO<sub>3</sub>, H<sub>2</sub>SO<sub>4</sub> and gas-phase sodium compounds using *in situ* mass spectrometry. (Arnold, 1984; Arijs *et al.*, 1982). Determination of absolute concentration by this method assumes local equilibrium between the ions and the cluster and requires a knowledge of the equilibrium constant.

Positive and negative ion concentrations in the stratosphere are of the order of 10<sup>3</sup>cm<sup>-3</sup>. Their lifetime is determined by mutual recombination and is typically approximately 10<sup>3</sup>s. While ions may recombine to form odd nitrogen species (HNO<sub>3</sub>) the limiting rate of a few cm<sup>-3</sup>s<sup>-1</sup> is negligible. Because these rates are so small, catalytic processes must be invoked for ion chemistry to significantly perturb the stratosphere. It is known that small ions can greatly enhance neutral reactions as, for example,



is four orders of magnitude faster at 250 K than the gas-phase reaction of O<sub>3</sub> with NO, and since the Na<sup>+</sup> is not removed the reaction is catalytic (Rowe *et al.*, 1982). The reaction of N<sub>2</sub>O<sub>5</sub> with NO is over nine orders of magnitude faster when N<sub>2</sub>O<sub>5</sub> is clustered to Li<sup>+</sup>. However, the effect decreases with ion size and there are no small ions in the stratosphere.

A reaction which was examined in great detail because of its potential impact is



No reaction was found with any ion X±(H<sub>2</sub>O) which is present in significant concentrations in the stratosphere (Bohringer *et al.*, 1983).

Some years ago it was proposed (Ruderman *et al.*, 1976) that the reaction



might destroy stratospheric ozone and thus account for a solar cycle variation in ozone, since there is a solar cycle variation in the galactic cosmic ionization rate. However, unsolvated  $\text{NO}_3^-$  is not a stratospheric ion, and in any case reaction (67) is slow ( $k < 10^{-13} \text{ cm}^3 \text{ s}^{-1}$ ) (Fehsenfeld *et al.*, 1976).

In summary, the stratospheric production rate of  $\text{HO}_x$  and  $\text{NO}_x$  from ionic processes is negligible due to the low production rate of ions. Moreover, efficient catalytic cycles for odd oxygen destruction involving ions have not yet been found.

### 2.2.3 Homogeneous Reactions Between Temporary Reservoir Species

The principal temporary reservoir species involved in stratospheric  $\text{HO}_x$ ,  $\text{NO}_x$  and  $\text{ClO}_x$  chemistry are shown in Table 2-1. These species serve to 'tie up' active radicals which would otherwise be involved in catalytic odd oxygen destruction (or production) cycles. Some species act as reservoir for two active types e.g.,  $\text{HNO}_3$  and  $\text{ClONO}_2$  act as reservoirs for  $\text{HO}_x$  and  $\text{ClO}_x$  respectively as well as  $\text{NO}_x$ . A common feature of these temporary reservoir species is that they are closed shell molecules and therefore their reactivity towards each other is generally expected to be much less than with atomic or radical species. However, concentrations of reservoir species can exceed those of active species by several orders of magnitude and consequently slow reactions between them may need to be considered because of the important consequences if active species are regenerated or more stable species are formed. For example the reaction of water with  $\text{N}_2\text{O}_5$  serves to release active  $\text{NO}_x$  species ( $\text{NO}_2$ ) and also provide a source of OH from  $\text{H}_2\text{O}$  through the reactions



The source of OH in the lower stratosphere would be comparable in magnitude to the reaction of  $\text{O}(^1\text{D})$  with water if the bimolecular rate coefficient for reaction of  $\text{H}_2\text{O}$  with  $\text{N}_2\text{O}_5$  was of the order of  $10^{-20}$

**Table 2-1.** Reservoir Species for Active  $\text{HO}_x$ ,  $\text{NO}_x$  and  $\text{ClO}_x$  Radicals in the Stratosphere

Family	Reservoir Species
$\text{HO}_x$	$\text{H}_2\text{O}$ , $\text{H}_2\text{O}_2$ $\text{HNO}_3$ , $\text{HO}_2\text{NO}_2$ , HONO
$\text{NO}_x$	$\text{N}_2\text{O}_5$ $\text{ClONO}_2$
$\text{ClO}_x$	HCl HOCl

## STRATOSPHERIC CHEMISTRY

$\text{cm}^3 \text{ molecule}^{-1} \text{ s}^{-1}$ . (Dak Sze, 1984). The upper limit room temperature value of  $k_{68} \leq 2 \times 10^{-21}$  is a factor of 5 lower than this, but measurement of such small rate coefficients presents considerable problems and there have been very few systematic studies of the kinetics and temperature dependencies of these slow reactions. Moreover the study of slow reactions in the gas phase is often complicated by heterogeneous reactions which may or may not have atmospheric significance (see Section 2.2.4).

Recently attention has been focussed on the reaction of chlorine nitrate with HCl, which has been known for some time to occur rapidly in laboratory gas and liquid phase reaction systems. Whilst a rationale can be made for a rapid reaction between these two species (Schmeisser and Brandle, 1961), the emerging consensus today is for a very slow bimolecular gas phase reaction (Molina *et al.*, 1985). However, a surface reaction occurs to produce  $\text{HNO}_3$  and  $\text{Cl}_2$  as products. Any impact of this reaction on stratospheric chemistry would be through the occurrence of the latter process.

The gas phase reactions of ozone with stable molecules has also to be considered in view of the relatively high concentrations of ozone in the mid stratosphere. Of particular interest is the reaction of ozone with water vapor via the exothermic pathway to yield hydrogen peroxide:



Subsequent photolysis of  $\text{H}_2\text{O}_2$  from this reaction would provide a significant source of OH even with a rate constant as low as  $10^{-23} \text{ cm}^3 \text{ molecule}^{-1} \text{ s}^{-1}$ . There are no data on the kinetics of this reaction.

A summary of the slow reactions involving temporary reservoirs which are potentially important for atmospheric chemistry is given in Table 2-2. The Table shows minimum values for the rate constants of these reactions that would be required to give significant effects on species distribution in the stratosphere, according to calculations with a 1D model using current chemistry. (Dak Sze, 1984). These rate constants are mostly approximately equal to or above the upper limit values that have been reported at room temperature.

### 2.2.4 Heterogeneous Reactions

The possibility that heterogeneous reactions involving trace species on the surface of atmospheric aerosol particles has been a subject of discussion for some time (Cadle *et al.*, 1975).

Aerosol particles are present in the stratosphere and are concentrated mainly in a layer centered at around 25 km altitude. They consist mainly of aqueous sulphuric acid (approximately 75% w/w  $\text{H}_2\text{SO}_4$ ) and originate from direct volcanic injection of sulphuric acid and from oxidation of sulphur-containing gases from both volcanic and other sources, e.g., COS. In the troposphere aerosol particles are widely distributed but the composition is very variable and depends on location.

The presence of aerosol particles can potentially impact on stratospheric ozone in several ways through gas surface interactions e.g., production and removal of active radical species, surface catalysis of chemical reactions and surface photochemical effects. The aerosol question now assumes more relevance in view of the 1982 eruption of the El Chichon volcano, which evidently increased the stratospheric aerosol loading by approximately an order of magnitude. There are other conditions in the stratosphere, for example polar high altitude clouds, which may provide potential heterogeneous chemistry effects.

**Table 2-2.** Minimum Values of Rate Coefficients for Significant Role of Homogeneous and Heterogeneous Reactions Involving Temporary Reservoir Species

Reaction	$k_{bi}$ (min) $\text{cm}^3\text{molec}^{-1}\text{sec}^{-1}$	$\gamma^*$ min.
**1. $\text{ClONO}_2 + \text{H}_2\text{O} \rightarrow \text{HOCl} + \text{HNO}_3$	$10^{-19}$	$5 \times 10^{-3}$
2. $\text{N}_2\text{O}_5 + \text{H}_2\text{O} \rightarrow 2\text{HNO}_3$	$10^{-20}$	$5 \times 10^{-4}$
3. $\text{HO}_2\text{NO}_2 + \text{H}_2\text{O} \rightarrow \text{HNO}_3 + \text{H}_2\text{O}_2$	$10^{-19}$	$5 \times 10^{-3}$
4. $\text{O}_3 + \text{H}_2\text{O} \rightarrow \text{H}_2\text{O}_2 + \text{O}_2$	$10^{-23}$	$1 \times 10^{-6}$
**5. $\text{HCl} + \text{ClONO}_2 \rightarrow \text{Cl}_2 + \text{HNO}_3$	$5 \times 10^{-17}$	$5 \times 10^{-4}$
**6. $\text{ClO} + \text{HO}_2\text{NO}_2 \rightarrow \text{HOCl} + \text{NO}_2 + \text{O}_2$	$5 \times 10^{-15}$	—
7. $\text{H}_2\text{O}_2 + \text{HNO}_3 \rightarrow \text{HO}_2\text{NO}_2 + \text{H}_2\text{O}$	$5 \times 10^{-15}$	$5 \times 10^{-3}$

\* In deriving  $\gamma(\text{min})$ , we assume that an air molecule collides with stratospheric aerosol about once in every  $10^4$  seconds.

\*\* The required  $k_{bi}(\text{min})$  and  $\gamma(\text{min})$  for the chlorine reactions (1), (5) and (6) may be lowered by an order of magnitude if the stratospheric ClX were to exceed 15 ppb.

The rate of removal or reaction of molecular species on the surface of aerosol particles is generally expressed in terms of the effective first order rate constant calculated from the product  $\gamma Z_s$  where  $Z_s$  is the collision frequency of gas molecules with the surface and  $\gamma$  the fraction of those collisions which lead to reaction. For the surface area corresponding to typical mid stratosphere aerosol  $Z_s$  is typically of the order  $10^{-4}$  to  $10^{-5} \text{ s}^{-1}$ . Most gas phase reactions of active species occur with much greater frequency. Thus even with unit efficiency for reaction at the surface, the heterogeneous reaction cannot be important in determining local partitioning of active species. Experimental studies indicate that  $\gamma$  values are normally in the range  $10^{-3}$  to  $10^{-5}$ , even for such active species as Cl, ClO (Martin *et al.*, 1980) and OH (Baldwin and Golden 1979), on sulphuric acid and other surfaces. It is concluded that for fast reacting radicals like Cl and OH, heterogeneous removal does not provide a significant sink. For slower reacting radicals such as ClO and perhaps  $\text{HO}_2$ , small perturbations on radical density may result from heterogeneous removal at high aerosol concentrations following volcanic eruptions. This process would compete with the slower processes by which active radicals are converted to reservoir species.

Heterogeneous effects are most likely to be significant for the slow reactions involving temporary reservoir species, particularly in their reactions with water which is present in the aerosol. For example the reaction of  $\text{N}_2\text{O}_5$  with water can occur on surfaces and if  $\text{HNO}_3$  were formed in  $\text{N}_2\text{O}_5$  and aerosol interactions with  $\gamma = 5 \times 10^{-4}$  this would have significant consequences for the  $\text{HO}_x$  budget in the lower stratosphere. This rate would be equivalent to a homogeneous bimolecular rate constant for the  $\text{N}_2\text{O}_5 + \text{H}_2\text{O}$  reaction of  $1 \times 10^{-20} \text{ cm}^3 \text{ molecule}^{-1} \text{ s}^{-1}$ .

The experimental data base at the present time does not allow identification of those reactions of stratospheric importance which can be catalyzed in this way and which are not. Moreover little is known about the  $\gamma$  values for the molecular species of interest,  $\text{N}_2\text{O}_5$ ,  $\text{ClONO}_2$ ,  $\text{HO}_2\text{NO}_2$  etc. In Table 2-2 are listed the  $\gamma$  values required to give a significant effect on the distribution of stratospheric species involved in the ozone budget, for those reactions between temporary reservoir species which are identified as potentially

## STRATOSPHERIC CHEMISTRY

significant in the stratosphere. In calculating the reaction rates it is assumed that the reaction partner present at higher concentration, is in sufficient excess for the overall removal of the minor reactant to follow pseudo first order kinetics.

The influence of surface adsorption on the visible and ultraviolet spectra of absorbed molecules has been considered in some detail in connection with the photodegradation of chlorofluoromethanes. Since these gases do not absorb at wavelengths above 300 nm they are not removed by direct photodissociation in the troposphere. However there is evidence that the electronic absorption spectra of molecules absorbed on surfaces may be red shifted in a similar way to electronic spectra in the liquid phase. Laboratory experiments have indicated that photodecomposition of these compounds by near UV radiation can occur in the presence of desert sand and other similar materials. (Ausloos *et al.*, 1977). No quantitative estimate of the rate of this process based on laboratory studies can be made at the present time. Due to the small surface area in the atmosphere, the fraction of any particular trace gas that is absorbed on the particles at a given time is extremely small. Thus an extremely large red-shift in the absorption spectrum would be required to give a significant effect. Indeed there is strong evidence from atmospheric measurements of chlorofluoromethanes that this process is of negligible importance as a sink for organochlorine species in the atmosphere.

The effect of light on the surface reaction efficiency parameter,  $\gamma$  has also been considered. Laboratory studies have shown that simulated sunlight has no effect on the heterogeneous reactivities of Cl and ClO (Martin *et al.*, 1980). There is no experimental information relating to this effect in the surface reaction of the temporary reservoir species.

In assessing the current evidence relating to the question whether or not aerosols perturb the homogeneous chemistry related to stratospheric ozone, it can be concluded that the effects are minor and are unlikely to change our overall picture of the chemistry of the stratosphere. Some modification of our detailed formulation of the behavior of temporary reservoir species may result from further characterization of their heterogeneous reactions in the laboratory. Local effects resulting from volcanic injections may be considerably more significant. Detection and understanding these effects is difficult, firstly, because the available baseline information does not allow unambiguous assignment of a given observation to the presence of enhanced aerosol loading and secondly the effects are expected to be subtle and of small magnitude.

### 2.2.5 Reactions with Complex Temperature and Pressure Functions

One outcome of the intensive research effort in stratospheric chemical kinetics has been the discovery that many radical-radical and radical-molecule reactions do not obey classical pressure and temperature behavior, i.e., positive Arrhenius activation energies and pressure-independent rate coefficients for bimolecular reactions. This departure from classical behavior can be explained by the absence of large (5 kcal mole<sup>-1</sup> or greater) energy barriers for these reactions and the presence of local minima in the potential energy surface which correspond to metastable reaction intermediates. In general, rate coefficients for reactions of this type decrease with increasing temperature and, over the limited temperature range encountered in the atmosphere, obey Arrhenius-type behavior, i.e.,

$$k(T) = A \exp(-E_a/RT)$$

where  $E_a$ , the Arrhenius activation energy, is negative. However, there are now several examples of reactions which show pronounced non-Arrhenius behavior and others which manifest unusual pressure and temperature behavior suggestive of more complex mechanisms. One objective of current research in reac-

tion rate theory is to express such behavior in a general analytical form which is suitable for use in atmospheric models.

There are four reactions of particular interest which show unusual pressure and temperature dependence behavior over atmospheric pressure and temperature conditions. These are:



While data on several of these reactions are incomplete, their experimentally observed rate coefficients can be expressed as a sum of pressure-dependent and pressure independent terms,

$$k_{\text{obsd}}([\text{M}], T) = k_{\text{II}}(T) + k_{\text{III}}(T)[\text{M}]$$

where  $k_{\text{II}}(T)$  = bimolecular component (zero-pressure intercept),  $k_{\text{III}}(T)$  = termolecular component and  $[\text{M}]$  = bath gas density. This empirical expression has a term which is directly proportional to  $[\text{M}]$  but falloff behavior is expected at higher pressures.

Table 2-3 summarizes the existing measurements of the bimolecular and termolecular components for these reactions. These reactions all have zero or negative values of E/R. For reactions 14, 30 and 71, the A-factors for the bimolecular component are considerably smaller than those expected for simple atom-transfer processes. Both of these observations are strongly suggestive of complex reaction behavior.

Considerable effort has been devoted to the understanding of these reactions and an explanation for their unusual pressure and temperature dependence is emerging (Just and Troe, 1980; Mozurkewich and Benson, 1984; Patrick, *et al.*, 1984; Kircher and Sander, 1984). Reactions such as the ones discussed

**Table 2-3.** A-factors and temperature dependence for bimolecular and termolecular components of reactions showing unusual behavior

Reaction	A*	$k_{\text{II}}$	E/R	A**	$k_{\text{III}}$	E/R
OH + HO <sub>2</sub>	$1.7 \times 10^{-11}$		-416	$3.0 \times 10^{-31}$		-500
OH + HNO <sub>3</sub>	$7.2 \times 10^{-15}$		-785	$1.9 \times 10^{-33}$		-725
OH + CO	$1.5 \times 10^{-13}$		0	$3.6 \times 10^{-33}$		?
HO <sub>2</sub> + HO <sub>2</sub>	$2.3 \times 10^{-13}$		-590	$1.7 \times 10^{-33}$		-1000

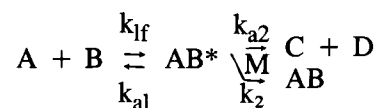
\* Units are cm<sup>3</sup> molecule<sup>-1</sup> s<sup>-1</sup>

\*\* Units are cm<sup>6</sup> molecule<sup>-2</sup> s<sup>-1</sup>, values are for M = N<sub>2</sub>

+ termolecular parameters are valid for  $[\text{M}] < 1 \times 10^{18}$  molecules cm<sup>-3</sup>, T > 260K.

## STRATOSPHERIC CHEMISTRY

above are believed to proceed through a bound intermediate having a sufficiently long lifetime to undergo collisional quenching. The reaction scheme may be written,



The overall rate constant may be divided into bimolecular and termolecular components under conditions where  $k_2[M] \ll k_{a1} + k_{a2}$ :

$$k_{\text{obsd}} = \frac{k_{1f}k_{a2}}{k_{a1} + k_{a2}} + \frac{k_{1f}k_2}{k_{a1} + k_{a2}} [M] \quad (\text{I})$$

Equation I has the correct functional form to describe the pressure dependence for most of these reactions. However, attempts to apply this theory at a detailed level to reactions of this kind have revealed inconsistencies which may point to a possible incompleteness in the model. Also the pressure dependence of the OH + HNO<sub>3</sub> reaction is not consistent with the form of equation I (NASA, 1985). Furthermore there is as yet no way to predict for which reactions we should expect complex  $k(p,T)$  behavior for conditions relevant to the atmosphere.

The stability of the complexes involved is not well known but is probably of the order of 10 kcal mol<sup>-1</sup>, implying that they decompose rather rapidly and do not undergo reactions with other species leading to new chemical pathways. A possible exception is HOCO, which probably reacts with O<sub>2</sub> to give CO<sub>2</sub> + HO<sub>2</sub>, the same products as for the "low pressure" bimolecular channel in the atmosphere.

Other familiar reactions such as the termolecular association reactions are special cases of this model, having only the collisional deactivation channel open ( $k_{a2} = 0$ ). Familiar "bimolecular" reactions such as NO + XO (X = F, Cl, Br, I), O + OH, N + NO and perhaps HO<sub>2</sub> + NO also proceed via intermediate bound complexes, but show no pressure dependence in the 0-1 atm pressure range because of the relatively short lifetime of the complex ( $k_{a1} + k_{a2} \gg k_2[M]$ ). These reactions would nevertheless be expected to exhibit a pressure dependence at sufficiently high pressure.

### 2.2.6 General Comments on Photodissociation Processes

The solar flux penetrating the stratosphere consists mainly of radiation with wavelength greater than 290 nm with a small amount of radiation in the 200 nm window. This short wavelength radiation is absorbed mainly by the small molecules with large atmospheric abundance such as O<sub>2</sub> and O<sub>3</sub> but is also important for the photolysis of halocarbons. The longer wavelength radiation is important for photolysis of the larger polyatomic species. The features responsible for absorption by polyatomic species in this region and the halocarbons near 200 nm are mainly the tails of absorption bands. Thus the absorption cross sections in this wavelength region may be dependent on temperature. To date, however, the majority of the absorption cross section measurements have been carried out at 298 K. Therefore, it is necessary to measure absorption cross sections at stratospheric temperatures particularly for molecules such as HNO<sub>3</sub>, ClONO<sub>2</sub> and HO<sub>2</sub>NO<sub>2</sub>. It is worth noting that these molecules are hard to manipulate in the laboratory. In general, the cross section measurements have not received the amount of attention commensurate with their importance.

It is assumed that the quantum yield for dissociation of the absorbing molecule is unity if its absorption spectrum is a continuum. It is necessary to confirm this assumption at least for important molecules such as  $\text{HNO}_3$  whose primary atmospheric degradation pathway is photolysis. The quantum yield measurements usually are not completely decoupled from the absorption cross section measurements. Consequently, in many instances the product of these two quantities ( $\sigma \times \Phi$ ) is better known than the individual quantities. In general, quantum yields for product formation have not been measured at the appropriate wavelengths, pressures, and temperatures for the atmosphere. In many cases, it is often assumed that the weakest bond breaks, but there are many known exceptions to this assumption; for example  $\text{ClONO}_2$  photolysis yields  $\text{Cl} + \text{NO}_3$  (Margitan, 1984a) rather than  $\text{ClO} + \text{NO}_2$  as was previously assumed. For the important species, the quantum yield for minor products must also be measured.

### 2.2.7 Errors and Uncertainties in Kinetic and Photochemical Data

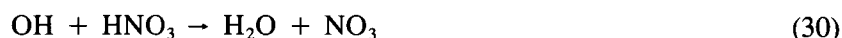
The uncertainties in the chemical and photochemical rate parameters and in the mechanisms involved in the atmospheric chemistry are one of the major factors in limiting the accuracy of model calculations of species concentration and ozone perturbations in the atmosphere. Most of the changes in the predicted ozone depletion due to chlorofluoromethanes that have occurred in recent years have resulted from changes in the values of kinetic parameters used in model calculations.

The uncertainty in the kinetic parameters for the key atmospheric reactions has been reduced greatly over the last 10-15 years due mainly to the rapid development of the techniques used for the direct measurement of radical species in the gas phase and for investigation of their reaction kinetics. Whereas 20 years ago the rates of most radical-molecule reactions were only known to within a factor of 10, today the room temperature rate constants of atmospherically important reactions of this type can be measured within an accuracy of  $\pm 10\%$ . Moreover the number of reactions for which good kinetic data are available have increased tremendously. The consistency in the experimental measurements gives confidence in the data base. There remain problems in reaction rate theory which is not able to explain some of the observed temperature and pressure dependencies. Although there is improved reliability of the data it should be recognized that the errors in the rate coefficients increase as the temperature diverges from room temperature and that certain reactions e.g., radical + radical reactions are intrinsically more difficult to study and consequently are always likely to carry more uncertainty than straightforward radical + molecule reactions.

Difficulties also arise in the study of very slow reactions between radicals and molecules, due to complications such as those arising from heterogeneous effects.

The uncertainty in the rate coefficients for atmospheric reactions results primarily from systematic errors arising from the chemical systems and the techniques used for their determination rather than measurement error of a statistical nature. Consequently it is not straightforward to assign uncertainties to preferred values given in an evaluation. Errors quoted in the NASA or CODATA evaluations are assessments based on such factors as the number of independent determinations made and the number and reliability of the different techniques employed. Furthermore in most cases, the probability of an error of a given magnitude falls off more slowly than a normal Gaussian function.

The problems of assignment of errors is illustrated by the development of our knowledge of the kinetic parameters for the two key reactions:



## STRATOSPHERIC CHEMISTRY

Initial investigations of these reactions apparently provided a sound data base with acceptable uncertainty limits for the  $k$  values and their temperature dependence. Subsequent studies have provided data which today gives recommended values for  $k_{298}$ , which lie significantly outside the  $\pm 20\%$  uncertainty limits proposed originally, and for the  $\text{OH} + \text{HNO}_3$  reaction a very different temperature dependence.

In determining an important atmospheric quantity such as the rate of generation of atmospheric radical species from a source gas, several elementary steps may be involved and cumulative errors in successive steps tend to increase the overall uncertainty for the process to an extent that meaningful interpretation of atmospheric observations cannot be made. The question arises whether it is possible to reduce these uncertainties by experiments or observations relating to the overall process. For example, if the process involved a kinetic competition which could be measured more accurately than the competing processes in isolation, the uncertainty might be reduced by such measurement. Competitive kinetic experiments have been widely used in the past for the determination of relative rate constants, but have now been largely superseded by direct techniques, where the potential for unrecognized systematic errors due to mechanistic and other difficulties is generally lower. For a limited number of simple chemical systems e.g. the production of  $\text{NO}$  from the  $\text{O}_3 - \text{N}_2\text{O} - \text{O}_2 - \text{N}_2$  photolysis system, some reduction in uncertainty could result from carefully designed measurements of overall reaction rates.

Not many rate coefficients have been measured in the laboratory under atmospheric conditions and extrapolation leads to a further source of uncertainty. Simple well characterized bimolecular and termolecular association reactions present no problem. Errors in extrapolated rate parameters can arise however with reactions exhibiting unexpected pressure and temperature dependence, reactions with more than one reaction channel, and reactions proceeding via complex intermediates which may react with other atmospheric constituents, particularly  $\text{O}_2$ . Well known examples are the reaction of  $\text{OH}$  with  $\text{CO}$ , the  $\text{HO}_2 + \text{HO}_2$  reaction, and the reaction of  $\text{OH}$  with  $\text{CS}_2$ . These uncertainties can be eliminated by rigorous experimental study focussed on measurements under conditions appropriate for the atmosphere. In the past, experimental difficulties restricted such kinetic investigations to use of indirect or modulated steady state techniques, but recent improvements in production techniques and detection sensitivity for radical species now allows direct measurements of rate coefficients under simulated atmospheric conditions. Further improvements in the reliability of the data base from this aspect, can be foreseen in the future.

For the key elementary reactions identified as being important for the stratosphere many of which are radical + radical reactions, the prospect of reducing uncertainties in the rate coefficients to less than  $\pm 10\%$  cannot be considered realistic. Some reduction in uncertainty can be expected from further temperature and pressure dependence studies, and a further understanding of product channels and reaction mechanisms can be anticipated in the future.

For the lower stratosphere, the data base for the important temporary reservoir species is slowly but surely improving. There are good prospects for further reduction in uncertainties in the photochemical and kinetic parameters for the gas phase processes involving these species, but formulation and parameterization of the heterogeneous chemistry remains problematical. There is a need for further field measurements to indicate the direction of future emphasis in this area, and further efforts in the development of laboratory techniques for production and study of the labile temporary reservoir species.

The prospects are good for improvement of the data base for homogeneous tropospheric chemistry. There is a need to establish with more reliability the kinetic parameters for certain elementary reactions in the oxidation of  $\text{CH}_4$  and  $\text{C}_2$  hydrocarbons, particularly those which are important (e.g. reactions forming and removing hydroperoxides) in the low  $\text{NO}_x$  situation prevailing in the background troposphere.

### 2.2.8 Identification of Gaps in the Chemical Description of the Atmosphere

The question of the completeness of the current models of stratospheric chemistry has been frequently raised, particularly when disagreement between model calculations and field measurements has appeared. For example at altitudes above 40 km it is believed that ozone is in photochemical equilibrium and its concentration is determined by relatively simple chemistry involving catalytic destruction by  $\text{HO}_x$  species, as described in Section 2.1. The rate parameters for these reactions are relatively well defined experimentally. Nevertheless comparison of theory and observations shows inconsistencies which cannot be assigned to a particular source of error. The differences may be accommodated within the combined uncertainty of the rate parameters; on the other hand slightly narrower uncertainty limits on the data would constrain the model such that unidentified chemical processes would need to be incorporated to reconcile theory and observation. Another example is the severe problem with the observations of abundance and seasonal variation of atmospheric  $\text{NO}_3$ , which are incompatible with currently known chemistry of this species.

These examples show that something is wrong with our description of the atmosphere and suggest that chemical processes may be missing. The specific source of the problem is not identified by these comparisons, however. All known reactions that are significant in the atmosphere have been included in the models to date, but there has been no systematic search for the reactions that could be important, but are as yet unidentified.

One possible approach to the identification of new and significant reactions is the application of a matrix technique. The starting point of this approach would be to construct a matrix of all currently proposed atmospheric constituents. The matrix will provide a formulation of all possible interactions between the individual constituents. Reactions of potential atmospheric significance, which have not already been established, can then be identified by application of criteria such as

- (1) The rate of the process should be significant when the concentrations of the reacting species in the atmosphere are at their upper limits and the reaction rate coefficient is at its maximum reasonable value.
- (2) The occurrence of the reaction should significantly alter the atmospheric trace gas composition.

If these criteria are met, a search for any previously reported information on the reaction should be made and further experimental investigation of the process carried out. If new species are formed as products of reactions identified as potentially important they would then be incorporated into an extended matrix, and their potential significance assessed. Their potential photochemical and thermal decomposition reactions should also be investigated.

Identification of novel aspects of atmospheric chemistry can also come from laboratory experiments. Most of our data base of atmospheric chemistry at the present time arises from laboratory investigations of isolated elementary reactions. This, however, has mainly concentrated on the determination of overall rate coefficients. The area of identification of reaction products has received less attention although this can provide insight into incomplete knowledge of the nature and kinetic behavior of significant atmospheric species.

Elucidation of some important aspects of atmospheric chemical mechanisms and also identification of new species of significance, has in the past resulted from laboratory studies of time dependence of stable reactants and products in more complex chemical systems under pseudo atmospheric conditions. These systems have often been designed to simulate selected components of atmospheric photochemical cycles and can provide a useful check on the completeness of our knowledge of these cycles. For example the

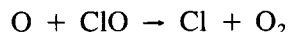
## STRATOSPHERIC CHEMISTRY

discovery of peroxyxynitric acid as a significant gas phase species resulted from steady state studies designed to investigate the oxidation of NO and NO<sub>2</sub> in the presence of HO<sub>2</sub> (Simonaitis and Heicklen, 1978) and FTIR spectroscopic investigation of this system at atmospheric pressure and room temperature (Niki *et al.*, 1977). Another example is the investigation of the photolysis of the O<sub>2</sub> - O<sub>3</sub> - H<sub>2</sub>O system (DeMore, 1973), which helped to clarify the then current issues concerning O<sub>3</sub> decomposition in gas mixtures containing water, through reactions with OH and HO<sub>2</sub>. This study also gave strong indication that knowledge of the very important radical loss reaction  $\text{OH} + \text{HO}_2 \rightarrow \text{H}_2\text{O} + \text{O}_2$  was incomplete.

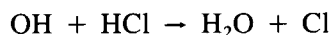
The utility of this type of experiment has clearly been established. Today as a result of dramatic improvements in spectroscopic methods, it will be possible to couple sensitive detection techniques for trace radicals and molecules with experiments on complex reaction systems. This coupling will facilitate a better control of the experimental system, thus providing improved prospects for accurate measurement of rate coefficients and branching ratios and the discovery of new chemistry. However it should be emphasized that true simulation of conditions in the free sunlit atmosphere in the laboratory is not a realistic or useful objective. Furthermore, the potential influence of heterogeneous effects needs to be carefully assessed in the interpretation of this type of laboratory experiment.

### 2.3. SUMMARY AND CONCLUSIONS

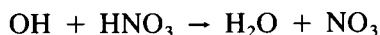
In the last few years, laboratory stratospheric chemistry has been characterized by steady improvements in the data base for reaction rate coefficients, product studies of elementary reactions, absorption cross sections and photodissociation quantum yields. While there have been no discoveries of fundamentally new catalytic cycles, radical or reservoir species, changes in the accepted rate coefficients for several important reactions have led to refinements in predictions of ozone depletion and have, in general, improved the agreement between measured and computed vertical profiles for trace species. With respect to odd oxygen depletion in the stratosphere, the most significant changes in the kinetics data base have concerned the reactions



and



the rates of which are now about 15% slower and 20% faster, respectively, under middle stratospheric conditions. These changes act in opposite directions as far as the chlorine-catalyzed ozone depletion is concerned. Minor changes have been reported in rate constants for the reaction

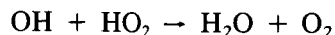
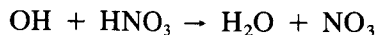


although these revisions are small compared to the major revision of a few years ago which increased the rate constant by a factor of three in the lower stratosphere. Re-evaluation of earlier kinetic data has also resulted in a decrease of about 40% in the rate constant for the reaction



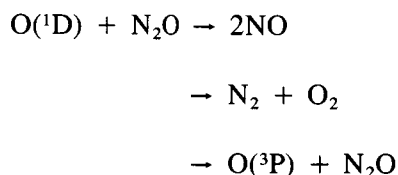
at 30 km.

For the most part, the list of chemical and photochemical processes identified in previous assessments as being the most important in stratospheric chemistry has not changed. In only a few cases are there serious gaps or inconsistencies in the data base, including a few extremely important reactions, e.g.,



for which the measured rate parameters are difficult to reconcile in terms of reaction rate theory. These and other reactions are examples of systems in which a relatively long-lived intermediate may be involved. The complex pressure and temperature dependence behavior which results has made it difficult to extrapolate rate constants beyond their range of measurement.

Although most of the reactions important in stratospheric chemistry have now been thoroughly studied, there are a number of important and potentially important processes which require attention. In the area of  $\text{NO}_x$  chemistry, the possible photolysis of  $\text{N}_2\text{O}$  to give  $\text{NO} + \text{N}$  would have a major impact on the odd nitrogen budget. Uncertainties associated with the rates and branching ratios of the reaction



as well as possible hot atom effects also have important consequences for modelling the  $\text{NO}_x$  source term.

Considerable progress has been made in understanding the reaction of  $\text{NO}_3$  but the reaction of  $\text{NO}_3$  with species such as  $\text{HCl}$  should be investigated. Additional work is required in the area of  $\text{NO}_3$  photochemistry focusing on the temperature dependences of primary quantum yields and absorption cross-sections.

In the area of  $\text{ClO}_x$  chemistry, additional work is necessary to clarify the branching ratio for the  $\text{OH} + \text{ClO}$  reaction and the role, if any, of the higher chlorine oxides. A number of uncertainties remain in the mechanism of  $\text{BrO}_x$ -catalyzed ozone destruction including the coupling with the  $\text{ClO}_x$  family through the  $\text{ClO} + \text{BrO}$  reaction and the reactions controlling  $\text{HBr}$ .

Many of the details of the atmospheric oxidation of methane and of halogenated hydrocarbons under stratospheric conditions have now been investigated and are moderately well understood.

In addition to the specific issues mentioned above, a number of other problem areas of a more speculative nature have been addressed. These include the effects of slow chemical reactions of non-radical reaction partners (e.g.,  $\text{ClONO}_2$ ,  $\text{HCl}$ ,  $\text{H}_2\text{O}$ ,  $\text{N}_2\text{O}_5$  and  $\text{HO}_2\text{NO}_2$ ), possibly occurring homogeneously or heterogeneously on aerosol particles, possible catalytic cycles involving sodium of mesospheric origin, reactions involving excited states of molecular oxygen and reactions of ions. None of these processes have so far been shown to have a significant effect on stratospheric ozone chemistry.

Two related questions of great significance for stratospheric chemistry concern the identification of possible missing reactions or species and the limits that can be placed on the accuracy of chemical and photochemical parameters in the mechanism. The ability of models to predict the response of the atmosphere to perturbations will always depend on both the accuracy of the rate coefficients used as input data and

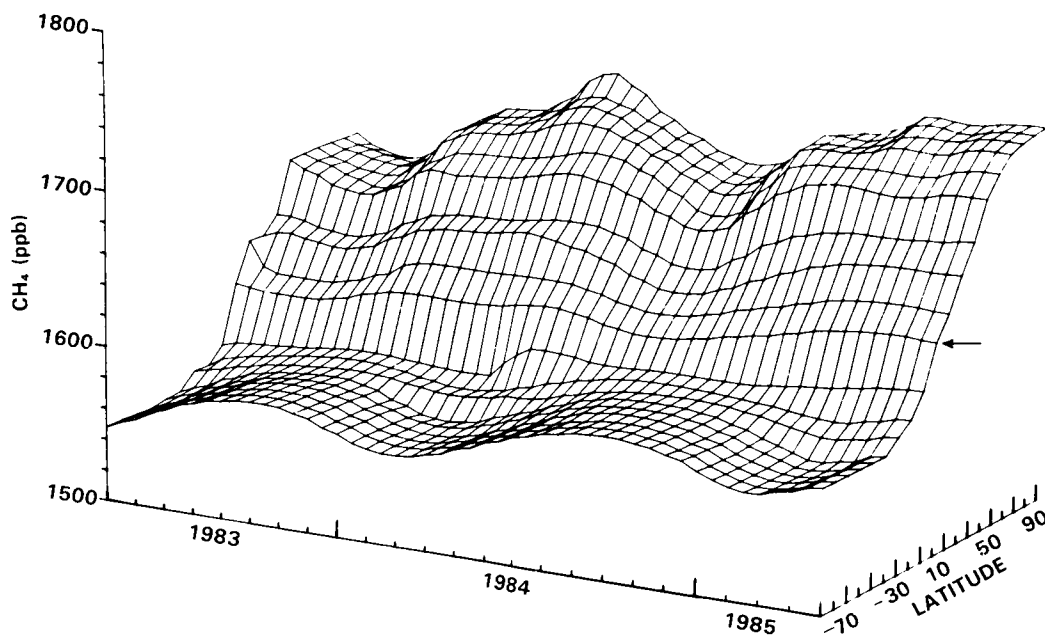
## STRATOSPHERIC CHEMISTRY

the completeness of the mechanism with regard to the interaction of known and hypothetical species. Although our understanding of the gas-phase chemistry has continued to improve, the prospects are low for further improvement of the accuracy with which the rate constants for certain sensitive reactions can be measured. Moreover, certain key elements of stratospheric models such as the production of  $\text{NO}_x$  and  $\text{HO}_x$  are driven by sequences of photochemical and kinetic processes each having a finite uncertainty. The combined effect of these uncertainties can be substantial even if the constituent parameters are well-determined.

One possible approach to this problem is to rely to a greater extent on experimental systems which mimic in a well-controlled fashion the same sequence of reaction steps that takes place in the atmosphere. These "integrated" experiments would focus on a narrow aspect of the overall mechanism such as  $\text{HO}_x$  or  $\text{NO}_x$  production. Such an approach has the potential for not only reducing the end-to-end uncertainty of a particular process but, with the use of sensitive diagnostic techniques, possibly reveal missing reactions and species.

With regard to omissions of important reactions from current models, the systematic use of the "matrix" approach could be useful. In this method, all known atmospheric species are tested, conceptually or experimentally, for reaction with one another. While this approach does not guarantee that important reactions will not be overlooked, it constitutes a systematic procedure for the consideration of all possible reactions, probable or improbable.

# TROPOSPHERIC TRACE GASES



## Panel Members

R. Gammon and S.C. Wofsy, Co-Chairmen

R.J. Cicerone

A.C. Delany

R.T. Harriss

M.A.K. Khalil

J.A. Logan

P. Midgley

M. Prather

## CHAPTER 3

### TROPOSPHERIC TRACE GASES: SOURCES, DISTRIBUTIONS AND TRENDS

#### TABLE OF CONTENTS

3.0	INTRODUCTION .....	57
3.1	HALOCARBONS .....	58
3.1.1	Distributions and Trends .....	58
3.1.2	Sources .....	69
3.1.3	Discussion .....	73
3.2	NITROUS OXIDE (N <sub>2</sub> O) .....	77
3.2.1	Global Atmospheric Trend and Distribution .....	77
3.2.2	Sources and Sinks .....	78
3.2.3	Discussion .....	84
3.3	OXIDES OF NITROGEN (NO <sub>x</sub> ) .....	85
3.3.1	Distributions and Trends .....	85
3.3.2	Sources and Sinks .....	85
3.3.3	Discussion .....	88
3.4	METHANE (CH <sub>4</sub> ) .....	88
3.4.1	Distributions and Trends .....	88
3.4.2	Sources and Sinks .....	89
3.4.3	Discussion .....	98
3.5	CARBON MONOXIDE (CO) .....	100
3.5.1	Distributions and Trends .....	100
3.5.2	Sources .....	105
3.5.3	Discussion .....	105
3.6	CARBON DIOXIDE (CO <sub>2</sub> ) .....	106
3.6.1	CO <sub>2</sub> Trends and Global Distribution .....	108
3.6.2	Discussion .....	109
3.7	SOURCE GASES FOR STRATOSPHERIC SULFATE AEROSOLS (OCS, CS <sub>2</sub> ) .....	112
3.8	VOLCANIC INJECTIONS OF CHLORINE INTO THE STRATOSPHERE .....	114
3.9	SECULAR TRENDS OF TRACE GASES FROM POLAR ICE CORES .....	115
3.10	SUMMARY AND RESEARCH RECOMMENDATIONS .....	115

### 3.0 INTRODUCTION

Trace gases released at the earth's surface into the lower atmosphere influence the chemistry of the stratosphere in several ways. Some tropospheric trace species participate directly in the ozone photochemistry in the stratosphere. Such gases as  $N_2O$  and the halocarbons are sufficiently long-lived and insoluble to reach the stratosphere. There they are destroyed by photochemical reactions which generate free radical products (e.g. NO, Cl, Br), and these enter into the catalytic cycles which control ozone abundance.

Water vapor is directly involved in the odd-hydrogen and odd oxygen chemical cycles in the stratosphere. Most of the water vapor in the troposphere is trapped at the temperature minimum which separates the troposphere from the stratosphere. The low water vapor content of the stratosphere (a few ppm) is controlled by freezing out processes at the tropical tropopause and by stratosphere-troposphere exchange processes. Oxidation of  $CH_4$  provides an important source of stratospheric  $H_2O$  which bypasses the cold trap. Another important role of  $CH_4$  in stratospheric chemistry termination of chlorine radical chain reactions, via  $(Cl + CH_4 \rightarrow HCl + CH_3)$ .

Trace gases may affect stratospheric chemistry indirectly by influencing the delivery of reactive species to the stratosphere, for example, by altering the tropospheric lifetime for a key species such as  $CH_4$ . In this sense, any tropospheric trace gas which significantly affects the photochemistry of the free troposphere (e.g., by altering local OH) indirectly affects the chemical balance in the stratosphere. Carbon monoxide, methane, oxides of nitrogen and other hydrocarbons all influence global tropospheric OH, and hence the major gas-phase scavenging process of the lower atmosphere.

There are several important species which influence stratospheric chemistry by altering the local physical conditions (temperature, insolation) in the stratosphere. For example, the "greenhouse" gases ( $CO_2$ ,  $H_2O$ , etc.) will affect stratospheric temperature, and hence temperature-dependent photochemical reaction rates. The trace gas carbonyl sulfide is a major gaseous source for the natural stratospheric sulfate aerosol layer.

Trace gas concentrations in the atmosphere reflect in part the overall metabolism of the biosphere, and in part the broad range of human activities such as agriculture, production of industrial chemicals, and combustion of fossil fuels and biomass. There is compelling evidence that the composition of the atmosphere is now changing, due to increased gaseous emissions associated at least in part with human activities. Observed trends in trace gas levels are reviewed and implications for the chemistry of the atmosphere are discussed in this chapter, with emphasis on those species influencing stratospheric chemistry and climate.

Species have been ordered in this discussion, beginning with gases derived from purely human sources and proceeding to those with both anthropogenic and natural sources. There are four principal classes of compounds for which emissions are affected by human activities: industrially manufactured gases (e.g. fluorocarbons), gases released in the production and consumption of fossil carbon fuels ( $CO_2$ , CO,  $N_2O$ , oxides of nitrogen), gases arising from biomass burning ( $CH_3Cl$ , OCS,  $NO_x$ ,  $N_2O$ ,  $CO_2$ , CO), and finally, biogenic gases released from agricultural lands, from soils or plants disturbed by development or exploitation, or from decomposing human or animal wastes. Throughout the discussion, particular emphasis is given to those species which are now increasing in the atmosphere, with a view towards understanding the causes of these important trends.

## SOURCE GASES

### 3.1 HALOCARBONS

#### 3.1.1 Distributions and Trends

Global baseline measurements of halocarbons CFC-11 ( $\text{CFCl}_3$ ), CFC-12 ( $\text{CF}_2\text{Cl}_2$ ),  $\text{CCl}_4$  and  $\text{CH}_3\text{CCl}_3$  were undertaken by the Atmospheric Lifetime Experiment, ("ALE", Prinn *et al.*, 1983a) beginning in 1978 and continuing to the present (now called the GAGE program). This study provided accurate descriptions of global distributions and trends for these key species, using careful calibration and intercomparison procedures to obtain self-consistent, absolute measurements at five coastal or island stations generally sampling unpolluted maritime air.

Figures 3-1 to 3-5 show results for these species (as monthly means) through June 1984 (Cunnold *et al.*, 1983a,b; Prinn *et al.*, 1983b; Simmonds *et al.*, 1983; all results are updated through 1984). The concentration for each gas is increasing with time, with growth rates averaging 5% per annum for CFC-11 and CFC-12, about 7% per annum for  $\text{CH}_3\text{CCl}_3$ , and 1% per annum for  $\text{CCl}_4$ . Concentrations of all species were observed to be higher in the Northern Hemisphere than in the Southern Hemisphere. Rates of increase, however, were larger in the Southern Hemisphere, indicating systematic gradual decline in the North-South asymmetry. The large excess of halocarbon concentrations in the North may be attributed to the dominant role of emissions from northern industrial areas and to the fact that the global distribution is far from a steady state. The decline of the North/South asymmetry reflects the slower growth rates for Northern emissions since the mid-1970's and increased importance for emissions in the Southern Hemisphere (see below).

One purpose of the ALE investigation was to determine the atmospheric lifetime for each gas, a key parameter controlling the ultimate impact of the gas on stratospheric chemistry. The largest uncertainties in analyzing lifetimes are associated with estimates of emission magnitude and/or estimates of the history of emission rates. The ALE investigators used two methods to assess lifetimes, one based on the atmospheric burden and on absolute source strength, the other based on the slope of the trend line and on the time history of emissions. Results using the extended data set (ALE + GAGE) may be summarized as follows (Prinn, Cunnold, Alyea, Rasmussen, Simmonds, Fraser, Crawford and Rosen, private communication, 1985):

CFC-11: The lifetime of  $\text{CFCl}_3$  is  $75^{+32}_{-17}$  years from the ALE trend analysis, consistent with estimates of removal rates in the stratosphere. It is unlikely that there is another globally significant removal process for this gas (Cunnold *et al.*, 1983a).

CFC-12: The trend lifetime estimate is  $111^{+289}_{-46}$  years, again consistent with removal only in the stratosphere. There is greater uncertainty in this case than for CFC-11, due to inadequate knowledge of release rates (see below) (Cunnold *et al.*, 1983b).

$\text{CH}_3\text{CCl}_3$ : Using the currently accepted calibration, the lifetime of this species is estimated using the inventory technique to be  $6.5^{+3}_{-2}$  years, in agreement with recent estimates by Khalil and Rasmussen (1984a). The inventory technique is strongly dependent on absolute calibration and very sensitive to estimated global emissions, both of which could be in error. Indeed, a change of 25% in either quantity could change the estimated lifetime by a factor of 2 (Logan *et al.*, 1981). For comparison, the lifetime estimate for trend analysis is 8.9 years. The major removal mechanism is almost certainly reaction with tropospheric OH. Current models for tropospheric photochemistry appear to give removal rates very close to the range given by the ALE analysis (Prinn *et al.*, 1983b).

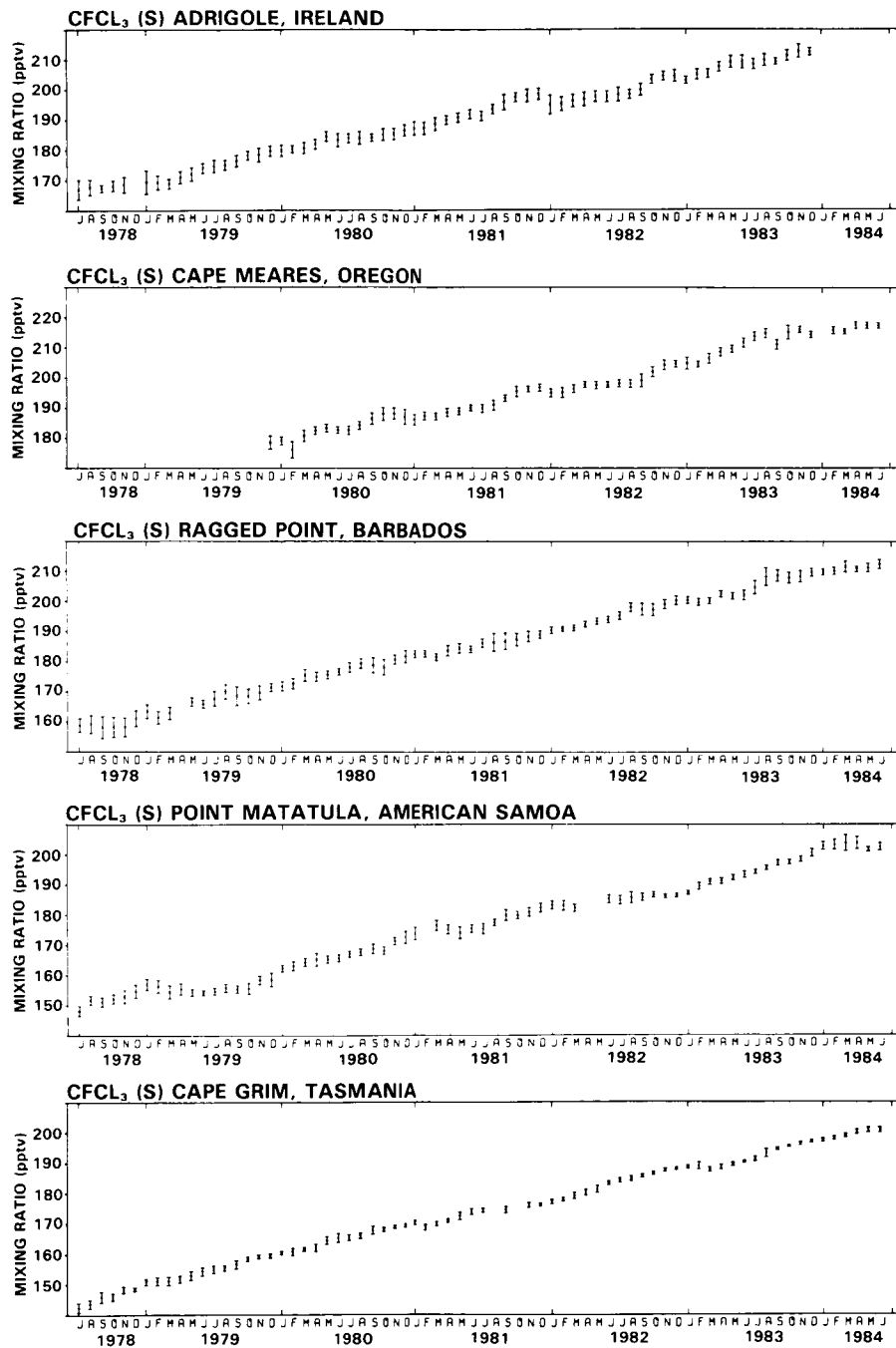


**Figure 3-1.** Monthly-mean mixing ratios and monthly variances of CFC-13 measured 4-times-daily on a gas chromatograph with a silicone column at the ALE/GAGE stations during the first 6 years of the ALE/GAGE network. The calibration factor used is 0.96 (see Prinn *et al.*, 1983a, 1983b; Rasmussen and Lovelock, 1983; Cunnold *et al.*, 1983a, 1983b; and Simmonds *et al.*, 1983 for further details). The CFC-13 trends based on the data from the first 5 years of the ALE/GAGE program (July, 1978-June, 1983) at Adrigole, Cape Meares, Ragged Point, Point Matatula, and Cape Grim are 4.4, 4.4, 5.0, 6.2 and 5.3% per year respectively. The Cape Meares trend is for 3.5 years of data while the other trends are for 5 years of data. The data for 7-83 to 6-84 are preliminary (R. Prinn, R. Rasmussen, F. Alyea, D. Cunnold, A. Crawford, P. Fraser, P. Simmonds and R. Rosen, private communication, 1985).

**SOURCE GASES**

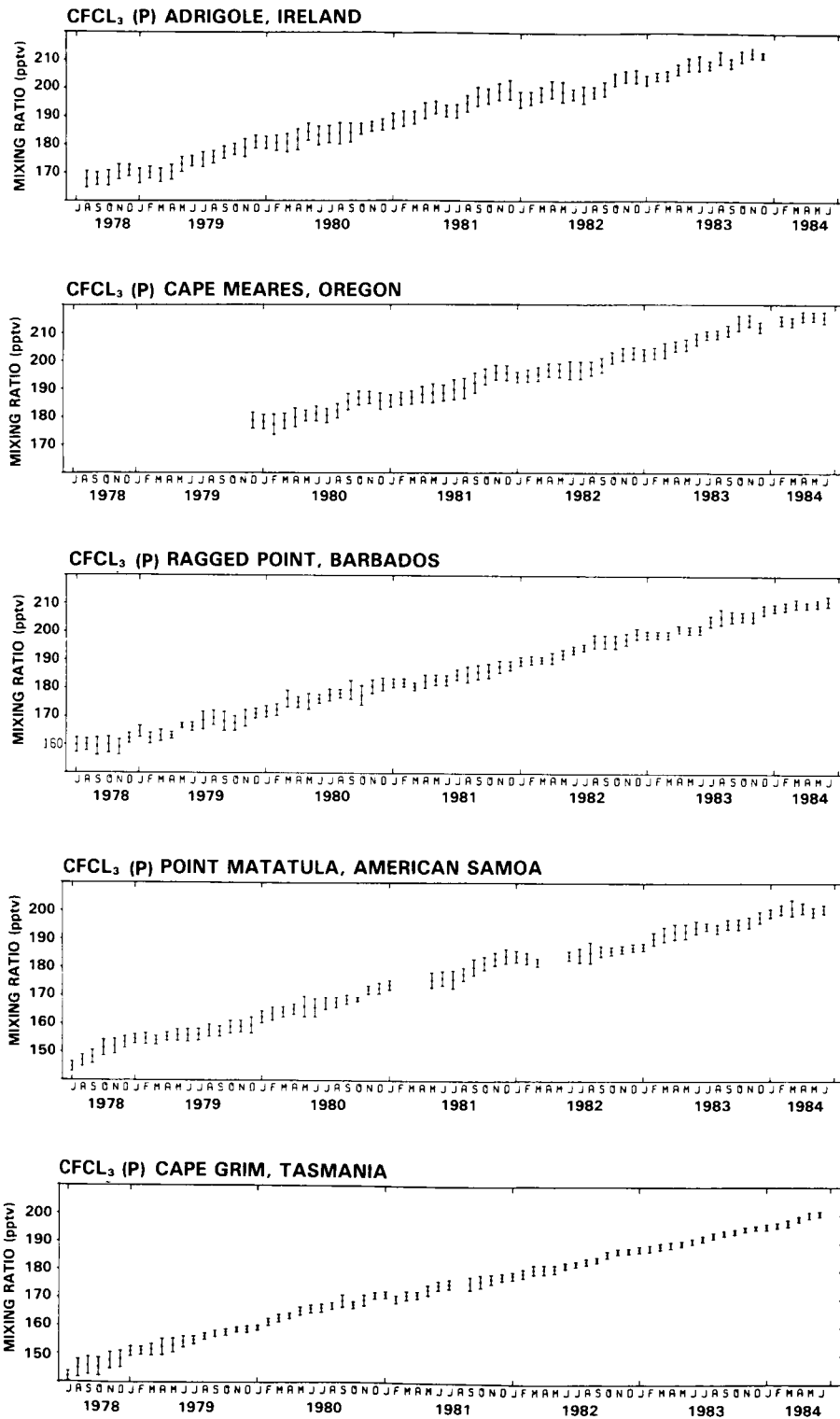


**Figure 3-2.** ALE/GAGE network data. As in Figure 1, but for CFC-11 measured on a Porasil column and with the 1978-1983 measured trends being 4.6, 4.3, 4.8, 5.7 and 5.2% per year at the 5 stations.

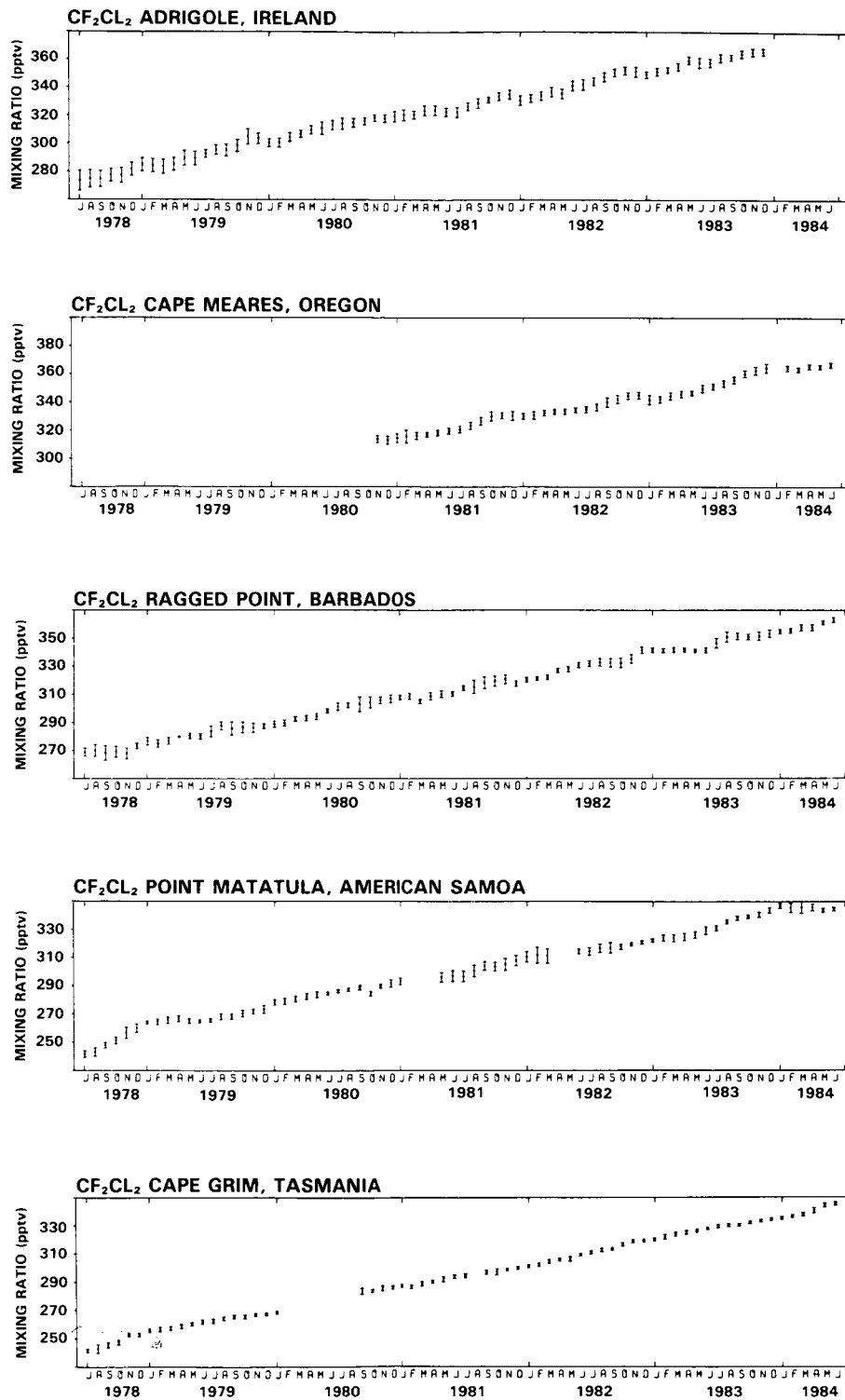
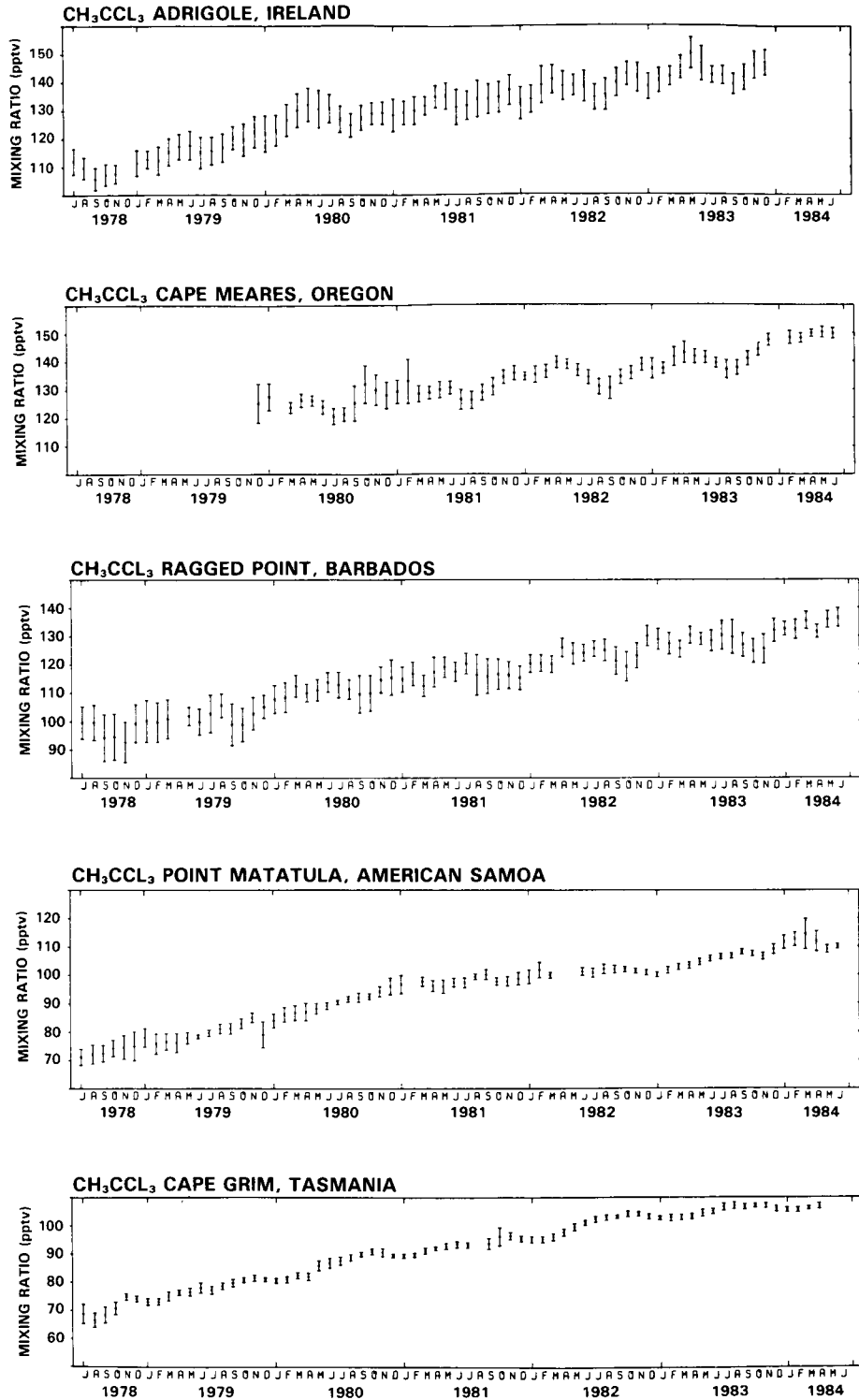


Figure 3-3. ALE/GAGE network data. As in Figure 1, but for CFC-12 measured on a Porasil column with a calibration factor of 0.95 and with the 1978-1983 measured trends being 4.7, 4.6, 5.2, 5.1 and 5.2% per year at the 5 stations.

**SOURCE GASES**



**Figure 3-4.** ALE/GAGE network data. As in Figure 1 but for CH<sub>3</sub>CCl<sub>3</sub> measured on a silicone column with a calibration factor of 0.8 and with the 1978-1983 measured trends being 4.9, 3.8, 6.2, 8.1 and 8.1% per year at the 5 stations.

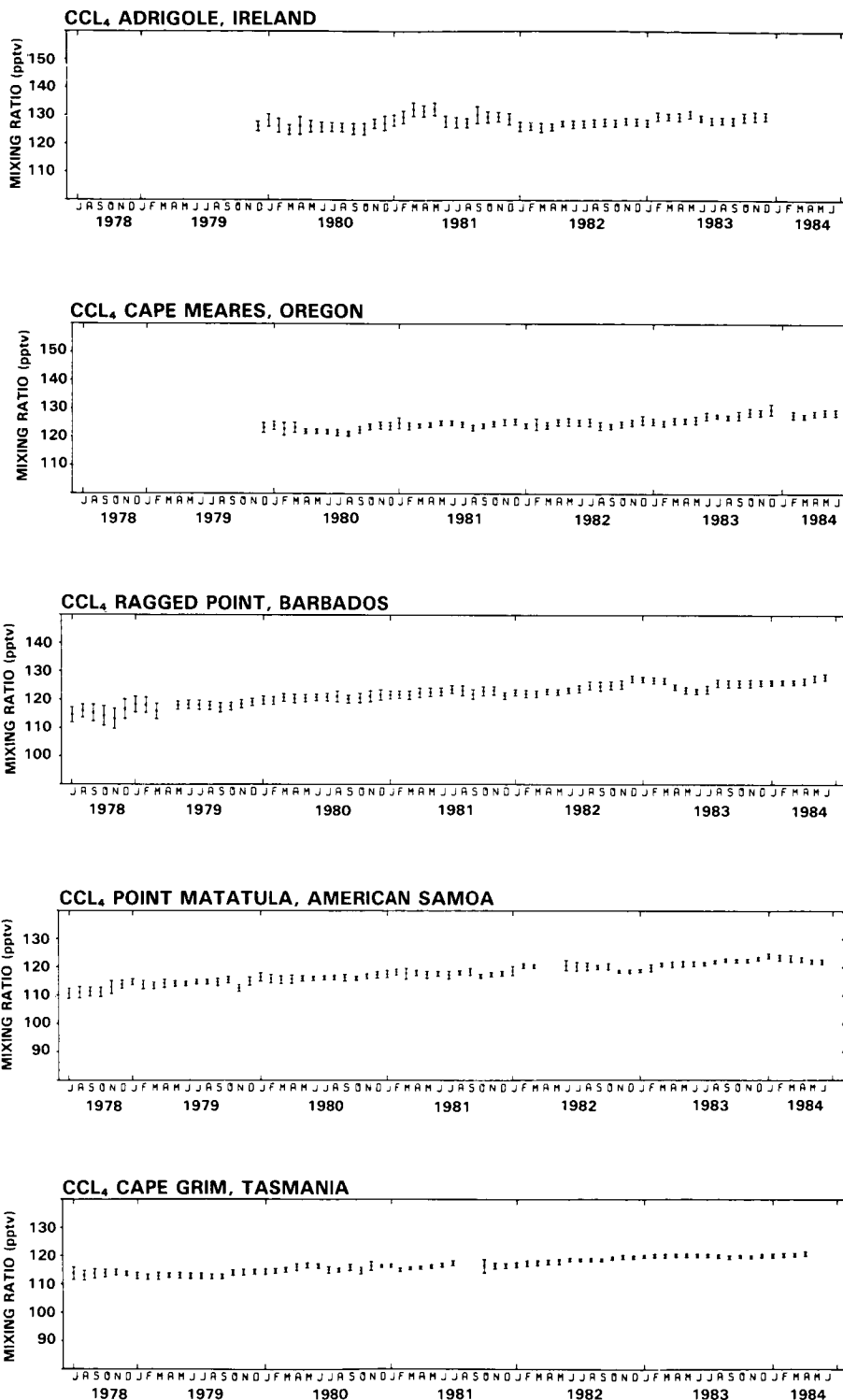


Figure 3-5. ALE/GAGE network data, as in Figure 1 but for CCl<sub>4</sub> measured on a silicone column with a calibration factor of 0.81 and with the 1978-1983 measured trends being 0.5, 0.8, 1.7, 1.4 and 1.3% per year at the 5 stations.

## SOURCE GASES

$\text{CCl}_4$ : Use of carbon tetrachloride has been nearly stable for many decades, thus the atmospheric burden is relatively close to steady state and annual increases are relatively small. Release rates are not well-documented, but atmospheric observations appear to be consistent with a lifetime of  $\sim 50$  yr., which could be explained by loss due to stratospheric photolysis with, perhaps, a contribution from hydrolysis in the oceans, (Simmonds *et al.*, 1983).

Distributions, trends and lifetimes for a wide range of halocarbons have been determined by various investigators, as summarized in Tables 3-1 and 3-2. Long-lived species presently at very low levels can potentially contribute significant concentrations of Cl and Br to the stratosphere, if release rates grow rapidly. As discussed below, CFC-113 ( $\text{C}_2\text{Cl}_3\text{F}_3$ ) and CFC-22 ( $\text{CHF}_2\text{Cl}$ ) are of particular interest, with their long lifetimes, increasing industrial applications, and rapidly rising atmospheric concentrations (Table 3-1B).

A number of bromine containing gases have been measured in the atmosphere remote from industrial or natural sources. Two brominated methane species,  $\text{CH}_3\text{Br}$  and  $\text{CHBr}_3$ , are found to be the most abundant bromine-containing compounds (Table 3-2). The concentrations of  $\text{CHBr}_3$  are quite variable because of its short atmospheric lifetime. Four other bromine containing trace gases are found at lower concentrations of around 1 to 4 pptv; these are  $\text{CH}_2\text{Br}_2$ ,  $\text{CHBr}_2\text{Cl}$ ,  $\text{CH}_2\text{BrCl}$  and  $\text{C}_2\text{H}_4\text{Br}_2$ . Finally there are two industrial gases present in the atmosphere at about 1 pptv; these are  $\text{CBrClF}_2$  (BCF) and  $\text{CF}_3\text{Br}$  both used as fire extinguishing compounds. Methyl bromide ( $\text{CH}_3\text{Br}$ ) and the two fire extinguishing compounds are more abundant in the Northern Hemisphere compared to the Southern Hemisphere. These compounds have known industrial sources. The presence of relatively large amounts of the other bromine containing trace gases in the Southern Hemisphere suggests that the oceans may be a source for these compounds, except for  $\text{C}_2\text{H}_4\text{Br}_2$ . Bromine compounds have recently served as tracers of pollution associated with arctic haze (Rasmussen and Khalil, 1984c; Berg *et al.*, 1984; Khalil and Rasmussen, 1985c).

Since bromine is a very efficient catalyst for recombination of ozone, concentrations of organobromine species as low as  $\sim 100$  ppt could be of interest to stratospheric chemists (Prather *et al.*, 1984). Current levels are below 25 ppt, but some species are increasing rapidly. The long-lived bromocarbons Halon 1301 ( $\text{CF}_3\text{Br}$ ) and Halon 1211 ( $\text{CBrClF}_2$ ), have enjoyed an expanding market in fire extinguishers for high technology, aircraft, and military applications. Hence, it might be expected that atmospheric concentrations may be increasing. Atmospheric concentration data for Halon 1301 are not available over a period of years. Concentrations of Halon 1211 in the atmosphere are rapidly rising, as documented by Khalil and Rasmussen (1985c) at the South Pole, the Arctic, and Cape Meares, Oregon (rate of increase 10–30% per year) and by Lal *et al.* (1985) in the upper stratosphere over France. Similarly, Lovelock (1985, private communication) observed ambient levels for Halon 1211 of only 0.16 pptv in 1978 at Cornwall, UK, but concentrations rose to 0.43 ppt in 1980 and 1.5 ppt in 1981.

There are no data establishing a trend for either  $\text{CH}_3\text{Br}$  or  $\text{C}_2\text{H}_4\text{Br}_2$  in the atmosphere. Ethylene dibromide ( $\text{C}_2\text{H}_4\text{Br}_2$ ) is an important industrial bromocarbon (see Table 3-2). Emissions arise from evaporation of leaded gasoline and from fumigation. Rates of use in both applications are declining, however, and the lifetime is relatively short ( $\sim 1$  yr.), hence concentrations of this species are unlikely to increase significantly in the near future. Methyl bromide ( $\text{CH}_3\text{Br}$ ), the second most abundant organobromine gas, has also a relatively short lifetime ( $\sim 3$  yr.) (Logan *et al.*, 1978; Yung *et al.*, 1980). Sources from leaded motor fuel are currently in decline (Bauer, 1979). It seems unlikely that use of  $\text{CH}_3\text{Br}$  in fumigation can grow rapidly, due to the high toxicity of the gas, and about half of methyl bromide emissions appear to be of natural origin (Yung *et al.*, 1975; Yung *et al.*, 1980). Hence there is not expected to be significant future increase in the concentration of  $\text{CH}_3\text{Br}$ .

## SOURCE GASES

Table 3-1A. Measured Distributions of Selected Halocarbons

COMPOUND	DATE	CONC $\pm$ SD pptv	LAT	NH AVE $\pm$ SD pptv	SH AVE $\pm$ SD pptv	GLBL AVE $\pm$ SD pptv	REF
CCl <sub>4</sub>	12/81			135	128		1
	2/81	150 $\pm$ 3	20				2
	6/81	100	53				11
	1/80			121	115	118	26
	5/82	150 $\pm$ 2	70	151			12
	11/81	146 $\pm$ 1	30°S-42°S		145		13
CHCl <sub>3</sub>				30	19	25	9
				45	16	26	24
	12/81			21	11		1
	2/81	32 $\pm$ 4	20	26			2
	11/81	21 $\pm$ 3	30°S-42°S		18 $\pm$ 2		13
	1978			29 $\pm$ 7.0	29 $\pm$ 4	29	15
CH <sub>2</sub> Cl <sub>2</sub>	12/81			38	21		1
CH <sub>3</sub> Cl	12/81	630	40°N-32°S				5
	1981	589 $\pm$ 43	71				3
	11/81	617 $\pm$ 9	30°S-42°S				13
CH <sub>3</sub> CCl <sub>3</sub>	12/81			156	116		1
	2/81	149 $\pm$ 3	20				2
	1981	170 $\pm$ 9	70				3
	11/81	123 $\pm$ 0.6	30°S-42°S				13
	1978			117 $\pm$ 4.0	90 $\pm$ 3		15
	1/80			114	83	98	25
C <sub>2</sub> HCl <sub>3</sub>	12/81			12	< 3		1
	1981		71	18			3
	1981	16 $\pm$ 15	70				3
				11			12,22
C <sub>2</sub> Cl <sub>4</sub>	12/81			29	5		1
	2/81	60 $\pm$ 7	20				2
	1981		71				3
	1981	87 $\pm$ 28	70	89			3
	11/81	9 $\pm$ 1	30°S-42°S		9 $\pm$ 1		13
	1978			56 $\pm$ 11	14 $\pm$ 3	35	15
			90			22	
CH <sub>2</sub> ClCH <sub>2</sub> CCl	12/81			37	14		1
CF <sub>4</sub> (CFC-14)	1979					70 $\pm$ 7	16
	1979	64 $\pm$ 2	90°S				23
	1984	72 $\pm$ 2	90°S				23
C <sub>2</sub> F <sub>6</sub> (CFC-116)	1979			4	3.5	4 $\pm$ 0.9	16

**SOURCE GASES**

**Table 3-1A.** Measured Distributions of Selected Halocarbons. — Continued

COMPOUND	DATE	CONC ± SD pptv	LAT	NH AVE ± SD pptv	SH AVE ± SD pptv	GLBL AVE ± SD pptv	REF
SF <sub>6</sub>	12/81			0.9	0.8		1
CClF <sub>3</sub> (CFC-13)	1979			3.2	3.6	3.4 ± 0.6	16
CCl <sub>2</sub> F <sub>2</sub> (CFC-12)	12/81			305	282		1
	2/81	326 ± 2	20				2
	1981	339 ± 6	70				3
	5/82	353 ± 3	70				12
	11/81	321 ± 1	30°S-42°S				13
	1978			274 ± 2	255 ± 4		15
	1/80			296	274	285	7
CCl <sub>3</sub> F (CFC-11)	12/81			186	172		1
	1/80					168	8
	1981	199 ± 3	70				3
	5/82	205 ± 2	70				12
	6/81	191	53				11
	11/81	186 ± 1	30°S-42°S				13
	1978			161 ± 1	148 ± 2		15
	1/80			174	160.5	168	6
CHClF <sub>2</sub> (CFC-22)	2/81	64 ± 1	20				2
	1981	71 ± 4	70				3
	11/81	58 ± 0.6	30°S-42°S				13
	1978			42 ± 1	36 ± 1	39	15
				73			12
C <sub>2</sub> ClF <sub>5</sub> (CFC-115)	1979	4.1					16
C <sub>2</sub> Cl <sub>2</sub> F <sub>4</sub> (CFC-114)	12/81			14	13		1
C <sub>2</sub> Cl <sub>3</sub> F <sub>3</sub> (CFC-113)	12/81			23	21		1
	2/81	21 ± 0.5	20	19 ± 0.4			2
	11/81	17 ± 1	30°S-42°S		17 ± 11		13
	1978			13 ± 0.8	12 ± 0.6		15
				17	11	14	19
				16	12	14	20,24
	5/82	23 ± 4	70				12

## SOURCE GASES

Table 3-1B. Reported Trends for Selected Halocarbon Concentrations

COMPOUND	DATE	INC %/yr $\pm$ SD	INC ppt/yr $\pm$ SD	LIFETIME $\pm$ SD (YEARS)	REF
CCl <sub>2</sub> F <sub>2</sub> (CFC-12)	12/81		26.0 $\pm$ 5	100 +100/-40	1
	1/80	6.0	17.1	greater than 81	7
			9.0 $\pm$ 2		19
	1980			135	17
	1980			120	14
CCl <sub>3</sub> F (CFC-11)	12/81		15.0 $\pm$ 3	60 + 40/-20	1
	1/80	5.7	9.6	78	6
	1/80			75	8
			10.0 + 1/-3		19
	75-81	6-7		60	14
				11	
CF <sub>4</sub> (CFC-14)	79-84	~2	1.3 $\pm$ 0.6	? ~ 10 <sup>4</sup>	27
CHClF <sub>2</sub> (CFC-22)		11.7			4
				75 + 15/-10	11
			10 - 11		11
C <sub>2</sub> Cl <sub>3</sub> F <sub>3</sub> (CFC-113)		10.0			20,24
CCl <sub>4</sub>	12/81		6.0		1
	1/80	1.8	2.1	52	26
CHCl <sub>3</sub>				0.50	9
	11/81			0.33	13
CH <sub>2</sub> Cl <sub>2</sub>	12/81			0.9 $\pm$ 0.3	1
CH <sub>3</sub> CCl <sub>3</sub>	12/81		13.0 $\pm$ 3	9 + 2/-1	1
			13.2 + .8/-1.2		19
	11/81				13
	1/80	8.7	8.6	6.5 to 9	25
C <sub>2</sub> Cl <sub>4</sub>	12/81			0.6 $\pm$ 0.2	1
CH <sub>2</sub> ClCH <sub>2</sub> CCl	12/81			0.6 $\pm$ 0.2	1

1. Singh, *et al.*, 1983a.
2. Rasmussen and Khalil, 1981a.
3. Rasmussen and Khalil, 1983a.
4. Khalil and Rasmussen, 1981.
5. Singh, *et al.*, 1983b.
6. Cunnold *et al.*, 1983a.
7. Cunnold *et al.*, 1983b.
8. Fraser *et al.*, 1983.
9. Khalil *et al.*, 1983.
11. Brice *et al.*, 1982.
12. Rasmussen and Khalil, 1983d.
13. Rasmussen *et al.*, 1982a.
14. Owens *et al.*, 1982.

15. Rasmussen and Khalil, 1982.
16. Penkett *et al.*, 1981.
17. Khalil and Rasmussen, 1983.
18. Rasmussen *et al.*, 1981c.
19. Rasmussen and Khalil, 1983c.
20. Rasmussen *et al.*, 1983b.
21. Rasmussen and Khalil, 1984a.
22. Khalil and Rasmussen, 1985d.
23. Khalil and Rasmussen, 1985e.
24. Prinn *et al.*, 1983a.
25. Prinn *et al.*, 1983b.
26. Simmonds *et al.*, 1983.
27. Cicerone, 1979.

## SOURCE GASES

Table 3-2. Atmospheric Concentrations of Bromo- and Iodo Carbons

COMPOUND	DATE	CONC $\pm$ SD pptv	LAT	NH AVE $\pm$ SD pptv	SH AVE $\pm$ SD pptv	GLBL AVE $\pm$ SD pptv	REF
CH <sub>3</sub> I	1981	1.3 $\pm$ 0.2	60°N			0.8	4
	1981	2.5 $\pm$ 0.8	22°N				4
	1981	3.4 $\pm$ 0.5	8°N				4
	1981	2.6 $\pm$ 0.9	14°S				4
	1981	2.4 $\pm$ 1.3	42°S				4
	1981	1.8 $\pm$ 0.4	90°S				4
	1981	7.0 $\pm$ 0.5	15°N				4
	1981	22.0 $\pm$ 5.0	60°N				4
	1981	12.0 $\pm$ 3.0	34°S				4
		1981			3.1 $\pm$ 0.3		2.2 $\pm$ 0.5
CH <sub>3</sub> Br	1981	10.9 $\pm$ 0.9	72°N				2
	1983	9 - 14	72°N				7
	3/83	11 $\pm$ 4	60-80°N				6
	11/84	7.5	90°S				1
CHBr <sub>3</sub>	3/83	2 - 46	60-80°N				6
	11/84	7.5	90°S				1
CH <sub>2</sub> Br <sub>2</sub>	1981	5.0 $\pm$ .3	72°N				2
	1983	4.7 - 5.6	72°N				7
	3/83	3 - 60	60-80°N				6
CH <sub>2</sub> BrCl	1981	2.5 $\pm$ .3	72°N				2
	1983	2.3 - 2.8	72°N				7
	11/84	2.5	90°S				1
CHBr <sub>2</sub> Cl	11/84	0.70	90°S				1
C <sub>2</sub> H <sub>4</sub> Br <sub>2</sub>	1981	1.24 $\pm$ .30	72°N				2
	1983	1.0 - 1.9	72°N				7
	3/83	1 - 37	60-80°N				6
CF <sub>3</sub> Br	11/84	1.0	90°S				1
CBrClF <sub>2</sub>	11/84	1.10	90°S				1
	1981	1.09 $\pm$ 0.10	72°N				2
	2/1985	2.00	44°N				3
	9/1982	1.03	72°N				3
	9/1983	1.31	72°N				3
	10/84	1.49	72°N				3
	1983	0.9 - 1.2	72°N				7
Br — total organic	1981	30	72°N				2
	11/82	7.6 $\pm$ 3.0	72°N				5

1. Khalil and Rasmussen, 1985c.
2. Rasmussen and Khalil, 1984c.
3. Lal *et al.*, 1985.
4. Rasmussen *et al.*, 1982b.

5. Berg and Sperry, 1983.
6. Berg *et al.*, 1984.
7. Rasmussen and Khalil, 1984c.

### 3.1.2 Sources

#### Industrial Production and Use

Table 3-3 presents a summary list of industrial halogenated species which have been observed in the free atmosphere, along with estimated source strengths. No organization currently has access to truly global industrial production data for halocarbons. The chlorofluoromethanes CFC 11 and 12 ( $\text{CFCl}_3$ ,  $\text{CF}_2\text{Cl}_2$ ) are the only compounds for which data covering a large fraction of the market are published, and for which emission estimates are routinely made. There is only very sparse information for the other halocarbons. Available data and estimates on production, current and historic, for the chemicals listed in Table 3-3 are described below and factors likely to influence future use are discussed. Of the industrially produced halocarbons considered here, only the methyl halides ( $\text{CH}_3\text{Cl}$ ,  $\text{CH}_3\text{Br}$ ,  $\text{CH}_3\text{I}$ ,  $\text{CH}_2\text{Br}_2$ , etc.) appear to have significant natural sources (Singh *et al.*, 1983a).

#### CFC 11 ( $\text{CFCl}_3$ ) and CFC 12 ( $\text{CF}_2\text{Cl}_2$ )

The Fluorocarbon Program Panel (FPP) of the Chemical Manufacturers Association (CMA) sponsors publication of an annual report of production for CFC 11 and CFC 12 by 20 companies representing production in North America, South America, Western Europe, Japan, Australia, Africa, and India. The data for 1960-1984 are summarized in Figure 3-6. The production of CFCs 11 and 12 by these companies fell by 7% in 1982 relative to 1981, to 599 kt, but rose by 8% in 1983 to 644 kt and rose by an additional 8% in 1984 to 694 kt (CMA, 1985). Thus in the last two years production rose by 16%, while remaining slightly below (~13%) the 810 kt produced by reporting companies in 1974, the peak year.

The FPP formerly attempted to estimate production in the rest of the world by extrapolation of data published for the USSR for the period 1968-75, which suggested 18% annual growth during that period. Continued use of this extrapolation could not be justified in the absence of more recent data for the USSR. Data for the People's Republic of China and the countries of Eastern Europe are lacking entirely. Consequently, no world production estimate was made for 1983 and the FPP does not plan to resume estimating world production until credible CFC production data for these countries become available. It is still considered that production by the companies reporting to CMA represents 80-85% of the world total, but this fraction is not well known and may be expected to change with time. Earlier FPP estimates of total world production of CFC-11 and CFC-12 showed 1982 values to be only 7% below the 1974 peak, and therefore by extension, the 7% growth in 1983 would result in values comparable to 1974. Since these estimates (CMA, 1983) probably overestimated growth in Soviet manufacture of CFC-12, world production of CFC's probably did not achieve levels of the peak year (1974) prior to 1984. The uncertainties in the world estimates are substantial, and we must fall back on careful monitoring of the atmosphere to provide the best information on worldwide emissions.

FPP production figures are broken down by use-category and CFC emissions to the atmosphere are then calculated. For each use an estimate has to be made for product lifetime, for rate of loss of CFC during use, and for fate upon disposal. The emission calculations are revised as new information becomes available (Gamlen *et al.*, 1985). For example, the rate of diffusion of CFC 11 from closed-cell foams has been reported recently to be slower than previously estimated (Khalil and Rasmussen, private communication, 1985). The CMA data show that the pattern of usage of CFC 11 and CFC 12 has changed substantially since 1976 with a decline in aerosol usage and an increase in other applications. Delay times between production and eventual release to the atmosphere have therefore grown somewhat.

## SOURCE GASES

Table 3-3. Atmospheric Halocarbons (partial list)

Substance	Measured concentration (pptv)	Time (year)	Est. global industrial production × 10 <sup>6</sup> kg	Year	Reference	Est. atmospheric lifetime years (NAS 1984)
CFC 11 (CCl <sub>3</sub> F)	200	1983	310	1982	1,8	65
CFC 12 (CCl <sub>2</sub> F <sub>2</sub> )	320	1983	444	1982	1,8	120
CFC 13 (CF <sub>3</sub> Cl)	~ 3.4	1980	—	—	10	400
CFC 22 (CHCl <sub>2</sub> F)	~ 52	1980	206	1984	2,7	20
CFC 113	~ 32	1/85	138-141	1984	2,5	90
CFC 114	—	—	13-14	1984	2	180
CFC 115	4	1980	—	—	10	380
CH <sub>3</sub> CCl <sub>3</sub>	~ 120	1983	545	1983	3,11	6.5
CFC 116	~ 4	1980	—	—	10	> 500
CCl <sub>4</sub>	~ 140	1979	~ 830	1983	3,12	50
CH <sub>3</sub> Cl	630	1980	~ 500	1984	3,6	~ 1.5
CH <sub>3</sub> I	~ 1	1981	—	—	9	0.02
CBrClF <sub>2</sub>	~ 1.2	1984	(~ 5?) <sup>‡</sup>	—	4	25
CBrF <sub>3</sub>	~ 1	1984	7-8	1984	2,4	110
CH <sub>3</sub> Br	9.0	1984	—	—	4	2.3
CH <sub>2</sub> BrCl	3.2	1984	—	—	4	—
CHBr <sub>2</sub> Cl	0.9	1984	—	—	4	—
C <sub>2</sub> H <sub>4</sub> Br <sub>2</sub>	~ 1	1984	—	—	4	~ 1
CHBr <sub>3</sub>	~ 2	1984	—	—	4	—

<sup>‡</sup> Estimated release from observed atmospheric increase, uncertain delay between industrial production and release to the atmosphere.

1. CMA, 1984.
2. DuPont, private communication, 1985.
3. ICI, private communication, 1985.
4. Khalil and Rasmussen, 1985a [mean of arctic and antarctic values, fall, 1984].
5. Khalil and Rasmussen, 1985d.
6. Rasmussen *et al.*, 1980.
7. Khalil and Rasmussen, 1981.
8. Cunnold *et al.*, 1983 a, b; Cunnold, 1984.
9. Rasmussen *et al.*, 1982.
10. Penkett *et al.*, 1981.
11. Prinn *et al.*, 1983b; Khalil and Rasmussen, 1984a.
12. Simmonds *et al.*, 1983; Rasmussen and Khalil, 1981.

### Other Halocarbons

Concern over depletion of stratospheric ozone by chlorine is not restricted to CFC-11 and 12 alone. Numerous other halocarbons discussed below contribute to the accumulation of chlorine in the stratosphere. Attention focuses generally on the long-lived CFCs (11, 12, 22, 113, 114) and on CH<sub>3</sub>CCl<sub>3</sub>, which are likely to become important sources of stratospheric chlorine in the next century. CFC-113 represents as much as 15% of the current production of long-lived halocarbons, due to rapid growth occurring since

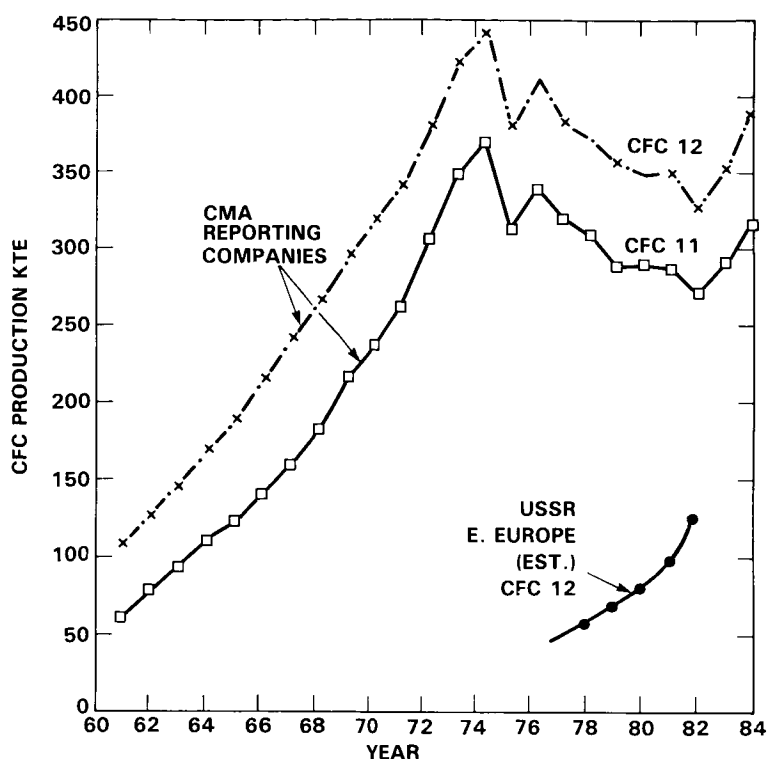


**Figure 3-6.** Chlorofluorocarbon production history for CFC-11 and CFC-12, 1961-84 for CMA reporting companies. Soviet Union/Eastern European production for CFC-12 is estimated separately. USSR production is based on Borisenkov and Kazadov, 1977 with estimates continued by CMA to include Eastern Europe from 1976 through 1982 (CMA, 1984).

1974. If CFC-113 is counted along with CFC-11 and CFC-12, it appears that there has been an overall increase in world-wide production of long-lived CFCs above that of the former peak year, 1974. We now discuss industrial sources of these species.

### CFC 22 ( $\text{CHClF}_2$ )

Refrigeration is the major use of CFC 22 but a significant portion, about 35% of total production, is used as a chemical intermediate to prepare tetrafluoroethylene, which in turn is polymerized to fluoropolymers. Limited CFC 22 production data have been reported for several years. Growth in fluoropolymer production (with little emission of CFC 22 to the atmosphere) accounts for much of the recent growth in CFC 22 production. It has been estimated that  $102$ ,  $163$ , and  $206 \times 10^6$  kg of CFC 22 were produced globally in 1977, 1981, and 1984 respectively (NASA 1979, DuPont, 1983).

### CFC 113 ( $\text{CCl}_2\text{FCClF}_2$ )

CFC 113 is used largely as a solvent to clean and deflux sophisticated electronic assemblies and components. Lower-cost cleaning systems, such as chlorocarbons and aqueous systems, also compete for this application. Historical production data are not available for CFC 113. DuPont (1981) estimated that about  $70$ ,  $79$ , and  $91 \times 10^6$  kg were produced globally in 1977, 1978, and 1979. Production of CFC 113 has increased rapidly in recent years, but its growth may level off as the market matures, and global production in 1984 has been estimated to be about  $140 \times 10^6$  kg (DuPont, private communication, 1985). Its future use is vulnerable to competing systems, changes in electronics technology, and possible requirements to reclaim the solvent.

## SOURCE GASES

Table 3-4. Global Production of CH<sub>3</sub>CCl<sub>3</sub> (excluding USSR and Eastern Europe)

Year	Production/Sales CH <sub>3</sub> CCl <sub>3</sub> (10 <sup>6</sup> kg)	
	ICI (1985) (Production)	Prinn <i>et al.</i> , (1983b) (Sales)
1976	475	—
1977	490	483.6
1978	520	497.5
1979	580	535.5
1980	580	544.2
1981	570	544.2
1982	540	—
1983	545	—

### CFC 114 (CClF<sub>2</sub> CClF<sub>2</sub>)

CFC 114 has limited use as an aerosol propellant of perfumes and colognes, as a refrigerant, and as an intermediate to prepare chloropentafluoroethane (CFC 115). Its production has remained relatively constant over the past 6 years at about  $13 \times 10^6$  kg (ICI, private communication, 1985).

### Methyl Chloroform (CH<sub>3</sub>CCl<sub>3</sub>)

Stabilized 1,1,1-trichloroethane (methyl chloroform) has been marketed since the early 1960's. Its principal use has always been the industrial degreasing of metallic or metaloplastic pieces. It is widely used for cold cleaning processes in the engineering industry. It is also used as a solvent in adhesives, varnishes and paints where low flammability and low toxicity are important. Sales of methyl chloroform grew rapidly in the 1960's and early 1970's when it replaced tri- and perchloroethylene and CCl<sub>4</sub> in many industrial applications. This replacement process is virtually complete in Western countries. Estimated global sales have leveled off since 1979, due at least in part to increasing efficiency of usage and to solvent reclamation (see Table 3-4).

### Carbon Tetrachloride (CCl<sub>4</sub>)

It is difficult to define the global capacity for production of carbon tetrachloride because it is co-produced with other chemicals. One industry estimate puts current capacity at  $1150 \times 10^6$  kg per annum. Carbon tetrachloride is used predominantly as a chemical intermediate in the production of CFCs 11 and 12, leading to relatively little emission of CCl<sub>4</sub> to the atmosphere. Using the reported CMA figures for 1983 production of CFCs, the quantity of CCl<sub>4</sub> used in this application is inferred to be  $778 \times 10^6$  kg. Various estimates put other uses and fugitive emissions of CCl<sub>4</sub> at 5–10% of total sales. This would indicate that the 1983 total production (excluding USSR, Eastern Europe and People's Republic of China) was  $830 \times 10^6$  kg, of which only  $40\text{--}80 \times 10^6$  kg would be likely to be emitted to the atmosphere (cf. Simmonds *et al.*, 1983). Sales of CCl<sub>4</sub> for direct use have declined significantly in the West because of concerns about its

toxicity. A small fraction is still used as a solvent in chemical and pharmaceutical production processes. Use as a grain fumigant is declining. However, there is some indication that release rates may still be substantial in Eastern Europe, the USSR or China. Annual release of at least  $90 \times 10^6$  kg is needed to explain atmospheric data for  $\text{CCl}_4$  from ALE (Simmonds *et al.*, 1983).

### Brominated Compounds

Atmospheric bromine (Table 3-3) is dominated by methyl bromide ( $\text{CH}_3\text{Br}$ ) and bromoform ( $\text{CHBr}_3$ ). The bromoform is believed to be mainly of natural origin, and  $\text{CH}_3\text{Br}$  about 50% natural. As discussed above, anthropogenic emissions of ethylene dibromide (EDB) and  $\text{CH}_3\text{Br}$  are probably declining. They have been used as grain fumigants, and both are emitted by automobiles using leaded gasoline.

As discovered earlier, two long-lived industrial brominated compounds (Halons 1211 and 1301) are currently of greater interest due to their rapidly increasing usage.

#### Halon 1211 ( $\text{CBrClF}_2$ )

The relatively high boiling point and low vapor pressure of Halon 1211 make it ideal for use in portable fire extinguishers. Flame extinction can be very rapid due to the high activity of Br atoms as combustion inhibitors. The growth of the Halon 1211 market has been as a replacement agent for  $\text{CCl}_4$  and  $\text{CO}_2$  extinguishers. Halon 1211 has been commercially available for more than 20 years but world sales did not reach significant volumes until the early 1970's. One industrial estimate (ICI, private communication, 1985) notes that the initially high growth rates of the 1970's have not been maintained. However, no data on current production for Halon 1211 are available from industry sources. The atmospheric data discussed in Section 3.1.1 imply release of about 5 kt per annum and rapid growth.

#### Halon 1301 ( $\text{CBrF}_3$ )

Halon 1301 is used almost exclusively as a fire extinguisher in total-flooding applications where water and carbon dioxide are unacceptable, such as in computer rooms, marine engines, art museums, etc. A small amount of the chemical is used as a refrigerant in special applications. DuPont (1978) estimated 1976 U.S. production to be about 1.4 kt which suggests 1976 global production was 1.4–3.0 kt. World production in 1984 was estimated to be 7–8 kt (DuPont, private communication, 1985). A large portion of increased use over recent years was for the fire protection of large oil and gas pipeline projects, and an industry estimate (DuPont, private communication, 1985) expects slower growth in fire protection applications of Halon 1301 in the future.

#### Methyl Chloride ( $\text{CH}_3\text{Cl}$ )

It is generally accepted that the industrial production of methyl chloride is far outweighed by releases from the oceans and from burning vegetation. Recent estimates of the total source are 2–5 MT per year (see for example, Logan *et al.*, 1981; Crutzen *et al.*, 1983), based on calculation of global reaction rates with OH. One estimate puts annual industrial production worldwide at 0.5 MT, or less than ~25% of global sources (ICI, private communication, 1984). Quantitation of the major sources is highly uncertain at present, and human activity (biomass burning) is likely to be a major contributor.

### 3.1.3 Discussion

#### Atmospheric Inventory

For a certain category of trace gases, observations of the changing atmospheric burden may be used to derive a globally integrated source for the gas. A requirement for such analysis is that the uncertainty in calculated atmospheric losses of the gas be much less than new releases to the atmosphere. These condi-

## SOURCE GASES

tions are applicable to most halocarbons whose atmospheric concentrations are far from steady-state levels, due either to long atmospheric lifetimes ( $\sim 100$  yrs.) and/or to rapid growth in release rates.

The CFCs 11 ( $\text{CFCl}_3$ ) and 12 ( $\text{CF}_2\text{Cl}_2$ ) have received the most attention. Their long lifetimes allow atmospheric observations to record cumulative release with moderate accuracy. Rowland (1982) pointed out disparities between estimated release for CFC-12 and the observed increase in atmospheric concentrations, based on surface measurements at two stations (Oregon and South Pole) for limited times over several years. This analysis has been confirmed by continued observations by more researchers using expanded observing networks. The observed atmospheric trend in CFC-11 is relatively consistent with CMA estimates of release (Cunnold *et al.*, 1983a; Fraser *et al.*, 1983a), whereas CFC 12 appears to require a substantial source from the USSR and Eastern Europe (Cunnold *et al.*, 1983b). The increase in the Eastern European source must, however, be less than the 18% compounded annual growth assumed since 1975 in pre-1983 CMA projections.

Inventories of methyl chloroform ( $\text{CH}_3\text{CCl}_3$ ) and carbon tetrachloride ( $\text{CCl}_4$ ) have also been analyzed using the ALE data (Prinn *et al.*, 1983b; Simmonds *et al.*, 1983). The global distribution and trend are consistent with previous flask measurements of  $\text{CH}_3\text{CCl}_3$  (Rasmussen and Khalil, 1981a,c,d). Global emissions may be determined for these gases with somewhat less accuracy than for the CFCs, since they are closer to a steady-state between emission and atmospheric loss. As noted earlier, the atmospheric lifetime for  $\text{CH}_3\text{CCl}_3$  is relatively short, 6.5–10 years (Khalil and Rasmussen, 1984a; ALE data updated) and thus photochemical losses (uncertain to at least  $\pm 25\%$ ) play a more dominant role in the global annual inventory than for CFC's. ALE analysis notes that industry estimates of  $\text{CH}_3\text{CCl}_3$  releases are consistent with observations over the 5 years of the ALE record if some delay in release of early production is considered in the early years. The derived range of lifetimes for  $\text{CH}_3\text{CCl}_3$ , 6.5–10 years, implies emissions of 500–600 kt per year.

Data for  $\text{CH}_3\text{CCl}_3$  from the ALE program have helped to define the global loss rates for other gases removed from the atmosphere by reaction with the OH radical, e.g.  $\text{CH}_4$ . The idea behind this analysis was proposed by Lovelock (1977) and followed up by a variety of authors (Crutzen and Fishman, 1977; Derwent and Eggleton, 1981; Makide *et al.*, 1981; Logan *et al.*, 1981). A lifetime of 5.5 yr. is calculated by the model of Logan *et al.* (1981), using updated chemical reaction rates, reasonably consistent with the ALE result of 6.5 yr. from the inventory method. Models using updated chemical rates may be expected therefore to provide fairly good estimates for the global OH distribution and hence for the removal rates of important trace gases such as  $\text{CH}_4$  (see below).

Global burdens of  $\text{CCl}_4$  are also close to steady state, despite a longer atmospheric lifetime ( $\sim 50$  yrs.), because the gas has a much longer history of sustained atmospheric release (Simmonds *et al.*, 1983). In this case industry estimates of release in the reporting (i.e., Western) countries can account for only half of the 90 kt per year needed to maintain the observed atmospheric increase.

As discussed above, CFC-113 ( $\text{C}_2\text{Cl}_3\text{F}_3$ ) is increasing rapidly in the earth's atmosphere. Recent measurements at Barrow, Alaska since mid-1983 yield a growth rate of  $14 \pm 1\%$   $\text{yr}^{-1}$ , while an earlier time-series at the South Pole (1/79–1/82) gave  $\sim 10\%$   $\text{yr}^{-1}$  (Khalil and Rasmussen, 1985b). Industrial production data (see above) suggest rapid growth in the manufacture of CFC-113,  $\sim 13\%$   $\text{yr}^{-1}$  during 1977–1979 and  $\sim 10\%$   $\text{yr}^{-1}$  1979–1984. The global burden is far from a steady state distribution and large increases in the atmospheric burden appear inevitable. Hence, even though present concentrations are less than 10% of CFC-11 and CFC-12, industrial emissions and atmospheric burdens of CFC-113 would appear to merit careful scientific scrutiny in the next 10 yrs.

The observed atmospheric growth rate of  $\text{CHClF}_2$  reported for the late 1970's (11–12%  $\text{yr}^{-1}$ , Khalil and Rasmussen, 1981) is quite consistent with the industrial production data cited above for this same period. Whether slower growth of industrial production in the present decade ( $\sim 8\% \text{ yr}^{-1}$  for 1981–1984, see above) is reflected in a turn-down in the rate of atmospheric increase has not yet been reported. If the change in end-use, away from refrigeration toward Teflon polymer production, has actually resulted in reduced fugitive emissions, a corresponding reduction in the atmospheric growth rate should now be discernible. However, use in the USSR and Eastern Europe is unknown and could be significant. CFC-22 is a major atmospheric halocarbon (Table 3-1) and it also merits careful scrutiny.

Six years of data at the South Pole (Khalil and Rasmussen, 1985c) indicated that atmospheric  $\text{CBrClF}_2$  (Halon 1211) is increasing very rapidly at  $\sim 22 (\pm 5)\% \text{ yr}^{-1}$ . The atmospheric level in late 1984 was 1.1 pptv at the South Pole, and 30% higher in the Arctic, consistent with production and use in high technology, fire-extinguishing applications in the industrialized Northern Hemisphere. Continued growth at the present rate for another decade would bring  $\text{CBrClF}_2$  levels to  $> 10$  pptv, surpassing identified natural sources of stratospheric bromine. Trend data for other atmospheric bromine gases have not yet been reported but rapid increases for  $\text{CF}_3\text{Br}$  might be anticipated based on estimates of production. Khalil and Rasmussen (1985) estimate total gaseous (organic) bromine at a current level 22 pptv in late 1984, of which perhaps 20–50% is of anthropogenic origin.

The recent advent of widespread use for  $\text{CBrClF}_2$  and  $\text{CF}_3\text{Br}$  ensure substantial growth in future atmospheric burdens, since lifetimes are long, 25 yr. for  $\text{CBrClF}_2$  and 100 yr. for  $\text{CF}_3\text{Br}$  (Molina *et al.*, 1982; Prather *et al.*, 1984), and present burdens are therefore much smaller than steady-state values. The atmospheric levels and industrial production of Halon fire suppressants therefore should be monitored closely, even though accumulation of damaging levels (50–100 ppt) would take a long time (Prather *et al.*, 1984).

### Regional Relative Source Strengths

Emissions of halocarbons from major source regions may be derived from the relative enhancement of trace gas concentrations in air masses influenced by these source areas. The sampled air mass may be viewed as an integrator of emissions on a regional scale. Such studies allow direct verification of source estimates. For example, a recent study attempted to derive the urban, combustion-related source of methane from the elevated concentrations of  $\text{CH}_4$  and CFC 11 in city centers around the world (Blake, *et al.* 1984).

Analysis of the reported ALE data by Prather (1985) has shown that, with a sufficient number of observations during pollution episodes, accurate relative source strengths may be derived for European emissions of CFC-11, CFC-12,  $\text{CCl}_4$  and  $\text{CH}_3\text{CCl}_3$  using data from Adrigole, Ireland. The temporal correlation of variations in the five ALE trace gases provides information on both the spatial association of sources and on the duration and recurrency of pollution events. Atmospheric measurements must be made at high frequency in order to obtain meaningful results using this analysis.

At Adrigole all the halocarbons exhibit similar patterns: the full width at half-height, of a pollution event averages 2 days although enhanced concentrations may persist for nearly a week. These events recur at roughly 5 to 8 day intervals. Variations of concentrations of the major halocarbons (CFC-11, CFC-12, and  $\text{CH}_3\text{CCl}_3$ ) are highly coherent. Evidently, major pollution events accumulate quantitatively comparable emissions of these gases. Carbon tetrachloride, on the other hand, is not fully coherent with the other halocarbons. One interpretation would place major  $\text{CCl}_4$  sources in spatially distant regions (e.g., Eastern Europe) as compared with those of major CFC sources (e.g., Western Europe).

## SOURCE GASES

European source strengths for CFC-12,  $\text{CH}_3\text{CCl}_3$ , and  $\text{CCl}_4$ , relative to that for CFC-11, are reported in Table 3-5, which also includes results of similar analyses for ALE data from Cape Meares, Oregon and Cape Grim, Tasmania (Prather, 1985). These latter two stations record pollution events less often and of smaller magnitude than observed at Adrigole, making the analyses there more uncertain. The data show that release patterns for the CFCs are similar for Europe, Western U.S. and Australia although Australian releases of CFC-12 are noticeably smaller with respect to CFC-11. More importantly, the global inventory for CFCs indicate a substantially larger source of CFC-12, relative to CFC-11, than is found by time series analysis of ALE data for any station. Since the effluents from the Soviet Union and developing countries are not sampled by ALE stations it appears that these countries play a relatively important role in world use of CFC-12, confirming suggestions made in earlier studies (Rowland, 1982; Cunnold *et al.*, 1983b) of the global inventory.

Emissions of  $\text{CH}_3\text{CCl}_3$ , measured relative to CFC-11, are clearly variable among the continents: Europe is about equal to the global mean value, the Western U.S. is a factor of 1.3 above global mean, and Australia a factor of 2 below. Carbon tetrachloride shows a relatively large European source with respect to CFC-11, but not large enough to account for the mean global source. Since the U.S. and Australia appear to contribute still lesser relative amounts of  $\text{CCl}_4$ , relative to CFC-11, we may conclude, as in the case of CFC-12, that substantial additional sources must exist in the USSR, China, Japan, or developing countries distant from ALE sites.

### Future Projections of Industrial Halocarbon Production

There is a need for projections of trends in atmospheric concentrations of trace gases into the future in order to calculate possible future changes in the stratosphere. There is no bar to developing forecasts for the next hundred years, but it is doubtful whether the result is meaningful. Projections require not only a complete understanding of the processes leading to the emission of a trace species and its atmospheric fate, but also detailed economic projections which must incorporate forecasts of population and GNP changes,

**Table 3-5.** Relative Molar Source Strengths Derived by Prather (1985) from Cross-Covariances of ALE Data (See Text for ALE References)

	CFC-11	CFC-12	$\text{CH}_3\text{CCl}_3$	$\text{CCl}_4$	$\text{N}_2\text{O}$
ALE (Ireland)*	1	1.1	1.8	0.28	30-70
ALE (Oregon)	1	1.2 ± .2	2.5 ± .3	0.15 ± .05	x
ALE (Tasmania)	1	0.9 ± .2	0.9 ± .2	0.15 ± .04	x
Global Estimate (flux in Gg/yr)	1 (265)	1.76 (410)	1.94 (500)	0.34 (100)	52 (2800 of N)

\* Error estimates are ± 10% for all but  $\text{N}_2\text{O}$  (see text).  
 Calibration factors for the ALE data have not been applied.  
 $\text{N}_2\text{O}$  flux estimates corresponds to 0.2% per annum.  
 $\text{N}_2\text{O}$  sources are undetectable (x) at Oregon and Tasmania.

regional development, and changes in technology. (Imagine a projection for today, rendered in 1885.) For gases of solely industrial origin such as CFCs, assessment must be made of the future availability of raw materials, capital for investment, possible new technology, and external constraints such as regulations, wars, famines, and economic depressions. We believe that it is not possible to render reliable, accurate long-term forecasts of this nature.

Forecasts for CFCs 11 and 12 up to 1995 have been prepared by CEFIC (European Fluorocarbon Technical Committee (EFCTC), A CEFIC Sector Growth Halocarbon Trend Study, 1983–1995). These forecasts cover Western Europe, Australia, New Zealand and South Africa and, in a separate forecast, the rest of the world (ROW) excluding North America, Japan and Eastern Bloc countries; i.e. the forecast covers areas of the world where European CFC producers have detailed market knowledge.

Although the CEFIC forecast is not globally complete it adds some perspective to a global view of CFC 11 and 12 usage in the next decade. High growth rates for CFCs 11 and 12 seen in OECD countries in the 1960's and 70's are not expected to return, even in developing countries where current demand is small. The overall growth rate is projected to be  $\sim 1.5\%$  per annum over the next ten years. Slightly higher growth rates in developing countries are not expected to significantly change the overall distribution of demand over the next ten years. The reliability of this forecast must be viewed in the context of recent events. Production of CFC-11 and CFC-12 by reporting companies increased 16% from 1982 to 1984 (Figure 3-6). This was a period of high economic growth in the USA and Japan, and economic stagnation in Europe, and one might speculate that growth would have been even faster if European economics were more robust. Thus world production can evidently increase very rapidly in favorable economic circumstances, in this case, five times faster than the regional CEFIC projections.

Projections are notoriously unreliable even over a short time span (less than 10 years). For example, several groups in the late 1970's made projections of the future growth of CFCs 11 and 12 in Western economies, ranging from 3–6% per year (Rand, 1980; SRI, 1982; OECD, 1983) whereas reported production for 1979–83 was in fact static (Figure 3-6). The latest Rand report (1986) estimates about 5% per year growth for CFC 11 and 2.6% per year for CFC 12 through 1990. Their estimates for long-term growth (through 2075), based on a variety of assumptions, range from 0.6–3% per year. Long term concentrations derived from these estimates span a very wide range, and any of the scenarios would appear to be feasible. It does not seem possible to single out any particular scenario as probable. Thus a range of assumptions needs to be explored in any assessment document. The resulting atmospheric conditions will span a correspondingly wide range, and a scientific assessment must concentrate on determining which part of the range presents significant environmental risks.

## 3.2 NITROUS OXIDE (N<sub>2</sub>O)

### 3.2.1 Global Atmospheric Trend and Distributions

The mean global concentration of N<sub>2</sub>O is about 300 ppbv, with very little geographic variation ( $< 1\%$  except near source regions) (Pierotti and Rasmussen, 1977). Nitrous oxide has a long atmospheric lifetime,  $\sim 150$  yrs., and large natural sources, hence atmospheric trends are expected to be small. A series of papers in the 1970's predicted important anthropogenic sources for N<sub>2</sub>O (for example, McElroy, 1976; Crutzen and Ehhalt, 1977; McElroy *et al.*, 1977; Weiss and Craig, 1976; Pierotti and Rasmussen, 1976), and suggested possible increases for the global concentration of the gas. Weiss (1981) presented convincing evidence for a steady increase of about  $0.7 \text{ ppb yr}^{-1}$  during the period 1977–1980, confirming these

## SOURCE GASES

ideas. Although the rate of increase is indeed small ( $0.2\% \text{ yr}^{-1}$ ), implications for the atmosphere are very significant (see below).

Recent data for  $\text{N}_2\text{O}$  from the ALE program are shown in Figure 3-7, along with trends observed at each station. The interhemispheric difference is small for  $\text{N}_2\text{O}$  ( $\sim 1$  ppb, N-S) (Weiss, 1982), but rates of increase appear to be larger in the Northern Hemisphere ( $0.25\text{--}0.7\% \text{ yr}^{-1}$ ) than in the Southern Hemisphere ( $0.1\text{--}0.2\% \text{ yr}^{-1}$ ). If shown to be statistically significant, this pattern would be counter to that for CFCs, indicating an increasing imbalance between northern sources and global sinks.

Recently, enhanced concentrations of  $\text{N}_2\text{O}$  have been observed in the lower atmosphere of Amazonia (Figure 3-8), a major source region as discussed below. The observed enhancement near the source is quite small, due to the large atmospheric burden of the gas. Nevertheless, this pilot study shows that considerable information about emissions from a large area can be derived from observations of geographical gradients. Measurements of temporal and spatial variations of  $\text{N}_2\text{O}$  could yield important insights into the atmospheric cycle of the gas, if the precision of routine measurements could be improved from the current value of  $\sim 1$  ppb to about  $0.1$  ppb (cf. Prather, 1985). It appears possible to develop technology for this purpose (e.g. using diode inset technology), and an important contribution to atmospheric science would result.

### 3.2.2 Sources and Sinks

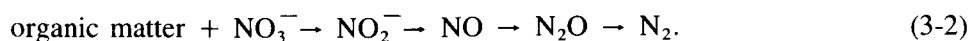
#### A. Natural Processes

Nitrous oxide is removed from the atmosphere mainly by photolysis in the stratosphere and secondarily by reaction with  $\text{O}(^1\text{D})$ .



The rate for destruction is calculated to be  $10.5 (\pm 3) \times 10^6$  tons  $\text{N yr}^{-1}$ , using observed distributions (e.g. Goldan *et al.*, 1980) and calculated rates for photochemical reactions in the stratosphere. The rate of increase in the atmosphere, currently  $0.7 \pm 0.1$  ppb  $\text{yr}^{-1}$ , corresponds to  $3.5 \times 10^6$  tons  $\text{N yr}^{-1}$ . Total emissions for  $\text{N}_2\text{O}$  amount therefore to  $14 \pm 3 \times 10^6$  tons  $\text{N yr}^{-1}$ . The magnitude of the annual increase, though small ( $0.2\%$  per year), implies a discrepancy in excess of  $30\%$  between current sources and sinks, (see Table 3-6). Since  $\text{N}_2\text{O}$  is the dominant precursor of stratospheric odd nitrogen, we expect gradual increases in the levels of  $\text{NO}_x$  in the stratosphere, adding up eventually to at least  $30\%$  above current levels.

Nitrous oxide is an obligatory free intermediate in microbial denitrification and other dissimilatory nitrogen reduction processes (Payne, 1983),



Sequential reduction of the nitrogen atom in (3-2) provides a respiratory electron sink for a wide variety of bacteria under anaerobic conditions. Denitrification is most often observed in environments isolated

SOURCE GASES

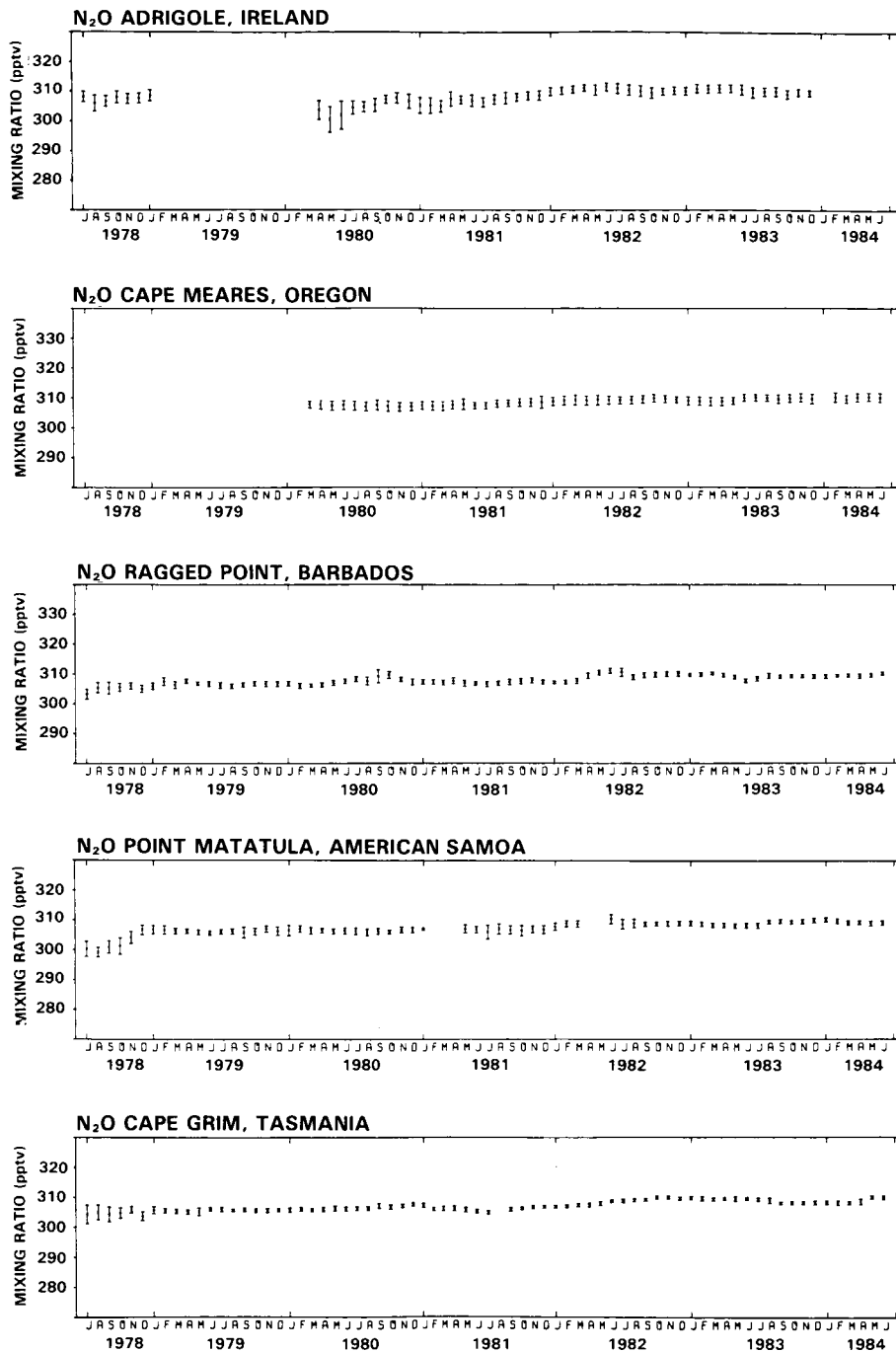
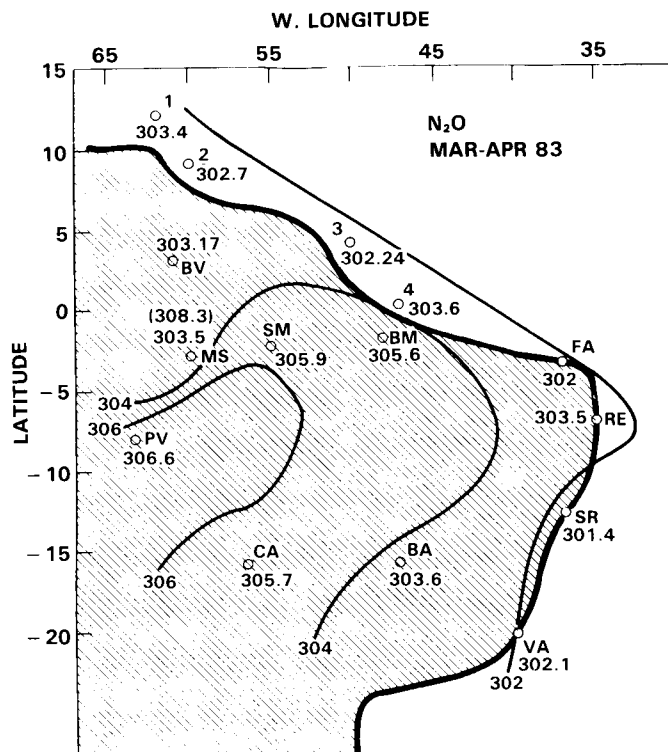


Figure 3-7. ALE/GAGE network data. As in Figure 3-1 but for N<sub>2</sub>O measured on Porasil column with a calibration factor of 0.92 and with the 1978-1983 measured trends being 0.77, 0.27, 0.24, 0.09 and 0.18% per year at the 5 stations.

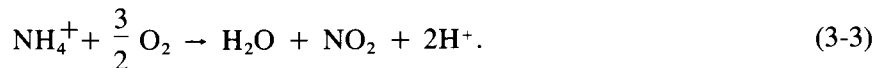
## SOURCE GASES



**Figure 3-8.** Isopleths of N<sub>2</sub>O mixing ratio (ppbv) over Brazil, March-April 1983 (Wofsy, personal communication, 1985).

from atmospheric oxygen and supplied with abundant sources of oxidizable detrital material; organic-rich sediments, flooded soils, and closed ocean basins, for example. Such systems were thought at one time to be the principal sources for atmospheric N<sub>2</sub>O, but this idea turned out to be incorrect. It has been observed that static anaerobic ecosystems contain typically very low concentrations of N<sub>2</sub>O, indicating that virtually all the N<sub>2</sub>O produced in denitrification is consumed *in situ* (Cohen and Gordon, 1978; Hashimoto *et al.*, 1983; Blackmer and Bremner, 1976; Firestone *et al.*, 1979; Firestone and Tiedje, 1979). These results reflect the ability of microorganisms to use N<sub>2</sub>O as an oxidant in systems which are prevented from exchanging gases with the environment.

Significant quantities of N<sub>2</sub>O are produced, however, by a variety of aerobic or partially aerobic environments, especially soils. Intense emissions are associated with rapid oxidation of organic matter or of reduced N in fertilizer (Bremner and Blackmer, 1978; Freney *et al.*, 1979; Hutchinson and Mosier, 1976; Breitenbeck *et al.*, 1980; Seiler and Conrad, 1981; Duxbury *et al.*, 1982; Slemr and Seiler, 1984; Robertson and Tiedje, 1984), and it appears primary nitrification is a major pathway for production of N<sub>2</sub>O (Yoshida and Alexander, 1970),



Nitrification is a key step in the aerobic degradation of organic detritus. It is carried out by a small group of autotrophic bacteria, and the process yields 1-3 molecules of N<sub>2</sub>O per 1000 nitrite molecules under fully aerobic conditions. The yield of N<sub>2</sub>O increases dramatically under low-oxygen conditions, rising to 10% of the nitrite production rate for partial pressures of O<sub>2</sub> below 0.01 atm (Goreau *et al.*, 1980).

**Table 3-6.** Nitrous Oxide Sources and Sinks (1984 concentration 303 ppb)  
(from McElroy and Wofsy, 1985)

A. <i>Atmospheric burden</i> ( $10^6$ tons as N)	1500
B. <i>Sinks + accumulation</i> ( $10^6$ tons N yr <sup>-1</sup> )	
stratospheric photolysis + reaction with O( <sup>1</sup> D)	10.5 ± 3
accumulation (0.7 ppb yr <sup>-1</sup> )	3.5 ± 0.5
total	14.0 ± 3.5
C. <i>Sources</i> ( $10^6$ tons N yr <sup>-1</sup> )	
oceans	2 ± 1
combustion: coal + oil, 4 ± 1	
biomass, 0.7 ± 0.2	4.7 ± 1.2
fertilized agricultural lands	0.8 ± 0.4
grasslands	< 0.1
~ boreal and temperate forests	0.1 - 0.5
tropical and subtropical forests and woodlands (extrapolation of soil data)	7.4 ± 4
total	15.3 ± 6.7
D. <i>Tropical Contribution</i> ( $10^6$ tons N yr <sup>-1</sup> )	
biomass burning	0.6
soil emissions	7.4
total	8.0

While it is clear that aerobic soils and waters are major sources of atmospheric N<sub>2</sub>O, reductive pathways may nevertheless be important. Studies by Robertson and Tiedje (1984) showed active denitrification in aerobic soil cores from forest environments. Using an oxygen microprobe, Sexstone *et al.* (1985) showed that soil aggregates contain active, anaerobic microsites where denitrification proceeds. This direct demonstration confirms ideas held by soil scientists for many years (cf. Arnold, 1955). Hence a significant source of N<sub>2</sub>O may be denitrification along a microscopic O<sub>2</sub> gradient, from which escape of N<sub>2</sub>O may be relatively rapid. Important modification of the N<sub>2</sub>O source may occur therefore when forests are converted to agriculture, since soil structure and organic content is radically changed. The nature of the effect on N<sub>2</sub>O has not yet been elucidated, however.

Soils in tropical forests emit N<sub>2</sub>O at rates far in excess of soils in most other environments, as shown by recent measurements from forest sites in the USA, Germany, Brazil, Ecuador, and elsewhere (see, for a review, Seiler and Conrad, 1985). Table 3-7 provides a summary of existing data for soils. Release rates for tropical forests average about  $2 \times 10^{10}$  molecules N<sub>2</sub>O cm<sup>-2</sup> sec<sup>-1</sup>, as compared for example, to  $1-2 \times 10^9$  cm<sup>-2</sup> sec<sup>-1</sup> in New Hampshire (Keller *et al.*, 1983, updated for other tropical sites, 1985). It is this large source whose signature is observed over South America, although biomass burning may

## SOURCE GASES

also contribute (Crutzen *et al.*, 1985, see below). Since the tropical forests of the world are being rapidly modified, this large natural source of N<sub>2</sub>O is likely to be changing. It would be of great interest to discover in what direction these changes might go.

### B. Anthropogenic Processes

Concerns arose during the 1970's (for example, McElroy *et al.*, 1977; Crutzen and Ehhalt, 1977) that use of nitrogenous fertilizer would artificially enhance biogenic emissions of N<sub>2</sub>O, leading to increased concentrations in the atmosphere. Recent investigations indicate that fertilization with NH<sub>4</sub><sup>+</sup> or urea does indeed stimulate emission of N<sub>2</sub>O, although the yield is relatively small (Hutchinson and Mosier, 1976; McKenney *et al.*, 1978; Breitenbeck *et al.*, 1980; Seiler and Conrad, 1981). Between 0.1 and 0.5% of the reduced nitrogen in fertilizer is converted to N<sub>2</sub>O within a few weeks of application, with highest efficiency for conversion at highest rates of fertilization. The ultimate release of N<sub>2</sub>O after fertilization could be higher, however, since fixed nitrogen is likely to be assimilated into organic material and re-oxidized a number of times before it is lost eventually from the soil.

**Table 3-7.** Nitrous Oxide Fluxes from Soils\* (Global mean value =  $2 \times 10^9 \text{ cm}^{-2} \text{ sec}^{-1}$ )

#### 1. Undisturbed soils

Mean Flux ( $10^9 \text{ cm}^{-2} \text{ sec}^{-1}$ )	Location	Environment	Duration	Reference
0.45, 1.0	New Hampshire	Northern Hardwood Forest	1 yr.	Keller <i>et al.</i> , 1983 Goreau, 1981
17	75 km N.E. of Manaus, Brazil	Tropical Moist Forest	8 mos., 4 dates	Keller <i>et al.</i> , 1985 Goreau and Demello, 1985
25	Puerto Rico	Subtropical Moist Forest	1 day, dry season	Keller <i>et al.</i> , 1985
5.7	Colorado	Natural Shortgrass Prairie	62 days, June	Mosier <i>et al.</i> , 1981
3.0	Louisiana	Salt, brackish and fresh marshes	2 yr.	Smith <i>et al.</i> , 1983
6.1	New York State	Northern Hardwood Forest, Mineral soil	1 yr.	Duxbury <i>et al.</i> , 1982
6.8	Florida Everglades	organic soil	1 yr.	Duxbury <i>et al.</i> , 1982

**Table 3-7.** Nitrous Oxide Fluxes from Soils\* (Global mean value =  $2 \times 10^9 \text{ cm}^{-2} \text{ sec}^{-1}$ ) — Continued  
2. Agricultural and disturbed soils

Mean Flux ( $10^9 \text{ cm}^{-2} \text{ sec}^{-1}$ )	Location	Environment	Duration	Reference
32	75 km N.E. of Manaus, Brazil	clearcut forest	8 mos.,	Keller <i>et al.</i> , 1985 Goreau and DeMello, 1985
8.2	Iowa	Soybean field	1 yr.	Bremner <i>et al.</i> , 1980
8.6	Iowa	farmland, fallow	June	Breitenbeack <i>et al.</i> , 1980
17.7	Colorado	cornfield, fertilized	growing season	Hutchinson and Mosier, 1976
2.9	California	cornfield	June, 1977	McKenney <i>et al.</i> , 1978
7.1	California	cornfield fertilized	June, 1977	McKenney <i>et al.</i> , 1978
11.2	California	tobacco field	June, 1977	McKenney <i>et al.</i> , 1978
51	California	tobacco field, fertilized	June, 1977	McKenney <i>et al.</i> , 1978
-2.7	U.K.	Field, fertilizers Perennial ryegrass	Aug.-Oct.	Ryden, 1981
430-1500	Florida Everglades	cultivated organic soils		Terry <i>et al.</i> , 1981
3.6	Canberra, Australia	clovergrass	5 mos.,	Freny <i>et al.</i> , 1979
19	New York State	alfalfa, fertilized cornfields (mineral soils)	1 yr.	Duxbury <i>et al.</i> , 1982

\*Table prepared by M. Keller

## SOURCE GASES

Combustion introduces another important anthropogenic source of N<sub>2</sub>O. Pierotti and Rasmussen (1976) and Weiss and Craig (1976) observed enhanced N<sub>2</sub>O in power plant plumes, and they measured the N<sub>2</sub>O/CO<sub>2</sub> ratio from coal and oil-fired plants. They argued that combustion of coal could be the dominant anthropogenic source of N<sub>2</sub>O. Crutzen *et al.* (1979) reported excess N<sub>2</sub>O in smoke plumes from biomass burning. Recent kinetic studies (Perry, 1984) have shown that N<sub>2</sub>O is produced in flames from fuel nitrogen by the rapid reaction,



Note that the NCO molecule is also the precursor for much of the NO<sub>x</sub> from combustion, by reactions with O<sub>2</sub> or O, and one might therefore expect a relationship between emissions of N<sub>2</sub>O and NO<sub>x</sub>. A recent investigation by W.M. Hao (Harvard University, Ph.D. thesis, 1985) confirms such a relationship in commercial power plant emissions and supports the views of Weiss and Craig, and of Pierotti and Rasmussen on the potential importance of coal-fired plants, since coal is a fuel rich in organic nitrogen. A preliminary report on N<sub>2</sub>O from biomass burning (Crutzen *et al.*, 1979) indicated very high emissions of N<sub>2</sub>O, but the same authors lowered their estimate by a factor of 10 in a recent article (Delany *et al.*, 1985a). Emissions from biomass burning now appear to be consistent with the nitrogen content of the fuel.

Table 3-6 summarizes current understanding of sources for atmospheric N<sub>2</sub>O (from McElroy and Wofsy, 1985). Estimates for the marine source are based on the nitrification process (Elkins *et al.*, 1978; Cohen and Gordon, 1979) using observations of accumulation of N<sub>2</sub>O and depletion of O<sub>2</sub> in marine waters, supported by extensive data showing small mean supersaturations for N<sub>2</sub>O dissolved in surface waters of the world's oceans (R. Weiss, private communication, 1983). The value for combustion is derived from the data discussed above, scaled to NO<sub>x</sub> emissions data from fossil fuel combustion and biomass burning (Seiler and Crutzen, 1980; Hao, 1985). The entry for fertilized agricultural lands assumes application of chemical fertilizer at the rate of 40 × 10<sup>6</sup> tons N yr<sup>-1</sup> and a similar rate for use of manures, with an overall yield for N<sub>2</sub>O of 1 ± 0.5%, based on the soil studies cited above. The value for forests reflects an average of measurements of forest soils in Europe, the USA, Puerto Rico, Ecuador and Brazil.

### 3.2.3 Discussion

It appears that anthropogenic processes account for about one third of current emissions. The table (3-6) implies a pre-industrial concentration of N<sub>2</sub>O (245-275 ppb) approximately 10-20% lower than today (304 ppb). Weiss (1981) has interpreted his atmospheric N<sub>2</sub>O data, including unpublished results for the period 1961-78, to estimate a slightly higher preindustrial N<sub>2</sub>O level, in the range 280-290 ppbv. Future studies of air bubbles in polar ice cores should eventually provide a history of atmospheric N<sub>2</sub>O for the period before the modern era of measurements. Preliminary data presented by Pearman *et al.* (1985) indicate an increase of 25 ppb from 1600 AD to the present.

The global N<sub>2</sub>O abundance is evidently lower than the steady-state value for current emissions. If the present pattern of emissions persisted, the abundance of atmospheric N<sub>2</sub>O would grow slowly to about 400 ppb. Khalil and Rasmussen (1983b) have estimated that atmospheric N<sub>2</sub>O will reach 380 ppbv about 50 years from now; likewise Ramanathan *et al.* (1985) estimated N<sub>2</sub>O levels of 375 ppbv by the 2030. However, there is little reason to project that emissions should remain constant in the future. Sources associated with combustion and with intensive agriculture are likely to increase, and we might expect temporarily increased fluxes of N<sub>2</sub>O from tropical forests disturbed by exploitation. On the other hand, the source from crop land and pasture may be smaller than from undisturbed systems. A much improved understanding is needed to predict future emissions of N<sub>2</sub>O and studies of tropical forests and industrial and agricultural sources are clearly important to this aim.

### 3.3 OXIDES OF NITROGEN

#### 3.3.1 Distribution and Trends

Oxides of nitrogen in the troposphere have an important, though indirect influence on the stratosphere by interacting with the chemistry of tropospheric radicals (i.e. OH) and by influencing biological activity in important ecosystems. The lifetime of odd nitrogen in the troposphere is short (1-7 days) and sources are geographically concentrated. Sinks are also variable in time and space; removal mechanisms are associated in part with photochemical activity and in part with wet and dry deposition. Hence ambient concentrations fluctuate over a wide range. The global distribution is highly complex, and poorly determined, and there is no direct information about trends. It may be inferred, however, that concentrations have probably increased substantially in important regions of the atmosphere (see below) due to anthropogenic activity.

Lowest concentrations of  $\text{NO}_x$  are found in the remote marine boundary layer, e.g. the central Pacific Ocean where NO mole fractions are only a few parts per trillion (McFarland *et al.*, 1979) and total  $\text{NO}_x$  (=NO +  $\text{NO}_2$ ) may be inferred to be 10-15 ppt. Measurements of  $\text{NO}_2$  by Noxon (1983) at 3 km in the same region indicate somewhat higher concentrations of this gas,  $\approx 30$  pptv. Levels of NO appear to increase in the upper troposphere, up to 50 pptv (Kley *et al.*, 1981; Carroll and Ridley, 1984; Torres, 1984; Bradshaw *et al.*, 1984) indicating a downward flux of this material to the subtropical ocean. This inverted gradient may reflect transport from the stratosphere, or from lightning or land sources in tropical convergence regions, with the  $\text{NO}_x$ -rich air in this case carried aloft by deep convection and deposited in the upper troposphere.

Data for  $\text{NO}_x$  in continental areas indicate higher concentrations than in marine areas, especially over populated lands. Nitric oxide concentrations in the middle troposphere vary from as low as a few ppt to more than 200 ppt, and levels may exceed 1000 ppt in the lower atmosphere at times (see reviews by Logan, 1983; Dickerson, 1984; Drummond *et al.*, 1985). Data for Niwot Ridge, Colorado, show an enormous range of concentrations for  $\text{NO}_x$ , as this rural site is influenced at times by urban pollution, while at other times it receives air transported from the very clean marine middle troposphere (Bollinger *et al.*, 1984). The Niwot Ridge data also show that organonitrates and peroxy nitrates may be very important in the tropospheric cycle of odd nitrogen (Singh *et al.*, 1985).

#### 3.3.2 Sources and Sinks

The focus of the present review is the influence of tropospheric  $\text{NO}_x$  on lifetimes for stratospheric source molecules ( $\text{CH}_3\text{CCl}_3$ ,  $\text{CH}_3\text{Cl}$ ,  $\text{CH}_4$ ) through interactions with tropospheric photochemistry. It would be of great interest to know whether global tropospheric  $\text{NO}_x$  levels are perturbed by human activities. Since direct information on trends is lacking, we must fall back on analysis of sources for  $\text{NO}_x$ .

##### *Combustion Sources*

The emission rate for fixed N from combustion of fossil fuels,  $\sim 20$  Tg  $\text{yr}^{-1}$ , may be assessed with some confidence using emission factors for  $\text{NO}_x$  and statistics for fuel use (see, for example, Logan, 1983 or Ehhalt and Drummond, 1982). Emissions in the U.S. doubled between 1950 and 1970, but have been relatively constant in the last decade due to levelling off of overall energy use (EPA, 1984). The impact of this  $\text{NO}_x$  on global tropospheric chemistry remains uncertain, however, because a significant fraction of  $\text{NO}_x$  from industrial emissions may be removed near the source. A number of papers have suggested that industrial emissions of  $\text{NO}_x$  are responsible for increasing the concentrations of OH and  $\text{O}_3$  in the

## SOURCE GASES

Northern Hemisphere (Crutzen, 1973; 1979; Chameides and Walker, 1973; Fishman *et al.*, 1979; Seiler and Fishman, 1981). Unfortunately, knowledge of the processes which disperse  $\text{NO}_x$  from industrial sources is inadequate for reliable assessment of this phenomenon. Note that, as mentioned above, combustion of relatively high-N, unrefined fuels (coal, agricultural residuals, residual oil) produce NO and  $\text{N}_2\text{O}$  largely through related chemical pathways involving NCO generated during fuel pyrolysis.

Fuel N is likely to be the major source of NO emitted from biomass burning since temperatures are thought to be too low for fixation of atmospheric  $\text{N}_2$ . Two independent studies suggest that the amount of biomass fuel burned annually is  $\sim 7 \times 10^{15}$  gm  $\text{yr}^{-1}$ , or  $\sim 3 \times 10^{15}$  gm C  $\text{yr}^{-1}$  (Seiler and Crutzen, 1980; Logan *et al.*, 1981), mostly in tropical regions. Logan (1983) used these assessments, in combination with data for the nitrogen content of vegetation and experimental determination of the conversion efficiency of fuel N to  $\text{NO}_x$ , to estimate that the source of  $\text{NO}_x$  from biomass burning could be as large as 12 tg N  $\text{yr}^{-1}$ . Delany *et al.* (1985a) recently reported measurements of  $\text{NO}_x$  in the polluted boundary layer in the vicinity of biomass fires. Their observed ratio of  $\Delta\text{NO}_x/\Delta\text{CO}_2 = 1.9 \pm 0.3 \times 10^{-3}$  may be used to estimate a global source of  $\text{NO}_x$ ,  $\sim 7$  tg N  $\text{yr}^{-1}$ , basically in agreement with earlier estimates.

Emissions from biomass burning are spatially and temporally concentrated, making the assessment of impacts on global chemistry difficult. In this respect, the problem is similar to that for urban emissions. The regions directly affected by fire plumes are too small to influence the global lifetimes of  $\text{CH}_4$  or  $\text{CH}_3\text{CCl}_3$ , for example. However, if a substantial fraction of this  $\text{NO}_x$  escapes to distant parts of the tropical troposphere, the lifetimes of these species could be significantly shortened, due to enhanced concentrations of OH, with potentially important consequences for stratospheric chemistry (Delaney *et al.*, 1985a).

### Natural Sources

Natural sources for  $\text{NO}_x$  include microbial activity in soils, lightning, and oxidation of stratospheric  $\text{N}_2\text{O}$ . The stratospheric source is only about 0.5 tg N  $\text{yr}^{-1}$  over the whole globe; while this is much smaller than the other sources discussed here, it is likely very important in the chemistry of the upper troposphere, especially in marine locations with negligible sources near the ground (Levy *et al.*, 1980).

There is no doubt that lightning produces  $\text{NO}_x$  in the atmosphere (Noxon, 1978b; Liu *et al.*, 1983), but there has been considerable dispute about the magnitude of the source. Most current estimates are  $< 10$  tg N  $\text{yr}^{-1}$  (Tuck, 1976; Chameides *et al.*, 1977; Dawson, 1980; Jackman *et al.*, 1980; Borucki and Chameides, 1984), and values significantly higher than this are inconsistent with the deposition rate of nitrate in precipitation (Logan, 1983; Ehhalt and Drummond, 1982; Borucki and Chameides, 1984). Lightning may provide the major source of  $\text{NO}_x$  in the middle and upper troposphere in the tropics (Liu *et al.*, 1983), and may even be important as a source of  $\text{NO}_x$  in the lower stratosphere (Ko *et al.*, 1985).

Odd nitrogen emissions from soils have attracted interest rather recently (Galbally and Roy, 1978; Galbally, 1985). A summary of available data is given in Table 3-8. Soils may either emit or consume NO and  $\text{NO}_2$ . A net positive flux of NO is the rule on average, except where NO levels in the air are very large ( $> 1$  ppb), while on average most soils consume  $\text{NO}_2$  (for a review, see Galbally, 1985). The global source of NO from soils may be roughly estimated as  $\sim 10$ – $15$  tg N  $\text{yr}^{-1}$ , a very significant contribution. Particular interest attaches to large emission rates observed from intensive agriculture and livestock operations, and from tropical forest soils. Both of these contribute  $\text{NO}_x$  to the atmosphere in areas distant from industrial sources, and both are being modified globally by human activities (increasing agriculture, declining areas of tropical forest). Noteworthy is the association between high emission rates for  $\text{N}_2\text{O}$  and for NO, which may derive from the fact that most biological processes producing one gas also produce the other (e.g., nitrification, Lipschultz *et al.*, 1981; denitrification, Payne, 1983).

Table 3-8. Measurements of NO Emissions from Soils

	Flux kg N m <sup>-2</sup> sec <sup>-1</sup>	References
Ungrazed pasture (average)	1.6 × 10 <sup>-12</sup>	Galbally and Roy, 1978
Grazed pasture (average)	3.5 × 10 <sup>-12</sup>	
Grazed pasture (range)	1–50 × 10 <sup>-12</sup>	Galbally and Roy, 1981
Fertilized grass (weighted annual average)	1.9 × 10 <sup>-12</sup>	Johansson and Granat, 1984
Unfertilized barley (weighted annual average)	0.6 × 10 <sup>-12</sup>	
Croplands (range)	0.1–62 × 10 <sup>-12</sup>	
Unfertilized forest soil (median) (range)	0.3 × 10 <sup>-12</sup> 0.1–0.8 × 10 <sup>-12</sup>	Johansson, 1984
Bare, unfertilized soil, Finthen (average) (range)	2.2 × 10 <sup>-12</sup> –5.8 to 14.2 × 10 <sup>-12</sup>	Slemr and Seiler, 1984
Bare, unfertilized soil, Utrera (range)	–2.2 to 107 × 10 <sup>-12</sup>	
Crested wheat grass (daily mean) (range)	7 × 10 <sup>-12</sup> –9.3 to 28.0 × 10 <sup>-12</sup>	Delany <i>et al.</i> , 1985
Amazon Tropical Forest	10 × 10 <sup>-12</sup>	NASA/ABLE II (W. Kaplan <i>et al.</i> , 1985)

Note: 1 × 10<sup>-12</sup> kg N m<sup>-2</sup> sec<sup>-1</sup> = 4.3 × 10<sup>9</sup> molecules cm<sup>-2</sup> sec<sup>-1</sup>

## SOURCE GASES

### 3.3.3 Discussion

The stratosphere will be indirectly affected by future changes in global levels of tropospheric  $\text{NO}_x$ . Many industrial, agricultural and natural sources of  $\text{NO}_x$  are closely associated with analogous production processes for  $\text{N}_2\text{O}$ . Automobiles and lightning are perhaps the principal exceptions. The observed imbalance ( $\sim 30\%$ ) between current sources and sinks for  $\text{N}_2\text{O}$  implies associated large increases in global emissions for both  $\text{N}_2\text{O}$  and  $\text{NO}_x$ . Unfortunately, it is not clear to what extent  $\text{NO}_x$  from industrial emissions, automobiles, or biomass burning affect remote regions of the atmosphere, and consequently the magnitude of the global influence of anthropogenic activities remains unclear. Resolution of this important issue requires careful experimental and theoretical investigation of transformations and transports of nitrogen oxides from industrial source areas and biomass burning areas to the global troposphere, as described for example in the recent Workshop Report from the proposed Global Tropospheric Chemistry Program. The expected sign of the effect for  $\text{NO}_x$  is clear, however: global levels of  $\text{NO}_x$  are almost certainly higher today than in preindustrial times. Global levels of OH could be either higher or lower, however, since increasing production of OH due to  $\text{NO}_x$  must be offset in part by anthropogenic CO (Wofsy, 1976; Sze, 1977; Chameides, *et al.*, 1977)(see below), which enhances the sink for OH; emissions of hydrocarbons may have an effect also. There is evidently a strong need for much better definition of the sources, sinks, and atmospheric cycles for  $\text{NO}_x$ .

## 3.4 METHANE ( $\text{CH}_4$ )

### 3.4.1 Distributions and Trends

Atmospheric measurements using GC/FID techniques, taken since 1965, have now clearly established that the concentration of methane is increasing (Rasmussen and Khalil, 1981b; Blake *et al.*, 1982; Fraser *et al.*, 1981, 1983, 1984; Khalil and Rasmussen, 1982, 1983b, 1984; Ehhalt *et al.*, 1983). Data have been obtained from at least six primary sites between 1979 and the present, including continuous measurements at Cape Meares, Oregon (Khalil and Rasmussen, 1983c). Methane concentrations have increased at every site consistent with the record from Cape Meares (see Figure 3-9). The record shows interannual variability in the trend of  $\text{CH}_4$  and there is evidence that recent variability is associated with the El Niño-Southern Oscillation (ENSO) phenomenon (Khalil and Rasmussen, 1985f). During the recent ENSO event (1982-83), concentrations of  $\text{CH}_4$  fell well below levels extrapolated from previous years (1978-81) and recovered with a rapid increase afterwards (Figure 3-9, 3-10), similar to behavior observed for  $\text{CO}_2$  (Gammon and Komhyr, 1983; Gammon *et al.*, 1984). The occurrence of this major El Niño reduced the estimated global long-term increase of  $\text{CH}_4$  to an average of about 1% per year for the period 1979-1984, whereas data from 1979-1982 had suggested a more rapid increase of about 1.8%  $\text{yr}^{-1}$ . Analysis of air trapped in polar ice (Craig and Chou, 1982; Rasmussen and Khalil, 1984b) shows that  $\text{CH}_4$  levels in the atmosphere have been increasing for several centuries, and have roughly doubled from values near 0.7 ppm that prevailed for thousands of years prior to the increase recorded in recent times. Analysis of Migeotte's plates by Rinsland *et al.* (1985a) indicates 1.14 ppm in Europe in 1951, with recent plates giving 1.58 ppm in 1981, corresponding to 1.1% mean annual increase over 30 yrs.

Seasonal cycles have been documented at various latitudes generally showing lowest concentrations in late summer and highest concentrations in winter and spring. At high northern latitudes there is a strong rise of  $\text{CH}_4$  during fall, probably caused by a seasonal peak of emissions from water-saturated soils that are frozen much of the year. Other features of the  $\text{CH}_4$  seasonality are generally consistent with the calculated seasonal cycles of OH. As with CO and  $\text{CO}_2$ , the amplitude of the seasonal cycle is largest at high northern latitudes and diminishes towards the equator (Khalil and Rasmussen, 1983c; Fraser *et al.*, 1983b).

The detailed global distribution and seasonal variation of  $\text{CH}_4$  has been recently synthesized from several thousand air samples collected by the global flask network operated by GMCC/NOAA, in a cooperative program with the Oregon Graduate Center and CSIRO (Australia) (Steele *et al.*, 1985, Figure 3-11). Weekly sample pairs from 17 sites allow the construction of a zonally averaged concentration surface, with a grid resolution of two weeks in time and  $10^\circ$  in latitude, for the two-year period 5/83-4/85. A remarkable feature of the concentration surface is the simple annual cycle of nearly constant seasonal amplitude and phase from southern mid-latitudes to the South Pole with a mid-summer minimum and fall and late-winter maxima. There is more complex seasonality at mid-to-high northern latitudes. The amplitude of the seasonal cycle increases poleward from the equator (arrow in Figure 3-11) in both hemispheres, and is highest in the Arctic. Neither the interannual variability of the local seasonality nor the latitude dependence of the secular increase can yet be recovered from the initial 24-month record. Annual mean  $\text{CH}_4$  concentrations as a function of latitude for 1984 are shown in Figure 3-12 (Steele *et al.*, 1985). In the future, coordinated interpretations of the seasonality and distributions of the carbon-cycle trace gases ( $\text{CO}_2$ ,  $\text{CO}$ ,  $\text{CH}_4$ ) should greatly clarify the role of regionally important sources (e.g. tropical biomass burning, tundra metabolism). Examination of isotopic data may also prove useful in this regard (see below).

### 3.4.2 Sources and Sinks

We now review present knowledge of the sinks and sources of atmospheric  $\text{CH}_4$  in order to lay the foundation for an analysis of the factors which may be responsible for the atmospheric trends. Summary tables give recent assessments of sinks (Table 3-9; McElroy and Wofsy, 1985) and sources (Tables 3-10 and 3-11; Seiler, 1984; Ehhalt and Schmidt, 1978; Khalil and Rasmussen, 1983c). As we shall see, the total sink is relatively well-known ( $\pm 35\%$ ) but apportionment among sources is highly uncertain.

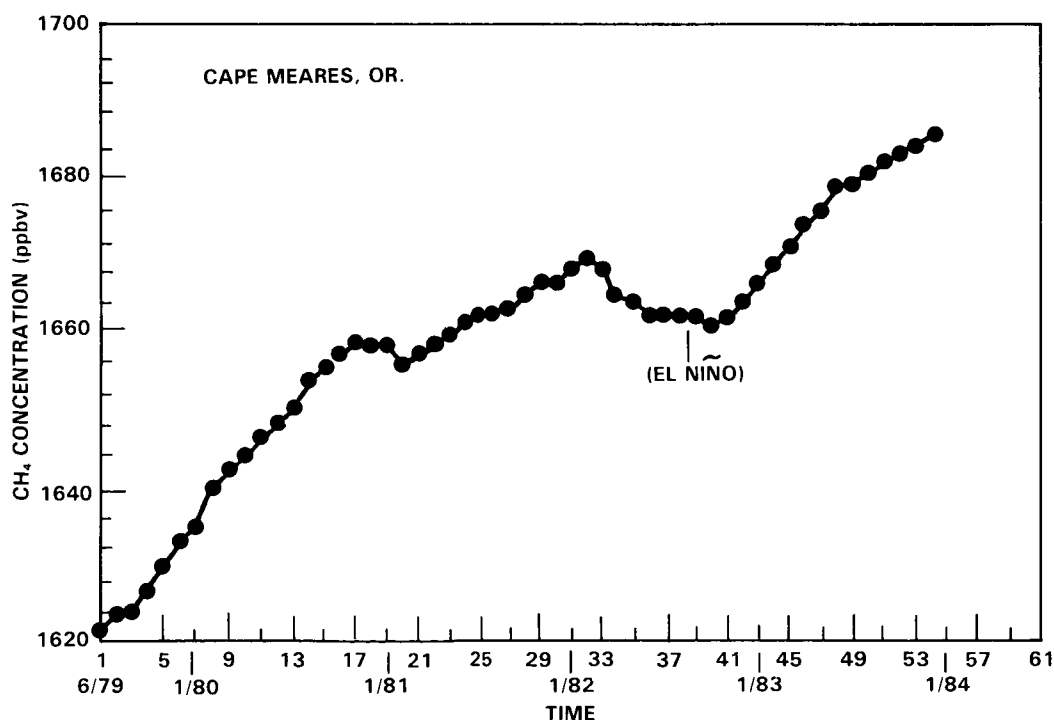


**Figure 3-9.** Trend of atmospheric  $\text{CH}_4$  concentration (ppbv) measured at Cape Meares, Oregon ( $45^\circ\text{N}$ ) for the period 6/79-1/84 (Khalil and Rasmussen, JGR, 1983 updated through 1984). Seasonal variation removed by 12-month running mean, interannual variations (El Nino, 1982/83) apparent.

SOURCE GASES

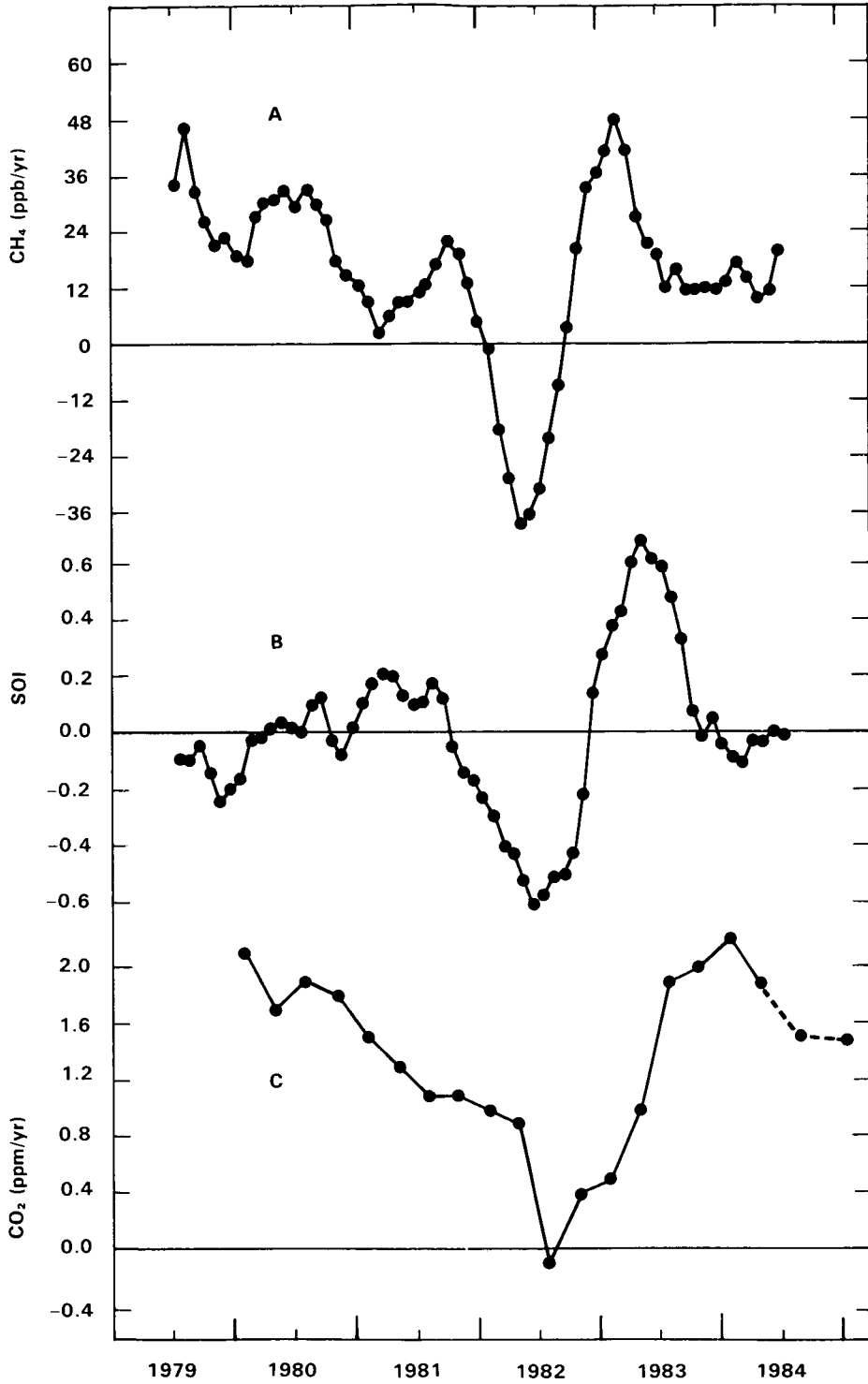


**Figure 3-10.** (Khalil and Rasmussen, 1985f) (a) Growth rate of atmospheric methane in ppbv/yr observed at Cape Meares, Oregon for successive 12-month overlapping intervals; (b) time derivative of the southern oscillation index (SOI) treated as in (a); (c) globally averaged year-to-year change in atmospheric  $\text{CO}_2$  by season, plotted in forward year (Gammon *et al.*, 1985b).

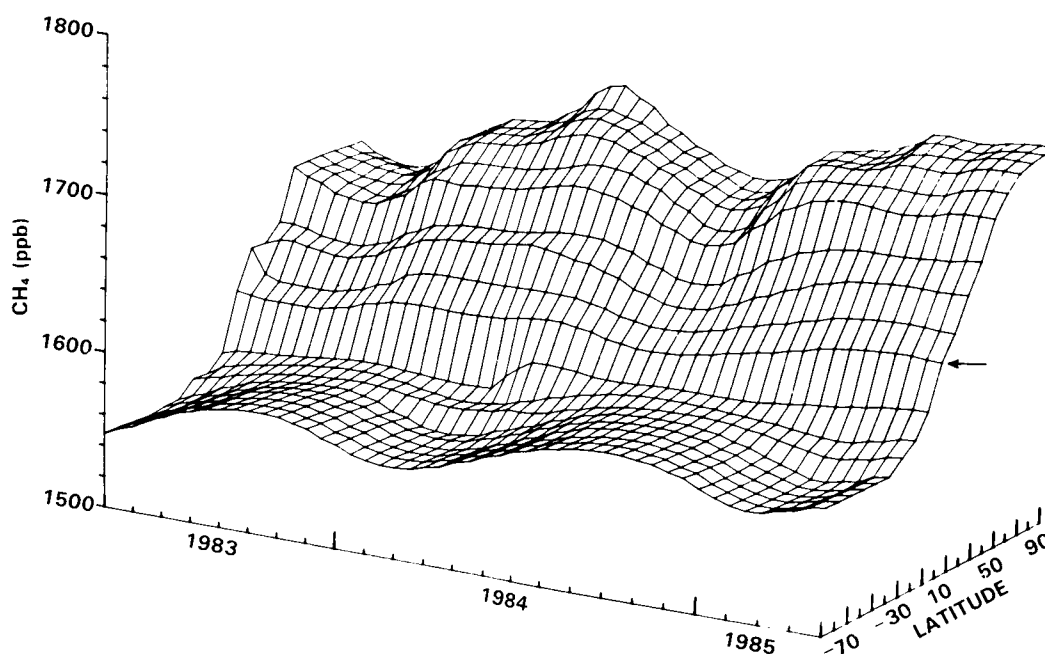


**Figure 3-11.** Zonally averaged global distribution of  $\text{CH}_4$  in the lower troposphere for the two-year period 5/83-4/85. Surface constructed from biweekly flask samples from 17 sites of the GMCC/OGC/CSIRO global network,  $76^\circ\text{N}$  to  $90^\circ\text{S}$  (Steele *et al.*, 1985). Arrow indicates equator, resolution is  $10^\circ$  in latitude, 14 days in time.

### Methane Sinks

The documented sinks for  $\text{CH}_4$  in the atmosphere are reactions with  $\text{OH}$  (Levy, 1971) and consumption by aerobic soils (Keller *et al.*, 1983; Seiler, 1984). The temperature dependence of the reaction rate for  $\text{OH} + \text{CH}_4$  (products) is not very different from that of the analogous reaction,  $\text{OH} + \text{CH}_3\text{CCl}_3 \rightarrow$  (products). Hence the experimental value for the lifetime of  $\text{CH}_3\text{CCl}_3$ ,  $6.5 (+3/-2)$  years from the ALE experiment (Prinn *et al.*, 1983a), provides an important constraint on the total removal rate for  $\text{CH}_4$  from the atmosphere. An updated version of the photochemical model by Logan *et al.* (1981), which gives a lifetime for  $\text{CH}_3\text{CCl}_3$  of  $\approx 5.5$  years, was used to derive the magnitude of the methane sink given in Table 3-9,  $425 \pm 125$  Tg  $\text{CH}_4$  per year. This value corresponds to a lifetime of 11 years.

Most unsaturated soils are sinks for atmospheric  $\text{CH}_4$ . Consumption rates in the dry subtropical areas studied by Seiler *et al.* (1984c) appear to be larger than in the wetter temperate and tropical forests studied by Keller *et al.* (1983). The value of  $10$  Tg  $\text{CH}_4 \text{ yr}^{-1}$  for the global sink in soils was derived assuming an average deposition of  $10^{10}$  molecules  $\text{cm}^{-2} \text{ sec}^{-1}$  over  $2/3$  of the earth's land area. The magnitude of this sink is evidently uncertain, but it seems unlikely to be of major importance in the global budget. According to the estimates in Table 3-9, soils remove much less than the annual accumulation of  $\text{CH}_4$  ( $65$  Tg  $\text{yr}^{-1}$ ).

Consideration of  $\text{CH}_4$  sinks appears to constrain the annual emissions to be  $500 \pm 145$  Tg  $\text{CH}_4 \text{ yr}^{-1}$ . This is probably one of the better-known quantities in the global  $\text{CH}_4$  budget, as it is tied to the empirical determination of the lifetime for  $\text{CH}_3\text{CCl}_3$ .

## SOURCE GASES

**Table 3-9.** Methane Sinks (from McElroy and Wofsy, 1985) (1984 concentration 1630 ppb)

A. <i>Atmospheric burden</i> ( $4700 \times 10^6$ tons CH <sub>4</sub> )	
B. <i>Sinks + atmospheric accumulation</i> (tg CH <sub>4</sub> yr <sup>-1</sup> )	
Reaction with OH	425 ± 125
Uptake by dry soils	10 ± 5
Accumulation (20 ppb/yr)	60 ± 15
total	495 ± 145

**Table 3-10.** Total CH<sub>4</sub> Emission into the Troposphere (Tg of CH<sub>4</sub> per year) (Seiler, 1984)

Source	1950	1960	1970	1980
Biogenic production	86-181	100-208	114-228	122-237
Abiogenic production	64-98	78-118	94-140	103-158
Total CH <sub>4</sub> production	146-285	178-336	208-368	225-395
Average CH <sub>4</sub> production	216	257	288	310
Biogenic/total (%)	62	60	59	58
<b>Sinks</b>				
Reactions with OH	210	230	270	290
Flux with stratosphere	44	48	56	60
Microorganisms	15	16	19	20
Total	269	294	345	370

### Atmospheric Methane from Natural Sources

Natural sources for atmospheric CH<sub>4</sub> are wetlands (including wet tundra and sedge, floodplains, peatlands, and associated open water areas), termites, wild fires, and enteric fermentation in wild ruminants. Estimates of these sources are uncertain (see below), but natural sources may be equivalent to approximately 5-35 percent of total annual production.

**Table 3-11.** Methane Sources ( $10^{12}$  gm yr<sup>-1</sup>) (multiply by 0.75 to obtain g C/yr)

	I	II
Enteric fermentation (cattle, sheep, etc.)	100 - 200	100 - 150
Rice paddies	~280	100 ± 50
Wetlands	90 - 300	150 ± 50
Biomass burning	—	10 - 60
Fresh water lakes	1 - 25	—
Oceans	1 - 17	—
Tundra	0.3 - 3	—
Anthropogenic/fossil fuel	16 - 50	—
Other	—	10 - 150
Total	586 - 825	390 - 765

Column I is taken from Ehhalt (1974) and Ehhalt and Schmidt (1978).

Column II is taken from Khalil and Rasmussen (1983).

The CH<sub>4</sub> flux from any wetland ecosystem can be influenced by a range of variables including the quantity and composition of the organic substrates being decomposed, soil moisture, soil temperature, and the types of vegetation present (e.g., see Baker-Blocker *et al.*, 1977; Dacey and Klug, 1979; Cicerone and Shetter, 1981; Harries *et al.*, 1982; Seiler *et al.*, 1984a,c). An important factor is the potential for oxidation of CH<sub>4</sub> in the source ecosystem before release to the atmosphere.

Currently there are only a few detailed studies of specific freshwater wetland ecosystems, for example in Michigan (Baker-Blocker *et al.*, 1977) and Virginia (Harries *et al.*, 1982). The studies in Michigan measured CH<sub>4</sub> efflux due to bubbling only, which may underestimate the CH<sub>4</sub> flux, since loss by diffusive processes and through (or along) stems of plants can also be important (Dacey and Klug, 1979; Cicerone and Shetter, 1981). The Virginia swamp that was studied had been highly modified by human land management practices (e.g. drainage and timber harvest). Thus published data on annual CH<sub>4</sub> emissions from major freshwater wetland ecosystems is very limited. Marine wetlands have been studied in more detail, but are not a major source of atmospheric CH<sub>4</sub> (Bartlett *et al.*, 1985) due to the inhibiting influence of high levels of SO<sub>4</sub><sup>2-</sup> in seawater.

The estimates for areal extent of global freshwater wetlands (see Table 3-12) are also uncertain. A generalized map of global wetland distribution is given in Figure 3-13 (Mathews, *et al.* 1986); estimated

## SOURCE GASES

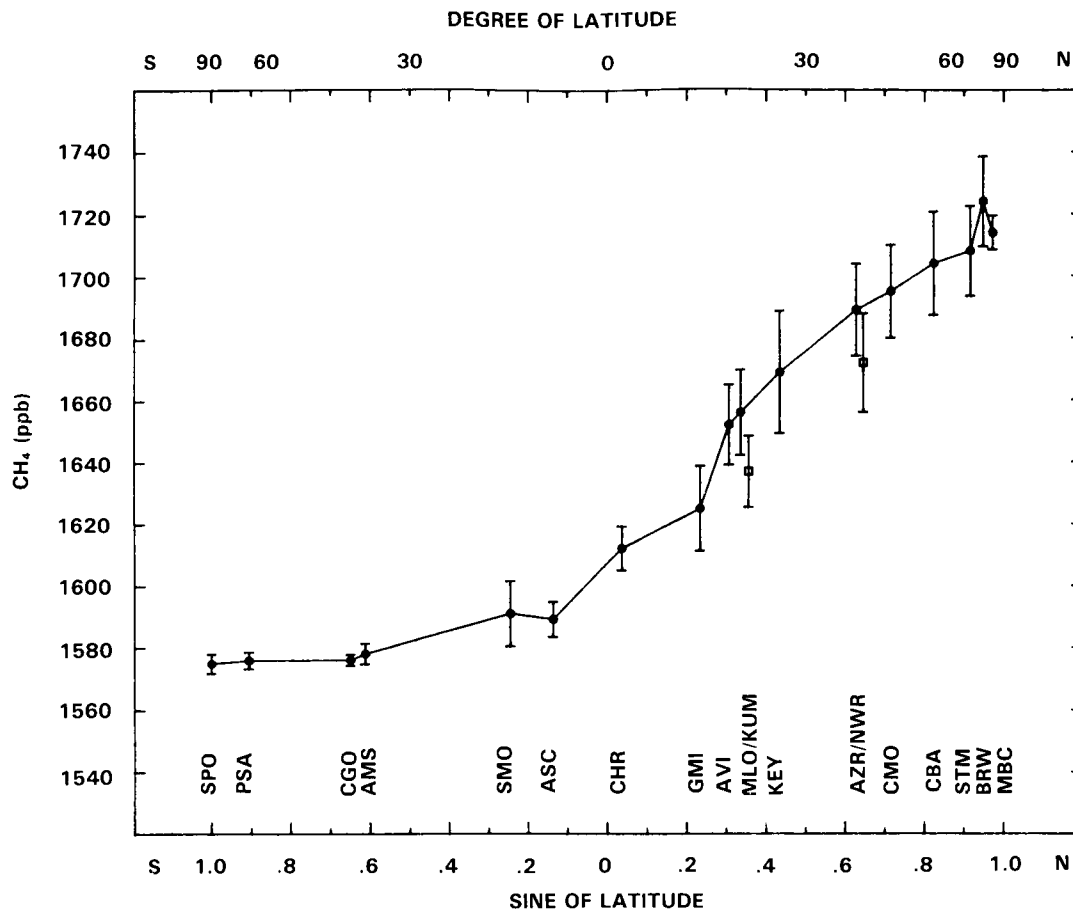


**Figure 3-12.** Latitudinal distribution of annual mean CH<sub>4</sub> concentration at 19 sampling sites from 76°N to 90°S (Steele *et al.*, 1985). The error bars reflect the relative noisiness of each site after seasonal and secular terms have been removed. High altitude sites MLO (Mauna Loa, Hawaii) and NWR (Niwot Ridge, Colorado) have lower mean CH<sub>4</sub> values than sea-level sites at the same latitude.

**Table 3-12.** Estimated Areas of Global Wetlands

Wetland areas (10<sup>3</sup> km<sup>2</sup>) by latitudinal zones (Mathews *et al.*, 1986). Natural wetlands include wet arctic meadows, mossy bogs, seasonally and permanently inundated grasslands, woodlands, shrublands and forests; irrigated rice is self explanatory.

	90°N-30°N	30°N-30°S	30°S-90°S	TOTAL
Natural wetlands	2932	1482	21	4435
Irrigated rice	276	1240	0	1516
<b>TOTAL</b>	<b>3208</b>	<b>2722</b>	<b>21</b>	<b>5951</b>

regional wetland areas are given in Table 3-12. Because wetlands are generally a small percentage of total land area in any region and are of low commercial interest they receive low priority for mapping.

A strategy for improving estimates of the global flux of  $\text{CH}_4$  from natural wetland ecosystems is urgently needed. The complex interplay of factors which influence  $\text{CH}_4$  emissions make a global budget uncertain, and estimates of the factors underlying global change from natural wetlands are based mostly on speculation. Studies are currently underway in a few major wetlands of North America which demonstrate how the combined use of *in situ*  $\text{CH}_4$  flux determinations and remote sensing of wetland areas and habitat distributions may produce quantitative, large-scale, long-term efflux data needed to make accurate global estimates. Such studies constitute a first step in the assessment of the causes of global  $\text{CH}_4$  changes. For example, Table 3-13 illustrates how measured values of net  $\text{CH}_4$  flux to the atmosphere from specific habitats in the Shark River area of the Florida Everglades are combined with Landsat-derived estimates of habitat area to derive a total flux of  $\text{CH}_4$  to the atmosphere. The table illustrates in this case the importance of identifying the extent of the sawgrass biome and the need to distinguish it from related landforms. (R. Harriss, personal communication, 1985).



Figure 3-13. World-wide distribution of natural wetlands (Mathews *et al.*, 1986).

## SOURCE GASES

The Shark River region is similar to other major seasonally flooded grasslands of the world such as the Pantanal region of Brazil and the Beni region of Bolivia, and one could extend the techniques to such areas with suitable international collaboration. Particular emphasis should be given also to the northern peatlands and tundra and to tropical floodplains and swamps, the major natural wetlands of the world. Coordination between remote sensing and *in situ* sampling is essential for such studies (see NAS, 1984).

Termites have been identified as a potentially important natural source of CH<sub>4</sub> (Zimmerman *et al.*, 1982). Many factors related to biology, ecology, and population of termites complicate the process of deriving an estimate for the associated global source of atmospheric CH<sub>4</sub> (Rasmussen and Khalil, 1983c; Khalil and Rasmussen, 1983d; Greenberg and Zimmerman, 1984). Systematic studies are now in progress which should reduce the uncertainty in emission factors for the major groups of termites, but there still remains the intractable problem of obtaining census data on termites of the world. Recent papers (Seiler *et al.*, 1984c; Rasmussen and Khalil, 1983c) argue that the global contribution of termites is smaller than projected by Zimmerman *et al.* (1982) but a lively controversy persists.

### Methane Sources in Agricultural Systems

Two major agricultural sources of atmospheric methane appear to be rice paddies and cattle. These sources were identified as early as 1963 and 1948, respectively. Globally significant amounts of carbon flow through these living systems under strongly reducing conditions. In rice agriculture, rich soils are covered with water during the growing season and become anoxic: O<sub>2</sub>, Fe<sup>+++</sup>, NO<sub>3</sub><sup>-</sup> and SO<sub>4</sub><sup>-</sup> are depleted in sequence, after which microbial methanogenesis accelerates. In cattle and sheep digestion, specialized microbes flourish in a reducing environment and methanogenesis occurs in the final stages of a long process of breaking down complex organic material. The methane is released in the breath of these animals and by eructation and flatulence. There is little opportunity for methane-oxidizing bacteria to decompose methane produced in the rumen of cattle and sheep, but oxidation *in situ* might be significant in rice paddies under some conditions.

Tables 3-10 and 3-11 give estimates of global methane release rates from enteric fermentation in cattle and sheep and from rice paddies. The 280 tg/year figure for rice is from Ehhalt (1974), based on measurements from laboratory incubations of paddy soils by Koyama (1964). Koyama extrapolated to global rice-growing areas and temperatures, and Ehhalt later scaled upward the estimate of areas under cultivation.

Figure 3-14 shows data on worldwide rice production and area harvested for 1940-1981. Multiple cropping of many areas of the Orient has permitted production to grow faster than area under cultivation. By holding paddy soils under water for two or three growing seasons annually instead of one, increased methanogenesis from these areas is guaranteed. If one were to extend Ehhalt's 1974 estimate to 1985, one would arrive at an annual release of over 300 tg CH<sub>4</sub>/year (225 tg C/yr.) from the world's rice paddies to the atmosphere. This estimate appears to be too large to be accommodated by the values adopted for the loss of CH<sub>4</sub> in Table 3-9, in combination with other source estimates.

In the past four years, new information has become available on CH<sub>4</sub> release from rice agriculture based on direct field studies. These support lower methane emissions than the Koyama laboratory studies, but they also point to complexities that challenge simple extrapolations. For example, Cicerone and Shetter (1981) reported field experiments in a California rice paddy from which they extrapolated a global source of only 60 tg CH<sub>4</sub>/year, about one-fourth the early values. They showed that the dominant transport mechanism moved methane from the soil to the atmosphere not by diffusion through the water or by rising

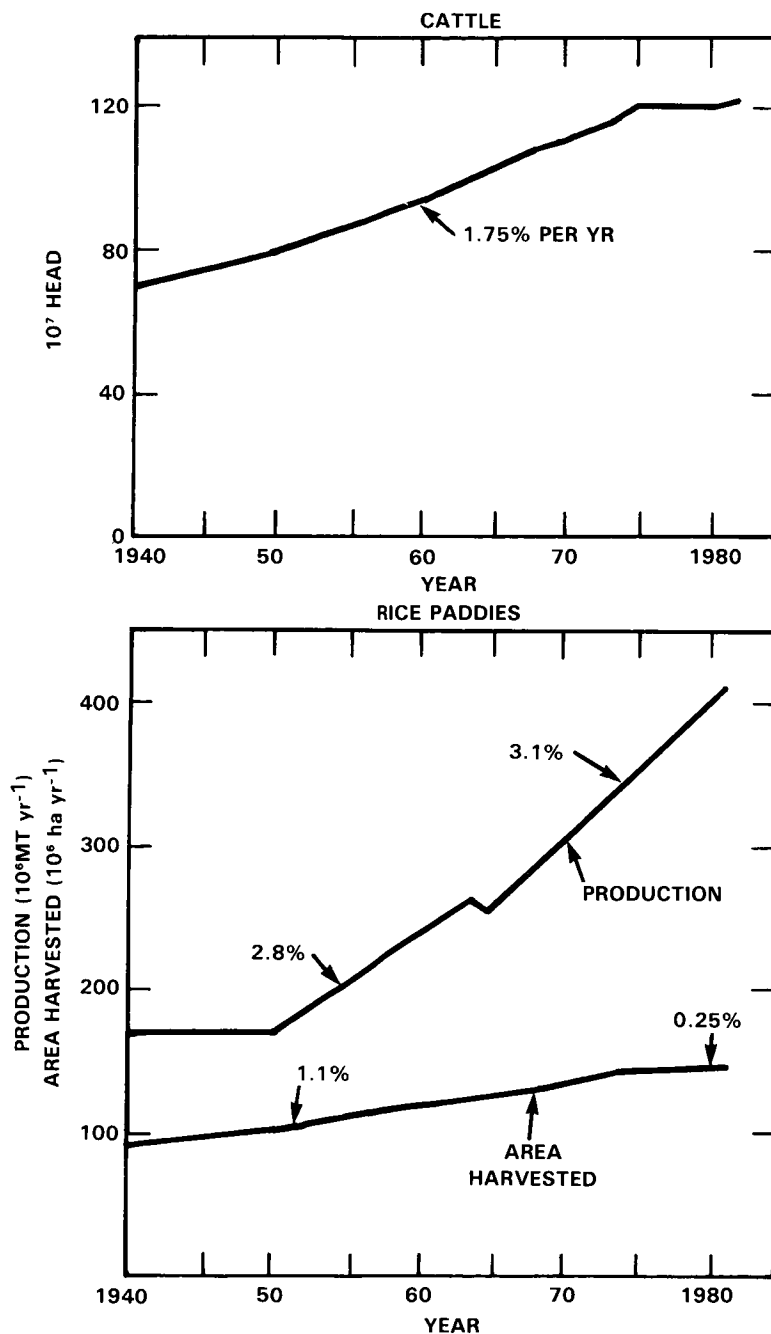


**Figure 3-14.** Temporal changes in the number of cattle in the world, and in the global production and area harvested of rice, taken from the United Nations FAO Production Yearbooks.

bubbles, but through (or along) the plant stems. Similar mechanisms were observed previously in littoral water litter (Dacy and Klug, 1979). Cicerone and Shetter also reported an apparent influence of nitrogen-fertilizer on methane release rates. A full-season experiment on rice emissions of methane was reported by Cicerone *et al.* (1983), indicating strong intraseasonal variation, with by far the largest fluxes occurring at the end of the growing season. The seasonally averaged methane flux, 0.25 g/m<sup>2</sup>/day, was higher than given by Cicerone and Shetter (1981).

## SOURCE GASES

In 1983 Seiler *et al.* (1984a) performed an extensive season-long experiment in Spanish rice fields. They found a less pronounced intraseasonal variation than that mentioned above, an average release rate of only 0.1 g CH<sub>4</sub>/m<sup>2</sup>/day and they confirm the role of gas transport by rice plants and found no influence of different nitrogen-fertilizer amounts. They sought and found a direct correlation between measured fluxes and soil temperatures and they derived a lower estimate for global fluxes from rice paddies, (35–59) tg CH<sub>4</sub>/year. Subsequently, Holzapfel-Pschorn and Seiler (Seiler *et al.*, 1985a) presented new field measurements from Italian rice paddies, indicating emission rates about four times larger than found in Spain by Seiler *et al.* (1984a). These data led Holzapfel-Pschorn and Seiler to propose revised estimates of methane fluxes from rice paddies: (70–170) tg CH<sub>4</sub>/year for 1984 and (39–94) tg CH<sub>4</sub>/year for year 1940. The oscillation of these recent global estimates indicates the need for a much improved understanding of methanogenesis and methane release in major rice-growing agricultural systems.

Methane emissions from cows and sheep have not been the subject of much recent research, except for conventional feeding experiments designed to evaluate the efficiency of milk production in US agricultural practice. Although entire books on this subject are available (e.g. Hungate, 1960) there is probably large uncertainty in the estimated global source. For example, the full impact of varying diet, grazing conditions, animal health and nutrition and enteric microbial ecology, should be investigated further. Special attention is needed on CH<sub>4</sub> emissions from cattle (including goats and sheep) in Africa, India and other relatively impoverished areas. We are not aware of any studies at all on such animals.

### 3.4.3 Discussion

The apparent doubling of CH<sub>4</sub> in historic times presents a serious challenge to stratospheric research. It is clear that concentrations of stratospheric CH<sub>4</sub>, H<sub>2</sub>O and H<sub>2</sub> must have been lower for centuries prior to ~1600 AD, and stratospheric photochemistry and ozone levels must have been different. Likewise, future levels of stratospheric ozone depend sensitively on future levels of CH<sub>4</sub>. Since we cannot quantitatively explain the current rise in CH<sub>4</sub>, we cannot predict future levels of CH<sub>4</sub> and, by extension, predictions of stratospheric O<sub>3</sub> are rendered uncertain.

Table 3-13. Calculated Methane Flux — Shark River Slough Study Area

Habitat Category	Area	Flux/Ha/Day**	Total Flux/day
Sawgrass < 3.0 m	76,024 ha	870 g/ha/day	66.1 × 10 <sup>6</sup> g/day
Sawgrass/Spikerush	17,747 ha	400 g/ha/day	7.1 × 10 <sup>6</sup> g/day
Sawgrass/Cypress	18,688 ha	130 g/ha/day	2.4 × 10 <sup>6</sup> g/day
Swamp Forest	5,151 ha	720 g/ha/day	3.7 × 10 <sup>6</sup> g/day
Unsampled/ Negligible Flux	20,588 ha	—	—

\*Area of individual habitats derived from a Landsat thematic mapper image obtained on 12/20/82.

\*\*Flux estimates are derived from a large number of individual measurements made at different times and sites.

Unravelling the mysteries of the global  $\text{CH}_4$  cycle will be very difficult. The present rise of  $\text{CH}_4$  levels represents the net effect of changes (up or down) in tropospheric OH, which controls the sink for  $\text{CH}_4$ , changes in wetland emissions due to land modification (reduced areas) and to climatic warming in the Arctic (increased source?), and changes in agricultural emissions from rice fields, cattle, and manure operations (increased source).

NASA recently initiated an interdisciplinary program to pursue this important problem. Determination of  $\text{CH}_4$  atmospheric trends at various latitudes is one important step in this direction. The study of carbon and hydrogen isotopes in methane is a promising new area being actively explored. Recent work by Stevens and Engelkemeir (1985) illustrate the basic ideas being pursued. Figure 3-15 shows isotopic compositions for  $^{13}\text{C}$  and  $^{12}\text{C}$  in  $\text{CH}_4$  (Stevens and Engelkemeir, 1985). Biogenic sources are generally depleted in  $^{13}\text{C}$  relative to atmospheric  $\text{CH}_4$ , while combustion and fossil fuel sources are isotopically heavier than atmospheric. One conclusion drawn from Figure 3-15 is that either non-biogenic sources must be unexpectedly important, or that presently unexplored biological sources must release relatively heavy  $\text{CH}_4$  (Stevens and Engelkemeir, 1985). The data suggest that much insight could be obtained from detailed analysis of  $^{13}\text{C}/^{12}\text{C}$  ratios of various sources combined with latitudinal, seasonal, and long-term trend data on the  $^{13}\text{C}/^{12}\text{C}$  ratio in atmospheric  $\text{CH}_4$ . Attention to detail is needed for this task since there could be seasonal or other variations of the  $^{13}\text{C}/^{12}\text{C}$  ratio for major sources.

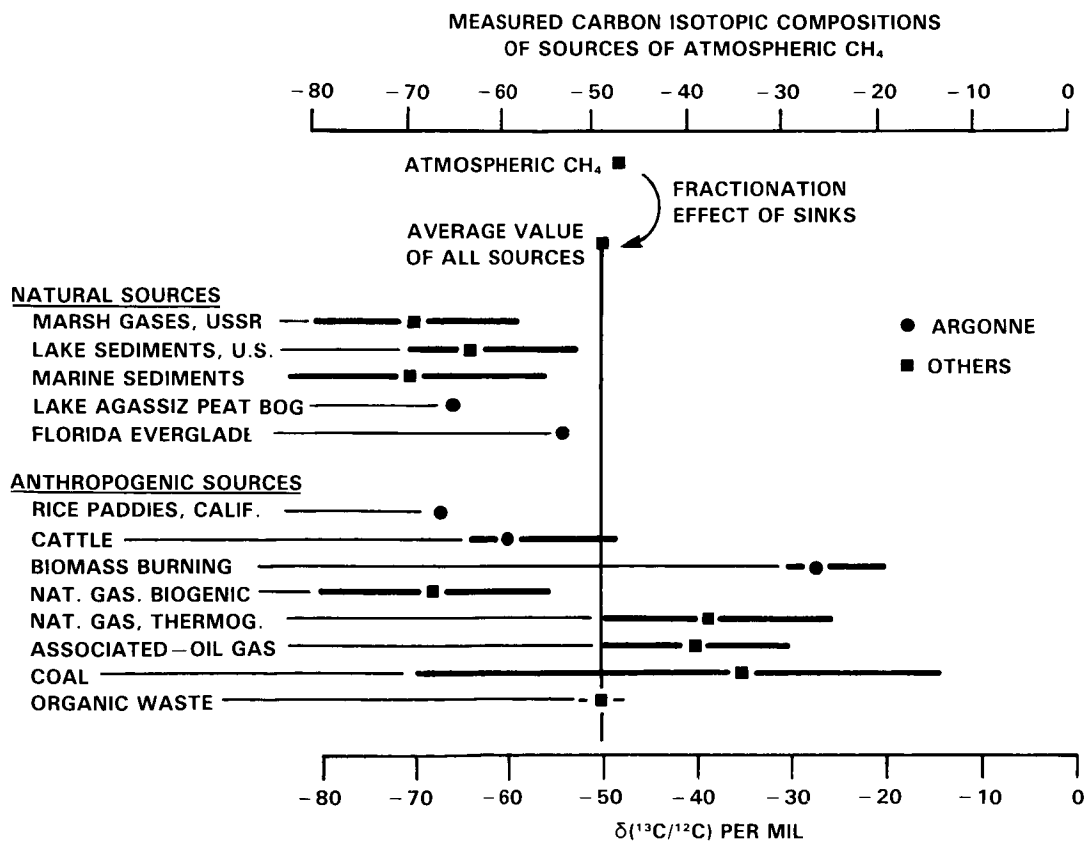


**Figure 3-15.** Summary of  $^{13}\text{C}/^{12}\text{C}$  isotopic composition of major sources of atmospheric methane (Stevens and Engelkemeir, 1985).

## SOURCE GASES

While the carbon isotopes offer promise for source analysis, the D/H ratio in CH<sub>4</sub> may provide useful diagnostics for the sink, since the OH reaction rate is much slower for CH<sub>3</sub>D than for CH<sub>4</sub>. Thus analysis of latitudinal and seasonal variations of CH<sub>3</sub>D in the atmosphere, together with source characterization, may help to define atmospheric distributions of OH.

While CH<sub>4</sub> (1.6 ppm) dominates among global atmospheric hydrocarbons, tropospheric photochemistry and OH-O<sub>3</sub>-CO global distributions are also strongly influenced by other, more reactive hydrocarbons, particularly isoprenes, terpenes, and the C<sub>2</sub>-C<sub>5</sub> alkenes. While the global fields of these non-methane hydrocarbons have not yet been well characterized, some recent, representative measurements are given in Table 3-14.

### 3.5 CARBON MONOXIDE (CO)

The influence of CO on stratospheric chemistry, while indirect, may be extremely important. Increasing levels of CO tend to suppress levels of atmospheric OH, leading to longer lifetimes and higher concentrations of CH<sub>4</sub>, CH<sub>3</sub>CCl<sub>3</sub>, and other species whose sinks are controlled by OH. Hence, factors controlling the atmospheric level of CO are vitally important to stratospheric chemistry as well as to tropospheric chemistry.

#### 3.5.1 Distributions and Trends

Figure 3-16 presents a reconstruction of the global CO distribution from available data through 1980. There is an evident north-south gradient, with more CO in the north. There is significant excess for CO in the lowest layers of the atmosphere in the Northern Hemisphere, while in the south the vertical gradient is very small, with perhaps a slight excess aloft.

More recent measurements have focused on better determination of the vertical gradients (Seiler and Fishman, 1981; Newell *et al.*, 1981), on definition of the seasonal cycles at various latitudes (Khalil and Rasmussen, 1984b,c; Seiler *et al.*, 1984a; GMCC, 1982), and on satellite observations to delineate major source regions (Reichle *et al.*, 1985).

The seasonal variation of CO has been measured at several locations and is shown here (Figure 3-17) for Cape Point, South Africa (Seiler *et al.*, 1984b). Highest concentrations are observed during winter and lowest levels are observed in the summer at ground level in non-urban locations. The amplitude of the seasonal cycle varies with latitude, being greatest at higher latitudes and smallest at the equator (GMCC, 1982; Seiler *et al.*, 1984b; Khalil and Rasmussen, 1984b.c). At northern mid-latitudes, the seasonal cycle amounts to  $\pm 25\%$  of the mean. These observations are in general agreement with the expected pattern, i.e. the inverse of the spatial and temporal variability of OH radicals which remove much of the CO from the atmosphere. Definition of the seasonal behavior has essentially resolved apparent inconsistencies among various data sets obtained at different times of year.

Satellite and aircraft data on mid-tropospheric CO clearly show expected enhancements due to industrial source regions in North America, Europe and Asia, as illustrated in Figure 3-16 to 3-18 (Fishman *et al.*, 1980; Reichle *et al.*, 1985). Important elevated regions were also found in the tropics, possibly associated with agricultural burning. Preliminary analysis of the tropical sources indicated a potentially large contribution to the global CO budget (Delaney *et al.*, 1984; Reichle *et al.*, 1984).

## SOURCE GASES

Table 3-14. Recent Measurements of Light Hydrocarbons

COMPOUND	DATE	CONC $\pm$ SD ppbv	LAT	REF	
C <sub>2</sub> H <sub>6</sub>	1/81	8.00 $\pm$ 1.60	40°N	1	
	6/80	2.97 $\pm$ 2.67	40°S	3	
	1982	1.67	26°S	2	
	12/18,1/79	2.37, 2.1	35°N	2,5	
	12/81	1.86, 2.0	25°N	2,5	
	12/81	0.64, 2.0	10°N	2,5	
	12/81	0.28, 2.0	10°S	2,5	
	12/81	0.23, 0.75	25°S	2	
	12/81	27.56	0-20°N	3	
	6/82	0.85	13-30°N	4	
	11/82	0.40	0-40°S	4	
	C <sub>3</sub> H <sub>8</sub>	1/81	8.50 $\pm$ 1.60	40°N	1
		6/80	0.42 $\pm$ 1.23	40°S	3
1982		0.42	26°S	2	
12/81,1/79		0.80, .85	35°N	2,5	
12/81		0.72, .90	25°N	2,5	
12/81		0.33, .50	10°N	2,5	
12/81		0.26, .20	10°S	2,5	
12/81		0.11	25°S	2	
12/82		10.86	0-20°N	3	
6/82		2.25	13-30°N	4	
11/82		0.10	0-40°S	4	
C <sub>4</sub> H <sub>10</sub>		1/81	3.00 $\pm$ 1.80	40°N	1
		6/80	0.34 $\pm$ 0.33	40°S	3
	1982	0.59	26°S	2	
	12/81	0.51	35°N	2	
	12/81	0.60	25°N	2	
	12/81	0.48	10°N	2	
	12/81	0.16	10°S	2	
	12/81	0.14	25°S	2	
	12/81	9.22	0-20°N	3	
	11/82	0.05	0-40°S	4	
	C <sub>5</sub> H <sub>12</sub>	1/81	3.00 $\pm$ 2.40	40°N	1
		6/80	0.43 $\pm$ 0.42	40°S	3
		1982	0.27	26°S	2
12/81		0.42	35°N	2	
12/81		0.43	25°N	2	
12/81		0.32	10°N	2	
12/81		0.33	10°S	2	
12/81		0.17		2	
12/81		0.99	0-20°N	3	
11/82		1.10	0-40°S	4	

**SOURCE GASES**

**Table 3-14.** Recent Measurements of Light Hydrocarbons — Continued

COMPOUND	DATE	CONC ± SD ppbv	LAT	REF
C <sub>2</sub> H <sub>2</sub>	12/81,1/79	0.46, 0.45	35°N	2,5
	12/81	0.42, 0.40	25°N	2,5
	12/81	0.23, 0.30	10°N	2,5
	12/81	0.25, 0.10	10°S	2,5
	12/81	0.13,	25°S	2,
	2/82	7.62	0-20°N	3
C <sub>2</sub> H <sub>4</sub>	6/80	2.70 ± 2.43	40°S	3
	1982	0.09	26°S	2
	12/81	0.12	35°N	2
	12/81	0.10	25°N	2
	12/81	0.08	10°N	2
	12/81	0.07	10°S	2
	12/81	0.08	25°S	2
	12/81	6.86	0-20°N	3
	6/82	2.10	13-30°N	4
11/82	0.20	0-40°N	4	
C <sub>3</sub> H <sub>6</sub>	1/81	1.00 ± 1.10	40°N	1
	12/81,1/79	0.05, .25	35°N	2,5
	12/81,1/79	0.18, .25	25°N	2,5
	12/81,1/79	0.23, .25	10°N	2,5
	12/81,1/79	0.22, .20	10°S	2,5
	12/81	0.07	25°S	2
	12/82	3.30	0-20°N	3
	12/82	0.20	0-40°N	4
C <sub>5</sub> H <sub>8</sub>		2.27 ± 2.23	40°S	3
C <sub>7</sub> H <sub>8</sub>	1/81	3.00 ± 1.80	40°N	1
	6/80	0.14 ± 0.13	40°S	3
	12/82	5.24	0-20°N	3
C <sub>8</sub> H <sub>10</sub>	1/81	3.00 ± 1.50	40°N	1
	6/80	0.14	40°S	3
	12/82	2.95	0-20°N	3

1. Sexton and Westberg, 1984.
2. Singh and Salas, 1982.
3. Greenberg and Zimmerman, 1984.
4. Bonsang and Lambert, 1985.
5. Rudolph and Ehhalt, 1981.

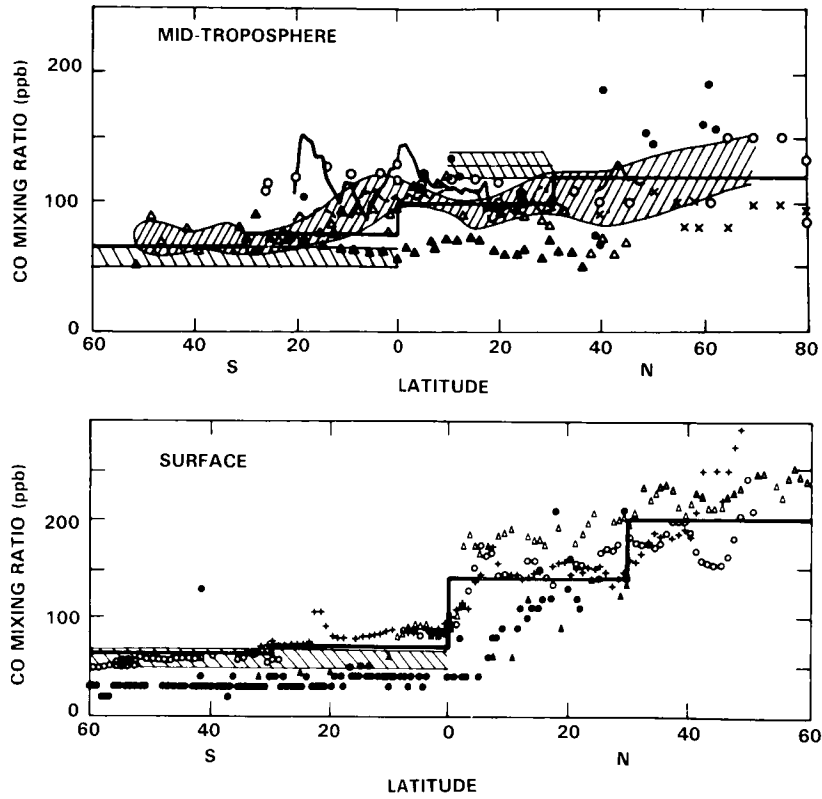


**Figure 3-16.** Summary of atmospheric CO measurements as a function of latitude for (a) mid-troposphere and (b) surface for the period 1967-78 (from Logan *et al.*, 1981). The heavy lines show average values for latitude zones 0, 30° (N,S) and 30, 90° (N,S).

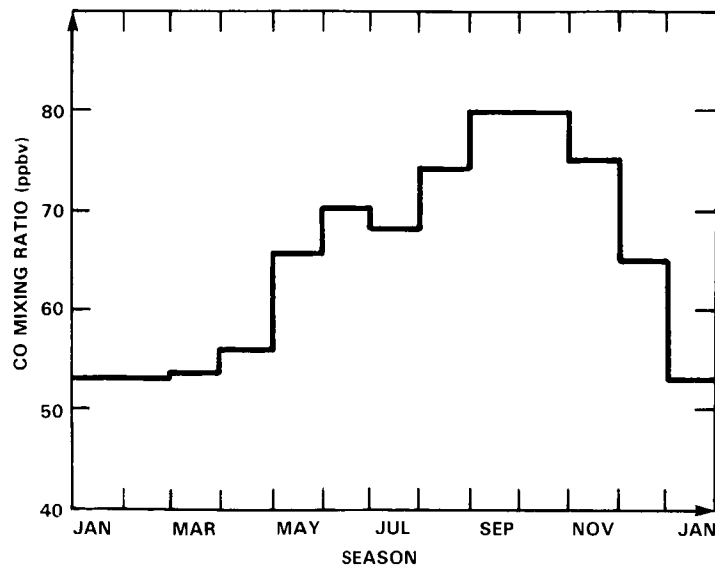


**Figure 3-17.** Seasonal variation of atmospheric CO mixing ratio (ppbv) measured at Cape Point, South Africa (34°S), 1978-81, (Seiler *et al.*, 1984b).

## SOURCE GASES

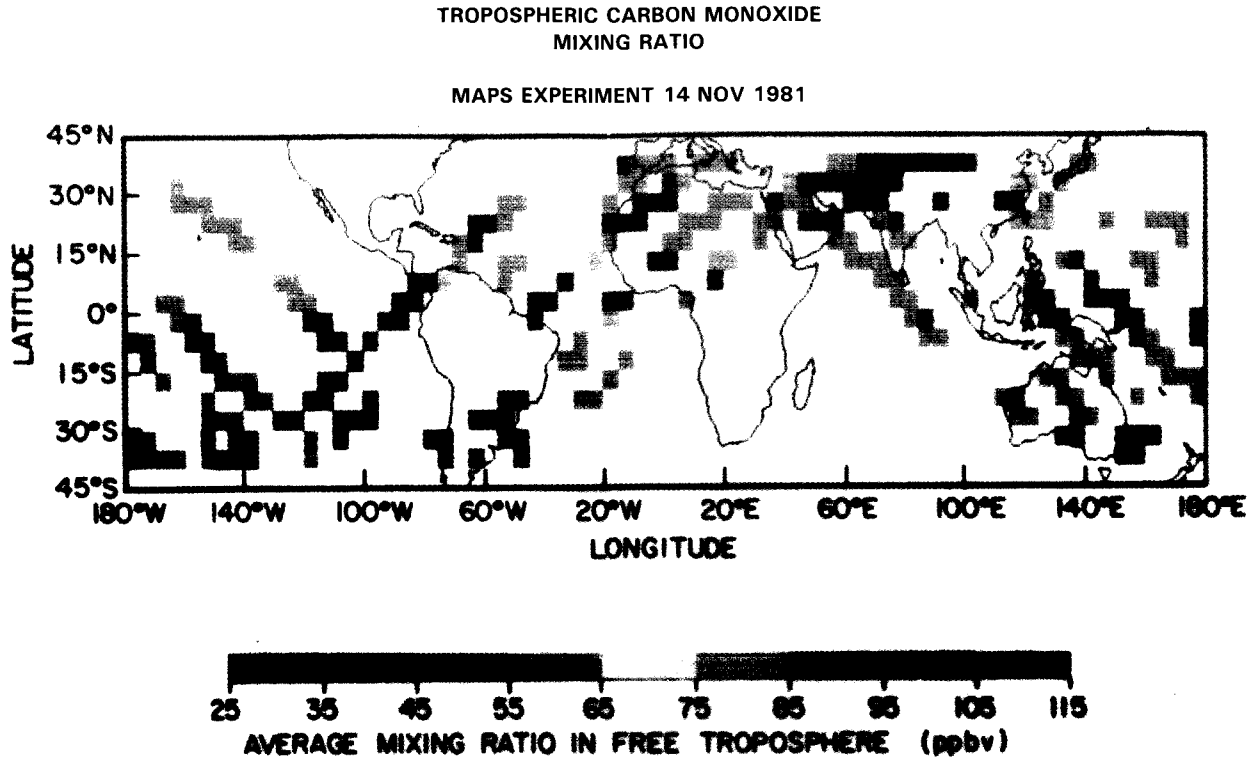


**Figure 3-18.** Average value of the volume mixing ratio of carbon monoxide in the free troposphere as measured by the Measurement of Air Pollution from Satellite (MAPS) experiment. The experiment was flown on  $5^\circ \times 5^\circ$  squares, and they have a precision of a few percent (Reichle *et al.*, 1985).

Since large anthropogenic sources of CO have been identified, it is expected that concentrations of CO may be increasing on a global scale. Carbon monoxide is emitted from a large number of primarily land-based sources as well as from the atmospheric oxidation of  $\text{CH}_4$  and other hydrocarbons. It reacts rather rapidly with OH radicals ( $\bar{\tau} \approx 0.4$  yrs,  $\tau_{\text{min}} \approx 0.1$  yrs in the tropics). The short atmospheric lifetime allows concentrations of CO to vary considerably in both space and time, making it difficult to isolate slow increases representative of the long-term trend. Trends may be quite dependent on latitude. Nevertheless, some recent data have shown an increase in the concentration of CO that may represent a long-term trend, although the magnitude is still quite uncertain. One study (Khalil and Rasmussen, 1984b,c) indicated CO increases of about  $5\% \text{ yr}^{-1}$  at Cape Meares, Oregon between 1979 and 1982. Subsequent measurements at this site lowered the estimated mean trend. Results presented by Dvoryashina *et al.* (1984) based on spectroscopic measurements of CO over the U.S.S.R. between 1971-1983, suggest a 1-2% increase during that period. Rinsland and Levine (1985) deduced values for CO over Switzerland in 1951 (from Migeotte's plates) and they estimated in mean annual increase of  $\approx 2\% \text{ yr}^{-1}$  between 1951 and 1981 at that site.

Mean concentrations and variability are smaller for CO in the Southern Hemisphere than in the north. The dominant sources of CO in the south may be the oxidation of  $\text{CH}_4$  and transport from the north. Comparison of recent measurements of CO at Cape Point, South Africa (1978-81) with shipboard data obtained in 1971-1972 indicates that CO in the Southern Hemisphere may have increased by  $0.5\text{-}1\% \text{ yr}^{-1}$  (Seiler *et al.*, 1984b). Measurements of CO taken at Tasmania and the South Pole do not yet show statistically significant increases (Fraser *et al.*, 1984).

It appears from these rather sparse data that CO may be increasing on a global scale, with the most significant increases at mid-to-high northern latitudes. It is not yet possible to estimate accurately the rate of CO increase, which is statistically more difficult than for CH<sub>4</sub> or CO<sub>2</sub> due to the greater spatial and temporal variability of CO.

### 3.5.2. Sources

Table 3-15 presents a recent budget for CO, adapted from Logan *et al.* (1981). Estimates for combustion are derived from detailed emissions inventories which incorporate the results of many field measurements. (Readers are referred to reviews by Seiler and Crutzen (1980) and Logan (1983) for detailed discussion.) The ranges given in Table 3-15 amount to "only" about  $\pm 50\%$ , reflecting the considerable attention paid by environmental agencies to this subject. Since much of the uncertainty is associated with estimates of the quantity of fuel consumed (especially in the case of biomass burning), it appears that better definition of the CO cycle must attend development and deployment of CO monitoring instruments, on satellites and on the ground, on refinement of the global OH distributions, and on remote sensing of agricultural burning. Development of a complete picture of CO sources requires coordinated research sampling a variety of spatial and temporal scales, in a manner analogous to that discussed for CH<sub>4</sub>.

### 3.5.3 Discussion

Anthropogenic activities account for about 40% of global CO emissions, and one would expect at least comparable increase in the global concentrations. High emissions of CO tend to suppress the concentration of OH (Wofsy, 1976), which can lead to positive feedback and more-than-proportionate increase in the CO abundance (Sze, 1977). However, it appears that elevated CO levels may be concentrated near the latitudes of maximum combustion sources, where NO<sub>x</sub> may also be elevated due to combustion (cf. Fishman *et al.*, 1980). Coincident elevations of CO and NO<sub>x</sub> may lead to enhanced photochemical activity, including significant ozone production (Crutzen, 1973; Chameides and Walker, 1973; Fishman *et al.*, 1979). Indeed, there is evidence of a correlation between high O<sub>3</sub> and high CO levels at northern midlatitudes indicative of enhanced photochemical activity (Fishman and Crutzen, 1978; Fishman *et al.*, 1980). It is possible that OH levels may actually be enhanced in the regions of high CO, due to excess NO<sub>x</sub>, O<sub>3</sub>, and other species. Thus, the possibility of OH-CO positive (or negative) feedback cannot be assessed without a good understanding of NO<sub>x</sub>, O<sub>3</sub> and hydrocarbon distributions in the atmosphere.

It is important to note that present day concentrations of CO (and CH<sub>4</sub>) are not in equilibrium with emissions, because CO and CH<sub>4</sub> are coupled, and the time constant for relaxation of the coupled OH-CO-CH<sub>4</sub> system may be several times longer than the 10 year lifetime of CH<sub>4</sub> (cf. Sze, 1977). This effect arises from the positive feedback discussed above: oxidation of CH<sub>4</sub> gives rise to an important source for CO, and CO and CH<sub>4</sub> are the dominant sinks for OH.

There is no direct evidence to define the time history for CO over past centuries, and hence one cannot accurately assess the extent of the CO rise due to anthropogenic activity. A number of factors suggest that increases probably are large, i.e. 2 or more times more CO today than in prehistoric times: the north/south gradient is of this order, present rates of increase appear to be substantial, and the source estimates break down to ~60/40 (natural/anthropogenic). If CO levels have indeed increased substantially over the globe, then atmospheric chemistry is very different today from the unperturbed state some centuries ago.

## SOURCE GASES

Table 3-15. Carbon Monoxide<sup>a</sup> (1984 concentrations 30–200 ppb)

A. <i>Atmospheric burden</i> ( $10^6$ tons as C)	200
B. <i>Sinks + accumulation</i> ( $10^6$ tons as C $\text{yr}^{-1}$ )	
reaction with OH	820 $\pm$ 300
soil uptake	110
accumulation (5.5% $\text{yr}^{-1}$ )	10
total	940 $\pm$ 330
C. <i>Sources</i> ( $10^6$ tons as C $\text{yr}^{-1}$ )	
fossil fuel combustion	190
oxidation of anthropogenic hydrocarbons	40
wood used as fuel	20
oceans	20
oxidation of $\text{CH}_4$	260
forest wild fires (temperate zone)	10
agricultural burning (temperate zone)	10
oxidation of natural hydrocarbons (temperate zone)	100
burning of savanna and agricultural land (tropics)	100
forest clearing (tropics)	160
oxidation of natural hydrocarbons (tropics)	150
total	1060
D. <i>Tropical Contribution</i> ( $10^6$ tons as C $\text{yr}^{-1}$ )	
burning	100
forest clearing	160
oxidation of hydrocarbons	150
total	410

<sup>a</sup> From Logan *et al.* (1981), updated by Logan *et al.* (private communication, 1984).

### 3.6 CARBON DIOXIDE ( $\text{CO}_2$ )

Although carbon dioxide is not itself a photochemically active species in either the troposphere or the stratosphere, it must be included in any discussion of source gases because it is the single most important greenhouse gas in the atmosphere. Hence it will have a strong influence on the temperature-dependent photochemistry in the stratosphere. A second reason to include  $\text{CO}_2$  is that it is the most abundant and best studied trace gas of the global carbon cycle. There are long, very precise and detailed time-series for atmospheric  $\text{CO}_2$  at different latitudes (Figures 3-19, 3-20). Such records offer a critical history of the evolution of atmospheric-biospheric exchange, and will greatly facilitate the interpretation of the cycling of related trace gases of the carbon cycle (e.g.  $\text{CH}_4$ , CO), whose secular increases have only very recently

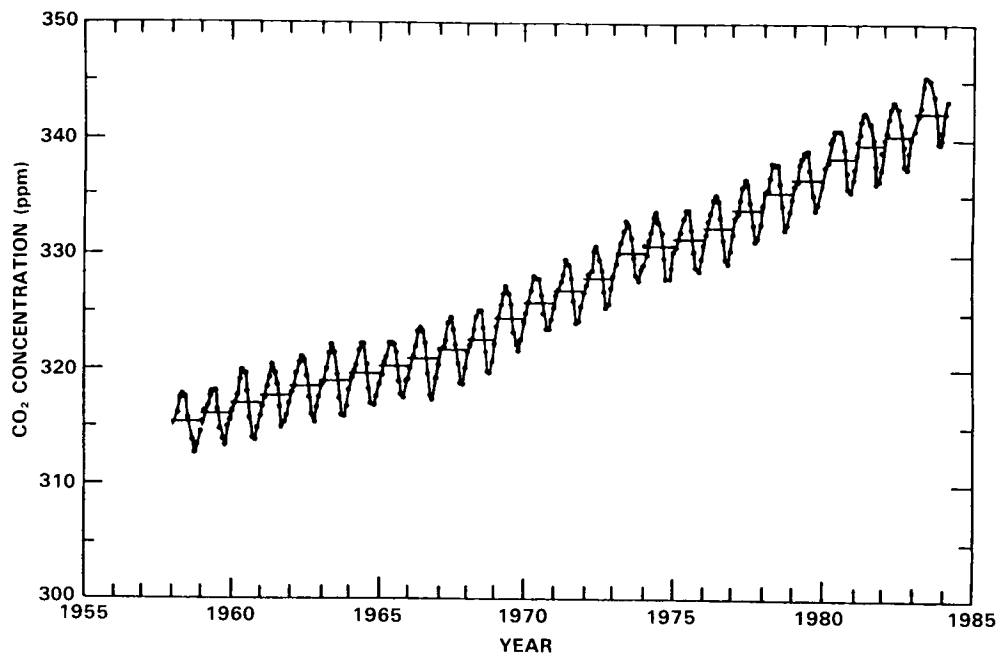


**Figure 3-19.** Concentration of atmospheric CO<sub>2</sub> at Mauna Loa Observatory, Hawaii, expressed as a mole fraction in ppm of dry air. The dots depict monthly averages of visually selected data which have been adjusted to the center of each month. The horizontal bars represent annual averages. Data obtained by C.D. Keeling, Scripps Institution of Oceanography, University of California, La Jolla, California, and are from files in the Carbon Dioxide Information Center, Oak Ridge National Laboratory, Oak Ridge, Tennessee.

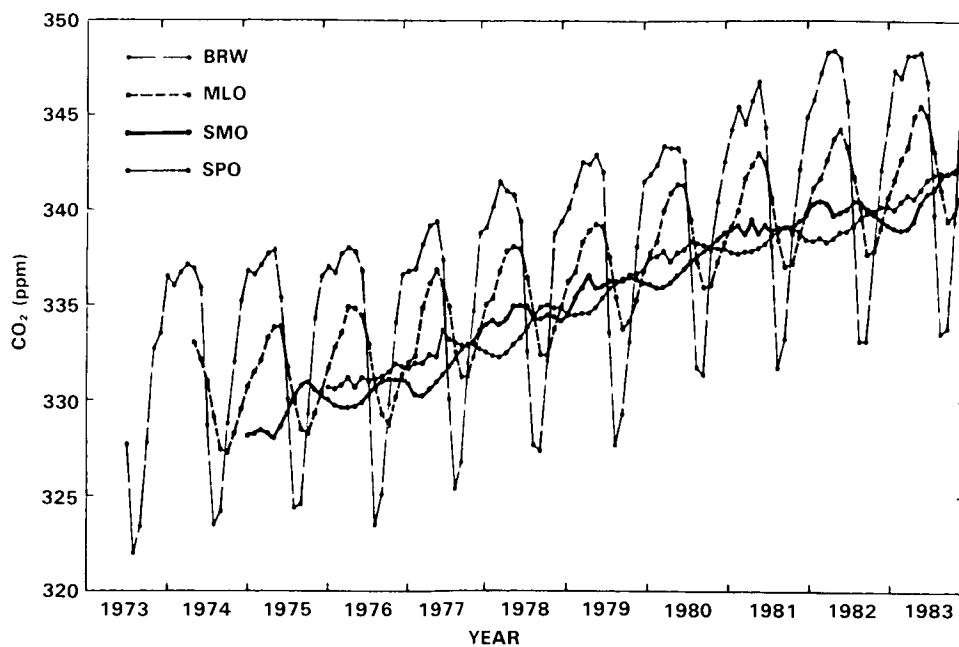


**Figure 3-20.** Provisionally selected monthly mean CO<sub>2</sub> concentrations from continuous measurements at the NOAA/GMCC baseline observatories (:Barrow, Alaska (BRW); Mauna Loa, Hawaii (MLO); American Samoa (SMO); South Pole (SPO). Values are in the WMO X81 mole fraction scale (Harries and Nicker-son, 1984).

## SOURCE GASES

been established, and for which the mechanisms of change are much less well understood. Unlike the industrial sources of fluorocarbon gases, the biogenic sources of several important species ( $\text{CO}_2$ ,  $\text{CH}_4$ ,  $\text{CO}$ ,  $\text{N}_2\text{O}$ ,  $\text{OCS}$ , etc.) will likely *respond to*, as well as promote, climatic change. The inferences drawn from  $\text{CO}_2$  studies on the working of the natural and perturbed carbon cycle will be essential for making accurate predictions of the evolving biogeochemical cycles of carbon, nitrogen, and sulfur under direct and indirect (climatic) human impact.

### 3.6.1 $\text{CO}_2$ Trends and Global Distribution

The modern period of direct, precise measurement of rising atmospheric  $\text{CO}_2$  levels began with C.D. Keeling's time-series at Mauna Loa Hawaii (Figure 3-19, MLO) and at the South Pole during IGY (1958). Before this time,  $\text{CO}_2$  measurements were of much lower quality, and of a less direct nature (see Gammon *et al.*, 1985a for a detailed review of the history of atmospheric  $\text{CO}_2$  measurements and methods). Since the early 1970's, continuous measurements of  $\text{CO}_2$  have been made by NOAA/GMCC at four remote stations: Barrow, Alaska; Mauna Loa, Hawaii; American Samoa, and the South Pole (Figure 3-20, Gammon *et al.*, 1985 a,b; Harries and Nickerson, 1984). The NOAA time-series at MLO agrees very well with the corresponding Keeling record. Recent interpretations of the global  $\text{CO}_2$  distributions have been presented by Keeling *et al.* (1984), Keeling (1983), Pearman *et al.* (1983), Fraser *et al.* (1984), Bacastow *et al.* (1985), Komhyr *et al.* (1985).

A more detailed representation of the spatial and temporal variability of  $\text{CO}_2$  near the earth's surface became possible in 1979 with the establishment of a global network of 20 cooperating air sampling sites coordinated by GMCC/NOAA. The  $\text{CO}_2$  results from this network through 1983 have been recently described by Komhyr *et al.* (1985); the global  $\text{CO}_2$  concentration surface for 1980-83 is shown in Figure 3-21. The observed  $\text{CO}_2$  seasonal amplitude is dominated by land plants and soils in the northern mid-latitudes. Figure 3-22 shows the latitude dependence of the  $\text{CO}_2$  seasonal amplitude (Gammon *et al.*, 1985b), which is strongly enhanced at northern middle and high latitudes.

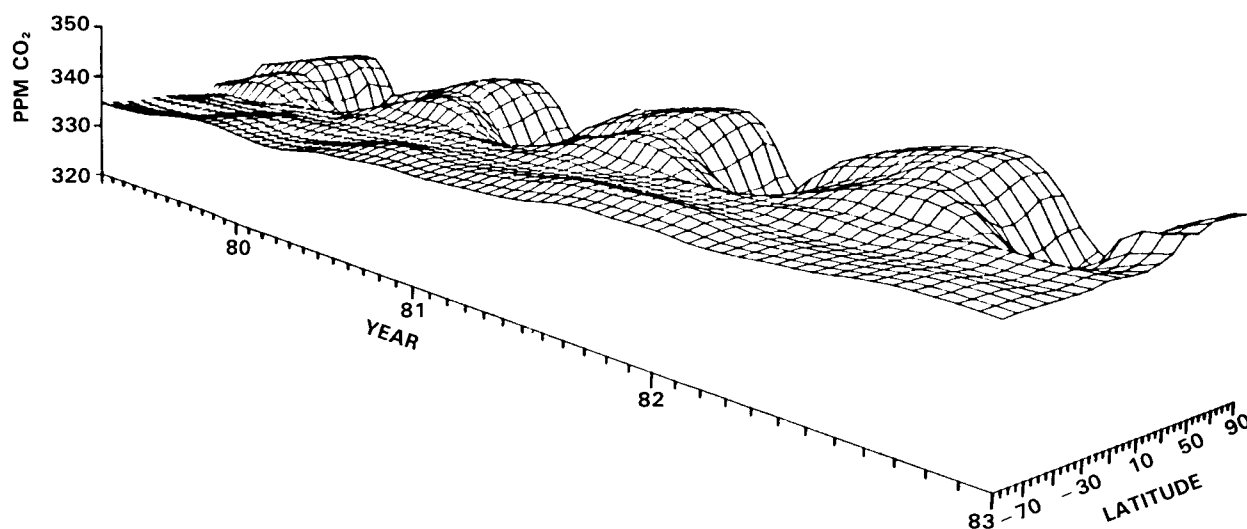


**Figure 3-21.** A three-dimensional perspective of the "pulse-of-the-planet," the variation of the global atmospheric  $\text{CO}_2$  concentration in latitude and time based on flask measurements for 1979-1982. This zonally averaged surface has a resolution of 20 days and  $10^\circ$  in latitude and was synthesized from results of  $\sim 10,000$  individual flask samples returned from 15 remote sea-level sites of the NOAA/GMCC sampling network (Komhyr *et al.*, 1985).

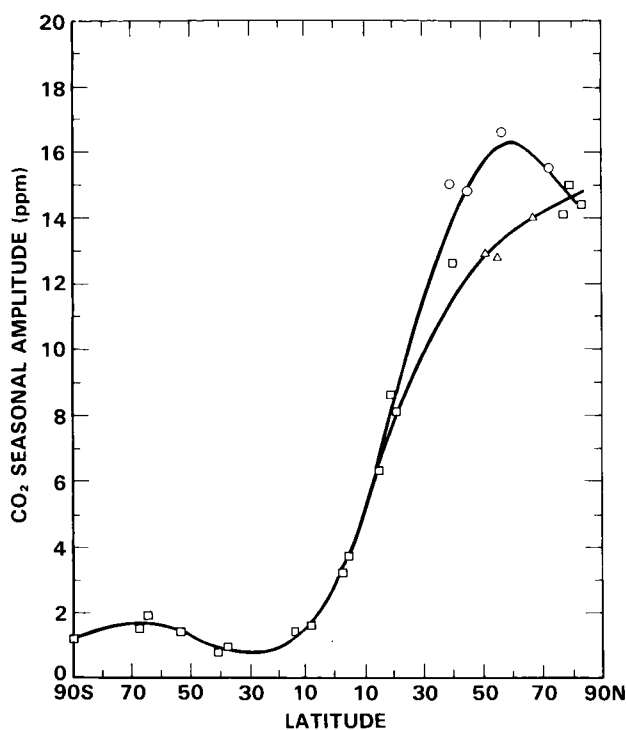


**Figure 3-22.** Latitude dependence of the atmospheric CO<sub>2</sub> seasonal amplitude as determined from surface stations (Komhyr *et al.*, 1985; Gammon *et al.*, 1985b). The separate curves at high northern latitude distinguished mid-ocean (Δ) from coastal (O) sites.

### 3.6.2 Discussion

Three examples are chosen below to illustrate: (1) the difficulty of establishing secular trends of biogenic trace gases in the presence of large interannual variability of natural origin; (2) the use of global trace gas data sets to interpret satellite remote sensing indices of global biospheric activity; and (3) the possibility that carbon cycle trace gas measurements offer a sensitive indicator of evolving atmosphere-biosphere exchanges in response to predicted climatic change. A summary of the temporal trends and variability observed for all three carbon cycle trace species (CO<sub>2</sub>, CH<sub>4</sub>, CO) is given in Table 3-16.

#### Natural Interannual Variability and El Nino:

The El Nino-Southern Oscillation perturbation of the global atmospheric CO<sub>2</sub> distribution is the strongest signal in the record after the local seasonal amplitude and long-term trends are removed. These CO<sub>2</sub> fluctuations are well correlated with both the Southern Oscillation Index and with regional sea surface temperature anomalies. The extraordinary 1982/83 ENSO event measurably perturbed the total global atmospheric burden of CO<sub>2</sub>. The amplitude of the natural CO<sub>2</sub> fluctuation associated with an ENSO event is of order  $\pm 0.5$  ppm; for comparison, background air is currently  $\sim 345$  ppm CO<sub>2</sub> in the global mean. Natural atmospheric CO<sub>2</sub> fluctuations of order 1 ppm (or 2 Gton carbon global atmospheric equivalent) correspond to small perturbations (1-2%) in the annual exchanges of the atmosphere-ocean (100 Gton C yr<sup>-1</sup>) and atmosphere-biosphere (60 Gton C yr<sup>-1</sup>) systems (Keeling, 1983). Fluctuations in the source-sink balance of either the biosphere or the ocean could be responsible for the observed atmospheric CO<sub>2</sub> fluctuations. Isotopic measurements (<sup>13</sup>CO<sub>2</sub>) are useful in distinguishing between these two possibilities (Mook *et al.*, 1983).

## SOURCE GASES

Table 3-16. Carbon Cycle Trace Gases: Summary of Measured Atmospheric Changes

Species	Tropospheric Concentration				Seasonality		Interannual Variability  (in growth rate or seasonal amplitude)
	Present Level (1984, ppm) global mean	Secular Increase (% change in period) during decades			% Increase in Seasonal amplitude during decades		
		Past Century	1965-75	1975-85	1965-75	1975-85	
		% decade <sup>-1</sup>	% decade <sup>-1</sup>	% decade <sup>-1</sup>	% decade <sup>-1</sup>	% decade <sup>-1</sup>	
CO <sub>2</sub>	343.8 ± 0.2		3	4	≤ 2	10-20	Yes (ENSO)
CH <sub>4</sub>	1.67 ± .01		< 5	10-15	- ? -	- ? -	Yes (ENSO)
CO	~0.09 ± .02		- ? -	5-50	- ? -	- ? -	Yes?

The globally averaged year-to-year change in atmospheric CO<sub>2</sub> plotted by season (Figure 3-10c) clearly shows the effect of the 1982/83 ENSO event on the global atmospheric burden of CO<sub>2</sub> over at least a two-year period, from mid-1982 to mid-1984. The summer of 1982, relative to the fall of the previous year, showed no increase ( $0.0 \pm 0.2$  ppm yr<sup>-1</sup>) in global CO<sub>2</sub> levels, implying that the equivalent of approximately  $5 \times 10^9$  tons of fossil carbon burned during that interval was removed from the atmospheric reservoir for temporary storage in the near surface ocean, and (probably) in the land biosphere as well. Now, more than a year after the minimum in the Southern Oscillation Index (1/83), this missing 5 Gtons of carbon has been returned to the global atmosphere; the year-to-year CO<sub>2</sub> increase peaked in early 1984 at  $2.2 \pm 0.2$  ppm yr<sup>-1</sup> before returning to the long-term mean growth rate of 1.4 ppm yr<sup>-1</sup> representative of the past decade. Since the past 5 years has been a period of nearly constant global combustion of fossil fuel  $\approx 5$  Gton yr<sup>-1</sup>, the observed large interannual variations in atmospheric CO<sub>2</sub> are clearly *not* the result of changing rates of fossil fuel usage. One important conclusion is that secular trends extracted from time series measurements of biogenic trace gases are only reliable when the time span covers one or more major ENSO cycles (4-7 years), since large interannual variations in the growth rate have been observed for both CO<sub>2</sub> and CH<sub>4</sub>. In the case of CO<sub>2</sub>, these interannual variations have been shown to be correlated with interannual variation in tropospheric temperature in that latitude band (Gammon *et al.*, 1985b). In the case of CH<sub>4</sub>, the oceanic content is only  $\sim 1/300$  of the atmospheric burden, and the variations shown in Figure 3-10 must therefore arise from variations in terrestrial sources.

### Atmospheric CO<sub>2</sub> and the Global Biosphere:

There is large uncertainty in assessing the global response of the land biosphere to the altered temperature and precipitation patterns which accompany a major El Nino event. While regional crop failures, floods and droughts are well documented, the globally integrated biospheric response and its effect on atmospheric CO<sub>2</sub> and other biogenic trace gases is harder to estimate. There is some recent evidence from satellite monitoring of the "vegetation index" of land plant activity that 1982 was a better growing season globally than 1983 (Fung *et al.*, 1985). This suggests that some fraction of the 5 Gtons of carbon missing from

the global atmosphere in the summer of 1982 may have been temporarily stored in the biosphere. Global surface measurements of seasonally varying CO<sub>2</sub> recently have been shown to relate directly to the seasonal photosynthetic activity of land plants as indicated by satellite indices of green-leaf matter (Tucker *et al.*, 1985; Fung *et al.*, 1985; Figure 3-23).

### Increasing Amplitude of the CO<sub>2</sub> Seasonal Cycle: A Climate Signal?

The regular variation of atmospheric CO<sub>2</sub> levels by season and latitude in the Northern Hemisphere is dominated by the seasonal exchange between the atmosphere and the land biosphere and soil carbon reservoirs (Figures 3-21, 3-22). Any major change in either photosynthetic uptake or respiratory release of carbon will alter the observed CO<sub>2</sub> seasonality, which represents the local imbalance of these two opposing processes. While the first attempt to find such secular changes in the CO<sub>2</sub> seasonal amplitude at Mauna Loa (Hall *et al.*, 1975) were not successful, more recent investigations *have* found large and significant growth rates in the seasonal amplitude at several Northern Hemisphere locations (MLO, 'P', BRW), especially during the past decade (Pearman and Hyson, 1980; Cleaveland *et al.*, 1983; Bacastow *et al.*, 1985; Komyr *et al.*, 1984; Keeling *et al.*, 1984). At Mauna Loa, the mean rate of increase has been  $\sim 0.7\% \text{ yr}^{-1}$  from 1958 to 1982, resulting in a 20% increase (5.5  $\rightarrow$  6.5 ppm) in the CO<sub>2</sub> seasonality over this interval (Bacastow *et al.*, 1984). For comparison, the corresponding percentage increase in CO<sub>2</sub> concentration has been only 9%. The amplitude increase before 1975 was slight ( $\sim 0.2\% \text{ yr}^{-1}$ ). However, since 1975, the increase in amplitude has been very rapid ( $\sim 2\% \text{ yr}^{-1}$  or  $\sim 0.1 \text{ ppm yr}^{-1}$ ). Similar rates of increase in the local CO<sub>2</sub> seasonality, have been recently reported for the long CO<sub>2</sub> records at more northerly stations (Weathership 'P', Keeling *et al.*, 1984; Barrow, Alaska, Bacastow *et al.*, 1985). While the NOAA/GMCC flask and continuous records at MLO and BRW extend only over the last decade, they also exhibit CO<sub>2</sub> seasonality growth rates of 1-2%  $\text{ yr}^{-1}$  over this period. The CO<sub>2</sub> amplitude changes at all northern latitudes have been similar in absolute terms (0.1-0.2 ppm  $\text{ yr}^{-1}$ ), the largest rates of increase ( $\sim 0.2 \text{ ppm yr}^{-1}$ ) observed in the Arctic (BRW).

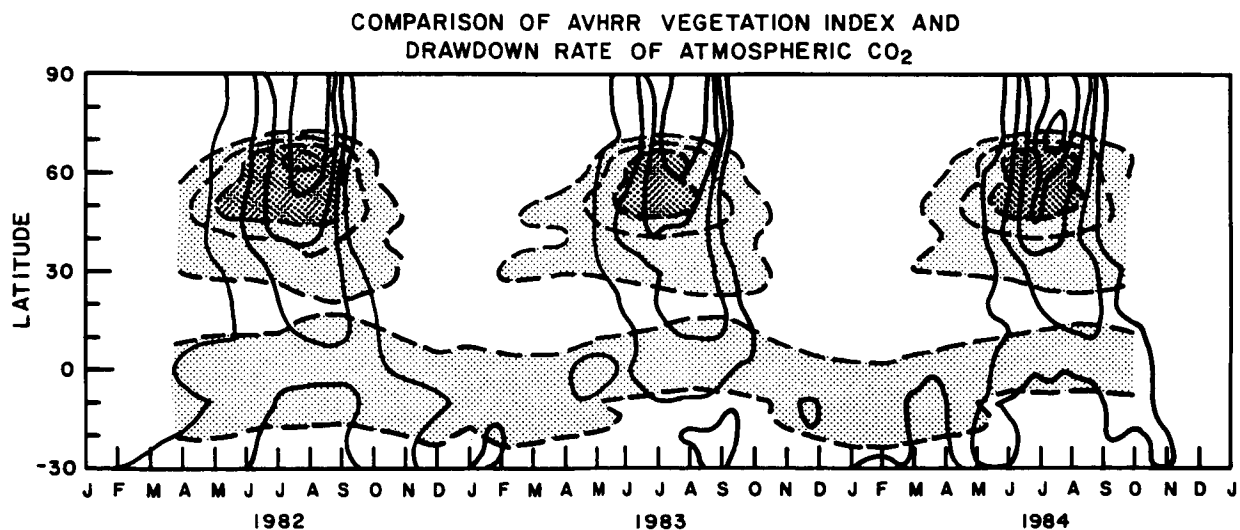


**Figure 3-23.** Overlay of the seasonal variation of atmospheric CO<sub>2</sub> with the seasonal variation of satellite-derived indices of photosynthetic activity of land plants ("normalized difference vegetation index") (Tucker *et al.*, 1986; Fung *et al.*, 1986). The dashed contours and the shaded regions represent the zonally averaged vegetation index; contour interval is 0.1. The solid contours represent negative values of  $d\text{CO}_2/dt$ , the rate of summer draw-down of atmospheric CO<sub>2</sub> by the land plants. Contour interval is  $-2 \text{ ppm/month}$ . Positive values of  $d\text{CO}_2/dt$  representing fall respiration are not reflected in corresponding variations of the vegetation index and are not plotted. Both CO<sub>2</sub> draw-down rates and vegetation indices peak at high (60°-70°N) northern latitudes in July-August.

## SOURCE GASES

As discussed by Keeling (1983) and Bacastow *et al.* (1985), an increasing CO<sub>2</sub> seasonal amplitude indicates 'increased plant activity,' but not necessarily increased net carbon storage. The observed percentage increase in northern hemisphere CO<sub>2</sub> seasonality is more than twice that of the CO<sub>2</sub> concentration, which suggests that any 'fertilization effect' (i.e. enhanced photosynthesis by the land biosphere in a higher CO<sub>2</sub> environment) could explain only a small fraction of the observed change in seasonal amplitude.

The seasonality of fossil fuel release is also insufficient to explain the increase (Pearman and Hyson, 1980). A more likely explanation is to be found in the strong temperature dependence of respiration of CO<sub>2</sub> from plants and soils and the observed warming trend over the last decade in the northern hemisphere. Harmonic analyses of the secular changes in CO<sub>2</sub> amplitude at each site may reveal whether enhanced photosynthesis (annual) or enhanced respiration (semi-annual) is more important. A first look at the NOAA/GMCC continuous CO<sub>2</sub> records since 1975 suggests that the changing seasonality of MLO is largely due to enhanced summer photosynthetic fixation of CO<sub>2</sub>, while at BRW, spring and fall respiration pulses contribute equally to an enhanced summer draw down as causes of the CO<sub>2</sub> amplitude increase. If the amplitude increase is proportional to the local amplitude, then the largest absolute changes are predicted to occur in the latitude band 50-60°N where the CO<sub>2</sub> seasonal amplitude itself is maximum.

As noted above, the second most important trace gas of the carbon cycle, methane, is now known to be increasing in the atmosphere at ~1% yr<sup>-1</sup>. There is evidence to suggest that the percentage rate of the CH<sub>4</sub> increase has become more rapid during the last decade (cf. Ehhalt *et al.*, 1983b). If the locus of the source region driving the atmospheric CH<sub>4</sub> increase is found to be the same as that for the CO<sub>2</sub> seasonal amplitude increase, then a strong argument can be made that both phenomena represent a response of the Northern Hemisphere biosphere and soil carbon pool to the incipient climate change predicted for the coming decades. Thus the change in CO<sub>2</sub> seasonality may be the first indication of a positive feedback loop involving atmospheric CO<sub>2</sub>, boreal climate, and soil carbon reservoirs. Increasing levels of CH<sub>4</sub> may also reflect these interactions, at least in part.

Table 3-16 summarizes current knowledge of the temporal behavior of the major gases of the carbon cycle (CO<sub>2</sub>, CH<sub>4</sub>, CO) during the past century and in particular during the past two decades. Clearly, CO<sub>2</sub> has been most intensively studied and is best understood. However, the relative roles of the ocean versus the land biota in producing the El Nino-related variability is very uncertain, as is the cause for the sudden onset of an increase in the seasonal amplitude during the past decade. For CH<sub>4</sub>, the seasonal amplitude is not yet well enough defined to detect secular amplitude changes, although the CH<sub>4</sub> concentration itself is observed to be increasing more rapidly since 1975 than in the previous decade. For CO, the observations are even more limited in space and time than for CH<sub>4</sub>, although some growth in the atmospheric CO level during the past decade has been reported, perhaps more rapid in far northern latitudes (1-4% yr<sup>-1</sup>) than in southern latitudes (0-0.5% yr<sup>-1</sup>). Of the carbon-cycle gases, the perturbation of the atmospheric concentration from pre-industrial levels seems to have been greater for CH<sub>4</sub> than for CO<sub>2</sub>. Preindustrial levels of CO are unknown. Levels and growth rates for N<sub>2</sub>O are included for comparison to illustrate that the primary biogenic trace gases of both the carbon (CH<sub>4</sub>, CO<sub>2</sub>) and nitrogen (N<sub>2</sub>O) cycles have experienced an acceleration in their rate of atmospheric increase during the past decade.

### 3.7 SOURCE GASES FOR STRATOSPHERIC SULFATE AEROSOLS (OCS, CS<sub>2</sub>)

While most sulfur gases emitted into the troposphere from natural and anthropogenic sources are too reactive and/or too soluble to reach the stratosphere, OCS is an important exception (Crutzen, 1976; Sze and Ko, 1979). Apart from volcanic injection, the major source of sulfur to the stratosphere is OCS from

## SOURCE GASES

the troposphere. Thus, as for CO<sub>2</sub>, the major role of OCS in stratospheric chemistry is indirect, via the role of the stratospheric sulfate aerosol layer in influencing the temperature structure in the lower stratosphere (18-22 km).

Carbonyl sulfide (OCS), has an atmospheric lifetime greater than one year. The OCS concentration in the free troposphere (500 ppt) is many times greater than other sulfur gases (Torres *et al.*, 1980), and therefore is a major source of sulfur to the background (non-volcanically perturbed) stratospheric sulfate layer (Crutzen, 1976; Turco *et al.*, 1980). The present anthropogenic sources appear to be a relatively small fraction of the total global emissions (Khalil and Rasmussen, 1985b, Table 3-17). Johnson (1985)

**Table 3-17.** Global Sources and Sinks of Carbonyl Sulfide and Carbon Disulfide\*

	OCS		CS <sub>2</sub>	
	Estimate	Range	Estimate	Range
<b>Sources (Tg y<sup>-1</sup>)</b>				
Oceans	0.60	0.3 - 0.9	0.6	0.2 - 0.7
Soils	0.40	0.2 - 0.6	0.9	0.5 - 2
Volcanoes	0.02	0.01 - .05	0.02	< 0.1
Marshes	0.02	0.01 - 0.06	0.1	0.05 - 0.2
Biomass burning	0.20	0.1 - 0.5	—	—
Coal-fired power plants	0.08	0.4 - 0.15	—	—
Automobiles, chemical industry and sulfur recovery processes	0.06	0.01 - 0.3	0.37	< 0.7
Subtotal	1.4	≤ 3	2	≤ 4
<b>CS<sub>2</sub> → OCS:</b>				
CS-photochemistry and OH reactions	0.60	0 - 2	0	0
Total	2	≤ 5	2	≤ 4
Global burdens (Tg)	4.6	3.8 - 5	0.07	0.04 - 0.1
	(500 pptv)		(20 pptv)	
Lifetime (y)	2-2.5	≥ 1	13 days	>4 days
<b>Sinks (Tg y<sup>-1</sup>)</b>				
OH reaction	0.8	0.1 - 1.5	0.6	≤ 4
Stratospheric photolysis	0.1	≤ 0.2	0	0
O atom reaction	0.03	—	0.1	< 0.2
Other	1.1	≤ 3.3	1.3	< 3

\* The estimated emissions are consistent with observed distributions of OCS and CS<sub>2</sub> according to a global mass balance (see text). All combinations of emissions within the ranges given above may not be consistent.

## SOURCE GASES

has reviewed remote tropospheric measurements of OCS over a seven year period by four different groups and estimated that the maximum secular trend was  $\pm 3\%$  per year and the most likely value was much closer to zero (Table 3-18). Torres *et al.* (1980) found the north-to-south interhemispheric gradient to be less than 10% from aircraft measurements in the free troposphere; from shipboard measurements in the marine boundary layer, Johnson (1985) set a limit on the meridional gradient within the Northern Hemisphere of less than 7%. Less is known about longitudinal gradients, expected to be smaller than latitudinal gradients except near strong regional sources.

Carbon disulfide ( $\text{CS}_2$ ) has an atmospheric lifetime of a few weeks, giving it an extremely low upper tropospheric concentration (6 ppt at 6 km, Tucker *et al.*, 1985), so that it does not directly affect the stratosphere. However, it appears that the atmospheric oxidation of  $\text{CS}_2$  by OH produces OCS, so that atmospheric  $\text{CS}_2$  is likely a major source of tropospheric OCS (Sze and Ko, 1979; Jones *et al.*, 1983; Barnes *et al.*, 1983). Hence, the OCS distribution may be influenced by emissions of  $\text{CS}_2$  from industrial sources. A detailed assessment is impossible at present due to the scant knowledge about actual source strengths for OCS or  $\text{CS}_2$  from natural and anthropogenic sources.

### 3.8 VOLCANIC INJECTIONS OF CHLORINE INTO THE STRATOSPHERE

Volcanoes have long been recognized as dominant sources of stratospheric sulfate and aerosol. It has also been clear for some time that volcanoes could be sources of stratospheric chlorine (Stolarski and Cicerone, 1974). Very little research has been done to quantify this source. Only a fraction of volcanic eruptions penetrate the stratosphere: The amount of volatile material in the pre-eruption magma varies from volcano to volcano, the amount of chlorine in the volatile material varies similarly, and soluble, polar compounds like HCl can be removed during the rapid rise (and condensation) of a volcanic plume. Hence volcanoes are sporadic sources not easily described by annual averages.

Two recent studies contribute new information. Johnston (1980) measured the amounts of chlorine in ashfall from the 1976 Augustine (Alaska) eruption and compared these amounts to those found in pre-eruption magmas. Johnston concluded that this volcano might have injected  $(82 \text{ to } 175) \times 10^9$  g of HCl into the stratosphere and that the potential injections of volcanoes have been underestimated in general.

**Table 3-18.** A History of Atmospheric OCS Measurements. All Measurements Were Made in the Spring of the Indicated Year Except for the First Set Which Was Made in the *Fall* of 1975. The OCS Concentration is Given in Units of ppt.

Investigator(s)	Location	Date	OCS
Sandalls and Penkett	England	1975	510
Maroulis <i>et al.</i>	USA	1977	467
Torres <i>et al.</i>	Pacific Ocean, 70°N-57°S	1978	512
Hoyt	Pacific Ocean, 46°N-12°N	1981	505
Johnson, 1985	Pacific Ocean, 53°N-16°N	1982	502
	Pacific Ocean, 50°N-6°S	1983	517

Following the 1982 El Chichon (Mexico) eruption, Mankin and Coffey (1984) detected an increase of about 40% in the stratospheric column of HCl between 20° and 40°N. Their measurements were by infrared absorption from aircraft, thus, their results are specific to HCl. Lacking observations below 18°N and above 41°N, they could only assume the spatial distribution of the HCl increase elsewhere. They estimated that the volcano injected about  $4 \times 10^{10}$  g HCl into the stratosphere. Based on their previous observations in northern midlatitudes, Mankin and Coffey have provided solid evidence of input from El Chichon but even so we do not know the initial form of the chlorine (Cl<sub>2</sub> or HCl), its altitude distribution and whether gas-particle interactions extended strong control over the partitioning of gaseous and aerosol chlorine.

### 3.9 SECULAR TRENDS OF TRACE GASES FROM POLAR ICE CORES

A recently developed technique for trace gas analysis of air bubbles trapped in polar ice now offers the promise of detailed atmospheric histories for climate-linked trace gases dating back hundreds to thousands of years ago. Thus the composition of the atmosphere may be inferred for times long before human activity had begun to alter it. So far concentrations of CO<sub>2</sub>, CH<sub>4</sub>, CCl<sub>3</sub>F and CCl<sub>2</sub>F<sub>2</sub> have been measured in the bubbles of ice cores (Delmas *et al.*, 1980; Berner *et al.*, 1980; Neftel *et al.*, 1982, 1985; Stauffer *et al.*, 1985; Oeschger, 1985; Robbins *et al.*, 1973; Khalil and Rasmussen, 1982; Craig and Chou, 1982; Rasmussen and Khalil, 1984b), and preliminary data have appeared for N<sub>2</sub>O (Pearman, *et al.* 1985).

The preindustrial levels of CO<sub>2</sub> have been determined to be between 260 and 280 ppmv (Delmas *et al.*, 1980; Neftel *et al.*, 1982, 1985; Zumbunn *et al.*, 1982; Raynaud and Barnola, 1985; Pearman *et al.*, 1985). Measurements of methane show that atmospheric concentrations before about 150-200 years ago were less than half of the present concentrations (Robbins *et al.*, 1973; Khalil and Rasmussen, 1982; Craig and Chou, 1982; Rasmussen and Khalil, 1984b).

The concentrations of CFC<sub>13</sub> and CF<sub>2</sub>Cl<sub>2</sub> were found to be below the detection limits of around 10 pptv in the ice cores, confirming that the present concentrations are due entirely to recent industrial emissions (Khalil and Rasmussen, 1982; Rasmussen and Khalil, 1984b).

It is expected that the concentrations of a large number of other trace gases, including N<sub>2</sub>O, CO, OCS and non-methane hydrocarbons may be obtained from the polar ice cores as better methods are developed for extracting the air without melting the ice. These measurements can provide unique information on the undisturbed natural state of the atmosphere. Recently reported measurements of <sup>13</sup>C/<sup>12</sup>C in CO<sub>2</sub> from Antarctic ice (Friedli *et al.*, 1984) suggest that isotopic time series for trace gases in ice cores may soon provide detailed information on the evolution of particular sources in recent centuries.

### 3.10 SUMMARY AND RESEARCH RECOMMENDATIONS

#### Overview of atmospheric trends

Halocarbons, methane, nitrous oxide, odd nitrogen, and carbon monoxide are the most important, globally distributed trace gases in the atmosphere, exerting powerful direct and indirect influence on stratospheric chemistry. Concentrations of all of these gases appear to be increasing at present on a global basis, by 5% yr<sup>-1</sup> for CFC-11 and CFC-12, 7% yr<sup>-1</sup> for CH<sub>3</sub>CCl<sub>3</sub>, 1% yr<sup>-1</sup> for CH<sub>4</sub>, 0.2% yr<sup>-1</sup> for N<sub>2</sub>O, and 1-2% yr<sup>-1</sup> for CO. Available evidence indicates that increases in levels of CH<sub>4</sub>, CO<sub>2</sub> and N<sub>2</sub>O have been sustained for long periods and the increases derive from nondiscretionary, large scale human activities, mainly food and energy production. From this viewpoint, it would be expected that trends in CO and

## SOURCE GASES

$\text{NO}_x$  may also have been sustained for a long time. It seems improbable, therefore, that present trends toward increasing concentrations will be arrested or reversed in the near future. On the contrary, analysis of the historical record and the present imbalances between sources and sinks suggest that we might anticipate a gradual acceleration of present increases, and that substantial rates of accumulation in the atmosphere should be sustainable for long periods. This view is conditioned on the postulate that global population and associated economic activity will continue to increase at appreciable rates for some time. We reach similar conclusions in the case of halocarbons which are purely of industrial origin.

### Research recommendations-tropospheric gases

The discussion in this chapter focusses attention on a number of important research needs.

1. Continued development of baseline measurements for  $\text{CH}_4$ ,  $\text{N}_2\text{O}$ , halocarbons and other species will play a major role in resolving questions raised here. Improved temporal and spatial resolution of the monitoring networks will require close cooperation between individuals, agencies and various national programs active in this field. Important information can be obtained by high frequency observations at sites near source regions (e.g. Adrigole).

2. It is important to undertake flux measurements of biogenic gases from representative ecosystems, especially for  $\text{CO}_2$ ,  $\text{CH}_4$ ,  $\text{N}_2\text{O}$  and  $\text{NO}$ , in order to understand past and future trends in the composition of the atmosphere. Studies of the underlying biological and geochemical processes are essential components of this effort, since we must understand the factors regulating observed fluxes.

3. The fate of  $\text{NO}_x$  from biomass burning and from industrial sources needs to be studied since addition of  $\text{NO}$  or  $\text{NO}_2$  to the middle troposphere can have a major influence on global OH levels. Much better definition of the  $\text{NO}_x$  distribution in the atmosphere is a prerequisite for this analysis. Studies of stratosphere-troposphere exchange are also needed.

4. Definition of trends and distributions for tropospheric CO is essential. A satellite-borne CO sensor, operating for extended periods ( $\sim$  years), could help enormously. This appears to be technically feasible. Expanded measurements of CO at baseline network stations should provide valuable data also.

5. Improved analytical precision, to  $\pm 1$  ppb, is needed in both synoptic and baseline studies of  $\text{N}_2\text{O}$ . Research on  $\text{N}_2\text{O}$  sources would benefit greatly from this instrumentation, which appears to be technically feasible using diode laser technology.

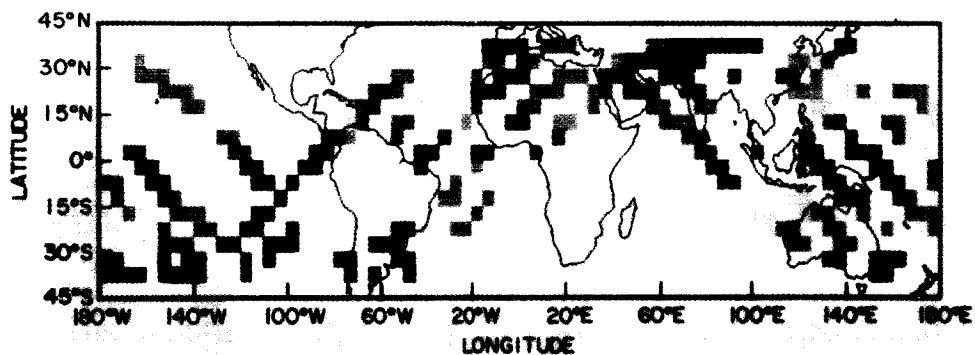
6. Methane isotopic studies promise to help define the relative contributions made by various sources.

7. Studies of trace gases in ice cores help enormously by putting present perturbed atmospheric gas concentrations in the context of the pre-industrial (i.e. natural) atmosphere, and by localizing the epoch when particular species began to increase.

8. Strong efforts should be made to obtain better release data for industrial halocarbons from all major producers, including the USSR, China and Eastern Europe.

Some of the above elements have been incorporated in the proposed Global Tropospheric Chemistry Program (NAS, 1984), and in components of NASA, NSF, and NOAA research programs. It should be clear from the discussion above that a high priority should be attached to these efforts in order to improve understanding of factors which influence stratospheric chemistry.

# TROPOSPHERIC CHEMISTRY



## Panel Members

V.A. Mohnen, Chairman

W. Chameides  
K.L. Demerjian  
D.H. Lenschow  
J.A. Logan  
R.J. McNeal

S.A. Penkett  
U. Platt  
U. Schurath  
P. da Silva Dias

## CHAPTER 4

### TROPOSPHERIC CHEMISTRY: PROCESSES CONTROLLING OZONE AND HYDROXYL RADICAL

#### TABLE OF CONTENTS

4.0	INTRODUCTION .....	117
4.1	PHOTOCHEMISTRY OF THE BACKGROUND TROPOSPHERE .....	117
4.1.1	The Chemistry of Ozone .....	118
4.1.2	The Chemistry of HO .....	120
4.1.3	The Chemistry of Oxides of Nitrogen .....	122
4.1.4	The Tropospheric Distribution of HO .....	123
4.1.5	Future Trends .....	125
4.2	CHEMISTRY OF OZONE FORMATION IN THE POLLUTED TROPOSPHERE .....	126
4.2.1	Source Region Chemistry .....	126
4.2.2	Night-time Chemistry of the Source Region .....	129
4.2.3	Ozone in the Non-Urban Tropospheric: "The Transition Region" .....	130
4.3	HETEROGENEOUS CHEMISTRY .....	132
4.3.1	Interactions with Aerosols and Particulates .....	133
4.3.2	Interactions with Hydrometeors .....	136
4.4	SURFACE EXCHANGE AND VERTICAL REDISTRIBUTION .....	141
4.4.1	Surface Exchange .....	141
4.4.2	Vertical Redistribution .....	145
4.5	RESEARCH NEEDS .....	147

**PRECEDING PAGE BLANK NOT FILMED**

## 4.0 INTRODUCTION

Recent concerns about changes in atmospheric ozone focus not only on the total column of ozone, but also on possible distortion of the vertical profile of ozone. Since approximately 10 percent of the total amount of ozone is present in the troposphere, this assessment includes processes governing tropospheric ozone. There is potential for climate modification resulting from changes in the ozone in both the troposphere and the stratosphere. The trace gases primarily responsible for the solar and long-wave radiative opacity of the present day atmosphere are  $\text{H}_2\text{O}$ ,  $\text{CO}_2$  and  $\text{O}_3$ . However, the long-wave opacity of several other radiatively active minor trace gases in the atmosphere, including  $\text{CH}_4$  and  $\text{CH}_3\text{CCl}_3$ , contribute significantly to the present day surface temperature. The sources of tropospheric ozone are transport from the stratosphere across the tropopause, and *in situ* photochemical production. Ozone is removed from the troposphere by surface deposition and by photochemical loss processes.

Photolysis of ozone leads to the formation of the hydroxyl radical (HO). Reaction with HO determines the atmospheric lifetime of many important gases in the troposphere, including those that are radiatively important. The troposphere can act as a "chemical filter" for numerous trace gases which are emitted at the earth's surface and transported into the stratosphere. Thus, tropospheric chemistry has an impact on ozone in the stratosphere by controlling HO levels in the troposphere. The tropospheric trace gases that contribute to *in situ* photochemical ozone production, or that influence tropospheric HO levels, include carbon monoxide, methane, oxides of nitrogen and nonmethane hydrocarbons. These gases are emitted at the earth's surface as a result of biogeochemical processes and fossil fuel combustion. There are additional tropospheric sources for  $\text{NO}_x$  from lightning and aircraft emissions. The source strengths for these trace gases are highly variable on geographic and temporal scales reflecting not only the inhomogeneity of the earth's surface, but also the efficiency of biological processes and the level of human activity.

The planetary boundary layer, PBL, is the initial recipient of substances from ground sources. Because of the dynamic character of the atmosphere, material from the PBL will mix into the free troposphere and can be transported horizontally over great distances. Vertical transport across the PBL is significantly enhanced in the presence of deep convective cloud systems. These dynamic processes provide a transition from high mixing ratios of trace gases near source regions to low mixing ratios in the remote troposphere. These changes in mixing ratios result in changes in chemical reaction paths, thus justifying a chemical classification of the troposphere into the background troposphere, the source region, and a "transition" regime between the two. The chemistry of the background troposphere is discussed in Section 4.1, and that of the source region and the transition region in Section 4.2. The troposphere is governed by heterogeneous chemistry far more so than the stratosphere. Heterogeneous processes of interest here involve scavenging of trace gases by aerosols, cloud and precipitation elements leading to aqueous phase chemical reactions and to temporary and permanent removal of material from the gas phase as discussed further in Section 4.4. They also include exchange of material with the earth's surface, such as dry deposition. Dry deposition is a major removal process for ozone, as well as for other gases of importance in tropospheric photochemistry (e.g.,  $\text{NO}_2$ ). These processes are discussed in Section 4.5.

### 4.1 PHOTOCHEMISTRY OF THE BACKGROUND TROPOSPHERE

The earliest theory of tropospheric ozone held that the gas was supplied by injection from the stratosphere and was removed by surface deposition (e.g., Junge, 1962). Over a decade ago, Crutzen (1973a, 1974) and Chameides and Walker (1973) showed that there are also important chemical sources and sinks for ozone in the troposphere. Recent modelling studies indicate that, averaged over the globe, chemical sources and sinks for ozone are in approximate balance, and are similar in magnitude to the source from the

## TROPOSPHERIC CHEMISTRY

stratosphere and the sink at the ground (Fishman *et al.*, 1979b; Logan *et al.*, 1981; Chameides and Tan, 1981). Several recent reviews (e.g., Bojkov, 1984; Fishman, 1985) present a detailed account of the debate over chemical versus transport control of tropospheric ozone. They conclude that both mechanisms play important roles, but that the relative importance of the chemical and physical processes controlling ozone in different environments are not well understood. Levy *et al.* (1985) used a general circulation model to investigate the influence of transport processes on tropospheric ozone; the model allowed for downward transport of ozone from the stratosphere and removal at the surface. They compared model simulations with available observations and found that the large scale circulation plays a major role in determining the behavior of ozone, particularly at remote locations. The model results also implied a significant role for chemical sources and sinks for ozone.

### 4.1.1 The Chemistry of Ozone

Ozone is formed by the association reaction of ground state O atoms with O<sub>2</sub>:



and is removed by photolysis



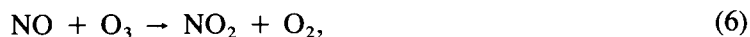
The metastable O(<sup>1</sup>D) is quenched by O<sub>2</sub> and N<sub>2</sub>



though it can also react with H<sub>2</sub>O to form the hydroxyl radical HO



Nitric oxide reacts with ozone to form NO<sub>2</sub>



with NO<sub>2</sub> removed by photolysis



Ozone removed by (6) is reconstituted by (7) followed by (1). It is convenient, because of the cyclic nature of the chemistry, to define a family of species undergoing rapid reactions leading to formation or removal of ozone. We define this family, odd oxygen, as the sum of O<sub>3</sub>, O(<sup>1</sup>D), O(<sup>3</sup>P) and NO<sub>2</sub>.

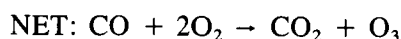
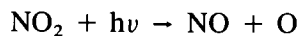
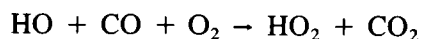
Odd oxygen is conserved in reactions (1)-(4), (6) and (7). It is formed by reactions of NO with HO<sub>2</sub>, CH<sub>3</sub>O<sub>2</sub>, and RO<sub>2</sub>.



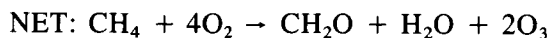
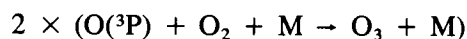
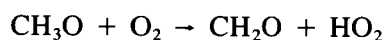
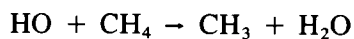
TROPOSPHERIC CHEMISTRY



The species  $\text{RO}_2$  represents a variety of complex organic peroxy radicals. These reactions occur during the photooxidation of  $\text{CO}$ ,  $\text{CH}_4$  and hydrocarbons, for example by



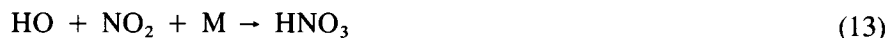
and by



Odd oxygen is removed by reaction of  $\text{O}({}^1\text{D})$  with  $\text{H}_2\text{O}$ , by reaction of  $\text{O}_3$  with  $\text{HO}_2$  and  $\text{HO}$ ,



by formation of nitric acid from  $\text{NO}_2$ ,



and by heterogeneous reactions of  $\text{O}_3$  and  $\text{NO}_2$  at the earth's surface.

## TROPOSPHERIC CHEMISTRY

Oxidation of CO, CH<sub>4</sub> and hydrocarbons leads to net production of odd oxygen in the presence of adequate NO<sub>x</sub>. The rate for production of ozone is roughly proportional to the concentration of NO, while the rate of loss is almost independent of NO<sub>x</sub> (NO + NO<sub>2</sub>) for concentrations below 200 ppt (Fishman *et al.*, 1979). Loss of odd oxygen, primarily by reactions (5) and (11) is balanced by production in reactions (8) and (9) for concentrations of NO near 30 ppt (Fishman *et al.*, 1979; Logan *et al.*, 1981; Crutzen, 1983). Hence, regions of the globe characterized by extremely low concentrations of NO, such as the remote Pacific, are likely to provide a net photochemical sink for odd oxygen (Liu *et al.*, 1983), while the continental boundary layer at midlatitudes, characterized by higher concentrations of NO, is likely to provide a net source. Measurements of NO<sub>x</sub> in the troposphere are few, and the lack of data for NO<sub>x</sub> contributes significantly to uncertainties in global estimates for the photochemical source of ozone.

Production of ozone in the troposphere is limited ultimately by supply of CO, CH<sub>4</sub>, and hydrocarbons, if NO<sub>x</sub> is available. One molecule of ozone may be formed for each molecule of CO (Crutzen, 1973b), while the yield of ozone from oxidation of CH<sub>4</sub> could be as large as 3.5 (e.g., Logan *et al.*, 1981). Production of ozone from nonmethane hydrocarbons is discussed in more detail later in this chapter.

### 4.1.2 The Chemistry of HO

Reaction with HO in the troposphere is the primary removal mechanism for many trace gases which influence the chemical composition and radiative balance of the stratosphere. Consequently, tropospheric and stratospheric chemistry are inextricably linked through the HO radical.

The hydroxyl radical is formed by reaction (2) followed by (5). It is removed by reaction with carbon monoxide and methane,



with reaction (14) dominant over (15). HO<sub>2</sub> is removed by reaction (8), and (16)



leading to regeneration of HO, or by



Hydrogen peroxide is photolysed,



it can react with HO,

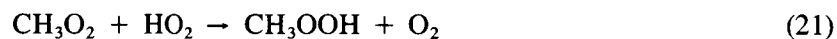
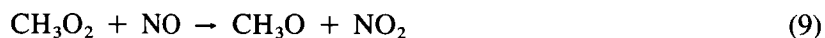


or may be removed by heterogeneous processes such as precipitation scavenging, as discussed below.



It is convenient, because of the fairly rapid interconversion of H, HO, HO<sub>2</sub> and H<sub>2</sub>O<sub>2</sub> to consider these species as a family, odd hydrogen (=H + HO + HO<sub>2</sub> + 2 × H<sub>2</sub>O<sub>2</sub>). Reaction (5) provides the dominant source for odd hydrogen, while reactions (19) and (20) provide important sinks for odd hydrogen. Reactions (8), (14) and (16)-(18) do not influence the concentration of odd hydrogen.

Atmospheric oxidation of methane (Figure 2-1) may also provide sources and sinks for odd hydrogen, in addition to providing a source for odd oxygen. CH<sub>3</sub>O<sub>2</sub>, formed in (15), is removed primarily by reaction with NO or HO<sub>2</sub>.



Subsequent reaction of methyl hydroperoxide with HO leads to loss of odd hydrogen.



Recent measurements of a relatively fast rate for reaction (22) (Niki *et al.*, 1983) indicate that this reaction may provide an important sink for odd hydrogen at low concentrations of NO<sub>x</sub> (Logan, 1985, private communication).

The net source of odd hydrogen is determined first by competition between reaction (9) and reaction (21), and second by competition between reactions (22)-(23) which remove odd hydrogen,



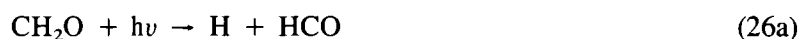
and reaction (24)



which recycles odd hydrogen. Reaction of the methoxy radical with oxygen yields formaldehyde.



Photolysis of CH<sub>2</sub>O



via path (26a) provides an important source for odd hydrogen in the upper troposphere, while path (26b) and reaction of HO with CH<sub>2</sub>O have no net effect on odd hydrogen.

The major pathways in the methane oxidation chain are thought to be understood fairly well. Recent kinetic data for some of the intermediate species have changed the net effect of the cycle on the budget of odd hydrogen. It should be emphasized that the influence of CH<sub>4</sub> chemistry on the budgets of both

## TROPOSPHERIC CHEMISTRY

odd hydrogen and odd oxygen depends critically on ambient concentrations of  $\text{NO}_x$ , because of competition between reactions (9) and (21). A discussion of the chemistry of HO and associated uncertainties may be found in Chameides and Tan (1981), Logan *et al.* (1981) and NRC (1984). Logan *et al.* (1981) present a detailed discussion of the potential influence of  $\text{CH}_4$  chemistry on odd hydrogen.

### 4.1.3. The Chemistry of Oxides of Nitrogen

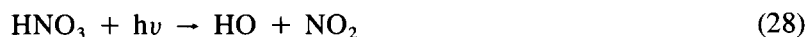
Nitrogen oxides act as catalysts in the photochemical production of ozone. Any reaction which converts NO to  $\text{NO}_2$ , other than the reaction of NO with ozone, provides a photochemical source of ozone. Present measurements of  $\text{NO}_x$  are inadequate for definition of its distribution. Preliminary data indicate that ambient concentrations are highly variable in space and time, as discussed in Chapter 3. The lack of data for  $\text{NO}_x$  precludes accurate quantification of the net global chemical source for ozone.

Nitrogen oxides are produced in the troposphere primarily in the form of NO. Nitric oxide and nitrogen dioxide are rapidly interconverted by reactions (6), (7), (8) and (9) on a time scale of minutes. Nitrogen oxides are removed from the atmosphere by conversion to nitric acid,



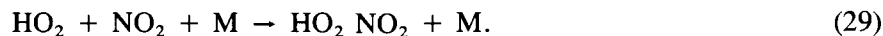
followed by heterogeneous processes, i.e., rainout or surface deposition of  $\text{HNO}_3$ . Surface deposition of  $\text{NO}_2$  could provide another important tropospheric sink. There have been few field studies of the rate of uptake of  $\text{NO}_x$  by surfaces, as discussed later in this chapter, and removal rates of  $\text{NO}_x$  are not well defined at present.

Current models suggest that  $\text{NO}_x$  is converted to  $\text{HNO}_3$  by reaction (13) within 1-2 days in summer. Nitric acid may be converted to aerosol nitrate, for example by reaction with sea-salt aerosol (Savoie and Prospero, 1982) or by reaction with ammonia (Tang, 1980). Nitric acid and aerosol nitrate are likely to be removed from the atmosphere by precipitation and surface deposition, with mean lifetimes of a few days (Junge, 1963; Levine and Schwartz, 1982). Nitric acid is converted back to  $\text{NO}_x$  by reactions (20) and (21) more slowly, with a time scale of 2-4 weeks.



These processes are significant primarily in the upper troposphere.

Nitric oxide and  $\text{NO}_2$  may be converted to  $\text{HNO}_2$ ,  $\text{HO}_2\text{NO}_2$ ,  $\text{NO}_3$ ,  $\text{N}_2\text{O}_5$  and organic nitrates in addition to  $\text{HNO}_3$ . Most of these molecules decompose thermally or photolytically and therefore provide temporary reservoirs for  $\text{NO}_x$ . Peroxynitric acid is formed by reaction of  $\text{HO}_2$  with  $\text{NO}_2$



It decomposes rapidly in the lower troposphere,



but it is thermally stable in the colder upper troposphere, where it is removed by photolysis and by reaction with HO. Current models suggest that a significant fraction of acidic nitrate may be present in the form of HO<sub>2</sub>NO<sub>2</sub> in the upper troposphere, but there are no observational data at present.

Peroxyacetyl nitrate (PAN) is formed during the degradation of hydrocarbons (see below). PAN is more stable than HO<sub>2</sub>NO<sub>2</sub> with respect to thermal decomposition, with a lifetime of about a day at 275 °K and several years at temperatures characteristic of the upper troposphere (Cox and Coffey, 1977; Hendry and Kenley, 1979). Recent kinetic data indicate that the lifetime of PAN towards photolysis is about four months (Senum *et al.*, 1984), with a similar value for attack by HO (Wallington *et al.*, 1984). Recent measurements of PAN show that it is an important reservoir for NO<sub>x</sub> in clean marine air (Singh and Salas, 1983a, b) and in rural air in North America (Bottenheim *et al.*, 1984; Spicer *et al.*, 1983) and in Europe (Brice *et al.*, 1984).

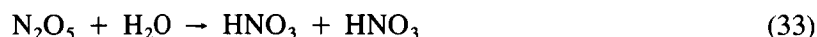
The nitrate radical (NO<sub>3</sub>) is formed by



and is photolysed rapidly during the day. At night a steady state should be established between NO<sub>3</sub> and N<sub>2</sub>O<sub>5</sub>.



The nitrate radical has been observed in a variety of "clean-air" locations including Hawaii and rural Colorado. In most cases the concentration of NO<sub>3</sub> at a given level of NO<sub>2</sub> was lower than predicted by model calculations (Noxon *et al.*, 1980; Platt *et al.*, 1980b, 1981, 1984; Platt and Perner, 1980; Noxon, 1983). Some processes, as yet unidentified, appear to be removing NO<sub>3</sub> and/or N<sub>2</sub>O<sub>5</sub> from the atmosphere at night. If these processes lead to removal of NO<sub>x</sub>, then nighttime removal of NO<sub>x</sub> by reactions involving NO<sub>3</sub> could be comparable to daytime by reaction (13). Platt *et al.* (1981, 1984) speculate that reactions of NO<sub>3</sub>, or more likely N<sub>2</sub>O<sub>5</sub>, on wet aerosols may account for rapid removal of NO<sub>3</sub> under conditions of high humidity, and may provide another sink for NO<sub>x</sub> in clouds and fog. A detailed discussion of NO<sub>3</sub> scavenging by cloud droplets, and its possible conversion to NO<sub>3</sub><sup>-</sup> by chemical reactions in the liquid phase is given in the section on heterogeneous chemistry. The rate of the homogeneous gas-phase reaction between N<sub>2</sub>O<sub>5</sub> and water vapor,



is extremely slow, but this reaction could provide an important source for HNO<sub>3</sub> if it proceeds at the upper limit ( $k < 1.3 \times 10^{-21} \text{ cm}^3 \text{ molecule}^{-1} \text{ sec}^{-1}$ ) given by Tuazon *et al.* (1983). The role of (33) in nighttime chemistry will remain uncertain until its rate constant is better defined.

#### 4.1.4. The Tropospheric Distribution of HO

Few reliable measurements of hydroxyl radicals have been made so far (e.g., Perner *et al.*, 1976; Huebler *et al.*, 1984; Hoell *et al.*, 1984; Beck *et al.*, personal communication) and these are insufficient to test photochemical theories. Indirect methods have been used, however, to test current models of tropospheric chemistry, and for the determination of average HO concentrations. These methods rely upon mass balance considerations for various trace gases, and they provide a globally averaged estimate for HO. Effective utilization of this approach for determination of HO requires that the tracer species satisfy a number of conditions:

## TROPOSPHERIC CHEMISTRY

1. Its atmospheric abundance in time and space must be defined accurately.
2. It must be known that removal occurs predominantly by reaction with HO and the rate constant must be determined accurately.
3. The sources and source distribution in time and space must be known accurately.

In recent decades, synthetic organic chemicals have been injected into the atmosphere in such large amounts that measurable background levels are present. Because of the exclusive manmade source of such chemicals, the major uncertainties associated in the source term could, in principle, be eliminated. A preliminary screening led to the selection of methylchloroform  $\text{CH}_3\text{CCl}_3$  (Singh, 1977; Lovelock, 1977) as the most suitable molecule for the following reasons:

1. Its atmospheric concentration was high enough and could be measured accurately.
2. The usage was such that emissions were similar to production.
3. The HO rate constant was available.

Analysis of data for methylchloroform therefore provides the best current test for global models of the HO distribution. Recent studies of data indicate that the lifetime of  $\text{CH}_3\text{CCl}_3$  is between 6 and 9 years (Prinn *et al.*, 1983a,b; Khalil and Rasmussen, 1984a). Results from the model for HO described in Logan *et al.* (1981) using kinetic data given in NASA-JPL (1983) are in good agreement with observations of  $\text{CH}_3\text{CCl}_3$ , in contrast to earlier analyses which underestimated  $\text{CH}_3\text{CCl}_3$  by about a factor of two (Logan *et al.*, 1981). The improved agreement is due in part to recent revisions in kinetic and solar flux data, which decrease calculated concentrations of HO by 20-30%, and in part to a recalibration of absolute concentrations of  $\text{CH}_3\text{CCl}_3$  by a factor of 0.8 (Khalil and Rasmussen, 1984a).

The atmospheric lifetime of  $\text{CH}_3\text{CCl}_3$  can be determined also from its historical emission rates, the observed trends in its atmospheric abundance and the global content. Prinn *et al.* (1983) estimated an atmospheric removal time of 10.2 years with an uncertainty range of +5.2 and -2.6 years from the first three years of data from the ALE network. The corresponding globally averaged HO concentration equals  $(5 \pm 2) \times 10^5 \text{ cm}^{-3}$ . The absolute concentration of  $\text{CH}_3\text{CCl}_3$  has since been revised downward about 20%, as discussed above, yielding revised lifetimes of 6.5 years with an uncertainty range of +3 and -2 years.

Other anthropogenic trace gases have been used in a similar manner to estimate HO, for example, dichloromethane, 1,2 dichloroethane and tetrachloroethane (Singh *et al.*, 1983a). A two box model shows that removal rates of these molecules are consistent with average HO concentrations of 4 to  $5 \times 10^5$  molecules  $\text{cm}^{-3}$ . Because of their relatively short lifetimes compared to methylchloroform, these chemicals can show HO latitudinal gradients with greater sensitivity. However, their source strengths are not as well defined as that of  $\text{CH}_3\text{CCl}_3$ .

Naturally occurring tracers, e.g.,  $^{14}\text{CO}$  and  $^{12}\text{CO}$ , have also been used to estimate HO levels. The  $^{12}\text{CO}$  sources however are so poorly defined that such an approach is at best unreliable. Sources of  $^{14}\text{CO}$  are somewhat better defined. The dominant source of  $^{14}\text{CO}$  is cosmic rays and this source is independent of season and latitude. Compared to the cosmic ray production rate, anthropogenic sources are negligible.

$^{14}\text{CO}$  is also produced in significant but uncertain quantities by the oxidation of organic matter. Current atmospheric  $^{14}\text{CO}$  data are all taken at ground level; seasonal and latitude gradients have been noted. These limited data have been analysed with the help of a 2-D model to suggest an average tropospheric HO abundance of  $7 \pm 3 \times 10^5$  molec  $\text{cm}^{-3}$  (Volz *et al.*, 1981). These values are a factor of 3 lower than those estimated by Weinstock and Niki (1972) almost a decade ago, largely because of their underestimate of the  $^{14}\text{CO}$  abundance. It must be realized, however, that the lifetime of  $^{14}\text{CO}$  is short ( $5 \pm 2$  months), and a better definition of the organic source term and vertical gradients are needed to improve these estimates.

Recently, Singh *et al.* (1983b) suggested that simpler and more easily measured molecules such as propane can be used to study the seasonal behavior of HO, provided the source term is characterized adequately. At present, poor characterization of source functions provides the major uncertainty in HO estimates derived from mass balance considerations.

While the budget of  $\text{CH}_3\text{CCl}_3$  provides one test of global models for HO, significant uncertainties remain in present understanding of tropospheric chemistry. For example, the methane oxidation scheme shown in Figure 2-1 may be an oversimplification of the mechanisms operative in the atmosphere, and the role of larger hydrocarbons in the chemistry of the remote atmosphere remains to be evaluated. Preliminary measurements indicate that nonmethane hydrocarbons (NMHC) may be of some importance for HO chemistry (Rudolph and Ehhalt, 1981; P. Warneck, 1974) even in the background troposphere.

#### 4.1.5. Future Trends

Recent measurements indicate that concentrations of  $\text{CH}_4$  and CO may be increasing, as discussed in Chapter 3. It was noted almost a decade ago that increases in these gases could lead to a decrease in HO, since reaction with CO and  $\text{CH}_4$  provides the major removal process for HO (Wofsy, 1976; Chameides *et al.*, 1977; Sze, 1977; Hameed *et al.*, 1979). The apparent increase in tropospheric levels of  $\text{CH}_4$  and CO over the last 35 years (Rinsland *et al.*, 1985) could have resulted from either an increase in the production rate of  $\text{CH}_4$  and/or CO, or a decrease in the destruction rate of these gases, since their concentrations are closely coupled via the methane oxidation chain and the hydroxyl radical. Photochemical model simulations attempting to predict the consequences of these trends are - at best - qualitative. A decrease in HO would imply longer lifetimes and higher concentrations for many chemically reactive and/or radiatively active species resulting in increased transport across the tropopause.

In a recent exploratory study, Levine *et al.* (1985) used a 1-D photochemical model to simulate present day concentrations of CO and  $\text{CH}_4$  at  $45^\circ\text{N}$  and concentrations for 1950 deduced from ground based infrared spectra. They suggest that the global source of  $\text{CH}_4$  may have increased by about 11%, the global surface source of CO may have increased by about 50%, and the tropospheric column of HO decreased by about 25%, from 1950 to the present day. These results should be regarded as extremely preliminary and speculative, however, since it is not clear how to infer changes in global fluxes from the results of a 1-D calculation representing  $45^\circ\text{N}$  in summer. There is a significant latitudinal gradient in CO, and data obtained in recent years suggest that trends in CO in the southern hemisphere are much smaller than at northern midlatitudes, as discussed in Chapter 3.

## TROPOSPHERIC CHEMISTRY

### 4.2 CHEMISTRY OF OZONE FORMATION IN THE POLLUTED TROPOSPHERE

#### 4.2.1 Source Region Chemistry

The discussion on clean tropospheric chemistry indicated that the oxidation of CO, CH<sub>4</sub>, and possibly other biogenic hydrocarbons leads to a net production of odd oxygen, if sufficient NO<sub>x</sub> is present (i.e., NO<sub>x</sub> > 30 ppt). In the polluted troposphere, unlike the clean troposphere, the rate of ozone formation is not necessarily proportional to the concentration of NO<sub>x</sub>, but varies in a complex way that is dependent upon the ratios and concentrations of the hydrocarbons and NO<sub>x</sub> as well as the chemical composition of the hydrocarbons themselves. The chemistry of ozone in the polluted troposphere has been studied for over thirty years. The research emphasis has been predominantly in elucidating the processes for oxidant/ozone formation in urban areas. The focus of interest in urban areas is due mainly to the high emission densities of ozone precursors (hydrocarbons and NO<sub>x</sub>) which result typically in very high ozone concentrations under summertime meteorological conditions. In many cases the concentration levels of ozone in urban areas exceed ambient air quality standards which have been set to protect public health and welfare.

Several reviews of the chemistry of polluted atmospheres are available (Leighton, 1961; Stern, 1977; Seinfeld, 1975; Heiklen, 1976), as are detailed discussions of reaction mechanisms (Demerjian *et al.*, 1974; Carter *et al.*, 1979; Baldwin *et al.*, 1977; Falls and Seinfeld, 1978; Whitten *et al.*, 1980) and reaction rate constant reviews (Baulch *et al.*, 1980; Demerjian *et al.*, 1980; Baulch *et al.*, 1982). The discussions which follows provides an overview of the chemistry of the polluted troposphere.

The chemistry that occurs in sunlight-irradiated polluted atmospheres involves the interaction of a host of chemical species. These include: hydrocarbons such as alkanes, alkenes, and aromatics; other organics such as aldehydes and ketones; nitric oxide (NO); nitrogen dioxide (NO<sub>2</sub>); ozone (O<sub>3</sub>); peroxyacetyl nitrate (PAN); nitric acid (HNO<sub>3</sub>); atomic oxygen (O<sup>3</sup>P) and its first electronic excited state O(<sup>1</sup>D); hydroxy radical (HO); hydroperoxyl radical (HO<sub>2</sub>); alkylperoxyl radicals (RO<sub>2</sub>); acylperoxyl radicals (R(O)O<sub>2</sub>); nitrogen trioxide (NO<sub>3</sub>); and dinitrogen pentoxide (N<sub>2</sub>O<sub>5</sub>).

This chemistry explains the rapid conversion of NO to NO<sub>2</sub> observed in the ambient polluted atmosphere (Leighton, 1961; Altshuller and Bufalini, 1965; Demerjian *et al.*, 1974). The key lies in a sequence of reactions involving the same free radical species thought to be important in the chemistry of the clean troposphere and a number of organic radicals derived from the host of more complex hydrocarbon and organic molecules present additionally in the polluted atmosphere.

The most important atmospheric reactions governing the decomposition of alkanes, alkenes, and aromatics involve their reaction with hydroxyl radical. Reaction sequences describing the pathways for their oxidation as a result of HO attack have been studied extensively (Demerjian *et al.*, 1974; Carter *et al.*, 1979; Niki, 1978; Falls and Seinfeld, 1978; Perry *et al.*, 1977; Atkinson *et al.*, 1985; Grosjean, 1984). In a very simplified form this may be represented as follows:



The alkyl radical (R) produced as a result of the HO attack on the hydrocarbon reacts with an oxygen molecule to form an alkylperoxyl radical (RO<sub>2</sub>)



The alkylperoxyl radical reacts with NO to form NO<sub>2</sub> and an alkoxy radical (RO)



Hydrogen abstraction from the alkoxy radical by molecular oxygen will produce a hydroperoxyl radical (HO<sub>2</sub>) and a carbonyl compound (R(C=O)H):



The aldehydes formed in the RO oxidation, or emitted as such from combustion sources, react with HO or photolyze, introducing another important source of radicals to the atmosphere.



The hydroperoxyl radical can then react with NO to form NO<sub>2</sub> and another hydroxyl radical, which re-enters the cycle.



Reactions (8) and (10) taken together provide an efficient mechanism for the rapid conversion of NO to NO<sub>2</sub>. This increase in the concentration of "odd oxygen" (previous section) results in an increase of ozone through the perturbation of the chemical steady state relationship (39) derived from the following reactions:



The chemical steady state relationship (39) has been shown to be a valid approximation over a considerable range of atmospheric pollutant conditions (Stedman and Jackson, 1975; Calvert, 1976).

$$[\text{O}_3] = \frac{J_7[\text{NO}_2]}{k_6[\text{NO}]} \quad (39)$$

Ratios of NO<sub>2</sub> and NO emitted into the atmosphere by man's activities are typically less than one and would lead to very low ozone steady state concentrations under typical atmospheric solar irradiation conditions. The impact of reactions (8) and (10) is to drive the ratio of NO<sub>2</sub> to NO up by oxidizing the NO to NO<sub>2</sub>, in direct competition with the ozone-nitric oxide reaction and thereby allowing ozone to build up in concentration.

Typical observations made in a polluted atmosphere of this phenomenon are shown in Figures 4-1a and b. The diurnal pattern begins with the emission of hydrocarbons, carbon monoxide and NO<sub>x</sub> from motor vehicles in the early morning. The NO is converted to NO<sub>2</sub> and ozone accumulation begins when

TROPOSPHERIC CHEMISTRY

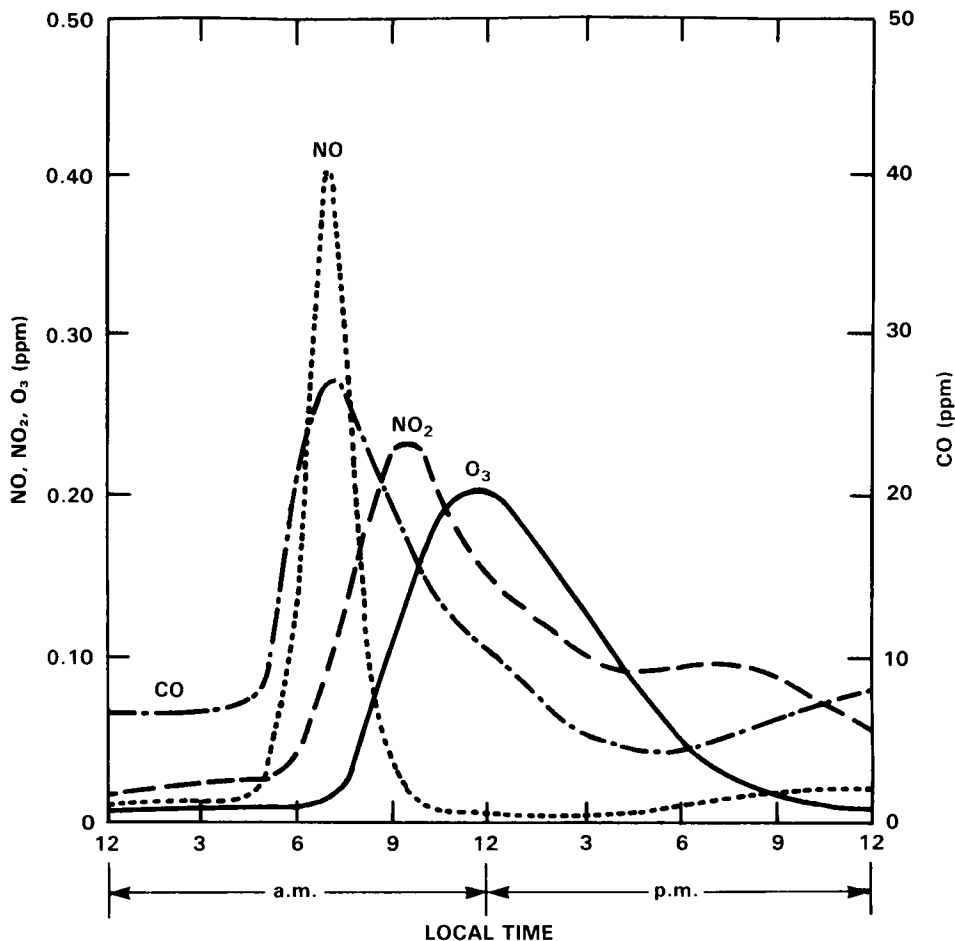


Figure 4-1a. Average daily 1-hour concentrations of selected pollutants in Los Angeles, California, July 19, 1965. From U.S. Department of Health, Education and Welfare.

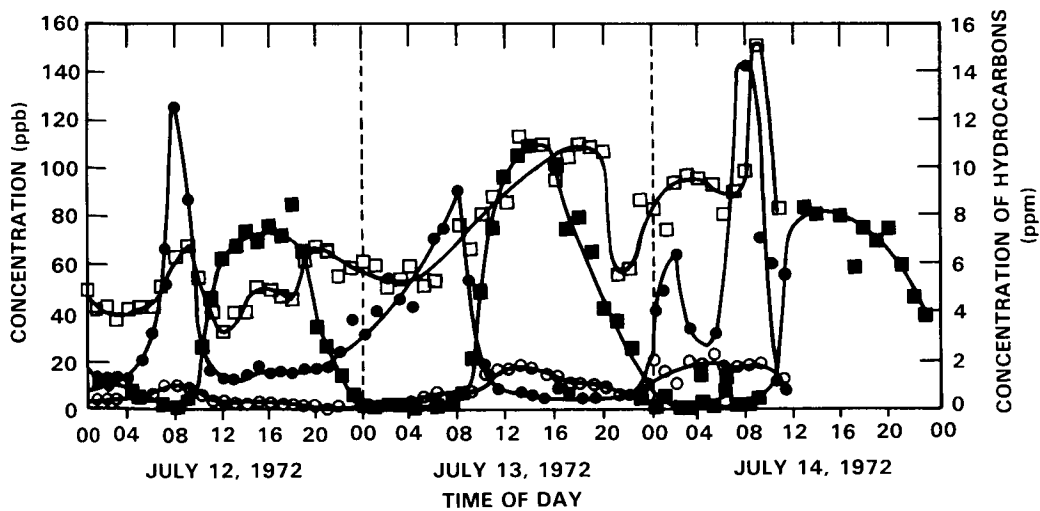


Figure 4-1b. Diurnal variations of air pollutants measured in London from July 12 to July 14, 1972. ■, Ozone ppb; ●, nitric oxide, ppb; □, nitrogen dioxide, ppb; ○, hydrocarbons, ppm. From Derwent and Steward.

most of the NO has been oxidized. The ozone concentration maximizes and then declines either as a result of reaction with additional emissions of NO through the day, dilution due to meteorology, or in the case of extended periods of time and transport, by interaction with the ground surface, which is a major sink for ozone in the atmosphere as will be discussed later in this chapter.

The interaction of organic free radicals produced by hydrocarbon oxidation with NO and NO<sub>2</sub> represents an important aspect of the chemistry of the oxides of nitrogen in the polluted atmosphere. They represent key processes in the conversion of NO to NO<sub>2</sub> and the formation of organic nitrates. It has recently been found that the more complex peroxyalkyl radicals formed during alkane photooxidation can add NO to form alkyl nitrates in non-negligible yields, in competition with reaction (10) (Atkinson *et al.*, 1985):



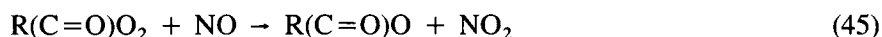
Also the hydroperoxyl radical formed from hydrocarbon oxidation in reaction (36) supplements that formed in reactions (12) and (14) to create hydrogen peroxide via reaction (17), and aldehydes react with the hydroxy radical to produce peroxyacyl radicals and ultimately peroxyacyl nitrates by reaction with NO<sub>2</sub>



A thermal equilibrium exists between the peroxyacyl nitrate and its components



and the peroxyacyl radical is removed from the atmosphere by reaction with NO (Cox and Coffey 1977)



The most commonly occurring peroxyacyl nitrate is peroxyacetyl nitrate or PAN and there is a great similarity between the behavior of PAN and ozone in polluted atmospheres. Their diurnal variations at ground based sites are virtually identical on many occasions (Garland and Penkett 1976) primarily because their formation and removal mechanisms are very similar. PAN is thus an excellent tracer of the photochemical reactivity of the troposphere and since it has no large stratospheric source it can be used in studies designed to investigate the seasonal behavior of tropospheric photochemical activity (Brice *et al.*, 1984).

#### 4.2.2 Night-time Chemistry of the Source Region

The nitrate radical NO<sub>3</sub> can be formed by reaction of NO<sub>2</sub> with ozone



During the day NO<sub>3</sub> is rapidly photolyzed back to its precursors but during the night an equilibrium with N<sub>2</sub>O<sub>5</sub> can be established



## TROPOSPHERIC CHEMISTRY

Night-time concentrations of  $\text{NO}_3$  as high as 355 pptv have been recorded in the Los Angeles basin (Platt *et al.*, 1980b, 1984). Some  $\text{NO}_3$  is converted to  $\text{HNO}_3$  by reactions with hydrocarbons and aldehydes,



but in the absence of  $\text{NO}$  no chain reactions can be initiated by the peroxy radicals, which will be rapidly lost. The  $\text{N}_2\text{O}_5$  which is formed will be stable until sunrise or it can be removed either by hydrolysis in deliquescent aerosols or by uptake on ground surfaces.

It is quite possible that heterogeneous chemistry is important in the overall  $\text{NO}_x$  cycle particularly in the formation of nitrous acid,  $\text{HONO}$ , which can act as an efficient source of  $\text{HO}$  radicals in conditions of low light intensity, but this is an area where much more research is required before definite statements can be made.

### 4.2.3 Ozone in the Non-Urban Troposphere; "The Transition Region"

Anthropogenic emissions of NMHC and  $\text{NO}_x$  may contribute significantly to photochemical production of ozone and other oxidants on a hemispheric scale, especially in the transition region, where the reactants are removed from their sources but there is still sufficient  $\text{NO}_2$  present for the chemistry described above to occur. The state of the science is such that a quantitative understanding of this contribution is not yet possible. Some phenomenological processes which may be important on the larger scales (continental to hemispheric) are: transport of ozone/oxidants formed within the confines of the urban plume followed by dispersal over regional and continental scales; photochemical production of ozone/oxidants from the remnants of aged urban air masses (partially oxidized hydrocarbons and slower reaction hydrocarbon species) which have been transported and dispersed over several days, and photochemical production of ozone/oxidants from low level emissions of non-methane hydrocarbons and  $\text{NO}_x$  (both natural and anthropogenic) over the continent. It is also possible that emissions of precursors in winter form a reservoir which can influence oxidant chemistry later in the year as photolytic processes become more efficient. Our understanding of the specific sources of ozone/oxidants is somewhat limited, due in part to difficulties in studying the reaction pathways for ozone formation for the less reactive hydrocarbon species, and in part to the lack of data for non-methane hydrocarbons and  $\text{NO}_x$  in aged polluted air masses and in background air.

The limited data base that exists for hydrocarbons suggests much larger concentrations for many species in the northern hemisphere than in the southern hemisphere. Figure 4-2 shows a latitudinal transect for ethane over the Eastern Pacific Ocean and similar data patterns have been observed over the Atlantic Ocean (Singh and Salas, 1983; Rasmussen and Khalil, 1983; Ehhalt and Rudolf, 1984). Larger differences between the two hemispheres are observed for more reactive hydrocarbons such as propane and butanes which are known to have large anthropogenic emissions. It has also been observed that the northern hemisphere concentrations of these various hydrocarbons vary greatly with season. Table 4-1 shows some average concentrations of hydrocarbons obtained in the vicinity of the Island of Spitzbergen at  $79^\circ\text{N}$  in the summer and at the end of the Arctic winter. All show much higher values in the winter than in the summer with the exception of  $\text{C}_2\text{H}_4$  and  $\text{C}_3\text{H}_6$  which are believed to have predominantly natural sources (Hov *et al.*, 1984). The decay with time from the spring peak in hydrocarbon concentrations at Point Barrow at  $70^\circ\text{N}$  in Alaska has been observed on a day-by-day basis and similar changes in the concentrations of many molecules were observed there (Rasmussen *et al.*, 1983). The variation at high latitudes in the northern hemisphere is also reflected in observations made at  $39^\circ\text{N}$  at Point Arena on the Pacific Coast of the U.S.A., particularly for  $\text{C}_3\text{H}_8$  and  $\text{C}_4\text{H}_{10}$  (Singh and Salas, 1982).

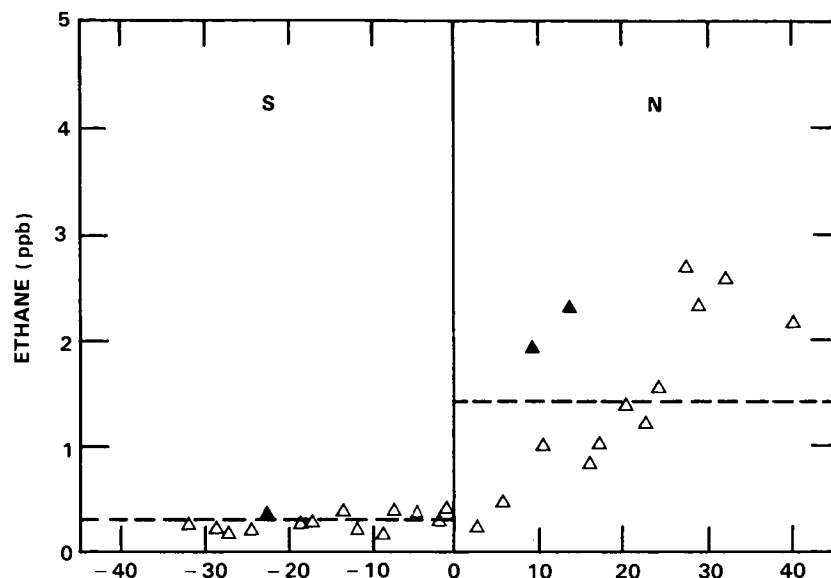


**Figure 4-2.** Ethane concentrations over eastern Pacific, darkened data points are excluded from the computation of averages for statistical reasons only. Dashed lines show the weighted hemispheric average. Source: Singh and Salas, 1982.

**Table 4-1.** Average concentrations and standard deviations (in parentheses) in pptv for 9 samples of pressurized air (5 from Bear Island, 2 from Hopen and 2 from Spitzbergen) in July 1982, and for 10 cryogenic samples from Ny-Alesund (Spitzbergen) spring 1983.

Hydrocarbons	July 1982	Spring 1983	Ratio Spring/ Summer
$C_2H_6$	1195 (27)	3950 (27)	3.3
$C_2H_4$	255.2 (84.4)	156 (37)	0.6
$C_2H_2$	66.5 (17.7)	954 (106)	14.3
$C_3H_8$	87.1 (30.1)	2156 (284)	24.8
$C_3H_6$	187 (111)	24 (7.7)	0.1
$iC_4H_{10}$	<20	390 (60)	>20
$nC_4H_{10}$	<20	805 (141)	>40
2-methyl butane	<20	346 (69)	>17
$nC_5H_{12}$	<20	339 (93)	>9
2-methyl pentane	<20	182 (34)	>9
3-methyl pentane	<20	160 (20)	>8
$nC_6H_{14}$	<20	172 (41)	>9
Cyclohexane	<20	54 (14)	>3
$C_6H_6$	65.6 (23.4)	307 (102)	4.7

Data from Hov *et al.*, 1984.

## TROPOSPHERIC CHEMISTRY

The extent of this large seasonal effect occurring throughout the northern hemisphere is not known although the studies made over the Atlantic and Pacific Oceans suggest that the largest concentrations of the hydrocarbons are to be found north of 20°N. It is also quite likely that higher concentrations will be observed over the continents. This would represent a large reservoir of gaseous carbon which would be capable of forming ozone when oxidized in the presence of NO<sub>2</sub>.

The NO<sub>x</sub> data base is even smaller than that for hydrocarbons and most is probably not directly applicable to the so-called "transitional region" between the truly remote troposphere and the easily identifiable polluted atmosphere adjacent to the source regions. It has been shown for instance that NO concentrations over the Equatorial Pacific Ocean are less than 5 pptv (McFarland *et al.*, 1979) which is less than the theoretical quantity required for ozone production to accompany methane and CO oxidation. Measurements made during the month of June at a coastal site in Ireland however show NO<sub>x</sub> concentrations up to 100 pptv (Helas and Warneck, 1981). Median concentrations of NO<sub>x</sub> are ~ 280 pptv in winter and ~ 300 pptv in summer at Niwot Ridge, Colorado, perhaps the only site in the transition region for which an extensive climatology for NO<sub>x</sub> is available. Measurements of NO<sub>x</sub> are discussed in greater detail in Chapter 3.

A further possible source of NO<sub>x</sub> is PAN, which is formed in regions of high NO<sub>x</sub> and could be carried to regions of low NO<sub>x</sub> before decomposing (reaction 44) (Crutzen, 1979). Measurements over the Pacific Ocean have been reported to be in the range of 100 pptv (Singh and Salas, 1983). As yet these are preliminary but they do suggest, along with the Irish data on NO<sub>x</sub>, that substantial amounts of NO<sub>2</sub> can be present on occasion. This is important since the only mechanism which can produce ozone on a large scale in the troposphere is photolysis of NO<sub>2</sub> (reaction 7) and possibly lightning.

There is a growing body of evidence to confirm that concentrations of ozone in the non-urban troposphere are influenced by human activity. Concentrations of ozone are larger at mid-latitudes of the northern hemisphere than at corresponding southern latitudes (Pittock, 1977; Fishman and Crutzen, 1978). Regional scale pollution episodes, during which ozone concentrations may exceed 100 ppbv for several days, indicate an extensive anthropogenic influence on ozone near the surface in both Europe and the United States (e.g., Cox *et al.*, 1975; Guicherit and Van Dop, 1977; Wolff and Lioy, 1980). Concentrations of ozone, both at the surface, and in the middle troposphere over Europe and North America, appear to be increasing (Warmbt, 1979; Angell and Korshover, 1983; Logan, 1985) as discussed further in Chapter 14.

In order to test the concepts about processes influencing ozone, and to evaluate future effects of combustion related emissions on tropospheric ozone, it will be necessary to develop rather sophisticated models for chemistry and transport. Such models must allow for the transformation and transport of pollutants from urban source regions to the middle troposphere. Future research is clearly needed into the photochemistry of the complex hydrocarbon/NO<sub>x</sub> mix which is found in non-urban air.

### 4.3 HETEROGENEOUS CHEMISTRY

Heterogeneous chemical reactions are normally defined as ones which occur at the interface between two phases, e.g., gas-liquid, gas-solid, or liquid-solid. In the atmosphere processes are considered to be heterogeneous as long as the overall reaction involves two phases even though specific steps in the reaction may be homogeneous. An example of this is the oxidation of SO<sub>2</sub> in cloudwater, i.e. the dissolution of gaseous SO<sub>2</sub> into a cloud droplet followed by the oxidation of aqeous SO<sub>2</sub> by homogeneous aqueous-phase reactions. Because SO<sub>2</sub> is transferred from the gas to the aqueous phase, this process is considered to be heterogeneous even though the actual oxidative reaction is homogeneous.

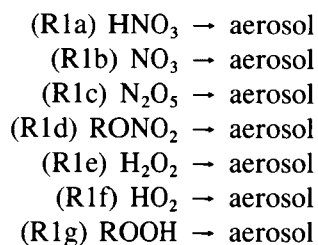
While heterogeneous reactions are not believed to have a significant direct impact upon the global levels of  $O_3$  and HO, they indirectly impact upon these species by affecting the levels of nitrogen oxide species such as  $HNO_3$ ,  $NO_3$ , and  $N_2O_5$  and hydrogen oxide species such as  $HO_2$ ,  $H_2O_2$ ,  $CH_3OOH$ , and other organic peroxides. In this section we briefly review the heterogeneous mechanisms that affect nitrogen oxide and hydrogen oxides.

#### 4.3.1 Interactions with Aerosols and Particulates

The presence of particles in the atmosphere raises the possibility that atmospheric gaseous species interact with these particles heterogeneously. In most cases this interaction results in a gas-to-particle conversion; i.e. the transfer of a chemical species from the gas phase to an aerosol or liquid droplet or the formation of a new particle from a gaseous species. Typically gas-to-particle conversion processes are classified into three categories (Kiang *et al.*, 1973; Schryer, 1982):

- 1) Homogeneous, homomolecular nucleation (the formation of a new stable liquid or solid ultrafine particle from a gas involving one gaseous species only);
- 2) Homogeneous, heteromolecular nucleation (the formation of a new particle from two or more gaseous species);
- 3) Heterogeneous, heteromolecular condensation (the growth of pre-existing particles due to deposition of molecules from the gas phase).

Of the above processes, the third, sometimes referred to as "aerosol scavenging", probably has the greatest impact upon the gas-phase levels of nitrogen oxides and hydrogen oxides and thus on the atmospheric abundances of ozone and HO (Turco *et al.*, 1982). Scavenging reactions that are most relevant in this regard are those involving  $HNO_3$ ,  $NO_3$ ,  $N_2O_5$ , organic nitrates ( $RONO_2$ ),  $H_2O_2$ ,  $HO_2$ , and organic peroxides ( $ROOH$ ). These reactions can be represented by



A complete understanding of scavenging reactions such as those listed above requires a thorough description of all the processes occurring at the surface interface and thus a knowledge of the aerosol surface structure and composition and its interaction with the relevant reactants and products. At the present time we have not yet developed this understanding; to do so will require the continued design and application of sophisticated experimental techniques used in conjunction with advanced theoretical studies of surface interactions. As a result present-day descriptions of heterogeneous reactions such as aerosol scavenging are quite rudimentary and involve the use of simple parameterizations to treat many of the complex molecular processes that occur but are not yet understood. One such simple description is described below.

The rate of scavenging of a gaseous species  $J$  is normally assumed to be proportional to the species ambient concentration,  $n_J$ , so that

$$\text{Rate of aerosol scavenging} = n_J k_{\text{part}} \quad (1)$$

## TROPOSPHERIC CHEMISTRY

where the proportionality constant,  $k_{\text{part}}$ , has units of  $\text{s}^{-1}$ . The parameter  $k_{\text{part}}$  can be represented by (Chameides and Davis, 1982; Heikes and Thompson, 1983),

$$k_{\text{part}} = \int \phi_J(r) n_p(r) dr \quad (2)$$

where  $n_p(r)$  is the concentration of aerosol particles having radii between  $r$  and  $r + dr$  and  $\phi_J(r)$  is the rate at which species  $J$  diffuses and sticks to an aerosol particle of radius  $r$ .  $\phi_J(r)$  can be represented by (Schwartz, 1983)

$$\phi_J(r) = \frac{4}{3} \pi \ell r V_j \left( 1 + \frac{4\ell^{-1}}{3r\alpha} \right) \frac{[n_J - n_J^0]}{n_J} \quad (3)$$

where  $\ell$  is the mean free path,  $V_j$  is the species thermal velocity,  $\alpha$  is the appropriate sticking or accommodation coefficient for species  $J$  impinging upon the aerosol surface, and  $n_J^0$  is the species' concentration at the surface of the aerosol. Typically,  $n_J^0$  is assumed to be zero for solid particles and  $(a_J/H_jRT)$  for wet particles, where  $a_J$  is the activity of  $J$  in solution,  $H_j$  is the species solubility constant in the appropriate aerosol solution,  $R$  is the gas constant, and  $T$  is the temperature.

While appearing to be quite straightforward, the application of Equations (1), (2), (3) to determine the rate of aerosol scavenging of a given species  $J$  is quite difficult. For one the value of  $\alpha$  is highly uncertain. The little data that does exist suggest that  $\alpha$  can vary widely depending upon the aerosol composition (i.e. basic or acidic), relative humidity (i.e. for hygroscopic aerosols, solid particles at low humidity and solution droplets at high humidity), and the nature of the impinging gas. For instance while sticking coefficients for species such as  $\text{HO}_2$ ,  $\text{H}_2\text{O}_2$ ,  $\text{NO}_3$  impinging upon water solutions with pH's above about 5 may approach unity, the  $\alpha$  for these species impinging upon  $\text{H}_2\text{SO}_4$  particles or similar highly acidic dry particles are likely of the order of  $10^{-6}$  to  $10^{-4}$  (cf. Chameides and Davis, 1982).

Another complication arises for hygroscopic aerosol particles which, provided the humidity is high enough, exist as small suspended solution droplets of relatively high ionic strength (i.e.  $\mu > 1$ ). At these ionic strengths, the particle can no longer be treated as an ideal solution as one does for lower ionic strengths. The appropriate values for  $a_j$  and  $H_j$  are generally not known and can only be accurately determined by detailed experimental studies such as those carried out by Pytkowicz (1984) for seawater.

In spite of these uncertainties, Equation (1), (2), and (3) can be used to obtain a preliminary indication of how important these scavenging reactions may be for a range of possible values for uncertain parameters such as  $\alpha$ . As an example, values for  $k_{\text{part}}$  for  $\text{NO}_3$  and  $\text{N}_2\text{O}_5$  as a function of  $\alpha$  and the total number density of aerosol particles (assuming a log-normal distribution) are illustrated in Figure 4-3 for the case when  $n_J^0 = 0$ . (Very similar scavenging coefficients would be obtained for other species such as  $\text{HNO}_3$ ,  $\text{HO}_2$ , and  $\text{H}_2\text{O}_2$ ). The results of Figure 4-3 suggest that for species with sufficiently long lifetimes (i.e. of the order of days or more), aerosol scavenging would represent a significant sink in regions of modest-to-large aerosol loadings if  $\alpha \geq 10^{-2}$ . Indeed the large levels of  $\text{NO}_3^-$  found in aerosols in the marine boundary layer would appear to confirm that scavenging of gaseous  $\text{HNO}_3$  by sea salt aerosol represents a major sink for this species in the marine atmosphere (Huebert and Lazrus, 1980; Liu *et al.*, 1983). At night when  $\text{NO}_3$  photochemical lifetimes become large, scavenging by aerosols could also be a significant sink for  $\text{NO}_3$ ; in fact this mechanism has been proposed to explain the low levels of  $\text{NO}_3$  observed at night (Noxon *et al.*, 1978; Platt *et al.*, 1980b; Heikes and Thompson, 1983). It is also interesting to note that in urban locations where aerosol number densities of  $10^4 - 10^5 \text{ cm}^{-3}$  are not uncommon, aerosol scavenging could also be an important sink for  $\text{HO}_2$ , whose photochemical lifetime is about 100s, if  $\alpha =$  values near 1 are appropriate.

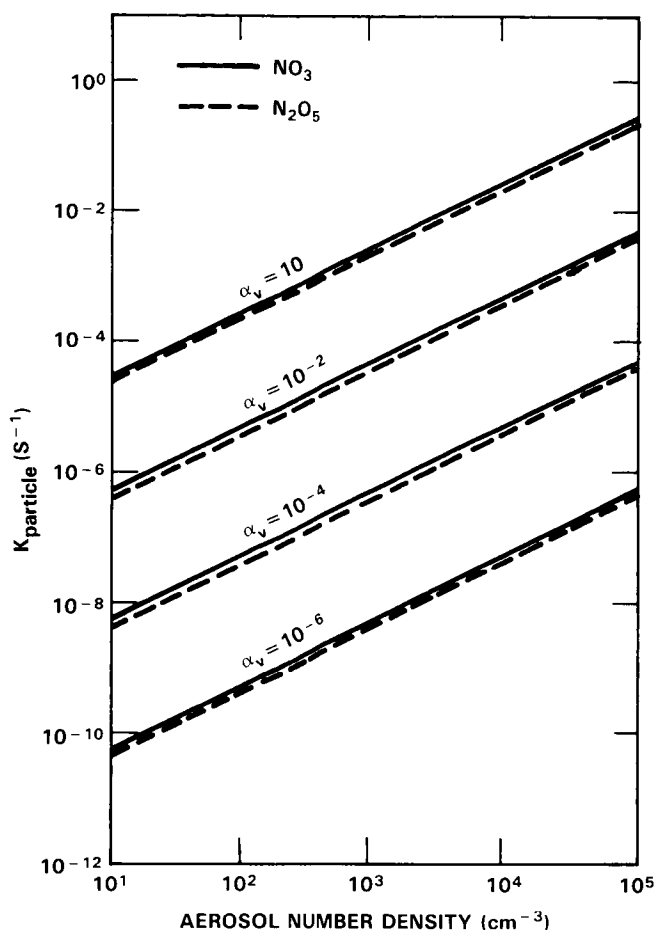


**Figure 4-3** Calculated values of aerosol  $k_{\text{part}}$  for  $\text{NO}_3$  and  $\text{N}_2\text{O}_5$  as a function of aerosol number density and sticking coefficient  $\alpha_v$ . After Heikes and Thompson (1983).

Thus these calculations imply that aerosol scavenging can be an important sink for  $\text{HNO}_3$  and  $\text{NO}_3$ , as well as  $\text{H}_2\text{O}_2$  and possibly  $\text{HO}_2$ . As such this process would represent a major heterogeneous sink for nitrogen oxides and hydrogen oxides. However, many uncertainties are associated with this assessment. Before a more definitive assessment of aerosol scavenging can be made, experimental studies establishing accurate values for  $\alpha$  as well as field measurements characterizing the chemical composition and structure of aerosol surfaces will be needed.

In addition to aerosol scavenging another potentially important heterogeneous sink of nitrogen oxides that needs to be considered is the formation of  $\text{NH}_4\text{NO}_3$  from gaseous  $\text{NH}_3$  and  $\text{HNO}_3$ , i.e.



In regions of high  $\text{NH}_3$  levels this process can represent a significant heterogeneous sink for nitrogen oxides. Studies by Stelson and Seinfeld (1982) have indicated that the levels of  $\text{NH}_4\text{NO}_3$  in the particulate phase relative to that of gas-phase  $\text{NH}_3$  and  $\text{HNO}_3$  can be accurately described in terms of the thermodynamic equilibrium between the phases. While the condensation of  $\text{NH}_4\text{NO}_3$  can occur via heteromolecular, homogeneous condensation as well as heteromolecular, heterogeneous condensation, observations indicate that the later process is the dominant one in the atmosphere.

## TROPOSPHERIC CHEMISTRY

### 4.3.2 Interactions with Hydrometeors

#### 4.3.2.1 Scavenging

Similar to the interactions of gases with aerosol particles, scavenging or heterogeneous removal is probably the most common process by which hydrometeors affect gas-phase species. This can occur via rainout (removal of gases by cloud droplets) as well as washout (removal of gases by raindrops). Of these two it is generally believed that rainout is more important than washout simply because of the longer lifetime and greater surface area afforded by cloud drops when compared to that of raindrops. With regard to nitrogen oxides and hydrogen oxides, removal of  $\text{HNO}_3$ ,  $\text{NO}_3$ ,  $\text{H}_2\text{O}_2$ , and  $\text{HO}_2$  are most relevant because of their high solubility or reactivity in clouds.

The rate of incorporation of a gaseous species J into a cloud droplet can be treated in much the same manner as that for aerosol particles described in the previous section. Thus

$$\text{Rate of cloud droplet scavenging} = n_J k_{\text{cloud}} \quad (4)$$

where

$$k_{\text{cloud}} = \int \phi_J(r) n_d(r) dr \quad (5)$$

and  $n_d$  is the number of cloud droplets with radii between  $r$  and  $r + dr$ .  $\phi_J(r)$  in Equation (5) is essentially the same as that given by Equation (3), except that now  $n_J^\circ = [J]/\text{HRT}$ , where  $[J]$  is the concentration of J in solution in units of moles (liter)<sup>-1</sup>. (Because ionic strengths in cloudwater are small, the solution can be treated as ideal so that  $a_J = [J]$  and  $H_J$  is given by the Henry Law constant for J in a pure water solution.) Values for  $\alpha$  for cloud drops, while not accurately known, are probably not nearly as uncertain or variable as those for aerosol particles since the water droplet surface is better defined. (On the other hand, the reader should note that the presence of organic films on droplets could further complicate the issue as discussed by Gill *et al.*, 1983). Sticking coefficients for most species of interest impinging on water are probably of the order of  $10^{-2}$  or higher although values as low as  $10^{-4}$  cannot be ruled out at this time (cf., Chameides and Davis, 1982).

Within a cloud, gaseous species are transferred to droplets until equilibrium is attained. Calculations simulating the transfer of gases to droplets indicates that, for reasonable values of  $\alpha$ , equilibrium between the two phases is rapidly attained. This fact is illustrated in Table 4-2 where equilibration times,  $\tau_{\text{eq}}$ , are listed for several species of interest as a function of  $\alpha$  and  $r$ . Because equilibrium does apply the concentration of a species J in solution can be related to its ambient gas-phase concentration in cloud-free regions via

$$[J] \cong [J]^{\text{eq}} = n_J / (A L \times 10^{-9} + (\text{HRT})^{-1}) \quad (6)$$

where  $[J]^{\text{eq}}$  is the concentration of J in the cloudwater at equilibrium, A is Avogadro's number, and L is the liquid water content in units of  $\text{gm}^{-3}$ .

Given Equation (6) as well as statistics for the average cloudiness of the atmosphere, the rate of precipitation from clouds, and the liquid water content of clouds, an expression for the rate of removal of a species via rainout can be obtained. The results of such an analysis are found in Figure 4-4a, where the rainout

Table 4-2. Values for  $H_{\text{eff}}$ ,  $(PF)_{\text{eq}}$ , and  $\tau_{\text{eq}}$  as a function of  $\alpha_w$  and  $r$  for selected soluble species.\*

Gas-Phase Species	$H_{\text{eff}}$ [M/atm]	$(PF)_{\text{eq}}$	$\tau_{\text{eq}}$ [sec]			
			$\alpha = 10^{-2}$ $r = 10\mu\text{m}$	$\alpha = 1$ $r = 10\mu\text{m}$	$\alpha = 10^{-4}$ $r = 10\mu\text{m}$	$\alpha = 10^{-2}$ $r = 30\mu\text{m}$
SO <sub>2</sub>	$4.1 \times 10^3$	0.06	2.1	0.93	120	12
HCHO	$1.3 \times 10^4$	0.16	4.3	1.9	250	24
HO <sub>2</sub>	$3.3 \times 10^4$	0.4	10	4.4	580	56
OH	$1 \times 10^5$	1.1	16	6.9	910	88
HCOOH	$1.5 \times 10^5$	1.7	33	14	$1.9 \times 10^3$	180
H <sub>2</sub> O <sub>2</sub>	$1.9 \times 10^5$	2.3	31	14	$1.8 \times 10^3$	180
NH <sub>3</sub>	$1.6 \times 10^6$	19	44	19	$2.5 \times 10^3$	240
HNO <sub>3</sub>	$7.3 \times 10^{11}$	$9 \times 10^6$	280	120	$1.6 \times 10^4$	$1.6 \times 10^3$

\*Values calculated for pH = 5.05, T = 291 °K, and L = 0.5g m<sup>-3</sup>. After Chameides (1984).

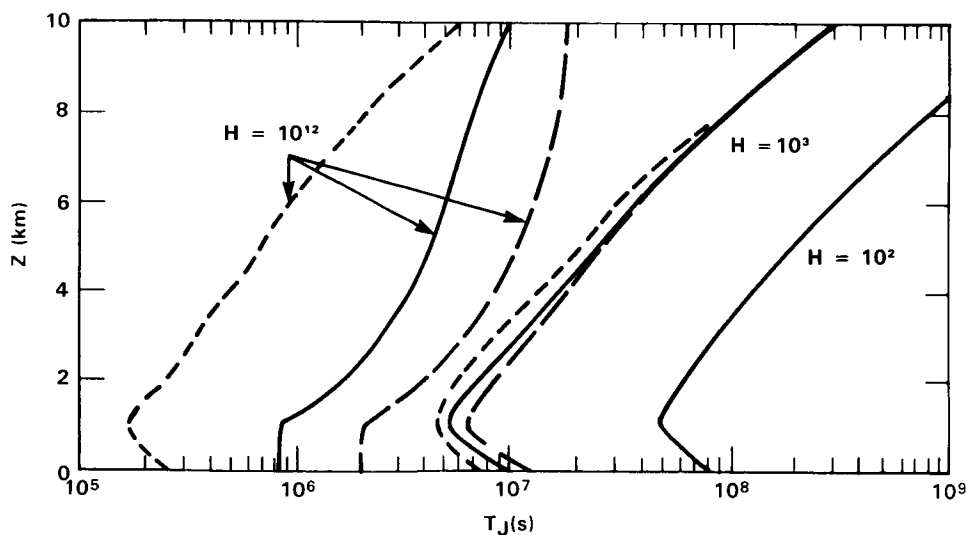
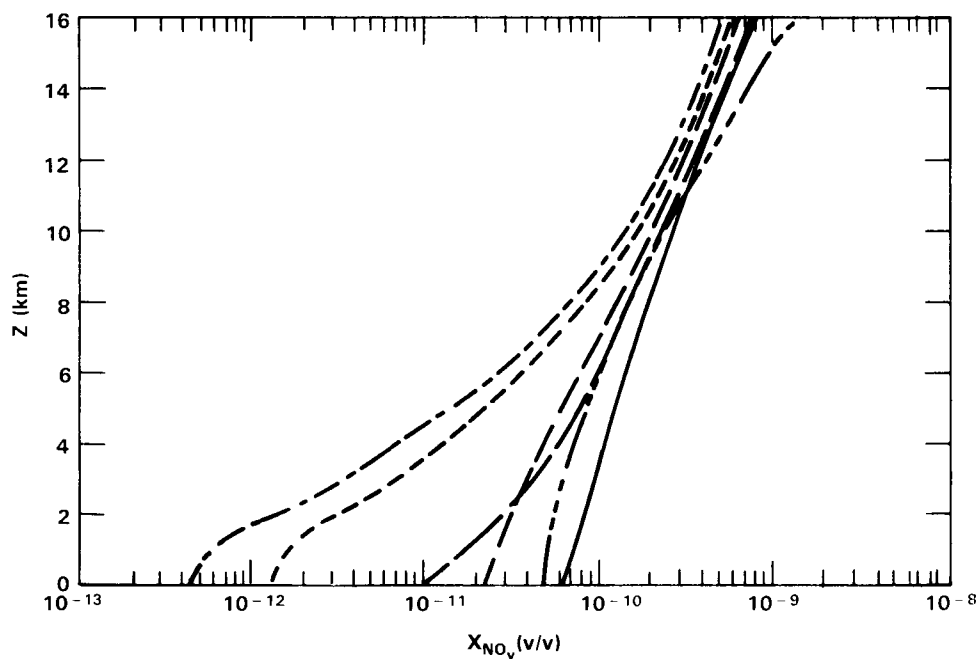


Figure 4-4a Effective rainout lifetimes,  $\tau_J^0$ , for  $H = 10^2$ ,  $10^3$ , and  $10^{12}$  (M atm<sup>-1</sup>) for different storm cycle periods. The dotted line is for a storm period (i.e. the time for a complete cycle of rain followed by a dry interval to transpire) of 1 day, the solid line is for a storm period of 10 days, and the dashed line is for a storm period of 25 days.

## TROPOSPHERIC CHEMISTRY

lifetimes,  $\tau_J$ , are illustrated as a function of  $z$  for different values of  $H$  and varying types of storm cycles. For species of low solubility,  $\tau_J$  is linearly related to  $H$  but independent of the length of time between storms. For species of high solubility which are virtually completely removed from the atmosphere during each storm,  $\tau_J$  is independent of  $H$  but linearly related to the time between storms; in this case  $\tau_J = T$  where  $T$  is the storm period.

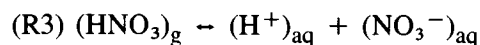
Thus in regions of long dry periods between storms, the rainout lifetimes for highly soluble species can become significantly longer than the average 10 day lifetime for water vapor that has been previously assumed to be representative of the lifetime of highly soluble species. It can be seen in Figure 4-4b that for nitrogen oxide species strikingly different profiles can be obtained in model calculations using this parameter for different assumed storm periods even though identical source strengths were assumed in each case. Thus, given the large seasonal and latitudinal variations in the water vapor-cycle, this result would seem to imply that in addition to  $\text{NO}_y$  sources,  $\text{NO}_y$  removal rates can also lead to large temporal and spatial variations in  $\text{NO}_y$  concentrations.



**Figure 4-4b** Model calculated profiles for "stratospheric  $\text{NO}_y$ " diffusing down into the troposphere. All profiles adopt a cross-tropopause flux of  $3.75 \times 10^8 \text{ cm}^{-2} \text{ s}^{-1}$  and a  $H = 10^{12} \text{ M (atm)}^{-1}$ . The dashed-dotted line, dotted line, and solid line adopt a deposition velocity of  $0.3 \text{ cm s}^{-1}$  and a storm period of 1, 10, and 25 days respectively. The broken line is the same as the solid line except a deposition velocity of  $1 \text{ cm s}^{-1}$  was used. The circles represent the average  $\text{NO}_y$  profile calculated by Kley *et al.* (1984) from the GFDL 3-D tracer-transport model. After Giorgi and Chameides (1985).

## 4.3.2.2 Chemical Effects

In addition to providing a liquid phase where soluble gases can be dissolved, clouds also offer an active chemical medium where aqueous-phase chemical reactions can occur which affect the removal rate of atmospheric species in general and nitrogen oxide and hydrogen oxide species in particular. For instance while the distribution of gaseous  $\text{HNO}_3$



provides a major rainout sink for atmospheric nitrogen oxides and source of dissolved  $\text{NO}_3^-$  in rainwater, another important sink can arise in regions where  $\text{NO}_x (= \text{NO} + \text{NO}_2)$  is large. This sink occurs via the production of gaseous  $\text{NO}_3$  radicals in clouds at night. Because  $\text{NO}_3$  radicals have long chemical lifetimes at night and can be rapidly scavenged by cloud droplets, their night time production in a cloud is followed by their incorporation into cloudwater. Once in the aqueous-phase,  $\text{NO}_3$  is rapidly converted to  $\text{NO}_3^-$ . A typical reaction sequence leading to  $\text{NO}_3^-$  production in cloudwater is

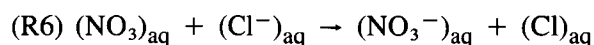
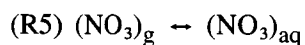
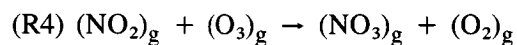
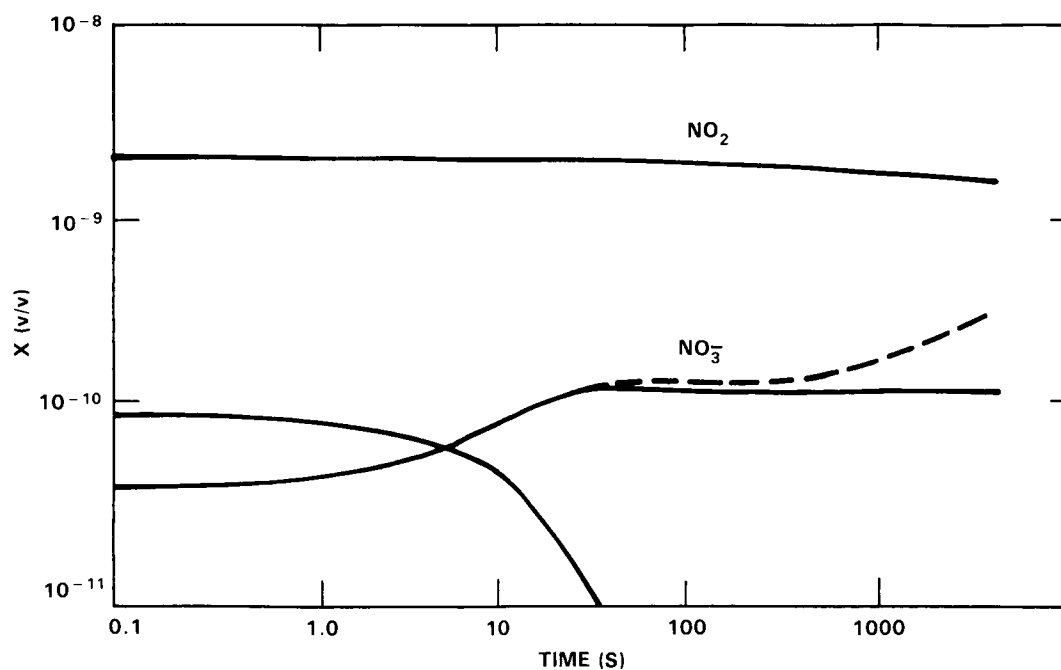


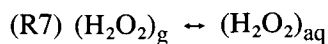
Figure 4-5 taken from a numerical simulation of the coupled gas- and aqueous-phase chemistry of a cloud, illustrates the enhanced levels of  $\text{NO}_3^-$  that can result from this process at night.



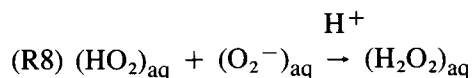
**Figure 4-5** The calculated mixing ratios for gaseous  $\text{NO}_2$  and  $\text{HNO}_3$  and aqueous-phase  $\text{NO}_3^-$  as a function of time for a stratiform cloud in a "High- $\text{NO}_x$ " region. The solid  $\text{NO}_3^-$  line is without scavenging of gaseous  $\text{NO}_3$  and dashed  $\text{NO}_3^-$  line is with scavenging of gaseous  $\text{NO}_3$ .

## TROPOSPHERIC CHEMISTRY

Whereas chemical processes in clouds can enhance the heterogeneous removal rate of nitrogen oxides, in the case of hydrogen oxides they may result in a net source. While the removal of gaseous  $\text{H}_2\text{O}_2$  and its incorporation in cloud water via



represent a sink for hydrogen oxides, the production of aqueous-phase  $\text{H}_2\text{O}_2$  via a variety of radical reactions such as



can produce  $\text{H}_2\text{O}_2$ . As illustrated in Figure 4-6, depending on the intensity of these radical sources, significant enhancements in  $\text{H}_2\text{O}_2$  can result. It is conceivable that clouds with intense  $\text{H}_2\text{O}_2$  production which evaporate could represent net sources of  $\text{H}_2\text{O}_2$  to the atmosphere. In order to determine if in fact this does occur it will be necessary to carry out further laboratory studies of radical processes relevant to cloud chemistry and to carry out field experiments which measure gas- and aqueous-phase  $\text{H}_2\text{O}_2$  levels in and out of a variety of clouds.

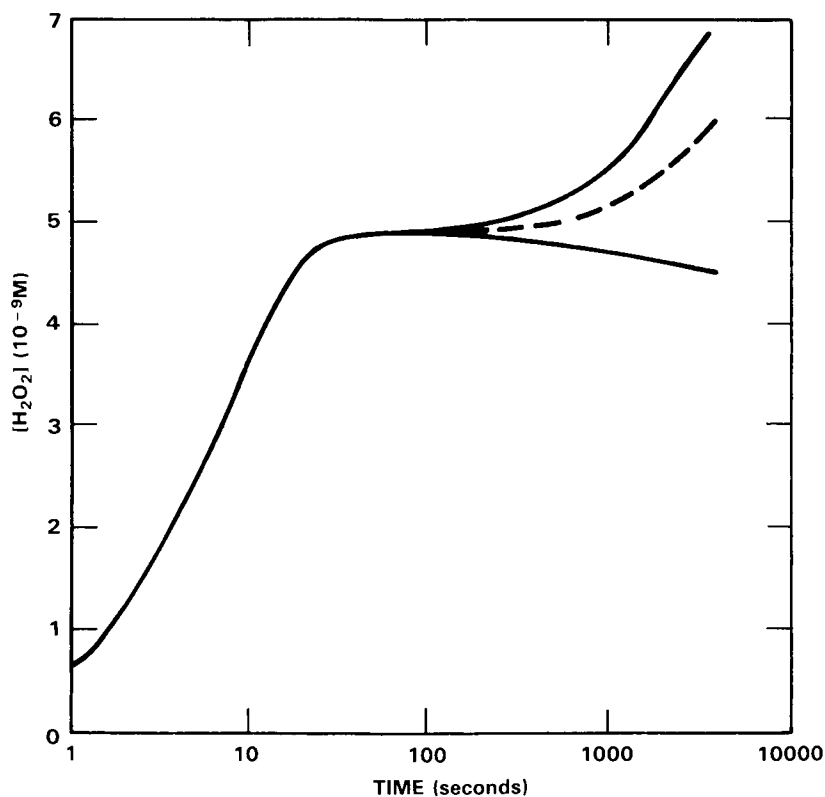


**Figure 4-6** Temporal variation in  $[\text{H}_2\text{O}_2]$  for a calculation in which all aqueous-phase sources of  $(\text{H}_2\text{O}_2)$  were neglected (solid line), for the standard model in which the aqueous-phase sources of  $(\text{H}_2\text{O}_2)_{aq}$  were included (dashed line), and for a calculation in which the cloud transmissivity  $\tau$  was taken to be 1.0 (dotted line). After Chameides (1984).

## 4.4 SURFACE EXCHANGE AND VERTICAL REDISTRIBUTION

### 4.4.1 Surface Exchange

Vertical transport in the boundary layer (i.e., the layer of air that is coupled directly to the surface by turbulent exchange processes on a time scale of about an hour or less), and between the boundary layer and the overlying free atmosphere, plays an important role in determining the fate of trace atmospheric species. At the surface, trace species may be both deposited and emitted, so that the flux at the surface is a net balance between the two processes. Deposition at the surface requires transport of the trace species to the surface by turbulent eddies.

Redistribution between the boundary layer and the overlying free atmosphere is mostly a result of highly intermittent cloud processes. Cycling of trace species through clouds can result in chemical transformations and loss through wet deposition (see section 4). The latent heat released by clouds can result in several kilometer ascents of boundary layer air into the free atmosphere within a few minutes. Compensating downward motions can transport air from the free atmosphere into the boundary layer. Eddy diffusivity models are not adequate for describing mixing of trace species over such large vertical displacements. Although some progress has been made in parameterizing these processes, much still remains to be done.

The subsequent sections discuss our current understanding of surface exchange of trace species important in estimating the tropospheric ozone budget, including both dry deposition and surface emission, as well as the exchange of trace species between the boundary layer and the overlying free atmosphere. Both are important in estimating the ozone budget throughout the troposphere.

Dry deposition is the transfer of an atmospheric constituent from the air directly to the earth's surface, regardless of whether the surface is wet or dry, or whether the loss is at the ground or in elements that are attached to, or touching the ground, such as a forest canopy or a snow cover. Because of the complexity of the earth's surface, and the variety of mechanisms for capturing species, precise physical descriptions of how this process takes place are difficult. Instead, the rate of dry deposition is commonly specified with a gross parameter such as a deposition velocity. The deposition velocity is defined as the ratio of the downward flux  $F_s$  of a species  $s$  to its mean concentration at some reference level  $s$

$$v_d = F_s / \bar{s} \quad (1)$$

Trace constituents are transferred from the atmospheric boundary layer to within a centimeter of the surface (or surface protrusions) by turbulent eddies. Below this, the transfer is predominantly by molecular diffusion. We can, therefore, define the downward flux through a particular level as the averaged product of instantaneous departures of the constituent concentration  $s'$  and vertical velocity  $w'$  from their means, measured at that level; i.e.,  $F_s = -\overline{w's'}$ , where the overbar denotes an average over a distance or time long enough to ensure a statistically reliable result.

Dry deposition is determined by the efficiency of the turbulence transport process, and the properties of both the constituent and the surface. The constituent may be either adsorbed or absorbed at the surface; that is, the constituent may either be stored on the surface without changing its identity, or it may combine chemically with the surface material. The deposition rate for constituents which are efficiently absorbed at the surface is controlled mainly by the ability of the turbulent eddies to transport the constituents to the surface, while for less reactive constituents, the rate is determined by the efficiency with which the

## TROPOSPHERIC CHEMISTRY

impinging constituents stick to the surface. As discussed by Wesely (1983) and Wesely and Hicks (1977), a convenient way to express this mathematically is to separate the effects of turbulence transport from constituent and surface properties by considering the reciprocal of the deposition velocity as a "resistance" to deposition, and equating it to the sum of the individual resistances contributed by (1) the turbulence transport process, commonly called the aerodynamic resistance  $r_a$ ; (2) that contributed by molecular transport through the quasilaminar layer within about a centimeter of the surface and surface elements  $r_s$ ; and (3) that contributed by how well the constituent sticks to the particular surface  $r_c$ :

$$v_d^{-1} = r_a + r_s + r_c \quad (2)$$

In this way, properties of the constituent and surface can, in principle, be separated from aerodynamic properties.

Many species are not only deposited, but are also emitted at the surface. Therefore, in these cases, the surface flux is the net result of both deposition and emission, and the concept of a surface resistance is no longer applicable for estimating surface flux, except when emission is negligible compared to deposition. Nitrogen oxides ( $\text{NO}_x = \text{NO} + \text{NO}_2$ ) for example, are emitted from vegetated surfaces. Depending upon the situation, either deposition or emission may dominate; thus the surface flux may be either positive or negative. Their emissions are mostly the result of the activity of various soil microbes, whose rates of production are governed mainly by soil composition, temperature, moisture and pH, available oxygen, and fertilization practices. Over water, nitrite photolysis is believed to be a source of NO emission (Zafiriou and McFarland, 1981). Surface emissions of  $\text{O}_3$  and  $\text{HNO}_3$  are considered to be negligible, so that the resistance concept can be used to estimate their surface flux.

The actual process of deposition depends upon many factors. Over vegetated surfaces, the condition of the vegetation can be important, particularly for reactive gas species. Ozone deposition, for example, is much larger when the leaf stomata are open than when they are closed. Thus, ozone deposition is maximized over vegetated areas in the daytime when plants are actively growing. Observations over the ocean indicate a deposition rate several times that predicted on the basis of laboratory studies over pure water. This indicates that trace constituents in the water and on the water surface are important in determining the actual deposition rate.

### 4.4.1.1 Techniques of Measurement

A variety of techniques have been developed and used for measuring dry deposition. A summary of techniques, and their advantages and disadvantages, is presented by Hicks *et al.* (1980). The most direct flux measurement technique is the eddy correlation technique. This requires fast response (on the order of 1 Hz bandwidth for ground-based measurements; 10 Hz bandwidth for airplane measurements) high resolution concurrent measurements of concentration and vertical velocity. Ozone sensors have been developed and used for this purpose (Pearson and Stedman, 1980; Eastman and Stedman, 1977; Wesely *et al.*, 1978). Instruments are also under development for measuring fast response nitric oxide fluctuations (e.g., Bradshaw and Davis, 1982). For ground-based sites, the height of measurement is typically a few meters above the ground, and averaging times of at least 20 minutes are required. The measured flux emanates as far as the order of a hundred meters or so upwind of the site; thus the flux is an average over a considerable area.

A common technique for measuring surface deposition and emission of trace species is to place an enclosure over the surface to be considered and measure the change in concentration within the box with time. This can then be related to the surface flux. Problems with this technique include (1) the enclosure modifies the turbulent transport process, and (2) the flux is measured only over the area covered by the enclosure.

Another technique for estimating surface flux is the profile method. The basis for this technique is the existence of a unique relationship between the flux of a species and its gradient near the surface. The eddy diffusivity, which is the negative of the ratio of the flux to the gradient, is a function of the surface roughness, wind speed and hydrodynamic stability. Therefore, additional micrometeorological measurements are required to obtain the flux from gradient or difference measurements. Fast response concentration measurements are not required, but concentration differences between levels need to be measured with an accuracy of about 1% of the mean concentration.

It may also be possible to estimate surface fluxes in some situations by estimating terms in the mean concentration budget. In this technique, the time rate of change of a constituent minus the net amount of a constituent advected into a volume through the top and sides is equated to that contributed by the flux at the surface. This technique cannot be used for constituents which are not conserved on a time scale of less than a day. As pointed out by Williams (1982), this method also requires accurate measurements of concentration differences.

Another factor to consider is that the chemical reactivity of some species is rapid enough that their flux may vary significantly between the measurement level and the ground. As pointed out by Fitzjarrald and Lenschow (1983), this can be the case for  $O_3$ ,  $NO$ , and  $NO_2$ , which react rapidly with each other in sunlight. They point out, for example, that for profile or eddy-correlation measurements of  $NO$  and  $NO_2$  flux, and also  $O_3$  flux when the mean concentration of  $NO_x$  is greater than about 20% of  $O_3$ , at least six measurements are needed to accurately estimate the fluxes. These measurements include combinations of the means and fluxes of all three species. The  $NO_x$  concentration, however, can be considered a conserved species near the surface.

#### 4.4.1.2 Results of Measurements

In this section, we briefly summarize results of previous studies on surface fluxes of  $O_3$ ,  $NO$  and  $NO_2$ , and  $HNO_3$ . Compared to these species, very little is known about the surface fluxes of  $H_2O_2$ , PAN and particulate nitrates, and thus they are not discussed further. Reviews of dry deposition rates for a variety of species are presented by Sehmel (1980) and McMahon and Denison (1979).

- **Ozone**

Ozone deposition has been measured over a variety of surfaces by the eddy correlation, profile and box techniques. Reviews of ozone deposition measurements are presented by Galbally and Roy (1980) and Wesely (1983). The results are summarized in the following Section.

#### Land surfaces

Surface resistance over vegetated areas has strong diurnal, seasonal and climatic variability, mainly due to the size of the leaf stomata. Resistances for water vapor transpiration and ozone uptake in vegetation have been found to be identical when allowance is made for their difference in molecular diffusivity (Turner *et al.*, 1974; Galbally and Roy, 1980). The median value for daytime surface resistance  $r_c$  over areas that are photosynthetically active, including both natural vegetation and crop lands, seems to be about  $100 \text{ s m}^{-1}$ . At the low end of the scale, Wesely (1983) reports values as low as  $20 \text{ s m}^{-1}$  over soybean fields; Lenschow *et al.* (1982) measured a value of  $50 \text{ s m}^{-1}$  over a forest.

## TROPOSPHERIC CHEMISTRY

At night, or when the vegetation is water stressed, the resistance of both naturally vegetated and cultivated surfaces increases by as much as a factor of two or more as the stomata close. The resistance of the leaves themselves becomes very large, and the deposition occurs mainly at the soil surface. However, even with senescent vegetation, a diurnal variation has been observed (Wesely, 1983). This may be partly due to greater efficiency in daytime for transporting air down to the underlying soil by the turbulence generated by surface heating. Since bare soil not saturated with water has a resistance of  $100 \text{ s m}^{-1}$  or less (Wesely, 1983; Galbally and Roy, 1980; Turner *et al.*, 1973), its resistance is smaller in daytime over an area with senescent vegetation than at night in an area with actively growing vegetation. Waterlogged bare soil, however, may have a resistance several times that of dry soil. Wesely *et al.* (1981), for example, measured a resistance of about  $1,000 \text{ s m}^{-1}$  for water-saturated bare soil just above freezing.

### Water

Deposition to water surfaces is observed to be much larger than predicted based on theoretical models of the exchange rate of soluble gases at the sea surface, and laboratory measurements of deposition to distilled water (Garland *et al.*, 1980). The reasons for this are still not completely understood, although it is thought to be the result of reactions of ozone with substances on or near the water surface. Galbally and Roy (1980) suggest an average of  $1000 \text{ s m}^{-1}$ , and present a summary of values measured by themselves and others using profile and box methods that range from 650 to  $4,400 \text{ s m}^{-1}$ . Lenschow *et al.* (1982) obtained a value of  $1,800 \text{ s m}^{-1}$  from direct eddy correlation measurements from aircraft. Over fresh water, Wesely *et al.* (1981) made eddy correlation measurements over Lake Michigan that give a surface resistance of about  $9,000 \text{ s m}^{-1}$ , which is somewhat closer to, but still considerably less than the calculated value for resistance of pure water.

Deposition to snow has been measured by Wesely *et al.* (1981) to have a resistance of about  $3,300 \text{ s m}^{-1}$  for crusty snow and snow on the ground for longer than a day, and somewhat less than this for fresh snow. Galbally and Roy (1980), on the other hand, measured a median value of  $1,600 \text{ s m}^{-1}$  and higher values for fresh snow.

### Total ozone surface destruction

Recent estimates of the total ozone destruction at the earth's surface are in the range of 0.5 to  $1.5 \times 10^{12} \text{ kg yr}^{-1}$  (Galbally and Roy, 1980). This is equivalent to an average surface flux of 60 to  $180 \text{ ng m}^{-2} \text{ s}^{-1}$  and, assuming a mean ozone concentration of  $60 \mu\text{g m}^{-3}$ , an average deposition velocity of 0.1 to  $0.3 \text{ cm s}^{-1}$ .

#### • Nitric acid

The only known published measurements of the deposition of nitric acid were obtained by Huebert (1985). He found that its surface resistance over grassland was virtually zero. Similarly, over water its surface resistance is expected to be negligible compared to the aerodynamic resistance (Levine and Schwartz, 1982). Although further experimental verification is important, it appears that specification of  $\text{HNO}_3$  deposition is relatively straightforward, with deposition velocities in the range of  $0.4$  to  $2 \text{ cm s}^{-1}$ .

#### • Nitrogen oxides

As discussed previously,  $\text{NO}_x$  is both emitted and deposited at many surfaces. During daytime over vegetated surfaces, the surface emission is typically larger than at night, and may exceed deposition because

the higher daytime soil temperature enhances microbial activity. In areas where anthropogenic activities enhance the  $\text{NO}_x$  concentration, surface deposition may become large enough that emission can be neglected. Because of the diversity of interactions that can occur near the surface, and the reactivity of  $\text{NO}_x$ , it is often difficult to separate emission and deposition, and parameterization of the surface flux is difficult. The mechanisms of nitrification and denitrification and the involvement of  $\text{N}_2$ ,  $\text{N}_2\text{O}$ ,  $\text{NO}$  and  $\text{NO}_2$  in these processes have been studied by, for example, Myers *et al.* (1979). Laboratory studies of soils to investigate the emissions of these gases under various conditions have been carried out by, for example, Lipschultz *et al.* (1981). On a global scale, the net result of these processes can, at present, be only roughly estimated. For example, Ehhalt and Drummond (1982) estimate that between 5 and 17% of the overall  $\text{NO}_x$  source is due to soil emission, Hahn and Crutzen (1982) estimate 0 to 50%, and Logan (1983) estimates 5 to 15%. Logan (1983) also estimates that dry deposition accounts for about 30% of  $\text{NO}_x$  removal.

Measurements of  $\text{NO}_x$  surface deposition are almost nonexistent. Wesely *et al.* (1982) have made eddy correlation measurements of  $\text{NO}_x$  flux over a field of soybeans, and found a minimum surface resistance of  $130 \text{ s m}^{-1}$  in daytime, with  $\text{NO}_2$  being the predominant species. At night they measured a resistance of about  $1500 \text{ s m}^{-1}$ . They estimated that the deposition velocity of  $\text{NO}_x$  was about 2/3 that of  $\text{O}_3$ . Over the ocean, there are no known measurements of  $\text{NO}_x$  surface flux. Thompson and Zafiriuou (1981), however, have estimated deposition velocities of  $0.00017 \text{ cm s}^{-1}$  and  $0.0012 \text{ cm s}^{-1}$  for  $\text{NO}$  and  $\text{NO}_2$ , respectively.

#### 4.4.1.3 Outlook

Instrumentation has been available for measuring ozone surface flux for several years, and our understanding of ozone deposition is now reasonably well understood over crop and range land. Deposition into forests and water is not as well understood, and further measurements would be desirable. In contrast, instruments for measuring  $\text{NO}_x$  surface flux are just now becoming available, and further technical development is essential—and forthcoming. Furthermore,  $\text{NO}_x$  surface flux is a combination of deposition and emission, and therefore is more difficult to parameterize. An additional complication in measuring the individual fluxes of  $\text{NO}$  and  $\text{NO}_2$  is their chemical reactivity, which can result in significant variation of their fluxes with height near the surface. As a result, our understanding of their surface fluxes is significantly less than for ozone. Almost nothing is known about surface fluxes of  $\text{H}_2\text{O}_2$ , PAN, and particulate nitrates.

#### 4.4.2. Vertical Redistribution

##### 4.4.2.1 Boundary Layer Transport

Transport in the boundary layer is dominated by turbulent eddies with length scales that extend over several decades. The entire spectrum of motions cannot be explicitly resolved by computer modeling. Therefore, simplifications are made to parameterize the transport process. One of the simplest and most widely used approaches is to assume that the transport occurs by eddy diffusion. This has serious limitations in many situations, since the scales important for transport are comparable to the depth of the boundary layer. Wyngaard (1984) has extended the simple eddy diffusion concept by splitting transport in the convective boundary layer into diffusion from the bottom up and from the top down, and in this way is able to obtain more realistic boundary layer structure. Fiedler (1984) has developed an integral closure model that accounts for exchange of parcels over finite vertical displacements, which again gives more

## TROPOSPHERIC CHEMISTRY

realistic results than simple eddy diffusion modeling. Another approach is to explicitly model the large eddies in the convective boundary layer, and parameterize only the small eddies which are relatively unimportant for transport. Moeng and Wyngaard (1984) have used this approach to calculate statistics of conservative scalars in the convective boundary layer. In the future, these models will likely be applied to chemically active species.

Parameterizations of the turbulent fluxes in the boundary layer using an eddy diffusion coefficient combined with one-dimensional photochemical models have been used to model trace gas concentrations in the boundary layer. One result of such a simulation, which included diurnal variation of the height of the mixed layer as well as the vertical diffusion coefficient, is that the concentrations of trace species in the troposphere are 20-30% higher than when mixing processes are described by a simple vertical eddy diffusion which is constant with time and height (Fishman and Carney, 1984). Thompson and Lenschow (1984) obtained similar results in the tropical marine boundary layer.

These models also include entrainment at the top of the mixed layer, implying a non-zero flux of the species at that level provided there is a jump in the concentration profile. However, the effects of clouds in intensifying the entrainment rate on top of the mixed layer have not been incorporated satisfactorily in the current one-dimensional models. This effect has been observed to be of importance over convectively active regions from the point of view of the temperature and moisture budgets (Fitzjarrald and Garstang, 1981).

### 4.4.2.2 Cloud Transport

Vertical motion in the free atmosphere is substantially more complex than a simple advective process at uniform speed. Convective clouds modify this simple view of vertical transport by very localized enhanced vertical transport coupled with heterogeneous removal of water soluble trace species. Vertical motion in a convectively unstable atmosphere cannot be considered as a single upward moving current; the average vertical motion within a certain area is the contribution of the vertical mass flux associated with the convective clouds (updrafts and downdrafts) and the compensating descending motion which occurs within and outside of clouds (Yanai *et al.*, 1976; Gray, 1973). In fact, over convectively active regions in the tropics, it has been shown that the cloud mass flux is about one order of magnitude larger than the average vertical motion at the cloud base (Yanai *et al.*, 1976; Houze, 1982; Nitta, 1977; Betts, 1975). Thus, deep clouds have a tremendous potential for redistributing mass in the troposphere, and transporting trace constituents from the boundary layer to the overlying free atmosphere (Chatfield and Crutzen, 1984).

Considerable progress has been attained in recent years in the development of parameterization schemes to simulate the role of clouds. A more realistic cloud model allows the possibility of taking trace constituents from one level to another where their lifetimes may be different. Individual cloud models with sophisticated microphysics are also available and can be used for vertical transport simulations of trace constituents. These results can then be generalized to provide an estimate of the transport produced by cloud ensembles. Field experiments that estimate heat and moisture budgets also provide observational evidence which can be checked against current results.

It has been also realized in recent years that the most important latent heat sources in the atmosphere are located over tropical land areas and in cloud clusters over the oceanic intertropical convergence zone (Riehl, 1979). Almost half of the earth's surface is in the tropics, and the tropical forests and savannas are important sources of trace constituents that react with or generate  $O_3$ . Thus, understanding the vertical

transport of trace constituents is closely associated with understanding the role of deep convective clouds. Trace constituents produced at the surface can be transported vertically and horizontally to long distances, once embedded in the Hadley and Walker circulations. Similarly, cloud transport in mid-latitude cyclones cannot be ignored because these systems also provide enhanced vertical transport depending on the availability of moisture near the surface.

The effect of cloud transports on the  $O_3$  cycle has been addressed from the point of view of the parameterization of the effects of moist convection on the large scale flow. Gidel's (1983) model extrapolates the Arakawa-Schubert (1974) cumulus parameterization theory to trace constituents. He shows that area averaged concentrations of the trace species which participate in the  $O_3$  chemistry are modified by (1) large scale horizontal and vertical advection; (2) detrainment of cloud mass, which can have different concentrations than the environment; (3) detrainment of liquid water which can then evaporate and release droplet constituents into the air; and (4) the compensating subsidence resulting from cloud convection. This simple cloud model captures some of the important physical mechanisms now ascribed to clouds. The main results of the extended Arakawa-Schubert parameterization theory in terms of trace species like  $O_3$  and  $NO_x$  are (1) an increasing mixing ratio with height can be obtained for a tracer with only a surface source especially if the photochemical lifetime of the tracer varies with height; (2) the predicted concentrations of some highly reactive lower tropospheric species in the upper troposphere are more realistic than eddy-diffusivity model predictions; and (3) the upper tropospheric distribution of trace species may depend more on surface sources than on upper tropospheric chemistry or stratospheric sources when clouds are present.

However, it is now realized that cumulus transports are considerably more complex than the Arakawa-Schubert parameterization used by Gidel (1983). The effects of cumulus downdrafts and lateral entrainment, the adequacy of the simple cloud model in describing the life cycle of clouds, and mesoscale circulations all have to be considered (Frank, 1983).

The concept of clouds being "vacuum cleaners" of anthropogenic and natural emissions at the surface has also been explored by Chatfield and Crutzen (1984) with a model based on the observed circulation in deep tropical convective systems. Again the role of recycling mass is emphasized but also with restrictions on the realism of the assumed cloud-induced circulation. Perhaps a slightly simpler problem of vertical transport by clouds is the role of small, non-precipitating cumulus clouds which are observed over the marine boundary layer. Carney and Fishman (1984) incorporated a photochemical model of the planetary boundary layer within the structure and mass flow characteristics of a layer of shallow, dispersed cumulus. Their comparisons with conventional flux parameterizations (enhanced eddy diffusivity) and with the available measured data for the remote marine troposphere provide further insight into the vertical distribution of trace gases.

The efficiency of clouds in transporting mass from the mixed layer to the free troposphere can now be estimated with observations. Since ozone is only weakly reactive with water, it is a possible tracer for cloud parcels on the time scale of convective clouds (15–30 min). Weaver and Pearson's (1984) results with ozone agree well with estimates of entrainment rate obtained from standard thermodynamic considerations. However, the available observational evidence is still tentative.

#### 4.5 RESEARCH NEEDS

Several important reports have been published over the past two years focusing on the current status of tropospheric and future research needs. These include the NAS/NRC reports, "A Strategy for Earth

## TROPOSPHERIC CHEMISTRY

Science from Space in the 1980's and 1990's" (National Academy Press, Washington, 1985, 149 pp.) and "Global Tropospheric Chemistry: A Plan for Action" (National Academy Press, Washington, 1984, 194 pp.). These reports develop recommendations for research in tropospheric chemistry including processes controlling ozone and hydroxyl radical, which is the specific focus of this assessment document. The NAS/NRC panel report (NAS 1984) concluded that a major international research program is necessary and feasible. The general scientific goals for this Global Tropospheric Chemistry Program (GTCP), defined by the N.A.S. (1984), are:

1. To understand the basic chemical cycles in the troposphere through field investigations, theory aided by numerical modeling, and laboratory studies.
2. To predict the tropospheric responses to perturbations, both natural and human-induced, to these cycles.
3. To provide the information required for the maintenance and effective future management of the atmospheric component of the global life support system.

Research in the Global Tropospheric Chemistry Program would be undertaken in five major research topics with the following specific research objectives:

1. To evaluate biological sources of chemical substances in the troposphere.
2. To determine the global distribution of tropospheric trace gases and aerosol particles and to assess relevant physical properties.
3. To test photochemical theory through field and laboratory investigations of photochemically driven transformation processes.
4. To investigate wet and dry removal processes for trace gases and aerosol particles.

The primary goal of the GTCP in its first decade is to measure, understand and predict changes in the chemistry of the global troposphere with particular emphasis on changes affecting the oxidizing capacity and radiative properties of the troposphere.

To address this goal the N.A.S. (1984) report has found it convenient to divide the study of tropospheric chemistry into five distinct yet interrelated areas:

- Global Distributions and Trends
- Biological and Surface Exchange Processes
- Gas Phase Photochemistry
- Condensed Phase Processes
- Theoretical Studies and Modeling

These areas were chosen both because they represent a natural breakdown of the overall research effort in tropospheric chemistry and because it was apparent that progress in all five areas would be necessary to achieve the overall GTCP goal.

The essential set of objectives pertinent to "tropospheric chemistry-processes controlling ozone and hydroxyl radical" are presented below (NAS 1984):

### (a) Gas Phase Photochemistry

The major scientific questions in gas phase photochemistry involve the need to understand better the fundamental oxidizing processes in the troposphere. Current theories point to the hydroxyl radical (HO)

and ozone ( $O_3$ ) as central players in the oxidizing processes. These theories must be tested and rejected or modified through an extensive field and laboratory measurements program. The essential objectives are:

- To determine through field measurements the tropospheric oxidation rates resulting from short-lived free radicals. The key free radical is HO.
- To understand through field measurements the key processes involved in the production and removal of ozone. The key measurements are of  $O_3$ , NO,  $NO_2$ ,  $HNO_3$ , peroxyacetyl nitrate,  $NH_3$ , abundant amines, and abundant hydrocarbons.
- To understand through laboratory experiments the mechanisms and kinetics of tropospheric oxidation of abundant alkanes (including  $CH_4$ ), olefins and terpenoids, and of isoprene.

(b) Heterogeneous Processes (Condensed Phase Processes)

Liquid and solid particles in the atmosphere play important roles in the overall atmospheric oxidation process as sinks and sources for atmospheric gases, in wet and dry deposition, and in the global radiative budget. The essential objectives are:

- To determine through a combination of field and laboratory studies, the mechanisms and kinetics of the major oxidation reactions in cloud and haze droplets.
- To determine through laboratory and field measurements the roles of atmospheric particles in addition, removal and long-range transport of chemically important species.

(c) Biological and Surface Exchange Processes

Emphasis in the study of exchange processes should be on those biological and surface environments and processes involved in determining the atmospheric levels of species important in atmospheric chemistry and radiation and in atmosphere-biota interactions. The essential objectives are:

- To measure the chemical exchanges of key species between the troposphere and dry and wet tropical land regions, certain agricultural regions, oceans, large areas of burning vegetation, and certain subpolar land regions. The key species are  $CH_4$  and other abundant hydrocarbons, CO,  $CO_2$ , abundant aldehydes and ketones, NO,  $NO_2$ , abundant organic nitrates, nitrites and acids,  $N_2O$ ,  $NH_3$ , dimethyl sulfide and other abundant organosulfur species,  $H_2S$ ,  $SO_2$ , OCS,  $CS_2$ ,  $O_3$ ,  $H_2O_2$ , abundant organoperoxy compounds, and abundant organohalides.
- To identify the environmental factors controlling the biological emission and uptake of the above key species by tropical forests and savannas, marshlands, rice paddies, boreal forests and peatlands, and wet tundra, and to determine the mechanisms for this control.

(d) Theoretical Studies and Modeling

Theory and models play important complementary roles in many of the experimentally-oriented objectives listed above. In addition, the complexity of the global tropospheric chemical-dynamical system demands the development of global three-dimensional models as essential tools for understanding and predicting changes in the system. The essential objectives are:

- To develop global chemical transport models capable of simulating the chemistry and circulation of atmospheric species on global and regional scales with sufficient spatial and temporal resolution

## TROPOSPHERIC CHEMISTRY

to include realistic treatment of the smaller-scale processes responsible for the large-scale inhomogeneities. One of these models should be available to and easily utilizable by the broader atmospheric chemistry community.

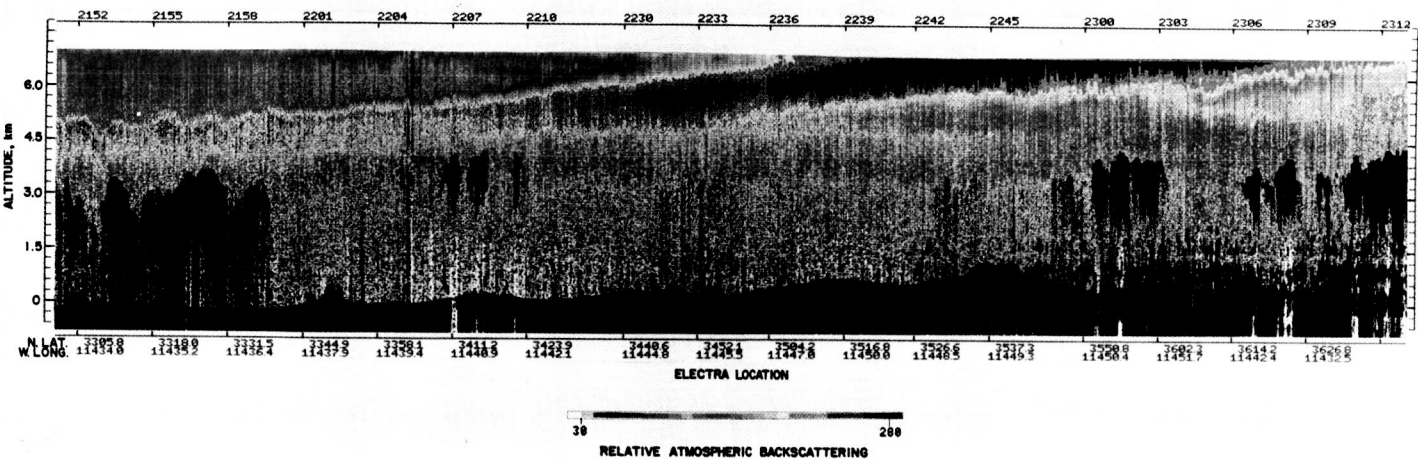
- To develop theories and models to aid in the interpretation of experimental data. Particular emphasis should be placed on understanding the processes of biological and surface exchange, gas-phase oxidation, and cloud and precipitation chemistry, and on synthesis and interpretation of global distribution and trend data.

ORIGINAL PAGE IS  
OF POOR QUALITY

CHAPTER

# STRAT-TROP EXCHANGE

AIRBORNE DIAL AEROSOL MEASUREMENT OF TROPOPAUSE FOLD EVENT  
APRIL 20, 1984  
TIME, GMT



## Panel Members

A.F. Tuck, Chairman

- |                |              |
|----------------|--------------|
| E.V. Browell   | D. Kley      |
| E.F. Danielsen | A.J. Krueger |
| J.R. Holton    | G. Megie     |
| B.J. Hoskins   | R.E. Newell  |
| D.R. Johnson   | G. Vaughan   |

## CHAPTER 5

### STRATOSPHERE-TROPOSPHERE EXCHANGE

#### TABLE OF CONTENTS

5.0 INTRODUCTION .....	151
5.1 EXCHANGE IN THE TROPICS .....	152
5.1.1 Meteorological Processes .....	152
5.1.2 Cumulonimbus Clouds .....	164
5.1.3 Aircraft Studies near Cumulonimbus Anvils in Panama .....	168
5.1.4 Discussion of Tropical Exchange .....	172
5.1.5 Summary of Tropical Exchange .....	173
5.2 EXTRATROPICAL EXCHANGE .....	174
5.2.1 Meteorological Processes .....	174
5.2.2 A Theoretical View of Mid-latitude Exchange .....	181
5.2.2.1 Deductions from Two-dimensional Models .....	181
5.2.2.2 Deductions from Three-dimensional Models .....	183
5.2.2.3 Diabatic Processes .....	184
5.2.3 A View Based on Isentropic FGGE Analyses .....	186
5.2.3.1 Systematic Meridional Exchange by Geostrophic Modes of Isentropic Mass Transport .....	188
5.2.3.2 Geostrophic Modes of Mass Transport and Quasi-horizontal Stratospheric- Tropospheric Exchange Within Middle Latitudes .....	190
5.2.3.3 Some Additional Aspects of Stratospheric-Tropospheric Exchange in Mid- latitudes .....	194
5.2.3.4 Summary of Isentropic Analyses .....	196
5.2.4 A Review of Past Work on Exchange in Mid-latitudes .....	197
5.2.5 Recent Aircraft Studies near the British Isles .....	202
5.2.6 Recent Aircraft Studies over the South Western United States .....	210
5.2.6.1 Analyses and Measurements at and below the Jet .....	212
5.2.6.2 Analyses and Measurements above the Jet .....	218
5.2.7 Ground Based Studies over France .....	222
5.2.8 Global Coverage: TOMS Ozone Column Measurements .....	227
5.2.8.1 Brewer Circulation/ITCZ Exchange/Stratospheric Fountain .....	228
5.2.8.2 Tropopause Folding near Jet Streams .....	228
5.2.8.3 Cut-off Lows .....	229
5.3 LARGE SCALE NUMERICAL MODELLING OF STRATOSPHERE-TROPOSPHERE EXCHANGE .....	230
5.3.1 General Circulation Models .....	230
5.3.2 Operational Weather Forecasting Models .....	235
5.4 ASSESSMENT OF STRATOSPHERE-TROPOSPHERE EXCHANGE .....	235
5.4.1 Unresolved Problems .....	238
5.4.2 Recommended Future Studies .....	239

## 5.0 INTRODUCTION

Exchange between the stratosphere and troposphere is important to the chemical composition of both regions; the export of ozone from the stratosphere provides the troposphere with a means of initiating photochemistry (Levy, 1971), and the precursor molecules originating from the planetary surface provide the stratosphere with its chemical feedstock from which the ozone-controlling  $\text{HO}_x$ ,  $\text{NO}_x$  and  $\text{Cl}_x$  photochemistries are driven (Hampson, 1965, Crutzen, 1971, Molina and Rowland, 1974).

The coarsely characterized morphology of the meteorological circulation governing the ingress of tropospheric air to the stratosphere in the tropics was deduced from the dryness apparent in mid-latitude measurements of stratospheric water vapour by Brewer (1949); the egress of air in mid-latitudes via tropopause folding during upper frontogenesis was demonstrated by Reed (1955), Reed and Danielsen (1959) and Staley (1960) using isentropic potential vorticity as a tracer for stratospheric air.

There have been several estimates of the annual mass exchange between the stratosphere and the troposphere. Reiter, (1975) has written a review, and has also (Reiter, 1979) emphasized the interannual variability which could exist as a result of fluctuations in the intensity of the Inter Tropical Convergence Zone. The annual average of the exchange of air for one hemisphere of the stratosphere was 89%, distributed as follows: Hadley Cell 43%, large scale eddies near jet stream regions 20%, seasonal changes in tropopause height 10%, horizontal exchange with the other hemispheric stratosphere 16%. These numbers were largely obtained by diagnostic studies using meridional stream functions relative to isobaric coordinates, combined with a cyclogenesis index and statistics of the conventionally defined (thermal) tropopause.

Such studies however do not provide a great deal of insight into the cross-tropopause flux of trace molecules, such as ozone and water vapour, which have their own particular distributions of sources and sinks. Some of the problems were outlined in an earlier report (WMO, 1982), pages 2-91 to 2-99. In particular, the laminar, correlated structure in ozone and water vapour profiles in the lower mid-latitude stratosphere, and the detailed physics and scale of the desiccation mechanism near the tropical tropopause are not well understood. It follows that quantitative estimates of the global distribution of cross-tropopause flux for specific molecules remains elusive.

A further unresolved issue is the extent of exchange associated with steady jet streams, i.e., those not involved in rapid upper cyclogenesis. Krishnamurti (1961) suggested that a thermally direct transverse circulation existed for the northern winter subtropical jet stream, while Mahlman (1973) drew a similar conclusion for a composite analysis of a polar front jet stream over North America, averaged relative to the flow. These transverse circulations imply upward air motion on the anticyclonic (equatorward) side and at the jet core, and downward motion on the cyclonic (poleward) side. If such circulations transfer air across the tropopause, there is a limited usefulness to estimates of exchange using cyclogenetic indices, a conclusion supported by the study of radioactive fallout by Mahlman (1969a).

An important result was the discovery of the "hygropause" in the tropics (Kley *et al.*, 1979); the existence of a decrease in water vapour mixing ratio above the tropopause in mid-latitudes had been evident from the first measurements (Dobson, Brewer and Cwilong, 1946; Brewer, 1949) and confirmed by higher and more frequent measurements (Foot, 1984). Water vapour mixing ratios decrease from the tropopause by a factor of 20 or 30 in mid-latitudes over an altitude of a half to one pressure scale height, and by a factor of 2 or 3 in the tropics over a similar depth. These facts, and the frequent occurrence of the layered structure in vertical profiles of ozone for at least two scale heights above the mid-latitude

## STRAT-TROP EXCHANGE

tropopause, suggest that for some purposes it may be necessary to draw a distinction between this transition region and the middle and upper stratosphere above it.

Indeed, if one assumes a mixing ratio of 2.5 and 6.5 ppmv at the hygropause and tropopause, respectively, between 30°N and 30°S, and of 4 and 25 ppmv poleward of these latitudes, it is a simple matter to show that something like a quarter to a half of all stratospheric water vapour is between the tropopause and the hygropause. Of course, in the mean this fraction probably has a much lower residence time than the remaining amount above it.

It has become apparent during the last decade that the transport of mass and tracers by the general circulation is conceptually simplified by using entropy (potential temperature) as the vertical coordinate. This point of view, originated by Shaw (1942), has been revived by Dutton (1976) and Johnson (1980) for the troposphere, by Tung (1982) for the stratosphere and consistently advocated by Danielsen (1961, 1968; Danielsen and Hipskind, 1980) for studies at tropopause level. The isentropic perspective suggests that past estimates of global cross-tropopause mass flux, made by zonal mean Eulerian streamline calculations relative to pressure surfaces, may not be particularly reliable.

It is necessary to obtain good data on the covariance of mass and the mixing ratio of species whose transport across the tropopause is of interest. This is so because while potential vorticity  $P_\theta$  may in future be calculable from the global analyses produced by high resolution primitive equation numerical weather prediction models, it will still be necessary to know the correlation between  $P_\theta$  and the various chemical species in order to compute fluxes; such knowledge is derived currently from a small number of high quality case studies using aircraft and balloons. At present, global estimates of downward cross-tropopause fluxes rely on a very crude count of upper tropospheric cyclogenetic events to give the case study data a global dimension. The estimates of the upward flux in the tropics are even cruder, since the knowledge of the detailed physical characteristics and scale of the meteorological processes responsible is less secure, although substantial progress has been made recently. It remains true that almost all local, high quality knowledge of cross-tropopause flux is confined to the Northern Hemisphere, in the North American and British Isles/Western European sectors. Most of these data, moreover, have been obtained in the March-May period.

In this chapter, the tropopause is defined both statistically and in a local, synoptic sense by the value  $P_\theta = 1.6 \times 10^{-5} \text{ K m}^2\text{kg}^{-1}\text{s}^{-1}$ , taken from an objective analysis of 8 years of zonal, temporal mean cross-sections of potential temperature, wind and potential vorticity by Danielsen (1984), see Figure 5-1. The definition applies from the pole to within 5° latitude of the equator, where  $P_\theta$  changes sign, and is coincident with the conventionally defined tropopause. The analyses are consistent with those obtained in the FGGE year by the ECMWF analyses, see Figure 5-2. A difficulty of isentropic coordinates for work on longer time scales is that the motion of  $\theta$  surfaces with respect to geometric heights has to be established.

### 5.1 EXCHANGE IN THE TROPICS

#### 5.1.1 Meteorological Processes

There is a wide spectrum of circulation features in the tropical troposphere which involve vertical motions and which may be of importance in the transfer of air from the troposphere to the stratosphere and therefore in the ozone budget. The long-term mean motions are dominated by the planetary scale Hadley and Walker circulations, which are essentially statistical entities; temporal variability occurs on a wide

STRAT-TROP EXCHANGE

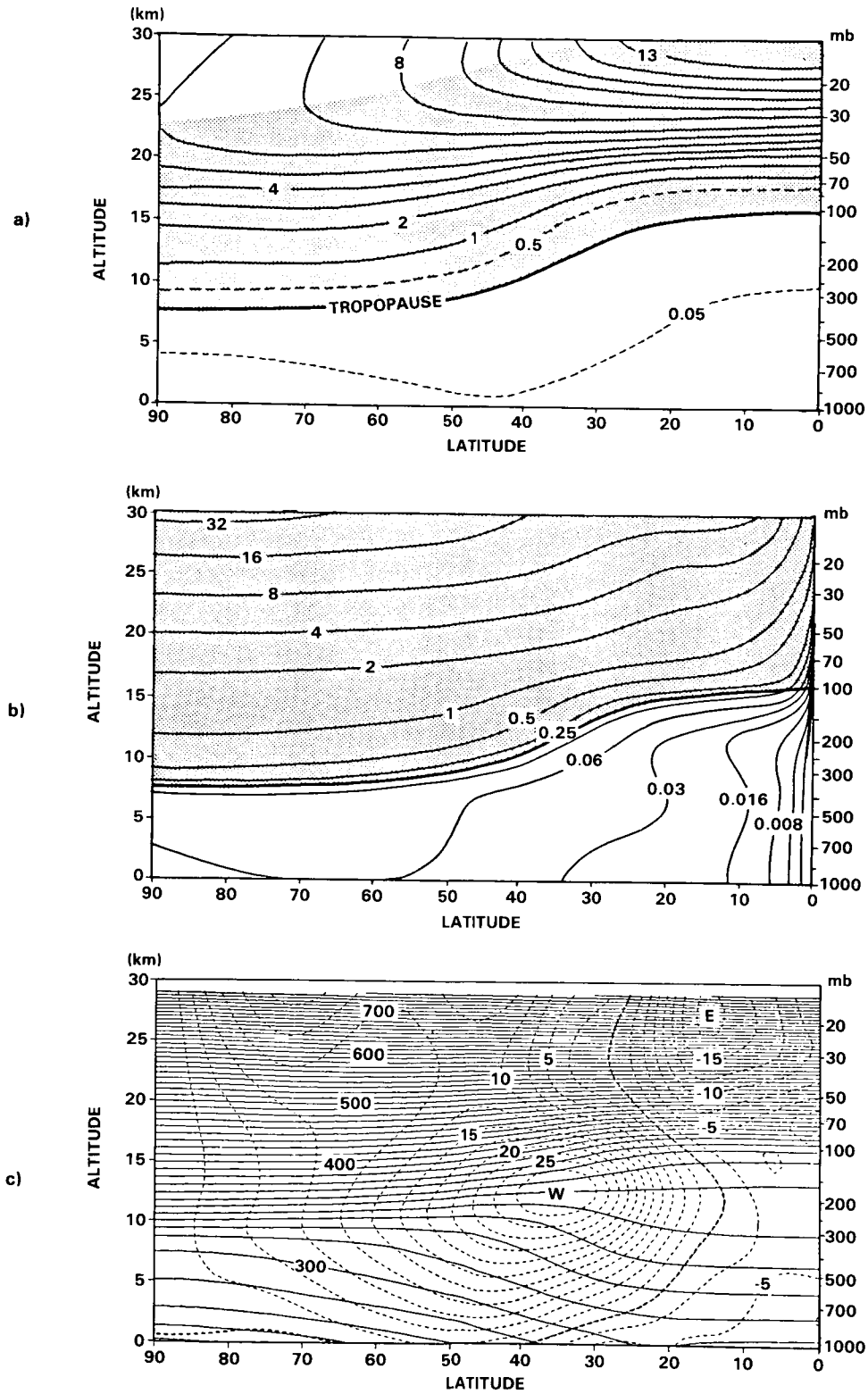
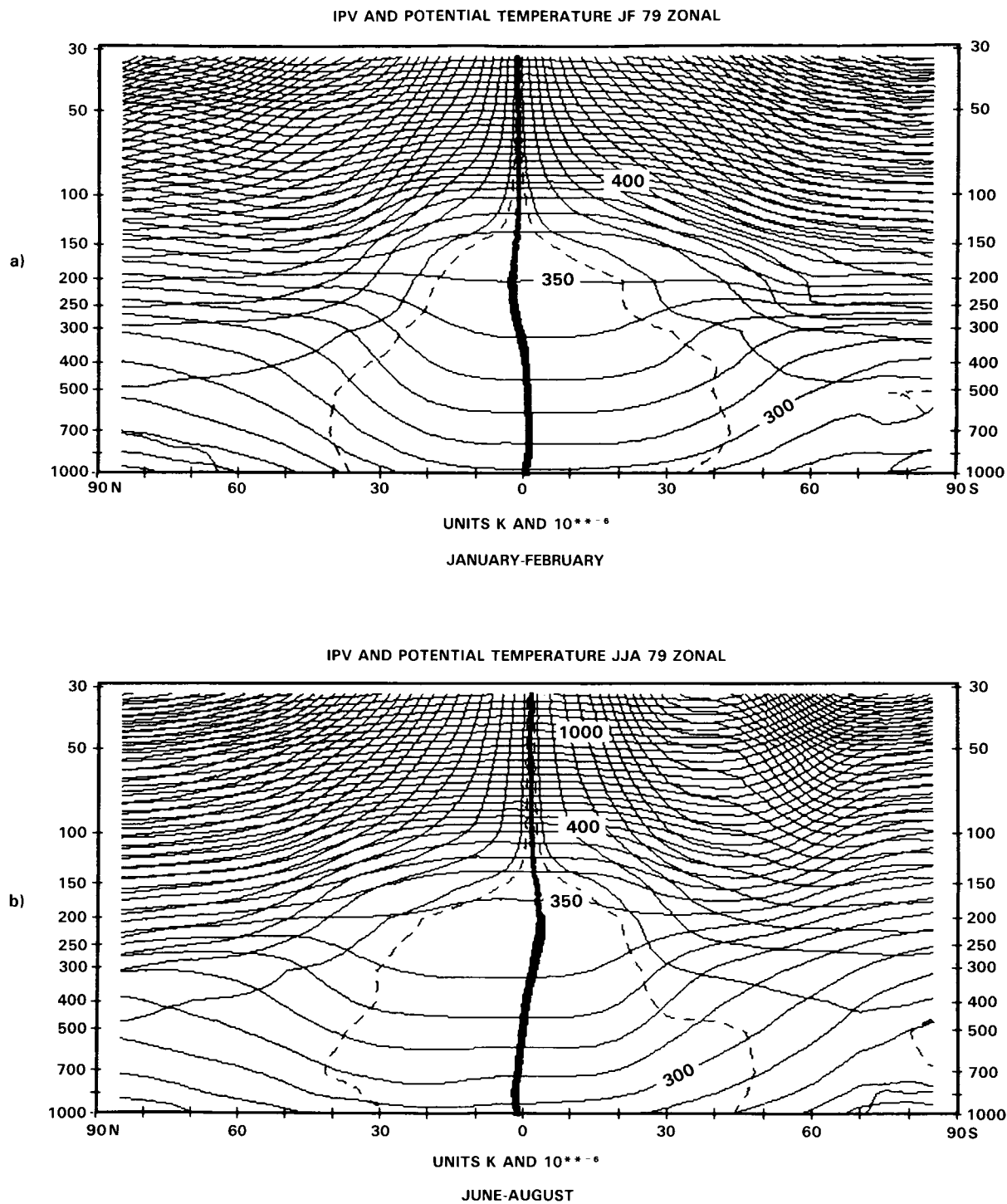


Figure 5-1. Zonal-annual mean distributions of: (a) ozone mixing ratio, ppmv; (b) potential vorticity,  $10^{-4} \text{ cm}^2 \text{ s}^{-1} \text{ K g}^{-1}$ ; (c) potential temperature, K, and westerly wind velocity,  $\text{m s}^{-1}$ .

# STRAT-TROP EXCHANGE



**Figure 5-2.** Zonal mean distributions of  $\theta$  and isentropic potential vorticity (IPV), ECMWF Analyses, FGGE year, 1979. Compare with Figures 5-1 b, c and 5-17. Data are (a) January and February, (b) June, July and August. The potential vorticity contours are 0,  $\pm 0.5$ ,  $\pm 1$ ,  $\pm 2 \dots$  in units of  $10^{-6} \text{ m}^2 \text{ s}^{-1} \text{ K kg}^{-1}$ ,  $\theta$  is contoured at 10 K up to 400 K and at 50 K when  $\theta > 400 \text{ K}$ . The 300 K contour touches the surface in the tropics.

variety of time and space scales down to the scale of the individual cumulonimbus clouds embedded in the larger circulation features. The annual cycles of the Hadley circulation and to a lesser extent the Walker circulation are evident in the north-south and east-west excursions of the tropical convergence zones which accompany the Asian and Australian monsoons as well as the cycles of rainy and dry weather elsewhere in the tropics.

Over much of the tropics, the nonseasonal variability of the Hadley and Walker circulations is primarily associated with the Southern Oscillation which is an interannual phenomenon although it is becoming apparent that there are prominent circulation changes at the subseasonal time scale of 40-50 days as well (Madden and Julian, 1971, 1972a; Anderson and Rosen, 1983; Lorenc, 1984). Synoptic scale disturbances in the tropical convergence zones include easterly waves and monsoon depressions which modulate the large-scale environment for the development of tropical storms and hurricanes and mesoscale disturbances such as squall lines and mesoscale cloud clusters. There are also important mesoscale circulations tied to localized interactions between the diurnal variation of solar heating and surface features; these include, for example, cloud clusters in the winter monsoon region and sea breeze circulations.

The long-term mean global scale flow in the upper tropical troposphere is well represented by the winds at the 150 mb level. Figure 5-3 shows the horizontal winds for January-February and June-August for the FGGE year 1979. The cross-equatorial flow in the western Pacific and the Indonesian region during northern winter and in the eastern Indian ocean in northern summer are the most important local contributions to the zonally symmetric meridional overturning known as the Hadley circulation. The zonal mean pattern of rising motion shifts from south of the equator in January-February to north of the equator in June-August.

Vertical motion is an extremely difficult quantity to estimate. At the synoptic scale it can be estimated kinematically from the divergence of the observed wind field; operational analyses now make use of reports from commercial airliners as well as cloud motion vectors to augment the conventional upper air network. Satellite measurements of tropical outgoing longwave radiation have also proved useful in identifying the spatial and temporal variability of the occurrence of the cold cloud tops associated with deep convection.

The zonal variability of rising motion in the tropics is part and parcel of a set of east-west overturnings which are known collectively as the Walker circulation. These overturnings are most easily seen in the divergent wind field and it has become customary to display the divergent winds in terms of the velocity potential from which it is derived. Figure 5-4 displays the fields of 150 mb velocity potential  $\chi$  for the northern winter and summer of 1979 derived from ECMWF analyses of the FGGE data set. Negative values of  $\chi$  may loosely be associated, in the large scale temporal mean, with rising motion, but should not be identified with vertical velocity. Relative minima in these maps correspond to regions of widespread rising motion; in January the negative center in the Indonesian and west Pacific region is associated with winter monsoon convection and in July the center over southern Asia is evidence of the rising motion due to the summer monsoon. It is worth noting that, as the contribution to the velocity potential from each wave component is inversely proportional to its squared wavenumber, a velocity potential field emphasizes the larger scale patterns of divergence and attendant rising motion; thus in these maps the Pacific-Indian Ocean Walker cells dominate.

The global wind analyses necessary to derive the transport potential fields implied in Figure 5-4 depend to a great extent on high level cloud motion estimates which are nominally applied to a single level only in the upper troposphere; unambiguous identification of penetration of the tropical tropopause in regions

STRAT-TROP EXCHANGE

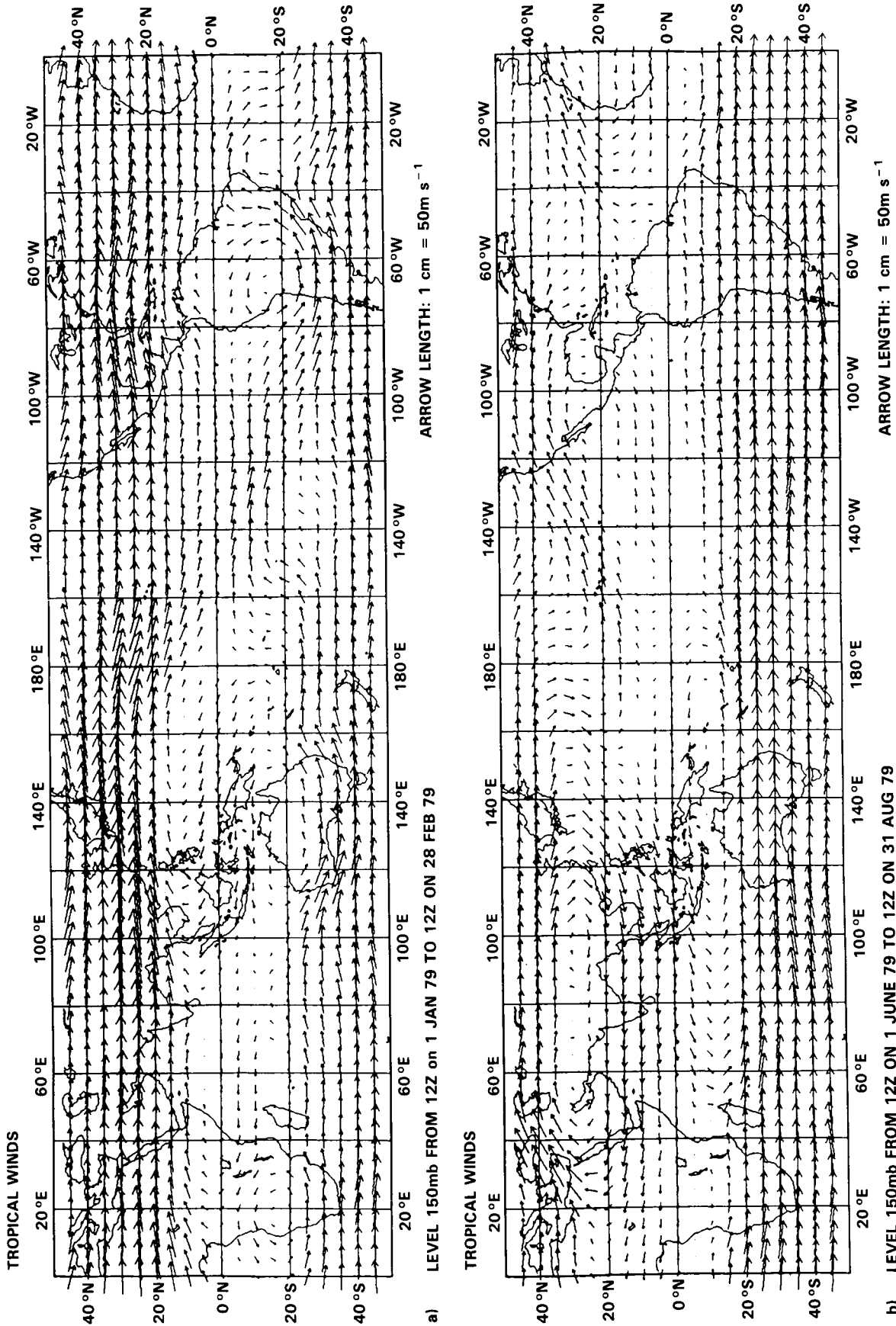
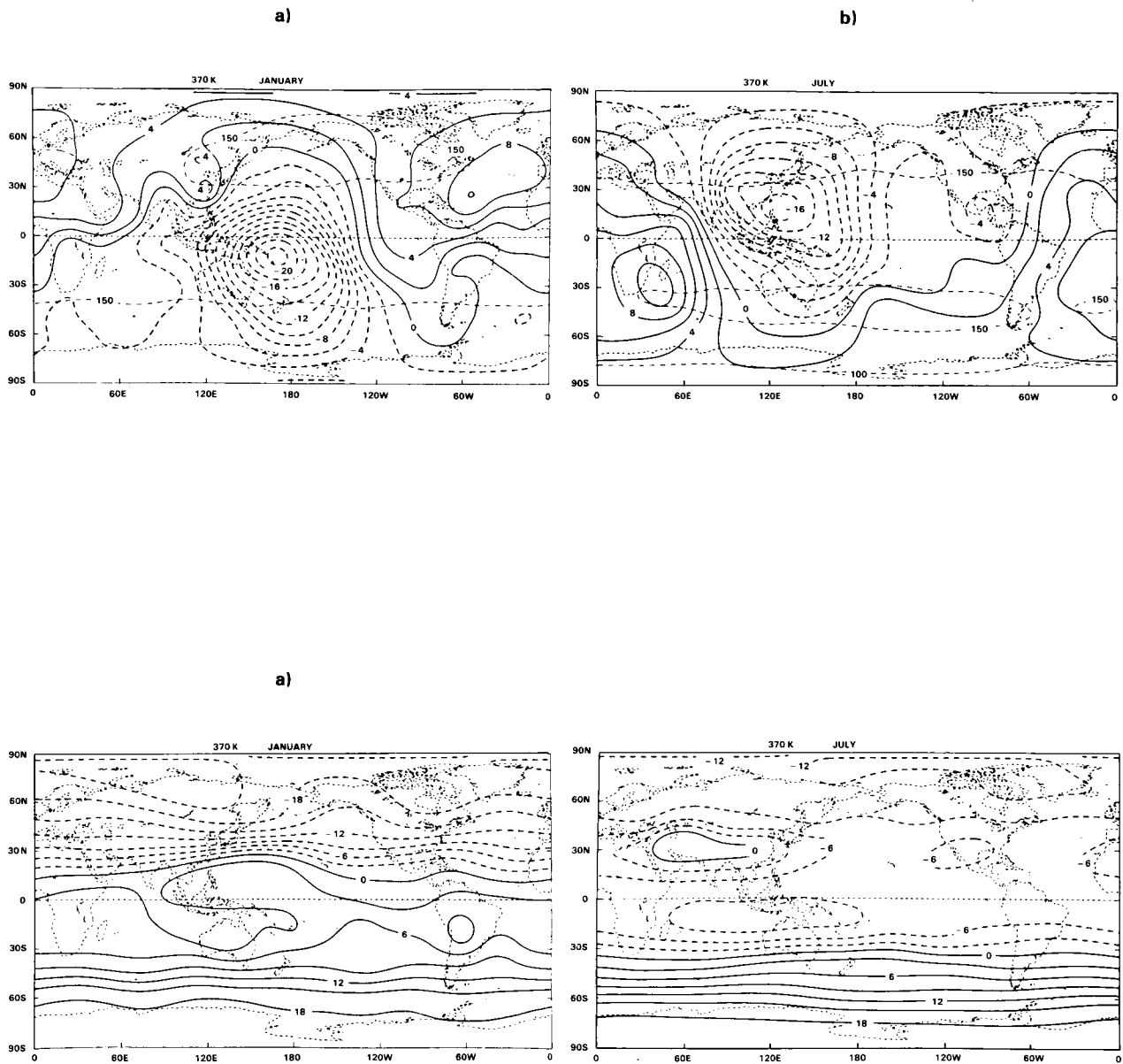


Figure 5-3. Streamlines of 150 mb winds in the tropics, ECMWF analyses, FGGE year, 1979. (a) January and February, (b) June, July and August. Note that some other analyses tend to show stronger cross-equatorial flow than those from ECMWF.

## STRAT-TROP EXCHANGE



**Figure 5-4.** Contours of velocity potential  $\chi$  (upper) and stream function  $\psi$  (lower) 370-380 K Level IIIb analyses, FGGE year, 1979.  $\mathbf{v} = \nabla\chi + \mathbf{k} \times \nabla\psi$ . Note that this decomposition of the velocity field accentuates the largest scales, particularly in  $\chi$ . Irrotational component of isentropic mass transport,  $\chi$ , is normal to contours in upper figures, from lower to higher values. Rotational component of isentropic mass transport,  $\psi$ , is parallel to contours in lower figures, with lower values on the left. (a) January, (b) July.

## STRAT-TROP EXCHANGE

of inferred vertical motion requires higher vertical resolution than is available in the conventional analyses.

Other indicators may suggest the passage of air upwards into the stratosphere. One readily available indicator is radiosonde temperature; cold temperatures are maintained at the tropical tropopause by the adiabatic expansion of air rising from below in deep convection. In the time mean the most vigorous convection is in longitudes 80°E to 180°E, as shown by the monthly 100 mb temperatures for 1979 in Figure 5-5, which was plotted for this report from radiosonde data. A study of 100 mb monthly mean temperatures by Newell and Gould-Stewart (1981) showed that these longitudes in November-February were cold enough to account for the dryness of the stratosphere, although this leaves open the question of the fate of the necessary ice crystals; in July the coldest areas are associated with the Indian monsoon although the 100 mb temperatures in this season are somewhat warmer than those in January. Temperatures at 100 mb below -82.4°C are low enough that the saturation moisture content is  $2 \times 10^{-6}$  mmr such as is observed in the stratosphere (see Chapter 9). Frederick and Douglass (1983) and Atticks and Robinson (1983) have come to the same general conclusion from studies of daily radiosonde data but find a considerably larger areal extent of the region of potential exchange.

As a means of measuring high cloud amount, outgoing longwave radiation measurements suffer from contamination with radiation from lower levels in the atmosphere; Barton (1983) has estimated high cloud frequency using two channels from the NIMBUS 5 radiometer data which are preferentially sensitive to high clouds. His results from the period December 1972 through February 1975 are shown in Figure 5-6. The main tropical regions where high clouds occur are the monsoon areas of the west Pacific and India with secondary regions over South America and Africa. From the three Januaries sampled, Barton found that the cloud was less confined to the west Pacific during the El Nino January of 1973. A similar El Nino dependence was found for rainfall (Rao, 1984), velocity potential (Climate Analysis Center, 1983, 1984) and outgoing longwave radiation (Lau and Chan, 1983), all pointing to a concentration of vertical motion in the west Pacific during cold periods.

Finally, another indicator of large-scale motion that influences the stratosphere is total ozone; this will clearly be lower where ozone-poor tropospheric air enters the lower stratosphere. The ozone data from the Nimbus 7 TOMS for the FGGE year 1979, January and July are shown in Figure 5-7. Lowest values occur in January in the west Pacific and South America with generally higher values occurring everywhere in the tropics in July. Ghazi (1980) has presented a series of total ozone maps that show a minimum in January in the west Pacific and over India in July, essentially in accordance with the findings of Newell and Gould-Stewart, and consistent with the annual cycles of tropopause temperature and total ozone at Gan (1°S, 73°E), Figure 5-8.

The network of upper air and surface stations in the tropics at best provides a grid of data that resolves motions on scales of several hundreds of kilometers; this data source as well as evidence from rainfall, cloud and total ozone measurements can be used to identify regions in which rising motion is occurring but they fall short of defining the scales on which the vertical motions are organized. Nevertheless, the contoured radiosonde data show coherent temperature structure on large scales at 100 mb (Figure 5-5). At the level of the tropical tropopause in particular a number of mechanisms for an exchange of air across the statistical boundary between the stratosphere and troposphere have been proposed to account for the dehydration which must occur as air becomes dry enough to be considered 'stratospheric'. Is penetrative vertical motion organized at the scale of individual overshooting cumulonimbus turrets? Or are there mesoscale regions of moderate ascent, driven by cloud heating from below and cooling at the top? Or is there gentle rising motion over a large area? With these questions in mind, and the fact that many scales

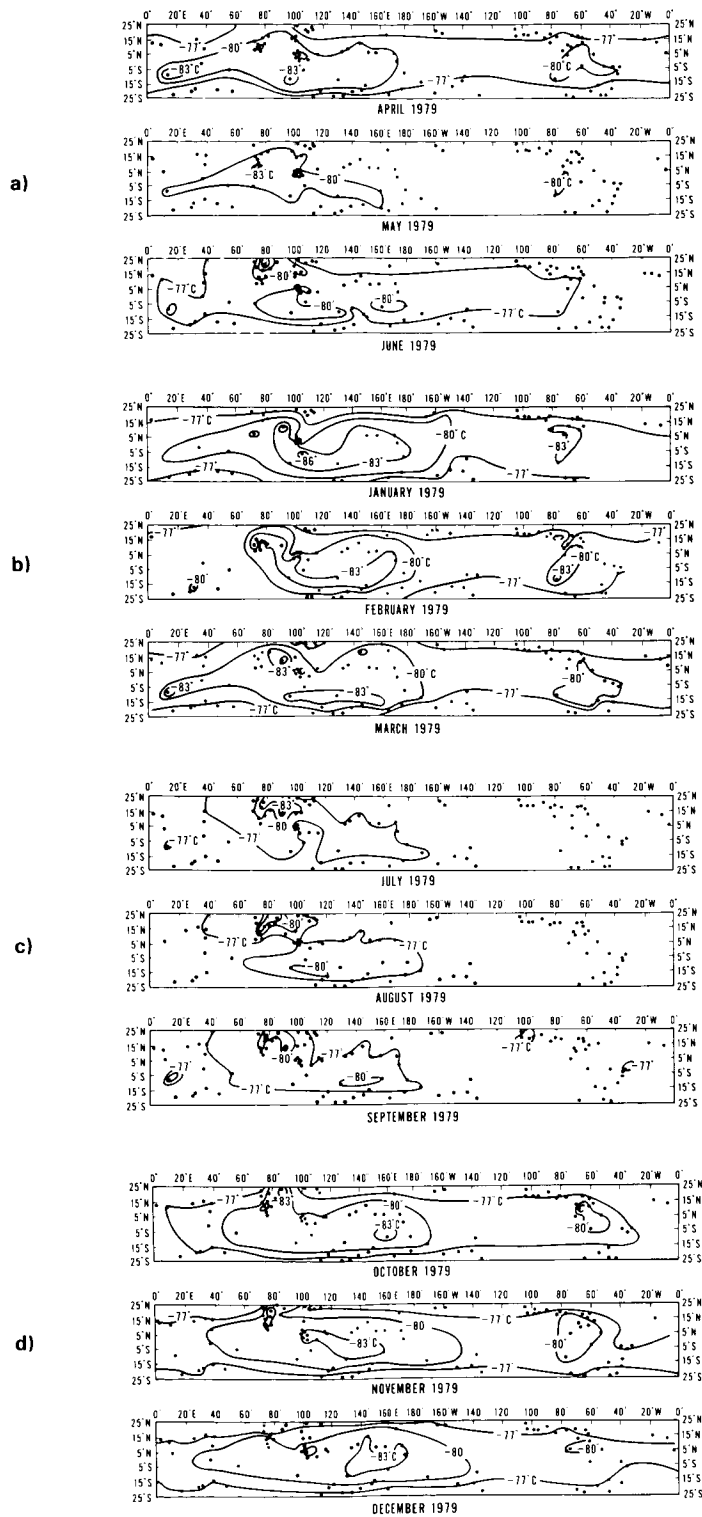


Figure 5-5. 100 mb tropical monthly mean temperatures for the FGGE year (1979), radiosonde data. (a) JFM, (b) AMJ, (c) JAS, (d) OND. Dots are radiosonde stations. Note especially the fluctuation of the area enclosed by the  $-80^{\circ}\text{C}$  contour over the year.

STRAT-TROP EXCHANGE

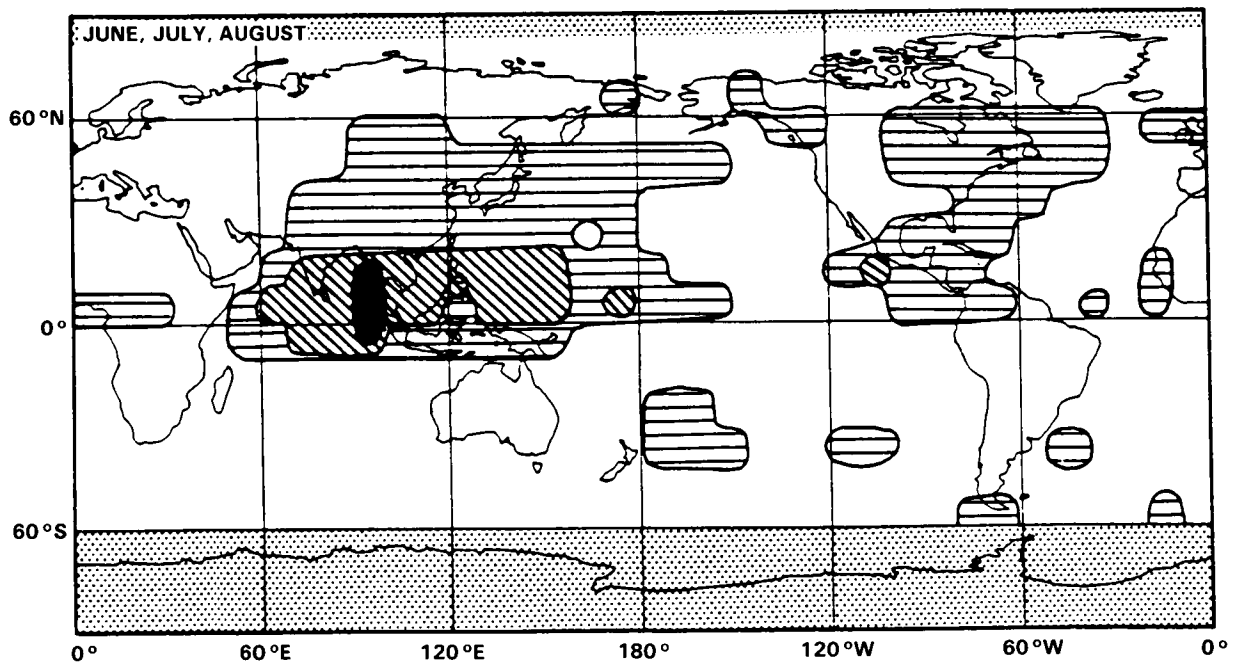
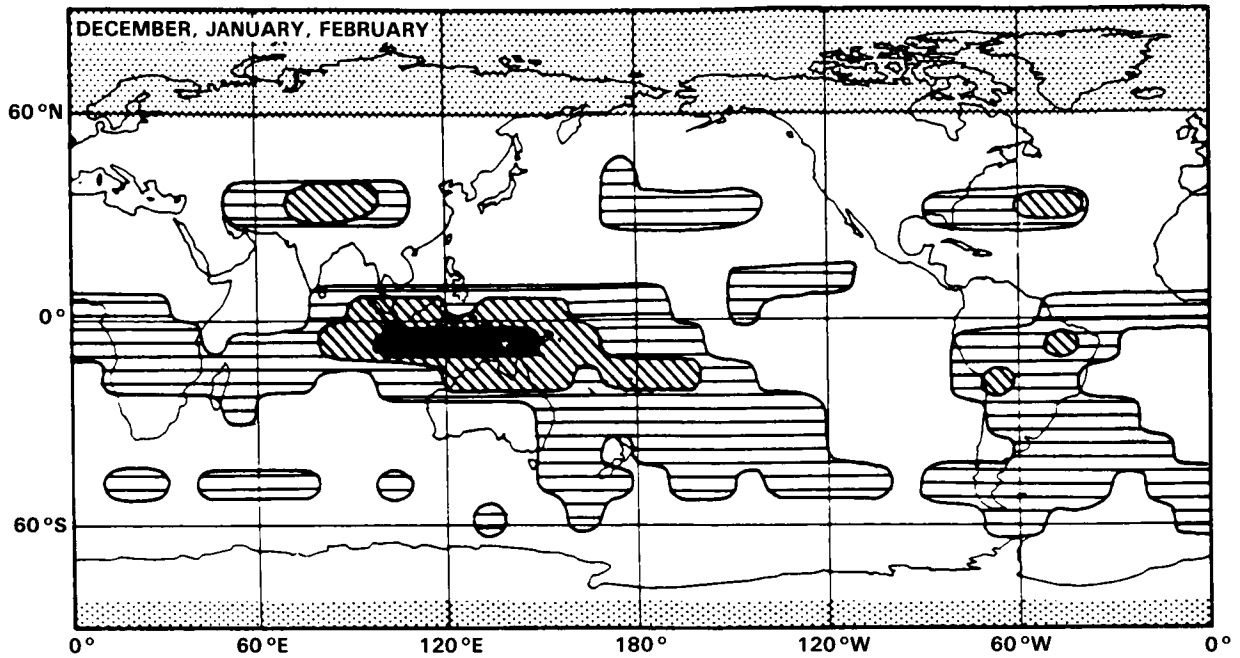
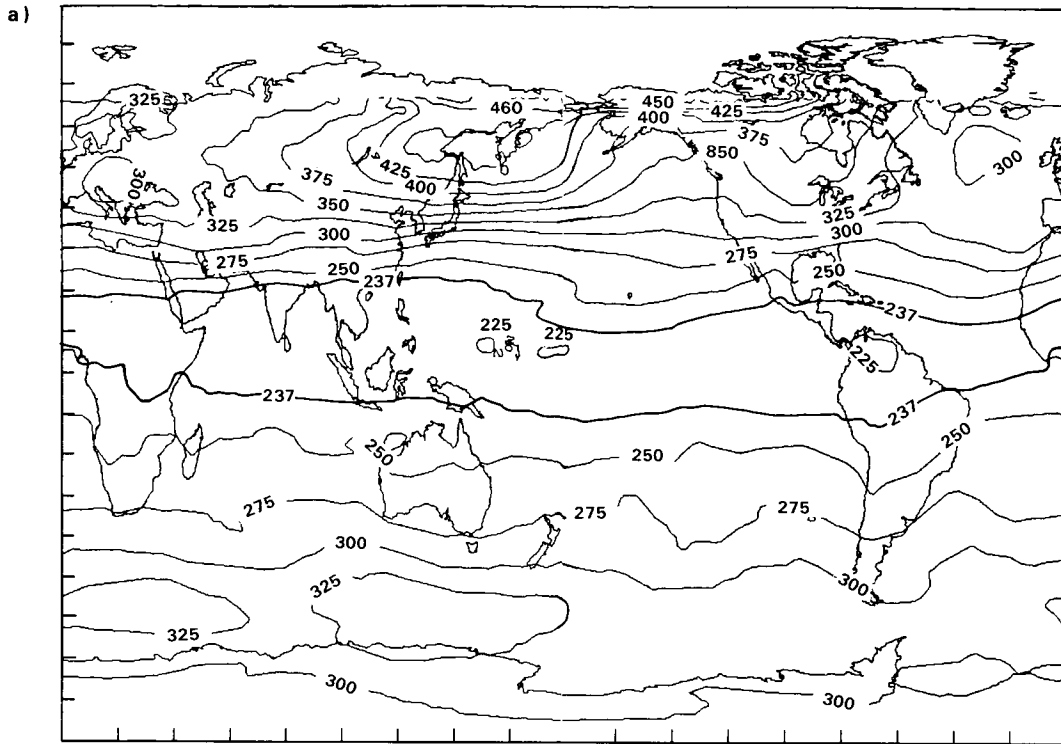


Figure 5-6. Frequencies of high clouds for the period January 1973-May 1975 from Barton (1983) for the seasons December-February (top) and June-August (bottom). Dark area is greater than 60% cloud cover; diagonal lines greater than 40%; horizontal lines, greater than 20%; clear, less than 20%; shaded, no observations.

STRAT-TROP EXCHANGE

JANUARY 1979



JULY 1979

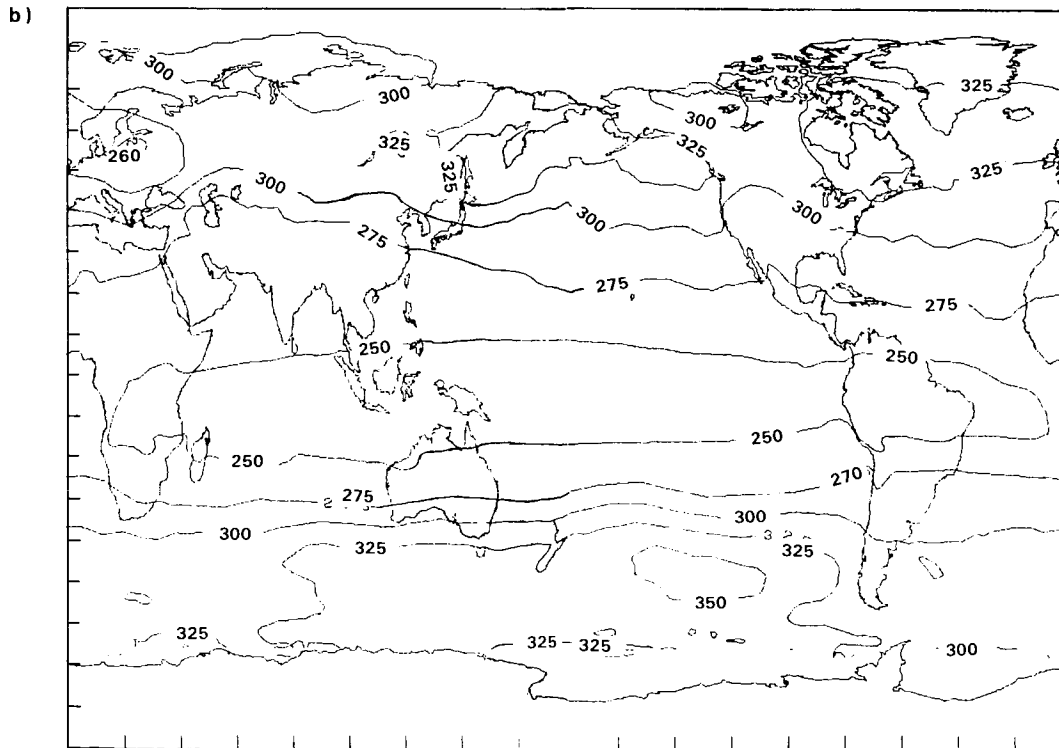
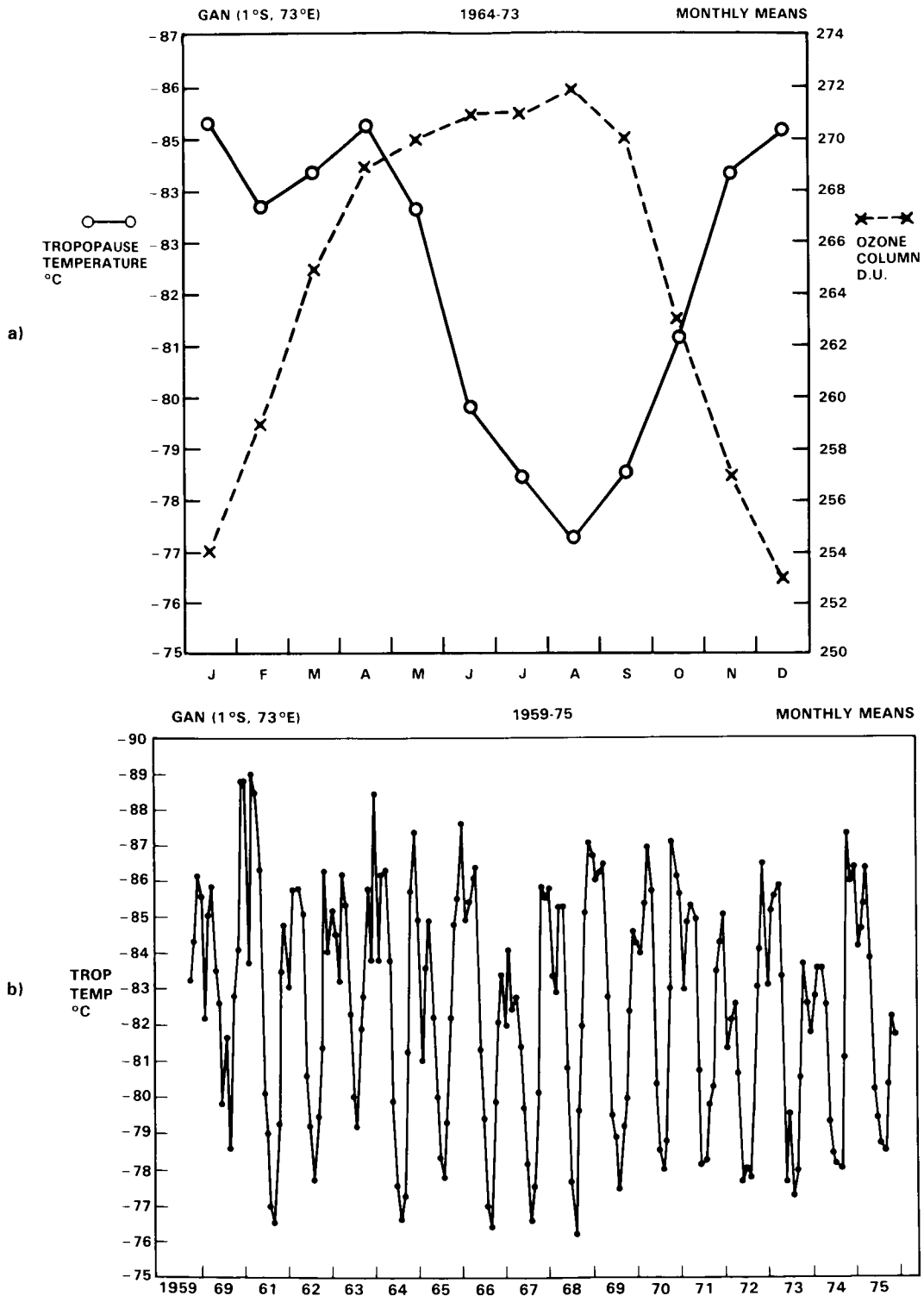


Figure 5-7. Monthly mean O<sub>3</sub> column observations, FGGE year, 1979. Data are from the Nimbus 7 TOMS instrument; (a) January, (b) July.

# STRAT-TROP EXCHANGE



**Figure 5-8.** (a) Annual cycle of tropopause temperature and ozone column density at Gan (1°S, 73°E). Data are monthly means, 1964-73. (b) Time series of monthly mean tropopause temperature, Gan, 1959-75. Note that there is a reproducible warming in February/March between cold peaks in December/January and April/May (on average). August is usually the warmest month.

of motion will have contained within them cumulonimbus clouds we proceed to discuss motions on scales other than the global circulation.

A whole series of synoptic-scale weather systems are present in the tropics, examples of which have been discussed by Riehl (1979). What is relevant here is whether these systems contribute to stratosphere-troposphere exchange. One such system is the easterly wave (Malkus, 1968); these seem to originate over Africa and propagate westward into the tropical Atlantic and Caribbean. Easterly waves are a feature also of the Pacific ITCZ. In some of these waves there is upper level divergence offset by rising motion from the lower troposphere and by sinking motion through the tropical tropopause as shown by Reed, *et al.* (1977). There are no statistics available on how many of these systems are accompanied by significant vertical motions at the level of the tropical tropopause.

Tropical storms are another major feature that may involve stratosphere-troposphere exchange. Gray (1968) has surveyed the region in which they occur and the criteria necessary for their development. Their structure is dealt with at length in Riehl (1979) and Palmen and Newton (1969). It is noteworthy that tropical cyclones in the western Pacific have a higher tropopause than those in the Atlantic; up to 8 °C colder than the average hurricane tropopause (Keenan and Templeton, 1983). It was pointed out above that the background temperature was also different in the same sense. But there is little direct evidence of vertical motion near the tropical tropopause in these severe tropical disturbances. Some of the schematic diagrams in Palmen and Newton (1969), imply subsidence in the eye and Riehl (1979) quotes some evidence from tritium measurements that stratospheric air is drawn down into the hurricane but there have been no systematic studies of this point.

Hurricanes have long been considered to be potential drivers of exchange but with little evidence. Penn (1964) observed the structure of the tropopause with aircraft flights. More recently, Rogers, Stout, and Nunez at Goddard Space Flight Center have analysed the TOMS data over Atlantic hurricanes and find low amplitude total ozone modulations (5 Dobson Units) in a partial ring surrounding the storm, together with larger scale features associated with the trough-ridge structure which steers the storm (Stout *et al.*, 1985). This study also made use of VAS 6.7 micrometer water vapour data to show that the region of higher total ozone in the forward sector of the storm was accompanied by dry air. These characteristics are evidence for tropopause deformation if not actual exchange of air. Evidence for very intense deformation of the tropopause (Holland *et al.*, 1984) is not supported by TOMS observations, which should show a localized ozone maximum. The event may, however, have been so short-lived that it had disappeared by the time that TOMS overflew the storm on the next day. The analyses of satellite observations of tropical storms are only beginning and the full extent of their value is still unknown.

It is essentially the moist static energy acquired near the surface that determines how high an air parcel can reach. This quantity is defined as  $c_p T + Lq + gz$  where  $c_p$  is the specific heat of air,  $T$  its temperature,  $L$  the latent heat of vaporization,  $q$  the specific humidity and  $gz$  the geopotential. Maps of moist static energy are shown in Hsiung and Newell (1985, paper in preparation); again some of the largest values occur in the west Pacific. As the latent heat is released within the rising parcel the air becomes warmer than the environment and therefore buoyant. This process operates on both the hurricane scale and that of the individual cumulonimbus. Parcels with moist static energy values of about  $350 \times 10^3$  J/kg can easily reach 16 km where they will have a temperature of about  $-83$  °C. The important point is that the tropical troposphere is potentially unstable to vertical motion. Roach and James (1973) show that parcel theory applied to soundings in the Bay of Bengal region in May can result in the rising air reaching altitudes of 21 km, with minimum temperatures of  $-90$  °C. Ludlam (1980) points out that dynamical forcing also plays a role in establishing the depth of cumulonimbus convection in this monsoon regime.

## STRAT-TROP EXCHANGE

Mesoscale cloud clusters have been observed in the tropics which seem to form independently of synoptic scale disturbances; over the South China Sea during Winter MONEX disturbances formed offshore in the early hours of each day apparently in response to convergence tied to a combination of local topographic features and the diurnal cycle of solar heating (Houze, *et al.*, 1981). Johnson and Kriete (1982) have shown that forced mesoscale vertical motions are associated with these systems. Similar mesoscale convective zones were observed during the wet season over Panama (Danielsen, 1982). These clusters tend to form extensive anvils and stratus decks at middle levels that may spread over several hundred kilometers. Radiative calculations by Webster and Stephens (1980), Doherty *et al.* (1984) and others indicate that these extensive cloud layers should experience IR warming from below and cooling above to space; the net heating could drive a number of processes including mesoscale ascent and turbulent overturning. These processes are enhanced by the release of latent heat associated with the precipitation observed from these cloud decks which often show a radar bright band similar to those seen in middle latitude stratiform precipitation (see Houze and Betts, 1981).

Radiative destabilization may operate also in other extensive high clouds; in fact although individual cumulonimbus clouds reach up to the tropopause many of the anvils are found well below the tropopause. The origin of some common cirrus clouds near the tropopause is not known; examples have been given by Platt (1983) for the region of northern Australia. Potential sources are synoptic scale motions or some type of radiative instability, both of which may be triggered by cumulonimbus activity.

### 5.1.2 Cumulonimbus Clouds

It is appropriate to discuss the individual cumulonimbus, a scale on which there seems to be a good potential for troposphere-stratosphere exchange as proposed by Danielsen (1982). This section is designed to set the stage for the case studies of Section 5.1.3. The mechanisms involved in cumulonimbus convection are discussed extensively in the textbooks of Riehl (1979) and Ludlam (1980). From the points of view of the present report it is desirable to know if this process can carry air into the stratosphere and if so, where and when. There is no question that large masses of air from the boundary layer are carried aloft to the upper troposphere by the cumulonimbus process. Although vertical motions in individual cells may range up to 30 m/sec, overall it takes an hour or more for significant quantities of air to be transferred to the upper troposphere. Whether the physical processes in the anvil then lead to penetration, as suggested by Danielsen, (1982) and reviewed by Holton (1984b) is an unsolved problem which is soon to be examined experimentally in NASA's STEP project. For the present discussion it is assumed that there is association between penetration and anvils. Frequency of occurrence of cumulonimbus is shown in Figure 5-9 for two seasons and may be compared with that of cirrus from the same marine data set down in Figure 5-10. The two are clearly related, especially in the west Pacific and the Indian Ocean. Cumulonimbus distribution thus matches the large-scale motion distribution discussed earlier. The release of latent heat that maintains the tropical circulation occurs primarily within these phenomena, termed by Malkus (1968), the "firebox of the circulation". If it turns out that experiments verify Danielsen's hypothesis, the correspondence between the most extensive cumulonimbus activity and the greatest large-scale vertical motion may allow stratosphere-troposphere exchange in the tropics to be monitored by means of the large-scale observables as we have discussed above.

We now consider some results of a case study which was designed to see how actual observations of large cumulonimbus tops compared with established climatologies. Airborne radar and cameras combined with horizon gyroscopes were used by Cornford and Spavins (1973) to study cumulonimbus tops during the April-June period in NE India. They concluded that tops extended to at least 20 km, and noted that Burnham (1970) had established that turbulence may extend into the clear air for 25-30 km around

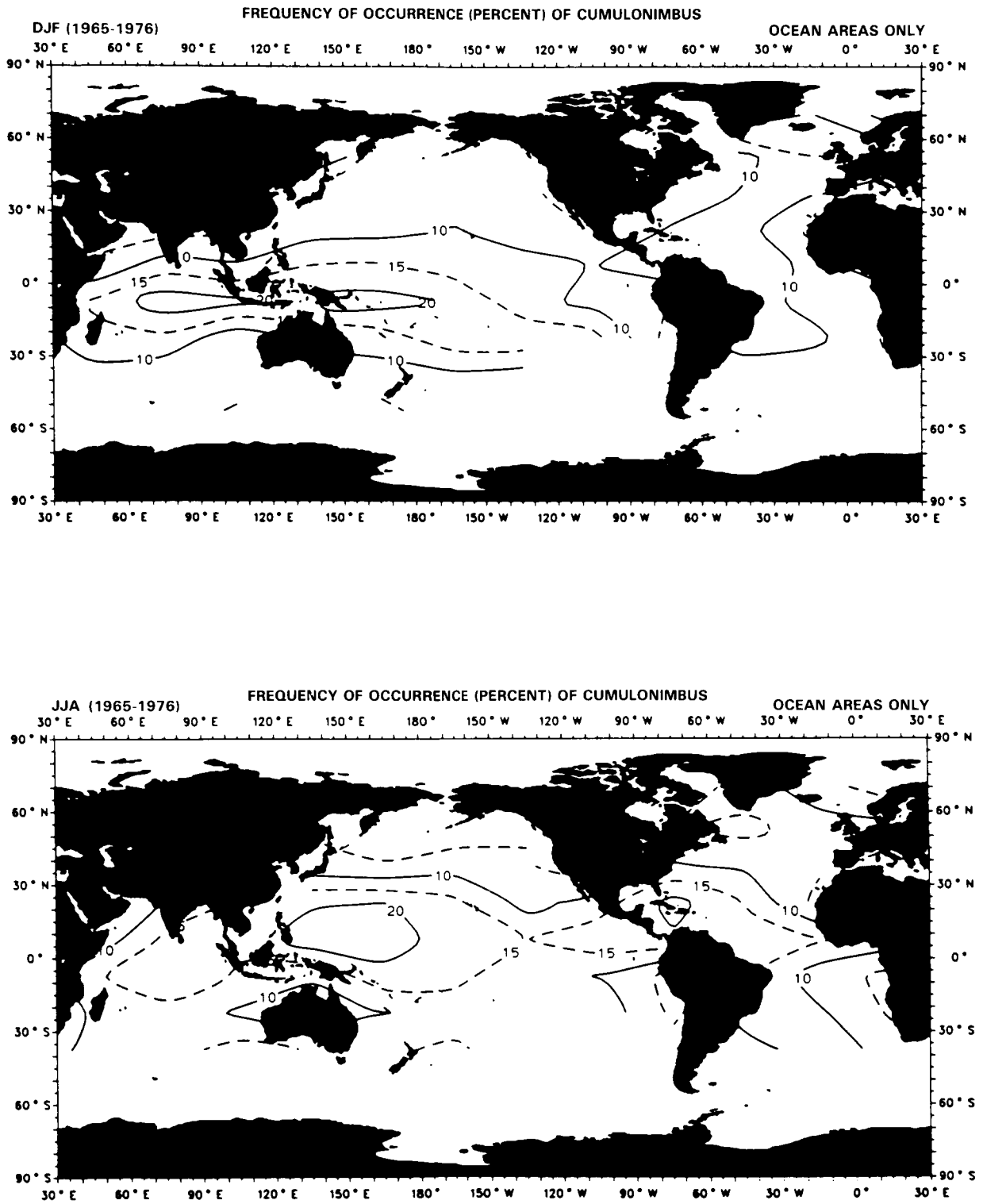


Figure 5-9. Frequencies of observation of cumulonimbus clouds over the ocean from Hahn, *et al.* (1982) for December-February (top) and June-August (bottom).

STRAT-TROP EXCHANGE

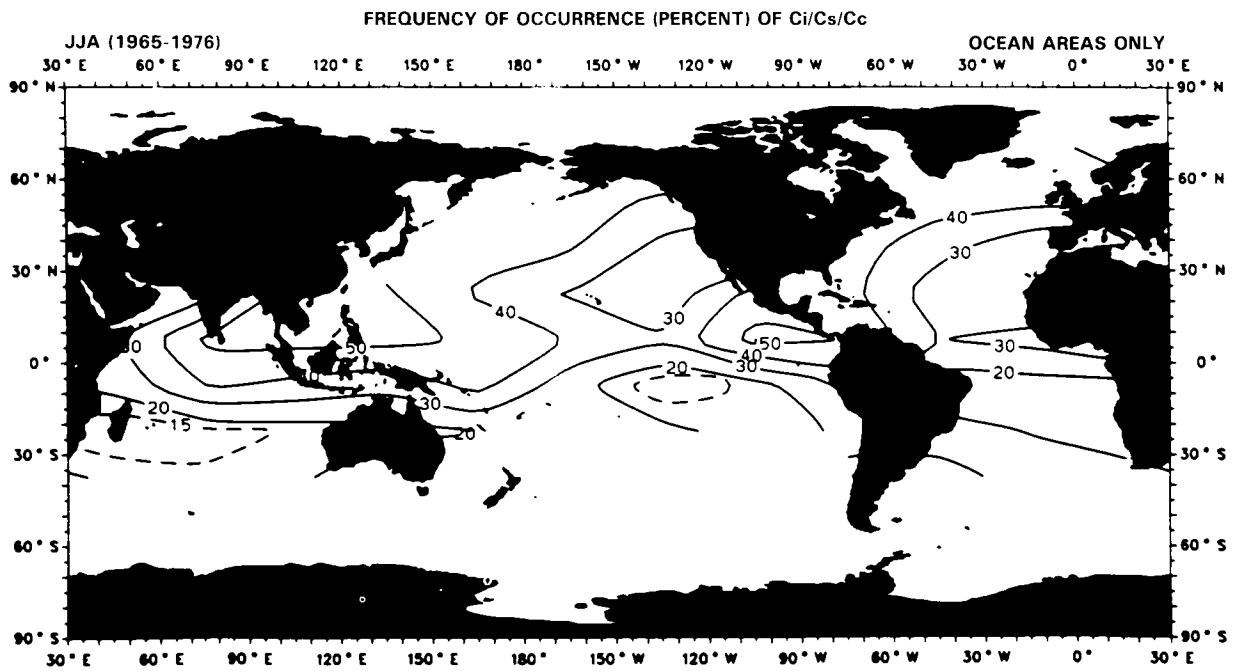
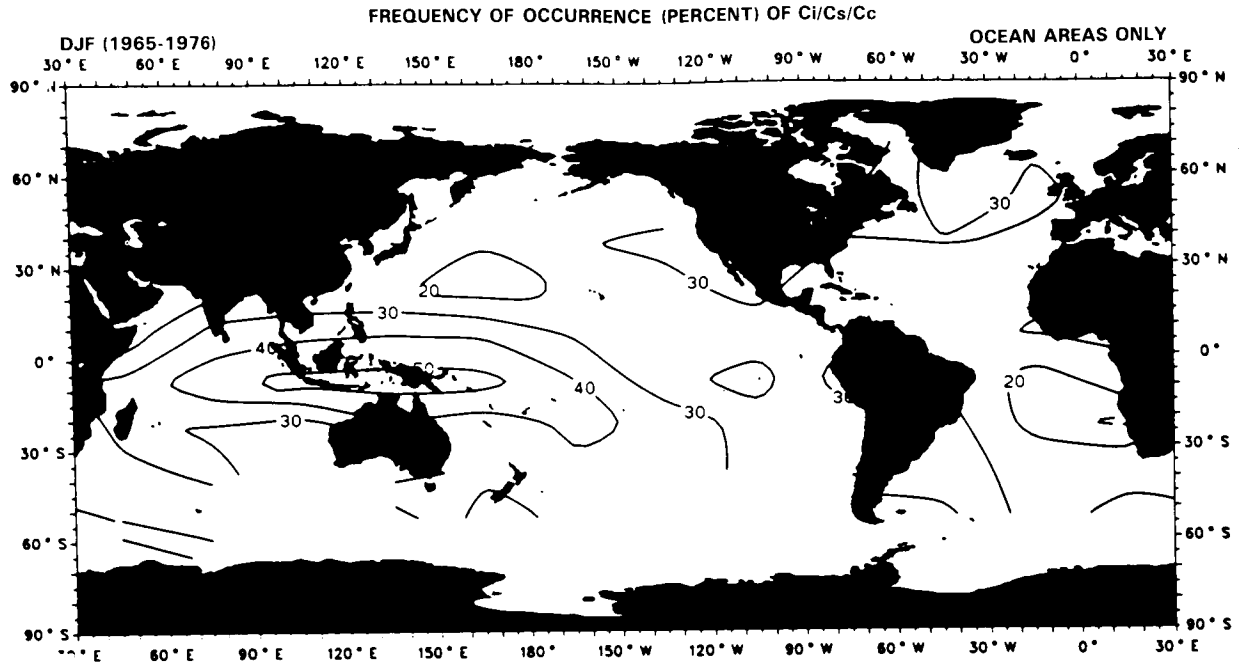


Figure 5-10. As in Figure 5-9 but for cirrus/cirrostratus/cirrocumulus.

a visible storm, and up to 1½-3 km above its top. Since parcel theory was the best statistical predictor of the observed top heights (although it was not reliable on a day to day basis), it is clear that near-surface air may be carried, on a time scale of hours, largely undiluted to up to 20 km, with potential for further mixing above this altitude. Mattingly (1977) noted a statistically significant tendency for the vertical extent of tops penetrating the tropopause in the Cornford and Spavins data to be correlated with the horizontal dimension: the bigger storms penetrated further, as shown in Figure 5-11.

It should be noted that upper level windshear frequently plays an important role in cumulonimbus development (Ludlam 1980), and the possibility of horizontal winds at the level of cumulonimbus tops and their associated anvils transporting water vapour and small ice crystals downwind must be considered. Aircraft studies in mid-latitudes (Barrett *et al.*, 1973) have apparently shown that this can occur.

Shipborne radiosonde launches during the winter MONEX experiment have also shown mesoscale temperature structure just above the tropopause near Borneo which was sufficiently cold to be compatible with the low mixing ratio associated with the stratosphere at and above the hygropause (Johnson and Kriete 1982), see Figure 5-12.

The production of nitric oxide during lightning discharges in cumulonimbus storms was calculated theoretically by Tuck (1976), Griffing (1977) and Chameides *et al.* (1977): a recent review is given by Borucki and Chameides (1984). Measurements of NO<sub>2</sub> production by Noxon (1976) confirmed this process, and he suggested that some of it could enter the stratosphere. Tuck (1976) calculated that there could be a flux of order 10<sup>34</sup> NO<sub>x</sub> molecules per year into the lower tropical stratosphere from cumulonimbi, which is of the same order as the stratospheric photochemical production from O(<sup>1</sup>D) + N<sub>2</sub>O → 2 NO.

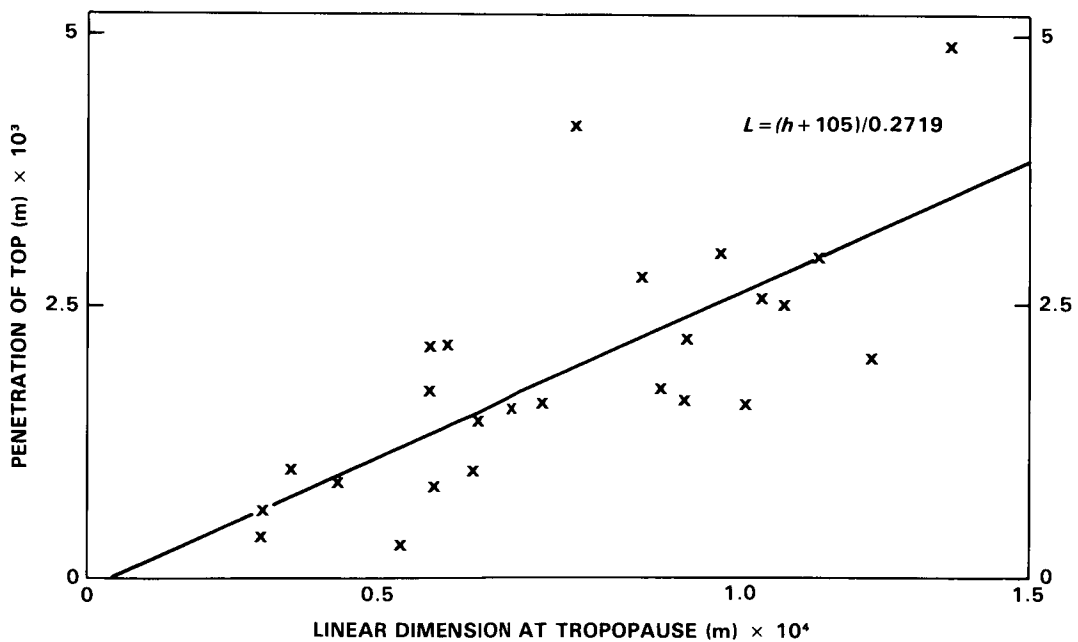
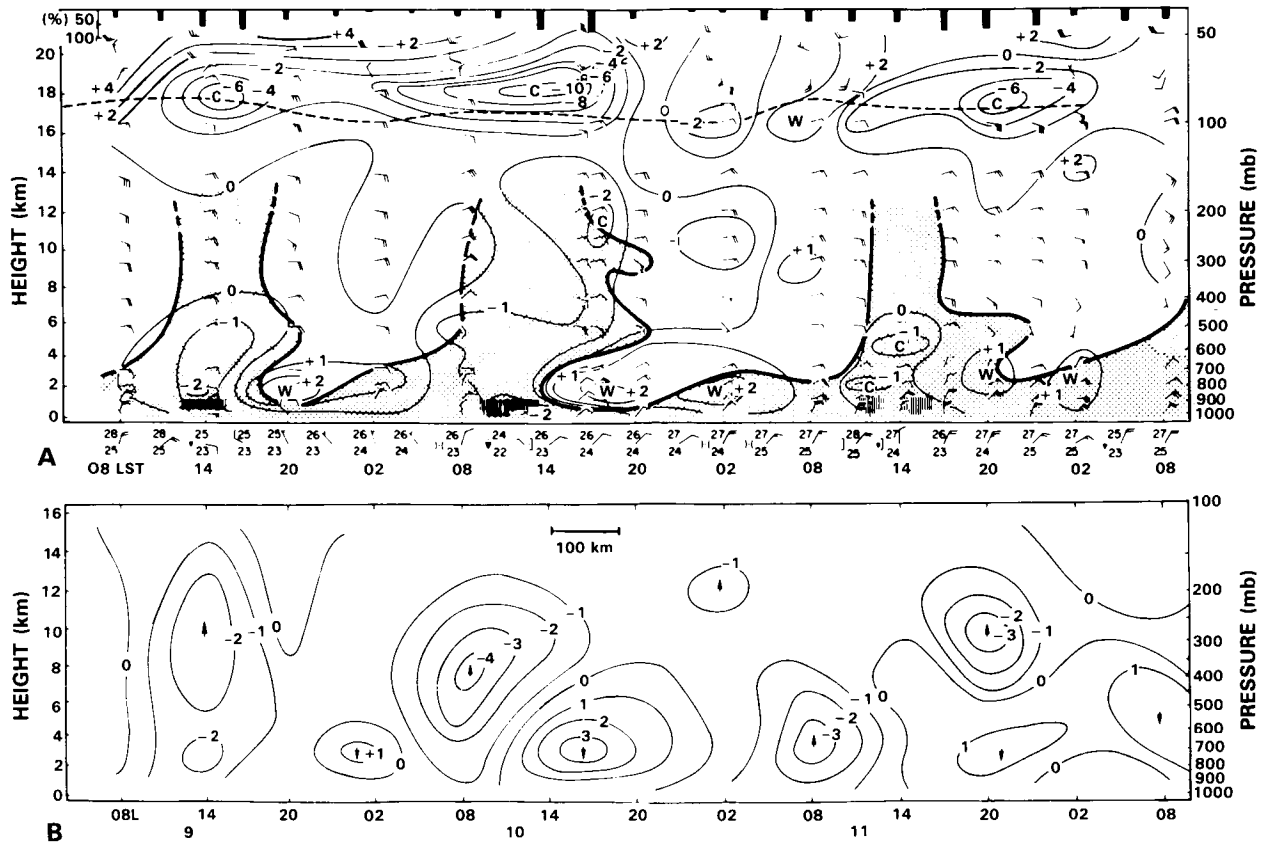


Figure 5-11. A diagram of the height of cumulonimbus tops above the tropopause versus horizontal dimension, from Mattingly (1977) using data from NE India obtained by Cornford and Spavins (1973).

## STRAT-TROP EXCHANGE



**Figure 5-12.** (a) Rawinsonde time series during winter MONEX for 9-11 December 1978. Stippling denotes regions of greater than 80% relative humidity. Solid contours are temperature deviations (K) from the 6-28 December mean. Wind speeds are in m/s (full barb - 5 m/s). Dashed line marks the tropopause. Bars at top indicate fraction of ship array covered by bright IR satellite cloudiness. (b) Vertical pressure velocity in units of 100 mb/day for the ship array computed by the kinematic method. Distance scale indicated represents advective length scale for 6 m/s motion of the anvil clouds. After Johnson and Kriete, 1982.

However, the degree of overlap between discharge channels and updrafts is unknown, and there is no reliable information on the partitioning of lightning-produced  $\text{NO}_x$  between stratosphere and troposphere.

It is clear from the large scale wind fields in the tropics that any volume of air at or a few km above the tropopause will not be simply transported zonally. Dynamical constraints dictate that there will be meridional components to the flow, consistent with the correlation observed by Reid and Gage (1984) between tropical tropopause height and the angular momentum of the atmosphere. Variations in the intensity of the Hadley Cell also show this (Reed and Vlcek, 1969, Newell *et al.*, 1974, Reiter, 1979); Section 5.2.3 also examines the connection between tropical and mid-latitude circulations.

### 5.1.3 Aircraft Studies near Cumulonimbus Anvils in Panama

In this section, we are concerned with the tracer aspect of water vapour. We show that from measurements of water vapour below and above the tropical tropopause it is possible to demonstrate that

tropopause-penetrating cumulonimbus clouds and subsequent anvil formation inject most, if not all, of the water that is found in the stratosphere above the tropopause.

In 1980, NASA conducted the second of a series of experiments to investigate the exchange of air from troposphere to stratosphere in a tropical region. A U2 aircraft was equipped with a multitude of instruments. Among these was a fast responding  $Ly(\alpha)$  hygrometer (Kley and Stone, 1978). Some initial results obtained from this experiment have been published earlier (Kley *et al.*, 1982). Whereas those results were basically a statistical analysis of height profiles of water vapour mixing ratios, detailed examination of individual profiles of total water mixing ratio (total water means the sum of water in all phases) and atmospheric temperature shows some prominent features.

1. The tropopause is well defined. Height and temperature show little variability.
2. Above tropopause, usually a little more than 2 km higher, there is a secondary temperature minimum. The temperature at the height of this minimum has values very similar to those at the tropopause.
3. Water vapour profiles decline sharply over a small height range to values around 6 ppmv at tropopause. At higher altitudes, this drop continues but the trend reverses soon to give rise to a relative maximum of the mixing ratio at the height of the secondary temperature minimum. Above the height of the relative maximum, there is another decline to an absolute minimum between 18 and 19 km. Finally, consistent on all profiles, the water mixing ratio increases above the height of the absolute minimum.

Figure 5-13 shows these prominent features enhanced. Also, Figure 5-14 was prepared. That figure presents the material of Figure 5-13 in a semi-log plot. The atmospheric temperature profile is drawn on frost point coordinates. Apparent supersaturation is shown as the cross-hatched area. Since total  $H_2O$  was measured, supersaturation of such magnitude implies ice crystals in the air. Plots, like Figure 5-14, were generated for all flights of the Panama Experiment and gave very similar results (Kley *et al.*, 1983). A cirrus deck from the tropopause on down to 12 or 11 km was therefore ubiquitous but never reached across the tropopause. Supersaturation, i.e., hydrometeors above the tropopause, was only observed on two occasions during penetration or "skimming" of active stratospheric anvils (Kley *et al.*, 1982; Knollenberg *et al.*, 1982). However, the observed water mixing ratios at the height of the temperature minimum above tropopause were mostly extremely close to saturation. As Figure 5-14 shows, the water mixing ratio comes within  $\sim 1.5^\circ C$  of being saturated at 16.7 km. Exceptions were encountered for flights 5 and 9 where temperatures were closer to an unperturbed stratospheric profile and the mixing ratios thus were farther away from saturation.

The key to the understanding of the injection mechanism of water into the stratosphere is in the interpretation of Figure 5-13 which serves as our standard case. If the Danielsen (1982) anvil formation hypothesis is accepted then the negative temperature anomalies at 17 km can be explained as being produced by this process. Figure 5-13 then shows that water injection is the result of anvil formation. One might even think of the relative water maximum at 17 km as giving proof of the Danielsen hypothesis. The profiles were all taken during aircraft descent, i.e., while not flying through active anvils. Therefore, the observations show the perturbed conditions that exist *after* the anvils have dissipated. It is not surprising that the water mixing ratio remains high because the layer is subsaturated and mixing ratio will be conserved since mixing will be inefficient due to the horizontal extent of the layer and the short elapsed time since dissipation of the anvil. It is possible to estimate this time if we use  $-83^\circ$  to  $-84^\circ C$  as initial anvil temperatures (Danielsen, 1982) and typical e-folding times for radiative cooling rates of five days for a dry atmosphere

STRAT-TROP EXCHANGE

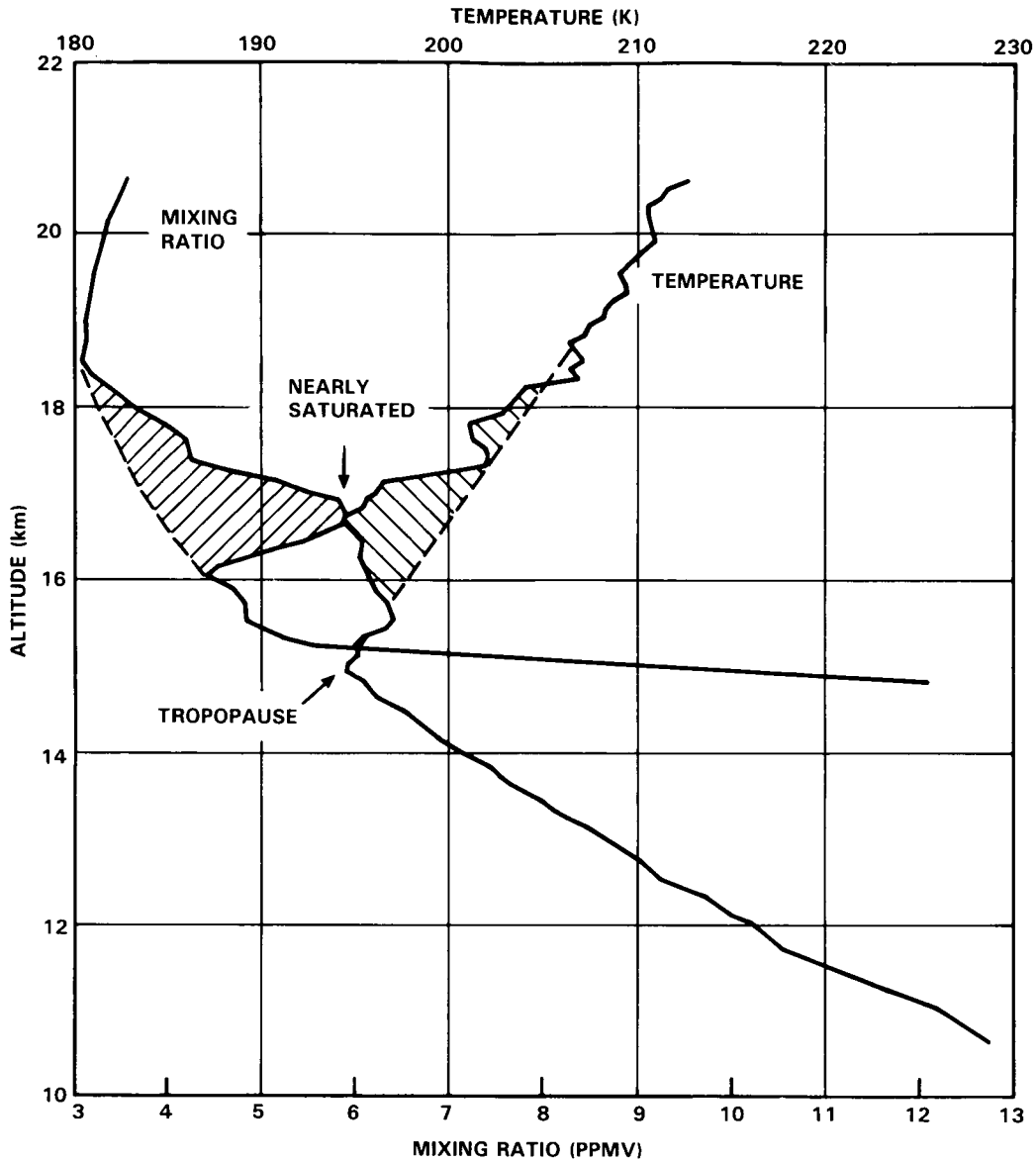
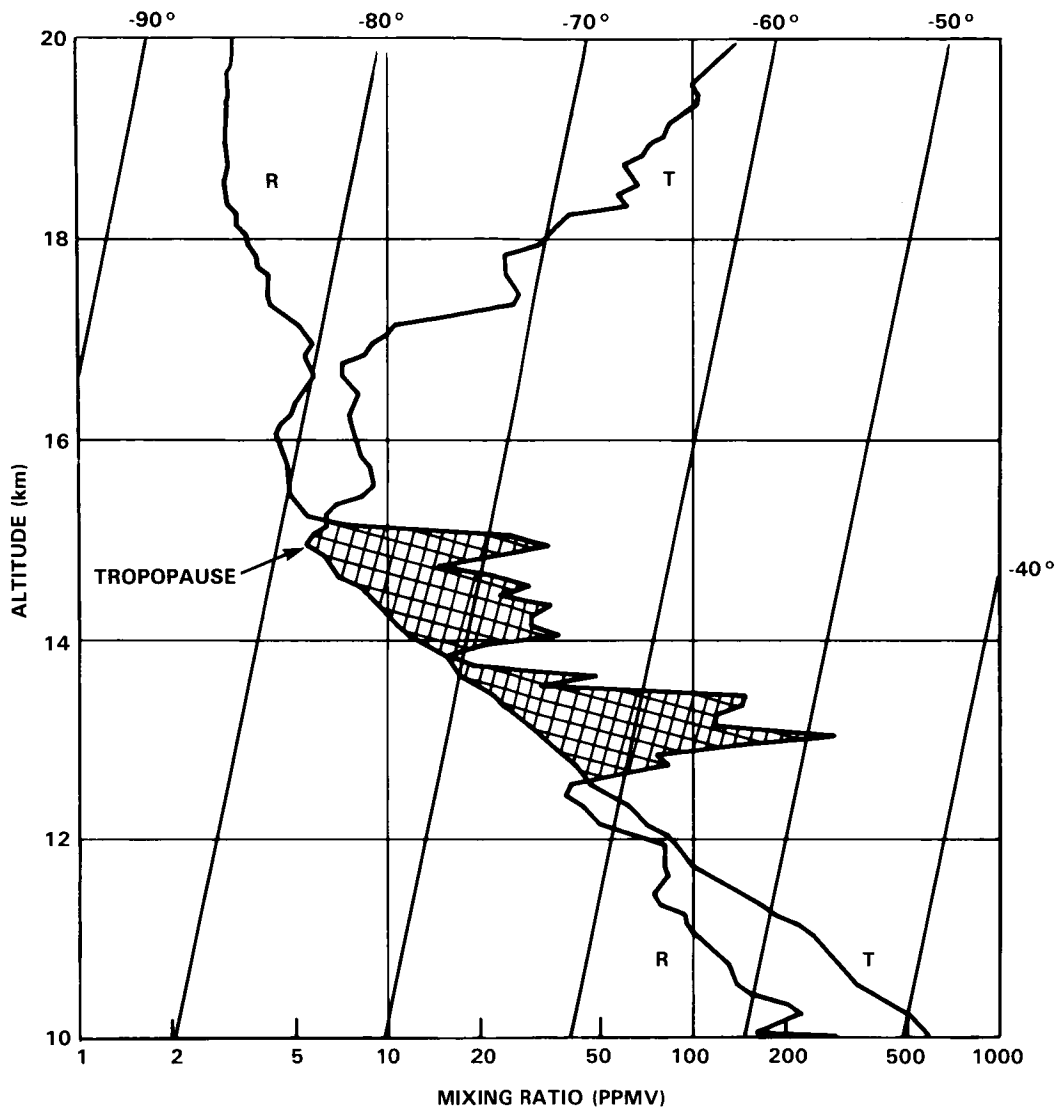


Figure 5-13. Water vapour mixing ratio and temperature, averaged over 100 m intervals, from U2 aircraft instrumentation at descent to Howard AFB on 11th September 1980.

(Fels, private communication). This implies that less than five days have passed since the air was part of an anvil. The enhanced mixing ratio with a maximum at ~17 km cannot have been produced below the layer and then diffused upward since there is a dryer layer between 16 and 15 km, followed by much higher mixing ratios below 15 km. The results typified by Figure 5-13 demonstrate that injection occurs at the altitude around 17 km. We must think of the process as one in which the turret overshoots and transports large amounts of ice into the stratosphere, and that the subsequent anvil formation distributes the ice quasi-horizontally. This process can lead to saturation while the excess ice precipitates out. There has been discussion on the thermodynamics (Danielsen, 1982) and the microphysics (Knollenberg *et al.*,



**Figure 5-14.** Mixing ratio (R) and temperature (T) for the 11th September data in Figure 5-13, on a semi-log plot. Cirrus deck indicated by cross-hatching. Temperature profile plotted on frost point coordinates.

1982) of water injection during cumulonimbus penetration and anvil formation. However, the answer, as far as injection of water into the stratosphere is concerned, is contained in Figure 5-13. These experimental results impose constraints on thermodynamics and microphysics of anvil formation. Whatever the microphysics are, they lead to saturated water conditions. Rather than asking the question whether the microphysical processes lead to hydration or dehydration of stratospheric air, it would perhaps be better to pose the question in a way as to ask what is the atmospheric temperature after anvil dissipation and what is the role of microphysics and radiative processes, modifying the initial anvil temperature after overshoot of the turret and entrainment of stratospheric air has taken place.

## STRAT-TROP EXCHANGE

### 5.1.4 Discussion of Tropical Exchange

We now turn to a discussion of the question whether or not anvils are sources or sinks of stratospheric water vapour above the hygropause level. We limit the discussion to this level, since the hygropause is well defined, both in altitude and water mixing ratio, and Danielsen (1982) has shown that the maximum height that anvils could reach is 19 km over the Eastern Pacific. There is direct experimental evidence of cumulonimbus tops reaching 21 km in May over the Bay of Bengal (Cornford and Spavins, 1973). We make the assumption that all water found in the tropical stratosphere has been anvil-processed or, in other words, there is no transfer of water to regions above the hygropause by diffusion or slow advection through the tropopause. Clearly, the anvils are a source of stratospheric water vapour by imposing boundary conditions of temperature and H<sub>2</sub>O saturation mixing ratio on the air in the anvil. This process can be called dehydration, if the air entrained during anvil formation has a mixing ratio higher than what is imposed as boundary conditions by the microphysical/radiative processes during the lifetime of the anvil. Such a source of water vapour would be methane oxidation. As Figure 5-13 shows, there is a slight increase of the H<sub>2</sub>O mixing ratio with height above the hygropause.

Our point made earlier that no water penetrates into the tropical stratosphere unless associated with overshooting thunderstorms is more than just an assumption. All flights of the Panama Experiment (Figure 5-14 and Figures 30 to 37 of Kley *et al.*, 1983) show saturation at the tropopause with mixing ratios around 6 ppmv, followed by the discussed decrease above the tropopause up to the level of anvil injection. A similar result was obtained during the only other sounding we made in the tropics (Kley *et al.*, 1979). It therefore seems appropriate, in the absence of counter-examples, to associate the physical source of stratospheric water vapour mainly with overshooting deep cumulonimbus convection. An alternative view may also be considered, in which, on some space scale, the low temperatures associated with overshooting Cb's and their anvils provide a source of dryness. Which of these is chosen depends upon the hypothetical reference state chosen for stratospheric humidity; if it is  $\chi_{\text{H}_2\text{O}} = 0$  then Cb's may be viewed as a source, if the reference is taken as the upper troposphere, it is more natural to think of a "source of dryness".

In the remainder of the discussion we will briefly investigate the longitudinal distribution of tropical lower stratospheric water vapour and the hygropause phenomenon. This part is more fragmentary and more observational work needs to be done. All the available information suggests that the water mixing ratio at the hygropause level shows little variability along a latitude circle in the tropics. The mean of the data typified by Figure 5-13 is  $\chi_{\text{HP}} = 3.4 \pm 0.2$  ppmv, where the subscript indicates altitude of the hygropause. Danielsen and Kley (1986, submitted for publication) analyzed a balloon sounding made on 31 January 1979. They show that air at 15 km over Laramie, WY with a mixing ratio of 3.2 ppmv had been isentropically transported on the 405 K potential temperature surface from a tropical sector (120°-140°E). Transport time from the source region to Laramie was only five days, during which time diffusion had not appreciably changed the mixing ratio of the layer. Mastenbrook (1968) reported monthly soundings over Trinidad (11°N, 61°W). His yearly mean at 60 mb was 3.4 ppmv. Remsberg *et al.* (1984) present zonal mean values of  $\sim 2.5$  ppmv at 60-70 mb and note that, due to retrieval uncertainties, these values might be too low by a margin equal to or less than 25%. In the absence of sufficient data it seems appropriate, at present, to adopt a hygropause mixing ratio around 3 ppmv with no justification to argue for a strong longitudinal asymmetry. However, it is not readily apparent that the assumption of little mixing during the 5-day passage to Wyoming is compatible with the implicit assumption of rapid mixing associated with no longitudinal asymmetry in the hygropause in the tropics despite the "source of dryness" being confined to, say, 70°-170°E.

If stratospheric anvils are the major source for stratospheric water vapour, then infrared enhanced satellite photography could be used to map injection areas. Danielsen (1982) shows that the intensity of

overshooting cumulonimbus convection is ultimately related to sea surface temperature and to the amount of latent heat stored in near-surface air. He points out that over the Micronesia area (centered on 150°E), sea surface temperatures are 3 K warmer than over other parts of the Pacific; this can produce 10 K colder temperatures during overshoot to 19 km. This implies that mixing ratios as low as 1.5 ppmv are possible, and could be lower than this (Cornford and Spavins, 1973).

Newell and Gould-Stewart (1981) have proposed a stratospheric fountain to occur during the winter season over Micronesia/Bay of Bengal. If the injection mixing ratio over Panama and other tropical areas with similar sea surface temperatures is 5.5 ppmv and the hygropause mixing ratio is 3 ppmv in the zonal mean, then the mass of air injected with a water mixing ratio of 1.6 ppmv needs to be 64% of the total. However, the area over which these very low mixing ratios at 19 km might occur is mainly located in a certain sector (i.e., Micronesia) and a strong zonal asymmetry of the hygropause mixing ratio would result. The available information does, therefore, not favour this concept. Alternatively, we could think of the process as one in which air that has been anvil processed at injection altitudes below the hygropause to resulting mixing ratios of  $\sim 5.5$  ppmv is entrained during anvil formation of the hygropause level and leaves with a resulting mixing ratio of 3 ppmv. Vertical diffusion times from 17 to 19 km would be about 46 days for  $K_{zz} = 5 \times 10^3 \text{cm}^2 \text{s}^{-1}$ . Adopting a mean zonal flow of 10 m/s it takes 23 days to advect material horizontally by 180° of longitude. Since  $K_{zz}$  could be lower than the value used here (Kida, 1983a, b), it seems justified to assume that freeze drying over the Micronesia/winter Monsoon area can account for the uniform mixing ratio of the hygropause. Anvil temperatures of  $-86.5^\circ\text{C}$  are required at 60 to 70 mb. These low temperatures are not found everywhere in the tropics. However, they do occur. Johnson and Kriete (1982) show temperature profiles over the winter monsoon area that exhibit characteristics of the Danielsen anvil mechanism at the height of the hygropause.

The results from the  $\text{Ly}(\alpha)$  hygrometer during the 1980 Panama Experiment show that water injection to the stratosphere occurs by overshooting cumulonimbus clouds and anvil formation above tropopause. The stratospheric water mixing ratio is determined by the anvil temperature at the time of dissipation, i.e., the transition from supersaturated to saturated conditions. The apparent uniformity of the hygropause represents a problem that needs further experimental and theoretical work. In the meantime, the experimental results are best explained by a cold trap of  $-86.5^\circ\text{C}$ , located at  $\sim 19$  km. The trap is provided by anvil spreading at that altitude from overshooting cumulonimbi. Injection of water vapour into the stratosphere occurs whenever anvils are formed above the tropopause. However, due to fast zonal flow, air with larger mixing ratio from lower altitude injection is entrained again at 19 km and leaves the hygropause with a mixing ratio of  $3 \pm 0.2$  ppmv.

As a consequence of the convective nature of this process, overshooting reverses positive surface temperature deviations of air parcels on the scale of convective events into negative temperature deviations above the tropopause. We like to suggest that an increase of the earth's surface temperature in the mean would, also, due to the increased amount of water in surface-near air, increase the intensity of overshooting. This would lead to a decrease in stratospheric water vapour. However, it must be remembered that it is very difficult to calculate the balance between radiative and convective processes near the tropical tropopause, and behaviour under such a perturbation is not yet predictable.

### 5.1.5 Summary of Tropical Exchange

There is a spatial and temporal correlation between the large scale tropical temperature minima at 100 mb (Figure 5-5) and the locations of the occurrence of the deepest cumulonimbus anvils. Although the lowest tropopause temperatures in the sector from 70°E to 170°E are low enough to account for the

## STRAT-TROP EXCHANGE

lowest water vapour mixing ratios observed in the stratosphere, quasi-uniform slow large scale ascent over this area of the tropical tropopause cannot account for the occurrence of the hygropause (minimum mixing ratios in the vertical water vapour profile) some 2-4 km above the tropopause. Appeal to some other mechanism must be made, and large cumulonimbus storms are the obvious candidate. Much remains to be learnt about the details however; tropical cumulonimbus frequently organise in clusters or on the mesoscale, for example. There may be cooperative interaction between deep local convection and large scale temperature minima at the tropopause, which could produce drier air for overshooting turrets collapsing back to mix with than would otherwise be the case. If a zonally symmetric hygropause is maintained throughout the year (and this is not established), there is a need to understand how the drying mechanism remains balanced with the horizontal mixing at subtropical and middle latitudes, particularly during the June-September period. It may be that both tropical convection depth and poleward motion in the subtropics are stronger in the northern winter, and weaker in the summer as a result of angular momentum conservation, but global scale observations are required.

One critical experiment which needs doing is to determine whether or not there are fine ice crystals (cirrus) near tropopause levels in the sector  $70^{\circ}\text{E}$  to  $170^{\circ}\text{E}$  in the tropics, and the areal extent of their occurrence. It is also necessary to do aircraft studies of the tallest cumulonimbus towers (which apparently occur during May/June over the Bay of Bengal and Ganges delta). If the explanation of the hygropause over Panama is correct (i.e., that it is produced by deeper convection elsewhere), then the hygropause should be coincident in altitude with the tops of the highest anvils. The odd nitrogen content of the stratospheric outflow from cumulonimbus storms needs to be measured.

## 5.2 EXTRATROPICAL EXCHANGE

### 5.2.1 Meteorological Processes

The exchange, or irreversible transfer of mass, trace gases and aerosols between the stratosphere and troposphere varies with latitude, longitude and season. Outflow from the stratosphere is predominantly by tropopause folding in association with large scale wave amplification and the formation of extratropical cyclonic storms. These storms amplify rapidly where the atmosphere has a large latitudinal temperature gradient and small static stability. Both conditions are more probable at low latitudes in the extratropics during late winter and early spring, and at high latitudes in late summer and early fall. The corresponding longitudinal variations are related to small static stability, produced by the passage of cold air over warm oceans or land surfaces. Thus during winter, cyclogenesis is more frequent and vigorous over the warmer oceans while in the spring the optimum conditions shift longitudinally to the high arid plateaus where surface heating is a maximum.

The outflow process was predicted by Reed (1955) and Reed and Danielsen (1959) who used potential vorticity as a quasiconservative tracer to identify air of recent stratospheric origin in the middle and upper troposphere. The process was verified by Briggs and Roach (1963), Danielsen (1964), and Reiter and Mahlman (1965) via aircraft measurements of ozone, water vapour and radioactivity of nuclear bomb test origin. Danielsen (1968) obtained direct correlations with the spatial distributions of potential vorticity. At that time, fast responding ozone and water vapour sensors were not available for aircraft experiments, but during the same spring a special ozone-sonde network was established in North America by Air Force Cambridge Research Laboratory (Hering and Borden, 1964-1966). Some of these sondes permitted indirect comparisons between ozone and radioactivity by relating both to computed distributions of potential vorticity (Danielsen, 1968). As anticipated, the three quantities were positively correlated in the lower stratosphere and in the folded tropopause layers in the middle and upper troposphere. These results are

consistent with the stratospheric sources of the three quantities and with a dominant influence of stratospheric mixing. The latter is required to explain the positive correlations despite the latitudinal and sometimes longitudinal differences in their upper or middle stratospheric sources (Danielsen, *op. cit.*).

Having direct *in situ* measurements of radioactive isotopes was a distinct advantage for identifying air of stratospheric origin and for establishing the relative importance of irreversible mixing. One can argue, as meteorologists and chemists do, about the nonconservation of potential vorticity and ozone and hence their use or misuse as stratospheric tracers. But, when radioactivity is corrected for radioactive decay it is unambiguously conserved. Only mixing processes can change the mixing ratio of a given isotope in an air parcel. By tracing three dimensional trajectories of these parcels and measuring changes in each parcel's mixing ratio one can evaluate the mixing. Furthermore, if the changes in potential vorticity and/or ozone are comparable to those of radioactivity, mixing processes are clearly responsible for the changes.

The mixing referred to here is small scale and irreversible. It is essentially independent of direction and tends to destroy gradients of any quantity including gradients of tracer  $i$ 's mixing ratio  $\chi_i$ . On the other hand, the larger scale motions from which trajectories are computed, in principle, are reversible. They are quasihorizontal and tend to create gradients by deformation, i.e., as illustrated in Figure 5-15, the flow increases the vertical gradient by convergence and spreads the gradient to a larger horizontal area by divergence. Steady state is maintained locally by a balance between flow deformation tending to increase the gradient and small scale mixing tending to decrease it.

In general, the stratosphere differs from the troposphere by having much larger vertical gradients of quasiconservative quantities. This characteristic is a consequence of the larger static stability of the stratosphere which acts to resist vertical motions and prevents large scale overturning, and also of chemical processes that generate vertical gradients. Conversely, in the troposphere, heating at the earth's surface reduces static stability and generates vertical overturning. Also, latent heat released by condensing water vapour in updrafts accelerates the updrafts, producing large cumulonimbus clouds that can traverse the entire depth of the troposphere. The prefix tropo - meaning to turn - implies vertical overturning, small vertical gradients, and a tendency for vertical homogeneity. These conditions are most clearly seen in the boundary layer but they are evident also in the vertical profiles of long-lived trace gases of lower tropospheric origin such as nitrous oxide and methane.

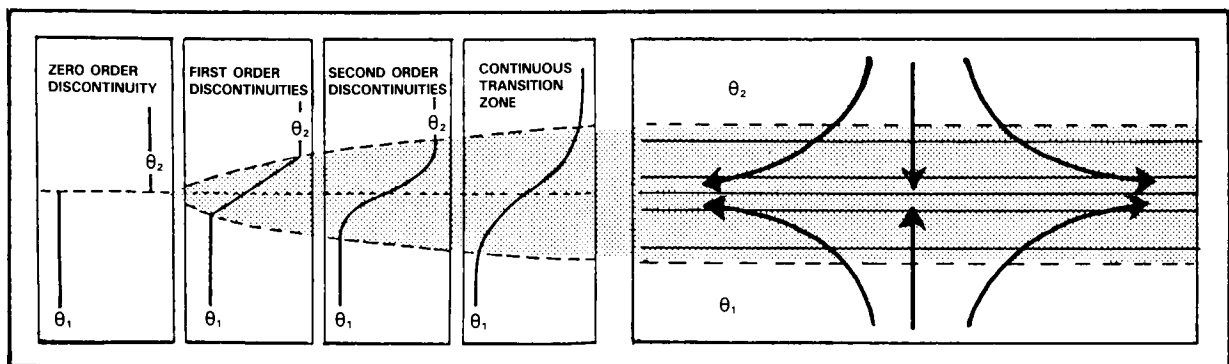


**Figure 5-15.** Continuous gradients of transition zone maintained by opposing actions of velocity deformations and small scale mixing. Discontinuities are physically unrealistic approximations. After Danielsen and Hipskind (1980).

## STRAT-TROP EXCHANGE

Relative to the troposphere, the much larger vertical gradients of the lower stratosphere resemble a transition zone whose lower boundary is the tropopause. When averaged zonally and/or temporally the distributions of stratospheric tracers support this concept. In particular, the surfaces of constant mixing ratio and potential vorticity are parallel to the mean tropopause. As seen in Figure 5-1a and 5-1b they slope downward from the equator to the pole with the maximum negative slopes at the latitude of the mean west wind jet stream, Figure 5-1c. It follows that the mean tropopause can be identified by a constant value of potential vorticity, except near the equator where a large meridional gradient occurs due to a sign reversal in the southern hemisphere.

Figure 5-1b was derived and contoured from the potential temperature and zonal velocity analyses of Figure 5-1c. They, in turn, were computer derived from the observations of temperature, pressure, humidity, zonal and meridional wind velocities provided by the global radiosonde network. The conversion from temperature  $T$  to potential temperature  $\theta$  by

$$\theta = T \left( \frac{1000}{p} \right)^{0.286} \quad (5.1)$$

incorporates the nonconservative effects of compression on  $T$ ;  $\theta$  is conserved in adiabatic parcel motion, whereas temperature is not. In Equation (5.1),  $p$  is expressed in millibars, thus  $\theta$  is the temperature an air parcel would attain if compressed adiabatically to 1000 mb. The specific entropy is proportional to the logarithm of  $\theta$ , so a surface of constant  $\theta$  is often referred to as an isentropic surface. Trajectories computed from the horizontal winds on a constant  $\theta$  surface also are called isentropic trajectories. They follow the three dimensional adiabatic motions of the air and therefore one can obtain reliable estimates of the unmeasurable vertical velocities.

Potential temperature is not conserved when the air is heated by radiation or by conduction. Generally these diabatic heating rates are small because air consists predominantly of diatomic molecules, poor radiators and absorbers in the visible and infrared. Triatomic molecules, aerosols and hydrometeors, the radiatively active entities, are always trace species. Thus, the adiabatic assumption is realistic for cloud free transports, at least on timescales of a few days. When cloud forms in ascending air the release of latent heat by condensing water vapour increases  $\theta$ ; therefore a diabatic heating rate must be incorporated into trajectory computations.

Potential vorticity, the quantity Reed (1955) used as a tracer for stratospheric air, can also be used to detect mixing. It is a quasi-conservative scalar derived from the vector equation of motion, the continuity and energy equations, and is defined by

$$P = \alpha \nabla \theta \cdot (\nabla \times \mathbf{V} + 2\Omega) \quad (5.2)$$

where  $\alpha$  is the specific volume,  $\nabla \theta$  is the three dimensional gradient of potential temperature and the term in parenthesis, the absolute vorticity, is the sum of the curl of the velocity and twice the angular velocity of the earth.

To an excellent approximation equation (5-2) can be reduced to

$$P_\theta = -g \frac{\delta \theta}{\delta p} (\zeta_\theta + f) \quad (5.3)$$

## STRAT-TROP EXCHANGE

where  $g$  is the acceleration of gravity,  $\delta\theta/\delta p$  is a measure of the stability of a parcel subject to a vertical displacement and  $(\zeta_\theta + f)$  (the sum of the horizontal curl or vorticity measured on a  $\theta$  map and the vertical component,  $f$ , of the earth's vorticity) is a measure of the stability of a parcel subject to a horizontal displacement.  $P_\theta$  combines as a product the two parcel stability criteria, namely hydrostatic stability and inertial stability. If both terms are positive, a displaced parcel is forced back to its equilibrium position. If either is negative, the displacement is amplified and mixing develops.

Reductions of static stability are produced by the horizontal convergence at constant  $\theta$  associated with propagating internal waves. The convergence reduces  $\delta\theta/\delta p$  by vertical stretching and simultaneously increases the vorticity  $(\zeta_\theta + f)$ . Conversely, divergence increases static stability and decreases inertial stability. Therefore, both vertical and horizontal mixing can occur with internal waves of large amplitude and long periods, but only locally where the waves have reduced the appropriate stability.

As shown by Reed (1955) and by Reed and Danielsen (1959), the values of  $P_\theta$  in the stratosphere exceed the tropospheric values by one, two or three orders of magnitude. In the absence of mixing,

$$\frac{dP_\theta}{dt} = -g (\zeta_\theta + f) \frac{\delta}{\delta p} \left( \frac{d\theta}{dt} \right) \quad (5.4)$$

From this we can easily account for the creation of large stratospheric and low tropospheric values. Heating above and cooling below increases  $P_\theta$ , thus the heating source of the ozone layer generates large values in the stratosphere. Conversely, heating at the earth's surface generates low values and leads to vertical mixing in the troposphere. When cloud or moisture layers extend up to the tropopause the radiative cooling at their top accentuates both trends.

Excluding radiative cooling at cloud tops,  $d\theta/dt$  is a small quantity in the free atmosphere, i.e., above the friction layer and below the ozone production layer. Therefore,  $P_\theta$  tends to be conserved as does  $\theta$ . For short periods both quantities approximate scalar invariants of the fluid and can be used as stationary Lagrangian coordinates.

This property permits one to trace and identify air of stratospheric properties. When the tropopause folds, tropospheric air with small values of  $P_\theta$  folds over an extruded layer of stratospheric air with large values of  $P_\theta$ . Since each parcel conserves its value of  $P_\theta$  during the folding process, the air of stratospheric origin can be readily identified even after it is considered a part of the troposphere.

Returning to Figure 5-1b, we can take advantage of the fact that the mean tropopause coincides with a constant  $P_\theta$  and define both the statistical mean tropopause and the synoptic tropopause by a threshold value of  $P_{\theta,T}$ . This definition, a generalization of the conventional definition avoids the concept of the tropopause as a discontinuity surface and the necessity for breaking such a surface when its slope becomes quasivertical. A discontinuity surface is an absolute barrier to mass exchange but, as discussed above, gradients that characterize the lower stratosphere are finite precisely because of small scale mixing and their associated mass exchange. Furthermore, the deformations maintaining the gradients imply divergence along the tropopause. This divergence demands an increase in area, which the tropopause can achieve only by folding. When the tropopause folds the gradients rotate but are not destroyed because potential vorticity is conserved in the folding process.

We can use  $P_{\theta,T}$  as a reference surface for computing irreversible mass transfers as the synoptic tropopause defined by  $P_\theta^h$  (the superscript denotes a local mean) oscillates relative to it. The displacements

## STRAT-TROP EXCHANGE

producing the oscillations can be reversible if they are stable but will become irreversible if they amplify exponentially with time. This type of irreversibility has been demonstrated by in situ and remote measurements of tropopause folding events described later.

These folds, which transfer air, trace gases and aerosols from the lower stratosphere into the mean troposphere, develop by a steepening of the tropopause at the jet core followed by a downward and southward stretching of the jet. Descending air on the north side of the jet is stratospheric, richer in ozone, potential vorticity and radioactivity but poorer in water vapour, carbon monoxide and aerosols than the descending tropospheric air on the south side of the jet. The atmosphere adjusts to this rapid downward and southward transport of horizontal momentum by forcing warmer air downward on the south side and cold air upward on the north side of the jet. This thermally indirect circulation, shown schematically in Figure 5-16, increases the horizontal pressure gradients in the upper and middle troposphere, balancing the increasing centrifugal accelerations of the developing cyclonic vortex. Thus, clouds and precipitation are generated in the cold air, in the core of the vortex, while clear skies predominate in the fold and in the tropospheric air southwest and south of the fold.

The streamlines in Figure 5-16 are similar to those in Figure 5-15 except for their inclined axes of convergence and divergence. Convergence normal to the fold counteracts diffusion by advecting tropospheric

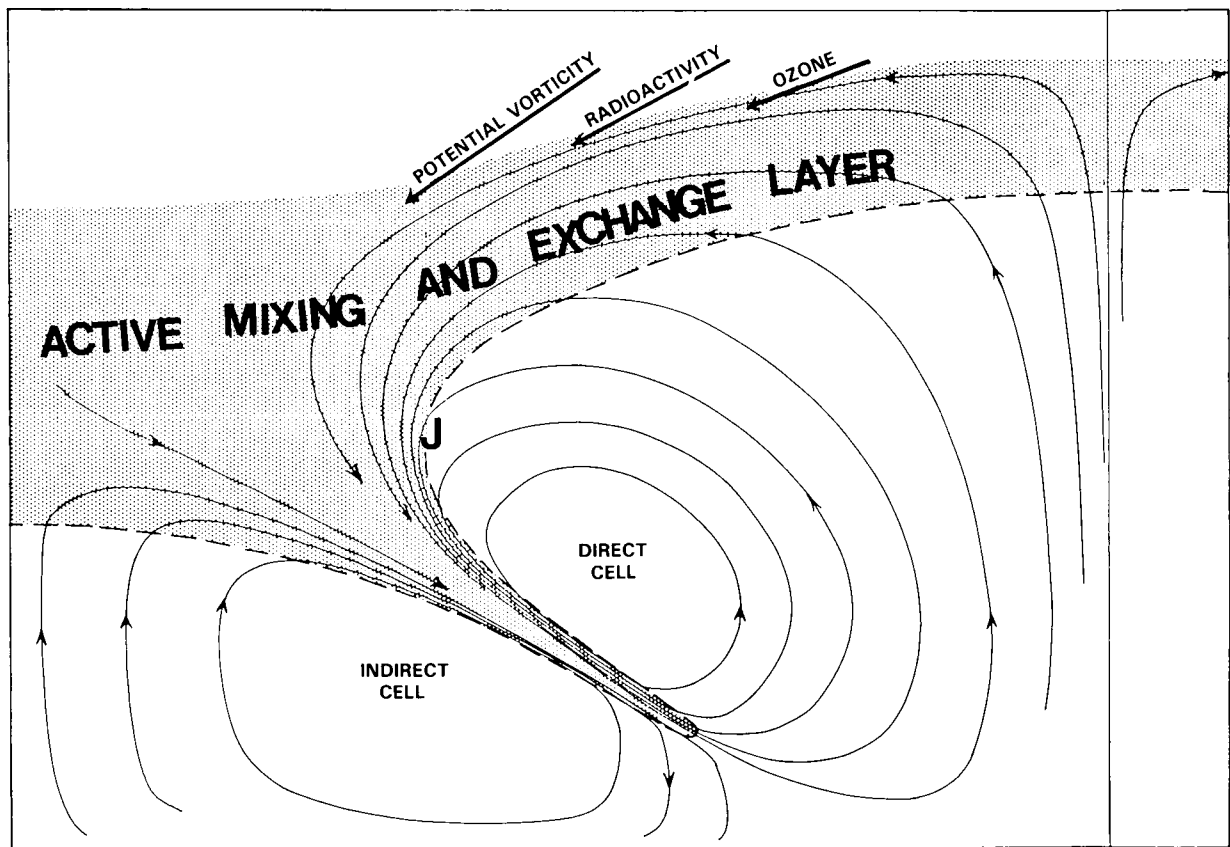


**Figure 5-16.** Thermally indirect and direct circulations which fold the tropopause and lead to irreversible transport from stratosphere to troposphere. Note entrainment of tropospheric air into fold along both boundaries, and that streamlines not trajectories are shown. From Danielsen (1968).

air into the fold. This entrained tropospheric air dilutes the mixing ratios of the stratospheric tracers - the mixture being advected southward and downward towards the surface boundary layer.

As the vortex continues to intensify, warm air to the east and north of the vortex ascends, producing more clouds and precipitation. This air turns anticyclonically (clockwise) away from the vortex, contributing to amplification of the ridge to the north and east of the vortex. The accelerating air resupplies momentum to the downstream jet, compensating for the momentum lost previously by the jet during the initial phase of cyclogenesis, and the amplifying ridge effectively cuts-off the vortex from its potential vorticity reservoir at high latitudes.

The result is an irreversible transfer of stratospheric air from the polar reservoir to lower latitudes and to lower altitudes. The process results in the formation of an isolated vortex at lower latitudes, each amplifying wave producing the same effect to varying degrees.

Less is known about the inflow of tropospheric air into the stratosphere. If there were no bulk transports associated with a large scale folding of the synoptic tropopause, the synoptic gradients of  $P_\theta$ ,  $\chi_{O_3}^1$ , and  $\chi_{Sr}^{1,0}$  in the stratosphere would be smooth and monotonic as are the zonal-annual means in Figures 5-1a and 5-1b. Analyses of  $\chi_\theta$  by Danielsen (1964, 1968) and vertical profiles of  $\chi_{O_3}^1$  from the AFCRL ozonesonde network (Hering and Borden, 1964-1966) demonstrate that such is not the case. There are well defined local maxima and minima in the lower stratosphere. Dobson (1973) postulated that the ozone minima were produced by ozone poor air from the upper subtropical troposphere entering the stratosphere at the conventional tropopause break and travelling northward at essentially constant altitude. The latter was based on statistical evidence of a maximum frequency of ozone partial pressure minima being  $15 \pm 1$  km from  $30^\circ$  to  $80^\circ$ N lat. There was also a similar maximum at higher latitudes at 23 km, for which Dobson could offer no explanation.

However, when the same data are analysed for ozone mixing ratio minima with  $\theta$  rather than  $z$  as the vertical coordinate, Danielsen and Kley (1986) show the maximum frequency occurs at  $\theta$ 's  $> 380$  K, i.e., much warmer than the  $\theta$ 's in the subtropical troposphere at the same height. In fact, the  $\theta$ 's are comparable to those in the lower tropical stratosphere. If the tropospheric air enters the stratosphere in the tropics and descends along constant  $\theta$  surfaces as it moves to the extratropics the adiabatic transport can be fast and effective in generating a sharply defined  $\chi_{O_3}$  minimum. Conversely, if the air enters at the subtropics and travels horizontally in the stratosphere the air must be diabatically heated by radiation to increase its  $\theta$  some 30 to 50 K. Much slower transports are then implied, with the transport times increasing greatly if the air is cloud free. Then one has difficulty explaining the well-defined minima given the evidence for ubiquitous small scale mixing in the stratosphere (but see Chapter 6).

However, an alternative view can also be taken. Figure 5-17 shows cross-sections of potential temperature and  $u$  from the climatology of Heastie and Stephenson (1960), for  $140^\circ$ E and  $75^\circ$ W in January. It is apparent that the isentropic surfaces in the 355-375 K range span the upper tropical troposphere and the middle and high latitude stratosphere, and that air can not only enter just above the core of the subtropical jet stream but can travel isentropically from  $30^\circ$ N to  $80^\circ$ N while maintaining an altitude of  $15 \pm 1$  km. This is consistent with the general circulation model results of Allam and Tuck (1984a, b), and the behaviour of the isentropic surfaces over the annual cycle is consistent with the maximum frequency of occurrence of the ozone-poor layers in late winter and early spring noted by Dobson (1973). Finally, inspection of ozonesonde ascents shows that ozone-poor minima in northern mid-latitudes are common in the range 350-380 K.

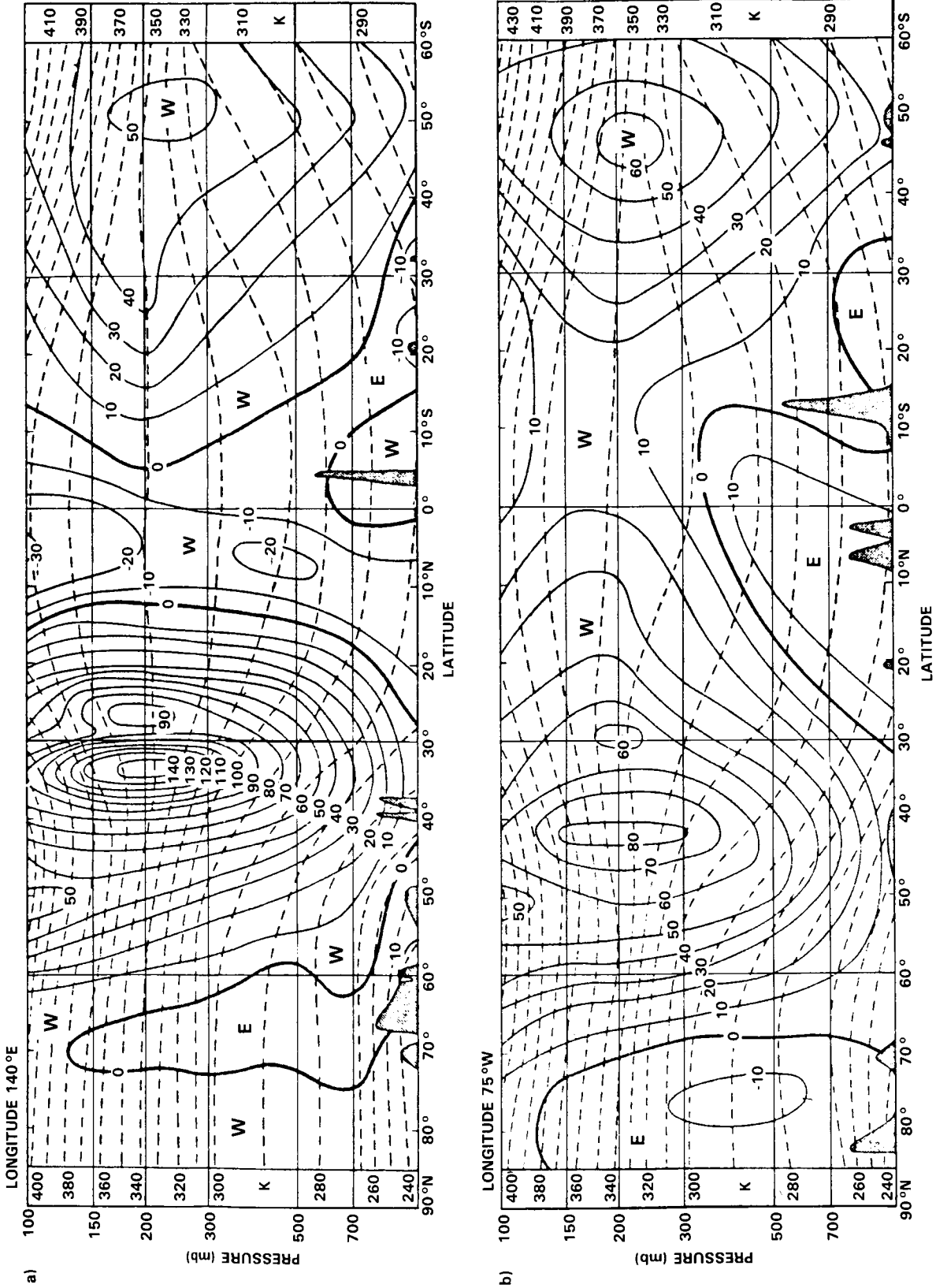


Figure 5-17. Vertical cross-section showing average zonal wind (knots) and potential temperature (K) in January. Isotachs are continuous lines, potential isotherms are dashed. (a) longitude 140°E, (b) longitude 75°W. From Heastie and Stephenson (1960).

In the case studied by Danielsen and Kley (*op. cit.*) the  $\chi_{O_3}$  minimum coincided with a  $\chi_{H_2O}$  minimum, i.e., it was cloud free and extremely dry. Also, their constant  $\theta$  trajectory analyses trace the air back to the tropics in 5 days. Furthermore, *in situ* observations made by the NASA U2 in the Spring 1984 STEP experiments show that the ozone-poor layers are dry and occur at  $\theta$ 's greater than 380 K. If these observations are statistically representative, then the bulk transports from troposphere to stratosphere must occur in the tropics. This however is subject to the counterarguments noted above, and to an absence of case studies near subtropical jet streams.

### 5.2.2 A Theoretical View of Mid-latitude Exchange

The dynamics of extra-tropical stratosphere - troposphere exchange are strongly influenced by two factors. The first is the contrast between the two regions in the very important quantity potential vorticity (PV):

$$\begin{aligned} P &= \frac{1}{\rho} \zeta_{\text{abs}} \cdot \nabla \theta \text{ in height coordinates} \\ &= -g \zeta_{\theta} / \frac{\partial p}{\partial \theta} \text{ in isentropic coordinates,} \end{aligned} \quad (5.5)$$

where  $\zeta_{\theta}$  is the vertical component of absolute vorticity evaluated in an isentropic surface. As discussed in detail in the review by Hoskins et al. (1985), in the absence of diabatic processes,  $P$  is conserved following the atmospheric motion. Further, the three dimensional isentropic potential vorticity (IPV) distribution plus the boundary temperature distribution at a particular time is sufficient to uniquely determine the atmospheric flow at that time provided only that the total mass between isentropic surfaces is known and the flow is in some sort of balance (e.g., quasi-geostrophic). A region of anomalously high IPV is generally associated with cyclonic vorticity in an extended region as well as compensating static stability changes (see Kleinschmidt, 1957 and refs). In the troposphere the PV has values below 1.5 units, where 1 PV unit equals  $10^{-6} \text{ K m}^2 \text{ s}^{-1} \text{ kg}^{-1}$ . The tropopause marks an abrupt transition to values of greater than 1.5 units and the magnitude increases rapidly with height in the lower stratosphere.

The second important factor is that there is significant potential temperature variation along the tropopause, which is therefore a sloping internal boundary when viewed in isentropic, as well as pressure and height, coordinates. Thus individual isentropic surfaces can sample both the stratospheric and tropospheric regions, and adiabatic flow on the surface can involve both regions. The lower stratosphere on such surfaces tends to move in association with synoptic disturbances that occur in the tropospheric region and it can indeed play a crucial role in the development of such disturbances.

#### 5.2.2.1 Deductions from Two-dimensional Models

Consideration of the stability of a 2-D flow  $v(x,z)$  in thermal wind balance with a temperature field  $\theta(x,z)$  to disturbances also independent of  $y$  yields (Ooyama 1966; Hoskins, 1974) an equation for the perturbation streamfunction in the  $x, z$  plane of the form

$$\frac{\partial}{\partial t^2} \left( \frac{\partial^2 \psi}{\partial x^2} + \frac{\partial^2 \psi}{\partial z^2} \right) = L(\psi) \quad (5.6)$$

## STRAT-TROP EXCHANGE

where  $L$  is an elliptic operator if  $P$  is positive. Analysis shows that the least stable direction is approximately along the isentropes and oscillations in this direction have a frequency

$$\sigma_{\min} = (f\xi_{\theta})^{1/2} \quad (5.7)$$

The most stable direction is approximately perpendicular to isentropic surfaces and their oscillation frequency  $\sigma_{\max}$  is such that

$$\sigma_{\max} \sigma_{\min} \propto P^{1/2} \quad (5.8)$$

Thus the large PV of the stratosphere implies markedly increased stability to motions perpendicular to isentropic surfaces, but no more resistance than the troposphere to motions along these surfaces.

In almost 2-D situations scaling arguments suggest that the flow  $v$  into the  $xz$  section should remain in geostrophic balance even for relative vorticities many times the Coriolis parameter. In this case the streamfunction for the ageostrophic flow ( $U_{ag,w}$ ) must be such as to maintain  $v$  in thermal wind balance with the temperature field, and consequently (Sawyer, 1956; Eliassen, 1962) must satisfy the equation

$$L(\psi) = 2Q_1. \quad (5.9)$$

Here  $L$  is the same elliptic operator as in Equation (5.6) and  $Q_1$  is a purely geostrophic term, being the tendency of the geostrophic wind to increase the  $x$ -temperature gradient. Synoptic disturbances in the troposphere will lead to non-zero values of  $Q_1$  and ageostrophic circulations. If the stratosphere was a high PV region with no isentropic gradient along the tropopause, it would act as a slightly flexible lid on the tropospheric circulation. However, since the isentropic gradient does exist and the stability of the stratosphere to motions along isentropes is not enhanced, the stratosphere tends to respond to tropospheric geostrophic forcing by ageostrophic motion along isentropes.

An example of a simple frontogenesis model in which this process occurs is shown in Figure 5-18. A temperature distribution which is independent of  $y$  contracts under the action of a geostrophic convergence  $u = -\alpha x$ .

Without any ageostrophic motions the tropopause slope would be gentle at this time. The tendency for the stratosphere to react to the forcing in the troposphere by moving along isentropic surfaces is marked. Equally marked is the tendency for the descent of stratospheric air to occur in a shallow tongue (as viewed in physical though not isentropic space), in contrast to the broad region of ascent of tropospheric air. This is in agreement with the scale analysis that suggests that the vertical scale of the response varies as  $P^{-1/2}$ . A further point of interest is that the Richardson number at the base of the tongue in Figure 5-18 has values as low as  $1/4$ , suggesting a high probability of mixing which would involve tropospheric and stratospheric air.

It is of interest to consider the applicability of quasi-geostrophic theory to the features discussed above. One of the basic assumptions of the theory is that static stability differences from those of a standard atmosphere, which is a function of the vertical coordinate only, are small. Thus it is not strictly applicable in the region of a sloping tropopause and, in particular, it would not give the development shown in Figure 5-18. In terms of Equation (5.6), the elliptic operator would be poorly approximated, but the geostrophic forcing  $Q_1$  would be correctly represented.

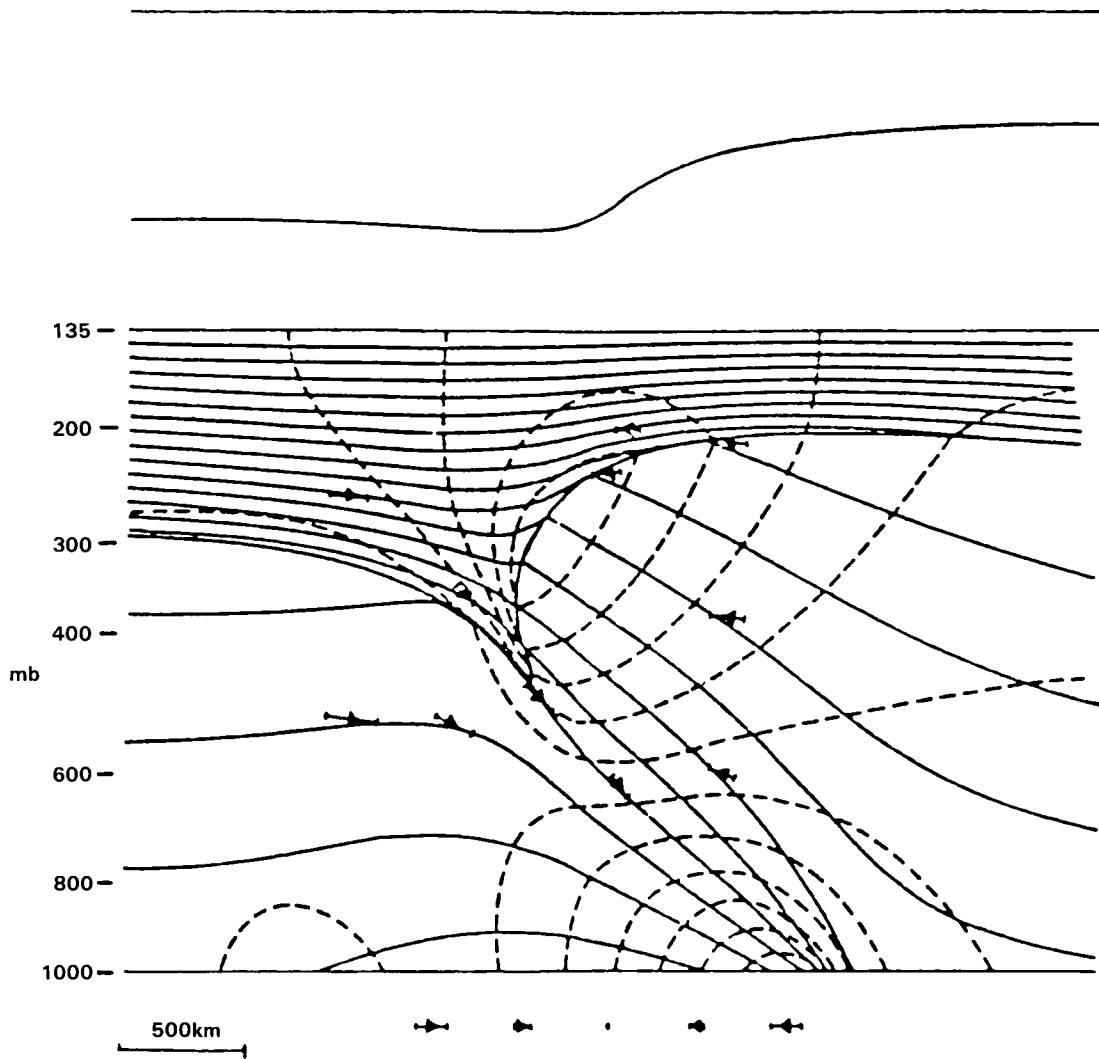


**Figure 5-18.** A simple frontogenesis model in which the basic deformation field shown below the lower axis acts on a 2-D situation with a tropopause which in the absence of any other motions would look as shown above. The actual tropopause position (heavy line), isentropes every 7.8 K (continuous lines), isolines of velocity into the section every  $10.5 \text{ ms}^{-1}$  (dashed contours) and particle motions (arrows) are shown in the centre. (After Hoskins, 1972).

### 5.2.2.2 Deductions from Three-dimensional Models

In three dimensions there are quasi-geostrophic (Hoskins *et al.*, 1978) and semi-geostrophic (Hoskins and Draghici, 1977) extensions of Equation (5.6), both describing the forcing of vertical circulations associated with a vector  $Q$  which is the tendency of the geostrophic wind to increase the vector temperature gradient on a fluid particle moving with the geostrophic wind. It is possible to find situations in the atmosphere (Shapiro, 1981) and understand them in these terms (Hoskins and Heckley, 1982) in which very strong descent of stratospheric air along isentropic surfaces is forced locally.

## STRAT-TROP EXCHANGE

As in two dimensions, quasi-geostrophic theory is wrong in its detailed prediction of tropopause movement. The semi-geostrophic equations (Hoskins, 1975) should be valid for motions whose Lagrangian time scale (time scale for change in  $v$  following a fluid particle) is much larger than  $f^{-1} \sim 3$  hours. Again they should be able to correctly treat movement of the tropopause because they do include a full vertical advection of PV. They have been used to model the growth to finite amplitude of a baroclinic wave or a basic zonal flow including a simple stratosphere as in the frontal example discussed above. As the wave grows, stratospheric air descends during its movement from the ridge towards the trough so that a vertical section across the trough shows the PV distribution given in Figure 5-19. The indication is that with more resolution in the numerical calculation it would become apparent that a standard synoptic development would exhibit marked tongues of stratospheric air descending along isentropes in upper air frontal structures. The model illustrated suffers from the numerical difficulty of accurately describing the advection of PV with its almost discontinuous structure at the tropopause.

The primitive equations have also been used to describe the growth of baroclinic waves to finite amplitude in situations with no diabatic heat sources. Shapiro (1975) used a 20-level isentropic coordinate model and showed the production in a strong synoptic development of very significant tongues of stratospheric air pushing into the troposphere. Another view of the probably irreversible mixing of stratospheric air into the troposphere in a baroclinic wave development is provided by the isentropic potential vorticity (IPV) and relative flow shown in Figure 5-20. The darkened region indicates the approximate location of the tropopause. As discussed in Hoskins and McIntyre (1985, paper in preparation), this picture is typical of the onset of decay in most, but not all simple baroclinic wave simulations. Sometimes the development is more similar to that in a cut-off low (Hoskins, *et al.*, 1985) in which, as viewed on an isentropic surface, a quasi-circular distribution of PV is separated from a near polar stratospheric vortex.

### 5.2.2.3 Diabatic Processes

The change of the IPV distribution in the presence of diabatic heating is approximately given by

$$\left( \frac{\partial}{\partial t} + \mathbf{v} \cdot \nabla_{\theta} \right) P = P^2 \frac{\partial}{\partial \theta} (\dot{\theta} P^{-1}) \quad (5.10)$$

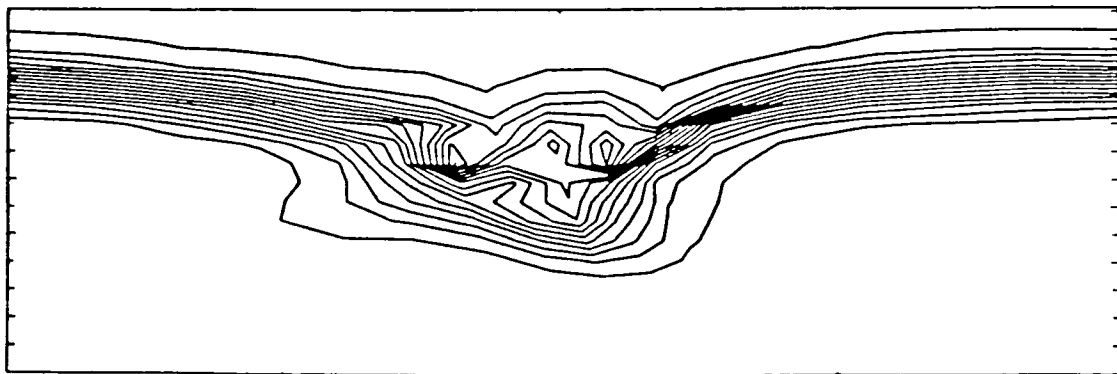


**Figure 5-19.** A vertical-zonal section across the trough of a non-linear baroclinic wave produced in a semi-geostrophic integration. The contours are those of potential vorticity defined for a Boussinesq fluid. The baroclinic wave had grown on a basic state with a narrow but finite transition from tropospheric to stratospheric values of potential vorticity. (After Hoskins and Heckley, 1982).

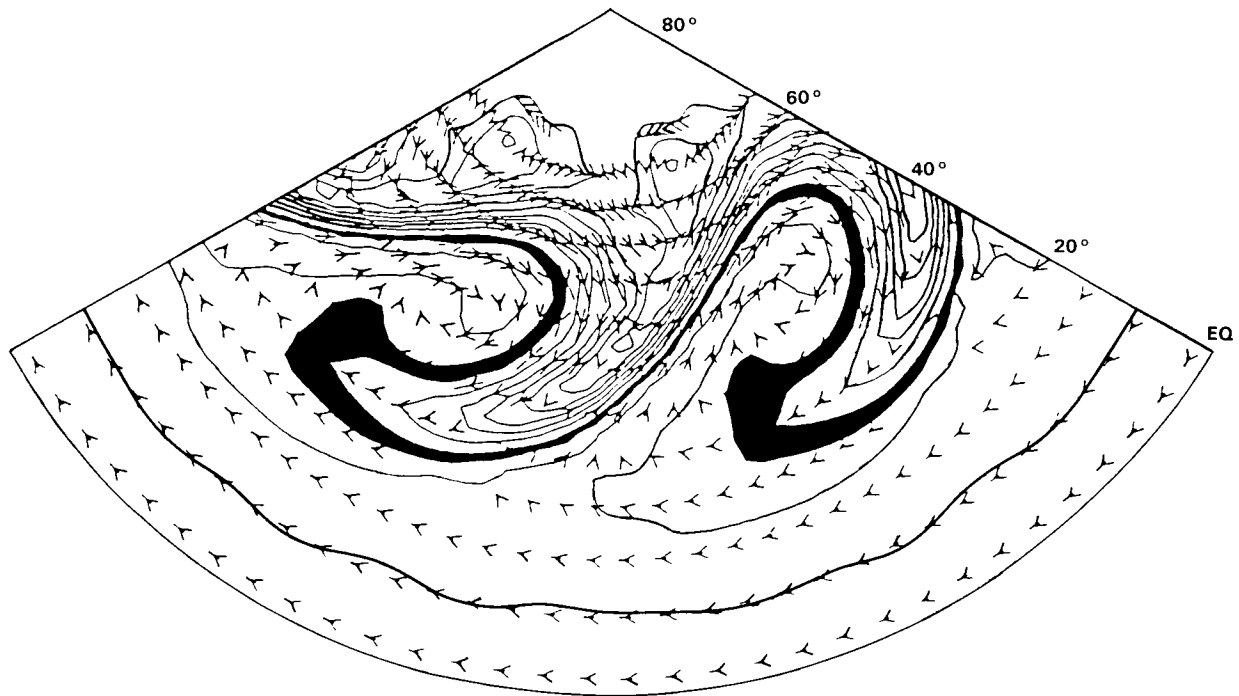


**Figure 5-20.** The day 8 350 K IPV map for a basic zonal wavenumber 6 baroclinic wave life-cycle experiment. The contour interval is  $0.8 \times 10^{-6} \text{ m}^2 \text{ s}^{-1} \text{ K kg}^{-1}$ . Also shown by arrows is the wind field on this isentropic surface in a frame of reference moving with the waves. The arrows nearest the equator represent a speed of  $16 \text{ ms}^{-1}$  (After Hoskins, *et al.*, 1985).

In the lower stratospheric polar vortex the radiative timescale determines the rate of change of  $P$  and indeed the maintenance of the vortex. However a descent of stratospheric PV along isentropes, as indicated above, induces cyclonic vorticity and reduced static stability in the underlying troposphere to an extent dependent on the surface temperature. If the anomalous IPV is moving relative to the low-level air, it also induces upward motion on its leading side. It thus leads to a region of much enhanced likelihood of moist convection, the extent of which depends on the low-level supply of moisture. The latent heating associated with this convection causes a change in the IPV distribution above it which occurs at a rate which may be deduced from Equation (5.10) as being sufficient to reduce the PV of the lower stratospheric air to tropospheric values in a matter of days. The descending stratospheric air therefore efficiently induces a process which usually absorbs it into the troposphere in a few days.

As in the 2-D models, one may also expect a 'lowered' tropopause to be a region of enhanced turbulent mixing. Shapiro (1976, 1978, 1980) produced evidence of such behaviour. However, as discussed by Shapiro (1978) and Gidel and Shapiro (1979), the result of this turbulence may not necessarily be a reduction in the PV contrast between air of stratospheric and tropospheric origin.

Upward motion of the middle latitude tropopause, on the other hand, is associated with anticyclonic vorticity and increased static stability in the troposphere. The chances of diabatic processes occurring on anything but the radiative timescale are reduced, and so it is not envisaged that these relatively broad regions will be favourable for major exchanges of tropospheric and stratospheric air. A blocking high, according

## STRAT-TROP EXCHANGE

to Hoskins *et al.* (1985), is the dynamical twin of the cut-off low, having such a raised tropopause associated with the poleward advection along isentropic surfaces of sub-tropical air. However as far as diabatic processes are concerned the nature of the two phenomena is very different, the blocking high tending to decay slowly on an advective or radiative timescale as opposed to the usually convection dominated, fast decay of the cut-off low.

Nevertheless, detailed studies of the relative rates of radiative lowering of the tropopause and advective decay in cut-off anticyclones have not been made, so exchange induced by radiative effects in such systems cannot be excluded.

### 5.2.3 A View Based on Isentropic FGGE Analyses

In this section a global scale view of the general circulation is developed, using isentropic analyses of the FGGE year (1979), as a context in which to see stratosphere-troposphere exchange, and to derive some constraints on the scales and location of exchange. The approach is to examine the scale of the mass circulation in the framework of the scale of the differential heating (taken to include radiation and latent heat release), by using Helmholtz's theorem to decompose the flow into irrotational ( $\nabla \times \mathbf{V} = 0$ ) and rotational ( $\nabla \cdot \mathbf{V} = 0$ ) components. Accordingly, the quasi-horizontal mass transport in an isentropic layer may be written as

$$\overline{\rho \mathbf{J} \mathbf{U}} = \nabla_{\theta} \bar{\chi} + (\mathbf{k} \times \nabla_{\theta} \bar{\psi}) \quad (5.11)$$

where  $\rho$  = density,  $\mathbf{J}$  is the Jacobian for transformation of vertical coordinate to potential temperature  $\theta (= | \delta z / \delta \theta | )$ ,  $\mathbf{U}$  is horizontal velocity,  $\chi$  = transport potential function,  $\psi$  = transport stream function and the overbars are time averages.

Then

$$(\overline{\rho \mathbf{J} \mathbf{U}})_{\chi} = \nabla_{\theta} \bar{\chi} \quad (5.12)$$

is the irrotational component of the flow, and

$$(\overline{\rho \mathbf{J} \mathbf{U}})_{\psi} = \mathbf{k} \times \nabla_{\theta} \bar{\psi} \quad (5.13)$$

is the rotational component.

The Poisson equations used to determine  $\chi$  and  $\psi$  are

$$\nabla_{\theta}^2 \bar{\chi} = \nabla_{\theta} \cdot (\overline{\rho \mathbf{J} \mathbf{U}}) = \delta \quad (5.14)$$

$$\nabla_{\theta}^2 \bar{\psi} = \mathbf{k} \cdot \nabla_{\theta} \times (\overline{\rho \mathbf{J} \mathbf{U}}) = \zeta \quad (5.15)$$

where  $\delta$  = divergence and  $\zeta$  = vorticity.

The approach is to calculate the divergence and curl of the mass transport from the NMC FGGE Level IIIa analysis.

By considering the time-averaged isentropic mass continuity equation (Johnson, Townsend and Wei, 1985) it is possible to show that, relative to isentropic surfaces, horizontal mass convergence (divergence) is balanced by an increase (decrease) of the upward mass flux in regions of heating, or a decrease (increase) of the downward mass flux in regions of cooling. It is thus possible to isolate thermodynamically coupled planetary circulations that connect regions of heat sources and heat sinks. It turns out that there is a component of such a circulation which is involved in stratosphere-troposphere exchange.

Considerable evidence exists regarding the extrusion of stratospheric air into the troposphere during cyclogenesis through circulations attending jet streams. Reed (1955), Briggs and Roach (1963), Danielsen (1964, 1967, 1968), Mahlman (1965), Reiter (1969, 1971 and 1972), Shapiro (1980), as well as others, clearly establish that stratospheric extrusions into the troposphere are maximized during cyclogenesis (see following section in this report). Return transport of tropospheric air into the stratosphere is required for the stratospheric balance of mass. Smith (1968), Reiter, Glasser and Mahlman (1969) and others have pointed out that quasi-horizontal transport processes serve to return tropospheric air to the stratosphere. Note however that Mahlman (1973) diagnosed transverse circulation in a steady (non-cyclogenetic) polar front jet stream which could produce exchange. Others have emphasized the importance of rising motion across the tropical tropopause (Brewer, 1949; Dobson, 1956) in conjunction with a "cold trap", tropical convection, and dehydration (Danielsen, 1982; Holton, 1984b). Details of the return of tropospheric air into the stratosphere however, are uncertain (Reiter, 1972; Ellsaesser, 1979; Holton, 1984b). The purpose of this discussion is to draw attention to physical processes associated with baroclinic phenomena and geostrophic motion in middle latitudes which provide for systematic stratospheric-tropospheric exchange (Johnson, 1979). While the importance of geostrophic modes of transport of properties has been established for decades, the systematic planetary nature of geostrophic mass transport, stratospheric-tropospheric exchange and differential heating within secondary and primary scales of atmospheric circulation has not been fully recognized.

In a recent study of the transport of water vapour within a stratospheric-tropospheric general circulation model, Allam and Tuck (1984a and b) concluded "that most of the water enters the stratosphere near the tropopause breaks by quasi-horizontal advection from the upper tropical troposphere into the lower extratropical stratosphere, although an appreciable amount moves vertically in the same region and at rather higher latitudes. This advection occurs chiefly through the action of eddies." They stated "that the simulated transport of water vapour by eddies in the stratosphere is greater in the northern than in the southern hemisphere" and that "the transport is greater during winter than during summer." Allam and Tuck (1984b) also noted from a trajectory analysis of general circulation model data that through quasi-horizontal transport, motions induced in regions of high shear and vorticity resulted in dry air from the upper tropical troposphere being mixed into the stratosphere. The evidence from these simulations substantiates suggestions that intrusion of tropospheric air into the stratosphere is associated with quasi-horizontal transport processes embedded within baroclinic waves and the meandering of polar and subtropical jet streams as well as with deep vertical convection in the tropics, a view emphasized by Reiter (1972).

From a dynamical point of view, this behaviour is to be expected. Within latitudinal regimes where rotation is important (i.e., scales large enough for the Coriolis force to largely balance the pressure gradient force), quasi-horizontal exchange processes through geostrophic motion are dominant. The important role that quasi-horizontal exchange within baroclinic waves plays in forcing meridional circulations in the troposphere is firmly established (Lorenz, 1967). The condition that quasi-horizontal exchange processes play an important role in the stratosphere is also established; however, the relative importance of quasi-horizontal exchange of trace constituents as opposed to exchange by mean meridional circulations is not well established, although a framework for providing a mechanistic means of doing this has been

## STRAT-TROP EXCHANGE

suggested recently (Mahlman *et al.*, 1984). Much of the uncertainty stems from lack of observations; however conceptual awkwardness also stems from averaging within coordinate systems that fail to permit degrees of freedom to isolate mass and energy transport processes within the atmosphere which are directly linked to the differential heating (Johnson, 1980, 1984b).

Within isentropic coordinates, the scale of the time-averaged mean mass circulation corresponds with the scale of the mean energy transport by differential heating. "Direct" planetary scale mass circulations exist in the sense that a branch of the circulation transports mass and energy from heat source to heat sink in upper isentropic layers and from heat sink to heat source in lower layers. Satisfaction of global energy balance requires that such mass circulations and transport processes exist apart from the distributions of atmosphere trace constituents. However, if within isentropic layers a correlation exists between a branch of a mass circulation and a trace constituent, it is likely that the isentropic mass circulation will be a key element in determining the scale and intensity of the quasi-horizontal transport of the trace constituent.

Before setting forth a simple model of stratospheric-tropospheric exchange, it is important to emphasize underlying reasons for systematic isentropic mass circulations in the atmosphere that serve to transport trace constituents. Concepts basic to the isolation of systematic isentropic mass circulations at the planetary scale were set forth by Shaw (1942). He noted that heating forced motion upward through isentropic surfaces while cooling forced motion downward, and that such motion constituted upward and downward branches of a mass circulation embedded within a stratified atmosphere. Horizontal branches linking heat sources and sinks through irrotational modes of mass transport are implied from the isentropic equation of continuity. The same mass circulations transport more dry static energy from heat source to sink in the upper layers than is returned in lower layers. Thus, net energy is transported from the heat source to the heat sink even though the net mass transport vanishes (Johnson and Townsend, 1981; Johnson, 1984a; Johnson, Townsend and Wei, 1985). As such, these global circulations are monsoonal in nature and will be at their maximum intensity in the winter season (Johnson, 1984a and b). These constraints, which require that within time-averaged circulations the scale of mass and energy transport corresponds with the scale of differential heating, permit no compromise, at least within hydrostatic atmospheres. While complexities are introduced by baroclinic, symmetric and convective instabilities, a fundamental premise for the development of monsoonal planetary circulation is that the transport processes during such instabilities should satisfy the basic requirement of net energy transport from heat source to heat sink, in the time-averaged sense.

### 5.2.3.1 Systematic Meridional Exchange by Geostrophic Modes of Isentropic Mass Transport

In their numerical simulation, Allam and Tuck (1984a,b) established that poleward and upward transport of water vapour from the troposphere into the stratosphere of each hemisphere occurred through eddies. These eddy circulations in their analyses are finite amplitude baroclinic features of middle latitudes. Johnson (1979) emphasized that systematic meridional mass exchange in finite amplitude baroclinic waves provided for intrusion of tropospheric air into the stratosphere by quasi-horizontal exchange and that this intrusion of tropospheric air would occur within an isentropic mass circulation that spanned the hemisphere. The combination of Allam and Tuck's results and the systematic nature of geostrophic transport processes point out the importance of isolating isentropic mass circulations embedded within baroclinic phenomena.

Recently Townsend and Johnson (1981, 1985) and Johnson (1984a) contrasted isobaric and isentropic zonally averaged meridional circulations; Figure 5-21 portrays isobaric and isentropic stream functions of the zonally averaged mass transport. Within the isentropic mass circulation the upward branch in tropical latitudes is associated with net heating while the downward branch in polar latitudes is associated with

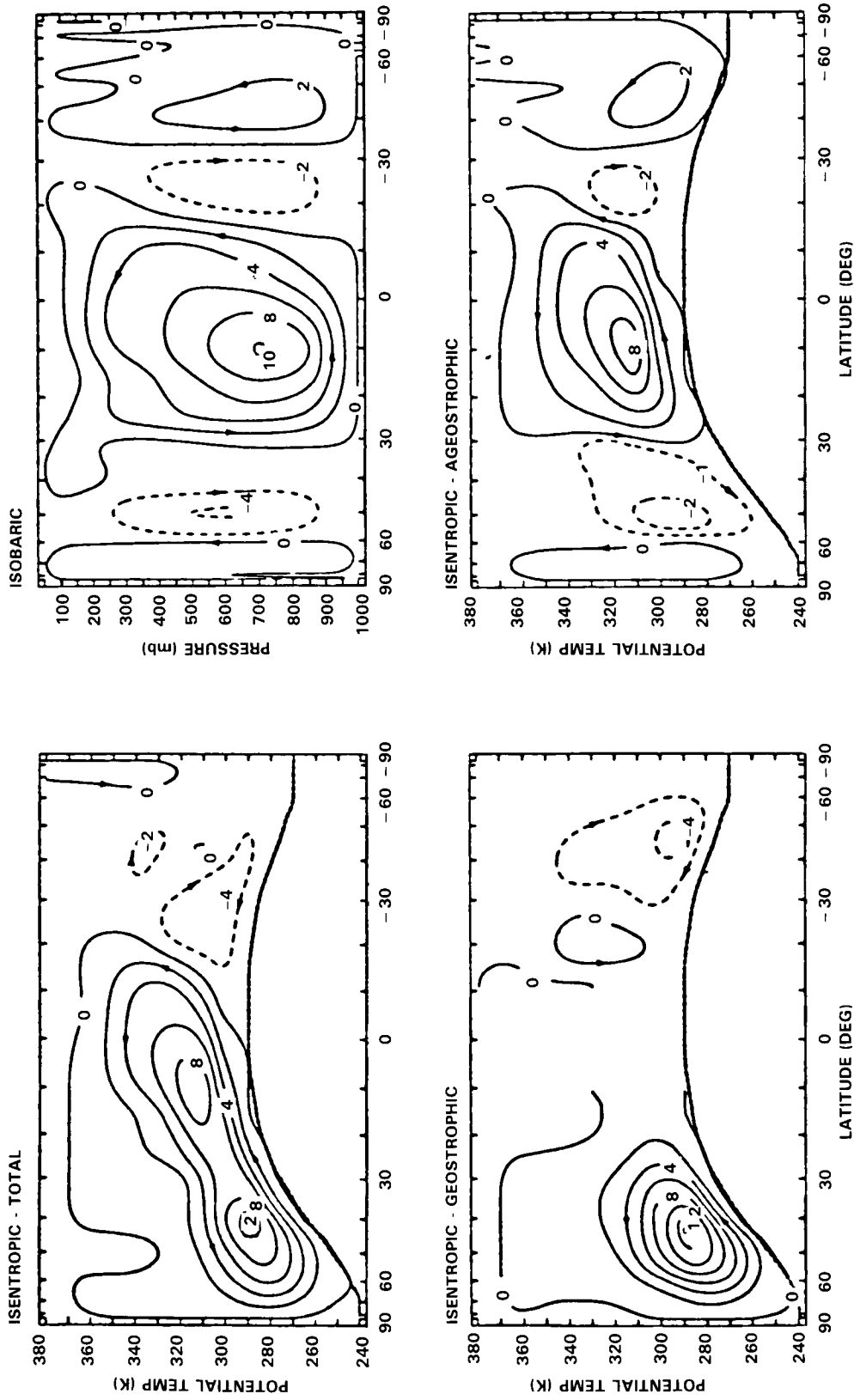


Figure 5-21. Mass stream function for the isobaric and isentropic mean meridional circulations for January (1979) (units,  $10^{10} \text{ kg s}^{-1}$ ). Arrows indicate the direction of the circulation. Note that a branch of the circulation spans the upper tropical troposphere and the lower stratosphere of middle and high latitudes.

## STRAT-TROP EXCHANGE

net cooling. As noted earlier, quasi-horizontal branches are required by mass continuity. These isentropic results verify Shaw's (1942) argument that the scale of the isentropic mass circulation corresponds with the scale of the differential heating.

While reasons for the differences between the scale of the meridional circulations in isobaric and isentropic coordinates involve several factors, one of the key factors is the degree of freedom for geostrophic mass transport in isentropic coordinates. Note in Figure 5-21 that the isentropic mass circulation can be partitioned into geostrophic and ageostrophic components. The scales of isentropic, ageostrophic meridional exchange are identical with the scales of meridional exchange in isobaric coordinates. Within low latitudes the mass transport within the isentropic Hadley circulation is through the ageostrophic mode while in extratropical latitudes it is through the geostrophic mode. Mean meridional velocities within this geostrophic circulation are of the order of a few meters per second and are of the same magnitude as the meridional velocities within the ageostrophic Hadley circulation. Isentropic mass circulations entail a handover between the ageostrophic and geostrophic modes of transport which does not require a change in the scale of horizontal transport within an isentropic layer (Johnson and Downey, 1975). This degree of freedom allows the establishment of a direct link between the global scale of differential heating and the scale of the atmospheric response, in the context of a temporally or zonally averaged mass circulation. The implication of this for stratosphere-troposphere exchange is that a portion of the meridional mass transport in upper isentropic layers begins in tropospheric regions of the tropics and subtropics and ends in the stratospheric regions of the extratropics and polar latitudes. One should note that within polar latitudes, the downward diabatic mass flux with respect to the isentropic stratification also provides for a systematic transfer of air from the polar stratosphere into the polar troposphere (Figure 5-21).

### 5.2.3.2 Geostrophic Modes of Mass Transport and Quasi-horizontal Stratospheric-Tropospheric Exchange Within Middle Latitudes

With regard to extratropical cyclones, jet streams, and baroclinic waves the quasi-horizontal stratospheric-tropospheric exchange will have characteristic features which are different within each of the phenomena and, as such, each of these phenomena deserves attention in order to understand their specific role. In summarizing atmospheric transport processes, Reiter (1972) reviews in detail the work of Reed, Danielsen, Staley, Reiter, Mahlman and others, and discusses exchange within each of these phenomena. Major emphasis has been placed on exchange processes attending jet streams. Viewed within a larger scale context however, none of these phenomena are independent since, within the structure of a large scale amplifying baroclinic wave in the westerlies (Newton and Palmen, 1963), all of these phenomena will be present. As a consequence all of the phenomena may be considered to be components of baroclinic instability or "sloping convection" (Hide and Mason, 1975) as it is realized in the actual atmosphere. Large scale meridional energy exchange within the amplifying baroclinic waves is accompanied by cyclo- and fronto-genesis in the lower troposphere in conjunction with jet stream circulations in the upper troposphere. In the following discussion the primary focus will be on physical processes within amplifying large scale baroclinic waves which provide for systematic stratospheric-tropospheric exchange through geostrophic modes of mass transport (Johnson, 1979).

Some physical insight into mean meridional motion within mid-latitude baroclinic waves is provided from the structure of a steady and an amplifying baroclinic wave (Charney, 1947; Eady, 1949). In the schematic (Johnson, 1979; Townsend and Johnson, 1985) showing the horizontal distribution of pressure and potential temperature of the steady baroclinic wave, the pressure and temperature are assumed to be in phase

(Figure 5-22). Within the zonal vertical cross-section of a layer extending from a lower isentropic surface  $\theta_1$  to an upper isentropic surface  $\theta_u$ , a midvalue isentropic surface  $\theta_m$  divides the hypothetical atmosphere into two regions. Ideally an isentropic surface  $\theta_m$  equal to 315 K would for the most part separate polar and subtropical air masses in the troposphere. In the cross-section, the dotted vertical lines designate trough and ridge positions that separate regions of poleward and equatorward geostrophic motion. The increase of wind with height reflects the thermal wind contribution from the baroclinic temperature distribution.

With a vertical scale linear in pressure, the relative position of the isentropes shows the greater mass ( $g^{-1}(\delta p/\delta\theta)d\theta$ ) in the layer between  $\theta_1$  and  $\theta_m$  to be positioned in the trough and lesser mass to be located in the ridge. The reverse mass distribution occurs in the layer above  $\theta_m$ . With the in-phase relation of the potential temperature and pressure fields, the intensity of the isentropic mass transport  $\rho Jv$  is symmetric about the trough line within each layer ( $J$  is the Jacobian of transformation,  $|\delta z/\delta\theta|$ ). The poleward mass transport forward of the trough is exactly balanced by equatorward transport to the rear of the trough. Thus, the mean meridional motion vanishes within each layer.

In the model of the amplifying baroclinic wave, the potential temperature is assumed to lag the surface pressure wave by a phase angle of  $90^\circ$  (see Figure 5-23). In the zonal cross-section, this lag of potential temperature introduces a westward tilt of the baroclinic wave in conjunction with the displacement of the coldest air to the inflection point of the surface pressure wave. A systematic structure results which provides for net poleward geostrophic mass transport above 315 K and an equatorward mass transport below 315 K. Ahead of the trough, poleward mass transport above 315 K located within a deeper layer of mass is greater than in the rear of the trough with its equatorward motion. Beneath 315 K the reverse

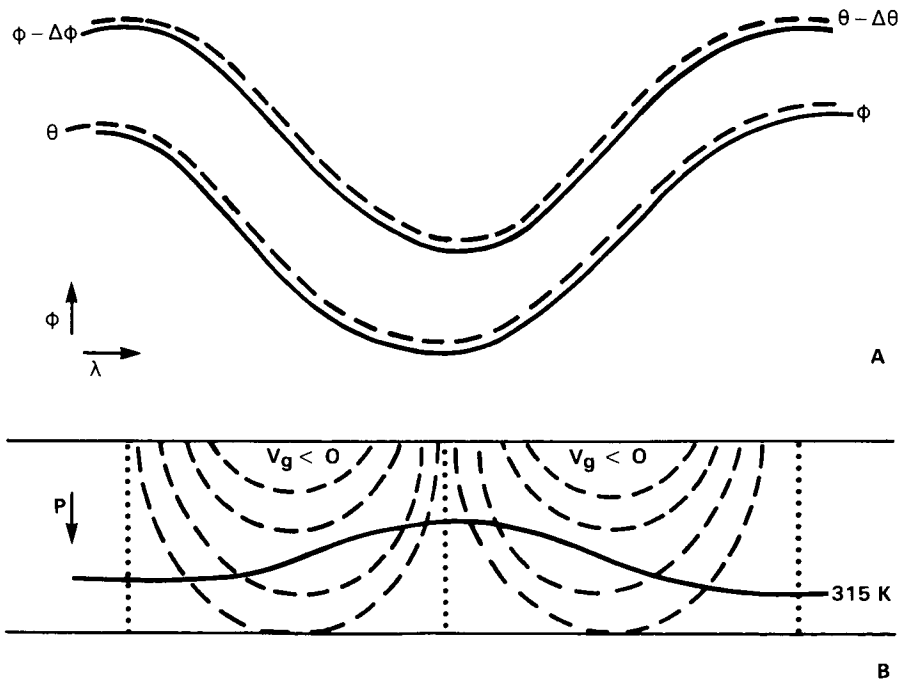


**Figure 5-22.** Schematics of horizontal ( $\lambda, \theta$ ) and vertical ( $\lambda, p$ ) distributions of geopotential and potential temperature within a steady baroclinic wave. In the zonal, vertical cross-section the dashed lines designate trough and ridge positions which separate regions of poleward and equatorward geostrophic motion within two isentropic layers. The layer in part (b) extends from a lower isentrope  $\theta_1$  to an intermediate isentrope  $\theta_m$  to an upper isentrope  $\theta_u$ . From Johnson (1979).

## STRAT-TROP EXCHANGE

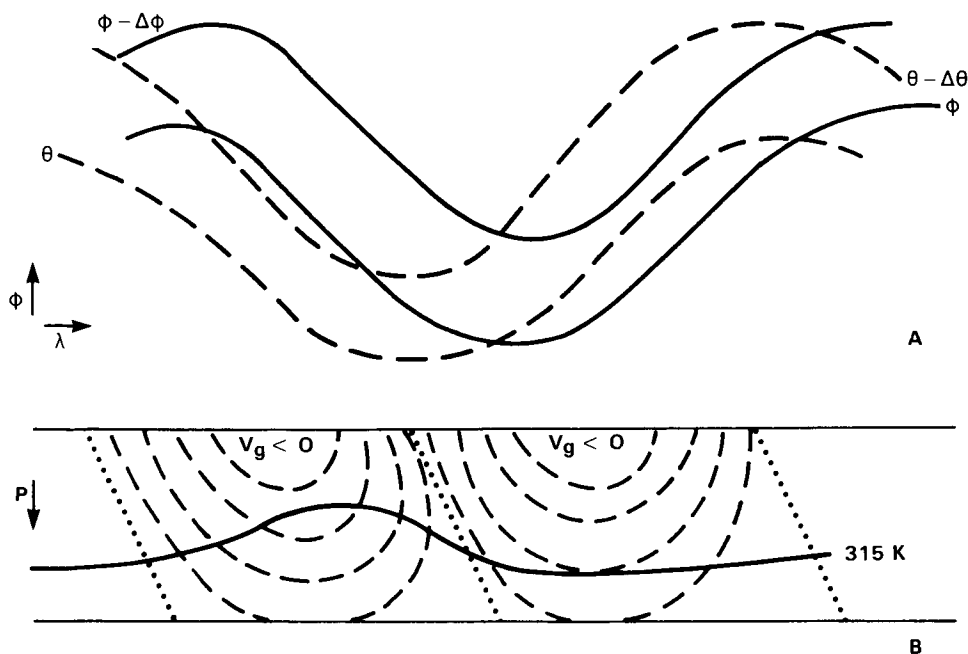


**Figure 5-23.** Schematic of amplifying baroclinic wave. See legend of Figure 5-22 for structural details.

occurs with more mass moving equatorward in the rear of the trough than ahead of the trough. As a consequence, the mean meridional mass transport within active baroclinic waves for this two-layered structure is poleward above 315 K and equatorward below 315 K.

The isentropic structure illustrated in Figure 5-24 transects a large amplitude wave that was studied extensively by Newton and Palmen (1963). This vertical cross-section is orientated nearly east-west along a line from Tucson to Bermuda. Newton and Palmen's analyses have been modified by rescaling the vertical coordinate. The layer extending from the earth's surface to 320 K contains more mass in regions of equatorward motion than in regions of poleward motion and reflects the strong equatorward movement of the polar air mass. Within the shaded area from 320 K to 335 K, more mass is located in the region of poleward motion (which is also more intense) than in the region of equatorward motion, reflecting the mean poleward movement of the subtropical air mass. The slope of the zero isotach indicates a westward tilt of the pressure wave with height in conjunction with the colder air to the rear of the surface pressure trough, the configuration of an intensifying baroclinic wave. Thus a mean meridional exchange occurring within this wave is similar to the exchange in the schematic of the amplifying wave. Since meridionally this layer spans the subtropical troposphere and the polar stratosphere, the structure indicates that the mean poleward motion is a mode of intrusion of tropospheric air into the polar stratosphere. It is interesting to compare Figure 5-24 with the cut off low described in Bamber *et al.* (1984), see also Section 5.2.6, where trace species profiles showed evidence of mixing over a considerable depth in the upper troposphere/lower stratosphere. This type of exchange would be suppressed in steady baroclinic waves. A similar structure of isentropic mass transport within an amplifying baroclinic wave is even more pronounced in Danielsen's cross-section through a baroclinic wave over the western United States for 1200 GMT, 13 April 1972 (see Danielsen's Figures 1 and 2, 1974). Geostrophic modes of mass transport exist within extratropical cyclones (Johnson and Downey, 1975), jet streams (Uccellini and Johnson, 1979) and baroclinic waves (Johnson, 1979, Townsend, 1980).

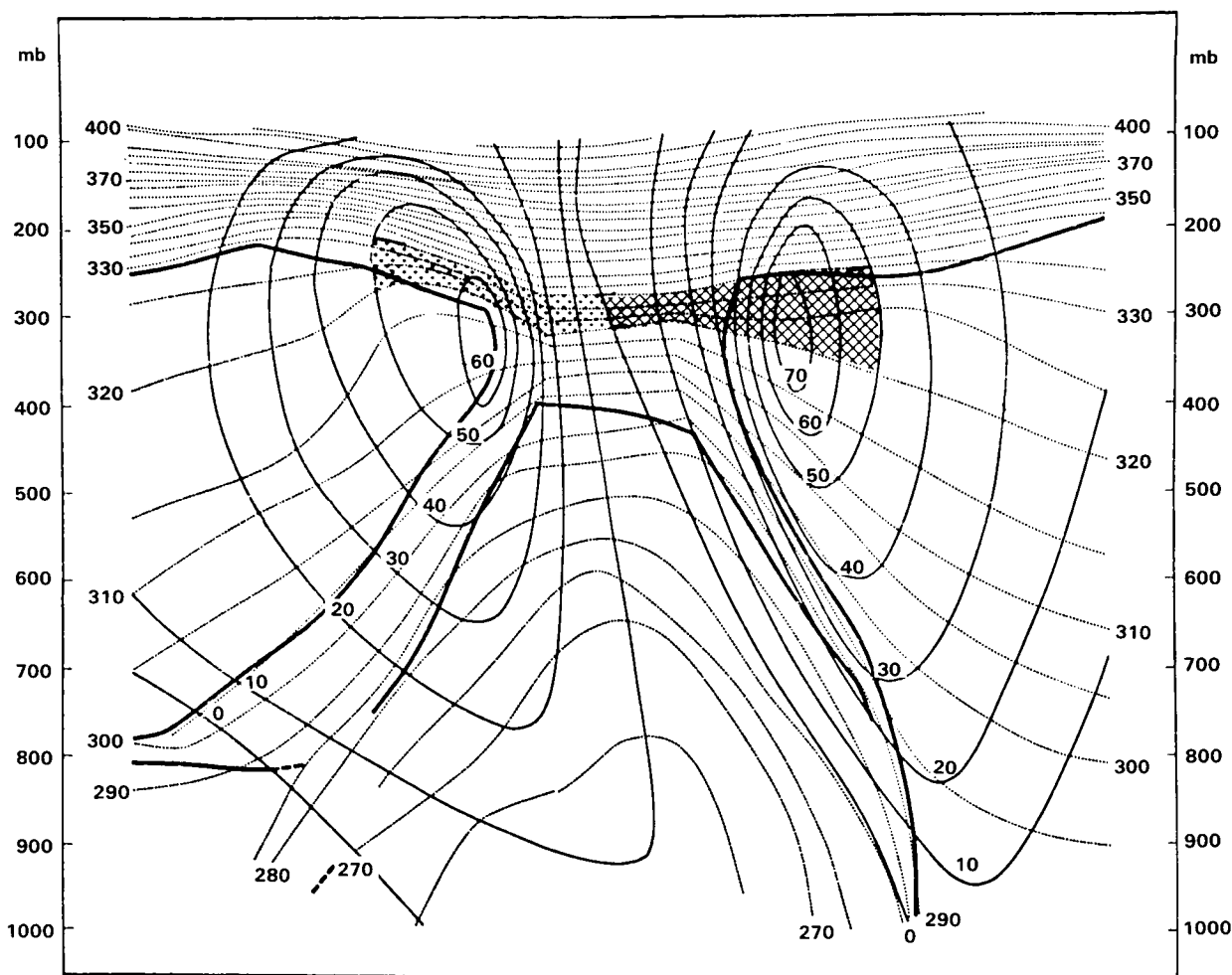


**Figure 5-24.** Vertical cross-section from Tucson to Bermuda through a large amplitude wave studied by Newton and Palmen (1963). Dotted lines are isentropes, solid lines are isotachs of the meridional wind while heavy lines are frontal boundaries and tropopause. Shaded regions show layer of positive covariance of mass and meridional motion embedded in wave structure.

In his study of the isobaric and isentropic circulation Townsend (1980) determined the isentropically time averaged mass transport along  $50^{\circ}\text{N}$  for the FGGE year (1979). Figure 5-25 shows results for the FGGE winter season from Townsend (1980). Note the systematic westward tilt of the zero isopleths of meridional velocity and the baroclinic structure that is indicative of the baroclinic instability process and a systematic geostrophic mode of mass transport. The tilt of the baroclinic disturbances extends upwards through the 360 K isentropic surface indicating that systematic stratospheric-tropospheric exchange is also present.

In interpreting the structure of the zonal cross-section of the isentropic meridional mass transport, one should realize the time averaged transport statistics are determined primarily by the isentropic geostrophic

## STRAT-TROP EXCHANGE

mass transport within all quasi-horizontal baroclinic circulations. As such, the isentropic statistics represent the average exchange occurring in what are commonly regarded to be both stationary and transient eddies in isobaric coordinates. Comparison with similar analyses in isobaric coordinates for 50°N would direct attention to transient components. For example, the embedded isentropic mass circulation in higher latitudes during the wintertime in Figure 5-21 is linked with propagating baroclinic disturbances which develop over the warm ocean currents off the east coasts of Asia and North America as cold polar air streams eastward and acquires latent and sensible energies from oceanic sources. The net meridional mass transport within the zonal cross-section (Figure 5-25) associated with such disturbances is located between 90°E and 90°W. Note that the equatorward mass transport in the low troposphere, which is part of the cold Asiatic winter monsoonal flow, is found between 90°E and 160°E while the poleward mass transport of warmer air is located between 160°E and 150°W.

The relatively large scale of the baroclinic feature from 90°E through 150°W and the depth also suggests that this feature is associated with a systematic poleward transport of tropical tropospheric air from the Philippine-Indonesia tropical convection zone within the Indonesian tropical belt. See Johnson and Townsend (1981, also Johnson, Townsend and Wei, 1985) for the mass and energy transport associated with these features at the planetary scale which within the three-dimensional structure provide for systematic intrusion of tropospheric air from the tropics into the stratosphere of higher latitudes.

### 5.2.3.3 Some Additional Aspects of Stratospheric-Tropospheric Exchange in Mid-latitudes

In studies of stratospheric-tropospheric exchange by quasi-horizontal transport processes, major emphasis has been devoted to the injection of ozone, radioactive debris and potential vorticity into the troposphere during cyclogenetic activity. With the higher concentration of these constituents in stratospheric air, these properties become excellent tracers of extrusions of stratospheric air into the troposphere. The condition that the concentration of ozone and radioactive debris in the troposphere is maximized during early spring has been associated with intense jet stream activity and deep convection during this season. Although these dynamic features partially explain the spring maximum of ozone concentration near the earth's surface in middle latitudes of the Northern Hemisphere, some aspects of this problem are related to seasonal variations of the isentropic structure of the stratosphere. During the winter an annual maximum of ozone develops in the polar stratosphere (Hering and Borden, 1965). With the energy deficit of the winter hemisphere and the development of an intense circumpolar vortex that extends from the troposphere upward into the stratosphere, isentropic layers climatologically located in the low polar stratosphere and the high troposphere of middle latitudes become entirely displaced into the stratosphere, though the effect of infrared cooling and consequent sinking of the isentropes and tropopause in regions where the mid-latitude upper tropospheric westerlies have moved equatorward. In the depth of winter such layers would not engage in stratospheric-tropospheric exchange in mid-latitudes. The lesser winter time extrusion of stratospheric air is also likely from the increased stratification which suppresses convective and symmetric modes of instability within or near hyperbaroclinic zones of jet streams. In spring, the troposphere of mid-latitudes rapidly warms, particularly over low-albedo land areas between 30° and 40°N, while the troposphere poleward of 50°N warms less rapidly. The result is that isentropic layers of the low stratosphere in winter become a part of the tropospheric circulation of the mid-latitudes during this season while within the troposphere the static and symmetric (inertial) stability of the atmosphere is decreased, in the sense that the horizontal wind shear on the anticyclonic side of the jet streams is increased. Active baroclinic waves in association with cyclogenesis and intensification of jet streams can now more actively tap the stratospheric reservoir of ozone through quasi-horizontal exchange processes which through increased inclination of isentropic surfaces transport ozone from the polar stratosphere into the lower troposphere of extratropical latitudes.

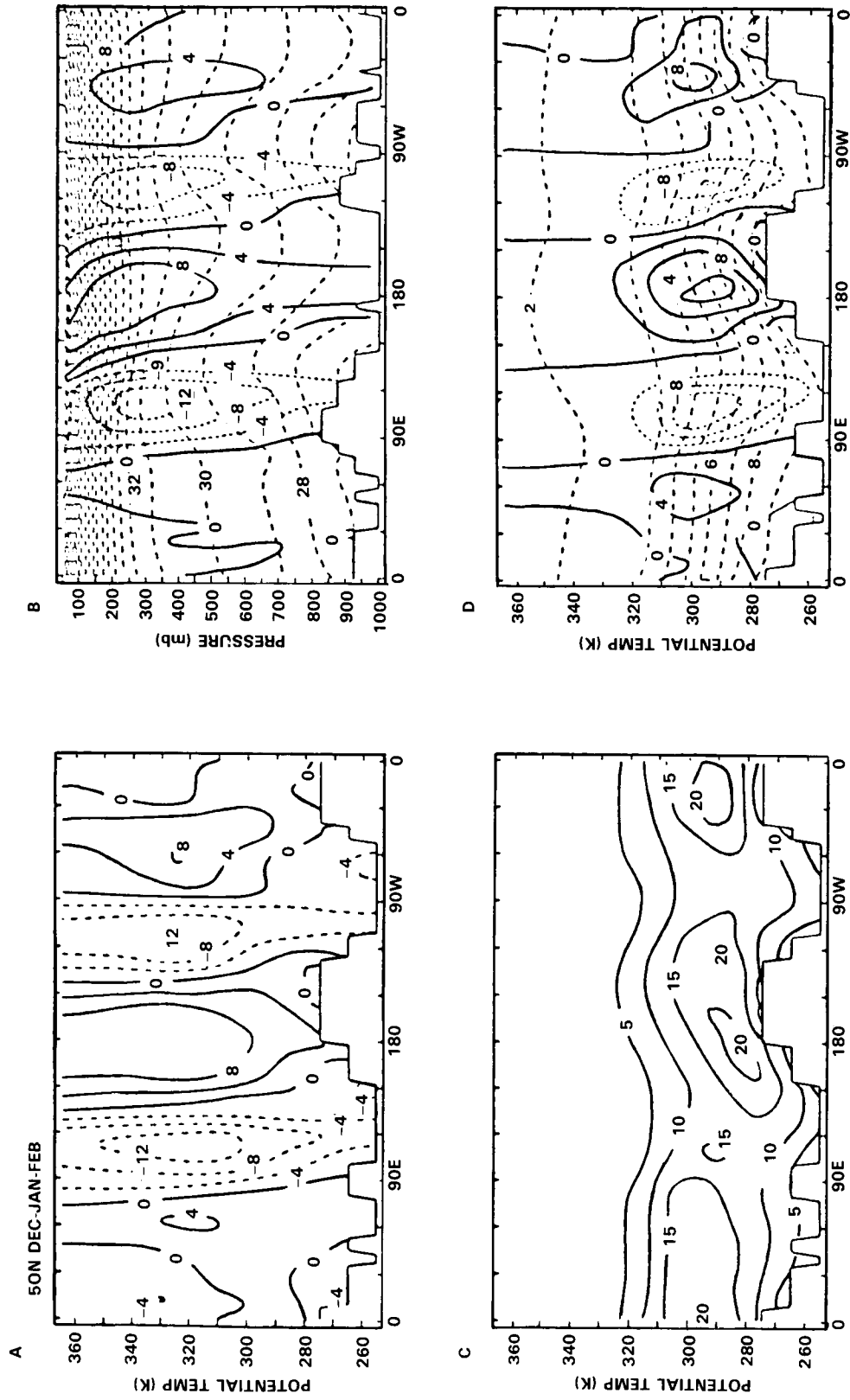


**Figure 5-25.** Zonal cross-sections along 50°N of the following: (a) Mass-weighted time-averaged meridional velocity,  $\langle v \rangle^t$  (units,  $\text{m s}^{-1}$ ), in isentropic coordinates; (b) Time-averaged potential temperature,  $\bar{\theta}^t$  (units, 10 K), and meridional velocity,  $V^t$  (units,  $\text{ms}^{-1}$ ) in isobaric coordinates; (c) Time-averaged mass distribution,  $\bar{e}J_{\theta}^t$  (units,  $10 \text{ kg m}^{-2} \text{ K}^{-1}$ ), in isentropic coordinates; (d) Time-averaged pressure,  $p^t$  (units,  $10^2 \text{ mb}$ ), and meridional mass transport,  $eJ_{\theta}^t$  (units,  $10 \text{ kg m}^{-1} \text{ K}^{-1} \text{ s}^{-1}$ ), in isentropic coordinates.

## STRAT-TROP EXCHANGE

The occurrence of the springtime maximum of injection of ozone into the troposphere which is associated with jet streams seems at first glance inconsistent with Allam and Tuck's (1984a and b) results that the maximum for the injection of water vapour into the stratosphere occurred in winter. The wintertime maximum of injection of water vapour into the stratosphere, however, is in accord with the wintertime maximum intensity of the isentropic Hadley mass circulation. The distribution of ozone with respect to the structure of isentropic mass transport depends on several factors. Thus, one should not expect that the maximum intensity of the extrusion of stratospheric ozone into the troposphere will occur at the same time as the maximum for the intrusion of tropospheric water vapour into the stratosphere.

In a recent study of the minor atmospheric constituents within a stationary low pressure circulation over the northeast Atlantic, Bamber *et al.* (1984) found substantial evidence for air of stratospheric origin in the upper troposphere of a cut-off, cold core polar low (i.e., one in which the upper troposphere has closed contours of geopotential height). On subsequent days moist convection within the troposphere of the cut-off low led to mixing of stratospheric and tropospheric air. Bamber *et al.* (1984) concluded that such circulations contribute to exchange of air between the stratosphere and troposphere; their case study is further described in Section 5.2.5.

An extratropical cyclone becomes a cut-off low through the process of occlusion. A cyclone occludes through developing a cold core vortex throughout its troposphere and a warm core vortex within the lower stratosphere. The development of the warm core vortex within the lower stratosphere entails isentropic mass convergence superimposed over isentropic mass divergence in the upper troposphere. Through the isentropic mass convergence within the lower stratosphere, stratospheric ozone-rich air descends into the climatological troposphere. Relative to other mechanisms the degree to which mixing within cut-off lows leads to irreversible transformation of stratospheric air into tropospheric air and a subsequent transfer of ozone into the troposphere remains to be determined. Finally, it is noted that the lapse rate of water vapour from the middle and high latitude tropopause to the hygropause, covering a factor of 30 decrease in mixing ratio, is good evidence of some return flow into the stratosphere (see Foot, 1984).

### 5.2.3.4 Summary of Isentropic Analyses

Stratospheric-tropospheric exchange within mid-latitudes, while occurring within baroclinic phenomena, extratropical cyclones, jet streams, and waves, involves planetary scale transport processes as well as deep convection. This exchange within mid-latitudes which primarily occurs through quasi-horizontal transport processes is in part determined by isentropic mass circulations which develop to transport energy from heat source to heat sink.

A primary objective of this discussion has been to relate large-scale quasi-horizontal transport within active baroclinic waves with systematic mass circulations which are forced by differential heating. Balance requirements inferred from zonally-averaged isentropic coordinates and results from FGGE dictate that the mass and energy transport within isentropic layers linking the polar stratosphere with the troposphere of the lower latitudes must be poleward. In lower isentropic layers the meridional mass transport and its geostrophic mode are equatorward. This net meridional mass transport in the isentropic zonally-averaged circulation structure occurs through a systematic covariance between the mass and meridional velocity within amplifying baroclinic waves. An analogy between concepts of sloping convection in a rotating fluid (Hide and Mason, 1975) and isentropic mass circulation occurring through geostrophic modes has been suggested by Johnson (1983, 1984a). The differing contexts provided by this large scale, averaged view and the detailed dynamical studies of exchange near mid-latitude jet streams will be discussed in Section 5.4.1.

#### 5.2.4 Review of Past Work on Exchange in Mid-Latitudes

Case studies of stratosphere-troposphere exchange have mostly consisted of aircraft flights near the polar front jet stream. By constructing wind and potential temperature cross-sections of jet streams from radiosonde data, Reed (1955) and Reed and Danielsen (1959) predicted on the basis of potential vorticity analyses that baroclinic zones beneath jet cores contain stratospheric air, and are therefore regions of active stratosphere-troposphere exchange. Most subsequent aircraft studies of jet streams were aimed at augmenting and lending detail to such cross-sections, making measurements by flying straight legs at constant pressure perpendicular to the maximum wind direction. Specially instrumented meteorological research aircraft have enabled a wide range of atmospheric parameters to be measured, with data from different flight levels combined by assuming no change in the jet stream structure during the mission (lasting about 6 hours).

Briggs and Roach (1963) reported 22 such flights in different regions of jet streams at various stages in their development. With measurements both of humidity and ozone concentration they could identify tracers for both tropospheric and stratospheric air. On all flights, a sharp gradient in tracer concentration was seen on the cyclonic side of the jet core, but only on a few flights did they observe a tongue of dry, ozone-rich air extending into the baroclinic zone beneath the core. This feature was most prominent in the entrance to middle regions of strong jet streams with straight or cyclonically curved contours. Frequently, the decrease in specific humidity within a baroclinic zone greatly exceeded the corresponding increase in ozone over background tropospheric concentrations, dry tongues being observed occasionally with no enhancement in ozone. Such results concur with more recent observations, where high values of potential vorticity were found to coincide with tropospheric concentrations of ozone (Shapiro, 1980; Vaughan and Tuck, 1985).

A systematic aircraft study of the extrusion of stratospheric air into the troposphere beneath jet entrances was coordinated by Danielsen (1964) in the early 1960s as a response to concern about anomalously severe episodes of radioactive fallout. Staley (1960, 1962) also analysed radioactivity data in this context. Mahlman (1965) examined the correlation between radioactivity deposition in the troposphere and a cyclogenesis index. Large atmospheric nuclear explosions prior to 1959 had deposited radioactive isotopes in the stratosphere. Effective mixing processes therein, combined with the moratorium on large nuclear tests after 1958, ensured that  $\text{Sr}^{90}$ , in particular, was by 1960 a reliable tracer for stratospheric air. By using several aircraft to collect filter samples of  $\text{Sr}^{90}$  around the same jet stream system Danielsen was able to investigate thoroughly the distribution of stratospheric air and the correlation between radioactivity and potential vorticity. An example of a cross-section showing both polar front and sub-tropical jet streams, taken from Danielsen (1968), is shown in Figure 5-26. Enhanced  $\text{Sr}^{90}$  concentrations occur beneath each jet stream, with some evidence of mixing also beneath the polar front jet core on its anticyclonic side. The distribution of potential vorticity calculated by hand from the cross-section displays a close correlation with radioactivity, verifying its use as a stratospheric tracer.

Danielsen uses the term 'tropopause fold' to describe the extrusion of stratospheric air beneath a jet stream. Such folds develop as part of the upper level frontogenetic process associated with an intensifying mid-latitude cyclone, and are initiated west of the upper-level trough behind a deepening surface vortex. Occurring thus beneath the entrance region of a strong cyclonically curved jet stream, the folds correspond to the conditions Briggs and Roach (1963) reported as favourable for the existence of dry, ozone-rich air beneath the jet core. The motion of air drawn into such folds was investigated by Danielsen using large-scale analyses of potential vorticity on isentropic surfaces drawn from radiosonde data, coupled with isentropic trajectory calculations. Maxima in potential vorticity, corresponding to tropopause folds, were



found to maintain their coherence in the tropospheric flow south of the jet stream system for a period of one or two days. Air from the fold depicted in Figure 5-26 was twice intercepted by aircraft as it traversed the United States. Radioactivity measurements demonstrated that the ratio of potential vorticity to  $Sr^{90}$  remained constant to within the accuracy of the observations. It was therefore concluded that potential vorticity and radioactivity could be used as tracers in the troposphere, with layers of high concentration gradually being eroded by small-scale mixing with ambient air. Cumulus and cumulonimbus entrainment on the cold side of the layer were identified as major agents in the mixing process, with mixing on the warm side being considered negligible by comparison. To compensate for the loss of air from the stratosphere in the folding process, Danielsen (1968) proposed a small mean inflow across the tropopause, which would also maintain the sharpness of the tropopause against the diffusive action of small-scale turbulence. A summary of his model of air flow during frontogenetic conditions, again taken from the 1968 paper, is shown in Figure 5-16. The analysis shown in Figure 5-27, due to Mahlman (1973) shows transverse mass transport diagnosed in a steady jet stream, and is consistent with Danielsen's idealized transverse circulation. Note that the region of ascent in this example includes the jet core. Its essential conclusions are supported by Reiter and Nania (1963) reporting several aircraft missions in the late 1950s to investigate clear air turbulence (CAT) near jet streams. Without tracer measurements, these flights can only illuminate the exchange problem indirectly but they do emphasise the role of the strong backing of wind direction with height beneath the jet core, observed in cyclogenetic troughs, in both the extrusion of stratospheric air and generation of CAT. CAT provides an additional process to mix the fold with tropospheric air, this time along the warm boundary where the wind shear is greatest.

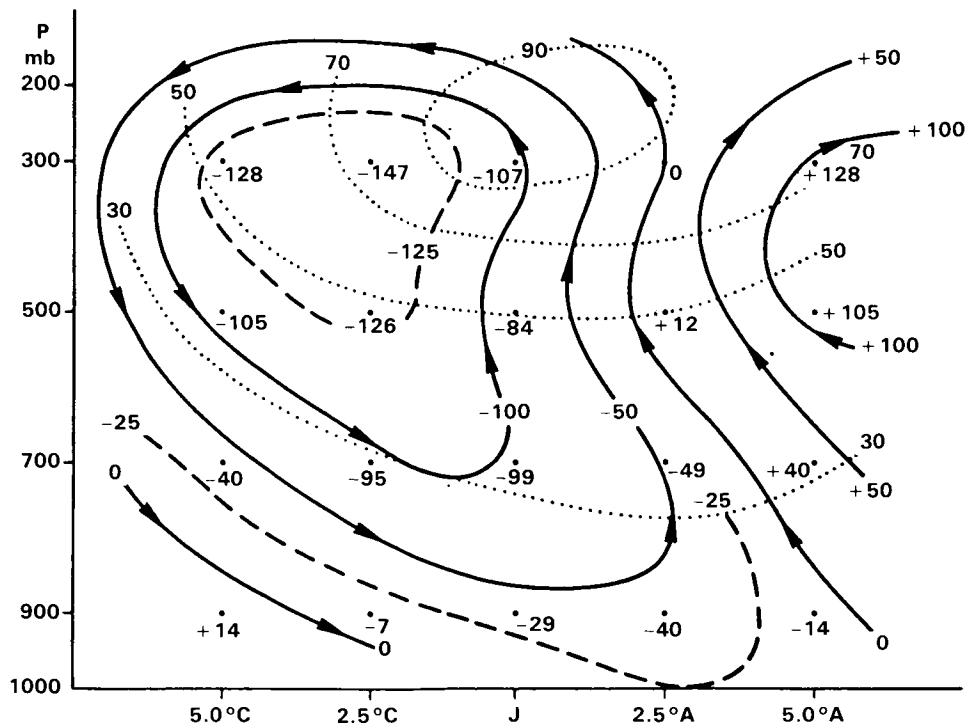


**Figure 5-27.** Mean mass transport stream function computed from vertical velocities in a steady polar front jet stream. Note vertical transport between 200 and 300 mb at and equatorward of the jet core. Units are  $mb\ m\ s^{-1}$ , the C and A labels on the abscissa refer to cyclonic and anticyclonic sides of the jet core, J. The averaging was performed relative to the flow, not fixed geographical coordinates. Mahlman (1973).

## STRAT-TROP EXCHANGE

With the instrumentation available in the 1960s, even aircraft-based investigations of jet streams were limited in their horizontal resolution, especially in the case of tracers - Briggs and Roach's ozone measurements, for instance, were 3-7 minutes apart, while Danielsen's radioactivity samples were taken every 20 minutes (although a cumulative count of  $\beta$  activity was recorded on his flights). The advent of inertial navigation systems and gust probes in the early 1970s allowed direct investigations of turbulence parameters, while the development of fast-response chemical sensors permitted a much more detailed delineation of tracer flow. Ozone, in particular, can now be measured reliably using chemiluminescent or ultraviolet absorption techniques with a time resolution of ten seconds or less, which corresponds to a horizontal resolution of a kilometre or better. Humidity, condensation nuclei and carbon monoxide concentrations have all been used as tracers of tropospheric air in recent studies. Good, fast-response measurements may be achieved of condensation nuclei and water vapour, especially by using a Lyman- $\alpha$  hygrometer for the latter (Kley *et al.*, 1979).

A comparison of ozone, radioactivity and potential vorticity on one jet stream cross-section flight was shown by Danielsen *et al.* (1970). Although broad agreement was claimed in the distribution of the three tracers, considerable structure was evident in both ozone and radioactivity above and on the cyclonic side of the jet core. This emphasises the difficulties encountered when investigating small-scale structure in potential vorticity with an aircraft. Although the absolute vorticity field may be resolved with confidence by flying across the mean flow, the stability must be estimated by interpolation between successive flight legs, with some guidance from nearby radiosonde ascents. Consequently, a derived potential vorticity field is both poorly resolved and subjective in nature. Objective local measurements of potential vorticity must await the development of aircraft-borne instruments to measure the local stability directly.

Further doubt of the suitability of potential vorticity as a tracer for stratospheric air was expressed by Shapiro and colleagues after a series of jet stream encounters with research aircraft in the 1970s. Shapiro (1974) found a close correlation between potential vorticity and ozone in both baroclinic zones beneath a double jet stream system, but deduced very high values of the former in the strong cyclonic shear zone on the stratospheric side of the maximum wind level. Four more research flights described by Shapiro (1976, 1978) also revealed a mesoscale region (about 100 km wide) of very strong cyclonic wind shear at the level of the jet core, leading him to deduce anomalously high values of potential vorticity there. As shown in Figure 5-28 (from Shapiro 1978), these do not correspond to anomalously high values of ozone. It must be emphasised that later, fast-response measurements of ozone ( $\tau < 10$ s) have revealed enormous variations in its concentration both in the fold region (Danielsen and Mohnen, 1977; Shapiro, 1980) and on the cyclonic side of the core (Vaughan and Tuck, 1985), which are presumably present also in the detailed potential vorticity field.

Reference has already been made to studies of the small-scale variations in ozone in cyclonic shear zones and tropopause folds. These, together with analyses of the turbulence parameters (Kennedy and Shapiro, 1975, 1980; Shapiro, 1980) have revealed a predominance of structures with length scales transverse to the wind direction of 10-20km (length scales along the wind direction are not known). This corresponds to about two minutes of flying time, and is much longer in horizontal scale than CAT. Turbulent fluxes may be calculated from gust probe and other fast-response instruments by the covariance method on the assumption that the motion is not ordered on the length scale chosen to calculate mean values (50-100km). Fluxes deduced in this way are completely dominated by components of the order of 10-20km in length. Shapiro (1980) suggests that these motions are wavelike phenomena with crests parallel to the jet stream axis, but further research is clearly necessary to determine both their nature and their net contribution to the turbulent transfer of heat and tracers.

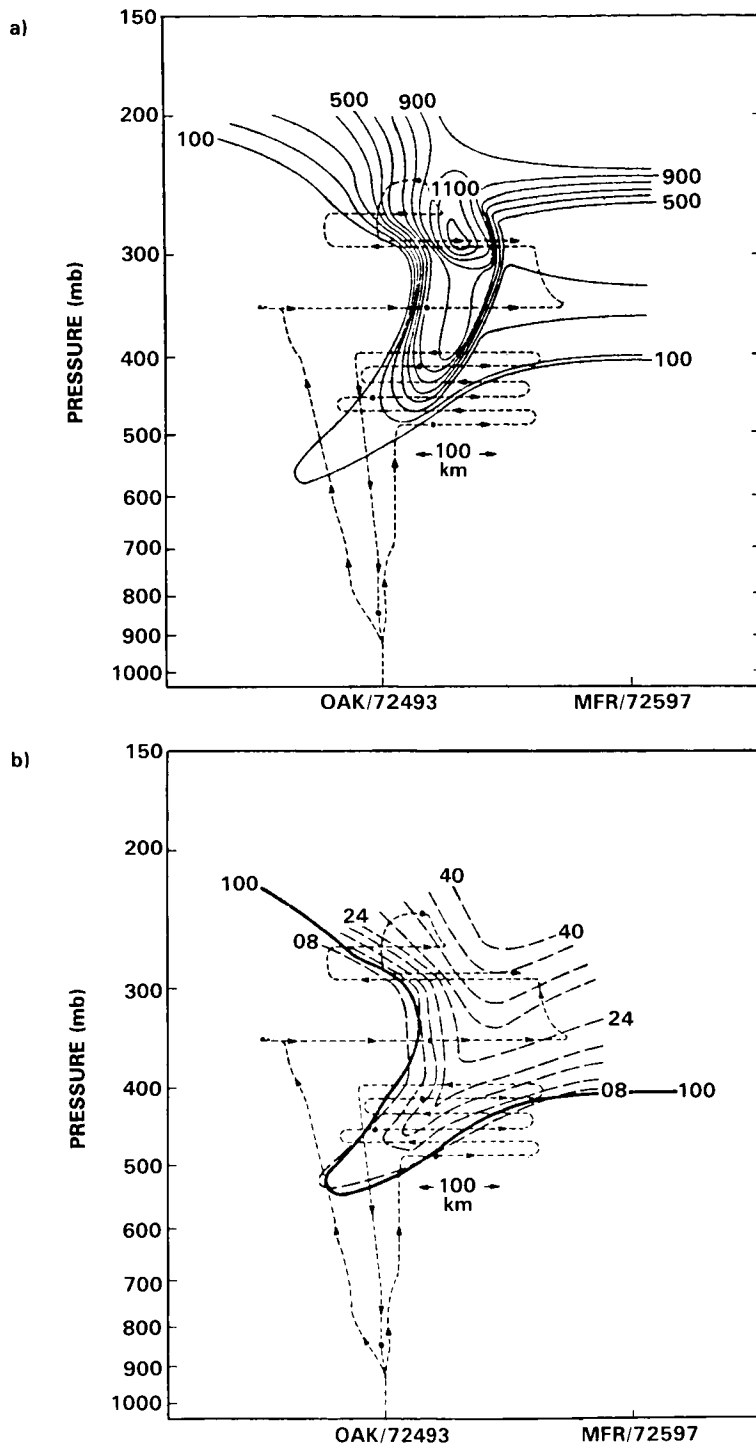


Figure 5-28. (a) Potential vorticity,  $10^7 \text{ K s}^{-1} \text{ mb}^{-1}$ , for 0000 GMT 16 April 1976. From Shapiro (1978).

(b) Ozone,  $10^{-8} \text{ vmr}$ , dashed lines;  $100 \times 10^{-7} \text{ K s}^{-1} \text{ mb}^{-1}$  isopleth of potential vorticity, solid line, same case as (a). Note that the region of high  $P_\theta$  gradient on the right of the intrusion is not accompanied by a similar anomaly of ozone. From Shapiro (1978).

## STRAT-TROP EXCHANGE

Observations with fast-response instrumentation revealed tropopause folds to be rather less homogeneous than previously believed. Incomplete correlation between ozone and potential vorticity and planetary boundary layer concentrations of condensation nuclei (Shapiro, 1980) as well as large horizontal variations in the ozone mixing ratio (Danielsen and Mohnen, 1977) suggest that these baroclinic zones can be regions of very active mixing. Direct flux calculations support Danielsen's (1968) view that most of the mixing occurs on the cold side of the fold.

Few estimates exist of the total mass of stratospheric air transferred into the troposphere in a folding event, and assume that air entering a tropopause fold in the cyclogenetic conditions described earlier is irreversibly removed from the stratosphere. The possibility that some of this air may be returned to the stratosphere at the jet exit (together with some entrained tropospheric air) has not been specifically investigated by aircraft flights, although humidity measurements in the lower stratosphere reported by Foot (1984) occasionally reveal very moist air - humidity mixing ratios greater than 15 ppm at 160 mb - well above the tropopause near the British Isles. Without isentropic trajectory analyses the source of this air could not be identified, although it did not appear to have originated near the polar front jet stream.

Measurements of reactive chemical species in regions of stratosphere - troposphere exchange can elucidate both the mixing of air and the chemical processes taking place as a consequence. Bamber *et al.* (1984) report hydrocarbon and ozone concentrations taken in a cut-off low with a cold core remaining in mid-latitudes after an intense period of meridional flow. Air between 7 and 10km was found to have chemical characteristics intermediate between those of the troposphere and stratosphere. The mixing of moist air from the former with ozone-rich air from the latter appears to have accelerated the removal rate of hydrocarbons, presumably by an enhancement of OH radical concentrations. Vigorous convective activity eventually eroded the intermediate layer, establishing a higher tropopause appropriate to its new latitude. More information is required on the extent of stratosphere-troposphere exchange in and around cut-off cold pools before a definitive estimate of their contribution to the total exchange can be made.

### 5.2.5 Recent Aircraft Studies near the British Isles

During April 1983, the C130 W Mk 2 aircraft of the Meteorological Research Flight was used to make 3 flights in a cut-off low (Figure 5-29) near the British Isles. Analysis of ozone traces and grab samples taken by the aircraft on the first two flights, on April 22 and 23, have shown this system to have two stratosphere-troposphere exchange events associated with it, which were found to have accelerated hydrocarbon oxidation, putatively by increasing [OH] (Bamber *et al.*, 1984). The vertical scale of the region of exchange at the centre of the low was 3-4 km (Figure 5-30), considerably deeper than the conventional picture of folds associated with jet streams. A third exchange event occurred in the cut-off low on April 23, as shown by a radiosonde ascent from weather ship C7R and the Total Ozone Mapping Spectrometer (TOMS) on board the Nimbus 7 satellite. Figure 5-31 shows the radiosonde ascents made on April 23 by C7R and the C130 aircraft, while Figure 5-32 shows a sequence of 6 days data from TOMS. Isentropic trajectories started at the point of origin of the large increases in O<sub>3</sub> column density track this feature in the TOMS data for 72 hours as it moves into the centre of the cut-off low (Figure 5-33). The aircraft flight on April 26 shows that the ozone mixing ratio below 5 km has increased, probably as a result of the earlier exchange events, and in the upper troposphere O<sub>3</sub> is almost identical with what it was on April 23 at the centre of the low. However, whereas on 23rd the air in this height range (6-9 km) was not clearly either stratospheric or tropospheric, by the 26th it was clearly beneath the tropopause, as shown by profiles of both temperature and CF<sub>2</sub>Cl<sub>2</sub> (Figures 5-34 and 5-35). By 26th, cumulonimbus clouds at the core of the low were reaching the tropopause, and presumably the updrafts and downdrafts

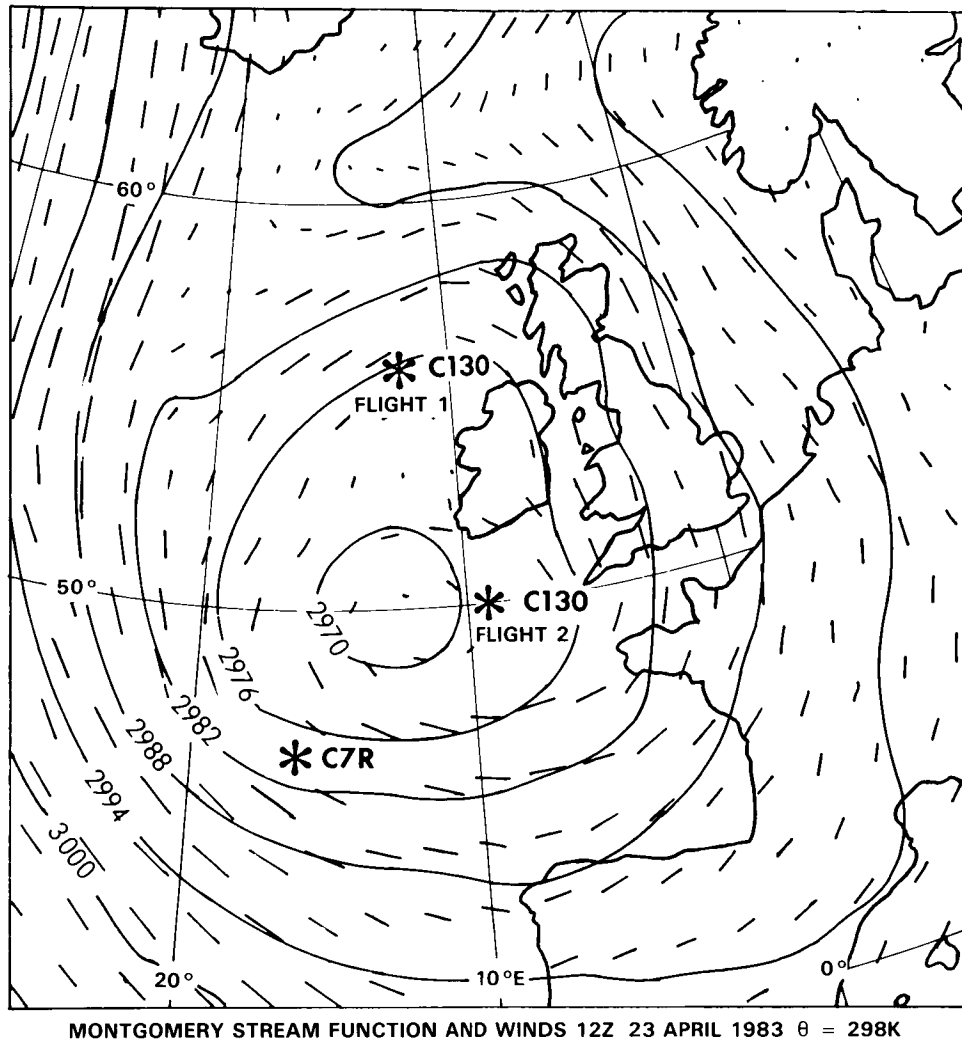


**Figure 5-29.** The cut-off low studied April 22-26. Montgomery stream function  $10^2 \text{ m}^2 \text{ s}^{-2}$  and winds ( $1 \cdot 1 \text{ cm} = 50 \text{ m s}^{-1}$ ) on the  $\theta = 298 \text{ K}$  surface are shown, 12 GMT, 23 April 1983. The feature persisted, with developments, until about 7 May.

involved were responsible for the changes in the  $\text{CF}_2\text{Cl}_2$  profile, which are consistent with the ozone changes in the lower troposphere. The fact that all three of these events are visible in the TOMS data and are supported as producing stratosphere-troposphere exchange by radiosonde profiles is encouraging. Two of the events clearly show evidence for extensive mixing of stratospheric air into the troposphere in the coincident trace gas and ozone data obtained by the aircraft; the third was just missed by the flight track on April 26. The meteorological assimilation field available in 1983 was the coarse mesh ( $1.875^\circ \text{ long} \times 1.5^\circ \text{ lat}$ ); it was used to produce isentropic trajectories at 6-hourly intervals which successfully tracked the enhanced column density feature in the TOMS data. By 1985, when further flights were attempted, in a NNW'ly jet stream in the Iceland-Scotland sector, the fine mesh ( $0.9375^\circ \text{ long} \times 0.75^\circ \text{ lat}$ ) was available and could resolve tongues of potential vorticity, well correlated and anticorrelated respectively, with the aircraft ozone and water vapour data. Again, note the vertical scale of the event (Figures 5-36 and 5-37). Note also that smaller scale features in the operational analysis potential vorticity field, to the

STRAT-TROP EXCHANGE

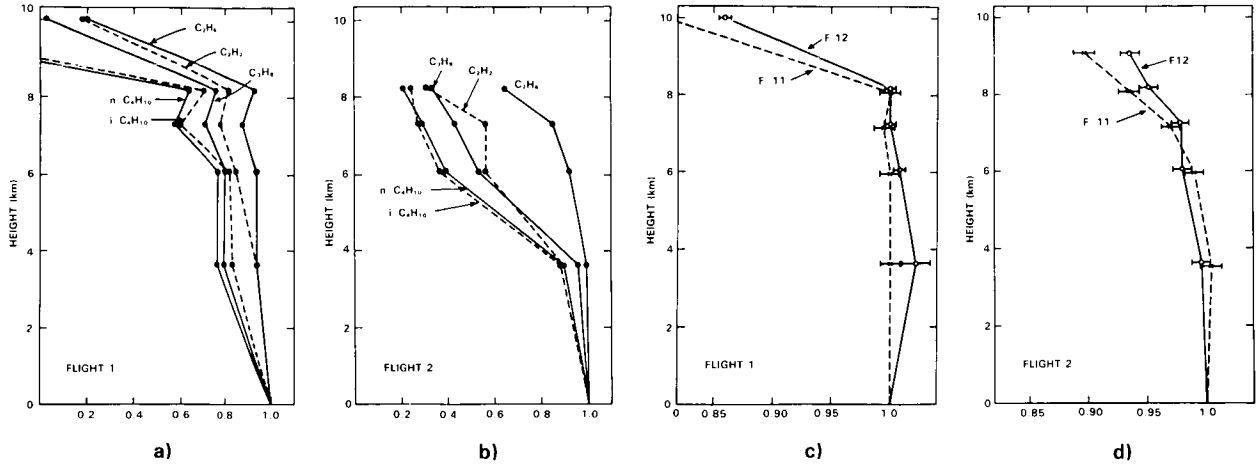


**Figure 5-30.** Flights made in the cut-off low shown in Figure 5-29. (a), (b) Vertical profiles expressed as fractions of the mixing ratios measured at 150 m for some light alkanes and acetylene. The dots represent measurements; lines joining them are included for illustrative purposes only. No butane isomers were detected in the top bottle on the first flight. For the second flight, a leak in the bottle containing air from 9.1 km prevented a hydrocarbon analysis. (c), (d) as (a), (b) but for F-11 ( $\text{CFCl}_3$ ) and F-12 ( $\text{CF}_2\text{Cl}_2$ ). Error bars are standard error estimates.

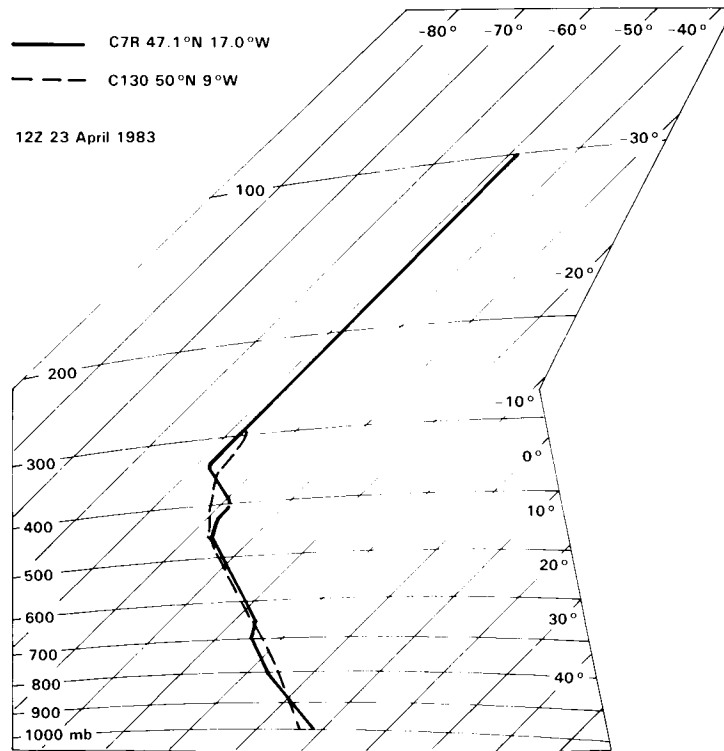
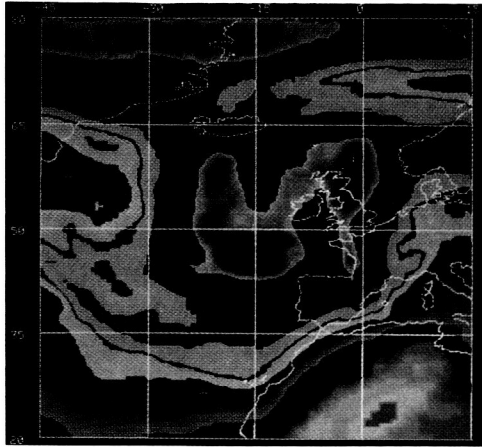


**Figure 5-31.** T- $\phi$  grams from weather ship C7R and the C130 (flight 2) in the cut-off low of Figure 5-29. The temperature curves are shown. Note the stable layer between 400 and 470 mb on the C7R ascent, and the layer between 300 and 500 mb on the C130 ascent with stability intermediate between typical tropospheric and stratospheric values.

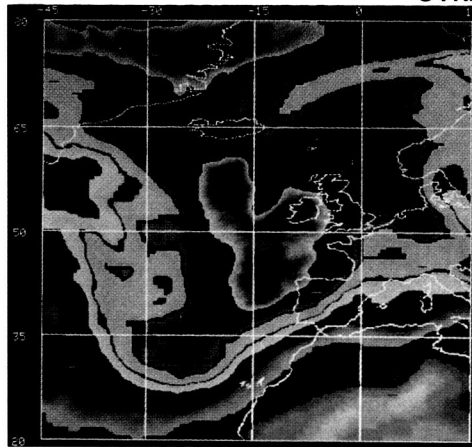
ORIGINAL PAGE  
COLOR PHOTOGRAPH

ORIGINAL PAGE  
COLOR PHOTOGRAPH

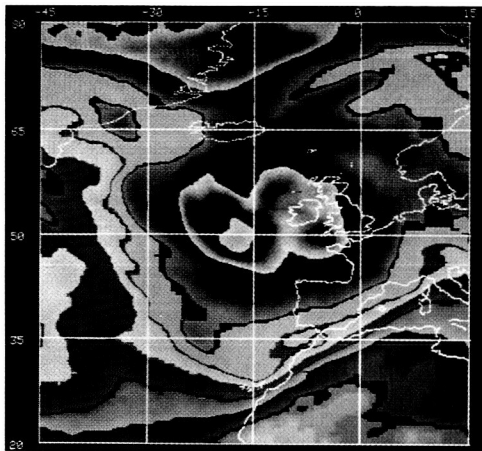
STRAT-TROP EXCHANGE



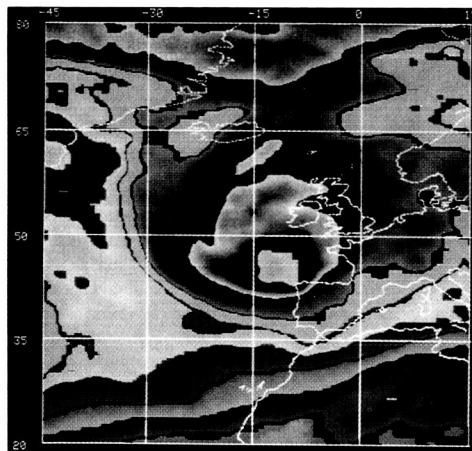
APRIL 21, 1983



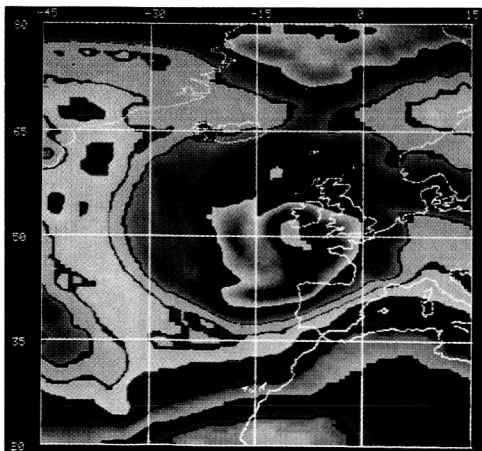
APRIL 22, 1983



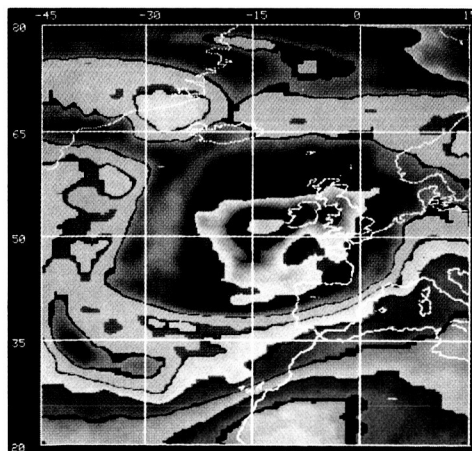
APRIL 23, 1983



APRIL 24, 1983



APRIL 25, 1983

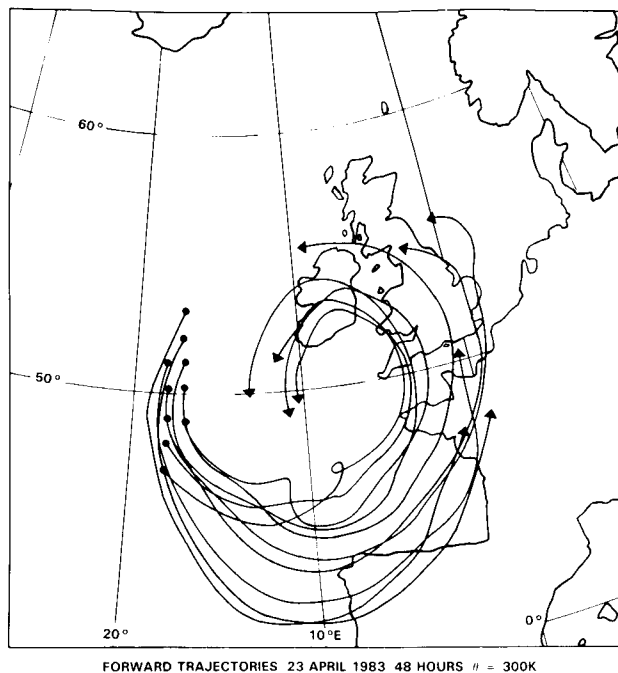


APRIL 26, 1983

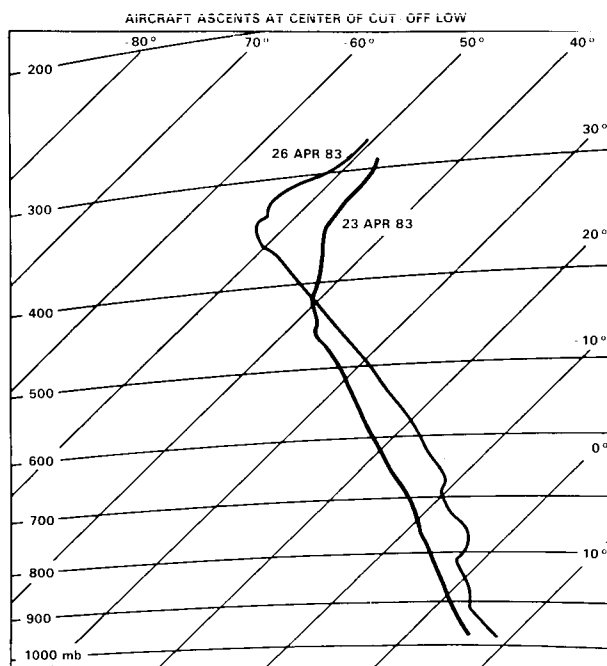


Figure 5-32. TOMS ozone data maps, illustrating cut-off low in the North Atlantic of Figure 5-29 using the color scale as shown. Diagrams are for 21-26 April 1983, in chronological order. By midday 27 April, the 500 DU contour at the center of the cut-off low had disappeared.

# STRAT-TROP EXCHANGE



**Figure 5-33.** Forward trajectories starting 12 GMT 23 April 1983, 48 hours on  $\theta = 300\text{ K}$  surface. Data are from coarse mesh assimilation; cf. Figure 5-32 for the behaviour of the area enclosed by the 500 DU contour.



**Figure 5-34.** C130 aircraft temperature profiles at centre of cut-off low, 23 and 26 April. Back trajectories for 26 April show air through the depth of the troposphere moving round the low centre.

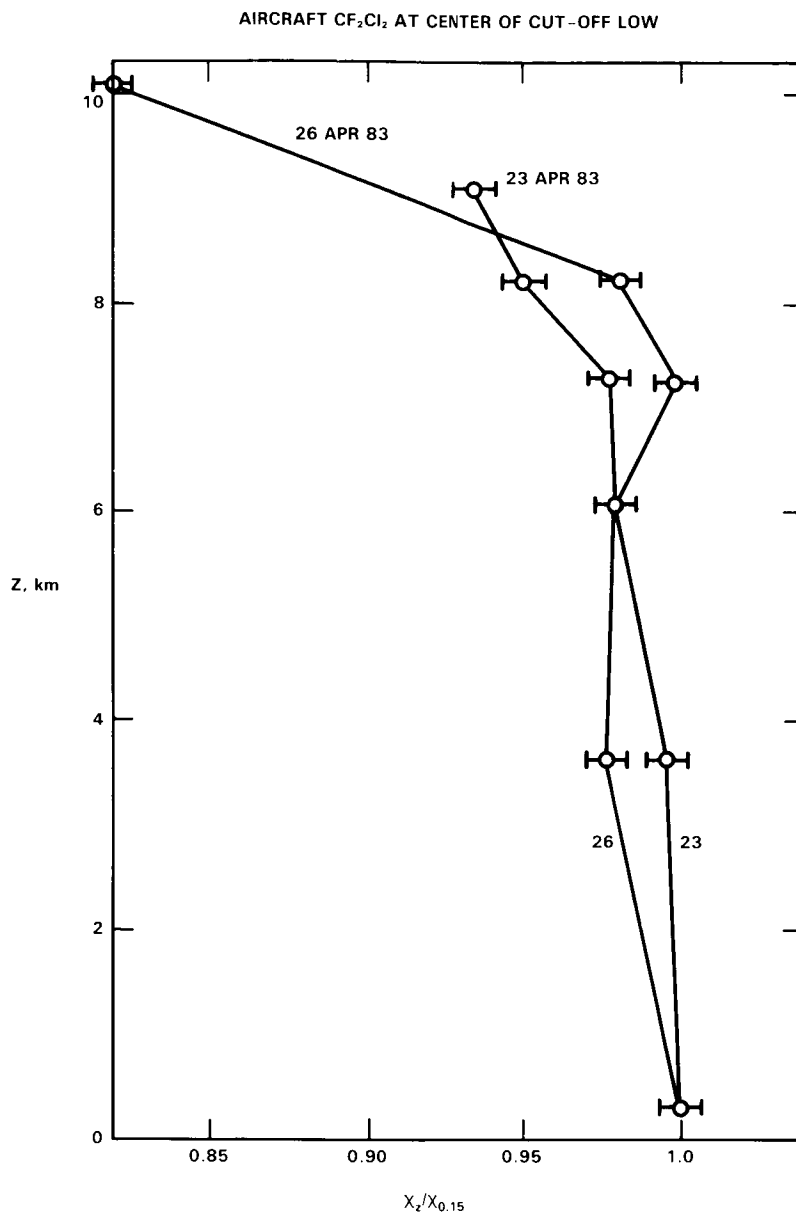


**Figure 5-35.** C130 aircraft CF<sub>2</sub>Cl<sub>2</sub> profiles at centre of cut-off low, 23 and 26 April; cf. Figure 5-34. The ozone profile changes were consistent with these, showing an ozone increase of 5-10 ppbv below 6 km by the later date (see text).

west and above the jet core in Figure 5-37, are independently corroborated by the aircraft data. This event was also studied by a flight parallel to the jet stream axis in the air bounded by the upper frontal surfaces (tropopause folds), and showed the ozone content to be very variable, but broadly increasing from ~60 ppbv beneath the jet exit to ~180 ppbv beneath the jet entrance. This development raises the possibility that if and when such resolution is available globally, it may be possible to combine meteorological analyses, TOMS data and aircraft studies to produce more reliable estimates of stratosphere-troposphere exchange on a global scale.

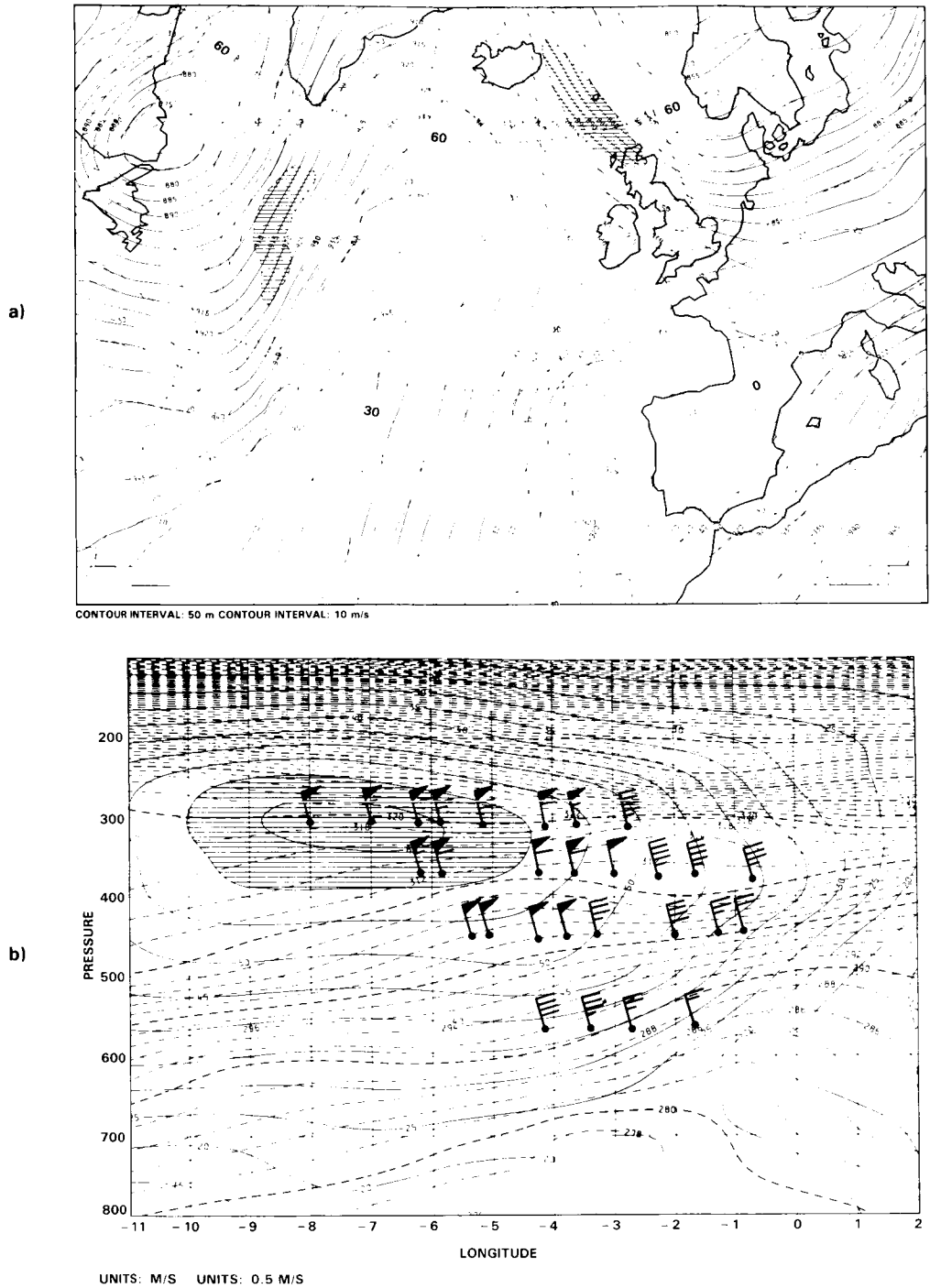


**Figure 5-36.** (a) Fine mesh analysis, 0000Z 27 April 1985, showing jetstream between Iceland and Scotland investigated by C130 aircraft. Dashed lines are isotachs,  $\text{ms}^{-1}$ , with values  $>60 \text{ m s}^{-1}$  shaded. Solid contours are 300 mb geopotential heights, dam. (b) Cross-section of wind speed ( $\text{m s}^{-1}$ , solid contours) and potential temperature (K, dashed contours) corresponding to the analysis in part (a). The section is along the  $60^\circ$  latitude circle; barbed arrows are aircraft winds, with fleches and triangles representing  $10$  and  $50 \text{ m s}^{-1}$ .

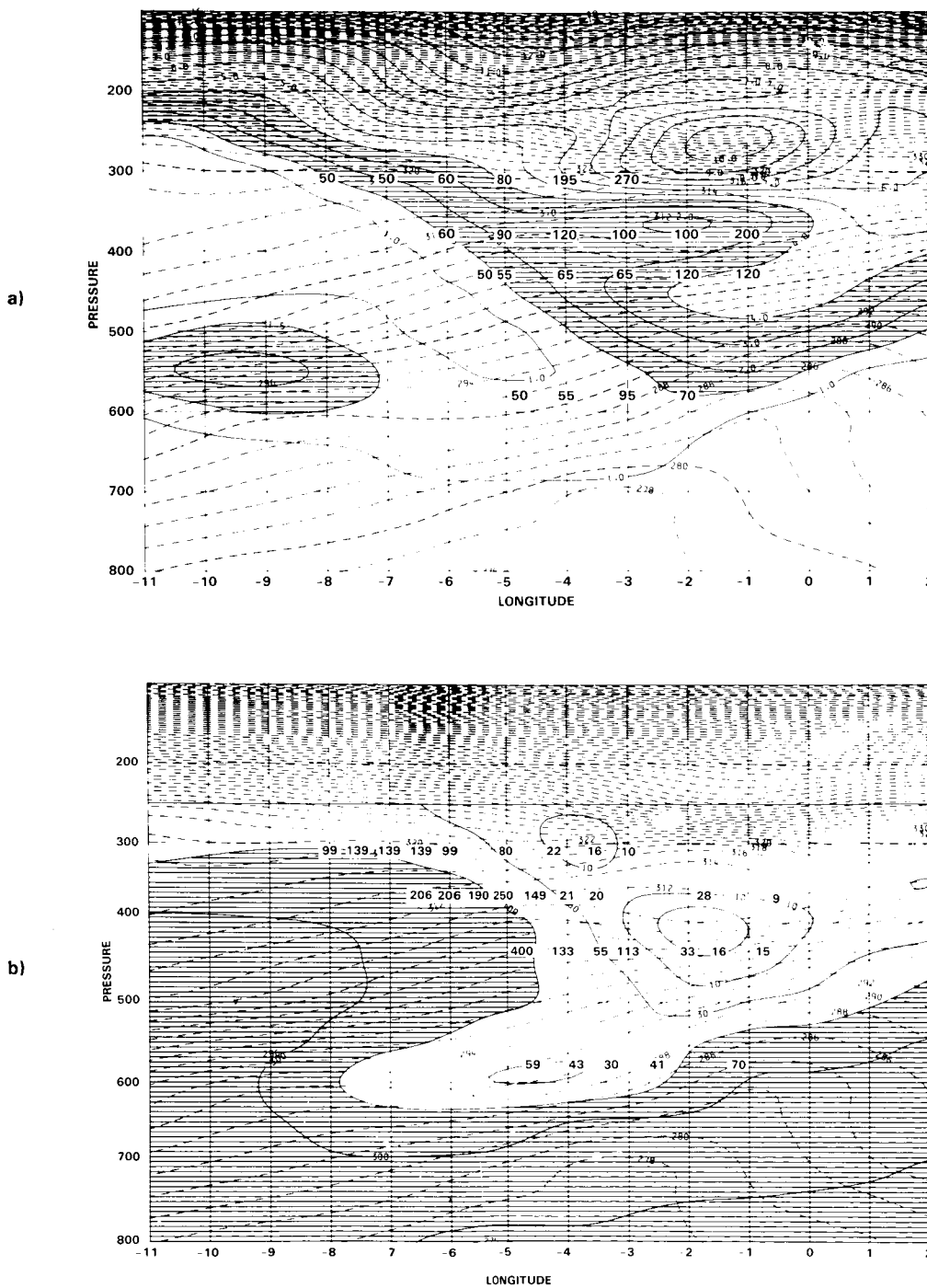


**Figure 5-37.** (a) Fine mesh cross-section of potential vorticity, derived from Figure 5-36(b); units are  $10^{-6} \text{ m}^2 \text{ s}^{-1} \text{ K kg}^{-1}$ ; values between 1.5 and 4.0 have been shaded horizontally. Spot values of aircraft ozone (ppbv) have been superposed as heavier numerals. (b) Fine mesh cross-section of water vapour mixing ratio ( $10^{-6}$  by mass), corresponding to Figure 5-36(b); values greater than 100 have been shaded horizontally. Spot values of aircraft water vapour, in the same units, have been superposed as heavier numerals.

## STRAT-TROP EXCHANGE

### 5.2.6 Recent Aircraft Studies over the South Western United States

During late April 1984, two NASA sponsored aircraft-experiments were coordinated to provide an extensive set of *in situ* and LIDAR measurements of tropopause folding events. Convair 990 and Electra aircraft, sponsored by the Global Tropospheric Experiment, GTE, made measurements in the troposphere and lower stratosphere, while a U2 aircraft, sponsored by the Stratospheric-Tropospheric Exchange Project, STEP, extended the stratospheric measurements to 21 km. These aircraft, equipped with fast responding sensors, made meteorological, trace gas and aerosol measurements of exceptional quality. Fast responding sensors are necessary to resolve the large gradients in the stratosphere and in the folds, and to permit cross correlations of all measured variables over a broad range of temporal and spatial scales.

Combining conventional meteorological analyses and numerical prognostic charts with special isentropic and cross-sectional analyses, Danielsen predicted the folding events and designed the aircraft flight paths. The U2 was flown above the jet core in a vertical plane oriented perpendicular to the wind, see Figure 5-38. It traversed this plane at four altitudes, separated by about 10,000 ft, making measurements on both sides of the jet, but skewed towards the cyclonic side. In approximately the same vertical plane the Electra was flown beneath the jet core, skewed towards the anticyclonic side. It traversed the tropopause fold and made essentially continuous vertical profile measurements of ozone and aerosol backscatter by a vertical (downward) pointing LIDAR. The objective here was to determine whether the ozone rich air in the fold descended towards the surface boundary layer and if it did, to measure the ozone dilution caused by the entrainment of tropospheric air at the boundaries of the fold. A much more complicated flight path was assigned to the CV-990, including a horizontal traverse across the jet core towards the center of the large scale cyclonic vortex, a descent into the ascending cold air, a traverse of the folded tropopause layer and then a return flight in the layer.

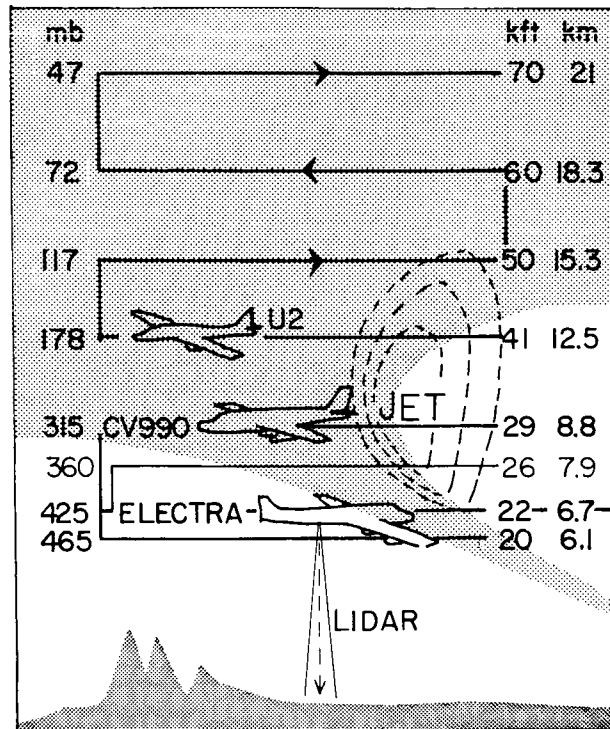


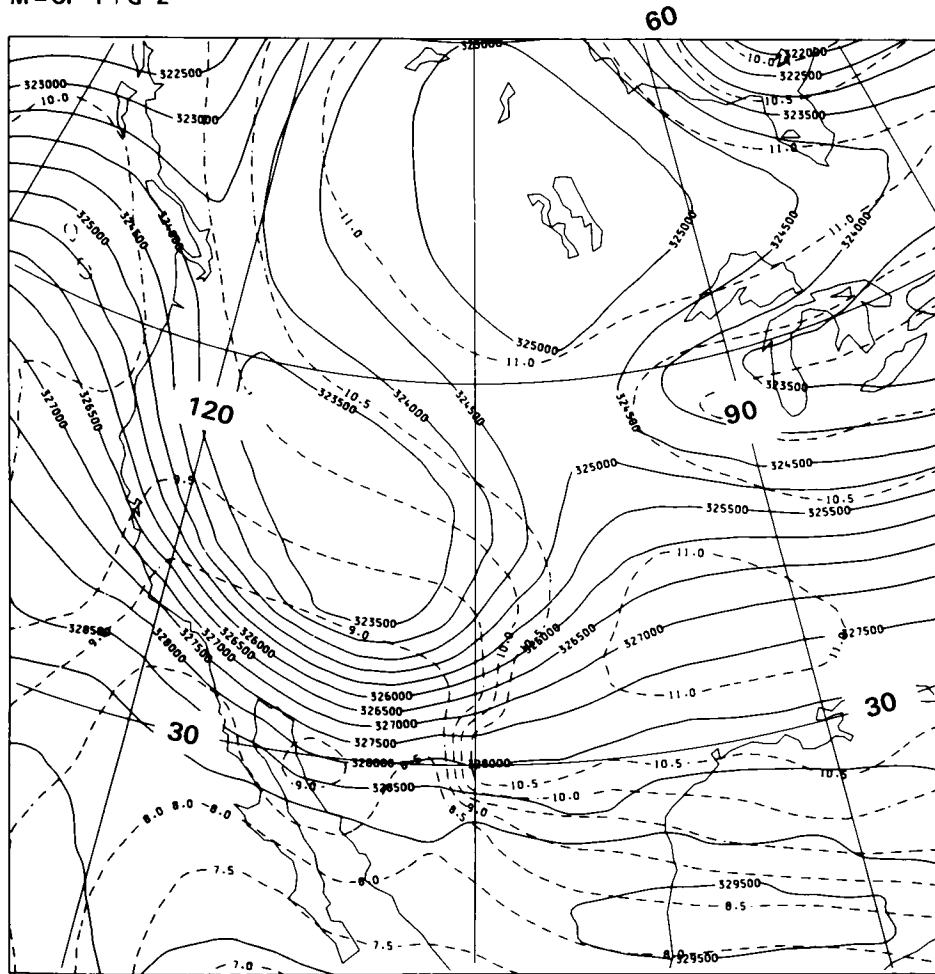
Figure 5-38. Flight paths in vertical plane relative to jet stream axis and tropopause fold.

## STRAT-TROP EXCHANGE

The cyclonic vortex which formed rapidly on April 20, 1984 over the southwestern United States is shown in Figure 5-39. The winds are approximately parallel to the contours of the Montgomery potential,  $\psi_M = c_p T + gz$ . Wind speeds are approximately inversely proportional to the spacing of the  $\psi_M$  contours. In this case, typical of the springtime cyclones, the jet wraps around the south side of the vortex, with speeds in excess of 130 kt. The detailed structure of this vortex is shown in the TOMS map of total ozone (see Figure 5-51).

Horizontal flight paths of the three aircraft are delineated in Figure 5-40. The letters along the CV-990 path identify reference points to be used in comparing trace gas measurements to the computed distribution of potential vorticity.

E.C.M.W.F. DATA FOR WESTERN U.S.A.  
 MONTGOMERY STREAMFUNCTION-THETA = 330.0  
 VALID AT 12Z ON 20/4/84 DAY 111  
 M = CP T + G Z



CONTOUR INTERVAL: 5 mb

**Figure 5-39.** Cyclonic vortex which developed rapidly over south western United States on 20 April 1984. Jet stream on this  $\theta = 330$  K surface is west and south of vortex where contour gradient is maximum. See text for description.

## STRAT-TROP EXCHANGE

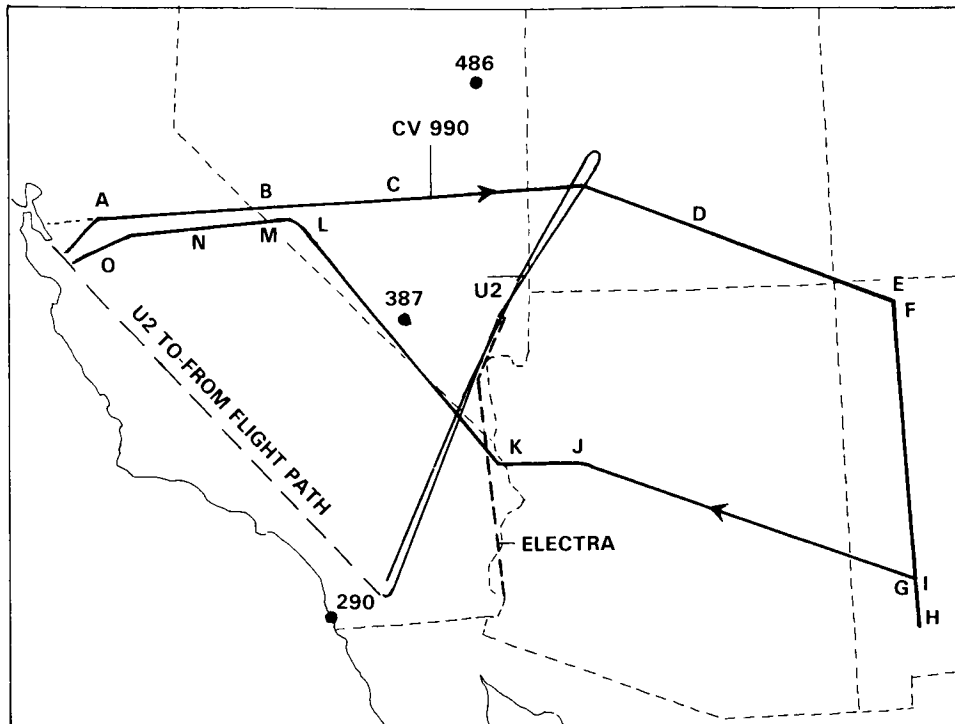


**Figure 5-40.** Flight paths (horizontal) of the three aircraft that made measurements in vortex on 20 April 1984. Letters on 990 path identify relative maxima and minima of tracers. Numbered dots identify 3 of 6 radiosonde stations used in analysing Figure 5-41.

### 5.2.6.1 Analyses and Measurements at and below the Jet

The distributions of potential temperature  $\theta$  in the vertical, from points A to I, and the wind speeds normal to the vertical planes are presented in Figure 5-41. These cross sections were prepared from a set of vertical and horizontal (constant pressure) analyses, mutually adjusted to assure spatial and temporal consistency. A total of nine vertical cross sections were prepared first along lines of radiosonde stations approximately perpendicular to the flow. Thermal and wind speed gradients were then transferred to a set of seven constant pressure charts and analysed. After adjustments were made these analyses were transferred to the vertical planes of the 990's flight path. Finally,  $P_{\theta}^{\dagger}$  was computed and contoured at a grid of points from Figure 5-41a. (The superscript denotes data subjected to a low pass filter). The distribution of  $P_{\theta}^{\dagger}$  (Figure 5-41) plus another 12 hours later were used to derive, by linear interpolation in time, the  $P_{\theta}^{\dagger}$  values for successive positions of the 990.

This labour intensive, time consuming effort was made to determine the diagnostic potentials of radiosonde data. Throughout the analysis only radiosonde observations were used. All flight data were reserved to test the final solutions. Could a three-dimensionally consistent analysis resolve a folded tropopause structure whose horizontal dimensions are less than the separation distance of radiosonde stations? Also, could a representative distribution of potential vorticity be computed from these analyses? The result of one such test is shown in Figure 5-42. The variations of  $P_{\theta}^{\dagger}$  versus time derived from the cross section analyses (continuous bold line) is plotted along with slightly smoothed ozone and carbon monoxide

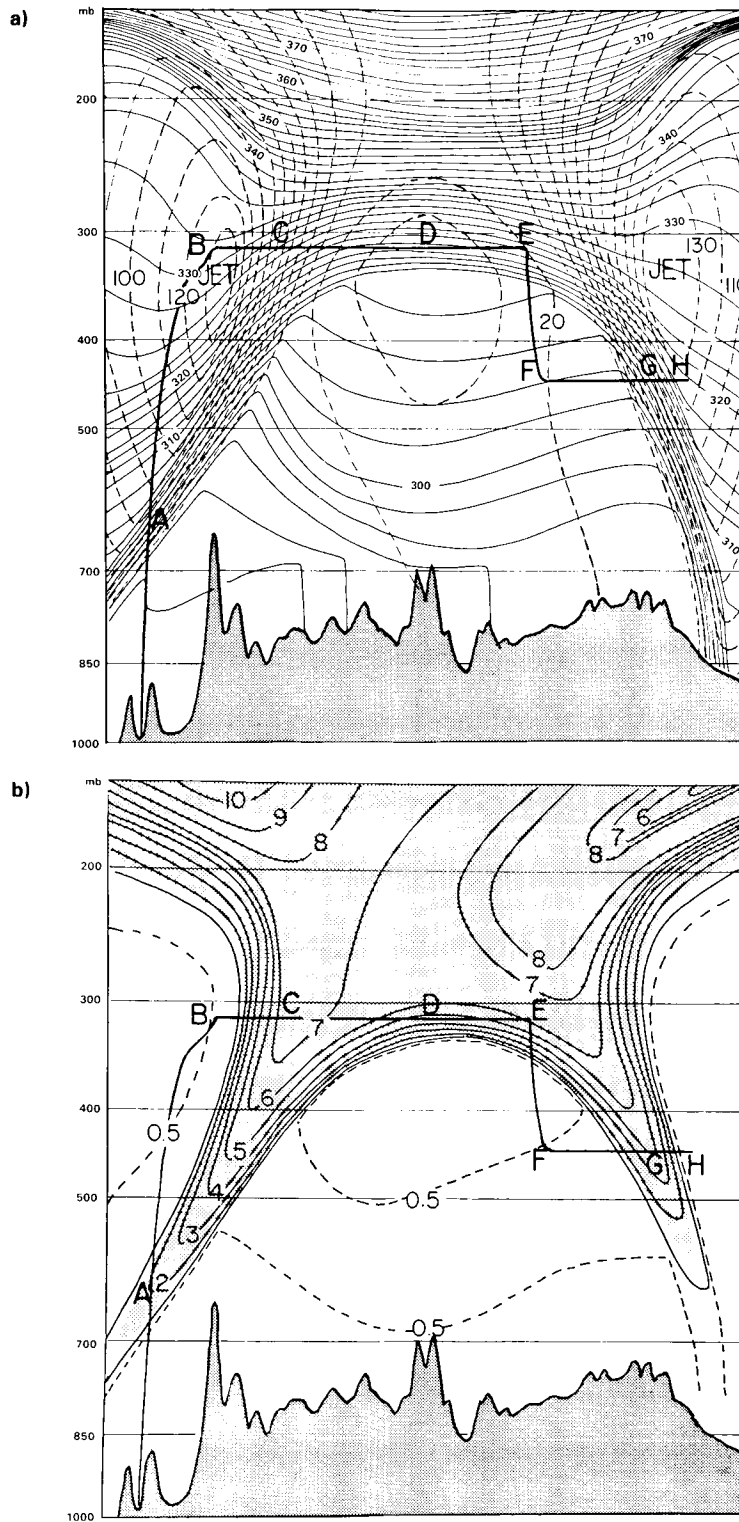


**Figure 5-41.** Vertical cross-sections along 990 flight for 1200 GMT, 20 April, 1984 including: (a) Potential temperature, 2K interval, and wind velocity normal to cross-section (10 knot contour interval). (b) Potential vorticity, along same cross-section, in units of  $10^{-5} \text{ cm}^2 \text{ s}^{-1} \text{ K g}^{-1}$ .

## STRAT-TROP EXCHANGE

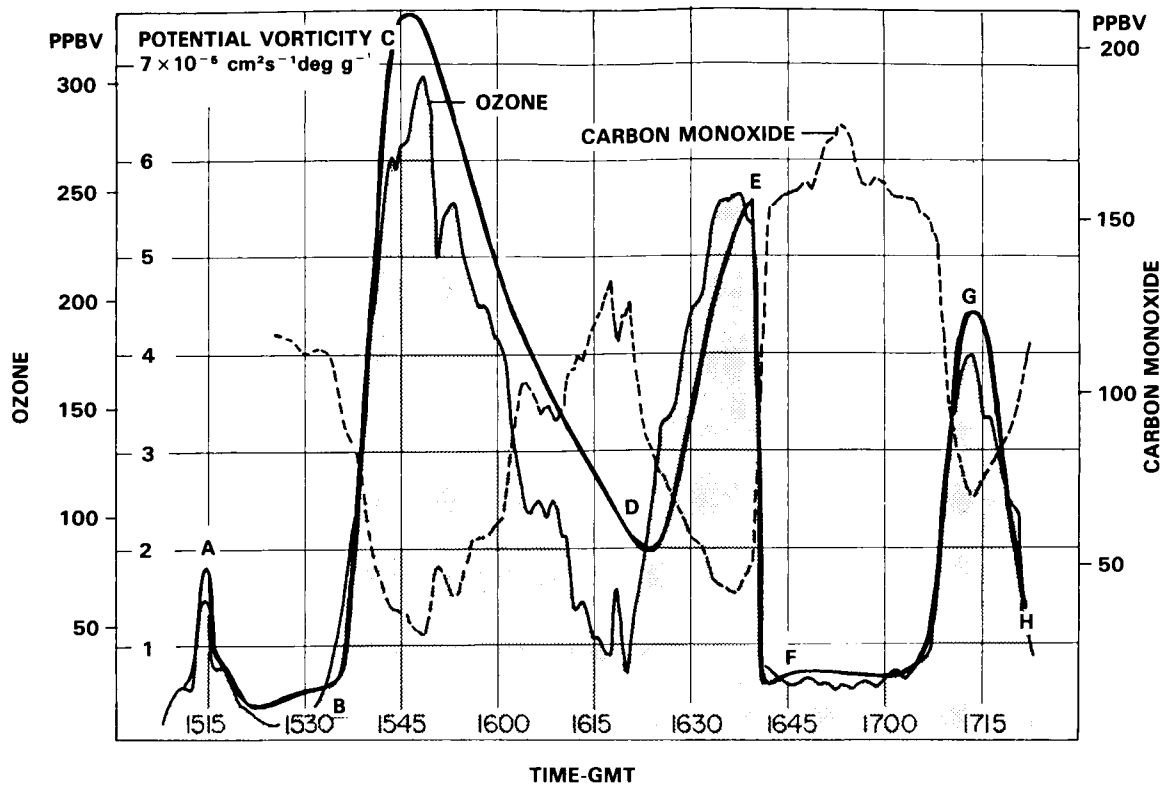


**Figure 5-42.** Potential vorticity  $P_\theta$  (bold line), derived solely from radiosonde data, versus lightly filtered ozone and carbon monoxide data from 990 flight.

measurements from the 990 aircraft. The ozone measurements are by courtesy of G. Gregory of Langley Research Center, the CO by G. Sachse, also of Langley.

Two results are obvious. Except for a small phase error near point D, where the linear interpolation was too crude,  $P_\theta$  and the ozone mixing ratio  $\chi_{O_3}^1$  are positively correlated and proportional to each other. Secondly,  $P_\theta$  and  $\chi_{O_3}^1$  are both negatively correlated with  $\chi_{CO}$ . Therefore  $P_\theta$  and  $\chi_{O_3}^1$  both function as representative stratospheric tracers while  $\chi_{CO}^1$  functions as a tropospheric tracer.

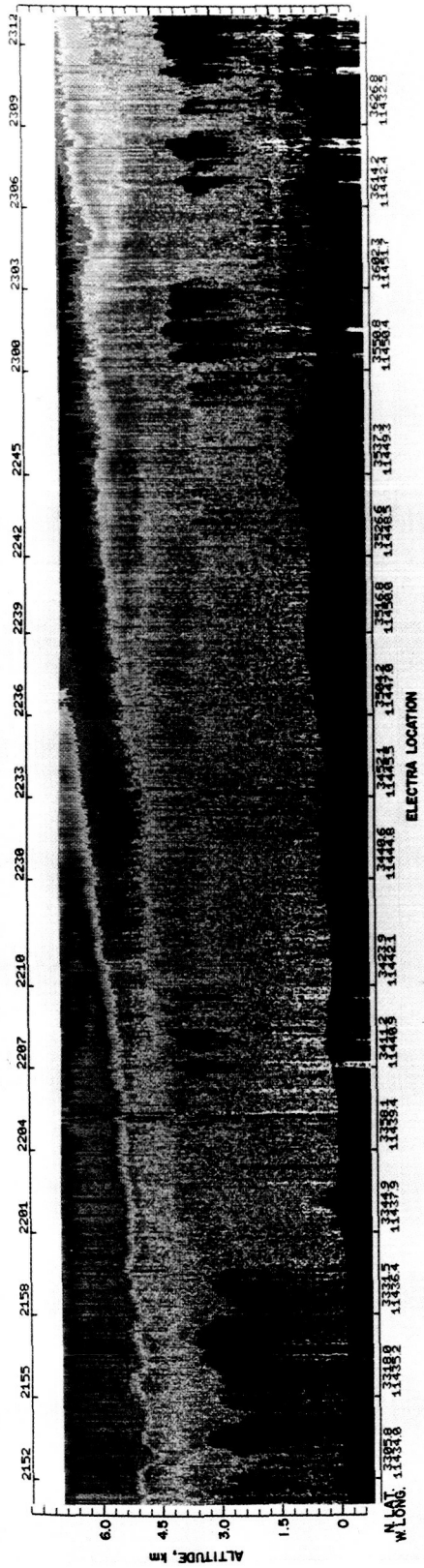
Another conclusion to be drawn from Figures 5-42 and 5-16 is that entrainment of tropospheric air and mixing are responsible for the decrease in  $P_\theta$  and  $\chi_{O_3}^1$  down the axis of the fold and, by implication, mixing is responsible for the gradients in the lower stratosphere. There is no evidence here of a loss of correlation as would be expected if  $P_\theta$  were independently changed by gradients of diabatic heating or if  $\chi_{O_3}$  were significantly changed by photochemistry.

Airborne DIAL measurements (Browell *et al.*, 1983) of aerosol distributions at 600 and 1064 nm were made from 1 km below the aircraft to the ground and ozone profiles were obtained over a 4 km altitude range also starting 1 km below the aircraft. *In situ* measurements of ambient temperature, dew point, ozone, and aerosol number density were made onboard the Electra.

Results of the first airborne DIAL aerosol and ozone measurements across a tropopause fold event are presented in Figure 5-43a and 5-43b. These data were obtained with the Electra flying at an altitude

AIRBORNE DIAL AEROSOL MEASUREMENT OF TROPOPAUSE FOLD EVENT  
 APRIL 20, 1984

TIME, GMT



## STRAT-TROP EXCHANGE

of 8.2 km ASL. The violet region at the bottom of Figure 5-43a is the topography along the Electra flight track. The planetary boundary layer (PBL) can be seen to rise to a depth of about 3.0 km above the surface. Convection in the PBL is associated with thermal plumes that originate at the surface and rise to the top of the PBL, where it gives rise to the irregular appearance of the boundary layer top. Several clouds are seen to be present near the top of the PBL, and a few of these clouds are optically thick to the laser beam which produces a shadow below them. The free troposphere typically has a lower aerosol loading than the PBL and this can also be seen in Figure 5-43a. Due to the enhanced aerosol loading from volcanically derived aerosols, the stratospheric air exhibited greater aerosol scattering than did air in the free troposphere. This contrast in scattering permitted the use of aerosols as a tracer of the stratospheric air mass. In Figure 5-43a the stratospheric air can be seen in a layer having a depth of  $\sim 1.5$  km from north of Las Vegas, Nevada, on the right side of the figure to near Yuma, Arizona, on the left. For the first time, the stratospheric air mass resulting from a tropopause fold was continuously traced down to the top of the PBL. Internal gravity waves were induced in the fold by the action of the PBL. It is expected that in addition to the mixing taking place across the boundaries of the fold in the free troposphere, mixing processes at the top of the PBL would mix the diluted stratospheric air into the PBL.

Calculations of the optical scattering properties of the tropospheric and stratospheric aerosols sampled *in situ* at 6.7 km altitude also show an enhancement of a factor of 2.2 in expected aerosol scattering from the stratospheric aerosols compared to the tropospheric aerosols at a laser wavelength of 1064 nm (Browell *et al.*, 1985). This enhancement in scattering resulted primarily from a factor of 4.3 increase in the total number density of aerosols in the 0.5 to 0.9  $\mu\text{m}$  diameter range and the presence of large aerosols in the 0.9 to 2.2  $\mu\text{m}$  diameter range.

The airborne DIAL system also obtained the distribution of ozone along the same flight track. The DIAL remote measurements of ozone are given in Figure 5-43b with higher ozone mixing ratios represented by the yellow and orange display. The maximum ozone level remotely measured in the stratospheric air was 240 ppbv in the centre of the layer near 2232 GMT. This agreed closely with the maximum value of 225 ppbv measured *in situ* at 6.7 km altitude. The concentration in the layer decreased to the 120 ppbv level in the layer above the PBL near 2152 GMT. The correlation coefficient between the DIAL derived aerosol and ozone distributions were calculated over 5 minute intervals with a vertical resolution of 210 m and a horizontal resolution of 2.1 km (105 shot average). The correlation coefficient between ozone and aerosol for each segment across the entire layer was greater than 0.8. This correlation reflects the high degree of spatial coincidence between the ozone and aerosol concentrations determined by the DIAL system.

Potential vorticity was calculated along a transect through the jet stream for 0000 GMT on 21 April 1984. A trajectory analysis was performed to determine the potential vorticity distribution in the cross section along the Electra flight track (see Figures 5-40, 5-41). A plot of potential vorticity isopleths which corresponds to the DIAL obtained aerosol and ozone cross-sections shown in Figure 5-43a and b is given in Figure 5-44. These results were obtained solely from the analysis of radiosonde data. The location of the boundary layer top corresponds closely to the lidar data in Figure 5-43a. The width and altitude of the potential vorticity levels indicating the location of stratospheric air near the top of the PBL on the left of Figure 5-44 agrees in general with the spatial location of the stratospheric air as determined by the DIAL system. Since the potential vorticity is calculated from widely spaced radiosonde data, the analysis cannot resolve the small scale gravity waves seen in the lidar data. In general, the potential vorticity analysis accurately defines the relative characteristics of the stratospheric intrusion. The depth of the layer as determined from the potential vorticity analysis agrees with the lidar measurements; however, the location of

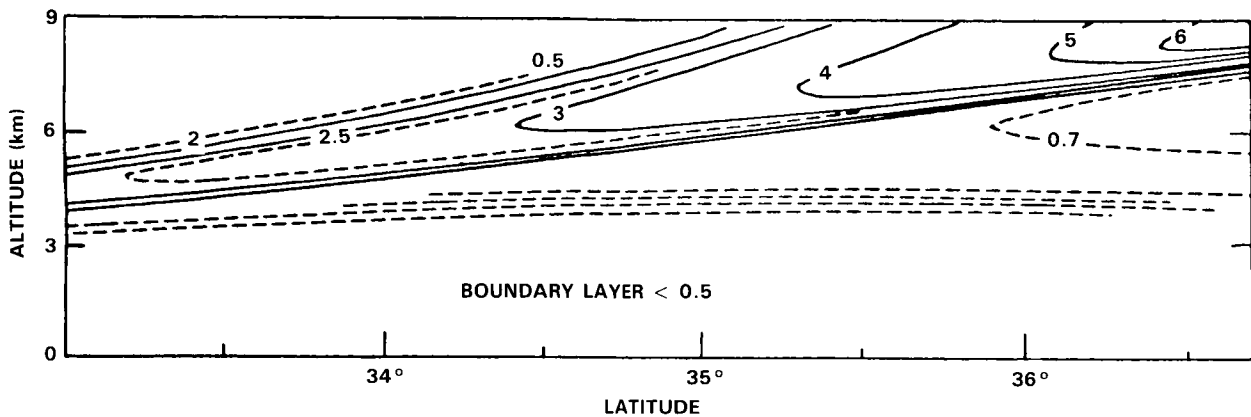


**Figure 5-44.** Isopleths of potential vorticity ( $10^{-5} \text{ cm}^2 \text{ s}^{-1} \text{ K g}^{-1}$ ) along Electra flight track on 20 April 1984. These data were calculated from an isentropic trajectory analysis from radiosonde data.

the warm boundary predicted from the potential vorticity information is higher than its actual location. Incorporation of *in situ* aircraft data into the potential vorticity analysis will improve the agreement with the DIAL data by constraining the location of the tropopause fold at altitudes of 6.7 and 8.2 km.

These results are consistent with the conservation of potential vorticity and ozone mixing ratio as deduced by Danielsen (1968) from simultaneous observations of potential vorticity and radioactive isotopes. They are inconsistent with the deductions by Shapiro (1980) and Gidel and Shapiro (1978). Eddy mixing processes are adiabatic - they redistribute energy, momentum, potential temperature and potential vorticity. When integrated or summed over infinitesimal volumes of a bulk system their effects cancel except at the surface of the bulk system, conversely diabatic heating rates and/or photochemical productions apply to each elemental mass of the bulk system. See Hoskins, McIntyre and Robertson (1985), equation (70b) for a mathematical statement: the mass integrated potential vorticity over a material volume can change only if there are non-zero values of  $d\theta/dt$  or the curl of a frictional force on its boundary. In practice in the atmosphere this means radiation, condensation or interaction with the planetary surface.

A fundamental difference between conservative and nonconservative processes in the atmosphere, is whether the surface integral of the property in question over a material volume is or is not constant in time. It is equally fundamental to our understanding of stratospheric-tropospheric exchange processes. In particular, it affects how we interpret correlations between trace species that we observe along the aircraft flight paths. With few exceptions, the nonconservative processes in the middle and lower stratosphere act slowly and are most effective in determining long term mean distributions. On the other hand, differential advectons by the winds and small scale mixing are most effective in determining instantaneous distributions. If this concept is correct, species whose large scale gradients are positively correlated will remain positively correlated as all internal wave induced velocities displace the larger scale gradients. Similarly, negatively correlated species will remain negatively correlated until small scale mixing becomes important. Then, their correlations will be systematically reduced in magnitude. Correlations computed from the  $\text{O}_3$  and  $\text{CO}$  measurements made on the 990 flight of April 20 confirm this assumption. The measurements were filtered by digital Fourier low-pass and successively higher band pass filters. Correlations approaching  $-1$  for the low pass approach 0 for the highest band pass.

The lowest correlations in the highest frequency band pass were found on the return flight in the folded tropopause zone. Here, tropospheric air is being entrained and mixed with the stratospheric air along both boundaries, as indicated by the streamlines of Figure 5-16.

## STRAT-TROP EXCHANGE

The distribution of ozone mixing ratio and aerosol backscatter obtained from the lidar measurements were presented earlier in this section. Again we see that as a direct result of the small scale mixing and the entrainment of tropospheric air by the velocity deformations that the values of all stratospheric tracers decrease down the fold as it is extended toward the surface boundary layer.

### 5.2.6.2 Analyses and Measurements above the Jet

Several factors conspire to make stratospheric analyses above the jet level much more difficult than those just presented. The time sequence of aircraft (U2) data was filtered, eliminating the short, high frequency waves, and the low pass filtered data combined with the radiosonde data. Analyses of this type based on temporal filtering along each horizontal flight leg will be presented below. However, they still include vertical structures of short vertical wave length associated with long horizontal wave lengths. Their vertical variations were deduced from the U2's ascent and descent profiles which were also incorporated in the analyses. To eliminate these waves, vertical profiles of temperature ( $T^1$ ) and zonal wind speed ( $U^1$ ) were constructed from the analysis at  $1^\circ$  latitude intervals and then these profiles were filtered vertically. The  $\theta$ ,  $U$ , and  $P_\theta$  analyses of Figures 5-45a and b were computed and drawn from the filtered profiles. These heavily filtered fields, denoted by an overbar, are considered representative of the undisturbed mean state. The 1 superscript will refer to the low passed filtered data. Figures 5-45a and b show  $\theta$  isotherms sloping downward to higher latitudes consistent with  $U$  decreasing with height. They also show that the maximum  $U$ , the jet axis, tilts with height toward lower latitudes. The  $P_\theta$  distribution, computed from analyses of Figure 5-45a plus estimated radii of curvature of the mean flow, includes a maximum on the cyclonic side of the jet, a minimum on the anticyclonic side. The horizontal gradient at constant  $\theta$  is largest in the lower stratosphere. It becomes negligibly small at  $\theta$ 's  $>450$  K, indicating that horizontal inhomogeneities produced by differential quasi-horizontal advections would be restricted to  $\theta$ 's  $<450$  K.

Examples of the horizontal inhomogeneities detected by the U2 at 50,000 ft (117 mb) (15.3 km) are presented in Figure 5-46 (a, b, c and d). Flying south-southwestward from the center of the vortex towards the jet,  $\theta$  decreases monotonically with many high frequency oscillations superimposed on the low pass profile. In marked contrast to these trends the  $\chi_{O_3}^1$ ,  $\chi_{H_2O}^1$  and  $\chi_{CN}^1$  oscillate from distinct maxima to minima. We were surprised to find  $\chi_{O_3}^1$  and  $\chi_{H_2O}^1$  positively correlated, and  $\chi_{H_2O}^1$  and  $\chi_{CN}^1$  negatively correlated. However, a comparison of the magnitudes indicates that the flight is in the dry stratosphere, above and to the north of the strong  $\chi_{H_2O}^1$  transition zone whose lower boundary is the tropopause. The flight at 41,000 ft crossed this transition zone and a positive correlation between  $\chi_{H_2O}^1$  and  $\chi_{CN}^1$  was observed where  $\chi_{H_2O}^1$  was large.

The spatial distributions of  $\chi_{O_3}^1$ ,  $\chi_{H_2O}^1$  and  $\chi_{CN}^1$  drawn from the low passed data and ascent-descent profiles are presented in Figures 5-47a, b and c. Here we see correlated relative maxima and minima of all three tracers sloping downward to higher latitude approximately parallel to  $\theta$ 's of Figure 5-45. A comparison of the toned areas reveals that the strong correlations observed at 50,000 ft extend over most of the dry stratosphere. In particular  $\chi_{H_2O}^1$  is positively correlated with  $\chi_{O_3}^1$  at  $\theta$ 's  $> 380$  K. This correlation implies an upper stratospheric source for  $H_2O$ , most probably that due to the oxidation of methane. Conversely the negative correlation at 41,000 ft is due to the surface source for  $H_2O$ .

These distributions combined with the absence of large variations in  $\theta$ , as seen in Figure 5-46a, are consistent with a folding of the  $P_\theta$ ,  $\chi$  etc distributions by a large amplitude, slow frequency, gravity modified inertial wave. In particular perturbation analyses show that waves of short vertical wave length whose wave fronts are parallel to the  $\theta$  surfaces will not disturb the  $\theta$  field but will advect the  $P_\theta$  gradients at

# STRAT-TROP EXCHANGE

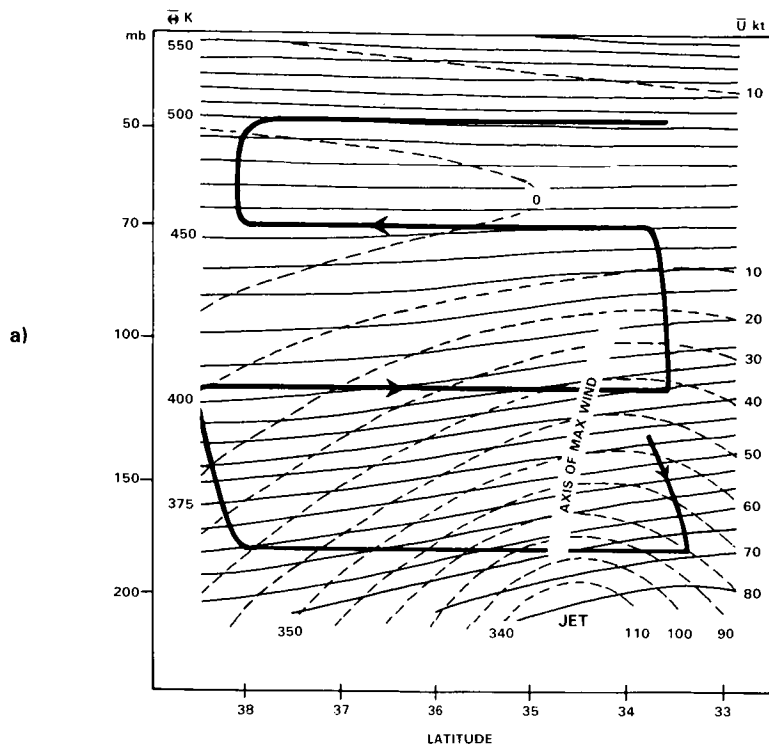


**Figure 5-45.** (a). Vertical cross-sections analysed only from meteorological measurements. See Figure 5-39 for the flow on the 330K surface, and Figure 5-40 for the U2 flight path. Data were heavily filtered to remove oscillations whose vertical wave lengths were  $\leq 3$  km. Note change in  $\theta$  contour interval at 400 K.

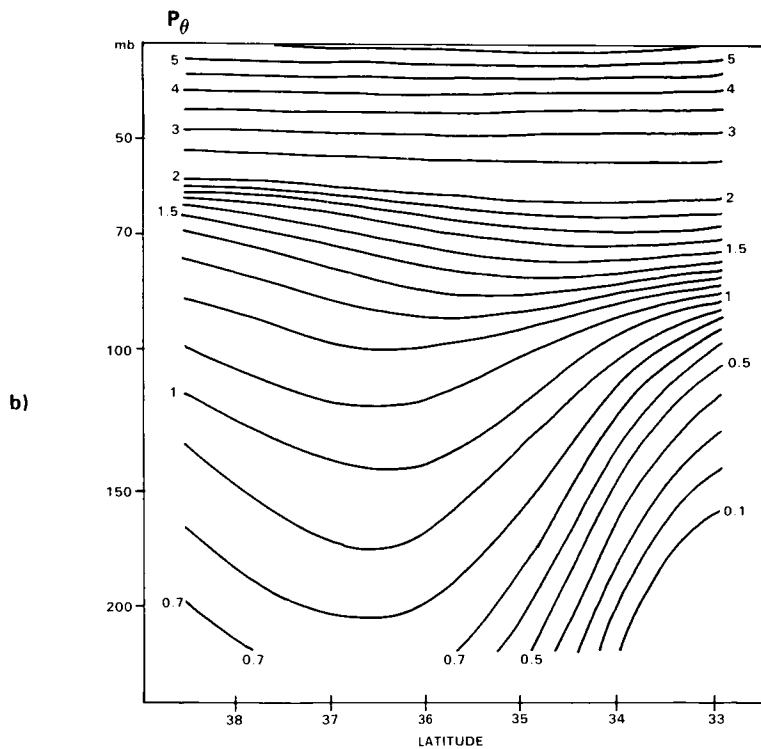
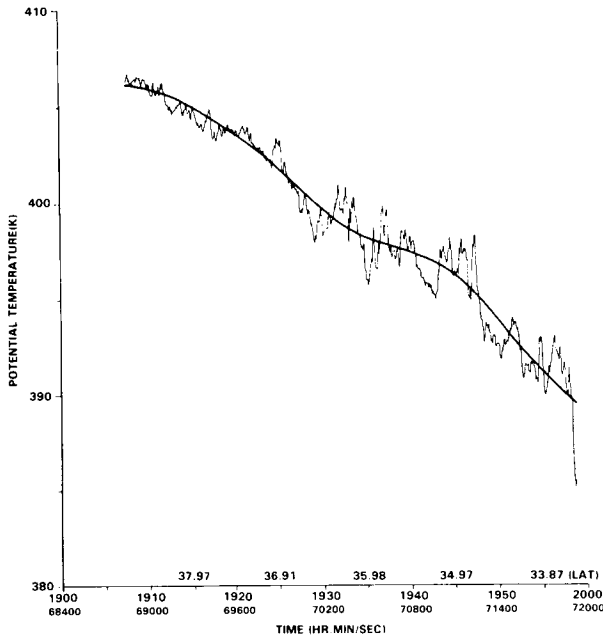
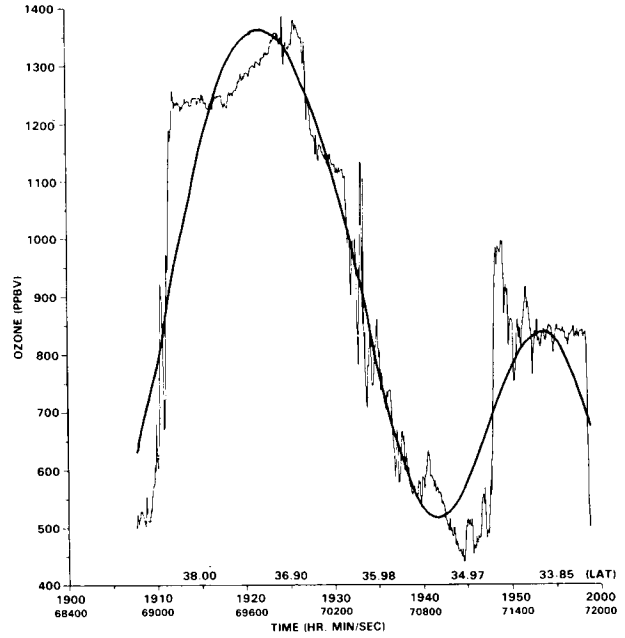


**Figure 5-45.** (b) As in part (a), but for potential vorticity. Note change in contour interval at  $2 \times 10^{-4} \text{ cm}^2 \text{ s}^{-1} \text{ kg}^{-1}$ .

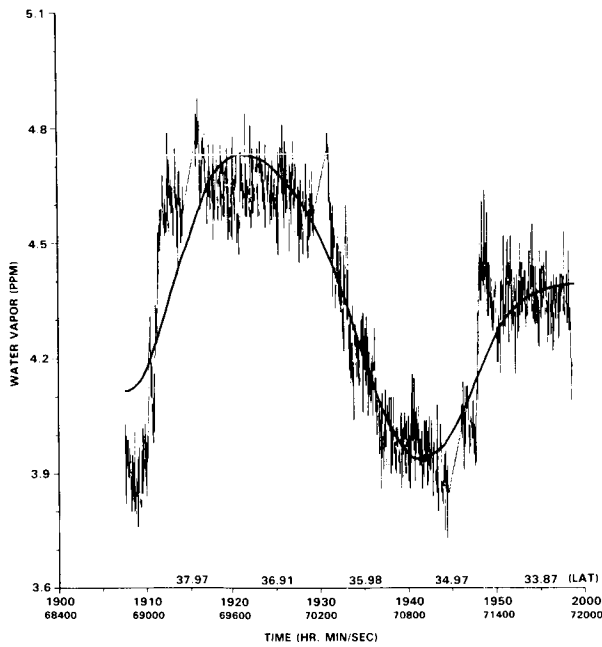
**STRAT-TROP EXCHANGE**



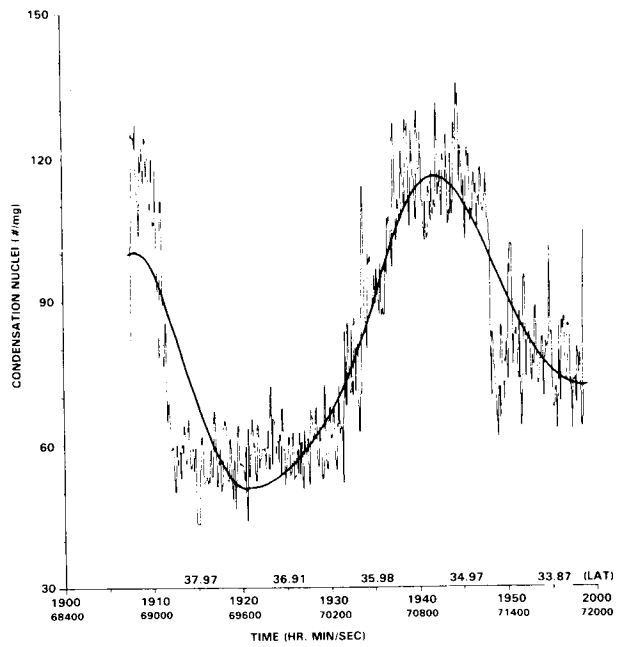
**a, potential temperature;**



**b, ozone mixing ratio;**

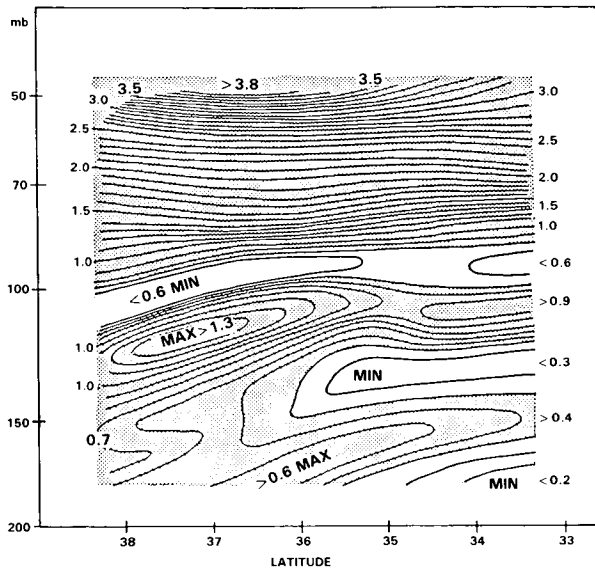


**c, water vapour mixing ratio**

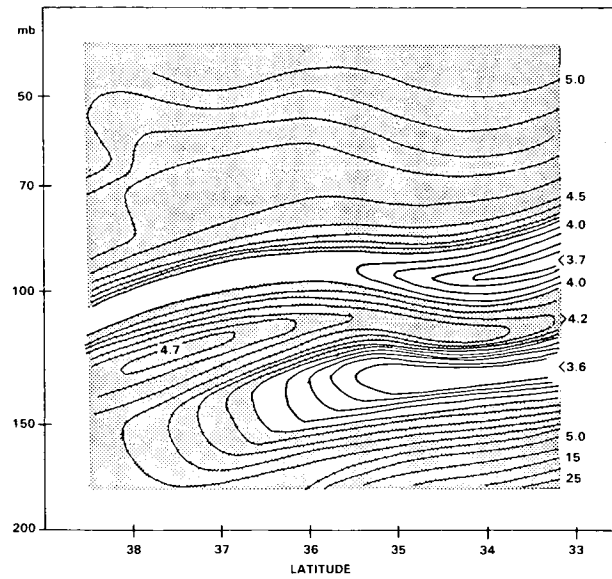


**d, condensation nuclei mixing ratio**

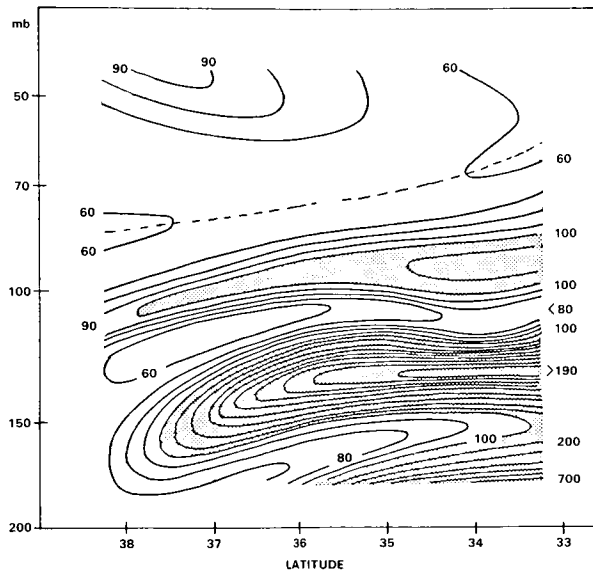
**Figure 5-46.** Temporal variations measured by U2 on 50,000 ft leg, 20 April 1984, including unfiltered and low pass filtered profiles of: (a) potential temperature; (b) ozone mixing ratio; (c) water vapour mixing ratio and (d) condensation nuclei mixing ratio.



a, ozone;



b, water vapour;



c, condensation nuclei mixing ratios

Figure 5-47. Vertical cross-sections analysed from low pass filtered data along flight legs and vertical ascent-descent profiles for: (a) ozone; (b) water vapour; and (c) condensation nuclei mixing ratios.

## STRAT-TROP EXCHANGE

constant  $\theta$ . These waves would be elliptically polarized and the hodographs plotted, during ascent and descent of the U2, from the observed winds confirm this necessary condition. The perturbation vectors,  $7-8 \text{ ms}^{-1}$  in amplitude, rotate anticyclonically with height, producing alternating northward and southward advectons.

These waves could fold and later unfold the distributions of conservative tracers. However, the observed high frequency oscillations indicate that instabilities of the Helmholtz type are generated along the boundaries of the folds. These produce small scale mixing which renders a potentially reversible transfer, irreversible. In this case the folding occurring above the jet is all in the stratosphere. Air from the anticyclonic side of the jet, having tropical (tropospheric) characteristics is folded over and under air from the cyclonic side with polar (upper or middle stratospheric) characteristics.

These high resolution experimental data show that potential vorticity and ozone are both positively correlated and proportional to each other; both are negatively correlated with carbon monoxide, which thus serves as a tropospheric tracer. It is also clear that mixing is an important process in folds.

### 5.2.7 Ground Based Studies over France

New ground based remote sensing instruments such as lidars and scidar have been developed during the last four years allowing a new insight into the relatively small scale phenomena associated with stratosphere-troposphere exchanges. These instruments are presently located in the Northern Hemisphere mid-latitude region and have been mainly used for the study of stratospheric air intrusions occurring primarily in association with the tropopause folding mechanisms taking place at the junction between frontal surfaces and the troposphere and related to the polar jet stream deformations. Their high spatial resolution is particularly well adapted to the vertical scale of such events ( $\sim 1 \text{ km}$ ) and the measurement temporal continuity leads to observations during long time periods compatible with the horizontal scale of a few hundred kilometers characteristic of these events. However the fixed location of the observing stations implies that the description of such an event will be dependent on the position and motion of the front as compared to the observation site and thus only a particular cross-section of the intrusion can be studied in detail. The data interpretation in terms of mixing between stratospheric and tropospheric air requires a synoptic analysis of potential vorticity and potential temperature cross-sections (Reed, 1955; Danielsen, 1968). Nevertheless as shown in the various examples given hereafter such an instrument as the lidar system in use at the Observatoire de Haute Provence Geophysical Station for ozone measurements since 1980 (Pelon and Megie, 1982a) may help to improve our understanding of the small scale processes involved in stratosphere-troposphere exchanges. Two case studies corresponding to different synoptic situations will be analysed hereafter.

The Figure 5-48 shows examples of lidar observations of the ozone vertical distribution taken on December 1 and 2, 1981. During this time period a meridional circulation was established over France due to a developing wave pattern in the jet stream associated with the descent of a low over southern Europe and the presence of an anticyclonic region over the Atlantic. This resulted in a main front located over Southern France at the 500 mb level during the second night of observation (December 2-3). The measurements reported on Figure 5-48b are thus representative of a vertical cross-section through the frontal zone in the southwest part of the low. The observed altitude decrease in the ozone number density maximum corresponds to the displacement of the front during the measurement period. At the lower edge of the front, simultaneous measurements using the star scintillometry technique (Scidar), Azouit and Vernin (1980), gave evidence for the presence of intense turbulent layers, at 5-6 km altitude just below the

# STRAT-TROP EXCHANGE

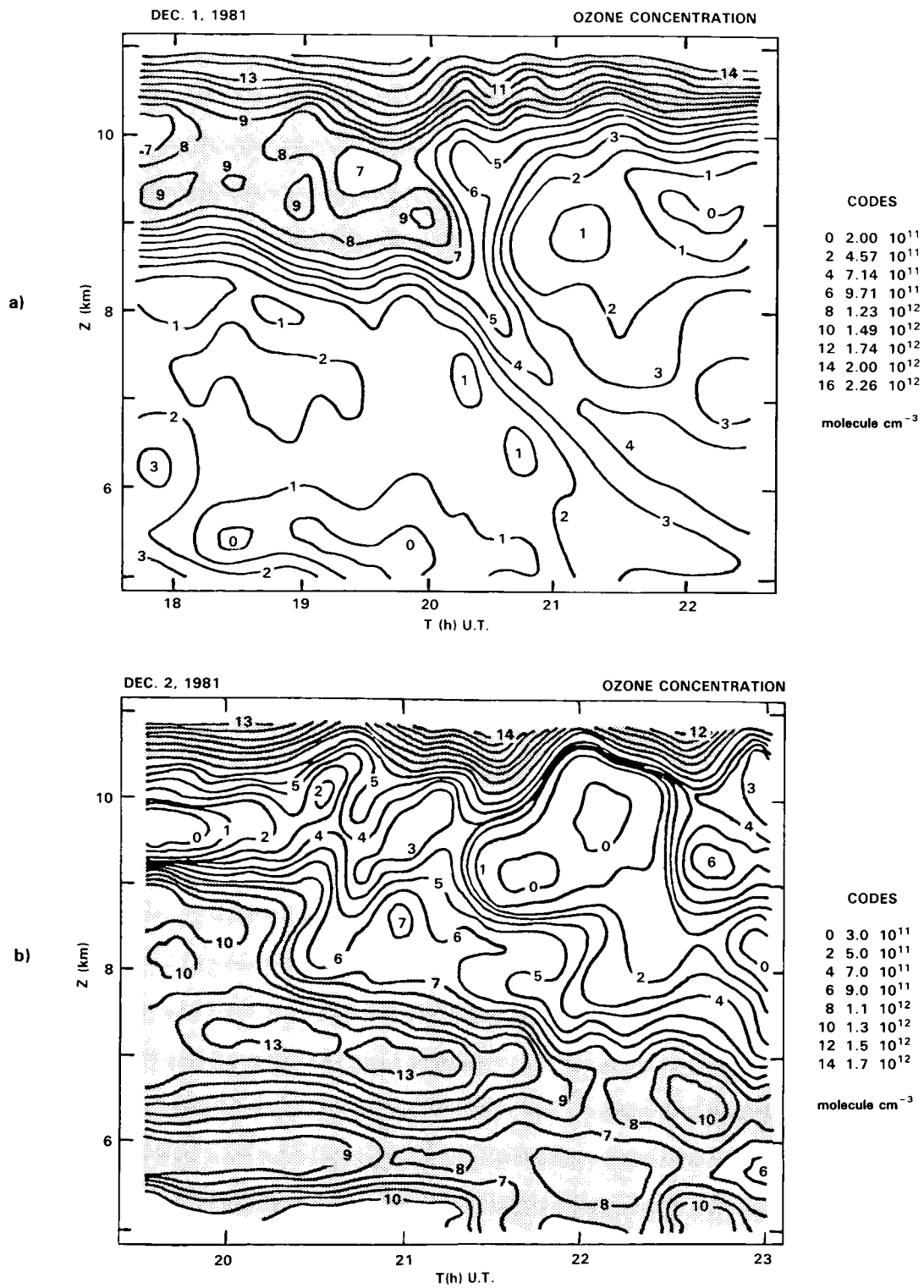


**Figure 5-48.** Ozone number density isocontours as a function of time (horizontal axis) and altitude (vertical axis) for the nights of December 1st and 2nd 1981. The hatched areas correspond to ozone concentrations larger than  $10^{12} \text{ cm}^{-3}$ .

## STRAT-TROP EXCHANGE

peak of the ozone distribution ( $1.5 \times 10^{12}$  mol cm<sup>-3</sup> i.e., 120 ppbv). If for the previous night (December 1-2) the shapes of the ozone isocontours (Figure 5-48a) are similar to the fingered structure observed in tropopause folding events, the observed evolution should not be attributed directly to the influence of the main front: in order to explain the origin of the high ozone content observed at tropospheric levels in both cases and to follow its ensuing evolution, air mass trajectories calculated from radiosonde observations, by the Meteorologie Nationale at the European Center have been used (Figure 5-49). Such trajectories are necessarily crude, especially in the region of frontal surfaces. The trajectories ending at the Observatoire de Haute Provence (OHP) on December 1 (6 pm and midnight UT) at the 300 and 500 mb levels (Figure 5-49a) show that the origin of the air masses four days before (November 28) are quite different. The one observed at 300 mb in the early night originated above Greenland at upper levels (225 mb) in the stratosphere (high ozone content), while those observed six hours later come from tropospheric levels at lower latitude. The synoptic situation on November 28 (0 h UT) corresponds to a very well developed frontal zone stretching from north-west of Southern England to the South of Iceland with a low over northern England and Western Scandinavia and a high over the Azores. The time resolved measurements at the OHP correspond thus to a transverse cross-section through this frontal zone: observed air masses originate at various altitudes with different ozone contents further modified by dispersion and small scale turbulence along the trajectories. Similarly, Figure 5-49b shows the trajectories ending on December 2 (midnight) at two points located at the 500 mb level in the frontal zone. Their origins are in the cyclonic zone above the North Sea four days before at the 400 mb level (points 5 and 6). The ozone rich air masses coming from this region have thus turned around the low in the associated frontal zone before reaching southern France (Figure 5-48b).

Considering the air mass trajectories calculated for the days following the observations, evidence is given that the air coming from points 2 and 3 on Figure 5-49a (December 1) is going back to higher latitudes (49°N and 57°N) and upper levels for point 2, whereas air originated from point 3 remains at the 500 mb level. On the second night (December 2-3), the trajectories originating at points (5 and 6) on Figure 5-49b are quite different: the air masses coming from point 5 continue to travel down to lower latitude (37°N) and higher pressure levels (630 mb). On the contrary air masses originating from point 6 reach a latitude of 68°N on December 7 at the 450 mb level. Such a behaviour illustrates the complexity of synoptic stratosphere-troposphere exchange processes: the air masses observed in the frontal zone can either be definitely transferred into the troposphere at mid-latitudes, or return to the stratosphere at higher latitudes in association with the polar jet stream. This latter conclusion must be tentative in view of the nature of the trajectory calculation. It is however an interesting possible behaviour.

Another example of the influence of cyclogenesis on ozone transfer can be given from observations performed on July 9, 1980 when large ozone concentrations were observed at the 300 mb level associated with a frontal zone located over Southern France and corresponding to a similar jet stream wave pattern as the one described above. The lidar measured ozone profiles give evidence for concentrations as high as  $3.5 \times 10^{12}$  mol cm<sup>-3</sup> (380 ppbv) at 9 km altitude, and  $2.5 \times 10^{12}$  mol cm<sup>-3</sup> (200 ppbv) at 7 km altitude, in the upper part of the frontal zone (Figure 5-50a). Considering the total ozone maps obtained from the TOMS experiment on board the Nimbus 7 satellite, the low observed over France corresponds to ozone total content up to 400 DU, the frontal zone being delimited by the 360 DU contours. Trajectories, calculated as before for the 300 and 500 mb levels, show that the air masses considered originated on July 6 from latitudes west of Ireland, close to 50°N (Figure 5-50b) and thus from the same cyclonic zone before it developed over Southern France. Related to the development of this low, the anticyclonic zone previously settled over the Northern Atlantic region is cut in two parts with a blocking high at 70°N latitude carrying low ozone content in the lower stratosphere as observed by TOMS. No direct correlation can then be

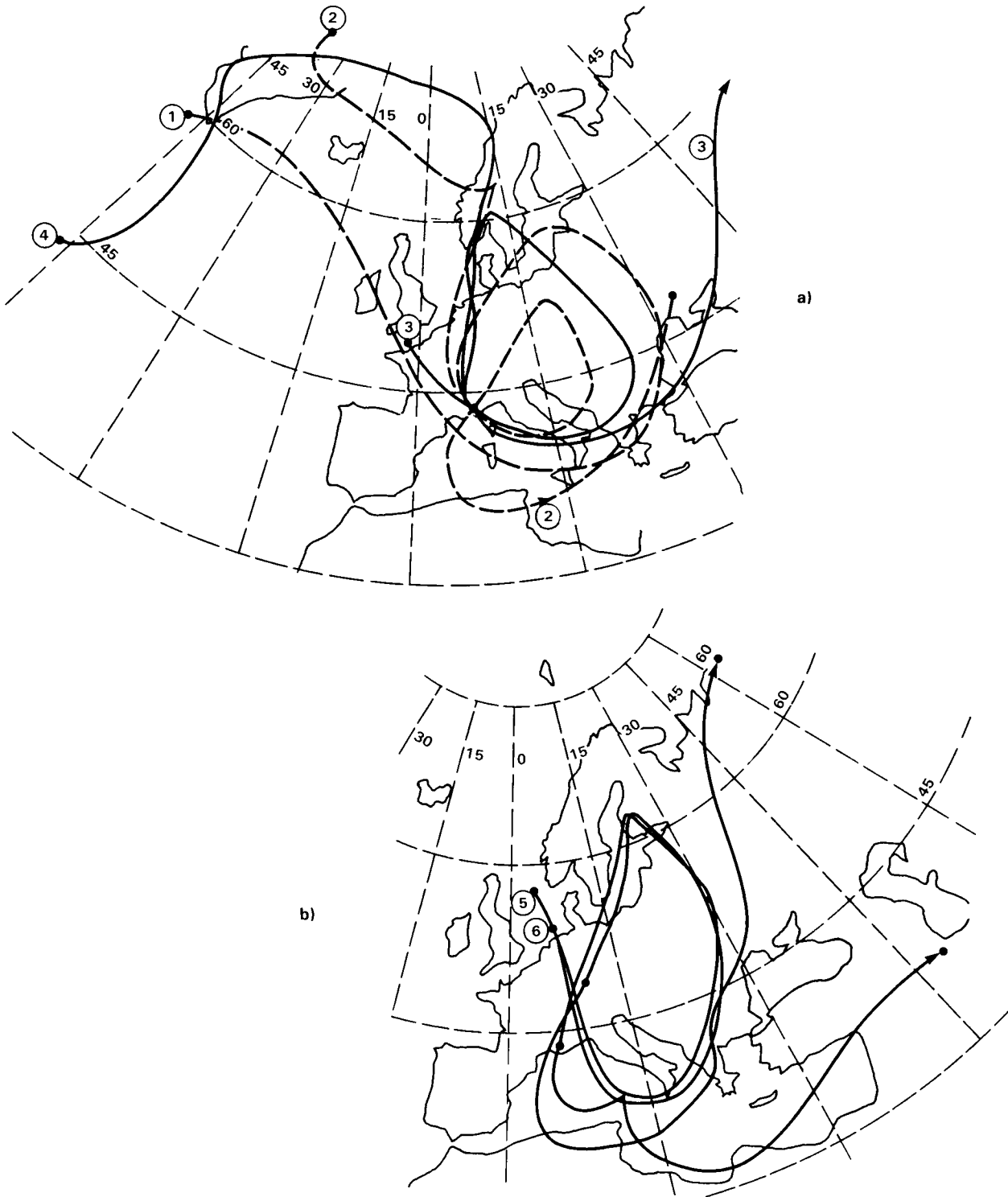


**Figure 5-49.** a) Air mass trajectories ending at the Observatoire de Haute Provence on December 1st, 6 pm ((1) 500 mb pressure level; (2) 300 mb and midnight; (3) 500 mb; (4) 300 mb). b) Air mass trajectories in the frontal zone at the 500 mb level originating at points 5 and 6 and ending at 49°N, 10°E and at the OHP (44°N, 5°E) on December 2nd (midnight) and their ensuing evolution.

# STRAT-TROP EXCHANGE

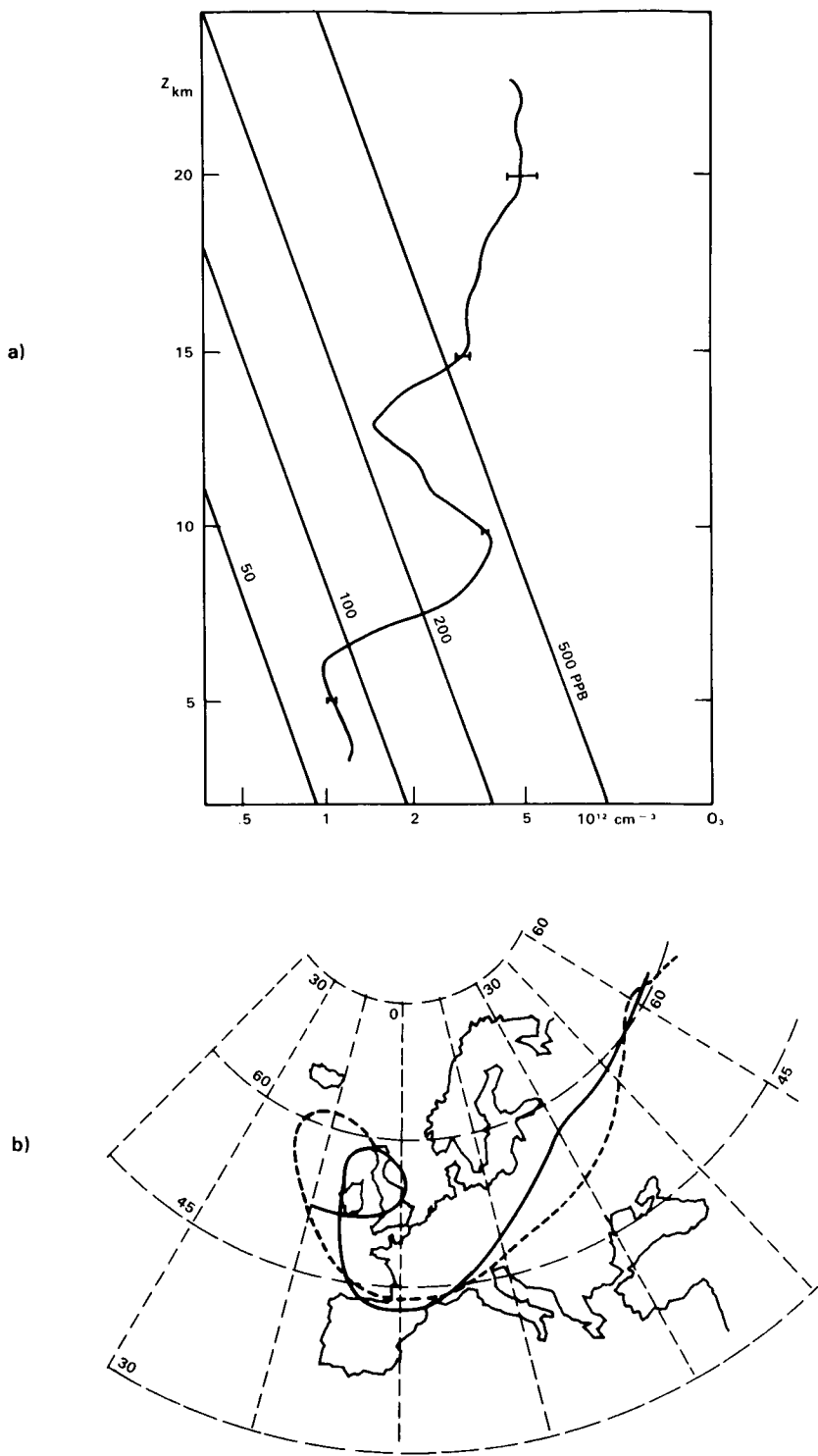


**Figure 5-50.** a) Ozone vertical distribution on July 9, 1980 at midnight as observed by lidar sounding at the OHP. b) Air mass trajectories ending at the OHP on July 9, 1980 (midnight) and their ensuing evolution: full line (500 mb), dotted line (300 mb).

further established between the location of the frontal zone and the ozone vertical distribution. It should also be pointed out that air masses, originating from this low, entered the associated frontal zone where it stayed on the following days, slowly ascending before reaching at higher latitudes on July 14 a cyclonic zone over Siberia (60°N, 70°E), returning thus to the polar stratosphere (Figure 5-50b). Again, the coarseness of these trajectories, together with an absence of measurements which would permit estimation of the rate of mixing, makes this an uncertain interpretation.

These two examples show the difficulty in quantifying the ozone transfer related to mid-latitude stratosphere-troposphere exchange processes. They did not give evidence for a large direct ozone transfer at 45°N from the stratosphere to the troposphere but rather indicated that such transfer occurred at higher latitude. The larger part of the transported ozone remains in the frontal zone for several days with a likely possibility for part of it to return to the polar stratosphere. Evaluation of the magnitude of the ozone transfer is also complicated by turbulent exchange processes in the frontal zone which are more intense than in the free troposphere. Further investigations are needed especially at the synoptic scale (using airborne lidar systems) to provide evaluation of ozone transfer within frontal zone, cutoff lows or blocking highs.

### 5.2.8 Global Coverage: TOMS Ozone Column Measurements

The total ozone column is a particularly sensitive indicator of vertical motions of air due to the peculiar vertical mixing ratio distribution of ozone. In the troposphere, the mixing ratio is small ( $\sim 0.04$  ppm) and nearly constant. Immediately above the tropopause the mixing ratio increases steeply ( $\sim 0.50$  ppm/km) with height in the stratosphere to a maximum near 35 km. Any vertical displacement produces a change in the total ozone due to convergence or divergence. Reed (1950) calculated that a well-developed upper tropospheric trough should contain 24 Dobsons of total ozone greater than the average of 300 Dobsons. An adjacent ridge will be depleted by a similar amount and 15% variations in total ozone should be found. Variations of this magnitude are observed with the Nimbus 7 TOMS in large scale planetary waves (Schoeberl and Krueger, 1983). Much larger changes (greater than 30%) are found in smaller scale troughs (Krueger, *et al.*, 1981). Information about the vertical structure of ozone would aid in diagnosis of exchange events, however, none of the current satellite-borne ozone profile sounding instruments is likely to provide any routine diagnostic coverage of exchange processes due to the lack of horizontal coverage and of vertical resolution.

The TOMS maps global total ozone each day with 50 km spatial resolution at nadir from a local noon orbit. The wavelengths of the instrument are selected for maximum penetration of the ozone region, with the Rayleigh scattering contribution functions peaking low in the troposphere. The precision of measurement, tested by comparison with coincident Dobson Spectrophotometer data (Bhartia, *et al.*, 1984a) is better than the average 2% rms difference and appears to be close to 1%. This figure is of the order of residual cloud biases and radiance measurements errors. Thus, total ozone differences of 3-5 Dobsons are at the limit of detection in individual samples but, by use of spatial coherence on mesoscale or synoptic dimensions, the limit of detection is less. Thus, measurement errors are generally trivial at extratropical latitudes.

At the present time, TOMS observations of total ozone show promise for investigation of exchange processes. The following discussion concentrates on these observations.

## STRAT-TROP EXCHANGE

### 5.2.8.1 Brewer Circulation/ITCZ Exchange/Stratospheric Fountain

The total ozone in the tropics is observed to have a general wavenumber 1 longitudinal variation. The zonal average ozone has a low variability (5-8 Dobsons) and exhibits a shallow minimum located in the winter hemisphere. The latitude of the minimum does not vary with longitude and is confined to within  $15^\circ$  of the equator. At the equinoxes the minimum jumps discontinuously to the opposite hemisphere. This behaviour is different from that of the ITCZ which tends to persist in the northern hemisphere throughout the oceanic areas, except for the western Pacific region where interhemispheric transitions are found. A direct association between the axes of the oceanic ITCZ and total ozone is not found.

The longitude of the minimum of tropical total ozone is, however, stationary and located over the western Pacific ( $150^\circ\text{E}$ ), coincident with the location of the "stratospheric fountain" of Newell and Gould-Stewart (1981), suggesting a possible decrease of lower stratospheric ozone in the fountain region. Alternatively it may only indicate a relation between the tropical tropopause height and total ozone, such as occurs in Figure 5-8.

An analysis of the detailed behaviour of total ozone over the ITCZ shows no relationship except for "superreflectivity" clouds. These clouds have apparent reflectivities greater than 100% and appear in the tropics and in severe storms. They are believed to be ice specularly-reflecting, capped cumulonimbus cloud masses. These clouds show an excess of ozone relative to the surroundings and may indicate subsidence of stratospheric air.

Tropical total ozone also exhibits small scale structure which is organized on scales larger than clouds and cloud masses, but seemingly located at random. Some features persist and migrate meridionally, indicating mass transport of ozone excess or deficit air between the tropics and subtropics. The transport of excess ozone into the tropics is found at Atlantic longitudes while ozone "minima" move out of the tropics at Indonesian longitudes. This behaviour appears to be consistent with the transport diagnosed in Section 5.2.2.2.

### 5.2.8.2 Tropopause Folding near Jet Streams

Aircraft observations of ozone and jet stream structure (Danielsen, 1968; Shapiro, 1980; Shapiro *et al.* 1982) indicate that the folds have typical vertical dimensions of 1-2 km. Recently exchange events with a vertical scale of 3 km have been observed (Figures 5-30 and 5-34). The integral amount of ozone in the fold is estimated to be on the order of 10 Dobsons based on a typical mixing ratio of 0.10 ppmv. This amounts to a 3% change which is well within the precision limits of the instrument. The shape of a fold in plan view can be seen in Figure 5-51, the TOMS data for the aircraft study case of April 20, 1984 described in Section 5.2.6. The fold observed with the airborne LIDAR (Figure 5-43) in the southwestern U.S. is found to coincide with the dark green band (325 - 350 Dobsons) that parallels the steep gradient in the yellow colors along the California-Nevada border. This high gradient band (25 Dobsons/100 km) is located exactly at the jet stream core as observed with the CV 990 aircraft at 310 mb over western Nevada (Figure 5-41).

The polar vortex boundary is another potential location for exchange of air. Polar vortex air masses are identified on TOMS maps by their extremely high total ozone values (450 - 550 Dobsons). The high total ozone would suggest low tropopause heights and, indeed, tropopause pressures of greater than 500 mb are found. The boundaries are also very steep with ozone gradients of 100 Dobsons/500 km typical.

Shapiro and associates investigated these features with aircraft flights across the vortex during the 1983 AGASP experiment. Jet stream winds were found at 300 - 400 mb and stratospheric air in the fold was traced by ozone, potential vorticity, and aerosols to as low as 700 mb (Shapiro, *et al.*, 1984). Other flights during this experiment investigated other folds with similar conclusions. The satellite observations of these features have yet to be investigated.

### 5.2.8.3 Cut-off Lows

In Section 5.2.5, evidence was presented that stratospheric air in cut-off low centres is mixed into the troposphere. TOMS showed an increase of about 50-60 DU associated with the low, and combined with the aircraft ozone data, it could be concluded that much or all of the ozone in this extension was probably mixed into the troposphere.

Cut-off lows always appear as isolated ozone maxima in TOMS maps, thus demonstrating that stratospheric air within the low centre is ozone enriched. In the Bamber *et al.* (1984) study the cut-off low was disrupted by convective activity. It is possible to follow the life cycle of other cut-off lows in the TOMS data. One often sees that a path is established to the main trough after a few days and at least part of the ozone is returned to the system that spawned the cut-off low. In other cases the low centre can be permanently absorbed. At the present time a systematic study of such features has not been made. It is apparent that combining the spatial information and quantitative ozone data in the TOMS maps with conventional radiosonde and aircraft observations and with numerical models will produce a better understanding of the importance of cut-off lows in the exchange budget.

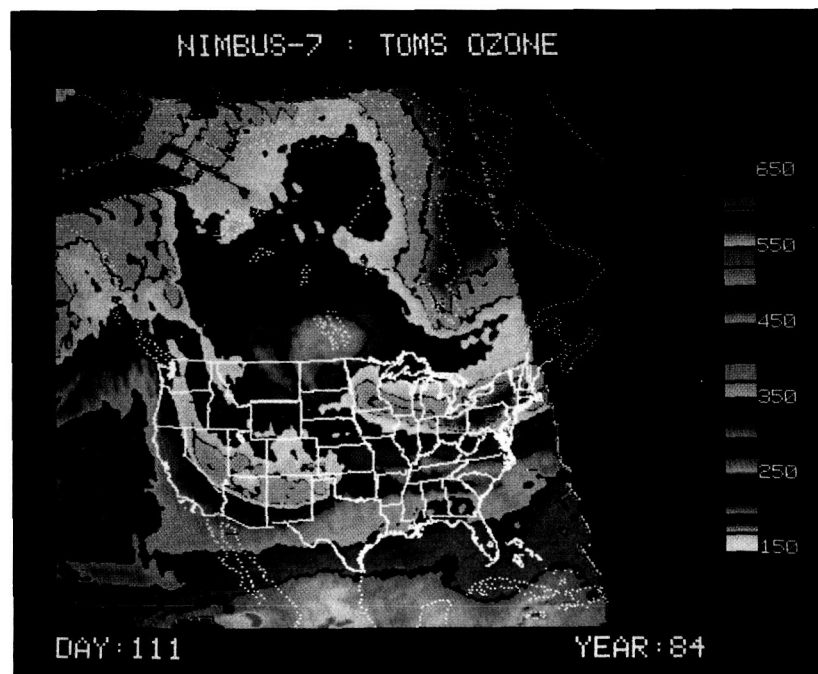


**Figure 5-51.** TOMS map of total ozone during the aircraft experiments over the western United States on 20 April 1984 (see section 5.2.6). Color boundaries are at 25 DU intervals as shown in color scale. The tropopause fold is in the dark green region south and west of the trough which is outlined in yellow color over Nevada and Arizona.

## STRAT-TROP EXCHANGE

### 5.3 LARGE SCALE NUMERICAL MODELLING OF STRATOSPHERE-TROPOSPHERE EXCHANGE

If it is accepted that understanding of the physical nature of the processes effecting exchange across the tropopause is necessary before successful modelling can be attempted, the basic difficulty is apparent from the case studies described in Sections 5.1 and 5.2. In the tropics and in many cases in the extratropics the scale of the individual processes is below the resolution of the global meteorological observing system. There were grounds for encouragement however, in the tropopause folding events reproduced by a limited area operational model, with  $0.9375^\circ \times 0.75^\circ$  longitude-latitude resolution (see Section 5.2.5). Nevertheless, some investigation with general circulation models has been done, because although such models parametrize mesoscale events and cumulonimbus storms, they can resolve the larger scale features of the sea-land contrast and the associated topography, jet streams and the horizontal temperature structure at the tropical tropopause, which arises from the preferential occurrence of the deepest cumulonimbi at longitudes in the western Pacific-Indian Ocean region.

#### 5.3.1 General Circulation Models

One consistent result from general circulation models which transport ozone (usually as a tracer with a parameterized chemistry) is that there is a greater flux from the stratosphere to the troposphere in the Northern than in the Southern Hemisphere. For this reason, and despite the inability of GCMs to adequately resolve the meteorological processes achieving the cross-tropopause flux, a table (5-1) has been given of available general circulation model estimates of the ozone flux to the troposphere. Other estimates of this flux from atmospheric data tend to be of the same general magnitude (Paetzold, 1955; Regener, 1957; Fabian and Junge, 1970; Danielsen and Mohnen, 1977). Figure 5-52 shows a model estimate of the Northern Hemisphere annual mean  $O_3$  cross-tropopause flux and mixing ratio at 500 mb; although these data show that the model is not completely equilibrated, it is nevertheless clear that the maxima are too early, occurring in late winter and early spring. Very recently, Levy *et al.* (1985) have published a more detailed consideration of tropospheric ozone in their GCM; it is discussed in Chapter 4.

(a) GCM estimates of ozone export to the troposphere. There are three model estimates of ozone fluxes from stratosphere to troposphere:

Table 5-1. General circulation model estimates of cross-tropopause  $O_3$  Flux

	NH	SH	
MLM	6.6	3.6	$O_3$ fluxes, $10^{10}$ molecules $cm^{-2} s^{-1}$
GS	4.9	2.5	
AT	3.8	3.0	

The references in the left hand column of Table 5-1 are, in order, Mahlman, Levy and Moxim (1980); Gidel and Shapiro (1979) and Allam and Tuck (1984a, b). The AT figure has not been previously published but was calculated with the same methodology as was used for water vapour in the reference.

The MLM estimate is actually  $O_3$  flux across the 240 mb surface, while the GS estimate assumes that the model zonal mean potential vorticity has a constant ratio to observed zonal mean ozone, and that

this ratio can be used to convert model potential vorticity flux to an ozone flux. The NH annual mean O<sub>3</sub> cross-tropopause flux and mixing ratio at 500 mb, are shown in Figure 5-47 for the AT model. The MLM model had horizontal resolution of 265 km and  $\sigma$  levels at pressures of 500, 315, 190 and 110 mb in the relevant region, while the GS model had 5° × 5° horizontal and 3 km vertical resolution. The AT model had horizontal resolution of ~320 km and similar  $\sigma$  levels to MLM at the relevant altitudes.

It could be argued that if a general circulation model does an acceptable job of getting the large scale dynamics right, the mass flux across the tropopause must be approximately correct, even if the detailed simulation of the synoptic, meso and cloud scale processes involved is poor. Such a view assumes that mass transport by the large scale dynamics is independent of the quality of representation of these smaller scales, and is by no means well established. Also, from the point of view of fluxes of particular chemical species, the case studies of Sections 5.1 and 5.2 show clearly that it is necessary to know the covariance of the species and the motion field on the active scales.

(b) Lagrangian diagnostics of GCM data

Kida (1983a,b) has used a hemispheric GCM, without topography and with annual mean forcing, to obtain trajectories from the 3 velocity components for many thousands of particles for periods of up to 5 years. Model resolution was 3° long × 2.5° lat with 12 levels from the surface to 1 mb, so the results must be dependent upon the treatment of sub grid scale processes. An analysis was used which produced a "spectrum" of ages of air particles in different regions of the model stratosphere. Particles in the tropical stratosphere were younger, and had a narrower spectrum of lifetimes since entry from the troposphere. At the poles, the model air particles were older, with a flat, broad spectrum of ages. Most particles entered the stratosphere across the tropical tropopause, but there was an identifiable fraction which entered the lower mid-latitude stratosphere from the upper tropical troposphere. It is difficult to see how Kida's results can be tested experimentally, since the only particles in the real atmosphere which retain their identity after 5 years in the stratosphere are likely to be N<sub>2</sub> or CF<sub>4</sub> molecules rather than fluid elements.

Allam & Tuck (1984a,b) have examined fluxes of mass and water vapour and associated trajectories across the "tropopause" in a 13-level global general circulation model, with 320 km horizontal resolution and vertical levels (at relevant heights) of 493, 319, 196, 117 and 74 mb. Ozone was available as a tracer, and its cross-tropopause transport calculated; the hemispheric average behaviour over a year is shown in Figure 5-52. Deep tropical convection over the Indian Ocean/Western Pacific and Central American sectors maintained a source of dryness at ~100 mb. Exchange of mass and water vapour occurred above the cores of the subtropical jet stream maxima, between the tropical upper troposphere and lower mid-latitude stratosphere. Some trajectories showed oscillatory behaviour with periods of the right order for inertial instability. A summary of the behaviour seen in all 400 trajectories is as follows.

(i) Within the limits of the model spatial and temporal scales, mixing was sufficiently effective that substantial development of the O<sub>3</sub>-H<sub>2</sub>O ratio of a parcel generally occurred during the 10-day period.

(ii) O<sub>3</sub>-H<sub>2</sub>O ratios developed strikingly around jet streams, particularly at exits and entrances.

(iii) Air parcels frequently underwent decreases in water vapour in the tropics during horizontal motion, especially when this was into the upper troposphere of the equatorial western Pacific; presumably this emphasizes the importance of mixing with drier air.

## STRAT-TROP EXCHANGE

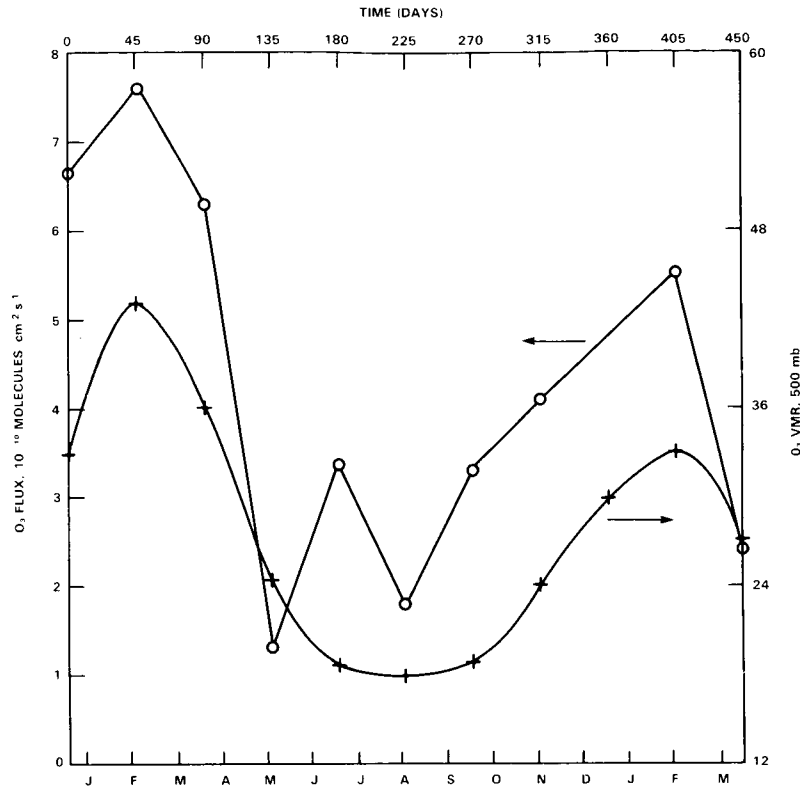


**Figure 5-52.** Northern hemisphere mean ozone flux stratosphere–troposphere (open circles) in the general circulation model described by Allam and Tuck (1984), and 500 mb ozone mixing ratio (crosses). Note that the behaviour is not completely equilibrated, and that the tropospheric ozone maximum occurs in late February.

(iv) There was little development of O<sub>3</sub>-H<sub>2</sub>O covariance in the anticyclonic circulations, particularly in the subtropical highs.

(v) Air entering the equatorial western Pacific region acquired a positive correlation between low values of ozone and low water vapour mixing ratios, presumably because of the co-location of ozone and temperature minima in this region.

(vi) The flow of air from about 100 to 200 mb in the equatorial western Pacific into the right entrance of the Japanese subtropical jet stream, above the core, resulted in low water vapour mixing ratios at the southern flank of the stratospheric Aleutian high, via the left exit.

(vii) Air moved, at about 100 mb, from the southern subtropical jet stream, at about 30°S, to about 15-20°N in a few days, at longitudes 180° to 160°W.

(viii) There were trajectories from subtropical and mid-latitudes at about 100 mb in the Northern Hemisphere which moved equatorward and upward in limited longitudinal zones, transporting relatively high water

vapour mixing ratios to the tropics and so tending to create an increase of water vapour with height above 100 mb. This did not occur in the Southern Hemisphere.

(ix) The proportion of trajectories which oscillated between 'stratosphere' and 'troposphere' was considerably higher than the proportion which directly ascended through the tropical tropopause. This is of course subject to bias in the initial distribution of rings of parcels, and to the difficulty in defining the model tropopause.

This model maintained a negative correlation between ozone and water vapour in the upper troposphere (200 mb level), but showed a positive correlation in the lower tropical stratosphere, with a negative correlation in the lower stratosphere of middle and high latitudes (Allam, Groves and Tuck, 1981). The negative correlations in the troposphere are readily explicable; the positive correlations were attributed to the drying action of deep cumulonimbus upon ozone-poor air from the lower tropical troposphere, a behaviour readily apparent in the time history of ozone and water vapour along appropriate model trajectories. Such predictions have yet to be tested against global scale data, but the lower stratospheric behaviour at high northern latitudes is consistent with old aircraft data obtained by Roach (1962), as may be seen from Figure 5-53.

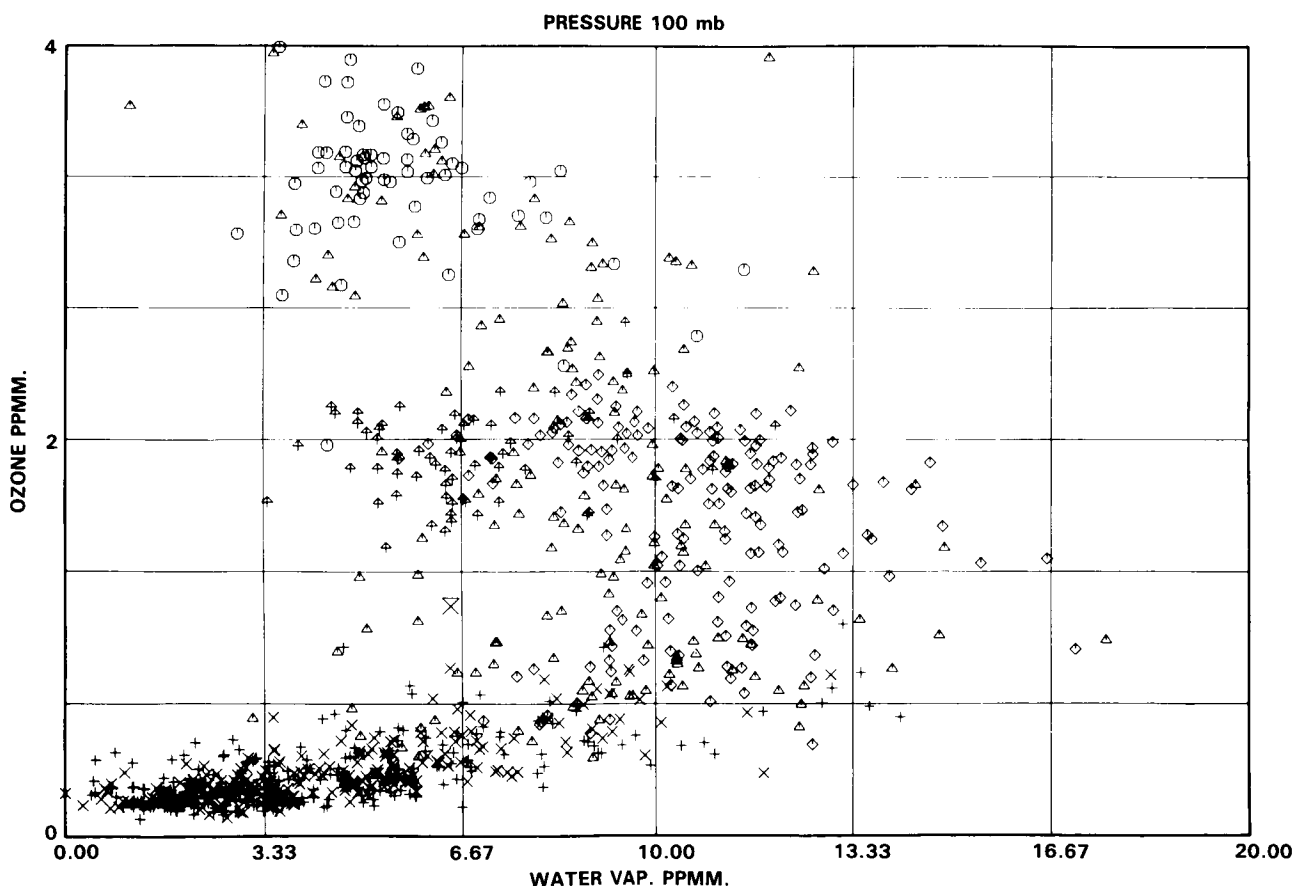


**Figure 5-53.** Ozone-water vapour correlation in the stratosphere. (a) From the general circulation model described by Allam, Groves and Tuck (1981), at 100 mb, January 1st. Circles are gridpoints situated between 90°N and 60°N, diamonds are between 60°N and 30°N, crosses between 30°N and 30°S, tailed triangles between 30°S and 60°S, and triangles are between 60°S and 90°S.

STRAT-TROP EXCHANGE

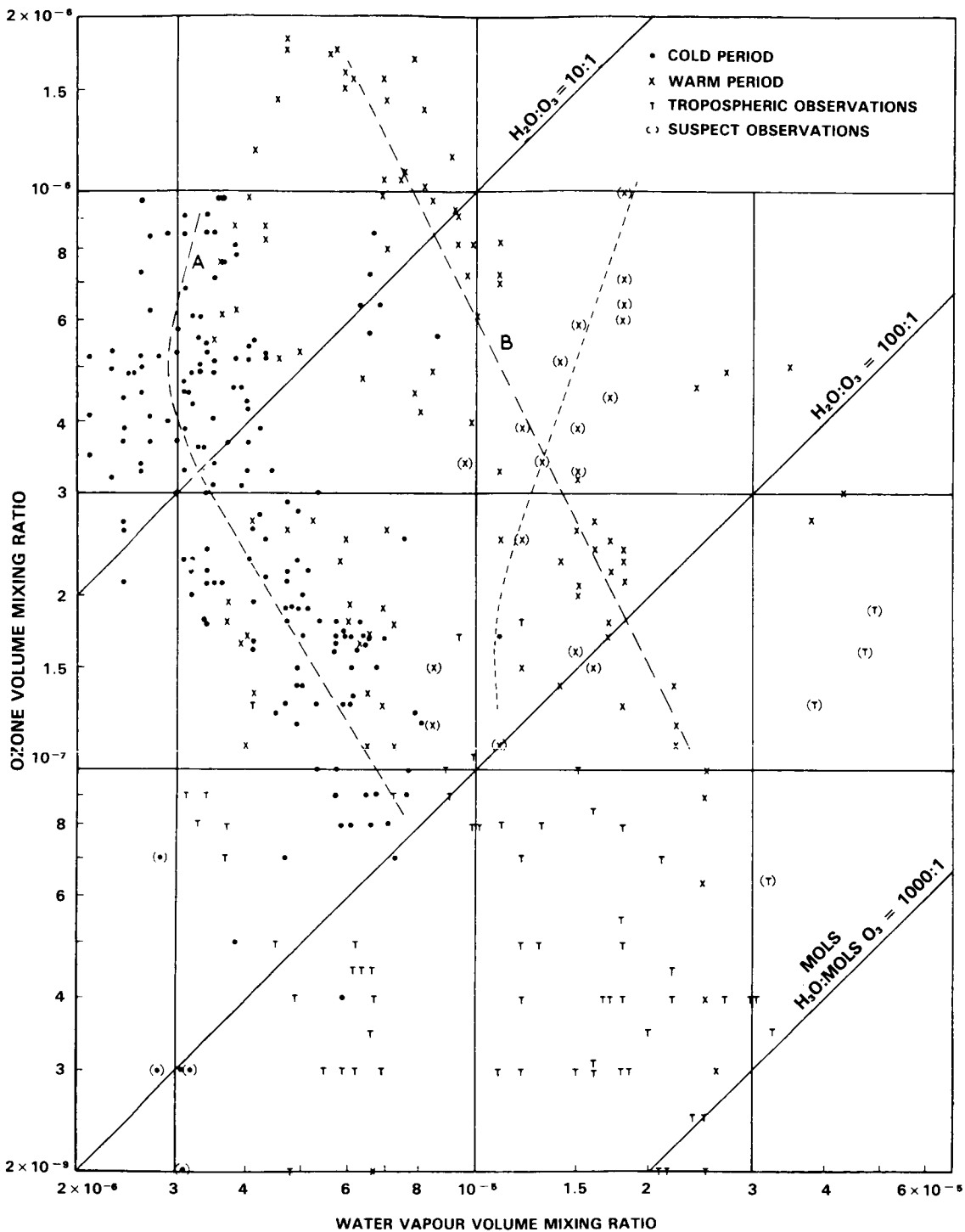


Figure 5-53. (b) from MRF Canberra flights, January-February 1962, 52°N-68°N, Greenwich meridian. Compare negative correlation in stratospheric air with that at high northern latitude points in part (a). From Roach (1962).

A feature common to all general circulation models is the difficulty of defining an objective, realistic tropopause. The representation at high latitudes is often poor, and it is extremely difficult to reproduce a temperature structure at the tropical tropopause which will dry the air there to the correct degree.

### 5.3.2 Operational Weather Forecasting Models

The Met Office global forecast model with levels at 1000, 950, 850, 700, 500, 400, 300, 250, 200, 150, 100, 70, 50 and 30 mb, and with lat.  $\times$  long. resolution  $1.5^\circ \times 1.875^\circ$  failed to produce good wind field analyses on the scale of polar front jet stream, as shown in Figures 5-54 and 5-55. The model's best analysis has the jet core speeds, and the wind shears on either side of it, seriously wrong and an attempt to compute potential vorticity shows that large errors are inherent, and that the horizontal contribution has to be considered. However, the limited area fine mesh of this model, covering  $30^\circ\text{N}$ - $80^\circ\text{N}$  and  $80^\circ\text{W}$ - $30^\circ\text{W}$  with a lat. long. grid of  $0.75^\circ \times 0.9375^\circ$  reproduced the aircraft observed wind shears much better, and in fact resolved a tropopause fold (Figure 5-37), with consistent trajectories, potential vorticity, ozone and water vapour structure. The potential vorticity and water vapour from the model were arrived at independently of the aircraft data, so the correlations between the  $\text{O}_3$  and PV, and between the 2 sets of humidities, are very significant.

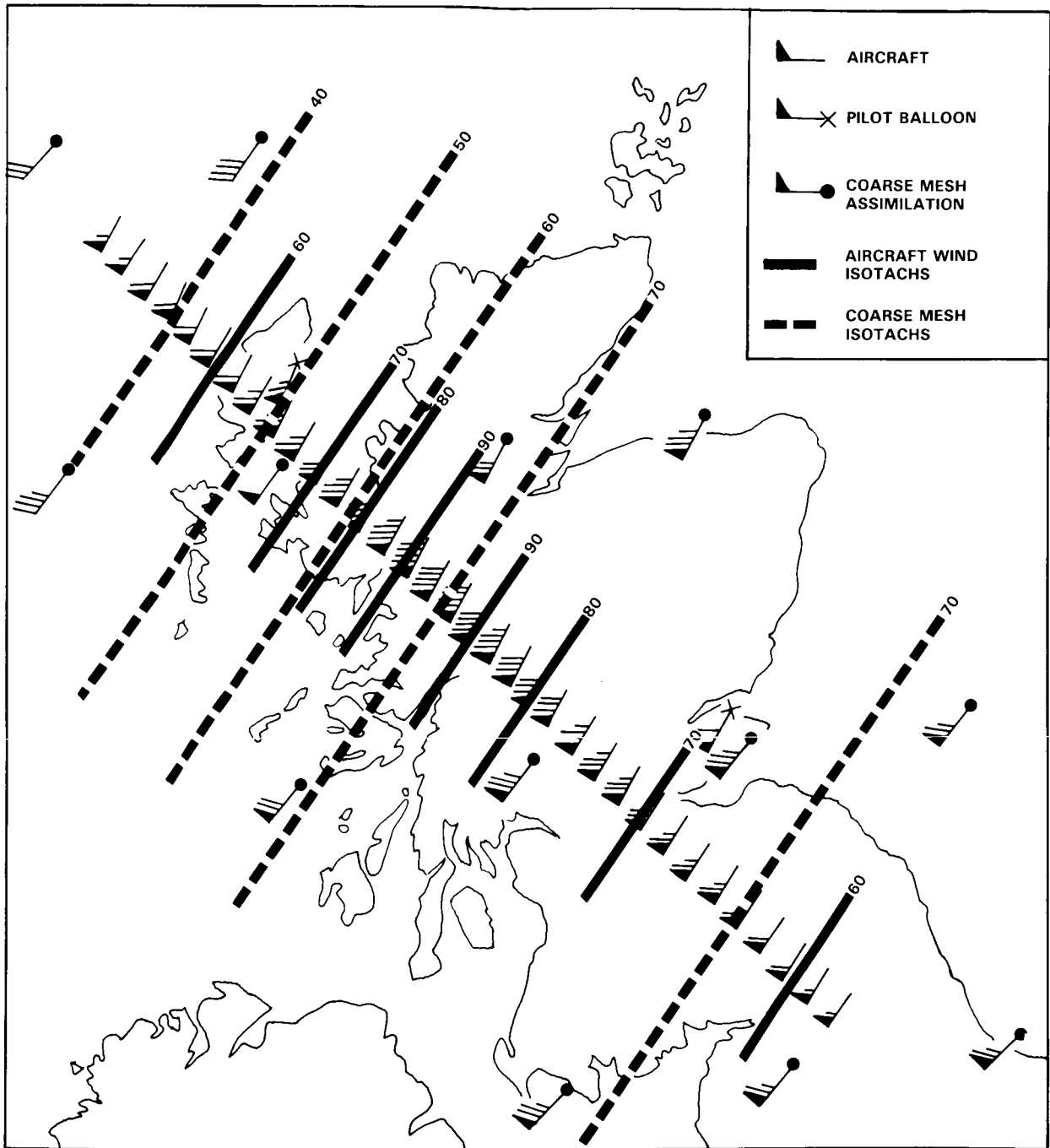
For reasons like those above present estimates of the annual average global transport of  $\text{O}_3$  across the tropopause from general circulation models cannot be considered to be completely reliable, let alone of the structure of the distribution in space and time, which is probably more important than the single number. The fine mesh results, however, give some reason to believe that better estimates will be possible in future.

## 5.4 ASSESSMENT OF STRATOSPHERE-TROPOSPHERE EXCHANGE

In both tropics and extratropics, recent high quality case studies have improved and amplified our detailed understanding of the processes effecting troposphere-stratosphere exchange, while reinforcing the basic correctness of the qualitative, gross mechanisms suggested for ingress by Brewer (1949) and for egress by Reed (1955). These case studies may in future be given global scope by combining them with measurement and analysis systems such as the TOMS observations, and with numerical weather prediction models, one of which has been shown to resolve extratropical tropopause folding events when its lat  $\times$  long resolution was improved from  $1.5^\circ \times 1.875^\circ$  to  $0.75^\circ \times 0.9375^\circ$ . However, for such an approach to work for a specific species, its covariance with potential vorticity in the lower stratosphere and upper troposphere must be known. In the absence of measured profiles of global extent at, above and below tropopause level, a start could be made by preparing correlograms of ozone and potential vorticity from all available data. In the tropics, it is likely to be more difficult to use operational meteorological models to obtain global scale estimates of cross tropopause flux. It may be possible to use satellite imagery of the ice crystal formations associated with deep tropical convection (anvils), but the methodology is not yet established.

Many substantial uncertainties remain. Previous studies used a body count of tropospheric cyclogenesis to compute the mass transfer out of the stratosphere in middle and high latitudes, despite some indications that this was unlikely to be a satisfactory procedure (Mahlman, 1965). Recent studies show that one cut-off low had three exchange events develop in the first three days; it existed as an entity for over 10 days, but no airborne studies were made after day 5. This, and the vertical extent of stratospheric extrusions revealed in some recent studies (3 and even 4 km) suggests that past estimates of ozone transfer to the troposphere may have been too small. Since cut-off lows are often associated with blocking anticyclones,

# STRAT-TROP EXCHANGE



H593 FL180 508MB 1800Z 16 APRIL 1983

**Figure 5-54.** Wind speeds measured from the C130 aircraft compared with the coarse mesh ( $1.5^\circ$  lat  $\times$   $1.875^\circ$  long) assimilation winds. Note the agreement of the aircraft data with the pilot balloon winds, and the model failure to resolve the wind shears. Dashed contours are the model assimilation; solid contours are the aircraft data. The fine mesh ( $0.75^\circ$  lat  $\times$   $0.9375^\circ$  long) did a much better job of reproducing the shears and core velocity.

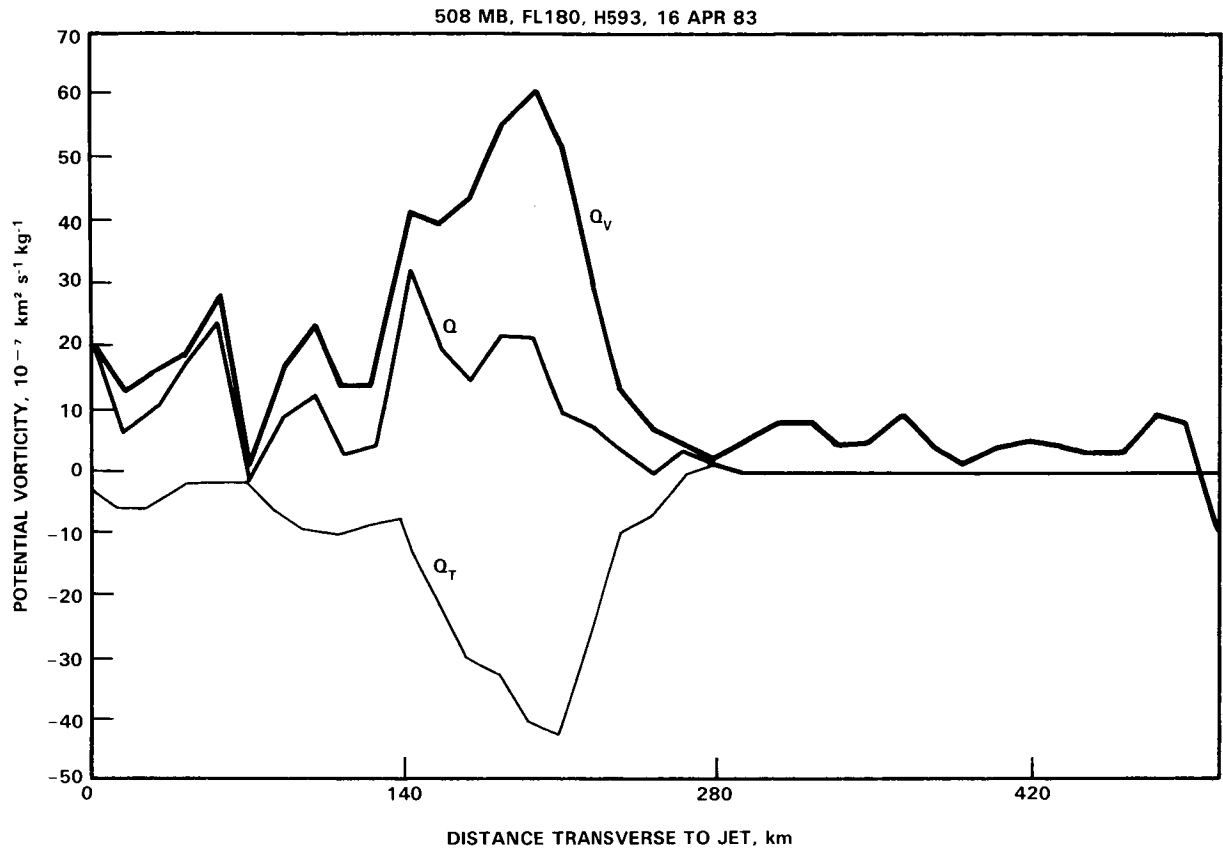


**Figure 5-55.** Potential vorticity from the aircraft winds of Figure 5-54. The vertical,  $Q_v$ , and transverse,  $Q_T$ , contributions to the total potential vorticity  $Q$  are shown. Note that  $Q_v$  is what meteorologists normally call "potential vorticity", and that the transverse component makes an important contribution near the core.

there could be substantial effects on the tropospheric ozone distribution. Blocking anticyclone/cut-off low systems occur preferentially in spring and autumn in the Northern Hemisphere in the NE American seaboard and Icelandic sectors, but in mid summer over the Central Pacific sector. They are also more intense and of longer duration in the Northern than in the Southern Hemisphere, where they are mostly confined to the New Zealand sector. There could thus be a systematic inter-hemispheric difference in tropospheric ozone content, and annual cycle variations which are a function of longitude arising purely from the dynamics of tropopause deformation during upper cyclogenesis. This supposition could be tested by assimilation analyses from a global weather model with adequate resolution (better than  $1^\circ \times 1^\circ$ ) with ozone treated as a tracer, possibly using TOMS data.

There is an apparent difficulty in reconciling the view that air enters the stratosphere solely in the tropics (which arises from recent case studies of water vapour profiles near cumulonimbus anvils in the Panama region) with the factor of 20 or 30 decrease in water vapour mixing ratio which occurs in a few kilometres above the mid-latitude tropopause. This is best resolved by saying that very little air above the hygropause cannot have entered in the tropics, but that air between the hygropause and the tropopause can have been mixed with extratropical tropospheric air moving quasi-horizontally, as suggested by dynamical and general circulation model studies. Whether or not air from this transition layer can be transported

## STRAT-TROP EXCHANGE

upward and equatorward in disturbed conditions, as predicted by a general circulation model, remains to be tested. Close examination of ozone, water vapour and methane profiles above the tropical hygropause is suggested. It is not securely established whether or not there is longitudinal variation in the water vapour mixing ratio at the tropical hygropause level. The matter is important, bearing in mind the potential of the deepest cumulonimbi for rapid vertical transport up to 20 km, with mixing extending up to 3 km higher.

There are two suggested explanations for the positive correlation observed in the stratosphere at and above hygropause level. One is that ozone and the component of water vapour coming from methane oxidation have a common source in the upper stratosphere. A second possibility arises from the general circulation model result of a positive correlation in ozone and water vapour between 30°N and 30°S at 70 mb, with no methane oxidation present. This was explained by deep convection in the western equatorial Pacific region drying ozone-poor air from near the surface.

It is possible that both mechanisms are effective; it might be expected that the first mechanism would give a positive correlation at high values of O<sub>3</sub> and H<sub>2</sub>O, while the second would maintain such a relationship at low values. This hypothesis clearly needs testing.

### 5.4.1 Unresolved Problems

An important unknown is connected with the extent to which tropopause folds are reversible. The data from recent studies in April 1983 and 1985 near the northern British Isles, and from April 1984 over the southwestern United States suggest that purely advective descriptions are incorrect, and that mixing is rapid. Nevertheless in some circumstances folds can be tracked for several days; if the mixed air is transported back to the stratosphere, then some tropospheric air may enter the stratosphere in mid-latitudes.

Both studies with global scale models and results from early aircraft studies in Project Springfield (Danielsen, 1964) suggest that some tropopause folds may split, with the supergeostrophic air to the right of the jet being decelerated and turned to the right, while the subgeostrophic air to the left of the jet is accelerated to the left. The supergeostrophic air descends into the south easterly flow around the upstream anticyclone, and is very unlikely to be reversible in the sense of return to the stratosphere. Such motion by folds has not been studied by aircraft with modern instrumentation, but is suggested by TOMS total ozone patterns in some troughs. Such volumes of air could reveal interesting chemical evolution. It is the subgeostrophic air which could re-enter the stratosphere. Figure 5-56 illustrates the splitting process.

There is a possible difficulty in need of resolution between the interpretation of the amplifying baroclinic wave given in Section 5.2.3.2 and the local dynamical constraint of potential vorticity conservation. It is shown that in such waves, subtropical air is transported poleward on isentropic surfaces that span the subtropical troposphere and the polar stratosphere, and that this transport exceeds that of polar air equatorward on the same surfaces. However, if the tropopause is advected with the air, exchange is not necessarily implied. The decrease in the water vapour profile, by roughly a factor of 30 within less than a scale height above the mid-latitude tropopause, argues that exchange does occur, but it is not clear how the large increase in potential vorticity needed to change tropospheric air into stratospheric air is achieved. In this context, the roles of radiative transfer and the presence of high cloud (cirrus), which occurs frequently in the warm sector of baroclinic lows, need examination; it may be also that the radiative time scale for the relaxation of cut-off highs which have moved to higher latitudes, as suggested in Section 5.2.3.2, needs further study. The time scales in actual cases have not as yet been established. There is one case study (Shapiro *et al.*, 1980), where in a split jet structure, tropospheric air with anticyclonic vorticity (i.e., low

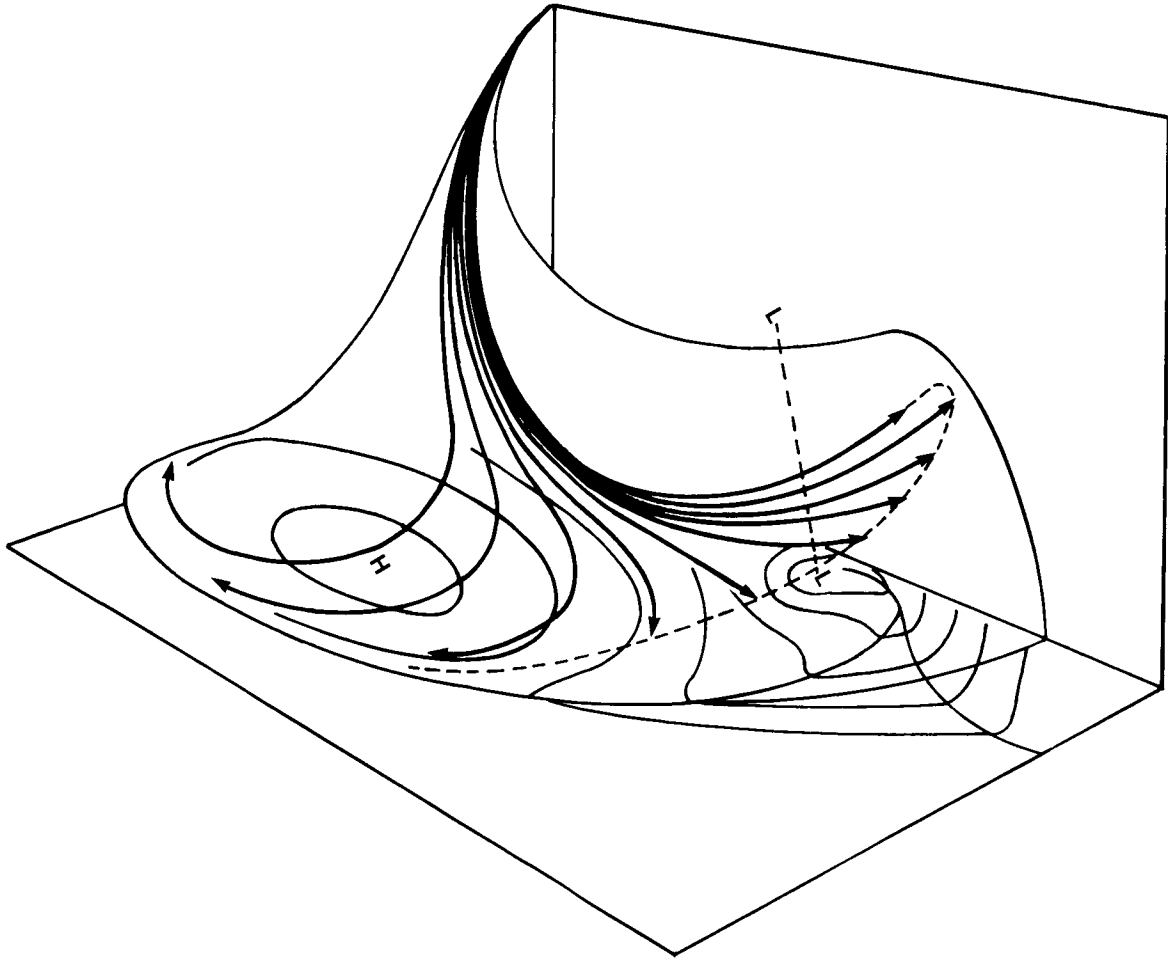


**Figure 5-56.** Schematic of trajectories of air extruded in a tropopause fold, relative to surface pressure pattern. The orthogonal planes are to lend a three-dimensional appearance. The air curving anticyclonically and downwards is unlikely to return to the stratosphere. The upward moving, cyclonically curved trajectories could return to the stratosphere, subject to constraints imposed by mixing processes.

potential vorticity) did move into the stratosphere, but which left open the question of how long it could stay there. Exchange from troposphere to stratosphere near jet streams needs more examination experimentally.

#### 5.4.2 Recommended Future Studies

There have as yet been no studies of exchange at the subtropical jet streams. In view of the considerable differences between such jets and polar front jet streams (see for example Newton and Trevisan, 1984), and the general circulation model results which suggest that partial inertial oscillations in the STJ could play a role in stratosphere-troposphere exchange, such studies are required, particularly of the E Eurasian jet stream in winter and spring.

It is not certain how much of the stratospheric air in cut-off lows is mixed into the troposphere after the system becomes isolated from the polar vortex. Similarly, the posited return of upper tropospheric

## STRAT-TROP EXCHANGE

air in baroclinic cyclogenesis to the stratosphere has not been characterized by detailed aircraft studies. A combination of upward looking DIAL ozone profiles and dropsondes to get  $u$ ,  $v$ ,  $w$ ,  $T$ ,  $P$  and humidity would be valuable, particularly in association with TOMS ozone mapping, which provides the means for a global extrapolation of local studies of each of the exchange processes.

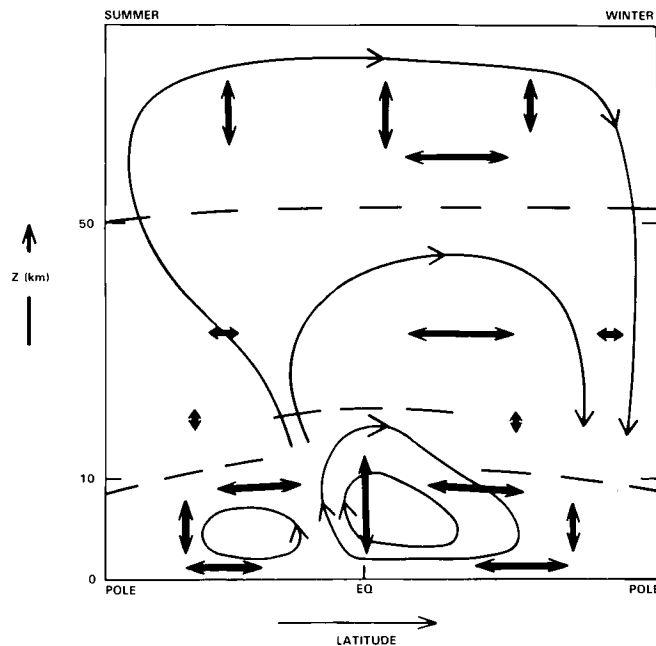
Investigation of the largest cumulonimbus storms, in the equatorial W Pacific Indian Ocean sector, the Bay of Bengal and at mid-latitudes in summer is required. The simple experiment of Barrett *et al.* (1973) could be very informative if repeated with modern instrumentation. It is also necessary to see if there is a widespread, thin layer of ice crystals in the region of low tropical tropopause temperatures (Figure 5-5).

There is also a clear need to examine the nitrogen oxide content of the air injected into the stratosphere by large Cb, and also that left behind by dissipating anvils. The ability of Cb to rapidly transport air from near the surface to tropopause level suggests that the whole range of the chemical composition of their inflow and outflow may need characterization. It is possible that suggestions made in 1976 that lightning may be an important source of  $\text{NO}_x$  for the lower stratosphere are correct, but better measurements are required.

There are instances in the literature where studies of the flow over mountains has revealed extremely steep slopes in the isentropes in the upper troposphere and lower stratosphere. Such situations should be investigated on a case study basis; the Himalayas and the Andes are outstanding examples of course.

Finally, if the global distribution of ozone flux across the tropopause is required in detail, satellite profiles in the lower stratosphere and upper troposphere will be required ultimately, as a check on techniques using global weather prediction models and potential vorticity.

# DYNAMICAL PROCESSES



## Panel Members

R.A. Plumb, Chairman

D.G. Andrews

A. O'Neill

M.A. Geller

M. Salby

W.L. Grose

R.A. Vincent

## CHAPTER 6

### DYNAMICAL PROCESSES

#### TABLE OF CONTENTS

6.0 INTRODUCTION .....	241
6.1 CLIMATOLOGICAL MEANS AND VARIABILITY OF THE MIDDLE ATMOSPHERE .....	243
6.1.1 Introduction .....	243
6.1.2 Zonally Averaged Structure of Wind and Temperature .....	246
6.1.3 Monthly Mean Wave Structure .....	250
6.1.4 Extratropical Transients .....	253
6.1.5 Equatorial Waves .....	258
6.1.6 Tides, Gravity Waves and Turbulence in the Middle Atmosphere .....	263
6.1.7 The Seasonal Cycle .....	268
6.1.8 Inter-Annual Variability .....	274
6.2 THEORY OF THE CIRCULATION OF THE MIDDLE ATMOSPHERE .....	278
6.2.1 Introduction .....	278
6.2.2 Some Simple Zonally-Averaged Models of the Middle Atmosphere .....	282
6.2.3 Aspects of Wave Mean-Flow Interaction Theory .....	286
6.2.4 Implications of the Theory .....	287
6.2.5 Stratospheric Sudden Warmings .....	290
6.2.6 The Non-Zonally-Averaged Climatological State .....	293
6.2.7 Theory of the Low-Latitude Zonal-Mean Circulation .....	294
6.3 MIDDLE ATMOSPHERE GENERAL CIRCULATION MODELS .....	297
6.3.1 Introduction .....	297
6.3.2 Current Status of Middle Atmosphere GCMs .....	298
6.3.3 GCM Deficiencies .....	307
6.3.4 Future Directions .....	308
6.3.5 Summary .....	311
6.4 OBSERVATIONS OF TRANSPORT PROCESSES .....	311
6.4.1 Introduction .....	311
6.4.2 Intercomparisons of Derived Quantities .....	311
6.4.3 Studies of Wave-Mean Flow Interaction and Stratospheric Warmings .....	313
6.4.4 Studies of Transport Processes .....	315
6.4.5 Conclusions .....	317

6.5 THEORY OF TRANSPORT PROCESSES .....	318
6.5.1 Introduction .....	318
6.5.2 Zonally-Averaged (2D) Formulations .....	318
6.5.3 Gross Characteristics of Atmospheric Transport .....	328
6.5.4 Some Outstanding Issues in 2D Modeling .....	334
6.5.5 Three-Dimensional Modeling .....	336
6.6 FUTURE NEEDS .....	337
6.6.1 Satellite Observation .....	337
6.6.2 Ground Based Studies .....	339
6.6.3 Dynamical Theory .....	340
6.6.4 General Circulation Models .....	341
6.6.5 Transport Theory and Modeling .....	342
6.7 SUMMARY .....	343
6.7.1 Observations of the Middle Atmosphere .....	343
6.7.2 General Circulation Modeling of the Middle Atmosphere .....	344
6.7.3 Theory of Dynamics and Transport .....	345

## 6.0 INTRODUCTION

The distribution of ozone is maintained by combined radiative, chemical and dynamical processes. In particular, transport processes determine the movement of ozone precursor constituents such as  $N_2O$  and  $CH_4$ . Dynamics also influences the distribution of constituents such as  $NO_x$ ,  $HO_x$  and  $Cl_x$  which determine ozone loss processes, and of course transport processes act on  $O_3$  itself determining its distribution throughout much of the atmosphere. For these reasons, it is crucial that models that aim to simulate present day ozone correctly as well as those that aim to make quantitatively correct predictions of future ozone distributions include quantitatively correct transport. This, in turn, requires that the atmospheric dynamics responsible for effecting this transport be modeled in a quantitatively correct manner.

Transport in the atmosphere can be effected by dynamical processes acting on all spatial and temporal scales. For instance, the Brewer-Dobson circulation is a global scale circulation consisting of rising motion in the tropics and descending motion at high latitudes. In this chapter, it is emphasized that this type of global-scale pattern of rising and descending motions owes its existence to the presence of asymmetric eddy motions. These can be large-scale eddies (e.g., baroclinic waves and planetary waves) or small-scale eddy motions (gravity waves and turbulence). The fact that the existence of the global scale overturning circulations is so intimately connected to eddy transport processes has important implications for the formulation of transport models.

The last comprehensive discussion of the state of research of the ozone problem took place four years ago [WMO, 1981]. Several notable advances in our understanding of dynamics and transport have been made during these four years. These have included new observational analyses, improvements in our modeling capabilities, and an enhanced theoretical basis for our understanding of transport. Brief discussion of some of these is given in this introductory section with a more complete discussion given in the body of the chapter.

On the observational side, there have been analyses of new satellite data. For instance, Salby *et al.* [1984] have used the high vertical resolution LIMS data to identify equatorial Kelvin waves in both the stratosphere and mesosphere. Also, the new availability of observations of  $O_3$ ,  $H_2O$ ,  $NO_2$  and  $HNO_3$  from LIMS and of  $N_2O$  and  $CH_4$  from SAMS has made it possible to use these observations to evaluate current ideas on the interplay between chemistry and transport. There have also been new analyses of more conventional nadir-viewing stratospheric satellite data. Perhaps, the analysis of this type that has had the greatest impact on our conceptual understanding was that of McIntyre and Palmer [1983] in which they showed observational evidence for Rossby wave breaking. Several multi-year climatological analyses have also appeared in the literature during this past four years. This has allowed the average annual cycle in Northern and Southern Hemisphere stratospheric climatological variables to be determined as well as the inter-annual variability in the climatology. Indeed, our knowledge of the circulation of the Southern Hemisphere stratosphere has improved dramatically in the recent years, principally as a result of global satellite coverage. Our understanding of this half of the globe, however, still lags behind that of the Northern Hemisphere.

Ground-based radar and lidar observations have also contributed significantly to our knowledge of gravity wave processes in the mesosphere. Vincent and Reid [1983] have provided measurements of vertical momentum fluxes that demonstrate consistency with the theoretical concepts of gravity-wave-induced drag on the mean zonal flow proposed by Lindzen [1981] and Matsuno [1982]. There have also been the beginnings of the assemblage of a radar-derived gravity wave climatology for the middle atmosphere. While little has yet appeared in the literature, these works have motivated researchers to become increasingly concerned about what role gravity waves might play in the stratosphere.

## DYNAMICAL PROCESSES

On the theoretical side, there has recently been a much greater appreciation of the balance between advective and dispersive transport processes [Mahlman, 1985; Plumb and Mahlman, 1986]. The latter work sets forth the framework from which a consistent specification of advection and dispersion can be made in two-dimensional photochemical models. A framework with which the one-dimensional eddy diffusion used by photochemical modellers can be reconciled with large-scale dynamics has also been given by Holton [1985] and Mahlman *et al.* [1985].

Along with the developing appreciation of the climatology of the middle atmosphere has come the realization that the traditional conceptual separation of the three-dimensional structure into zonal mean and eddy components may have severe limitations. This is especially true during Northern winter, when the polar vortex may be shifted well off the pole. In the absence of any theoretical framework to simplify the transport problem, the full implications of this three-dimensionality can only be addressed via direct analysis of the observed circulation and constituent distributions or in three-dimensional models.

There has been a great deal of activity in middle atmosphere modeling over the last four years. Among other things, this has led to an increasing realization that, despite the large scale of flow patterns typical of stratospheric maps, general circulation models of the middle atmosphere need to use horizontal resolutions that were previously thought to be necessary only in the troposphere. There has been a slow, but appreciable, advancement in the inclusion of transport and photochemical processes in three-dimensional models. A continuing problem with middle atmosphere general circulation models is their pathology in producing excessively cold polar night temperatures with associated excessively strong westerlies. There remains some uncertainty over the role of improved parameterization of radiative processes versus inadequate dynamics in giving rise to this discrepancy. Even if the source of this problem is taken to be inadequacies in dynamics, it is unclear what role is played in this by gravity waves as opposed to large-scale waves.

Such shortcomings place limitations on the use of current models for assessment studies. However a more serious practical limitation is that inclusion of complex, realistic photochemistry into such models remains prohibitively expensive (except for short integration times), even for the fastest present day computers. It seems we must await a future generation of computers, or a theoretical advance in the simplification of three-dimensional transport, before three-dimensional assessments become a reality.

The remainder of this chapter is organized as follows. Section 6.1 deals with the observed structure of the middle atmosphere. In this section, there is a brief discussion of the techniques used to observe the middle atmosphere. This is followed by discussions of the zonally-averaged and eddy structure of the middle atmosphere; in particular, our rapidly expanding appreciation of transient motions is discussed in some detail. Discussions of observed middle atmosphere seasonal variations and interannual variability follow. Section 6.2 contains a discussion of our theoretical understanding of the middle atmosphere circulation. The point is made very strongly that our present understanding of middle atmosphere dynamics tells us a great deal about middle atmosphere transport processes. In particular, the relationship between the residual mean circulation and eddy processes is underscored. The present status of general circulation models of the middle atmosphere is discussed in Section 6.3. Section 6.4 reviews some recent satellite-based observational studies of stratospheric transport processes, as revealed by the behavior of constituents and of potential vorticity (a dynamical tracer). The theory of global transport and its representation in transport models is discussed in Section 6.5. Finally, Sections 6.6 and 6.7 contain some comments on future directions in this field of research and a summary of the main points of the chapter.

## 6.1 CLIMATOLOGICAL MEANS AND VARIABILITY OF THE MIDDLE ATMOSPHERE

### 6.1.1 Introduction

Climatologies of the middle atmosphere have been constructed from radiosonde/rocket soundings and other surface-based information. The set of observations due to Groves [1970] was adopted as the CIRA [1972] standard atmosphere. Few radiosondes reach levels above the lower stratosphere and rocket data are very sparse. It is therefore impossible to obtain a complete global picture of the structure and dynamics of the middle atmosphere from these types of observations alone. With the launch of satellite-borne radiometers, it became possible to map the temperature distribution in three dimensions and to follow its changes from day to day. From the thermal wind relation between the temperature and motion fields, the wind field in the extratropics can be derived to a good approximation if the height of some base pressure level in the atmosphere is available, and a wide range of dynamical studies can then be conducted. One major advantage of satellite measurements is their global coverage. Note however that the process of building up the height/wind analysis from some base level means that errors in the base height field (and there remain substantial gaps in ground-based observations, especially over the Southern oceans) permeate the entire analysis. Further major advantages of satellite measurements are their approximate spatial uniformity and the fact that they are made with a single instrument. These features are particularly important for dynamical studies as relevant diagnostic quantities can involve a high order of spatial differentiation, and global analyses based on readings of uniform reliability are consequently vital. Recent climatological studies of the middle atmosphere which have employed satellite data are those of Labitzke and Barnett [1979], McGregor and Chapman [1979], Hamilton [1982b], Geller *et al.* [1983, 1984], and Hirota *et al.* [1983a]. A new interim CIRA atmosphere is to be published in the Handbook for MAP, Vol. 16.

Confidence in the reliability of satellite-derived data has been increased through comparison of quantities derived from satellite data with equivalent quantities obtained from conventional meteorological analyses and/or other, independent, satellite data. Smith [1982] compared wind fields, wave structures and other derived quantities using SCR and LIMS satellite data and NMC analyses based on conventional (radiosonde) data below, and satellite data above, 10mb. The comparisons showed good qualitative agreement, although SCR and LIMS data could not be compared directly since the instruments were not operating at the same time. Kohri [1981] had earlier performed similar studies using a single month (Dec. 1975) of LRIR data.

A somewhat more stringent and systematic attempt at intercomparison was made by the PMP-1 working group using SAMS and LIMS data from the Nimbus 7 satellite, SSU data from TIROS-N and conventional analyses (mostly based on radiosonde data) from NMC, ECMWF and the Free University of Berlin. The study focused on 8 individual days, including quiet and disturbed times; results are discussed in Rodgers [1984]. Overall the study found good qualitative agreement and, in some cases, good quantitative agreement between the various data sources. However, differences in horizontal and/or vertical gradients can produce marked differences in derived quantities; significant differences were apparent for momentum flux. A second study by this working group [Rodgers and Grose, 1985] has focused on monthly mean comparisons for periods between 1979-81 using the same data sources. Conclusions were similar to those of the earlier study.

Noticeably absent to date is a detailed comparison focusing on the Southern Hemisphere. This situation is perhaps a result of the sparseness of radiosonde data for the Southern Hemisphere and the fact that many of the sampling strategies for remote measurements from satellites have focused on the dynamically more active Northern Hemisphere.

## DYNAMICAL PROCESSES

Satellite measurements do not give readings at a point but are averages over a volume of the atmosphere [see Houghton *et al.*, 1984, Chapter 6]. Moreover, they are made asynchronously: measurements at different points are taken at different times, so that some form of time interpolation is also implied. During periods when the circulation is highly contorted important features may not be adequately resolved and other measuring techniques with higher spatial and temporal resolution then provide useful supplementary information. Two such techniques are lidar and radar which give good vertical and temporal resolution from ground sites, though clearly not global coverage.

Ground-based techniques offer refined vertical and temporal resolution, which makes them well suited to studying small-scale phenomena such as gravity waves. Their value in observing large-scale processes is limited by the localness of the measurements. An important development has been that of the MST (Mesosphere-Stratosphere-Troposphere) radar technique introduced by Woodman and Guillen [1974]. Radars of this type operating at VHF (30-300 MHz) and UHF (0.3-3 GHz) have the capability of measuring winds, waves and turbulence parameters with time and vertical resolutions of the order of 1 to 2 min and 50 to 300 m, respectively. Echoes are obtained from refractive index irregularities caused by temperature and density fluctuations in the troposphere and stratosphere and by fluctuations in electron density in the mesosphere. The Doppler shift of the echoes gives the line-of-sight velocity. Three radar beams enable the measurement of the complete velocity vector, as these radars have the unique ability to measure vertical velocities with reasonable accuracy. Depending on the radar sensitivity, it is possible to make almost continuous wind soundings at heights up to 25 to 30 km. In the mesosphere, echo occurrence is, however, often intermittent with diurnal, seasonal and geographic changes being found. Because of their excellent temporal and spatial resolutions MST radars have provided invaluable information about short period gravity waves and turbulent motions. However, long term studies of the dynamics of the mesosphere have so far been restricted to a few sites. Rottger [1980] and Gage and Balsley [1984] have provided recent reviews of MST techniques and their capabilities.

Partial reflection (PR) radars which operate at frequencies near 2 MHz share with the MST technique the ability to measure the structure of tides, gravity waves and the time-mean flow in the mesosphere. Although their time and height resolutions are moderate (a few min and a few km) PR radars have proved very reliable and, at some stations, almost continuous observations have been made over several years, giving insight into the morphology of mesospheric waves and winds [Vincent, 1984b].

Lidars which use Rayleigh scattering from atmospheric molecules to measure neutral density and temperature constitute an important new development since they provide information about the wave parameters which is complementary to that provided by radars [Chanin and Hauchecorne, 1981]. Time and height resolutions of 15 min to 1 hr and 100 m to 1 km can be achieved and since lidars can observe much of the stratosphere and mesosphere, they can study the 'gap' region between 30 and 55 km, which is the most difficult region to investigate with MST radars. To date, most information about small-scale dynamics in this range has come from infrequent rocket and balloon soundings.

This section on climatology is an account of the global structure of the large-scale circulation of the middle atmosphere that has been inferred from satellite measurements, and includes a description of the small-scale wave and turbulence processes determined by radar. The section begins with a discussion of the basic state of the middle atmosphere as represented by the zonal mean structure of temperature and winds at the solstices (Section 6.1.2). This zonal mean structure is, of course, an incomplete description of the three-dimensional state. Even on a monthly-averaged basis, the wintertime stratospheric wind field may depart substantially from zonally uniform flow, because of the presence of large-amplitude quasi-stationary waves. While it has become almost conventional to describe the climatology of stratospheric

waves in terms of these time-averaged components, day-to-day variations are in fact substantial. Estimates of the ratio of variance in transient wave components to that in the time-mean waves range from 1 to 1 [Tomatsu, 1979] to 3 to 1 [Geller *et al.*, 1984; Hirota *et al.*, 1983a]. Consequently any meaningful description of climatology must account for fluctuations about the time-averaged state of the stratosphere. The emergence of continuous global satellite observations in recent years has greatly facilitated our knowledge of such features. Understanding has been advanced by these measurements for both transient extratropical disturbances and for equatorial wave modes. Many of these features were previously unobserved; indeed the identification of some of these modes has been a major success of limb-viewing satellite measurements.

The extratropical planetary wave field may be characterised, at least qualitatively, in terms of two basic contributions to frequency spectra of individual wavenumbers. At low frequencies, variance has the form of a red continuum, falling off more or less systematically with decreasing period, representing the baroclinic, "quasi-stationary" waves, which are largely confined to midlatitudes of the winter hemisphere. These disturbances propagate upwards through the stratosphere and play a central role in coupling the stratosphere with the troposphere. They are "quasi-stationary" in the sense that they fluctuate, in amplitude and phase, about climatologically preferred values. Their climatological structures are presented as monthly mean waves in Section 6.1.3. It must be emphasised, however, that the departures of the actual wave field from these means can be dramatic, especially during high-latitude warming events (see Section 6.1.7).

Adjacent to and superimposed on this red continuum are discrete spectral peaks appearing at westward frequencies for the smallest zonal wavenumbers. As will be discussed in Section 6.1.4, several of these discrete peaks may be manifestations of planetary normal modes. These waves are of global extent (at least at the lowest levels) and their vertical structure is for the most part barotropic.

Most of the wave activity of the middle atmosphere is believed to originate in the troposphere. Forcing of the large-scale, quasi-stationary waves is ultimately provided by the orographic effects of large mountain ranges and the thermal effect of longitudinal variations in diabatic heating. However the tropospheric planetary wave field incorporates a substantial transient component. While the nature of these disturbances has not been addressed in stratospheric studies, such considerations have been examined extensively in tropospheric investigations. A number of these [Eliassen and Machenhauer, 1965; 1969; Ahlquist, 1982; Lindzen *et al.*, 1984] indicate that a sizable fraction of the unsteady planetary wave activity at periods shorter than two weeks is associated with the planetary normal modes. Some of these studies [also Hirooka and Hirota, 1985] suggest that during sporadic amplifications, these transient components in combination may attain amplitudes as large as the stationary components. It is important that the relative contribution from these two elements of planetary wave activity be more fully understood.

A distinct set of wave motions is observed in the tropics. These "equatorial waves" are of large zonal scale, but confined in latitude about the equator. They have large horizontal phase speeds and short vertical wavelengths, which precluded their observation from satellites until the advent of limb-viewing instruments. These waves, which play a fundamental role in the momentum budget of the tropical middle atmosphere, are described in Section 6.1.5.

Gravity waves and tides are of relatively small amplitude in the lower stratosphere. Because of their high frequency and rapid vertical propagation they are, in the main, attenuated relatively little as they propagate upwards and therefore they attain large amplitudes in the mesosphere, where they become dominant influences on the mean circulation. Section 6.1.6 discusses our current knowledge of these motions and of the turbulence which they generate in the mesosphere.

## DYNAMICAL PROCESSES

The final two sections describe the variability of the circulation. The account of the seasonal cycle in Section 6.1.7 draws attention to the extreme departures from time-averaged fields that can occur in the middle atmosphere. On longer time scales, it has come to be recognised that the year-to-year variability of the circulation is more marked in the stratosphere than in the troposphere. Therefore, the circulation in any one year or small group of years should not be taken as fully representative; some findings on the inter-annual variability of the middle atmosphere are presented in Section 6.1.8.

### 6.1.2 Zonally Averaged Structure of Wind and Temperature

The zonal mean temperatures and zonal winds of the stratosphere and mesosphere for January and July are shown in Figures 6-1. and 6-2. Except at high latitudes in the lower stratosphere during winter, the temperature increases with height in the stratosphere (due to ozone heating) and decreases with height in the mesosphere. In the middle and upper stratosphere, the temperature decreases monotonically from the summer to the winter pole, whereas the temperature gradient has the opposite sign in the mesosphere.

In Section 6.2, below, this climatological temperature structure will be compared with that predicted on the basis of a radiative-convective equilibrium calculation. Some of the differences are substantial, with the winter pole as much as 100 K warmer than the radiative-convective equilibrium value. As will be discussed in Section 6.2, these differences are indicative of dynamical influences.

There are pronounced differences between hemispheres during winter in the stratosphere and lower mesosphere at high latitudes, which reflect different levels of dynamical activity. In the northern hemisphere, the polar temperatures are warmer through most of the stratosphere and colder near the stratopause than they are in the southern hemisphere. During summer, the stratopause in the southern hemisphere is about 5 K warmer than in the northern hemisphere, probably because the Earth is closer to the Sun in January than it is in July.

Zonal winds in winter and summer are westerly and easterly, respectively, with maxima located at mid latitudes in the lower mesosphere. Easterlies occupy equatorial latitudes in the stratosphere at the solstices, except in the lower stratosphere during the westerly phase of the quasi-biennial oscillation (Section 6.1.8). The middle and upper mesosphere are marked by a rapid decrease with height of both the westerly and easterly winds. This is thought to be due to the drag imposed by the dissipation of gravity waves, which propagate upwards from the troposphere [e.g., Lindzen, 1981]. Another major feature of the wind distribution is that zonal winds are typically much stronger during winter in the southern hemisphere than they are in the winter northern hemisphere. This is consistent (through thermal wind balance) with the colder polar temperatures in the southern hemisphere.

The zonal-mean meridional velocity  $\bar{v}$  in the middle atmosphere can only be inferred indirectly from satellite measurements of radiance. In the mesosphere, however, long term-radar measurements have been used to obtain  $\bar{v}$ . Figure 6-3 shows an example of the annual changes of the meridional and zonal flow in the mesosphere observed with a partial reflection radar. It illustrates the variability due to the passage of large-scale waves but overall the mean meridional flow is from the summer to winter pole, in agreement with theoretical expectations (see 6.2.4). The peak magnitudes are between 5 and 20  $\text{ms}^{-1}$  and occur at the mesopause [Nastrom *et al.*, 1982; Vincent, 1984b]. Mean vertical velocities,  $\bar{w}$ , are extremely difficult to measure because of their small magnitudes. However, Nastrom *et al.* [1985] found reasonable agreement in the lower atmosphere between MST radar measurements of  $\bar{w}$  and values computed by other

DYNAMICAL PROCESSES

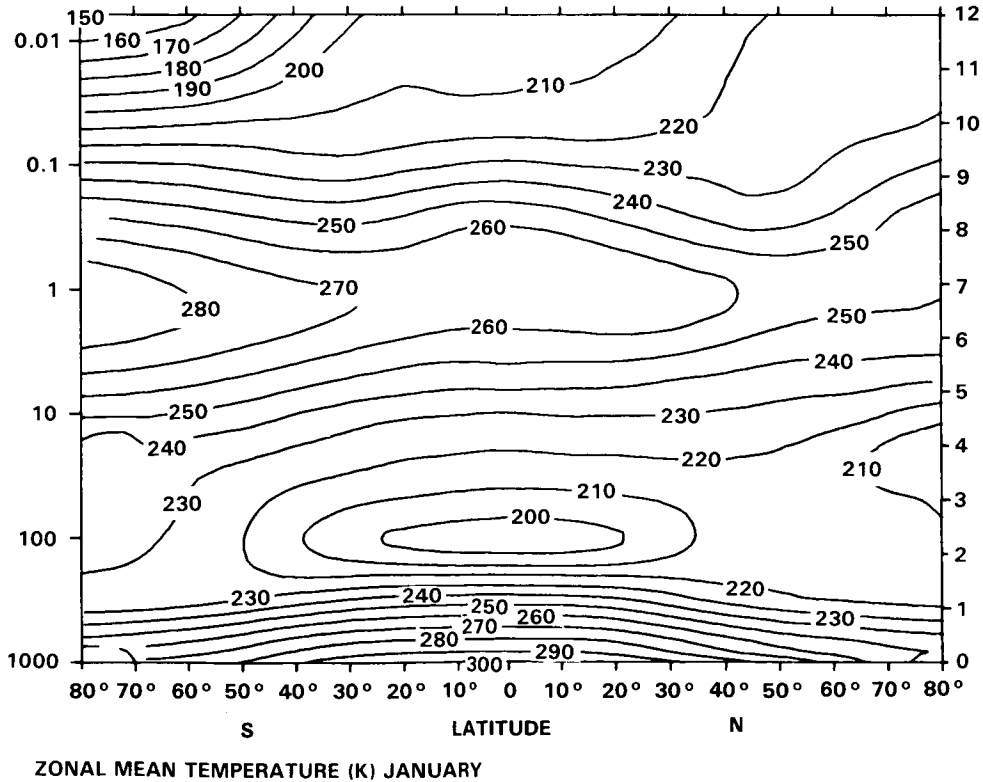
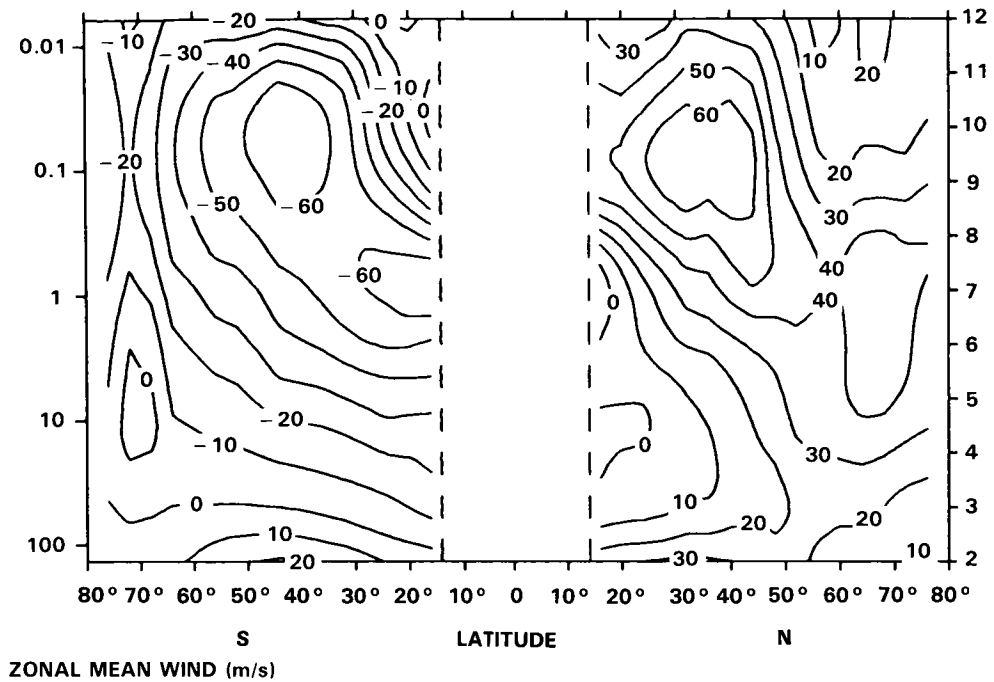


**Figure 6-1.** Cross sections [pressure (mbar)-latitude] of zonal mean geostrophic wind ( $\text{ms}^{-1}$ ) and zonal mean temperature (K) for the average over 5 years of the monthly means for January. The data are from the combined SCR/PMR retrieval made at the University of Oxford for the period January 1973 to December 1974 and July 1975 to June 1978. (Supplied by J.J. Barnett and M. Corney).

DYNAMICAL PROCESSES

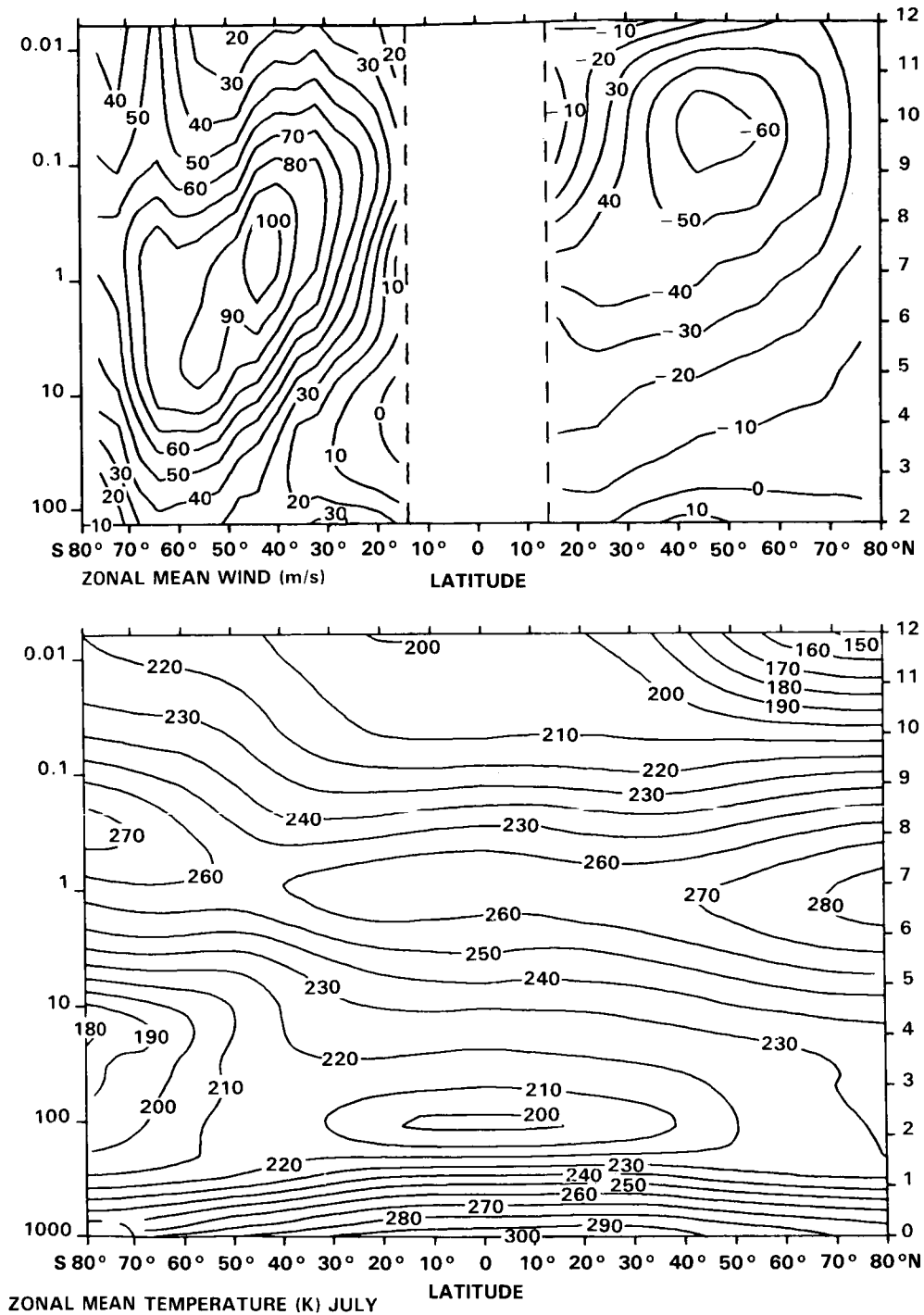


Figure 6-2. As Figure 6-1 but for July.

means. In the mesosphere, Balsley and Riddle [1984] measured long-term velocities of about  $25 \text{ cm s}^{-1}$  with the Poker flat [65°N] MST radar which are much larger in magnitude and opposite in sign to the values expected from the observed  $\bar{v}$  and temperature structure. Theory predicts a rising circulation over the summer pole and sinking motion over the winter pole (Section 6.2.4).



## DYNAMICAL PROCESSES

### 6.1.3 Monthly-Mean Wave Structure

Departures of the circulation of the middle atmosphere from zonal symmetry are conventionally summarized by presenting the structure of harmonic waves around latitude circles. Whereas any zonally varying field can be represented mathematically as a Fourier spectrum of waves, such descriptions are most valuable when the field contains only the gravest components, e.g., wavenumbers 1 and 2, as is typically the case for the stratospheric height field. Such behavior is consistent with the planetary wave theory of Charney and Drazin [1961] who showed that only the longest waves generated in the troposphere can penetrate well into the middle atmosphere in winter. Recent studies, however, caution against an over-reliance on linear theory when interpreting the complete behavior of the wave components [McIntyre and Palmer, 1983, 1984; Clough *et al.*, 1985].

The amplitudes and phases of wavenumbers 1 and 2 are shown in Figure 6-4 and 6-5. They are computed for the solstices from the monthly-mean geopotential height field. Maximum amplitudes are at high latitudes near the stratopause and decay with height in the mesosphere. This decrease may be due to a number of factors: dissipation of disturbances is more rapid in the mesosphere than in the stratosphere [Dickinson, 1973]; the vertical penetration of disturbances may be limited by the wind distribution resulting in equatorward refraction [Karoly and Hoskins, 1982]; large-scale disturbances may be dissipated to some extent in the stratosphere by the generation of small scales of motion during 'wave breaking' [McIntyre and Palmer, 1983, 1984]. In summer, monthly-mean amplitudes are very small since large-scale quasi-stationary disturbances are confined to the troposphere by easterly winds in the stratosphere [Charney and Drazin, 1961]. In both hemispheres during winter, the amplitudes of wave 2 are less than those of wave 1. Both waves exhibit a westward tilt with height at midlatitudes in the stratosphere and less tilt in the mesosphere. The ridges and troughs associated with the waves are aligned from the south-west to the north-east in the northern hemisphere, and from the south-east to the north-west in the southern hemisphere. The tilt with height and the trough/ridge alignment correspond to poleward eddy momentum and heat fluxes, and upward and equatorward Eliassen-Palm fluxes (see Section 6.2).

There are inter-hemispheric differences in the amplitudes of the monthly-mean waves that can be associated with the differences in zonal mean temperatures and winds mentioned earlier (see Section 6.2). The northern hemisphere winter stratosphere is more disturbed than is that of the southern hemisphere, reflecting the more asymmetric circulation in the northern hemisphere winter troposphere. As a consequence of this difference, theoretical arguments (Section 6.2) predict warmer polar temperatures and weaker zonal winds for the northern hemisphere during winter than during the southern winter. In the stratosphere, there is a stronger meridional gradient of the phase of the waves in the southern hemisphere (Eliassen-Palm fluxes tilt more equatorwards). This is consistent with the prediction of linear theory that waves will be more strongly refracted equatorwards in the broader and stronger westerly jet of the southern hemisphere.

The time-averaged waves (principally waves 1 and 2) combine with the zonal mean flow in the middle stratosphere to produce the monthly-mean winter circulation shown in Figures 6-6 and 6-7. The main features of the circulation are of a much larger scale than in the troposphere. In the northern hemisphere (Figure 6-6), a persistent feature near 180°E is the so-called Aleutian High. It is an anticyclonic circulation containing air drawn polewards from lower latitudes [Clough *et al.* 1985]. Strong fluctuations in its intensity occur throughout winter, particularly during sudden warmings. The circulation in the southern hemisphere (Figure 6-7) is far less disturbed and the pole is correspondingly colder. There is, however, a smaller interhemispheric difference in the temperature of the coldest air near the center of the westerly vortex.

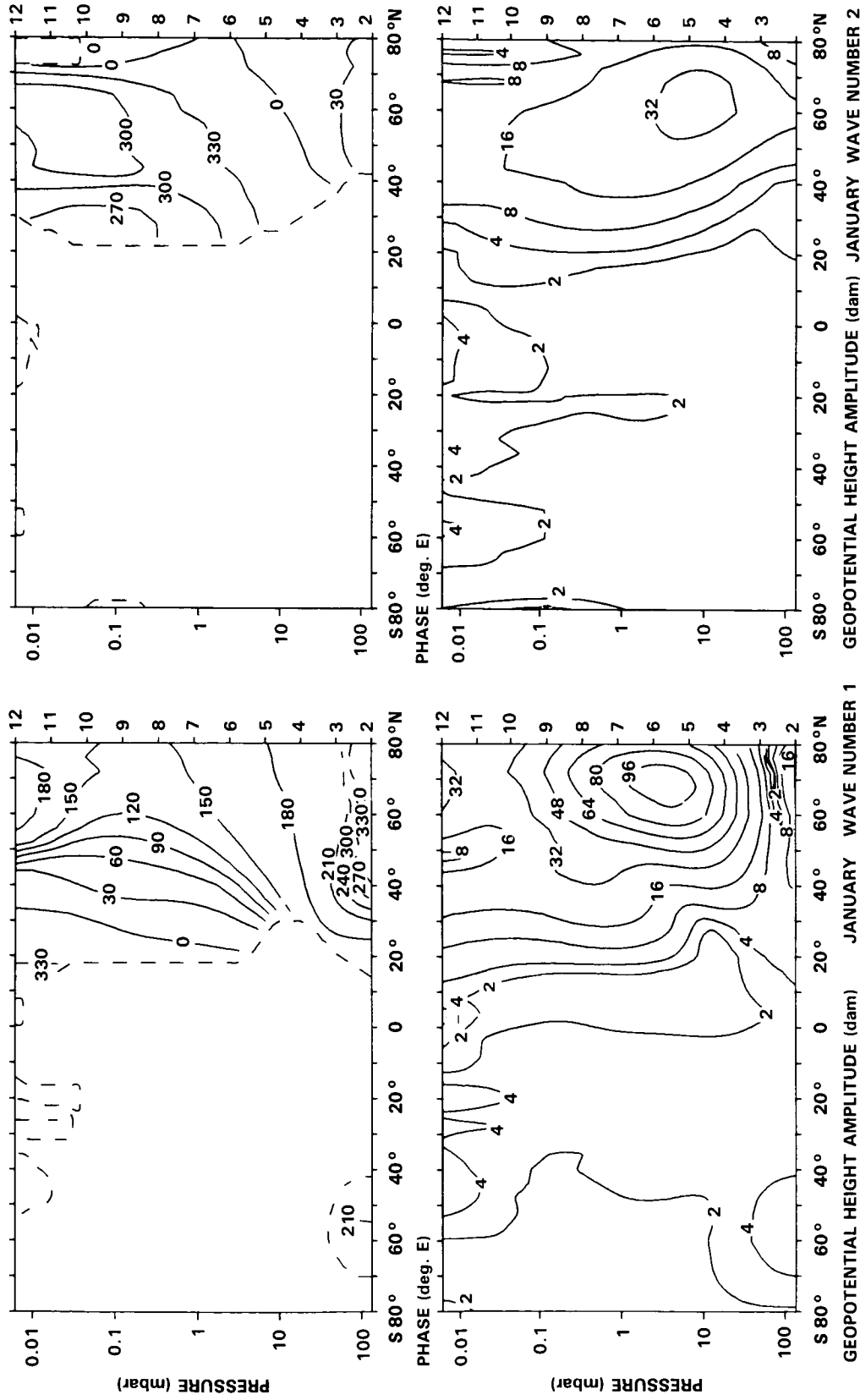


Figure 6-4. Cross sections of the amplitudes (dam) and phases (degrees east) of geopotential height waves 1 and 2 computed for January using the same data used for Figures 6-1 and 6-2. Scale on left is pressure (mbar). Courtesy of J.J. Barnett and M. Corney.





## DYNAMICAL PROCESSES

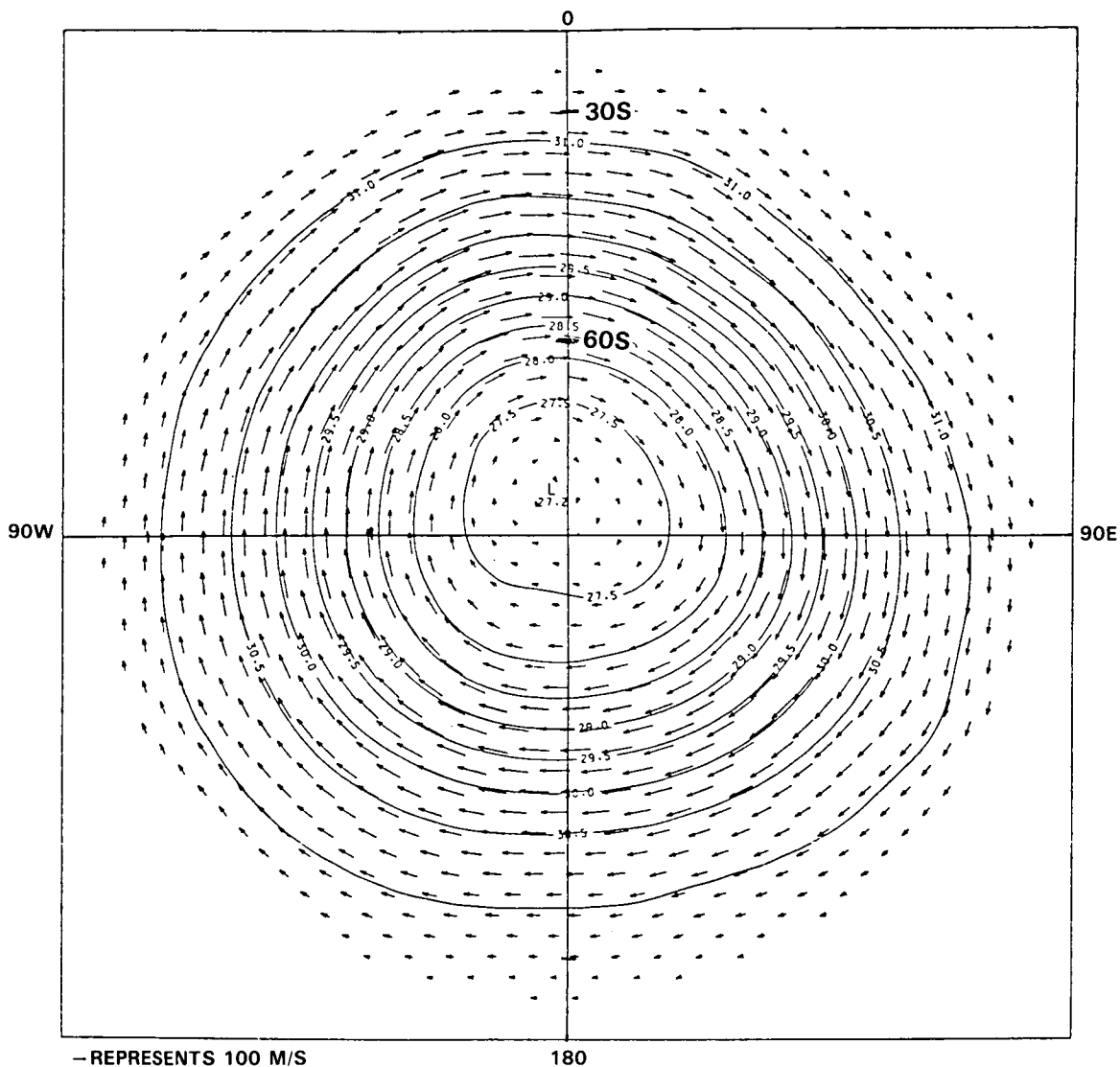
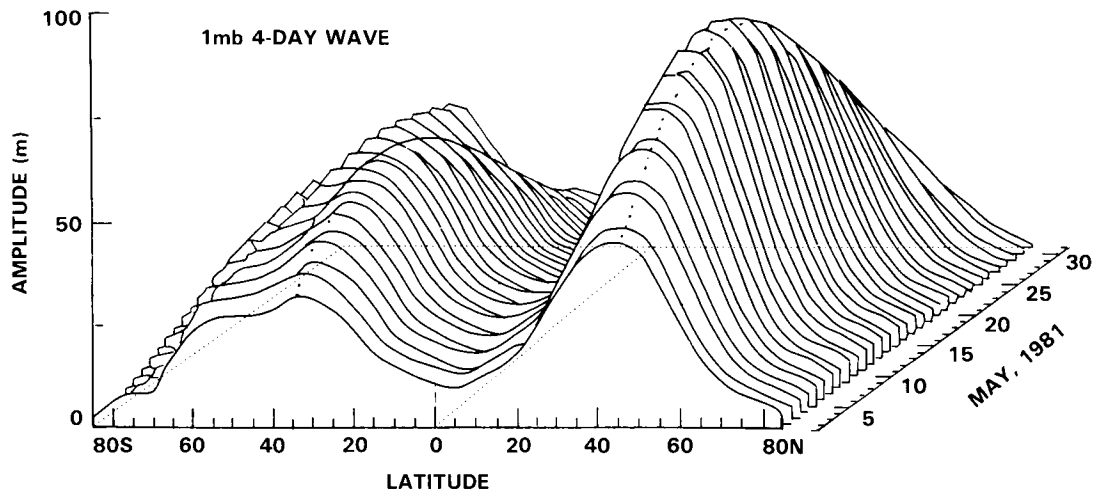


Figure 6-7. As Figure 6-6 but for the southern hemisphere for July 1981.

The first normal mode to be convincingly identified and the most widely documented is the 5-day wave [Madden and Julian, 1972b; 1973]. It has a wavenumber 1 global structure which is symmetric about the equator and propagates westward around the earth once in 5 days. Evidence for the disturbance has emerged from meteorological analyses [Madden, 1978], global satellite temperature retrievals [Rodgers, 1976a; Hirota and Hirooka, 1984], and from radar wind measurements [Salby and Roper, 1980; Hirota *et al.*, 1983b]. The last study indicated a sizable perturbation of the zonal mean flow by this component, particularly in the summer easterlies where quasi-stationary wave activity is absent.

With the increased availability of global satellite measurements, additional normal modes have been identified. Figure 6-8 shows the wavenumber 2 analogue of the 5-day wave, the 4-day wave at the stratopause, as derived from Tiros-N SSU by Hirota and Hirooka [1984]. The satellite observations have provided a fairly compelling picture of a global disturbance, nearly symmetric between the hemispheres. Higher



**Figure 6-8.** Structure and evolution of the 4-day wave at stratopause level, observed by Tiros-N SSU and NOAA-A HIRS. Corresponds to wavenumber 2 at 1 mb, bandpassed between 3.8-4.5 days over May 1981. Systematic retrogression is simultaneously observed. [After Hirota and Hirooka, 1984.]

degree normal modes have also emerged in Nimbus-5 SCR, Nimbus-6 PMR, Tiros-N SSU, NOAA-A HIRS data [Chapman and Peckham, 1980; Venne, 1984; Hirooka and Hirota, 1985]. Figure 6-9 shows the antisymmetric 10-day wave of wavenumber 1 at stratopause derived from Tiros-N SSU by Hirooka and Hirota [1985]. These features agree rather well with the theoretical properties of normal modes.

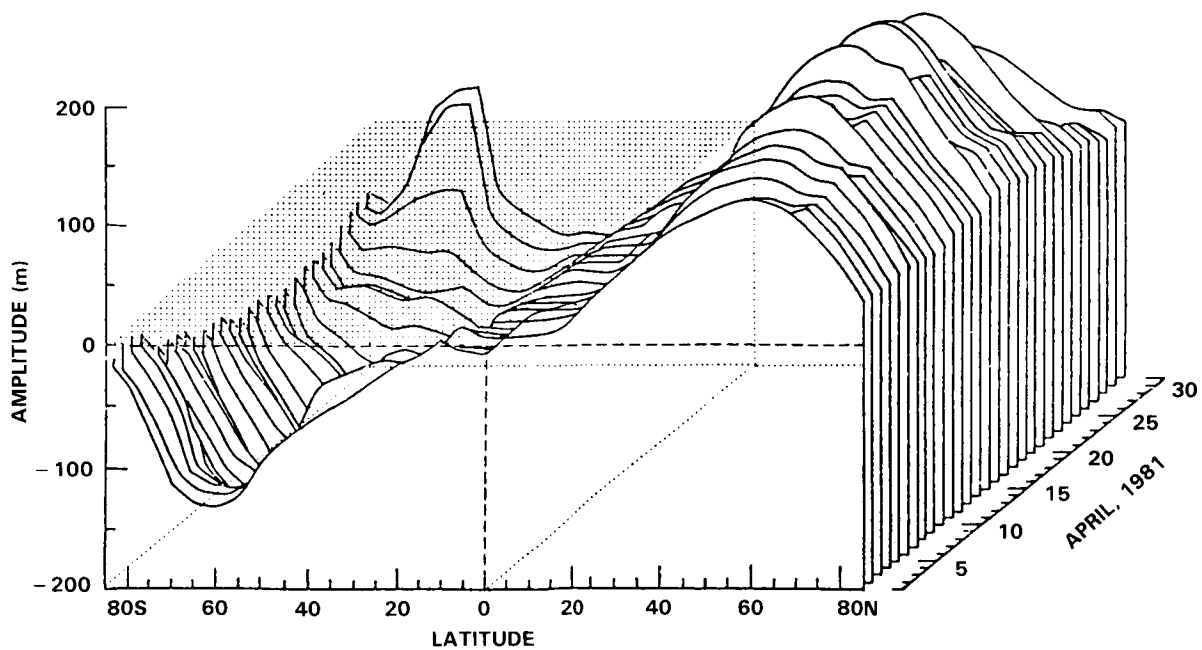


**Figure 6-9.** Structure and evolution of the 10-day wave at stratopause level, observed by Tiros-N SSU. Wavenumber 1 geopotential at 1 mb band passed about 9.2 days during April 1981. [Adapted from Hirooka and Hirota, 1985.]

## DYNAMICAL PROCESSES

Higher degree modes have larger amplitudes than the graver modes, which may be explained on the basis of their longer periods [Salby, 1984a]. Their structures, however, become markedly asymmetric in the solstice stratosphere as a result of their exclusion from the summer hemisphere by strong easterlies. Hirooka and Hirota [1985] have presented evidence of the amplification of slower modes prior to disturbed conditions in the stratosphere. In some respects this association with stratospheric warmings parallels the suggestion of Lindzen *et al.* [1984] that such components may play a role in blocking phenomena in the troposphere. However, considerably more study will be needed to establish such relationships.

One transient feature, which has attracted considerable attention, is the 16-day wave [Miller, 1974; Madden, 1978]. This disturbance is most evident in Northern Hemisphere winter; however it has been documented by both observations and GCM integrations in all seasons [Speth and Madden, 1983; Hayashi and Golder, 1983; Hirooka and Hirota, 1985]. Northern Hemisphere statistics [Madden, 1978; 1983] indicate a structure and evolution quite similar to the second symmetric normal mode of wavenumber 1. At least some studies have been able to document a global modal structure. Madden and Labitzke [1981] have identified the disturbed period of January 1979 as a manifestation of this phenomenon; this conclusion is supported by Lindzen *et al.*'s [1984] analysis of tropospheric behavior. In addition to its sizable amplitude, the 16-day wave is notable for being a recurrent climatological feature. It populates over half of an eight-winter ensemble of Northern Hemisphere winter dates [Madden, 1983]. Interference between this traveling wave and the stationary forced wave has been suggested as being responsible for the quasi-regular fluctuations which have been observed in eddy transports at stratospheric levels [Hirota and Sato, 1969; Madden, 1975] and upward migration of wave amplitude vacillations [Madden, 1977]. The same mechanism has been offered in connection with the switching of the EP flux vector prior to stratospheric warmings [Palmer, 1981a]. Quiroz [1979b] proposed a similar interference process, but involving different wavenumbers.

In wavenumber 1, the observed vacillations take the form of pulsations in wave amplitude, spaced 2-3 weeks apart. The fluctuations in eddy amplitude and attending transports which occur at various levels are not in phase, but rather tend to migrate upwards. Madden [1983] has recently shown that the observed behavior of such eddy transport vacillations is captured reasonably well by a simple barotropic normal mode propagating across the observed westward tilting stationary wave. Figure 6-10 shows the phase lag of the observed vacillation in heat and momentum fluxes as functions of height. The same quantities, shown for the simple model (solid line) are in reasonable agreement. Hirooka and Hirota [1985] have demonstrated with global TIROS-N SSU data that such fluctuations can induce vacillations in the zonal-mean circulation. Similar results were obtained from numerical calculations with a baroclinic beta-plane model [Garcia and Geisler, 1981]. From the synoptic viewpoint such oscillations in wavenumber 1 and their response in the zonal-mean flow correspond to a wobbling and perhaps translation of the vortex about the pole. Leovy *et al.* [1985] have reported such behavior in connection with the scavenging of ozone-rich air in low latitudes by the vortex when it is displaced off the pole. Once material is entrained into the perturbed flow configuration, a substantial transport to high latitudes is facilitated.

Conceptually such vacillations in eddy transports may be viewed as the traveling wave modulating the stationary wave fluxes. Its effect is to transform a steady uniform field of eddy fluxes into one which is localized into "capsules" which migrate upwards [Salby and Garcia, 1985]. Observations at a fixed level thus indicate a succession of pulses in wave activity and transport. At a particular point, the EP flux has a transient component which orbits about the time-mean vector (Figure 6-11). During the vacillation, eddy fluxes increase and decrease and may reverse direction, e.g., equatorward switching to poleward. Such behavior promotes mean flow deceleration through enhanced EP flux convergence which follows from the poleward convergence of meridians and focusing of wave activity [O'Neill and Youngblut, 1982].

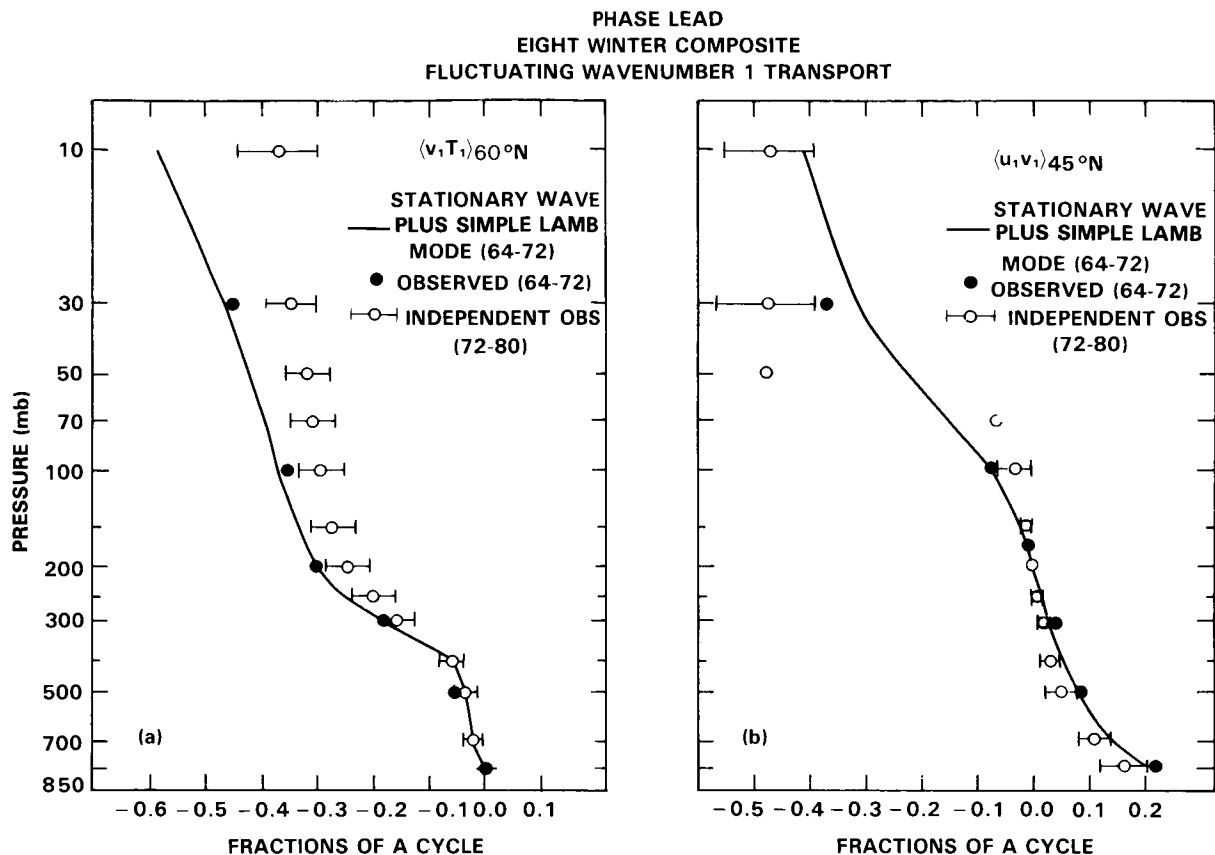


**Figure 6-10.** Vacillations in eddy transports induced by interference between traveling and stationary waves. (a) phase lead of heat flux vacillation at  $60^\circ N$ ; (b) phase lead of momentum flux vacillation at  $45^\circ N$ . Vacillation resulting from interference between observed 8-winter (1964-1972) composite 16-day wave and stationary wave (closed circle). Vacillation resulting from interference between simple Lamb mode and observed (1964-1972) stationary wave (solid line). Vacillation resulting from interference between *independent* 8-winter (1972-1980) 16-day wave derived from cross spectral analysis (1/23-1/12 cpd) and previous stationary wave (open circle). [Adapted from Madden, 1983].

Since this process is responsible for local and instantaneous wave amplifications, it may lead to strong nonlinearity in the form of wave breaking [McIntyre and Palmer, 1984] at upper levels [Salby, 1984b].

Although the extratropical stratosphere is largely believed to be dynamically stable, it is important to recognize that such conditions may be violated locally. Polar regions where the stabilizing influence of the planetary vorticity gradient is weak are particularly prone to such behavior. In such regions, the potential vorticity gradient will always be susceptible to being reversed by curvature in the local flow field and thus satisfy the conditions for instability [Charney and Stern, 1962]. A disturbance which may fall into this category is the polar eastward moving 4-day wave, discussed by Venne and Stanford [1982] in Nimbus-4 and Nimbus-5 SCR data. Prata [1984] has recently documented the wavenumber 2 component of this disturbance with Nimbus-5 SCR and Nimbus-6 PMR data. Calculations performed in realistic zonal shear [Hartmann, 1983] yield unstable polar modes which are not dissimilar to these observations.

Another disturbance possibly arising out of instability is the eastward travelling wavenumber 2 anomaly of the Southern Hemisphere [Harwood, 1975; Hartmann, 1976a], as suggested by Hartmann [1984]. The

## DYNAMICAL PROCESSES

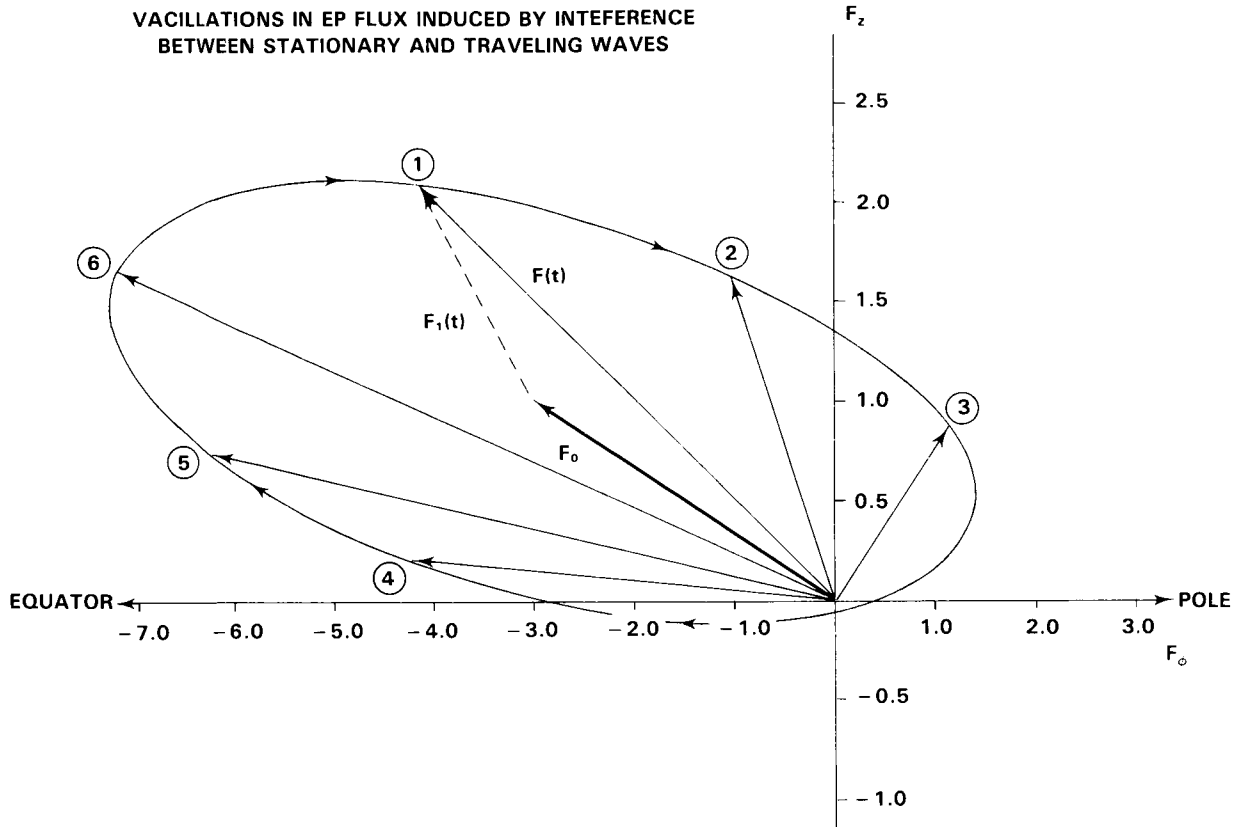


**Figure 6-11.** Modulation of EP flux vector by barotropic traveling wave migrating over a westward tilting stationary wave. Transient component orbits about time-mean vector. Both instantaneous EP flux components are modulated to zero and double their time-mean values, and reverse direction somewhere during the vacillation. Equatorward propagation switching poleward; upward flux driven between zero and double its time-mean value. [After Salby and Garcia, 1985].

2-day wave, a westward propagating wavenumber 3 disturbance [Muller, 1972; Rodgers and Prata, 1981] has likewise been suggested as arising out of baroclinic instability [Plumb, 1983a], although a normal mode explanation has also been proposed [Salby 1981c]. Velocity amplitudes in excess of  $50 \text{ m s}^{-1}$  have been observed in the Southern Hemisphere [Craig *et al.*, 1980]; a wave of this magnitude would be expected to induce closed streamlines and therefore to be highly nonlinear, perhaps playing an important role in large-scale transport (Craig *et al.* [1985]; see Section 6.5).

We have concerned ourselves here chiefly with disturbances which are most evident in the stratosphere. However tropospheric transients may be equally important if they induce transport near the tropopause. For example the pentagonal wave [Salby, 1982a; Hamilton, 1983b; Randal and Stanford, 1983], a regularly propagating feature of the Southern Hemisphere troposphere, was shown to induce sizable convergences of total ozone column abundances [Schoeberl and Krueger, 1983].

### 6.1.5 Equatorial Waves

Since their identification in radiosonde observations [Wallace and Kousky, 1968], Kelvin waves have been recognised as an important ingredient of the momentum budget of the tropical middle atmosphere

(see Section 6.2.7). Another equatorial mode, the westward-propagating Rossby gravity wave, was diagnosed in radiosonde observations by Maruyama [1969]. Both of these classical waves are confined to the tropics and propagate vertically with wavelengths of 10 km or less. They are presumably excited by convective heating in the tropical convergence zone [Hayashi, 1970; Holton, 1972; Murakami, 1972; Hayashi, 1974; Hayashi and Golder, 1978]. While such heating is indicative of a broad-band process, Holton [1973] demonstrated a natural discrimination of Kelvin waves in the range of periods 10-20 days [phase speeds of 20-40  $\text{ms}^{-1}$ ] as is observed in the lower stratosphere. Chang [1976], Hayashi [1976], and Itoh [1977] have shown that the vertical scale of diabatic forcing favors vertical wavelengths twice the depth of the heating, more or less consistent with early observations of equatorial waves.

In addition to these waves, there are considerably faster eastward-propagating disturbances which have recently been recorded at upper stratospheric levels. These were first identified in rocketsonde data by Hirota [1978], although evidence of their existence dates back to Maruyama [1969], and may also be found in Holton [1973] and in Zangvil and Yanai [1980]. They correspond to Kelvin waves with periods of 5-10 days, phase speeds of 50-70  $\text{ms}^{-1}$  (twice that of the Wallace and Kousky variety) and vertical wavelengths of about 20 km. Their presence is clearly seen in time-height sections of temperature and zonal wind over Ascension Island (Figure 6-12). Downward phase migration corresponds to upward group propagation. Evidence for the faster, longer vertical wavelength disturbances has also been derived from Nimbus-5 SCR data [Hirota, 1979]. Because of their higher frequency, these fast Kelvin waves are better able to traverse the strong radiative damping of the stratosphere [Dunkerton, 1979] and hence are more likely to play a role in the semi-annual oscillation at upper levels (Hirota, [1980]; see section 6.2.7).

Historically, satellite observation of equatorial waves has not met with great success, largely because of the deep vertical weighting functions and coarse resolution inherent to nadir viewing instruments. However recent limb-viewing configurations, with their narrower weighting functions, have provided an unprecedented opportunity to observe such disturbances. Tropical temperature fields derived with Nimbus-7 LIMS exhibit pronounced eastward variance over the entire stratosphere [Salby *et al.*, 1984]. Many aspects of this

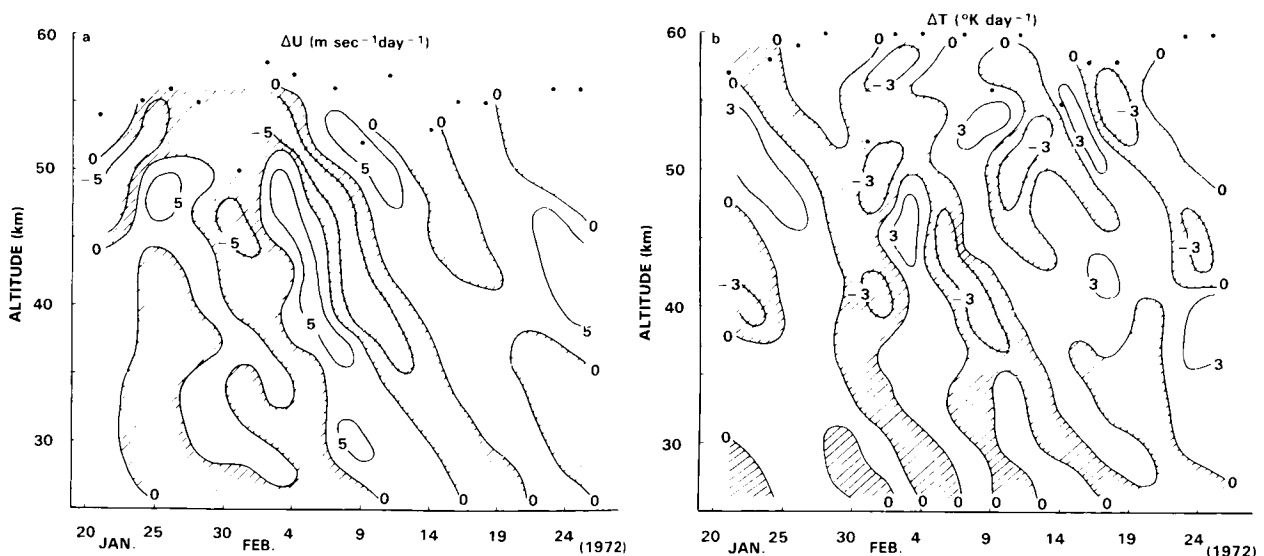


**Figure 6-12.** Signatures of two-day differenced (a) zonal wind, and (b) temperature over Ascension Island (8°S, 14°W), derived from rocketsonde measurements. [After Hirota, 1978].

## DYNAMICAL PROCESSES

wave activity are in accord with dispersion characteristics of equatorial Kelvin waves, although not solely the Wallace and Kousky [1968] variety or even the Hirota [1978] variety. Figure 6-13 shows wavenumber 1 temperature power as a function of latitude for three stratospheric levels. At each of these, unsteady behavior is dominated over the tropics by eastward propagating variance which is localized in particular bands of frequency. Each of these features is nearly symmetric about the equator. The slower of the two is evident at all three levels. It lies in the period-range 6.7-8.6 days, corresponding to phase speeds of  $55\text{-}70\text{ ms}^{-1}$  and Hirota's variety of Kelvin waves. In the uppermost level shown, a second, apparently distinct, eastward feature emerges in the band 3.5-4.0 days, corresponding to phase speeds of  $115\text{-}135\text{ ms}^{-1}$ , considerably faster than either the Wallace and Kousky or the Hirota variety.

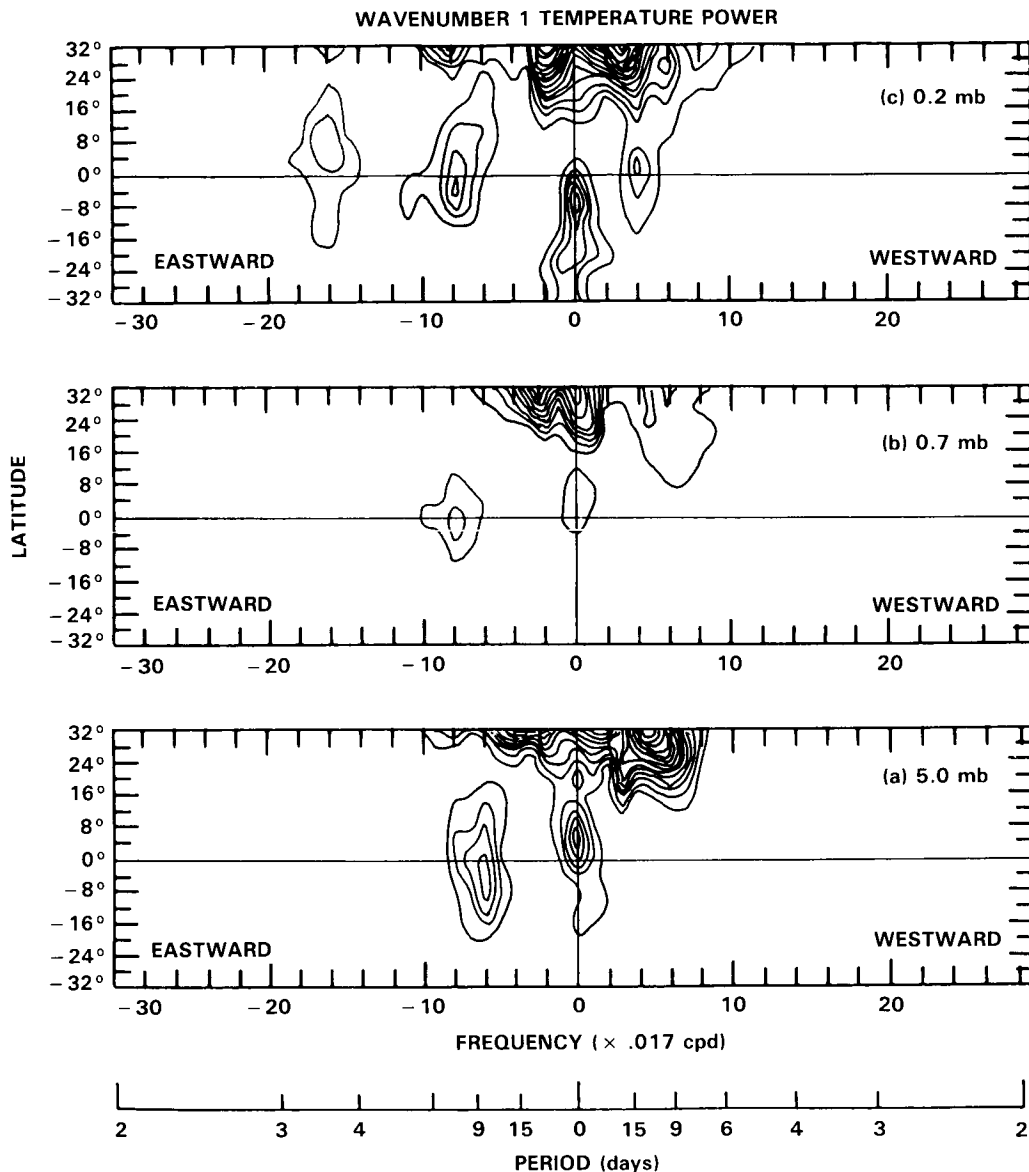


**Figure 6-13.** Temperature power for wavenumber 1 as a function of frequency and latitude at (a) 5.0 mb, contour increment =  $0.2\text{ K}^2$ ; (b) 0.7 mb, contour increment =  $0.1\text{ K}^2$ ; (c) 0.2 mb, contour increment =  $0.04\text{ K}^2$ . [After Salby *et al.*, 1984].

Similar features are evident for wavenumber 2. The slowest has phase speeds of 30-40  $\text{ms}^{-1}$  commensurate with the variety first reported by Wallace and Kousky [1968]. Its latitude-height structure, decomposed into components symmetric and antisymmetric about the equator (Figure 6-14), has virtually all of the variance captured by the symmetric contribution and maximizes on the equator, consistent with the behavior of Kelvin waves. The observed downward phase migration is consistent with upward wave activity propagation. Vertical wavelengths vary from 7-13 km, in agreement with the observed phase speed and the dispersion relationship for Kelvin waves. By comparison, the ultra-fast feature has a much deeper vertical wavelength, 41 km, and broader structure. However, its behavior is also consistent with the dispersion characteristics of Kelvin waves. The vertical growth of this mode is unabated through the highest level monitored by LIMS, 0.05 mb. This characteristic led Dunkerton [1982b] to speculate upon its role in the momentum budget of the mesosphere. Whereas these recent satellite observations have permitted a rather detailed description of Kelvin wave behavior in the stratosphere, Rossby-gravity waves have yet to be detected in satellite retrievals. Whether they are simply not present at these levels or they remain unresolved in limb-viewing measurements is unclear.

Features strikingly similar to the Kelvin waves derived from satellite retrievals have been diagnosed in GCM integrations (Figure 6-15) by Hayashi *et al.* [1984]. Maxima in each of the three ranges of phase speed appear in tropical temperature spectra. Lateral and vertical structures are similar to those shown from LIMS. In addition the barotropic 16-day wave is prominent at westward frequencies. It has a symmetric global structure similar to that of the classical normal mode [Hayashi and Golder, 1983].

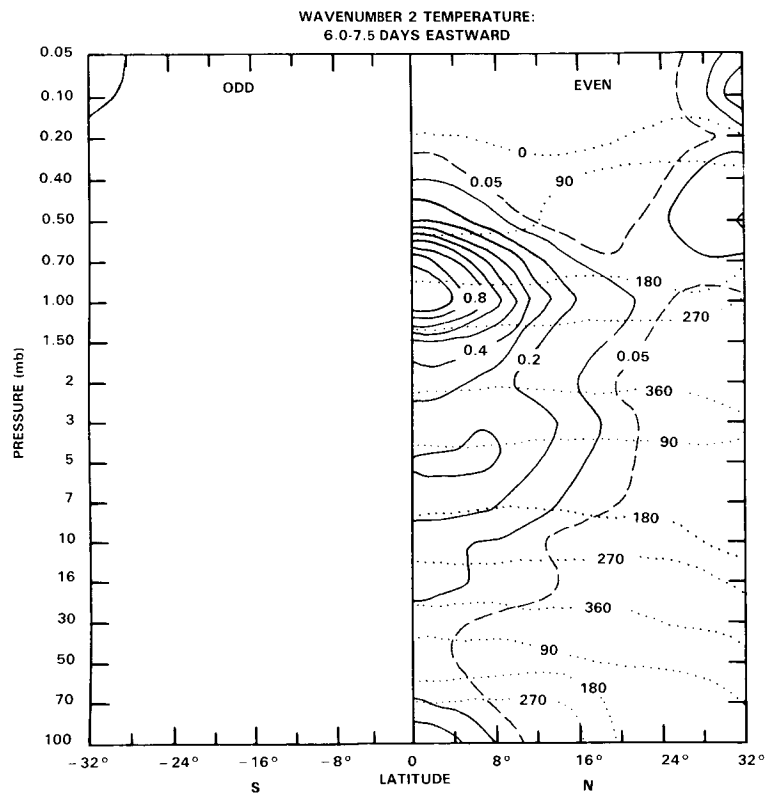


**Figure 6-14.** Wavenumber 2 temperature power (solid) and phase (dotted) corresponding to eastward periods between 6.0-7.5 days, as functions of latitude and pressure. Decomposed into latitudinal components symmetric and antisymmetric about the equator. Symmetric components displayed at positive latitudes, antisymmetric components at negative latitudes. Power in  $\text{K}^2$ . [After Salby *et al.*, 1984].

DYNAMICAL PROCESSES

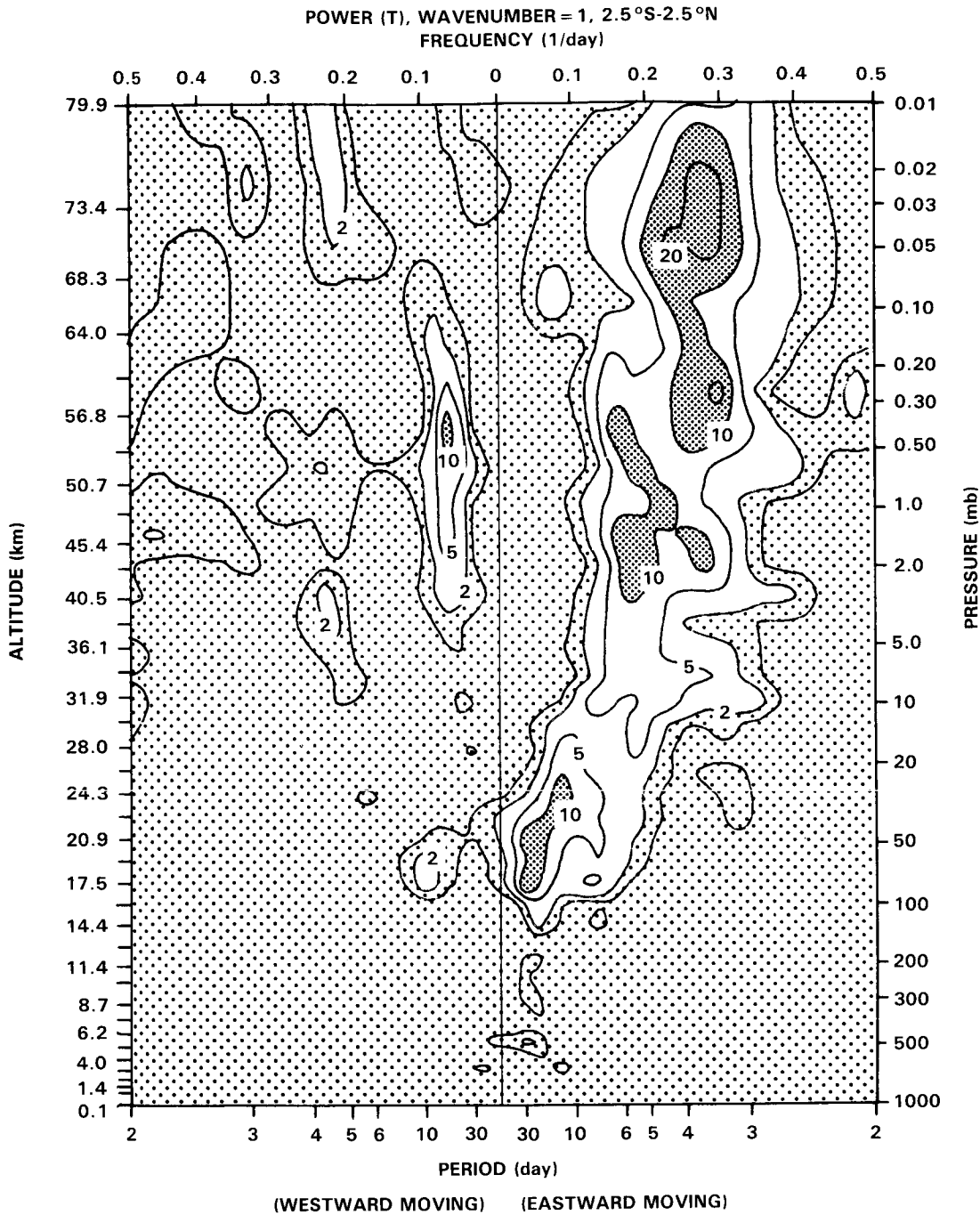


**Figure 6-15.** Temperature power spectral density for wavenumber 1, as a function of frequency and altitude over the equator, derived from 40-level GCM integration in annual-mean conditions. [After Hayashi *et al.*, 1984].

In combination, these Kelvin disturbances can lead to temperature perturbations of several degrees. From photochemical considerations, it follows that similar perturbations should develop in ozone at upper levels. If such features can be identified, they might serve to validate temperatures derived from UV constituent measurements at upper levels where signal/noise in IR measurements deteriorates.

### 6.1.6 Tides, Gravity Waves and Turbulence in the Middle Atmosphere

Tides, and gravity waves in particular, are believed to play an important role in determining the large-scale circulation and temperature structure of the middle atmosphere (see Section 6.2) as well as being the predominant source of small-scale turbulence in this region. Solar tides are thermally forced in the troposphere through infrared absorption by water vapor and in the stratosphere through UV absorption by ozone. Although the broad details of the forcing are well understood there are a number of aspects which require further study [Forbes, 1984]. Gravity wave sources are less well known, but the major sources are thought to be in the lower atmosphere and to include topographic forcing, frontal disturbances, convective activity, geostrophic adjustment and shear instabilities. As the waves propagate upwards, their exponential growth, in the absence of reflection and dissipation, leads eventually to wave breakdown and the generation of turbulence.

Much of the early information about gravity waves in the middle atmosphere came from rocket studies which, although somewhat limited because of their infrequency, provided evidence for seasonal and geographic variations in wave activity. In the mesosphere, Theon *et al.* [1967] found a large seasonal variation in wave activity at high latitudes with the maximum activity occurring in winter. At midlatitudes there is less evidence of seasonal changes. Hirota [1984], in a comprehensive study of the climatology of waves in the 20 to 60 km height range made with data taken at the Meteorological Rocket Network stations in the northern hemisphere, found similar seasonal changes as well as evidence for a semiannual cycle at low latitudes (Figure 6-16). High resolution rocket investigations have provided information about the gravity wave structures, although, of course, rocket soundings are too infrequent to resolve their behavior in time. For example, the vertical wavelength of the waves tends to increase as a function of height, with a minimum of about 1.5 km near 60 km increasing to about 3 km near 100 km [Philbrick, 1981]. Both rocket and radar studies suggest a dominant vertical wavelength of about 10 to 15 km in the mesosphere. From these values an intrinsic phase speed  $|c - \bar{u}| = N/k_z$  of about  $30 \text{ ms}^{-1}$  may be inferred [Fritts, 1984] where  $N$  is the buoyancy frequency and  $k_z$  is the vertical wavenumber. There are only a few indirect estimates of phase velocity in the middle atmosphere but what measurements there are give values in the range 20 to  $100 \text{ ms}^{-1}$  for mesospheric waves [Vincent and Reid, 1983; Meek *et al.*, 1985a; Vincent, 1985].

Radars are now providing a large amount of information about gravity waves in the mesosphere, albeit with a somewhat limited geographical coverage. Morphologies of wave activity are now becoming available [Meek *et al.*, 1985b]. Power spectral studies of the wave motions show that, averaged over long periods, the energy densities observed at widely separated locations agree well in form and amplitude. Typically the wave energy decreases with frequency  $f$ , as  $f^{-k}$ , with  $k \sim 1.5-2.0$  [Balsley and Carter, 1982; Vincent, 1984a; Meek *et al.*, 1985b]. The rms amplitudes for each wind component are in the range 15 to  $20 \text{ ms}^{-1}$  so that the total perturbation velocity is approximately 25 to  $30 \text{ ms}^{-1}$ ; rms amplitudes of vertical motions are much smaller than this, being about 1 to  $2 \text{ ms}^{-1}$ . Most studies show that there is usually little, if any, amplitude growth with height so that the energy density  $\rho_0 \overline{v'^2}$  decays as  $\exp(-z/h_0)$ , where  $\rho_0$  is the neutral density and  $\overline{v'^2}$  is the mean square perturbation velocity. The decay scale  $h_0$ , may change with season [Manson *et al.*, 1981] but is in the range 5 to 12 km. The comparable values of  $|v'|$  and  $|c - \bar{u}|$  as well as the energy decay with height are often taken as indirect evidence of wave saturation in the mesosphere [Fritts, 1984] although wind shears can also cause variations in wave amplitude.

With the data now available, estimates can be made of a number of important wave and turbulence parameters in the mesosphere. From the energy distribution as a function of frequency, Vincent [1984a] found seasonally averaged energy densities of about  $5$  to  $10 \times 10^{-3} \text{ Jm}^{-3}$  and vertical fluxes of

## DYNAMICAL PROCESSES

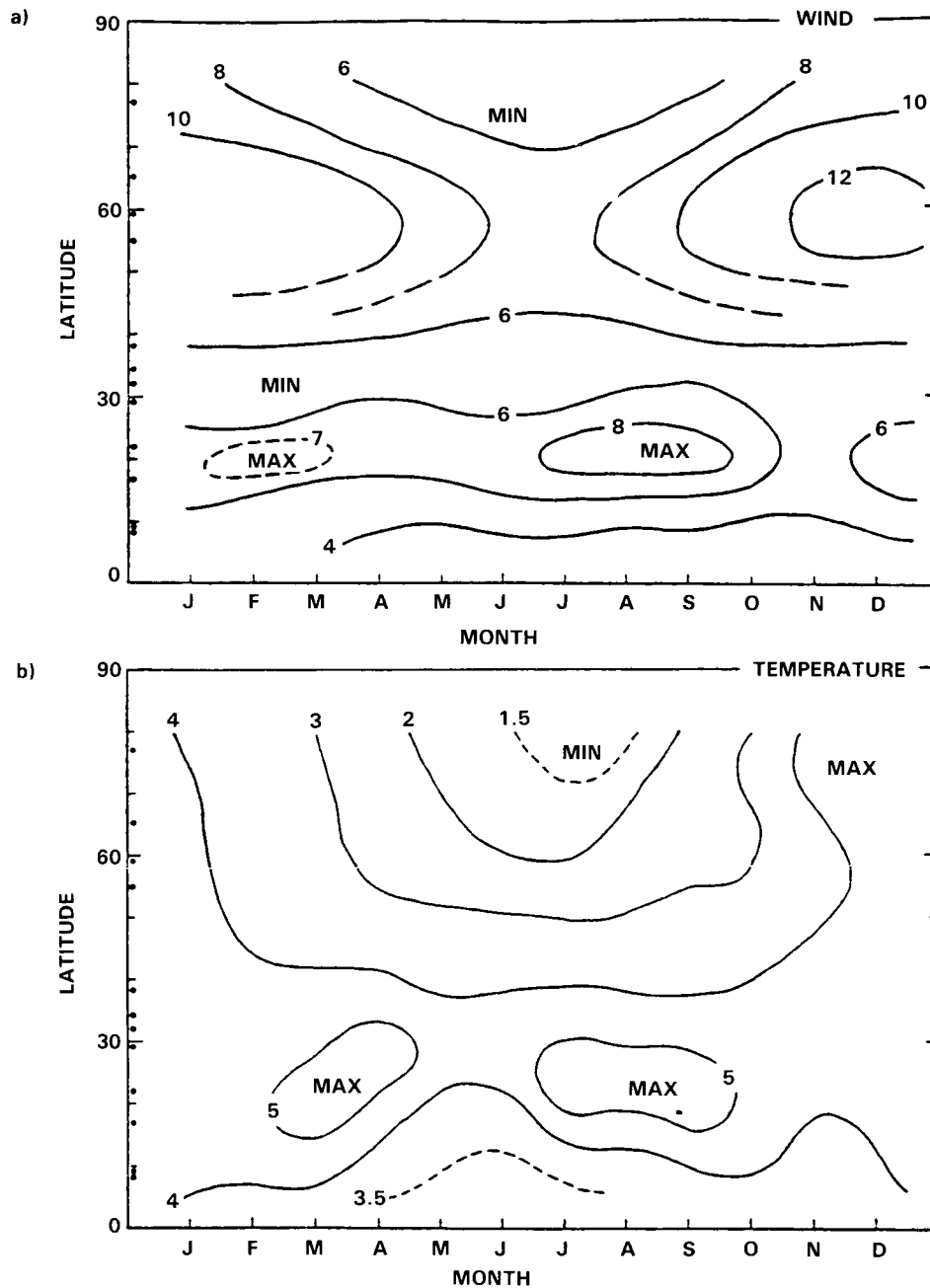


**Figure 6-16.** Latitude-time cross-sections of rms fluctuations in (a) wind ( $\text{ms}^{-1} \text{ km}^{-2}$ ) and (b) temperature ( $\text{K km}^{-2}$ ) [After Hirota, 1984].

$\approx 10^{-2} \text{ Wm}^{-2}$ . The rate of decay of wave energy has been used to determine energy dissipation rates and diffusion coefficients by the method of Hines [1965]. Typical values for the 80 to 100 km height range are  $\epsilon \approx 0.01$  to  $0.2 \text{ Wkg}^{-1}$  for energy dissipation rates and  $D \approx 100$  to  $500 \text{ m}^2\text{s}^{-1}$  for the eddy diffusion coefficients.

More direct evidence for wave saturation and measurements of the associated momentum flux convergence came with the development of a technique in which the momentum fluxes could be measured

directly [Vincent and Reid, 1983]. The method uses two coplanar radar beams which point at equal and opposite angles to the zenith and the vertical flux of horizontal momentum is given by the difference between the mean square Doppler velocities observed along the two beams. So far, measurements have been made only at Adelaide but observations tend to support theoretical predictions. Figure 6-17 shows  $\overline{u'w'}$  and the inferred flux convergence measured at Adelaide in May 1981 [Vincent and Reid, 1983] and these and other observations show that, averaged over several days, values of  $[\overline{u'w'}]$  in the mesosphere are in the range of 1 to 5  $\text{m}^2\text{s}^{-2}$  and the momentum flux  $\rho_0 \overline{u'w'}$  decreases approximately exponentially with increasing height, indicating a flux convergence. The wave drag is:

$$G = - \rho_0^{-1} \frac{d}{dz} \left[ \rho_0 \overline{u'w'} \right]$$

Thus, on the basis of these measurements,  $G$  is found to be of the order of 20 to 80  $\text{m s}^{-1} \text{ day}^{-1}$  and is in the correct sense to balance the Coriolis torques induced by the observed mean meridional flow (see Section 6.2.3). More indirect estimates of wave drag also support these findings [Meek *et al.*, 1985b].

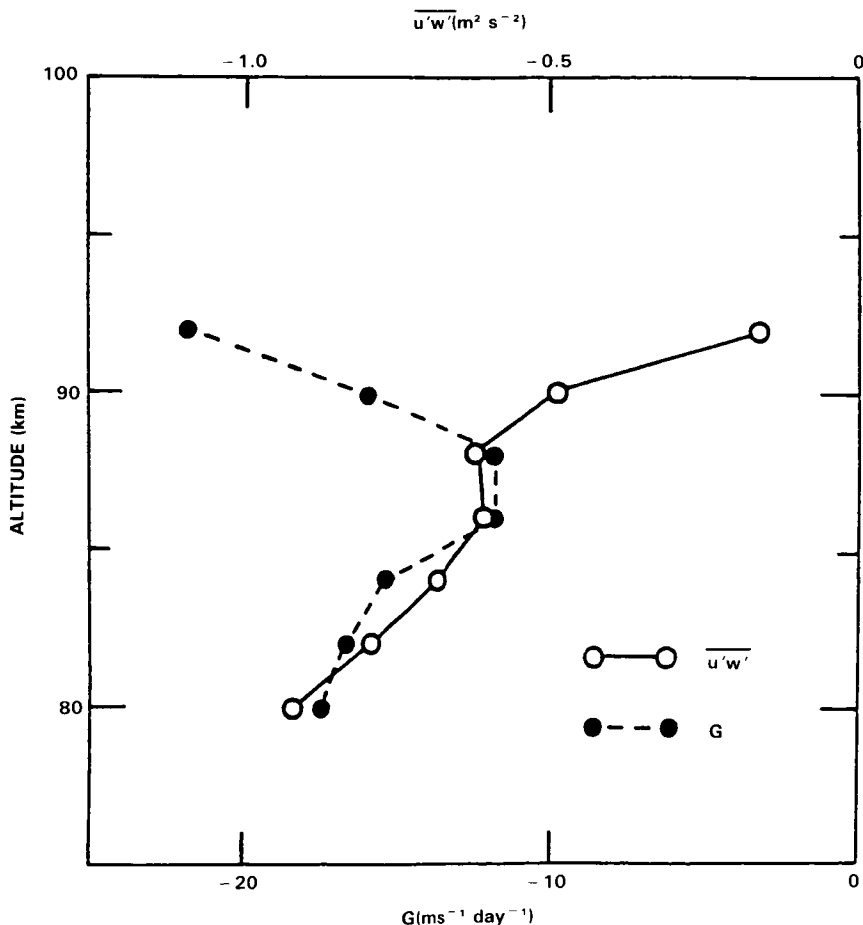


**Figure 6-17.** Height profiles of  $\overline{u'w'}$  and zonal drag,  $G$ , observed at Adelaide in May 1981 [After Vincent and Reid, 1983].

## DYNAMICAL PROCESSES

However, there can be significant variability of  $\overline{u'w'}$  over time scales ranging from hours to days and (presumably) in space so that extended measurements at more locations are required to understand fully the role gravity waves play in the momentum budget of the mesosphere. One interesting and potentially important feature of the measurements is that high frequency waves (periods less than 1 hour) appear to carry a substantial fraction of the energy and momentum fluxes. This is because their large vertical group velocities more than compensate for their smaller amplitudes in the lower atmosphere relative to the long period waves. Short-term variations in wave energy and the associated fluctuations in mesospheric heating have been investigated by Clark and Morone [1981].

Variability or intermittency in wave activity in the mesosphere is also evident in observations of small-scale turbulent motions. High resolution MST radar measurements show that the scattering regions appear as blobs, sheets and layers, with vertical thicknesses ranging from 150 m or less up to a few km [Rottger, 1980]. Horizontal scales are estimated to extend from 1 km up to hundreds of km. Some of the layers are observed to descend with time, which suggests the turbulent structures are associated with dissipating gravity waves. By measuring the Doppler spectral widths of the echoes it is possible, with care, to estimate the turbulent intensity directly and so infer eddy dissipation rates and diffusivities [Sato and Woodman, 1982; Hocking, 1983]. Applications of this technique to the mesosphere give values comparable to those inferred from gravity wave decay rates (viz.  $\epsilon \cong 0.01$  to  $0.2 \text{ W kg}^{-1}$  and  $D \cong 100$  to  $500 \text{ m}^2\text{s}^{-2}$ ). Figure 6-18 shows vertical profiles of 'global averages' of  $\epsilon$  and  $D$  in the upper mesosphere constructed from all available data [Hocking, 1985]. To date, there are insufficient data to deduce a seasonal and geographic climatology of turbulence in the mesosphere. It is possible that satellite measurements of ozone densities at the 80 km level could be used to monitor indirectly the amount of turbulence and wave activity. Thomas *et al.* [1984b] found equinoctial maxima in ozone concentrations at 80 km, which they attributed to reductions in the turbulent transport from lower levels of water vapor, probably the most active agent for ozone destruction in the mesosphere. The reduction in turbulence at the equinoxes is presumed to be due to the attenuation of gravity waves propagating through the weak zonal winds in the middle atmosphere and a corresponding reduction in wave breaking in the mesosphere. Some support for these ideas has come from studies of Meek *et al.* [1985b] who found an attenuation of wave activity in the mesosphere at the time of the equinoctial reversal of the zonal circulation at Saskatoon.

High-resolution radar and balloon studies show that turbulent processes in the lower stratosphere are also intermittent in space and time with the turbulence confined to thin layers. Layer thicknesses range from a few tens to a few hundred metres and horizontal scales are inferred to range from a few kilometres up to a few hundred kilometres in extent. The association of the turbulent layers with regions of high wind shear caused by the wave-like features of the wind profile is especially evident. The persistence of these features and their slow downward movement with time strongly indicates that much of the stratospheric turbulence is generated by dynamically unstable inertio-gravity waves [Barat, 1982; Sato and Woodman, 1982]. Estimates of mean dissipation rates vary between  $5 \cdot 10^{-6}$  and  $10^{-4} \text{ W kg}^{-1}$  with corresponding mean diffusivities ranging between  $0.01$ - $0.2 \text{ m}^2 \text{ s}^{-1}$ . Aircraft measurements show highest turbulence activity over the mountains [Lilly *et al.*, 1974]. Radar estimates of diffusivity in the stratosphere ( $0.2 \text{ m}^2 \text{ s}^{-1}$ ) are about an order of magnitude larger than those inferred from aircraft observations [Lilly *et al.*, 1974]. The reasons for this difference are not yet resolved. As will become apparent below (Section 6.5), however, even these larger values are probably unimportant for large-scale transport.

Long-term radar measurements of horizontal wave motions show that, similar to the situation in the mesosphere, the energy is distributed with a  $f^{-5/3}$  power law [Balsley and Carter, 1982]. In contrast to what is often assumed in theory, these and other studies are starting to indicate that the wave energy density does not remain constant with increasing height in the stratosphere but rather shows an exponential

ENERGY DISSIPATION (GLOBAL)

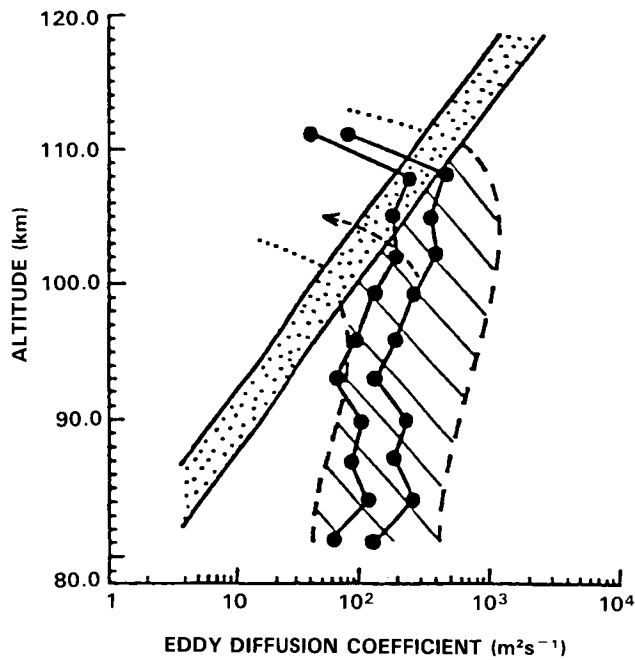
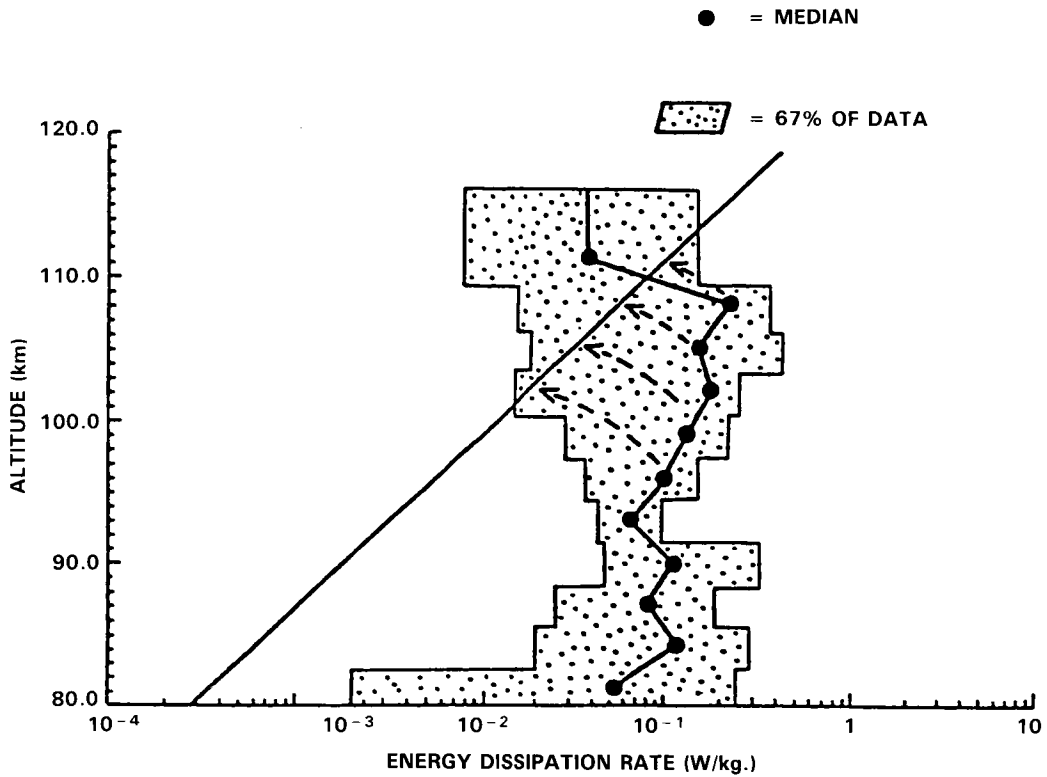


Figure 6-18. Profiles of global eddy dissipation rates and diffusion coefficients as function of height above 80 km [After Hocking, 1985].

## DYNAMICAL PROCESSES

decay, again similar to the mesospheric situation. While there are a number of reasons (including reflection and the effect of the background wind) why the wave amplitudes may not grow with height, saturation processes are possibly important, which suggests that gravity waves may contribute to the momentum budget of the stratosphere. Massman [1981], using southern hemisphere constant pressure balloon measurements, found large upward fluxes of wave energy and momentum in the upper troposphere but significantly smaller values in the stratosphere, which indicates flux convergence across the tropopause. The convergence of the vertical momentum flux, which is approximately equal to the Eliassen-Palm flux for small-scale gravity waves (see Section 6.2), suggests destruction of wave activity in the tropopause region. The maximum fluxes were near the Andes. Schoeberl [1985] has shown theoretically that topographically forced waves may superpose in the stratosphere to form unstable regions.

The amplitude of the solar diurnal and semidiurnal tides in the stratosphere are small ( $< 1 - 5 \text{ ms}^{-1}$ ) and they do not appear to play a significant role in the dynamics of this region. In the mesosphere, however, tidal motions can be large and, at latitudes of less than  $30^\circ$ , the migrating diurnal tide is probably an important source of heat, momentum and turbulence. Theory predicts that the fundamental (1,1) diurnal mode will become convectively unstable in the equatorial mesosphere [Lindzen, 1968] and because of its short vertical wavelength (25-30 km) this mode is strongly damped by turbulent processes in the mesosphere at higher latitudes. Observations show that the wave amplitudes maximize near 90 km altitude. Calculations suggest that the dissipating tide generates easterly winds of up to  $60 \text{ ms}^{-1}$  in the equatorial upper mesosphere and westerly winds of  $35 \text{ ms}^{-1}$  at  $30^\circ$  latitude [Miyahara, 1984]. Estimates put the upward energy flux into the mesosphere at about  $1.5 \text{ Wm}^{-2}$  and the most recent calculations indicate that the (1,1) mode generates large heating rates near 80 km [Groves and Forbes, 1984], which could be significant on a global scale. Finally, it is noted that the tides can affect the concentration of minor constituents such as ozone in the mesosphere not only by direct transport but also by their reversible temperature fluctuations, which can produce significant variations in the photochemistry [Forbes, 1984].

### 6.1.7 The Seasonal Cycle

The march of solar heating drives a seasonal cycle in the middle atmosphere; in the stratosphere, cold polar temperatures and a strong westerly vortex in winter are replaced in summer by warm polar temperatures and a weak easterly vortex. Because of dynamical disturbances, however, the seasonal cycle does not proceed uniformly.

Figure 6-19 shows the annual march of zonal mean radiance near the north and south poles in the upper stratosphere. Maximum temperatures (proportional to the radiances) are achieved in mid-summer and minimum in mid-winter. Winter temperatures are more variable in the Northern Hemisphere because of stratospheric warmings. The seasonal increase of temperatures in the Southern Hemisphere is highly oscillatory from midwinter to summer, whereas in the Northern Hemisphere temperatures increase gradually in spring after abrupt changes in winter. After mid-winter, upper stratospheric temperatures in the polar region are higher in the southern than in the Northern Hemisphere, except during major warmings in the Northern Hemisphere [Barnett, 1974]. The meridional temperature gradient reverses at high latitudes in the upper stratosphere of the Southern Hemisphere as a warm pool forms over the pole after mid-winter [Hartmann, 1976a; Hirota *et al.*, 1983]. These changes are related to the observed poleward and downward movement of the zonal mean jet in the Southern Hemisphere during late winter [Harwood, 1975; Hartmann, 1976a; Leovy and Webster, 1976].

Figure 6-20 shows the evolution of the zonal mean wind in the upper stratosphere. In the Northern Hemisphere, the zonal mean westerlies are strongly disrupted by disturbances (e.g. during January-February

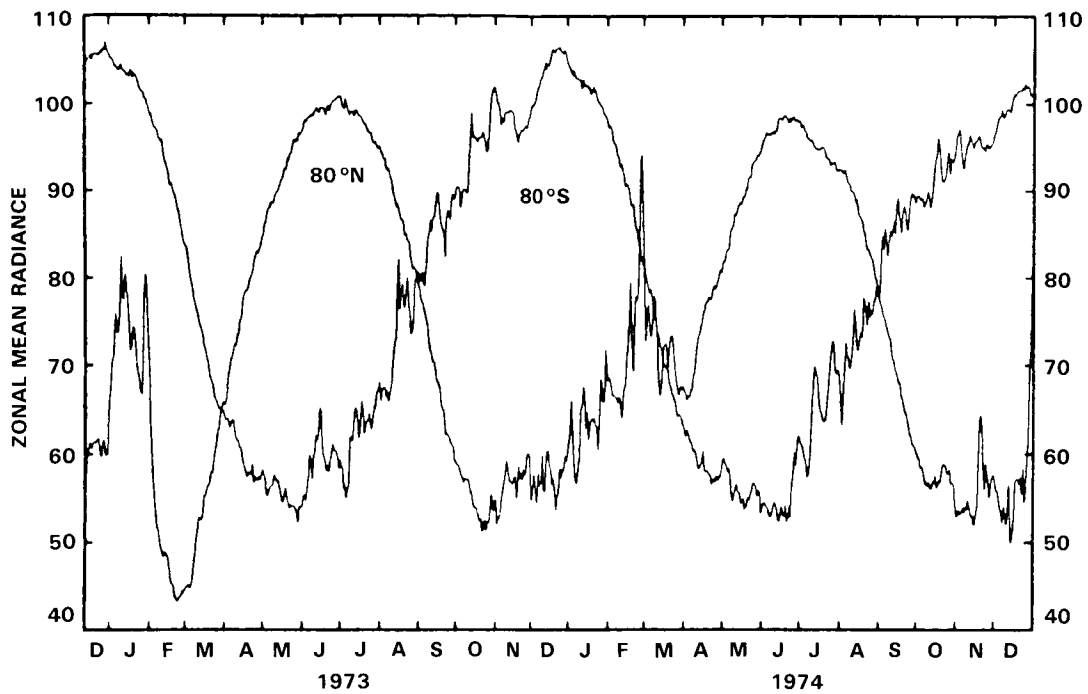


Figure 6-19. Annual march of zonal mean radiance observed by the Nimbus 5 SCR channel B12 for 80°N and 80°S. Units are  $\text{mW m}^{-2} \text{ster}^{-1} (\text{cm}^{-1})^{-1}$ . Taken from Hirota *et al.* [1983a].

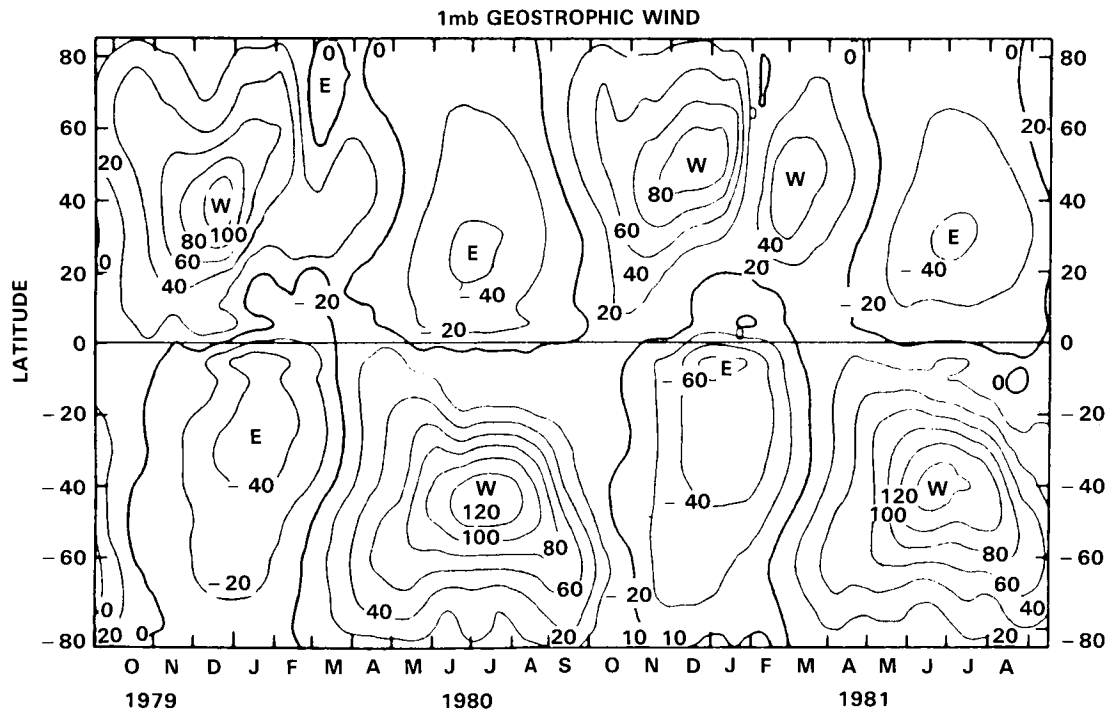


Figure 6-20. Latitude-time section on the zonal mean geostrophic wind at the 1 mb level estimated from the 20-day average height field observed by the Tiros N SSU. Units are  $\text{ms}^{-1}$ . Positive values denote westerly winds. Taken from Hirota *et al.* [1983a].

## DYNAMICAL PROCESSES

1981). Should these disturbances occur in late winter, the westerly circulation may never recover before summer easterlies are introduced by the evolving radiation field. These 'final warmings' occur earlier in the seasonal cycle in the Northern Hemisphere than in the Southern Hemisphere where the winds evolve more regularly. The zonal winds in the Southern Hemisphere are strongest at high latitudes in early winter, at mid latitudes in mid-winter and then, as the zonal mean jet moves polewards and downwards, at high latitudes again in late winter.

In equatorial regions the annual cycle is weak and the seasonal cycle in the upper stratosphere becomes dominated by a semiannual oscillation (SAO). The SAO was originally discovered by Reed [1965, 1966] and further observational evidence has been presented by Belmont and Dartt [1973], Hirota [1978, 1980] and Hamilton [1982a]. While a substantial semiannual component exists at middle and high latitudes, this appears to be largely a reflection of the non-sinusoidal character of the seasonal cycle there; in the tropics, however, a distinct maximum in the zonal wind SAO occurs, reaching amplitudes of about  $30 \text{ ms}^{-1}$  near the stratopause, with maximum westerlies just after equinox (Figure 6-21). Easterly zonal winds penetrate from the summer hemisphere into the winter hemisphere twice a year; the easterlies spread further across the equator during the southern hemisphere summer. As is evident from Figure 6-21, there is a second maximum of the SAO near the mesopause, out of phase with that in the upper stratosphere [Hirota, 1980; Hamilton, 1982a].

Figure 6-22 shows the evolution in the upper stratosphere of the amplitudes of waves 1 and 2 computed from the monthly mean fields of geopotential height. The distinct seasonal cycle of wave amplitudes is linked to that of the zonal mean winds. Large-scale disturbances in the troposphere can only penetrate into the stratosphere during winter when winds are westerly (although the seasonal cycle in planetary wave activity may also reflect changes in tropospheric forcing). Except for wave 1 in the northern hemisphere winter, the position of the maximum wave amplitudes is close to the latitude of strongest zonal mean westerlies (marked by broken lines on the figures). The maximum amplitude of wave 1 in the Northern Hemisphere winter is at higher latitudes. While amplitudes tend to be at their maximum in the Northern Hemisphere in mid-winter, wave 1 amplitudes (and to a lesser extent wave 2 amplitudes) show a relative minimum in mid-winter in the Southern Hemisphere. The poleward and downward movement of the jet in the Southern Hemisphere in spring is associated with an enhancement of wave 1 [Hartmann *et al.*, 1984; Shiotani and Hirota, 1985]. Transient waves at extra-tropical latitudes show similar seasonal variations in amplitude to those of the time-averaged waves, with largest amplitudes in winter and smaller amplitudes in summer.

The most spectacular departures from a regular seasonal cycle in the middle atmosphere occur near the winter pole during sudden warmings. Wave amplitudes can double and temperatures can rise locally by 80 K or more in a week or so. This dramatic phenomenon, which occurs sporadically in the winter stratosphere, is associated, in extreme cases, with a reversal of the zonal-mean westerly flow. The picture of a zonally symmetric flow which undergoes a deceleration and possibly a reversal in direction may, in some respects, be misleading. Such phenomena may be manifested in the total flow field (i.e., zonal mean plus waves) by a displacement of the vortex off the pole in the case of a "wave 1" warming [e.g., Palmer and Hsu, 1983], or by a split in the vortex in the case of a "wave 2" warming [e.g., Palmer, 1981a]. A recent example of this latter type of warming is that of Figure 6-23, which shows two cyclonic vortices separated by a warm anticyclone over the pole. The atmospheric disturbance can often be detected at the mesopause and above [e.g., Muller *et al.*, 1985]. Warmings are believed to be triggered by changes in the large-scale circulation in the troposphere, although the precise nature of these changes has not been adequately documented.

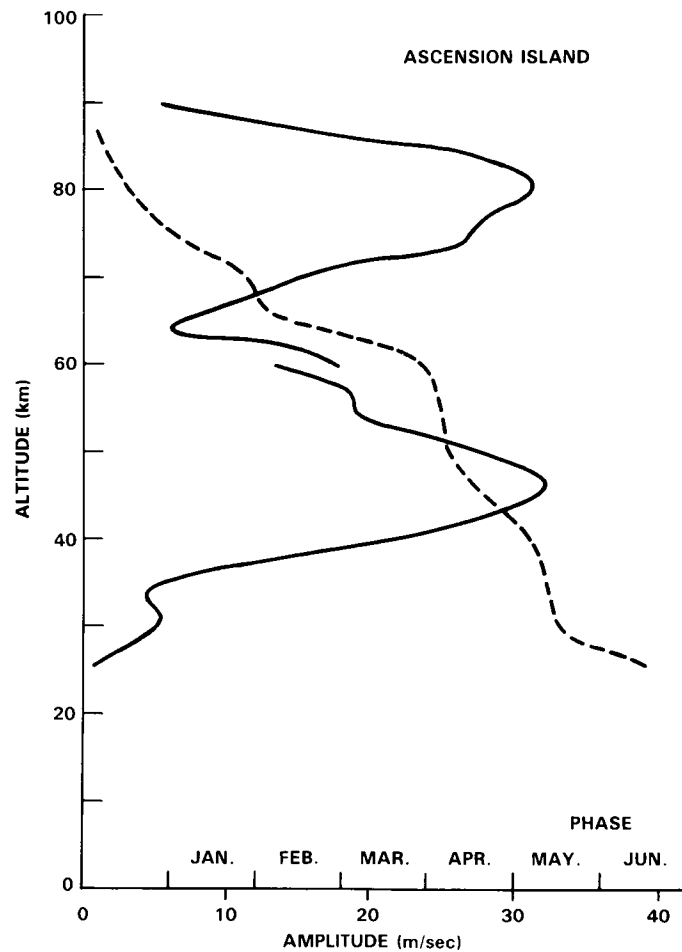


**Figure 6-21.** Vertical distribution of the amplitude (solid) and phase (time of the maximum westerly component [dashed]) of the semiannual cycle of zonal wind at Ascension Island. [After Hirota, 1978].

During warmings there is a large exchange of material between high and low latitudes. Not all this exchange will be permanent, but strong warmings may effect considerable poleward transport of trace chemical species. The poleward advection of air from low latitudes during warmings is indicated by maps of Ertel's potential vorticity on isentropic surfaces (see Section 6.2). (Over short periods, contours of potential vorticity on such surfaces are approximately material lines.) An example for an early winter warming in the Northern Hemisphere is shown in Figure 6-24. The area of low potential vorticity was drawn around the westerly vortex into the polar cap from low latitudes. McIntyre and Palmer [1983, 1984] have applied the term "wave breaking" to extreme and irreversible buckling of potential vorticity contours such as that depicted in Figure 6-24.

Major warmings involving the replacement of polar westerlies by easterlies do not occur in mid-winter in the Southern Hemisphere. This is probably because the circulation in the troposphere does not contain such persistent large-scale disturbances as it does in the northern hemisphere. In late winter, however, the final stratospheric warming is similar to the wave 1 type of minor warming that occurs in the northern hemisphere, when the zonally averaged jet moves polewards and downwards.

DYNAMICAL PROCESSES

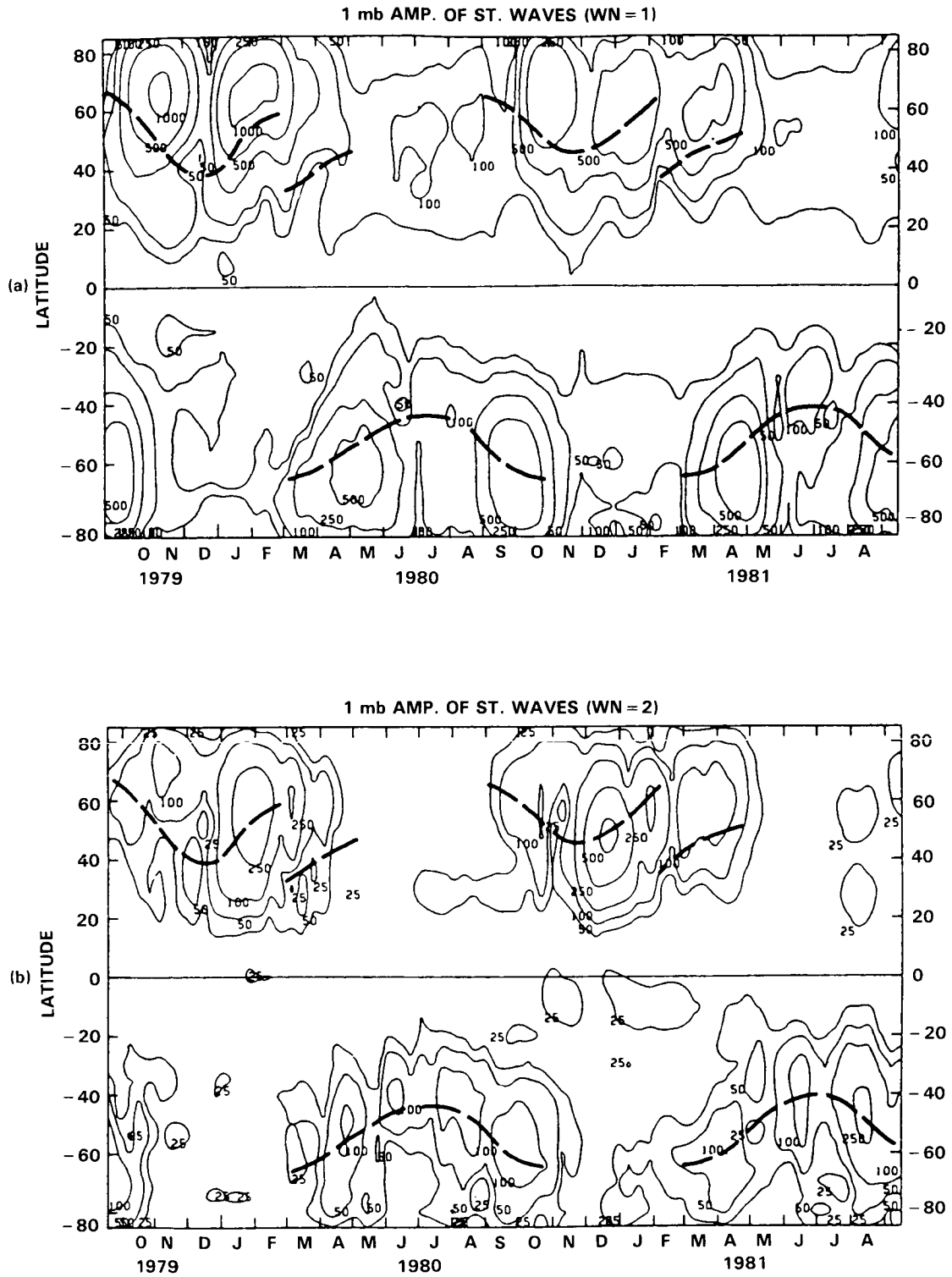


**Figure 6-22.** Latitude-time section of amplitude of quasi-stationary (a) wavenumber 1, and (b) wavenumber 2. Units are metres. Heavy broken lines denote axes of maximum westerlies. [After Hirota *et al.*, 1983].

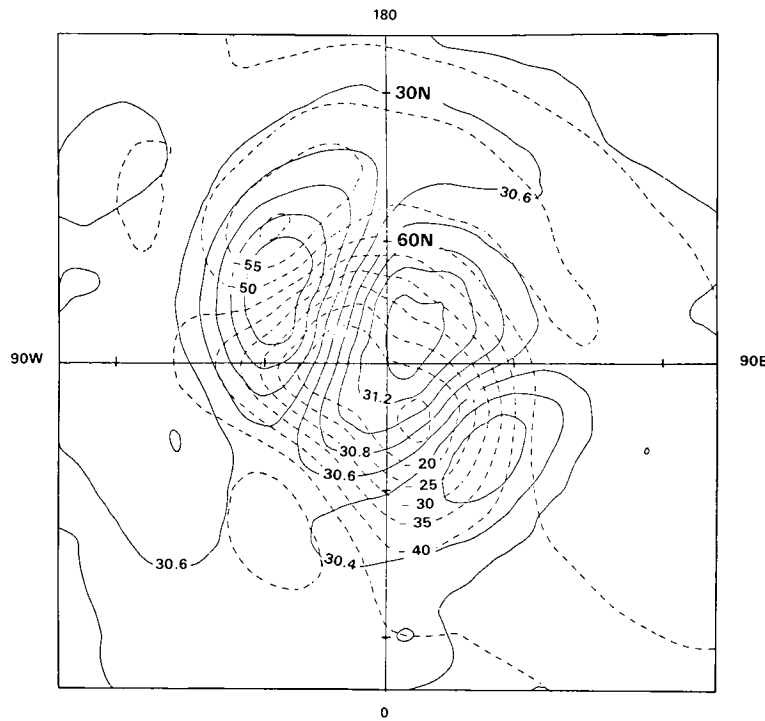


**Figure 6-23.** Polar stereographic maps at 10 mb of geopotential height (km solid lines) and temperature (K dashed lines) on 2 January 1985 at the height of a major stratospheric warming. Data obtained from a stratospheric sounding on the satellite NOAA-7. [Analysis made by the Middle Atmosphere Group, Meteorological Office, U.K.].

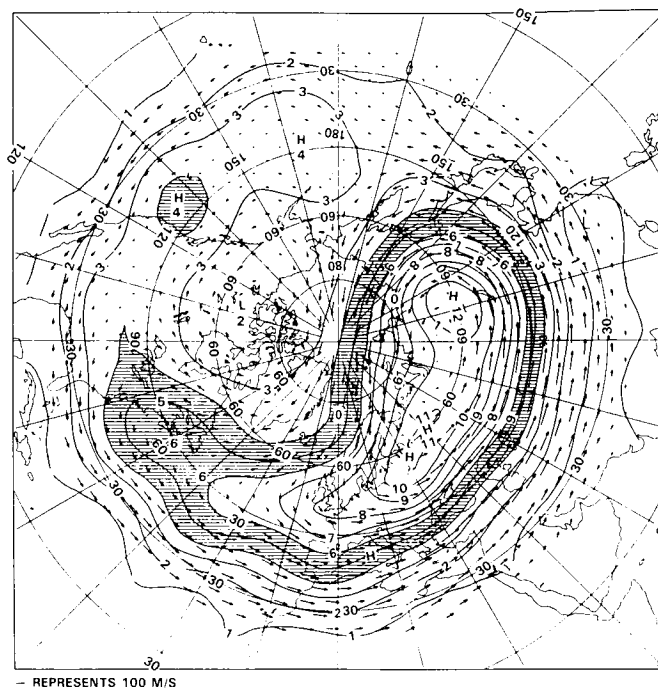


**Figure 6-24.** Ertel's potential vorticity and geostrophic winds evaluated on the 850 K isentropic surface near 10 mb for 4 December 1981. Units are  $\text{km}^2 \text{kg}^{-1} \text{s}^{-1} \times 10^{-4}$ . [After Clough *et al.*, 1985].

## DYNAMICAL PROCESSES

### 6.1.8 Inter-Annual Variability

The circulation of the middle atmosphere exhibits strong interannual variability in winter, which can be observed up to the mesopause. Labitzke and Naujokat [1983] have used the long record of radiosonde data (nearly 30 years) to study the inter-annual variability of the lower stratosphere. Figure 6-25 is a frequency distribution of the temperature at 30 mb for both poles. During summer when the prevailing winds are from the east, tropospheric disturbances do not penetrate far into the stratosphere. Therefore, conditions are quiet and the inter-annual variability is small, particularly at mid latitudes. In the northern winter and spring, the frequency distribution is broad. Labitzke [1982] has noted that the circulation is dominated by different zonal harmonic waves in different years: "disturbed" winters have a pronounced wave 1 pattern, often leading to major mid winter warmings and thus a warm polar region; and undisturbed winters with a pronounced wave 2 and a very cold polar region (vortex more symmetrically placed with respect to the pole), and only minor warmings in the stratosphere.

In the middle stratosphere, the variability is much smaller during the southern midwinters because large-scale waves are weaker than in the northern hemisphere. Wave amplitudes increase in spring (Figure 6-22) and are associated with increased variability of polar temperatures in October and November.

Geller *et al.* [1984] have noted significant inter-annual variability in the monthly mean zonal winds in the northern hemisphere. This is shown for four winters in Figure 6-26. Despite the variability, however, the same general pattern emerges during each of the winters as winter proceeds from December to February.

Even a rather superficial inspection of the circulation statistics of the equatorial middle atmosphere reveals characteristics, particularly long-period variations, which are profoundly different from those of the mid-latitude circulation. The variability of the latter is dominated by the seasonal cycle; in tropical latitudes (within about  $15^\circ$  of the equator) the annual cycle disappears, to be replaced by a quasi-biennial cycle in the lower stratosphere and, as has already been noted, a semiannual cycle in the upper stratosphere and mesosphere.

Between about 20 and 35 km altitude the monthly-mean zonal winds at tropical stations are seen to exhibit strong quasi-cyclic behavior (see Figure 6-27); the winds alternate between easterlies and westerlies of  $20\text{--}30\text{ ms}^{-1}$  with a period which ranges between 23 and 34 months (with a mean value of about 28 months). This phenomenon, which was first reported by Reed [1960] and Veryard and Ebdon [1961], has become known as the "quasi-biennial oscillation" [QBO]. Further description of its observed properties are to be found in Reed [1965], Wallace [1973], Coy [1979, 1980], Hamilton [1984], Dunkerton and Delisi [1985]. The wind oscillation is observed to be remarkably symmetric in longitude and dominated by the zonal component, so that it takes the form of alternating easterly and westerly jets over the equator; these jets descend slowly, successively being replaced from above by one of the opposite sign (Figure 6-28). The jets are confined to within about  $15^\circ$  of the equator [Wallace, 1973; Dunkerton and Delisi, 1984] although there is some evidence for a signal at higher latitudes, and perhaps in the planetary wave component of the winter hemisphere as well as in the zonal flow [Holton and Tan, 1980, 1982; Labitzke, 1982]. During the westerly phase of the QBO, the polar region tends to be colder and wave 2 amplitudes larger with less likelihood of a major warming; during the easterly phase, wave 1 amplitudes tend to be emphasized, leading to warmer polar temperatures and sometimes major warmings. This inter-annual variability in the middle latitudes may also be linked to the tropospheric Southern Oscillation [van Loon *et al.*, 1981], which in turn is thought to be connected with feedbacks between the atmosphere and local anomalies in sea surface temperature [e.g. Gill, 1982].

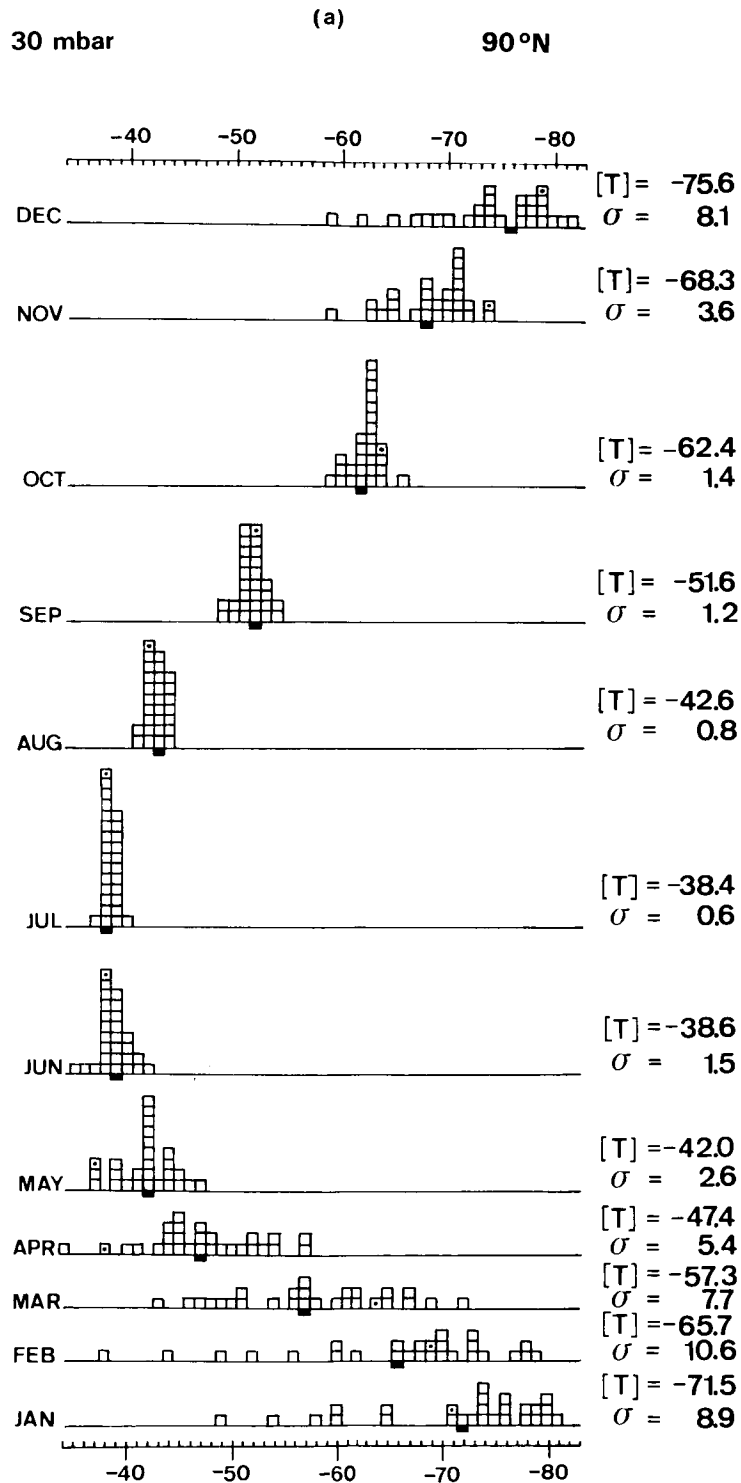


**Figure 6-25.** Frequency distribution of the monthly mean 30 mb temperatures ( $^{\circ}\text{C}$ ). The interval is  $1^{\circ}\text{C}$ . The long-term average  $[T]$  is given on the right hand side of the picture together with the standard deviation  $\sigma$ , and  $[T]$  is also marked as a black box in the frequency distribution. (a) is for the North Pole using radiosonde data for the period July 1955-Dec. 1982,

DYNAMICAL PROCESSES

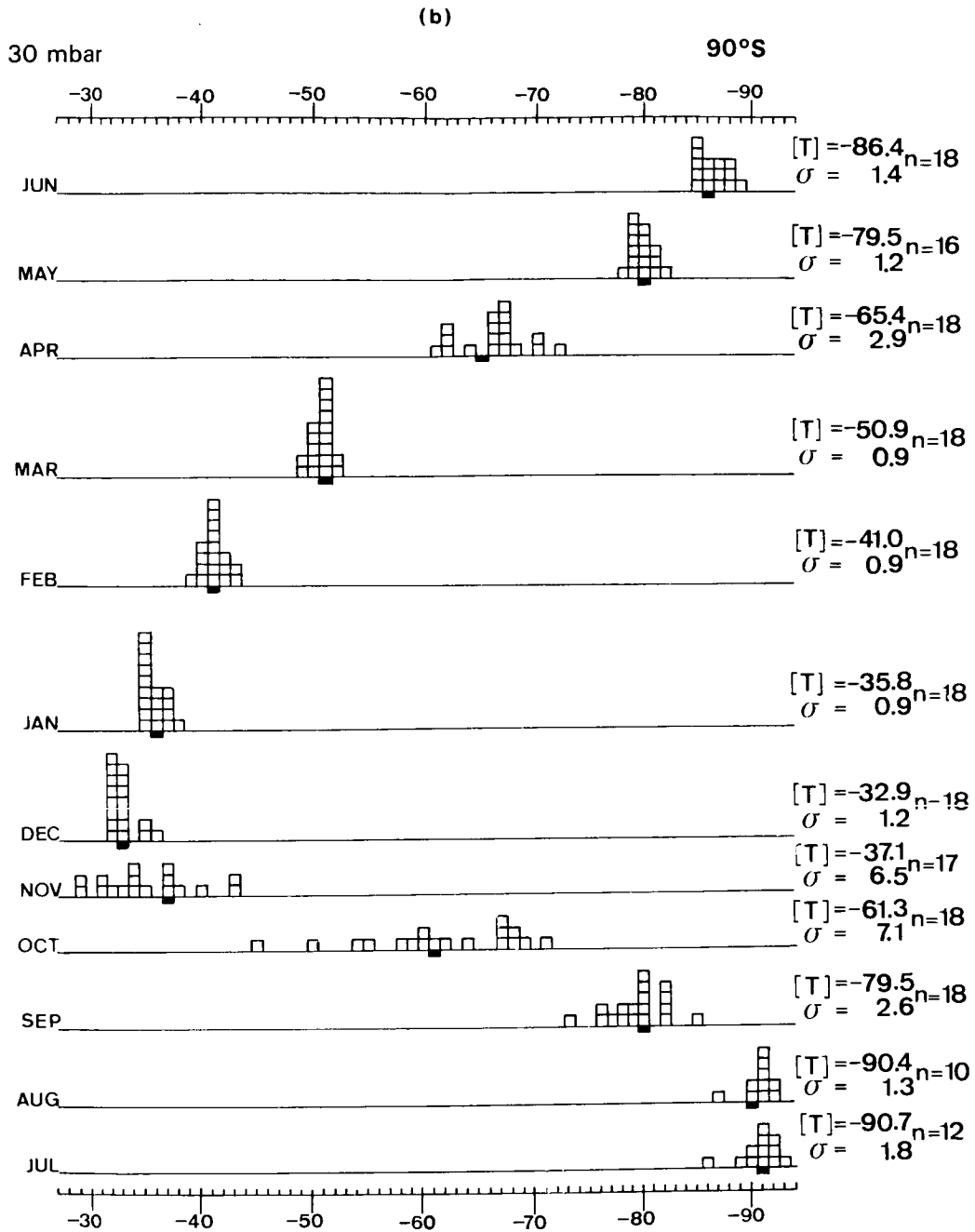
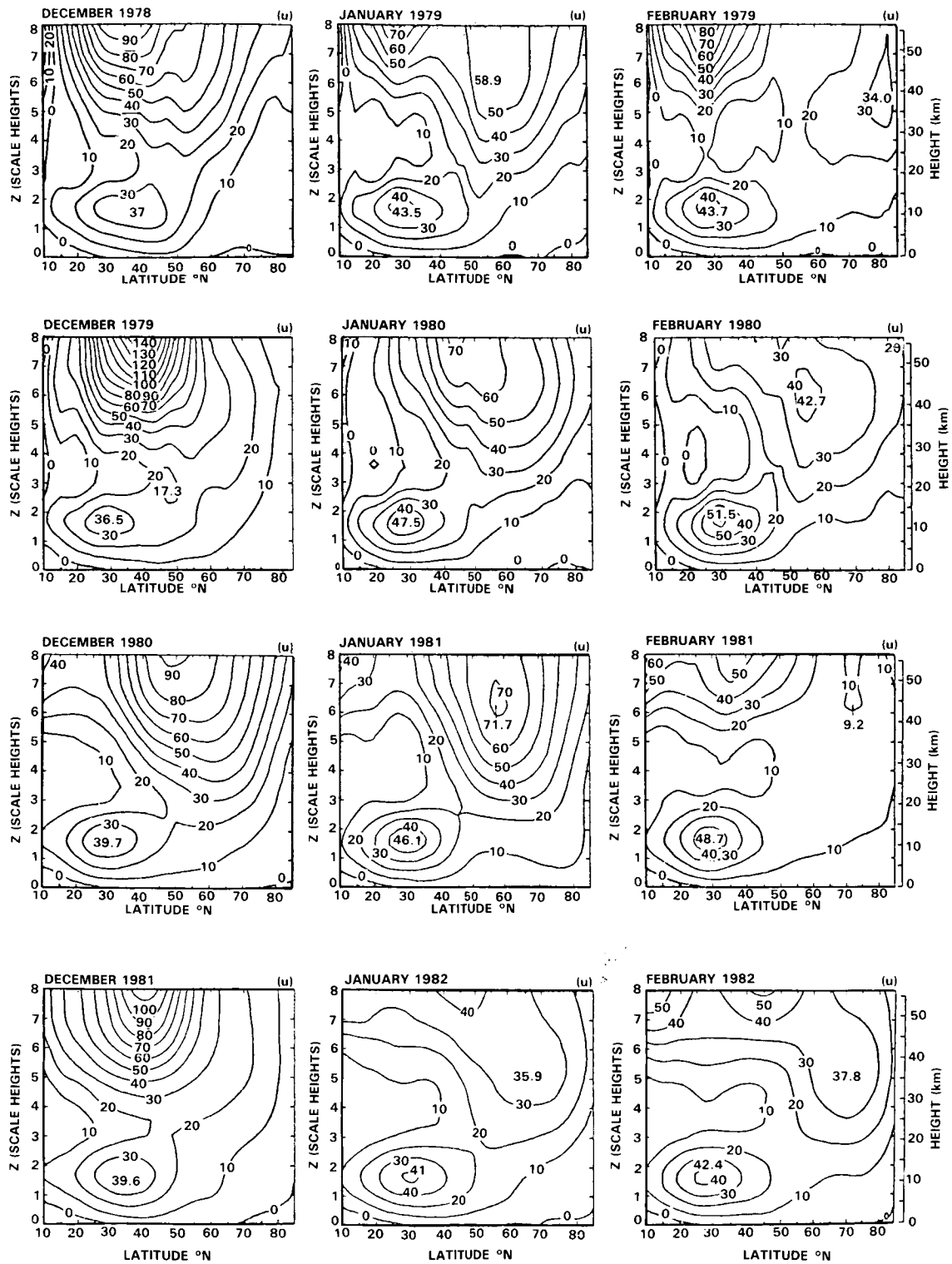


Figure 6-25. (b) is for the South Pole for the period 1961-1978 using, for each month, data for the number of years specified by n. [After Naujokat, 1981, and Labitzke and Naujokat, 1983].

Consistent with thermal wind balance, given the observed zonal wind structure, a temperature QBO (amplitude 1-2 K) is also observed [Reed 1962, 1964; Newell *et al.*, 1974; Angell and Korshover, 1978b]. Like the wind oscillation, the thermal component appears to be primarily confined to the tropics. However, a QBO in total ozone, first identified by Funk and Garnham [1962] and recently clarified by Hasebe [1983, 1984] in an analysis of Nimbus 4 BUUV and ground-based observations, is more prominent in middle latitudes, especially in the Southern Hemisphere (Figure 6-29).



**Figure 6-26.** Northern hemisphere, monthly mean, zonally averaged geostrophic winds ( $\text{ms}^{-1}$ ) for the months of December, January and February for the winters 1978-79 through 1981-82. Regions of easterlies are shaded. [After Geller *et al.*, 1984].

## DYNAMICAL PROCESSES

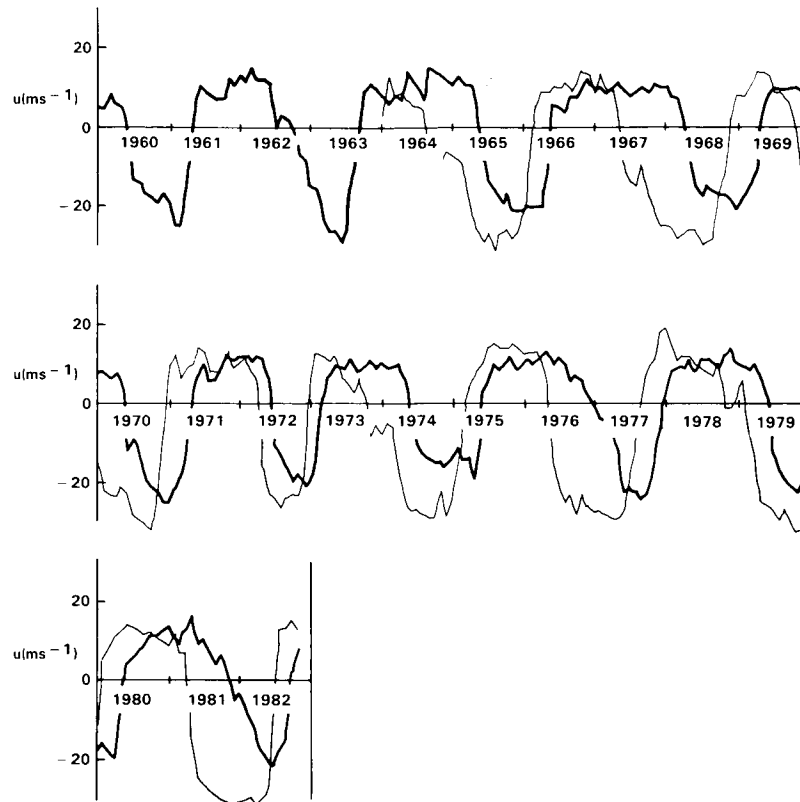


**Figure 6-27.** Monthly mean zonal winds at Singapore ( $1^{\circ}20'N$ ) at 50 mb (thick line) and 30 mb (thin line). Westerly wind is positive. [After Plumb, 1984].

An implication of the inter-annual variability of the middle atmosphere is that observations covering a single winter or even a small group of winters may be unrepresentative of the circulation of the middle atmosphere in a longer term mean. This should be borne in mind when verifying numerical simulations of the circulation or of the transport of trace species; this point will be addressed further in Section 6.6.

## 6.2 THEORY OF THE CIRCULATION OF THE MIDDLE ATMOSPHERE

### 6.2.1 Introduction

This section discusses the dynamical processes which maintain the observed large-scale circulation of the middle atmosphere in a state that is often far from radiative-photochemical equilibrium. It mostly concentrates on the maintenance of the climatological *zonal-mean* state, although some dynamical aspects of the climatological, non-zonally-averaged state are mentioned. The dynamics of stratospheric sudden warmings and long-period oscillations in the tropical middle atmosphere are also discussed briefly. (The adjective “climatological” here refers to those features which vary slowly from month to month during the annual cycle and recur regularly from year to year. They can be isolated, for example, by taking time averages over the individual calendar months in a data record extending over many years.)

To investigate the role played by dynamical processes in producing the observed middle atmospheric circulation it is first useful to consider what form the circulation would take if dynamical processes were

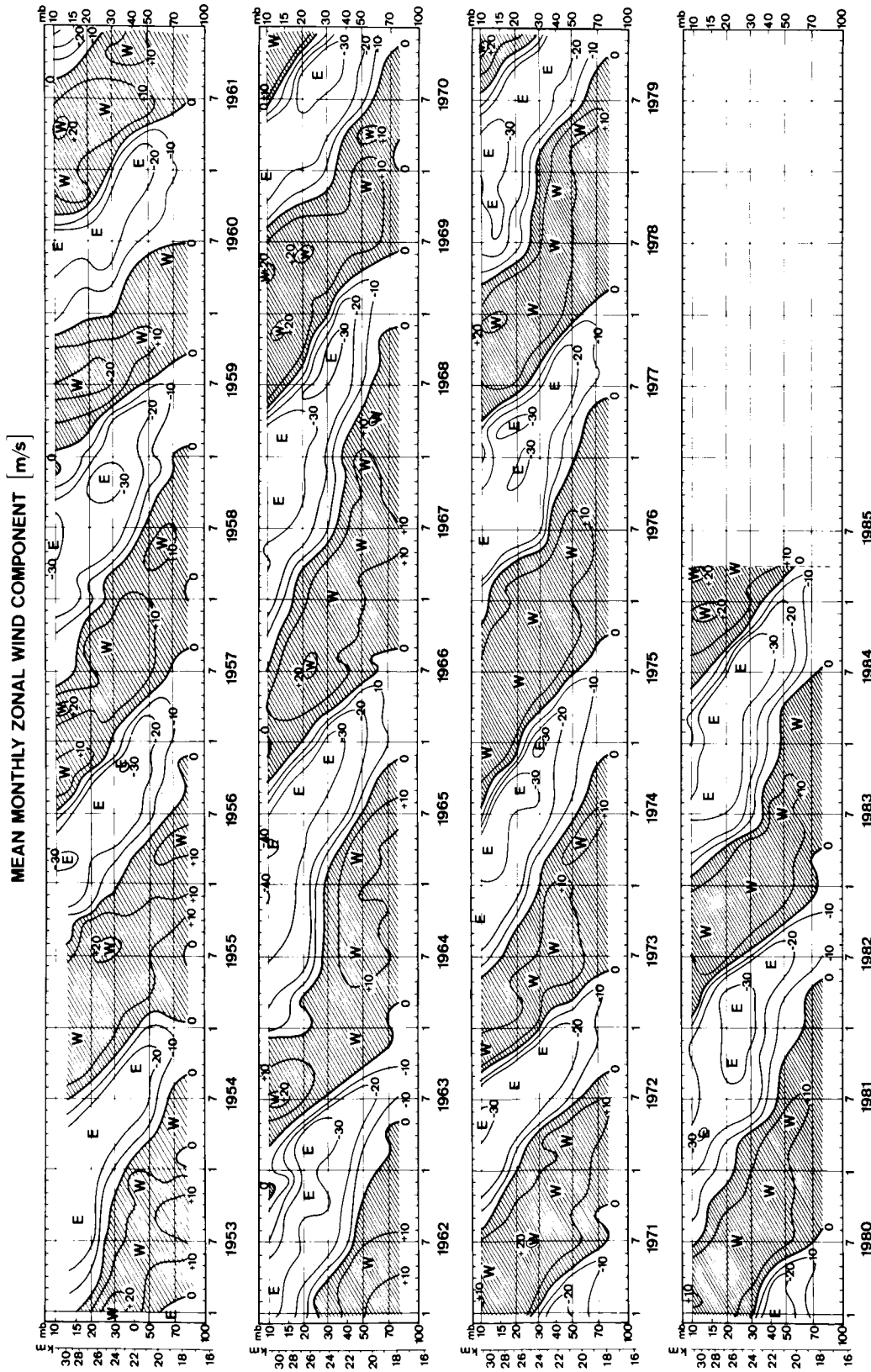
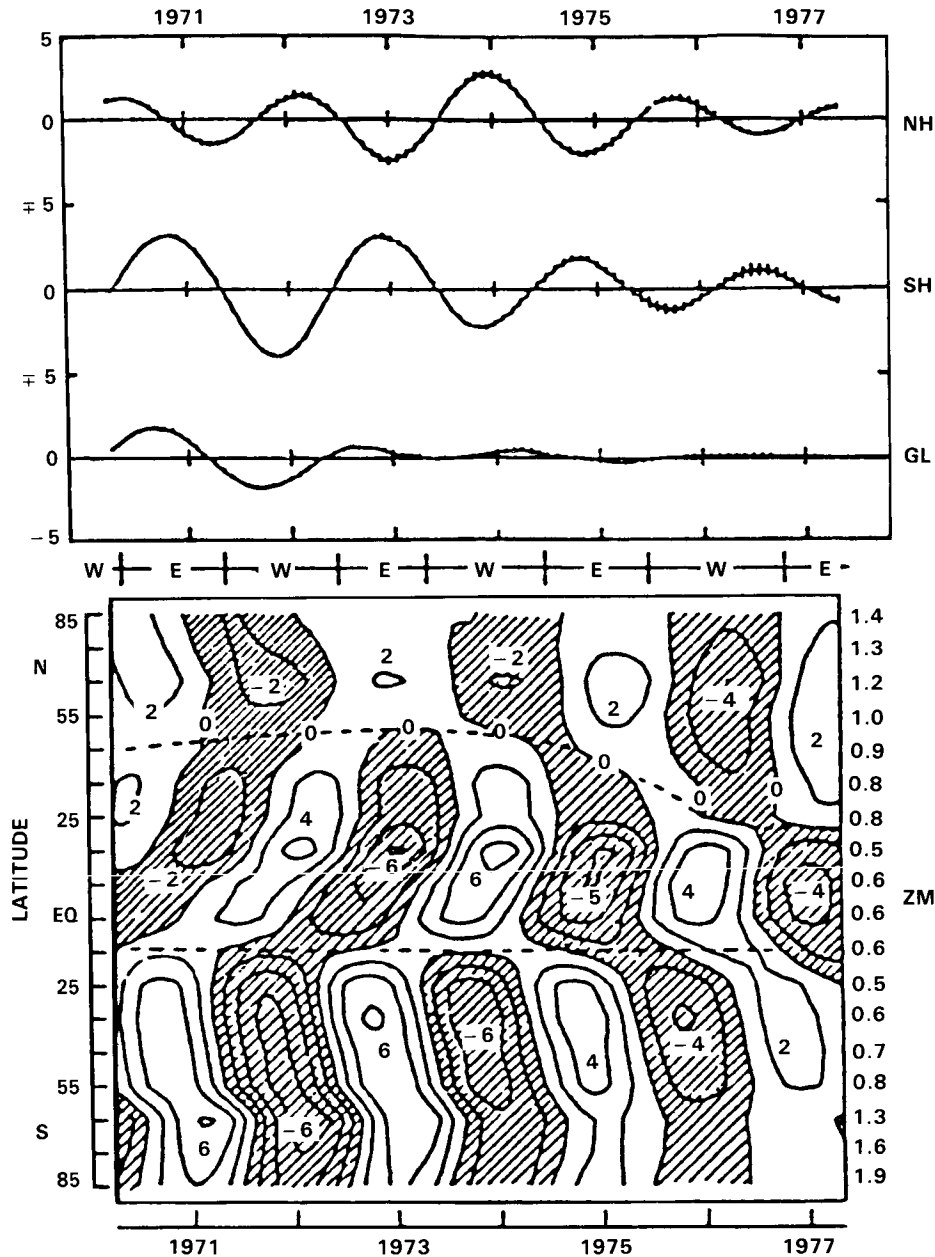


Figure 6-28. Time-height cross section of mean monthly zonal winds (m/s) at equatorial stations, calculated from all available daily values:

- Jan 1953 - Aug 1967 Canton Island, 3°S/172°W
- Sep 1967 - Dec 1975 Gan/Maledive Islands, 1°S/73°E
- Jan 1976 - Apr 1985 Singapore, 1°N/104°E (After Naujokat, 1985).

DYNAMICAL PROCESSES



**Figure 6-29.** Quasi-biennial oscillation of total ozone (matm-cm) in the mean values of (NH) Northern Hemisphere, (SH) Southern Hemisphere, and (GL) globe, and (ZM) zonal mean values. The isopleths in ZM are drawn with the interval of 2 matm-cm, and the shaded areas correspond to negative deviations. The tick mark is January of the given year. [After Hasebe, 1983].

absent (except for some representation of convection, and perhaps baroclinic wave activity, in the troposphere). The temperature field associated with such a circulation can be calculated from a radiative-photochemical model of the stratosphere and mesosphere, together with a radiative-convective model of the troposphere. An example for near-solstice conditions is shown in Figure 6-30, from Fels and Schwarzkopf [1985] [reported in Mahlman and Umscheid, 1984], whose model is time-marched through an annual cycle. The figure shows strong latitude and height variations of the resulting zonally-symmetric tem-

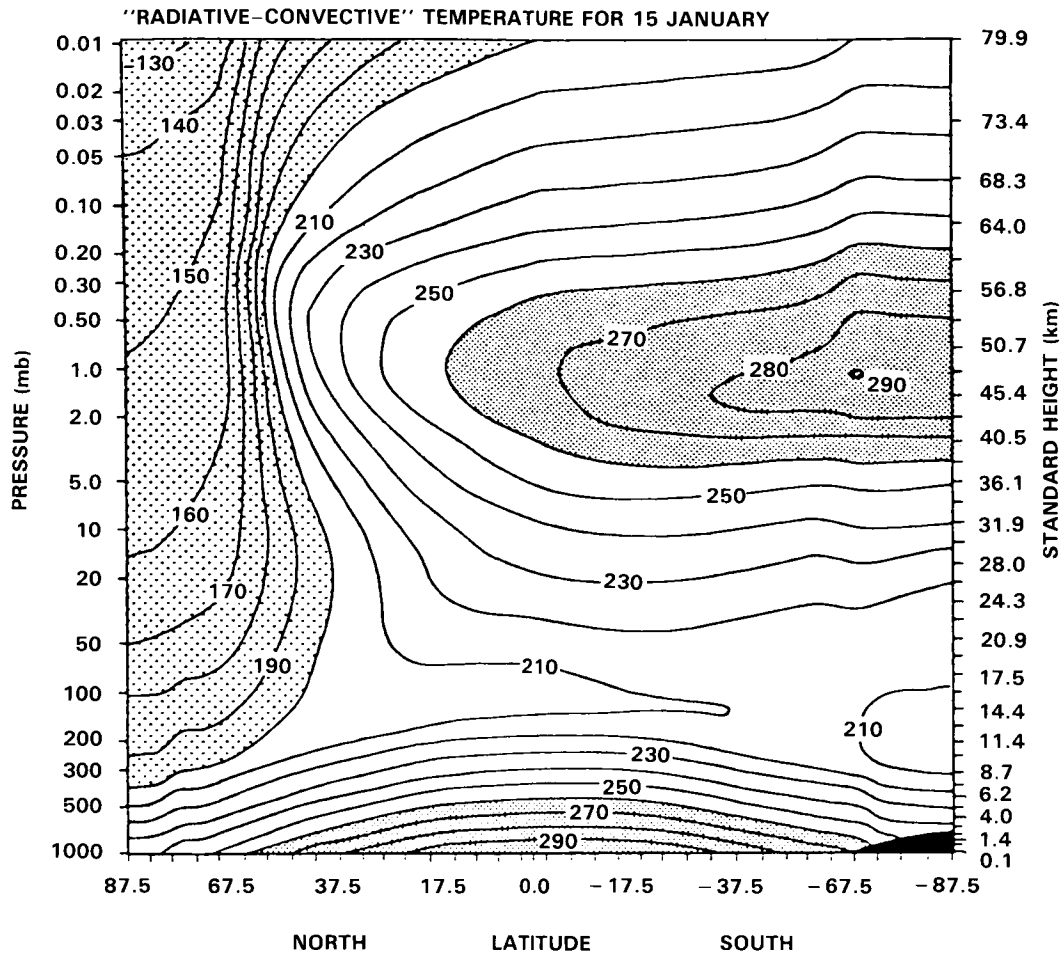


**Figure 6-30.** Time-dependent "radiatively-determined" temperature  $T_r$  for 15 January 1982 from the calculation of Fels and Schwarzkopf (1985). The surface temperatures are prescribed at their seasonally-varying observed values. Cloudiness, and ozone below 35 km, are prescribed at annual-mean values, as in Fels *et al.* (1980); ozone above 35 km is allowed to "float", in response to temperature variations, towards a crude photochemical equilibrium. Details of the water vapor prescription are relatively standard and are described in Fels and Schwarzkopf (1985). [From Mahlman and Umscheid, 1984].

perature  $T_r$ , with a maximum of about 280 K at the summer stratopause and temperatures below 180 K throughout the middle atmosphere at the winter pole, decreasing to 130 K at the winter mesopause. The temperature field  $T_r$  calculated in this way will be referred to below as the "radiatively-determined temperature". A comparison of this calculated temperature field with a typical observed January-mean zonally-averaged temperature (Figure 6-1) shows some overall similarities, but also some strikingly different features. In particular, the observed north polar night is much warmer (by about 20 K in the in the lower stratosphere, increasing to about 100 K in the mesosphere) than the corresponding  $T_r$ , while the observed equatorial tropopause is a little colder than  $T_r$  and the lower stratosphere in winter mid-latitudes is a little warmer. The July-mean zonally-averaged temperature (Figure 6-2) is roughly a mirror image of January, except that the southern winter polar midstratosphere, at about 180 K, is only just above the radiatively-determined value.

## DYNAMICAL PROCESSES

It is also of some interest to consider what zonal winds would be associated with a radiatively-determined temperature field like that of Figure 6-30. From thermal-wind balance, assuming zero wind (or the observed zonal mean winds of a few  $\text{ms}^{-1}$ ) at the ground, one would calculate extremely strong westerlies in the winter polar night and quite strong easterlies in the summer hemisphere (see Figure 6-31). In both hemispheres the magnitude of the winds would increase with height throughout the stratosphere and mesosphere. The observed zonal mean winds for January are close to being in thermal wind balance with the zonal-mean temperatures (at least in extratropical regions), and hence show a rather more moderate growth with height, peaking near 60 km and decreasing to small values at the mesopause (Figure 6-1). In July the Southern Hemisphere winter winds are stronger than their Northern Hemisphere winter counterparts of January.

Although some of the differences between the observations and the time-marched radiative-photochemical-convective calculations may be due to deficiencies in the radiative aspects of the model, by far the most important cause of these differences is the presence of *in situ* dynamical processes, which are deliberately ignored in this particular model. The extra heating or cooling that must be provided by the presence of dynamical effects is often called the “dynamical heating” [e.g. Fels *et al.*, 1980]. Some of the dynamical processes contributing to this heating would occur in a middle atmosphere whose circulation was zonally-symmetric; however, simple arguments suggest that the dynamical processes that are most important in accounting for departures from  $T_r$  (in the extra-tropics, at least) are associated with deviations from zonal symmetry – the “eddies” or “waves”. The details of how eddies can accomplish this task are discussed in Sections 6.2.2-6.2.4. (A basic caveat to be noted here is that, although this definition of an eddy or wave is convenient mathematically, it may not always be the most suitable from a physical point of view).

### 6.2.2 Some Simple Zonally-Averaged Models of the Middle Atmosphere

To gain insight into the ways in which dynamical processes can lead to departures of the zonal-mean temperature from the temperature  $T_r$  of a hypothetical atmosphere controlled by radiative, photochemical and convective effects, it is helpful to begin by considering some rather simple models of the extratropical middle atmosphere. A convenient starting-point is the quasigeostrophic set of zonal-mean equations on a mid-latitude beta-plane, in log pressure coordinates. The “transformed Eulerian-mean” versions of these equations [e.g., Edmon *et al.*, 1980; Dunkerton *et al.*, 1981] can be written

$$\frac{\partial \bar{u}}{\partial t} - f_0 \bar{v}_* = \rho_0^{-1} \bar{\nabla} \cdot \bar{\mathbf{F}} + \bar{X} \equiv G, \quad (1a)$$

$$\frac{\partial \bar{T}}{\partial t} + N^2 H R^{-1} \bar{w}_* = \bar{J}/c_p, \quad (1b)$$

$$\frac{\partial \bar{v}_*}{\partial y} + \frac{1}{\rho_0} \frac{\partial}{\partial z} [\rho_0 \bar{w}_*] = 0, \quad (1c)$$

$$f_0 \frac{\partial \bar{u}}{\partial z} + R H^{-1} \frac{\partial \bar{T}}{\partial y} = 0. \quad (1d)$$

Here  $z = -H \ln [p/p_0]$ , where  $p$  is pressure,  $p_0$  a constant reference pressure and  $H$  a representative pressure scale height (typically about 7 km, in which case  $z$  is approximately equal to geometric height throughout the middle atmosphere).  $x$  and  $y$  denote eastward and northward distance, respectively, from some mid-latitude origin,  $R$  is the gas constant for dry air and  $c_p$  the specific heat at constant pressure.  $f_0$  is a mean

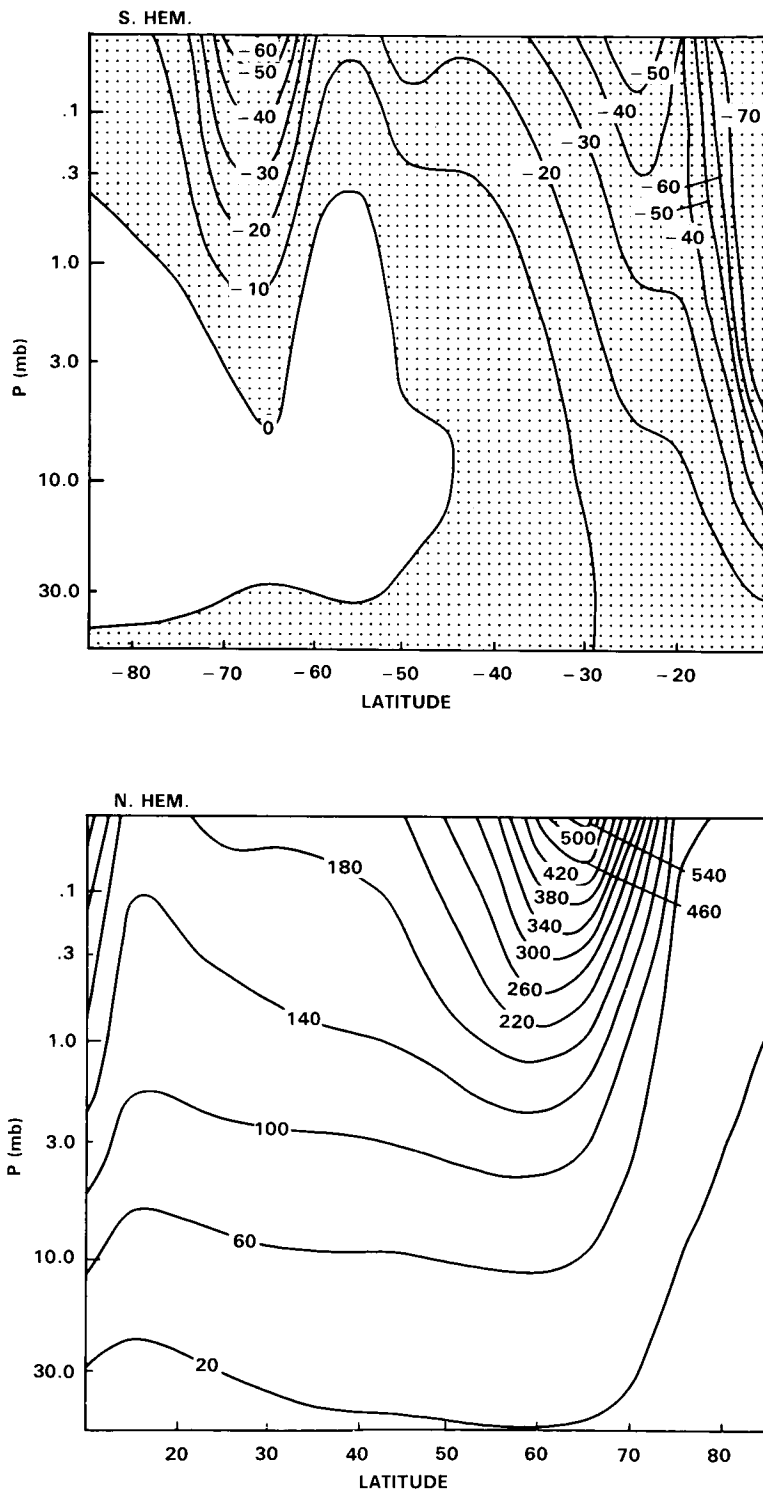


**Figure 6-31.** Geostrophic winds  $U(\theta, P)$  calculated from the January 15 temperatures of Figure 6-30. The value of  $U(\theta, 50 \text{ mb})$  is taken from Oort and Rasmussen, and the thermal wind equation integrated upward from 50 mb. The contours have been modestly handsmoothed. [After Fels and Schwarzkopf, 1985].

## DYNAMICAL PROCESSES

Coriolis parameter,  $\bar{u}$  is the zonal mean wind and  $\bar{T}$  the zonal-mean temperature.  $(\bar{v}_*, \bar{w}_*)$  is the "residual mean meridional circulation", defined by:

$$\bar{v}_* \equiv \bar{v} - \frac{1}{\rho_0} \frac{\partial}{\partial z} \left[ \frac{\rho_0 \bar{v}'T'}{N^2HR^{-1}} \right], \quad \bar{w}_* \equiv \bar{w} + \frac{\partial}{\partial y} \left[ \frac{\bar{v}'T'}{N^2HR^{-1}} \right] \quad (2)$$

where  $(\bar{v}, \bar{w})$  is the zonal-mean meridional circulation and  $\bar{v}'T'$  is the northward eddy temperature flux.  $\rho_0[z]$  is a basic density, proportional to  $p$ , and  $N^2HR^{-1} = dT_0/dz + \kappa T_0/H$ , where  $T_0[z]$  is a reference temperature profile and  $\kappa = R/c_p$ .

The eddy forcing of the mean flow is represented in (1) by an effective force, equal to  $\nabla \cdot \underline{\underline{F}}$ , acting on the mean zonal flow. The vector  $\underline{\underline{F}}$  is called the Eliassen-Palm [EP] flux [Eliassen and Palm, 1961]; its full definition in log-pressure coordinates is given, for example, by Dunkerton *et al.*, [1981, eqs (A1)]. For quasigeostrophic, planetary-scale waves, it reduces to:

$$\underline{\underline{F}} = (F_y, F_z) = [-\rho_0 \overline{u'v'}, \rho_0 f_0 \overline{v'T'}/N^2HR^{-1}] \quad (3a)$$

where  $\rho_0 \overline{u'v'}$  is the northward eddy flux of zonal momentum, while for small-scale, vertically-propagating internal gravity waves it is given by:

$$\underline{\underline{F}} = [0, -\rho_0 \overline{u'w'}] \quad (3b)$$

where  $\rho_0 \overline{u'w'}$  is the vertical eddy flux of zonal momentum. The quantity  $\bar{X}$  represents all other contributions to the zonal force per unit mass acting on the mean flow.  $\bar{J}$  represents mean diabatic effects and, if small-scale or molecular diffusion of heat is negligible, equals the zonal-mean net radiative heating rate.

One advantage of the transformed set (1) over the standard "Eulerian-mean" equations [e.g., eqs (2) of Dickinson, 1969] is that no "eddy heating" terms appear in the mean thermodynamic equation (1b), under quasigeostrophic scaling. The only (large-scale) "eddy forcing" is then  $\rho_0^{-1} \nabla \cdot \underline{\underline{F}}$ , in (1a). Another advantage is that  $\nabla \cdot \underline{\underline{F}}$ , unlike the "eddy-forcing" terms in the standard equations, can be related directly to certain rather general physical properties of the eddies, as will be discussed in Section 6.2.3.

Consider now a hypothetical steady-state atmosphere in which the seasonal cycle is absent; with time derivatives set to zero, (1a,b) give:

$$-f_0 \bar{v}_* = G, \quad N^2HR^{-1} \bar{w}_* = \bar{J}/c_p, \quad (4)$$

and substitution into (1c) yields

$$-f_0^{-1} \frac{\partial G}{\partial y} + \frac{1}{\rho_0} \frac{\partial}{\partial z} \frac{\rho_0 \bar{J} \kappa}{N^2H} = 0. \quad (5)$$

This shows how the net heating  $\bar{J}$  must be related to  $G \equiv \rho_0^{-1} \nabla \cdot \underline{\underline{F}} + \bar{X}$  in this hypothetical state. If  $\nabla \cdot \underline{\underline{F}}$  and  $\bar{X}$  both vanish then  $\bar{J}$  must also vanish [provided that  $\bar{w}_* = 0$  at the lower boundary]; the atmosphere is then in radiative equilibrium (if small-scale thermal diffusion is negligible), with the long-wave cooling balancing the solar heating everywhere. Then  $\bar{T} = T_r(y, z)$ , say,  $u = u_r(y, z)$  [where  $f_0 \partial u_r / \partial z + RH^{-1} \partial T_r / \partial y = 0$  by (1d)] and  $\bar{v}_* = \bar{w}_* = 0$  by (4), i.e., the residual mean meridional circulation vanishes.

Suppose next that  $G = 0$  still, but that time-dependence is allowed by letting the solar heating take on an annual variation  $\bar{J}_s(y,z,t)$ . Further progress is aided by a parameterization of  $\bar{J}$  in terms of  $\bar{T}$ ; as a simple example consider the Newtonian cooling form

$$\frac{\bar{J}}{c_p} = - \frac{(\bar{T} - T_r)}{\tau_r(z)} \quad (6)$$

where  $T_r(y,z,t)$  is the temperature calculated from a time dependent radiative-photochemical model (such as that from which Figure 6-30 was obtained) with specified solar heating  $\bar{J}_s(y,z,t)$ , and  $\tau_r(z)$  is a radiative relaxation time. This parameterization is not expected to be quantitatively accurate for large departures of  $\bar{T}$  from  $T_r$ ; however, it does contain the important physical feature of relating the net heating to departures from a radiatively-determined  $T_r$ . From Equations (1) and (6) it can then be shown that:

$$\left[ \frac{\partial^2}{\partial y^2} + \frac{\partial}{\partial z} \left( \rho_0^{-1} \frac{\partial}{\partial z} \rho_0 \epsilon \right) \right] \frac{\partial \bar{T}}{\partial t} + \frac{\partial}{\partial z} \left[ \rho_0^{-1} \frac{\partial}{\partial z} \left( \frac{\rho_0 \epsilon}{\tau_r} [\bar{T} - T_r] \right) \right] = 0, \quad (7)$$

where  $\epsilon(z) \equiv f_0^2/N^2(z)$ . In this equation the term in  $T_r$  (related to the solar heating  $\bar{J}_s$ ) provides the *forcing*, while  $\bar{T}$  represents the *response*. In general,  $\bar{T}$  will follow  $T_r(y,z,t)$ , but will be somewhat lagged in time and somewhat differently distributed in space; the zonally-symmetric dynamics provides a kind of ‘‘inertia’’. Since  $\bar{T} \neq T_r$  in general,  $\bar{J} \neq 0$  by (6) and  $(\bar{v}_*, \bar{w}_*) \neq 0$  by Equations (1a,b,c,d). It should be emphasized that the non-vanishing of the *net* heating  $\bar{J}$  is essentially due to the presence of this ‘‘dynamical inertia’’, and cannot be regarded as imposed by external agencies. To put it another way, although the solar heating has been specified in advance in this model, the long-wave cooling must be determined as part of the solution.

Simple order-of-magnitude arguments, assuming height scales of order  $H$  and horizontal scales of order  $L$ , where  $f_0^2 L^2 \sim H^2 N^2$  (this fails near the equator, where  $f_0^2 L^2 \ll N^2 H^2$ , and where quasigeostrophic theory generally breaks down in any case) show that:

$$\left[ \frac{\partial \bar{T}}{\partial t} \right] \sim \left[ \frac{\bar{T} - T_r}{\tau_r} \right]$$

approximately, in this model. If  $\Delta \bar{T}(y,z)$  is the maximum annual variation of  $\bar{T}$  in the model and  $\tau$  is a seasonal timescale (say 3 months), we have  $\partial \bar{T} / \partial t \sim \Delta \bar{T} / \tau$ . However, typical radiative relaxation times are mostly less than about 20 days in the middle atmosphere, so that  $\tau_r \ll \tau$ , whence

$$\bar{T} - T_r \sim \frac{\tau_r}{\tau} \Delta \bar{T} \ll \Delta \bar{T}, \quad (8)$$

and departures of  $\bar{T}$  from the radiatively-determined value  $T_r(y,z,t)$  are much less in this model than the actual annual swing  $\Delta \bar{T}$ . The model therefore predicts extratropical temperatures  $\bar{T}(y,z,t)$  that are always close to the temperatures  $T_r(y,z,t)$  determined from radiative-convective considerations. (Note that this conclusion does not depend on the details of the parameterization (6)). It is therefore clear that this simple model fails to predict the observed *large* departures of  $\bar{T}$  from  $T_r$  in certain parts of the extratropical middle atmosphere (e.g., the polar night and the summer upper mesosphere). Additional effects must be included if a basic understanding of the annual variations of the temperatures structure of these regions is to be obtained.

## DYNAMICAL PROCESSES

Now, if  $G \equiv \rho_0^{-1} \nabla \cdot \mathbf{F} + \bar{X}$  is retained, the set (1), with parameterization (6) yields:

$$\begin{aligned} & \left[ \frac{\partial^2}{\partial y^2} + \frac{\partial}{\partial z} \left[ \rho_0^{-1} \frac{\partial}{\partial z} \rho_0 \epsilon \right] \right] \frac{\partial \bar{T}}{\partial t} + \frac{\partial}{\partial z} \left[ \rho_0^{-1} \frac{\partial}{\partial z} \left[ \frac{\rho_0 \epsilon}{\tau_r} [\bar{T} - T_r] \right] \right] \\ & \quad [1] \qquad \qquad \qquad [2] \\ & \quad + \left[ \frac{f_0 H}{R} \frac{\partial^2 G}{\partial y \partial z} \right] = 0. \\ & \quad \qquad \qquad [3] \end{aligned} \tag{9}$$

Suppose that  $G$  varies on a timescale  $\tau_w$ : except for rapid events like sudden warmings we have  $\tau_w \sim \tau \gg \tau_r$ . (If rapid events of this kind are present, they can be removed by averaging over a time  $\tau_w = O(\tau)$ : see Andrews *et al.*, [1983].) A scaling gives the ratio of terms as:

$$[1] : [2] : [3] = \frac{\Delta \bar{T}}{\tau} : \frac{\bar{T} - T_r}{\tau_r} : \frac{f_0 L \Delta G}{R} \tag{10}$$

if  $f_0^2 L^2 \sim N^2 H^2$  (thus excluding equatorial regions again) and  $\Delta G$  is the variation in  $G$  over time  $\tau_w$ . In the polar night stratosphere and in the upper mesosphere it is found that  $(\bar{T} - T_r)/\tau_r \gg \Delta \bar{T}/\tau$  in general, so here the effects represented by  $G$  must be large enough to give a balance between terms [2] and [3]. The term in  $\partial \bar{T}/\partial t$  in (9) is therefore small in these regions: equivalently the time derivatives in (1a) and (1b) are small, so that (according to this model) the balances expressed by (4) and (5) hold approximately, at each  $t$ , in those regions where  $\bar{T}$  exhibits large departures from  $T_r$ .

This simple model suggests that dynamical effects which contribute to the mean zonal force per unit mass  $G \equiv \rho_0^{-1} \nabla \cdot \mathbf{F} + \bar{X}$  may be responsible for maintaining the large departures of  $\bar{T}$  from  $T_r$  that are observed in parts of the middle atmosphere. Conversely, it also suggests that those regions – such as parts of the midlatitude lower stratosphere and the summer stratopause – which are observed to be close to radiative equilibrium [e.g. Houghton, 1978; Wehrbein and Leovy, 1982] may be in that state because of the absence of dynamical effects that can produce a significant  $G$ .

### 6.2.3 Aspects of Wave, Mean-Flow Interaction Theory

We now discuss the dynamical processes that are likely to contribute importantly to the forcing term  $G \equiv \rho_0^{-1} \nabla \cdot \mathbf{F} + \bar{X}$ . First consider  $\nabla \cdot \mathbf{F}$ : it was mentioned in Section 6.2.2 that one advantage of the transformed Eulerian-mean equations (1) is that the ‘‘eddy-forcing’’ term  $\nabla \cdot \mathbf{F}$  depends on certain physical properties of the eddies. This dependence is expressed by the ‘‘generalized Eliassen-Palm Theorem’’ (Andrews and McIntyre, 1976, 1978a; Boyd, 1976) which, for eddies on a flow that is basically zonal, takes the form:

$$\frac{\partial A}{\partial t} + \nabla \cdot \mathbf{F} = D + \left[ \begin{array}{l} \text{terms that are cubic} \\ \text{in wave amplitude} \end{array} \right] \tag{11}$$

which is of a standard form expressing the conservation of some quantity, here a measure of wave activity,  $A$ .  $A$  and  $D$ , like  $\mathbf{F}$ , are zonal-mean quadratic functions of eddy quantities, while the term that is cubic in eddy amplitude is negligible for waves whose amplitudes are small enough for linear theory to be valid.  $D$  involves wave dissipation or forcing, and thus vanishes if the waves are conservative;  $\partial A/\partial t$  vanishes

if the waves are steady. Thus (11) states that  $\nabla \cdot \mathbf{F}$  depends on wave transience, nonconservative wave effects and wave nonlinearity. If all of these are absent then  $\nabla \cdot \mathbf{F} = 0$ . Conversely, if waves are strongly transient, nonconservative or nonlinear (or any combination of these), we can anticipate large values of  $\nabla \cdot \mathbf{F}$  and perhaps large departures of  $\bar{T}$  from  $T_r$ . It should be noted that  $\bar{A}$  generally involves Lagrangian quantities like the northward particle displacement: “transience” thus means “Lagrangian transience” in this context (see Section 6.5.2). Important contributions to  $\bar{X}$  are likely to be produced for example by turbulent mixing associated with the “breaking” of large-amplitude gravity waves (see Section 6.2.4).

#### 6.2.4 Implications of the Theory

The theory sketched in the two previous sections, involving the use of a quasigeostrophic beta-plane model for the mean flow and restrictions to small amplitude waves in Equation (11), is clearly too crude for accurate quantitative comparisons with observations. (Some of these constraints can in fact be relaxed: for instance, similar ideas can be formulated for the primitive equations on the sphere – in the extratropics – by using isentropic coordinates.) However, perhaps a more important use of the theory is to provide qualitative insights into the physical mechanisms which maintain the zonal-mean climatological state of the middle atmosphere. It suggests how eddy motions on various scales can keep certain parts of the middle atmosphere far from the state predicted by radiative-convective models, and throws light on the physical eddy processes that may be responsible for this. It thus helps to clarify the role of the eddies in the maintenance of the climatological mean state. For instance, if in a climatological average certain eddies are found to exhibit a significant  $\nabla \cdot \mathbf{F}$ , then, under the scaling described at the end of Section 6.2.2, the corresponding eddy forcing  $G = \rho_0^{-1} \nabla \cdot \mathbf{F}$  is responsible for driving a climatological residual circulation ( $\bar{v}_*, \bar{w}_*$ ) and thence inducing a net radiative heating  $\bar{J}$ , by preventing  $\bar{T}$  from relaxing to  $T_r$  [see Kurzeja, 1981; Plumb, 1982; Apruzese *et al.*, 1982]. (This point was originally made by Dickinson [1969] using the northward eddy flux of quasigeostrophic potential vorticity  $\bar{v}'\bar{Q}'$  as a measure of eddy forcing. Under quasigeostrophic scaling this flux equals  $\rho_0^{-1} \nabla \cdot \mathbf{F}$ : cf. Section 6.5.3). In general, therefore, it is clearly misleading to regard the residual circulation as a “diabatic circulation”, *driven* by an externally-imposed net radiative heating  $\bar{J}$  [Kurzeja *et al.*, 1984].

Of course, not all situations in the middle atmosphere will be as simple as this: for example, one cannot generally regard the eddy structure, and therefore  $\nabla \cdot \mathbf{F}$ , as independent of the mean flow, nor, indeed, of radiative processes, since these contribute to the nonconservative dissipation of the waves. However, the case just described does caution against too naive an application of names like “eddy transport” and “mean transport” to the various terms in the mean equations of motion. Not only may such terms differ between one particular formulation and another – e.g., between the transformed set (1) and the standard Eulerian-mean set or the Lagrangian-mean set (Andrews and McIntyre, [1978b]; see also Plumb [1983b], for a slightly different example) – but they may none of them be entirely consistent with results of thought-experiments or model calculations in which eddies are artificially excluded from the middle atmosphere [e.g., Andrews *et al.*, 1983].

These insights have already proved useful in the interpretation of tracer transport [e.g., Mahlman *et al.*, 1981, 1984] and the behavior of numerical models of the middle atmosphere (see Section 6.3). They should also help in the future investigation of the observed middle atmosphere, not only by providing a basic theoretical framework for interpretation but also by indicating specific aspects of wave motions, in specific regions of the middle atmosphere, which may require particular attention. These aspects will now be considered in more detail.

## DYNAMICAL PROCESSES

The first question to ask is what kinds of eddy or wave motion could be responsible for the large observed climatological departures of  $\bar{T}$  from  $T_r$  in the polar night stratosphere (especially in the northern hemisphere) and in the upper mesosphere.

Taking first the polar winter stratosphere, obvious candidates are the planetary-scale wave disturbances, including the quasi-stationary planetary waves that are familiar features of the northern winter stratosphere but are of smaller amplitude in the southern winter (Section 6.1.3). The theory sketched above indicates that the effectiveness of the waves in driving  $\bar{T}$  away from  $T_r$  depends mainly on the Eliassen-Palm flux divergence  $\nabla \cdot \mathbf{F}$ , and that  $\nabla \cdot \mathbf{F}$  in turn depends on the waves being transient, nonconservative or nonlinear. One class of event in which all three of these processes are probably significant, namely the "breaking" of planetary waves, has recently been identified from satellite-derived measurements of the stratosphere [McIntyre and Palmer, 1983, 1984; Clough *et al.*, 1985]. This phenomenon involves the rapid, irreversible deformation of otherwise wavy material contours, and is most clearly depicted in terms of maps on isentropic surfaces of Ertel's potential vorticity  $P$  ( $\equiv \rho^{-1} \zeta_a \cdot \nabla \theta$ , where  $\rho$  is density,  $\zeta_a$  is absolute vorticity and  $\theta$  is potential temperature or entropy). Like  $\theta$ ,  $P$  is approximately conserved following fluid particles (it is exactly conserved for adiabatic, frictionless flow), and the maps therefore give a picture (which is somewhat blurred, owing to the finite resolution of satellite measurements) of the behavior of distorting, quasi-material lines of fluid particles in the stratosphere. During "breaking" planetary-wave events, long "tongues" of potential vorticity are strung out on isentropic surfaces in an apparently irreversible manner (see Figure 6-24), and significant mixing of potential vorticity may then occur. Several key aspects of this process have yet to be clarified, however, including the role of radiative effects and the extent to which the mixing is irreversible [Clough *et al.*, 1985].

If such planetary-wave breaking events are common in the northern winter stratosphere, they could well lead to systematically large climatological contributions to  $\nabla \cdot \mathbf{F}$  there. This contribution is in addition to that expected in the absence of wave breaking from the effects of wave dissipation through radiative damping, which may be particularly important in the upper stratosphere where the damping rates become large. Further research is needed to understand the relative contribution of these effects and to determine whether their net contribution to  $\nabla \cdot \mathbf{F}$  is large enough to account for the observed departures of the climatological temperatures from radiative equilibrium (see Section 6.4.2). However, some support for the application of the simple theory given here comes from the general circulation model results of Mahlman and Umscheid [1984] (in which the model's polar night stratosphere being too close to  $T_r$  may be associated with over-weak planetary wave amplitudes: cf. Section 6.3.3). Also relevant is the observation that the southern hemisphere winter stratosphere is closer to the radiatively-determined state than is the northern winter stratosphere: this may be due to the weaker southern winter planetary wave amplitudes mentioned above.

Consider now the departure of  $\bar{T}$  from  $T_r$  in the upper mesosphere. In the summer hemisphere, at least, these cannot be due to quasi-stationary planetary waves, since such waves are essentially absent there. Following a suggestion of Houghton [1978], it is now generally believed that gravity waves provide the major part of the forcing in the upper mesosphere. In the absence of significant dissipation or reflection, the velocity and temperature amplitudes of such waves grow roughly exponentially with height as they propagate upwards from the lower atmosphere. Eventually nonlinear effects become important, leading to wave "breaking", as signalled by the overturning of isentropic surfaces, and hence turbulence, small-scale mixing and dissipation; as a result the wave growth with altitude is halted [Hodges, 1967]. This "saturation" process leads, as seen in Section 6.1.6, to a vertical momentum flux convergence, and thus a contribution to  $\nabla \cdot \mathbf{F}$  (by (3b)), which in fact tends to accelerate the mean flow towards the phase speed of the waves (Figure 6-32). The turbulence also causes diffusion of mean momentum and thus contributes to  $\bar{X}$ ; diffusion of heat and chemical constituents is likely to occur in the same way (see Section 6.5).

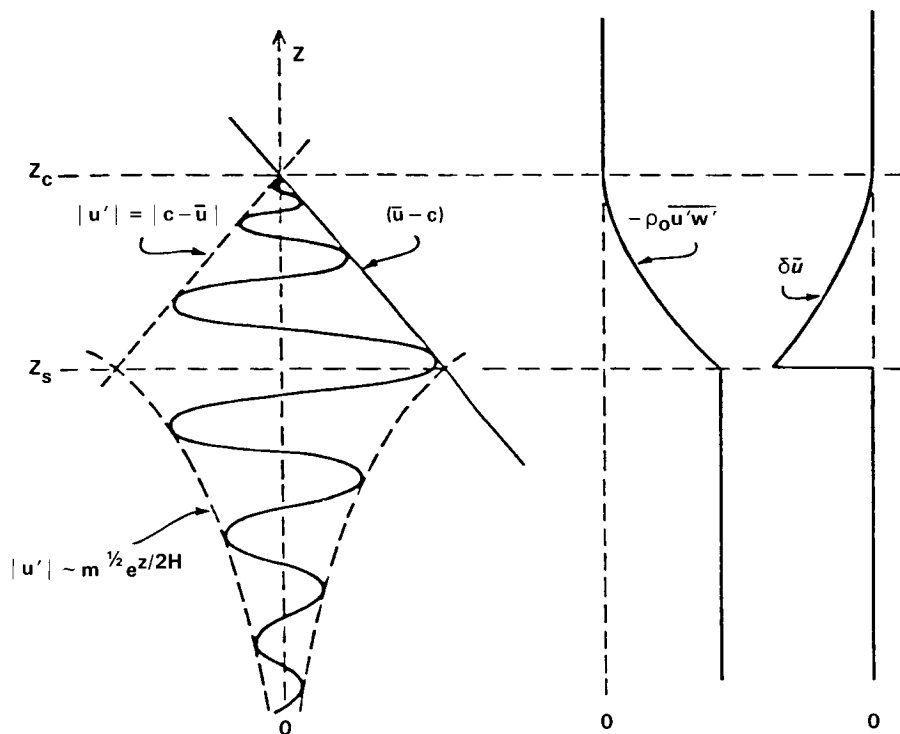


**Figure 6-32.** Schematic of the growth with height and saturation of a gravity wave due to convective instability. Wave damping produces both a divergence of the vertical flux of horizontal momentum and an acceleration of the mean flow toward the phase speed of the wave. Deceleration and diffusion cease above the critical level ( $z = z_c$ ) in the linear theory. [After Fritts, 1984].

A simple model of this process was suggested by Lindzen [1981], who estimated the range of zonal phase speeds  $c$  of gravity waves that might be expected to propagate through the mean zonal wind, avoiding absorption at critical levels where  $\bar{u} = c$ , and reach the mesosphere (Figure 6-33). He then used a linear theory to estimate the altitude at which these waves would break and to calculate  $\nabla \cdot \mathbf{F}$  and the diffusion associated with the breaking waves. He found that  $G = \rho_0^{-1} \nabla \cdot \mathbf{F} + X$  could equal several tens of metres per second per day above a "breaking level" in the middle or upper mesosphere. This is of the right order of magnitude to account for the observed departures of the upper mesosphere from its radiatively determined state.

Further work in this area, and application to simple mechanistic models, includes the papers by Matsuno [1982], Holton [1982, 1983], Dunkerton [1982a,b], Weinstock [1982], Schoeberl *et al.* [1983], Holton, and Zhu [1984] and Miyahara [1984]. The mechanistic models have been fairly successful in simulating the observed mean temperature and zonal wind in the upper mesosphere: mean north-south winds also seem to agree reasonably well with the limited number of observations (Section 6.1). The possible importance of the refraction of small-scale waves by planetary waves has also been considered [Dunkerton and Butchart, 1984] as has the possible damping or forcing of planetary waves by gravity waves [Miyahara, 1985; Schoeberl and Strobel, 1984; Holton, 1984].

The development of reliable parameterizations of the mean momentum forcing  $G$  due to mesospheric gravity waves will require an improved understanding of the mechanics of the breaking process and much more observational information on the global morphology of gravity waves in the middle atmosphere. Other wave motions which may contribute to the maintenance of climatological mean departures of  $\bar{T}$

## DYNAMICAL PROCESSES

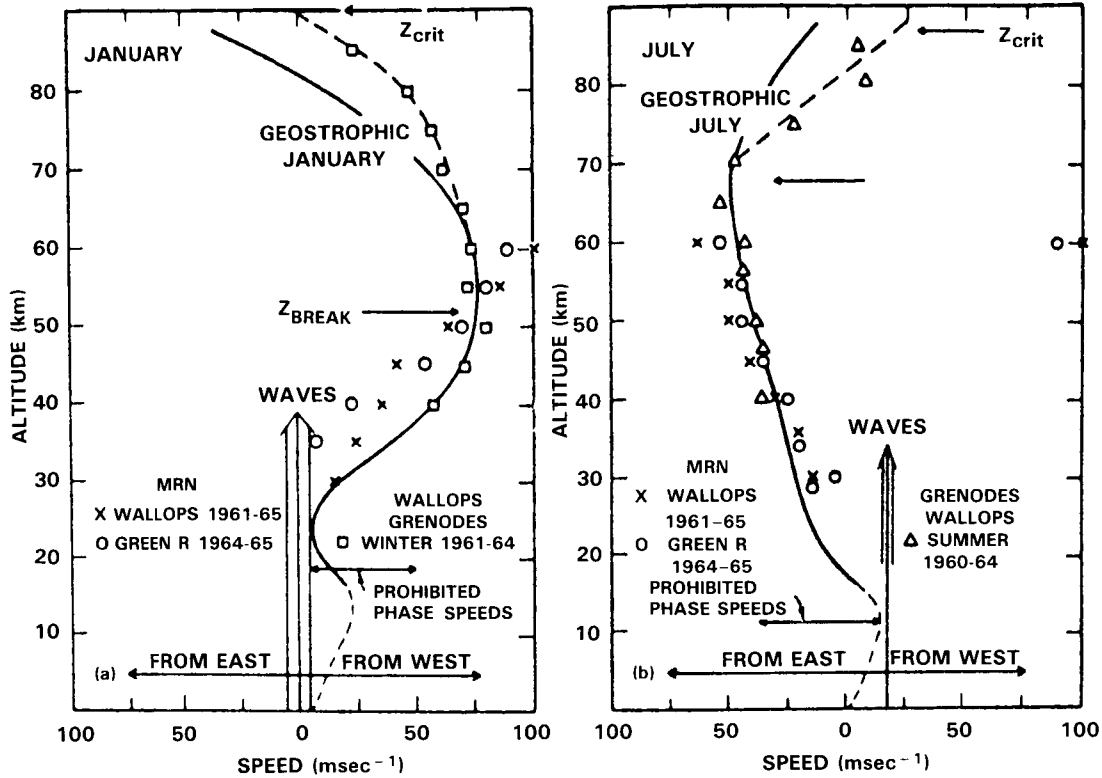


**Figure 6-33.** Profiles of the zonal wind as a function of height at mid-latitudes for winter and summer and the permitted and prohibited phase speeds for tropospheric gravity waves reaching the mesosphere. [After Lindzen, 1981].

from  $T_r$  include atmospheric tides, which may also break in the mesosphere and could contribute to G below and above their breaking altitudes [Lindzen, 1981; Hamilton, 1981a; Miyahara, 1984]. Gravity waves may perhaps break under some circumstances in the stratosphere and lower mesosphere, and may make some significant contributions to G at these levels [Hamilton, 1983a].

### 6.2.5 Stratospheric Sudden Warmings

The stratospheric sudden warming is a spectacular phenomenon which is observed to occur in certain northern hemisphere winters; a "major" warming occurs roughly every second year. It is manifested by a breakdown and (often) reversal of the basic zonal-mean polar westerly vortex, accompanied by a rapid rise in temperature in the stratospheric polar cap. Minor warmings of lesser amplitude occur more frequently in both hemispheres during their respective winters. In a sense, the major warming is just a large-amplitude example of a fairly frequent event. The advent of satellite measurements and the development of numerical models of the middle atmosphere have contributed enormously to our knowledge of sudden warmings. Recent reviews of the phenomenon include those by Labitzke [1981] (dealing mostly with observations) and McIntyre [1982] (dealing mostly with theory).

There is now little doubt that sudden warmings are intimately linked with the propagation from the troposphere into the stratosphere of some form of large-amplitude planetary-wave disturbance (indeed, there appears to be an association between major warmings and large-amplitude blocking events in the

troposphere). This kind of dynamical mechanism was originally proposed by Matsuno [1971], although some of the details of his hypothesis have since required modification. A standard procedure for investigating observed and modeled sudden warmings has been to split each variable into a zonal-mean and an ‘‘eddy’’ part, and to study the resulting wave, mean-flow interaction [e.g., Dunkerton *et al.*, 1981; Palmer, 1981a,b; Butchart *et al.*, 1982; O’Neill and Youngblut, 1982; Simmons and Struening, 1983]. In this case, theory of the type introduced in Sections 6.2.2 and 6.2.3 is helpful: thus the EP vector  $\underline{F}$  can be regarded as giving an indication of the direction of propagation of the planetary waves through the existing mean flow structure. Under normal climatological conditions a cross-section showing the direction of  $\underline{F}$  at various points in the meridional plane [Hamilton, 1982b; Geller *et al.*, 1983] suggests a general propagation of planetary waves from the mid- and high-latitude troposphere up into the stratosphere, followed by a tendency for such waves to propagate equatorwards (see Figure 6-34).

There is evidence, however, that this tendency reverses prior to sudden warmings, with  $\underline{F}$  being refracted poleward, causing some focusing of the waves into the high-altitude polar cap (see Figure 6-35). This may be due to refraction of the waves by a changing mean flow structure, although similar effects can be produced independent of mean flow changes by interference between stationary and transient waves (see Section 6.1.4). Whatever the cause, there are good theoretical grounds to believe that this ‘‘focusing’’ is an important precursor to the subsequent polar warming.

The effect of the mean flow of such focusing can be investigated with Equations (1a,b,c,d). In spherical coordinates, (1a) is replaced by:

$$\frac{\partial \bar{u}}{\partial t} - 2\Omega \sin \phi \bar{v}_* = \frac{1}{\rho_0 a \cos \phi} \nabla \cdot \underline{F} \tag{12}$$

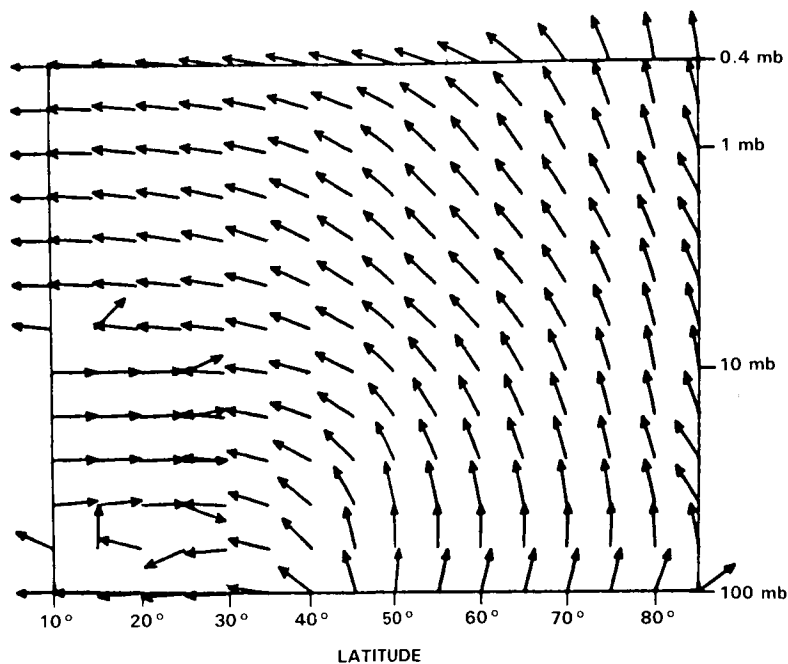


**Figure 6-34.** The climatological January-mean directions of the geostrophic Eliassen-Palm flux  $\underline{F}$ , defined by equation (3), at various latitudes and heights in the northern hemisphere, based on four years of stratospheric data. [From Hamilton, 1982b].

## DYNAMICAL PROCESSES

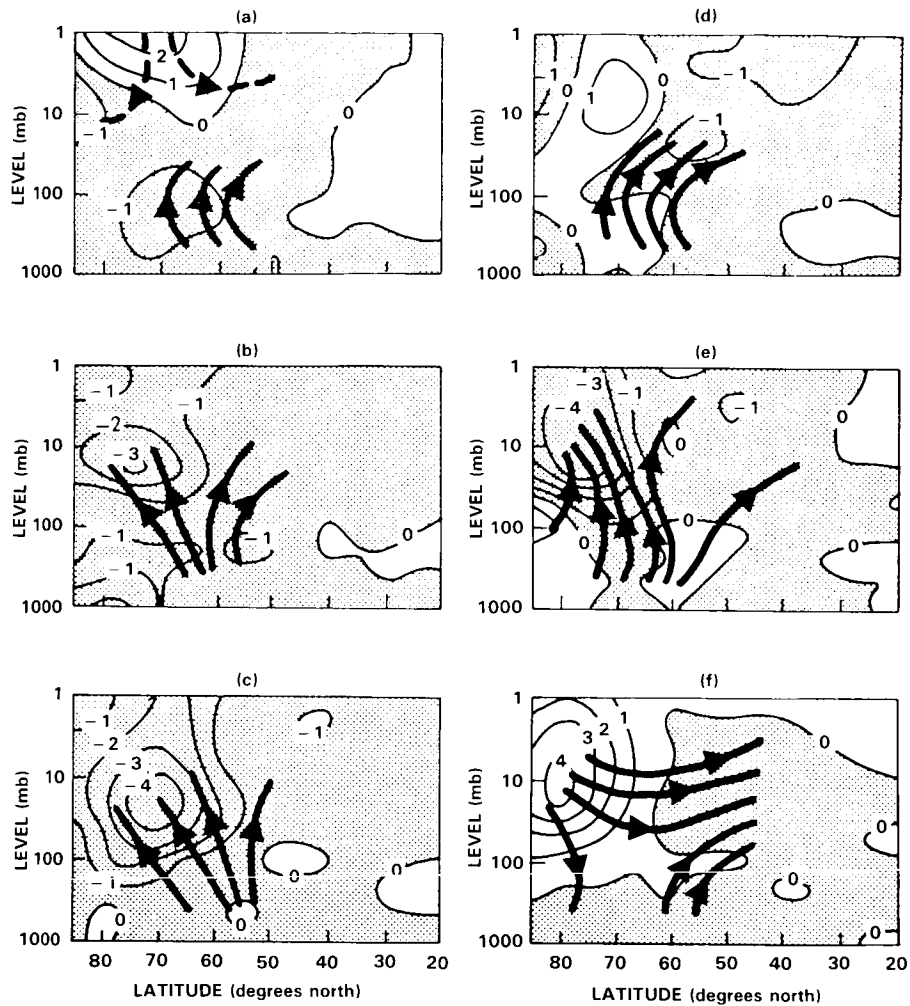


**Figure 6-35.** “Integral curves” giving the local direction of  $\underline{F}$ , and contours of  $(\rho_0 a \cos \phi)^{-1} \nabla \cdot \underline{F}$  labelled in units of  $10^{-4} \text{ ms}^{-2}$  (negative values stippled) for several days in February 1979; (a) 17th, (b) 19th, (c) 21st, (d) 23rd, (e) 26th, (f) 28th. (Dashed integral curves are dominated by zonal wavenumber 1 disturbances; full integral curves are dominated by wavenumber 2). [From Palmer, 1981a].

(neglecting  $\bar{X}$ ), where  $\phi$  is latitude and  $\Omega$  and  $a$  are the earth’s rotation rate and radius, respectively. If waves are transient, nonconservative or nonlinear, then significant values of  $\nabla \cdot \underline{F}$  are expected, by Equation (11). The “transience” contribution ( $-\partial A/\partial t$ ) to  $\nabla \cdot \underline{F}$  (and also possibly the dissipation contribution  $D$ ) will be negative as waves first penetrate into the high polar cap and, while there is no simple way of estimating the nonlinear contribution, model calculations and observational data show that the net result of all these processes is to produce a negative  $\nabla \cdot \underline{F}$  there (see Figure 6-35). The effect of this negative forcing on the right of (12) will be enhanced by the small values of  $\rho_0$  and  $\cos \phi$  in the high-altitude polar regions. Consideration of a full set of equations analogous to (1) shows that this large negative zonal force leads to a rapid deceleration ( $\partial \bar{u}/\partial t < 0$ ), despite the mitigating effect of the Coriolis term  $2\Omega \sin \phi \bar{v}_*$ . By thermal-wind balance this deceleration is associated with a rapid rise in temperature, as observed in the sudden warming. In terms of the thermodynamic equation (1b) we find  $\partial \bar{T}/\partial t = -N^2 H \bar{w}_*/R > 0$ , with  $\bar{J}$  negligible on the timescale of the warming: thus the temperature increase is associated with a residual mean descent ( $\bar{w}_* < 0$ ), although the Eulerian-mean vertical velocity  $\bar{w}$  is often found to be positive. It

is observed that air parcels are descending, on average, too [Mahlman, 1969b; Dunkerton *et al.*, 1981]. (But note that  $\bar{w}_*$  is not generally equal to the Lagrangian-mean vertical velocity during transient wave events).

This description of sudden warmings leaves a number of questions to be answered. First, how important are changes in the mean flow structure in favoring focusing of planetary waves into the polar cap, and how do these changes arise? Such "preconditioning" appears in some (but not all) cases to be due to an earlier wave event. Second, what is the cause of the anomalous amplification of planetary wave activity? It may be a result of as yet poorly understood processes in the troposphere; other possibilities are near-resonance of the stationary waves [Tung and Lindzen, 1979], which may even be self-induced by nonlinear "self-tuning" [Plumb, 1981], or constructive interference between stationary and traveling wave components.

Very recent studies suggest that for some planetary-wave events, especially those of large amplitude, the separation into zonal mean and eddy parts may be an unnecessarily complicated way of viewing the dynamics and may perhaps give misleading impressions of causality [see Clough *et al.*, 1985]. As an alternative, the use of isentropic potential vorticity maps (Hoskins *et al.*, 1985; see Sections 6.2.4 and 6.4.4) may provide a simpler method of analysing sudden warmings and other transient phenomena involving large departures from a zonally-symmetric state. However, a body of theory, comparable to that described above for the "zonal-mean, eddy" separation, and capable of showing how to analyse such maps in a quantitative way, has yet to be developed.

### 6.2.6 The Non-Zonally-Averaged Climatological State

In Sections 6.2.2-6.2.4 the maintenance of the climatological *zonal-mean* state of the middle atmosphere was discussed. A rather different process will be briefly considered in this section, namely the control of the climatological state in which the zonal mean is not taken. This question needs to be looked at in a different way, since the time-mean state now contains stationary (or quasi-stationary) planetary-wave deviations from zonal symmetry. These "stationary eddies" were included among those wave motions which were invoked to explain departures of the zonal-mean climatology from a radiatively-determined state.

The discussion of the maintenance of a zonally-asymmetric time-mean state is hampered by the lack, at present, of a comprehensive theoretical framework for the dynamical evaluation and interpretation of the processes involved. As in the zonal-mean case, one must not give too much weight to naive physical interpretations of the various terms in the time-averaged equations of motion. However, some general qualitative remarks can be made. In the first place, monthly-mean climatological data would presumably be zonally-symmetric in an idealized atmosphere whose lower boundary contained no zonal asymmetries, since any traveling-wave structures would tend to be removed by the climatological time-averaging and the phases of any disturbances that happened to be stationary would tend to be randomly distributed in longitude. It thus follows that any zonal asymmetries in the climatological fields will be linked in some way with zonal asymmetries in the earth's surface.

It is now generally accepted that the observed stationary waves in the *troposphere* are ultimately associated with orography and with thermal aspects of the land-sea difference [e.g., Wallace, 1983; Held, 1983; Donner and Kuo, 1984]. Since stationary disturbances of the longest wavelengths can propagate from the troposphere into the stratosphere in the winter hemisphere [Charney and Drazin, 1961], it is to be expected that some, at least, of the climatological zonal asymmetries in the middle atmosphere can be attributed to the orographic and thermal forcing in the troposphere. This expectation is partly confirmed by studies with numerical models of linear stationary waves in climatological zonal-mean states. Some of these [e.g., Matsuno, 1970; Schoeberl and Geller, 1977] impose as a lower boundary condition an observed monthly-mean geopotential height field in the middle or upper troposphere (without enquir-

## DYNAMICAL PROCESSES

ing into the precise cause of this field) and compute the linearized response of the stratosphere and mesosphere. These models have achieved a fair degree of success in simulating observed monthly-mean zonally-asymmetric fields in the middle atmosphere. Others [e.g., Lin, 1982; Alpert *et al.*, 1983] include details of the tropospheric forcing as well; in this case it appears to be more difficult to achieve a satisfactory simulation of stationary waves in the middle atmosphere. This reflects our poor understanding of the forcing of the stationary waves. One possibly important failing of such linear models may be the neglect of the time-averaged nonlinear effects of "transient eddies" (departures from the monthly-mean fields) on the stationary eddies. Given some basic flow that is zonally asymmetric (perhaps because of the influence of tropospheric thermal or orographic forcing) these transient eddies may help to enhance, or alternatively diminish, the zonal asymmetry. Recent studies [e.g., Hoskins, 1983] suggest that these effects may be important in the troposphere; whether they also take place to a significant degree in the middle atmosphere has not yet been investigated.

### 6.2.7 Theory of the Low-Latitude Zonal-Mean Circulation

It was mentioned in Section 6.1 that zonal-mean circulation of the equatorial middle atmosphere is dominated by long-period variations, namely the quasi-biennial oscillation (QBO) and semi-annual oscillation (SAO), rather than the annual cycle that predominates in extra-tropical regions. What makes the dynamics of these low-latitude zonal circulations so intriguing and so different from those of high latitudes is that while the latter are qualitatively similar to those expected on the basis of a simple atmospheric response to seasonal thermal driving, albeit with sometimes dramatic modulations induced by tropospheric-forced eddy activity, the former appear to be dependent on eddy transport in a more fundamental way. A major clue that this is so comes from the observation of strong equatorial westerlies during the westerly phases of both the QBO and the SAO. Since inviscid zonally symmetric circulations conserve absolute angular momentum, they would inevitably tend to drive easterlies at the equator by bringing in air of relatively low absolute angular momentum from higher latitudes; therefore zonally asymmetric eddies are required to achieve the implied angular momentum transport. The major eddy motions observed in the tropical middle atmosphere and described in Section 6.1.5 are depicted schematically in Figure 6-36. Of these, only the equatorial Kelvin waves appear capable of transporting westerly momentum into the equatorial stratosphere and it therefore seems clear these motions must be responsible for the westerly phase of the QBO and of the stratopause SAO.

In fact, it is now believed that *both* westerly and easterly phases of the QBO are wave-driven. This belief stems from a suggestion of Lindzen and Holton [1968], updated by Holton and Lindzen [1972], that the QBO results from an interplay between westerly forcing by slow equatorial Kelvin waves and easterly forcing by mixed Rossby-gravity waves, both of which dissipate (and therefore interact with the mean flow) primarily in the lower stratosphere. Their theory, which was discussed further by Plumb [1977] and is reviewed in Plumb [1984], predicts well the major features of the observed time/height structure of the QBO (Figure 6-37; cf. Figure 6-28) and was further supported by the generation of an analogous oscillation in a laboratory experiment of Plumb and McEwan [1978] and by an analysis of the observed momentum budget of the equatorial lower stratosphere [Lindzen and Tsay, 1975]. Therefore the Holton-Lindzen theory has become widely accepted; a few modifications have been proposed, perhaps the most substantial of which is the suggestion of Dunkerton [1983a] (see also Dickinson [1968] and Andrews and McIntyre [1976]) that lateral momentum transport by the quasi-stationary planetary waves of the winter hemisphere may contribute substantially to the driving of the easterly regime.

The thermal structure of the QBO and, correspondingly, the associated (Lagrangian-mean) meridional circulation were investigated in a two-dimensional model by Plumb and Bell [1982]. Their results, depicted

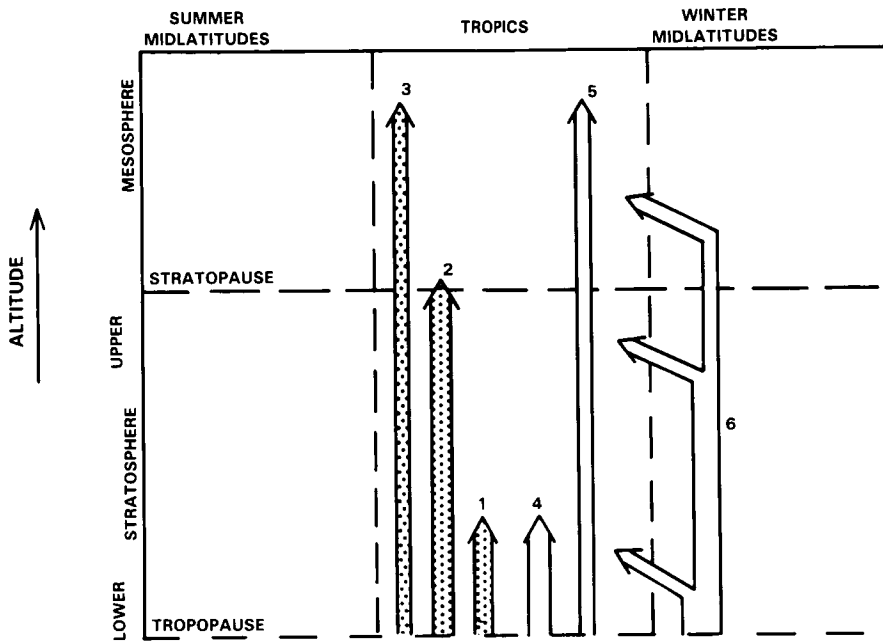


**Figure 6-36.** Schematic illustration of the propagation of wave motions into the tropical stratosphere and mesosphere. Arrows terminate where waves dissipate and interact with the mean flow. Stippled arrows (open arrows) represent waves which produce an effective westerly (easterly) force on the flow in these regions. 1. Slow Kelvin waves, 2. Fast Kelvin waves, 3. Ultra-fast Kelvin waves and internal gravity waves, 4. Mixed Rossby-gravity waves, 5. Internal gravity waves and tides, 6. Quasi-stationary planetary waves.

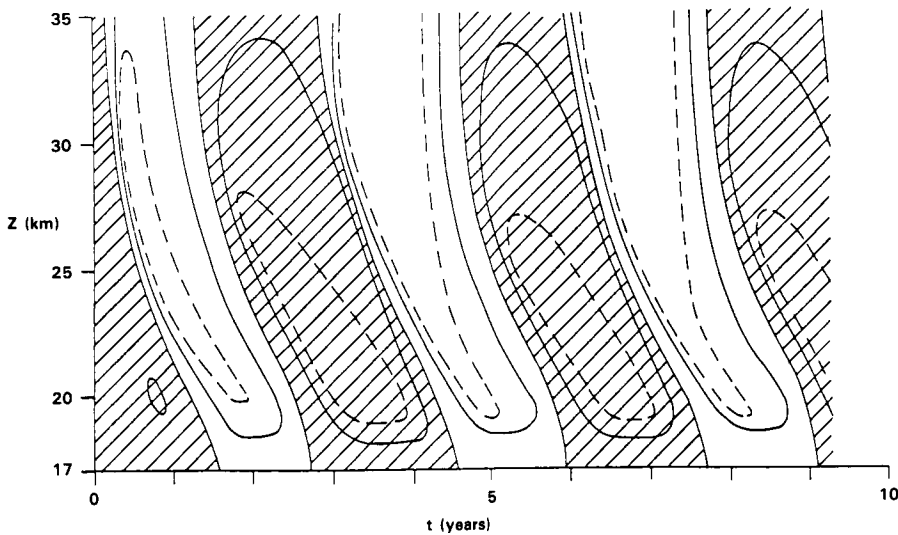


**Figure 6-37.** Theoretical evolution of mean zonal flow  $\bar{u}$  at the equator according to the Holton-Lindzen model. Solid contours are at intervals of  $15 \text{ ms}^{-1}$ , dashed contours represent  $\pm 22.5 \text{ ms}^{-1}$ . Westerlies are shaded. [After Plumb, 1977].

## DYNAMICAL PROCESSES

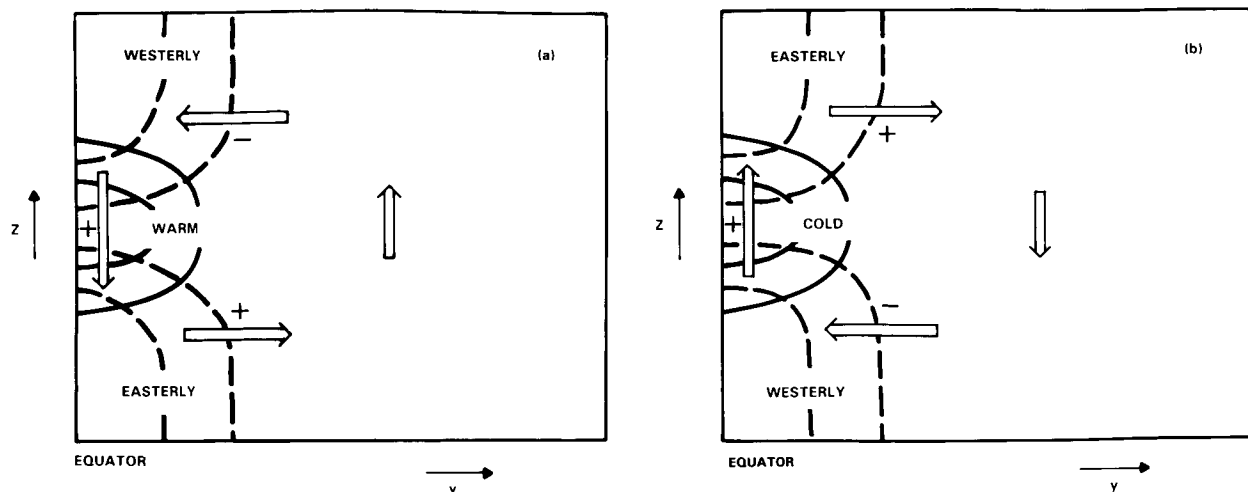


**Figure 6-38.** Schematic representation of the mean meridional circulation driven by an equatorial thermal anomaly, and the consequent acceleration of the mean zonal wind. Solid contours: Potential isotherms. Dashed contours: Isopleths of zonal velocity.  $\pm$  Sign of zonal acceleration. (a) Warm anomaly, (b) Cold anomaly. [After Plumb and Bell, 1982].

schematically in Figure 6-38, show the meridional circulation to be an important determinant of the structure of the zonal wind QBO. Advection by this meridional circulation is also likely to contribute to trace species transport in low latitudes; Hasebe [1984] and Ling and London [1985] have discussed this in the context of the QBO in total ozone.

The driving of the SAO is in some ways similar to that of the QBO. The westerly SAO regime at the stratopause again appears to be driven by Kelvin waves, as suggested by Holton [1975], Hirota [1978] and Dunkerton [1979]; the fast Kelvin waves described in Section 6.1.5 propagate to these levels where they are observed to be of sufficiently large amplitude to account for the observed westerly accelerations [Coy and Hitchman, 1984]. Unlike the QBO, however, the easterly phase of the stratopause SAO appears to be driven not by equatorial waves but by the effects of the seasonal meridional circulation [Holton and Wehrbein, 1980b; Mahlman and Sinclair, 1980; Takahashi, 1984] or planetary waves propagating from the winter hemisphere [Hopkins, 1975; Dunkerton, 1979]. Indeed, on the basis of a successful simulation of the stratopause SAO in the GFDL "SKYHI" model, Mahlman and Umscheid [1984] concluded that both effects are important in producing the observed structure. Note that the periodicity of the SAO is thus externally imposed by the semiannual variability of mean angular momentum advection and planetary wave circulations in the tropics, whereas that of the QBO is internal to the dynamics of the wave mean-flow interaction [Plumb, 1977].

The mesopause SAO has been explained by Dunkerton [1982b] as a secondary phenomenon, produced as a "shadow" of the stratopause oscillation. He suggested that selective absorption of vertically-propagating internal gravity waves through the stratopause region so modulates the spectrum of waves propagating to higher levels as to force an oscillation of opposite sign to that at the stratopause. As yet there is no direct evidence to support this prediction.

## 6.3 MIDDLE ATMOSPHERE GENERAL CIRCULATION MODELS

### 6.3.1. Introduction

Quantitative assessment of our understanding of the middle atmosphere circulation relies on numerical models of varying degrees of complexity. These range from highly simplified models such as radiative-convective models (which neglect dynamics) through so-called "mechanistic" dynamical models (which neglect radiative effects, or represent them in a very crude fashion) to general circulation models (GCMs) which are defined here, following Mahlman and Umscheid [1984], as models which aim to include all major physical processes in a self-consistent manner. However, at present no models fully meet this criterion. While most GCMs use similar radiation schemes, for example, the manner in which momentum transfer by small-scale motions is parameterized ranges from very crude forms such as Rayleigh friction to more sophisticated schemes which are nonetheless highly simplified representations of a very complex process. Mahlman and Umscheid [1984] have pointed out that the important differences between GCMs and "mechanistic" models of the middle atmosphere relate to the inclusion of realistic radiative transfer (i.e., the radiative transfer should agree well with modern line-by-line calculations), a self-determined troposphere (including moist convection effects) and, perhaps, a "sufficient" model spatial resolution. Following the discussion of Section 6.2, it is clear that one of the major scientific challenges is the explanation of the maintenance of the observed large departures from radiative equilibrium in the mesosphere and in the winter stratosphere. It is therefore of particular importance that radiative processes which, in the absence of dynamical effects, would drive the system back to radiative equilibrium be represented as accurately as possible.

Given the fact that GCMs are typically much more expensive to run than are "mechanistic" models, it is important to note for which types of middle atmosphere scientific problems mechanistic models are appropriate and for which classes of problems GCMs are appropriate. Mechanistic models can be used to test specific physical hypotheses. For example, Matsuno's [1971] classic paper used such a model to illustrate the role of stationary planetary waves in giving rise to sudden stratospheric warmings. Such mechanistic studies focus on limited aspects of a problem and leave other aspects unaddressed. For instance, in Matsuno's model, the question of what gives rise to the tropospheric planetary wave activity or the basic state zonal wind in the first place is not addressed. However, the role of radiation in preventing such warmings from taking place in the real atmosphere is severely underestimated in such models. GCM experiments can be used to address these points.

One difficulty with the use of GCMs is associated with their large amount of output. The volume that emerges from a GCM integration is comparable to that of an atmospheric data set (and can even be greater depending on the frequency at which it is retained). This makes diagnostic studies of GCM behavior a formidable task. Moreover, the multiplicity of physical effects in a GCM, compared with a mechanistic model, makes GCM results sometimes difficult to interpret. Given these circumstances, both GCMs and mechanistic models need to be used cooperatively in middle atmosphere studies.

GCMs are very useful in studying the coupling of middle atmosphere dynamics with radiative and chemical processes. Examples are studies of the coupling of middle atmosphere dynamics with radiation by Ramanathan *et al.* [1983] and of the coupling of dynamics with chemical processes by Mahlman *et al.* [1980].

Tropospheric GCMs have also been used to examine the sensitivity of tropospheric climate and/or weather forecasting to inclusion of the middle atmosphere. Simmons and Struening [1983] have looked

## DYNAMICAL PROCESSES

at the sensitivity of tropospheric weather forecasts to extending the top of the European Centre for Medium-Range Weather Forecasting model from 50 to 10 mb and using a hybrid vertical coordinate system instead of sigma coordinates. Mechoso *et al.* [1982] used the UCLA GCM to study the sensitivity of numerical forecasts to moving the top level of the model from the lower stratosphere to the stratopause.

Middle atmosphere GCMs can also be used to understand the limitations of more simplified models or to develop more proper parameterizations for such models. For instance, Mahlman [1975] and Tuck [1979] have used tracer transport experiments with GCMs to study some of the shortcomings of simplified transport formulations commonly used in one- and two-dimensional photochemical models. Plumb and Mahlman [1985] have used tracer transport experiments with GCMs to establish the formulation of transport for two-dimensional photochemical models on a firmer physical basis.

GCM results can also be used as proxy for atmospheric data to examine the representativeness of present observational networks as well as to look at the impact of proposed future systems. Moxim and Mahlman [1980] have used the results of GCM transport studies to look at the representativeness of globally averaged ozone amounts that are inferred from the ground-based ozone network.

Middle atmosphere GCMs are just beginning to be used in the analysis of satellite data. Such forecast-analysis methods are already used extensively for tropospheric studies [e.g., McPherson *et al.*, 1979]. In this system, data are analyzed, a forecast is run, and the results of the forecast are used to help in the analysis at a later time. The cycle is then repeated. This type of analysis yields a complete data set, constrained by all available observations, that is dynamically and energetically consistent with the GCM formulation. Stratospheric forecast-analysis methods are now beginning to be applied to stratospheric satellite data by the British Meteorological Office and by groups in the United States.

### 6.3.2. Current Status of Middle Atmosphere GCMs

GCMs have modeled several aspects of observed middle atmosphere structure. In the following, we will look into some of the contributions of GCMs to our understanding of middle atmospheric behavior. We will also look at some model shortcomings. In this discussion, we shall confine attention to model studies for which the upper model boundary is at the stratopause or above.

#### a) Climatology

Several recent middle atmosphere GCMs have appeared recently in the published literature. These include the model results presented by Schlesinger and Mintz [1979], Hunt [1981], O'Neill *et al.* [1982], Mahlman and Umscheid [1984], and Rind *et al.* [1985]. A typical deficiency that appears in most middle atmosphere GCM results is that of excessive winter westerly and summer easterly zonal winds together with excessively cold winter polar temperatures as required by thermal wind balance. Figure 6-39 gives examples of these results from the works of Schlesinger and Mintz [1979], Hunt [1981], Mahlman and Umscheid [1984], and Rind *et al.* [1985]. All four of these results are for the month of January although Schlesinger and Mintz' and Hunt's result are for perpetual January integrations while the Mahlman and Umscheid and Rind *et al.* results are from annual cycle integrations. The four results shown in Figure 6-39 all use different formulations for radiative transfer as well as different parameterizations for the diffusion and drag resulting from subgrid scale processes. Nevertheless, certain features are found to be common to all of these results. All four simulations give middle atmosphere winter hemisphere westerlies and summer hemisphere easterlies as are observed. However, all have winter westerlies too strong compared to

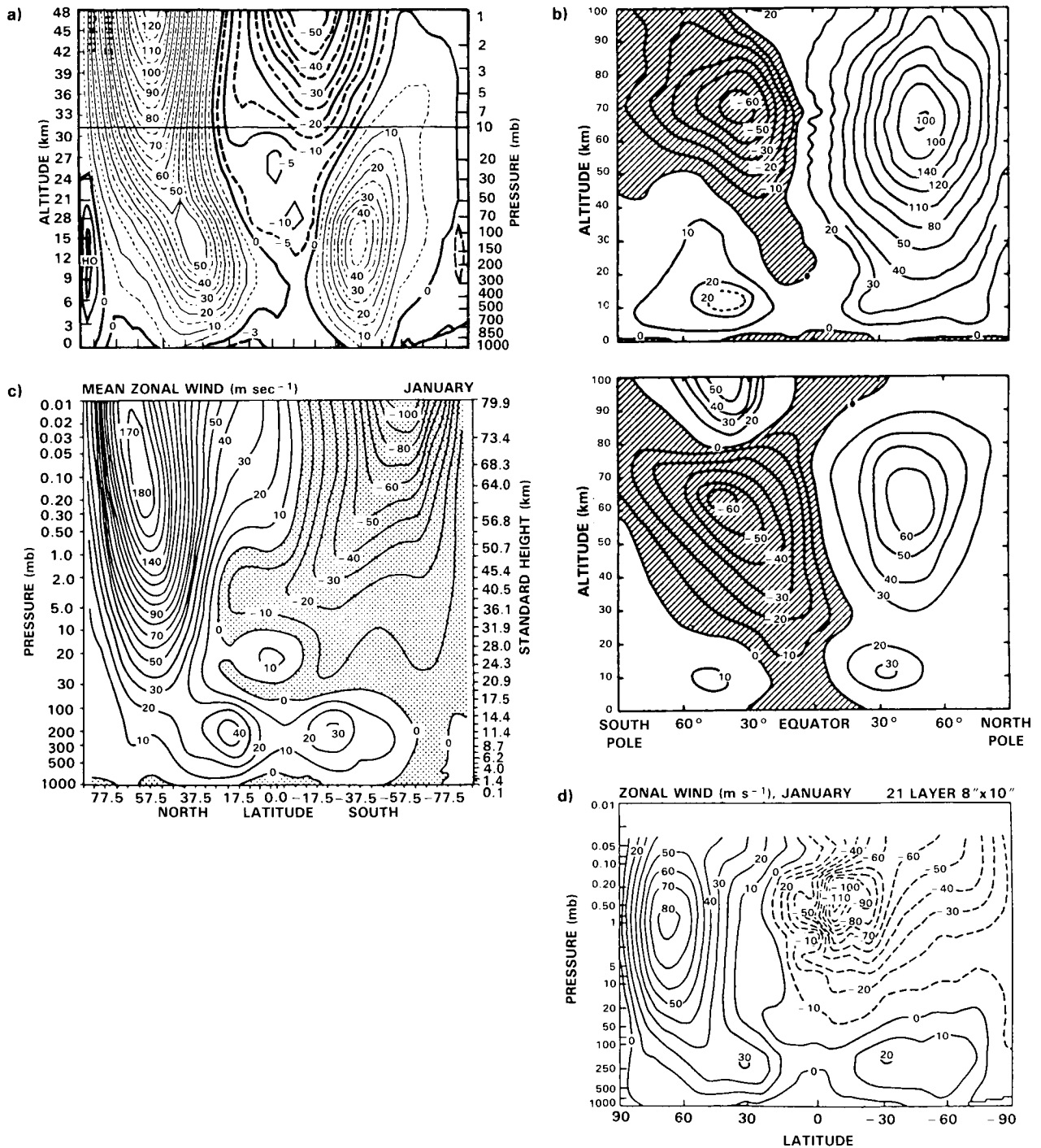


**Figure 6-39.** (a) Mean zonal wind in m/s as modeled with perpetual January insolation by Schlesinger and Mintz [1979]

(b) Mean zonal wind in m/s as modeled with perpetual January insolation by Hunt [1981] in top panel and "observed" mean zonal wind for Northern Hemisphere January and July conditions from Newell [1968] in bottom panel

(c) Mean zonal wind for January from the model of Mahlman and Umscheid [1984]

(d) Mean zonal wind for January from the model of Rind *et al.* [1985].

## DYNAMICAL PROCESSES

observations. One way to see this is to compare the maximum westerly wind values at 10 mb (about 30 km) in the three simulation results with observations. In the results of Schlesinger and Mintz, Hunt, and Mahlman and Umscheid, the maximum westerly wind at 10 mb is about  $70 \text{ ms}^{-1}$ . Rind *et al.*'s maximum westerly wind at 10 mb is about  $60 \text{ ms}^{-1}$ . For comparison, we see that the "observations" show maximum westerly wind values at 10 mb of about  $20 \text{ ms}^{-1}$ . (More recent analysis of a four year data set by Geller *et al.* [1984] indicates maximum mean January winds at 10 mb in the Northern Hemisphere ranging from about 30 to  $50 \text{ ms}^{-1}$ ).

We see then that all middle atmospheric GCMs (given our definition that GCMs must include proper radiative transfer calculations) give excessive winter westerlies. Mahlman and Umscheid [1984] discussed extensively this aspect of the behavior of the GFDL SKYHI model and attributed this problem to a combination of underestimation of the upward flux of planetary waves out of the troposphere and the neglect of the effects of small-scale gravity waves in their model.

### b) Perturbation Studies

Middle atmospheric GCMs have also been used to test for their response to imposed perturbations. Fels *et al.* [1980] investigated the effects of doubling  $\text{CO}_2$  and halving  $\text{O}_3$  in a low resolution model extending up to about 80 km with annual average insolation and boundary conditions. Figure 6-40 shows their modeled zonally averaged temperatures for the control (unperturbed) case and for the doubled  $\text{CO}_2$  and halved  $\text{O}_3$  cases. They found for the doubled  $\text{CO}_2$  case that the resulting middle atmosphere cooling was quite independent of latitude; little change was found therefore in the mean zonal wind. The halved  $\text{O}_3$  case gave much more latitudinal structure in the cooling and consequently a much greater effect on the mean zonal flow, mostly above 30 km. No significant changes in tropospheric planetary wave structure were found in either of the perturbation experiments. This last result is consistent with that found in studies of the effects of middle atmosphere changes on tropospheric planetary waves using simpler mechanistic models [Schoeberl and Strobel, 1978a; and Geller and Alpert, 1980]. One result that did emerge from the Fels *et al.* study that would not have been easy to obtain with a mechanistic model was the sensitivity of the tropical tropopause temperature to the imposed  $\text{O}_3$  changes. The strong cooling found at the tropical tropopause in the halved  $\text{O}_3$  experiment should result in much less stratospheric water vapor by increasing the freezing out of water in the rising branch of the Hadley circulation.

### c) Comparison with Simpler Models

Another application of middle atmosphere GCMs is in comparing the results of full GCMs with more simplified models for the purposes of seeing the limitations of the simpler models and improving their parameterizations. Two examples of this type of application of middle atmospheric GCMs are the works of Fels *et al.* [1980] and Plumb and Mahlman [1985]. Fels *et al.* [1980] used the GFDL SKYHI model to explore the applicability of the simpler Radiative-Convective-Equilibrium (RCE) and Fixed-Dynamical-Heating (FDH) models to the doubled  $\text{CO}_2$  and halved  $\text{O}_3$  experiments that were discussed in the previous section.

The RCE model is one in which the solar heating is taken to balance the long wave cooling at each point in the model except where the computed temperature lapse rate exceeds some critical value, in which case the lapse rate is fixed at this value; the surface temperature is usually calculated self-consistently. Fels *et al.* fixed the surface temperatures, however, so that the response to the imposed perturbation is purely radiative above the convective zone and purely dynamical below.

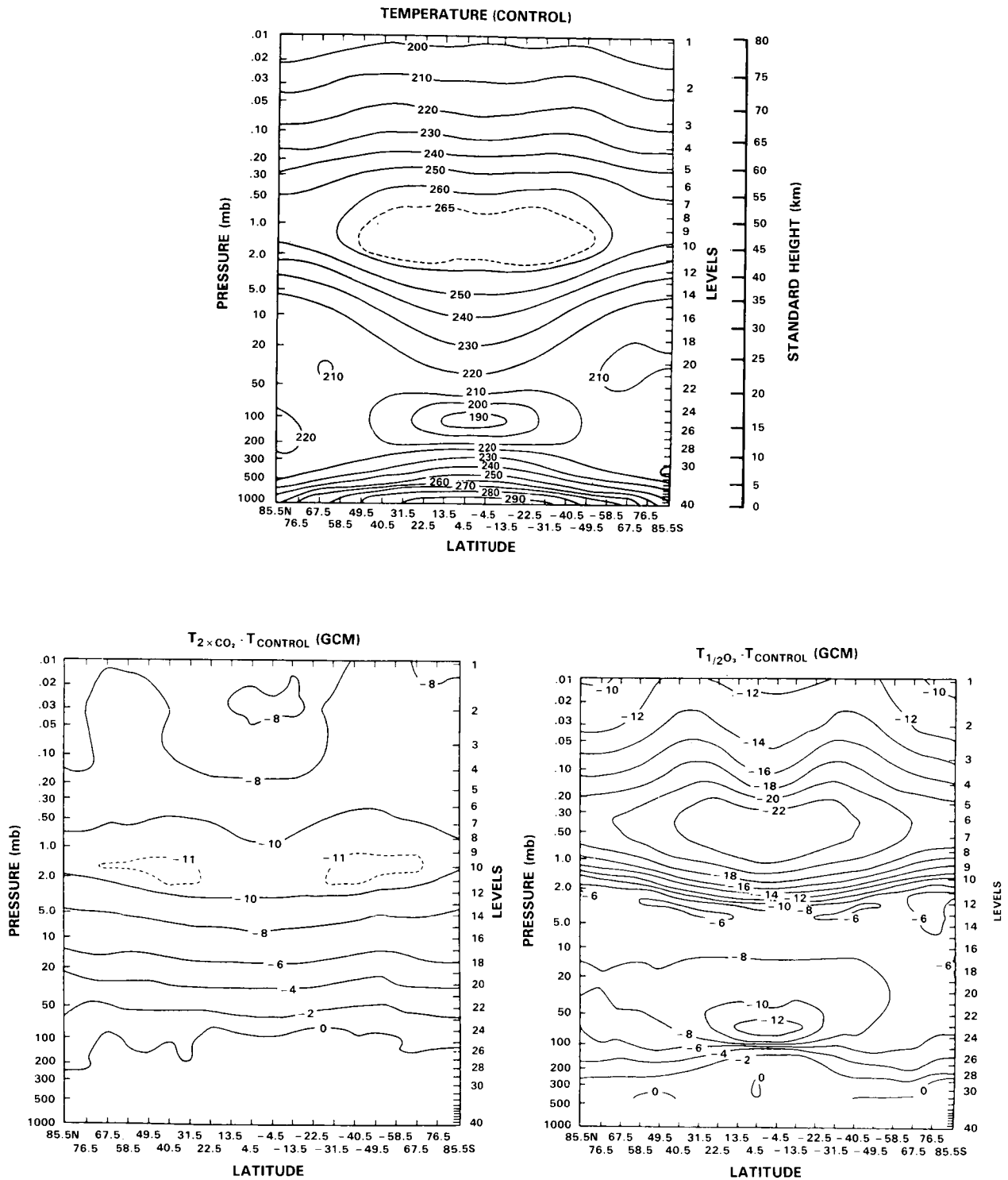


Figure 6-40. (Top) Modeled zonally averaged temperature in degress Kelvin; (lower left) difference between modeled zonally averaged temperatures and those with uniformly doubled CO<sub>2</sub> concentrations; (lower right) difference between modeled zonally averaged temperatures and those with uniformly halved O<sub>3</sub> concentrations. All are general circulation model results from Fels *et al.* [1980].

## DYNAMICAL PROCESSES

The FDH model is one in which the dynamical heating is taken to remain unchanged when the distribution of radiatively active constituents is perturbed. Thus, given Fels *et al.* [1980] GCM results for annual averaged insolation, the equilibrium solution is one where the sum of the solar heating, long wave cooling, and dynamical heating rates are everywhere known and the distribution of dynamical heating rates is easily determined. In performing the perturbation experiments, the new FDH temperature distribution is one for which the new local net radiative heating rate plus the unchanged dynamical heating rate is everywhere zero.

Figure 6-41 shows the RCE and FDH modeled temperature differences for the halved O<sub>3</sub> perturbation experiment. This is to be compared with the full GCM results for this case that were shown in Figure 6-40. From the comparison, we see that above 35 km there is qualitative similarity among all three model results with maximum cooling of 22-25 K near the tropical stratopause; however, larger horizontal gradients in the amount of cooling are seen in the FDH results. Below about 25 km, there are substantial differences among the three results that can be attributed, in part, to the fixed lapse rate constraint in the troposphere and to the different "control" temperature distribution of the RCE model [see Fels *et al.*, 1980]. There is a qualitative difference between the FDH and GCM results in the tropics between about 55 and 75 km where the dynamical cooling has apparently changed in the GCM case. There are also significant differences in the cooling results just above the tropical tropopause among the GCM, RCE, and FDH results. Fels *et al.* point out that this region is particularly sensitive to very small changes in the heating or cooling rates. Quite similar results are obtained in all of the three models (GCM, RCE, and FDH) for the doubled CO<sub>2</sub> case (not shown here). The only very significant difference is in the shape of the perturbation response in the lower stratosphere in the RCE model compared with those of the GCM and FDH models. This is due to the fixed lapse rate constraint in the RCE case. The fact that the FDH model does so well in the doubled CO<sub>2</sub> case is consistent with the rather flat response in the GCM perturbation experiment with latitude. Such a flat response should not produce greatly altered dynamics.

Thus, the Fels *et al.* [1980] investigation showed that for perturbation experiments involving changes of concentrations of long wave radiatively active constituents such as CO<sub>2</sub>, which give a flat distribution of temperature change with latitude, the FDH, and, in fact, the RCE models give fairly good simulations of temperature change. In cases where the altered constituent is a strong solar radiation absorber such as ozone, the GCM gives a temperature response with more latitudinal structure and more altered dynamics. Even in this case, however, the FDH model does well except in the tropical lower stratosphere and mesosphere. Investigations of this type show the utility of middle atmosphere GCMs in seeing the limitations of simpler models.

Plumb and Mahlman [1986] have used the GFDL tracer model (with its top at 10 mb) to investigate better ways in which to parameterize transport in two-dimensional photochemical models. They have derived the two-dimensional transport tensor by performing two transport experiments that allow them to solve for the four components of the "diffusion" tensor. They do this by calculating the zonally-averaged meridional and vertical tracer fluxes in the GCM. This, together with the calculated meridional and vertical gradients of the computed zonally averaged distributions allows solution for the transport tensor. Plumb and Mahlman have used this transport tensor in a two-dimensional model to show that they can mimic reasonably well the zonal average of the three-dimensional transport of the GCM. Thus, they demonstrate an internally consistent manner in which a transport formulation can be developed for two-dimensional models to give equivalent transport to a GCM in a zonally averaged sense. Plumb and Mahlman's GCM study underscores the importance of including consistent advection and diffusion in two-dimensional transport models (see Section 6.5).

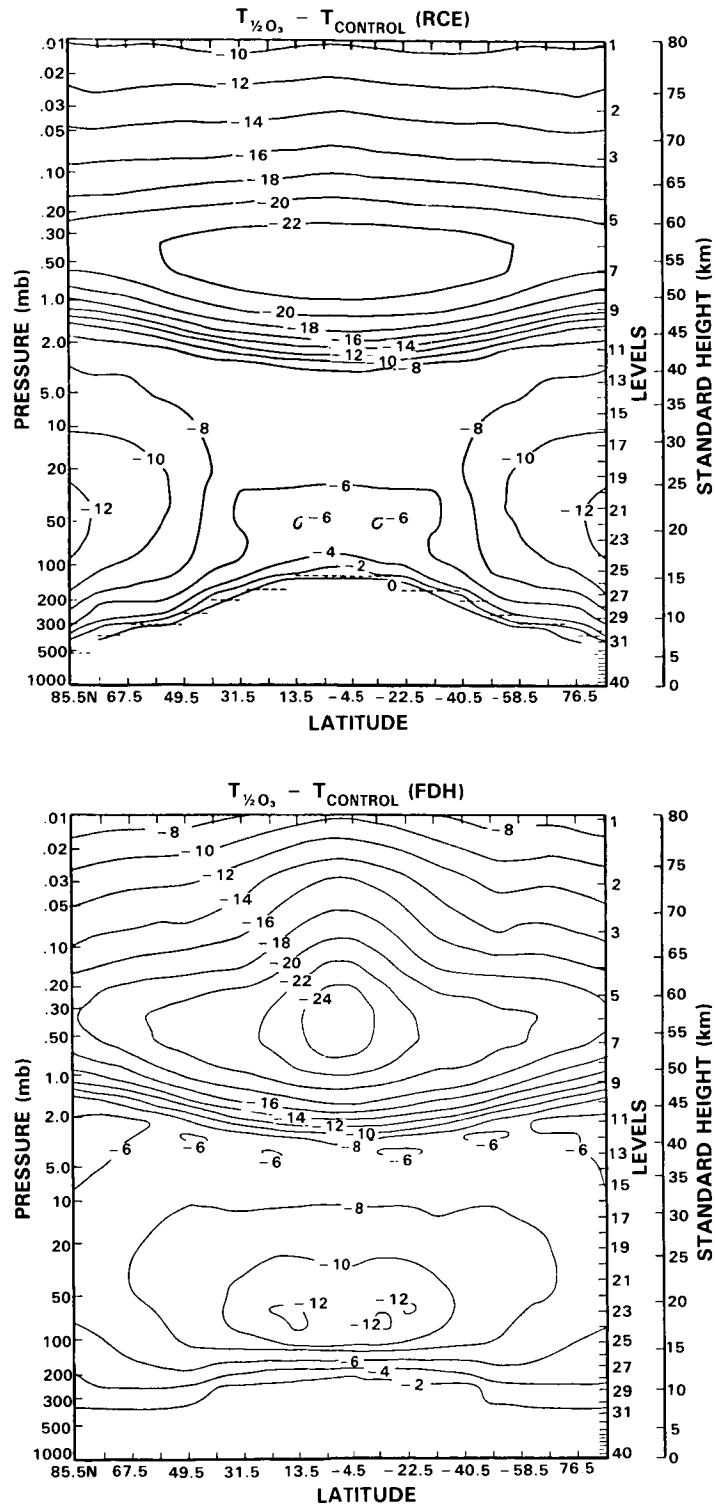


Figure 6-41. Difference in zonally averaged temperatures (in degrees Kelvin) between halved  $O_3$  case and control case using a radiative-convective-equilibrium (RCE) model (top) and fixed-dynamical-heating (FDH) model (bottom). From Fels *et al.* [1980].

## DYNAMICAL PROCESSES

### d) Transport and Photochemistry Studies

Middle atmosphere GCMs have been very useful for studies of transport and photochemistry. Two very different types of studies have been accomplished by the use of marked parcels and by tracer transport formulations, some of which have involved photochemistry while others have not. Examples of middle atmosphere transport studies using marked parcels are those of Kida [1977, 1983a,b], and Hsu [1980]. Examples of transport studies without photochemistry include Mahlman and Moxim [1978] while those with some degree of photochemistry include Cunnold *et al.* [1975, 1980], Mahlman *et al.* [1980], Levy *et al.* [1979], and Golombek [1982].

As examples of these two types of investigations, we will briefly discuss the work of Kida [1983a,b] and Mahlman *et al.* [1980]. Kida used a 12-level hemispheric GCM extending from the ground to 1 mb. Its horizontal grid was 3 degrees of longitude by 2.5 degrees of latitude. It had no topography but did include a parameterization of thermal forcing of planetary waves. Kida examined the very long term motion of air parcels into and out of the stratosphere by performing trajectory analyses on a large number of marked air parcels. In this work, he defined the age of a stratospheric air parcel as the length of time elapsed since the parcel first entered the stratosphere. Figure 6-42 shows parcel age spectra for 5 degree latitude by 1 km altitude domains for three separate latitude bands: 5-10 degrees (tropics), 45-50 degrees

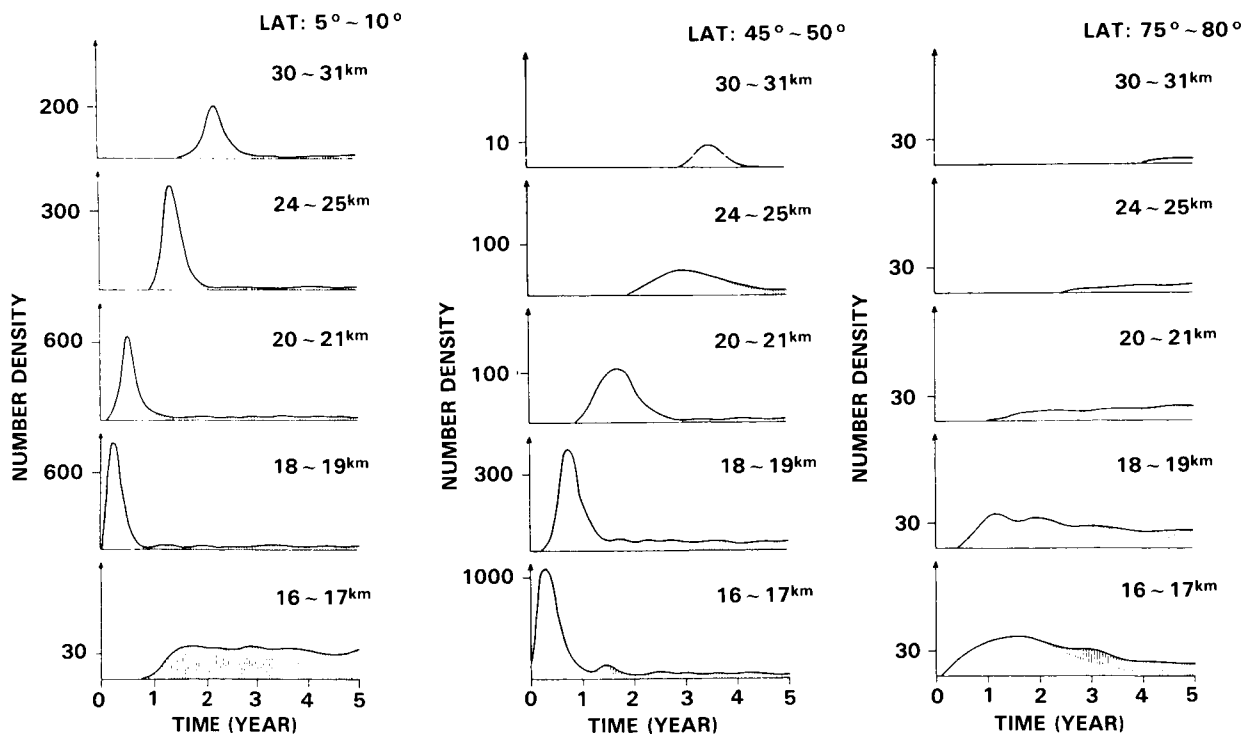


**Figure 6-42.** The age spectrum of air parcels whose initial location was just below the tropical tropopause for selected domains in the lower stratosphere. Left - 5-10 degrees; middle - 45-50 degrees; right - 75-80 degrees. Each domain covers 5 degrees in latitude and 1 km in altitude. Shaded portions are due to parcels that have once entered the troposphere and, after a long time, re-entered the stratosphere or remained in the troposphere. From Kida [1983b].

(mid-latitudes), and 75-80 degrees (polar latitudes). These are given for five altitude ranges. At the start of this experiment, the parcels are all located just beneath the tropical tropopause. In the tropics, the tropopause altitude is about 17 km, so we may interpret the age spectra as showing strongly peaked distributions above the tropopause with the peak in age spectra occurring at later times at increasing altitude consistent with the speed of the rising motion in the Hadley circulation of  $\sim 5$  km/year. Below the tropopause, the distribution is flat indicating that after about a year the marked parcels start reentering the troposphere and build up to a steady state number density. At middle latitudes, one sees less sharp stratospheric distribution peaks than was the case for the tropics. The broader peak in the age spectra at longer times with increasing altitude indicates that it has taken longer for stratospheric air parcels to reach these higher altitudes and that the trajectories taken are more diverse. Note that all five altitudes are in the stratosphere at middle latitudes. Finally, the high latitudes have very flat distributions indicating that it takes a long time for "new" stratospheric air parcels to reach the polar stratosphere, and that the trajectories followed by these polar stratospheric air parcels were very diverse.

Another very different use of a middle atmospheric GCM in investigating transport and photochemistry is that of Mahlman *et al.* [1980] who used the GFDL 11-level tracer model [see Manabe and Mahlman, 1976 and Mahlman and Moxim, 1978] for two idealized ozone experiments. The first of these experiments, the Stratified Tracer Experiment, specified instant relaxation of the ozone concentration at the top level (10 mb) to 7.5 ppmv. Ozone was then treated as inert tracer at all levels below this top level until it was removed in the lower troposphere. In the second experiment, the Simple Ozone Experiment, a simplified ozone photochemistry is used at the top model level, and again ozone is taken to be inert at lower levels and is removed in the lower troposphere. Mahlman *et al.* [1980] found that both experiments gave remarkably similar results. For example, Figure 6-43 shows the zonal-mean ozone mixing ratio [ppmv] from the fourth year of both experiments. These results suggest that the details of middle stratosphere ozone chemistry exert very little influence on the distribution of ozone in the lower stratosphere compared with the influence of transport processes.

#### e) Modeling of Stratospheric Warmings

Two types of GCM studies of stratospheric warmings have been undertaken. These are the analysis of stratospheric warmings that have spontaneously arisen in the course of climatological runs with GCMs and GCM forecasting of observed stratospheric warming events. The first spontaneous appearance of a stratospheric warming in a GCM was reported by Newson [1974] using an early version of the British Meteorological Office stratospheric model. Similar results were found with the NASA/Langley quasi-geostrophic stratospheric model by Haggard and Grose [1981]. Neither of these models meets our present definition of a GCM since the model used by Newson used Newtonian cooling in place of an infrared radiative transfer treatment, and Haggard and Grose's model was quasi-geostrophic and contained a parameterized troposphere. Nonetheless, these were two of the earliest reports of stratospheric warming events arising spontaneously in stratospheric circulation models. Mahlman and Umscheid [1984] have recently reported the spontaneous appearance of a sudden warming-type event in the GFDL SKYHI GCM. So far, middle atmosphere GCMs have not produced simulations of stratospheric warming events as intense as those observed in the actual atmosphere.

The pioneering attempt at forecasting stratospheric warming events with a GCM was by Miyakoda *et al.* [1970]. This effort showed some success but failed to produce a true warming event. More recent attempts by Simmons and Struening [1983], Mechoso *et al.* [1985], and Geller *et al.* [1985] have shown greater success.

DYNAMICAL PROCESSES

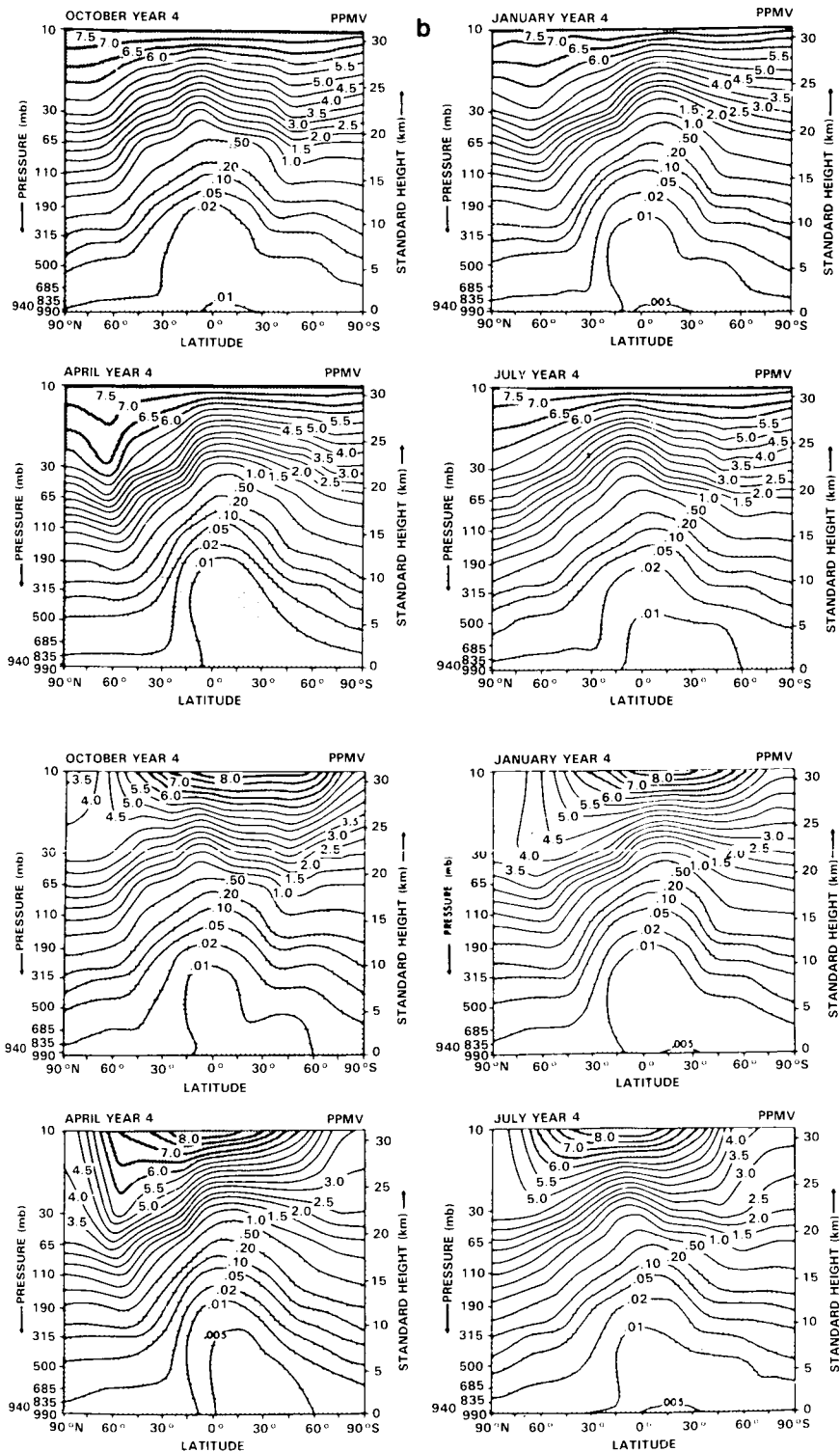


Figure 6-43. Zonal mean mixing ratio (ppmv) for selected months from the fourth year of the Stratified Tracer Experiment (top four panels) and the Simple Ozone Experiment (bottom four panels) of Mahlman *et al.* [1980].

In summary then, troposphere-middle atmosphere GCMs have had a number of successes in simulating some middle atmospheric phenomena. They reproduce many of the observed features of the middle atmosphere [see NASA, 1979, pages 79-91]. Some of the successfully simulated features are the following: the reversed meridional temperature gradient in the lower stratosphere [Smagorinsky *et al.*, 1965]; scale filtering of disturbances with increasing altitude [Manabe and Hunt, 1968]; equatorial tropopause structure [Manabe and Mahlman, 1976]; midlatitude warm belt [Manabe and Mahlman, 1976]; interhemispheric asymmetries [Manabe and Mahlman, 1976]; stratospheric tracer structure [Hunt and Manabe, 1968]; seasonal variation of lower stratospheric temperature [Manabe and Mahlman, 1976]; cancellation between mean cell and eddies [Smagorinsky *et al.*, 1965]; gross features of stratospheric-tropospheric mass exchange [Mahlman and Moxim, 1978]; summertime easterly flow [Manabe and Mahlman, 1976]; identification of Kelvin and mixed Rossby-gravity wave modes in the lower stratosphere [Hayashi, 1974; Tsay, 1974]; phase relationships between ozone and pressure perturbations [Schlesinger and Mintz, 1979]; simulation of the semi-annual oscillation [Mahlman and Sinclair, 1980]; identification of upper stratospheric and mesospheric Kelvin waves [Hayashi *et al.*, 1984]; identification of the effects of gravity waves on the mean zonal flow and planetary waves [Miyahara, *et al.*, 1985]; spontaneous stratospheric warmings [Newson, 1974]; and successful forecasting of stratospheric warmings up to the lower stratosphere [Simmons and Struening, 1983]. References given above are for the first apparent publication reporting each achievement.

### 6.3.3. GCM Deficiencies

#### a) Cold Pole

As discussed in the previous section, all middle atmosphere GCMs (using our definition that they must contain state-of-the-art radiation calculations and a self-determined troposphere) suffer from producing a winter polar night stratosphere that is too cold. Along with this, by the thermal wind relation, the winter westerlies are too strong. This problem typically exists in middle atmosphere GCMs from the tropopause to the mesopause. There is some uncertainty about the cause for this, although it appears that the causes in the lower and upper stratosphere may differ. As discussed in Section 6.2, the climatological state of the winter stratosphere arises from a balance between dynamical effects, driving the system away from radiative equilibrium, and the restoring influence of radiation. In the lower stratosphere, where both effects are weak, the balance is a very sensitive one and the results of Ramanathan *et al.* [1983] suggest that an accurate representation of radiation is crucial to a proper simulation of this region. This conclusion is confirmed by the results of Mahlman and Umscheid [1984]. In the middle and upper stratosphere, however, the balance is less sensitive to small changes in radiation and it seems most likely that the models are in some way underestimating dynamical heat transport. This deficiency may arise from deficient planetary-wave transports or from the failure of current models to represent small-scale motions such as internal gravity waves. The importance of gravity wave transports in maintaining the climatological balance of the stratosphere is currently not well understood.

#### b) Interannual Variability

Typically, stratospheric GCMs exhibit considerably less interannual variability than does the actual atmosphere [e.g., Geller *et al.*, 1984]. This is almost certainly a planetary wave, mean flow interaction problem. Mahlman [personal communication] has noted that the GFDL SKYHI model at 5° resolution shows deficient tropospheric disturbances on all scales (both standing and transient); the representation is improved at 1° resolution. Deficient planetary waves will lead to underestimation of the planetary wave effects on the mean flow.

## DYNAMICAL PROCESSES

### c) Quasi-biennial Oscillation

To date, no GCM has successfully simulated the quasi-biennial oscillation of the equatorial stratosphere. This is to be compared with the relatively successful simulation of the equatorial semi-annual oscillation that was discussed above. The reason for this is probably (see Section 6.2.7) that the equatorial wave modes responsible for the quasi-biennial oscillation have shorter vertical wavelengths than those responsible for the semi-annual oscillation, and the vertical grid spacing in current GCMs cannot resolve these shorter wavelengths. It should be pointed out also that most middle atmosphere GCMs are probably too dissipative to support a quasi-biennial oscillation [see Plumb, 1984].

### d) Tropical Tropopause and Stratospheric Water Vapor

Several middle atmosphere GCMs with relatively high vertical resolution have simulated a tropical tropopause that is too cold by  $\sim 3\text{-}10$  K. Lower vertical resolution models with incomplete radiative transfer schemes have sometimes been too warm. Since stratospheric water vapor is very drastically sensitive to the equatorial tropopause temperature, models that attempt to calculate stratospheric water vapor get too high or too low values depending on their bias in the model tropical tropopause temperatures. Also, numerical simulation of water vapor advection is very difficult due to its extreme vertical gradients in the upper troposphere.

### e) Inclusion of Chemistry

It is an expensive proposition to include relatively complete chemistry schemes in middle atmosphere GCMs. This is due to several factors. One is the number of extra prognostic equations that must be included. A GCM without chemistry calculates four prognostic variables: the two horizontal wind components, temperature, and water vapor. Without treating chemistry by chemical families, one has to calculate about fifteen constituent prognostic equations for transported species. Using chemical families might only imply doubling to tripling the number of prognostic variables. Thus, the number of prognostic equations is greater by about a factor between two and five when chemistry is included.

Furthermore, several of the previously discussed deficiencies of middle atmosphere GCMs in calculating the proper dynamical structure of the middle atmosphere will lead to deficiencies in calculating proper constituent distributions. For instance, if the GCM-calculated tropical tropopause temperature is too cold, the dryness of the air entering the stratosphere will be increased. This will reduce production of the OH radical and thence, ultimately, affect the modeled ozone chemistry. Also, if the "cold winter pole bias" is due to inadequate dynamical heating then the diabatic circulation, and by inference, the transport circulation (see Section 6.5), and the nonadvective eddy transport will be too weak.

Thus we see that some of the problems in calculating proper middle atmosphere structure with GCMs are expected to lead to difficulties in simulating the interactive chemistry of the stratosphere. In particular, if the GCM has difficulty in simulating the  $\text{NO}_x$  and  $\text{HO}_x$  distributions due to dynamical and related deficiencies, then problems must be expected in the representation of ozone, even if by some miracle the model chemistry were to be perfect.

## 6.3.4. Future Directions

### a) Model formulations

We have touched on a variety of GCM applications for both theoretical and observational problems. Differences in model formulations may lead to discrepancies between results obtained from different models.

It is important to understand how the characteristics of a GCM influence its behavior and, in particular, to distinguish those aspects of GCM results which are robust from those which are influenced by details of the model formulation.

A number of features distinguish one GCM from another. These include the numerical scheme (grid-point or spectral), vertical and horizontal resolution, the radiation scheme, parameterization of sub-grid-scale mixing, convection and gravity wave transports and, for transport applications, the means by which conservation of tracer amount is ensured and occurrence of negative mixing ratios is avoided. The level of sophistication of the parameterization schemes used in GCMs varies greatly and their impact on model performance is not well understood.

b) Comparison of GCMs with Observations

Given the problems that middle atmosphere GCMs have had in reproducing some of the most basic features of the observed middle atmosphere (i.e., zonally averaged temperatures and winds) and, until recently, the scarcity of analyses of the middle atmosphere general circulation, middle atmosphere GCM comparison with data has largely been on the basis of morphology comparisons. More sophisticated comparisons are now possible. For instance, GCM diabatic circulations can be compared with that derived from atmospheric data. There are also methods that can be used to compare the effective diffusion in GCMs and the observed atmosphere. In a two-dimensional sense, these two quantities (the diabatic circulation and the effective diffusion) are the two quantities that should be compared if a GCM is to properly transport species [see Mahlman *et al.* 1984, for example].

c) Horizontal and Vertical Resolution

There has been a persistent belief in middle atmosphere modeling that lesser horizontal resolution is required in simulating the middle atmosphere than for the troposphere. Experience is showing otherwise. Both the GFDL experience and the British Meteorological Office experience have indicated the necessity for using higher horizontal resolution than was previously thought to be needed in middle atmosphere GCMs. Mahlman's research group at GFDL has found that their GCM dynamics become progressively more active as they go to finer and finer horizontal resolutions. This leads to progressively better simulations as horizontal resolutions are increased. O'Neill's group at the U.K. Meteorological Office has found in stratospheric warming simulations that higher horizontal resolutions are required during circumstances of more active dynamics.

d) Gridpoint versus Spectral Models

A number of modeling deficiencies have been attributed to fundamental differences between finite difference and spectral transform models. Each modeling architecture has its advantages. The spectral transform method computes horizontal derivatives exactly whereas the finite difference methods used in gridpoint models have their associated errors. (Of course, spectral models have their own truncation errors, entering the calculation in a different way). Spectral transform models are set up for efficient implementation of semi-implicit time differencing which make them more efficient to run. On the other hand, the semi-implicit time differencing makes the model's gravity waves propagate more slowly. This may imply that gravity wave effects must be completely parameterized rather than treated explicitly in these models. A true comparison between middle atmosphere spectral and gridpoint GCMs at the present time is impeded by the different manner in which these two modeling communities have treated dissipative processes. One area that needs to be explored in gridpoint models, however, is the effect of polar filtering

## DYNAMICAL PROCESSES

on GCM middle atmosphere dynamics. This, potentially, could be an area where spectral models would have a distinct advantage over gridpoint models.

### e) Gravity Wave and Turbulence Effects

Perhaps the most important area in which progress is needed in modeling the middle atmosphere is in understanding the proper methods to include the effects of gravity waves and turbulence on the large-scale flow. The pioneering works of Lindzen [1981] and Matsuno [1982] have shown that the effects of gravity waves must be included for proper simulation of the mesosphere. Hunt [1985] has included Lindzen's [1981] parameterization for gravity wave breaking in a GCM that extends upward to 100 km. He has also explicitly included the effects of the diurnal tide in this model. He finds that inclusion of these effects improves his model results significantly. Kida [1985] has constructed a simplified GCM-type model which was meant to study the effects of explicitly simulating gravity wave effects on the middle atmosphere. This model extended from 15 km to 135 km and from the South Pole to the North Pole but extends only ten degrees in longitude (with periodic boundary conditions). His gridspacing was chosen to be able to simulate eddy motions with zonal length scales down to 100 km. He specified a random forcing of gravity waves at the model's lower boundary. These gravity waves will break higher up in the model by virtue of their exponential growth together with the GCM's treatment of convective adjustment. Kida's results show that explicitly modeling the effects of gravity waves in his model gives a simulation that, qualitatively, at least, agrees with middle atmosphere observations. Miyahara *et al.* [1985] have carried out a study of the role of gravity waves in the high-resolution GFDL SKYHI GCM and have also shown the very important role of the model's gravity waves in the mesosphere.

One of the most significant questions in middle atmospheric dynamics at the present time is whether or not gravity waves play an important role in the stratosphere. Tenenbaum [1982] has pointed out the nearly omnipresent problem of GCMs producing too little negative shear on the topside of the subtropical jet stream. Schoeberl [1985] has carried out an idealized study of the linear gravity wave spectrum that is produced by airflow over topography. He found that the superposition of several gravity waves produced regions of shear instability in the lower stratosphere, but that gravity wave instability in the mesosphere usually was the result of a single wave breaking. Thus, parameterization schemes for gravity waves in the stratosphere may have to be more complex than those currently used for the mesosphere.

Observational analyses of gravity waves and turbulence are needed to understand more about the sources of gravity waves, their climatology, and their effects on large-scale middle atmospheric flow.

### e) Radiative Transfer

All of the previous discussion assumes that present day treatments of radiative transfer in the middle atmosphere are sufficient for inclusion into GCMs. If our ability to calculate heating rates in the middle atmosphere is found to be deficient, this would affect all of our perceptions about general circulation modeling of the middle atmosphere. Our understanding of these radiative processes has been discussed in detail in Chapter 7.

Middle atmosphere GCMs that extend sufficiently far upward (above 70 km) must include the effects of the breakdown of local thermodynamic equilibrium. That is to say collisions at this altitude become insufficiently frequent to fully populate the Boltzmann distribution so that the formulation for infrared transfer must be altered [see Dickinson, 1984].

### 6.3.5. Summary

In summary then, present day middle atmosphere GCMs have shown considerable success in modeling certain aspects of the observed circulation. They also have severe problems (e.g., the cold winter pole bias). These problems are sufficiently great that GCM transport studies, while probably being representative of actual atmospheric processes, cannot be taken to give quantitatively correct values for atmospheric transport. It is desirable that middle atmosphere GCMs be developed to the point where they can be taken to be quantitatively correct atmospheric surrogates since data quality may never be sufficient for such transport studies to be carried out without model intervention.

## 6.4 OBSERVATIONS OF TRANSPORT PROCESSES

### 6.4.1 Introduction

Observations which reveal information about the processes responsible for the transport of constituents in the middle atmosphere must necessarily provide the foundation upon which a sound theoretical description of constituent transport can be developed. Historically, it has been the process of seeking agreement between observation and theory that has led to advances in our understanding. Quite often, observations have dictated major revisions in existing theories. Significantly, the earliest example of the latter process with respect to constituents in the middle atmosphere relates to ozone. Measurement of total ozone column by Dobson *et al.* [1929] indicated a distribution that contradicted the photochemical theories developed by Chapman [1930] and subsequent investigators. It soon became apparent that poleward and downward transport of ozone from the photochemical source region in the high equatorial stratosphere was required for consistency with the observations. There followed some 40 years during which the interplay between observations and theory greatly increased our understanding of transport phenomena. Mahlman *et al.* [1984] provide an extensive discussion of this period.

In the 1970's the advent of satellite observations dramatically enhanced our knowledge of the atmospheric circulation, thermal structure, and constituent distributions by providing near-global measurements of temperature and species concentrations continuously over long periods. The impact of these measurements on our understanding of the structure and climatology has been discussed in Section 6.1; here we specifically address observations (both direct and indirect) of processes which determine the transport of dynamic and thermodynamic quantities (momentum, heat and potential vorticity) and of trace constituents.

### 6.4.2 Intercomparisons of Derived Quantities

Many recent studies of stratospheric transport processes and their impact on the structure and dynamics of the stratosphere rely on the determination of potential vorticity and eddy fluxes of potential vorticity (or, equivalently, the divergence of Eliassen-Palm fluxes; cf. Section 6.2) from analyses based on satellite data. Given the degree of differentiation in the vertical and horizontal required to derive potential vorticity from temperature retrievals, it is pertinent to question the accuracy of these determinations. Since errors in potential vorticity depend in a complex way on the magnitude and structure of the errors in temperature and geopotential analyses, the simplest avenue for the assessment of the reliability of potential vorticity calculations (or of the EP flux divergence) is via comparison of results from different data sources.

Grose [1984] reported excellent agreement for Ertel's potential vorticity (EPV) derived from LIMS data with that derived from SSU data reported in McIntyre and Palmer [1983, 1984]. A comparison be-

## DYNAMICAL PROCESSES

tween SSU and LIMS results for January 27, 1979, is presented in Figure 6-44. Additional comparisons for the entire period January and February 1979 exhibit equally good agreement. The differences between the two sets of results are largely due to the differences in resolution of the nadir viewing SSU [Pick and Brownscombe, 1981] and the limb viewing LIMS [Gille and Russell, 1984].

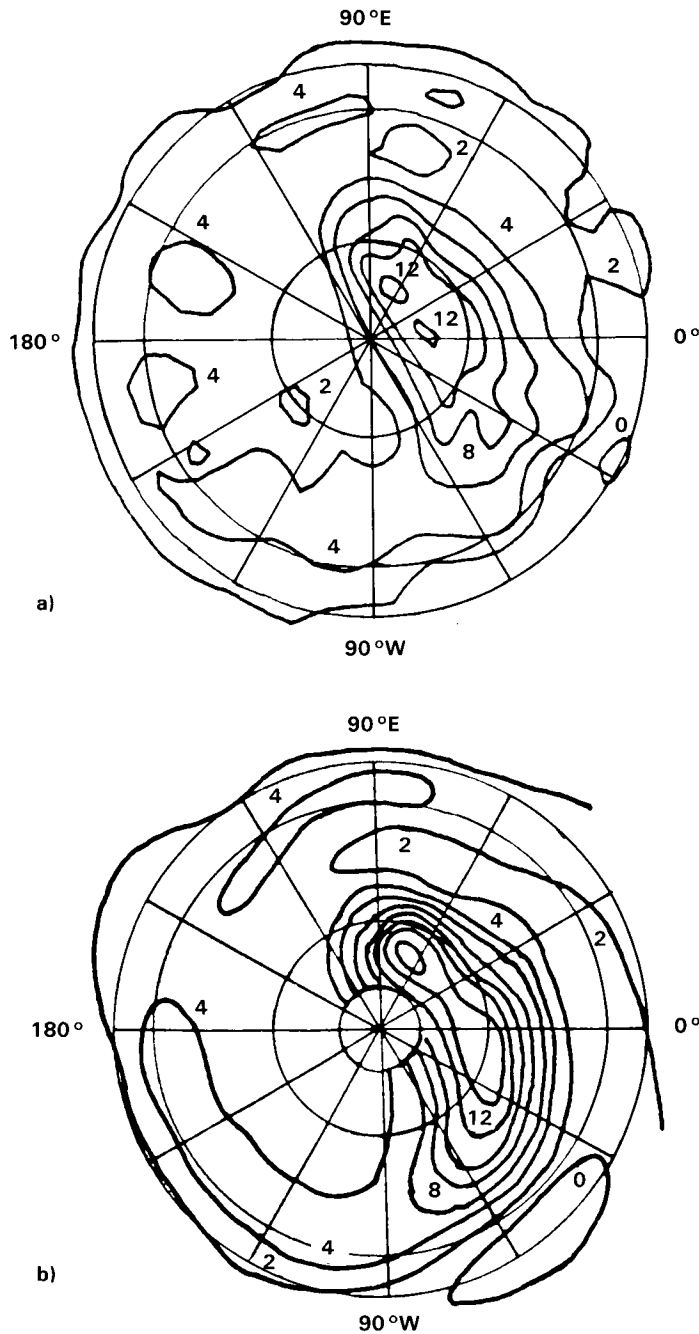


**Figure 6-44.** Ertel's potential vorticity ( $\text{K m}^{-1} \text{s}^{-1}$ ) on the 850 K isentropic surface (average pressure about 10mb) for January 27, 1979. (a) SSU data [from McIntyre and Palmer, 1984], (b) LIMS data [from Grose, 1984].

Another intercomparison study for the Northern Hemisphere winter stratosphere using satellite and radiosonde/rocketsonde measurements was carried out by Miles and Chapman [1984]. This study utilized Nimbus 5 SCR data and conventional data from NMC and Berlin to derive zonal mean winds, time-mean wave structure and Eliassen-Palm cross sections for the period December 1973-February 1974. The results exhibited good qualitative agreement with the exception of the Eliassen-Palm flux divergence in the stratosphere. The disagreement between the EP flux divergences for the different sources could be traced to differences in the horizontal eddy momentum flux distributions. Although all three data sources were found to give somewhat different results, the SCR results are more compatible with those from Berlin data. Surprisingly, the NMC results are quite different from the Berlin results. One factor which could explain the NMC-Berlin differences is the incorporation of vector wind reports in the Berlin analysis although several other factors could be responsible. These results demonstrate that useful derived quantities can be obtained from satellite data, but emphasise the difficulty of accurate determination of quantities requiring several orders of differentiation.

#### 6.4.3 Studies of Wave-Mean Flow Interaction and Stratospheric Warmings

##### (a) Heat and momentum budgets and the mean circulation

Hartmann [1976b] utilized Nimbus 5 Selective Chopper Radiometer (SCR) data to examine the dynamical climatology of the winter stratosphere in the Southern Hemisphere for 1973. This study was significant in that derived quantities were used in conservation equations to study zonal mean budgets of heat, momentum, and energy. The mean meridional velocity was independently inferred from both heat and momentum balance considerations. For the lower and middle stratosphere, the two results were qualitatively similar and the differences were most probably a result of errors in the data or errors introduced from the approximations used in the analysis. However, in the upper stratosphere the results were qualitatively dissimilar. One implication of these results is that momentum dissipation on scales unresolved by the satellite instrument might be important in the upper stratosphere. Crane *et al.* [1980] came to similar conclusions on the basis of an analysis of heat and momentum budgets for the stratosphere and mesosphere using Nimbus 6 Pressure Modulator Radiometer (PMR) data.

Hamilton [1983a] utilized NMC data from four Northern Hemisphere winters and evaluated the terms in the zonally averaged heat and momentum budgets. Vertical velocity was inferred from the thermodynamic equation and then utilized in the mass continuity equation to evaluate the meridional velocity. The terms in the momentum equation were then evaluated with the residual needed to balance the equation interpreted as the momentum dissipation by unresolved waves (such as gravity waves). These results suggested that an easterly acceleration was required to balance the momentum budget in the region near the stratopause.

Smith and Lyjak [1985] performed a similar study, but utilized LIMS data extending into the mesosphere. The results were broadly consistent with those of Hamilton for Northern Hemisphere winter, indicating a requirement for an easterly acceleration to account for the evaluated residual momentum deficit. Their results also demonstrated a requirement for a westerly acceleration in the springtime Northern Hemisphere. The momentum deficits were then utilized to evaluate an equivalent Rayleigh friction coefficient. The calculated values, however, were substantially larger than the values typically utilized in numerical circulation models.

The results of Hamilton [1983a] and Smith and Lyjak [1985] are qualitatively consistent with current theories for momentum dissipation from breaking gravity waves, although they suggest a possibly significant role for gravity wave stresses in the upper stratosphere as well as in the mesosphere. However, the

## DYNAMICAL PROCESSES

quantitative estimates of this effect are uncertain because errors inherent in the data set, as well as those introduced by the approximations utilized in the analysis, are also incorporated into the evaluated momentum residual term.

### (b) Stratospheric warmings in the Northern Hemisphere

Numerous investigators have utilized satellite data to investigate stratospheric warming phenomena. Palmer [1981a,b] studied the stratospheric major warmings of 1979 and 1980 employing SSU data and the transformed Eulerian-mean formulation of Andrews and McIntyre [1976, 1978a]. Palmer diagnosed the thermal and momentum budgets of the stratosphere during the warming events. Calculated Eliassen-Palm cross sections were used to study the evolving wave-mean flow interactions. Based upon the results of these analyses, Palmer speculated upon the idea of preconditioning of the stratosphere with formation of a high-latitude jet core prior to a major warming. This study generally supports the concept advanced by Kanzawa [1980, 1982, 1984] (and foreshadowed by Quiroz *et al.* [1975]) of a minor warming preconditioning the polar latitudes for a subsequent major warming.

Additional studies of the 1979 warming analyzed by Palmer [1981a,b] have been performed by Gille and Lyjak [1984], Gille *et al.* [1983], and Grose [1984] using LIMS data. The results are consistent with those of Palmer. Minor differences between the various results are attributable to the different data sets (SSU and LIMS) and differences in the analyses.

O'Neill and Youngblut [1982] used NMC data to perform an analysis of the 1976/1977 warmings. They also adopted the transformed Eulerian-mean formulation and Eliassen-Palm cross sections as a diagnostic in their analysis. Ray tracing was used in conjunction with quasi-geostrophic refractive index to study the propagation of wave disturbances. Their analysis concluded that a strong jet at high latitudes favored focusing of wave activity into the polar region with subsequent deceleration of the zonal jet; this process was discussed in Section 6.2.

### (c) Southern Hemisphere studies

Relatively fewer diagnostic studies of the Southern Hemisphere have been conducted using satellite data. One inhibiting factor is the relatively poorer upper tropospheric base level analyses that must be used to build up the geopotential heights with the satellite temperature data. Larger ocean areas and fewer radiosonde stations (in comparison to the Northern Hemisphere) make accurate base level analyses for the Southern Hemisphere more difficult. Hartmann *et al.* [1984] utilized SSU data (NMC analysis) to study wave-mean flow interaction for the Southern Hemisphere winter of 1979. Their results showed evidence for a dipole structure in the Eliassen-Palm flux divergence centered near 65°S corresponding to acceleration of the mean-flow, perhaps suggestive of a local source of wave activity. The origin of this source is unclear, although Hartmann *et al.* suggest barotropically unstable modes as the cause.

Yamazaki and Mechoso [1985] investigated the Southern Hemisphere final warming, when the winter westerlies give way to summer easterlies, of 1979. The evolution of the flow during this period was mostly a gradual process, suggestive of radiative control, but with some contribution from intermittent planetary wave events.

The evolution of a stratospheric minor warming during Southern Hemisphere mid-winter was examined by Al-Ajmi *et al.* [1985] using SCR data. This study highlighted some fundamental differences between

Southern Hemisphere warmings and their counterparts in the Northern Hemisphere. This warming was confined to higher levels and lower latitudes than typical for Northern Hemisphere warmings. The jet shifted poleward and downward. The calculated Eliassen-Palm cross sections exhibit the dipole structure of high latitude divergence and low latitude convergence similar to that noted by the Hartmann *et al.* [1984] study. The deceleration of the zonal mean wind associated with the region of convergence was comparable with that of Northern Hemisphere major warmings. Isentropic maps of potential vorticity suggest low latitude air being irreversibly mixed into middle latitudes.

#### 6.4.4. Studies of Transport Processes

##### (a) Potential vorticity

Hartmann [1976b] studied the zonal mean budget of potential vorticity for the Southern Hemisphere winter of 1973 utilizing SCR, ITPR, and NEMS data from the Nimbus 5 satellite. As noted in Section 6.2, Ertel's potential vorticity is a conserved tracer under the assumptions of adiabatic, frictionless flow [Ertel, 1942]. In the lower to middle stratosphere, both ozone and potential vorticity are quasi-conserved for a few days, at least. Therefore, potential vorticity serves as a proxy for studying the transport of quasi-conserved trace species in this region of the atmosphere. Hartmann concluded in this study that the eddy transport of potential vorticity was consistent with observations of ozone transport and calculations conducted with general circulation models.

McIntyre and Palmer [1983, 1984] utilized maps of Ertel's potential vorticity on isentropic surfaces in the middle stratosphere to study transport and mixing in the winter stratosphere during the period of January-February 1979. The data used in this study were from the SSU instrument on the Tiros-N satellite. In contrast to the zonal mean potential vorticity calculations of Hartmann [1976b], these hemispheric maps vividly depicted the large-scale transport processes occurring during a minor and major warming in this period. McIntyre and Palmer utilized these maps of potential vorticity to show evidence of "wave breaking" or irreversible deformation of the isentropic potential vorticity contours. They suggested that the breaking waves act to erode the polar vortex (a region of high potential vorticity with strong meridional gradients) and produce a mixed region in middle latitudes (or "surf zone") with relatively weak gradients. These results suggest that isentropic potential vorticity maps can provide extremely valuable insight and further understanding of transport processes.

Hoskins *et al.* [1985] have advocated mapping of potential vorticity distributions as a powerful diagnostic technique for studies of dynamics and transport in both stratosphere and troposphere. The power of potential vorticity as a dynamical diagnostic stems not only from the conservation property, but also from an "invertibility" principle which states that knowledge of the isentropic potential vorticity fields with suitable boundary information is sufficient to determine all of the dynamical variables of interest.

The concept of using isentropic mapping potential vorticity as a diagnostic has received impetus from the study of Clough *et al.* [1985], who produced potential vorticity maps from SSU data to study the evolution of a Canadian warming in Dec. 1981. Butchart and Remsberg [1986] utilized LIMS data and developed the concept of "area diagnostics" (time evolution of the area contained within a contour of either constant potential vorticity or species mixing ratio on an isentropic surface) advanced by McIntyre and Palmer [1983, 1984]. They demonstrate the use of the area diagnostics as a means of delineating the mixed or surf zone from the polar vortex, and for detecting when nonconservative effects such as diabatic heating or photochemistry become important.

## DYNAMICAL PROCESSES

### (b) Constituents

Leovy *et al.* [1985] studied the transport of ozone in the stratosphere using LIMS data for the period Oct. 1978 to May 1979. These results were supportive of the wave breaking hypothesis of McIntyre and Palmer [1983, 1984]. Leovy *et al.* noted that the ozone displayed a strong negative correlation with isentropic potential vorticity maps. Ozone mixing ratio from LIMS on the 850 K isentropic surface of January 27, 1979, is presented in Figure 6-45 for comparison with the potential vorticity maps in Figure 6-44. Both ozone and EPV maps display the signature of a “breaking wave”. The core of high EPV (low ozone) is being drawn out clockwise around an intensifying Aleutian anticyclone. Concomitantly, a tongue of lower EPV (higher ozone) is being drawn from low latitudes poleward in the region of confluence between the anticyclone and the polar low. This result is to be anticipated since both ozone and potential vorticity are quasi-conserved over times of a few days in the lower to middle stratosphere. Leovy *et al.* suggested that observed differences in the ozone and potential vorticity arose from differing nonconservative processes affecting the two tracers and from their different gradients. The results of the analysis provide support for the idea of the ozone hole associated with the polar vortex being filled as the episodes of wave breaking produce irreversible mixing of tongues of higher ozone mixing ratio from the tropics into high latitudes. The contribution of this process to the seasonal evolution of ozone needs further study.

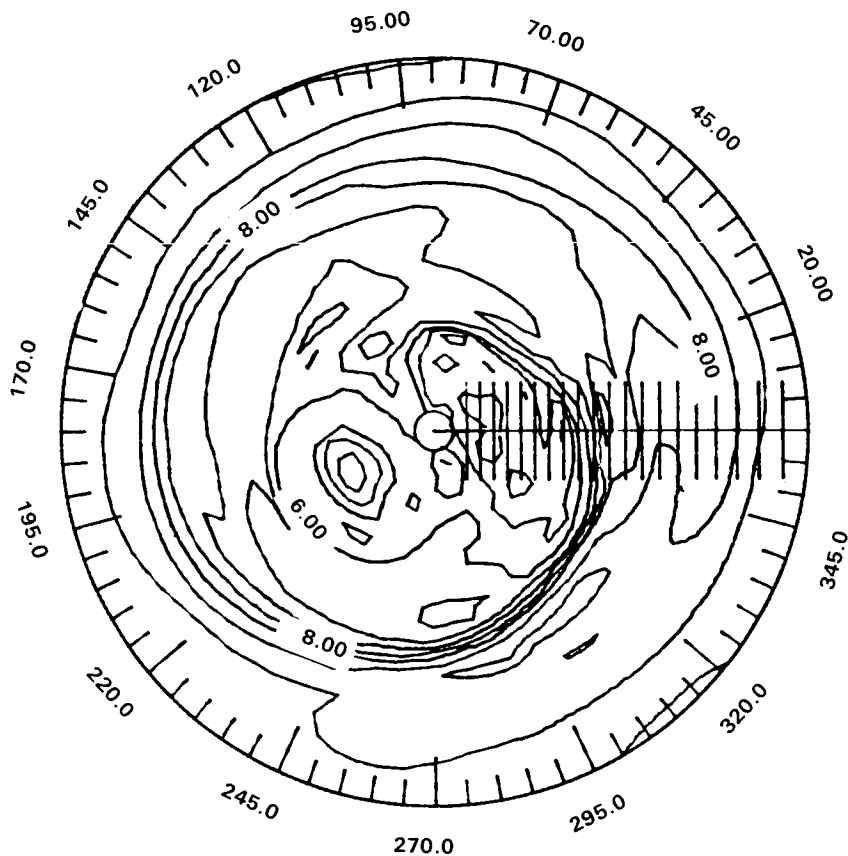


**Figure 6-45.** Ozone mixing ratio (ppmv) on the 850 K isentropic surface, (~ 10 mbar), January 26, 1979. LIMS data [from Grose and Russell, 1985].

Grose [1984] and Grose and Russell [1985] also point out the correspondence between potential vorticity and quasi-conserved species. In particular, water vapor shows a strong correlation with potential vorticity as shown in Figure 6-46. The results suggest that fields of isentropic potential vorticity and quasi-conserved species in combination have the potential for providing a wealth of information on dynamical, chemical and radiative processes.

Calculation of parcel trajectories using satellite data has great potential for studying the coupling of radiative, chemical, and dynamical processes. For example, Austin and Tuck [1985] and Austin [1985] have used SSU and LIMS data to calculate parcel trajectories in the stratosphere. Solomon and Garcia [1983b] and Callis *et al.* [1983b] illustrated the use of trajectory analysis to show the coupling between dynamics and photochemistry responsible for producing the “Noxon cliff” or strong latitudinal gradient in column  $\text{NO}_2$  observed during displacement of the polar vortex during so-called “wave 1 events”.

#### 6.4.5. Conclusions

The recent availability of satellite data of sufficient quality to derive dynamical quantities has stimulated many diagnostic studies. The uncertainties associated with derived quantities remain to be evaluated. However, there is little doubt that they provide much useful qualitative insight into dynamics and transport processes. The use of isentropic maps of potential vorticity as a diagnostic is only beginning to be

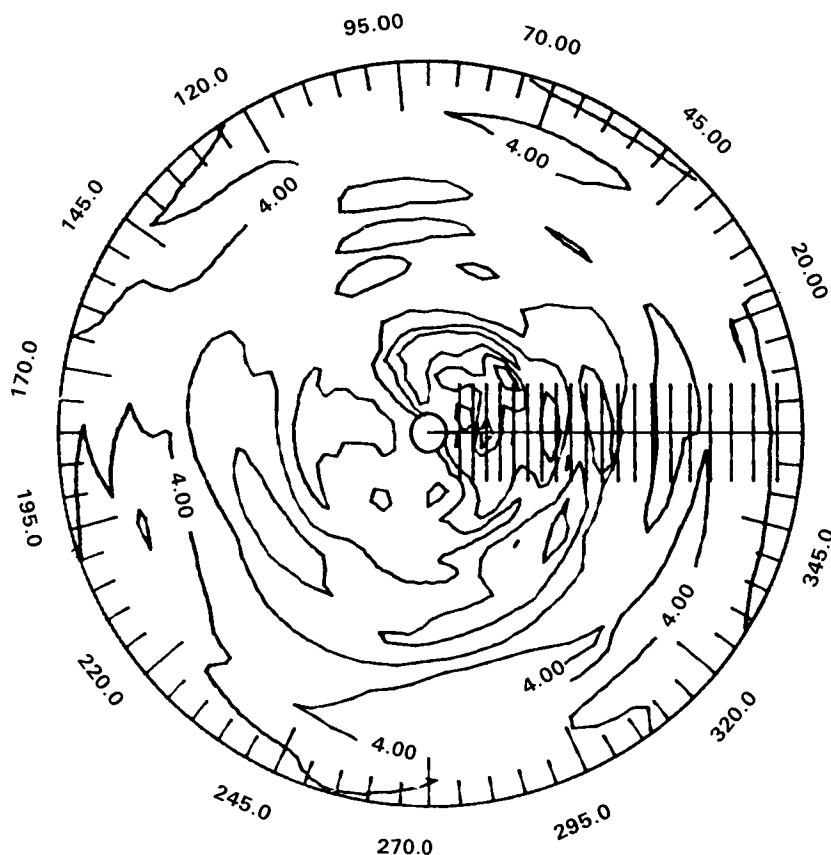


**Figure 6-46.** Water vapor mixing ratio (ppmv) on the 850 K isentropic surface ( $\sim 10$  mbar), January 27, 1979. LIMS data [from Grose and Russell, 1985].

## DYNAMICAL PROCESSES

explored, but promises to greatly expand our understanding of fundamental processes, particularly when used in conjunction with fields of trace chemicals measured simultaneously.

### 6.5 THEORY OF TRANSPORT PROCESSES

#### 6.5.1 Introduction

The problem of transport of a conserved tracer – the amount of which is constant with time within a given material parcel of air – is in principle simply a matter of tracking parcel movements. Over short periods of time, this may be a useful approach – and indeed has proved to be so in some such cases [e.g., Allam and Tuck, 1984b; Austin and Tuck, 1985]. However, given the complexity of the atmospheric trajectories, this is not in itself a practical avenue for understanding the global transport of atmospheric constituents. Nevertheless this simple property of *Lagrangian* conservation (i.e., following material elements) is the root of all transport processes and must not be hidden in any analysis procedure if we wish to retain insight into global transport mechanisms.

The global transport problem has for twenty years or more been reduced to one of manageable (though still difficult) proportions by limiting the aim to one of explaining the behavior of zonally-averaged atmospheric constituent structures on long time scales (say, a month and longer). The restriction to zonal averages greatly reduces the number of degrees of freedom in the problem, without a profound loss of information, since the strong quasi-zonal flow in most regions of the atmosphere ensures that much of the seasonal-mean structure of long-lived constituents is in the meridional (latitude-height) plane. In fact it is only relatively recently, with the advent of satellite monitoring of atmospheric constituents, that our knowledge of their structure has been comprehensive enough to demand anything more sophisticated than a zonal-mean conceptual framework. As noted in Sections 6.1 and 6.4, it is now recognised that even the monthly-mean flow in the winter stratosphere may be highly asymmetric in the zonal direction and therefore that the zonally-averaged approach may have severe limitations. These limitations and possible avenues for avoiding the restriction to zonal averages will be addressed later in this section. However at the present time the zonal-mean formulation forms the basis of assessment modeling (Chapters 12 and 13) and we therefore begin this Section with a detailed discussion of recent developments in zonal-mean transport theory.

#### 6.5.2 Zonally-Averaged (2D) Formulations

A quasi-conserved tracer of mixing ratio  $q$  satisfies a conservation relation of the form:

$$\frac{dq}{dt} = S \quad (13)$$

where  $d/dt$  is the derivative following the flow and  $S$  represents sources and/or sinks of  $q$ . For a quasi-conserved quantity,  $S$  is normally small although it is important to recognize that the transport processes themselves may ensure that  $S$  becomes large, even though a naive scaling analysis may indicate otherwise. (For example, the importance of local diffusion of  $q$  may be greatly intensified as a result of the shearing of  $q$  gradients by the flow and the consequent cascade to small scales). The traditional zonal mean budget equation for  $\bar{q}$  then follows from the zonal mean of (13), viz.,

$$\left[ \frac{\partial}{\partial t} + \bar{\mathbf{u}} \cdot \bar{\nabla} \right] \bar{q} + \frac{1}{e_0} \bar{\nabla} \cdot e_0 \bar{\mathbf{u}}' \bar{q}' = \bar{S} \quad (14)$$

where  $\rho_0$  is the basic atmospheric density. Thus the zonal-mean transport of  $q$  is mathematically split into two components: advection of  $q$  by the mean meridional circulation  $(\bar{v}, \bar{w})$  and an "eddy flux"  $\rho_0 \overline{u'q'}$ . Attempts to arrive at a simple description of transport on this basis, however, proved confusing (e.g., see the discussion of McIntyre [1980b] and Mahlman *et al.* [1984]). It is now recognized following the work of Andrews and McIntyre [1976, 1978b] that the simplicity of (14) is deceptive and that the mathematical separation of transport into "mean" and "eddy" components is an arbitrary procedure which may not (and in practice does not) yield the simplest picture of transport [McIntyre, 1980a]. The formulation (14) proves to be less straightforward than it might appear simply because this separation has masked the three-dimensional Lagrangian conservation properties of (13). These properties are more faithfully preserved in an alternative formulation, which is even simpler in form than (14), viz., the budget equation for the generalized Lagrangian-mean mixing ratio  $\bar{q}^L$ , as defined by Andrews and McIntyre [1978b], which is

$$\left[ \frac{\partial}{\partial t} + \bar{\mathbf{u}}^L \cdot \nabla \right] \bar{q}^L = \bar{S}^L \quad (15)$$

[McIntyre, 1980a]. Thus transport of the Lagrangian-mean mixing ratio resides solely in the term representing advection by the Lagrangian-mean meridional circulation  $\bar{\mathbf{u}}^L = (\bar{v}^L, \bar{w}^L)$  and there are no explicit eddy transport terms (apart from any effects implicit in  $\bar{S}^L$ ).

The reason for the greater simplicity of the generalized Lagrangian-mean approach is evident from Figure 6-47. The generalized Lagrangian-mean mixing ratio  $\bar{q}^L$  at reference latitude and height  $(y_L, z_L)$  is, by definition, the average along a material tube of air whose center of mass in the latitude/height plane is at  $(y_L, z_L)$ , as shown in Figure 6-47a. After a time  $\delta t$  (Figure 6-47b) this material tube is displaced by mean motions to a new reference (center of mass) position  $(y_L + \bar{v}^L \delta t, z_L + \bar{w}^L \delta t)$  and is distorted by eddy motions. However, if  $S = 0$ , then every element in the tube conserves its value of  $q$  and therefore the Lagrangian mean  $\bar{q}^L$  evaluated at the new reference position  $(y_L + \bar{v}^L \delta t, z_L + \bar{w}^L \delta t)$  is identical to that at  $(y_L, z_L)$  at the outset, independent of the wavy distortions of the tube. Therefore, in a frame of reference moving with the center of mass of the tube (which by definition moves with the Lagrangian-mean velocity  $\bar{\mathbf{u}}^L$ ),  $\bar{q}^L$  is constant if  $S = 0$ . This is the essence of Equation (15).

Despite the simplicity of this description – which has led to profound conceptual advances in atmospheric transport theory – its practical application is beset by many problems [McIntyre, 1980b] not the least of which is the determination of the Lagrangian-mean flow  $(\bar{v}^L, \bar{w}^L)$  itself. Dunkerton [1978] argued that a reasonable estimate of this circulation could be obtained via the diabatic circulation (see Table 6-1, below). Thus Dunkerton obtained a picture of the circulation of the middle atmosphere (Figure 6-48a) which differs substantially from the Eulerian-mean picture – cf. Figure 6-48b. The implied transport characteristics of the flow depicted in Figure 6-48a are, unlike those which would be inferred from Figure 6-48b, consistent with the global structure of trace constituent distributions (and, indeed, flow patterns similar to 6-48a had earlier been inferred from observed tracer distributions [Brewer 1949, Dobson, 1956]). For one thing the upward motion into the lower stratosphere occurs solely in low latitudes, as has been inferred from the observed dryness of the stratosphere (see Chapter 5). Further, the poleward/downward flow in the winter hemisphere is consistent with the observed structure of long-lived stratospheric tracers, including ozone and potential temperature, the circulation transporting ozone from the tropical middle and upper stratosphere to lower levels in the winter high latitudes and the subsidence at the winter high latitudes maintaining the temperature above its radiative equilibrium, as observed.

While this conceptual picture of large-scale transport processes represents a considerable advance over the traditional viewpoint embodied in Equation (14) it is not as such a complete description. The main

## DYNAMICAL PROCESSES

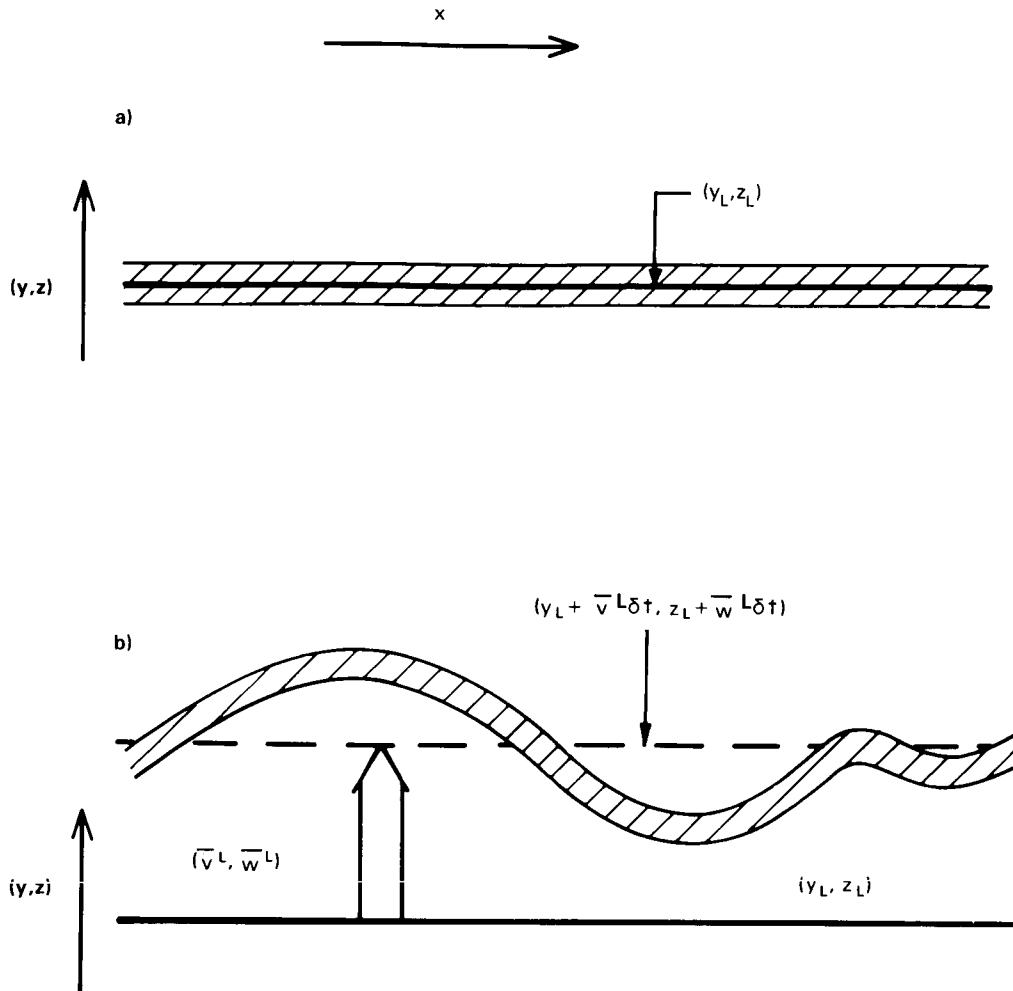


**Figure 6-47.** Schematic illustration of the conservation of the generalized Lagrangian-mean mixing ratio of a conserved tracer. The hatched region is a material tube of air which moves from its location shown in (a) at some time to that shown in (b) a time  $\delta t$  later. See text for discussion.

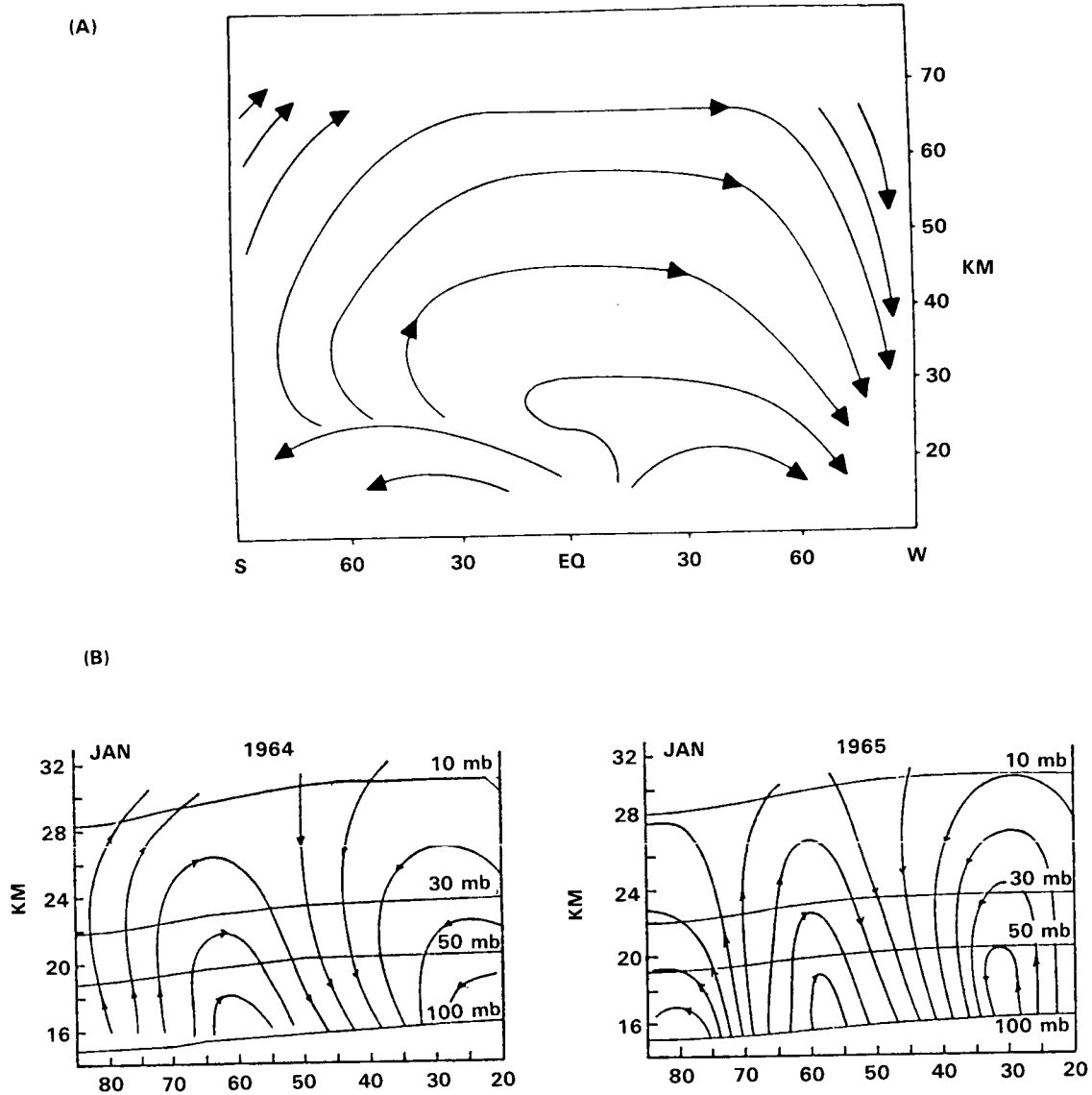
reason for this is that (15) is a prediction equation for the Lagrangian-mean mixing ratio  $\bar{q}^L$  whereas what is usually required is a description of the evolution of Eulerian measures of  $q$ , which may be quite different from the evolution of  $\bar{q}^L$ . Consider, for example, a wave breaking event as depicted schematically in Figure 6-49, in which, for simplicity of argument, it is assumed that  $\bar{v}^L$  and  $\bar{w}^L$  are zero. The mixing ratio isopleths of a conserved tracer  $q$  (it is further assumed that  $S = 0$ ) are initially aligned zonally, with, say high values to the south. A transient breaking wave event distorts these isopleths to such an extent that the reference material curve  $C$  (on which  $q = q_c$  is constant) is fractured leaving, after the passage of the event, an isolated pool of high  $q$  to the north of its initial latitude and a pool of low  $q$  to the south. This irreversible dispersion of material contours clearly achieves a very real (Eulerian) transport in latitude which is not explicitly revealed by the Lagrangian-mean budget, since (15) tells us, under the present assumptions that  $\partial \bar{q}^L / \partial t = 0$ . The point is, of course, that transport has been achieved, not by any change in  $\bar{q}^L$ , but by an irreversible deformation of the contour  $C$  along with  $\bar{q}^L$  is determined. Mathematically, this transport is implicit in (15) only through the mapping  $\bar{q}^L \rightarrow \bar{q}$  which must be performed in order to apply (15) to practical problems [Plumb, 1979; McIntyre, 1980b].

Table 6-1. Measures of the mean meridional circulation

(i)	Eulerian mean circulation ( $\bar{v}, \bar{w}$ )	Conventional, Eulerian, zonal average
(ii)	Generalized Lagrangian-mean circulation ( $\bar{v}^L, \bar{w}^L$ )	Zonal average along (wavy) material lines. Velocity of center of mass of material tubes of fluid. The only circulation on this list which is not, in general, nondivergent.
(iii)	Residual circulation ( $\bar{v}_*, \bar{w}_*$ )	Defined by Equation (2). The mean circulation of "transformed Eulerian-mean" theory. This formulation greatly simplifies the quasigeostrophic zonal-mean budget equations for heat and momentum.
(iv)	Diabatic circulation ( $\bar{v}_D, \bar{w}_D$ )	The mean circulation in isentropic coordinates. Equals (iii) for quasigeostrophic flow if mean isentropes are stationary.
(v)	Transport circulation ( $V_T, W_T$ )	Defined by Equation (17). The "advective mass flux" of Kida [1983a]. The non-diffusive component of transport in the formulation (16). Equals (ii) if eddy-induced dispersion is spatially homogeneous; equals (iii) for small-amplitude, adiabatic eddies.

Another serious problem with the practical application of (15) has been brought to light by determination of the Lagrangian-mean circulation in the stratosphere of numerical models [Kida, 1977, 1983a; Plumb and Mahlman, 1986]. Andrews and McIntyre [1978b] pointed out that  $\bar{u}^L$  is not a nondivergent velocity (i.e., it does not satisfy the usual continuity equation) and discussed the reasons for this. Now, our concept of an advective process – one that displaces the center of mass of a tracer distribution without, to first order, affecting the spread of the distribution about the center of mass (unlike dispersive processes such as that discussed above in the context of Figure 6-49) is implicitly based on an assumption that the advecting velocity is nondivergent. However, Kida [1983a] and Plumb and Mahlman [1986] found the Lagrangian-mean meridional circulation in the numerical models they investigated to include a large divergent component, so much so that the Lagrangian-mean flow, shown in Figure 6-50, bears limited resemblance to Figure 6-48a.

# DYNAMICAL PROCESSES



**Figure 6-48.** (a) Streamlines (schematic) of the diabatic circulation of the middle atmosphere at the solstices. 'S' and 'W' denote summer and winter pole, respectively. [After Dunkerton, 1978]. (b) Eulerian-mean meridional circulation (schematic) of the Northern Hemisphere winter stratosphere [After Vincent, 1968].

Plumb [1979] showed that, for small-amplitude eddies, the zonal-mean constituent budget equation could be written:

$$\frac{\partial \bar{q}}{\partial t} + V_T \frac{\partial \bar{q}}{\partial y} + W_T \frac{\partial \bar{q}}{\partial z} = \frac{\partial}{\partial y} \left[ K_{yy} \frac{\partial \bar{q}}{\partial y} + K_{yz} \frac{\partial \bar{q}}{\partial z} \right] + \frac{1}{e_0} \frac{\partial}{\partial z} \left[ e_0 K_{zy} \frac{\partial \bar{q}}{\partial y} + e_0 K_{zz} \frac{\partial \bar{q}}{\partial z} \right] + \bar{S} \quad (16)$$

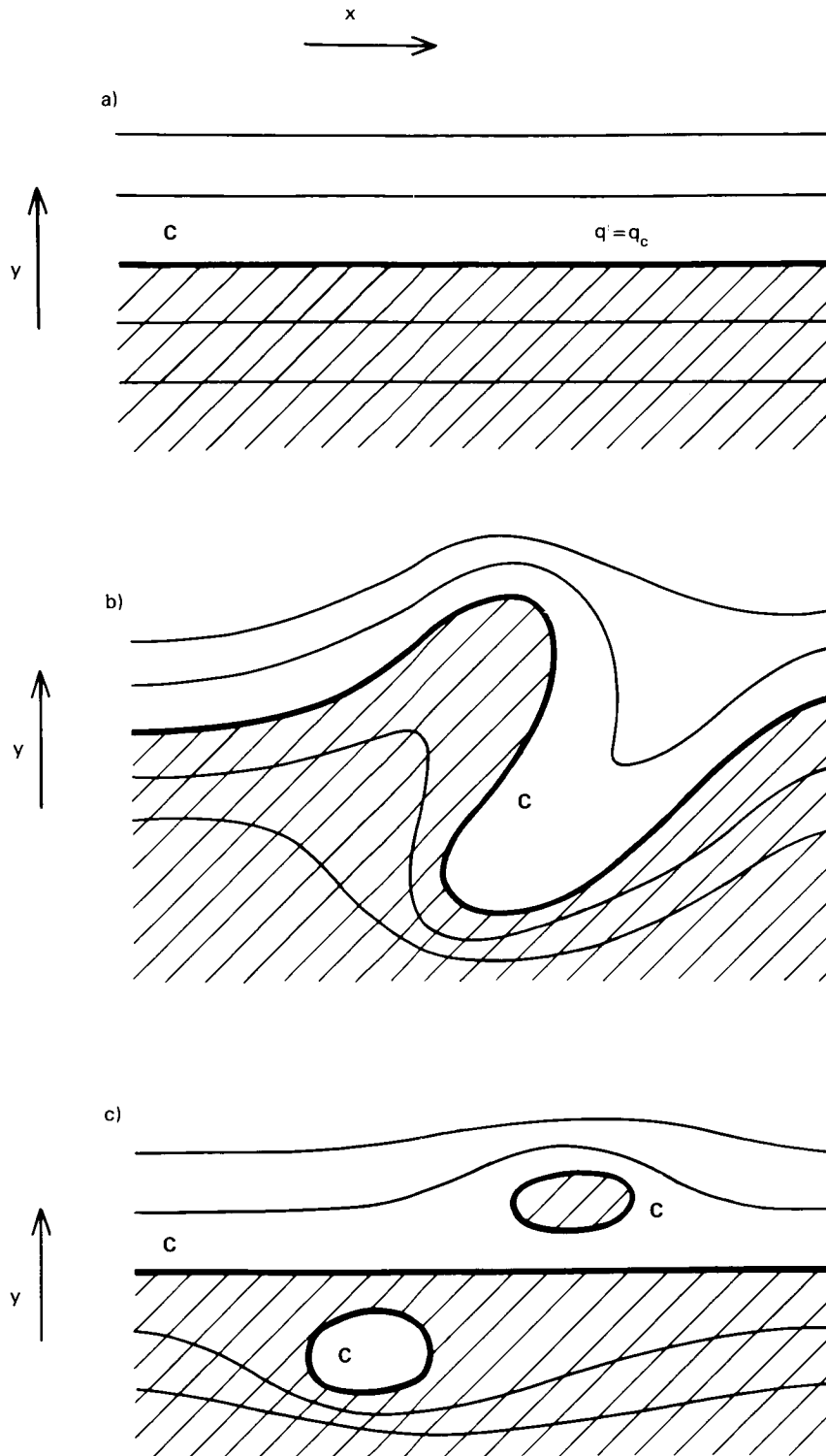


**Figure 6-49.** Schematic illustration of the irreversible distortion of material lines (a) before, (b) during and (c) after a breaking wave event. The heavy curve C is an isoline of a tracer  $q = q_c$ . Regions of  $q > q_c$  are shaded. See text for discussion.

## DYNAMICAL PROCESSES

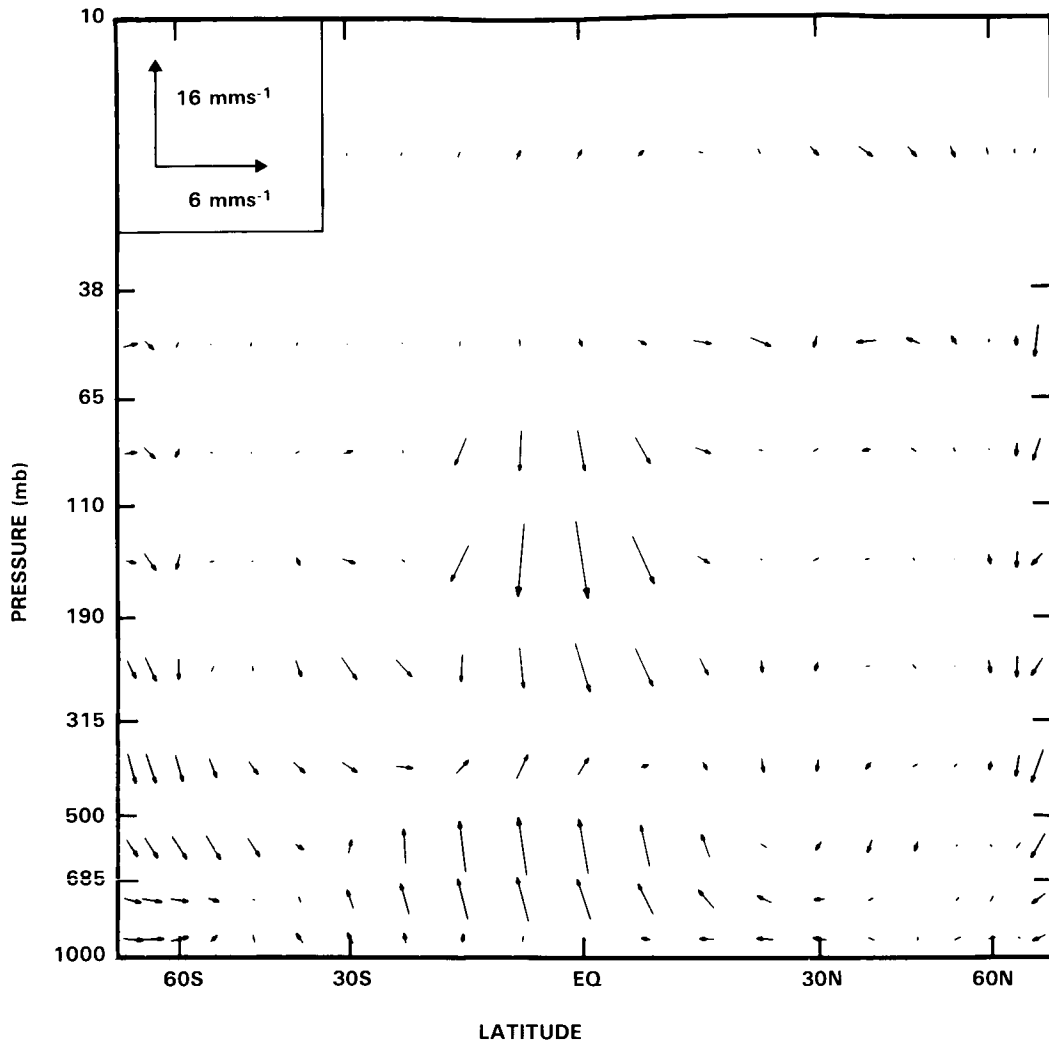


**Figure 6-50.** Lagrangian-mean circulation ( $\overline{v^L}, \overline{w^L}$ ) in the GFDL general circulation/tracer model [Mahlman and Moxim, 1978] as determined by Plumb and Mahlman [1986].

where  $(V_T, W_T)$  is a nondivergent meridional circulation defined by

$$\begin{bmatrix} V_T \\ W_T \end{bmatrix} = \begin{bmatrix} \overline{v} + \frac{\partial L}{\partial y} \\ \overline{w} - \frac{1}{\rho_0} \frac{\partial}{\partial z} (\rho_0 L) \end{bmatrix} \quad (17)$$

with  $L = \frac{1}{2} (\overline{v'\xi} - \overline{w'\eta})$ , and  $\mathbf{K}$  is a diffusivity tensor which, for conserved tracers, is defined by

$$\begin{bmatrix} K_{yy} & K_{yz} \\ K_{yz} & K_{zz} \end{bmatrix} = \begin{bmatrix} \frac{1}{2} \frac{\partial \overline{\eta^2}}{\partial t} & \frac{1}{2} \frac{\partial \overline{(\eta\xi)}}{\partial t} \\ \frac{1}{2} \frac{\partial \overline{(\eta\xi)}}{\partial t} & \frac{1}{2} \frac{\partial \overline{\xi^2}}{\partial t} \end{bmatrix} \quad (18)$$

where  $(\eta, \zeta)$  are the eddy displacements in the  $(y, z)$  directions as defined by Andrews and McIntyre [1978b]. These terms in (18) describe not only the effects of dispersion relative to the Lagrangian-mean flow as discussed above, but also the transport by the divergent part of the Lagrangian-mean circulation. Then the advection by the nondivergent "transport circulation"  $(V_T, W_T)$  is truly advective, in the normal sense.

Since the pioneering work of Andrews and McIntyre [1976, 1978b] brought about a breaking away from the conventional definition of the "mean" circulation as the basis of transport formulations, several new definitions of "mean circulation" have appeared, of which the transport circulation is one of four. Each of these measures of the mean meridional circulation has its own particular application. There has, however, been a confusing tendency in the recent literature of transport modeling to overlook the differences between some of these. The different circulations are listed in Table 6-1, in which some of their interrelationships are noted. The transport circulation differs from the Lagrangian-mean velocity unless the diffusivity  $\mathbf{K}$  is spatially homogeneous [Andrews and McIntyre, 1978b; Plumb, 1979; Matsuno, 1980; Kida, 1983a]. While  $(V_T, W_T)$  may be defined by Equation (17), this is not a practical avenue for its determination. Kida [1983a] refers to this velocity as the "advective mass flux" and determined it from a numerical model as that part of the circulation which is asymmetric with respect to a time-reversal, while Plumb and Mahlman [1986] derived it by inverting a flux-gradient relation for trace constituent fluxes; their results are illustrated in Figure 6-51. This circulation is very similar to that obtained by Dunkerton [1978] as shown in Figure 6-49; reasons for this will be discussed below.

The same formalism can be used to help understand the variability of trace constituents. The perturbation concentration of a conserved tracer is related to the eddy displacements through

$$q' = -\eta \frac{\partial \bar{q}}{\partial y} - \zeta \frac{\partial \bar{q}}{\partial z}$$

If  $\gamma = -(\partial \bar{q} / \partial y) / (\partial \bar{q} / \partial z)$  is the slope of the mean isopleths of  $q$ , then

$$q' = -\frac{\partial \bar{q}}{\partial z} (\zeta - \gamma \eta).$$

Therefore the variance of  $q$  around a latitude circle is

$$\overline{q'^2} = \left[ \frac{\partial \bar{q}}{\partial z} \right]^2 \overline{(\zeta - \gamma \eta)^2}. \quad (19)$$

Ehhalt *et al.* [1983] defined an "equivalent displacement height"

$$\Delta = \overline{(q'^2)^{1/2}} / \left| \frac{\partial \bar{q}}{\partial z} \right| \quad (20)$$

and found this quantity to be essentially the same for a range of long-lived constituents in the lower stratosphere. (Actually the variance used in (20) by Ehhalt *et al.* was the variance in time at a fixed point). This result can be understood from (19) under two conditions: that the constituents are conserved on the time scale of the eddies (so that (19) is valid) and that the mean isopleth slope of all long-lived constituents is the same. The latter condition has been argued and discussed by Mahlman [1985] and Mahlman *et al.*

# DYNAMICAL PROCESSES

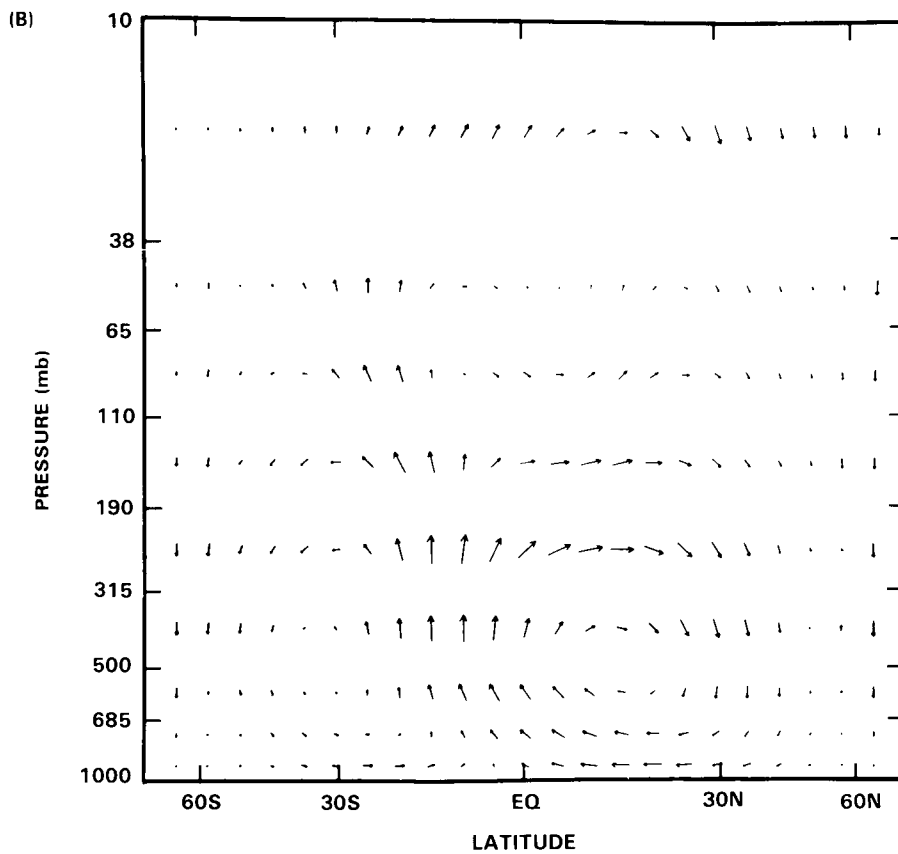
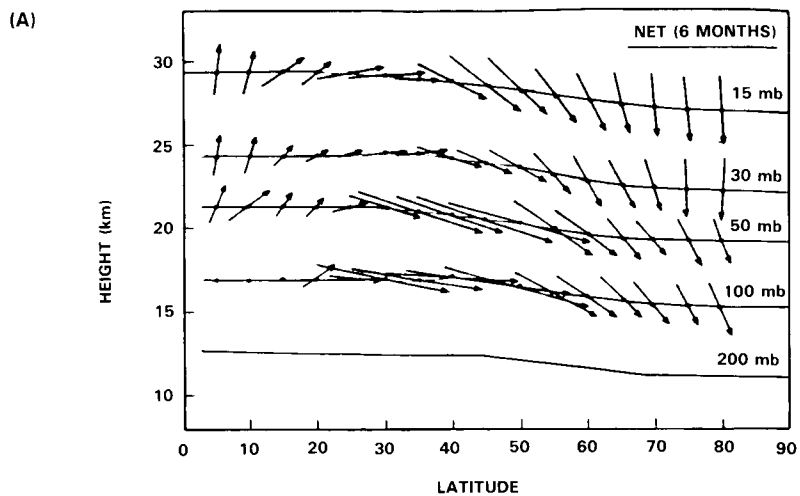


**Figure 6-51.** Model-determined transport circulation ( $V_T, W_T$ ) for Northern winter according to (a) Kida [1983a]; (b) Plumb and Mahlman [1986].

[1985]. Under these circumstances, we can equate  $\Delta^2$  in (20) with  $(\overline{\xi - \gamma\eta})^2$  in (19);  $\Delta$  is just the eddy displacement normal to the mean isopleths.

For small-amplitude eddies, then, (16) describes the transport of exactly conserved constituents in terms of advection by the transport circulation  $(V_T, W_T)$  and diffusion with a diffusivity defined by (17). This approach has been discussed further by Matsuno [1980] and Danielsen [1981]. Note that, as described thus far, these diffusivities are purely *kinematic*, i.e., they depend solely on the properties of the flow field and are independent of the constituent field. However, for non-conserved constituents, this is no longer the case. The reason for this is that additional transport effects arise – the so-called “chemical eddy” terms – which depend on the nonconservative effects. For a weak sink of the form  $s = -\lambda(q - q_0)$ , Plumb [1979] showed that (16) needs to be modified by the inclusion of an additional diffusivity  $\mathbf{K}^{(c)}$  where:

$$\begin{bmatrix} K_{yy}^{(c)} & K_{yz}^{(c)} \\ K_{zy}^{(c)} & K_{zz}^{(c)} \end{bmatrix} = \begin{bmatrix} \overline{\lambda\eta^2} & \overline{\lambda\eta\xi} \\ \overline{\lambda\eta\xi} & \overline{\lambda\eta^2} \end{bmatrix} \quad (21)$$

Similar, but more general, expressions are given by Matsuno [1980], Pyle and Rogers [1980b] and Tung [1984]. The reason for this additional effect, which is implicit in the Lagrangian-mean budget of (15) via the term  $\overline{S^L}$ , can be understood with reference to Figure 6-52. Consider a steady, laminar, non-dispersing flow (in which the kinematic tracer dispersion effects discussed above do not occur) for which the streamline is a trajectory. Consider now the mixing ratio  $q$  of a parcel moving along this trajectory; it is assumed that  $q$  has a background gradient such that high values of  $q$  are to the south. If  $q$  were exactly conserved then any parcel moving along the trajectory C would move northward at A and then return southward at B with exactly the same value of  $q$ . Thus there is no net northward transport. If  $q$  is allowed to relax toward its local mean value, however, then in that part of the trajectory between A and B, where  $q$  is greater than the local mean value (since the parcel is northward of its mean position),  $q$  decreases and therefore the parcel returns southward at B with a smaller mixing ratio than it took northward at A. Therefore there is a net northward (downgradient) flux of  $q$  induced by the nonconservative term. Since this effect is dependent on the chemistry of the constituent (or, for the quasi-conservative quantities entropy and potential vorticity, effects such as radiation) then in principle the transport properties differ from one constituent to another. As Pyle and Rogers [1980b] showed, the situation is even more complicated

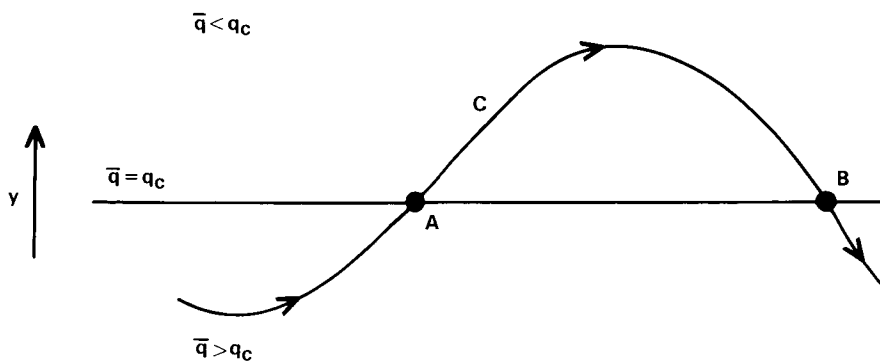


**Figure 6-52.** Illustrating the impact of nonconservative effects on eddy transport. The curve C is a trajectory. If the mixing ratio  $q$  is caused by nonconservative effects to relax toward the local mean value, then parcels move northward at A with a greater value of  $q$  than that with which they return southward at B, thus achieving a net northward transport of  $q$ . See text for discussion.

## DYNAMICAL PROCESSES

if the constituents interact with one another, since the transport properties of each constituent then depend on the structure of the others; they showed, however, that this additional complication may be avoided by restricting attention to the transport of families of interacting constituents. Further, as Tung [1984] has noted, within the range of validity of the simplified expression (21), the appropriate values of  $\mathbf{K}^{(c)}$  may be easily determined for any constituent given the kinematic statistics  $\eta^2$ ,  $\eta\zeta$  and  $\zeta^2$  (which are dependent only on the flow characteristics) and the relaxation rate coefficient  $\lambda$  for the particular constituent.

Comparing (18) and (21), it is clear that the relative contribution of kinematic dispersion and non-conservative effects to constituent diffusion depends on the ratio of timescales on which these processes act. The transport of all constituents whose chemistry is much slower than the parcel dispersion rate is governed by the same kinematic effects; those constituents with faster chemistry must be treated differently. An indication of the actual value of the critical time scales in the middle atmosphere will be discussed below.

Together, (18) and (21) reveal explicitly the now well-known dependence of transport on eddy transience and nonconservative effects. If the eddies are steady [in the Lagrangian sense demanded by the vanishing of (18)] and the constituent is conserved ( $\lambda=0$ ) then  $\mathbf{K}=0$ ; if, further, the transport circulation vanishes (which, as will be discussed below, depends on similar conditions on potential vorticity transport) then there is no transport of the constituent at all. This corollary of the celebrated "non-acceleration" theorem of Andrews and McIntyre [1976, 1978a] and Boyd [1976] has been called the "non-transport" theorem by Mahlman *et al.* [1980]. The power of this theorem stems not so much from the fulfillment of these conditions (since they are never exactly satisfied in real situations) as from the fact that it highlights those processes which are important (viz. transience and nonconservative effects) to constituent transport. It cannot be over-emphasized that the transience as defined by (17) is *Lagrangian* transience (i.e. the time derivative of Lagrangian displacement statistics) which is not necessarily related in a simple way to the properties of Eulerian statistics such as velocity variances. This distinction between Lagrangian and Eulerian behavior has on some occasions been overlooked in recent literature on stratospheric transport, even though it has long been recognized as fundamental in classical turbulent transport theory. For example, the integrated transience  $\{(\partial\alpha^2/\partial t)\cdot dt\}$  over a wave pulse (whether a temporary event or an entire winter season) necessarily vanishes if  $\alpha$  is an Eulerian quantity which is sufficiently small before and after the event. However the same is clearly not true of Lagrangian statistics as exemplified by the hypothetical example of Figure 6-49 where a wave event leaves a *permanent* distortion of material lines. A related point is that the structure of Eulerian eddy statistics is not in general a good guide to the structure of transport processes.

### 6.5.3 Gross Characteristics of Atmospheric Transport

Formulations of the form of (16) have now been used for two decades as the basis of two-dimensional transport modeling, since the pioneering work of Reed and German [1965]. The parameterization problem thus posed will be specifically addressed in Chapter 12; however a discussion of the properties of atmospheric transport as represented by such formulations is in order here. The major qualitative question that arises is whether, in practice, the meridional transport of atmospheric constituents is primarily advective or diffusive in character (or both). Reed and German [1965] made assumptions which led to the conclusion that the eddy fluxes are diffusive. More recently, however, it has been shown that these fluxes are, in the midlatitude stratosphere, better represented by an effective advection [Clark and Rogers, 1978; Plumb, 1979; Matsuno, 1980; Pyle and Rogers, 1980b; Danielsen, 1981] which to a first approximation achieves the now well-known cancellation between mean and eddy transport in the traditional formulation of (14) [Hunt and Manabe, 1968; Mahlman and Moxim, 1978] and which is thus a manifestation of the

“non-transport” theorem. These developments have led to suggestions that midlatitude stratospheric transport is primarily advective in character [Holton, 1981; Garcia and Solomon, 1983; Guthrie *et al.*, 1984; Solomon and Garcia, 1984b; Tung, 1984]. However, one needs to be careful here; as already emphasised in Section 6.2, the mean circulation - however one defines it - can never be regarded as independent of the eddies. In fact if we assume, following Plumb and Mahlman [1986], that the eddy forcing  $G$  discussed in Section 6.2 is dominated by quasigeostrophic eddy transport (a reasonable assumption for the midlatitude stratosphere) then, since  $\rho_0^{-1} \nabla \cdot \mathbf{F} = \overline{v'Q'}$  for such motions [Edmon *et al.* 1980] where  $Q$  is the quasigeostrophic potential vorticity, the steady state balance of momentum in Equation (4) becomes

$$-f_0 \bar{v}_* = \overline{v'Q'} \quad (22)$$

If it can be assumed that  $Q$  is sufficiently well conserved, its transport characteristics are the same as those of any other conserved tracer and then  $\overline{v'Q'} \cong -K_{yy} \partial \bar{Q} / \partial y$  (other terms being negligible for quasigeostrophic flow). Therefore the steady momentum budget becomes

$$f_0 \bar{v}_* = K_{yy} \frac{\partial \bar{Q}}{\partial y} \quad (23)$$

What (23) expresses is that for a steady circulation (e.g., in solstice conditions, at least) the dynamical effects of *advection* by the residual circulation and *diffusion* of potential vorticity must balance. Plumb and Mahlman [1986] used this result to argue that, globally [if not locally], the effects of advection and diffusion of long-lived tracers as expressed by (16) must be formally comparable, *provided*  $Q$  is a good enough tracer for  $K_{yy}$  in (20) to be approximated by the kinematic value appropriate to longlived tracers. A more direct practical indication of the importance of both influences is the accumulation of evidence from observations and numerical model studies that very long-lived stratospheric tracers appear to exhibit a “slope equilibrium” whereby their isopleths of constant zonally-averaged mixing ratio have almost the same shape (e.g., Figure 6-43); Mahlman [1985] and Mahlman *et al.* [1985] explain this characteristic as a balance between the steepening effects of advection and the slope-flattening effects of quasi-horizontal diffusion - certainly advection alone by a circulation such as Figure 6-48a or 6-51 would be expected to produce much steeper slopes, especially at high latitudes.

The argument that advective and diffusive transport must be formally comparable rests on the assumptions of quasigeostrophy and potential vorticity conservation [so that (22) and (23) respectively are valid]. If planetary waves are the primary vehicles for stratospheric transport (which seems very likely, notwithstanding the possible contribution from gravity waves noted elsewhere in this chapter) then the first assumption is justifiable. The second, however, may be suspect where radiative effects contribute significantly to wave dissipation and hence to  $\overline{v'Q'}$ . Indeed, in theory one can conceive of situations of a non-dispersing wave ( $K_{yy} = 0$ ) which exhibits a nonzero potential vorticity flux by virtue of radiative dissipation; then, by (22), the wave would drive a nonzero residual circulation without any accompanying diffusion of conserved constituents. In general, diffusive transport will be comparable with advective transport whenever dispersion is a significant contributor to potential vorticity transport. This appears to be a safe assumption in the lower stratosphere where radiative time scales are long (20 days or so) and where the mixing processes described in Section 6.4 are quite intense (during winter - all transport processes are weak in the summer stratosphere). The situation is less clear in the upper stratosphere, where radiative time scales are only a few days. However planetary wave mixing is also intense in the winter upper stratosphere and so, even here, dispersive effects may be a major component of potential vorticity transport. It is clearly conceptually important to establish whether this is so.

## DYNAMICAL PROCESSES

In the mesosphere, where gravity waves become the dominant vehicle for momentum transport, the quasigeostrophic assumption breaks down. However, as will be discussed below, estimates of diffusivities in the mesosphere imply that here also diffusion (in this case, in the vertical) is a major component of constituent transport.

In order to represent transport processes satisfactorily, it is necessary to know their structure as well as their intensity. McIntyre and Palmer [1983, 1984] noted that quasi-horizontal mixing events in the northern winter stratosphere, revealed in potential vorticity maps of Figures 6-24 and 6-44, occur primarily in a mid-latitude "surf zone", associated with the deformation of material lines, e.g., in the vicinity of the Aleutian anticyclone. Studies of tracer diffusion in numerical models [Kohno, 1984; Mahlman, 1985; Plumb and Mahlman, 1986] have also revealed such a zone of maximum mixing in this region; the morphology of the process, discussed by Mahlman [1985] and illustrated in Figure 6-53 is, not surprisingly, similar to that revealed by McIntyre and Palmer's potential vorticity maps. An example of Plumb and Mahlman's results for the horizontal diffusion coefficient in the GFDL model is shown in Figure 6-54. The result that the diffusion is weak in high latitudes (where Eulerian measures of planetary wave amplitude such as geopotential height or northward velocity maximize) and strong in the subtropics (where Eulerian amplitudes are weak) illustrates the point made earlier about the importance of distinguishing between Eulerian and Lagrangian eddy statistics. The dispersion of material lines tends to be strongest where the mean zonal winds are weak; in fact, for small amplitude stationary waves, the northward displacement amplitude  $|\eta|$  is related to the geopotential amplitude  $|\phi'|$  by  $|\eta| \cong |\phi'|/(\bar{u})$ . Therefore, although  $|\phi'|$  maximizes at middle-to-high latitudes where the zonal winds are strong (cf. Figures 6-4 and 6-5),  $|\phi|$  maximizes in the subtropics where  $\bar{u}$  is weak. In fact the location of the  $\bar{u} = 0$  surface, which is indicated on Figure 6-54, seems largely to determine the locations of strong horizontal diffusion in the GFDL model. This suggests that the transport processes are dominated by the quasi-stationary waves, although in reality the transports will be strongly modulated by the transients discussed in Section 6.1.4 (cf. Figure 6-11).

In both the studies of Kohno [1984] and Plumb and Mahlman [1986] the mixing was found to be weak in high latitudes. However, as discussed in Section 6.3, general circulation models apparently underrepresent high-latitude dynamical activity in the stratosphere; therefore it seems likely that transport is underestimated here. In a mechanistic model of a high-latitude warming event, Hsu [1980] demonstrated strong high-latitude dispersion of air parcels; synoptic potential vorticity and ozone maps at the time of such events appear to confirm substantial latitudinal transport at these times.

Of course, planetary wave mixing does not take place purely in the horizontal plane. Mahlman *et al.* [1981] and Tung [1982, 1984] suggested that, for the almost adiabatic conditions typical of much of the stratosphere on the time scales of interest, the mixing should occur along the isentropic surfaces. Mahlman [1985], however, has noted some caveats in this argument; Plumb and Mahlman [1986] in fact found the mixing to occur along directions a little steeper than the mean isentropes. Since the residual and transport circulations are equal if the mixing is isentropic [Holton, 1981; Plumb and Mahlman, 1986], this result explains the similarity between these circulations evident from Figures 6-48a and 6-51.

A schematic summary of our current view of zonally-averaged transport phenomena in the troposphere, stratosphere and mesosphere is shown in Figure 6-55. This figure is based on that of Kida [1983b] with modifications incorporating results of Plumb and Mahlman [1986] and the characteristics of mesospheric advection and diffusion described in Section 6.2. We shall here summarize the major characteristics of transport in the troposphere, stratosphere and mesosphere as we currently understand them; the important and complex issue of troposphere-stratosphere exchange is considered separately in Chapter 5.

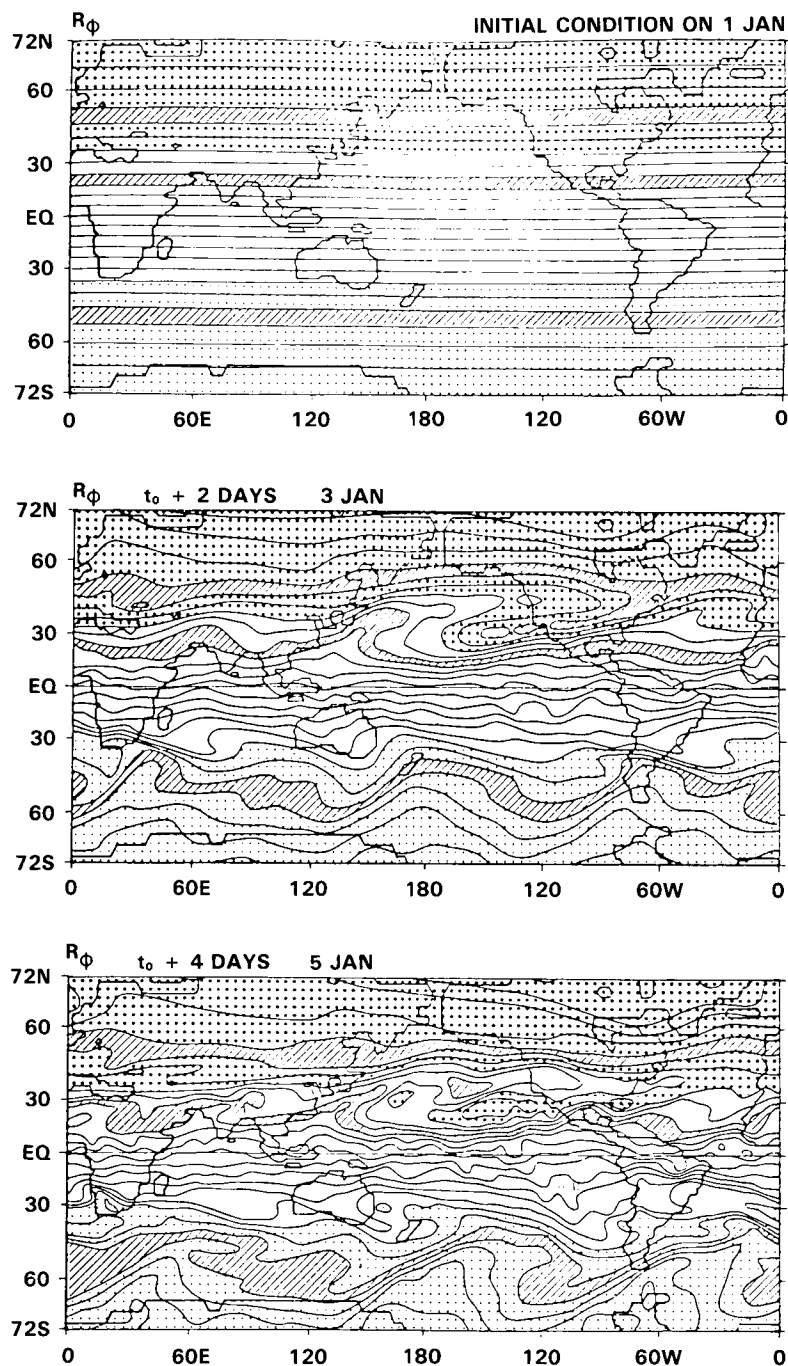


**Figure 6-53.** Isopleths of modeled evolution of mixing ratio on the 480 K isentropic surface of a conserved tracer initially (1 Jan) stratified uniformly in latitude. [After Mahlman, 1985].

Tropospheric transport is the most complex, with advection by the Hadley circulation, quasi-horizontal mixing associated with planetary and synoptic eddies and vertical convective mixing all significant contributors to large-scale transport. On the whole, transport time scales are relatively short - for example, Plumb and Mahlman's [1986] estimates for  $K_{zz}$  give time scales for vertical diffusion over the tropospheric

DYNAMICAL PROCESSES

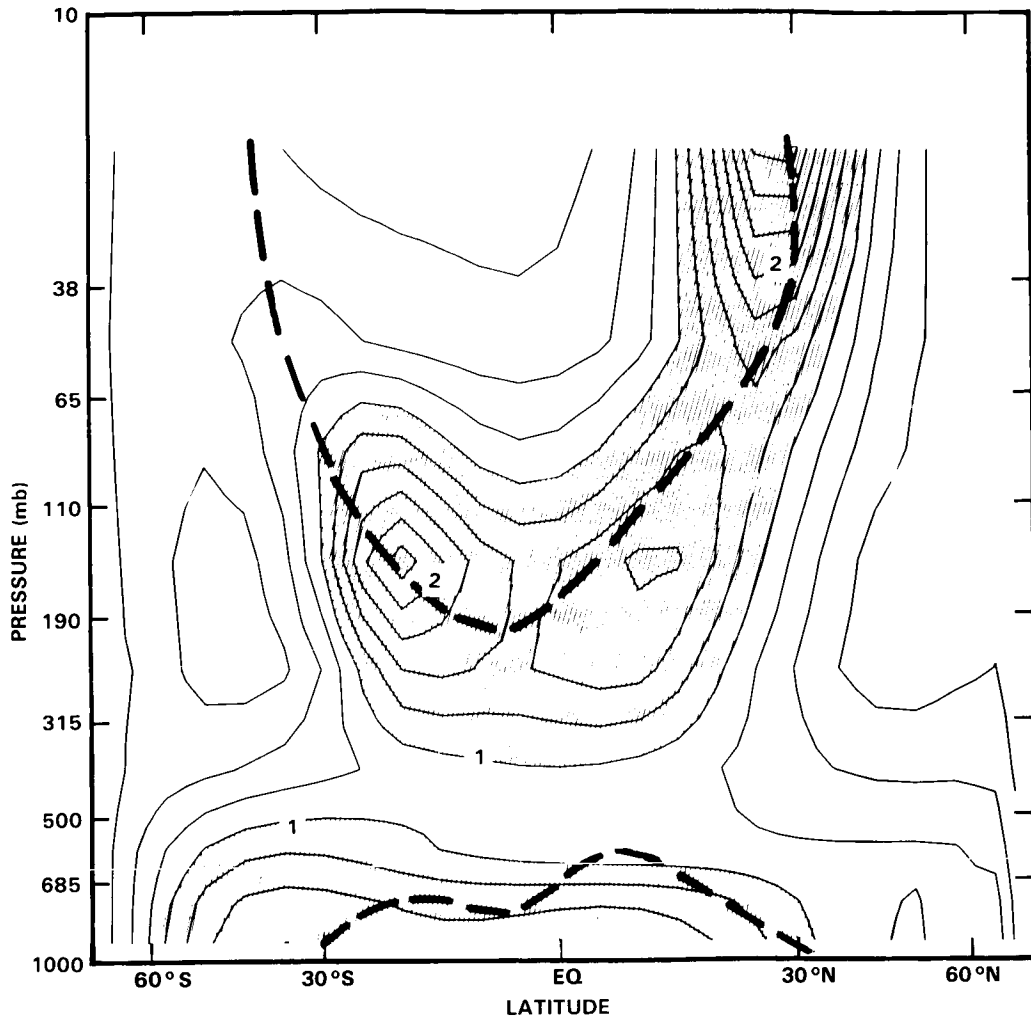


**Figure 6-54.** Calculated horizontal diffusivities ( $10^6 \text{ m}^2 \text{ s}^{-1}$ ) for the GFDL general circulation/tracer model in January [after Plumb and Mahlman, 1986]. The dashed curve is the line of zero zonal-mean wind.

depth ranging from 10-30 days in the tropics to 30-100 days at middle and high latitudes - so that long-lived tracers with weak local sources and sinks will be well-mixed through the troposphere.

The stratospheric situation seems simpler, with transport largely dictated by the quasi-stationary eddies (via direct quasi-horizontal mixing and indirectly via the wave-driven meridional circulation). Vertical diffusion is relatively unimportant here. In Section 6.2 it was estimated that the contribution to  $K_{zz}$  from small-scale turbulence is at most  $0.2 \text{ m}^2 \text{ s}^{-1}$ , and Kida [1983a] and Plumb and Mahlman [1986] found similar values for large-scale transport in their model studies; these values give vertical mixing times over one scale height of a few years or more, too long to be competitive with the processes noted above. (An independent upper limit on the vertical diffusion rate for momentum in the equatorial lower stratosphere comes from the existence of the QBO, which, as discussed by Plumb [1984], requires the momentum mixing timescale to exceed about 2 years). Kida [1983a] noted that the relative importance of advection and quasi-horizontal diffusion for any particular tracer depends on the meridional slope of the tracer isopleths; for slopes characteristic of long-lived tracers, both he and Plumb and Mahlman [1986] estimated the two

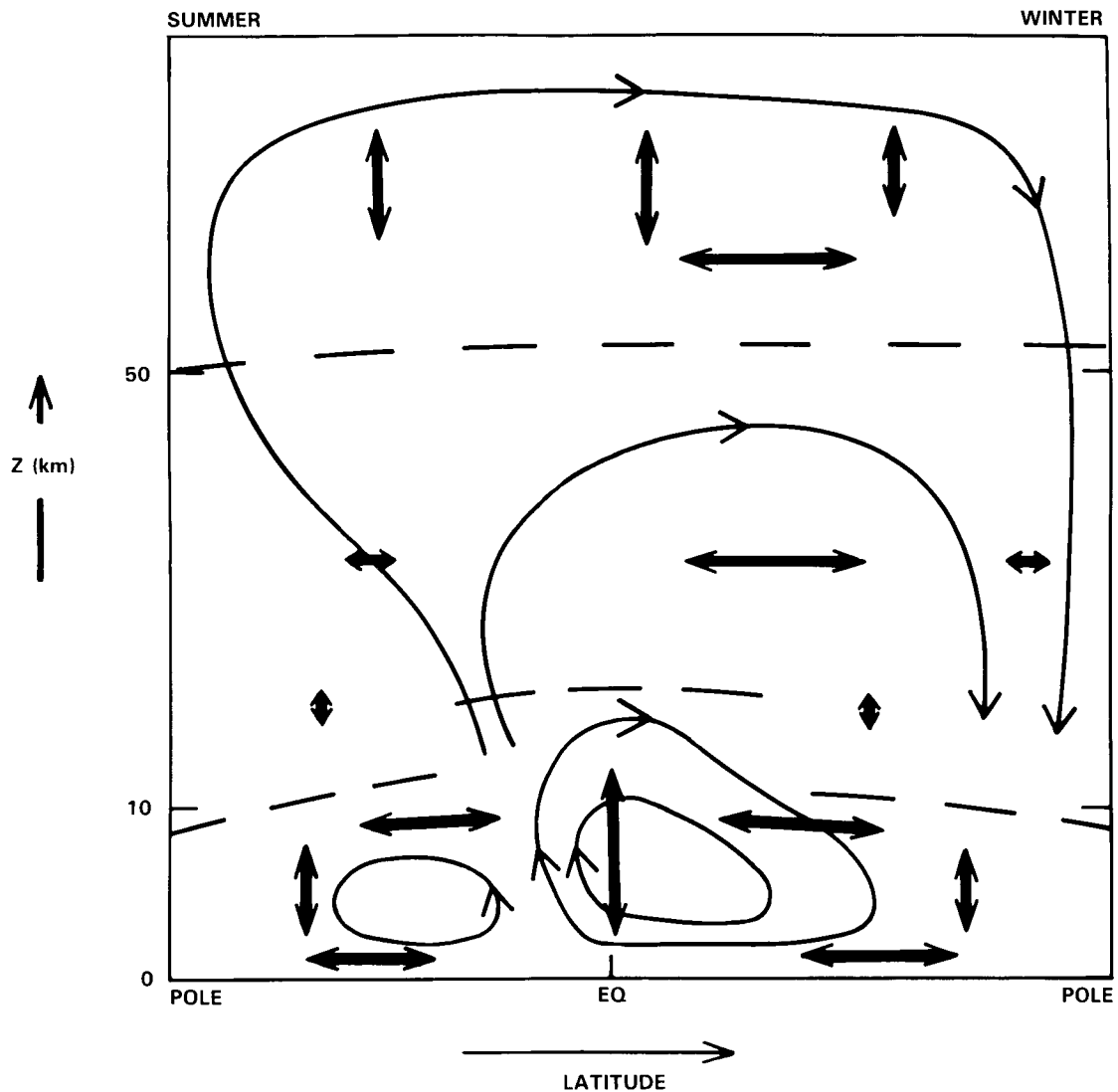


**Figure 6-55.** Schematic illustration of zonally-averaged transport processes up to the mesopause. Single arrows: mean circulation; double arrows: quasi-horizontal and vertical diffusion. See text for discussion.

to be of comparable importance. (Indeed, as noted above, it seems to be this balance that determines the isopleth slopes). Kida estimated a typical global value in the lower stratosphere of  $K_{yy} \cong 3 \times 10^5 \text{ m}^2 \text{ s}^{-1}$ , although, since his model stratosphere is dynamically less active than the observed stratosphere, this is likely to be an underestimate. Plumb and Mahlman's results, shown in Figure 6-54, are similar to this value in the summer hemisphere and in winter middle and high latitudes but much larger (up to  $2 \times 10^6 \text{ m}^2 \text{ s}^{-1}$ ) in the "surf-zone" of the winter subtropics.

In the mesosphere, planetary wave amplitudes decrease and control of transport processes appears to be dominated by gravity waves, through vertical mixing and the strong wave-driven pole-to-pole circulation. These processes are very rapid, with a characteristic hemispheric advection time scale, given  $V_T \cong 10 \text{ m s}^{-1}$ , of about 10 days and a similar time scale for vertical mixing over a scale height, given  $K_{zz} \cong 10^2 \text{ m}^2 \text{ s}^{-1}$  (comparable with the values estimated in Section 6.1 for momentum mixing). However,

## DYNAMICAL PROCESSES

one should note the suggestion of Chao and Schoeberl [1984] and Fritts and Dunkerton [1985] that the diffusivity associated with breaking gravity waves for heat and, by implication, long-lived constituents, may be much smaller than that for momentum. It might also be mentioned in passing that quasi-horizontal mixing processes may not be altogether negligible; in particular Craig *et al.* [1985] have noted the probable impact on tracer distributions of summertime pulses of "two-day wave" activity.

### 6.5.4 Some Outstanding Issues in 2D Modeling

Following the discussion in Section 6.5.2 it would be fair to conclude that a profound change has taken place over the past ten years in our conceptual formulation and understanding of zonally-averaged transport problems. More recently, this has begun to impact on the practice of 2-D modeling, in particular in models using the residual circulation, rather than the Eulerian mean circulation, as a basis [e.g., Holton, 1981; Garcia and Solomon, 1983; Ko *et al.*, 1985; Rogers and Pyle, 1984]. This circulation should be a good approximation to the transport circulation in the stratosphere, though less so in the troposphere [Plumb and Mahlman, 1986]. More recently still, we have seen objective assessments of transport processes and their magnitudes in numerical models and, as discussed in preceding sections of this chapter (particularly 6.4.4), we are beginning to understand the morphology of large-scale transport processes. Together, these advances are for the first time permitting real insight into the dynamics of these phenomena and have, amongst other things, led us to appreciate the practical importance of kinematic transport effects (i.e., large-scale turbulence), which in some recent literature has been played down in favor of the so-called "chemical eddy" terms.

While some of these GCM-based parameterizations are being applied in 2-D models [Enting, 1985; Pitari and Visconti, 1985; Plumb and Mahlman, 1986] it would seem desirable (in view of the shortcomings of GCMs discussed in Section 6.3) to obtain similarly objective representations of the actual atmospheric circulation. Deriving the full set of transport coefficients from first principles requires accurate information on horizontal *and* vertical winds or constituent fluxes - hence the dependence hitherto on GCM data, since accurate observations of vertical winds or fluxes on a global scale are just not available (nor are they likely to be in the foreseeable future). However, some progress may be attainable on the basis of assumptions about the characteristics of eddy transport. The most promising such assumption is that the eddy motions are almost adiabatic [Mahlman *et al.*, 1981; Tung, 1982, 1984]. Under these conditions, the transport circulation may be represented by the residual circulation [Holton, 1981; Plumb and Mahlman, 1986] - which can, at least at the solstices, be approximated by the diabatic circulation, which in turn may be determined from a radiation calculation - while the diffusion tensor collapses to a scalar diffusivity representing mixing along the isentropes, whose determination then only requires quasi-horizontal (isentropic) information on the flow or constituent fluxes. Thus the problem of deriving the transport coefficients from atmospheric data becomes practicable - though still difficult. A preliminary effort in this direction has been made by Newman *et al.* [1986] using satellite-based analyses to derive potential vorticity fluxes and thence to estimate the quasi-horizontal diffusivities. However, there are some problems with the calculation of potential vorticity fluxes in the stratosphere (this flux is proportional to the divergence of the EP flux; intercomparisons of this quantity were discussed in Section 6.4.2), and, at least in the upper stratosphere, potential vorticity may not be representative of long-lived tracers. Perhaps studies of long-lived trace constituents (satellite observations of which are now becoming available as discussed in Section 6.4) will provide alternative avenues.

These procedures - and, indeed, most of the body of the theory outlined in Section 6.5.2 - rely on a complete knowledge of a *given* (real or model) atmospheric circulation. It must be emphasized, of course,

because of the relation between the advective and diffusive components and of the dependence of equilibrium tracer isopleth slopes on the balance between the two, that the two should be represented in a mutually consistent way. There appear to be two ways of achieving this; the first is simply to calculate the two from the same circulation data (e.g., the GCM-based calculations discussed above). A second approach is, given the diffusivities  $K$ , to calculate diagnostically the residual circulation corresponding to this eddy transport (via Equation (23) or via the coupled heat and momentum budgets as in, for example, the model of Garcia and Solomon [1983]). The latter approach, however, implicitly invokes the assumption that entropy and/or potential vorticity may be regarded as long-lived tracers and, as noted above, this assumption may be suspect above the middle stratosphere.

Another, less direct, way of estimating the diffusivities from the observed atmospheric behaviour is to tune 2-D models to reproduce the observed distributions of long-lived constituents [e.g., Ko *et al.*, 1985]. However, this procedure is not suitable for revealing more than the gross magnitudes of the diffusivities. Moreover, if the mean circulation used in the model is in error, similar errors will be produced in the calculated diffusivities, in order to give the "correct" balanced state.

The detailed formulation of 2-D models currently in use for assessment purposes is discussed in Chapter 12 of this document and a comparison of model assessments is presented in Chapter 13. Differences between the various models - in the model chemistries as well as transport formulations - are manifested in such comparisons; it is not easy to determine, however, to what extent the differences in representation of transport are responsible for differences in results. From a dynamical point of view, it would be desirable to compare the behavior of models with identical chemistries. The easiest way of achieving this is to bypass the model chemistries altogether by running an experiment with an inert tracer, spreading out from an initially localized source. An ideal case would be the "instantaneous midlatitude source" experiment of Mahlman and Moxim [1978] (cf. Plumb and Mahlman [1986]; not only would this allow comparison of the transport characteristics of the 2-D models with a 3-D model, but also with the observed behavior of the radioactive debris from the atmospheric bomb tests in the early 1960s. Such a comparison would highlight any major inadequacies in model transport formulations.

For practical as well as theoretical reasons, transport parameterizations are usually designed to represent monthly or seasonally averaged transport. Thus such representations are incapable of modeling transport variability on time scales less than about a month or longer than the annual cycle. We have seen in Section 6.1 that wave amplitudes and fluxes can fluctuate markedly on time scales as short as 1-2 weeks, especially (but not only) during winter warming events. In principle - given the required circulation data - the transport coefficients could be determined day by day to enable this variability to be incorporated into 2-D models. Plumb and Mahlman [1986] have argued, however, that 2-D models are not well posed on these time scales, and it may therefore be necessary to rely on three-dimensional studies [e.g. Rose and Brasseur, 1985].

On interannual time scales, 2-D models are in principle better suited to representing transport variability. The approach has been applied, with some success, to modeling the QBO in ozone, driven by the QBO in tropical winds and temperatures [Hasebe, 1984; Ling and London, 1985]. The more general question of the impact of year to year variations in the circulation of the winter middle atmosphere is more difficult to address. The problem is not so much theoretical - given an adequate (real or model-generated) multiyear data set, one could in principle generate transport coefficients month by month or season by season - as philosophical, viz., to define what it is that one is trying to model (a particular year or a "typical" year?). This issue, which is not confined to 2-D transport models, becomes particularly acute for model validation.

## DYNAMICAL PROCESSES

We are now beginning to appreciate the large interannual variability of wind and temperature fields in the winter stratosphere [Labitzke and Naujokat, 1983; Geller *et al.*, 1984; see Section 6.1.8]. The impact of this variability on constituent transport needs to be addressed; since the wind and temperature variability is presumably indicative of variability of the transport processes, this impact is likely to be major. A related question, since the frequency and intensity of warming events are variable from year to year, is how much of the "average" wintertime transport is associated with such events. If they account for a substantial fraction of the net transport, then the adequacy of current models (including most GCMs) is open to question.

A further issue arises in long-term assessment studies. If a model is being used to predict changes in the distribution of radiatively active constituents such as ozone, should the model be "interactive" in the sense that some attempt be made to allow the model to respond to the changing climate? This question can be answered in part from the discussion of Section 6.2. From this discussion and the results of Fels *et al.* [1980] described in Section 6.3, we have seen that both the distribution of mean diabatic heating  $\bar{J}$  and the residual circulation  $\bar{w}_*$  are, to a good approximation, outside the tropics, determined by the eddy transport. If the latter is fixed, then so are  $\bar{J}$  and  $\bar{w}_*$ . Therefore, they are - to a first approximation - unaffected by changes in radiatively active constituents, as the results of Fels *et al.* [1980] clearly demonstrate. The mean temperature will, in general, change in order to maintain  $\bar{J}$  as will the mean zonal wind, to maintain thermal wind balance with the temperature distribution. (A detailed assessment of the impact of changing trace gas distributions on climate is given in Chapter 15). It may well be important to allow these temperature changes to impact on model chemistry. However, changes in *transport* can only occur if the mean temperature and zonal wind distributions change so much as to impact significantly on the eddy motions themselves (via altered propagation or dissipation characteristics) and, of course, that is a three-dimensional problem. Therefore it is futile in a 2-D model to attempt to predict changes in the residual circulation, for example, rather than specifying it at the outset, simply because 2-D models are by their nature incapable of addressing situations where such effects are important.

### 6.5.5 Three-Dimensional Modeling

The recent advances in the theory and practice of 2-D transport modeling which have been reviewed above have brought the zonally-averaged model to the level of a sophisticated assessment tool. At the same time, however, fundamental limitations of the zonally averaged approach have become increasingly apparent. We must look to three-dimensional models to overcome these limitations. As we have seen in Section 6.3.3, however, even three-dimensional models are not without their limitations, particularly in regard to their deficient climatology in the winter stratosphere and the prohibitive cost of including full chemistry for extended integrations.

On short time scales, the use of such models for data assimilation in forecast mode offers an exciting avenue for exploiting the detailed, global observations of constituent distributions now available from satellites and described in Section 6.4. Thus, we can expect to learn much about mixing events on these time scales and, by implication, of long-term transport since this is to a large degree the aggregate of these events.

For seasonal time scales and longer, three-dimensional models with simplified chemistry have taught us much about large-scale transport processes, as well as providing data bases from which to derive parameterized transport formulations for 2-D models. In order for the models to reach their full usefulness, however, the deficiencies in GCM climatologies noted in Section 6.3.3 will need to be overcome.

The use of three-dimensional models (with realistic chemistry) for long-term assessment experiments appears to be out of the question in the foreseeable future and there is therefore a continuing need for zonally-averaged models, despite their shortcomings. It is possible that some of these shortcomings could be overcome through the development of three-dimensional models that seek not to represent the transport associated with every eddy, in the way a GCM does, but rather to represent the aggregate effects of eddy transport in a similar way to a 2-D model, but relative to a slowly evolving, nonzonal basic state. This approach, which is similar to that suggested by McIntyre and Palmer [1983], would involve models with lower spatial and temporal resolution than GCMs and which would therefore be capable of incorporating more complex chemistry and of being integrated for longer times. However, developments in transport theory will be needed. While some progress is being made in the understanding of three-dimensional processes in tropospheric dynamics [e.g., Hoskins, 1983] we are still a long way from a simple understanding of transport relative to spatially nonuniform basic states.

## 6.6 FUTURE NEEDS

### 6.6.1 Satellite Observation

With the emergence of continuous global satellite measurements our picture of dynamical and transport processes in the middle atmosphere has sharpened considerably. They have made possible the identification of a number of transient waves hitherto unresolved, and have vividly exposed the complexity of transport as the westerly vortex evolves during disturbed conditions. Our knowledge of the morphology of a number of chemical constituents has also been advanced by these observations. Unfortunately with this improved focus on stratospheric behavior so too has emerged a recognition of the limitations posed by current observations and the need for even more sophisticated measurements. Perhaps the most striking demand of this sort stems from the possibility of planetary wave breaking, which may lead to a significant cascade to smaller scales. An irregular distribution of some quantity such as potential vorticity implies not only a high degree of spatial variance but also temporal variability through the advection of parcels by the flow field. Dynamical features such as the fast equatorial waves (Section 6.1.5) also place constraints on the quality of observations required. Such considerations appear to be increasingly significant at upper levels due to the tendency for the wave spectrum to be dominated by higher frequencies and the increasing amplitudes of gravity waves and tidal oscillations.

One of the chief difficulties in applying satellite data is dealing with their asynoptic nature. A "transience error" arises from the fact that measurements are not made simultaneously [Hartmann, 1976a], but rather are taken at different locations at different times. Their analysis therefore presumes some form of space-time interpolation. Several methods of estimating synoptic fields from asynoptic data have been employed [Rodgers, 1976b; Hirota, 1976]. These range in sophistication from presuming simultaneity over a day of measurements to four-dimensional assimilation in numerical forecast models.

The latter approach, although considerably more involved, has some advantages, such as the the ability to provide the ageostrophic velocity components. Whether these and higher order quantities are more of a reflection of the data or of the model, however, is unclear. Alternative approaches of deriving such quantities directly from temperature retrievals have also been proposed [Salby, 1982b]. Recently it has been shown [Salby, 1982b] that synoptic maps may be recovered uniquely from asynoptic data provided that the observed field is adequately sampled. The temporal scales that can be resolved in asynoptic measurements depend on whether single or combined node (ascending and/or descending) data are used. In the former case, frequencies up to 0.5 cpd can in principle be recovered, while in the latter synoptic irregularities at middle and high latitudes, intrinsic to asynoptic data, are explicitly accounted for [Salby,

## DYNAMICAL PROCESSES

1982a]. By taking into account these sampling irregularities of combined node data, Prata [1984] was able to obtain the wavenumber 2 component of the 4-day wave, previously unobserved. The aforementioned issues determine how frequently it is sensible to map synoptic data.

Considerations of synoptic sampling and resolution are more general than applying solely to dynamical quantities. They pertain equally to unsteady disturbances in any field, e.g., distributions of chemical species. The question of resolution then reduces to how much of the spatial and temporal variability is captured by the sampling. For example, localised features in potential vorticity or a constituent will not be resolved if their dimensions are comparable to the spacing of the data or if the feature moves appreciably over the time it takes the satellite to circle the globe.

Another important example arises in connection with diurnal variations, which may accompany tidal oscillations or a photochemically active species. Such features are not resolved by observations from a single sun-synchronous satellite because the orbit drifts westward at the same rate as the feature and thus views the same relative point on the feature with each latitude crossing. Global observation of such phenomena will require measurements from multiple satellites.

Many quantities central to dynamical and hence transport considerations, e.g., motion fields, potential vorticity, Eliassen-Palm flux divergence, are not measured directly but rather must be derived from observed temperature behavior. Such quantities are higher order in that they involve one or more derivatives of observed fields. The availability of direct velocity measurements such as will be made on UARS should be of great value in obtaining such quantities. Differentiation has the effect of increasing the spatial variability of the fields and eroding the signal to noise ratio, perhaps below useful values. Of course, fields such as potential vorticity are themselves of inherently richer structure than lower order quantities, making it difficult to distinguish legitimate features from observational error. Multiple satellite observations and scanning radiometers may be valuable in alleviating this problem. However the assimilation of such data will require that spatial and temporal irregularities of the combined sampling be accounted for, in order that the full information content of the data be recovered.

There also exists a need for refined vertical resolution. Rocketsonde and radiosonde measurements suggest that dramatic changes in temperature can occur within quite a thin layer of the stratosphere during sudden warmings. In order to capture such behavior in global analyses, it may be necessary to make use of different observing systems, both satellite- and ground-based. Rocketsonde measurements have historically been invaluable in validating remote temperature retrievals. Their waning in recent years presents a problem for future missions. As was noted above, one of the prime virtues of satellite observations is their homogeneity. The importance of long-term continuity with regard to the monitoring of trends and expanding our understanding of the complex realm of stratospheric behavior cannot be overstated. It is hoped that further remote sensing missions will be planned to succeed UARS following 1989.

Despite some recent examples to the contrary, most studies of the middle atmospheric circulation are still focused on midlatitudes of the Northern Hemisphere. What we have learned of the climatology and transient behavior of the Southern Hemisphere has confirmed and indeed strengthened the impression of significant differences between the two hemispheres during their respective winters, and a fuller exploitation of the contrast between these two regions will surely help to further our understanding of both. Southern Hemisphere analyses are currently undermined to some extent by the relatively poor quality of low level analyses upon which to build; this is another area where direct wind measurements (such as will be provided by UARS) will prove invaluable.

The middle atmosphere tropics have received even less attention than the Southern midlatitudes. To some extent this is a result of the weak temperature structure in low latitudes; again, direct wind measurements will be needed before much of the tropical circulation is visible in satellite observations. Equatorial wave motions, with their small vertical scales, have been revealed by limb-viewing instruments and there is a continuing need for such observations.

### 6.6.2 Ground Based Studies

The use of radars and more recently lidars has led to a significant improvement in our understanding of wave and turbulence processes in the middle atmosphere. Radars offer the capabilities of measuring important time-mean quantities such as  $\bar{u}$ ,  $\bar{v}$  and  $\bar{w}$  as well as the eddy flux terms  $\overline{u'^2}$ ,  $\overline{u'w'}$  etc., while lidars give information on  $\bar{q}$ ,  $\bar{T}$ ,  $T'$  etc. Although the usefulness in studying large-scale phenomena is limited by the local nature of radar measurements, they offer the advantage over satellite retrievals that they measure the velocity field directly. This feature makes them particularly attractive in the tropics where geostrophy breaks down. There they may serve as independent verification of velocities derived from remotely monitored temperatures.

If the potential of ground-based techniques is to be fully realised, then a number of deficiencies need to be rectified. At present many radars operate on an irregular basis and it is desirable that their operation be made continuous to make long-term measurements throughout as much of the middle atmosphere as possible. In particular, the possible influence of gravity waves on the stratospheric circulation (see Section 6.2.4) needs to be investigated. Coordination of observations is also important; this is an issue being partially addressed by projects organized under the auspices of the Middle Atmosphere Program.

At present most radars are located in continental areas where the effect of topographically forced waves may be significant. In order to assess the global role of gravity waves it is therefore important that radar measurements be made in oceanic regions. Observations in equatorial regions are almost non-existent and the establishment of radars near the equator is crucial for the study of gravity and tropical waves. The predicted breakdown of the diurnal tide in the equatorial mesosphere has yet to be investigated experimentally.

The construction of radar networks will help with the identification of wave sources and with the measurement of important wave parameters such as horizontal phase velocities and wavelengths. For example, a valuable application would be the construction of an array of sounders along the equator downfield from a convective center such as Indonesia. Cross-spectral analyses could then be performed on the combined array of velocity profiles to derive structural and temporal behavior of the motion field. This would facilitate the analysis of particular wavenumber-frequency bands so that individual components (e.g., Kelvin waves) could be discriminated for.

The widespread use of lidar investigations of density and temperature is to be encouraged. As well as providing complementary information to the radars, lidars give information in the 30 to 60 km height range (the so-called 'gap'). By colocating radars and lidars it will be possible for the first time to measure heat fluxes, albeit locally, in the mesosphere.

Finally, it is noted that the more widespread use of lidar measurements of temperature and density may help to compensate for the decreasing number of rocket measurements due to the reduction in the meteorological rocket network. This would be especially the case if lidar techniques can be extended to wind measurements.

## DYNAMICAL PROCESSES

### 6.6.3 Dynamical Theory

Section 6.2 has discussed the importance of eddy motions – especially planetary waves in the winter stratosphere and gravity waves in the mesosphere – in maintaining the climatological state of the middle atmosphere. It has also been emphasized that it is misleading to regard the residual circulation as independent of the eddy forcing or as a “diabatic circulation” *driven* by an externally-imposed net radiative heating. Some general questions in this area which will require particular attention in the near future include the following:

#### (a) Planetary-Wave Breaking

McIntyre and Palmer [1983, 1984] have suggested that breaking planetary waves (Section 6.2.4) may bring about substantial mixing of potential vorticity in the stratosphere and may thereby be responsible for the region of weak potential vorticity gradient (which they call the “surf zone”) often observed to surround the main cyclonic vortex in the northern winter mid-stratosphere. A combination of theoretical and observational studies will be required to confirm this mixing hypothesis and to assess the impact of diabatic processes on the breaking-wave phenomenon. Indeed, improved understanding of the relative roles of mixing and diabatic processes in net potential vorticity transport is important not only to our understanding of the dynamical structure of the middle atmosphere, but also to our conceptual picture of stratospheric transport. The feedback effects of the wave-induced mean flow changes on the wave propagation characteristics also need further study. For example it has been speculated [McIntyre, 1982; McIntyre and Palmer, 1983, 1984] that the weakened potential vorticity gradients in the subtropics may inhibit the meridional propagation of planetary waves and thus form “resonant cavities” which may enhance the local growth of the wave amplitudes. A related requirement is for a careful combination of theoretical and observational studies of sudden warmings and a clearer understanding of the relationship between the “zonal-mean, eddy” approach and the “synoptic map” approach mentioned in Section 6.2.5.

#### (b) Gravity Wave Drag

An increased understanding of the basic mechanics of gravity-wave breaking is needed for the development of improved parameterizations of the effects of such breaking on the zonal-mean flow and on planetary waves. For example, more account may need to be taken of the effects on the parameterizations of including a broad-band spectrum of gravity waves, rather than the small discrete sets of wavenumbers and phase speeds that have mostly been used hitherto. The relative magnitudes of the gravity-wave induced diffusivities of momentum, heat and constituents [Chao and Schoeberl, 1984; Fritts and Dunkerton, 1985] also need to be investigated.

It is particularly important that the role of gravity waves in the stratosphere be better understood. The “cold pole” problem of middle atmosphere GCMs is suggestive of weak wave drag in these models, and one process that could be lacking in these models is gravity wave drag.

#### (c) General Theory

There is a need for a basic theoretical framework, perhaps analogous to the “zonal-mean, eddy” framework, but more suitable for the organization and interpretation of data concerning strongly zonally-asymmetric planetary-scale disturbances in the middle atmosphere.

#### 6.6.4 General Circulation Models

While there have been several notable successes that have been associated with middle atmosphere GCMs, considerable caution should be exercised in carrying over GCM-derived results to the actual atmosphere. This is so because there are several well known deficiencies in middle atmosphere GCM simulations. These include the cold winter pole/excessive westerlies problem (and the associated problem that middle atmosphere GCMs do not produce stratospheric warming episodes of sufficient intensity). From these deficiencies, we conclude that existing middle atmosphere GCMs are probably deficient in eddy transport effects and in the strength of their residual mean circulation. Thus, we expect that 2-D transport parameters calculated from GCMs will be too small compared with those that are representative of the actual atmosphere. Furthermore, since the derivation of those transport parameters formally depends on the assumptions of small amplitude theory, it is possible that 2-D representations of 3-D dynamical transport may be less applicable and work less well in the real atmosphere than in GCMs.

The wintertime "cold pole" problem is perhaps the most serious deficiency of current middle atmosphere GCMs. As we have seen, dynamical theory ascribes this problem to an under-representation in the models of wave drag on the flow. This could be a result of the forcing of planetary waves in the model being too weak because of inadequate representation of orography or an inadequate parameterization of convective heating in the troposphere, or because of the importance in the real world of other wave motions which are not adequately resolved in the models. Indeed, the underlying problem - one which the shortcomings of GCMs may be helping to solve - is our incomplete understanding of the momentum budget of the middle atmosphere. As discussed in Section 6.4, several studies have highlighted the difficulty in balancing the momentum budget from analyses of the observed circulation. It is not clear whether these results indicate data inaccuracies on the large scale or whether small-scale, unresolved motions are making a significant contribution. The crucial role of gravity wave drag in the mesosphere is now appreciated and it is essential that its role, if any, in the stratosphere be fully clarified. Improved understanding of this process is a prerequisite to improved parameterization in models.

As mentioned previously, the application of GCM-derived parameters to the actual atmosphere is limited by the fact that middle atmosphere GCMs show some very significant modeling deficiencies. There is an alternative to using a GCM for middle atmosphere studies. This is the forecast/analysis sense in which available data is continually inserted into the GCM, which is then used as an analysis tool to produce regular gridded analyses of both observed and unobserved variables. That is to say, the GCM governing equations are used to both provide both continuity in the observables and to derive such unobservables as the ageostrophic wind components. Thus, using the output from GCM forecast/analysis will give the balanced dynamic fields that are needed for transport studies but are consistent with observations. It must not be overlooked, however, that results of such procedures will be model-dependent and it is important that their robustness be assessed.

Several groups in the world are now attempting to perform transport-chemistry studies using GCMs. Most of this work has been aimed at understanding the dynamical and chemical processes that maintain observed species distributions. Complex chemistry schemes have not been used in GCMs for several reasons. One is the great expense and complexity in doing so. Another is related to the problems that GCMs have in reproducing the observed atmospheric structure. The use of GCMs to forecast multidecade ozone scenarios is not envisaged in the near future.

## DYNAMICAL PROCESSES

### 6.6.5 Transport Theory and Modeling

Theoretical developments over the past decade have *in principle* provided a stronger theoretical basis for the parameterization of eddy transport of trace constituents in 2-D (zonally averaged) models, although it must be emphasized that the approach rests on the basic assumption that departures from zonal symmetry are small. One important lesson to come out of the basic theoretical considerations discussed in Sections 6.2 and 6.5 is the interdependence of advective and diffusive transport processes, and the fact that these should therefore be represented in transport models in a mutually consistent way. It is also now recognised that mixing processes are spatially inhomogeneous – most dramatically illustrated by the stratospheric “surf zone” – and that models using latitudinally constant diffusivities may not simulate correct latitudinal constituent structures.

The practical problem of determination of appropriate transport coefficients for a given flow climatology is still not entirely satisfactory. Those derived from general circulation models have the attribute of being self-consistent but of course these can reflect the properties of the real atmosphere no better than the models themselves, and we have seen that at the present state of the art these have serious shortcomings, especially in the representation of dynamical activity in the stratosphere. It is possible to estimate the residual (ageostrophic) circulation diagnostically from the heat budget as done (implicitly) by Murgatroyd and Singleton [1961] and indeed, their results are currently used in some 2-D models [e.g., Miller *et al.*, 1981; Guthrie *et al.*, 1984]; given the advances in our knowledge of the climatology of the middle atmosphere since this calculation, it would seem desirable to update this calculation.

Estimation of the diffusivities from atmospheric circulation data is more difficult since reliable ageostrophic wind data is not generally available. Newman *et al.* [1986] have applied Plumb and Mahlman's [1986] technique to estimate  $K_{yy}$  via inversion of a flux-gradient relation for quasi-geostrophic potential vorticity, although this approach breaks down in low latitudes. With the rapidly improving coverage of trace constituent distributions, it may become practicable to estimate gross mixing rates from observed global fields, or by tuning 2-D models to match observations [e.g., Ko *et al.*, 1984] although the success of this approach depends on having a good model of the transport circulation (since the modeled constituent fields will represent a balance between advection and diffusion).

Of particular interest, since GCM approaches have been unable to address the matter, is an assessment of transport characteristics during warming events in winter high latitudes. Indeed a basic question is what proportion of the net wintertime transport is associated with these events. Ozone records and, indeed, the observed temperature increases suggest that the effects are significant. Therefore incorporation of such phenomena into transport models appears desirable. However, given the extreme convolution of streamlines during such events (Figure 6-23), one must question the ability of 2-D models to represent them to any useful degree; even if such models can predict the zonal mean adequately, the relevance of zonal mean predictions in such cases, at least on the time scale of a single event, is not clear.

Perhaps to a lesser extent the same is true throughout the winter and it is to be hoped that advances in 3-D modeling, either via full GCM treatments or in low resolution models, will enhance our ability to model more meaningfully the structure of trace constituents, especially in the winter stratosphere. We can also look forward to an increased understanding of 3-D transport processes via analyses of the behavior of global constituent fields from observations and in three-dimensional numerical models run in forecast mode.

## 6.7 SUMMARY

### 6.7.1 Observations of the Middle Atmosphere

The advent of global satellite monitoring of the middle atmosphere has had a profound impact on our appreciation of the structure and dynamics of the region. In recent years we have seen the emergence of multiyear, global, satellite-based climatologies of the stratosphere and mesosphere and, correspondingly, recognition of the substantial interannual variability of the circulation. The development of a Southern Hemisphere climatology has, of course, been very much dependent on satellite observations and is of particular importance, as the contrast between the two hemispheres (especially in winter) is substantial and presents a challenge to dynamical theories. The observed differences between the two hemispheres have provided valuable input to theoretical developments, but have yet to be exploited to the full, and our understanding of the Southern Hemisphere middle atmosphere still lags behind that of the Northern Hemisphere.

Analyses of transient events have also advanced remarkably, partly because of improved data coverage in time and space and partly because of the application of more sophisticated analysis procedures. Thus a number of transient planetary wave modes have been identified, several of which can be associated with theoretically-predicted normal mode oscillations. The improved vertical resolution of limb-viewing instruments has permitted, for the first time from satellites, identification of equatorial waves in the stratosphere and mesosphere and, indeed, of "ultrafast" Kelvin waves, which were previously unobserved in the atmosphere (but which had been found in a general circulation model). As yet, however, there is no satellite-based observation of the mixed Rossby-gravity waves, which have been postulated to provide the driving for the easterly phase of the Quasi-Biennial Oscillation (although it has been suggested that this driving could be provided by other means).

Sudden warming events continue to be a source of dynamical interest. Although progressively more events are being monitored by satellite, much of our understanding is based on analysis of the event of February 1979. While it is understandable that this well-observed event (it occurred during the FGGE year) should receive considerable attention, there are dangers in ascribing too much significance to a single case. However other occurrences are also being studied, including the final warming in the Southern Hemisphere. The improved data base, together with theoretical developments, have led to an improving description of warmings but we are still far short of a complete understanding of the dynamical processes involved.

Diagnostic techniques have advanced in parallel with improving data coverage. In particular, evaluation of the Eliassen-Palm flux (both in observed data sets and in numerical models) has proved an illuminating means of elucidating the meridional propagation of stratospheric planetary waves and, through transformed Eulerian mean theory, the interaction of these waves with the zonal mean flow. Thus, the switching of wave propagation from equatorward to poleward prior to sudden warmings, with the associated tendency to deceleration of the high latitude westerlies, has been claimed to be an important precursor of such events. However, it is becoming increasingly apparent that the stratospheric flow is highly three-dimensional (especially during warming events) and that the "zonal-mean, eddy" separation inherent in such approaches may not always be appropriate. One more generally applicable technique which has aroused considerable recent interest is that of mapping Ertel's potential vorticity (EPV) on isentropic surfaces. EPV is a function of dynamical variables (importantly, most dynamical quantities of interest can be recovered from the EPV distribution) which acts as a tracer for adiabatic, frictionless flow. This fact has been known to theoreticians for many years, but it is only in the last few years that it has come to be applied to the large-scale stratospheric circulation. Despite the demands this technique places on data quality (the second horizontal

## DYNAMICAL PROCESSES

derivative of satellite radiance data is required) its use has led to the identification of the "breaking" of planetary waves in the subtropical winter stratosphere, where the deformation field associated with the wave motion acts to distort, perhaps irreversibly, the material surfaces mapped by the EPV contours.

This new insight into large-scale stratospheric transport has been complemented by the recent availability of satellite observations of the global distributions of a number of trace constituents. Features similar to those evident in EPV maps have been observed in the distribution of ozone and water vapor. In this respect, as in others, exploitation of the wealth of new material which has become available with these new observations promises to enhance profoundly our understanding of the distribution of middle atmosphere constituents and of the transport processes which influence them.

Not all motions of dynamical interest in the middle atmosphere have been, nor are they likely to be, observed by satellite-borne instruments. Ground-based radar and, to a lesser extent, rocket and lidar measurements provide the only means of observing gravity waves in the region, as well as yielding other information currently unattainable from satellites such as ageostrophic wind data. Gravity wave observations are of particular importance, in view of their role in driving the mesospheric circulation. This role has recently been quantified (in support of theoretical predictions) following the development of a technique to measure gravity wave momentum fluxes using a twin-beam radar. In this application, as in many other respects, interpretation of the results of such experiments is clouded by the question of the global relevance of observations made at a single site. While a global synoptic network of ground-based observing facilities is inconceivable, it is desirable that a more representative coverage be achieved.

Ground-based observations play another crucial role, viz., as "ground truth" for calibration of satellite measurements. This aspect is important in maintaining continuity between successive satellite instruments, and especially so if satellites are to be used to detect long-term trends such as those which may occur in response to trends in constituent concentrations. It is therefore essential that ground-based networks, such as they are, be maintained and even augmented (thus reversing recent trends).

Satellite observations have become such an important source of information on the circulation of the middle atmosphere that it goes without saying that their continuation is crucial to the progress of the subject. Continuity of monitoring is particularly important; ideally, this requires not only that each monitoring satellite be replaced before the end of its useful life, but also that both old and new instruments operate simultaneously for some time, in order that intercalibrations may be carried out. Most of our routine data has come, and will continue to come, from nadir-viewing radiometers. However, the value of limb-viewing instruments has been noted above and elsewhere in this chapter; it is highly desirable that such instruments should operate on a continuous basis. Finally, the potential value of direct wind velocity measurements cannot be overstressed. Such data would be profoundly valuable, particularly in the tropics, where the temperature signal is weak and the derivation of wind from temperature is unsound, and in the Southern Hemisphere, where the low-level analysis required to build up the wind field from temperature retrievals is of poor quality.

### 6.7.2 General Circulation Modeling of the Middle Atmosphere

The application of general circulation models (GCMs) to the middle atmosphere has so far met with mixed success. Many key aspects of the observed dynamical behavior of the region have been reproduced successfully (at least qualitatively) in these models and their use in both climatological (long-term) and forecast (short term) integrations, in transport experiments and as experimental tools for the conduct of

perturbation experiments has contributed greatly to recent advances in our understanding of the middle atmosphere circulation. However, GCM results still exhibit serious deficiencies. The most serious of these concerns the climatology of the winter stratosphere, where the models consistently predict a polar night that is much colder (and therefore closer to radiative equilibrium) than that observed. While it has been shown that this problem can be alleviated in the lower stratosphere through improved representations of radiation, it seems clear that the more serious and more robust error in the middle stratosphere and above reflects inadequacies in the representation of dynamical transports. Other shortcomings of current GCMs include a failure to generate a Quasi-Biennial Oscillation in the equatorial stratosphere, errors in predicted tropical tropopause temperatures and an inability to resolve internal gravity waves. Since these latter motions are a crucial component of the mesospheric circulation, the fact that they must be parameterized in GCMs is rather unsatisfactory.

Successes of GCM simulations have included several examples of forecasts of stratospheric warmings. While these forecasts are only useful for a limited period (because of climate drift associated with the models' "cold pole" problem) their success has presented us with an additional tool for investigations of such phenomena. GCMs have also been used as vehicles for the conduct of perturbation experiments, for the investigation of large-scale transport processes and, in the absence of an adequate observational data set, as a source of data for the derivation of transport coefficients required by two-dimensional transport models. While what is learned from these exercises is very much model-dependent, there are good reasons to believe that the insight thereby gained is meaningful. It should also be noted that even the failures of GCM simulations have been of considerable benefit in guiding research priorities. As the GCM is the most complete synthesis of our quantitative understanding, the failure of such a model to represent correctly the observed atmospheric state (in circumstances where factors such as resolution are considered satisfactory) is an indication of the inadequacy of that understanding. Thus, identification of the causes of GCM errors is of considerable scientific value; for example, the "cold pole" problem has led us to question our understanding of planetary wave generation processes and the role of gravity waves in the stratospheric momentum budget.

Despite the availability of ever-faster computers, we have still not reached the stage where it is possible to incorporate a comprehensive chemistry into middle atmosphere GCMs in order to undertake long-term assessment experiments. Moreover, the climatological inadequacies of current models would in any case limit the usefulness of such assessments. Nevertheless, GCM experiments with highly simplified chemistry have proved valuable in complementing other approaches in the investigation of global transport processes in the middle atmosphere. In the foreseeable future, however, assessment studies will continue to rely on the use of simplified transport models.

### 6.7.3 Theory of Dynamics and Transport

Over the past eight years or so we have seen a considerable improvement in our conceptual picture of the dynamics of the middle atmosphere circulation and of the transport processes which maintain it. It has become recognized that the "Brewer-Dobson" picture of an equator-to-pole circulation in the lower stratosphere and a summer-pole-to-winter-pole circulation in the upper stratosphere and mesosphere is, in a dynamical and transport sense, a more meaningful description of the mean meridional circulation than that obtained by simple zonal averaging of the local meridional winds. The former was originally inferred from observed distributions of ozone and water vapor in the stratosphere and we now know that the transport of constituents such as these is not well depicted by the latter, Eulerian mean, representation but is described more simply in terms of what has here been called the "transport circulation" which,

## DYNAMICAL PROCESSES

in the middle atmosphere at least, is similar to the now more familiar "residual" and "diabatic" circulations. The Brewer-Dobson circulation is therefore an estimate of the transport circulation, which is what we need to know for understanding the global transport of constituents, and which is in turn a close approximation to the residual circulation; the latter is the appropriate measure of the mean circulation for dynamical investigations via transformed Eulerian-mean theory.

A description of meridional exchange in the middle atmosphere solely in these terms, however, is incomplete. The existence of this meridional circulation has in the literature (and in textbooks) frequently been described as a simple response to diabatic heating. This view is, however, logically unsound since the departures of the atmosphere from radiative equilibrium which give rise to this heating must be maintained by dynamical effects, in fact by eddy momentum transport (as expressed by the divergence of the Eliassen-Palm flux). This theoretical result has been in the literature for many years now, but its significance has only recently become widely appreciated. For one thing, it offers a simple diagnostic approach to the determination of where, and to what degree, these eddy processes act; thus it can be inferred from the Brewer-Dobson circulation that such processes must be acting in the winter stratosphere and in the mesosphere.

It is now widely accepted that the mesospheric driving is provided largely by internal gravity waves, with perhaps some contribution from planetary waves in the winter hemisphere and from tides in the tropics. These waves, propagating upward from the troposphere, reach large amplitude in the mesosphere, where they may break and thus act as *in situ* forcing on the mean flow. Much theoretical effort has been directed recently at understanding this phenomenon and its parameterization in numerical models. However, apart from a measurement of the magnitude of the effect by radar supporting this general picture, these developments have proceeded largely unconstrained by experimental evidence and there remains a need for a deeper understanding of the properties of atmospheric gravity waves and of the breaking process.

In the winter stratosphere, quasi-stationary planetary waves are the most likely driving mechanism. It has until recently been supposed that this interaction must derive from the dissipation of these waves by radiative effects, although this view presented problems in the lower stratosphere where such effects are weak. However it is now realised that planetary wave breaking, a process that has been identified from the observed behavior of potential vorticity maps, may be an important factor (and perhaps the dominant one, at least in the lower stratosphere). Thus, strong eddy mixing processes in the "surf zone" of the winter subtropics may be a powerful influence on the dynamical structure and evolution of the winter stratosphere. However, a number of crucial issues need clarification, including the efficiency of this mixing and the relative contribution of radiative dissipation; the latter question is particularly important for our conceptual picture of constituent transport.

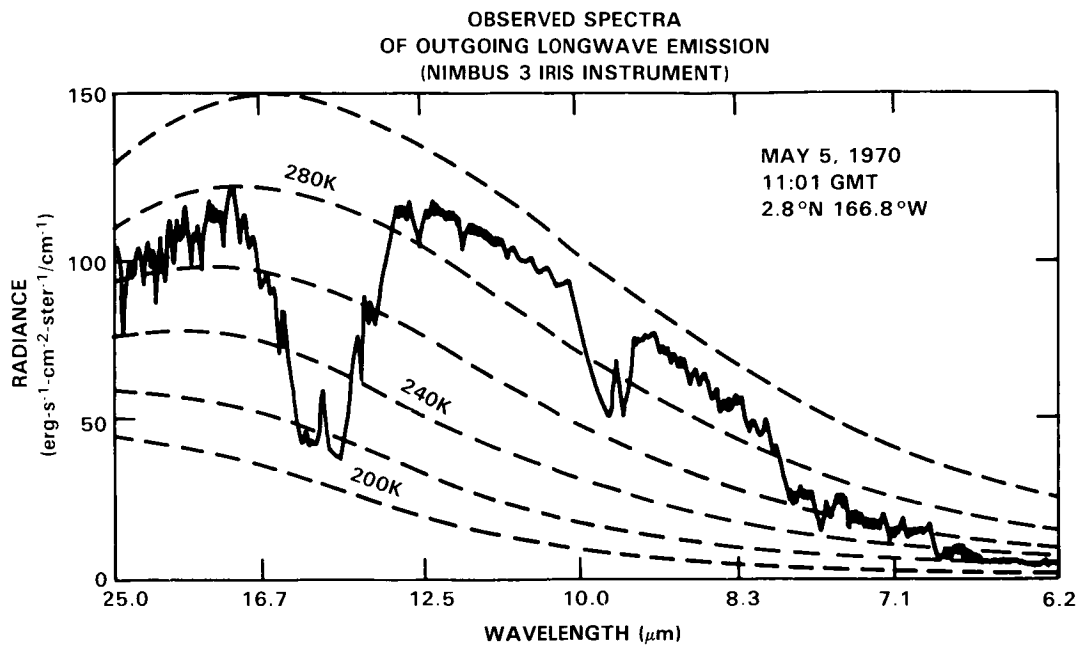
During high-latitude warming events the location of this planetary wave driving switches from the subtropics to the polar cap, apparently as a consequence of the focusing of waves into that region. The reasons for this focusing and for the characteristic amplification of planetary wave activity at such times are not well understood, although it has been speculated that both these effects may be a consequence of the changes in the dynamical structure of the stratosphere brought about by previous low-latitude mixing processes.

Another outstanding issue - one that is raised by the apparent failure of current GCMs to generate sufficient eddy driving in the winter stratosphere as well as observational indications of a deficit in the large-scale stratospheric momentum budget - is the role of gravity waves in driving the stratospheric cir-

ulation. At present there is little consensus amongst theoreticians on this issue and little or no relevant observational evidence. It is to be hoped that stratospheric observations of gravity waves (by MST radars, for example) will be forthcoming to help resolve this question.

Recognition of the existence of large-scale mixing (i.e. quasi-horizontal turbulence) in the stratosphere has had an impact on our conceptual picture of zonally-averaged constituent transport. Until recently, this picture comprised advection by the Brewer-Dobson circulation, with some diffusion superimposed on this for nonconservative constituents (the so-called "chemical eddy" contribution). Large-scale mixing events will also impact (as an effective diffusion) on even conserved constituents. Indeed, if the eddy momentum transport is dominated by this mixing (rather than the effects of radiative dissipation), then it can be argued that advective and diffusive transport of constituents must be formally comparable, so that an adequate representation of both is necessary in two-dimensional transport models. More generally, recognition of the central role of eddy transports in driving the mean meridional circulation implies that such models are incapable of being "interactive" in the sense of predicting meridional circulation changes.

# RADIATIVE PROCESSES



## Panel Members

J.E. Frederick and C. Leovy, Co-Chairmen

D.E. Anderson, Jr.	J.E. Mentall
G.P. Anderson	G.H. Mount
R.E. Dickinson	M. Nicolet
S.R. Drayson	C.D. Rodgers
S. Fels	G. Rottman
L.A. Hall	P.C. Simon
J. Kiehl	

## CHAPTER 7

### RADIATIVE PROCESSES: SOLAR AND TERRESTRIAL

#### TABLE OF CONTENTS

7.0 INTRODUCTION .....	349
7.1 SOLAR RADIATION AND ITS ABSORPTION IN THE STRATOSPHERE AND MESOSPHERE .....	349
7.1.1 The Solar Spectral Irradiance: Overview .....	349
7.1.2 Irradiance at Wavelengths Shorter Than 175 nm .....	350
7.1.2.1 The Lyman alpha line (121.6 nm) and its variability .....	350
7.1.2.2 The wavelength range 130-175 nm .....	351
7.1.3 A Reference Solar Spectral Irradiance for Wavelengths Longer Than 175 nm .....	352
7.1.3.1 The spectral region 175-210 nm .....	352
7.1.3.2 The spectral region 210-327.5 nm .....	354
7.1.3.3 The spectral region 327.5-852.5 nm .....	363
7.1.4 Solar Variability at Wavelengths Greater Than 175 nm .....	363
7.1.5 Rayleigh Scattering .....	367
7.1.6 Absorption by Molecular Oxygen .....	368
7.1.6.1 Absorption at the Lyman alpha line (121.6 nm) .....	368
7.1.6.2 The Schumann-Runge bands and underlying continuum .....	368
7.1.6.3 Absorption by the Herzberg continuum .....	370
7.1.7 Absorption by Ozone .....	375
7.1.7.1 General characteristics of ozone absorption .....	375
7.1.7.2 The Hartley region .....	375
7.1.7.3 The Huggins bands .....	376
7.1.7.4 The Chappuis bands .....	376
7.1.8 Solar Heating Rates .....	377
7.2 TERRESTRIAL RADIATION .....	378
7.2.1 Overview and Major Issues .....	378
7.2.2 Line-by-line Calculations, Band Transmittances, and Spectroscopic Data .....	380
7.2.3 Radiative Damping .....	382
7.2.4 Longwave Radiation in the Stratosphere .....	384
7.2.5 Longwave Radiation in the Mesosphere .....	388
7.2.6 The Distribution of Net Radiative Heating .....	390
7.3 CONCLUSIONS AND FUTURE RESEARCH NEEDS .....	391

## 7.0 INTRODUCTION

Solar radiation incident on the Earth and its atmosphere provides the ultimate driving force for all chemical and dynamical processes addressed in this assessment. Acting to counter the extraterrestrial energy source, longwave terrestrial radiation escapes to space thereby cooling the planet. On a globally and annually averaged basis a near balance exists between solar heating and longwave cooling. However, at any particular location and time of year a nonzero net heating, positive or negative, can exist, and this imbalance acts as a source term for the mean global circulation of the middle atmosphere. While the solar radiative heating depends only weakly on temperature, this is not true of the longwave cooling. Net radiative heating is therefore strongly influenced by the dynamical processes. In the middle atmosphere radiative and dynamical processes are inextricably coupled. Knowledge of the processes affecting both solar and terrestrial radiation is also essential for the remote sensing of middle atmosphere composition, but the emphasis of this chapter is the heat balance.

The first major subdivision of this chapter considers solar radiation and the processes that control its deposition in the Earth's atmosphere. The published data obtained since 1978 define a reference solar spectral irradiance for use in atmospheric chemical and dynamical studies, while long term satellite measurements are now providing information on variations in the Sun's output over a range of time scales. As concerns absorption of solar radiation in the atmosphere, new cross section data for molecular oxygen and ozone are now available. In the case of O<sub>2</sub> the revised values differ significantly from those used in atmospheric modeling at the time of WMO Report No. 11 (1982).

The second portion of this chapter addresses terrestrial longwave radiation. Major issues here relate to the accuracy of line-by-line calculations used to predict infrared flux divergences, both as regards assumptions made in radiative transfer calculations and in the spectroscopic parameters used as inputs. A valid line-by-line treatment of longwave transfer must utilize accurate line profile shapes including, for example, the temperature dependence of the half width and pressure effects on the wings. Additional topics include the influence of radiative processes on planetary scale wave activity, photochemical acceleration of radiative damping, and the breakdown of local thermodynamic equilibrium at mesospheric altitudes.

## 7.1 SOLAR RADIATION AND ITS ABSORPTION IN THE STRATOSPHERE AND MESOSPHERE

### 7.1.1 The Solar Spectral Irradiance: Overview

This section assesses the present knowledge of the solar spectral irradiance and its temporal variations at wavelengths relevant to the stratosphere and mesosphere. Since the last comprehensive NASA assessment report (WMO No. 11, 1982) and the detailed review of Simon (1981) there has been a substantial increase in the quantity of data available in the wavelength region  $\lambda = 175$  to 320 nm, which is the critical portion of the spectrum for stratospheric modeling. Simon and Brasseur (1983) reviewed the information available here through the end of 1982. In addition to several rocket-borne irradiance measurements, orbiting spectrometers on the Solar Mesosphere Explorer (SME) and Nimbus 7 satellites have provided data that give an indication of irradiance variability over the 27 day solar rotation period and somewhat longer time scales. However, the state of knowledge concerning irradiance variations over the 11 year solar cycle remains inadequate, and estimates are not yet sufficiently precise. Reflecting the expanding data base, this portion of the report presents a new reference spectrum for use in stratospheric modeling. The following sections review the present knowledge of the solar irradiance, first at wavelengths less than 175 nm focusing on the Lyman alpha line and solar emission in the spectral range of the Schumann-Runge continuum. A

## RADIATIVE PROCESSES

reference solar spectral irradiance for the region 175 to 850 nm is then presented, followed by a summary of solar variability including estimates of the magnitude of the 11 year cycle at these wavelengths.

### 7.1.2 Irradiance at Wavelengths Shorter than 175 nm

#### 7.1.2.1 The Lyman Alpha Line (121.6 nm) and its Variability

Figure 7-1 illustrates the behavior of the Lyman alpha line at 121.6 nm over the 3-year period 1982-1984 as measured by the SME satellite. Values are of the integrated line emission expressed in photons  $\text{cm}^{-2}\text{s}^{-1}$ . The short term variations are related to the presence of active regions situated at different solar longitudes. This gives rise to periods related to the solar rotation of 27 days. The evolution of these active regions leads to irregular behavior in the amplitude of the short term variability as is evident in Figure 7-1. The straight line is a simple least squares fit to the measurements and indicates a significant decrease over the observing period corresponding to a declining level of solar activity. An estimate of the trend arising from instrument sensitivity changes has been removed from the data shown.

A change in the integrated Lyman alpha irradiance of roughly a factor of 2 over the 11 year solar cycle now has wide acceptance (Bossy and Nicolet, 1981; Lean and Skumanich, 1983). Table 7-1 lists measurements reported over the period June 1979 through July 1983 by Mount *et al.* (1980) and Mount and Rottman (1981, 1983a, 1983b, 1985) together with the 10.7 cm solar radio flux appropriate to the day of each measurement. Error bars on the two earlier flights are  $\pm 15\%$  and for the latter three results

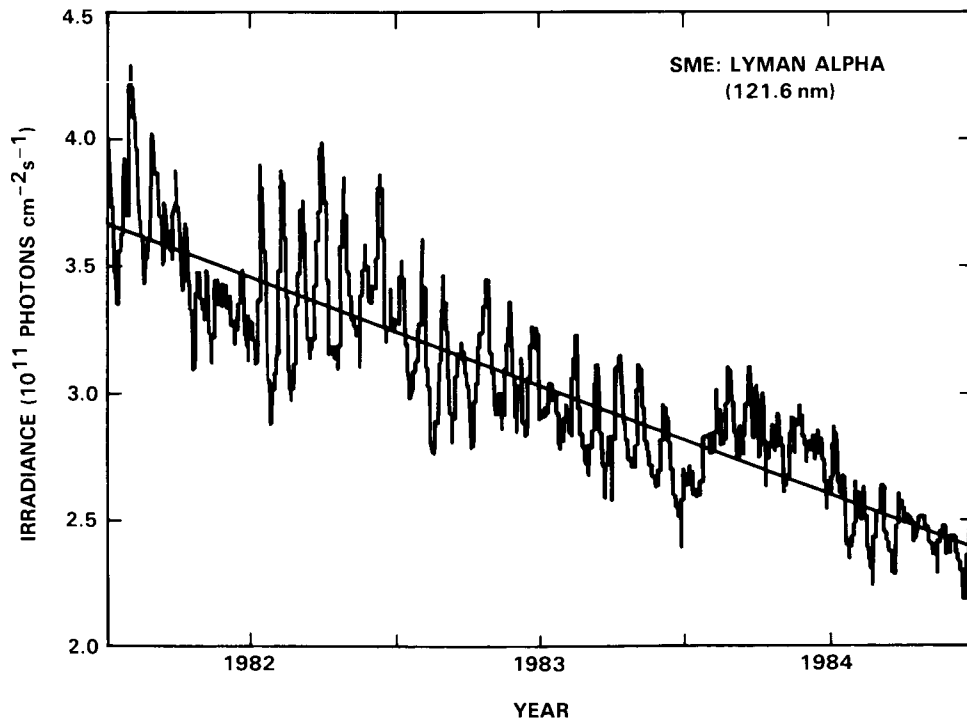


**Figure 7-1.** Variation in the integrated irradiance of the Lyman alpha line (121.6 nm) over the period 1982 through 1984 observed from the Solar Mesosphere Explorer satellite. The straight line is a least squares fit to the measurements. (Data provided by G.J. Rottman.)

are somewhat smaller. The factor of 2 decrease in flux from mid-1980 to mid-1983 is real. Note also that the SME measurements, extending through 1984, show Lyman alpha decreasing to values less than reported in Table 7-1. If such values are accepted, a quiet Sun value of  $2.25 \times 10^{11}$  photons  $\text{cm}^{-2}\text{s}^{-1}$  is obtained with uncertainty limits of  $\pm 15\%$ . Integrated Lyman alpha flux values larger than those in Table 7-1 have appeared in the literature (Hinteregger, 1981). Although there is no obvious basis to dismiss such results, the smaller values are recommended here for use in atmospheric modeling. It is clear from a study of the experimental techniques that systematic errors can arise and great care must be taken to interpret the measurements properly (Nicolet, 1984a, 1985).

For estimates of the flux at any level of solar activity, the analytic form of Bossy and Nicolet (1981) is adequate, although the numerical constants should be altered slightly to accommodate a revised solar minimum value and the variations of Table 7-1. The recommended relationship is:

$$q(\text{Ly}\alpha) = (2.25 \times 10^{11}) + (0.014 \times 10^{11})[S_a(10.7) - 65] \tag{7.1}$$

This expression reproduces each of the values in Table 7-1 to an accuracy of  $\pm 20\%$  or better. Caution is advised in accepting a simple formula as an accurate predictor of the true solar irradiance variation. Although the parameterization of Equation 7.1 predicts the gross variations in the Lyman alpha flux, the SME measurements reveal a complicated temporal variation that cannot be reproduced in detail by simple statistical relationships based on proxy solar indices. Continuing direct observations of the Lyman alpha flux, accounting for any instrumental artifacts, are required to fully define the temporal behavior.

### 7.1.2.2 The Wavelength Range 130-175 nm

Solar energy at wavelengths between 130 and 175 nm is deposited at altitudes above the mesopause where it dissociates molecular oxygen in the Schumann-Runge continuum. A variation in the integrated

Table 7-1. Measured Values of the Integrated Lyman Alpha Line Flux<sup>1</sup>

Date	Lyman Alpha Flux (photons $\text{cm}^{-2}\text{s}^{-1}$ )	10.7 cm Radio Flux
June 5, 1979	$5.0 \times 10^{11}$	230.2
July 15, 1980	$5.5 \times 10^{11}$	218.4
May 12, 1982	$3.3 \times 10^{11}$	142.2
January 12, 1983	$3.0 \times 10^{11}$	135.7
July 25, 1983	$2.7 \times 10^{11}$	136.7

<sup>1</sup>Values from Mount *et al.* (1980) and Mount and Rottman (1981, 1983a,b, 1985).

## RADIATIVE PROCESSES

130-175 nm flux over the solar cycle of a factor of two is indicated by the rocket measurements of Table 7-2 based on Mount *et al.* (1980) and Mount and Rottman (1981, 1983a, 1985). Values reported near the last solar minimum prior to 1979, as reported in WMO No. 11 (1982), are considered less reliable than subsequent data because of improvements in calibration techniques. Error bars on the more recent results are typically  $\pm 20\%$ . In view of the increasing quality now obtainable, high priority should be placed on new measurements during the minimum of the present solar cycle.

Figure 7-2 presents the integrated 130-175 nm radiance derived from SME for the period 1982-1984. The percentage magnitude of the short term variation is less than that at Lyman alpha and most values lie between  $7.6 \times 10^{11}$  and  $8.7 \times 10^{11}$  photons  $\text{cm}^{-2}\text{s}^{-1}$  for prevailing solar activity levels.

### 7.1.3 A Reference Solar Spectral Irradiance for Wavelengths Longer than 175 nm

#### 7.1.3.1 The Spectral Region 175-210 nm

The objective of this section is to compile a reference solar spectrum for use in atmospheric modeling without regard to changes in the Sun's output over time. However, it is now universally accepted that solar irradiance in the 175 to 210 nm spectral region varies with the 27 day solar rotation period and the 11 year solar cycle (Rottman, 1983; London *et al.*, 1984; Heath and Schlesinger, 1985). At wavelengths longer than 210 nm, the threshold of the  $A^l$  I continuum, the percentage variability with solar rotation drops sharply as shown by the Nimbus 7 SBUV measurements of Heath *et al.* (1984). Unfortunately uncertainties in the absolute calibration of rocket-borne sensors and drifts in satellite-based instruments over long periods in orbit still inhibit definitive observations of irradiance variations over time scales of many years. To circumvent these experimental problems empirical models of solar variability have been proposed based on readily observable indices of solar activity (Cook *et al.*, 1980; Lean *et al.*, 1982; Lean, 1984) and extrapolations from observed 27 day irradiance changes to the 11 year cycle (Heath and Schlesinger, 1985).

**Table 7-2.** Measured Values of the Integrated Solar Irradiance Over the Wavelength Range 130-175 nm\*

Date	Integrated Irradiance 130-175 nm (photons $\text{cm}^{-2}\text{s}^{-1}$ )	10.7 cm Solar Radio Flux
June 5, 1979	$1.5 \times 10^{12}$	230.2
July 15, 1980	$1.3 \times 10^{12}$	218.4
May 17, 1982	$8.0 \times 10^{11}$	142.2
July 25, 1983	$7.2 \times 10^{11}$	136.7

\*Values from Mount *et al.* (1980) and Mount and Rottman 1981, 1983a, 1985).

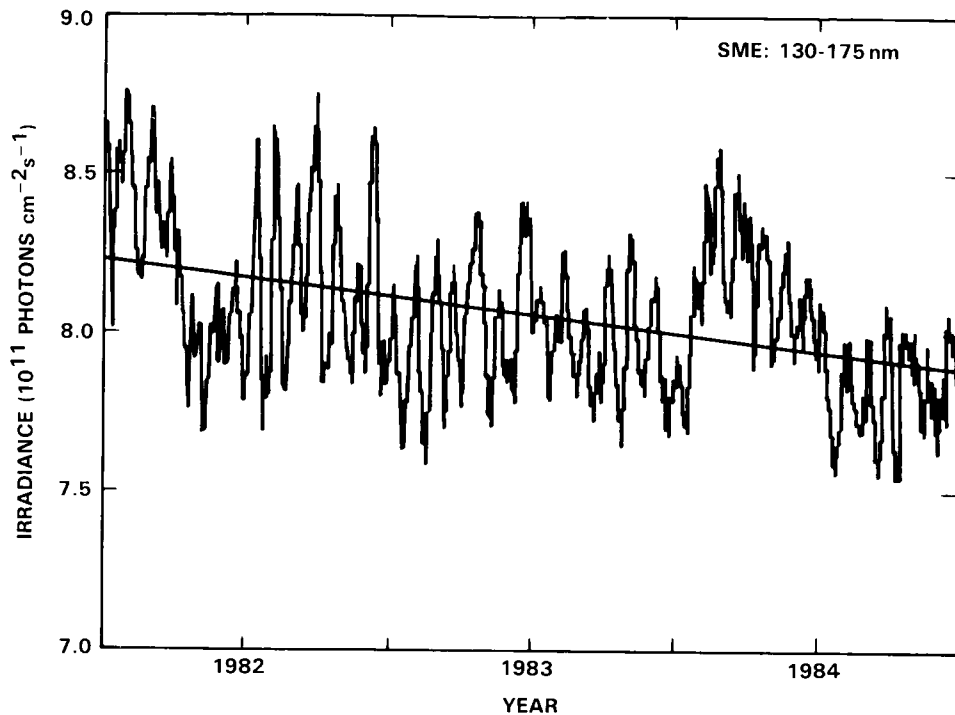


**Figure 7-2.** Variation in the 130-175 nm integrated irradiance over the period 1982 through 1984 observed from the Solar Mesosphere Explorer satellite. The straight line is a least squares fit to the measurements. (Data provided by G.J. Rottman.)

Table 7-3 lists the published solar irradiance measurements performed in 1978 and later. Also given are the 10.7 cm solar radio flux,  $S_a(10.7)$ , adjusted to one astronomical unit for the day of each measurement. Data obtained prior to 1978 have been discussed by Simon (1981) and in WMO No. 11 (1982). Examination of the data corresponding to the entries of Table 7-3 shows no clear relationship between absolute irradiance and the solar activity indices. This certainly reflects experimental uncertainties rather than the absence of a solar cycle dependence since the theoretical basis for irradiance variations is firm. Given no definitive information showing that one measurement is superior to another, the best estimate for a reference solar irradiance in a given spectral interval is the mean of all available data. However, if one measurement is known to be deficient in some respect, it is acceptable to eliminate this data set when compiling the final spectrum. The approach used to define the reference spectrum is therefore as follows: All data corresponding to the entries of Table 7-3 were placed on the  $500 \text{ cm}^{-1}$  wavenumber grid that has become standard in atmospheric modeling since its first use by Ackerman (1971). The mean of all available data was then computed. The final reference spectrum in Table 7-4 is denoted by  $F_{\text{REF}}(i)$  where the spectral intervals  $i = 1, 2, \dots, 19$  correspond to wavelengths from 175.439 to 210.526 nm. In generating the spectrum, the data of June 5, 1979 were eliminated for wavelengths longer than 180 nm as recommended by G.H. Mount. A useful index of the scatter in the available data is the root mean square (RMS) deviation from the mean reference spectrum. For spectral intervals  $i_1$  to  $i_2$  this is defined as:

$$\epsilon(i_1, i_2) = 100 \left[ \frac{1}{(i_2 - i_1 + 1)} \sum_{i=i_1}^{i_2} \left\{ \frac{F(i) - F_{\text{REF}}(i)}{F_{\text{REF}}(i)} \right\}^2 \right]^{1/2}$$

## RADIATIVE PROCESSES

Here  $F(i)$  is the irradiance in interval  $i$  from a data source listed in Table 7-3 and  $F_{REF}(i)$  is the mean of all acceptable measurements. Table 7-3 includes the computed RMS deviations for  $(i_1, i_2) = (1, 19)$ . In most cases these values are less than 10% although the quoted uncertainty in any single measurement is typically  $\pm 15\%$ - $20\%$ . The mean 10.7 cm radio flux for all measurements entering the final reference spectrum is approximately 185, corresponding to a moderate level of solar activity.

### 7.1.3.2 The Spectral Region 210-327.5 nm

The solar irradiance in the spectral region 210-330 nm is responsible for dissociating ozone and other trace gases significant in the photochemistry of the stratosphere and mesosphere. In addition, photons at wavelengths up to 240 nm dissociate molecular oxygen via the Herzberg continuum. The data available to define the absolute solar spectral irradiance in this wavelength range were sparse for many years, the single comprehensive spectrum being Broadfoot (1972) derived from a rocket measurement made on June 15, 1970. Simon (1981) has presented a detailed discussion of data available as of 1980. The only measurements that spanned the entire wavelength region 210-330 nm at that time were by Broadfoot (1972) and Heath (1980), although several other data sets covered portions of this interval (Simon, 1975; Mount *et al.*, 1980; Simon *et al.*, 1982; Arvesen *et al.*, 1969). Since Simon's (1981) review a significant number of

**Table 7-3.** Solar Spectral Irradiance Measurements for Wavelengths 175.439 – 210.526 nm Considered in Developing the Reference Spectrum\*

Date of Measurement	$S_a(10.7 \text{ cm})$ Radio Flux	RMS Deviation $\epsilon(1,19)\%$	Reference
Nov. 7, 1978	174.6	9.6	Heath (1980)
Nov. 16, 1978	128.8	7.8	Mentall <i>et al.</i> (1985)
June 5, 1979 <sup>1</sup>	230.2	14.2	Mount <i>et al.</i> (1980)
May 22, 1980	276.6	11.4	Mentall <i>et al.</i> (1985)
July 15, 1980	218.4	6.5	Mount and Rottman (1981)
Sept. 15, 1980	153.8	7.8	Mentall <i>et al.</i> (1981)
Oct. 16, 1981	302.4	11.9	Mentall <i>et al.</i> (1985)
May 17, 1982	142.2	4.6	Mount and Rottman (1983a)
Jan. 12, 1983	135.7	6.2	Mount and Rottman (1983b)
July 25, 1983	136.7	7.2	Mount and Rottman (1985)

\*Data from this measurement at wavelengths greater than 180 nm were not included in computing the final reference spectrum of Table 6-4.

rocket-borne measurements that very nearly cover the entire 210-330 nm wavelength range have been reported in the literature. The present assessment focuses on measurements made in the years 1978 and later. This limited scope reflects the belief that improvements in measurement techniques make the more recent results preferable to early data and that sufficient data exist in the 1978-1984 time frame to assemble a useful reference spectrum for atmospheric modeling irrespective of the earlier results. Table 7-5 lists the measurements considered here. The accuracy of the irradiance values derived by Mount and Rottman (1981, 1983a,b, 1985) degrades at wavelengths above 296 nm, and results beyond this limit were therefore excluded from the average. Typical uncertainty limits including both systematic and random errors are  $\pm 15-20\%$ . The RMS deviations from the reference spectrum,  $\epsilon(i=20, 53)$  as defined in Equation 7.2, for all data sets listed in Table 7-5 were less than 10%. The systematic differences between the results of Mount and Rottman (1981, 1983a,b, 1985), Heath (1980), and Mentall *et al.* (1981) are 5-10%. The results are given as the reference spectrum in Table 7-4 for spectral intervals  $i=20$  to 53.

**Table 7-4.** Reference Solar Irradiance, Rayleigh Scattering, O<sub>2</sub> and O<sub>3</sub> Cross Sections

Spectral Interval	Wavelength* Range (nm)	Irradiance (Photons cm <sup>-2</sup> s <sup>-1</sup> )	Ray. Scat. $\sigma_{RS}(cm^2)$	O <sub>2</sub> Herzberg $\sigma_{HZ}(O_2)$ (cm <sup>2</sup> )	Ozone $\sigma(O_3)$ (cm <sup>2</sup> )	
					T=203K	T=273K
1	175.439 - 176.991	1.74E+11	6.79E-25	4.61E-24	8.11E-19	
2	176.991 - 178.571	2.10E+11	6.49E-25	5.03E-24	7.99E-19	
3	178.571 - 180.180	2.38E+11	6.20E-25	5.46E-24	7.86E-19	
4	180.180 - 181.818	3.04E+11	5.93E-25	5.88E-24	7.63E-19	
5	181.818 - 183.486	3.19E+11	5.66E-25	6.29E-24	7.29E-19	
6	183.486 - 185.185	2.93E+11	5.41E-25	6.68E-24	6.88E-19	
7	185.185 - 186.916	3.62E+11	5.16E-25	7.04E-24	6.40E-19	
8	186.916 - 188.679	4.73E+11	4.93E-25	7.36E-24	5.88E-19	
9	188.679 - 190.476	5.61E+11	4.70E-25	7.64E-24	5.31E-19	
10	190.476 - 192.308	6.63E+11	4.49E-25	7.87E-24	4.80E-19	
11	192.308 - 194.175	6.90E+11	4.28E-25	8.04E-24	4.38E-19	
12	194.175 - 196.078	9.56E+11	4.08E-25	8.14E-24	4.11E-19	
13	196.078 - 198.020	1.15E+12	3.89E-25	8.17E-24	3.69E-19	
14	198.020 - 200.000	1.27E+12	3.71E-25	8.13E-24	3.30E-19	

## RADIATIVE PROCESSES

**Table 7-4.** Reference Solar Irradiance, Rayleigh Scattering, O<sub>2</sub> and O<sub>3</sub> Cross Sections (Continued)

Spectral Interval	Wavelength* Range (nm)	Irradiance (Photons cm <sup>-2</sup> s <sup>-1</sup> )	Ray. Scat. $\sigma_{RS}$ (cm <sup>2</sup> )	O <sub>2</sub> Herzberg $\sigma_{HZ}$ (O <sub>2</sub> ) (cm <sup>2</sup> )	Ozone $\sigma$ (O <sub>3</sub> ) (cm <sup>2</sup> )	
					T=203K	T=273K
15	200.000 - 202.020	1.52E+12	3.53E-25	8.01E-24	3.26E-19	
16	202.020 - 204.082	1.78E+12	3.36E-25	7.84E-24	3.26E-19	
17	204.082 - 206.186	2.20E+12	3.20E-25	7.63E-24	3.51E-19	
18	206.186 - 208.333	2.69E+12	3.05E-25	7.33E-24	4.11E-19	
19	208.333 - 210.526	4.54E+12	2.90E-25	6.99E-24	4.84E-19	
20	210.526 - 212.766	7.14E+12	2.76E-25	6.45E-24	6.26E-19	
21	212.766 - 215.054	8.35E+12	2.62E-25	5.81E-24	8.57E-19	
22	215.054 - 217.391	8.39E+12	2.49E-25	5.23E-24	1.17E-18	
23	217.391 - 219.780	1.08E+13	2.36E-25	4.71E-24	1.52E-18	
24	219.780 - 222.222	1.18E+13	2.24E-25	4.26E-24	1.97E-18	
25	222.222 - 224.719	1.60E+13	2.13E-25	3.80E-24	2.55E-18	
26	224.719 - 227.273	1.34E+13	2.02E-25	3.35E-24	3.24E-18	
27	227.273 - 229.885	1.41E+13	1.92E-25	2.90E-24	4.00E-18	
28	229.885 - 232.558	1.57E+13	1.82E-25	2.45E-24	4.83E-18	
29	232.558 - 235.294	1.38E+13	1.72E-25	2.05E-24	5.79E-18	
30	235.294 - 238.095	1.60E+13	1.63E-25	1.69E-24	6.86E-18	
31	238.095 - 240.964	1.45E+13	1.54E-25	1.30E-24	7.97E-18	
32	240.964 - 243.902	2.20E+13	1.46E-25	0.93E-24	9.00E-18	
33	243.902 - 246.914	1.99E+13	1.38E-25	0.00E-00	1.00E-17	
34	246.914 - 250.000	1.97E+13	1.31E-25		1.08E-17	
35	250.000 - 253.165	1.94E+13	1.23E-25		1.13E-17	

RADIATIVE PROCESSES

Table 7-4. Reference Solar Irradiance, Rayleigh Scattering, O<sub>2</sub> and O<sub>3</sub> Cross Sections (Continued)

Spectral Interval	Wavelength* Range (nm)	Irradiance (Photons cm <sup>-2</sup> s <sup>-1</sup> )	Ray. Scat. $\sigma_{RS}(\text{cm}^2)$	O <sub>2</sub> Herzberg $\sigma_{HZ}(\text{O}_2)$ (cm <sup>2</sup> )	Ozone $\sigma(\text{O}_3)$ (cm <sup>2</sup> )	
					T=203K	T=273K
36	253.165 - 256.410	2.91E+13	1.17E-25		1.15E-17	
37	256.410 - 259.740	4.95E+13	1.10E-25		1.12E-17	
38	259.740 - 263.158	4.53E+13	1.04E-25		1.06E-17	
39	263.158 - 266.667	1.07E+14	9.78E-26		9.59E-18	9.65E-18
40	266.667 - 270.270	1.20E+14	9.22E-26		8.31E-18	8.34E-18
41	270.270 - 273.973	1.10E+14	8.68E-26		6.89E-18	6.92E-18
42	273.973 - 277.778	1.04E+14	8.17E-26		5.35E-18	5.42E-18
43	277.778 - 281.690	8.24E+13	7.68E-26		3.91E-18	4.02E-18
44	281.690 - 285.714	1.52E+14	7.22E-26		2.67E-18	2.77E-18
45	285.714 - 289.855	2.15E+14	6.78E-26		1.73E-18	1.79E-18
46	289.855 - 294.118	3.48E+14	6.36E-26		1.04E-18	1.09E-18
47	294.118 - 298.507	3.40E+14	5.97E-26		5.85E-19	6.24E-19
48	298.507 - 303.030	3.22E+14	5.59E-26		3.16E-19	3.43E-19
49	303.030 - 307.692	4.23E+14	5.24E-26		1.66E-19	1.85E-19
50	307.692 - 312.5	4.95E+14	4.90E-26		8.67E-20	9.80E-20
51	312.5 - 317.5	5.44E+14	4.58E-26		4.33E-20	5.01E-20
52	317.5 - 322.5	5.93E+14	4.28E-26		2.09E-20	2.49E-20
53	322.5 - 327.5	6.95E+14	4.01E-26		9.37E-21	1.20E-20
54	327.5 - 332.5	8.15E+14	3.75E-26		4.71E-21	6.17E-21
55	332.5 - 337.5	7.81E+14	3.52E-26		1.98E-21	2.74E-21
56	337.5 - 342.5	8.35E+14	3.31E-26		7.77E-22	1.17E-21

**RADIATIVE PROCESSES**

**Table 7-4.** Reference Solar Irradiance, Rayleigh Scattering, O<sub>2</sub> and O<sub>3</sub> Cross Sections (Continued)

Spectral Interval	Wavelength* Range (nm)	Irradiance (Photons cm <sup>-2</sup> s <sup>-1</sup> )	Ray. Scat. $\sigma_{RS}(\text{cm}^2)$	Ozone	
				$\sigma(\text{O}_3)$ (cm <sup>2</sup> ) T=203K	$\sigma(\text{O}_3)$ (cm <sup>2</sup> ) T=273K
57	342.5 - 347.5	8.14E+14	3.11E-26	1.77E-22	5.88E-22
58	347.5 - 352.5	8.53E+14	2.92E-26	—	2.66E-22
59	352.5 - 357.5	9.17E+14	2.75E-26	—	1.09E-22
60	357.5 - 362.5	8.38E+14	2.60E-26	—	5.49E-23
61	362.5 - 367.5	1.04E+15	2.45E-26	—	—
62	367.5 - 372.5	1.10E+15	2.31E-26	—	—
63	372.5 - 377.5	9.79E+14	2.19E-26	—	—
64	377.5 - 382.5	1.13E+15	2.07E-26	—	—
65	382.5 - 387.5	8.89E+14	1.96E-26	—	—
66	387.5 - 392.5	1.14E+15	1.86E-26	—	—
67	392.5 - 397.5	9.17E+14	1.76E-26	—	—
68	397.5 - 402.5	1.69E+15	1.67E-26	—	—
69	402.5 - 407.5	1.70E+15	1.59E-26	—	—
70	407.5 - 412.5	1.84E+15	1.51E-26	2.91E-23	
71	412.5 - 417.5	1.87E+15	1.44E-26	3.14E-23	
72	417.5 - 422.5	1.95E+15	1.37E-26	3.99E-23	
73	422.5 - 427.5	1.81E+15	1.30E-26	6.54E-23	
74	427.5 - 432.5	1.67E+15	1.24E-26	6.83E-23	
75	432.5 - 437.5	1.98E+15	1.18E-26	8.66E-23	
76	437.5 - 442.5	2.02E+15	1.13E-26	1.25E-22	
77	442.5 - 447.5	2.18E+15	1.08E-26	1.49E-22	

C - B

RADIATIVE PROCESSES

Table 7-4. Reference Solar Irradiance, Rayleigh Scattering, O<sub>2</sub> and O<sub>3</sub> Cross Sections (Continued)

Spectral Interval	Wavelength* Range (nm)	Irradiance (Photons cm <sup>-2</sup> s <sup>-1</sup> )	Ray. Scat. $\sigma_{RS}$ (cm <sup>2</sup> )	O <sub>2</sub> Herzberg $\sigma_{HZ}(O_2)$ (cm <sup>2</sup> )	Ozone	
					$\sigma(O_3)$ (cm <sup>2</sup> ) T=203K	$\sigma(O_3)$ (cm <sup>2</sup> ) T=273K
78	447.5 - 452.5	2.36E+15	1.03E-26		1.71E-22	
79	452.5 - 457.5	2.31E+15	9.85E-27		2.12E-22	
80	457.5 - 462.5	2.39E+15	9.42E-27		3.57E-22	
81	462.5 - 467.5	2.38E+15	9.01E-27		3.68E-22	
82	467.5 - 472.5	2.39E+15	8.63E-27		4.06E-22	
83	472.5 - 477.5	2.44E+15	8.26E-27		4.89E-22	
84	477.5 - 482.5	2.51E+15	7.92E-27		7.11E-22	
85	482.5 - 487.5	2.30E+15	7.59E-27		8.43E-22	
86	487.5 - 492.5	2.39E+15	7.28E-27		8.28E-22	
87	492.5 - 497.5	2.48E+15	6.99E-27		9.09E-22	
88	497.5 - 502.5	2.40E+15	6.71E-27		1.22E-21	
89	502.5 - 507.5	2.46E+15	6.44E-27		1.62E-21	
90	507.5 - 512.5	2.49E+15	6.19E-27		1.58E-21	
91	512.5 - 517.5	2.32E+15	5.95E-27		1.60E-21	
92	517.5 - 522.5	2.39E+15	5.72E-27		1.78E-21	
93	522.5 - 527.5	2.42E+15	5.50E-27		2.07E-21	
94	527.5 - 532.5	2.55E+15	5.30E-27		2.55E-21	
95	532.5 - 537.5	2.51E+15	5.10E-27		2.74E-21	
96	537.5 - 542.5	2.49E+15	4.91E-27		2.88E-21	
97	542.5 - 547.5	2.55E+15	4.73E-27		3.07E-21	
98	547.5 - 552.5	2.53E+15	4.56E-27		3.17E-21	

## RADIATIVE PROCESSES

Table 7-4. Reference Solar Irradiance, Rayleigh Scattering, O<sub>2</sub> and O<sub>3</sub> Cross Sections (Continued)

Spectral Interval	Wavelength* Range (nm)	Irradiance (Photons cm <sup>-2</sup> s <sup>-1</sup> )	Ray. Scat. $\sigma_{RS}(\text{cm}^2)$	Ozone $\sigma(\text{O}_3)$ (cm <sup>2</sup> )	
				T=203K	T=273K
99	552.5 - 557.5	2.54E+15	4.34E-27	3.36E-21	
100	557.5 - 562.5	2.50E+15	4.18E-27	3.88E-21	
101	562.5 - 567.5	2.57E+15	4.04E-27	4.31E-21	
102	567.5 - 572.5	2.58E+15	3.90E-27	4.67E-21	
103	572.5 - 577.5	2.67E+15	3.76E-27	4.75E-21	
104	577.5 - 582.5	2.67E+15	3.63E-27	4.55E-21	
105	582.5 - 587.5	2.70E+15	3.51E-27	4.35E-21	
106	587.5 - 592.5	2.62E+15	3.39E-27	4.42E-21	
107	592.5 - 597.5	2.69E+15	3.28E-27	4.61E-21	
108	597.5 - 602.5	2.63E+15	3.17E-27	4.89E-21	
109	602.5 - 607.5	2.68E+15	3.06E-27	4.84E-21	
110	607.5 - 612.5	2.66E+15	2.96E-27	4.54E-21	
111	612.5 - 617.5	2.59E+15	2.87E-27	4.24E-21	
112	617.5 - 622.5	2.69E+15	2.77E-27	3.90E-21	
113	622.5 - 627.5	2.61E+15	2.68E-27	3.60E-21	
114	627.5 - 632.5	2.62E+15	2.60E-27	3.43E-21	
115	632.5 - 637.5	2.62E+15	2.52E-27	3.17E-21	
116	637.5 - 642.5	2.63E+15	2.44E-27	2.74E-21	
117	642.5 - 647.5	2.60E+15	2.36E-27	2.61E-21	
118	647.5 - 652.5	2.55E+15	2.29E-27	2.42E-21	
119	652.5 - 657.5	2.48E+15	2.22E-27	2.20E-21	

RADIATIVE PROCESSES

Table 7-4. Reference Solar Irradiance, Rayleigh Scattering, O<sub>2</sub> and O<sub>3</sub> Cross Sections (Continued)

Spectral Interval	Wavelength* Range (nm)	Irradiance (Photons cm <sup>-2</sup> s <sup>-1</sup> )	Ray. Scat. $\sigma_{RS}$ (cm <sup>2</sup> )	Ozone $\sigma(O_3)$ (cm <sup>2</sup> )	
				T=203K	T=273K
120	657.5 - 662.5	2.57E+15	2.15E-27	2.02E-21	
121	662.5 - 667.5	2.61E+15	2.09E-27	1.85E-21	
122	667.5 - 672.5	2.61E+15	2.03E-27	1.67E-21	
123	672.5 - 677.5	2.62E+15	1.97E-27	1.54E-21	
124	677.5 - 682.5	2.62E+15	1.91E-27	1.42E-21	
125	682.5 - 687.5	2.57E+15	1.85E-27	1.25E-21	
126	687.5 - 692.5	2.52E+15	1.80E-27	1.12E-21	
127	692.5 - 697.5	2.60E+15	1.75E-27	1.02E-21	
128	697.5 - 702.5	2.58E+15	1.70E-27	9.20E-22	
129	702.5 - 707.5	2.52E+15	1.65E-27	8.40E-22	
130	707.5 - 712.5	2.51E+15	1.60E-27	7.70E-22	
131	712.5 - 717.5	2.48E+15	1.56E-27	6.90E-22	
132	717.5 - 722.5	2.45E+15	1.52E-27	6.30E-22	
133	722.5 - 727.5	2.48E+15	1.47E-27	5.70E-22	
134	727.5 - 732.5	2.45E+15	1.43E-27	5.25E-22	
135	732.5 - 737.5	2.44E+15	1.39E-27	4.75E-22	
136	737.5 - 742.5	2.39E+15	1.36E-27	4.47E-22	
137	742.5 - 747.5	2.40E+15	1.32E-27	4.20E-22	
138	747.5 - 752.5	2.41E+15	1.29E-27	3.75E-22	
139	752.5 - 757.5	2.40E+15	1.25E-27	3.25E-22	
140	757.5 - 762.5	2.38E+15	1.22E-27	2.92E-22	

## RADIATIVE PROCESSES

**Table 7-4.** Reference Solar Irradiance, Rayleigh Scattering, O<sub>2</sub> and O<sub>3</sub> Cross Sections (Continued)

Spectral Interval	Wavelength* Range (nm)	Irradiance (Photons cm <sup>-2</sup> s <sup>-1</sup> )	Ray. Scat. $\sigma_{RS}$ (cm <sup>2</sup> )	Ozone $\sigma(O_3)$ (cm <sup>2</sup> )	
				T=203K	T=273K
141	762.5 - 767.5	2.34E+15	1.19E-27	2.76E-22	
142	767.5 - 772.5	2.32E+15	1.16E-27	2.70E-22	
143	772.5 - 777.5	2.30E+15	1.13E-27	2.80E-22	
144	777.5 - 782.5	2.33E+15	1.10E-27	2.85E-22	
145	782.5 - 787.5	2.34E+15	1.07E-27	2.52E-22	
146	787.5 - 792.5	2.29E+15	1.04E-27	2.20E-22	
147	792.5 - 797.5	2.29E+15	1.02E-27	1.82E-22	
148	797.5 - 802.5	2.27E+15	9.90E-28	1.63E-22	
149	802.5 - 807.5	2.27E+15	9.66E-28	1.75E-22	
150	807.5 - 812.5	2.20E+15	9.42E-28	1.90E-22	
151	812.5 - 817.5	2.22E+15	9.19E-28	1.85E-22	
152	817.5 - 822.5	2.18E+15	8.96E-28	1.70E-22	
153	822.5 - 827.5	2.20E+15	8.75E-28	1.52E-22	
154	827.5 - 832.5	2.14E+15	8.53E-28	1.42E-22	
155	832.5 - 837.5	2.14E+15	8.33E-28	1.40E-22	
156	837.5 - 842.5	2.13E+15	8.13E-28	1.40E-22	
157	842.5 - 847.5	2.09E+15	7.94E-28	1.42E-22	
158	847.5 - 852.5	2.05E+15	7.75E-28	1.45E-22	

\* Wavelength range for spectral intervals 1-49 correspond to 500 wavenumbers. Wavelength range for remainder of spectral intervals is 5 nm.

**Table 7-5.** Solar Spectral Irradiance Measurements for Wavelengths 210.526 – 327.5 nm Considered in Developing the Reference Spectrum

Date of Measurement	RMS Deviation $\epsilon(20,53)\%$	Reference
Nov. 7, 1978	3.3	Heath (1980)
July 15, 1980	5.3	Mount and Rottman (1981) <sup>1</sup>
Sept. 15, 1980	6.2	Mentall <i>et al.</i> (1981)
May 17, 1982	3.1	Mount and Rottman (1983a) <sup>1</sup>
Jan. 12, 1983	3.0	Mount and Rottman (1983b) <sup>1</sup>
July 25, 1983	3.3	Mount and Rottman (1985) <sup>1</sup>

<sup>1</sup>Values at wavelengths greater than 296 nm were excluded in compiling the reference spectrum.

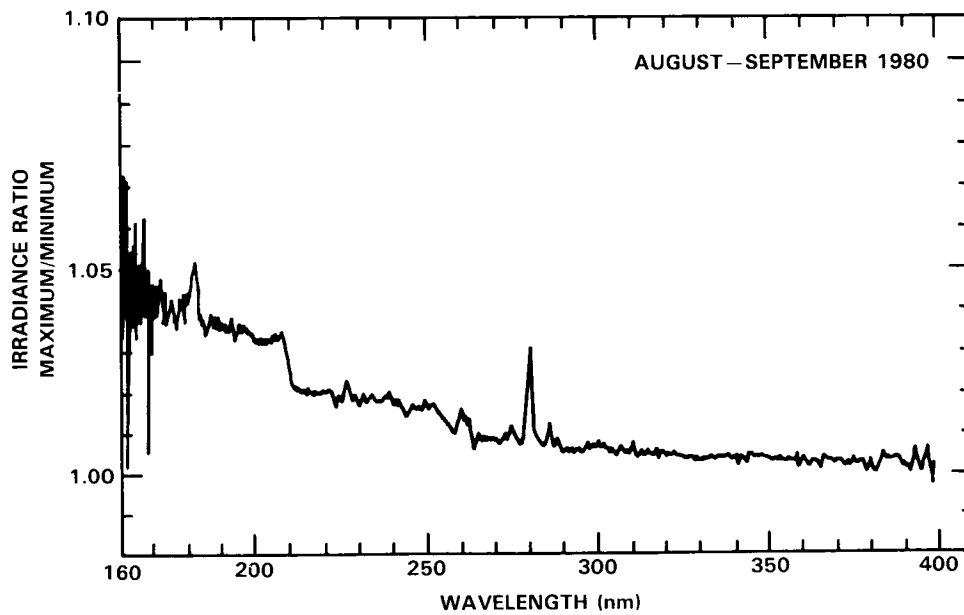
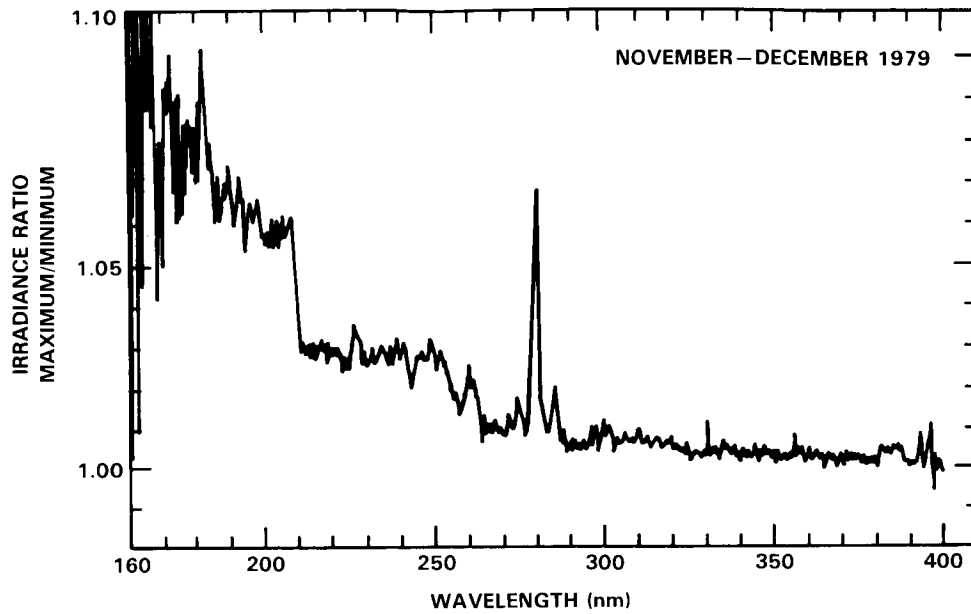
### 7.1.3.3 The Spectral Region 327.5 - 852.5 nm

Recommended values of the solar irradiance at wavelengths greater than 327.5 nm have not changed significantly since the comprehensive review of Nicolet (1981) and WMO No. 11 (1982). The available data sets here are the Nimbus 7 SBUV results of Heath (1980) extending to 400 nm and the results of Arvesen *et al.* (1969) and Neckel and Labs (1984). The values in Table 7-4 from 327.5 to 397.5 nm ( $i = 54$  to 67) are based on Heath (1980) and at longer wavelengths are the same as given in WMO No. 11 (1982) which includes a discussion of the uncertainties. In the visible the accuracy is  $\pm 3\%$ , but this degrades somewhat toward the ultraviolet.

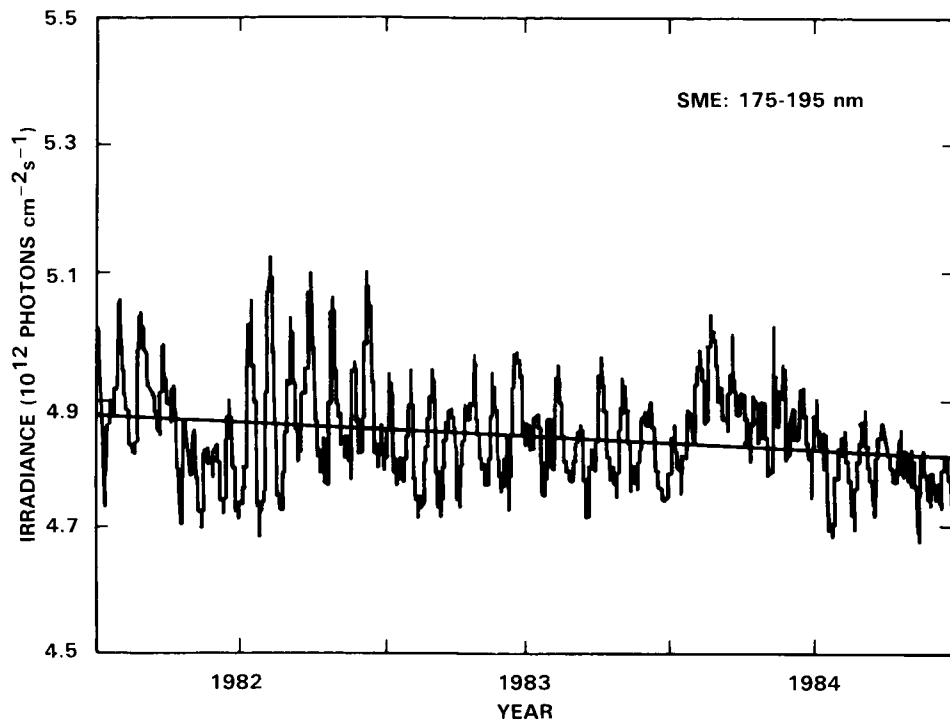
### 7.1.4 Solar Variability at Wavelengths Greater than 175 nm

Figure 7-3 illustrates the variation in irradiance received at the Earth as a function of wavelength over two 27 day solar rotation periods in November/December 1979 and August/September 1980 as observed by the Nimbus 7 SBUV instrument (Heath *et al.*, 1984). Between 175 and 210 nm, the spectral region important for production of atmospheric odd oxygen, the maximum irradiance during the December 1979 rotation tends to be 1.05 to 1.07 times the minimum value with a peak ratio approaching 1.10. The  $A^1 I$  edge near 210 nm is an obvious feature longward of which the fractional variations decrease markedly. Between 210 and 250 nm the maximum to minimum irradiance ratio is typically 1.03 and beyond 260 nm drops to 1.01 or less. An exception is the large variation in the core of the Mg II absorption feature near 280 nm. The changes observed during the September rotation are much less pronounced. Figures 7-4, 7-5, and 7-6 for the wavelength regions 175-195 nm, 195-208 nm, and 240-260 nm respectively show that the variability of the irradiance is not exactly repeatable from one solar rotation to another, as would be expected from the evolution of active regions.

## RADIATIVE PROCESSES



**Figure 7-3.** Variation in the solar irradiance over two 27 day rotation periods in November-December 1979 and August-September 1980. The ratio is of the maximum irradiance observed during the rotation to the mean of the preceding and following minima. Values are from the Nimbus 7 SBUV experiment (Heath *et al.*, 1984).



**Figure 7-4.** Variation in the 175-195 nm integrated irradiance over the period 1982 through 1984 observed from the Solar Mesosphere Explorer satellite. The straight line is a least squares fit to the measurements. (Data provided by G.J. Rottman.)

A linear fit to the values in Figures 7-4 through 7-6 and extrapolation provides a rough measure of solar variations over time scales of years. Table 7-6 presents estimates of the solar cycle variability in selected wavelength bins spanning the region 175 to 300 nm. The reported quantity,  $R_{sc}$ , is a measure of the ratio of solar maximum irradiance to solar minimum irradiance obtained from a linear fit to all of the SME measurements. The uncertainty limits account for possible instrument drifts that may still influence the results after a correction for this has been applied. Caution is advised in a physical interpretation of the  $R_{sc}$  values. The tabulated results give the ratio of a typical irradiance averaged over a 27 day rotation period at solar maximum to the same average performed at solar minimum. Also included in Table 7-6 is an estimate of the 27 day irradiance variation,  $R_{27}$ , from the data of Figure 7-3. If this is taken as a typical mean solar rotation, then the ratio of maximum to minimum irradiance during a solar cycle is the product  $R_{27}R_{sc}$ . For model calculations of atmospheric response to an 11 year solar variability, the maximum and minimum irradiances,  $F_{MAX}(i)$  and  $F_{MIN}(i)$ , are related to the mean reference spectrum of Table 7-4 by:

$$F_{MAX}(i) = F_{REF}(i) \left[ \frac{2 R_{27}(i) R_{sc}(i)}{1 + R_{27}(i) R_{sc}(i)} \right] \quad (7.3)$$

and

$$F_{MIN}(i) = F_{REF}(i) \left[ \frac{2}{1 + R_{27}(i) R_{sc}(i)} \right] \quad (7.4)$$

where  $R_{27}(i)$  and  $R_{sc}(i)$  must be derived for each spectral interval based on Table 7-6.

## RADIATIVE PROCESSES

**Table 7-6.** Parameters for Estimating Irradiance Variability over the 11 Year Solar Cycle

Wavelength Range	$R_{sc}^1$ (max/min)	$R_{27}^2$ (max/min)
175 - 190	1.020 ( $\pm 0.020$ )	1.07
190 - 210	1.030 ( $\pm 0.020$ )	1.06
210 - 240	1.026 ( $\pm 0.020$ )	1.03
240 - 300	1.005 ( $\pm 0.020$ )	1.01

$R_{sc}^1$  is the ratio of a 27 day mean irradiance near solar maximum to a 27 day mean at solar minimum.

$R_{27}^2$  is the ratio of the maximum irradiance observed during a typical 27 day solar rotation to the minimum irradiance during this rotation.

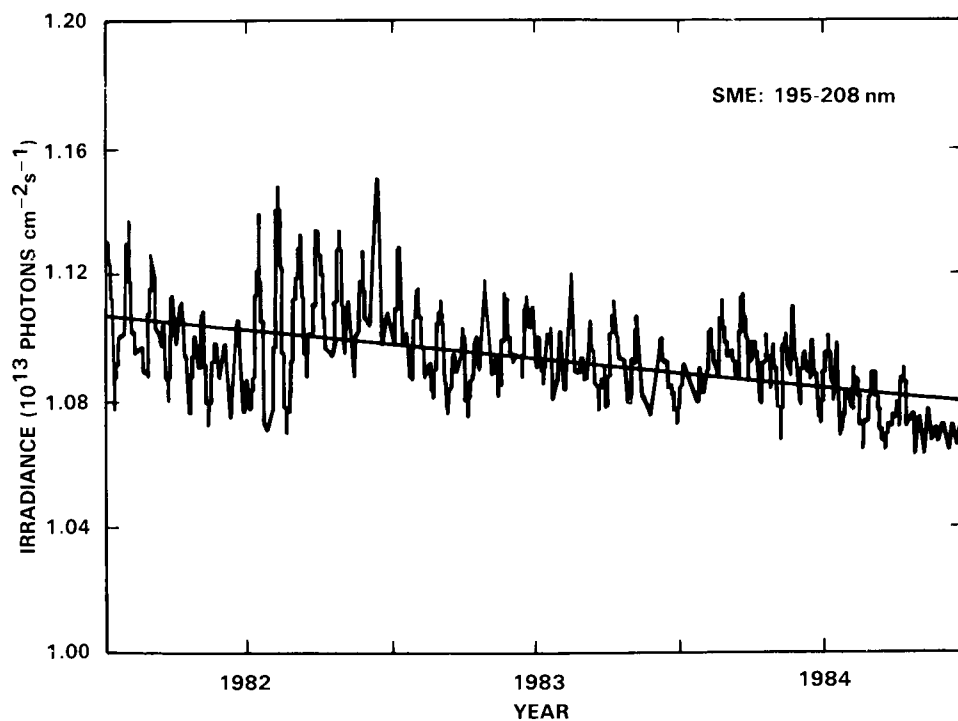


**Figure 7-5.** Variation in the 195-208 nm integrated irradiance over the period 1982 through 1984 observed from the Solar Mesosphere Explorer satellite. The straight line is a least squares fit to the measurements. (Data provided by G.J. Rottman.)

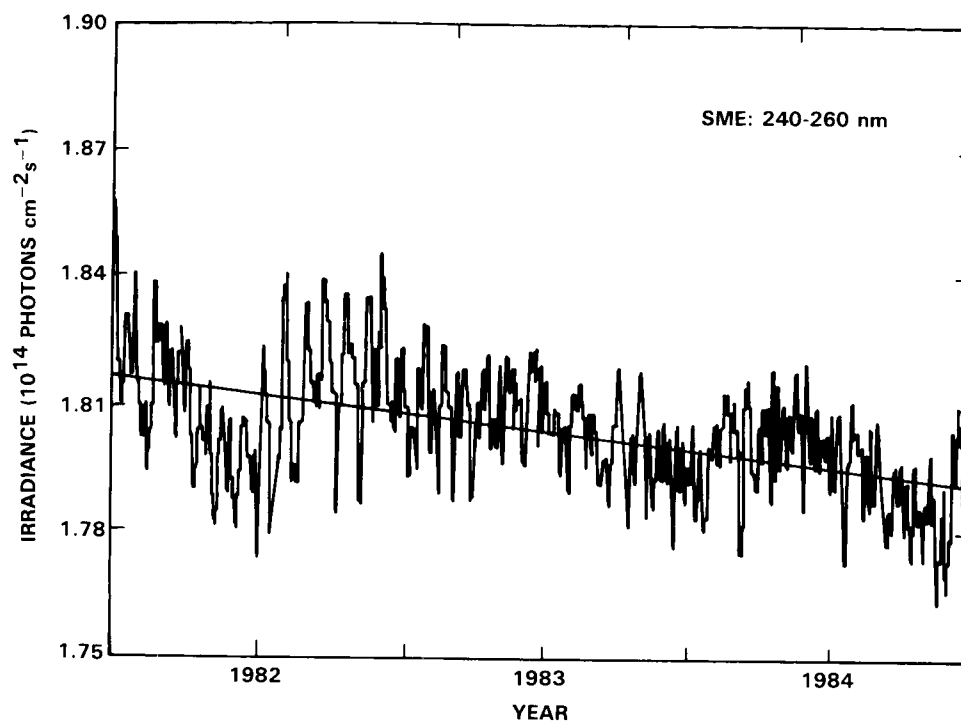


**Figure 7-6.** Variation in the 240-260 nm integrated irradiance over the period 1982 through 1984 observed from the Solar Mesosphere Explorer satellite. The straight line is a least squares fit to the measurements. (Data provided by G.J Rottman.)

It must be recognized that any estimate of solar cycle variability based on the available measurements contains a large uncertainty, and the recommendations given above will surely change as more information becomes available. Estimates of solar variability from Table 7-6 are much smaller than recent predictions derived from empirical models of solar activity. The model of Lean (1984) uses Nimbus 7 SBUV observations of short term irradiance changes and from this infers the behavior over an 11 year cycle. This procedure predicts a 25% minimum to maximum variation at 200 nm, decreasing to 10% between 210 and 250 nm. As the long term data base increases, further empirical modeling to relate observed irradiance behavior to readily measured indices of solar activity is strongly encouraged. However, in view of the complex behavior displayed by the solar irradiance, the major emphasis must be on the acquisition of a long term data base that is essentially free of instrumental artifacts.

### 7.1.5 Rayleigh Scattering

An accurate calculation of the solar radiation field reaching the lower stratosphere and troposphere at wavelengths greater than 290 nm requires inclusion of multiple Rayleigh scattering and reflection from the lower boundary, particularly cloud decks (Meier *et al.*, 1982; Nicolet *et al.*, 1982). In addition, at wavelengths near 210 nm the optical depth for Rayleigh scattering is approximately 20% of that associated with the Herzberg continuum of O<sub>2</sub>. Recently Bates (1984) re-evaluated the cross section for Rayleigh scattering in air and using these results Nicolet (1984a) has derived analytic expressions for use in aeronomic calculations. With wavelength  $\lambda$  expressed in microns the following formula applies:

## RADIATIVE PROCESSES

$$\sigma_{RS}(\lambda) = \frac{4.02 \times 10^{-28}}{\lambda^4 + \chi} \quad (7.5)$$

where  $\sigma_{RS}(\lambda)$  is the Rayleigh scattering cross section in  $\text{cm}^2$  and the parameter  $\chi$  is given by:

$$\chi = 0.389\lambda + \frac{0.09426}{\lambda} - 0.3228 \quad (7.6)$$

for  $0.20\mu \leq \lambda \leq 0.55\mu$  and:

$$\chi = 0.04 \quad (7.7)$$

for  $0.55\mu < \lambda \leq 1.0\mu$ . Nicolet (1984) notes that Equations 7.5 and 7.6 produce accurate results at least to a wavelength of  $0.190\mu$ . Table 7-4 includes values of the Rayleigh scattering cross section for use in atmospheric modeling.

### 7.1.6 Absorption by Molecular Oxygen

#### 7.1.6.1 Absorption at the Lyman Alpha Line (121.6 nm)

Absorption by  $\text{O}_2$  controls the penetration of the H Lyman alpha line into the mesosphere. The primary complication involved in treating the transfer of this radiation concerns the need to convolve the Lyman alpha self-reversed profile with the  $\text{O}_2$  absorption cross section, which varies significantly over an interval of  $\pm 0.1$  nm about line center (Frederick and Hudson 1980a; Lewis *et al.*, 1983; Nicolet, 1985). Early laboratory measurements showed the  $\text{O}_2$  cross section to vary in the range  $1 \times 10^{-20}$  to  $3 \times 10^{-20} \text{cm}^2$  over the line profile (Ogawa, 1971) and more recent data have defined the temperature dependence (Carver *et al.*, 1977). The change in profile shape with optical depth can be incorporated into transmission calculations by use of an effective cross section which depends on  $\text{O}_2$  column content,  $N$ , measured along the path of the solar beam. For a temperature of 230K Nicolet (1985) derived the expression

$$T(\text{Ly}\alpha) = \exp[-2.115 \times 10^{-18} N^{0.8855}] \quad (7.8)$$

where  $T$  is the Lyman alpha transmission and  $N$  is in  $\text{cm}^{-2}$ . The effective  $\text{O}_2$  cross section is  $\sigma_{\text{eff}} = 2.115 \times 10^{-18} N^{-0.1145}$ . For  $N = 1 \times 10^{20} \text{cm}^{-2}$  this gives  $\sigma_{\text{eff}} = 1.08 \times 10^{-20} \text{cm}^2$  which is close to the laboratory measurements. Equation 7.8 is recommended for use in atmospheric calculations.

#### 7.1.6.2 The Schumann-Runge Bands and Underlying Continuum

At wavelengths shortward of 205 nm extending to 175 nm the Schumann-Runge bands of molecular oxygen are a major absorption feature, corresponding to the transition  $\text{B}^3\Sigma_u^- \leftarrow \text{X}^3\Sigma_g^-$ . Predissociation yielding two  $\text{O}(^3\text{P})$  atoms occurs via one or more repulsive states in more than 99% of the absorptions (Hudson and Mahle, 1972). Because a predissociation is involved, the cross section consists of thousands of individual rotational lines. The Schumann-Runge band absorption is generally viewed as the dominant source of atmospheric odd oxygen at altitudes greater than 60 km; however, this transition is significant at stratospheric altitudes for a different reason. At discrete wavelengths situated in between the rotational peaks the cross section drops to small values ( $\sim 10^{-24} - 10^{-23} \text{cm}^2$ ) and solar radiation at these selected

wavelengths, particularly above 190 nm, can then penetrate into the middle stratosphere. Several source molecules, such as nitrous oxide and the chlorofluorocarbons, have large cross sections in the 175-200 nm spectral region and significant fractions of their total dissociation rates arise from absorption here. Hence, in modeling the Schumann-Runge band system it is critical to consider details of the line shapes since the overlapping wings of thousands of lines sum to form the smooth pseudo-continuum cross section located between the rotational peaks.

The Schumann-Runge bands are not the only transition that contributes to the total O<sub>2</sub> dissociation cross section between 175 and 205 nm. The Herzberg continuum extends throughout this spectral region, while absorption by excited vibrational levels in the Schumann-Runge continuum leads to a highly temperature dependent cross section that increases in importance relative to the bands as wavelength decreases toward 175 nm (Hudson and Mahle, 1972). These underlying continua must be considered when computing the solar energy that penetrates to any given level of the mesosphere and stratosphere.

The molecular parameters used to characterize the Schumann-Runge band cross section are (1) an oscillator strength for each vibrational transition and (2) a rotational line width in wavenumber units reflecting predissociation broadening for each band. Intercomparisons of the available laboratory data by Nicolet and Peetermans (1980), Nicolet (1983), and Frederick *et al.* (1983) show that significant discrepancies still exist. Of the measurements made over the last decade only those of Yoshino *et al.* (1983) have sufficient spectral resolution to yield the absolute cross section directly for the (1,0) - (12,0) bands. The cross sections of Yoshino *et al.* (1983) are recommended here as the preferred data set for future use in stratospheric modeling. However, these data, obtained at a temperature of 300 K, are not currently in a form that is directly applicable to atmospheric studies, although the necessary work is proceeding. The extraction of predissociation line widths from high resolution photoabsorption data for the (13,0) - (16,0) bands has been accomplished (Smith *et al.*, 1984) and the determination of line widths for the (1,0) - (12,0) bands is in progress (D. E. Freeman, personal communication, 1985).

Given band oscillator strengths and rotational line widths, it is necessary to compute the detailed cross section using the wavenumber and strength of each spectral line (Frederick and Hudson, 1979, 1980a). The total line width consists of contributions from predissociation and Doppler broadening while the line shape is described by a Voigt profile. Although Doppler broadening leads to a temperature dependent cross section, the major source of temperature sensitivity arises from absorption by O<sub>2</sub>(X<sup>3</sup>Σ<sub>g</sub><sup>-</sup>) in the excited v=1 and 2 levels. Band oscillator strengths for these transitions are typically an order of magnitude larger than for absorption by v=0 (Blake, 1979) leading to a temperature dependence in the total cross section that reflects a changing thermal population of the ground electronic state. In atmospheric applications this temperature dependence should be accounted for.

The atmospheric transmission of solar radiation in the i-th spectral interval for i=1,2,...,17 as defined in Table 7-4 is:

$$T(i,N) = T_{SR}(i,N) T_{HZ}(i,N) T_{O_3}(i,N) \quad (7.9)$$

where T<sub>HZ</sub>(i,N) is the transmission as controlled by the Herzberg continuum of O<sub>2</sub>, T<sub>O<sub>3</sub></sub>(i,N) accounts for the effect of absorption by ozone, and T<sub>SR</sub>(i,N) refers to the combined effects of the Schumann-Runge bands and the underlying Schumann-Runge continuum. Here N is the slant path O<sub>2</sub> column abundance measured along the path of the incoming solar beam. Because the O<sub>2</sub> Herzberg continuum σ<sub>HX</sub> and ozone σ<sub>O<sub>3</sub></sub> cross sections vary smoothly with wavelength one can use the mean values of Table 7-4 directly in the expressions

## RADIATIVE PROCESSES

$$T_{\text{HZ}}(i,N) = \exp[-\sigma_{\text{HZ}}(i)N] \quad (7.10)$$

and

$$T_{\text{O}_3}(i,N) = \exp[-\sigma_{\text{O}_3}(i) N_{\text{O}_3}(N)] \quad (7.11)$$

where  $N_{\text{O}_3}(N)$  is the slant path  $\text{O}_3$  column at the location where  $N$  gives the slant column  $\text{O}_2$ . However, the rapid variation in the Schumann-Runge band cross section over small wavelength intervals makes it impractical, if not impossible, to include all spectral detail in photochemical calculations. For this reason simple parameterizations giving the transmission in a spectral interval or an effective cross section as a function of slant path molecular oxygen column content,  $N$ , are useful. An alternate approach is to present molecular oxygen dissociation rates and transmission values in tabular form. The transmission through the  $i$ -th spectral interval extending from wavenumber  $\nu(i)$  to  $\nu(i) + \Delta\nu(i)$  in the Schumann-Runge region is:

$$T_{\text{SR}}(i,N) = \frac{1}{\Delta\nu(i)} \int_{\nu(i)}^{\nu(i)+\Delta\nu(i)} d\nu \exp\left[-\int_0^N dN \sigma_{\text{SR}}(\nu,N)\right] \quad (7.12)$$

The cross section  $\sigma_{\text{SR}}$  depends on  $N$  because of temperature variations along the slant path of the incoming solar beam. As used here, the cross section,  $\sigma_{\text{SR}}$ , includes both the Schumann-Runge bands and Schumann-Runge continuum, but not the Herzberg continuum. Values of  $T_{\text{SR}}(i,N)$  for the spectral range 57000–48500  $\text{cm}^{-1}$  ( $\lambda = 175.439 - 206.186$  nm) split into 17 intervals ( $i=1,2,\dots, 17$ ) appear in Table 7-7. These calculations utilize the cross sections of Frederick and Hudson (1979, 1980a,b) applied to an overhead Sun and the temperature profile of the *U.S. Standard Atmosphere, 1976*. The temperature dependent Schumann-Runge continuum cross sections are from Hudson and Mahle (1972). The results of Table 7-7 can be applied to any solar zenith angle with acceptable accuracy by taking the tabulated  $\text{O}_2$  column abundances to be measured along the slant path of incoming sunlight. In addition, the transmission values in Table 7-7 include an estimate of the effects of the (1,0) Schumann-Runge band covering intervals  $i=14$  and 15. Absorption by this band was neglected by Frederick and Hudson (1979a, 1980a,b) since there was uncertainty as to whether predissociation occurs here, but it clearly appears in the high resolution stratospheric balloon spectra of Anderson and Hall (1983). Parameterizations incorporating varying levels of complexity have been presented by Blake (1979), Nicolet and Peetermans (1980), and Allen and Frederick (1982). Simon and Brasseur (1983) have reviewed the various approaches taken in this type of work. It would be of value to derive a new set of transmission functions and dissociation rates based on the cross sections of Yoshino *et al.* (1983) since these data are preferable to previous laboratory results because of their high spectral resolution. Such work has not yet been performed. Until this is done, the parameterizations of Nicolet and Peetermans (1980) or Allen and Frederick (1982), corrected to include currently accepted values of the Herzberg continuum cross section, are acceptable for atmospheric modeling.

### 7.1.6.3 Absorption by the Herzberg Continuum

Absorption by molecular oxygen in the Herzberg continuum,  $\text{A}^3\Sigma_u^+ \leftarrow \text{X}^3\Sigma_g^-$ , followed by dissociation is the dominant source of odd oxygen in the Earth's atmosphere at altitudes below approximately 60 km. The relevant wavelengths in the solar spectrum lie shortward of 242.4 nm. Despite the importance of this absorption in the formation of the ozone layer, the transition is strictly forbidden by electric dipole selection rules and the cross section is less than  $1 \times 10^{-23} \text{ cm}^2$  at all wavelengths.

**RADIATIVE PROCESSES**

**Table 7-7.** Transmission in the Schumann-Runge System (SR Bands Plus SR Continuum) Versus Slant Path O<sub>2</sub> Column

O <sub>2</sub> Column N(cm <sup>-2</sup> )*	Transmission In 500 cm <sup>-1</sup> Intervals**					
	(1) 57000-56500	(2) 56500-56000	(3) 56000-55500	(4) 55500-55000	(5) 55000-54500	(6) 54500-54000
3.922E+16	9.919E-01	9.947E-01	9.974E-01	9.979E-01	9.982E-01	9.994E-01
7.262E+16	9.851E-01	9.903E-01	9.952E-01	9.962E-01	9.967E-01	9.989E-01
1.555E+17	9.690E-01	9.807E-01	9.904E-01	9.920E-01	9.934E-01	9.977E-01
3.901E+17	9.274E-01	9.589E-01	9.784E-01	9.808E-01	9.849E-01	9.947E-01
1.060E+18	8.324E-01	9.183E-01	9.509E-01	9.533E-01	9.654E-01	9.868E-01
2.905E+18	6.666E-01	8.571E-01	9.003E-01	8.993E-01	9.291E-01	9.675E-01
7.718E+18	4.512E-01	7.698E-01	8.288E-01	8.166E-01	8.754E-01	9.294E-01
1.960E+19	2.416E-01	6.504E-01	7.398E-01	7.118E-01	8.045E-01	8.715E-01
4.716E+19	9.681E-02	5.013E-01	6.334E-01	5.910E-01	7.149E-01	7.989E-01
1.078E+20	2.584E-02	3.364E-01	5.087E-01	4.566E-01	6.060E-01	7.100E-01
2.358E+20	3.290E-03	1.823E-01	3.657E-01	3.160E-01	4.793E-01	6.014E-01
4.939E+20	8.669E-05	7.037E-02	2.140E-01	1.187E-01	3.422E-01	4.744E-01
9.919E+20	6.006E-08	1.479E-02	8.532E-02	7.962E-02	2.118E-01	3.365E-01
1.919E+21	0.000E-00	9.174E-04	1.636E-02	2.227E-02	1.050E-01	2.042E-01
3.607E+21	0.000E-00	4.659E-06	8.035E-04	2.992E-03	3.585E-02	1.003E-01
6.756E+21	0.000E-00	3.945E-10	5.405E-06	1.454E-04	7.271E-03	3.853E-02
1.299E+22	0.000E-00	0.000E-00	2.674E-09	1.750E-06	7.493E-04	1.085E-02
2.595E+22	0.000E-00	0.000E-00	0.000E-00	1.250E-09	2.147E-05	1.557E-03
5.382E+22	0.000E-00	0.000E-00	0.000E-00	0.000E-00	3.0380E-08	4.294E-05
1.145E+23	0.000E-00	0.000E-00	0.000E-00	0.000E-00	0.000E-00	3.130E-08
2.480E+23	0.000E-00	0.000E-00	0.000E-00	0.000E-00	0.000E-00	0.000E-00

## RADIATIVE PROCESSES

**Table 7-7.** Transmission in the Schumann-Runge System (SR Bands Plus SR Continuum) Versus Slant Path O<sub>2</sub> Column (Continued)

O <sub>2</sub> Column N(cm <sup>-2</sup> )*	Transmission In 500 cm <sup>-1</sup> Intervals**					
	(7) 54000-53500	(8) 53500-53000	(9) 53000-52500	(10) 52500-52000	(11) 52000-51500	(12) 51500-51000
3.922E+16	9.997E-01	9.998E-01	9.999E-01	9.999E-01	9.999E-01	9.999E-01
7.262E+16	9.994E-01	9.997E-01	9.998E-01	9.999E-01	9.999E-01	9.999E-01
1.555E+17	9.989E-01	9.994E-01	9.997E-01	9.999E-01	9.999E-01	9.999E-01
3.901E+17	9.974E-01	9.987E-01	9.994E-01	9.997E-01	9.998E-01	9.999E-01
1.060E+18	9.933E-01	9.968E-01	9.986E-01	9.994E-01	9.994E-01	9.998E-01
2.905E+18	9.829E-01	9.918E-01	9.964E-01	9.984E-01	9.984E-01	9.996E-01
7.718E+18	9.598E-01	9.804E-01	9.910E-01	9.962E-01	9.959E-01	9.989E-01
1.960E+19	9.178E-01	9.588E-01	9.788E-01	9.908E-01	9.898E-01	9.974E-01
4.716E+19	8.567E-01	9.245E-01	9.560E-01	9.795E-01	9.763E-01	9.938E-01
1.078E+20	7.785E-01	8.745E-01	9.207E-01	9.581E-01	9.496E-01	9.862E-01
2.358E+20	6.828E-01	8.058E-01	8.741E-01	9.254E-01	9.035E-01	9.713E-01
4.939E+20	5.668E-01	7.158E-01	8.152E-01	8.759E-01	8.361E-01	9.452E-01
9.919E+20	4.302E-01	6.020E-01	7.404E-01	8.083E-01	7.516E-01	9.047E-01
1.919E+21	2.802E-01	4.603E-01	6.449E-01	7.167E-01	6.530E-01	8.493E-01
3.607E+21	1.455E-01	3.380E-01	5.272E-01	6.002E-01	5.427E-01	7.781E-02
6.756E+21	6.039E-02	2.227E-01	4.011E-01	4.720E-01	4.303E-01	6.917E-01
1.299E+22	2.027E-02	1.315E-01	2.827E-01	3.478E-01	3.273E-01	5.932E-01
2.595E+22	4.384E-03	6.138E-02	1.761E-01	2.296E-01	2.360E-01	4.831E-01
5.382E+22	2.953E-04	1.664E-02	8.453E-02	1.210E-01	1.532E-01	3.604E-01
1.145E+23	1.365E-06	1.443E-03	2.309E-02	4.147E-01	8.007E-02	2.306E-01
2.480E+23	0.000E-00	1.279E-05	1.948E-03	6.263E-03	2.716E-02	1.119E-01

**RADIATIVE PROCESSES**

**Table 7-7.** Transmission in the Schumann-Runge System (SR Bands Plus SR Continuum) Versus Slant Path O<sub>2</sub> Column (Continued)

O <sub>2</sub> Column N(cm <sup>-2</sup> )*	Transmission In 500 cm <sup>-1</sup> Intervals**				
	(13) 51000-50500	(14) 50500-50000	(15) 50000-49500	(16) 49500-49000	(17) 49000-48500
3.922E+16	9.999E-01	9.999E-01	9.998E-01	9.998E-01	9.999E-01
7.262E+16	9.999E-01	9.999E-01	9.998E-01	9.998E-01	9.999E-01
1.555E+17	9.999E-01	9.999E-01	9.998E-01	9.998E-01	9.999E-01
3.901E+17	9.999E-01	9.999E-01	9.998E-01	9.998E-01	9.999E-01
1.060E+18	9.999E-01	9.999E-01	9.998E-01	9.998E-01	9.999E-01
2.905E+18	9.998E-01	9.999E-01	9.998E-01	9.998E-01	9.999E-01
7.718E+18	9.997E-01	9.999E-01	9.998E-01	9.998E-01	9.999E-01
1.960E+19	9.993E-01	9.998E-01	9.998E-01	9.998E-01	9.999E-01
4.716E+19	9.983E-01	9.998E-01	9.996E-01	9.997E-01	9.998E-01
1.078E+20	9.962E-01	9.996E-01	9.996E-01	9.997E-01	9.998E-01
2.358E+20	9.921E-01	9.990E-01	9.994E-01	9.997E-01	9.998E-01
4.939E+20	9.846E-01	9.979E-01	9.984E-01	9.996E-01	9.996E-01
9.919E+20	9.728E-01	9.954E-01	9.977E-01	9.993E-01	9.995E-01
1.919E+21	9.546E-01	9.901E-01	9.954E-01	9.987E-01	9.990E-01
3.607E+21	9.274E-01	9.789E-01	9.910E-01	9.974E-01	9.983E-01
6.756E+21	8.881E-01	9.618E-01	9.827E-01	9.949E-01	9.970E-01
1.299E+22	8.365E-01	9.362E-01	9.679E-01	9.908E-01	9.944E-01
2.595E+22	7.687E-01	8.974E-01	9.403E-01	9.830E-01	9.891E-01
5.382E+22	6.763E-01	8.326E-01	8.859E-01	9.673E-01	9.783E-01
1.145E+23	5.511E-01	7.220E-01	7.810E-01	9.348E-01	9.553E-01
2.480E+23	3.896E-01	5.441E-01	5.947E-01	8.693E-01	9.076E-01

\*O<sub>2</sub> column is measured along the slant path of incoming solar radiation.

\*\*The numbering of intervals 1 through 17 is the same as that used in Table 7-4.

## RADIATIVE PROCESSES

The small magnitude of the absorption poses major experimental problems, and it now appears that laboratory data used in atmospheric modeling prior to 1982 significantly overestimated the true cross section. A primary complication concerns the dependence of measured cross sections on the molecular oxygen concentration present in the laboratory apparatus. This arises from a combination of pressure-induced absorption and formation of the O<sub>4</sub> dimer whose absorption cross section differs from that of O<sub>2</sub>. Historically, large O<sub>2</sub> column abundances were required to accurately measure the weak Herzberg continuum absorption, and in the laboratory this implied large concentrations as well. Data collected under such conditions require extrapolation to low pressure limiting values for application to upper atmospheric calculations. Apparently this pressure dependent behavior was not adequately corrected for in the early measurements, and published values for the zero pressure limit were not appropriate to atmospheric conditions. As an example of this pressure dependence, the data of Johnston *et al.* (1984) show a linear relationship between the measured absorption cross section and O<sub>2</sub> concentration. At a wavelength of 225 nm the cross section at one atmosphere is more than a factor of two greater than the zero pressure extrapolated value. An additional problem that may have degraded early data concerns unwanted formation of ozone in the laboratory system. Between 200 and 230 nm the absorption cross section of ozone exceeds that of molecular oxygen by factors ranging from 4 × 10<sup>4</sup> to 2 × 10<sup>6</sup>. Hence a very small ozone mixing ratio in the laboratory system, if not corrected for, would seriously contaminate the derived Herzberg cross section, particularly at wavelengths greater than 220 nm. Further discussion of these issues appears in Frederick *et al.* (1983a) together with an intercomparison of cross section values published prior to 1980.

Balloon-borne spectrometer measurements of the attenuated solar irradiance reaching the middle stratosphere reported by Frederick and Mentall (1982) indicated more ultraviolet light reaching these levels than predicted on the basis of Herzberg continuum cross section values generally accepted at the time (e.g., Hasson and Nicholls, 1971; Ditchburn and Young, 1962; Ogawa, 1971; Shardanand and Prasad Rao, 1977; Hudson and Reed, 1979). Interpretation of the in situ measurements in terms of O<sub>2</sub> absorption cross sections by Herman and Mentall (1982a) implied values significantly less than the laboratory results. More recent balloon measurements by Anderson and Hall (1983) support these small cross sections, although the data of Pirre *et al.* (1984) suggest somewhat larger values. In addition, new laboratory work has been reported by Cheung *et al.* (1984a) and Johnston *et al.* (1984), taking care to derive the low pressure limiting cross sections properly. These support small values as inferred from the attenuated solar radiation measurements. However, a comparison of the results of Cheung *et al.* (1984a) and Johnston *et al.* (1984) in the wavelength region of near overlap shows a significant disagreement. In the wavelength range 204-205 nm Cheung *et al.* (1984a) report a cross section of  $(5.5 \pm 1.0) \times 10^{-24} \text{cm}^2$  while at 205 nm the Johnston *et al.* (1984) value is  $(7.7 \pm 0.3) \times 10^{-24} \text{cm}^2$ . Both data sets are allegedly free of contamination from the long wavelength end of the Schumann-Runge bands. In yet unpublished work with longer path lengths and lower pressure A.S.C. Cheung and colleagues have examined in detail the extrapolation to the low pressure limit and obtain, at 205 nm, a cross section of  $(7.2 \pm 0.2) \times 10^{-24} \text{cm}^2$ . These cross sections include a calculated Rayleigh scattering contribution (Bates, 1984) of  $0.35 \times 10^{-24} \text{cm}^2$  at 205 nm.

The Herzberg continuum cross sections recommended in Table 7-4 are based on the laboratory results of Johnston *et al.* (1984) combined with a theoretical continuum shape to extrapolate in wavelength beyond the limits of the measurements, being 205 and 225 nm. The equation used for extrapolation is:

$$\sigma_{\text{HZ}}(\lambda) = \sigma_0 \left( \frac{\lambda_0}{\lambda} \right) \exp\{-\alpha[\ln(\lambda_0/\lambda)]^2\} \quad (7.13)$$

where  $\sigma_{\text{HZ}}$  is the desired Herzberg continuum cross section at wavelength  $\lambda$  in nm. In the spectral range 205-225 nm Equation 7.13 was used to interpolate between the grid points of Johnston *et al.* (1984) using

$\sigma_0$  and  $\alpha$  values obtained by fitting the measured cross sections at adjacent wavelengths. It is noted that the Herzberg continuum cross sections of Johnston *et al.* (1984) include contributions from Rayleigh scattering.

### 7.1.7 Absorption by Ozone

#### 7.1.7.1 General Characteristics of Ozone Absorption

Absorption of incoming solar radiation by ozone occurs in the strong Hartley region at wavelengths less than 308 nm while the weaker, temperature dependent Huggins bands extend to longer wavelengths terminating near 360 nm. An additional absorption region, the Chappuis bands, lie in the visible from approximately 410 nm out through wavelengths exceeding 850 nm. Absorption in the Hartley region peaks close to 255 nm with a cross section near  $1 \times 10^{-17}$  cm<sup>2</sup> and is accompanied by the process  $O_3 + h\nu \rightarrow O_2(a^1\Delta_g) + O(^1D)$  plus a small yield of  $O(^3P)$ . Absorption in the Huggins and Chappuis bands produces only ground state oxygen atoms. Simons *et al.* (1973) analyzed high resolution ozone spectra showing that the Hartley region is dominated by a continuum with weak band structure superimposed. The electronic transition is  $^1B_2 \leftarrow X^1A_1$ . The Huggins bands involve the same upper and lower states where absorption here populates  $^1B_2$  below the dissociation limit followed by predissociation.

#### 7.1.7.2 The Hartley Region

Absorption in the Hartley region is by far the dominant mechanism for dissociating ozone in the stratosphere and mesosphere. Over the past 35 years there have been several measurements of the cross section as reviewed by Hudson (1971) up through 1970. Hearn (1961) reported absolute measurements of the Hartley region cross section at the wavelengths of several mercury lines, 253.7, 289.4, 296.7, and 302.1 nm, and these results have served as the basis for normalizing relative measurements that cover the entire spectrum. Absolute values of the Hartley region cross section are generally considered known to an accuracy of  $\pm 2.5\%$  at room temperature.

The recommended cross section values in Table 7-4 are based on the following original data sources and previous tabulations. For spectral intervals  $i=1$  to 14 ( $\lambda = 175.439 - 200.000$  nm) the values are based on the data of Watanabe *et al.* (1953) as tabulated by Ackerman (1971). There appears to have been no new measurements reported in this wavelength region since 1953. Recommended cross sections for intervals  $i=15$  to 33 ( $\lambda = 200.000 - 246.914$  nm), also taken from Ackerman (1971), are based on the results of Inn and Tanaka (1953) which are supported by the later measurements of DeMore and Raper (1964) and Griggs (1968). New measurements for spectral intervals  $i=34$  to 57 ( $\lambda = 246.914 - 347.5$  nm) encompassing essentially all of the remaining Hartley region have been made by A.M. Bass of the National Bureau of Standards and R.J. Paur of the Environmental Protection Agency (Bass and Paur, 1984; Paur and Bass, 1985). These results, which are not yet published in full, include the temperature dependence of the cross section and use the 253.7 nm measurement of Hearn (1961) to establish an absolute scale. The cross section at 253.7 nm is assumed to be independent of temperature. Table 7-4 lists the Bass and Paur cross sections at temperatures of 203 and 273 K, a range that encompasses that encountered in the stratosphere. The temperature dependence seems to arise from absorption by excited modes of  $O_3(X^1A_1)$  in the thermal population (Simons *et al.*, 1973). Near the long wavelength limit of the Hartley region ( $i=49$ ) the ratio of cross sections for 273 K and 203 K is 1.11. While this variation is not large compared to many uncertainties in photochemical modeling, the temperature dependence of the Hartley region should likely be included in future atmospheric calculations at wavelengths greater than 295 nm. At wavelengths

## RADIATIVE PROCESSES

greater than 300 nm where the quantum yield of O(<sup>1</sup>D) in ozone photodissociation is temperature dependent, simultaneous measurements of the absolute cross section and of the production of O(<sup>1</sup>D) are still needed as functions of temperature.

### 7.1.7.3 The Huggins Bands

At wavelengths greater than 310 nm the vibrational structure of the Huggins bands becomes pronounced and the cross section displays a significant temperature dependence as illustrated at low spectral resolution by Table 7-4. When the spectral structure associated with bending and symmetric stretching sequences is resolved as in the data of Simons *et al.* (1973), the cross section at locations in between the sharp peaks shows a large temperature dependence with much smaller changes in the immediate vicinity of cross section maxima. These variations reflect a changing thermal population of vibrational levels in the ground electronic state.

Early cross section determinations in the Huggins bands by Inn and Tanaka (1953) and Griggs (1968) show generally good agreement, although the fine structure in the spectrum makes the measured result dependent on details of the instrument bandpass. Results obtained at high spectral resolution (0.003 nm) by Freeman *et al.* (1984) reveal structure in the Huggins bands on wavelength scales of 0.01 to 0.02 nm. Freeman *et al.* (1984) also intercompared various high resolution data sets over the wavelength range 323-327 nm and found differences between absolute values that can be 20 percent or more. This is indicative of a temperature dependence and, to a lesser extent, discrepancies in reported absolute values. Because of fine structure in the ozone absorption cross section and the temperature dependence, the level of agreement between different data sets in the Huggins bands is not yet satisfactory.

Since for use in photochemical modeling cross sections averaged over broad spectral intervals are required, the values in Table 7-4 are adopted. However, this totally obscures the fine structure in the true cross section. For application to atmospheric ozone measurements it is essential to consider details of the Huggins bands cross section that lie within the instrument bandpass. Table 7-4 lists the recommended Huggins band cross section values for temperatures of 203 and 273 K beginning with spectral interval  $i=50$ . The reported values are derived from the high resolution results of Bass and Paur (1984). Tabulated cross sections for  $i=58$  to 60 are based on Inn and Tanaka (1953) as tabulated by Ackerman (1971). Based on the analysis of Simons *et al.* (1973) the cross section in these last three spectral intervals arises entirely from absorption by thermally excited O<sub>3</sub>(X<sup>1</sup>A<sub>1</sub>) and rapidly becomes negligible below typical room temperatures. Over the wavelength range 362.5 to 407.5 nm ( $i=61$  to 69) absorption by ozone is weak and is insignificant at stratospheric and mesospheric temperatures. A new set of accurate, absolute cross section measurements covering the entire Huggins bands, including temperature dependence, would be of value for atmospheric applications.

### 7.1.7.4 The Chappuis Bands

Ozone absorbs weakly in the visible region of the spectrum via the Chappuis bands that extend longward of 407.5 nm and peak near 600 nm with a cross section close to  $5 \times 10^{-21}$  cm<sup>2</sup>. The original data source for the cross sections of Table 7-4, beginning with interval  $i=70$ , is Vigroux (1953) whose results have been confirmed by Griggs (1968). The values of Table 7-4 for  $i=70$  to 117 are as given by Ackerman (1971) and for  $i=118$  to 158 are from Nicolet (1981). The accuracy of the available data, as indicated by the agreement between Vigroux (1953) and Griggs (1968), is sufficient for applications to atmospheric modeling.

For many atmospheric applications it is not necessary to include the spectral detail of Table 7-4 at Chappuis band wavelengths. Therefore, Table 7-8 presents the Rayleigh scattering cross sections, and ozone absorption cross sections averaged over 50 nm intervals extending from 375 to 875 nm. The values are as given by Nicolet *et al.* (1982).

**Table 7-8.** Reference Rayleigh Scattering and Ozone Absorption Cross Sections Averaged Over 50 nm Intervals

Central Wavelength (nm)	Rayleigh Scattering $\sigma_{RS}(\text{cm}^2)$	Ozone Absorption $\sigma(\text{O}_3) (\text{cm}^2)$
400 $\pm$ 25	1.67E-26	—
450	1.03E-26	2.34E-22
500	6.66E-27	1.25E-21
550	4.51E-27	3.39E-21
600	3.17E-27	4.46E-21
650	2.29E-27	2.47E-21
700	1.70E-27	9.75E-22
750	1.28E-27	3.85E-22
800	9.88E-28	2.05E-22
850	7.74E-28	—

### 7.1.8 Solar Heating Rates

The calculation of accurate atmospheric heating rates by absorption of solar radiation is, in principle, straightforward provided the proper input data are available. For an aerosol-free atmosphere the required information consists of the incident solar spectral irradiance, the absorption cross sections of  $\text{O}_3$  and  $\text{O}_2$ , the Rayleigh scattering cross section, and the vertical distribution of ozone at all locations. The dominant processes for heating the stratosphere and mesosphere are dissociation of  $\text{O}_3$  and  $\text{O}_2$  where calculations assume that all excess energy above that needed to break the molecular bond is thermalized. Absorption of solar radiation by  $\text{NO}_2$  also makes a small contribution to stratospheric heating, being up to 0.1 K per day. Complications inherent in the heating rate evaluation concern the need to include multiple scattering and reflection from the lower boundary of the atmosphere. The parameterization of Lacis and Hansen (1974), which includes all of the above processes, has wide acceptance here, although the availability of improved values of the solar irradiance, the relevant cross sections, and of vertical profiles of ozone in the stratosphere and mesosphere would make a new evaluation of value. Such work has recently been performed by Kiehl and Solomon (1986) using LIMS measurements.

## RADIATIVE PROCESSES

When volcanic aerosols are present in the stratosphere the problem of evaluating the heating rate becomes much more complex. Pollack and Ackerman (1983) have shown that a lower stratospheric aerosol layer like that from El Chichon could lead to an extra heating of several tenths of a degree per day.

Figure 7-7 from London (1980) illustrates the latitudinal and seasonal pattern in the heating rate by  $O_3$  and  $O_2$ . Large values exist in the high latitude summer with the maximum absorption per unit mass occurring near 50 km where the heating is 18 K per day. This peak value determines the location of the stratopause (London, 1980). The increase in heating rate at altitudes above 70 km arises from absorption by molecular oxygen. Finally, the heating rate in the mid-to-high latitude winter is generally less than 2 K per day. Although use of more recent data would alter the values in Figure 7-7, the overall patterns with latitude and season are well-established. However, the relevant quantity for dynamical modeling is the difference between the heating and cooling rates, the latter arising from terrestrial emission. Small errors in either calculation could have a significant impact on the accuracy of the final net heating rate. Therefore, as improved data become available they should be used to generate updated heating rates in a timely manner. This is especially true of the global distribution of ozone for which an ever increasing data base exists.

## 7.2 TERRESTRIAL RADIATION

### 7.2.1 Overview and Major Issues

In the absence of motions the thermal structure of the stratosphere and mesosphere would be determined solely by a balance between heating arising from absorption of solar radiation and cooling by infrared emission. Because of the circulation, the actual thermal structure departs greatly from this state of radiative equilibrium and is determined by all three components. Accurate treatments of both solar and infrared radiation are therefore critical components of general circulation models. Furthermore, infrared emission exerts a significant influence over the evolution of atmospheric eddies via radiative damping. This section assesses the present knowledge of terrestrial longwave radiation and identifies the major issues requiring additional study.

Several recent studies illustrate the effect of the interplay between net heating and circulation on trace gas distributions. Transport by the large-scale circulation can be decomposed into two components: meridional mixing on isentropic surfaces and zonal mean cross-isentropic transport due to net radiative heating of air parcels, the *mean diabatic circulation* (Mahlman *et al.*, 1981, Tung, 1982). Harwood and Pyle (1980), using a zonally symmetric model, calculated the change in total ozone caused by changing the radiation and the corresponding diabatic circulation in the lower stratosphere. The change in radiation was accomplished by incorporating Rodgers' (1967) heating rates in the lower stratosphere where they had previously assumed no heating. The magnitude of this change was only a few tenths  $K\ day^{-1}$ . The corresponding change in ozone is substantial, especially near 30N and 30S in July-September where changes of 20% in total ozone column are found. This change is significant compared with current model estimates of decreased ozone column due to increases in CFC's of roughly 5%.

Haigh (1984, also see Haigh and Pyle, 1982) has examined the differences in ozone distribution and total ozone in the Harwood-Pyle model between a case with fixed heating rate and a case with the heating rate calculation fully coupled to the modeled variations of temperature and ozone. In the lower stratosphere between 150 and 30 mb, total column ozone differences of 10-20% were produced even though heating rate differences were only a few tenths of a degree Kelvin per day. These differences were attributed to differences in the strength of the zonally symmetric meridional circulation.

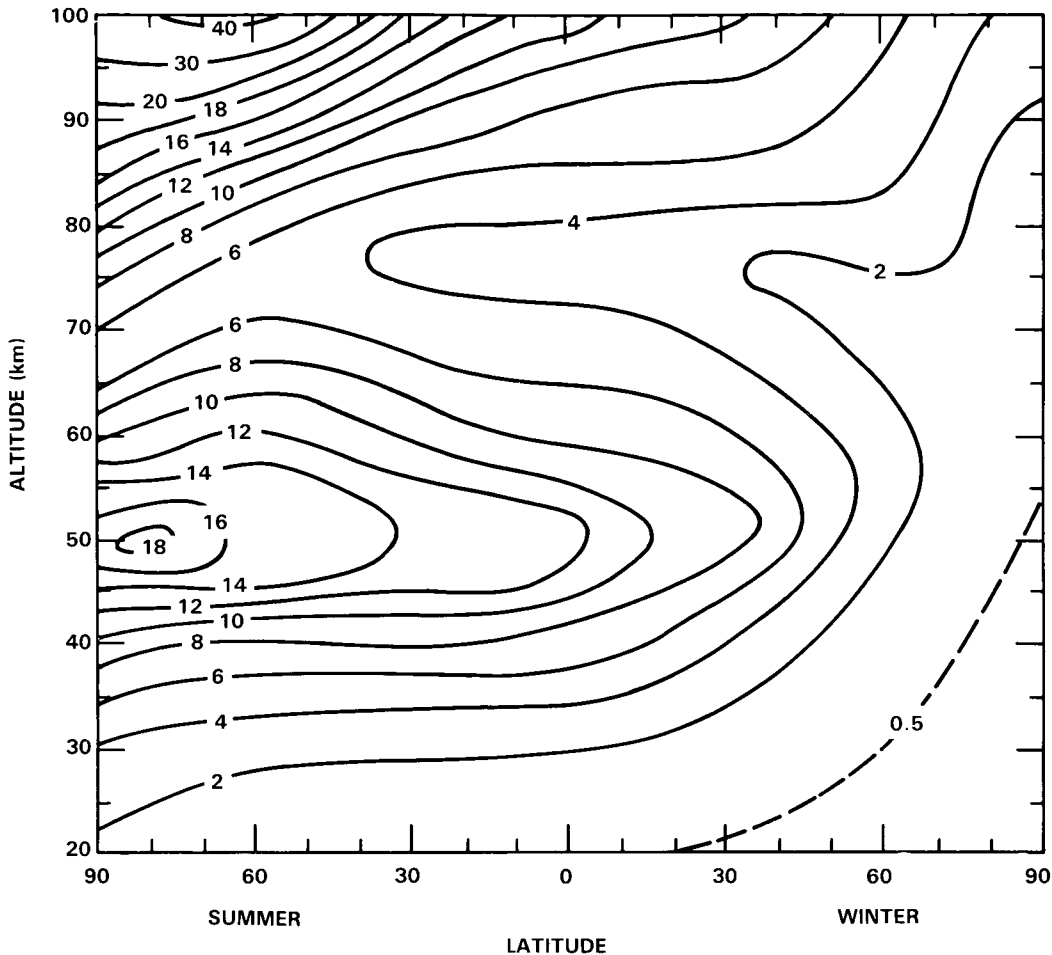


**Figure 7-7.** Heating rate arising from absorption of solar radiation by ozone and molecular oxygen. Values are in K per day from London (1980).

Simulations of the circulation of the middle atmosphere depend on a delicate interplay between the modeling of radiative forcing and forcing by eddies. The latter is often described quantitatively as the *Eliassen-Palm flux divergence* (EPFD). Experiments by Ramanathan *et al.* (1983) using the NCAR Community Climate Model have demonstrated model sensitivities to relatively modest changes in the treatment of radiative forcing in the lower stratosphere. They degraded the model radiation scheme by altering the upper boundary condition for solar absorption, eliminating the temperature dependence of the CO<sub>2</sub> hot bands and changing the temperature dependence of H<sub>2</sub>O emissivity. The largest changes occurred in the polar night region of the stratosphere where temperatures decreased by as much as 25K.

The objective of longwave radiation calculations is to predict the heating or cooling at a given location in the atmosphere associated with absorption and emission of terrestrial radiation in the infrared. Numerical simulations of longwave heating and cooling must treat details of radiation transfer in the infrared bands of CO<sub>2</sub>, O<sub>3</sub>, H<sub>2</sub>O, and other trace gases. This requires either lengthy line-by-line calculations or accurate band models to treat the transmission of thermal radiation through a broad spectral region containing numerous individual lines. The major issues in these investigations involve (1) the accuracy of line-by-line computations,

## RADIATIVE PROCESSES

(2) the accuracy and completeness of spectroscopic data required in the evaluations, and (3) the availability and accuracy of band models. These topics together with an assessment of the role of terrestrial radiation in atmospheric dynamical modeling receive attention in the following sections.

### 7.2.2 Line-by-Line Calculations, Band Transmittances, and Spectroscopic Data

The transmittance of terrestrial radiation through a wavenumber interval  $\Delta\nu$  is defined as:

$$A = \int_{\Delta\nu} [1 - \exp(-\int k_\nu(s)\rho(s)ds)]d\nu \quad (7.14)$$

where  $\rho(s)$  is absorbing gas density,  $k_\nu$  is the mass absorption coefficient and integrations are over path-length elements  $ds$  and bandwidth  $\Delta\nu$ . The complexity in applying Equation 7.14 to atmospheric radiation transfer derives from the fact that  $k_\nu$  varies rapidly over the interval  $\Delta\nu$  displaying a line structure characteristic of the molecular band under consideration, for example, the 15 micron band of  $\text{CO}_2$  or the 9.6 micron band of ozone. The absorption coefficient is also a function of pressure and temperature and varies along the inhomogeneous paths that occur in the atmosphere.

Presently, there are three general techniques available for examining longwave radiation transfer in the atmosphere. First, calculations that accurately resolve the structure of each rotational line in the infrared spectrum can be carried out. These line-by-line methods can be very accurate, but they are computationally very expensive. For this reason, the line-by-line models are most often used as 'benchmarks' to gauge how well parameterized methods are able to capture the important radiative properties of the atmosphere. Secondly, calculations can be performed for narrow spectral intervals that do not resolve the structure of each rotational line. These narrow band models make certain assumptions regarding the distribution of line strengths and positions within each narrow spectral interval. The definition of 'narrow' interval has in the past been very subjective. Intervals ranging from  $2 \text{ cm}^{-1}$  to  $200 \text{ cm}^{-1}$  have been employed to model the absorption of a given gas. Recently, Kiehl and Ramanathan (1983) have shown that narrow band model results are quite sensitive to interval size. It was found that an interval size of a few  $\text{cm}^{-1}$  ( $5 \text{ cm}^{-1}$  for the case of  $\text{CO}_2$ ) led to good agreement between observed and calculated absorption. A more detailed discussion of the problems involved with the narrow band model appears in Chapter 15 of this report. Finally, the third method available for examining the radiative budget is the broadband model. Because of their dependence on a number of assumptions regarding the structure of the band and the treatment of temperature and pressure dependence, the exact formulations of these models tend to differ from one another. The advantage of these models is their great computational speed. Thus, they are well suited for large general circulation models. They have also been shown to be in good agreement with observed absorptances and higher resolution models (Kiehl and Ramanathan, 1983, Ramanathan and Downey, 1985; Fels and Schwarzkopf, 1981). For the stratosphere, there is good agreement between these models. Cooling rates generated by both narrow and broadband models are within 5-10% of one another throughout the stratosphere.

The objective of line-by-line calculations is to construct a detailed model of  $k_\nu$  as a function of  $\nu$  in Equation 7.14 including all temperature, pressure, and path length dependencies. The major scientific concerns involve the accuracy with which such models represent the actual transfer of radiation in the Earth's atmosphere. The parameters needed to construct  $k_\nu$  are the position in wavenumbers of the center of each line in the band, the intensity of each line, the line widths, and the shapes of the line profiles. The positions of the lines can be computed from standard formulae tailored to each molecule, although reliable molecular constants must be based on accurate spectroscopic data. It is important to include the

variation of line widths with temperature, and this is not necessarily a simple square root dependence as is often assumed. It is also necessary to obtain line widths at typical atmospheric pressures to circumvent possible errors encountered in extrapolation from laboratory conditions.

Figure 7-8 from Chedin and Scott (1984) illustrates the fact that transmittances computed for the 15 micron  $\text{CO}_2$  band using laboratory measurements of line half-width and assuming a Lorentzian shape can overestimate transmittance. At low pressures characteristic of the upper stratosphere, synthetic spectra based on Lorentz or Voigt line shapes are generally in good agreement with observed spectra. However, depending on the particular molecule, this agreement degrades toward higher pressure. This issue is particularly important for remote sensing of atmospheric composition. The situation is less delicate for energy balance calculations. Fels (1985) notes that the product of line strengths and line widths in transmission calculations is less uncertain than either quantity individually, and as a consequence, these uncertainties are not the limiting factor in heating rate calculations for the middle atmosphere.

A good indirect indication of the reliability with which the spectroscopic parameters of  $\text{CO}_2$ ,  $\text{O}_3$ , and  $\text{H}_2\text{O}$  are known can be obtained by considering the problem of stratospheric remote sensing. In general, remote sensing places more stringent requirements on the accuracy of spectroscopic parameters than do heating rate calculations. Although there are some systematic discrepancies, some of which may be due in part to errors in spectroscopic data, agreement between limb sounding retrievals and correlative measurements of temperature, ozone, and water vapor are generally excellent (Gille *et al.*, 1984a; Remsberg *et al.*, 1984a; Russell *et al.*, 1984c), and this result lends strong credence to the accuracy of the spectroscopic parameters used in these retrievals.

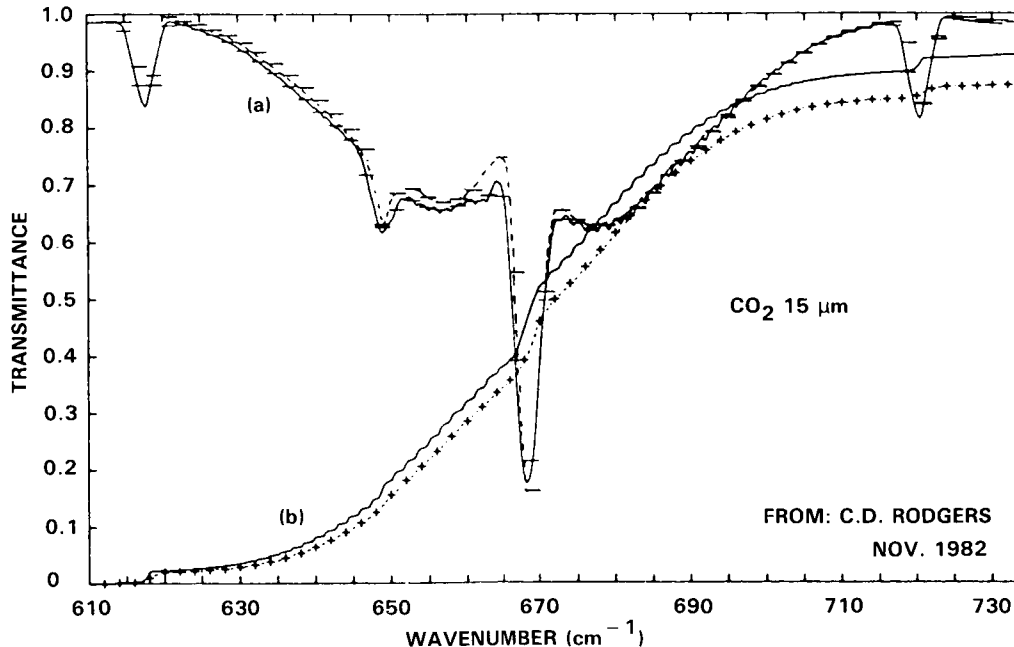


**Figure 7-8.** Laboratory and synthetic spectra of  $\text{CO}_2$  in the 15 micron spectral region. (a) Solid curve: synthetic spectrum; dashes: observations. (b) Integrated absorption. Solid curve: synthetic; dashes: observations. (from Chedin and Scott, 1984; figure originally from C. D. Rodgers, private communication, 1982).

## RADIATIVE PROCESSES

Drayson *et al.* (1984) have discussed the spectroscopic data used in these calculations. For CO<sub>2</sub>, the AFGL tape (1975 version) was used and proved to be satisfactory. The principle uncertainties are in the precise strengths of the bands and in the shape of the pressure broadened lines in the far wings. These are known to be sub-Lorentzian (Fels and Schwarzkopf, 1981). Overall, the accuracy of the spectroscopic data base for the 15  $\mu\text{m}$  CO<sub>2</sub> bands should be sufficient to allow transmission function calculations that are accurate to within at least 10%, and probably better than 5%, throughout the middle atmosphere.

The water vapor rotation band and 6.3  $\mu\text{m}$  band parameters are also well known, and the parameters on the AFGL tape are probably as accurate as those for CO<sub>2</sub>. The water vapor lines are super-Lorentzian in the far wings, but the effect of this on heating rate calculations is very small (Thomas and Nordstrum, 1982).

Spectroscopic parameters for O<sub>3</sub> are the least well known of the three gases. Drayson *et al.* used the data of Flaud *et al.* (1980) with a modification to band strength recommended by Secroun *et al.* (1981). The line strengths and positions in the isotopic bands of O<sup>16</sup>O<sup>16</sup>O<sup>18</sup> and O<sup>16</sup>O<sup>18</sup>O<sup>16</sup> are not very well known, and there is still some uncertainty about the temperature dependent line half-widths and line shapes. Nevertheless, the overall accuracy of transmission functions for this band should exceed 10% (Drayson *et al.*, 1984). Because the ozone contribution to the middle atmosphere cooling rate is generally less than 1/3 as large as that for CO<sub>2</sub>, uncertainty in ozone spectroscopic parameters should make a relatively small contribution to heating rate errors.

For modeling of atmospheric energetics and dynamics the required quantity is the transmittance over an entire band. It would be of great value to measure these quantities directly in the laboratory using broadband instruments over the range of pressure and temperature characteristic of the atmosphere. At typical laboratory temperatures "hot bands" arising from absorption by thermally excited states are present and would alter the measured transmittance from that applicable to the stratosphere and mesosphere. Broadband measurements would provide an important constraint on line-by-line calculations. Once given line-by-line results that are accurate over a range of atmospheric conditions, it is then possible to develop reliable band models. Spectroscopic properties of such trace gases as CH<sub>4</sub>, N<sub>2</sub>O, HNO<sub>3</sub> and CFC11 and 12 are not as well known as those of CO<sub>2</sub>, H<sub>2</sub>O, and O<sub>3</sub>. Although the contribution of these gases to the net cooling rate is now relatively small, their concentrations are expected to increase and laboratory measurements of broadband transmittance over the proper range of temperature and pressure would be of direct use in climate studies as well as remote sensing.

### 7.2.3 Radiative Damping

Under suitable conditions, the behavior of eddies can be strongly influenced by the damping effect of long wave radiative emission. This problem has been the subject of a number of studies in the last several years (Fels, 1982; Wehrbein and Leovy, 1982; Schoeberl, *et al.*, 1983; Fels, 1984; Apruzese and Strobel, 1984). After a period of some initial disagreement, when it seemed that there was a substantial spread in the theoretical relaxation rates calculated by different investigators, there now seems to be a satisfactory consensus on this subject. A major concern in this research has been an evaluation of the dependence of the damping rate on the vertical scale of the wave. A second issue, important for mesospheric calculations, has been the incorporation of effects due to the breakdown of local thermodynamic equilibrium.

The results of the above studies show that scale dependent radiative damping is of considerable importance in the dynamics of waves whose vertical wavelength is shorter than 30 km. At 50 km, for example, a disturbance of wavelength 12 km will decay about three times as rapidly as will one whose wavelength

is infinite (Fels, 1984). This and other cases are illustrated in Figure 7-9. These effects can be of considerable importance not only for the waves themselves, but also for related large scale phenomena whose behavior depends on wave damping, such as the quasi-biennial oscillation (Holton and Lindzen, 1972; Hamilton, 1981b), the zonal mean momentum budget of the mesosphere (Holton, 1982), and the semiannual oscillation (Hitchman and Leovy, 1986).

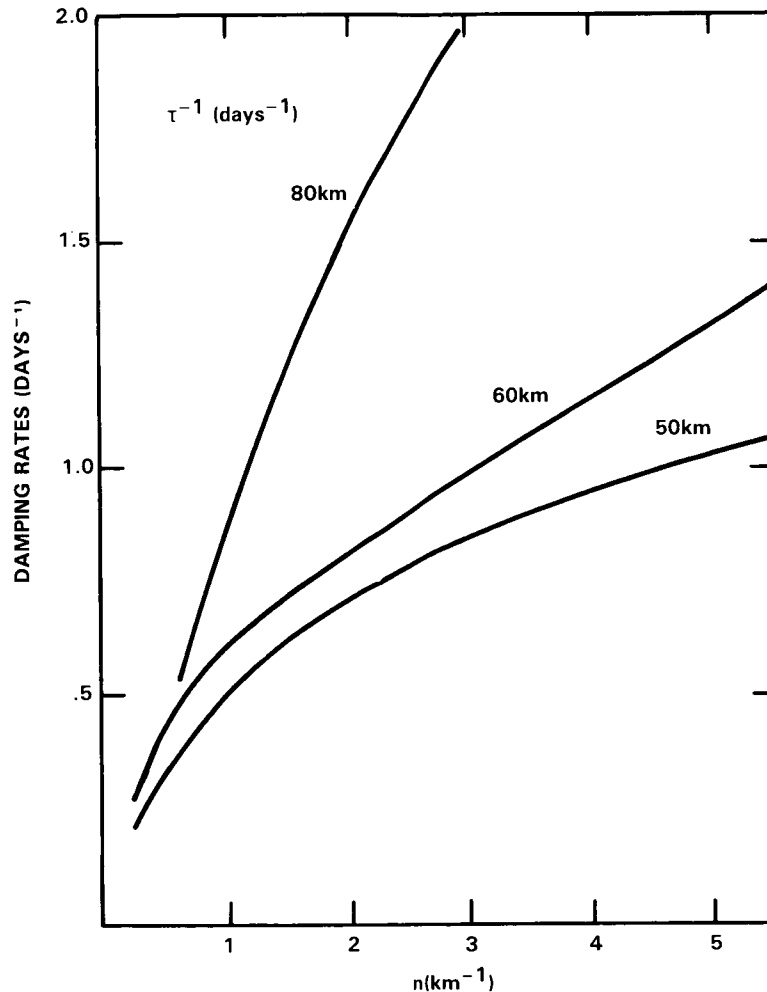


**Figure 7-9.** Middle atmosphere damping rates (ordinate,  $\text{days}^{-1}$ ) versus vertical wavenumber  $n$  ( $\text{km}^{-1}$ ). From the calculations of Fels (1982, 1984).

For internal gravity waves whose vertical scale is on the order of a kilometer or less, the decrease of damping time with decreasing wavelength is slow. To the extent that turbulent mixing behaves as a diffusive process, radiative decay should not play an important role in the damping of disturbances of very small vertical scale in the middle atmosphere. In contrast to internal gravity waves and most classes of equatorial waves, planetary waves have vertical scales large enough that radiative damping is dominated by radiation to space and is therefore essentially scale independent (vertical wavelengths  $\geq 30$  km). It is therefore likely to be less important for these waves. However, an interesting question arises in connection with the influence of radiative damping of the potential vorticity field (McIntyre and Palmer, 1984). As

## RADIATIVE PROCESSES

inferred from global satellite radiance measurements, this field appears to show rather rapid nonconservative changes in the middle and upper stratosphere during disturbed wintertime conditions (major and minor warmings). Detailed calculations of the extent to which these changes are due to diabatic processes as opposed to turbulent motions at scales that are not resolved by the available data have not been published.

A final issue concerns the photochemical acceleration of radiative damping. Physically, a temperature perturbation which alters the local thermal emission also influences the ozone abundance via a change in the reaction rates that govern odd oxygen loss. The effect is to alter the local solar heating rate in a manner to accelerate the decay of the initial perturbation. Recently, Ghazi *et al.* (1985) have used simultaneous ozone and temperature measurements to study radiative damping in the stratosphere. Empirically they show that changes in upper stratospheric solar heating accelerate the damping rate in a manner that supports the more recent theoretical predictions of Hartmann (1978) and Strobel (1978) and previous atmospheric observations (Ghazi *et al.*, 1979).

### 7.2.4 Longwave Radiation in the Stratosphere

The calculation of long wave cooling is relatively straightforward near the stratopause, but becomes increasingly difficult as one descends into the lower stratosphere. In part, the difficulty arises from the contributions of species other than CO<sub>2</sub>, O<sub>3</sub>, and H<sub>2</sub>O, particularly aerosols. It is also due to the relatively great contribution in the lower stratosphere of upwelling radiation from the troposphere. Below about 25 km the net radiative imbalance is determined by a small difference between several heating and cooling contributions each of which is individually very small.

Variable tropospheric cloudiness is an additional problem in net heating calculations. Between 20 and 25 km, two of the largest contributors are heating due to absorption of solar radiation in the visible and ultraviolet bands of ozone and exchange of long wave radiation by ozone in the 9.6  $\mu\text{m}$  band which is also generally a heating effect below 25 km. The former can vary by up to 30% as a result of variations in the albedo of underlying surface and cloud, while the latter can vary by as much as 100% as a result of variations in the height, coverage, and emissivity of clouds. Each of these factors can contribute up to 0.5 K day<sup>-1</sup> to heating in the 20–25 km layer (London, 1980a).

The spatial distribution of the total longwave cooling can be calculated with any of the methods mentioned in Section 7.2.2. The zonally averaged longwave cooling for the month of January is shown in Figure 7-10. A narrow band Malkmus model employing an interval size of 5 cm<sup>-1</sup> and using the Voigt line profile of Fels (1979) was used for these cooling rate calculations (Kiehl and Solomon, 1986). The temperature and gas distributions are from the monthly and zonally averaged January LIMS data (Gille and Russell, 1984). The lower stratosphere is radiatively cooling everywhere except near the tropical tropopause region. The relative magnitude of the cooling/heating in the lower stratosphere is only a few tenths K per day. Note that the maximum latitudinal range of cooling near 26 km is larger than a factor of 2. The region of warming around the tropical tropopause is very sensitive to the mean thermal state. If the temperatures in this region were increased by 5 K this region would radiatively cool.

As pointed out above, this region is also affected by the presence of clouds. In the tropics cirrus clouds occur not only below the tropopause, but also at times just above the mean tropopause. The presence of cirrus in this region can greatly change the local radiative energy budget. The results of Stephens and Webster (1979) for a layer of cirrus imply large longwave cooling at the cloud top and moderate solar heating in this region. The net radiative effect for their high cloud case is a cloud top cooling of a few

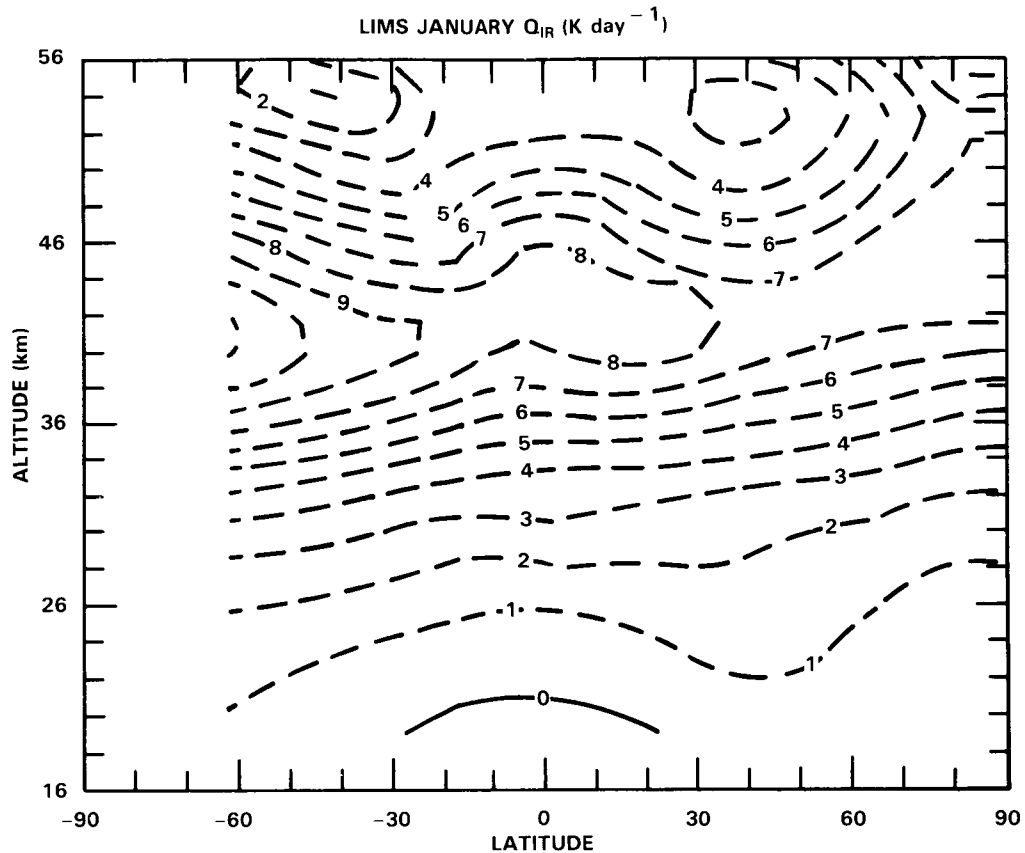


**Figure 7-10.** Zonally averaged longwave cooling rates for the mean January LIMS data in  $\text{K day}^{-1}$  (Kiehl and Solomon, 1985).

$\text{K per day}$ . Since the solar heating is present only during the daytime, large diurnal variations in this cooling will exist. The cooling due to cirrus is strongly dependent on the height of the cloud as well. The emissivity of these clouds is also an important radiative property. Cirrus are not black as is commonly assumed for cloud forms at lower levels. Another important property which affects the cloud top cooling is the cloud microphysics. Ramaswamy and Detwiler (1985) have calculated the cloud top cooling of a cirrus layer as a function of the crystal length. Their results indicate that this cooling is dependent on cloud microstructure. These studies show that an accurate knowledge of the cloud morphology and microphysics is necessary for a detailed determination of the radiative cooling in and above the cloud and into the lower stratosphere. Figure 7-11 shows the results of the calculations of Ramanathan *et al.* (1983) of the effects of cirrus on net radiative heating.

The presence of volcanic aerosols can also affect the radiative balance of this region. The computed change in net longwave radiative heating based on the radiation model of Ramaswamy and Kiehl (1985) due to background aerosols (McClatchey *et al.*, 1971) and El Chichon aerosols (Hoffman and Rosen, 1983) is shown in Figure 7-12. The change due to the background aerosol layer is very small ( $0.003 \text{ K per day}$ ), but the magnitude of change due to the El Chichon volcanic cloud is comparable in magnitude to the net longwave heating of the unperturbed stratosphere ( $0.4 \text{ K per day}$ ). The predicted effect of El Chichon volcanic aerosols on the heating rate due to absorption of solar radiation was also found to be significant

## RADIATIVE PROCESSES

if the aerosols contained 10% or more ash by volume. Radiative-convective equilibrium calculations for the El Chichon cloud with 10% ash give a temperature increase of 3.5K at 24 km, (Pollack and Ackerman, 1983) in agreement with the observational estimate of Labitzke *et al.* (1983). These calculations also indicate that the El Chichon cloud had a non-negligible influence on the heat balance of the troposphere. Such large stratospheric changes could affect the quasi-biennial oscillation (Dunkerton, 1983b). Kiehl (1984) has also pointed out the importance of stratospheric aerosols in changing radiative damping rates in this region of the stratosphere. Thus, knowledge of the transient volcanic events is of great importance in understanding the radiative balance of the lower stratosphere.

Though less important than volcanic aerosols following major eruptions, polar stratospheric clouds can also influence the net radiative heating. These clouds occur frequently in the Southern Hemisphere winter polar vortex and occasionally in the Northern Hemisphere polar vortex in the 15-25 km layer

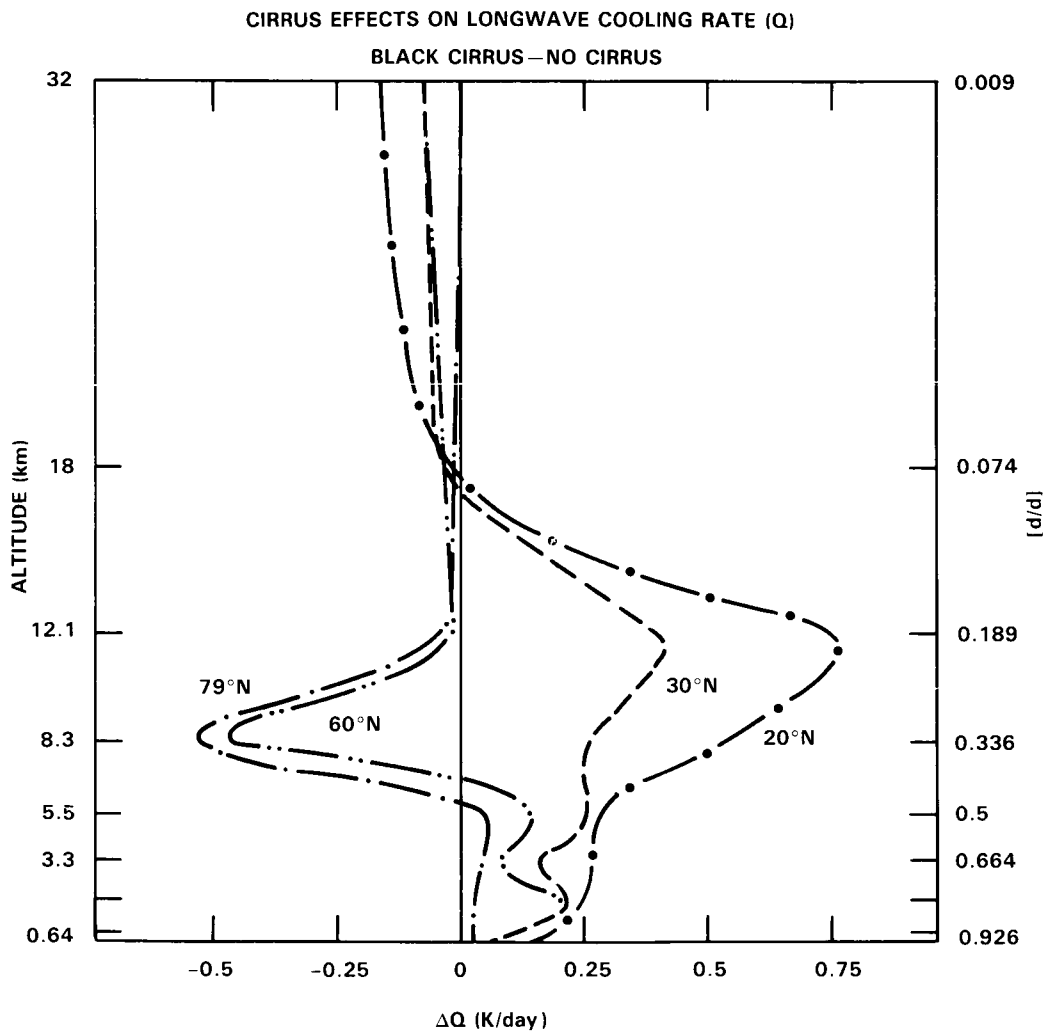


**Figure 7-11.** Change in net radiative heating due to the effect of prescribed black cirrus at various latitudes (Ramanathan *et al.*, 1983).

(McCormick *et al.*, 1982). Their effect on the radiation is ordinarily small, but they might occasionally make a significant contribution to the budget in the Antarctic (Pollack and McKay, 1985). More work to define the radiative properties of these clouds would be of value.

The role that other gases can play in determining the radiative and thermal structure of the lower stratosphere and tropopause region must also be considered. The change in the tropical longwave cooling due to the presence of  $\text{CH}_4$ ,  $\text{N}_2\text{O}$ ,  $\text{CF}_2\text{Cl}_2$  and  $\text{CFCl}_3$  is only a few hundredths of a degree per day, but due to the spectral position of the absorption bands of these gases, they tend to radiatively heat the tropopause region. Thus, an increase in the amount of any of these gases will lead to an increase in heating in this region. This effect could have important implications for the abundance of  $\text{H}_2\text{O}$  in the stratosphere.

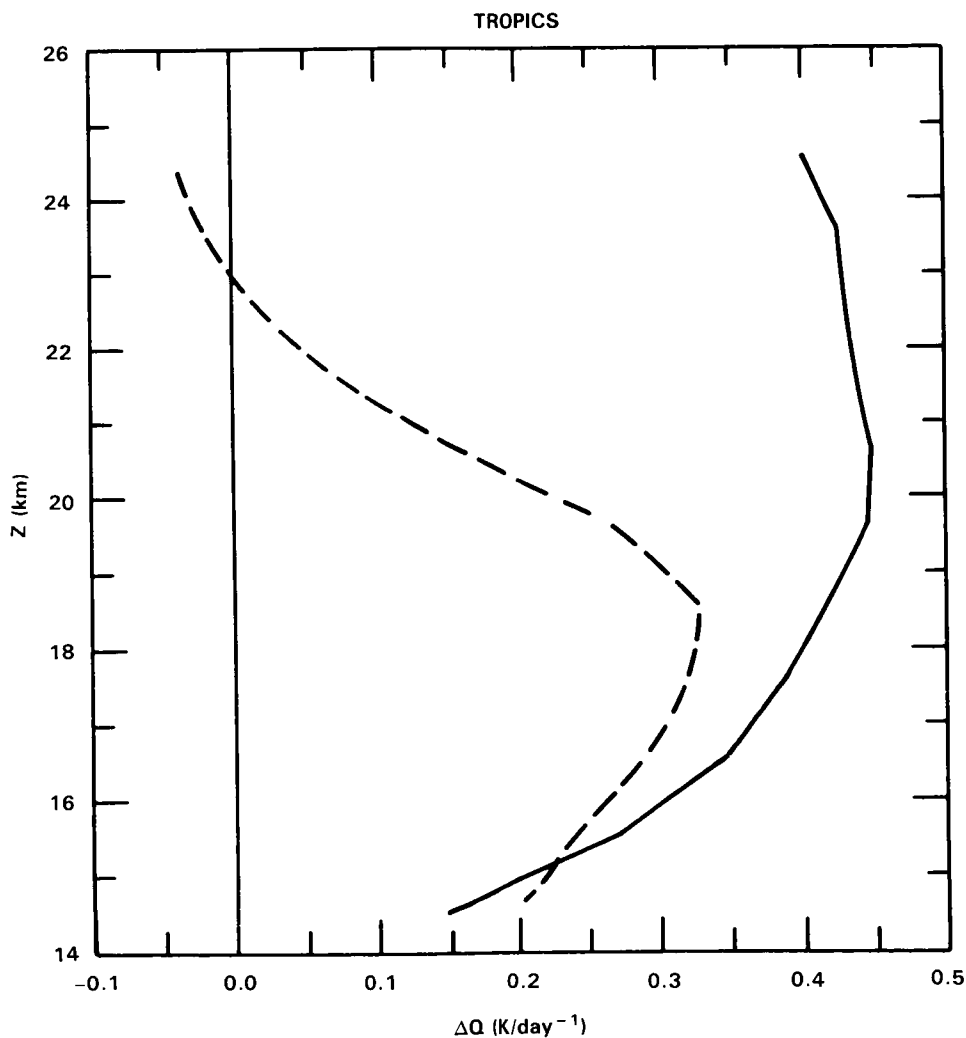


**Figure 7-12.** The change in net longwave heating rates due to the presence of background aerosols (dashed: for this case cooling has been multiplied by a factor of 100), and the El Chichon aerosol layer (solid).

## RADIATIVE PROCESSES

The accuracy of radiative cooling calculations depends on the accuracy of the input data used to evaluate the radiative fluxes. As discussed in Section 7.2.2, the input data for these calculations are the line strength, width, and position. An estimate of how inaccuracies in these parameters can affect the radiative cooling can be obtained by varying any one of these parameters by a given amount, and then evaluating the cooling for the new 'adjusted' line parameters. The results of a calculation where the line strengths of CO<sub>2</sub> were increased by 10% are shown in Figure 7-13 using the model described by Kiehl and Solomon (1986). In general, cooling rate errors of ~3% result from the 10% inaccuracy; however, there are two regions where the errors are as large as 6%, just above the stratopause and near the equatorial tropopause.

Uncertainties in gas concentration also affect the accuracy of radiative calculations. An uncertainty of 15% in the H<sub>2</sub>O concentration produces a cooling rate uncertainty of about 0.05K day<sup>-1</sup>, while uncertainties in ozone concentration ranging from 15% below 10 mb to 7% above 10 mb produce 9.6 micron band cooling rate uncertainties of up to 0.13K day<sup>-1</sup> (Fels and Schwarzkopf, 1985 unpublished). On the other hand, such ozone concentration uncertainties produce ultraviolet heating rate uncertainties that are larger by as much as an order of magnitude.

### 7.2.5 Longwave Radiation in the Mesosphere

Moving upward from the stratopause to the vicinity of the mesopause, the problem of accurately calculating longwave cooling rates increases in complexity. Just below the stratopause, longwave transfer is dominated by cooling-to-space from the wings of nonoverlapping strong Lorentz lines of the  $\nu_2$  - funda-

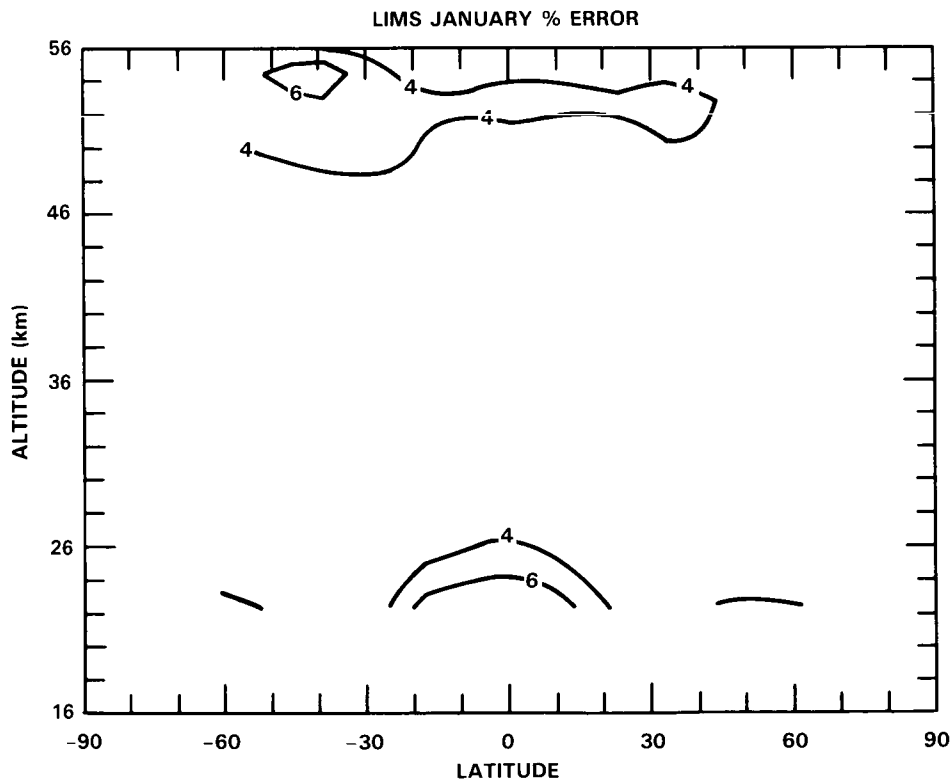
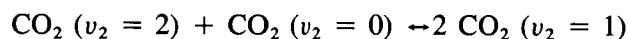


**Figure 7-13.** The percentage change in the LIMS January longwave cooling rates due to a 10% increase in the CO<sub>2</sub> line strengths.

mental of CO<sub>2</sub>. Above the stratopause, Voigt line shapes become important, and the hot and isotopic bands of CO<sub>2</sub> play an increasingly important role (Dickinson, 1972, 1984; Kutepov and Shved, 1978). As the bands become more transparent looking downward as well as upward, flux divergence is no longer dominated by cooling to space, but is determined by the difference between cooling to space and warming from upwelling flux, an imbalance that can depend delicately on the vertical temperature profile. The relative contribution due to upwelling flux is strongest for the weak bands, so that this effect further enhances the importance of the hot and isotopic bands (Dickinson, 1973, 1984). However, the most important complication arises from breakdown of local thermodynamic equilibrium (LTE) for the CO<sub>2</sub> vibrational bands.

Since the pioneering work of Murgatroyd and Goody (1958), there have been many calculations of the longwave cooling of the mesosphere by CO<sub>2</sub> (e.g., Leovy, 1964b; Kuhn and London, 1969; Kutepov and Shved, 1978; Drayson, 1967; Apruzese *et al.*, 1982; Wehrbein and Leovy, 1982). All of these have followed the lead of Murgatroyd and Goody in modeling the non-LTE problem in terms of the interaction of a single vibrationally excited level and the ground state, and broadly similar cooling rate distributions have been calculated in all of these studies.

Dickinson (1984) has pointed out that this approximation may be inadequate because of the importance of the hot and isotopic bands between 60 and 85 km. These bands begin to depart noticeably from LTE around 70 km, while the more opaque fundamental remains close to LTE up to almost 80 km. Consequently a model which separately accounts for populations of  $\nu_2 > 1$  levels of C<sup>12</sup>O<sub>2</sub><sup>16</sup> and  $\nu_2 = 1$  populations of minor isotopes is needed. Dickinson has carried out cooling rate calculations using a model which explicitly calculates the collisional and radiative coupling between the ground state, and the excited  $\nu_2 = 1$  and  $\nu_2 = 2$  levels of C<sup>12</sup>O<sub>2</sub><sup>16</sup>, as well as the  $\nu_2 = 1$  levels of the minor CO<sub>2</sub> isotopes. Collisional coupling coefficients for vibrational-thermal energy exchange between  $\nu_2 = 1$  and the ground state followed the work of Allen *et al.* (1979, 1980). The collisional coefficient coupling the  $\nu_2 = 2$  and  $\nu_2 = 1$  levels was taken from Taine and Lepoutre (1979). The rate for vibration-vibration exchanges of the forms



and



were based on a measurement of Huddleston and Weitz (1981). One vibration-vibration coupling coefficient was assumed for all of these cases, and its value is highly uncertain. Coupling between CO<sub>2</sub> vibrational energy and thermal energy of atomic oxygen was also included following the suggestion of Crutzen (1970), and using a coefficient based on an observation of Sharma and Nadile (1981). This coefficient is also quite uncertain, but for climatological studies the effect of atomic oxygen should be unimportant below the mesopause.

Results of Dickinson's calculation for the CIRA 1972 January-July temperature distribution are shown in Figure 7-14. It is encouraging to note that, despite the considerably greater sophistication of the model, the results are generally quite consistent with those of London (1980a), and are qualitatively similar to those of the original Murgatroyd and Goody (1958) calculations. The major uncertainties include: the temperature distribution, the vibration-vibration collisional coupling coefficients, the effect of temperature fluctuations on the calculation of climatological mean cooling rates, and the effects of collisions between atomic oxygen and CO<sub>2</sub> above the mesopause. Based on the uncertainties in Dickinson's calculation and the agreement between different sets of calculations, it seems that the accuracy with which long wave cooling rates due to CO<sub>2</sub> in the mesosphere can be calculated is about 10% or 1 K per day whichever is greater.

## RADIATIVE PROCESSES

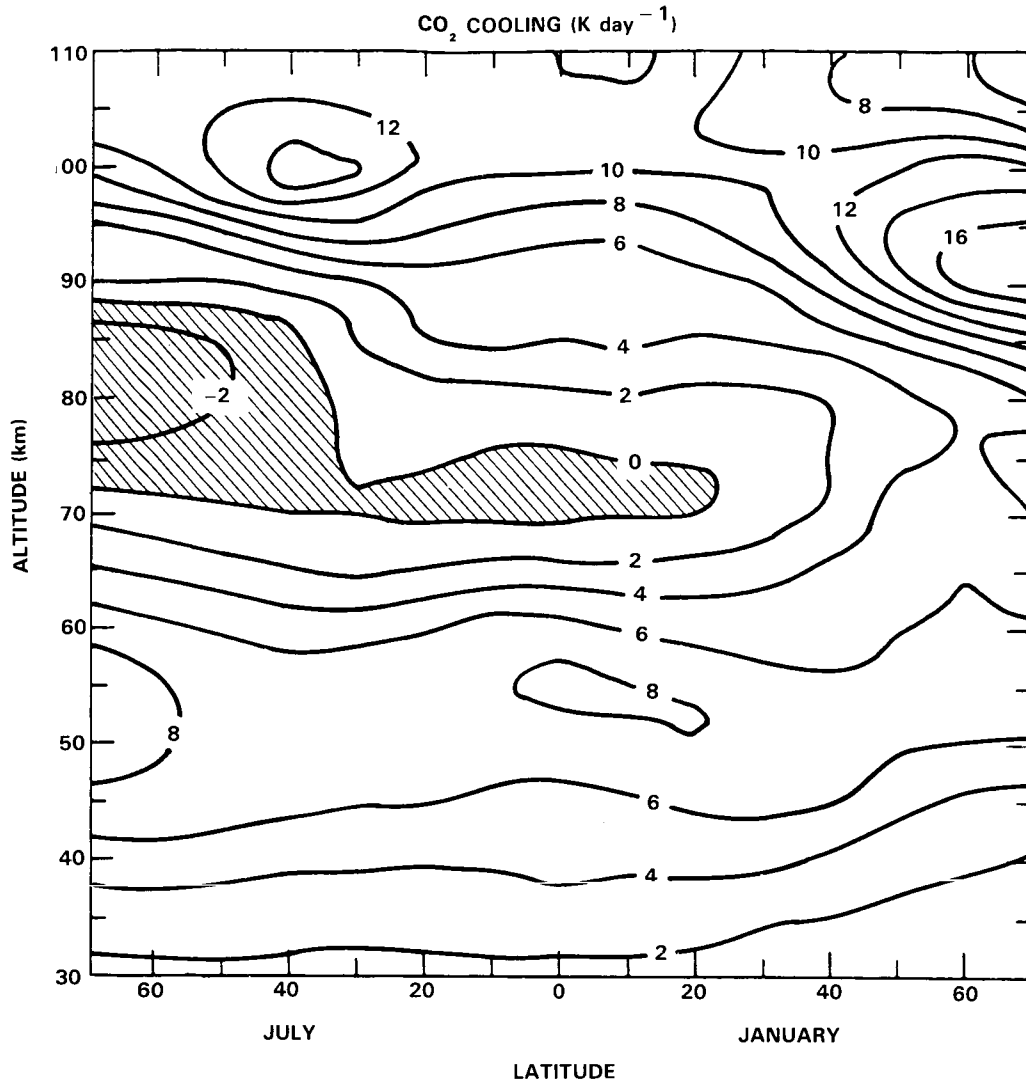


Figure 7-14. Longwave heating rate due to CO<sub>2</sub> in the upper stratosphere, mesosphere, and lower thermosphere for the January-July CIRA atmosphere (from Dickinson, 1984).

### 7.2.6 The Distribution of Net Radiative Heating

Net atmospheric heating is obtained by combining the computed long and short wave contributions. The contributions to long wave cooling and solar energy absorption have been reviewed by London (1980). It would be of interest to calculate the net heating from temperature, ozone, and water vapor distributions from a consistent global data set such as LIMS. Since the global mean net heating at any level is expected to be very close to zero, evaluation of this quantity would provide a check on the internal consistency of the data set and the other factors entering the calculations. Such a study has recently been carried out by Krehl and Solomon (1986). Except in the region between 55 and 65 km, they find global mean net cooling rate magnitudes are only a few tenths degrees Kelvin per day or less. The larger magnitudes between 55 and 65 km could be due to errors in LIMS temperatures at these altitudes. The largest uncertainty in these calculations arises from uncertainties in constituent concentrations, particularly ozone. Dickinson (1984) has evaluated the globally integrated net heating resulting from such a calculation in the mesosphere, and finds that its magnitude is generally less than 1K day<sup>-1</sup>.

A second test of the accuracy of such calculations has been suggested by Fels (1985). In the summer polar stratosphere, the Eliassen-Palm flux divergence (EPFD) due to large-scale motions is very small and one expects that the net radiative heating will also be small,  $\leq 2\text{K day}^{-1}$  near the stratopause. The LIMS data do not extend to the summer pole, but Fels has used a state-of-the-art radiative model to make this calculation for both a coupled radiative-photochemical model, and for observed (SBUV) ozone data. In both cases, he finds small net radiative heating rates,  $< 2\text{K day}^{-1}$ , near the summer stratopause.

### 7.3 CONCLUSIONS AND FUTURE RESEARCH NEEDS

The data base for the solar ultraviolet irradiance received at the Earth has increased tremendously both in size and quality over the last several years. This results from improved calibration techniques for rocket-borne sensors and the long term operation of instruments carried on satellites. The uncertainties in individual measurements have been estimated by the experimenters themselves and by intercomparison of results obtained by different groups. This indicates that at wavelengths between 175 and 210 nm the irradiances are known to an accuracy of  $\pm 10\text{-}15\%$  for average levels of solar activity, while between 210 and 330 nm typical error bars are 10% or less. At longer wavelengths, where measurements are obtainable from the ground, a typical uncertainty is 5% or smaller.

Instruments carried on Nimbus 7 and the Solar Mesosphere Explorer satellite have now defined the variability in solar irradiance over the 27 day rotation period of the Sun. At wavelengths between 175 and 210 nm, the spectral region important for production of odd oxygen below the mesopause, the maximum irradiance observed during a single solar rotation can be 6 to 7% above the minimum value. Longward of 210 nm out to 240 nm the minimum to maximum variation drops to 3% and by 300 nm is on the order of 1%. The variations in the core of solar emission and absorption lines can exceed these ranges. However, these fluctuations are confined to very small wavelength intervals and are therefore not important for driving variations in the Earth's atmosphere. Nonetheless, the behavior of discrete solar absorption or emission features can be valuable proxies for changes in irradiance over broad wavelength regions.

Present knowledge of variations in the 175-330 nm irradiance over the 11 year solar cycle remains inadequate. A key problem here involves identifying instrumental artifacts in the long term record obtained by satellites. As such, the reference solar cycle variation presented in this chapter should be viewed as tentative and subject to change in the future. An adequate investigation of solar cycle variability must utilize instrumentation capable of yielding a drift free data record over time scales of years to decades. The development and implementation of such a capability is identified as the major need in this research area. However, additional studies of the fundamental physical processes underlying solar variability and empirical modeling to relate observed variations to readily measurable indices of solar activity are also required.

Significant changes have taken place in accepted values of the molecular oxygen absorption cross sections at wavelengths relevant to the stratosphere and mesosphere. New laboratory data are available that provide accurate oscillator strengths and rotational line widths for the Schumann-Runge bands. These molecular parameters should now be processed into a form that allows easy use in atmospheric models. Two independent laboratory experiments have now produced consistent values of the Herzberg continuum cross section of  $\text{O}_2$ . The small values that result, being  $7\text{-}8 \times 10^{-24}\text{cm}^2$  near 205 nm, are compatible with most deductions from *in situ* measurements of the attenuated solar irradiance.

Absolute values of the ozone absorption cross section in the Hartley region are known to an accuracy estimated to be  $\pm 2.5\%$ . However, at wavelengths greater than 308 nm, in the Huggins bands, a compli-

## RADIATIVE PROCESSES

cated line structure in the spectrum and a substantial temperature dependence exist. Different measurements here are difficult to compare because of the dependence of results on instrument spectral response functions. A definitive, absolute cross section measurement at very high spectral resolution would be of value here, especially for application to ground-based atmospheric ozone measurements.

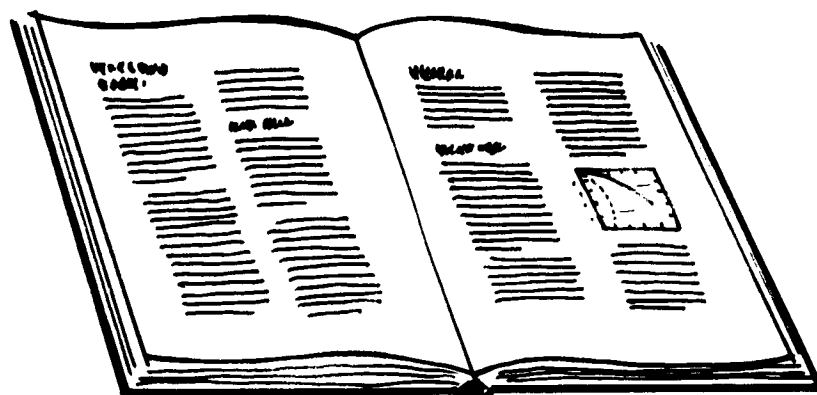
For use in calculating atmospheric heating rates by solar radiation, the error bars on the incident irradiance and on the ozone and molecular oxygen absorption cross sections combine to produce a larger uncertainty in the final result than exists in any of the inputs taken alone. The error bar on the available ozone measurements themselves is probably the largest error source. A careful evaluation of the confidence level for calculated global scale solar heating rate distributions should be done based on an error analysis of all input information required in the calculations. This is especially important since dynamical models require the *net* radiative heating which is the difference between solar heating and terrestrial cooling. At many locations this difference is small compared to either component alone, and the computational errors here assume great significance.

As concerns the transfer of terrestrial radiation, present knowledge of the molecular processes and of the data required in line-by-line calculations is not completely satisfactory. The line shapes that exist in the atmosphere are determined by complex molecular interactions that are poorly modeled in the far wings. Present calculations tend to adopt Lorentz, Doppler, and Voigt line shapes that are not always accurate representations of the true state of affairs. Related to this, the pressure dependence of line shapes needs additional laboratory and theoretical study. While simple models can duplicate observed atmospheric spectra at low pressures, the agreement deteriorates as pressure increases. This issue is especially important in remote sensing of lower stratospheric composition. In addition to problems involving the shapes of atmospheric lines, additional measurements are needed of the line widths and their temperature dependencies. Additional laboratory measurements of the transmittance of bands that are relevant to the middle atmosphere would be valuable for constraining line by line calculations. The uncertainty in transmittance for some bands of minor constituents limits the accuracy with which their radiative effects can be calculated.

Calculations of longwave radiation in the stratosphere and mesosphere contain numerous uncertainties in addition to the molecular processes discussed above. The influence of clouds on the radiation balance is not yet well-defined, both as concerns the distribution and variations in cloudiness and the radiation microphysics of cloud composition. The long term significance of perturbations to the radiation budget from volcanic aerosols and stratospheric clouds is not well understood. Finally, the radiative role of trace gases such as  $N_2O$  and the chlorofluorocarbons as well as the implications of their changes over time merits further study. It is important to develop a solid quantitative understanding of all of these topics, both to adequately define all components of the radiation budget and to generate accurate net heating rates for use in studies of the atmospheric circulation.

The availability of satellite data sets for ozone, temperature, the solar irradiance, and the outgoing terrestrial emission is leading to a great increase in our understanding of the global radiation budget. It is essential that long term, accurate data sets for these important quantities continue to be collected and analyzed. This global scale information, together with information on molecular processes, is essential for developing a complete understanding of radiative processes in the Earth's stratosphere and mesosphere.

# REFERENCES



## Research Panel

C. Meetre — Database Designer

M.A. Baldauf

K. Taylor

## APPENDIX: REFERENCES

- Abbas, M. M., T. Kostiuk, M. J. Mumma, D. Buhl, V. G. Kunde, and L. W. Brown, Stratospheric ozone measurement with an infrared heterodyne spectrometer, *Geophys. Res. Lett.*, *5*, 317-320, 1978.
- Ackerman, M., Ultraviolet solar radiation related to mesospheric processes, in *Mesospheric Models and Related Experiments*, edited by G. Fiocco, pp. 149-159, D. Reidel, Dordrecht, 1971.
- Ackerman, M., and C. Muller, Stratospheric methane and nitrogen dioxide from infrared spectra, *Pure Appl. Geophys.*, *106-108*, 1325-1335, 1973.
- Ackerman, M., J. C. Fontanella, D. Frimout, A. Girard, N. Louisnard, and C. Muller, Simultaneous measurements of NO and NO<sub>2</sub> in the stratosphere, *Planet. Space Sci.*, *23*, 651-660, 1975.
- Ackerman, M., D. Frimout, A. Girard, A. Gottignies, and C. Muller, Stratospheric HCl from infrared spectra, *Geophys. Res. Lett.*, *3*, 81-83, 1976.
- Ackerman, M., D. Frimout, C. Muller, and D. J. Wuebbles, Stratospheric methane measurements and predictions, *Pure Appl. Geophys.*, *117*, 367-380, 1978/79.
- Ackerman, M., C. Lippens, C. Muller, J. Vercheval, J. Besson, A. Girard, J. Laurent, and M. P. Lemaitre, Observations of middle atmosphere CH<sub>4</sub> and N<sub>2</sub>O vertical distributions by the Spacelab one grille spectrometer, *Geophys. Res. Lett.*, submitted, 1985.
- Ahlquist, J., Normal-mode global Rossby waves, theory and observations, *J. Atmos. Sci.*, *39*, 193-202, 1982.
- Aikin, A. C., B. Woodgate, and H. J. P. Smith, Equatorial ozone profiles from the solar maximum mission - A comparison with theory, *Planet. Space Sci.*, *32*, 503-513, 1984.
- Aimedieu, P., P. Rigaud, and J. Barat, The sunrise ozone depletion problem of the upper stratosphere, *Geophys. Res. Lett.*, *8*, 787-789, 1981.
- Aimedieu, P., A. J. Krueger, D. E. Robbins, and P. C. Simon, Ozone profile intercomparison based on simultaneous observations between 20 and 40 km, *Planet. Space Sci.*, *31*, 801-807, 1983.
- Al-Ajmi, D. N., R. S. Harwood, and T. Miles, A sudden warming in the middle atmosphere of the Southern Hemisphere, *Quart. J. Roy. Meteorol. Soc.*, *111*, 359-389, 1985.
- Allam, R. J., and A. F. Tuck, Transport of water vapour in a stratosphere-troposphere general circulation model I. Fluxes, *Quart. J. Roy. Meteorol. Soc.*, *110*, 321-356, 1984a.
- Allam, R. J., and A. F. Tuck, Transport of water vapour in a stratosphere-troposphere general circulation model II. Trajectories, *Quart. J. Roy. Meteorol. Soc.*, *110*, 357-392, 1984b.
- Allam, R. J., K. S. Groves, and A. F. Tuck, Global OH distribution derived from general circulation model fields of ozone and water vapor, *J. Geophys. Res.*, *86*, 5303-5320, 1981.
- Allen, D. C., J. D. Haigh, J. T. Houghton, and C. J. S. M. Simpson, Radiative cooling near the mesopause, *Nature*, *281*, 660-661, 1979.
- Allen, D. C., T. Scragg, and C. J. S. M. Simpson, Low temperature fluorescence studies of the deactivation of the bend-stretch manifold of CO<sub>2</sub>, *Chem. Phys.*, *51*, 279-298, 1980.
- Allen, M., and J. E. Frederick, Effective photodissociation cross sections for molecular oxygen and nitric oxide in the Schumann-Runge bands, *J. Atmos. Sci.*, *39*, 2066-2075, 1982.
- Allen, M., J. I. Lunine, and Y. L. Yung, The vertical distribution of ozone in the mesosphere and lower thermosphere, *J. Geophys. Res.*, *89*, 4841-4872, 1984.
- Alpert, J. C., M. A. Geller, and S. K. Avery, The response of stationary planetary waves to tropospheric forcing, *J. Atmos. Sci.*, *40*, 2467-2483, 1983.
- Altshuller, A. P., and J. J. Bufalini, Photochemical aspects of air pollution: A review, *Environ. Sci. Technol.*, *5*, 39-64, 1971.
- Anderson, G. P., and L. A. Hall, Attenuation of solar irradiance in the stratosphere: Spectrometer measurements between 191 and 207 nm, *J. Geophys. Res.*, *88*, 6801-6806, 1983.
- Anderson, J. G., The absolute concentration of OH (X<sup>2</sup>π) in the Earth's stratosphere, *Geophys. Res. Lett.*, *3*, 165-168, 1976.

## REFERENCES

- Anderson, J. G., Free radicals in the earth's stratosphere: A review of recent results, in *Proceedings of the NATO Advanced Study Institute on Atmospheric Ozone: Its Variation and Human Influences*, Rep. FAA-EE-80-20, edited by A. C. Aikin, pp. 233-251, DOT, FAA, Washington, DC, 1980.
- Anderson, J. G., The past five years-the next five years, paper presented at the International Workshop on Current Issues in our Understanding of the Stratosphere and the Future of the Ozone Layer, BMFT, NASA, FAA, WMO, Feldafing, FRG, June 11-16, 1984.
- Anderson, J. G., J. J. Margitan, and D. H. Stedman, Atomic chlorine and the chlorine monoxide radical in the stratosphere: Three in-situ observations, *Science*, *198*, 501-503, 1977.
- Anderson, J. G., H. J. Grassl, R. E. Shetter, and J. J. Margitan, Stratospheric free chlorine measured by balloon-borne in situ resonance fluorescence, *J. Geophys. Res.*, *85*, 2869-2887, 1980.
- Anderson, J. G., H. J. Grassl, R. E. Shetter, and J. J. Margitan, HO<sub>2</sub> in the stratosphere: Three in situ observations, *Geophys. Res. Lett.*, *8*, 289-292, 1981.
- Anderson, J. R., and R. D. Rosen, The latitude-height structure of 40-50 day variations in atmospheric angular momentum., *J. Atmos. Sci.*, *40*, 1584-1591, 1983.
- Anderson, P. W., Pressure broadening in the microwave and infrared regions, *Phys. Rev.*, *76*, 647-661, 1949.
- Andrews, D. G., and M. E. McIntyre, Planetary waves in horizontal and vertical shear: The generalized Eliassen-Palm relation and the mean zonal acceleration, *J. Atmos. Sci.*, *33*, 2031-2048, 1976.
- Andrews, D. G., and M. E. McIntyre, Generalized Eliassen-Palm and Charney-Drazin theorems for waves on axisymmetric mean flows in compressible atmospheres, *J. Atmos. Sci.*, *35*, 175-185, 1978a.
- Andrews, D. G., and M. E. McIntyre, An exact theory of nonlinear waves on a Lagrangian mean flow, *J. Fluid. Mech.*, *89*, 609-646, 1978b.
- Andrews, D. G., J. D. Mahlman, and R. W. Sinclair, Eliassen-Palm diagnostics of wave-mean flow interaction in the GFDL "SKYHI" general circulation model, *J. Atmos. Sci.*, *40*, 2768-2784, 1983.
- Angell, J. K., and J. Korshover, Recent rocketsonde-derived temperature variations in the Western Hemisphere, *J. Atmos. Sci.*, *35*, 1758-1764, 1978a.
- Angell, J. K., and J. Korshover, Estimate of global temperature variations in the 100-30 mb layer between 1958 and 1977, *Mon. Weather Rev.*, *106*, 1422-1432, 1978b.
- Angell, J. K., and J. Korshover, Global temperature variations in the troposphere and stratosphere, *Mon. Weather Rev.*, *111*, 901-921, 1983a.
- Angell, J. K., and J. Korshover, Global variations in total ozone and layer-mean ozone: An update through 1981, *J. Clim. Appl. Meteor.*, *22*, 1611-1627, 1983b.
- Angell, J. K., J. Korshover, and W. G. Planet, Ground-based and satellite evidence for a pronounced total-ozone minimum in early 1983 and responsible atmospheric layers, *Mon. Weather Rev.*, *113*, 641-646, 1985.
- Apruzese, J., and D. F. Strobel, Radiative relaxation rates for individual 15-micron CO<sub>2</sub> lines in the upper stratosphere and lower mesosphere, *J. Geophys. Res.*, *89*, 7187-7194, 1984.
- Apruzese, J. P., M. R. Schoeberl, and D. F. Strobel, Parameterization of IR cooling in a middle atmosphere dynamics model. 1. Effect on the zonally averaged circulation, *J. Geophys. Res.*, *87*, 8951-8966, 1982.
- Arakawa, A., and W. H. Schubert, Introduction of cloud ensemble with the large scale environment, *J. Atmos. Sci.*, *31*, 674-701, 1974.
- Arijs, E., D. Neverjans, and J. Ingles, Unambiguous mass determination of major stratospheric positive ions, *Nature*, *288*, 684-686, 1980.
- Arijs, E., D. Neverjans, and J. Ingels, Stratospheric positive ion composition measurements, ion abundances and related trace gas detection, *J. Atmos. Terr. Phys.*, *44*, 43-53, 1982.
- Arnold, F., Multi-ion complexes in the stratosphere-Implications for trace gases and aerosol, *Nature*, *284*, 610-611, 1980.

## REFERENCES

- Arnold, F., Stratospheric trace gas detection by rocket-, balloon-, and aircraft-borne chemical ionization mass spectrometry, paper presented at the International Workshop on Current Issues in our Understanding of the Stratosphere and the Future of the Ozone Layer, BMFT, NASA, FAA, WMO, Feldafing, FRG, June 11-16, 1984.
- Arnold, F., and G. Henschen, First mass analysis of stratospheric negative ions, *Nature*, 275, 521-522, 1978.
- Arnold, F., and S. Qiu, Upper stratosphere negative ion composition measurements and inferred trace gas abundances., *Planet. Space Sci.*, 32, 169-177, 1984.
- Arnold, F., H. Bohringer, and G. Henschen, Composition measurements of stratospheric positive ions, *Geophys. Res. Lett.*, 5, 653-656, 1978.
- Arnold, P. W., Losses of nitrous oxide from soil, *J. Soil*, 5, 116-128, 1955.
- Arrhenius, S., On the influence of carbonic acid in the air upon the temperature of the ground, *Philos. Mag.*, 41, 237, 1896.
- Arvesen, J. C., R. N. Griffin, and B. D. Pearson, Jr., Determination of extraterrestrial solar spectral irradiance from a research aircraft, *Appl. Optics*, 8, 2215-2232, 1969.
- Asai, K., T. Itabe, and T. Igarashi, Range-resolved measurements of atmospheric ozone using a differential-absorption CO<sub>2</sub> laser radar, *Appl. Phys. Lett.*, 35, 60-62, 1979.
- Atkinson, R., and A. C. Lloyd, Evaluation of kinetic and mechanistic data for modeling of photochemical smog, *J. Phys. Chem. Ref. Data*, 13, 315-444, 1984.
- Atkinson, R., S. M. Aschmann, A. M. Winer, and W. P. L. Carter, Rate constants for the gas-phase reactions of NO<sub>3</sub> with furan, thiophene and pyrole at 295 K and atmospheric pressure, *Environ. Sci. Technol.*, 19, 87-90, 1985.
- Atticks, M. G., and G. D. Robinson, Some features of the structure of the tropical tropopause, *Quart. J. Roy. Meteorol. Soc.*, 109, 295-308, 1983.
- Attmannspacher, W., and H. U. Duetsch, International ozone sonde intercomparison at the Observatory Hohenpeissenberg 5-20 April 1978, *Ber. Deutschen Wetterdienstes*, Nr. 20, 1970.
- Attmannspacher, W., and H. U. Duetsch, Second international ozone sonde intercomparison at the Observatory Hohenpeissenberg 5-20 April 1978, *Ber. Deutschen Wetterdienstes*, Nr. 157, 1981.
- Augustsson, T., and V. Ramanathan, A radiative-convective model study of the CO<sub>2</sub> climate problem, *J. Atmos. Sci.*, 34, 448-451, 1977.
- Ausloos, P., R. E. Rebert, and L. Glasgow, Photodecomposition of chloromethane absorbed on silica surfaces, *J. of Res. of Nat. Bureau of Standards*, 82, 1-8, 1977.
- Austin, J., Comparison of stratospheric air parcel trajectories calculated from SSU and LIMS satellite data, *J. Geophys. Res.*, in press, 1985.
- Austin, J., and A. F. Tuck, The calculation of stratospheric air parcel trajectories using satellite data, *Quart. J. Roy. Meteorol. Soc.*, 111, 279-307, 1985.
- Austin, J., R. R. Garcia, J. M. Russell III, S. Solomon, and A. F. Tuck, On the atmospheric photochemistry of nitric acid, *J. Geophys. Res.*, in press, 1985a.
- Austin, J., R. C. Pallister, J. A. Pyle, A. F. Tuck, and A. M. Zarody, Photochemical model comparisons with LIMS observations in a stratospheric trajectory coordinate system, *Quart. J. Roy. Meteorol. Soc.*, in press, 1985b.
- Azouit, M., and J. Vernin, Remote investigation of tropospheric turbulence by two dimensional analysis of stellar scintillation, *J. Atmos. Sci.*, 37, 1550-1557, 1980.
- Bacastow, R. B., C. D. Keeling, and T. P. Whorf, Seasonal amplitude increase in atmospheric CO<sub>2</sub> concentration at Mauna Loa, Hawaii, 1959-1982, *J. Geophys. Res.*, 90, 10529-10540, 1985.
- Baker, C. B., W. R. Kuhn, and E. Ryzner, Effects of the El Chichon volcanic cloud on direct and diffuse irradiances, *J. Clim. Appl. Meteor.*, 23, 449-452, 1984.
- Baker-Blocker, A., T. M. Donahue, and K. H. Mancy, Methane flux from wetlands areas, *Tellus*, 29, 245-250, 1977.

## REFERENCES

- Baldecchi, M. G., B. Carli, F. Mencaraglia, A. Bonetti, and M. Carlotti, Atlas of stratospheric submillimeter lines: 1. The 7-20  $\text{cm}^{-1}$  interval, *J. Geophys. Res.*, **89**, 11689-11704, 1984.
- Baldwin, A. C., and D. M. Golden, Heterogeneous atmospheric reactions-Sulphuric acid aerosols as tropospheric sinks, *Science*, **206**, 562-563, 1979.
- Baldwin, A. C., J. R. Barker, D. M. Golden, and D. G. Hendry, Photochemical smog. Rate parameter estimates and computer simulation, *J. Phys. Chem.*, **81**, 2483-2492, 1977.
- Ballard, H. N., A review of seven papers concerning the measurement of temperature in the stratosphere and mesosphere, *Tech. Rep. ECOM-5125*, 67 pp., U.S. Atmos. Sci. Lab., White Sands Missile Range, NM, 1967.
- Balsley, B. B., and D. A. Carter, The spectrum of atmospheric velocity fluctuations at 8 km and 86 km, *Geophys. Res. Lett.*, **9**, 465-468, 1982.
- Balsley, B. B., and A. C. Riddle, Monthly mean values of the mesospheric wind field over Poker Flat, Alaska, *J. Atmos. Sci.*, **41**, 2368-2375, 1984.
- Baluteau, J. P., A. Marten, E. Bussoletti, M. Anderegg, J. E. Beckman, A. F. M. Moorwood, and N. Coron, High resolution infrared spectra of the Earth's atmosphere-II. Ground-based observations in the 500-570  $\text{cm}^{-1}$  range, *Infrared Phys.*, **17**, 211-224, 1977.
- Bamber, D. J., P. G. W. Healey, B. M. R. Jones, S. A. Penkett, A. F. Tuck, and G. Vaughan, Vertical profiles of tropospheric gases: Chemical consequences of stratospheric intrusions, *Atmos. Environ.*, **18**, 1759-1766, 1984.
- Barat, J., Some characteristics of clear-air turbulence in the middle atmosphere, *J. Atmos. Sci.*, **39**, 2553-2564, 1982.
- Barbe, A., P. Marche, C. Secroun, and P. Jouve, Measurements of tropospheric and stratospheric  $\text{H}_2\text{CO}$  by an infrared high resolution technique, *Geophys. Res. Lett.*, **6**, 463-465, 1979.
- Barnes, I., K. H. Becker, E. H. Fink, A. Reimer, F. Zabel, and H. Niki, Rate constant and products of the reaction  $\text{CS}_2 + \text{OH}$  in the presence of  $\text{O}_2$ , *Int. J. Chem. Kinet.*, **15**, 631-645, 1983.
- Barnes, R. A., A. R. Bandy, and A. T. Torres, ECC ozonesonde accuracy and precision, *J. Geophys. Res.*, **90**, 7881-7887, 1985.
- Barnett, J. J., The mean meridional temperature behaviour of the stratosphere from November 1970 to November 1971 derived from measurements by the selective chopper radiometer on Nimbus 4, *Quart. J. Roy. Meteorol. Soc.*, **100**, 505-530, 1974.
- Barnett, J. J., and M. Corney, Temperature comparisons between the NIMBUS 7 SAMS, rocket/radiosondes and the NOAA-6 SSU, *J. Geophys. Res.*, **89**, 5294-5302, 1984.
- Barnett, J. J., and M. Corney, A middle atmosphere temperature reference model from satellite measurements, *Adv. Space Res.*, **5**, 125-134, 1984.
- Barnett, J. J., J. T. Houghton, and J. A. Pyle, The temperature dependence of the ozone concentration near the stratopause, *Quart. J. Roy. Meteorol. Soc.*, **101**, 245-257, 1975a.
- Barnett, J. J., R. S. Harwood, J. T. Houghton, C. G. Morgan, C. D. Rodgers, and E. J. Williamson, Comparison between radiosonde, rocketsonde and satellite observations of atmospheric temperatures, *Quart. J. Roy. Meteorol. Soc.*, **101**, 423-436, 1975b.
- Barrett, E. W., P. M. Kuhn, and A. Shlanta, Recent measurements of the injection of water vapor and ozone into the stratosphere by thunderstorms, in *Proceedings of the 2nd Conference on the Climatic Impact Assessment Program, DOT-TSC-OST-73-4*, edited by A. J. Broderick, pp. 34-46, Transportation Systems Center, Cambridge, MA, 1973.
- Barth, C. A., D. W. Rusch, R. J. Thomas, G. H. Mount, G. J. Rottman, G. E. Thomas, R. W. Sanders, and G. M. Lawrence, Solar Mesosphere Explorer: Scientific objectives and results, *Geophys. Res. Lett.*, **10**, 237-240, 1983.
- Barton, I. J., Upper level cloud climatology from an orbiting satellite, *J. Atmos. Sci.*, **40**, 435-447, 1983.

## REFERENCES

- Basco, N., and J. E. Hunt, Mutual combination of ClO radicals, *Int. J. Chem. Kin.*, *11*, 649-664, 1979.
- Bass, A. M., and R. J. Paur, The ultraviolet cross sections of ozone: I. The measurements, in *Atmospheric Ozone*, edited by C. S. Zerefos and A. Ghazi, pp. 606-610, D. Reidel, Dordrecht, 1984.
- Bates, D. R., Rayleigh scattering by air, *Planet. Space Sci.*, *32*, 785-790, 1984.
- Bauer, E., A catalog of perturbing influences on stratospheric ozone, 1955-1975, *J. Geophys. Res.*, *84*, 6929-6940, 1979.
- Baulch, D. L., R. A. Cox, R. F. Hampson, Jr., J. A. Kerr, J. Troe, and R. T. Watson, Evaluated kinetic and photochemical data for atmospheric chemistry, *J. Phys. Chem. Ref. Data*, *9*, 295-471, 1980.
- Baulch, D. L., R. A. Cox, P. J. Crutzen, R. F. Hampson, J. A. Kerr, J. Troe, and R. T. Watson, Evaluated kinetic and photochemical data for atmospheric chemistry: Supplement I. CODATA Task Group on Chemical Kinetics, *J. Phys. Chem. Ref. Data*, *11*, 327-496, 1982.
- Baulch, D. L., R. A. Cox, R. F. Hampson, Jr., J. A. Kerr, J. Troe, and R. T. Watson, Evaluated kinetic and photochemical data for atmospheric chemistry supplement II. CODATA Task Group on Gas Phase Chemical Kinetics, *J. Phys. Chem. Ref. Data*, *13*, 1259-1380, 1984.
- Belmont, A. D., and D. G. Dartt, Semiannual variation in zonal wind from 20 to 65 kilometers, at 80°N-10°S, *J. Geophys. Res.*, *78*, 6373-6376, 1973.
- Belmont, A. D., D. G. Dartt, and G. D. Nastrom, Periodic variations in stratospheric zonal winds from 20 to 65 km, at 80°N to 70°S, *Quart. J. Roy. Meteorol. Soc.*, *100*, 203-211, 1974.
- Berg, W. W., and P. D. Sperry, Atmospheric bromine in the Arctic, *J. Geophys. Res.*, *88*, 6719-6736, 1983.
- Berg, W. W., P. J. Crutzen, F. E. Grahek, S. N. Gitlen, and W. A. Sedlacek, First measurements of total chlorine and bromine in the lower stratosphere, *Geophys. Res. Lett.*, *7*, 937-940, 1980.
- Berg, W. W., L. E. Heidt, W. Pollock, P. D. Sperry, R. J. Cicerone, and E. S. Gladney, Brominated organic species in the Arctic atmosphere, *Geophys. Res. Lett.*, *11*, 429-432, 1984.
- Berner, W., H. Oeschger, and B. Stauffer, Information on the CO<sub>2</sub> cycle from ice-core studies, *Radiocarbon*, *22*, 227-235, 1980.
- Betts, A. K., Parametric interpretation of trade wind cumulus budget studies, *J. Atmos. Sci.*, *32*, 1934-1945, 1975.
- Bevilacqua, R. M., J. J. Olivero, P. R. Schwartz, C. J. Gibbins, J. M. Bologna, and D. L. Thacker, An observational study of water vapor in the mid-latitude mesosphere using ground-based microwave techniques, *J. Geophys. Res.*, *88*, 8523-8534, 1983.
- Bevilacqua, R. M., W. J. Wilson, W. B. Ricketts, P. R. Schwartz, and R. J. Howard, Possible seasonal variability of mesospheric water vapor, *Geophys. Res. Lett.*, *12*, 397-400, 1985.
- Bhartia, P. K., K. F. Klenk, A. J. Fleig, C. G. Wellemyer, and D. Gordon, Intercomparison of Nimbus 7 Solar Backscattered Ultraviolet ozone profiles with rocket, balloon and Umkehr profiles, *J. Geophys. Res.*, *89*, 5227-5238, 1984a.
- Bhartia, P. K., K. F. Klenk, C. K. Wong, D. Gordon, and A. J. Fleig, Intercomparison of the Nimbus 7 SBUV/TOMS total ozone data sets with Dobson and M83 results, *J. Geophys. Res.*, *89*, 5239-5248, 1984b.
- Bhartia, P. K., D. F. Heath, and A. J. Fleig, Observation of anomalously small ozone densities in South Polar Stratosphere during October 1983 and 1984, paper presented at 5th General Assembly, IAGA Symposium, Prague, Czechoslovakia, July, 1985.
- Blackmer, A. M., and J. M. Bremner, Potential of soil as a sink for atmospheric nitrous oxide, *Geophys. Res. Lett.*, *3*, 739-742, 1976.
- Blackshear, W. T. W. L. Grose, and R. E. Turner, Simulated sudden stratospheric warmings: Synoptic evaluations, *Quart. J. Roy. Meteorol. Soc.*, in press, 1986.
- Blake, A. J., An atmospheric absorption model for the Schumann-Runge bands of oxygen, *J. Geophys. Res.*, *84*, 3272-3282, 1979.

## REFERENCES

- Blake, A. J., S. T. Gibson, and D. G. McCoy, Photodissociation of  $^{16}\text{O}^{18}\text{O}$  in the atmosphere, *J. Geophys. Res.*, **89**, 7277-7284, 1984.
- Blake, D. R., Increasing concentrations of atmospheric methane, 1979-1983, Ph.D. thesis, 213 pp., U. of California, Irvine, CA, 1984.
- Blake, D. R., and F. S. Rowland, World-wide increase in tropospheric methane, *J. Atmos. Chem.*, in press, 1985.
- Blake, D. R., W. E. Mayer, S. C. Tyler, Y. Makide, D. C. Montaque, and F. S. Rowland, Global increase in atmospheric methane concentrations between 1978 and 1980, *Geophys. Res. Lett.*, **9**, 477-480, 1982.
- Blake, D. R., V. H. Woo, S. C. Tyler and F. S. Rowland, Methane concentrations and source strengths in urban locations, *Geophys. Res. Lett.*, **11**, 1211-1214, 1984.
- Blanchet, J. P., and R. List, On the optical properties of Arctic haze, in *Aerosols and Their Climate Effects*, edited by H. E. Gerber and A. Deepak, pp. 179-196, A. Deepak Publ., Hampton, VA, 1984.
- Blatherwick, R. D., A. Goldman, D. G. Murcray, F. J. Murcray, G. R. Cook, and J. W. Van Allen, Simultaneous mixing ratio profiles of stratospheric NO and NO<sub>2</sub> as derived from balloon-borne infrared solar spectra, *Geophys. Res. Lett.*, **7**, 471-473, 1980.
- Blatherwick, R. D., F. J. Murcray, F. H. Murcray, A. Goldman, and D. G. Murcray, Atlas of South Pole IR solar spectra, *Appl. Opt.*, **21**, 2658-2659, 1982.
- Bloomfield, P., M. L. Thompson, and S. Zeger, A statistical analysis of Umkehr measurements of 32-46 km ozone, *J. Appl. Meteorol.*, **21**, 1828-1837, 1982.
- Bloomfield, P., G. Oehlert, M. L. Thompson, and S. Zeger, A frequency domain analysis of trends in Dobson total ozone records, *J. Geophys. Res.*, **88**, 8512-8522, 1983.
- Blumenthal, D. L., W. S. Keifer, and J. A. McDonald, Aircraft measurements of pollutants and meteorological parameters during the Sulphate Regional Experiment (SURE), *Rep. EPRI-EA-1909*, 230 pp., Meteorology Research, Santa Rosa, CA, 1981.
- Bohringer, H., D. W. Fahey, F. C. Fehsenfeld, and E. E. Ferguson, The role of ion molecule reactions in conversion of N<sub>2</sub>O<sub>5</sub> to HNO<sub>3</sub> in the stratosphere, *Planet. Space Sci.*, **31**, 185-191, 1983.
- Bojkov, R. D., Some characteristics of the total ozone deduced from Dobson-spectrophotometer and filter-ozonometer data and their application to determination of the effectiveness of the ozone station network, *Ann. Geoph.*, **25**, 293-299, 1969.
- Bojkov, R. D., Tropospheric ozone, its changes and possible radiative effect, *WMO Special Environment Report 16*, 1983.
- Bojkov, R. D., and G. C. Reinsel, Trends in tropospheric ozone concentration, in *Atmospheric Ozone*, edited by C. S. Zerefos and A. Ghazi, pp. 775-781, D. Reidel, Dordrecht, 1984.
- Bollinger, M. J., C. J. Hahn, D. D. Parrish, P. C. Murphy, D. L. Albritton, and F. C. Fehsenfeld, NO<sub>x</sub> measurements in clean continental air and analysis of the contributing meteorology, *J. Geophys. Res.*, **89**, 9623-9631, 1984.
- Bonsang, B., and G. Lambert, Nonmethane HC in an oceanic atmosphere, *J. Atmos. Chem.*, **2**, 257-271, 1985.
- Borchers, R., P. Fabian, and S. A. Penkett, First measurements of the vertical distribution of CCl<sub>4</sub> and CH<sub>3</sub>CCl<sub>3</sub> in the stratosphere, *Naturwiss.*, **70**, 514-516, 1983.
- Borchers, R., P. Fabian, B. C. Krueger, S. Lal, U. Schmidt, D. Knapska, and S. A. Penkett, The vertical distribution of CCl<sub>2</sub>F-CClF<sub>2</sub> (CFC-113) and CClF<sub>2</sub>-CClF<sub>2</sub> (CFC-114) in the stratosphere, paper presented at 5th General Assembly, International Association of Geomagnetism and Aeronomy, Prague, 5-17 August 1985.
- Borden, T. R., and W. S. Hering, Ozonesonde observations over North America, Vol I, 525 pp., II, 286 pp., III, 266 pp., IV, 376 pp., *Report AFCRL-65-913*, Air Force Cambridge Res. Labs., Hanscom AFB, MA, 1964.

## REFERENCES

- Borden, T. R., and W. S. Hering, Mean distributions of ozone density over North America 1963-1964, *Environmental Research Paper No. 162, Report AFCRL-65-913*, 28 pp., Air Force Cambridge Research Labs., Hanscom AFB, MA, 1965.
- Borghini, R., D. Cariolle, A. Girard, J. Laurent, and N. Louisnard, Comparison entre les resultats d'un modele une dimensionnel et des resultats de mesures stratospheriques de CH<sub>4</sub>, H<sub>2</sub>O et des oxydes d'azote, *Rev. Phys. Appl.*, 18, 229-237, 1983.
- Borisenkov, Ye. P., and Yu. Ye. Kazakov, Effect of freons and halocarbons on the ozone layer of the atmosphere and climate, typed manuscript, USSR, 1977.
- Borucki, W. J., and W. L. Chameides, Lightning: Estimates of the rates of energy dissipation of nitrogen fixation, *Res. Geophys. and Space Phys.*, 22, 363-372, 1984.
- Bossy, L., and M. Nicolet, On the variability of Lyman alpha with solar activity, *Planet. Space Sci.*, 29, 907-914, 1981.
- Bottenheim, J. W., K. A. Brice, and K. G. Anlauf, Discussion of a Lagrangian trajectory model describing long-range transport of oxides of nitrogen, the incorporation of PAN in the chemical mechanism, and supporting measurements of PAN and nitrate species at rural sites in Ontario, Canada, *Atmos. Environ.*, 18, 2609-2619, 1984.
- Boughner, R. E., The effect of increased carbon dioxide concentrations on stratospheric ozone, *J. Geophys. Res.*, 83, 1326-1332, 1978.
- Boughner, R. E., and V. Ramanathan, Climatic consequence of increasing CO<sub>2</sub>: A study of the feedback mechanism between increasing CO<sub>2</sub> concentrations and the atmospheric ozone, water vapor, and thermal structure balance, paper presented at Second Conf. Atmospheric Radiation, Amer. Meteor. Soc., Arlington, VA, 29-31 October, 1975.
- Boughner, R., J. C. Larsen, and M. Natarajan, The influence of NO and ClO variations at twilight on the interpretation of solar occultation measurements, *Geophys. Res. Lett.*, 7, 231-234, 1980.
- Bowman, K. P., and A. J. Krueger, A global climatology of total ozone from the Nimbus 7 Total Ozone Mapping Spectrometer (TOMS), *J. Geophys. Res.*, 90, 7967-7976, 1985.
- Boyd, J. P., The noninteraction of waves with the zonally averaged flow on a spherical Earth and the interrelationships of eddy fluxes of energy, heat and momentum, *J. Atmos. Sci.*, 33, 2285-2291, 1976.
- Bradford, C. M., F. H. Murcray, J. W. Van Allen, J. N. Brooks, D. G. Murcray, and A. Goldman, Ground level detection and feasibility for monitoring of several trace atmospheric constituents by high resolution infrared spectroscopy, *Geophys. Res. Lett.*, 3, 387-390, 1976.
- Bradshaw, J. D., and D. D. Davis, Sequential two-photon laser-induced fluorescence—A new method for detecting atmospheric trace levels of NO, *Optics Letters*, 7, 224-226, 1982.
- Bradshaw, J. D., S. KeSheng, M. O. Rodgers, S. T. Sandholm, and D. D. Davis, Measurements of tropospheric NO concentrations as part of the NASA GTE/CITE program, *Eos Trans. AGU*, 65, 835, 1984.
- Brasseur, G., *Physique et chimie de l'atmosphere moyenne*, Masson, Paris, 1982.
- Brasseur, G., and M. Bertin, The action of chlorine on the ozone layer as given by a zonally averaged two-dimensional model, *Pure Appl. Geophys.*, 117, 436-450, 1978/79.
- Brasseur, G., and M. Nicolet, Chemospheric process of nitric oxide in the mesosphere and stratosphere, *Planet. Space Sci.*, 21, 939-961, 1973.
- Brasseur, G., and P. C. Simon, Stratospheric chemical and thermal response to long-term variability in solar UV irradiance, *J. Geophys. Res.*, 86, 7343-7362, 1981.
- Brasseur, G., and S. Solomon, *Aeronomy of the Middle Atmosphere: Chemistry and Physics in the Stratosphere and Mesosphere*, 441 pp., D. Reidel, Dordrecht, 1984.
- Brasseur, G., P. De Baets, and A. De Rudder, Solar variability and minor constituents in the lower thermosphere and in the mesosphere, *Space Sci. Rev.*, 34, 377-385, 1983a.

## REFERENCES

- Brasseur, G., A. De Rudder, and P. C. Simon, Implication for stratospheric composition of a reduced absorption cross section in the Herzberg continuum of molecular oxygen, *Geophys. Res. Lett.*, **10**, 20-23, 1983b.
- Brasseur, G., A. De Rudder, and C. Tricot, Stratospheric response to chemical perturbations, *J. Atmos. Chem.*, **3**, 261-288, 1985.
- Bremner, J. M., and A. M. Blackmer, Nitrous oxide: Emission from soils during nitrification of fertilizer nitrogen, *Science*, **199**, 295-298, 1978.
- Bremner, J. M., S. G. Robbins, and A. M. Blackmer, Seasonal variability in emission of nitrous oxide in soil, *Geophys. Res. Lett.*, **7**, 611-643, 1980.
- Bretherton, F. P., Momentum transport by gravity waves, *Quart. J. Roy. Meteorol. Soc.*, **95**, 213-243, 1969.
- Brewer, A. W., Evidence for a world circulation provided by the measurements of helium and water vapour distribution in the stratosphere, *Quart. J. Roy. Meteorol. Soc.*, **75**, 351-363, 1949.
- Brewer, A. W., and J. R. Milford, The Oxford-Kew ozonesonde, *Proc. Roy. Soc. London A*, **256**, 470-495, 1960.
- Brewer, A. W., and A. W. Wilson, The regions of formation of atmospheric ozone, *Quart. J. Roy. Meteorol. Soc.*, **94**, 249-265, 1968.
- Brice, K. A., R. G. Derwent, A. E. J. Eggleton, and S. A. Penkett, Measurements of CCl<sub>3</sub>F and CCl<sub>4</sub> at Harwell 1/75-6/81, *Atmos. Environ.*, **16**, 2543-2554, 1982.
- Brice, K. A., S. A. Penkett, D. H. F. Atkins, F. J. Sandalls, D. J. Bamber, A. F. Tuck, and G. Vaughan, Atmospheric measurements of peroxyacetyl nitrate (PAN) in rural, South-East England: Seasonal variations, Winter photochemistry, and long-range transport, *Atmos. Environ.*, **18**, 2691-2702, 1984.
- Brietenbeck, G. A., A. M. Blackmer, and J. M. Bremner, Effects of different nitrogen fertilizers on emissions of nitrous oxide from soil, *Geophys. Res. Lett.*, **7**, 85-88, 1980.
- Briggs, J., and W. T. Roach, Aircraft observations near jet streams, *Quart. J. Roy. Meteorol. Soc.*, **89**, 225-247, 1963.
- Broadfoot, A. L., The solar spectrum 2100-3200 Å, *Astrophys. J.*, **173**, 681-689, 1972.
- Broecker, W. S., T. H. Peng, and R. Engh, Modeling the carbon system, *Radiocarbon*, **22**, 565-598, 1980.
- Browell, E. V., A. F. Carter, and S. T. Shipley, An airborne lidar system for ozone and aerosol profiling in the troposphere and lower stratosphere, in *Proceedings of the Quadrennial International Ozone Symposium, Vol. I*, edited by J. London, pp. 99-107, IAMAP, NCAR, Boulder, CO, 1981.
- Browell, E. V., A. F. Carter, S. T. Shipley, R. J. Allen, C. F. Butler, M. N. Mayo, J. H. Siviter, Jr, and W. M. Hall, NASA multi purpose airborne DIAL system and measurements of ozone and aerosol profiles, *Appl. Opt.*, **22**, 522-534, 1983.
- Browell, E. V., S. Ismail, E. F. Danielsen, G. L. Gregory, and S. M. Beck, Airborne lidar and in situ measurements of a tropopause fold event, in press, 1985.
- Bruehl, C. H., and P. J. Crutzen, A radiative-convective model to study the sensitivity of climate and chemical composition to a variety of human activities, *Stratosphere*, Proceedings of a working party meeting, Brussels, May 18, 1984, *Commission of European Communities*, edited by A. Ghazi, pp. 85-94, 1984.
- Brune, W. H., E. M. Weinstock, J. J. Schwab, R. M. Stimpfle, and J. G. Anderson, Stratospheric ClO: In situ detection with a new approach, *Geophys. Res. Lett.*, **12**, 441-444, 1985.
- Bryan, K., F. G. Komro, S. Manabe, and M. J. Spelman, Transient climate response to increasing atmospheric carbon dioxide, *Science*, **215**, 56-58, 1982.
- Bryan, K., F. G. Komro, and C. Rooth, The ocean's transient response to global surface temperature anomalies, in *Climate Processes and Climate Sensitivity, Geophysical Monograph 29*, Maurice Ewing Series Vol. 5, edited by J. E. Hansen and T. Takahashi, pp. 29-38, American Geophysical Union, Washington, DC, 1984.

## REFERENCES

- Bufton, J. L., R. W. Stewart, and Chi Weng, Remote measurement of tropospheric ozone, *Appl. Opt.*, **18**, 3363-3364, 1979.
- Buijs, H. L., G. L. Vail, G. Tremblay, and D. J. W. Kendall, Simultaneous measurements of the volume mixing ratio of HCl and HF in the stratosphere, *Geophys. Res. Lett.*, **7**, 205-208, 1980.
- Burkhardt, E. G., C. A. Lambert, and C. K. N. Patel, Stratospheric nitric oxide: Measurements during daytime and sunset, *Science*, **188**, 1111-1113, 1975.
- Burnett, C. R., and E. B. Burnett, Spectroscopic measurements of the vertical column abundance of hydroxyl (OH) in the Earth's atmosphere, *J. Geophys. Res.*, **86**, 5185-5202, 1981.
- Burnett, C. R., and E. B. Burnett, Vertical column abundance of atmospheric OH at solar maximum from Fritz Peak, Colorado, *Geophys. Res. Lett.*, **9**, 708-711, 1982.
- Burnett, C. R., and E. B. Burnett, OH PEPSIOS, *Appl. Opt.*, **22**, 2887-2892, 1983a.
- Burnett, C. R., and E. B. Burnett, OH column abundance measurements from Boca Raton, FL, Fritz Peak, CO, and Poker Flat, AK, *Eos Trans. AGU*, **64**, 781, 1983b.
- Burnett, C. R., and E. B. Burnett, Observational results on the vertical column abundance of atmospheric hydroxyl: Description of its seasonal behavior 1977-1982 and of the 1982 El Chichon perturbation, *J. Geophys. Res.*, **89**, 9603-9611, 1984.
- Burnett, C. R., and E. B. Burnett, Atmospheric hydroxyl response to the partial solar eclipse of May 30, 1984, *Geophys. Res. Lett.*, **12**, 263-266, 1985.
- Burnham, J., Atmospheric gusts-A review of the results of some recent research at the Royal Aircraft Establishment, *Mon. Weather Rev.*, **98**, 723-734, 1970.
- Burrows, J. P., T. J. Wallington, and R. P. Wayne, Kinetics of the reaction of OH with ClO, *J. Chem. Soc. Faraday Trans. 2*, **80**, 957-971, 1984.
- Burrows, J. P., D. W. T. Griffith, G. K. Moortgat, and G. S. Tyndall, Matrix isolation Fourier transform infrared study of the products of the reaction between ClO and NO<sub>2</sub>, *J. Phys. Chem.*, 266-271, 1985.
- Butchart, N., and E. E. Remsberg, The area of the stratospheric polar vortex as a diagnostic for tracer transport on an isentropic surface, *J. Atmos. Sci.*, in press, 1985.
- Butchart, N., S. A. Clough, T. N. Palmer, and P. J. Trevelyan, Simulations of an observed stratospheric warming with quasi-geostrophic refractive index as a model diagnostic, *Quart. J. Roy. Meteorol. Soc.*, **108**, 475-502, 1982.
- Butler, D. M., Earth observing system. Science and mission requirements. Working group report, Volume I, Part 2, *NASA Technical Memorandum 86129*, NASA Goddard Space Flight Center, Greenbelt, MD, 1984.
- Cadle, R. D., and G. W. Grams, Stratospheric aerosol particles and their optical properties, *Reviews of Geophysics and Space Physics*, **13(4)**, 475-501, 1975.
- Cadle, R. D., P. J. Crutzen, and D. H. Ehhalt, Heterogeneous chemical reactions in the stratosphere, *J. Geophys. Res.*, **80**, 3381-3385, 1975.
- Cahen, C., J. Pelon, P. Flamant, and G. Megie, Mesure de la vapeur d'eau tropospherique par absorption differentielle laser, *C. R. Acad. Sci.*, Paris, **292**, 29, 1981.
- Callis, L. B., and M. Natarajan, Stratospheric ozone and temperature perturbations: An examination of synergistic effects, in *Proceedings of the Quadrennial International Ozone Symposium, Vol. II*, edited by J. London, pp. 910-917, IAMAP, NCAR, Boulder, CO, 1981.
- Callis, L. B., and M. Natarajan, Atmospheric carbon dioxide and chlorofluoromethanes: Combined effects on stratospheric ozone, temperature, and surface temperature, *Geophys. Res. Lett.*, **8**, 587-590, 1981.
- Callis, L. B., M. Natarajan, and R. E. Boughner, On the relationship between the greenhouse effect, atmospheric photochemistry and species distribution, *J. Geophys. Res.*, **88**, 1401-1426, 1983a.

## REFERENCES

- Callis, L. B., J. M. Russell III, K. V. Haggard, and M. Natarajan, Examination of winter-time latitudinal gradients in stratospheric NO<sub>2</sub> using theory and LIMS observations, *Geophys. Res. Lett.*, *10*, 945-948, 1983b.
- Callis, L. B., M. Natarajan, and J. M. Russell III, Estimates of the stratospheric distributions of odd nitrogen from the LIMS data, *Geophys. Res. Lett.*, *12*, 259-262, 1985a.
- Callis, L. B., M. Natarajan, R. E. Boughner, J. M. Russell III, and J. D. Lambeth, Stratospheric photochemical studies using Nimbus 7 data, Part II: Development of infrared trace species distributions, *J. Geophys. Res.*, in press, 1985b.
- Calvert, J. G., Test of the theory of ozone generation in Los Angeles atmosphere, *Environ. Sci. Technol.*, *10*, 248-256, 1976.
- Camy-Peyret, C., J.-M. Flaud, L. Delbouille, G. Roland, J. W. Brault, and L. Testerman, Quadrupole transitions of the 1-0 band of N<sub>2</sub> observed in high resolution atmospheric spectrum, *J. Physique Lett.*, *42*, 279-283, 1981.
- Camy-Peyret, C., J.-M. Flaud, J. Laurent, and G. M. Stokes, First infrared measurement of atmospheric NO<sub>2</sub> from the ground, *Geophys. Res. Lett.*, *10*, 35-38, 1983.
- Cariolle, D., and D. Brard, The distribution of ozone and active stratospheric species: Results of a two-dimensional atmospheric model, in *Atmospheric Ozone*, edited by C. S. Zerefos and A. Ghazi, pp. 77-81, D. Reidel, Dordrecht, 1984.
- Cariolle, D., and M. Deque, A GCM study of the transport of heat, momentum and ozone in the stratosphere, in *Atmospheric Ozone*, edited by C. S. Zerefos and A. Ghazi, pp. 24-27, D. Reidel, Dordrecht, 1984.
- Carli, B., F. Mencaraglia, and A. Bonetti, Fourier spectroscopy of the stratospheric emission, *Int. J. Infrared mm Waves*, *1*, 253-276, 1980.
- Carli, B., F. Mencaraglia, and A. Bonetti, New assignments in the submillimeter emission of the stratosphere, *Int. J. Infrared mm Waves*, *3*, 385-394, 1982.
- Carli, B., F. Mencaraglia, A. Bonetti, B. M. Dinelli, and F. Forni, Submillimeter detection of stratospheric OH and further line assignments in the stratospheric emission spectrum, *Int. J. Infrared mm Waves*, *4*, 475-488, 1983.
- Carli, B., F. Mencaraglia, and A. Bonetti, Submillimeter high resolution FT spectrometer for atmospheric studies, *Appl. Opt.*, *23*, 2534-2603, 1984.
- Carli, B., F. Mencaraglia, A. Bonetti, M. Carlotti, and I. Nolt, Detection of atomic oxygen and further line assignments in the far infrared stratospheric spectrum, *Int. J. Infrared mm Waves*, *6*, 149-176, 1985a.
- Carli, B. M. Carlotti, D. M. Dinelli, F. Mencaraglia, and I. Nolt, Further evidence of stratospheric chlorine monoxide, in press, 1985b.
- Carney, T. A., and J. Fishman, An investigation of the vertical distribution of trace constituents in the troposphere with a one-dimensional photochemical model and a model of the trade-wind boundary layer, *Eos Trans. AGU*, *65*, 836, 1984.
- Carroll, M. A., and B. A. Ridley, Tropospheric NO<sub>x</sub> measurements, *Eos Trans. AGU*, *65*, 834, 1984.
- Carter, W. P. L., A. C. Lloyd, J. L. Sprung, and J. N. Pitts, Jr., Progress in the validation of a detailed mechanism for the photooxidation of propene and nebutane in photochemical smog, *Int. J. Chem. Kinet.*, *11*, 45-111, 1979.
- Carver, J. H., B. H. Horton, and F. G. Burger, Nocturnal ozone distribution in the upper atmosphere, *J. Geophys. Res.*, *71*, 4189-4191, 1966.
- Carver, J. H., H. P. Giess, T. H. Hobbs, B. R. Lewis, and J. H. McCoy, Temperature dependence of the molecular oxygen photoabsorption cross section near the H Lyman alpha line, *J. Geophys. Res.*, *82*, 1955-1960, 1977.
- CDAC: See National Research Council, *Changing Climate*, Carbon Dioxide Assessment Committee.
- Cess, R. D., Climatic change: An appraisal of atmospheric feedback mechanisms employing zonal climatology, *J. Atmos. Sci.*, *33*, 1831-1843, 1976.

## REFERENCES

- Cess, R. D., and S. C. Chen, The influence of ethane and acetylene upon the thermal structure of the Jovian atmosphere, *Icarus*, 26, 444-450, 1975.
- Cess, R. D., and S. D. Goldenberg, The effect of ocean heat capacity upon global warming due to increasing atmospheric carbon dioxide, *J. Geophys. Res.*, 86, 498-502, 1981.
- Cess, R. D., and G. L. Potter, A commentary on the recent CO<sub>2</sub>-climate controversy, *Climatic Change*, 6, 365-376, 1984.
- Cess, R. D., and L. S. Wang, A band absorptance formulation for nonisothermal gaseous radiation, *Int. J. Heat Mass Transfer*, 13, 547-555, 1970.
- Cess, R. D., B. P. Briegleb and M. S. Lian, Low-latitude cloudiness and climate feedback: Comparative estimates from satellite data, *J. Atmos. Sci.*, 39, 53-59, 1982.
- Cess, R. D., D. P. Kratz, S. J. Kim and J. Caldwell, Infrared band models for atmospheric methane, *J. Geophys. Res.*, in press, 1985.
- Chamberlin, T. C., An attempt to frame a working hypothesis of the cause of glacial periods on an atmospheric basis, *J. Geol.*, 7, 545, 1899.
- Chameides, W. L., The photochemistry of a remote marine stratiform cloud, *J. Geophys. Res.*, 89, 4739-4755, 1984.
- Chameides, W. L., and D. D. Davis, The free radical chemistry of cloud droplets and its impact upon the composition of rain, *J. Geophys. Res.*, 87, 4863-4877, 1982.
- Chameides, W. L., and A. Tan, The two dimensional diagnostic model for tropospheric OH: An uncertainty analysis, *J. Geophys. Res.*, 86, 5209-5223, 1981.
- Chameides, W. L., and J. C. G. Walker, A photochemical theory of tropospheric ozone, *J. Geophys. Res.*, 78, 8751-8760, 1973.
- Chameides, W. L., D. H. Stedman, R. R. Dickerson, D. W. Rusch, and R. J. Cicerone, NO<sub>x</sub> production in lightning, *J. Atmos. Sci.*, 34, 143-149, 1977a.
- Chameides, W. L., S. C. Liu, and R. J. Cicerone, Possible variations in atmospheric methane, *J. Geophys. Res.*, 82, 1795-1798, 1977b.
- Chan, S. H., and C. L. Tien, Total band absorptance of nonisothermal infrared-radiating gases, *J. Quant. Spectrosc. Radiat. Transfer*, 9, 1261-1271, 1969.
- Chance, K. V., and W. A. Traub, An upper limit for stratospheric hydrogen peroxide, *J. Geophys. Res.*, 89, 11655-11660, 1984.
- Chance, K. V., and W. A. Traub, to be published under BIC I, BIC II, 1986.
- Chance, K. V., J. C. Brasunas, and W. A. Traub, Far infrared measurement of stratospheric HCl, *Geophys. Res. Lett.*, 9, 704-706, 1980.
- Chandra, S., Solar-induced oscillations in the stratosphere: A myth or reality?, *J. Geophys. Res.*, 90, 2331-2339, 1985.
- Chang, C. P., Forcing of stratospheric Kelvin waves by tropospheric heat sources, *J. Atmos. Sci.*, 35, 740-744, 1976.
- Chang, J. S., A. C. Baldwin, and D. M. Golden, An explanation of the preferential formation of less stable isomers in threebody reactions: Cl + NO<sub>2</sub> + M, ClO + NO<sub>2</sub> + M, *J. Chem. Phys.*, 71, 2021-2024, 1979.
- Chanin, M. L., The Intercomparison Ozone Campaign held in France in June 1981: Description of the campaign, *Planet. Space Sci.*, 31, 707-715, 1983a.
- Chanin, M. L., The Ozone Intercomparison Campaign, 1981: Concluding remarks, *Planet. Space Sci.*, 31, 811-812, 1983b.
- Chanin, M. L., and A. Hauchecorne, Lidar observations of gravity and tidal waves in the middle atmosphere, *J. Geophys. Res.*, 86, 9715-9721, 1981.

## REFERENCES

- Chao, W. C., and M. R. Schoeberl, On the linear approximation of gravity wave saturation in the mesosphere, *J. Atmos. Sci.*, *41*, 1893-1898, 1984.
- Chapman, S., A theory of upper atmospheric ozone, *Mem. Roy. Met. Soc.*, *3*, 103-125, 1930.
- Chapman, W., and G. Peckham, Spectral analysis of wave motions in the middle atmosphere, *Phil. Trans. Roy. Soc. London*, *A296*, 59-63, 1980.
- Charlock, T. P., Cloud optical feedback and climate stability in a radiative-convective model, *Tellus*, *34*, 245-254, 1982.
- Charney, J. G., The dynamics of long waves in a baroclinic westerly current, *J. Meteorol.*, *4*, 135-162, 1947.
- Charney, J. G. (Chairman), *Carbon Dioxide and Climate: A Scientific Assessment*, 33 pp., National Academy Press, Washington, DC, 1979.
- Charney, J. G., and P. G. Drazin, Propagation of planetary-scale disturbances from the lower into the upper atmosphere, *J. Geophys. Res.*, *66*, 83-109, 1961.
- Charney, J. G., and M. E. Stern, On the stability of internal baroclinic jets in a rotating atmosphere, *J. Atmos. Sci.*, *19*, 159-172, 1962.
- Chatfield, R. B., and P. J. Crutzen, Sulfur dioxide in remote oceanic air: Cloud transports of reactive precursors, *J. Geophys. Res.*, *89*, 7111-7132, 1984.
- Chedin, A., and N. A. Scott, The impact of spectroscopic parameters on the comparison of the Jovian atmosphere discussed in connection with the recent laboratory, earth and planetary observation programs, *J. Quant. Spectrosc. Radiat. Transfer*, *32*, 453-461, 1984.
- Chedin, A., N. Husson, N. A. Scott, I. Jobard, I. Cohen-Hallaleh, and A. Berroir, La Banque de données GEISA, Description et logiciel d'utilisation, Laboratoire de Meteorologie Dynamique du C.N.R.S., *Internal Note 108*, Ecole Polytechnique, 91128 Palaiseau Cedex, France, October, 1980.
- Chedin, A., N. Husson, N. A. Scott, I. Cohen-Hallaleh, and A. Berroir, The GEISA data bank: 1984 version, Laboratoire de Meteorologie Dynamique du C.N.R.S., *Internal Note 127*, Ecole Polytechnique, 91128 Palaiseau Cedex, France, February, 1985.
- Chemical Manufacturers Association, CMA, *Effect of chlorofluorocarbons on the atmosphere, revision 17*, edited by B. P. Block, H. Magid, and R. B. Ward, 98 pp., Washington, DC, 1982.
- Chemical Manufacturers Association, CMA, *Production, sales and calculated release of CFC 11 and CFC 12 through 1983*, October, 1984.
- Chemical Manufacturers Association, CMA, *Production, sales and calculated release of CFC 11 and CFC 12 through 1984*, October, 1985.
- Chemical Manufacturers Association-National Bureau of Standards, CMA-NBS, *Proceedings of CMA-NBS workshop on atmospheric spectra*, November 3-4, 1983, Gaithersburg, MD, edited by A. Weber, June, 1985.
- Cheung, A.S.C., K. Yoshino, W. H. Parkinson, and D. E. Freeman, Herzberg continuum cross section of oxygen in the wavelength region 193.5-204.0 nm and band oscillator strengths of the (0,0) and (1,0) Schumann-Runge bands, *Can. J. Phys.*, *62*, 1752-1762, 1984a.
- Cheung, A. S. C., K. Yoshino, W. H. Parkinson, and D. E. Freeman, Herzberg continuum cross-section of oxygen in the wavelength region 193.5-204 nm: New laboratory measurements and stratospheric implications, *Geophys. Res. Lett.*, *11*, 580-582, 1984b.
- Chou, C. C., R. J. Milstein, W. S. Smith, H. Veraruiz, M. J. Molina, and F. S. Rowland, Stratospheric photodissociation of several saturated perhalo- chlorofluorocarbon compounds in current technological use (Fluorocarbons -13, -113, -114, and -115), *J. Phys. Chem.*, *82*, 1-7, 1978.
- Chou, M.-D., L. Peng, and A. Arking, Climate studies with a multilayer energy balance model. Part III: Climatic impact of stratospheric volcanic aerosols, *J. Atmos. Sci.*, *41*, 759-767, 1984.
- Chu, W. P., and M. P. McCormick, Inversion of stratospheric aerosol and gaseous constituents from spacecraft solar extinction data in the 0.38 - 1.0  $\mu\text{m}$  wavelength region, *Appl. Opt.*, *18*, 1404-1413, 1979.
- CIAP: See Climatic Impact Assessment Program.

## REFERENCES

- Cicerone, R. J., Atmospheric carbon tetrafluoride: A nearly inert gas, *Science*, **206**, 59-61, 1979.
- Cicerone, R. J., Methane in the atmosphere, in *Global Environment Problems*, edited by S. F. Singer, Paragon House, New York, in press, 1985.
- Cicerone, R. J., and J. L. McCrumb, Photodissociation of isotopically heavy O<sub>2</sub> as a source of atmospheric O<sub>3</sub>, *Geophys. Res. Lett.*, **7**, 251-254, 1980.
- Cicerone, R. J., and J. D. Shetter, Sources of atmospheric methane: Measurements in rice paddies and a discussion, *J. Geophys. Res.*, **86**, 7203-7209, 1981.
- Cicerone, R. J., and R. Zellner, The atmospheric chemistry of hydrogen cyanide, *J. Geophys. Res.*, **88**, 10689-10696, 1983.
- Cicerone, R. J., S. Walters, and S. C. Liu, Non-linear response of stratospheric ozone column to chlorine injections, *J. Geophys. Res.*, **88**, 3647-3661, 1983a.
- Cicerone, R. J., J. D. Shetter, and C. C. Delwiche, Seasonal variation of methane flux from a California rice paddy, *J. Geophys. Res.*, **88**, 11022-11024, 1983b.
- Cieslik, S., and M. Nicolet, The aeronomic dissociation of nitric oxide, *Planet. Space Sci.*, **21**, 925-930, 1973.
- Clancy, R. T., D. O. Muhleman, and G. L. Berge, Microwave spectra of terrestrial mesospheric CO, *J. Geophys. Res.*, **87**, 5009-5014, 1982.
- Clark, J.H.E., and L. T. Morone, Mesospheric heating due to convectively excited gravity waves. A case study, *Mon. Weather Rev.*, **109**, 990-1001, 1981.
- Clark, J.H.E., and T. G. Rogers, The transport of conservative trace gases by planetary waves, *J. Atmos. Sci.*, **35**, 2232-2235, 1978.
- Clark, T. A., and D. J. W. Kendall, Far infrared emission spectrum of the stratosphere from balloon altitudes, *Nature*, **260**, 31-32, 1976.
- Clark, T. A., and D. J. W. Kendall, Line positions and strengths of magnetic dipole transitions of molecular oxygen from stratospheric emission spectra, *J. Quant. Spectrosc. Radiat. Transfer*, **24**, 65-73, 1980.
- Clark, T. A., D. A. Naylor, R. T. Boreiko, J. M. Hoogerdijk, B. Fitton, M. F. Kessler, and R. J. Emery, Downward flux of atmospheric 63  $\mu$ m emission from atomic oxygen at balloon altitudes, *Nature*, **313**, 206-207, 1985.
- Climate Analysis Center, *Climate Diagnostics Bulletin*, Published monthly by the Climate Analysis Center, NOAA/NMC/NWS, Washington, DC, 1983.
- Climate Analysis Center, *Climate Diagnostics Bulletin*, Published monthly by the Climate Analysis Center, NOAA/NMC/NWS, Washington, DC, 1984.
- Climatic Impact Assessment Program, Report of findings: The effects of stratospheric pollution by aircraft, *DOT-TST-75-50*, edited by A. J. Grobecker, S. C. Coroniti, and R. H. Cannon, Jr., 551 pp., Department of Transportation, Washington, DC, 1974.
- Clough, S. A., N. S. Grahame, and A. O'Neill, Potential vorticity in the stratosphere derived using data from satellites, *Quart. J. Roy. Meteorol. Soc.*, **111**, 335-358, 1985.
- CMA: See Chemical Manufacturer's Association.
- Coakley, J. A. Jr., and R. D. Cess, The effect of tropospheric aerosols on the earth's radiation budget: A parameterization for climate models, *J. Atmos. Sci.*, **40**, 116-138, 1983.
- Coffey, M. T., W. G. Mankin, and A. Goldman, Simultaneous spectroscopic determination of the latitudinal, seasonal, and diurnal variability of stratospheric N<sub>2</sub>O, NO, NO<sub>2</sub>, and HNO<sub>3</sub>, *J. Geophys. Res.*, **86**, 7331-7341, 1981a.
- Coffey, M. T., W. G. Mankin, and R. J. Cicerone, Spectroscopic detection of stratospheric hydrogen cyanide, *Science*, **214**, 333-335, 1981b.
- Coffey, M. T., W. G. Mankin, A. Goldman, C. P. Rinsland, G. A. Harvey, V. Malathy Devi, and G. M. Stokes, Infrared measurements of atmospheric ethane (C<sub>2</sub>H<sub>6</sub>) from aircraft and ground based solar absorption spectra in the 3000 cm<sup>-1</sup> region, *Geophys. Res. Lett.*, **12**, 199-202, 1985.

## REFERENCES

- Coffey *et al.*, 1985: See Roscoe *et al.*, 1985.
- Cohen, Y., and L. I. Gordon, Nitrous oxide in the oxygen minimum of the eastern tropical North Pacific: Evidence for its consumption during denitrification and possible mechanisms for its production, *Deep Sea Res.*, **6**, 509-524, 1978.
- Cohen, Y., and L. I. Gordon, Nitrous oxide production in the ocean, *J. Geophys. Res.*, **84**, 347-353, 1979.
- Cole, A. E., and A. J. Kantor, Air Force Reference Atmospheres, *Rep. AFGL-TR-78-0051*, 78 pp., Air Force Geophys. Lab., Hanscom AFB, MA, 1978.
- Connell, P. S., D. J. Wuebbles, and J. S. Chang, Stratospheric hydrogen peroxide-The relationship of theory and observation, *J. Geophys. Res.*, **90**, 10726-10732, 1985.
- Cook, J. W., G. E. Brueckner, and M. E. Van Hoosier, Variability of the solar flux in the far ultraviolet 1175-2100 Å, *J. Geophys. Res.*, **85**, 2257-2268, 1980.
- Cornford, S. G., and C. S. Spavins, Some measurements of cumulonimbus tops in the pre-monsoon season in the north-east of India, *Met. Mag.*, **102**, 314-332, 1973.
- COSPAR International Reference Atmosphere*, CIRA, edited by A. C. Strickland, Akademie-Verlag, Berlin, 1972.
- Cowley, J. R., and G. M. Lawrence, Earth Limb altitude determination for the Solar Mesosphere Explorer, paper presented at AIAA Aerospace Sciences Meeting, *AIAA Paper 83-0429*, 9 pp., Reno, Nevada, January 10-13, 1983.
- Cox, R. A., and M. J. Coffey, Thermal decomposition of peroxyacetyl nitrate in the presence of NO, *Environ. Sci. Tech.*, **11**, 900-906, 1977.
- Cox, R. A., and R. G. Derwent, Kinetics of chlorine oxide radical reactions using modulated photolysis, Part I, Disproportionation of ClO, *J. Chem. Soc. Far. I*, **75**, 1635-1647, 1979.
- Cox, R. A., A.E.J. Eggleton, R. G. Derwent, J. E. Lovelock, and D. H. Pack, Long-range transport of photochemical ozone in north-western Europe, *Nature*, **255**, 118-121, 1975.
- Cox, R. A., R. G. Derwent, A. E. J. Eggleton, and H. J. Reid, Kinetics of chlorine oxide radical reactions using modulated photolysis, Part 2, ClO and ClOO radical kinetics, *J. Chem. Soc. Far. I*, **75**, 1648-1666, 1979.
- Cox, R. A., J. P. Burrows, and G. B. Coker, Product formation in the association reaction of ClO with NO<sub>2</sub> investigated by diode laser spectroscopy, *Int. J. Chem. Kinet.*, **16**, 445-467, 1984.
- Coy, L., An unusually large westerly amplitude of the quasi-biennial oscillation, *J. Atmos. Sci.*, **36**, 174-176, 1979.
- Coy, L., An unusually large westerly amplitude of the quasi-biennial oscillation, corrigendum, *J. Atmos. Sci.*, **37**, 913, 1980.
- Coy, L., and M. Hitchman, Kelvin wave packets and flow acceleration: A comparison of modeling and observation, *J. Atmos. Sci.*, **41**, 1875-1880, 1984.
- Craig, H., and C. C. Chou, Methane: The record in polar ice cores, *Geophys. Res. Lett.*, **9**, 1221-1224, 1982.
- Craig, R. A., *The Upper Atmosphere: Meteorology and Physics*, 209 pp., Academic Press, New York, 1965.
- Craig, R. L., R. A. Vincent, G. J. Fraser, and M. J. Smith, The quasi 2-day wave in the Southern Hemisphere mesosphere, *Nature*, **287**, 319-320, 1980.
- Craig, R. L., R. A. Vincent, and R. A. Plumb, On the interaction between the quasi 2-day wave and the mean flow, in *Handbook for MAP, Vol. 18*, edited by S. Kato, pp. 76-79, SCOSTEP Secretariat, Univ. of Illinois, Urbana, 1985.
- Crane, A. J., Uses of satellite data in studies of stratospheric dynamics, Ph.D. thesis, Oxford University, Oxford, 1977.
- Crane, A. J., Aspects of the energetics of the upper stratosphere during the January-February 1973 major sudden warming, *Quart. J. Roy. Meteorol. Soc.*, **105**, 185-206, 1979.

## REFERENCES

- Crane, A. J., J. D. Haigh, J. A. Pyle, and C. F. Rogers, Mean meridional circulations of the stratosphere and mesosphere, *Pure Appl. Geophys.*, 118, 307-328, 1980.
- Crutzen, P. J., discussion of "Absorption and emission by carbon dioxide in the mesosphere", *Quart. J. Roy. Meteorol. Soc.*, 96, 767-769, 1970.
- Crutzen, P. J., Ozone production rates in an oxygen, hydrogen, nitrogen-oxide atmosphere, *J. Geophys. Res.*, 76, 7311-7327, 1971.
- Crutzen, P. J., Gas phase nitrogen and methane chemistry in the atmosphere, in *Physics and Chemistry of Upper Atmospheres*, edited by B. M. McCormac, D. Reidel, Boston, MA, 1973a.
- Crutzen, P. J., A discussion of the chemistry of some minor constituents in the stratosphere and troposphere, *Pure Appl. Geophys.*, 106-108, 1385-1399, 1973b.
- Crutzen, P. J., Photochemical reactions initiated by and influencing ozone in unpolluted tropospheric air, *Tellus*, 26, 47-57, 1974.
- Crutzen, P. J., The possible importance of CSO for the sulfate layer of the stratosphere, *Geophys. Res. Lett.*, 3, 73-76, 1976.
- Crutzen, P. J., The role of NO and NO<sub>2</sub> in the chemistry of the stratosphere and troposphere, *Ann. Rev. Earth Pl. Sci.*, 7, 443-472, 1979.
- Crutzen, P. J., Atmospheric interactions--Homogeneous gas reactions of C, N and S containing compounds, in *The Major Biogeochemical Cycles and Their Interactions*, edited by B. Bolin and R. Cook, pp. 67-112, Wiley, New York, 1983.
- Crutzen, P. J., The role of the tropics in atmospheric chemistry, in *Geophysiology of Amazonia*, edited by R. Dickinson, Wiley, New York, in press, 1985.
- Crutzen, P. J., and D. H. Ehhalt, Effects of nitrogen fertilizers and combustion on the stratospheric ozone layer, *Ambio*, 6, 112-117, 1977.
- Crutzen, P. J., and J. Fishman, Average concentrations of OH in the troposphere and the budgets of CH<sub>4</sub>, CO, H<sub>2</sub>, and CH<sub>3</sub>CCl<sub>3</sub>, *Geophys. Res. Lett.*, 4, 321-324, 1977.
- Crutzen, P. J., and L. T. Gidel, A two dimensional photochemical model of the atmosphere. 2. The tropospheric budgets of the anthropogenic chlorocarbons, CO, CH<sub>4</sub>, CH<sub>3</sub>Cl and the effect of various NO<sub>x</sub> sources on tropospheric ozone, *J. Geophys. Res.*, 88, 6641-6661, 1983.
- Crutzen, P. J., and U. Schmailzl, Chemical budgets of the stratosphere, *Planet. Space Sci.*, 31, 1009-1032, 1983.
- Crutzen, P. J., and S. Solomon, Response of mesospheric ozone to particle precipitation, *Planet. Space Sci.*, 28, 1147-1153, 1980.
- Crutzen, P. J., I. S. A. Isaksen, and G. C. Reid, Solar proton events: Stratospheric sources of nitric oxide, *Science*, 189, 457-459, 1975.
- Crutzen, P. J., L. E. Heidt, J. P. Krasnec, W. H. Pollock, and W. Seiler, Biomass burning as a source of atmospheric gases CO, H<sub>2</sub>, N<sub>2</sub>O, NO, CH<sub>3</sub>Cl and COS, *Nature*, 282, 253-256, 1979.
- Crutzen, P. J., W. Seiler, A. C. Delany, J. Greenburg, P. Haagensen, L. Heidt, R. Lueb, W. Pollock, A. Wartburg, and P. Zimmerman, Tropospheric chemical composition measurements in Brazil during the dry seasons, *J. Atmos. Chem.*, 2, 233-256, 1983.
- Cunnold, D., Fluorocarbon lifetime and releases from 5 years of ALE data, paper presented at CSIRO symposium, The Scientific Application of Baseline Observations of Atmospheric Composition, Aspendale, Australia, 7-9 November, 1984.
- Cunnold, D., F. N. Alyea, N. Phillips, and R. G. Prinn, A three-dimensional dynamical chemical model of atmospheric ozone, *J. Atmos. Sci.*, 32, 170-194, 1975.
- Cunnold, D. M., F. N. Alyea, and R. G. Prinn, Relative effects on atmospheric ozone of latitude and altitude of supersonic flight, *AIAA Journal*, 15, 337-345, 1977.

## REFERENCES

- Cunnold, D. M., F. N. Alyea, and R. G. Prinn, Preliminary calculations concerning the maintenance of the zonal mean ozone distribution in the Northern Hemisphere, *Pure Appl. Geophys.*, 118, 329-354, 1980.
- Cunnold, D. M., R. G. Prinn, R. A. Rasmussen, P. G. Simmonds, F. N. Alyea, C. A. Cardelino, A. J. Crawford, P. J. Fraser, and R. D. Rosen, The atmospheric lifetime experiment, 3, Lifetime methodology and application to 3 years of  $\text{CFCl}_3$  data, *J. Geophys. Res.*, 88, 8379-8400, 1983a.
- Cunnold, D. M., R. G. Prinn, R. A. Rasmussen, P. G. Simmonds, F. N. Alyea, C. A. Cardelino, and A. J. Crawford, The atmospheric lifetime experiment, 4, Results for  $\text{CF}_2\text{Cl}_2$  based on 3 years of data, *J. Geophys. Res.*, 88, 8401-8414, 1983b.
- Curtis, P. D., J. T. Houghton, G. D. Peskett, and C. D. Rodgers, The pressure modulator radiometer for Nimbus F, *Proc. Roy. Soc. London A*, 337, 135-150, 1974.
- Dacey, J., and M. J. Klug, Methane efflux from lake sediments through water lilies, *Science*, 203, 1253-1255, 1979.
- Danielsen, E. F., Trajectories: Isobaric, Isentropic and Actual, *J. Meteorol.*, 18, 479-493, 1961.
- Danielsen, E. F., *Project Springfield Report*, Defense Atomic Support Agency, DASA 1517, Washington, DC, 1964.
- Danielsen, E. F., Transport and diffusion of stratospheric radioactivity based on synoptic hemispheric analyses of potential vorticity, Final report, *Report NYO-3317-3*, 97 pp., Pennsylvania State University, University Park, PA, 1967.
- Danielsen, E. F., Stratospheric-tropospheric exchange based on radioactivity, ozone and potential vorticity, *J. Atmos. Sci.*, 25, 502-518, 1968.
- Danielsen, E. F., The relationship between severe weather, major dust storms and rapid large-scale cyclogenesis (II), in *Subsynchronous Extratropical Weather Systems: Observations, Analysis, Modeling, and Prediction, Notes from a colloquium, Summer, 1974, Volume II: Seminars and workshops*, Report PB-247286/8, pp. 226-241, NCAR, Boulder, CO, 1974.
- Danielsen, E. F., An objective method for determining the generalized transport tensor for two-dimensional Eulerian models, *J. Atmos. Sci.*, 38, 1319-1339, 1981.
- Danielsen, E. F., Statistics of cold cumulonimbus anvils based on enhanced infrared photographs, *Geophys. Res. Lett.*, 9, 601-604, 1982.
- Danielsen, E. F., Meteorological context for Global Tropospheric Experiments' instruments tests, paper presented to American Geophysical Union, San Francisco, California, December 3-7, 1984, *Eos Trans. AGU*, 65, 834, 1984.
- Danielsen, E. F., and R. S. Hipskind, Stratospheric-tropospheric exchange at polar latitudes in summer, *J. Geophys. Res.*, 85, 393-400, 1980.
- Danielsen, E. F., and D. Kley, A tropical cumulonimbus source for correlated water vapor and ozone minima in extratropical stratosphere, *J. Geophys. Res.*, in press, 1985.
- Danielsen, E. F., and V. A. Mohnen, Project Dustorm Report: Ozone transport, in situ measurements and meteorological analyses of tropopause folding, *J. Geophys. Res.*, 82, 5867-5877, 1977.
- Danielsen, E. F., R. Bleck, J. Shedlovsky, A. Wartburg, P. Haagensen and W. Pollock, Observed distribution of radioactivity, ozone and potential vorticity associated with tropopause folding, *J. Geophys. Res.*, 75, 2353-2361, 1970.
- Dave, J. V., J. J. DeLuisi, and C. L. Mateer, Results of a comprehensive theoretical examination of the optical effects of aerosols on the Umkehr measurements, *Spec. Environ. Rep. 14*, pp. 15-22, WMO, Geneva, 1979.
- Davies, R. W., Many body treatment of pressure shifts associated with collisional broadening, *Phys. Rev.*, A12, 927-946, 1975.
- Dawson, G. A., Nitrogen fixation by lightning, *J. Atmos. Sci.*, 37, 174-178, 1980.

## REFERENCES

- De La Noe, J., A. Baudry, M. Perault, P. Dierich, N. Monnanteuil, and J. M. Colmont, Measurements of the vertical distribution of ozone by ground-based microwave techniques at the Bordeaux Observatory during the June 1981 intercomparison campaign, *Planet. Space Sci.*, *31*, 737-741, 1983.
- De More: See DeMore.
- De Muer, D., Vertical ozone distributions over Uccle, Belgium from six years of soundings, *Beit. Phys. Atmos.*, *49*, 1-16, 1976.
- De Rudder, A., and G. Brasseur, Ozone in the 21st century: Increase or decrease?, in *Atmospheric Ozone*, edited by C. S. Zerefos and A. Ghazi, pp. 92-96, D. Reidel, Dordrecht, 1984.
- De Rudder, A., and G. Brasseur, A model calculation of the ozone response to the increase in the atmospheric emission of several gases, *Internal Report*, Inst. Aeronomie Spatiale de Belgique, Brussels, 1985.
- de Zafra, R. L., A. Parrish, P. M. Solomon, and J. W. Barrett, A measurement of stratospheric HO<sub>2</sub> by ground-based millimeter-wave spectroscopy, *J. Geophys. Res.*, *89*, 1321-1326, 1984.
- de Zafra, R. L., A. Parrish, P. M. Solomon, and J. W. Barrett, Quantitative observations of stratospheric chlorine monoxide as a function of latitude and season during the period 1980-1983, in *Atmospheric Ozone*, edited by C. S. Zerefos and A. Ghazi, pp. 206-209, D. Reidel, Dordrecht, 1985a.
- de Zafra, R. L., A. Parrish, J. Barrett, and P. Solomon, An observed upper limit on stratospheric hydrogen peroxide, *J. Geophys. Res.*, *90*, 13087-13090, 1985b.
- Deguchi, S., and D. O. Muhleman, Mesospheric water vapor, *J. Geophys. Res.*, *87*, 1343-1346, 1982.
- Delany, A. C., P. J. Crutzen, P. Haagenen, S. Walters, and A. F. Wartburg, Photochemically produced ozone in the emission from large-scale tropical vegetation fires, *J. Geophys. Res.*, *90*, 2425-2429, 1985.
- Delany, A. C., D. R. Fitzjarrald, D. Pearson, D. H. Lenschow, G. J. Wendel, and B. Woodruff, Direct measurements of fluxes of oxides of nitrogen and of ozone over grasslands, *J. Atmos. Chem.*, in press, 1986.
- Delbouille, L., G. Roland, J. W. Brault, and L. Testerman, Photometric atlas of the solar spectrum from 1850 to 10,000 cm<sup>-1</sup>, preliminary data, Kitt Peak National Observatory, 1981.
- Delmas, R. J., J. M. Ascencia, and M. Legrand, Polar ice evidence that atmospheric CO<sub>2</sub> 20,000 B.P. was 50% of present, *Nature*, *284*, 155-157, 1980.
- DeLuisi, J. J., Umkehr vertical ozone profile errors caused by the presence of stratospheric aerosols, *J. Geophys. Res.*, *84*, 1766-1770, 1979.
- Demerjian, K. L., J. A. Kerr, and J. G. Calvert, Mechanism of photochemical smog formation, *Adv. Environ. Sci. Technol.*, *10*, 1-262, 1974.
- Demerjian, K. L., K. L. Schere, and J. T. Peterson, Theoretical estimates of active (spherically integrated) flux and photolytic rate constants of atmospheric species in the lower troposphere, *Adv. Environ. Sci. Technol.*, *10*, 369-459, 1980.
- DeMore, W. B., Rate constants for the reactions of hydroxyl and hydroperoxyl radicals with ozone, *Science*, *180*, 735-737, 1973.
- DeMore, W. B., Rate constant and possible pressure dependence of the reaction OH + HO<sub>2</sub>, *J. Phys. Chem.*, *86*, 121-126, 1982.
- DeMore, W. B., and O. Raper, Hartley band extinction coefficients of ozone in the gas phase and in liquid nitrogen, carbon monoxide and argon, *J. Phys. Chem.*, *68*, 412-414, 1964.
- DeMore, W. B., M. J. Molina, R. T. Watson, D. M. Golden, R. F. Hampson, M. J. Kurylo, C. J. Howard, and A. R. Ravishankara, Chemical kinetics and photochemical data for use in stratospheric modeling, Evaluation number 6, *JPL Publication 83-62*, 219 pp., Jet Propulsion Lab., Pasadena, CA, 1983.
- DeMore, W. B., J. J. Margitan, M. J. Molina, R. T. Watson, D. M. Golden, R. F. Hampson, M. J. Kurylo, C. J. Howard, and A. R. Ravishankara, Chemical kinetics and photochemical data for use in stratospheric modeling, Evaluation Number 7, *JPL Publication 85-37*, 226 pp., Jet Propulsion Lab., Pasadena, CA, 1985.

## REFERENCES

- Derwent, D. G., Two-dimensional model studies of the impact of aircraft emission on tropospheric ozone, *Atmos. Environ.*, *16*, 1997-2007, 1982.
- Derwent, R. G., and A. E. J. Eggleton, Two dimensional model studies of methyl chloroform in the troposphere, *Quart. J. Roy. Meteorol. Soc.*, *107*, 231-242, 1981.
- Derwent, R. G., and H. N. M. Steward, Elevated ozone levels in the air of central London, *Nature*, *241*, 342-343, 1973.
- Dickerson, R. R., Measurements of reactive nitrogen compounds in the free troposphere, *Atmos. Chem.*, *18*, 2585-2593, 1984.
- Dickenson, R. E., Planetary Rossby waves propagating vertically through weak westerly wind wave guides, *J. Atmos. Sci.*, *25*, 984-1002, 1968.
- Dickinson, R. E., Theory of planetary wave-zonal flow interaction, *J. Atmos. Sci.*, *26*, 73-81, 1969.
- Dickinson, R. E., Infrared radiative heating and cooling in the Venusian mesosphere, 1, Global mean radiative equilibrium, *J. Atmos. Sci.*, *29*, 1551-1556, 1972.
- Dickinson, R. E., Method of parameterization for infrared cooling between altitudes of 30 and 70 kilometers, *J. Geophys. Res.*, *78*, 4451-4457, 1973.
- Dickinson, R. E., Energetics of the stratosphere, *J. Atmos. Terr. Phys.*, *37*, 855-864, 1975.
- Dickinson, R. E., Modeling climate changes due to carbon dioxide increases, in *Carbon Dioxide Review*, edited by W. C. Clark, pp. 101-133, Clarendon Press, New York, 1982.
- Dickinson, R. E., Infrared radiative cooling in the mesosphere and lower thermosphere, *J. Atmos. Terr. Phys.*, *46*, 995-1008, 1984.
- Dickinson, R. E., Modeling of future climate. WMO/ICSU/UNEP international assessment of the impact of an increased atmospheric concentration of carbon dioxide on the environment, in press, 1985.
- Dickinson, R. E., S. C. Liu, and T. M. Donahue, Effect of chlorofluoromethane infrared radiation on zonal atmospheric temperature, *J. Atmos. Sci.*, *35*, 2142-2152, 1978.
- Ditchburn, R. W., and P. A. Young, The absorption of molecular oxygen between 1850 and 2500 Å, *J. Atmos. Terr. Phys.*, *24*, 127-139, 1962.
- Dobson, G. M. B., Origin and distribution of polyatomic molecules in the atmosphere, *Proc. Roy. Soc. London*, *A236*, 187-193, 1956.
- Dobson, G. M. B., The laminated structure of the ozone in the atmosphere, *Quart. J. Roy. Meteorol. Soc.*, *99*, 599-607, 1973.
- Dobson, G. M. B., D. N. Harrison, and J. Lawrence, Measurements of the amount of ozone in the Earth's atmosphere and its relation to other geophysical conditions: Part III, *Proc. Roy. Soc. London*, *A122*, 456-486, 1929.
- Dobson, G. M. B., A. W. Brewer, and B. M. Cwilong, Meteorology of the lower stratosphere, *Proc. Roy. Soc. London*, *A185*, 144-175, 1946.
- Dodge, M. C., Combined effects of organic reactivity and NMHC/NO<sub>x</sub> ratio on photochemical oxidant formation--a modeling study, *Atmos. Environ.*, *18*, 1657-1665, 1984.
- Dognon, A. M., F. Caralp, and R. Lesclaux, Reactions of chlorofluoromethyl peroxy radicals with NO: A kinetic study in the temperature range 230-430K, *J. Chem. Phys. Phys. Biol.*, in press, 1985.
- Doherty, G. M., R. E. Newell, and E. F. Danielsen, Radiative heating rates near the stratospheric fountain, *J. Geophys. Res.*, *89*, 1380-1384, 1984.
- Donner, L. J., and H.-L. Kuo, Radiative forcing of stationary planetary waves, *J. Atmos. Sci.*, *41*, 2849-2868, 1984.
- Donner, L. J., and V. Ramanathan, Methane and nitrous oxide: Their effects on the terrestrial climate, *J. Atmos. Sci.*, *37*, 119-124, 1980.
- Dopplick, T. G., Radiative heating of the global atmosphere: Corrigendum, *J. Atmos. Sci.*, *36*, 1812-1817, 1979.

## REFERENCES

- Douglass, A. R., R. B. Rood, and R. S. Stolarski, Interpretation of ozone temperature correlations, 2. Analysis of SBUV ozone data, *J. Geophys. Res.*, 90, 10693-10708, 1985.
- Drayson, S. R., Calculation of long-wave radiative transfer in planetary atmospheres, Ph.D. thesis, *Rep. 07584-1-T*, 110 pp., College of Engineering, University of Michigan, Ann Arbor, MI, 1967.
- Drayson, S. R., P. L. Bailey, H. Fischer, J. C. Gille, A. Girard, L. L. Gordley, J. E. Harries, W. G. Planet, E. E. Remsberg, and J. M. Russell, III, Spectroscopy and transmittances for the LIMS experiment, *J. Geophys. Res.*, 89, 5141-5146, 1984.
- Drummond, J. R., and R. F. Jarnot, Infrared measurements of stratospheric composition II. Simultaneous NO and NO<sub>2</sub> measurements, *Proc. Roy. Soc. London A*, 364, 237-254, 1978.
- Drummond, J. R., J. T. Houghton, G. D. Peskett, C. D. Rodgers, M. J. Wale, J. Whitney, and E. J. Williamson, The stratospheric and mesospheric sounder on Nimbus 7, *Phil. Trans. Roy. Soc. London*, A296, 219-241, 1980.
- Drummond, J. W., J. M. Rosen, and D. J. Hofmann, Balloon borne chemiluminescent measurement of NO to 45 km, *Nature*, 265, 319-320, 1977.
- Drummond, J. W., A. Volz, and D. H. Ehhalt, An optimized chemiluminescence detector for tropospheric NO measurements, *J. Atmos. Chem.*, 2, 287-306, 1985.
- Duce, R. A., V. A. Mohnen, P. R. Zimmerman, D. Grosjean, W. Cautreels, R. Chatfield, R. Jaenicke, J. A. Ogren, E. D. Pellizzari, and G. T. Wallace, Organic material in the global troposphere, *Revs. Geophys. Space Phys.*, 21, 921-952, 1983.
- Duetsch, H. U., Two years of regular ozone soundings over Boulder, Colorado, *NCAR Tech. Note No. 10*, 449 pp., NCAR, Boulder, CO, 1966.
- Duetsch, H. U., Vertical ozone distribution on a global scale, *Pure Appl. Geophys.*, 116, 511-529, 1978.
- Duetsch, H. U., Total ozone trend in the light of ozone soundings, The impact of El Chichon, in *Atmospheric Ozone*, edited by C. S. Zerefos and A. Ghazi, pp. 263-268, D. Riedel, Dordrecht, 1985.
- Duetsch, H. U., C. Ling, and W. Zuellig, Regular ozone observation at Thalwill, Switzerland and at Boulder, Colorado, *Rept. LAPETH-1*, 279 pp., Eidgenoessische Technische Hochschule, Zurich, 1970.
- Dunkerton, T. J., On the mean meridional mass motions of the stratosphere and mesosphere, *J. Atmos. Sci.*, 35, 2325-2333, 1978.
- Dunkerton, T. J., On the role of Kelvin waves in the westerly phase of the semi-annual zonal wind oscillation, *J. Atmos. Sci.*, 36, 32-41, 1979.
- Dunkerton, T. J., Stochastic parameterization of gravity wave stresses, *J. Atmos. Sci.*, 39, 1711-1725, 1982a.
- Dunkerton, T. J., Theory of the mesopause semi-annual oscillation, *J. Atmos. Sci.*, 39, 2681-2690, 1982b.
- Dunkerton, T. J., Laterally-propagating planetary waves in the easterly phase of the quasi-biennial oscillation, *Atmosphere-Ocean*, 21, 55-68, 1983a.
- Dunkerton, T. J., Modification of stratospheric circulation by trace constituent changes?, *J. Geophys. Res.*, 88, 10831-10836, 1983b.
- Dunkerton, T. J., and N. Butchart, Propagation and selective transmission of internal gravity waves in a sudden warming, *J. Atmos. Sci.*, 41, 1443-1460, 1984.
- Dunkerton, T. J., and D. P. Delisi, Climatology of the equatorial lower stratosphere, *J. Atmos. Sci.*, 42, 376-396, 1984.
- Dunkerton, T. J., C. P. F. Hsu, and M. E. McIntyre, Some Eulerian and Lagrangian diagnostics for a model stratospheric warming, *J. Atmos. Sci.*, 38, 819-843, 1981.
- Dutton, J. A., *The Ceaseless Wind*, 579 pp., McGraw-Hill, New York, 1976.
- Duxbury, J. M., D. R. Bouldin, R. E. Terry, and R. L. Tate, Emissions of nitrous oxide from soils, *Nature*, 298, 462-464, 1982.
- Dvoryashina, Y. V., V. I. Dianov-Klokov, and L. N. Yurganov, On the variations of atmospheric total column carbon monoxide abundance for 1970-1982, *Phys. Atmos. Oceans*, 20, 40-47, 1984.
- Eady, E. T., Long waves and cyclone waves, *Tellus*, 1, 35-42, 1949.

## REFERENCES

- Eastman, J. A., and D. H. Stedman, A fast response sensor for eddy-correlation flux measurement, *Atmos. Environ.*, *11*, 1209-1211, 1977.
- Eaton, F., and G. Wendler, Some environmental effects of forest fires in interior Alaska, *Atmos. Environ.*, *17*, 1331-1337, 1983.
- Edmon, Jr., H. J., B. J. Hoskins, and M. E. McIntyre, Eliassen-Palm cross sections for the troposphere, *J. Atmos. Sci.*, *37*, 2600-2616, 1980.
- Edmonds, J. A., J. Reilly, J. R. Trabalka, and D. E. Reichle, An analysis of possible future atmospheric retention of fossil fuel CO<sub>2</sub>, *DOE/OR-21400/1*, 169 pp., Institute for Energy Analysis, Washington, DC, 1984.
- Edwards, D. K., and S. J. Morizumi, Scaling of vibration-rotation band parameters for nonhomogeneous gas radiation, *J. Quant. Spectrosc. Radiat. Transfer*, *10*, 175-188, 1970.
- Ehhalt, D. H., The atmospheric cycle of methane, *Tellus*, *26*, 58-70, 1974.
- Ehhalt, D. H., and J. W. Drummond, The tropospheric cycle of NO<sub>x</sub>, in *Chemistry of the Unpolluted and Polluted Troposphere*, edited by H. W. Georgii and W. Jaeschke, D. Reidel, Hingham, MA, 1982.
- Ehhalt, D. H., and J. Rudolph, On the importance of light hydrocarbons in multiple atmospheric systems, in *Berichte der Kernforschungsanlage*, Julich GmbH, Juli, 1984.
- Ehhalt, D. H., and U. Schmidt, Sources and sinks of atmospheric methane, *Pure Appl. Geophys.*, *116*, 452-464, 1978.
- Ehhalt, D. H., and A. Toennissen, Hydrogen and carbon compounds in the stratosphere, in *Proceedings of the NATO Advanced Study Institute on Atmospheric Ozone: Its Variation and Human Influences*, Rep. No. FAA-EE-80-20, edited by A. C. Aikin, pp. 129-151, DOT, FAA, Washington, DC, 1980.
- Ehhalt, D. H., L. E. Heidt, R. H. Lueb, and E. A. Martell, Concentrations of CH<sub>4</sub>, CO, CO<sub>2</sub>, H<sub>2</sub>, H<sub>2</sub>O, and N<sub>2</sub>O in the upper stratosphere, *J. Atmos. Sci.*, *32*, 163-169, 1975.
- Ehhalt, D. H., E. P. Roeth, and U. Schmidt, On the temporal variance of stratospheric trace gas concentrations, *J. Atmos. Chem.*, *1*, 27-51, 1983a.
- Ehhalt, D. H., R. J. Zander, and R. A. Lamontagne, On the temporal increase of tropospheric CH<sub>4</sub>, *J. Geophys. Res.*, *88*, 8442-8446, 1983b.
- Ehhalt, D. H., J. Rudolph, F. Meixner, and U. Schmidt, Measurements of selected C<sub>2</sub>-C<sub>5</sub> hydrocarbons in the background troposphere: Vertical and latitudinal variations, *J. Atmos. Chem.*, *3*, 29-52, 1985.
- Elansky, N. F., A. Ya. Arabov, A. S. Elskhov, and I. A. Senik, Spatial and temporal variability of the NO<sub>2</sub> total content based on annual observation data in *Atmospheric Ozone*, edited by C. S. Zerefos and A. Ghazi, pp., 157-162, D. Reidel, Dordrecht, 1984.
- Eliassen, E., and B. Machenhauer, A study of the fluctuations of atmospheric planetary flow patterns represented by spherical harmonics, *Tellus*, *17*, 220-238, 1965.
- Eliassen, E., and B. Machenhauer, On the observed large-scale atmospheric wave motions, *Tellus*, *21*, 149-165, 1969.
- Eliassen, A., On the vertical circulation in frontal zones, *Geofys. Pub.*, *24* (4), 147-160, 1962.
- Eliassen, A., and E. Palm, On the transfer of energy in stationary mountain waves, *Geofys. Publ.*, *22*, No. 3, 1-23, 1961.
- Elkins, J. W., S. C. Wofsy, M. B. McElroy, C. E. Kolb, and W. A. Kaplan, Aquatic sources and sinks for nitrous oxide, *Nature*, *275*, 602-606, 1978.
- Ellingson, R. G., and G. N. Serafino, Observations and calculations of aerosol heating over the Arabian Sea during MONEX, *J. Atmos. Sci.*, *41*, 575-589, 1984.
- Elliott, W. P., L. Machta and C. D. Keeling, An estimate of the biotic contribution to the atmospheric CO<sub>2</sub> increase based on direct measurements at Mauna Loa Observatory, *J. Geophys. Res.*, *90*, 3741-3746, 1985.

## REFERENCES

- Ellis, P., G. Holah, J. T. Houghton, T. S. Jones, G. Peckham, G. D. Peskett, D. R. Pick, C. D. Rodgers, H. K. Roscoe, R. Sandwell, The selective chopper radiometer for Nimbus 5, *Proc. Roy. Soc. London A*, 334, 149-170, 1973.
- Ellsaesser, H. W., Sources and sinks of stratospheric water vapor, in *Proceedings of the NATO Advanced Study Institute on Atmospheric Ozone: Its Variation and Human Influences*, Rep. FAA-EE-80-20, edited by A. C. Aikin, pp. 283-300, DOT, FAA, Washington, DC, 1980.
- Ellsaesser, H. W., J. E. Harries, D. Kley and R. Penndorf, Stratospheric H<sub>2</sub>O, *Planet Space Sci.*, 28, 827-835, 1980.
- Enting, I. G., Preliminary studies with a two-dimensional model using transport fields derived from a GCM, *J. Atmos. Chem.*, in press, 1985.
- National air pollutant emission estimates, 1940-1983, EPA-450/4-84-028, Environmental Protection Agency, Research Triangle Park, NC, 1984.
- EPA: See National Air Pollutant Estimates.
- Ertel, H., Ein neuer hydrodynamischer wirbelsatz, *Meteor. Z.*, 59, 277-281, 1942.
- Evans, W. F. J., C. I. Lin, and C. L. Midwinter, The altitude distribution of nitric acid at Churchill, *Atmosphere*, 14, 172-179, 1976.
- Evans, W. F. J., J. B. Kerr, C. T. McElroy, R. S. O'Brien, and J. C. McConnell, Measurements of NO<sub>2</sub> and HNO<sub>3</sub> during a stratospheric warming at 54 degrees N. in February, 1979, *Geophys. Res. Lett.*, 9, 493-496, 1982a.
- Evans, W. F. J., C. T. McElroy, J. B. Kerr, and J. C. McConnell, Simulations of the October 23, 1980 stratoprobe flight, *Geophys. Res. Lett.*, 9, 223-226, 1982b.
- Fabian, P., Halogenated hydrocarbons in the atmosphere, in *The Handbook of Environmental Chemistry*, Vol. 4, Springer-Verlag, Heidelberg, in press, 1985.
- Fabian, P., and C. E. Junge, Global rate of ozone destruction at the earth's surface, *Arch. Met. Geophys. Bioklim.*, A19, 161-172, 1970.
- Fabian, P., J. A. Pyle, and R. J. Wells, The August 1972 solar proton event and the atmospheric ozone layer, *Nature*, 277, 458-460, 1979.
- Fabian, P., R. Borchers, S. A. Penkett, and N. J. D. Prosser, Halocarbons in the stratosphere, *Nature*, 294, 733-735, 1981a.
- Fabian, P., R. Borchers, G. Flentje, W. A. Matthews, W. Seiler, H. Giehl, K. Bunse, F. Muller, U. Schmidt, A. Volz, A. Khedim, and F. J. Johnen, The vertical distribution of stable trace gases at mid-latitudes, *J. Geophys. Res.*, 86, 5179-5184, 1981b.
- Fabian, P., J. A. Pyle, and R. J. Wells, Diurnal variation of minor constituents in the stratosphere modeled as a function of latitude and season., *J. Geophys. Res.*, 87, 4981-5000, 1982.
- Fabian, P., R. Borchers, B. C. Krueger, S. Lal, and S. A. Penkett, The vertical distribution of CHClF<sub>2</sub> (CFC-22) in the stratosphere, *Geophys. Res. Lett.*, 12, 1-3, 1985a.
- Fabian, P., G. Flentje, and W. A. Mathews, Stratospheric NO profiles from simultaneous measurements of two chemiluminescent balloon-borne sondes, *Planet. Space Sci.*, in press, 1985b.
- Fabian, P., R. Borchers, B. C. Krueger, and S. Lal, The vertical distribution of CFC-114 (CClF<sub>2</sub>-CClF<sub>2</sub>) in the atmosphere, *J. Geophys. Res.*, 90, 13091-13093, 1985c.
- Falls, A. H., and J. H. Seinfeld, Continued development of a kinetic mechanism for photochemical smog, *Environ. Sci. Technol.*, 12, 1398-1400, 1978.
- Farman, J. C., B. G. Gardiner, and J. D. Shanklin, Large losses of total ozone in Antarctica reveal seasonal ClO<sub>x</sub>/NO<sub>x</sub> interaction, *Nature*, 315, 207-210, 1985.
- Farmer, C. B., and O. F. Raper, The HF:HCl ratio in the 14-38 km region of the stratosphere, *Geophys. Res. Lett.*, 4, 527-529, 1977.

## REFERENCES

- Farmer, C. B., O. F. Raper, and R. H. Norton, Spectroscopic detection and vertical distribution of HCl in the troposphere and stratosphere, *Geophys. Res. Lett.*, **3**, 13-16, 1976.
- Farmer, C. B., O. F. Raper, B. D. Robbins, R. A. Toth, and C. Mueller, Simultaneous spectroscopic measurements of stratospheric species: O<sub>3</sub>, CH<sub>4</sub>, CO, CO<sub>2</sub>, N<sub>2</sub>O, HCl, and HF at northern and southern mid-latitudes, *J. Geophys. Res.*, **85**, 1621-1632, 1980.
- Farmer, C. B., B. Carli, A. Bonetti, M. Carlotti, B. M. Dinelli, H. Fast, N. Louisnard, C. Alamichel, W. Mankin, M. Coffey, I. G. Nolt, D. G. Murcray, A. Goldman, G. Stokes, D. Johnson, W. Traub, K. Chance, R. Zander, L. Delbounille, and G. Roland, Balloon Intercomparison Campaigns: Results of remote sensing measurements of HCl, to be published, 1986.
- Fast, H., W.F.J. Evans, G. L. Vail, and H. L. Buijs, A measurement of the stratospheric HCl profile at 82°N on November 8, 1978, *J. Geophys. Res.*, in press, 1985.
- FCM: See *The National plan for stratospheric ozone monitoring*.
- Feely, H. W., and J. Spar, Tungsten-185 from nuclear bomb tests as a tracer for stratospheric meteorology, *Nature*, **188**, 1062-1064, 1960.
- Fehsenfeld, F. C., E. E. Ferguson, G. E. Streit, and D. L. Albritton, Stratospheric ion chemistry and the 11-year variation in polar ozone, *Science*, **194**, 544-545, 1976.
- Fels, S. B., Simple strategies for inclusion of Voigt effects in infrared cooling rate calculations, *Appl. Opt.*, **18**, 2634-2637, 1979.
- Fels, S. B., A parameterization of scale dependent radiative damping rates in the middle atmosphere, *J. Atmos. Sci.*, **39**, 1141-1152, 1982.
- Fels, S. B., The radiative damping of short vertical scale waves in the mesosphere, *J. Atmos. Sci.*, **41**, 1755-1764, 1984.
- Fels, S. B., Radiative-dynamical interactions in the middle atmosphere, in *Issues in Atmospheric and Oceanic Modeling*, edited by B. Saltzman, Advances in Geophysics 28, Part A, in press, 1985.
- Fels, S. B., and L. D. Kaplan, A test of the role of longwave radiative transfer in a general circulation model, *J. Atmos. Sci.*, **33**, 779-789, 1975.
- Fels, S. B., and M. D. Schwartzkopf, An efficient, accurate algorithm for calculating CO<sub>2</sub> 15 μm band cooling rates, *J. Geophys. Res.*, **86**, 1205-1232, 1981.
- Fels, S. B., J. D. Mahlman, M. D. Schwarzkopf, and R. W. Sinclair, Stratospheric sensitivity to perturbations in ozone and carbon dioxide: Radiative and dynamical response, *J. Atmos. Sci.*, **37**, 2265-2297, 1980.
- Fiedler, B. H., An integral closure model for the vertical turbulent flux of a scalar in a mixed layer, *J. Atmos. Sci.*, **41**, 674-680, 1984.
- Finger, F. G., M. E. Gelman, F. J. Schmidlin, R. Leviton, and B. Kennedy, Compatibility of meteorological rocketsonde data as indicated by International Comparison Tests, *J. Atmos. Sci.*, **32**, 1705-1714, 1975.
- Firestone, M. K., and J. M. Tiedje, Temporal change in nitrous oxide and dinitrogen following the onset of an aerobiosis, *Appl. Environ. Microbiol.*, **38**, 673-679, 1979.
- Firestone, M. K., M. S. Smith, R. B. Firestone, and J. M. Tiedje, The influence of nitrate, nitrite and oxygen on the gaseous products of denitrification in soil, *Soil Sci. Soc. Am. J.*, **43**, 1140-1144, 1979.
- Fischer, H., F. Fergg, D. Rabus, and P. Burkert, Stratospheric H<sub>2</sub>O and HNO<sub>3</sub> profiles derived from solar occultation measurements, *J. Geophys. Res.*, **90**, 3831-3835, 1985a.
- Fischer, H., E. Redemann, F. Fergg, and D. Rabus, Measurements of stratospheric NO<sub>2</sub> profiles using a gas correlation radiometer in the solar occultation mode, *J. Atmos. Chem.*, in press, 1985b.
- Fishman, J., Ozone in the troposphere, in *Ozone in the Free Atmosphere*, edited by R. C. Whitten and S. S. Prasad, pp. 161-194, Van Nostrand Reinhold, New York, 1985.
- Fishman, J., and T. A. Carney, A one-dimensional photochemical model of the troposphere with planetary boundary-layer parameterization, *J. Atmos. Chem.*, 351-376, 1984.

## REFERENCES

- Fishman, J., and P. J. Crutzen, The origin of ozone in the troposphere, *Nature*, 274, 855-858, 1978.
- Fishman, J., and W. Seiler, Correlative nature of ozone and carbon monoxide in the troposphere: Implications for the tropospheric ozone budget, *J. Geophys. Res.*, 88, 3662-3670, 1983.
- Fishman, J., V. Ramanathan, P. J. Crutzen, and S. C. Liu, Tropospheric ozone and climate, *Nature*, 282, 818-820, 1979a.
- Fishman, J., S. Solomon, and P. J. Crutzen, Observational and theoretical evidence in support of a significant in-situ photochemical source of tropospheric ozone, *Tellus*, 31, 432-446, 1979b.
- Fishman, J., W. Seiler, and P. Haagenen, Simultaneous presence of O<sub>3</sub> and CO bands in the troposphere, *Tellus*, 32, 456-463, 1980.
- Fitzjarrald, D. R., and M. Garstang, Boundary-layer growth over the tropical ocean, *Mon. Weather Rev.*, 109, 1762-1772, 1981.
- Fitzjarrald, D. R., and D. H. Lenschow, Mean concentration and flux profiles for chemically reactive species in the atmospheric surface layer, *Atmos. Environ.*, 17, 2505-2512, 1983.
- Flaud, J.-M., C. Camy-Peyret, and L. S. Rothman, Improved ozone line parameters in the 10- and 4.8  $\mu\text{m}$  regions, *Appl. Opt.*, 19, 655, 1980.
- Flaud, J.-M., C. Camy-Peyret, D. Cariolle, J. Laurent, and G. M. Stokes, Daytime variations of atmospheric NO<sub>2</sub> from ground-based infrared measurements, *Geophys. Res. Lett.*, 10, 1104-1107, 1983.
- Fleig, A. J., K. F. Klenk, P. K. Bhartia, K. D. Lee, C. G. Wellemeyer, and V. G. Kaveeshwar, Vertical ozone profile results from Nimbus 4 data, in *Proc. 4th Conf. Atmos. Radiation*, pp. 20-26, AMS, Toronto, Canada, 1981.
- Fleig, A. J., K. F. Klenk, P. K. Bhartia, D. Gordon, and W. H. Schneider, Users guide for the Solar Backscattered Ultraviolet (SBUV) instrument first-year ozone-S data set, *NASA Ref. Publ. 1095*, 72 pp., NASA Goddard Space Flight Center, Greenbelt, MD, 1982.
- Fontanella, J., A. Girard, L. Gramont, and N. Louisnard, Vertical distribution of NO, NO<sub>2</sub>, and HNO<sub>3</sub> as derived from stratospheric absorption infrared spectra, *Appl. Opt.*, 14, 825-839, 1975.
- Foot, J. S., Aircraft measurements of the humidity in the lower stratosphere from 1977 to 1980 between 45°N and 60°N, *Quart. J. Roy. Meteorol. Soc.*, 110, 303-320, 1984.
- Forbes, J. M., Middle atmosphere tides, *J. Atmos. Terr. Phys.*, 46, 1049-1067, 1984.
- Fouquart, Y., B. Bonnel, G. Brogniez, A. Cerf, M. Chaoui, L. Smith, and J. C. Vanhooote, Size distribution and optical properties of Saharan aerosols during Eclats, in *Aerosols and their Climate Effects*, edited by H. E. Gerber and A. Deepak, pp. 35-62, A. Deepak Publ., Hampton, VA, 1984.
- Frank, W. M., The cumulus parameterization problem, *Mon. Weather Rev.*, 111, 1859-1871, 1983.
- Fraser, P. J., M. A. K. Khalil, R. A. Rasmussen, and A. J. Crawford, Trends of atmospheric methane in the Southern Hemisphere, *Geophys. Res. Lett.*, 8, 1063-1066, 1981.
- Fraser, P. J., G. I. Pearman, and P. Hyson, The global distribution of atmospheric CO<sub>2</sub>: II. A review of provisional background observations 1978-1980, *J. Geophys. Res.*, 88, 3591-3598, 1982.
- Fraser, P. J., P. Hyson, I. G. Enting, and G. I. Pearman, Global distribution and Southern Hemisphere trend of atmospheric CCl<sub>3</sub>F, *Nature*, 302, 692-695, 1983a.
- Fraser, P. J., M. A. K. Khalil, R. A. Rasmussen, and L. P. Steele, Tropospheric methane in the mid-latitudes of the Southern Hemisphere, *J. Atmos. Chem.*, 1, 125-135, 1983b.
- Fraser, P. J., P. Hyson, M. A. K. Khalil, and R. A. Rasmussen, Conference on Scientific Application of Baseline Observations on Atmospheric Composition, Aspendale, Australia, 7-9 November, 1984.
- Frederick, J. E., Solar corpuscular emission and neutral chemistry in the Earth's middle atmosphere, *J. Geophys. Res.*, 81, 3179-1976, 1976.
- Frederick, J. E., Radiative-photochemical response of the mesosphere to dynamical forcing, *J. Geophys. Res.*, 86, 5224-5230, 1981.
- Frederick, J. E., and R. J. Cicerone, Dissociation of metastable O<sub>2</sub> as a potential source of atmospheric odd oxygen, *J. Geophys. Res.*, 90, 10733-10738, 1985.

## REFERENCES

- Frederick, J. E., and A. R. Douglass, Atmospheric temperatures near the tropical tropopause: Temporal variations, zonal asymmetry and implications for stratospheric water vapor, *Mon. Weather Rev.*, **111**, 397-1403, 1983.
- Frederick, J. E., and R. D. Hudson, Predissociation linewidths and oscillator strengths for the 2-0 to 13-0 Schumann-Runge bands of O<sub>2</sub>, *J. Molec. Spectrosc.*, **74**, 247-258, 1979a.
- Frederick, J. E., and R. D. Hudson, Predissociation of nitric oxide in the mesosphere and stratosphere, *J. Atmos. Sci.*, **36**, 737-745, 1979b.
- Frederick, J. E., and R. D. Hudson, Dissociation of molecular oxygen in the Schumann-Runge bands, *J. Atmos. Sci.*, **37**, 1099-1106, 1980a.
- Frederick, J. E., and R. D. Hudson, Atmospheric opacity in the Schumann-Runge bands and the aeronomic dissociation of water vapor, *J. Atmos. Sci.*, **37**, 1088-1098, 1980b.
- Frederick, J. E., and J. E. Mentall, Solar irradiance in the stratosphere: Implications for the Herzberg continuum absorption of O<sub>2</sub>, *Geophys. Res. Lett.*, **9**, 461-464, 1982.
- Frederick, J. E., and N. Orsini, The distribution and variability of mesospheric odd nitrogen: A theoretical investigation, *J. Atmos. Terr. Phys.*, **44**, 479-1982, 1982.
- Frederick, J. E., and G. N. Serafino, Satellite observations of the nitric oxide dayglow: Implications for the behavior of mesospheric and lower thermospheric odd nitrogen, *J. Geophys. Res.*, **90**, 3821-3830, 1985.
- Frederick, J. E., R. D. Hudson, and J. E. Mentall, Stratospheric observations of the attenuated solar irradiance in the Schumann-Runge band absorption region of molecular oxygen, *J. Geophys. Res.*, **86**, 9885-9890, 1981.
- Frederick, J. E., A. J. Blake, D. E. Freeman, R. W. Nicholls, T. Ogawa, and P. C. Simon, MSG-7: Molecular absorption processes related to the penetration of ultraviolet solar radiation into the middle atmosphere, in *Handbook for MAP, Vol. 8*, edited by C. F. Sechrist, Jr., pp. 53-74, SCOSTEP Secretariat, Univ. of Illinois, Urbana, 1983a.
- Frederick, J. E., F. T. Huang, A. R. Douglass, and C. A. Reber, The distribution and annual cycle of ozone in the upper stratosphere, *J. Geophys. Res.*, **88**, 3819-3828, 1983b.
- Frederick, J. E., G. N. Serafino, and A. R. Douglass, An analysis of the annual cycle in upper stratospheric ozone, *J. Geophys. Res.*, **89**, 9547-9555, 1984.
- Fredriksson, K., B. Galle, K. Nystrom, and S. Svanberg, Lidar system applied in atmospheric pollution monitoring, *Appl. Optics*, **18**, 2998-2998, 1979.
- Freeman, D. E., K. Yoshino, J. R. Esmond, and W. H. Parkinson, High resolution absorption cross section measurements of ozone at 195 K in the wavelength region 240-350 nm, *Planet. Space Sci.*, **32**, 239-248, 1984.
- Freney, J. R., O. T. Denmead, and J. R. Simpson, Nitrous oxide emissions from soils at low moisture contents, *Soil Biol. Biochem.*, **11**, 167-173, 1979.
- Frerking, M. A., and D. J. Muehlner, Infrared heterodyne spectroscopy of atmospheric ozone, *Appl. Opt.*, **16**, 526-528, 1977.
- Friedl, R. R., W. H. Brune, and J. G. Anderson, Kinetics of SH with NO<sub>2</sub>, O<sub>3</sub>, O<sub>2</sub>, and H<sub>2</sub>O<sub>2</sub>, *J. Phys. Chem.*, **89**, 5505-5510, 1985.
- Friedli, H., E. Moore, H. Oeschger, U. Siegenghler, and B. Stauffer, <sup>13</sup>C/<sup>12</sup>C ratios in CO<sub>2</sub> extracted from antarctic ice, *Geophys. Res. Lett.*, **11**, 1145-1148, 1984.
- Fritts, D. C., Gravity wave saturation in the middle atmosphere: A review of theory and observations, *Rev. Geophys. and Space Phys.*, **22**, 275-308, 1984.
- Fritts, D. C., and T. J. Dunkerton, Fluxes of heat and constituents due to convectively unstable gravity waves, *J. Atmos. Sci.*, **42**, 549-556, 1985.
- Fritz, B., and R. Zellner, Reaction rate and equilibrium constant for ClO + O<sub>2</sub> → OClOO, presented at CMA Chemistry Workshop, Goettingen, 1984.

## REFERENCES

- Froidevaux, L., Photochemical modeling of the earth's stratosphere, Ph.D. thesis, 275 pp., California Institute of Technology, Pasadena, CA, 1983.
- Froidevaux, L., and Y. L. Yung, Radiation and chemistry in the stratosphere: Sensitivity to O<sub>2</sub> absorption cross-sections in the Herzberg continuum, *Geophys. Res. Lett.*, **9**, 854-857, 1982.
- Froidevaux, L., M. Allen, and Y. L. Yung, A critical analysis of ClO and O<sub>3</sub> in the mid-latitude stratosphere, *J. Geophys. Res.*, **90**, 12999-13030, 1985a.
- Froidevaux, L., M. Allen, S. Berman, and A. Daughton, Analysis of LIMS observations in the upper stratosphere and lower mesosphere, I. The mean O<sub>3</sub> profile and its temperature sensitivity at mid-latitudes in May, 1979, in press, 1985b.
- Funk, J. P., and G. J. Garnham, Australian ozone observations and a suggested 24-month cycle, *Tellus*, **14**, 378-382, 1962.
- Gage, K. S., and B. B. Balsley, MST radar studies of wind and turbulence in the middle atmosphere, *J. Atmos. Terr. Phys.*, **46**, 739-753, 1984.
- Galbally, I. E., Emission of fixed nitrogen compounds to the atmosphere in remote areas, in *Biogeochemical Cycling of Sulfur and Nitrogen in Remote Areas*, edited by J. N. Galloway, D. Reidel, Dordrecht, in press, 1985.
- Galbally, I. E., and C. R. Roy, Loss of fixed nitrogen from soils by nitric oxide exhalation, *Nature*, **275**, 734-735, 1978.
- Galbally, I. E., and C. R. Roy, Destruction of ozone at the earth's surface, *Quart. J. Roy. Meteorol. Soc.*, **106**, 599-620, 1980.
- Galbally, I. E., and C. R. Roy, Ozone and nitrogen oxides in the Southern Hemisphere troposphere, in *Proceedings of the Quadrennial International Ozone Symposium, Vol. I*, edited by J. London, pp. 431-438, IAMAP, NCAR, Boulder, CO, 1981.
- Galbally, I. E., C. R. Roy, R. S. O'Brien, B. A. Ridley, D. R. Hastie, W. F. J. Evans, C. T. McElroy, J. B. Kerr, P. Hyson, W. Knight, and J. E. Laby, Measurements of the trace composition of the Austral stratosphere: Chemical and meteorological data, *Technical Paper No. 1*, CSIRO, Div. of Atmos. Res., Australia, 1983.
- Galindo, I., Anthropogenic aerosols and their regional scale climatic effects, in *Aerosols and their Climatic Effects*, edited by H. E. Gerber and A. Deepak, pp. 245-260, A. Deepak Publ., Hampton, VA, 1984.
- Gallagher, C. C., C. A. Forsberg, A. S. Mason, B. W. Gandrud, and M. Janghorbani, Total chlorine content in the lower stratosphere, *J. Geophys. Res.*, **90**, 10747-10752, 1985.
- Gamache, R. R., and R. W. Davies, Theoretical N<sub>2</sub><sup>-</sup>, O<sub>2</sub><sup>-</sup>, and air broadened halfwidths of O<sub>3</sub> calculated by quantum Fourier transform theory with realistic collision dynamics, *J. Molec. Spec.*, **109**, 283-299, 1985.
- Gamlen, P. H., B. C. Lane, P. M. Midgley, and J. J. Steed, The production and release to atmosphere of CHCl<sub>3</sub> and CCl<sub>2</sub>F<sub>2</sub>, *Atmos. Environ.*, in press, 1985.
- Gammon, R. H., and W. D. Komhyr, Response of the global atmospheric CO<sub>2</sub> distribution to the atmospheric/oceanic circulation perturbation in 1982, in *IUGG Symposium 19 (Oceans and CO<sub>2</sub> Climate Response)*, Vol. 2, 828 pp., Hamburg, FRG, 1983.
- Gammon, R. H., W. D. Komhyr, L. Waterman, T. Conway, K. Thoning, and D. Gillette, The 1982/83 ENSO event: Response of the global atmospheric CO<sub>2</sub> distribution, paper presented at Conference on Scientific Application of Baseline Observations of Atmospheric Composition, CSIRO, Aspendale, Australia, 7-9 November, 1984.
- Gammon, R. H., E. T. Sandquist, and P. J. Fraser, History of carbon dioxide in the atmosphere, *U.S. Department of Energy State-of-the-Art Report on the Global Carbon Cycle (DOE)*, Chapter 3, in press, 1985a.

## REFERENCES

- Gammon, R. H., W. D. Komhyr, and J. T. Peterson, The global atmospheric CO<sub>2</sub> distribution 1968-83: Interpretation of the results of the NOAA/GMCC measurement program, in *The Global Carbon Cycle: Analysis of the Natural Cycle and Implications of Anthropogenic and Alterations for the Next Century*, edited by J. R. Trabalka and D. E. Reichle, Springer-Verlag, New York, in press, 1985b.
- Garcia, R. R., and J. Geisler, Stochastic forcing of small amplitude oscillations in the stratosphere, *J. Atmos. Sci.*, **38**, 2187-2197, 1981.
- Garcia, R. R., and S. Solomon, A numerical model of the zonally averaged dynamical and chemical structure of the middle atmosphere, *J. Geophys. Res.*, **88**, 1379-1400, 1983.
- Garcia, R. R., and S. Solomon, The effect of breaking gravity waves on the dynamics and chemical composition of the mesosphere and lower thermosphere, *J. Geophys. Res.*, **90**, 3850-3868, 1985.
- Garcia, R. R., S. Solomon, R. G. Roble, and D. W. Rusch, A numerical response of the middle atmosphere to the 11-year solar cycle., *Planet. Space Sci.*, **32**, 411-423, 1984.
- Garland, J. A., and S. A. Penkett, Absorption of peroxyacetyl nitrate and ozone by natural surfaces, *Atmos. Environ.*, **10**, 1127-1131, 1976.
- Garland, J. A., A. W. Elzerman, and F. A. Penkett, The mechanism for dry deposition of ozone to sea water surfaces, *J. Geophys. Res.*, **85**, 7488-7492, 1980.
- Gates, W. L., Modeling the ice-age climate, *Science*, **191**, 1138-1144, 1976.
- Gates, W. L., K. H. Cook, and M. E. Schlesinger, Preliminary analysis of experiments on the climatic effects of increased CO<sub>2</sub> with an atmospheric general circulation model and a climatological ocean, *J. Geophys. Res.*, **86**, 6385-6393, 1981.
- Geisler, J. E., and R. E. Dickinson, The five-day wave on the sphere with realistic zonal winds, *J. Atmos. Sci.*, **33**, 632-641, 1976.
- Geller, M. A., Dynamics of the middle atmosphere, *Space Sci. Rev.*, **34**, 359-375, 1983.
- Geller, M. A., Modelling the middle atmosphere circulation, in *Dynamics of the Middle Atmosphere*, edited by J. R. Holton and T. Matsuno, pp. 467-500, Terrapub, Tokyo, 1984.
- Geller, M. A., and J. C. Alpert, Planetary wave coupling between the troposphere and the middle atmosphere as a possible sun-weather mechanism, *J. Atmos. Sci.*, **37**, 1197-1215, 1980.
- Geller, M. A., M. F. Wu, and M. E. Gelman, Troposphere-stratosphere (Surface-55 km) monthly winter general circulation statistics for the Northern Hemisphere-four year averages, *J. Atmos. Sci.*, **40**, 1334-1352, 1983.
- Geller, M. A., M. F. Wu, and M. E. Gelman, Troposphere-stratosphere (Surface-55 km) monthly winter general circulation statistics for the Northern Hemisphere-interannual variations, *J. Atmos. Sci.*, **41**, 1726-1744, 1984.
- Gelman, M. E., A. J. Miller, R. M. Nagatani, and H. D. Bowman II, Mean zonal wind and temperature structure during the PMP-1 winter periods, *Adv. Space Res.*, **10**, 159-162, 1983.
- Geophysical Monitoring for Climatic Change: See Harris, J. M.
- Georgii, H.-W., and F. X. Meixner, Measurement of the tropospheric and stratospheric SO<sub>2</sub> distribution, *J. Geophys. Res.*, **85**, 7433-7438, 1980.
- Ghazi, A., *Atlas der Globalverteilung des Gesamt Ozonbetrages nach Satellitenmessungen (April 1970-Mai 1972)*, Mitteilungen aus dem Institut fuer Geophysik and Meteorologie der Universitat zu Koln, 1980.
- Ghazi, A., and J. J. Barnett, Ozone behavior and stratospheric thermal structure during Southern Hemispheric spring, *Contr. to Atmos. Phys.*, **53**, 1-13, 1980.
- Ghazi, A., A. Ebel, and D. F. Heath, A study of satellite observations of ozone and stratospheric temperatures during 1970-1971, *J. Geophys. Res.*, **81**, 5365-5373, 1976.
- Ghazi, A., V. Ramanathan, and R. E. Dickinson, Acceleration of upper stratospheric radiative damping: Observational evidence, *Geophys. Res. Lett.*, **6**, 437-440, 1979.
- Ghazi, A., R. H. Wang, and M. P. McCormick, A study on radiative damping of planetary waves utilizing stratospheric observations, *J. Atmos. Sci.*, **42**, 2032-2042, 1985.

## REFERENCES

- Gibbins, C. J., P. R. Schwartz, D. L. Thacker, and R. M. Bevilacqua, The variability of mesospheric water vapor, *Geophys. Res. Lett.*, **9**, 131-134, 1982.
- Gidel, L. T., Cumulus cloud transport of transient tracers, *J. Geophys. Res.*, **88**, 6587-6599, 1983.
- Gidel, L. T., and M. A. Shapiro, The role of clear air turbulence in the production of potential vorticity in the vicinity of upper tropospheric jetstream-frontal systems., *J. Atmos. Sci.*, **36**, 2125-2138, 1979.
- Gidel, L. T., and M. A. Shapiro, General circulation model estimates of the net vertical flux of ozone in the lower stratosphere and the implications for the tropospheric ozone budget, *J. Geophys. Res.*, **85**, 4049-4058, 1980.
- Gidel, L. T., P. J. Crutzen, and J. Fishman, A two-dimensional photochemical model of the atmosphere. 1: Chlorocarbon emissions and their effect on stratospheric ozone, *J. Geophys. Res.*, **88**, 6622-6640, 1983.
- Gill, A. E., *Atmosphere-Ocean Dynamics*, 662 pp., Academic Press, New York, 1982.
- Gill, P. S., T. E. Graedel, and C. J. Weschler, Organic films on atmospheric aerosol particles, fog droplets, cloud droplets, raindrops and snowflakes, *Rev. Geophys. Space Phys.*, **21**, 903-920, 1983.
- Gille, J. C., and F. B. House, On the inversion of Limb radiance measurements, I, Temperature and thickness., *J. Atmos. Sci.*, **28**, 1427-1442, 1971.
- Gille, J. C., and L. V. Lyjak, An overview of wave-mean flow interactions during the winter of 1978-1979 derived from LIMS observations, in *Dynamics of the Middle Atmosphere*, edited by J. R. Holton and T. Matsuno, pp. 289-306, Terrapub, Tokyo, 1984.
- Gille, J. C., and J. M. Russell III, The Limb Infrared Monitor of the Stratosphere: Experiment description, performance, and results, *J. Geophys. Res.*, **89**, 5125-5140, 1984.
- Gille, J. C., P. L. Bailey, R. A. Craig, F. B. House, and G. P. Anderson, Sounding the stratosphere and mesosphere by infrared Limb scanning from space, *Science*, **208**, 397-399, 1980a.
- Gille, J. C., P. L. Bailey, and J. M. Russell III., Temperature and composition measurements from the LRIR and LIMS experiments on Nimbus 6 and 7, *Phil. Trans. Roy. Soc. London*, **A296**, 205-218, 1980b.
- Gille, J. C., P. L. Bailey, L. V. Lyjak, and J. M. Russell III, Results from the LIMS experiment for the PMP-1 winter 1978/79, *Adv. in Space Res.*, **2**, 163-167, 1983.
- Gille, J. C., J. M. Russell III, P. L. Bailey, L. L. Gordley, E. E. Remsberg, J. H. Lienesch, W. G. Planet, F. B. House, L. V. Lyjak, and S. A. Beck, Validation of the temperature retrievals obtained by the Limb Infrared Monitor of the Stratosphere (LIMS) experiment on NIMBUS 7, *J. Geophys. Res.*, **89**, 5147-5160, 1984a.
- Gille, J. C., J. M. Russell III, P. L. Bailey, E. E. Remsberg, L. L. Gordley, W. F. J. Evans, H. Fischer, B. W. Gandrud, A. Girard, J. E. Harries, and S. A. Beck, Accuracy and precision of the nitric acid concentrations determined by the Limb Infrared Monitor of the Stratosphere experiment on NIMBUS 7, *J. Geophys. Res.*, **89**, 5179-5190, 1984b.
- Gille, J. C., C. M. Smythe, and D. F. Heath, Observed ozone response to variations in solar ultraviolet radiation, *Science*, **225**, 315-317, 1984c.
- Giorgi, F., and W. L. Chameides, The rainout parameterization in a photochemical model, *J. Geophys. Res.*, **90**, 7872-7880, 1985.
- Girard, A., and N. Louisnard, Stratospheric water vapor, nitrogen dioxide, nitric acid and ozone measurements deduced from spectroscopic observations, *J. Geophys. Res.*, **89**, 5109-5114, 1984.
- Girard, A., J. Besson, R. Giraudet, and L. Gramont, Correlated seasonal and climatic variations of trace constituents in the stratosphere, *Pure Appl. Geophys.*, **117**, 381-393, 1978/79.
- Girard, A., L. Gramont, N. Louisnard, S. Le Boiteux, and G. Fergant, Latitudinal variation of HNO<sub>3</sub>, HCl, and HF vertical column density above 11.5 km, *Geophys. Res. Lett.*, **9**, 135-138, 1982.
- Girard, A., G. Ferganti, L. Gramont, O. Lado-Bordowsky, J. Laurent, S. LeBoiteux, M. P. Lemaitre, and N. Louisnard, Latitudinal distribution of ten stratospheric species deduced from simultaneous spectroscopic measurements, *J. Geophys. Res.*, **88**, 5377-5392, 1983.

## REFERENCES

- GMCC: See Harris, J. M.
- Godson, W. L., Total ozone in the middle stratosphere over Arctic and sub-Arctic areas in winter and spring, *Quart. J. Roy. Meteorol. Soc.*, **86**, 301-317, 1960.
- Goldan, P. D., W. C. Kuster, D. L. Albritton, and A. L. Schmeltekopf, Stratospheric  $\text{CFCl}_3$ ,  $\text{CF}_2\text{Cl}_2$ , and  $\text{N}_2\text{O}$  height profile measurements at several latitudes, *J. Geophys. Res.*, **85**, 413-423, 1980.
- Goldman, A., D. G. Murcray, F. H. Murcray, W. J. Williams, and F. S. Bonomo, Identification of the  $\nu_3$   $\text{NO}_2$  band in the solar spectrum observed from a balloon-borne spectrometer, *Nature*, **225**, 443-444, 1970.
- Goldman, A., R. N. Stocker, D. Rolens, W. J. Williams, and D. G. Murcray, Stratospheric  $\text{HNO}_3$  distributions from balloon-borne infrared atmospheric emission measurements from 1970-75, *Scientific Report*, University of Denver, Denver, CO, 1976.
- Goldman, A., F. G. Fernald, W. J. Williams, and D. G. Murcray, Vertical distribution of  $\text{NO}_2$  in the stratosphere as determined from balloon measurements of solar spectra in the 4500 Å region, *Geophys. Res. Lett.*, **5**, 257-260, 1978.
- Goldman, A., D. G. Murcray, F. J. Murcray, G. R. Cook, J. W. Van Allen, F. S. Bonomo, and R. D. Blatherwick, Identification of the  $\nu_3$  vibration rotation band of  $\text{CF}_4$  in balloon-borne infrared solar spectra, *Geophys. Res. Lett.*, **6**, 609-612, 1979.
- Goldman, A., D. G. Murcray, F. J. Murcray, and E. Niple, High resolution IR balloon-borne solar spectra and laboratory spectra in the  $\text{HNO}_3$  1720  $\text{cm}^{-1}$  region: An analysis, *Appl. Opt.*, **19**, 3721-3724, 1980.
- Goldman, A., F. J. Murcray, R. D. Blatherwick, J. R. Gillis, F. S. Bonomo, F. H. Murcray, D. G. Murcray, and R. J. Cicerone, Identification of acetylene ( $\text{C}_2\text{H}_2$ ) in infrared atmospheric absorption spectra, *J. Geophys. Res.*, **86**, 12143-12146, 1981a.
- Goldman, A., J. Reid, and L. S. Rothman, Identification of electric quadrupole  $\text{O}_2$  and  $\text{N}_2$  lines in the infrared atmospheric absorption spectrum due to the vibration-rotation fundamentals, *Geophys. Res. Lett.*, **8**, 77-78, 1981b.
- Goldman, A., F. J. Murcray, J. R. Gillis, and D. G. Murcray, Identification of new solar OH lines in the 10-12 micron region, *Astrophys. J.*, **248**, L133-L135, 1981c.
- Goldman, A., F. J. Murcray, R. D. Blatherwick, F. S. Bonomo, F. H. Murcray, and D. G. Murcray, Spectroscopic identification of  $\text{CHClF}_2$  (F-22) in the lower stratosphere, *Geophys. Res. Lett.*, **8**, 1012-1014, 1981d.
- Goldman, A., R. D. Blatherwick, F. J. Murcray, J. W. Van Allen, F. H. Murcray, and D. G. Murcray, *New Atlas of Stratospheric Infrared Absorption Spectra*, Univ. of Denver, Denver, CO, 1982.
- Goldman, A., F. G. Fernald, F. J. Murcray, F. H. Murcray, and D. G. Murcray, Spectral least squares quantification of several atmospheric gases from high resolution infrared solar spectra obtained at the South Pole, *J. Quant. Spectrosc. Radiat. Transfer*, **29**, 189-204, 1983a.
- Goldman, A., D. G. Murcray, D. L. Lambert, and J. F. Dominy, The pure rotation spectrum of the hydroxyl radical and the solar oxygen abundance, *Mon. Not. R. Astr.*, **203**, 767-776, 1983b.
- Goldman, A., F. H. Murcray, D. G. Murcray, and C. P. Rinsland, A search for formic acid in the upper troposphere: A tentative identification of the 1105  $\text{cm}^{-1}$   $\nu_6$  band Q branch in high-resolution balloon-borne solar absorption spectra, *Geophys. Res. Lett.*, **11**, 307-310, 1984a.
- Goldman, A., C. P. Rinsland, F. J. Murcray, D. G. Murcray, M. T. Coffey, and W. G. Mankin, Balloon-borne and aircraft infrared measurements of ethane ( $\text{C}_2\text{H}_6$ ) in the upper troposphere and lower stratosphere, *J. Atmos. Chem.*, **2**, 211-221, 1984b.
- Goldman, A., J. R. Gillis, C. P. Rinsland, F. J. Murcray, and D. G. Murcray, Stratospheric  $\text{HNO}_3$  quantification from line-by-line nonlinear least-squares analysis of high-resolution balloon-borne solar absorption spectra in the 870  $\text{cm}^{-1}$  region, *Appl. Opt.*, **23**, 3252-3255, 1984c.

## REFERENCES

- Golombek, A., A global three-dimensional model of the circulation and chemistry of long-lived atmospheric species, Ph.D. thesis, 201 pp., Dept. of Meteor. and Phys. Oceanography, MIT, Cambridge, MA, 1982.
- Goody, R. M., A statistical model for water vapor absorption, *J. Meteorol.*, **78**, 165-169, 1952.
- Goody, R. M., *Atmospheric Radiation*, 436 pp., Oxford University Press, London, 1964.
- Goreau, T. J., The biogeochemistry of nitrous oxide, Ph.D. thesis, Harvard Univ., Boston, MA, 1981.
- Goreau, T. J., and W. Z. DeMello, Effects of deforestation on sources and sinks of atmospheric carbon dioxide, nitrous oxide and methane from some Amazonian biota and soils, in press, 1985.
- Goreau, T. J., W. A. Kaplan, S. C. Wofsy, M. B. McElroy, F. W. Valois, and S. W. Watson, Production of NO<sub>2</sub> and N<sub>2</sub>O by nitrifying bacteria at reduced concentrations of oxygen, *Appl. Environ. Microbiology*, **40**, 526-532, 1985.
- Gotz, F. W. P., A. R. Meetham, and G. M. B. Dobson, The vertical distribution of ozone in the atmosphere, *Proc. Roy. Soc. London*, **A145**, 416-446, 1934.
- Graedel, T. E., and J. R. McRae, On the possible increase of the atmospheric methane and carbon monoxide concentrations during the last decade, *Geophys. Res. Lett.*, **7**, 977-979, 1980.
- Grant, K. E., P. S. Connell, and D. J. Wuebbles, Monte Carlo uncertainty analysis of atmosphere ozone concentrations from large trace gas perturbations, in press, 1985.
- Gray, L. J., and J. A. Pyle, Semi-annual oscillation and equatorial tracer distributions, *Quart. J. Roy. Meteorol. Soc.*, in press, 1986.
- Gray, W. M., Global view of the origin of tropical disturbances and storms, *Mon. Weather Rev.*, **26**, 653-700, 1968.
- Gray, W. M., Cumulus convection and large-scale circulations, Part I: Broad-scale and mesoscale considerations, *Mon. Weather Rev.*, **101**, 839-855, 1973.
- Greenberg, J. P., and P. R. Zimmerman, Nonmethane HC in remote tropical, continental, and marine atmospheres, *J. Geophys. Res.*, **89**, 4767-4778, 1984.
- Greenberg, J. P., P. R. Zimmerman, L. Heidt, and W. Pollock, Hydrocarbons and carbon monoxide emissions from biomass burning in Brazil, *J. Geophys. Res.*, **89**, 1350-1354, 1984.
- Grevesse, N., A. J. Sauval, and E. F. Van Dishoeck, An analysis of vibration-rotation lines of OH in the solar infrared spectrum, *Astron. Astrophys.*, **141**, 10-16, 1984.
- Griffing, G. W., Ozone and nitrogen oxides production during thunderstorms, *J. Geophys. Res.*, **82**, 943-950, 1977.
- Griggs, M., Absorption coefficients of ozone in the ultraviolet and visible regions, *J. Chem. Phys.*, **49**, 857-859, 1968.
- Grose, W. L., Recent advances in understanding stratospheric dynamics and transport processes: Application of satellite data to their interpretation, *Adv. in Space Res.*, **4**, 19-28, 1984.
- Grose, W. L., and J. M. Russell III, The use of isentropic potential vorticity in conjunction with quasi-conserved species in the study of stratospheric dynamics and transport, in press, 1985.
- Grose, W. L., R. E. Turner, and J. E. Nealy, Transport processes in the stratosphere: Model simulations and comparisons with satellite observations, in *Proceedings of the International Middle Atmosphere Symposium*, Kyoto, Japan, in press, 1984.
- Grose, W. L., R. E. Turner, and J. E. Nealy, Coupling between photochemistry and transport: Simulations with a 3-D model, *J. Atmos. Terr. Phys.*, in press, 1985.
- Grosjean, D., Atmospheric reactions of ortho cresol: Gas phase and aerosol products, *Atmos. Environ.*, **18**, 1641-1652, 1984.
- Groves, G. V., Seasonal and latitudinal models of atmospheric temperature, pressure and density, 25 to 100 km, *AFCRL-70-0261*, 78 pp., Air Force Cambridge Research Labs., Hanscom AFB, MA, 1970.
- Groves, G. V., and J. M. Forbes, Equinox tidal heating of the upper atmosphere, *Planet. Space Sci.*, **32**, 447-436, 1984.

## REFERENCES

- Guedalia, D., C. Estournel, and R. Vehil, Effects of Sahel dust layers upon nocturnal cooling of the atmosphere, *ECLATS Experiment*, 644-650, 1984.
- Guicherit, R., and H. Van Dop, Photochemical production of ozone in Western Europe (1971-1978) and its relation to meteorology, *Atmos. Environ.*, *11*, 145-155, 1977.
- Guthrie, P. D., C. H. Jackman, J. R. Herman, and C. J. McQuillan, A diabatic circulation experiment in a two-dimensional photochemical model, *J. Geophys. Res.*, *89*, 9589-9602, 1984.
- Hack, W., and H. Kurzke, The production of H-atoms in the energy transfer reaction of  $O_2(^1\Delta_g)$  with  $HO_2(X^2A'')$ , *Chem. Phys. Lett.*, *104*, 93-96, 1984.
- Hack, W., and H. Kurzke, Kinetic study of the elementary chemical reaction  $H(^2S) + O_2(^1\Delta_g) \rightarrow OH(^2\pi) + O(^3P)$  in the gas phase, *J. Phys. Chem.*, in press, 1985.
- Haggard, K. V., and W. L. Grose, Numerical simulation of a sudden stratospheric warming with a three-dimensional spectral, quasi-geostrophic model, *J. Atmos. Sci.*, *38*, 1480-1497, 1981.
- Hahn, J., and P. J. Crutzen, The role of fixed nitrogen in atmospheric photochemistry, *Phil. Trans. Roy. Soc. London*, *B296*, 521-541, 1982.
- Haigh, J. D., and J. A. Pyle, Ozone perturbation experiments in a two-dimensional circulation model, *Quart. J. Roy. Meteorol. Soc.*, *108*, 551-574, 1982.
- Haigh, J. D., Radiative heating in the lower stratosphere and the distribution of ozone in a two-dimensional model, *Quart. J. Roy. Meteorol. Soc.*, *110*, 167-185, 1984.
- Hall, C. A. S., C. A. Ekdahl, and D. E. Wartenberg, A fifteen-year record of biotic metabolism in the Northern Hemisphere, *Nature*, *255*, 136-138, 1975.
- Hameed, S., and R. D. Cess, The impact of a global warming on biospheric sources of methane and its climatic consequences, *Tellus*, *35*, 1-7, 1983.
- Hameed, S., J. P. Pinto, and R. W. Stewart, Sensitivity of the predicted CO-OH-CH<sub>4</sub> perturbation to tropospheric NO<sub>x</sub> concentrations, *J. Geophys. Res.*, *84*, 763-768, 1979.
- Hameed, S., R. D. Cess, and J. S. Hogan, Response of the global climate to changes in atmospheric chemical composition due to fossil fuel burning, *J. Geophys. Res.*, *85*, 7537-7545, 1980.
- Hamilton, K., Studies of wave-mean flow interaction in the stratosphere, mesosphere and lower thermosphere, Ph.D. thesis, Princeton University, Princeton, NJ, 1981a.
- Hamilton, K., The vertical structure of the quasi-biennial oscillation and its theory, *Atmos.-Ocean*, *19*, 236-250, 1981b.
- Hamilton, K., Rocketsonde observation of the mesospheric semiannual oscillation at Kwajalein, *Atmos.-Ocean*, *20*, 281-286, 1982a.
- Hamilton, K., Some features of the climatology of the Northern Hemisphere stratosphere revealed by NMC upper atmosphere analyses, *J. Atmos. Sci.*, *39*, 2737-2749, 1982b.
- Hamilton, K., Diagnostic study of the momentum balance in the Northern Hemisphere winter stratosphere, *Mon. Weather Rev.*, *111*, 1434-1441, 1983a.
- Hamilton, K., Aspects of wave behavior in the mid and upper troposphere of the Southern Hemisphere, *Atmos.-Ocean*, *21*, 40-54, 1983b.
- Hamilton, K., Mean wind evolution through the quasi-biennial cycle in the tropical lower stratosphere, *J. Atmos. Sci.*, *41*, 2113-2125, 1984.
- Hampson, J., Chemiluminescent emissions observed in the stratosphere and mesosphere, in *Les Problemes Meteorologiques de la Stratosphere et de la Mesosphere*, edited by CNES, Presses Universitaires de France, Paris, 1965.
- Handwerk, V., and R. Zellner, Laboratory study of the reaction  $ClO + O_2(^1\Delta) \rightarrow$  products, Final report to CMA, 1984.
- Hanel, R. A., B. J. Conrath, V. G. Kunde, C. Prabhakara, I. Revah, V. V. Salomonson, and G. Wolford, The Nimbus 4 infrared spectroscopy experiment 1. Calibrated thermal emission spectra, *J. Geophys. Res.*, *77*, 2629-2641, 1972.

## REFERENCES

- Hansen, J., D. Johnson, A. Lacis, S. Lebedeff, P. Lee, D. Rind, and G. Russell, Climate impact of increasing atmospheric carbon dioxide, *Science*, 213, 957-966, 1981.
- Hansen, J., A. Lacis, D. Rind, G. Russell, P. Stone, I. Fung, R. Ruedy, and J. Lerner, Climate sensitivity: Analysis of feedback mechanisms, in *Climate Processes and Climate Sensitivity*, Maurice Ewing Series 5, edited by J. E. Hansen and T. Takasashi, 368 pp., American Geophysical Union, Washington, DC, 1984.
- Hao, W. M., Sources of N<sub>2</sub>O from combustion, Ph.D. thesis, Harvard University, Boston, MA, 1985.
- Harries, J. E., Ratio of HNO<sub>3</sub> to NO<sub>2</sub> concentrations in daytime stratosphere, *Nature*, 274, 235, 1978.
- Harries, J. E., Stratospheric composition measurements as tests of photochemical theory, *J. Atmos. Terr. Phys.*, 44, 591-597, 1982.
- Harries, J. E., D. G. Moss, N. R. W. Swann, G. F. Neill, and P. Gildwarg, Simultaneous measurements of H<sub>2</sub>O, NO<sub>2</sub>, and HNO<sub>3</sub> in the daytime stratosphere from 15 to 35 km, *Nature*, 259, 300-302, 1976.
- Harries, R. C., D. I. Sebacher, and F. P. Day, Methane flux in the Great Dismal Swamp, *Nature*, 297, 673-674, 1982.
- Harris, J. M. and B. A. Bodhaine (Eds.), *Geophysical Monitoring for Climatic Change, Summary Report 1982*, 160 pp., NOAA Air Resources Laboratory, Boulder, CO, 1983.
- Harris, J. M., and E. C. Nickerson (Eds.), *Geophysical Monitoring for Climatic Change, No. 12, Summary Report, 1983*, 199 pp., NOAA Air Resources Laboratory, Boulder, CO, 1984.
- Harshvardhan, A. Arking, M. D. King and M.-D. Chou, Impact of the El Chichon stratospheric aerosol layer on N. H. temperatures, paper presented at WMO(CAS)/IAMAP Workshop on Aerosols and Their Climatic Effects, Williamsburg, VA, 28-30 March 1983.
- Hartmann, D. L., The structure of the stratosphere in the Southern Hemisphere during late winter 1973 as observed by satellite, *J. Atmos. Sci.*, 33, 1141-1154, 1976a.
- Hartmann, D. L., The dynamical climatology of the stratosphere in the Southern Hemisphere during late winter 1973, *J. Atmos. Sci.*, 33, 1789-1802, 1976b.
- Hartmann, D. L., A note concerning the effect of variable extinction on radiative-photochemical relaxation, *J. Atmos. Sci.*, 35, 1125-1130, 1978.
- Hartmann, D. L., Barotropic instability of the polar night jet stream, *J. Atmos. Sci.*, 40, 817-835, 1983.
- Hartmann, D. L., and R. R. Garcia, A mechanistic model of ozone transport by planetary waves in the stratosphere, *J. Atmos. Sci.*, 36, 350-364, 1979.
- Hartmann, D. L., C. R. Mechoso, and K. Yamazaki, Observations of wave mean-flow interaction in the Southern Hemisphere, *J. Atmos. Sci.*, 41, 351-362, 1984.
- Harwood, R. S., The temperature structure of the Southern Hemisphere stratosphere: August-October, 1971, *Quart. J. Roy. Meteorol. Soc.*, 102, 757-770, 1975.
- Harwood, R. S., and J. A. Pyle, A two-dimensional mean circulation model for the atmosphere below 80 km, *Quart. J. Roy. Meteorol. Soc.*, 101, 723-747, 1975.
- Harwood, R. S., and J. A. Pyle, Studies of the ozone budget using a zonal mean circulation model and linearized photochemistry, *Quart. J. Roy. Meteorol. Soc.*, 103, 319-343, 1977.
- Harwood, R. S., and J. A. Pyle, The dynamical behaviour of a two-dimensional model of the stratosphere, *Quart. J. Roy. Meteorol. Soc.*, 106, 395-420, 1980.
- Hasebe, F., Interannual variations of global total ozone revealed from Nimbus 4 BUUV and ground-based observations, *J. Geophys. Res.*, 88, 6819-6834, 1983.
- Hasebe, F., The global structure of the total ozone fluctuations observed on the time scales of two to several years, in *Dynamics of the Middle Atmosphere*, edited by J. R. Holton and T. Matsuno, pp. 445-464, Terrapub, Tokyo, 1984.
- Hashimoto, L. K., W. A. Kaplan, S. C. Wofsy, and W. B. McElroy, Transformations of fixed nitrogen in the Cariaco Trench, *Deep Sea Res.*, 30, 575-590, 1983.

## REFERENCES

- Hasson, V., and R. W. Nicholls, Absolute spectral absorption measurements in molecular oxygen from 2640-1920 Å: II. Continuum measurements 2430-1920 Å, *J. Phys. B.: Atom. Mol. Phys.*, **4**, 1789-1797, 1971.
- Hastie, D. R., and M. D. Miller, A balloon-borne tunable diode laser absorption spectrometer for multi-species trace gas measurements in the stratosphere, *Appl. Opt.*, in press, 1985.
- Hayashi, Y., A theory of large-scale equatorial waves generated by condensation heat and accelerating the zonal wind, *J. Meteorol. Soc. Japan*, **48**, 140-160, 1970.
- Hayashi, Y., Spectral analysis of tropical disturbances appearing in a GFDL general circulation model, *J. Atmos. Sci.*, **31**, 180-218, 1974.
- Hayashi, Y., Non-singular resonance of equatorial waves under the radiation condition, *J. Atmos. Sci.*, **33**, 183-201, 1976.
- Hayashi, Y., D. Golder, and J. Mahlman, Stratospheric and mesospheric Kelvin waves simulated by the GFDL "SKYHI" general circulation model, *J. Atmos. Sci.*, **41**, 1971-1984, 1984.
- Hayashi, Y., and D. Golder, Transient planetary waves simulated by GFDL spectral general circulation models. Part I: Effects of mountains, *J. Atmos. Sci.*, **40**, 941-950, 1983.
- Hayashi, Y., D. Golder, and J. Mahlman, Stratospheric and mesospheric Kelvin waves simulated by the GFDL "SKYHI" general circulation model, *J. Atmos. Sci.*, **41**, 1971-1984, 1984.
- Heaps, W. S., and T. J. McGee, Balloon borne lidar measurements of the stratospheric hydroxyl radical, *J. Geophys. Res.*, **88**, 5281-5285, 1983.
- Heaps, W. S., and T. J. McGee, Progress in stratospheric hydroxyl measurement by balloon-borne lidar, *J. Geophys. Res.*, **90**, 7913-7922, 1985.
- Heaps, W. S., T. J. McGee, R. D. Hudson, and L. O. Caudill, Stratospheric ozone and hydroxyl radical measurements by balloon-borne lidar, *Applied Opt.*, **21**, 2265-2274, 1982.
- Hearn, A. G., The absorption of ozone in the ultraviolet and visible regions of the spectrum, *Proc. Phys. Soc. (London)*, **78**, 932-940, 1961.
- Heaseman, C. H., Satellite observations of mesospheric wind structure, Ph.D. thesis, Oxford University, Oxford, 1981.
- Heastie, H., and P. M. Stephenson, Upper winds over the world, *Geophys. Mem.*, No. 103, London: HMSO, **13**, 1-217, 1960.
- Heath, D. F., A review of observational evidence for short and long term ultraviolet flux variability of the sun, in *Proceedings of the International Conference on Sun and Climate*, Centre National d'Etudes Spatiales, Toulouse, Sept. 30-Oct. 3, 445-450, 1980.
- Heath, D. F., and B. M. Schlesinger, Temporal variability of the UV solar spectral irradiance from 160-400 nm over periods of the evolution and rotation of active regions from maximum to minimum phases of the sunspot cycle, in press, 1985.
- Heath, D. F., A. J. Krueger, H. A. Roeder, and B. D. Henderson, The solar backscatter ultraviolet and total ozone mapping spectrometer (SBUV/TOMS) for Nimbus G, *Opt. Eng.*, **14**, 323-331, 1975.
- Heath, D. F., A. J. Krueger, and P. J. Crutzen, Solar proton event: Influence on stratospheric ozone, *Science*, **197**, 886-889, 1977.
- Heath, D. F., T. P. Repoff, and R. F. Donnelly, Nimbus-7 SBUV observations of solar UV spectral irradiance variations caused by solar rotation and active-region evolution for the period November 7, 1978-November 1, 1980, *NOAA-TM-ERL-ARL-129*, 78 pp., NOAA Air Resources Laboratory, Rockville, MD, September, 1984.
- Heicklen, J., *Atmospheric Chemistry*, 406 pp., Academic Press, New York, 1976.
- Heidt, L. E., J. P. Krasnec, R. A. Lueb, W. H. Pollack, B. E. Henry, and P. J. Crutzen, Latitudinal distributions of CO and CH<sub>4</sub> over the Pacific, *J. Geophys. Res.*, **85**, 7329-7336, 1980.

## REFERENCES

- Heikes, B., and A. M. Thompson, Effects of heterogeneous processes on NO<sub>3</sub>, HONO, and HNO<sub>3</sub> chemistry in the troposphere, *J. Geophys. Res.*, *10*, 10883-10895, 1983.
- Helas, G., and P. J. Warneck, Background NO<sub>x</sub> mixing ratios in air masses over the North Atlantic Ocean, *J. Geophys. Res.*, *86*, 7283-7290, 1981.
- Held, I. M., Stationary and quasi-stationary eddies in the extratropical troposphere: Theory, in *Large-scale Dynamical Processes in the Atmosphere*, edited by B. J. Hoskins and R. Pearce, pp. 127-168, Academic Press, New York, 1983.
- Helten, M., W. Patz, M. Trainer, H. Fark, E. Klein, and D. H. Ehhalt, Measurements of stratospheric HO<sub>2</sub> and NO<sub>2</sub> by matrix isolation and ESR spectroscopy, *J. Atmos. Chem.*, *2*, 191-202, 1984a.
- Helten, M., W. Patz, D. H. Ehhalt, and E. P. Roeth, Measurements of nighttime NO<sub>3</sub> and NO<sub>2</sub> in the stratosphere by matrix isolation and ESR spectroscopy, in *Atmospheric Ozone*, edited by C. S. Zerefos and A. Ghazi, pp. 196-200, D. Reidel, Dordrecht, 1984b.
- Hendry, D. G., and R. A. Kenley, Chapter 7, in *Atmospheric chemistry of peroxy nitrates, nitrogen air pollutants: Chemical and biological implications*, edited by D. Grosjean, Ann Arbor Science, Ann Arbor, MI, 1979.
- Hering, W. S. and T. R. Borden: See Borden, T. R. and W. S. Hering.
- Herman, J. R., and C. J. McQuillan, Atmospheric chlorine and stratospheric ozone nonlinearities and trend detection, *J. Geophys. Res.*, *90*, 5721-5732, 1985.
- Herman, J. R., and J. E. Mentall, O<sub>2</sub> absorption cross sections (187-225 nm) from stratospheric solar flux measurements, *J. Geophys. Res.*, *87*, 8967-8975, 1982a.
- Herman, J. R., and J. E. Mentall, The direct and scattered solar flux within the stratosphere, *J. Geophys. Res.*, *87*, 1319-1330, 1982b.
- Hess, P. H., and J. R. Holton, The origin of temporal variance in long-lived trace constituents in the summer stratosphere, *J. Atmos. Sci.*, *42*, 1455-1463, 1985.
- Hicks, B. B., M. L. Wesely, and J. L. Durham, *Critique of Methods to Measure Dry Deposition*, 83 pp., Environmental Sciences Research Laboratory, Office of Research and Development, U. S. Environmental Protection Agency, Research Triangle Park, NC, 1980.
- Hidalgo, H., and P. J. Crutzen, The tropospheric and stratospheric composition perturbed by NO<sub>x</sub> emissions of high-altitude aircraft, *J. Geophys. Res.*, *82*, 5833-5866, 1977.
- Hide, R., and P. J. Mason, Sloping convection in a rotating fluid, *Advances in Physics*, *24*, 47-100, 1975.
- Hill, W. J., P. N. Sheldon, and J. J. Tiede, Analyzing worldwide total ozone for trends, *Geophys. Res. Lett.*, *4*, 21-24, 1977.
- Hills, A. J., and C. J. Howard, Rate coefficient temperature dependence and branching ratio for the OH + ClO reaction, *J. Chem. Phys.*, *81*, 4458-4465, 1984.
- Hilsenrath, E., and B. M. Schlesinger, Total ozone seasonal and interannual variations derived from the 7 year Nimbus 4 data, *J. Geophys. Res.*, *86*, 12087-12096, 1981.
- Hilsenrath, E., T. Seiden, and P. Goodman, An ozone measurement in the mesosphere and stratosphere by means of a rocketsonde, *J. Geophys. Res.*, *71*, 1385-1397, 1969.
- Hilsenrath, E., J. Ainsworth, A. Holland, J. Mentall, A. Torres, W. Attmannspacher, A. Bass, W. Evans, W. Komhyr, K. Mauersberger, A. J. Miller, M. Proffitt, D. Robbins, S. Taylor, and E. Weinstock, Results from the balloon ozone intercomparison campaign (BOIC), in *Atmospheric Ozone*, edited by C. S. Zerefos and A. Ghazi, pp. 454-459, D. Reidel, Dordrecht, 1985.
- Hilsenrath, E., J. Ainsworth, W. Attmannspacher, A. Bass, W. F. J. Evans, A. Holland, W. Komhyr, K. Mauersberger, J. Mentall, M. Proffitt, D. Robbins, S. Taylor, A. Torres, and E. Weinstock, Results from the Balloon Ozone Intercomparison Campaign (BOIC), to be published, 1986.
- Hines, C. O., Dynamical heating of the upper atmosphere, *J. Geophys. Res.*, *70*, 177-183, 1965.

## REFERENCES

- Hinteregger, H. E., Representations of solar EUV fluxes for aeronomical applications, in *The Mesosphere and Thermosphere*, edited by G. Schmidtke and K. S. W. Champion, pp. 39-52, Pergamon Press, Oxford, 1981.
- Hirooka, T., and I. Hirota, Normal mode Rossby waves observed in the upper stratosphere. Part II. Second antisymmetric and symmetric modes of zonal wavenumbers 1 and 2, *J. Atmos. Sci.*, **42**, 536-548, 1985.
- Hirota, I., Seasonal variation of planetary waves in the stratosphere observed by the Nimbus 5 SCR, *Quart. J. Roy. Meteorol. Soc.*, **102**, 757-770, 1976.
- Hirota, I., Equatorial waves in the upper stratosphere and mesosphere in relation to the semi-annual oscillation of the zonal wind, *J. Atmos. Sci.*, **35**, 714-722, 1978.
- Hirota, I., Kelvin waves in the equatorial middle atmosphere observed by the Nimbus-5 SCR, *J. Atmos. Sci.*, **36**, 217-222, 1979.
- Hirota, I., Observational evidence of the semiannual oscillation in the tropical middle atmosphere-A review, *Pure Appl. Geophys.*, **118**, 217-238, 1980.
- Hirota, I., Climatology of gravity waves in the middle atmosphere, *J. Atmos. Terr. Phys.*, **46**, 767-773, 1984.
- Hirota, I., and T. Hirooka, Normal mode Rossby waves observed in the upper stratosphere. Part I: First symmetric modes of wavenumbers 1 and 2, *J. Atmos. Sci.*, **41**, 1253-1267, 1984.
- Hirota, I., and Y. Sato, Periodic variation of the winter circulation and intermittent vertical propagation of planetary waves, *J. Meteorol. Soc. Japan*, **47**, 390-402, 1969.
- Hirota, I., T. Hirooka, and M. Shiotani, Upper stratospheric circulation in the two hemispheres observed by satellites, *Quart. J. Roy. Meteorol. Soc.*, **109**, 443-454, 1983a.
- Hirota, I., Y. Maekawa, S. Fukao, K. Fukuyama, M. P. Sulzer, J. L. Fellous, T. Tsudo, and S. Kato, Fifteen-day observation of mesospheric and lower thermospheric motions with the aid of the Arecibo UHF radar, *J. Geophys. Res.*, **88**, 6835-6842, 1983b.
- Hitchman, M. H., An observational study of wave-mean flow interaction in the equatorial middle atmosphere, Ph.D. thesis, 360 pp., Dept. of Atmospheric Sciences, University of Washington, Seattle, WA, 1985.
- Hitchman, M. H., and C. B. Leovy, Evolution of the zonal mean state in the equatorial middle atmosphere during October, 1978-May, 1979, *J. Atmos. Sci.*, **43**, in press, 1986.
- Hocking, W. K., Mesospheric turbulence intensities measured with a HF radar at 35° S - II, *J. Atmos. Terr. Phys.*, **45**, 103-114, 1983.
- Hocking, W. K., Turbulence in the region 80-120 km, in *Handbook for MAP, Vol. 16*, edited by K. Labitzke, J. J. Barnett, and B. Edwards, pp. 290-304, SCOSTEP Secretariat, Univ. of Illinois, Urbana, 1985.
- Hodges, Jr., R. R., Generation of turbulence in the upper atmosphere by internal gravity waves, *J. Atmos. Sci.*, **72**, 3455-3458, 1967.
- Hoell, J. M., C. N. Harward, and B. S. Williams, Remote infrared heterodyne radiometer measurements of atmospheric ammonia profiles, *Geophys. Res. Lett.*, **7**, 313-316, 1980.
- Hoell, J. M., G. L. Gregory, M. A. Carroll, M. McFarland, B. A. Ridley, D. D. Davis, J. Bradshaw, M. O. Rodgers, A. L. Torres, G. W. Sachse, G. F. Hill, E. P. Condon, R. A. Rasmussen, M. C. Campbell, J. C. Farmer, J. C. Sheppard, C. C. Wang, and L. I. Davis, An intercomparison of carbon monoxide, nitric oxide, and hydroxyl measurement techniques: Overview of results, *J. Geophys. Res.*, **89**, 11819-11825, 1984.
- Hoffert, M. I., A. J. Callegari, and C. T. Hsieh, The role of deep sea storage in the secular response to climate forcing, *J. Geophys. Res.*, **85**, 6667-6679, 1980.
- Hoffman-Sievert, R., and A. W. Castleman, The reaction of SO<sub>3</sub> with water clusters and the formation of H<sub>2</sub>SO<sub>4</sub>, *J. Phys. Chem.*, **88**, 3329-3333, 1984.
- Hofmann, D. J., and J. M. Rosen, Balloon-borne observations of stratospheric aerosol and condensation nuclei during the year following the Mt. St. Helens eruption, *Geophys. Res. Lett.*, **87**, 11039-11061, 1982.

## REFERENCES

- Hofmann, D. J., and J. M. Rosen, Sulfuric acid droplet formation and growth in the stratosphere after the 1982 eruption of El Chichon, *Science*, 222, 325-327, 1983.
- Holland, A. J., T. D. Keenan, and G. D. Crane, Observations of a phenomenal temperature perturbation in tropical cyclone Kerry (1979), *Mon. Weather Rev.*, 112, 1074-1082, 1984.
- Holstein, K. J., E. H. Fink, J. Wildt, R. Winter, and F. Zabel, Mechanisms of HO<sub>2</sub>(A<sub>2</sub>A') excitation in various chemical systems, *J. Phys. Chem.*, 87, 3943-3948, 1983.
- Holton, J. R., Waves in the equatorial stratosphere generated by tropospheric heat sources, *J. Atmos. Sci.*, 29, 368-375, 1972.
- Holton, J. R., A note on the frequency distribution of atmospheric Kelvin waves, *J. Atmos. Sci.*, 30, 499-501, 1973.
- Holton, J. R., *The Dynamical Meteorology of the Stratosphere and Mesosphere*, 216 pp., American Meteorological Society, Boston, MA, 1975.
- Holton, J. R., Wave propagation and transport in the middle atmosphere, *Phil. Tran. Roy. Soc. London*, A296, 73-85, 1980.
- Holton, J. R., An advective model for two-dimensional transport of stratospheric trace species, *J. Geophys. Res.*, 86, 11989-11994, 1981.
- Holton, J. R., The role of gravity wave induced drag and diffusion in the momentum budget of the mesosphere, *J. Atmos. Sci.*, 39, 791-799, 1982.
- Holton, J. R., The influence of gravity wave breaking in the circulation of the middle atmosphere, *J. Atmos. Sci.*, 40, 2497-2507, 1983.
- Holton, J. R., The generation of mesospheric planetary waves by zonally asymmetric gravity wave breaking, *J. Atmos. Sci.*, 41, 3427-3430, 1984a.
- Holton, J. R., Troposphere-stratosphere exchange of trace constituents: The water vapor puzzle, in *Dynamics of the Middle Atmosphere*, edited by J. R. Holton and T. Matsuno, pp. 369-385, Terrapub, Tokyo, 1984b.
- Holton, J. R., A dynamically based transport parameterization for one-dimensional photochemical models, in *Handbook for MAP, Vol. 18*, edited by S. Kato, Chap. 4, SCOSTEP Secretariat, Univ. of Illinois, Urbana, 1985.
- Holton, J. R., A dynamically based transport parameterization for one-dimensional photochemical models of the stratosphere, *J. Geophys. Res.*, in press, 1986.
- Holton, J. R., and R. S. Lindzen, An updated theory of the quasi-biennial oscillation of the tropical stratosphere, *J. Atmos. Sci.*, 29, 1076-1080, 1972.
- Holton, J. R., and H. C. Tan, The influence of the equatorial quasi-biennial oscillation on the global circulation at 50 mb, *J. Atmos. Sci.*, 37, 2200-2208, 1980.
- Holton, J. R., and H. C. Tan, The quasi-biennial oscillation in the Northern Hemisphere lower stratosphere, *J. Meteorol. Soc. Japan*, 60, 140-148, 1982.
- Holton, J. R., and W. M. Wehrbein, The role of forced planetary waves in the annual cycle of zonal mean circulation of the middle atmosphere, *J. Atmos. Sci.*, 37, 1968-1983, 1980a.
- Holton, J. R., and W. M. Wehrbein, A numerical model of the zonal mean circulation of the middle atmosphere, *Pure Appl. Geophys.*, 118, 284-306, 1980b.
- Holton, J. R., and X. Zhu, A further study of gravity wave induced drag and diffusion in the mesosphere, *J. Atmos. Sci.*, 41, 2653-2662, 1984.
- Hood, L. L., The temporal behavior of upper stratospheric ozone at low latitudes: Evidence from Nimbus 4 BUUV data for short-term responses to solar ultraviolet variability, *J. Geophys. Res.*, 89, 9557-9568, 1984.
- Hopkins, R. H., Evidence of polar-tropical coupling in upper stratospheric zonal wind anomalies, *J. Atmos. Sci.*, 32, 712-719, 1975.

## REFERENCES

- Horvath, J. J., J. E. Frederick, N. Orsini, and A. R. Douglass, Nitric oxide in the upper stratosphere: Measurements and geophysical interpretation, *J. Geophys. Res.*, **88**, 10809-10817, 1983.
- Hoskins, B. J., Non-Boussinesq effects and further development in a model of upper tropospheric frontogenesis, *Quart. J. Roy. Meteorol. Soc.*, **98**, 532-541, 1972.
- Hoskins, B. J., The role of potential vorticity in symmetric stability and instability, *Quart. J. Roy. Meteorol. Soc.*, **100**, 480-482, 1974.
- Hoskins, B. J., The geostrophic momentum approximation and the semi-geostrophic equations, *J. Atmos. Sci.*, **32**, 233-242, 1975.
- Hoskins, B. J., Modelling of the transient eddies and their feedback on the mean flow, in *Large-scale Dynamical Processes in the Atmosphere*, edited by B. J. Hoskins and R. Pearce, pp. 169-199, Academic Press, New York, 1983.
- Hoskins, B. J., and I. Draghici, The forcing of ageostrophic motion according to the semi-geostrophic equations and in an isentropic coordinate model, *J. Atmos. Sci.*, **34**, 1859-1867, 1977.
- Hoskins, B. J., and W. A. Heckley, Baroclinic waves and frontogenesis in a non-uniform potential vorticity semi-geostrophic model, *J. Atmos. Sci.*, **39**, 1999-2016, 1982.
- Hoskins, B. J., I. Draghici, and H. C. Davies, A new look at the omega equation, *Quart. J. Roy. Meteorol. Soc.*, **104**, 31-38, 1978.
- Hoskins, B. J., M. E. McIntyre, and A. W. Robertson, On the use and significance of isentropic potential vorticity maps, *Quart. J. Roy. Meteorol. Soc.*, **111**, 877-946, 1985.
- Houghton, J. T., *The Physics of Atmospheres*, 203 pp., Cambridge University Press, Cambridge, 1977.
- Houghton, J. T., The stratosphere and mesosphere, *Quart. J. Roy. Meteorol. Soc.*, **104**, 1-30, 1978.
- Houghton, J. T., F. W. Taylor, and C. D. Rodgers, Remote sounding of atmospheres, *Cambridge Planetary Science Series No. 5*, 343 pp., Cambridge University Press, Cambridge, 1984.
- Houze, Jr., R. A., Cloud clusters and long-scale vertical motions in the tropics, *J. Meteorol. Soc. Japan*, **60**, 396-409, 1982.
- Houze, R. A., and A. K. Betts, Convection in GATE, *Rev. Geophys. Space Phys.*, **19**, 541-576, 1981.
- Houze, R. A., S. G. Geotis, F. D. Marks, and A. K. West, Winter monsoon convection in the vicinity of North Borneo. Part I: Structure and time evolution of the clouds and precipitation, *Mon. Weather Rev.*, **109**, 1595-1614, 1981.
- Hov, O., S. A. Penkett, I. S. A. Isaksen, and A. Semb, Organic gases in the Norwegian Arctic, *Geophys. Res. Lett.*, **11**, 425-428, 1984.
- Hoyt, S. D., The air-sea exchange of carbonyl sulfide (OCS) and halocarbons, Ph.D. thesis, Oregon Graduate Center, Beaverton, Oregon, 1982.
- Hsu, C. P. F., Air parcel motions during a numerically simulated sudden stratospheric warming, *J. Atmos. Sci.*, **37**, 2768-2792, 1980.
- Hubler, G., D. Perner, U. Platt, A. Tonnisson, and D. H. Ehhalt, Ground-level OH radical concentrations: New measurements by optical absorption, *J. Geophys. Res.*, **89**, 1309-1319, 1984.
- Huddleston, R. K., and E. Weitz, A laser-induced fluorescence study of energy transfer between the symmetric stretching and bending modes of CO<sub>2</sub>, *Chem. Phys. Lett.*, **83**, 174-179, 1981.
- Hudson, R. D., Critical review of ultraviolet photoabsorption cross sections for molecules of astrophysical and aeronomic interest, *Rev. Geophys. Space Phys.*, **9**, 305-406, 1971.
- Hudson, R. D. (Ed.), *The Stratosphere 1981. Theory and Measurements*, WMO Global Ozone Research and Monitoring Project Report No. 11, 516 pp., WMO, Geneva, 1982.
- Hudson, R. D., and S. H. Mahle, Photodissociation rates of molecular oxygen in the mesosphere and lower thermosphere, *J. Geophys. Res.*, **77**, 2902-2914, 1972.
- Hudson, R. D., and E. I. Reed (Eds.), *The Stratosphere: Present and Future*, NASA Reference Publication 1049, 432 pp., NASA Goddard Space Flight Center, Greenbelt, MD, 1979.

## REFERENCES

- Huebert, B. J., The dry deposition of nitric acid to grass, *J. Geophys. Res.*, **90**, 2085-2090, 1985.
- Huebert, B. J., and A. L. Lazrus, Tropospheric gas-phase and particulate nitrate measurements, *J. Geophys. Res.*, **85**, 7322-7328, 1980.
- Hungate, R. E., *The Rumen and Its Microbes*, 533 pp., Academic Press, New York, 1960.
- Hunt, B. G., Experiments with a stratospheric general circulation model. III. Large-scale diffusion of ozone including photochemistry. *Mon. Weather Rev.*, **97**, 287-306, 1969.
- Hunt, B. G., The maintenance of the zonal mean state of the upper atmosphere as represented in a three-dimensional general circulation model extending to 100 km, *J. Atmos. Sci.*, **38**, 2172-2186, 1981.
- Hunt, B. G., The impact of gravity wave drag and diurnal variability on the general circulation of the middle atmosphere, *J. Atmos. Sci.*, in press, 1985.
- Hunt, B. G., and S. Manabe, Experiments with stratospheric general circulation model, II. Large-scale diffusion of tracers in the stratosphere, *Mon. Weather Rev.*, **96**, 503-539, 1968.
- Hunten, D., The philosophy of one-dimensional modeling, in *Proceedings Fourth Conference Climatic Impact Assessment Program, DOT-TSC-OST-75-38*, edited by T. M. Hard and A. J. Broderick, pp. 147-155, Transportation Systems Center, Cambridge, MA, 1975.
- Huntress, W. T. Jr., Upper Atmosphere Research Satellite Program—to study the chemistry, energetics, and dynamics, Final Report, *JPL Publ. 78-54*, 62 pp., Jet Propulsion Lab., Pasadena, CA, 1978.
- Husson, N., A. Chedin, N. A. Scott, I. Cohen-Hallaleh, and A. Berroir, La Banque de donnees GEISA. Mise a jour no. 3, Laboratoire de Meteorologie Dynamique du C.N.R.S., *Internal Note 116*, Ecole Polytechnique, 91128 Palaiseau Cedex, France, July 1982.
- Husson, N., A. Chedin, N. A. Scott, D. Bailly, G. Graner, N. Lacombe, A. Levy, C. Rossetti, G. Tarra-go, C. Camy-Peyret, J. M. Flaud, A. Bauer, J. M. Colmont, N. Monnanteuil, J. C. Hilico, G. Pierre, M. Loete, J. P. Champion, L. S. Rothman, L. R. Brown, G. Orton, P. Varanasi, C. P. Rinsland, M. A. H. Smith, and A. Goldman, The GEISA spectroscopic line parameters data bank in 1984, *Annales Geophysicae*, Fasc. 2, Series A, 1986.
- Hutchinson, G. E., and A. R. Mosier, Nitrous oxide emissions from an irrigated cornfield, *Science*, **205**, 1125-1127, 1976.
- Hyson, P., Stratospheric water vapor over Australia, *Quart. J. Roy. Meteorol. Soc.*, **109**, 285-294, 1983.
- Idso, S. B., The climatological significance of a doubling of earth's atmospheric carbon dioxide concentration, *Science*, **207**, 1462-1463, 1980.
- Iman, R. L., and M. J. Shortencarier, A Fortran 77 program and user's guide for the generation of Latin hypercube and random samples for use with computer models, *SAND 83-2365*, Sandia National Laboratories, Albuquerque, NM, 1984.
- Iman, R. L., J. C. Helton, and J. E. Campbell, An approach to sensitivity analysis of computer models: Part I-Introduction, Input variable selection and preliminary variable assessment, *J. Quality Tech.*, **13**, 174-183, 1981.
- Imbrie, J., and K. P. Imbrie, *Ice Ages, Solving the Mystery*, 224 pp., Enslow Pub., Short Hills, NJ, 1979.
- Inn, E. C. Y., and Y. Tanaka, Absorption coefficient of ozone in the ultraviolet and visible regions, *J. Opt. Soc. Am.*, **43**, 870-873, 1953.
- Inst. fur Met. des Frei Universiteit Berlin, Meteorologische Abhandlungen, Tagliche Hohenkarten der 30-Mbar-flache sowie monatliche mittelkarten fur das jahr 1980, Verlag Von Dietuch Reiner, Berlin, 1980.
- Isaksen, I. S. A., Tropospheric ozone budget and possible man made effects, in *Quadrennial International Ozone Symposium, Vol. II*, edited by J. London, pp. 845-852, IAMAP, NCAR, Boulder, CO, 1981.
- Isaksen, I. S. A., and O. Hov, Calculations of trends in the tropospheric concentration of O<sub>3</sub>, OH, CO, CH<sub>4</sub> and NO<sub>x</sub>, in press, 1985.

## REFERENCES

- Isaksen, I. S. A., and F. Stordal, Ozone perturbations by enhanced levels of CFCs, N<sub>2</sub>O and CH<sub>4</sub>: A two-dimensional diabatic circulation study including uncertainty estimates, *J. Geophys. Res.*, in press, 1985.
- Ishiwata, T., I. Fujiwara, Y. Naruge, K. Obi, and I. Tanaka, Study of NO<sub>3</sub> by laser induced fluorescence, *J. Phys. Chem.*, *87*, 1349-1352, 1983.
- Itoh, H., The response of equatorial waves to thermal forcing, *J. Meteorol. Soc. Japan*, *55*, 222-239, 1977.
- Jackman, C. H., and P. D. Guthrie, Sensitivity of N<sub>2</sub>O, CFC<sub>13</sub> and CF<sub>2</sub>Cl<sub>2</sub> two-dimensional distributions to O<sub>2</sub> absorption cross sections, *J. Geophys. Res.*, *90*, 3919-3923, 1985.
- Jackman, C. H., and R. D. McPeters, The response of ozone to solar proton events during solar cycle 21: A theoretical interpretation, *J. Geophys. Res.*, *42*, 90, 7955-7966, 1985.
- Jackman, C. H., J. E. Frederick, and R. S. Stolarski, Production of odd nitrogen in the stratosphere and mesosphere: An intercomparison of source strengths, *J. Geophys. Res.*, *85*, 7495-7505, 1980.
- Jackman, C. H., J. A. Kaye, and P. D. Guthrie, LIMS HNO<sub>3</sub> data above 5 mbar: Corrections based on simultaneous observations of other species, *J. Geophys. Res.*, *90*, 7923-7930, 1985.
- Jackman, C. H., R. S. Stolarski, and J. A. Kaye, Two-dimensional monthly average ozone balance from Limb Infrared Monitor of the stratosphere and stratospheric and mesospheric sounder data, *J. Geophys. Res.*, *91*, 1103-1116, 1986.
- Jesson, J. P., Release of industrial halocarbons and tropospheric budget, in *Proceedings of the NATO Advanced Study Institute on Atmospheric Ozone: Its Variation and Human Influences, Rep. FAA-EE-80-20*, edited by A. C. Aikin, pp. 373-396, DOT, FAA, Washington, DC, 1980.
- Johansson, C., Field measurements of emission of nitric oxide from fertilized and unfertilized forest soils in Sweden, *J. Atmos. Chem.*, *1*, 429-442, 1984.
- Johansson, C., and L. Granat, Emission of nitric oxide from arable land, *Tellus*, *36B*, 25-37, 1984.
- Johnson, D. R., Systematic stratospheric-tropospheric exchange through quasi-horizontal transport within active baroclinic waves, in *The Long-Range Transport of Pollutants and its Relation to General Circulation including Stratospheric/Tropospheric Exchange Processes—Conference Proceedings, WMO No. 538*, pp. 401-408, WMO, Geneva, 1979.
- Johnson, D. R., A generalized transport equation for use with meteorological coordinate systems, *Mon. Weather Rev.*, *108*, 733-745, 1980.
- Johnson, D. R., On the forcing and maintenance of the isentropic zonally averaged circumpolar vortex, paper presented at *IAMAP-WMO Symposium on Maintenance of the Quasi-Stationary Components of the Flow in the Atmosphere and in Atmospheric Models*, pp 19-22, WMO, Geneva, Paris, August 30-September 2, 1983.
- Johnson, D. R., On the global distribution of heat sources and sinks and their relation to mass and energy transport, paper presented at *WMO Proceedings of the FGGE Tropics Seminar*, Tallahassee, Florida, October 8-12, 1984a.
- Johnson, D. R., The global circulation during the FGGE year: On the balance of mass, energy, and angular momentum within isentropic and isobaric coordinates as revealed by different FGGE data sets, paper presented at *WMO Proceedings of the Global Weather Experiment Scientific Seminar*, Helsinki, Finland, August 29-31, 1984b.
- Johnson, D. R., and W. K. Downey, Azimuthally averaged transport and budget equations for storms: Quasi-Lagrangian diagnostics 1, *Mon. Weather Rev.*, *103*, 967-979, 1975.
- Johnson, D. R., and R. D. Townsend, Diagnostics of the heat sources and sinks of the Asiatic monsoon and the thermally-forced planetary scale response, M. S. thesis, *AD-A119755*, 72 pp., Wisconsin Univ., Madison, WI, 1981.
- Johnson, D. R., R. D. Townsend, and M-Y Wei, The thermally forced responses of the planetary scale circulation to the global distribution of heat sources and sinks, *Tellus*, *37A*, 106-125, 1985.

## REFERENCES

- Johnson, F. S., J. D. Purcell, R. Tourey, and K. Watanabe, Direct measurements of the vertical distribution of atmospheric ozone to 70 kilometers altitude, *J. Geophys. Res.*, **57**, 157-176, 1952.
- Johnson, J. E., The role of the oceans in the atmospheric cycle of carbonyl sulfide, Ph.D. thesis, University of Washington, Seattle, WA, 1985.
- Johnson, K. W., and M. E. Gelman, Trends in the upper stratospheric temperatures as observed by rocketsondes (1965-1983), in *Handbook for MAP, Vol. 18*, edited by S. Kato, pp. 24-27, SCOSTEP Secretariat, Univ. of Illinois, Urbana, 1985.
- Johnson, R. H., and D. C. Kriete, Thermodynamic circulation characteristics of winter monsoon tropical mesoscale convection, *Mon. Weather Rev.*, **110**, 1898-1911, 1982.
- Johnston, D. A., Volcanic contribution of chlorine to the stratosphere: More significant to ozone than previously estimated?, *Science*, **209**, 491-493, 1980.
- Johnston, H. S., Reduction of stratospheric ozone by nitrogen oxide catalysts from supersonic transport exhaust, *Science*, **173**, 517-522, 1971.
- Johnston, H. S., Human effects on the global atmosphere, *Ann. Rev. Phys. Chem.*, **35**, 481-505, 1984.
- Johnston, H. S., and J. Podolske, Interpretations of stratospheric photochemistry, *Rev. Geophys. Space Phys.*, **16**, 491-519, 1978.
- Johnston, H. S., D. Kattenhorn, and G. Whitten, Use of excess carbon 14 data to calibrate models of stratospheric ozone depletion by supersonic transports, *J. Geophys. Res.*, **78**, 368-380, 1976.
- Johnston, H. S., M. Paige, and F. Yao, Oxygen absorption cross sections in the Herzberg continuum and between 206 and 326 K, *J. Geophys. Res.*, **89**, 11661-11665, 1984.
- Johnston, H. S., C. A. Cantrell, and J. G. Calvert, Unimolecular decomposition of NO<sub>3</sub> to NO and O<sub>2</sub>, *J. Geophys. Res.*, in press, 1985.
- Jones, B. M. R., J. P. Burrows, R. A. Cox, and S. A. Penkett, OCS formation in the reaction of OH with CS<sub>2</sub>, *Chem. Phys. Lett.*, **88**, 372-376, 1982.
- Jones, B. M. R., R. A. Cox, and S. A. Penkett, Atmospheric chemistry of carbon disulfide, *J. Atmos. Chem.*, **1**, 65-86, 1983.
- Jones, R. L., Satellite measurements of atmospheric composition: Three years' observations of CH<sub>4</sub> and N<sub>2</sub>O, *Adv. Space Res.*, **4**, 121-130, 1984.
- Jones, R. L., and J. A. Pyle, Observations of CH<sub>4</sub> and N<sub>2</sub>O by the Nimbus 7 SAMS: A comparison with in-situ data and two-dimensional numerical model calculations, *J. Geophys. Res.*, **89**, 5263-5279, 1984.
- Jones, R. L., J. A. Pyle, J. E. Harries, A. M. Zavody, J. M. Russell III, and J. C. Gille, The water vapour budget of the stratosphere studied using LIMS and SAMS satellite data, *Quart. J. Roy. Meteorol. Soc.*, in press, 1985.
- Joseph, J. H., The sensitivity of a numerical model of the global atmosphere to the presence of desert aerosols, Dept. of Geophysics and Planetary Sciences, Tel-Aviv Univ., Ramat Aviv, Israel, 6997, 1983.
- JPL: See DeMore, et al. and NASA-JPL listings.
- Junge, C., W. Seiler, and P. Warneck, The atmospheric <sup>12</sup>CO and <sup>14</sup>CO budget, *J. Geophys. Res.*, **76**, 2866-2879, 1971.
- Junge, C. E., Global ozone budget and exchange between stratosphere and troposphere, *Tellus*, **14**, 363-377, 1962.
- Junge, C. E., *Air chemistry and radioactivity*, 380 pp., Academic Press, New York, 1963.
- Just, T., and J. Troe, Theory of two-channel unimolecular reactions. 1. General formulation, *J. Phys. Chem.*, **84**, 3068-3072, 1980.
- Kagann, R. H., J. W. Elkins, and R. L. Sams, Absolute band strengths of halocarbons F-11 and F-12 in the 8 to 16 $\mu$ m region, *J. Geophys. Res.*, **88**, 1427-1432, 1983.
- Kanzawa, H., The behavior of mean zonal wind and planetary-scale disturbances in the troposphere and stratosphere during the 1973 sudden warming, *J. Meteorol. Soc. Japan*, **58**, 329-356, 1980.

## REFERENCES

- Kanzawa, H., Eliassen-Palm flux diagnostics and the effect of the mean zonal wind on planetary wave propagation for an observed sudden stratospheric warming, *J. Meteorol. Soc. Japan*, *60*, 1063-1073, 1982.
- Kanzawa, H., Four observed sudden warmings diagnosed by the Eliassen-Palm flux and refractive index, in *Dynamics of the Middle Atmosphere*, edited by J. R. Holton and T. Matsuno, pp. 307-331, Terrapub, Tokyo, 1984.
- Karoly, D. J., and B. J. Hoskins, Three dimensional propagation of planetary waves, *J. Meteorol. Soc. Japan*, *60*, 109-123, 1982.
- Katz, M., *Methods of Air Sampling and Analysis*, edited by M. Katz, pp. 549-555, American Public Health Assoc., Washington, DC, 1977.
- Kawahira, K., A quasi-one-dimensional model of the ozone transport by planetary waves in the winter stratosphere, *J. Meteorol. Soc. Japan*, *60*, 831-849, 1982.
- Keating, G. M., The response of ozone to solar activity variations. A review, *Solar Physics*, *74*, 321-347, 1981.
- Keating, G. M., and D. F. Young, Interim reference ozone models for the middle atmosphere, in *Handbook for MAP, Vol. 16*, edited by K. Labitzke, J. J. Barnett, and B. Edwards, pp. 205-229, SCOSTEP Secretariat, Univ. of Illinois, Urbana, 1985.
- Keating, G. M., G. P. Brasseur, J. Y. Nicholson III, and A. De Rudder, Detection of the response of ozone in the middle atmosphere to short-term solar ultraviolet variations, *Geophys. Res. Lett.*, *12*, 449-452, 1985.
- Keeling, C. D., The Global Carbon Cycle: What we know and could know from atmospheric, biospheric, and oceanic observations, in *Proceedings of the CO<sub>2</sub> Research Conference: Carbon Dioxide, Science and Consensus, DOE CONF-820970*, pp. II.3-II.62, U.S. Dept. of Energy, Washington, DC, 1983.
- Keeling, C. D., A. F. Carter, and W. G. Mook, Seasonal, latitudinal and secular variations in the abundance and isotopic ratios of atmospheric CO<sub>2</sub>, *J. Geophys. Res.*, *89*, 4615-4628, 1984.
- Keenan, T. D., and J. I. Templeton, A comparison of tropical cyclone, hurricane and typhoon mass and moisture structure, *Mon. Weather Rev.*, *111*, 320-327, 1983.
- Keller, M., T. J. Goreau, S. C. Wofsy, W. A. Kaplan, and M. B. McElroy, Production of nitrous oxide and consumption of methane by forest soils, *Geophys. Res. Lett.*, *10*, 1156-1159, 1983.
- Keller, M., W. A. Kaplan, and S. C. Wofsy, Emissions of N<sub>2</sub>O, CH<sub>4</sub> and CO from tropical forest soils, in press, 1985.
- Kelly, P. M., P. D. Jones, T. M. L. Wigley, R. S. Bradley, H. F. Diaz, and C. M. Goodess, The extended Northern Hemisphere surface air temperature record: 1851-1984, *Proceedings, AMS Conference on Climate Variations*, Boston, MA, 190 pp., 1984.
- Kendall, D. J. W., and H. L. Buijs, Stratospheric NO<sub>2</sub> and upper limits of CH<sub>3</sub>Cl and C<sub>2</sub>H<sub>6</sub> from measurements at 3.4 μm, *Nature*, *303*, 221-222, 1983.
- Kendall, D. J. W., and T. A. Clark, Balloon-borne far infrared atmospheric emission studies, *Infrared Phys.*, *18*, 803-813, 1978.
- Kendall, D. J. W., and T. A. Clark, The pure rotational atmospheric lines of hydroxyl, *J. Quant. Spectrosc. Radiat. Transfer*, *21*, 511-526, 1979.
- Kendall, D. J. W., and T. A. Clark, Detection of minor constituents of the stratosphere by far infrared emission spectroscopy, *Int. J. Infrared mm Waves*, *3*, 783-808, 1981.
- Kennedy, P. J., and M. A. Shapiro, The energy budget in a clear air turbulence zone as observed by aircraft, *Mon. Weather Rev.*, *111*, 650-993, 1975.
- Kennedy, P. J., and M. A. Shapiro, Further encounters with clear air turbulence in research aircraft, *J. Atmos. Sci.*, *37*, 986-993, 1980.
- Kerr, J. B., and C. T. McElroy, Measurement of stratospheric nitrogen dioxide from the AES stratospheric balloon program, *Atmosphere*, *14*, 166-171, 1976.

## REFERENCES

- Kerr, J. B., C. L. Mateer, C. T. McElroy, and D. I. Wardle, Intercomparison of the Dobson and grating ozone spectrophotometers, in *Proc. Joint Symp. on Atm. Ozone, Vol. 1*, pp. 109-120, Dresden, GDR, 1976.
- Kerr, J. B., C. T. McElroy, and W. F. J. Evans, Mid-latitude summertime measurements of stratospheric  $\text{NO}_2$ , *Can. J. Phys.*, **60**, 196-200, 1982.
- Keyser, L. F., High pressure flow kinetics. A study of the  $\text{OH} + \text{HCl}$  reaction from 2 to 100 torr, *J. Phys. Chem.*, **88**, 4759-4759, 1984.
- Khalil, M. A. K., and R. A. Rasmussen, Increase of  $\text{CHClF}_2$  in the earth's atmosphere, *Nature*, **292**, 823-824, 1981.
- Khalil, M. A. K., and R. A. Rasmussen, Secular trends of methane, *Chemosphere*, **12**, 877-883, 1982.
- Khalil, M. A. K., and R. A. Rasmussen, Gaseous tracers of Arctic haze, *Environ. Sci. and Tech.*, **17**, 157-164, 1983a.
- Khalil, M. A. K., and R. A. Rasmussen, Increase and seasonal cycles of nitrous oxide in the Earth's atmosphere, *Tellus*, **35B**, 161-169, 1983b.
- Khalil, M. A. K., and R. A. Rasmussen, Sources, sinks and seasonal cycles of atmospheric methane, *J. Geophys. Res.*, **88**, 5131-5144, 1983c.
- Khalil, M. A. K., and R. A. Rasmussen, Termites and methane, *Nature*, **302**, 355, 1983d.
- Khalil, M. A. K., and R. A. Rasmussen, The atmospheric lifetime of methylchloroform ( $\text{CH}_3\text{CCl}_3$ ), *Tellus*, **36B**, 317-332, 1984a.
- Khalil, M. A. K., and R. A. Rasmussen, Global increase of carbon monoxide, in *Transactions of the APCA Specialty Conference on Environmental Impacts of Natural Emissions*, edited by V. P. Aneja, 1984b.
- Khalil, M. A. K., and R. A. Rasmussen, Carbon monoxide in the Earth's atmosphere: Increasing trend, *Science*, **224**, 54-56, 1984c.
- Khalil, M. A. K., and R. A. Rasmussen, Causes of increasing atmospheric methane: Depletion of hydroxyl radicals and the rise of emissions, *Atmos. Environ.*, **19**, 397-407, 1985a.
- Khalil, M. A. K., and R. A. Rasmussen, Global sources, lifetimes and mass balances of carbonyl sulfide ( $\text{OCS}$ ) and carbon disulfide ( $\text{CS}_2$ ) in the earth's atmosphere, *Atmos. Environ.*, **18**, 1805-1813, 1985b.
- Khalil, M. A. K., and R. A. Rasmussen, The trend of bromodifluoromethane ( $\text{CBrClF}_2$ ) and the concentration of other bromine containing gases at the South Pole, *Antarctic Journal of the U.S.*, in press, 1985c.
- Khalil, M. A. K., and R. A. Rasmussen, Trichlorotrifluoroethane (F-113) trends at Pt. Barrow, Alaska, in *Geophysical Monitoring for Climate Change, No. 13, Summary Report 1984*, U.S. Department of Commerce, ERL/NOAA, Boulder, CO, in press, 1985d.
- Khalil, M. A. K., and R. A. Rasmussen, Atmospheric carbon tetrafluoride ( $\text{CF}_4$ ): Sources and trends, *Geophys. Res. Lett.*, **12**, 671-672, 1985e.
- Khalil, M. A. K., and R. A. Rasmussen, Interannual variability of atmospheric methane, *Science*, in press, 1985f.
- Khalil, M. A. K., R. A. Rasmussen, and S. D. Hoyt, Atmospheric chloroform ( $\text{CHCl}_3$ ): Ocean-air exchange and global mass balance, *Tellus*, **35B**, 266-274, 1983.
- Kiang, C. S., D. Stauffer, V. J. Mohnen, J. Bricard, and D. Vigla, Heteromolecular nucleation theory applied to gas-to-particle conversion, *Atmos. Environ.*, **7**, 1279-1283, 1973.
- Kida, H., A numerical investigation of the atmospheric general circulation and stratospheric-tropospheric mass exchange. I. Long-term integration of a simplified general circulation model. II. Lagrangian motion of the atmosphere, *J. Meteorol. Soc. Japan*, **55**, 52-88, 1977.
- Kida, H., General circulation of air parcels and transport characteristics from a hemispheric GCM, Part 1. A determination of advective mass flow in the lower stratosphere, *J. Meteorol. Soc. Japan*, **61**, 171-188, 1983a.

## REFERENCES

- Kida, H., General circulation of air parcels and transport characteristics derived from a hemispheric GCM. Part 2. Very long-term motions of air parcels in the troposphere and stratosphere, *J. Meteorol. Soc. Japan*, *61*, 510-523, 1983b.
- Kida, H., A numerical experiment on the general circulation of the middle atmosphere with a three-dimensional model explicitly representing internal gravity waves and their breaking, *Pure Appl. Geophys.*, *122*, 731-746, 1985.
- Kiehl, J. T., The effect of aerosols on radiative damping rates in the stratosphere, paper presented at *Proceedings of the International Radiation Symposium*, Perugia, Italy, Aug. 21-26, 1984.
- Kiehl, J. T., The results cited under this citation refer to calculations performed by J. T. Kiehl employing the narrow band model described in Ramaswamy, V. and J. T. Kiehl, Sensitivities of the radiative forcing due to large loadings of smoke and dust aerosols, *J. Geophys. Res.*, *90*, 5597-5613, 1985.
- Kiehl, J. T., and V. Ramanathan, CO<sub>2</sub> radiative parameterization used in climate models: Comparison with narrow band models and with laboratory data, *J. Geophys. Res.*, *88*, 5191-5202, 1983.
- Kiehl, J. T., and S. Solomon, On the radiative balance of the stratosphere, *J. Atmos. Sci.*, *43*, in press, 1986.
- Kircher, C., and S. P. Sander, Kinetics and mechanism of HO<sub>2</sub> and DO<sub>2</sub> disproportionations, *J. Phys. Chem.*, *88*, 2082-2091, 1984.
- Kleinschmidt, E., Dynamic meteorology, in *Handbuch der Physik*, edited by A. Eliassen and E. Kleinschmidt, pp. 1-154, 1957.
- Kley, D., Ly( $\alpha$ ) absorption cross section of H<sub>2</sub>O and O<sub>2</sub>, *J. Atmos. Chem.*, *2*, 203-210, 1984.
- Kley, D., and E. J. Stone, A measurement of water vapor in the stratosphere by photodissociation with Ly ( $\alpha$ ) (1216Å) light, *Rev. Sci. Instrum.*, *49*, 691-697, 1978.
- Kley, D., E. J. Stone, W. R. Henderson, J. W. Drummond, W. Harrop, A. L. Schmeltekopf, and T. L. Thompson, *In situ* measurements of the mixing ratio of water vapor in the stratosphere, *J. Atmos. Sci.*, *36*, 2513-2534, 1979.
- Kley, D., J. W. Drummond, and A. L. Schmeltekopf, On the structure and microstructure of stratospheric water vapor, in *Atmospheric Water Vapor* edited by A. Deepak, T. D. Wilkinson, and L. H. Ruhke, pp. 315-327, Academic Press, New York, 1980.
- Kley, D., J. W. Drummond, M. McFarland, and S. C. Liu, Tropospheric profiles of NO<sub>x</sub>, *J. Geophys. Res.*, *86*, 3153-3161, 1981.
- Kley, D., A. L. Schmeltekopf, K. Kelley, R. H. Winkler, T. L. Thompson, and M. McFarland, Transport of water vapor through the tropical tropopause, *Geophys. Res. Lett.*, *9*, 617-620, 1982.
- Kley, D., A. L. Schmeltekopf, K. Kelly, R. H. Winkler, T. L. Thompson, and M. McFarland, The U2 Lyman-alpha hygrometer results from the 1980 Panama experiment, in *The 1980 Stratospheric-Tropospheric Exchange Experiment, NASA Tech Memo 84297*, edited by A. Margozzi, NASA Ames Research Center, Moffett Field, CA, 425 pp., 1983.
- Knapska, D., U. Schmidt, C. Jebsen, G. Kulesa, J. Rudolph and S. A. Penkett, Vertical profiles of chlorinated source gases in the mid-latitude stratosphere, in *Atmospheric Ozone*, edited by C. S. Zerefos and A. Ghazi, pp. 117-121, D. Reidel, Dordrecht, 1985a.
- Knapska, D., U. Schmidt, C. Jebsen, F. J. Johnen, A. Khedim, and G. Kulesa, A laboratory test of cryogenic sampling of long lived trace gases under simulated stratospheric conditions, in *Atmospheric Ozone*, edited by C. S. Zerefos and A. Ghazi, pp. 122-128, D. Reidel, Dordrecht, 1985b.
- Knight, W., D. R. Hastie, and B. A. Ridley, Measurements of nitric oxide during a stratospheric warming, *Geophys. Res. Lett.*, *9*, 489-492, 1982.
- Knittel, J., Ein Beitrag zur Klimatologi der Stratosphaere der Suedhalbkugel, *Meteor. Abh. der F.U., Berlin*, A2, Nr.1, 1976.
- Knollenberg, R. G., A. J. Dasher, and D. Huffman, Measurements of the aerosol and ice crystal population in tropical stratospheric cumulonimbus anvils, *Geophys. Res. Lett.*, *9*, 613-616, 1982.

## REFERENCES

- Knop, G., and F. Arnold, Nitric acid vapor measurements in the troposphere and lower stratosphere by chemical ionization mass spectrometry, *Geophys. Res. Lett.*, in press, 1985.
- Ko, M. K. W., and N. D. Sze, A 2-D model calculation of atmospheric lifetimes for N<sub>2</sub>O, CFC-11 and CFC-12, *Nature*, 297, 317-319, 1982.
- Ko, M. K. W., and N. D. Sze, Effect of recent data revisions on stratospheric modeling, *Geophys. Res. Lett.*, 10, 341-344, 1983.
- Ko, M. K. W., and N. D. Sze, Diurnal variation of ClO: Implications for the stratospheric chemistries of ClONO<sub>2</sub>, HOCl, and HCl, *J. Geophys. Res.*, 89, 11619-11632, 1984.
- Ko, M. K. W., N. D. Sze, M. Livshits, M. B. McElroy, and J. A. Pyle, The seasonal and latitudinal behavior of trace gases and O<sub>3</sub> as simulated by a two-dimensional model of the atmosphere, *J. Atmos. Sci.*, 41, 2381-2408, 1984.
- Ko, M. K. W., K. K. Tung, D. K. Weinstein, and N. D. Sze, A zonal-mean model of stratospheric tracer transport in isentropic coordinates: Numerical simulations for nitrous oxide and nitric acid, *J. Geophys. Res.*, 90, 2313-2329, 1985.
- Kobayashi, J., and Y. Toyama, On various methods of measuring the vertical distribution of atmospheric ozone 2, *Papers in Meteor. and Geoph.*, 17, 97-112, 1966.
- Kobayashi, J., M. Kyozuka, and H. Muamatsu, On various methods of measuring the vertical distribution of atmospheric ozone 1, *Papers in Meteor. and Geoph.*, 17, 76-96, 1966.
- Kohno, J., Stratospheric ozone transport due to transient large-amplitude planetary waves, *J. Meteorol. Soc. Japan*, 62, 413-439, 1984.
- Kohri, W. J., LRIR observations of the structure and propagation of the stationary planetary waves in the Northern Hemisphere during December 1975, Ph.D. thesis, *Cooperative Thesis No. 63*, Drexel Univ. and National Center for Atmospheric Research, Boulder, CO, 1981.
- Komhyr, W. D., A carbon-iodine sensor for atmospheric soundings, paper presented at *Proc. Ozone Symp.*, Albuquerque, NM, pp. 26-30, 1965.
- Komhyr, W. D., Electrochemical concentration cells for gas analysis, *Ann. Geoph.*, 25, 203-210, 1969.
- Komhyr, W. D., R. H. Gammon, J. Harriss, L. W. Waterman, T. J. Conway, W. R. Taylor, and K. W. Thoning, Global atmospheric CO<sub>2</sub> distribution and variation from 1968-1982 NOAA/GMCC flask sample data, *J. Geophys. Res.*, 90, 5567-5596, 1985.
- Kondo, Y., W. A. Matthews, A. Iwata, and M. Takagi, Measurements of nitric oxide from 7 to 32 km and its diurnal variation in the stratosphere, *J. Geophys. Res.*, 90, 3813-3820, 1985.
- Koyama, T., Gaseous metabolism in lake sediments and paddy soils and the production of atmospheric methane and hydrogen, *J. Geophys. Res.*, 68, 3971-3973, 1963.
- Koyama, T., Biogeochemical studies on lake sediments and paddy soils and the production of atmospheric methane and hydrogen, in *Recent Researches in the Fields of Hydrosphere, Atmosphere and Nuclear Geochemistry*, edited by Y. Miyake and T. Koyama, Water Research Laboratory, Nagoya University, Nagoya, Japan, 1964.
- Krey, P. W., R. J. Lagomarsino, and L. E. Toonkel, Gaseous halogens in the atmosphere in 1975, *J. Geophys. Res.*, 82, 1753-1766, 1977.
- Krishnamurti, T. N., The subtropical jet stream of winter, *J. Meteorol.*, 18, 172-191, 1961.
- Krueger, A. J., Rocket measurements of ozone over Hawaii, *Ann. Geoph.*, 25, 307-311, 1969.
- Krueger, A. J., and R. A. Minzner, A mid-latitude ozone model for the 1976 U.S. standard atmosphere, *J. Geophys. Res.*, 81, 4477-4481, 1976.
- Krueger, A. J., B. Guenther, A. J. Fleig, D. F. Heath, E. Hilsenrath, R. McPeters, and C. Prabakhara, Satellite ozone measurements, *Phil. Trans. Roy. Soc. London*, A296, 191-204, 1980a.
- Krueger, A. J., A. J. Fleig, J. A. Gatlin, D. F. Heath, P. K. Bhartia, V. G. Kaveeshwar, K. F. Klenk, and P. M. Smith, First results from the Nimbus 7 total ozone mapping spectrometer, in *Proceedings*

## REFERENCES

- Quadrennial International Ozone Symposium, Vol. I*, edited by J. London, pp. 322-327, IAMAP, NCAR, Boulder, CO, 1981.
- Krumins, M. V., and W. C. Lyons, Corrections for the upper atmosphere temperatures using a thin-film loop mount, *Tech. Rep. NOLTR 72-152*, 46 pp., U.S. Nav. Ordnance Lab., White Oak, MD, 1972.
- Kuhn, W. R., and J. London, Infrared radiative cooling in the middle atmosphere (30-110 km), *J. Atmos. Sci.*, *26*, 189-204, 1969.
- Kulcke, W., and H. K. Paetzold, Uber eine radiosonde zur bestimmung der vertikalen ozonverteilung, *Ann. Meteorol.*, *8*, 47-53, 1957.
- Kunde, V., B. Conrath, R. Hanel, J. Herman, D. Jennings, W. Maguire, J. Brasunas, H. Buijs, J. Berike, and J. McKinnon, Measurement of lower stratosphere gaseous constituents with a balloon-borne cryogenic spectrometer, *J. Geophys. Res.*, in press, 1985.
- Kurzeja, R. J., The transport of trace chemicals by planetary waves in the stratosphere. Part 1: Steady waves, *J. Atmos. Sci.*, *38*, 2779-2788, 1981.
- Kurzeja, R. J., K. V. Haggard, and W. L. Grose, Numerical experiments with a general circulation model concerning the distribution of ozone in the stratosphere, *J. Atmos. Sci.*, *41*, 2029-2051, 1984.
- Kutepov, A. A., and G. M. Shved, Radiative transfer in the 15  $\mu\text{m}$  CO<sub>2</sub> band with non-LTE in the Earth's atmosphere, *Izves. Atmos. and Ocean. Phys.*, *14*, 28-43, 1978.
- Labitzke, K., The interaction between stratosphere and mesosphere in winter, *J. Atmos. Sci.*, *29*, 1395-1399, 1972.
- Labitzke, K., The temperature in the upper stratosphere: Differences between hemispheres, *J. Geophys. Res.*, *79*, 2171-2175, 1974.
- Labitzke, K., Comparison of the stratospheric temperature distribution over Northern and Southern Hemispheres, *COSPAR Space Research, XVII*, 159-165, 1977.
- Labitzke, K., The major stratospheric warming during January/February 1979, *Beilage zur Berliner Wetterkarte*, *8.5*, 1979.
- Labitzke, K., Stratospheric-mesospheric midwinter disturbances: A summary of observed characteristics, *J. Geophys. Res.*, *86*, 9665-9678, 1981.
- Labitzke, K., On the interannual variability of the middle stratosphere during the northern winters, *J. Meteorol. Soc. Japan*, *60*, 124-139, 1982.
- Labitzke, K., A survey over the PMP-1 winters 1978/79-1981/82 in comparison with earlier winters, *Adv. Space Res.*, *2*, 149-157, 1983.
- Labitzke, K., On the interannual variability of the middle atmosphere during winter, in *Handbook for MAP, Vol. 18*, edited by S. Kato, pp. 1-9, SCOSTEP Secretariat, Univ. of Illinois, Urbana, 1985.
- Labitzke, K., and J. J. Barnett, Review of climatological information obtained from remote sensing of the stratosphere and mesosphere, *Space Res.*, *19*, 97-106, 1979.
- Labitzke, K., and B. Naujokat, On the variability and on trends of temperature in the middle stratosphere, *Beitr. Phys. Atmosph.*, *56*, 495-507, 1983.
- Labitzke, K., and B. Naujokat, An update of the observed QBO of the stratospheric temperatures over the Northern Hemisphere, *Geophys. Res. Lett.*, in press, 1986.
- Labitzke, K., R. Lenschow, B. Naujokat, and K. Petzoldt, The second winter of PMP-1: 1979/80, *Beilage zur Berliner Wetterkarte*, *2.4*, 1980.
- Labitzke, K., R. Lenschow, and B. Naujokat, The third winter of PMP-1: 1980/81, *Beilage zur Berliner Wetterkarte*, *16.7*, 1981.
- Labitzke, K., B. Naujokat, and M. P. McCormick, Temperature effects on the stratosphere of the April 4, 1982 eruption of El Chichon, Mexico, *Geophys. Res. Lett.*, *10*, 24-26, 1983.
- Labitzke, K., J. J. Barnett and B. Edwards (Eds.), *Draft of a New Reference Middle Atmosphere, Handbook for MAP, Vol. 16*, 318 pp., SCOSTEP Secretariat, Univ. of Illinois, Urbana, 1985.

## REFERENCES

- Labitzke, K., G. Brasseur, B. Naujokat, and A. de Rudder, Long-term temperature trends in the stratosphere: Possible influence of antropogenic gases, *Geophys. Res. Lett.*, *13*, 1152-1155, 1986.
- Lacis, A., Chlorofluorocarbons and stratospheric ozone, in *Global Environmental Problems*, edited by S. F. Singer, Paragon House, New York, in press, 1985.
- Lacis, A. A., and J. E. Hansen, A parameterization for the absorption of solar radiation in the Earth's atmosphere, *J. Atmos. Sci.*, *31*, 118-133, 1974.
- Lacis, A., J. Hansen, P. Lee, T. Mitchell, and S. Lebedeth, Greenhouse effect of trace gases, *Geophys. Res. Lett.*, *8*, 1035-1038, 1981.
- Lacome, N., A. Levy, and C. Boulet, Air broadened line width of nitrous oxide: An improved calculation, *J. Mol. Spectrosc.*, *97*, 139-153, 1983.
- Lal, S., R. Borchers, P. Fabian, and B. C. Krueger, Increasing abundance of CBrClF<sub>2</sub> in the atmosphere, *Nature*, *316*, 135-136, 1985.
- Lau, K-M, and P. H. Chan, Short term climate variability and atmospheric teleconnections from satellite-observed outgoing longwave radiation. Part I: Simultaneous relationships, *J. Atmos. Sci.*, *40*, 2735-2750, 1983.
- Laurent, J., M. P. Lemaître, C. Lippens, and C. Muller, *L'Aeronautique et l'Astronautique*, *98*, 60-61, 1983.
- Laurent, J., M. P. Lemaître, J. Besson, A. Girard, C. Lippens, C. Muller, J. Vercheval, and M. Ackerman, Middle atmosphere NO and NO<sub>2</sub> observed by means of the Spacelab 1 grille spectrometer, *Nature*, in press, 1985.
- Lazrus, A. L., and B. W. Gandrud, Distribution of stratospheric nitric acid vapor, *J. Atmos. Sci.*, *31*, 1102-1108, 1974.
- Lazrus, A. L., B. W. Gandrud, R. N. Woodard, and W. A. Sedlacek, Direct measurements of stratospheric chlorine and bromine, *J. Geophys. Res.*, *81*, 1067-1090, 1976.
- Lean, J. L., Estimating the variability of the solar flux between 200 and 300 nm, *J. Geophys. Res.*, *89*, 1-9, 1984.
- Lean, J. L., and A. Skumanich, Variability of the Lyman alpha flux with solar activity, *J. Geophys. Res.*, *88*, 5751-5759, 1983.
- Lean, J. L., O. R. White, W. C. Livingston, D. F. Heath, R. F. Donnelly, and A. Skumanich, A three component model of the variability of the solar ultraviolet flux: 145-200 nm, *J. Geophys. Res.*, *87*, 10307-10317, 1982.
- Leifer, R., R. Larsen, and L. Toonkel, Stratospheric distributions and inventories of trace gases in the Northern Hemisphere for 1976, *Report EML-349, I-211*, Environmental Measurements Lab., New York, 1979a.
- Leifer, R., L. Toonkel, and R. Larsen, Project airstream, trace gases in the stratosphere, *Report EML-349, II-107*, Environmental Measurements Lab., New York, 1979b.
- Leifer, R., K. C. Sommers, and S. F. Guggenheim, Atmospheric trace gas measurements with a new clean air sampling system, *Geophys. Res. Lett.*, *8*, 1079-1081, 1981.
- Leighton, H., Influence of Arctic haze on the solar radiation budget, *Atmos. Environ.*, *17*, 2065-2068, 1983.
- Leighton, P. A., *Photochemistry of Air Pollution*, Academic Press, New York, 1961.
- Lemaître, M. P., J. Laurent, J. Besson, A. Girard, C. Lippens, C. Muller, J. Vercheval, and M. Ackerman, Sample performance of the grille spectrometer, *Science*, *225*, 171-172, 1984.
- Lenoble, J., A general survey of the problem of aerosol climatic impact, in *Aerosols and Their Climatic Effects*, edited by H. E. Gerber and A. Deepak, pp. 279-294, A. Deepak Publ., Hampton, VA, 1984.
- Lenoble, J., D. Tanre, P. Y. Deschamps, and M. Hessman, A simple method to compute the change in earth-atmosphere radiative balance due to a stratospheric aerosol layer, *J. Atmos. Sci.*, *39*, 2565-2576, 1982.

## REFERENCES

- Lenschow, D. H., R. Pearson, Jr., and B. B. Stankov, Measurements of ozone vertical flux to ocean and forest, *J. Geophys. Res.*, **87**, 8833-8837, 1982.
- Leone, J. A., and J. H. Seinfeld, Analysis of the characteristics of complex chemical reaction mechanisms: Application to photochemical smog chemistry, *Environ. Sci. Technol.*, **18**, 280-287, 1984a.
- Leone, J. A., and J. H. Seinfeld, Updated chemical mechanism for atmospheric photooxidation of toluene, *Int. J. Chem. Kinet.*, **16**, 159-193, 1984b.
- Leovy, C. B., Simple models of thermally driven mesospheric circulations, *J. Atmos. Sci.*, **21**, 327-341, 1964a.
- Leovy, C. B., Radiative equilibrium of the mesosphere, *J. Atmos. Sci.*, **21**, 238-248, 1964b.
- Leovy, C. B., and P. J. Webster, Stratospheric long waves: Comparison of thermal structure in the northern and southern hemispheres, *J. Atmos. Sci.*, **33**, 1624-1638, 1976.
- Leovy, C. B., C. R. Sun, M. H. Hitchman, E. E. Remsberg, J. M. Russell III, L. L. Gordley, J. C. Gille, and L. V. Lyjak, Transport of ozone in the middle stratosphere: Evidence for planetary wave breaking, *J. Atmos. Sci.*, **42**, 230-244, 1985.
- Lesclaux, R., and F. Caralp, Determination of the rate constants for the reactions of  $\text{CFCl}_2\text{O}_2$  radical with NO and  $\text{NO}_2$  by laser photolysis and time resolved mass spectrometry, *Int. J. Chem. Kinet.*, **16**, 1117-1128, 1984.
- Leu, M. T., Kinetics of the reaction  $\text{O} + \text{ClO} \rightarrow \text{Cl} + \text{O}_2$ , *J. Phys. Chem.*, **88**, 1394-1398, 1984.
- Levine, J. S., C. P. Rinsland, and G. M. Tennille, The photochemistry of methane and carbon monoxide in the troposphere in 1950 and 1985, *Nature*, **318**, 254-257, 1985.
- Levine, S. Z., and S. E. Schwartz, In-cloud and below-cloud scavenging of nitric acid vapor, *Atmos. Environ.*, **16**, 1725-1734, 1982.
- Levy II, H., Normal atmosphere: Large radical and formaldehyde concentrations predicted, *Science*, **173**, 141-143, 1971.
- Levy II, H., Photochemistry of the lower troposphere, *Planet. Space Sci.*, **20**, 919-935, 1972.
- Levy II, H., J. D. Mahlman, and W. J. Moxim, A preliminary report on the numerical simulation of the three-dimensional structure and variability of atmospheric  $\text{N}_2\text{O}$ , *Geophys. Res. Lett.*, **6**, 155-158, 1979.
- Levy II, H., J. D. Mahlman, and W. J. Moxim, A stratospheric source of reactive nitrogen in the unpolluted troposphere, *Geophys. Res. Lett.*, **7**, 441-444, 1980.
- Levy II, H. B., J. D. Mahlman, W. J. Moxim, and S. C. Liu, Tropospheric ozone: The role of transport, *J. Geophys. Res.*, **90**, 3753-3771, 1985.
- Lewis, B. R., I. M. Vardavas, and J. H. Carver, The aeronomic dissociation of water vapor by H Lyman alpha radiation, *J. Geophys. Res.*, **88**, 4935-4940, 1983.
- Lilly, D. K., D. E. Waco, and S. I. Adelfang, Stratospheric mixing estimated from high-altitude turbulence measurements, *J. Appl. Meteorol.*, **13**, 488-493, 1974.
- Lin, B. D., The behavior of winter stationary planetary waves forced by topography and diabatic heating, *J. Atmos. Sci.*, **39**, 1206-1226, 1982.
- Lindzen, R. S., Some speculations on the roles of critical level interactions between internal gravity waves and mean flows, in *Acoustic-Gravity Waves in the Atmosphere-Symposium Proceedings*, edited by T. M. Georges, Environmental Science Services Administration, Boulder, CO, 427 pp., 1968.
- Lindzen, R. S., Turbulence and stress owing to gravity and tidal breakdown, *J. Geophys. Res.*, **86**, 9707-9714, 1981.
- Lindzen, R. S., and J. R. Holton, A theory of the quasi-biennial oscillation, *J. Atmos. Sci.*, **25**, 1095-1107, 1968.
- Lindzen, R. S., and C. Y. Tsay, Wave structure of the tropical stratosphere over the Marshall Islands area during 1 April-1 July 1958, *J. Atmos. Sci.*, **22**, 2008-2021, 1975.

## REFERENCES

- Lindzen, R. S., D. M. Straus, and B. Katz, An observational study of large-scale atmospheric Rossby waves during FGGE, *J. Atmos. Sci.*, *41*, 1320-1335, 1984.
- Ling, X., and J. London, A theoretical study of the quasi-biennial oscillation in the tropical stratosphere, in *Atmospheric Ozone*, edited by C. S. Zerefos and A. Ghazi, pp. 53-58, D. Reidel, Dordrecht, 1985.
- Lippens, C., and C. Muller, Atmospheric nitric acid and chlorofluoromethane 11 from interferometric spectra obtained at the Observatoires du Pic du Midi, *J. Optics (Paris)*, *12*, 331-336, 1981.
- Lippens, C., C. Muller, J. Vercheval, M. Ackerman, J. Laurent, M. P. Lemaitre, J. Besson, and A. Girard, Trace constituents measurements deduced from spectrometric observations onboard Spacelab, *Adv. Space Res.*, *4*, 75-79, 1984.
- Lipschultz, F., O. C. Zafiriou, S. C. Wofsy, M. B. McElroy, F. W. Valois, and S. W. Watson, Production of NO and N<sub>2</sub>O by soil nitrifying bacteria: A source of atmospheric nitrogen oxides, *Nature*, *294*, 641-643, 1981.
- Liu, S. C., and G. C. Reid, Sodium and other minor constituents of meteoric origin in the atmosphere, *Geophys. Res. Lett.*, *6*, 283-286, 1979.
- Liu, S. C., T. M. Donahue, R. J. Cicerone, and W. L. Chameides, Effect of water vapor on the destruction of ozone in the stratosphere perturbed by Cl<sub>x</sub> or NO<sub>x</sub> pollutants, *J. Geophys. Res.*, *81*, 3111-3118, 1976.
- Liu, S. C., D. Kley, M. McFarland, J. D. Mahlman, and H. Levy II, On the origin of tropospheric ozone, *J. Geophys. Res.*, *85*, 7546-7552, 1980.
- Liu, S. C., M. McFarland, D. Kley, O. Zafiriou, and B. J. Huebert, Tropospheric NO<sub>x</sub> and O<sub>3</sub> budgets in the equatorial Pacific, *J. Geophys. Res.*, *88*, 1360-1368, 1983.
- Loewenstein, M., W. J. Starr, and D. G. Murcray, Stratospheric NO and HNO<sub>3</sub> observations in the Northern Hemisphere for three seasons, *Geophys. Res. Lett.*, *5*, 531-534, 1978a.
- Loewenstein, M., W. J. Borucki, H. F. Savage, J. G. Borucki, and R. C. Whitten, Geographical variations of NO and O<sub>3</sub> in the lower stratosphere, *J. Geophys. Res.*, *83*, 1874-1882, 1978b.
- Logan, J. A., Nitrogen oxides in the troposphere: Global and regional budgets, *J. Geophys. Res.*, *88*, 10785-10807, 1983.
- Logan, J. A., Tropospheric ozone: Seasonal behavior, trends and anthropogenic influence, *J. Geophys. Res.*, *90*, 10463-10482, 1985.
- Logan, J. A., M. J. Prather, S. C. Wofsy, and M. B. McElroy, Atmospheric chemistry: Response to human influence, *Phil. Trans. Roy. Soc. London*, *A290*, 187-234, 1978.
- Logan, J. A., M. J. Prather, S. C. Wofsy, and M. B. McElroy, Tropospheric chemistry: A global perspective, *J. Geophys. Res.*, *86*, 7210-7254, 1981.
- London, J., Radiative energy sources and sinks in the stratosphere and mesosphere, in *Proceedings of the NATO Advanced Study Institute on Atmospheric Ozone: Its Variation and Human Influences, Rep. FAA-EE-80-20*, edited by A. C. Aikin, pp. 703-721, DOT, FAA, Washington, DC, 1980a.
- London, J., The observed distribution and variations of total ozone, in *Proceedings of the NATO Advanced Study Institute on Atmospheric Ozone: Its Variation and Human Influences, Report FAA-EE-80-20*, edited by A. C. Aikin, pp. 31-44, DOT, FAA, Washington, DC, 1980b.
- London, J., and J. Park, Application of general circulation models to the study of stratospheric ozone, *Pure Appl. Geophys.*, *106-108*, 1611-1617, 1973.
- London, J., and J. Park, The interaction of ozone photochemistry and dynamics in the stratosphere: A three-dimensional stratospheric model, *Can. J. Chem.*, *62*, 1599-1609, 1974.
- London, J., B. D. Bojkov, S. Oltmans, and J. F. Kelly, Atlas of the global distribution of total ozone, July 1957-July 1967, *Tech. Note NCAR/TN/113 + STR*, Nat. Center for Atmos. Res., Boulder, CO, Jan., 1976.

## REFERENCES

- London, J., J. E. Frederick, and G. P. Anderson, Satellite observations of the global distribution of stratospheric ozone, *J. Geophys. Res.*, 82, 2543-2556, 1977.
- London, J., G. G. Bjarnason, and G. J. Rottman, 18 months of UV irradiance observations from the Solar Mesosphere Explorer, *Geophys. Res. Lett.*, 11, 54-56, 1984.
- Lorenc, A. C., The evolution of the planetary scale 200 mb divergent flow during the FGGE year, *Quart. J. Roy. Meteorol. Soc.*, 110, 427-441, 1984.
- Lorenz, E. N., The nature and theory of the general circulation of the atmosphere, *WMO No 218*, WMO, 1967.
- Louis, J. F., A two-dimensional transport model of the atmosphere, Ph.D. thesis, Univ. of Colorado, Boulder, CO, 1974.
- Louisnard, N., and O. Lado-Bordowsky, Spectroscopic measurements of carbon monoxide in the stratosphere, *J. Geophys. Res.*, 88, 3781-3797, 1983.
- Louisnard, N., and S. Pollitt, Measurements of neutral constituents using infrared and visible remote sensing, in *Handbook for MAP, Vol. 15*, edited by D. G. Murcray, pp. 37-70, SCOSTEP Secretariat, Univ. of Illinois, Urbana, 1985.
- Louisnard, N., A. Girard, and G. Eichen, Mesures du profil vertical de concentration de la vapeur d'eau stratospherique, *C. R. Acad. Sc. Paris*, 290, 385-388, 1980.
- Louisnard, N., G. Fergant, A. Girard, L. Gramont, O. Lado-Bordowsky, J. Laurent, S. Le Boiteau, and M. P. Lemaitre, Infrared absorption spectroscopy applied to stratospheric profiles of minor constituents, *J. Geophys. Res.*, 88, 5365-5376, 1983.
- Lovelock, J. E., Atmospheric halocarbons and stratospheric ozone, *Nature*, 252, 292-294, 1974.
- Lovelock, J. E., Methyl chloroform in the troposphere as an indicator of OH radical abundance, *Nature*, 267, 32, 1977.
- Ludlam, F. H., *Clouds and Storms, Chapter 8*, Pennsylvania State University Press, University Park, PA, 1980.
- Luther, F., Commentary on climatic effects of minor atmospheric constituents, in *Carbon Dioxide Review*, edited by W. C. Clark, pp. 290-294, Clarendon Press, New York, 1982.
- Luther, F. M., and Y. Fouquart, *WMO Report WCP-93*, 37 pp., Geneva, 1984.
- Luther, F., D. J. Wuebbles, and J. S. Chang, Temperature feedback in a stratospheric model, *J. Geophys. Res.*, 82, 4935-4942, 1977.
- Madden, R. A., Oscillations in the winter stratosphere. 2: The role of horizontal heat transport and the interaction of transient and stationary planetary-scale waves, *Mon. Weather Rev.*, 103, 717-719, 1975.
- Madden, R. A., Evidence for large-scale regularly propagating waves in a 73-year data set, in *Extended Summaries of Contributions, IAGA/IAMAP*, Seattle, Washington, International Assoc. for Atmos. Phys., NCAR, Boulder, CO, 1977.
- Madden, R. A., Further evidence of traveling planetary waves, *J. Atmos. Sci.*, 35, 1605-1618, 1978.
- Madden, R. A., The effect of the interference of traveling and stationary waves on time variations of the large-scale circulation, *J. Atmos. Sci.*, 40, 1110-1125, 1983.
- Madden, R. A., and P. R. Julian, Detection of a 40-50 day oscillation in the zonal wind in the tropical Pacific, *J. Atmos. Sci.*, 28, 702-708, 1971.
- Madden, R. A., and P. R. Julian, Descriptions of global scale circulation cells in the tropics with a 40-50 period, *J. Atmos. Sci.*, 29, 1109-1123, 1972a.
- Madden, R. A., and P. Julian, Further evidence of global-scale 5-day pressure waves, *J. Atmos. Sci.*, 29, 1464-1469, 1972b.
- Madden, R. A., and P. Julian, Reply to comments by R. Deland, *J. Atmos. Sci.*, 30, 935-940, 1973.
- Madden, R. A., and K. Labitzke, A free Rossby wave in the troposphere and stratosphere during January 1979, *J. Geophys. Res.*, 86, 1247-1254, 1981.

## REFERENCES

- Madronich, S., D. R. Hastie, B. A. Ridley, and H. I. Schiff, Measurement of the photodissociation coefficient of NO<sub>2</sub> in the atmosphere, I. Method and surface measurements, *J. Atmos. Chem.*, *1*, 3-25, 1983.
- Mahlman, J. D., Relation of stratospheric-tropospheric mass exchange mechanisms to surface radioactivity peaks, *Arch. Met. Geoph. Biokl. A.*, *15*, 1-25, 1965.
- Mahlman, J. D., Long-term dependence of surface fallout fluctuations upon tropopause-level cyclogenesis, *Arch. Met. Geoph. Biokl. A.*, *18*, 299-311, 1969a.
- Mahlman, J. D., Heat balance and mean meridional circulations in the polar stratosphere during the sudden warming of January 1958, *Mon. Weather Rev.*, *97*, 534-540, 1969b.
- Mahlman, J. D., On the maintenance of the polar front jet stream, *J. Atmos. Sci.*, *30*, 544-557, 1973.
- Mahlman, J. D., Some fundamental limitations of simplified transport models as implied by results from a three-dimensional general circulation/tracer model, in *Proceedings Fourth Conference Climatic Impact Assessment Program, DOT-TSC-OST-75-38*, edited by T. M. Hard and A. J. Broderick, pp. 132-146, Transportation Systems Command, Cambridge, MA, 1975.
- Mahlman, J. D., Coupling in atmospheric observations with comprehensive numerical models, *Proc. of ICMUA Sessions and IUGG Symposium 18, XVII IUGG General Assembly, Canberra, Australia*, *18*, pp. 253-259, 1980.
- Mahlman, J. D., "Strategies for equatorial lower stratospheric measurements" and "The status of stratospheric general circulation models", papers presented at International Workshop on Current Issues in our Understanding of the Stratosphere and the Future of the Ozone Layer, BMFT, NASA, FAA, WMO, Feldafing, FRG, June 11-16, 1984.
- Mahlman, J. D., Mechanistic interpretation of stratospheric tracer transport, *Issues in Atmos. and Oceanic Modelling, J. Smagorinsky Comm. Vol.*, 1985.
- Mahlman, J. D., and W. J. Moxim, Tracer simulation using global circulation model: results from a midlatitude instantaneous source experiment, *J. Atmos. Sci.*, *35*, 1340-1374, 1978.
- Mahlman, J. D., and R. W. Sinclair, Recent results from the GFDL troposphere-stratosphere-mesosphere general circulation model, *Proc. of ICMUA Sessions and IUGG Symposium 18, XVII IUGG General Assembly, Canberra, Australia*, 11-18, 1980.
- Mahlman, J. D., and L. J. Umscheid, Dynamics of the middle atmosphere: Successes and problems of the GFDL "SKYHI" general circulation model, in *Dynamics of the Middle Atmosphere*, edited by J. R. Holton and T. Matsuno, pp. 501-525, Terrapub, Tokyo, 1984.
- Mahlman, J. D., H. B. Levy II, and W. J. Moxim, Three-dimensional tracer structure and behavior as simulated in two ozone precursor experiments, *J. Atmos. Sci.*, *37*, 655-685, 1980.
- Mahlman, J. D., D. G. Andrews, H. U. Duetsch, D. L. Hartmann, T. Matsuno, R. J. Murgatroyd, and J. F. Noxon, Transport of trace constituents in the stratosphere, in *Handbook for MAP, Vol. 3*, edited by C. F. Sechrist, Jr., pp. 14-43, SCOSTEP Secretariat, Univ. of Illinois, Urbana, 1981.
- Mahlman, J. D., D. G. Andrews, D. L. Hartmann, T. Matsuno, and R. G. Murgatroyd, Transport of trace constituents in the stratosphere, in *Dynamics of the Middle Atmosphere*, edited by J. R. Holton and T. Matsuno, pp. 387-416, Terrapub, Tokyo, 1984.
- Mahlman, J. D., H. B. Levy II, and W. J. Moxim, Three dimensional simulations of stratospheric N<sub>2</sub>O: Predictions for other trace constituents, *J. Geophys. Res.*, in press, 1985.
- Maier, E. J., A. C. Aikin, and J. E. Ainsworth, Stratospheric nitric oxide and ozone measurements using photoionization mass spectrometry and UV absorption, *Geophys. Res. Lett.*, *5*, 37-40, 1978.
- Maki, A. G., F. J. Lovas, and W. B. Olson, Infrared frequency measurements on the ClO fundamental band, *J. Mol. Spectros.*, *92*, 410-418, 1982.
- Makide, Y., and F. S. Rowland, Tropospheric concentrations of methyl chloroform, CH<sub>3</sub>CCl<sub>3</sub>, in January 1978 and estimates of atmospheric residence times for hydrocarbons, *Proceedings Natl. Acad. Sci., USA*, 5933-5937, 1981.

## REFERENCES

- Malcolm, K. W., K. O. Nien, and D. A. K. Sze, A 2-D model calculation of atmospheric lifetimes for  $N_2O$ , CFC-11 and CFC-12, *Nature*, 297, 317-319, 1982.
- Malko, M. W., and J. Troe, Analysis of the unimolecular reaction  $N_2O_5 + M \rightarrow NO_2 + NO_3 + M$ , *Int. J. Chem. Kinet.*, 14, 399-416, 1982.
- Malkmus, W., Random Lorentz band model with exponential tailed  $S^{-1}$  line-intensity distribution, *J. Opt. Soc. Amer.*, 57, 323-329, 1967.
- Malkus, J. S., Large-scale interactions, in *The Sea, Vol. 1*, edited by M. N. Hill, Interscience Publishers, New York, 1962.
- Manabe, S., and B. G. Hunt, Experiments with a stratospheric general circulation model: I. radiative and dynamic effects, *Mon. Weather Rev.*, 96, 477-539, 1968.
- Manabe, S., and J. D. Mahlman, Simulation of seasonal and interhemispheric variations in the stratospheric circulation, *J. Atmos. Sci.*, 33, 2185-2217, 1976.
- Manabe, S., and R. J. Stouffer, Sensitivity of a global climate model to an increase of  $CO_2$  concentration in the atmosphere, *J. Geophys. Res.*, 85, 5529-5554, 1980.
- Manabe, S., and R. T. Wetherald, Thermal equilibrium of the atmosphere with a given distribution of relative humidity, *J. Atmos. Sci.*, 24, 241-259, 1967.
- Manabe, S., and R. T. Wetherald, The effects of doubling the  $CO_2$  concentration on the climate of a general circulation model, *J. Atmos. Sci.*, 32, 3-15, 1975.
- Manabe, S., and R. T. Wetherald, On the distribution of climate change resulting from an increase in  $CO_2$ -content of the atmosphere, *J. Atmos. Sci.*, 37, 99-118, 1980.
- Mankin, W. G., and M. T. Coffey, Latitudinal distributions and temporal changes of stratospheric HCl and HF, *J. Geophys. Res.*, 88, 10776-10784, 1983.
- Mankin, W. G., and M. T. Coffey, Increased stratospheric hydrogen chloride in the El Chichon cloud, *Science*, 226, 170-172, 1984.
- Mankin, W. G., M. T. Coffey, D. W. T. Griffith, and S. R. Drayson, Spectroscopic measurement of carbonyl sulfide (OCS) in the stratosphere, *Geophys. Res. Lett.*, 6, 853-856, 1979.
- Mankin, W. G., M. T. Coffey, K. V. Chance, W. A. Traub, B. Carli, A. Bonetti, I. G. Nolt, R. Zander, D. W. Johnson, G. Stokes, and C. B. Farmer, Intercomparison of measurements of stratospheric hydrogen fluoride, to be published, 1986.
- Manson, A. H., C. E. Meek, and J. G. Gregory, Winds and waves (10 min - 30 days) in the mesosphere and lower thermosphere at Saskatoon ( $32^\circ N$ ,  $107^\circ W$ ,  $L=4.3$ ) during the year October 1979 to July 1980, *J. Geophys. Res.*, 86, 9615-9625, 1981.
- Marche, P., and C. Meunier, Atmospheric trace species measured above Haute-Provence Observatory, *Planet. Space Sci.*, 31, 731-733, 1983.
- Marche, P., A. Barbe, C. Secroun, J. Corr, and P. Jouve, Ground based spectroscopic measurements of HCl, *Geophys. Res. Lett.*, 7, 869-872, 1980a.
- Marche, P., A. Barbe, C. Secroun, J. Corr, and P. Jouve, Mesures des acides fluorhydrique et chlorhydrique dans l'atmosphère par spectroscopie infrarouge a partir du sol, *C. R. Acad. Sc. Paris*, 290B, 369-371, 1980b.
- Marche, P., C. Meunier, A. Barbe, and P. Jouve, Total atmospheric ozone measured by ground based high resolution infrared spectra-comparison with Dobson measurements, *Planet. Space Sci.*, 31, 723-727, 1983.
- Margitan, J. J., Chlorine nitrate: The sole product of the  $ClO + NO_2 + M$  recombination, *J. Geophys. Res.*, 88, 5416-5420, 1983.
- Margitan, J. J., Kinetics of the reaction  $O + ClO \rightarrow Cl + O_2$ , *J. Phys. Chem.*, 88, 3638-3643, 1984a.
- Margitan, J. J., Mechanisms of the atmospheric oxidation of sulfur dioxide catalysis by hydroxyl radicals, *J. Phys. Chem.*, 88, 3314-3318, 1984b.

## REFERENCES

- Maroulis, P. J., A. I. Torres, and A. R. Bandy, Atmospheric concentrations of carbonyl sulfide in the southwestern and eastern United States, *Geophys. Res. Lett.*, 4, 510-512, 1977.
- Martin, L. R., H. S. Judeikis, and M. Wu, Heterogeneous reactions of Cl and ClO in the stratosphere, *J. Geophys. Res.*, 85, 5511-5518, 1980.
- Maruyama, T., Long-term behavior of Kelvin waves and mixed Rossby-gravity waves, *J. Meteorol. Soc. Japan*, 47, 245-254, 1969.
- Mason, C. J., and J. J. Horvath, The direct measurement of nitric oxide concentration in the upper atmosphere by a rocket-borne chemiluminescent detector, *Geophys. Res. Lett.*, 3, 391-394, 1976.
- Massman, W. J., An investigation of gravity waves on a global scale using TWERLE data, *J. Geophys. Res.*, 86, 4072-4082, 1981.
- Mastenbrook, H. J., Water vapor distribution in the stratosphere and high troposphere, *J. Atmos. Sci.*, 25, 299-311, 1968.
- Mastenbrook, H. J., and S. J. Oltmans, Stratospheric water vapor variability for Washington, DC/Boulder, CO: 1964-82, *J. Atmos. Sci.*, 40, 2157-2165, 1983.
- Mateer, C. L., and I. A. Asbridge, On the appropriate haze correction for direct sun total ozone measurements with the Dobson spectrophotometer, in *Proceedings of the Quadrennial International Ozone Symposium, Vol. I*, edited by J. London, pp. 236-242, IAMAP, NCAR, Boulder, CO, 1981.
- Mateer, C. L., and J. J. DeLuisi, The estimation of the vertical distribution of ozone by the short Umkehr method, in *Proceedings of the Quadrennial International Ozone Symposium, Vol. I*, edited by J. London, pp. 64-73, IAMAP, NCAR, Boulder, CO, 1981.
- Mateer, C. L., and H. U. Duetsch, Uniform evaluation of Umkehr observations from the World Ozone Network: Part 1, Proposed standard Umkehr evaluation technique, Nat'l Center for Atmos. Res., Boulder, Colorado, 1964.
- Mathews, E. I. Fung, and S. Ross, Atmospheric methane: Global distributions of biogenic source locations, in press, 1986.
- Matson, M., Eruptions of El Chichon volcano, in *Radiative Effects of the El Chichon Volcanic Eruption: Preliminary Results Concerning Remote Sensing, NASA Tech. Memo. 84959*, edited by W. R. Bandeen and R. S. Fraser, 103 pp., NASA Goddard Space Flight Center, Greenbelt, MD, 1982.
- Matsuno, T., Vertical propagation of stationary planetary waves in the winter Northern Hemisphere, *J. Atmos. Sci.*, 27, 871-883, 1970.
- Matsuno, T., A dynamical model of the stratospheric sudden warming, *J. Atmos. Sci.*, 28, 1479-1494, 1971.
- Matsuno, T., Lagrangian motion of air parcels in the stratosphere in the presence of planetary waves, *Pure Appl. Geophys.*, 118, 189-216, 1980.
- Matsuno, T., A quasi one-dimensional model of the middle atmosphere circulation interacting with internal gravity waves, *J. Meteorol. Soc. Japan*, 60, 215-226, 1982.
- Mattingly, S. R., The contribution of extratropical severe storms to the stratospheric water vapour budget, *Met. Mag.*, 106, 256-262, 1977.
- Mayer, E. W., D. R. Blake, S. C. Tyler, Y. Makide, D. C. Montague, and F. S. Rowland, Methane: Interhemispheric concentration gradient and atmospheric residence time, *Proc. Nat. Acad. Sci., USA*, 79, 1366-1370, 1982.
- McClatchey, R. S., R. W. Fenn, J. E. A. Selby, F. E. Volz, and J. S. Garing, Optical properties of the atmosphere, *AFCRC-71-0279*, 85 pp., Air Force Cambridge Res. Lab., Bedford, MA, 1971.
- McClatchey, R. A., W. S. Benedict, S. A. Clough, D. E. Burch, R. F. Calfee, K. Fox, L. S. Rothman, and J. S. Garing, AFCRL atmospheric absorption line parameters compilation, *AFCRL-TR-73-0096*, 83 pp., Air Force Cambridge Research Laboratory Report, Hanscom AFB, MA, 1973.
- McCormick, M. P., and T. J. Swisler, Stratospheric aerosol mass and latitudinal distribution of the El Chichon eruption cloud for October 1982, *Geophys. Res. Lett.*, 10, 877-880, 1983.

## REFERENCES

- McCormick, M. P., P. Hamill, T. J. Pepin, W. P. Chu, T. J. Swissler, and L. R. McMaster, Satellite studies of the stratospheric aerosol, *Bull. Amer. Meteor. Soc.*, **60**, 1038-1046, 1979.
- McCormick, M. P., H. M. Steele, P. Hamill, W. P. Chu, and T. J. Swissler, Polar stratospheric cloud sightings by SAM II, *J. Atmos. Sci.*, **39**, 1387-1397, 1982.
- McCormick, M. P., T. J. Swissler, E. Hilsenrath, A. J. Krueger, and M. T. Osborn, Satellite and correlative measurements of stratospheric ozone; Comparison of measurements made by SAGE, ECC balloons, chemiluminescent and optical rocketsondes, *J. Geophys. Res.*, **89**, 5315-5320, 1984.
- McCormick, M. P., T. J. Swissler, W. H. Fuller, W. H. Hunt, M. T. Osborn, Airborne and ground-based lidar measurements of the El Chichon stratospheric aerosol from 90N to 56S, *Geof. Int.*, **23-2**, 187-221, 1984.
- McElroy, M. B., Chemical processes in the solar system, in *Chemical Kinetics*, edited by D. R. Hershebach, pp. 127-211, Int. Review of Science, Butterworths, London, 1976.
- McElroy, M. B., and S. C. Wofsy, Tropical forests: Interactions with the atmosphere, in *Symposium volume on 'Tropical Forests and World Atmospheres'*, edited by G. T. Prance, in press, 1985.
- McElroy, M., S. C. Wofsy, J. Penner and J. McConnell, Atmospheric ozone: Possible impact of stratospheric aviation, *J. Atmos. Sci.*, **31**, 287-303, 1974.
- McElroy, M. B., S. C. Wofsy, and Y. L. Yung, The nitrogen cycle: Perturbations due to man and their impact on atmospheric N<sub>2</sub>O and O<sub>3</sub>, *Phil. Trans. Roy. Soc. London*, **A277**, 159-181, 1977.
- McFarland, J., D. Kley, J. W. Drummond, A. L. Schmeltekopf, and R. H. Winkler, Nitric oxide measurements in the Equatorial Pacific region, *Geophys. Res. Lett.*, **6**, 605-608, 1979.
- McFarland, M., B. A. Ridley, M. Profitt, and D. L. Albritton, Simultaneous in-situ measurements of stratospheric O<sub>3</sub>, NO<sub>2</sub>, and NO, in press, 1985.
- McGregor, J., and W. A. Chapman, Stratospheric temperatures and geostrophic winds during 1973-1974, *Quart. J. Roy. Meteorol. Soc.*, **105**, 241-261, 1979.
- McInturff, R. M. (Ed.), Stratospheric warmings: Synoptic, dynamic and general-circulation aspects, *NASA Ref. Publ. 1017*, 166 pp., NASA, Washington, DC, 1978.
- McIntyre, M. E., Towards a Lagrangian-mean description of stratospheric circulations and chemical transports, *Phil. Trans. Roy. Soc. London*, **A296**, 129-148, 1980a.
- McIntyre, M. E., An introduction to the generalized Lagrangian-mean description of wave, mean-flow interaction, *Pure Appl. Geophys.*, **118**, 152-176, 1980b.
- McIntyre, M. E., How well do we understand the dynamics of stratospheric warmings?, *J. Meteorol. Soc. Japan*, **60**, 37-65, 1982.
- McIntyre, M. E., and T. N. Palmer, Breaking planetary waves in the stratosphere, *Nature*, **305**, 593-600, 1983.
- McIntyre, M. E., and T. N. Palmer, The 'surf zone' in the stratosphere, *J. Atmos. Terr. Phys.*, **46**, 825-850, 1984.
- McKay, M. D., R. J. Beckman, and W. J. Conover, A comparison of three methods for selecting values of input variables in the analysis of output from a computer code, *Technometrics*, **21**, 239-245, 1979.
- McKenney, D. J., D. L. Wade, and W. I. Findlay, Rates of N<sub>2</sub>O evolution from N fertilized soil, *Geophys. Res. Lett.*, **5**, 777-780, 1978.
- McKenney, D. J., K. F. Shuttleworth, J. R. Vriesacker, and W. T. Findlay, Production and loss of nitric oxide from denitrification in anaerobic Brookstone clay, *Appl. Env. Microbiol.*, **43**, 534-541, 1982.
- McKenzie, R. L., and P. V. Johnston, Seasonal variation in stratospheric NO<sub>2</sub> at 45 degrees S, *Geophys. Res. Lett.*, **9**, 1255-1258, 1982.
- McMahon, T. A., and P. J. Denison, Empirical atmospheric deposition parameters—A survey, *Atmos. Environ.*, **13**, 571-585, 1979.

## REFERENCES

- McMillin, L. M., and C. Dean, Evaluation of a new operational technique for producing clear radiances, *J. Appl. Meteorol.*, *21*, 1005-1014, 1982.
- McPeters, R. D., and C. H. Jackman, The response of ozone to solar proton events during solar cycle 21: The observations, *J. Geophys. Res.*, *90*, 7945-7954, 1985.
- McPeters, R. D., C. H. Jackman, and E. G. Stassinopoulos, Observations of ozone depletion associated with solar proton events, *J. Geophys. Res.*, *86*, 12071-12081, 1981.
- McPeters, R. D., D. F. Heath, and P. K. Bhartia, Average ozone profiles for 1979 from the NIMBUS 7 SBUV instrument, *J. Geophys. Res.*, *89*, 5199-5214, 1984.
- McPherson, R. D., K. H. Bergman, R. E. Kistler, G. E. Rasch, and D. S. Gordon, The NMC operational global data assimilation system, *Mon. Weather Rev.*, *107*, 1445-1461, 1979.
- Mechoso, C. R., M. J. Suarez, K. Yamazaki, J. Spahr, and A. Arakawa, A study of the sensitivity of numerical forecasts to an upper boundary condition in the lower stratosphere, *Mon. Weather Rev.*, *110*, 1984-1993, 1982.
- Mechoso, C. R., K. Yamazaki, A. Kitch, and A. Arakawa, Numerical forecasts of stratospheric warming events during the winter of 1979, *J. Atmos. Sci.*, in press, 1985.
- Meek, C. E., I. M. Reid, and A. H. Manson, Observations of mesospheric wind velocities. I. Gravity wave horizontal scale and phase velocities determined from spaced wind observations, *Rad. Sci.*, in press, 1985a.
- Meek, C. E., I. M. Reid, and A. H. Manson, Observations of mesospheric wind velocities. II. Cross sections of power spectral density for 48-8h, 8-1h, 1h-10 min over 60-110 km for 1981, *Rad. Sci.*, in press, 1985b.
- Megie, G., and J. E. Blamont, Laser sounding of atmospheric sodium, Interpretation in terms of global atmospheric parameters, *Planet. Space Sci.*, *25*, 1093-1109, 1977.
- Megie, G., and R. T. Menzies, Complementarity of UV and IR differential absorption lidar for global measurements of atmospheric species, *Appl. Optics*, *19*, 1173-1183, 1980.
- Megie, G., J. Y. Allain, M. L. Chanin, and J. E. Blamont, Vertical profile of stratospheric ozone by lidar sounding from the ground, *Nature*, *270*, 329-331, 1977.
- Meier, R. R., D. E. Anderson, Jr., and M. Nicolet, Radiation field in the troposphere and stratosphere from 240-1000 nm - I. General analysis, *Planet. Space Sci.*, *30*, 923-933, 1982.
- Mentall, J. E., J. E. Frederick, and J. R. Herman, The solar irradiance from 200-330 nm, *J. Geophys. Res.*, *86*, 9881-9884, 1981.
- Mentall, J. E., B. Guenther, and D. Williams, The solar spectral irradiance between 150 and 200 nm, *J. Geophys. Res.*, *90*, 2265-2272, 1985.
- Menzies, T., Remote measurement of ClO in the stratosphere, *Geophys. Res. Lett.*, *6*, 151-154, 1979.
- Menzies, T., A re-evaluation of laser heterodyne radiometer ClO measurements, *Geophys. Res. Lett.*, *10*, 729-732, 1983.
- Michalsky, J. J., B. M. Herman and N. R. Larson, Mid-latitude stratospheric aerosol layer enhancement by El Chichon: The first year, *Geophys. Res. Lett.*, *11*, 76-79, 1984.
- Mihelic, D., D. H. Ehhalt, G. F. Kulesa, J. Klomfass, M. Trainer, U. Schmidt, and H. Rohrs, Measurements of free radicals in the atmosphere by matrix isolation and electron paramagnetic resonance, *Pure Appl. Geophys.*, *116*, 530-536, 1978.
- Miles, T., and W. A. Chapman, Intercomparison of planetary-scale diagnostics derived from separate satellite and radiosonde time-mean temperature fields, *Quart. J. Roy. Meteorol. Soc.*, *110*, 1003-1021, 1984.
- Miller, A. J., Periodic variation of atmospheric circulation at 14-16 days, *J. Atmos. Sci.*, *31*, 720-726, 1974.
- Miller, A. J., T. G. Rogers, R. M. Nagatani, D. F. Heath, A. J. Krueger, W. Planet, and D. Crosby, Preliminary comparisons of daily total ozone fields derived from SBUV, TOMS and HIRS-2 satellite

## REFERENCES

- instruments, in *Proc. XVII General Assembly of the International Union of Geodesy and Geophysics*, pp. 153-164, 1979.
- Miller, A. J., R. M. Nagatani, T. G. Rogers, A. J. Fleig, and D. F. Heath, Total ozone variations 1970-1974 using Backscattered Ultraviolet (BUV) and ground-based observations, *J. Appl. Meteorol.*, *21*, 621-630, 1982.
- Miller, A. J., R. M. Nagatani and J. E. Frederick, Ozone-temperature relationships in the stratosphere, in *Proceedings of the International Ozone Symposium*, pp. 321-324, Thessaloniki, Greece, D. Reidel, Dordrecht, 1985.
- Miller, C., D. L. Filken, A. J. Owens, J. M. Steed, and J. P. Jesson, A two-dimensional model of stratospheric chemistry and transport, *J. Geophys. Res.*, *86*, 12039-12065, 1981.
- Mitchell, J. F. B., The seasonal response of a general circulation model to changes in CO<sub>2</sub> and sea temperatures, *Quart. J. Roy. Meteorol. Soc.*, *109*, 113-152, 1983.
- Mitchell, J. M., El Chichon: Weather-maker of the century?, *Weatherwise*, *35*, 252-261, 1982.
- Miyahara, S., A numerical simulation of the zonal mean circulation of the middle atmosphere including effects of solar diurnal tidal waves and internal gravity waves; solstice condition, in *Dynamics of the Middle Atmosphere*, edited by J. R. Holton and T. Matsuno, pp. 271-287, Terrapub, Tokyo, 1984.
- Miyahara, S., Suppression of stationary planetary waves by internal gravity waves in the mesosphere, *J. Atmos. Sci.*, *42*, 100-107, 1985.
- Miyahara, S., Y. Hayashi, and J. D. Mahlman, Interactions between gravity waves and planetary scale flow simulated by GFDL "SKYHI" general circulation model, *J. Atmos. Sci.*, in press, 1985.
- Miyakoda, K., R. F. Strickler, and G. D. Hembree, Numerical simulation of the breakdown of a polar-night vortex in the stratosphere, *J. Atmos. Sci.*, *27*, 139-154, 1970.
- Moeng, C.-H., and J. C. Wyngaard, Statistics of conservative scalars in the convective boundary layer, *J. Atmos. Sci.*, *41*, 3161-3169, 1984.
- Molina, L. T., M. J. Molina, and F. S. Rowland, Ultraviolet absorption cross sections of several brominated methanes and ethanes of atmospheric interest, *J. Phys. Chem.*, *86*, 2672-2676, 1982.
- Molina, L. T., M. J. Molina, R. A. Stachnik and R. D. Tom, An upper limit to the rate of HCl + ClONO<sub>2</sub> reaction, *J. Phys. Chem.*, *89*, 3779-3781, 1985.
- Molina, M. J., and F. S. Rowland, Stratospheric sink for chlorofluoromethanes: chlorine atom catalyzed destruction of ozone, *Nature*, *249*, 810-814, 1974.
- Molina, M. J., L. T. Molina, and T. Ishiwata, Kinetics of the ClO + NO<sub>2</sub> + M reaction, *J. Phys. Chem.*, *84*, 3100-3104, 1980.
- Molina, M. J., L. T. Molina, and C. A. Smith, The rate of the reaction of OH with HCl, *Int. J. Chem. Kinet.*, *16*, 1151-1160, 1984.
- Mook, W. M., M. Koopmans, A. F. Carter, and C. D. Keeling, Seasonal, latitudinal, and secular variations in the abundance and isotopic ratios of atmospheric carbon dioxide (1): Results from land stations, *J. Geophys. Res.*, *88*, 915-933, 1983.
- Morel, O., R. Simonaitis, and J. Heicklen, Ultraviolet absorption spectra of HO<sub>2</sub>NO<sub>2</sub>, CCl<sub>3</sub>O<sub>2</sub>NO<sub>2</sub>, CCl<sub>2</sub>FO<sub>2</sub>NO<sub>2</sub> and CH<sub>3</sub>O<sub>2</sub>NO<sub>2</sub>, *Chem. Phys. Lett.*, *73*, 38-42, 1980.
- Mount, G. H., and G. J. Rottman, The solar spectral irradiance 1200-3184 Å near solar maximum: 15 July 1980, *J. Geophys. Res.*, *86*, 9193-9198, 1981.
- Mount, G. H., and G. J. Rottman, Solar absolute spectral irradiance 1150-3173 Å: May 17, 1982, *J. Geophys. Res.*, *88*, 5403-5410, 1983a.
- Mount, G. H., and G. J. Rottman, The solar absolute spectral irradiance at 1216 Å and 1800-3173 Å: January 12, 1983, *J. Geophys. Res.*, *88*, 6807-6811, 1983b.
- Mount, G. H., and G. J. Rottman, The solar absolute spectral irradiance 118-300 nm: July 25, 1983, *J. Geophys. Res.*, *90*, 13031-13036, 1985.

## REFERENCES

- Mount, G. H., G. J. Rottman, and J. G. Timothy, The solar spectral irradiance 1200-2550 Å at solar maximum, *J. Geophys. Res.*, 85, 4271-4274, 1980.
- Mount, G. H., D. W. Rusch, J. M. Zawodny, J. F. Noxon, C. A. Barth, G. J. Rottman, R. J. Thomas, G. E. Thomas, R. W. Sanders, and G. M. Lawrence, Measurements of NO<sub>2</sub> in the Earth's stratosphere using a Limb scanning visible light spectrometer, *Geophys. Res. Lett.*, 10, 265-268, 1983.
- Mount, G. H., D. W. Rusch, J. F. Noxon, J. M. Zawodny, and C. A. Barth, Measurements of stratospheric NO<sub>2</sub> from the solar mesosphere explorer satellite, 1. An overview of the results, *J. Geophys. Res.*, 89, 1327-1340, 1984.
- Moxim, W. J., and J. D. Mahlman, Evaluation of the various total ozone sampling networks using the GFDL 3-D tracer model, *J. Geophys. Res.*, 85, 4527-4539, 1980.
- Mozurkewich, M., and S. Benson, Negative activation energies and curved Arrhenius plots. I. Theory of reaction over potential wells, *J. Phys. Chem.*, 88, 6429-6435, 1984.
- Mueller, P. K., and G. M. Hidy, The sulfate regional experiment: Report of findings, *EPRI-EA-1901*, Electric Power Research Institute, Palo Alto, CA, March, 1983.
- Muller, C., J. Vercheval, M. Ackerman, C. Lippens, J. Laurent, M. P. Lamaitre, J. Besson, and A. Girard, Observations of middle atmospheric CH<sub>4</sub> and N<sub>2</sub>O vertical distributions by the Spacelab 1 grille spectrometer, *Geophys. Res. Lett.*, 12, 667-670, 1985.
- Muller, H. G., Long period meteor wind oscillations, *Phil. Trans. Roy. Soc. London*, A271, 585-598, 1972.
- Muller, H. G., G. A. Whitehurst, and A. O'Neill, Stratospheric warmings and their effects on the winds in the upper atmosphere during the winter of MAP/WINE 1983-1984, *J. Atmos. Terr. Phys.*, in press, 1985.
- Mumma, M. J., J. D. Rogers, T. Kostiuik, D. Deming, J. J. Hillman, and D. Zipoy, Is there any chlorine monoxide in the stratosphere?, *Science*, 221, 268-271, 1983.
- Murad, E., W. Swider, and S. W. Benson, Possible role for metals in stratospheric chlorine chemistry, *Nature*, 289, 273-275, 1981.
- Murakami, T., Equatorial stratospheric waves induced by diabatic heat sources, *J. Atmos. Sci.*, 29, 1129-1137, 1972.
- Murcray, D. G., T. G. Kyle, F. H. Murcray, and W. J. Williams, Nitric acid and nitric oxide in the lower stratosphere, *Nature*, 218, 78-79, 1968.
- Murcray, D. G., A. Goldman, A. Csoeke-Poekkh, F. H. Murcray, W. J. Williams, and R. N. Stocker, Nitric acid distribution in the stratosphere, *J. Geophys. Res.*, 78, 7033-7038, 1973.
- Murcray, D. G., D. B. Barker, J. N. Brooks, A. Goldman, and W. J. Williams, Seasonal and latitudinal variations of the stratospheric concentration of HNO<sub>3</sub>, *Geophys. Res. Lett.*, 6, 223-225, 1975.
- Murcray, D. G., A. Goldman, C. M. Bradford, G. R. Cook, J. W. Van Allen, F. S. Bonomo, and F. H. Murcray, Identification of the  $\nu_2$  vibration-rotation band of ammonia in ground level solar spectra, *Geophys. Res. Lett.*, 5, 527-530, 1978.
- Murcray, D. G., A. Goldman, F. H. Murcray, F. J. Murcray, and W. J. Williams, Stratospheric distribution of ClONO<sub>2</sub>, *Geophys. Res. Lett.*, 6, 857-859, 1979.
- Murcray, D. G., F. J. Murcray, A. Goldman, F. H. Murcray, and J. J. Kusters, Balloon-borne remote sensing of stratospheric constituents, 22, 2629-2640, 1983.
- Murcray, D. G., A. Goldman, J. Kusters, R. Zander, W. Evans, N. Louisnard, C. Alamichel, M. Bangham, S. Pollitt, B. Carli, B. Dinelli, S. Piccioli, A. Volboni, W. Traub, and K. Chance, Intercomparison of stratospheric water vapor profiles obtained during the balloon intercomparison campaign, in *Atmospheric Ozone*, edited by C. S. Zerefos and A. Ghazi, pp. 144-148, D. Riedel, Dordrecht, 1985a.
- Murcray, D. G., L. S. Rottman, G. A. Vanasse, F. H. Murcray, F. J. Murcray, and A. Goldman, Atmospheric emission spectra from the stratospheric cryogenic interferometer balloon experiment, paper presented at the Ninth colloquium on High Resolution Molecular Spectroscopy, Riccione, Italy, 1985b.

## REFERENCES

- Murcray, D. G., A. Goldman, J. Kusters, R. Zander, W. F. J. Evans, N. Louisnard, D. Alamichel, M. Bangham, S. Pollitt, B. Carli, B. Dinelli, S. Piccioli, A. Volboni, W. Traub, and K. Chance, Intercomparison of stratospheric water vapor profiles obtained during the balloon intercomparison campaign, to be published, 1986.
- Murcray, F. J., A. Goldman, D. G. Murcray, G. R. Cook, J. W. Van Allen, and R. D. Blatherwick, Identification of isolated NO lines in balloon-borne infrared solar spectra, *Geophys. Res. Lett.*, **7**, 673-676, 1980.
- Murgatroyd, R. J., Recent progress in studies of the stratosphere, *Quart. J. Roy. Meteorol. Soc.*, **108**, 271-312, 1982.
- Murgatroyd, R. J., and R. M. Goody, Sources and sinks of radiative energy from 30 to 90 km, *Quart. J. Roy. Meteorol. Soc.*, **84**, 225-234, 1958.
- Murgatroyd, R. J., and F. Singleton, Possible meridional circulations in the stratosphere and mesosphere, *Quart. J. Roy. Meteorol. Soc.*, **87**, 125-135, 1961.
- Murray, E. R., Remote measurement of gases using discretely tunable infrared lasers, *Opt. Eng.*, **16**, 284-290, 1977.
- Myers, R. J. K., J. R. Simpson, R. Wetselaar, and G. T. McKinney, Problems in modelling the environmental aspects of the nitrogen cycle in agro-ecosystems, SCOPE workshop on "Dynamic Aspects of Nitrogen Cycling in the Australian Ecosystems," Aspendale, Vic., Australia, 1979.
- Nagata, T., T. Tohmatsu, and T. Ogawa, Sounding rocket measurement of atmospheric ozone density, 1965-1970, *Space Res.*, **11**, 849-855, 1971.
- NAS: See National Academy of Sciences.
- NASA, Man's impact on the troposphere: Lectures in tropospheric chemistry, *NASA Reference Publication 1022*, edited by J. S. Levine and D. R. Schryer, Hampton, VA, Sept. 1978.
- NASA, *The Stratosphere: Present and Future*, *NASA Reference Publication 1049*, edited by R. D. Hudson and E. I. Reed, 432 pp., NASA Goddard, Greenbelt, MD, 1979.
- NASA-JPL, Chemical kinetics and photochemical data for use in stratospheric modeling, Evaluation No. 7, NASA Panel for Data Evaluation, *JPL Publication 85-37*, Jet Propulsion Laboratory, Pasadena, CA, 1982.
- Nastrom, G. D., B. B. Balsley, and D. A. Carter, Mean meridional winds in the mid- and high-latitude summer mesosphere, *Geophys. Res. Lett.*, **9**, 139-142, 1982.
- Nastrom, G. D., W. L. Ecklund, and K. S. Gage, Direct measurements of synoptic scale vertical velocities using clear air radars, *Mon. Weather Rev.*, **113**, 708-718, 1985.
- Natarajan, M., L. B. Callis, and J. E. Nealy, Solar UV variability: Effects on stratospheric ozone, trace constituents and thermal structure, *Pure Appl. Geophys.*, **119**, 750-779, 1980/81.
- National Academy of Sciences, NAS, *Halocarbons: Effect on Stratospheric Ozone*, National Academy Press, Washington, DC, 1976.
- The National plan for stratospheric ozone monitoring and early detection of change, 1981-1986, *FCM-P17-1982*, 79 pp., Federal Coordinator for Meteorological Services and Supporting Research, NOAA, Rockville, MD, 1982.
- National Research Council, *Environmental Impact of Stratospheric Flight*, National Academy of Sciences, Washington, DC, 1975.
- National Research Council, *Effects on Stratospheric Ozone*, National Academy of Sciences, Washington, DC, 1976.
- National Research Council, *Stratospheric Ozone Depletion by Halocarbons: Chemistry and Transport*, National Academy of Sciences, Washington, DC, 1979.
- National Research Council, *Protection Against Depletion of Stratospheric Ozone by Chlorofluorocarbons*, Committee on Impacts of Stratospheric Change, 392 pp., National Academy of Sciences, Washington, DC, 1979.

## REFERENCES

- National Research Council, *Changing Climate: Report of the Carbon Dioxide Assessment Committee*, CDAC, 496 pp., National Academy Press, Washington, DC, 1983.
- National Research Council, *Causes and Effects of Changes in Stratospheric Ozone: Update 1983*, National Academy Press, Washington, DC, 1984.
- National Research Council, *Global Tropospheric Chemistry, A Plan for Action*, National Academy Press, Washington, DC, 1984.
- Naudet, J. P., P. Rigaud, and D. Huguenin, Stratospheric NO<sub>2</sub> at night from balloons, *J. Geophys. Res.*, **89**, 2583-2587, 1984.
- Naudet, J. P., P. Rigaud, and D. Huguenin, Variabilite temporelle du NO<sub>3</sub> stratospherique, in *Atmospheric Ozone*, edited by C. S. Zerefos and A. Ghazi, pp. 201-205, D. Reidel, Dordrecht, 1985.
- Naujokat, B., Long-term variations in the stratosphere of the Northern Hemisphere during the last two sunspot cycles, *J. Geophys. Res.*, **86**, 9811-9816, 1981.
- Naujokat, B., An update of the observed QBO of the stratospheric winds over the tropics, *J. Atmos. Sci.*, in press, 1986.
- Nava, D. F., J. V. Michael, and L. J. Stief, Rate constant for the reaction of atomic bromine with formaldehyde from 223 to 480K, *J. Phys. Chem.*, **85**, 1896-1899, 1981.
- Naylor, D. A., T. A. Clark, and R. T. Boreiko, Determination of stratospheric H<sub>2</sub>O and O<sub>3</sub> column densities from balloon altitude far infrared absorption spectra by a curve of growth method, *Infrared Phys.*, **21**, 271-281, 1981.
- Naylor, D. A., R. T. Boreiko, T. A. Clark, R. J. Emery, B. Fitton, and M. F. Kessler, Atmospheric emission in the 20 μm window from Mauna Kea, *Pub. Astron. Soc. Pacific*, **96**, 167-173, 1984.
- Naylor, D. A., J. M. Hoogerdijk, R. T. Boreiko, T. A. Clark, B. Fitton, M. F. Kessler, and R. J. Emery, Observations of 63 micron atomic oxygen emission in the earth's atmosphere from balloon altitudes: Astronomical implications, in press, 1985.
- Neckel, H., and D. Labs, Improved data of solar spectral irradiance from 0.33 to 1.25 μm, *Solar Physics*, **74**, 231-249, 1981.
- Neckel, H., and D. Labs, The solar radiation between 3300 and 12500 Å, *Solar Physics*, **90**, 205-258, 1984.
- Neftel, A., H. Oeschger, J. Schwander, B. Stauffer, and R. Zumbunn, Ice core measurements give atmospheric CO<sub>2</sub> content during the past 40,000 years, *Nature*, **295**, 220-223, 1982.
- Neftel, A., E. Moor, H. Oeschger, and B. Stauffer, Evidence from polar ice cores for the increase in atmospheric CO<sub>2</sub> in the past two centuries, *Nature*, **315**, 45-47, 1985.
- Nelson, H. H., L. Pasternack, and J. R. McDonald, Laser-induced excitation and emissions spectra of NO<sub>3</sub>, *J. Phys. Chem.*, **87**, 1286-1266, 1983.
- Newell, R. E., The general circulation of the atmosphere and its effects on the movement of trace substances, *J. Geophys. Res.*, **68**, 3949-3962, 1963a.
- Newell, R. E., The general circulation of the stratosphere above 60 km, *Meteor. Monogr.*, Amer. Meteor. Soc., Boston, **31**, 98-113, 1963b.
- Newell, R. E., Further ozone transport calculations and the spring maximum in ozone amount, *Pure Appl. Geophys.*, **59**, 191-206, 1964.
- Newell, R. E., and T. G. Dopplick, Questions concerning the possible influence of anthropogenic CO<sub>2</sub> on atmospheric temperature, *J. Appl. Meteor.*, **18**, 822-825, 1979.
- Newell, R. E., and S. Gould-Stewart, A stratospheric fountain?, *J. Atmos. Sci.*, **38**, 2789-2796, 1981.
- Newell, R. E., J. W. Kidson, D. G. Vincent, and G. J. Boer, *The General Circulation of the Tropical Atmosphere, Vol. 1*, MIT Press, Cambridge, MA, 1969.
- Newell, R. E., J. W. Kidson, D. G. Vincent, and G. J. Boer, *The General Circulation of the Tropical Atmosphere, Vol. 2*, MIT Press, Cambridge, MA, 1974.

## REFERENCES

- Newell, R. E., E. P. Condon, and H. G. Reichle, Measurements of CO and CH<sub>4</sub> in the troposphere over Saudi Arabia, India and the Arabian Sea during the 1979 International Summer Monsoon Experiment (MONEX), *J. Geophys. Res.*, **86**, 9833-9838, 1981.
- Newman, P. A., M. R. Schoeberl, and R. A. Plumb, A computation of the horizontal mixing coefficients calculated from NMC data, *Geophys. Res. Lett.*, in press, 1986.
- Newson, R. L., An experiment with a tropospheric and stratospheric three-dimensional general circulation model, in *Proceedings Third Conference on the Climatic Impact Assessment Program, DOT-TSC-OST-74-15*, edited by A. J. Broderick and T. M. Hard, pp. 461-474, Dept. of Transp., Washington, DC, 1974.
- Newton, C. W., and E. Palmén, Kinematic and thermal properties of a large amplitude wave in the westerlies, *Tellus*, **15**, 99-119, 1963.
- Newton, C. W., and A. Trevisan, Clinogenesis and frontogenesis in jet stream waves. Part I: Analytical relation, *J. Atmos. Sci.*, **41**, 2717-2734, 1984.
- Nicolet, M., On the production of nitric oxide by cosmic rays in the mesosphere and stratosphere, *Planet. Space Sci.*, **23**, 637-649, 1975.
- Nicolet, M., The solar spectral irradiance and its action in the atmospheric photodissociation processes, *Planet. Space Sci.*, **29**, 951-974, 1981.
- Nicolet, M., The influence of solar radiation on atmospheric chemistry, *Annales Geophysicae*, **1**, 493-502, 1983.
- Nicolet, M., On the molecular scattering in the terrestrial atmosphere: An empirical formula for its calculation in the homosphere, *Planet. Space Sci.*, **32**, 1467-1468, 1984a.
- Nicolet, M., On the photodissociation of water vapor in the mesosphere, *Planet. Space Sci.*, **32**, 871-880, 1984b.
- Nicolet, M., Aeronomical aspects of mesospheric photodissociation: Processes resulting from the H Lyman-alpha line, *Planet. Space Sci.*, **33**, 69-80, 1985.
- Nicolet, M., and S. Cieslik, The photodissociation of nitric oxide in the mesosphere and stratosphere, *Planet. Space Sci.*, **28**, 105-115, 1980.
- Nicolet, M., and W. Peetermans, Atmospheric absorption in the O<sub>2</sub> Schumann-Runge band spectral region and photodissociation rates in the stratosphere and mesosphere, *Planet. Space Sci.*, **28**, 85-103, 1980.
- Nicolet, M., R. R. Meier, and D. E. Anderson, Jr., Radiation field in the troposphere and stratosphere. II. Numerical analysis, *Planet. Space Sci.*, **30**, 935-983, 1982.
- Niki, H., P. D. Maker, C. M. Savage, and L. P. Breitenbach, Fourier transform IR spectroscopic observation of pernitric acid formed via  $\text{HOO} + \text{NO}_2 \rightarrow \text{HOONO}_2$ , *Chem. Phys. Lett.*, **45**, 564-566, 1977.
- Niki, H., P. D. Maker, C. M. Savage, and L. P. Breitenbach, A fourier transform infrared study of the kinetics and mechanisms for the reaction  $\text{HO} + \text{CH}_3\text{OOH}$ , *J. Phys. Chem.*, **87**, 2190-2193, 1983.
- Niple, E., W. G. Mankin, A. Goldman, D. G. Murcray, and F. J. Murcray, Stratospheric NO<sub>2</sub> and H<sub>2</sub>O mixing ratio profiles from high resolution infrared solar spectra using nonlinear least squares, *Geophys. Res. Lett.*, **7**, 489-492, 1980.
- Nitta, T., Response of cumulus updraft and downdraft to GATE A/B-scale motion systems, *J. Atmos. Sci.*, **34**, 1163-1186, 1977.
- Nordhaus, W. D., and G. W. Yohe, Future paths of energy and carbon dioxide emissions, in *Changing Climate*, pp. 87-153, National Academy of Sciences, Washington, DC, 1983.
- North, G. R., R. F. Cahalan and J. A. Coakley, Energy-balance climate models, *Rev. Geophys. Space Phys.*, **19**, 91-122, 1981.
- Norton, R. B., and J. F. Noxon, The dependence of stratospheric NO<sub>3</sub> upon latitude and season, *J. Geophys. Res.*, in press, 1985.
- Noxon, J. F., Atmospheric nitrogen fixation by lightning, *Geophys. Res. Lett.*, **3**, 463-465, 1976.

## REFERENCES

- Noxon, J. F., Stratospheric NO<sub>2</sub> in the Antarctic winter, *Geophys. Res. Lett.*, 5, 1021-1022, 1978a.
- Noxon, J. F., Tropospheric NO<sub>2</sub>, *J. Geophys. Res.*, 83, 3051-3057, 1978b.
- Noxon, J. F., Stratospheric NO<sub>2</sub>, 2, Global behavior, *J. Geophys. Res.*, 84, 5067, 1979.
- Noxon, J. F., Tropospheric NO<sub>2</sub> (Correction), *J. Geophys. Res.*, 85, 4560-4561, 1981a.
- Noxon, J. F., NO<sub>x</sub> in the mid-Pacific troposphere, *Geophys. Res. Lett.*, 8, 1223-1226, 1981b.
- Noxon, J. F., NO<sub>3</sub> and NO<sub>2</sub> in the mid-Pacific troposphere, *J. Geophys. Res.*, 88, 11017-11021, 1983.
- Noxon, J. F., R. B. Norton, and W. R. Henderson, Observation of atmospheric NO<sub>3</sub>, *Geophys. Res. Lett.*, 5, 675-678, 1978.
- Noxon, J. F., E. C. Whipple Jr., and R. S. Hyde, Stratospheric NO<sub>2</sub> 1. Observational method and behavior at mid-latitude, *J. Geophys. Res.*, 84, 5047-5065, 1979a.
- Noxon, J. F., E. Marovich, and R. B. Norton, Effect of a major warming upon stratospheric NO<sub>2</sub>, *J. Geophys. Res.*, 84, 7883, 1979b.
- Noxon, J. F., R. B. Norton, and E. Marovich, NO<sub>3</sub> in the troposphere, *Geophys. Res. Lett.*, 7, 125-128, 1980.
- Noxon, J. F., W. R. Henderson, and R. B. Norton, Stratospheric NO<sub>2</sub>, 3. The effects of large scale horizontal transport, *J. Geophys. Res.*, 88, 5240-5248, 1983.
- NRC: See National Research Council.
- Oeschger, H., The contribution of ice core studies to the understanding of environmental processes, in *Green Ice Core: Geophysics, Geochemistry, and the Environment*, American Geophysical Union Monograph No. 33, edited by C. C. Langway, H. Oeschger, and W. Dansgaard, pp. 9-17, 33, 1985.
- Oeschger, H., U. Siegenthaler, U. Schotterer and A. Gugelmann, A box diffusion model to study the carbon dioxide exchange in nature, *Tellus*, 27, 168-192, 1975.
- Ogawa, M., Absorption cross sections of O<sub>2</sub> and CO<sub>2</sub> continua in the Schumann and far-UV regions, *J. Chem. Phys.*, 54, 2550-2556, 1971.
- Ogawa, T., K. Shibasaki, and K. Suzuki, Balloon observation of the stratospheric NO<sub>2</sub> profile by visible absorption spectroscopy, *J. Meteorol. Soc. Japan*, 59, 410-416, 1981.
- Oltmans, S. J., and J. London, The quasi-biennial oscillation in atmospheric ozone, *J. Geophys. Res.*, 87, 8981-8989, 1982.
- O'Neill, A., and C. Youngblut, Stratospheric warmings diagnosed using the transformed Eulerian-mean equations and the effect of the mean state on wave propagation, *J. Atmos. Sci.*, 39, 1370-1386, 1982.
- O'Neill, A., R. L. Newson, and R. J. Murgatroyd, An analysis of the large-scale features of the upper troposphere and the stratosphere in a global, three-dimensional, general circulation model, *Quart. J. Roy. Meteorol. Soc.*, 108, 25-53, 1982.
- Ongstad, A. P., and J. W. Birks, Studies of reactions of importance in the stratosphere. V. Rate constants for the reactions  $O + NO_2 \rightarrow NO + O_2$  and  $O + ClO \rightarrow Cl + O_2$  at 298K, *J. Chem. Phys.*, 81, 3922-3930, 1984.
- Oort, A. H., Global Atmospheric Statistics, 1958-1973, *NOAA Professional Paper*, 14, 1983.
- Ooyama, K., On the stability of the baroclinic circular vortex: A sufficient criterion for instability, *J. Atmos. Sci.*, 23, 43-53, 1966.
- Oran, E. S., P. S. Julienne, and D. F. Strobel, The aeronomy of odd nitrogen in the thermosphere, *J. Geophys. Res.*, 80, 3068-3076, 1975.
- Orton, G. S., and A. G. Robiette, A line parameter list for the  $\nu_2$  and  $\nu_4$  bands of <sup>12</sup>CH<sub>4</sub> and <sup>13</sup>CH<sub>4</sub>, extended to J<sup>1</sup>=25 and its application to planetary atmospheres, *J. Quant. Spectrosc. Radiat. Transfer*, 24, 81-95, 1980.
- Ostlund, H. G., H. G. Dorsey and R. Brescher, GEOSECS Atlantic radiocarbon and tritium results, *Report No. 5*, Univ. Miami Tritium Laboratory Data, 1976.

## REFERENCES

- Owens, A. J., J. M. Steed, D. L. Filkin, C. Miller, and J. P. Jesson, The potential effects of increased methane on atmosphere ozone, *Geophys. Res. Lett.*, **9**, 1105-1108, 1982a.
- Owens, A. J., J. M. Steed, C. Miller, D. L. Fillim, and J. P. Jesson, The atmospheric lifetime of CFC-11 and CFC-12, *Geophys. Res. Lett.*, **9**, 700-703, 1982b.
- Owens, A. J., C. H. Hales, D. L. Filkin, C. Miller, and M. McFarland, Multiple scenario ozone change calculations: The subtractive perturbation approach, in *Atmospheric Ozone*, edited by C. S. Zerefos and A. Ghazi, pp. 82-86, D. Reidel, Dordrecht, 1985a.
- Owens, A. J., C. H. Hales, D. L. Filken, C. Miller, J. M. Steed, and J. P. Jesson, A coupled one-dimensional radiative-convective, chemistry-transport model of the atmosphere 1. Model structure and steady-state perturbation calculations, *J. Geophys. Res.*, **90**, 2283-2311, 1985b.
- Paetzold, H. K., New experimental and theoretical investigation on the atmospheric ozone layer, *J. Atmos. Terr. Phys.*, **7**, 128-140, 1955.
- Pallister, R. C., and A. F. Tuck, The diurnal variation of ozone in the upper stratosphere as a test of photochemical theory, *Quart. J. Roy. Meteorol. Soc.*, **109**, 271-284, 1983.
- Palmen, E., and C. W. Newton, *Atmospheric Circulation Systems*, 603 pp., Academic Press, New York, 1969.
- Palmer, T. N., Diagnostic study of wavenumber-2 stratospheric sudden warming in a transformed Eulerian mean formalism, *J. Atmos. Sci.*, **38**, 844-855, 1981a.
- Palmer, T. N., Aspects of stratospheric sudden warmings studied from a transformed Eulerian-mean viewpoint, *J. Geophys. Res.*, **86**, 9679-9687, 1981b.
- Palmer, T., and C. Hsu, Stratospheric sudden coolings and the role of nonlinear wave interactions in preconditioning the circumpolar flow, *J. Atmos. Sci.*, **40**, 909-928, 1983.
- Park, J. H., D. J. W. Kendall, and H. L. Buijs, Stratospheric HF mixing ratio profiles in the Northern and Southern Hemispheres, *J. Geophys. Res.*, **89**, 11645-11653, 1984.
- Parker, D. E., and J. L. Brownscombe, Stratospheric warming following the El Chichon volcanic eruption, *Nature*, **301**, 406-408, 1983.
- Parrish, A., R. L. De Zafra, P. M. Solomon, J. W. Barrett, and E. R. Carlson, Chlorine oxide in the stratospheric ozone layer: Ground-based detection and measurement, *Science*, **211**, 1158-1161, 1981.
- Patel, C. K. N., E. G. Burkhardt, and C. A. Lambert, Spectroscopic measurements of stratospheric nitric oxide and water vapor, *Science*, **184**, 1173-1176, 1974.
- Patrick, R., J. R. Barker, and D. M. Golden, Computational study of the  $\text{HO}_2 + \text{HO}_2$  and  $\text{DO}_2 + \text{DO}_2$  reactions, *J. Phys. Chem.*, **88**, 128-136, 1984.
- Patterson, E. M., B. T. Marshall and K. A. Rahn, Radiative properties of the Arctic aerosol, *Atmos. Environ.*, **16**, 2967-2977, 1982.
- Paur, R. J., and A. M. Bass, The ultraviolet cross sections of ozone II. Results and temperature dependence, in *Atmospheric Ozone*, edited by C. S. Zerefos and A. Ghazi, pp. 611-616, D. Reidel, Dordrecht, 1985.
- Payne, W. J., *Denitrification*, 214 pp., Wiley, New York, 1983.
- Pearman, G. I., P. Hyson, and P. J. Fraser, The global distribution of atmospheric carbon dioxide: I. Aspects of observation and modelling, *J. Geophys. Res.*, **88**, 3581-3590, 1983.
- Pearman, G. I., D. Etheridge, F. deSilva, and P. J. Fraser, Evidence of changing concentrations of atmospheric  $\text{CO}_2$ ,  $\text{N}_2\text{O}$  and  $\text{CH}_4$  from air bubbles in antarctica, *Nature*, 1985.
- Pearman, G. I., and P. Hyson, Activities of the global biosphere as reflected in atmospheric  $\text{CO}_2$  records, *J. Geophys. Res.*, **85**, 4457-4467, 1980.
- Pearson, Jr., R., and D. H. Stedman, Instrumentation for fast response ozone measurements from aircraft, *Atmos. Techn.*, National Center for Atmospheric Research, Boulder, CO, **12**, 51-55, 1980.

## REFERENCES

- Pelon, J., and G. Megie, Ozone monitoring in the troposphere and lower stratosphere: Evaluation and operation of a ground based lidar station, *Geophys. Res.*, **87**, 4947-4955, 1982a.
- Pelon, J., and G. Megie, Ozone vertical distribution and total content using a ground-based active remote sensing technique, *Nature*, **299**, 137-139, 1982b.
- Pelon, J., and G. Megie, Ozone monitoring in the troposphere and lower stratosphere: Evaluation and operation of a ground-based lidar station, *J. Geophys. Res.*, **87**, 4947-4955, 1982c.
- Pelon, J., and G. Megie, Lidar measurements of the vertical ozone distribution during the June 1981 intercomparison campaign GAP/OHP, *Planet. Space Sci.*, **31**, 717-721, 1983.
- Penkett, S. A., The application of analytical techniques to the understanding of chemical processes occurring in the atmosphere, *Toxicol. Environ. Chem.*, **3**, 291-321, 1981.
- Penkett, S. A., R. G. Derwent, P. Fabian, R. Borchers, and U. Schmidt, Methyl chloride in the stratosphere, *Nature*, **283**, 58-60, 1980.
- Penkett, S. A., N. J. D. Prosser, R. A. Rasmussen, and M. A. K. Khalil, Atmospheric measurements of CF<sub>4</sub> and other fluorocarbons containing the CF<sub>3</sub> grouping, *J. Geophys. Res.*, **86**, 5172-5178, 1981.
- Penn, S., A case study using ozone to determine structure and air motions at the tropopause, *J. Appl. Meteorol.*, **3**, 581-586, 1964.
- Perner, D., D. H. Ehhalt, H. W. Paetz, U. Platt, E. P. Roeth, and A. Volz, OH radicals in the lower troposphere, *Geophys. Res. Lett.*, **3**, 466-468, 1976.
- Perry, R., Kinetics of the reactions of NCO radicals with H<sub>2</sub>, NO and O<sub>2</sub> using laser photolysis-laser induced fluorescence, paper presented at 16th Informal Conference on Photochemistry, *Abstract T-12*, Cambridge, MA, August, 1984.
- Perry, R. A., R. Atkinson, and J. N. Pitts, Jr., Kinetics and mechanism of the gas phase reactions of OH radicals with aromatic hydrocarbons over the temperature range 296 - 435K, *J. Phys. Chem.*, **82**, 296-304, 1977.
- Philbrick, C. R., Measurements of structural features in profiles of mesospheric density, in *Handbook for MAP, Vol. 2*, edited by S. K. Avery, pp. 333-340, SCOSTEP Secretariat, Univ. of Illinois, Urbana, 1981.
- Pick, D. R., and J. L. Brownscombe, Early results based on the stratospheric channels of TOVS on the TIROS-N series of operational satellites, *Adv. in Space Res.*, **1**, 247-260, 1981.
- Pickett, H. M., D. E. Brinza, and E. A. Cohen, Pressure broadening of ClO by nitrogen, *J. Geophys. Res.*, **86**, 7279-7282, 1981.
- Pierotti, D., and R. A. Rasmussen, Combustion as a source of nitrous oxide in the atmosphere, *Geophys. Res. Lett.*, **3**, 265-267, 1976.
- Pierotti, D., and R. A. Rasmussen, The atmosphere distribution of nitrous oxide, *J. Geophys. Res.*, **82**, 5823-5832, 1977.
- Pirre, M., P. Rigaud, and D. Huguenin, New in-situ measurements of the absorption cross section of O<sub>2</sub> in the Herzberg continuum, *Geophys. Res. Lett.*, **11**, 1199-1202, 1984.
- Pirre, M., P. Rigaud, and D. Huguenin, Mesure de l'absorption par la haute atmosphere dans le domaine de l'ultraviolet de la fenetre atmospherique au voisinage de 200 nm, in *Atmospheric Ozone*, edited by C. S. Zerefos and A. Ghazi, pp. 630-634, G. Reidel, Dordrecht, 1985.
- Pitari, G., and G. Visconti, Two-dimensional tracer transport: Derivation of residual mean circulation and eddy transport tensor from a 3-D model data set, *J. Geophys. Res.*, **90**, 8019-8032, 1985.
- Pittock, A. B., Climatology of the vertical distribution of ozone over Aspendale, *Quart. J. Roy. Meteorol. Soc.*, **103**, 575-584, 1977.
- Planet, W. G., D. S. Crosby, J. H. Lienesch, and M. L. Hill, Determination of total ozone amounts from TIROS radiance measurements, *J. Clim. and Appl. Meteor.*, **23**, 308-316, 1984.

## REFERENCES

- Platt, C. M. R., Cirrus clouds in tropical Australia, *Weatherwise*, 36, 132-133, 1983.
- Platt, U., and D. Perner, Direct measurements of atmospheric CH<sub>2</sub>O, HNO<sub>2</sub>, O<sub>3</sub>, NO<sub>2</sub>, and SO<sub>2</sub> by differential optical absorption in the near UV, *J. Geophys. Res.*, 85, 7453-7458, 1980.
- Platt, U., D. Perner, G. W. Harris, A. M. Winer, and J. N. Pitts, Jr., Observations of nitrous acid in an urban atmosphere by differential optical absorption, *Nature*, 285, 312-314, 1980a.
- Platt, U., D. Perner, A. M. Winer, G. W. Harris, and J. N. Pitts, Jr., Detection of NO<sub>3</sub> in the polluted troposphere by differential optical absorption, *Geophys. Res. Lett.*, 7, 89-92, 1980b.
- Platt, U., D. Perner, J. Schroder, C. Kessler, and A. Toennissen, The diurnal variation of NO<sub>3</sub>, *J. Geophys. Res.*, 86, 11965-11970, 1981.
- Platt, U. F., A. M. Winer, H. W. Biermann, R. Atkinson, and J. H. Pitts, Jr., Measurement of nitrate radical concentrations in continental air, *Environ. Sci. Technol.*, 18, 365-369, 1984.
- Plumb, R. A., The interaction of two internal waves with the mean flow: Implications for the theory of the quasi-biennial oscillation, *J. Atmos. Sci.*, 34, 1847-1858, 1977.
- Plumb, R. A., Eddy fluxes of conserved quantities by small-amplitude waves, *J. Atmos. Sci.*, 36, 1699-1704, 1979.
- Plumb, R. A., Instability of the distorted polar night vortex: A theory of stratospheric warmings, *J. Atmos. Sci.*, 38, 2514-2531, 1981.
- Plumb, R. A., The circulation of the middle atmosphere, *Aus. Meteorol. Mag.*, 30, 107-121, 1982.
- Plumb, R. A., Baroclinic instability of the summer mesosphere: A mechanism for the quasi-two-day-wave?, *J. Atmos. Sci.*, 40, 262-270, 1983a.
- Plumb, R. A., A new look at the energy cycle, *J. Atmos. Sci.*, 40, 1669-1688, 1983b.
- Plumb, R. A., The quasi-biennial oscillation, in *Dynamics of the Middle Atmosphere*, edited by J. R. Holton and T. Matsuno, pp. 217-251, Terrapub, Tokyo, 1984.
- Plumb, R. A., and R. C. Bell, A model of the quasi-biennial oscillation on an equatorial beta-plane, *Quart. J. Roy. Meteorol. Soc.*, 108, 335-352, 1982.
- Plumb, R. A., and J. D. Mahlman, The zonally-averaged transport characteristics of the GFDL general circulation/tracer model, *J. Atmos. Sci.*, in press, 1986.
- Plumb, R. A., and A. D. McEwan, The instability of a forced standing wave in a viscous stratified fluid: A laboratory analogue of the quasi-biennial oscillation, *J. Atmos. Sci.*, 35, 1827-1839, 1978.
- Pollack, J. B., and T. P. Ackerman, Possible effects of the El Chichon volcanic cloud on the radiation budget of the northern tropics, *Geophys. Res. Lett.*, 10, 1057-1060, 1983.
- Pollack, J. B., and C. P. McKay, The impact of polar stratospheric clouds on the heating rates of the winter polar stratosphere, *J. Atmos. Sci.*, 42, 245-262, 1985.
- Pollitt, S., M. Coffey, W. Evans, A. Goldman, J. J. Kusters, N. Louisnard, W. G. Mankin, D. G. Murcray, and W. J. Williams, Intercomparative measurements of stratospheric nitric acid, in *Atmospheric Ozone*, edited by C. S. Zerefos and A. Ghazi, pp. 151-156, D. Reidel, Dordrecht, 1985.
- Pollitt, S., D. G. Murcray, A. Goldman, J. J. Kusters, W. J. Williams, N. Louisnard, W. F. J. Evans, M. Coffey, W. G. Mankin, R. Zander, D. W. Johnson, G. Stokes, and R. K. Seals, BIC nitric acid intercomparison, to be published, 1986.
- Pollock, W., L. E. Heidt, R. Lueb, and D. H. Ehhalt, Measurement of stratospheric water vapor by cryogenic collection, *J. Geophys. Res.*, 85, 5555-5568, 1980.
- Pommereau, J. P., Observation of NO<sub>2</sub> diurnal variation in the stratosphere, *Geophys. Res. Lett.*, 9, 850-853, 1982.
- Porch, W. M., and M. C. MacCracken, Parametric study to the effects of Arctic soot on solar radiation, *Atmos. Environ.*, 16, 1365-1371, 1982.
- Posey, J., J. Sherwell, and M. Kaufman, Kinetics of the reactions of atomic bromine with HO<sub>2</sub> and H<sub>2</sub>O<sub>2</sub>, *Chem. Phys. Lett.*, 77, 476-479, 1981.

## REFERENCES

- Poulet, G., G. Laverdet, and G. Le Bras, Discharge flow-mass spectrometric determination of the rate coefficient for the reactions of formaldehyde with bromine atoms and chlorine atoms, *J. Phys. Chem.*, **85**, 1891-1895, 1981.
- Poulet, G., G. Laverdet, and G. Le Bras, Kinetics of the reactions of atomic bromine with HO<sub>2</sub> and HCO at 298K, *J. Chem. Phys.*, **80**, 1922-1928, 1984.
- Poulet, G., G. Laverdet, and G. LeBras, Rate constant and branching ratio for the reaction of OH with ClO, *J. Phys. Chem.*, in press, 1985.
- Poynter, R. L., and H. M. Pickett, Submillimeter, millimeter, and microwave spectral line catalogue, *JPL Publication 80-23, Revision 1*, 151 pp., Jet Propulsion Laboratory, California Institute of Technology, Pasadena, CA, 1981.
- Poynter, R. L., and H. M. Pickett, Submillimeter, millimeter, and microwave spectral line catalogue, *JPL Publication 80-23, Revision 2*, 171 pp., Jet Propulsion Laboratory, California Institute of Technology, Pasadena, CA, 1984.
- Prabhakara, C., Effects of non-photochemical processes on the meridional distribution and total amount of ozone in the atmosphere, *Mon. Weather Rev.*, **91**, 411-431, 1963.
- Prasad, S. S., Possible existence and chemistry of ClO.O<sub>2</sub> in the stratosphere, *Nature*, **285**, 152-154, 1980.
- Prata, A., The 4-day wave, *J. Atmos. Sci.*, **41**, 150-155, 1984.
- Prather, M. J., Ozone in the upper stratosphere and mesosphere, *J. Geophys. Res.*, **86**, 5325-5338, 1981.
- Prather, M. J., Continental sources of halocarbons and nitrous oxide, *Nature*, **317**, 221-225, 1985.
- Prather, M. J., M. B. McElroy, and S. C. Wofsy, Reductions in ozone at high concentrations of stratospheric halogens, *Nature*, **312**, 227-231, 1984.
- Prinn, R. G., P. G. Simmonds, R. A. Rasmussen, R. D. Rosen, F. N. Alyea, C. A. Cardelino, A. J. Crawford, D. M. Cunnold, P. J. Fraser, and J. E. Lovelock, The atmospheric lifetime experiment, 1, Introduction, instrumentation and overview, *J. Geophys. Res.*, **88**, 8353-8367, 1983a.
- Prinn, R. G., R. A. Rasmussen, P. G. Simmonds, F. N. Alyea, D. M. Cunnold, B. C. Lane, C. A. Cardelino, and A. J. Crawford, The atmospheric lifetime experiments, 5, Results for CH<sub>3</sub>CCl<sub>3</sub> based on three years of data, *J. Geophys. Res.*, **88**, 8415-8426, 1983b.
- Pugh, L. A., and K. N. Rao, Intensities from infrared spectra, *Mol. Spectros., Mod. Res.*, **2**, 165-225, 1976.
- Pyle, J. A., A calculation of the possible depletion of ozone by chlorofluorocarbons using a two-dimensional model, *Pure Appl. Geophys.*, **118**, 355-377, 1980.
- Pyle, J. A., and C. F. Rogers, A modified diabatic circulation model for stratospheric tracer transport, *Nature*, **287**, 711-714, 1980a.
- Pyle, J. A., and C. F. Rogers, Stratospheric transport by stationary planetary waves: The importance of chemical processes, *Quart. J. Roy. Meteorol. Soc.*, **106**, 421-446, 1980b.
- Pyle, J. A., and C. F. Rogers, Modelling tracer budgets in the stratosphere, *Quart. J. Roy. Meteorol. Soc.*, **110**, 1097-1106, 1984.
- Pyle, J. A., and A. M. Zavody, The derivation of near-global fields of hydrogen containing radical concentrations from satellite data sets, *Quart. J. Roy. Meteorol. Soc.*, in press, 1985a.
- Pyle, J. A., and A. M. Zavody, The variability of stratospheric radicals, paper presented at the 5th General Assembly, International Association of Geomagnetism and Aeronomy, Prague, 5-17 August 1985b.
- Pyle, J. A., A. M. Zavody, J. E. Harries, and P. H. Moffat, Derivation of OH concentration from satellite infrared measurements of NO<sub>2</sub> and HNO<sub>3</sub>, *Nature*, **305**, 690-692, 1983.
- Quinn, T. H., K. A. Wolf, W. E. Mooz, J. K. Hammitt, T. W. Chesnutt and S. Sarma, Projected use, emissions, and banks of potential ozone depleting substances, *N-2282-EPA*, Rand Corp., Santa Monica, CA, 1985.
- Quiroz, R. S., Stratospheric temperatures during solar cycle 20, *J. Geophys. Res.*, **84**, 2415-2420, 1979a.
- Quiroz, R. S., Tropospheric-stratospheric interaction in the major warming event of January-February 1979, *Geophys. Res. Lett.*, **6**, 645-648, 1979b.

## REFERENCES

- Quiroz, R. S., The isolation of stratospheric temperature change due to the El Chichon volcanic signals, *J. Geophys. Res.*, **88**, 6773-6780, 1983a.
- Quiroz, R. S., The climate of the "El Nino" winter of 1982-83. A season of extraordinary climatic anomalies, *Mon. Weather Rev.*, **111**, 1685-1706, 1983b.
- Quiroz, R. S., and M. E. Gelman, An evaluation of temperature profiles from falling sphere soundings, *J. Geophys. Res.*, **81**, 406-412, 1976.
- Quiroz, R. S., A. J. Miller, and R. M. Nagatani, A comparison of observed and simulated properties of sudden stratospheric warmings, *J. Atmos. Sci.*, **32**, 1723-1736, 1975.
- Ramanathan, V., Greenhouse effect due to chlorofluorocarbons: Climatic implications, *Science*, **190**, 50-52, 1975.
- Ramanathan, V., Radiative transfer within the Earth's troposphere and stratosphere: A simplified radiative-convective model, *J. Atmos. Sci.*, **33**, 1330-1346, 1976.
- Ramanathan, V., Climatic effects of anthropogenic trace gases, in *Energy/Climate Interactions*, pp. 269-280, D. Reidel, Dordrecht, 1980.
- Ramanathan, V., The role of ocean-atmosphere interactions in the CO<sub>2</sub> climate problem, *J. Atmos. Sci.*, **38**, 918-930, 1981.
- Ramanathan, V., and J. A. Coakley, Jr., Climate modeling through radiative-convective models, *Rev. Geophys. Space Phys.*, **16**, 465-490, 1978.
- Ramanathan, V., and R. E. Dickinson, The role of stratospheric ozone in the zonal and seasonal radiative energy balance of the earth-troposphere system, *J. Atmos. Sci.*, **36**, 1084-1104, 1979.
- Ramanathan, V., and P. Downey, A non-isothermal emissivity and absorptivity formulation for water vapor, *J. Geophys. Res.*, **91**, in press, 1986.
- Ramanathan, V., L. B. Callis and R. E. Boughner, Sensitivity of atmospheric and surface temperature to perturbations in the stratospheric concentration of ozone and nitrogen dioxide, *J. Atmos. Sci.*, **33**, 1092-1112, 1976.
- Ramanathan, V., M. S. Lian and R. D. Cess, Increased atmospheric CO<sub>2</sub>: Zonal and seasonal estimates of the effect on the radiation energy balance and surface temperature, *J. Geophys. Res.*, **84**, 4949-4958, 1979.
- Ramanathan, V., E. J. Pitcher, R. C. Malone and M. L. Blackmon, The response of a spectral general circulation model to refinements in radiative processes, *J. Atmos. Sci.*, **40**, 605-630, 1983.
- Ramanathan, V., R. J. Cicerone, H. B. Singh and J. T. Kiehl, Trace gas trends and their potential role in climate change, *J. Geophys. Res.*, **90**, 5547-5566, 1985.
- Ramaswamy, V., and A. Detwiler, Interdependence of radiation and microphysics in cirrus clouds, *J. Atmos. Sci.*, **43**, in press, 1985.
- Ramaswamy, V., and J. T. Kiehl, Sensitivities of the radiative forcing due to large loadings of smoke and dust aerosols, *J. Geophys. Res.*, **90**, 5597-5613, 1985.
- Randal, W. J., and J. L. Stanford, Structure of medium-scale atmospheric waves in the Southern Hemisphere summer, *J. Atmos. Sci.*, **40**, 2312-2318, 1983.
- Randhawa, J. S., Ozonesonde for rocket flight, *Nature*, **213**, 53-54, 1967.
- Rao, M. S. V., Retrieval of worldwide precipitation and allied parameters from satellite microwave observations, in *Advances in Geophysics*, Vol. 26, edited by B. Saltzman, pp. 1238-1336, Academic Press, New York, 1984.
- Rao (Vupputuri), R. K., Numerical experiment on the steady state meridional structure and ozone distribution in the stratosphere, *Mon. Weather Rev.*, **101**, 510-527, 1973.
- Raper, O. F., C. B. Farmer, R. A. Toth, and B. D. Robbins, The vertical distribution of HCl in the stratosphere, *Geophys. Res. Lett.*, **4**, 531-534, 1977.

## REFERENCES

- Rasmussen, R. A., and M. A. K. Khalil, Atmospheric halocarbons: Measurements and analyses of selected trace gases, in *Proceedings of the NATO Advanced Study Institute on Atmospheric Ozone: Its Variation and Human Influences, Rep. FAA-EE-80-20*, edited by A. C. Aikin, pp. 209-231, DOT, FAA, Washington, DC, 1980.
- Rasmussen, R. A., and M. A. K. Khalil, Global atmospheric distribution and trend of methylchloroform ( $\text{CH}_3\text{CCl}_3$ ), *Geophys. Res. Lett.*, **8**, 1005-1007, 1981a.
- Rasmussen, R. A., and M. A. K. Khalil, Atmospheric methane ( $\text{CH}_4$ ); Trends and seasonal cycles, *J. Geophys. Res.*, **86**, 9826-9832, 1981b.
- Rasmussen, R. A., and M. A. K. Khalil, Differences in the concentrations of atmospheric trace gases in and above tropical boundary layer, *Pure Appl. Geophys.*, **119**, 990-997, 1981c.
- Rasmussen, R. A., and M. A. K. Khalil, Increase in the concentration of atmospheric methane, *Atmos. Environ.*, **15**, 883-886, 1981d.
- Rasmussen, R. A., and M. A. K. Khalil, Latitudinal distributions of trace gases in and above the boundary layer, *Chemosphere*, **11**, 227-235, 1982.
- Rasmussen, R. A., and M. A. K. Khalil, Natural and anthropogenic trace gases in the lower troposphere of the Arctic, Dept. of Environ. Sci., Beaverton, OR, 1983a.
- Rasmussen, R. A., and M. A. K. Khalil, Atmospheric fluorocarbons and methyl chloroform at the South Pole, *1982 Annual Issue of the Antarctic Journal of the United States*, **17**, 203-205, 1983b.
- Rasmussen, R. A., and M. A. K. Khalil, Global production of methane by termites, *Nature*, **301**, 700-702, 1983c.
- Rasmussen, R. A., and M. A. K. Khalil, Natural and anthropogenic trace gases in the lower troposphere in the arctic, *Chemosphere*, **12**, 371-375, 1983d.
- Rasmussen, R. A., and M. A. K. Khalil, Trace gases at Point Barrow and Arctic haze, in *Geophysical Monitoring for Climatic Change Annual Report 10*, edited by B. A. Bodhaine and J. M. Harris, NOAA/ERL, U.S. Dept. of Commerce, Boulder, CO, 1983e.
- Rasmussen, R. A., and M. A. K. Khalil, Rare trace gases at the South Pole:  $\text{CHClF}_2$ ,  $\text{CH}_3\text{I}$ ,  $\text{CHCl}_3$  and  $\text{SF}_6$ , 1984a.
- Rasmussen, R. A., and M. A. K. Khalil, Atmospheric methane in recent and ancient atmospheres: Concentrations, trends and interhemispheric gradients, *J. Geophys. Res.*, **89**, 11599-11605, 1984b.
- Rasmussen, R. A., and M. A. K. Khalil, Gaseous bromine in the Arctic and Arctic haze, *Geophys. Res. Lett.*, **11**, 433-436, 1984c.
- Rasmussen, R. A., S. A. Penkett, and N. Prosser, Measurements of carbontetrafluoride in the atmosphere, *Nature*, **277**, 549-550, 1979.
- Rasmussen, R. A., L. E. Rasmussen, M. A. K. Khalil, and R. W. Dalluge, Concentration distribution of methyl chloride in the atmosphere, *J. Geophys. Res.*, **85**, 7350-7356, 1980.
- Rasmussen, R. A., M. A. K. Khalil, and R. W. Dalluge, Atmospheric trace gases in Antarctica, *Science*, **211**, 285-287, 1981.
- Rasmussen, R. A., M. A. K. Khalil, A. J. Crawford, and P. J. Fraser, Natural and anthropogenic trace gases in the Southern Hemisphere, *Geophys. Res. Lett.*, **9**, 704-707, 1982a.
- Rasmussen, R. A., M. A. K. Khalil, R. Gunawardena, and S. D. Hoyt, Atmospheric methyl iodide ( $\text{CH}_3\text{I}$ ), *J. Geophys. Res.*, **87**, 3086-3090, 1982b.
- Rasmussen, R. A., M. A. K. Khalil, and R. J. Fox, Altitudinal and temporal variations of hydrocarbons and other gaseous tracers of Arctic haze, *Geophys. Res. Lett.*, **10**, 144-147, 1983.
- Ravishankara, A. R., and P. H. Wine, Absorption cross sections for  $\text{HNO}_3$  between 565 and 673 nm, *Chemical Physics Letters*, **101**, 73-78, 1983.
- Ravishankara, A. R., P. H. Wine, A. Torabi, C. A. Smith, and R. Wells, Photodissociation of  $\text{N}_2\text{O}_5$ , *J. Phys. Chem.*, in press, 1985.

## REFERENCES

- Rayez, J. C., B. Veyret, and R. Lesclaux, Thermodynamical and structural data of free radicals of atmospheric interest calculated by MNDO-CI, paper presented at XVth Int. Symp. on Free Radicals, Lauzelle-Ottignies, Belgium, 1983.
- Raynaud, D., and J. M. Barnola, An Antarctica ice core reveals atmospheric CO<sub>2</sub> variations over the past few centuries, *Nature*, *315*, 309-311, 1985.
- Reagan, J. B., R. E. Meyerott, R. W. Nightingale, R. C. Gunton, R. G. Johnson, J. E. Evans, W. L. Imhof, D. F. Heath, and A. J. Krueger, Effects of the August 1972 solar particle events on stratospheric ozone, *J. Geophys. Res.*, *86*, 1473-1494, 1981.
- Reber, C. A., Upper Atmosphere Research Satellite (UARS) Mission, *NASA Goddard Space Flight Center Publication 430-1003-001*, NASA Goddard Space Flight Center, Greenbelt, MD, 1985.
- Reck, R. A., Stratospheric ozone effects on temperature, *Science*, *192*, 557-559, 1976.
- Reck, R. A., Atmospheric temperature calculated for ozone depletion, *Nature*, *263*, 116-117, 1976.
- Reck, R. A., Thermal effect of stratospheric ozone depletion at 85° latitude as influenced by airborne particles, *Geophys. Res. Lett.*, *5*, 361-364, 1978.
- Reck, R. A., and D. L. Fry, The direct effect of chlorofluoromethanes on the atmospheric surface temperature, *Atmos. Environ.*, *12*, 2501-2503, 1978.
- Reck, R. A., and J. R. Hummel, Influence of aerosol optical properties on surface temperatures computed with a radiative-convective model, *Atmos. Environ.*, *15*, 1727-1731, 1981.
- Reed, R. J., The role of vertical motions in ozone-weather relationships, *J. Meteorol.*, *7*, 263-267, 1950.
- Reed, R. J., A study of a characteristic type of upper level frontogenesis, *J. Meteorol.*, *12*, 226-237, 1955.
- Reed, R. J., The structure and dynamics of the 26-month oscillation, paper presented at 40th anniv. meeting of the Amer. Met. Soc., Boston, 1960.
- Reed, R. J., Evidence of geostrophic motion in the equatorial stratosphere, *Quart. J. Roy. Meteorol. Soc.*, *88*, 324-327, 1962.
- Reed, R. J. A tentative model of the 26-month oscillation in tropical latitudes, *Quart. J. Roy. Meteorol. Soc.*, *90*, 441-466, 1964.
- Reed, R. J., The quasi-biennial oscillation of the atmosphere between 30 and 50 km over Ascension Island, *J. Atmos. Sci.*, *22*, 331-333, 1965.
- Reed, R. J., Zonal wind behaviour in the equatorial stratosphere and lower mesosphere, *J. Geophys. Res.*, *71*, 4223-4233, 1966.
- Reed, R. J., and E. F. Danielson, Fronts in the vicinity of the tropopause, *Arch. Met. Geophys. Bioklim.*, *11*, 1-17, 1959.
- Reed, R. J., and K. E. German, A contribution to the problem of stratospheric diffusion by large-scale mixing, *Mon. Weather Rev.*, *93*, 313-321, 1965.
- Reed, R. J., and C. L. Vlcek, The annual temperature variation in the lower tropical stratosphere, *J. Atmos. Sci.*, *26*, 163-167, 1969.
- Reed, R. J., D. C. Norquist, and E. F. Recker, The structure and properties of African wave disturbances as observed during Phase III of GATE, *Mon. Weather Rev.*, *105*, 317-333, 1977.
- Regener, V. H., Vertical flux of atmospheric ozone, *J. Geophys. Res.*, *62*, 221-228, 1957.
- Regener, V. H., Measurement of ozone with the chemiluminescent method, *J. Geophys. Res.*, *69*, 3795-3800, 1964.
- Reid, G. C., and K. S. Gage, A relation between the height of the tropical tropopause and the global angular momentum of the atmosphere, *Geophys. Res. Lett.*, *11*, 840-842, 1984.
- Reinsel, G., G. C. Tiao, M. N. Wang, R. Lewis, and D. Nychka, Statistical analysis of stratospheric ozone data for the detection of trend, *Atmos. Environ.*, *15*, 1569-1577, 1981.
- Reinsel, G., G. C. Tiao, R. Lewis, and M. Bobkoski, Analysis of upper stratospheric ozone profile data from the ground-based Umkehr method and the Nimbus-4 BUV satellite experiment, *J. Geophys. Res.*, *88*, 5393-5403, 1983.

## REFERENCES

- Reinsel, G. C., G. C. Tiao, J. L. De Luisi, C. L. Mateer, A. J. Miller, and J. E. Frederick, Analysis of upper stratospheric Umkehr ozone profile data for trends and the effects of stratospheric aerosols, *J. Geophys. Res.*, **89**, 4833-4840, 1984.
- Reiter, E. R., Atmospheric transport processes. Part 1: Energy transfers and transformation, *USAEC Report TID-24868*, 253 pp., Colorado State Univ., Fort Collins, CO, 1968.
- Reiter, E. R., Atmospheric transport processes. Part 2: Chemical tracers, *USAEC Report TID-25314*, 382 pp., Colorado State Univ., Fort Collins, CO, 1971.
- Reiter, E. R., Atmospheric transport processes. Part 3: Hydrodynamic tracers, *USAEC Report TID-25731*, 212 pp., Colorado State Univ., Fort Collins, CO, 1972.
- Reiter, E. R., Stratospheric-tropospheric exchange processes, *Rev. Geophys. Space Phys.*, **13**, 459-474, 1975.
- Reiter, E. R., Tropospheric-stratospheric transport processes: Indications of their interannual variability, paper presented at WMO Symp. on Long Range Transport of Pollutants and its Relation to General Circulation including Stratosphere/Troposphere Exchange Processes, *WMO No. 538*, pp. 393-400, 1979.
- Reiter, E. R., and H. J. Kanter, Time behavior of CO<sub>2</sub> and O<sub>3</sub> in the lower troposphere based on recordings from neighbouring mountain stations between 0.7 and 3.0 km ASL including the effects of meteorological parameters, *Arch. Met. Geoph. Biokl. Ser. B*, **30**, 191-225, 1982.
- Reiter, E. R., and J. D. Mahlman, A case study of mass transport from stratosphere to troposphere not associated with surface fallout, in *Atmospheric Science Paper No. 70*, pp. 54-83, Colorado State University, Ft. Collins, CO, 1971.
- Reiter, E. R., and M. P. McCormick, SAGE-European ozonesonde comparison, *Nature*, **300**, 337-339, 1982.
- Reiter, E. R., and A. Nania, Jet stream structure and clear air turbulence (CAT), *J. Appl. Meteorol.*, **3**, 247-260, 1963.
- Reiter, E. R., M. E. Glasser, and J. D. Mahlman, The role of the tropopause in stratospheric-tropospheric processes, *Pure Appl. Geophys.*, **75**, 185-218, 1969.
- Remsberg, E. E., and L. L. Gordley, Analysis of differential absorption lidar from the Space Shuttle, *Appl. Optics*, **17**, 624-630, 1978.
- Remsberg, E. E., J. M. Russell III, J. C. Gille, L. L. Gordley, P. L. Bailey, W. G. Planet, and J. E. Harries, The validation of Nimbus 7 LIMS measurements of ozone, *J. Geophys. Res.*, **89**, 5161-5178, 1984a.
- Remsberg, E. E., J. M. Russell III, L. L. Gordley, J. C. Gille, and P. L. Bailey, Implications of stratospheric water vapor distribution as determined from the Nimbus 7 LIMS experiment, *J. Atmos. Sci.*, 2934-2945, 1984b.
- Ridley, B. A., and D. R. Hastie, Stratospheric odd nitrogen: NO measurements at 51°N in summer, *J. Geophys. Res.*, **86**, 3162-3166, 1981.
- Ridley, B. A., and H. I. Schiff, Stratospheric odd nitrogen: Nitric oxide measurements at 32°N in autumn, *J. Geophys. Res.*, **86**, 3167-3172, 1981.
- Ridley, B. A., J. T. Bruin, H. I. Schiff, and J. C. McConnell, Altitude profile and sunset decay measurements of stratospheric nitric oxide, *Atmosphere*, **14**, 180-188, 1976.
- Ridley, B. A., M. McFarland, J. T. Bruin, H. I. Schiff, and J. C. McConnell, Sunrise measurements of stratospheric nitric oxide, *Can. J. Phys.*, **55**, 212-221, 1977.
- Ridley, B. A., S. H. Luu, D. R. Hastie, H. I. Schiff, J. C. McConnell, W. F. J. Evans, C. T. McElroy, J. B. Kerr, H. Fast, and R. S. O'Brien, Stratospheric odd nitrogen: Measurements of HNO<sub>3</sub>, NO, NO<sub>2</sub> and O<sub>3</sub> near 54° N. in winter, *J. Geophys. Res.*, **89**, 4797-4820, 1984.
- Riehl, H., *Climate and Weather in the Tropics*, Academic Press, New York, 611 pp., 1979.
- Rigaud, P., J. P. Naudet, and D. Huguenin, Simultaneous measurements of vertical distribution of stratospheric NO<sub>3</sub> and O<sub>3</sub> at different periods of the night, *J. Geophys. Res.*, **88**, 1463-1467, 1983.

## REFERENCES

- Rind, D., and S. Lebedeff, Potential climatic impacts of increasing atmospheric CO<sub>2</sub> with emphasis on water availability and hydrology in the United States, *NASA-TM-87479*, 106 pp., NASA Goddard Space Flight Center, Greenbelt, MD, 1984.
- Rind, D., R. Suozzo, A. Lacis, G. Russell, and J. Hansen, 21 layer troposphere-stratosphere climate model, *Mon. Weather Rev.*, in press, 1985.
- Rinsland, C. P., and J. S. Levine, Free tropospheric carbon monoxide concentrations in 1950 and 1951 deduced from infrared total column amount measurements, *Nature*, *318*, 250-254, 1985.
- Rinsland, C. P., M. A. H. Smith, J. M. Russell, J. H. Park, and C. B. Farmer, Stratospheric measurements of continuous absorption near 2400 cm<sup>-1</sup>, *Appl. Opt.*, *20*, 4167-4171, 1981.
- Rinsland, C. P., M. A. H. Smith, P. L. Rinsland, A. Goldman, J. W. Brault, and G. M. Stokes, Ground-based infrared spectroscopic measurements of atmospheric hydrogen cyanide, *J. Geophys. Res.*, *87*, 1119-1124, 1982a.
- Rinsland, C. P., M. A. H. Smith, R. K. Seals, Jr., A. Goldman, F. J. Murcray, D. G. Murcray, J. C. Larsen, and P. L. Rarig, Stratospheric measurements of collision-induced absorption by molecular oxygen, *J. Geophys. Res.*, *87*, 3119-3122, 1982b.
- Rinsland, C. P., A. Goldman, F. J. Murcray, D. G. Murcray, M. A. H. Smith, R. K. Seals, Jr., J. C. Larsen, and P. L. Rinsland, Stratospheric N<sub>2</sub>O mixing ratio profile from high-resolution balloon-borne solar absorption spectra and laboratory spectra near 1880 cm<sup>-1</sup>, *Appl. Opt.*, *21*, 4351-4355, 1982c.
- Rinsland, C. P., R. E. Boughner, J. C. Larsen, G. M. Stokes, and J. W. Brault, Diurnal variations of atmospheric nitric oxide: Ground-based infrared spectroscopic measurements and their interpretation with time-dependent photochemical model calculations, *J. Geophys. Res.*, *89*, 9613-9622, 1984a.
- Rinsland, C. P., A. Goldman, V. M. Devi, B. Fridovich, D. G. S. Snyder, G. D. Jones, F. J. Murcray, D. G. Murcray, M. A. H. Smith, R. K. Seals, Jr., M. T. Coffey, and W. G. Mankin, Simultaneous stratospheric measurements of H<sub>2</sub>O, HDO, and CH<sub>4</sub> from balloon-borne and aircraft infrared solar absorption spectra and tunable diode laser laboratory spectra of HDO, *J. Geophys. Res.*, *89*, 7259-7266, 1984b.
- Rinsland, C. P., R. E. Boughner, J. C. Larsen, A. Goldman, F. J. Murcray, and D. G. Murcray, Stratospheric NO and NO<sub>2</sub> profiles at sunset from analysis of high resolution balloon-borne infrared solar absorption spectra obtained at 33°N. and calculations with a time-dependent photochemical model, *NASA Tech. Memo 86285*, 46 pp., NASA Langley Research Center, Hampton, VA, 1984c.
- Rinsland, C. P., J. S. Levine, and T. Miles, Concentration of methane in the troposphere deduced from 1951 solar spectra, *Nature*, *318*, 245-249, 1985a.
- Rinsland, C. P., A. Goldman, D. G. Murcray, F. J. Murcray, F. S. Bonomo, R. D. Blatherwick, V. M. Devi, M. A. H. Smith, and P. L. Rinsland, Tentative identification of the 780 cm<sup>-1</sup> v<sub>4</sub> band Q branch of chlorine nitrate in high-resolution solar absorption spectra of the stratosphere, *J. Geophys. Res.*, *90*, 7931-7943, 1985b.
- Rinsland, C. P., V. M. Devi, J.-M. Flaud, C. Camy-Peyret, M. A. H. Smith, and G. M. Stokes, Identification of <sup>18</sup>O-isotopic lines of ozone in infrared ground-based solar absorption spectra, *J. Geophys. Res.*, *90*, 10719-10725, 1985c.
- Rinsland, C. P., A. Goldman, and G. M. Stokes, Identification of atmospheric C<sub>2</sub>H<sub>2</sub> lines in the 3230-3340 cm<sup>-1</sup> region of high resolution solar absorption spectra recorded at the National Solar Observatory, *Appl. Opt.*, *24*, 2044-2046, 1985d.
- Rippel, H., A helium cooled balloon experiment for measuring infrared emission from stratospheric gases, Ph.D. Thesis, Univ. Wuppertal, Dept. of Atmospheric Physics, W. Germany, 1984a.
- Rippel, H., Ein Heliumgekühltes Ballonexperiment zur Messung der Infrarotemissionen stratosphärischer Spurengase., Ph.D. Thesis, University of Wuppertal, F.R.G., 1984b.

## REFERENCES

- Roach, W. T., Aircraft observations in the lower sub-arctic stratosphere in winter, *Meteorological Research Committee Paper 121*, (available at National Meteorological Library, UK Meteorological Office), 1962.
- Roach, W. T., and B. F. James, A climatology of the potential vertical extent of giant cumulonimbus clouds in some selected areas, *Met. Mag.*, *101*, 161-181, 1973.
- Robbins, D., W. Evans, N. Louisnard, S. Pollitt, W. Traub, and J. Waters, Ozone intercomparisons from the balloon intercomparison campaign, in *Atmospheric Ozone*, edited by C. S. Zerefos and A. Ghazi, pp. 465-469, D. Reidel, Dordrecht, 1985.
- Robbins, D., J. Waters, P. Zimmermann, R. Jarnot, J. Hardy, H. Pickett, S. Pollitt, W. Traub, K. Chance, N. Louisnard, W. F. J. Evans, and J. Kerr, Ozone measurements during the balloon intercomparison campaign, to be published, 1986.
- Robbins, R. C., L. A. Cavanagh, and L. J. Salas, Analysis of ancient atmospheres, *J. Geophys. Res.*, *78*, 5341-5344, 1973.
- Robert, D., and J. Bonamy, Short range force effects in semiclassical molecular line broadening calculations, *Jl. de Physique*, *40*, 923-943, 1979.
- Robertson, J. P., and J. M. Tiedje, Denitrification and nitrous oxide production in successful and old growth Michigan forests, *Soil Sci. Soc. Am. J.*, *48*, 383-389, 1984.
- Robinson, E., and R. C. Robbins, Sources, abundance and fate of gaseous atmospheric pollutants, *Res. Proj. PR-6755*, Suppl. rep., Stanford Res. Inst., Menlo, CA, 1969.
- Robinson, E., R. A. Rasmussen, J. Krasnec, D. Pierotti, and M. Jakubovic, Halocarbon measurements in the Alaskan troposphere and lower stratosphere, *Atmos. Environ.*, *11*, 215-218, 1977.
- Roche, A. E., *UARS Spectroscopy Requirements: Report of the UARS Spectroscopy Working Group*, in press, 1985.
- Rodgers, C. D., The radiative heat budget of the troposphere and lower stratosphere, Planet. Circ. Project, MIT Dept. Meteorol., *Rep. #A2*, 1967.
- Rodgers, C. D., Evidence for the five-day wave in the upper stratosphere, *J. Atmos. Sci.*, *33*, 710-711, 1976a.
- Rodgers, C. D., Retrieval of atmospheric temperature and composition from remote measurements of thermal radiation, *Rev. Geophys. Space Phys.*, *14*, 609-624, 1976b.
- Rodgers, C. D., Statistical principles of inversion theory., in *Inversion Methods in Atmospheric Remote Sounding*, edited by A. Deepak, pp. 117-138, Academic Press, New York, 1977.
- Rodgers, C. D. (Ed.), Coordinated Study of the Behavior of the Middle Atmosphere in Winter (PMP-1), *Handbook for MAP, Vol. 12*, 154 pp., SCOSTEP Secretariat, Univ. of Illinois, Urbana, 1984.
- Rodgers, C. D., and W. L. Grose, PMP-1 Data Comparison Workshop, Part II, in *Handbook for MAP*, SCOSTEP Secretariat, Univ. of Illinois, Urbana, in press, 1985.
- Rodgers, C. D., and A. J. Prata, Evidence for a travelling 2-day wave in the middle atmosphere, *J. Geophys. Res.*, *86*, 9661-9664, 1981.
- Rodgers, C. D., and C. D. Walshaw, The computation of infra-red cooling rate in planetary atmospheres, *Quart. J. Roy. Meteorol. Soc.*, *92*, 67-92, 1966.
- Rodgers, C. D., R. L. Jones, and J. J. Barnett, Retrieval of temperature and composition from Nimbus 7 SAMS measurements, *J. Geophys. Res.*, *89*, 5280-5286, 1984.
- Rogers, C. F., and J. A. Pyle, Stratospheric tracer transport: A modified diabatic circulation model, *Quart. J. Roy. Meteorol. Soc.*, *110*, 219-237, 1984.
- Rood, R. B., and A. R. Douglass, Interpretation of ozone temperature correlations 1. Theory, *J. Geophys. Res.*, *90*, 5733-5743, 1985.
- Roscoe, H., Tentative observation of stratospheric N<sub>2</sub>O<sub>5</sub>, *Geophys. Res. Lett.*, *9*, 901-902, 1982.
- Roscoe, H. K., J. R. Drummond, and R. F. Jarnot, Infrared measurements of stratospheric composition III. The daytime changes of NO and NO<sub>2</sub>., *Proc. Roy. Soc. London A*, *375*, 507-528, 1981.
- Roscoe, H. K., B. J. Kerridge, S. Pollitt, M. Bingham, N. Louisnard, C. Alamichel, J. P. Pommereau, T. Ogawa, N. Iwagami, M. T. Coffey, W. Mankin, J. M. Fland, C. Camay-Peret, F. J. Murcray,

## REFERENCES

- A. Goldman, W. F. J. Evans, and T. McElroy, Intercomparison of stratospheric measurements of NO and NO<sub>2</sub>, in *Atmospheric Ozone*, edited by C. S. Zerefos and A. Ghazi, pp. 149-156, D. Reidel, Dordrecht, 1985a.
- Roscoe, H. K., B. J. Kerridge, J. A. Pyle, L. J. Gray, and R. J. Wells, Simultaneous measurements of stratospheric NO and NO<sub>2</sub> and their comparison with model predictions, *J. Geophys. Res.*, in press, 1985b.
- Roscoe, H. K., B. J. Kerridge, S. Pollitt, M. Bangham, N. Louisnard, C. Alamichel, J. M. Flaud, C. Camy-Peyret, J. R. Pommereau, T. Ogawa, N. Iwagami, M. T. Coffey, W. Mankin, F. J. Murcray, A. Goldman, W. F. J. Evans, T. McElroy, and J. Kerr, Intercomparison of remote measurements of stratospheric NO and NO<sub>2</sub>, to be published, 1986.
- Rose, K., and G. Brasseur, Ozone during sudden stratospheric warmings: A three-dimensional simulation, in *Atmospheric Ozone*, edited by C. S. Zerefos and A. Ghazi, pp. 28-32, D. Reidel, Dordrecht, 1985.
- Rothman, L. S., *AFGL atmospheric absorption line parameters compilation: 1985 Edition*, in press, 1985.
- Rothman, L. S., A. Goldman, J. R. Gillis, R. R. Gamache, H. M. Pickett, R. L. Poynter, N. Husson, and A. Chedin, AFGL trace gas compilation: 1982 version, *Appl. Opt.*, 22, 1616-1627, 1983a.
- Rothman, L. S., R. R. Gamache, A. Barbe, A. Goldman, J. R. Gillis, L. R. Brown, R. A. Toth, J. M. Flaud, and C. Camy-Peyret, AFGL atmospheric absorption line parameters compilation: 1982 Edition, *Appl. Opt.*, 22, 2247-2256, 1983b.
- Rothman, L. S., G. A. Vanasse, Murcray, D. G., F. H. Murcray, F. J. Murcray, and A. Goldman, Atmospheric emission spectra from the stratospheric cryogenic interferometer balloon experiment, in *Ninth Colloquium on High Resolution Molecular Spectroscopy*, pp. 19, University Press, Bologna, Italy, 1985.
- Rottger, J., Structure and dynamics of the stratosphere and mesosphere revealed by VHF radar investigations, *Pure Appl. Geophys.*, 118, 494-527, 1980.
- Rottman, G. J., 27-day variations observed in solar ultraviolet (120-300 nm) irradiance, *Planet. Space Sci.*, 31, 1001-1007, 1983.
- Rowe, B. R., A. A. Viggiano, F. C. Fehsenfeld, D. W. Fahey, and E. E. Ferguson, Reactions between neutrals clustered on ions, *J. Chem. Phys.*, 76, 742-743, 1982.
- Rowland, F. S., and M. J. Molina, Chlorofluoromethanes in the environment, *Rev. of Geophys. Space Phys.*, 13, 1-36, 1975.
- Rowland, F. S., and P. J. Rogers, Upper stratospheric photolysis of NaCl and KCl, *Proc. Natl. Acad. Sci. USA*, 79, 2737-2739, 1982.
- Rowland, F. S., E. W. Mayer, D. R. Blake and Y. Makide, Trends in atmospheric methane concentrations since 1978, paper presented at Proc. Symp. Composition of the Non-urban Troposphere, Williamsburg, VA, 25-28 May 1982.
- Rowland, F. S., D. R. Blake, and E. W. Mayer, World-wide increase in concentration of atmospheric methane since 1978, in *Symposium Proceedings of WMO Technical Conference on Observation and Measurement of Atmospheric Contaminants*, in press, 1984.
- Roy, C. R., I. E. Galbally, and B. A. Ridley, Measurements of nitric oxide in the stratosphere of the Southern Hemisphere, *Quart. J. Roy. Meteorol. Soc.*, 106, 887-894, 1980.
- Ruderman, M. A., H. M. Folet, and J. W. Chamberlain, Eleven-year variation in polar ozone and stratospheric-ion chemistry, *Science*, 192, 555-557, 1976.
- Rudolph, J., and D. H. Ehhalt, Measurements of C<sub>2</sub>-C<sub>5</sub> hydrocarbons over the North Atlantic, *J. Geophys. Res.*, 86, 11959-11964, 1981.
- Rudolph, J., D. H. Ehhalt, and A. Toennissen, Vertical profiles of ethane and propane in the stratosphere, *J. Geophys. Res.*, 86, 7267-7272, 1981.

## REFERENCES

- Rundel, R. D., D. M. Butler, and R. S. Stolarski, Uncertainty propagation in a stratospheric model 1. Development of a concise stratospheric model, *J. Geophys. Res.*, **83**, 3063-3072, 1978.
- Rusch, D. W., and R. S. Eckman, Implications of the comparison of ozone abundances measured by the Solar Mesosphere Explorer to model calculations, *J. Geophys. Res.*, **90**, 12991-12998, 1985.
- Rusch, D. W., J. C. Gerard, S. Solomon, P. J. Crutzen, and G. C. Reid, The effect of particle precipitation on the neutral and ion chemistry of the middle atmosphere—I. Odd nitrogen, *Planet. Space Sci.*, **29**, 767-774, 1981.
- Rusch, D. W., G. H. Mount, C. A. Barth, G. J. Rottman, R. J. Thomas, G. E. Thomas, R. W. Sanders, G. M. Lawrence, and R. S. Eckman, Ozone densities in the lower mesosphere measured by a Limb Scanning Ultraviolet Spectrometer, *Geophys. Res. Lett.*, **10**, 241-244, 1983.
- Rusch, D. W., G. H. Mount, C. A. Barth, and M. Callan, Global measurements of ozone in the 1.0 to 0.1 mb region by an ultraviolet spectrometer on the Solar Mesosphere Explorer, *J. Geophys. Res.*, **89**, 11677-11687, 1984.
- Rusch, D. W., R. J. Thomas, and E. Hilsenrath, Satellite-rocket ozone profile comparisons over Natal, *J. Geophys. Res.*, in press, 1985.
- Russell III, J. M., Global distribution and variability of stratospheric constituents measured by LIMS, *Adv. Space Res.*, **4**, 107-116, 1984.
- Russell III, J. M., and J. C. Gille, The Limb Infrared Monitor of the Stratosphere (LIMS) experiment, in *The Nimbus 7 Users' Guide*, edited by C. R. Madrid, pp. 71-103, NASA Goddard Space Flight Center, Greenbelt, MD, 1978.
- Russell III, J. M., J. C. Gille, E. E. Remsberg, L. L. Gordley, P. L. Bailey, S. R. Drayson, J. Fischer, A. Girard, J. E. Harries, and W. F. J. Evans, Validation of nitrogen dioxide results measured by the Limb Infrared Monitor of the Stratosphere (LIMS) experiment on Nimbus 7, *J. Geophys. Res.*, **89**, 5099-5107, 1984a.
- Russell III, J. M., S. Solomon, L. L. Gordley, E. E. Remsberg, and L. B. Callis, The variability of stratospheric and mesospheric NO<sub>2</sub> in the polar winter night observed by LIMS, *J. Geophys. Res.*, **89**, 7267-7275, 1984b.
- Russell III, J. M., J. C. Gille, E. M. Remsberg, L. L. Gordley, P. L. Bailey, H. Fischer, A. Girard, S. R. Drayson, W. F. J. Evans, and J. E. Harries, Validation of water vapor results measured by the Limb Infrared Monitor of the Stratosphere experiment on NIMBUS 7, *J. Geophys. Res.*, **89**, 5115-5124, 1984c.
- Russell III, J. M., S. Solomon, M. P. McCormick, A. J. Miller, D. W. Rusch, and J. J. Barnett, Middle atmosphere composition revealed by satellite observations, in *Handbook for MAP*, in press, 1986.
- Ryden, J. C., N<sub>2</sub>O exchange between grassland and the atmosphere, *Nature*, **292**, 235-237, 1981.
- SRI International, *Chemical Economics Handbook Product Review: Fluorocarbons*, August, 1982.
- Salby, M. L., Rossby normal modes in nonuniform background configurations. I: Simple fields, *J. Atmos. Sci.*, **38**, 1803-1826, 1981a.
- Salby, M. L., Rossby normal modes in nonuniform background configurations. II: Equinox and solstice conditions, *J. Atmos. Sci.*, **38**, 1827-1840, 1981b.
- Salby, M. L., The 2-day wave in the middle atmosphere—Observations and theory, *J. Geophys. Res.*, **86**, 9654-9660, 1981c.
- Salby, M. L., A ubiquitous wavenumber-5 anomaly in the Southern Hemisphere during FGGE, *Mon. Weather Rev.*, **110**, 1712-1720, 1982a.
- Salby, M. L., Sampling theory for synoptic satellite observations. Part I. Space-time spectra, resolution and aliasing. Part II. Fast Fourier synoptic mapping, *J. Atmos. Sci.*, **39**, 2577-2614, 1982b.
- Salby, M. L., Survey of planetary-scale traveling waves: The state of theory and observations, *Rev. Geophys. Space. Phys.*, **22**, 209-236, 1984a.

## REFERENCES

- Salby, M. L., Transient disturbances in the stratosphere: Implications for theory and observing systems, *J. Atmos. Terr. Phys.*, **46**, 1009-1047, 1984b.
- Salby, M. L., and R. Garcia, Vacillations induced by interference of stationary and traveling waves, in *Handbook for MAP, Vol. 18*, edited by S. Kato, pp. 170-174, SCOSTEP Secretariat, Univ. of Illinois, Urbana, 1985.
- Salby, M. L., and R. G. Roper, Long-period oscillations in the meteor region, *J. Atmos. Sci.*, **37**, 237-244, 1980.
- Salby, M. L., D. L. Hartmann, P. L. Bailey, and J. C. Gille, Evidence for equatorial Kelvin modes in Nimbus-7 LIMS, *J. Atmos. Sci.*, **41**, 220-235, 1984.
- Samain, D., and P. C. Simon, Solar flux determination in the spectral range 150-210 nm, *Solar Physics*, **49**, 33-41, 1976.
- Sandalls, F. J., and S. A. Penkett, Measurements of carbonyl sulfide and carbon disulfide in the atmosphere, *Atmos. Environ.*, **11**, 197-199, 1977.
- Sander, S. P., and M. Peterson, Kinetics of the reaction  $\text{HO}_2 + \text{NO}_2 + \text{M} \rightarrow \text{HO}_2\text{NO}_2 + \text{M}$ , *J. Phys. Chem.*, **88**, 1566-1571, 1984.
- Sanheuzza, E., and J. Heicklen, Chlorine atom sensitized oxidation of dichloromethane and chloromethane, *J. Phys. Chem.*, **79**, 7-11, 1975.
- Sato, T., and R. F. Woodman, Fine altitude resolution observations of stratospheric turbulent layers by the Arecibo 430 MHz radar, *J. Atmos. Sci.*, **39**, 2546-2552, 1982.
- Savoie, D. L., and J. M. Prospero, Particle size distribution of nitrate and sulfate in the marine atmosphere, *Geophys. Res. Lett.*, **9**, 1207-1210, 1982.
- Sawyer, J. S., The vertical circulation at meteorological fronts and its relation to frontogenesis, *Proc. Roy. Soc. London*, **A234**, 346-362, 1956.
- Schenkel, A., and B. Broder, Interference of some trace gases with ozone measurements by the KI method, *Atmos. Environ.*, **16**, 2187-2190, 1982.
- Schlesinger, M. E., A review of climate model simulations of  $\text{CO}_2$ -induced climatic change, *Rep. No. 41*, 135 pp., Climatic Research Institute, Oregon State University, Corvallis, OR, 1983.
- Schlesinger, M. E., Climate model simulation of  $\text{CO}_2$ -induced climatic change, in *Advances in Geophysics*, **26**, edited by B. Saltzman, pp. 141-235, Academic Press, New York, 1984.
- Schlesinger, M. E., and Y. Mintz, Numerical simulation of ozone production, transport and distribution with a global general circulation model, *J. Atmos. Sci.*, **36**, 1325-1361, 1979.
- Schlesinger, M. E., and J. F. B. Mitchell, Model projections of equilibrium climate response to increased  $\text{CO}_2$ , edited M. C. MacCracken and F. M. Luther, U.S. Department of Energy, in press, 1985.
- Schlesinger, M. E., W. L. Gates, and Y. J. Han, The role of the ocean in  $\text{CO}_2$ -induced climate change: Preliminary results from the OSU coupled atmosphere-ocean general circulation model, in *Coupled Ocean Atmosphere Models*, edited by J. C. Nichol, pp. 447-478, Elsevier Science, New York, 1985.
- Schmailzl, U., and P. J. Crutzen, Budgets of stratospheric trace gases from 2-D-model calculations and satellite observations, in *Atmospheric Ozone*, edited by C. S. Zerefos and A. Ghazi, pp. 43-47, D. Reidel, Dordrecht, 1985.
- Schmeisser, M., and K. Brandle, Halogennitrate und ihre Reaktionen, *Angew. Chem.*, **73**, 388-393, 1961.
- Schmidt, U., G. Kulessa, A. Khedim, D. Knapska, and J. Rudolph, Sampling of long lived trace gases in the middle and upper stratosphere, in *Sixth ESA Symposium on European Rocket and Balloon Programmes and Related Research—Conferences*, *ESA SP-183*, edited by W. R. Burke, pp. 141-145, European Space Agency, Paris, 1983.
- Schmidt, U., A. Khedim, D. Knapska, G. Kulessa, and F. J. Johnen, Stratospheric trace gas distributions observed in different seasons, *Adv. Space Res.*, **4**, 131-134, 1984.

## REFERENCES

- Schmidt, U., D. Knapska, and S. A. Penkett, A study of the vertical distribution of methyl chloride ( $\text{CH}_3\text{Cl}$ ) in the midlatitude stratosphere, *J. Atmos. Chem.*, in press, 1985a.
- Schmidt, U., P. Fabian, and R. Borchers, Intercomparison of balloon-borne cryogenic whole air samplers during the MAP/Globus campaign, *Planet. Space Sci.*, in press, 1985b.
- Schneider, S. H., On the carbon dioxide-climate confusion, *J. Atmos. Sci.*, 32, 2060-2066, 1975.
- Schneider, S. H., and S. L. Thompson, Atmospheric  $\text{CO}_2$  and climate: Importance of the transient response, *J. Geophys. Res.*, 86, 3135-3147, 1981.
- Schneider, W. H., P. K. Bhartia, K. F. Klenk, and C. L. Mateer, An optimum statistical technique for ozone profile retrieval from backscattered UV radiances, paper presented at Fourth Conference on Atmospheric Radiation, Am. Meteorol. Soc., Toronto, Ontario, Canada, June 16-18, 1981.
- Schoeberl, M. R., Stratospheric warmings: Observations and theory, *Rev. Geophys. Space Phys.*, 16, 521-538, 1978.
- Schoeberl, M. R., Medium-scale disturbances in total ozone during Southern Hemisphere summer, *Bull. Amer. Meteorol. Soc.*, 64, 1358-1365, 1983.
- Schoeberl, M. R., On the penetration of mountain waves into the middle atmosphere, *J. Atmos. Sci.*, 42, 2856-2864, 1985.
- Schoeberl, M. R., and M. A. Geller, A calculation of the structure of stationary planetary waves in winter, *J. Atmos. Sci.*, 34, 1235-1255, 1977.
- Schoeberl, M. R., and D. F. Strobel, The response of the zonally averaged circulation to stratospheric ozone reductions, *J. Atmos. Sci.*, 35, 1751-1757, 1978a.
- Schoeberl, M. R., and D. F. Strobel, The zonally averaged circulation of the middle atmosphere, *J. Atmos. Sci.*, 35, 577-591, 1978b.
- Schoeberl, M. R., and D. F. Strobel, Nonzonal gravity wave breaking in the winter mesosphere, in *Dynamics of the Middle Atmosphere*, edited by J. R. Holton and T. Matsuno, pp. 45-64, D. Reidel, Dordrecht, 1984.
- Schoeberl, M. R., D. F. Strobel, and J. Apruzese, A numerical model of gravity wave breaking and stress in the mesosphere, *J. Geophys. Res.*, 88, 5249-5259, 1983.
- Schryer, D. R., *Heterogeneous Atmospheric Chemistry, Geophysical Monograph 26*, American Geophysical Union, Washington, DC, 1982.
- Schwab, J. J., D. W. Toohey, W. H. Brune, and J. G. Anderson, Reaction kinetics of  $\text{O} + \text{ClO} \rightarrow \text{Cl} + \text{O}_2$  between 252-347K, *J. Geophys. Res.*, 89, 9581-9587, 1984.
- Schwartz, P. R., C. L. Croskey, R. M. Bevilacqua, and J. J. Olivero, Microwave spectroscopy of  $\text{H}_2\text{O}$  in the stratosphere and mesosphere, *Nature*, 305, 294-295, 1983.
- Schwartz, S. E., Gas- and aqueous-phase chemistry of  $\text{HO}_2$  in liquid-water clouds, paper presented at the meeting of the American Chemical Society, Division of Environmental Chemistry, Washington, DC, September, 1983.
- Secroun, C., A. Barbe, P. Jouve, P. Arcas, and E. Arie, Intensity of the  $\nu_3$  band of ozone from a study of its anomalous dispersion at  $10 \mu\text{m}$ , *J. Molec. Spectrosc.*, 85, 8-15, 1981.
- Schmel, G. A., Particle and gas dry deposition: A review, *Atmos. Environ.*, 14, 983-1011, 1980.
- Seiler, W., The cycle of carbon monoxide in the atmosphere, in *Proceedings of the ICESA Conference, Vol. 2*, I.E.E.E., New York, 1976.
- Seiler, W., Contributions of biological processes to the global budget of  $\text{CH}_4$  in the atmosphere, in *Current Perspectives in Microbial Ecology*, American Soc. for Microbiology, Washington, DC, edited by M. J. Klug and C. A. Reddy, 710 pp., 1984.
- Seiler, W., and R. Conrad, Field measurements of natural and fertilizer-induced  $\text{N}_2\text{O}$  release rates from soils, *APCA Journal*, 31, 767-772, 1981.

## REFERENCES

- Seiler, W., and R. Conrad, Contributions of tropical ecosystems to the global budgets of trace gases, especially CH<sub>4</sub>, H<sub>2</sub>, CO and N<sub>2</sub>O, in *Geophysiology of Amazonia*, edited by R. Dickinson, Wiley, New York, in press, 1985.
- Seiler, W., and P. Crutzen, Estimates of the gross and net flux of carbon between the biosphere and the atmosphere from biomass burning, *Climate Change*, 2, 207-247, 1980.
- Seiler, W., and J. Fishman, The distribution of carbon monoxide and ozone in the free troposphere, *J. Geophys. Res.*, 86, 7255-7265, 1981.
- Seiler, W., and U. Schmidt, New aspects of CO and H<sub>2</sub> cycles in the atmosphere, in *Proceedings of the Int'l Conf. on the Structure, Composition, and Gen'l Circulation of the Upper and Lower Atmospheres and Possible Anthropogenic Perturbations*, pp. 192-222, IAMAP, Melbourne, 1974.
- Seiler, W., F. Muller, and H. Oeser, Vertical distribution of chlorofluoromethanes in the upper troposphere and lower stratosphere, *Pure Appl. Geophys.*, 116, 554-566, 1978.
- Seiler, W., A. Holzapfel-Pschorn, R. Conrad, and D. Scharffe, Methane emissions from rice paddies, *J. Atmos. Chem.*, 1, 241-268, 1984a.
- Seiler, W., H. Giehl, E. Brunke, and E. Halliday, The seasonality of CO abundance in the Southern Hemisphere, *Tellus*, 36B, 219-231, 1984b.
- Seiler, W., R. Conrad, and D. Scharffe, Field studies of CH<sub>4</sub> emissions from termite nests into the atmosphere and measurements of CH<sub>4</sub> uptake by tropical soils, *J. Atmos. Chem.*, 1, 171-187, 1984c.
- Seinfeld, J. H., *Air Pollution: Physical and Chemical Fundamentals*, 523 pp., McGraw-Hill Book Co., New York, 1975.
- Senum, G. I., Y. N. Lee, and Gaffrey, Ultraviolet absorption spectrum of peroxyacetyl nitrate and peroxypropionyl nitrate, *J. Phys. Chem.*, 88, 1269-1270, 1984.
- Sexstone, A. J., N. P. Reusbeck, T. B. Parkin, and J. M. Tiedje, Direct measurement of oxygen profiles and denitrification rates in soil aggregates, *Soil Sci. Am. J.*, 49, 645-651, 1985.
- Sexton, K. and H. Westberg, Nonmethane HC composition of urban and rural atmospheres, *Atmos. Environ.*, 18, 1125-1132, 1984.
- Shapiro, M. A., A multiple-structured frontal zone-jet stream system as revealed by meteorologically instrumented aircraft, *Mon. Weather Rev.*, 102, 244-253, 1974.
- Shapiro, M. A., Simulation of upper level frontogenesis with a 20-level isentropic coordinate primitive equation model, *Mon. Weather Rev.*, 103, 591-604, 1975.
- Shapiro, M. A., The role of turbulent heat flux in the generation of potential vorticity in the vicinity of upper level jetstream systems, *Mon. Weather Rev.*, 102, 892-896, 1976.
- Shapiro, M. A., Further evidence of the mesoscale and turbulent structure of upper jet stream-frontal zone systems, *Mon. Weather Rev.*, 106, 1101-1111, 1978.
- Shapiro, M. A., Turbulent mixing within tropopause folds as a mechanism for exchange of chemical constituents between the stratosphere and troposphere, *J. Atmos. Sci.*, 37, 994-1004, 1980.
- Shapiro, M. A., Frontogenesis and geostrophically forced secondary circulations in the vicinity of jetstream-frontal zone systems, *J. Atmos. Sci.*, 38, 954-973, 1981.
- Shapiro, M. A., E. R. Reiter, R. D. Cadle, and W. A. Sedlacek, Vertical mass and trace constituent transports in the vicinity of jet streams, *Arch. Met. Geoph. Biokl.*, B28, 193-206, 1980.
- Shapiro, M. A., A. J. Krueger, and P. J. Kennedy, Nowcasting the position and intensity of jet streams using a satellite-borne total ozone mapping spectrometer, in *Nowcasting*, edited by K. A. Browning, pp. 137-145, Academic Press, New York, 1982.
- Shapiro, M. A., R. C. Schnell, F. P. Parungo, S. J. Oltmans, and B. A. Bodhaine, El Chichon volcanic debris in an Arctic tropopause fold, *Geophys. Res. Lett.*, 11, 421-424, 1984.
- Shardanand, and A. D. Prasad Rao, Collision induced absorption of O<sub>2</sub> in the Herzberg continuum, *J. Quant. Spectrosc. Radiat. Transfer*, 17, 433-439, 1977.

## REFERENCES

- Sharma, R. D., and R. M. Nadile, Carbon dioxide ( $v_2$ ) radiative results using a new non-equilibrium model, *AIAA 81-0426*, paper presented at AIAA 19th Aerospace Sciences meeting, St. Louis, MO, 1981.
- Shaw, Napier Sir, *Manual of Meteorology, The Physical Processes of Weather, Vol. III*, 445 pp., Cambridge University Press, Cambridge, 1942.
- Shiotani, M., and I. Hirota, Planetary wave-mean flow interaction in the stratosphere: A comparison between the Northern and Southern Hemisphere, *Quart. J. Roy. Meteorol. Soc.*, *111*, 309-334, 1985.
- Siegenthaler, U., and H. Oeschger, Transient temperature changes due to increasing  $\text{CO}_2$  using simple models, *Ann. of Glaciology*, *5*, 153-159, 1984.
- Silver, J. A., and C. E. Kolb, Measurement of molecular sodium species in the upper atmosphere, *Report No. ARI-RP-199*, Aerodyne Research, Inc., Billerica, MA, May, 1985.
- Silver, J. A., A. C. Stanton, M. S. Zahniser, and C. E. Kolb, Gas phase reaction rate of sodium hydroxide with hydrochloric acid, *J. Phys. Chem.*, *88*, 3123-3129, 1984a.
- Silver, J. A., M. S. Zahniser, A. C. Stanton, and C. E. Kolb, Temperature dependent thermolecular reaction rate constants for potassium and sodium superoxides formation, paper presented at 20th Symposium (International) on Combustion, Ann Arbor, MI, August, 1984b.
- Simmonds, P. G., F. N. Alyea, C. A. Cardelino, A. J. Crawford, D. M. Cunnold, B. C. Lane, J. E. Lovelock, R. G. Prinn, and R. A. Rasmussen, The atmospheric lifetime experiment, 6, Results for carbon tetrachloride based on 3 years data, *J. Geophys. Res.*, *88*, 8427-8441, 1983.
- Simmons, A. J., and R. Struefing, Numerical forecasts of stratospheric warming events using a model with a hybrid vertical coordinate, *Quart. J. Roy. Meteorol. Soc.*, *109*, 81-111, 1983.
- Simon, P. C., Balloon measurements of solar fluxes between 1960 and 2300 Å, in *Proceedings of the Third Conference on the Climatic Impact Assessment Program, DOT-TSC-OST-74-15*, edited by A. J. Broderick and T. M. Hard, pp. 137-140, Dept. of Transp., Washington, DC, 1975.
- Simon, P. C., Solar irradiance between 120 and 400 nm and its variations, *Solar Physics*, *74*, 273-291, 1981.
- Simon, P. C., and G. Brasseur, Photodissociation effects of solar UV radiation, *Planet. Space Sci.*, *31*, 987-999, 1983.
- Simon, P. C., R. Pastiels, and D. Nevejans, Balloon observations of solar ultraviolet irradiance at solar minimum, *Planet. Space Sci.*, *30*, 68-71, 1982.
- Simonaitis, R., Oxidation of the  $\text{CH}_3$  radical and some halomethyl and haloethyl radicals of atmospheric interest, in *Proceedings of the NATO Advanced Study Institute on Atmospheric Ozone, Rep. FAA-EE-80-20*, edited by A. C. Aikin, pp. 501-515, DOT, FAA, Washington, DC, 1980.
- Simonaitis, R., and J. Heicklen, Temperature dependence of the reactions of  $\text{HO}_2$  with  $\text{NO}$  and  $\text{NO}_2$ , *Int. J. Chem. Kinet.*, *10*, 67-87, 1978.
- Simons, J. W., R. J. Paur, H. A. Webster III, and E. J. Bair, Ozone ultraviolet photolysis. VI. The ultraviolet spectrum, *J. Chem. Phys.*, *59*, 1203-1208, 1973.
- Singh, H. B., Atmospheric halocarbons: Evidence in favour of reduced average hydroxyl radical concentration in the troposphere, *Geophys. Res. Lett.*, *4*, 101-104, 1977a.
- Singh, H. B., Preliminary estimates of average tropospheric OH concentrations in the Northern and Southern Hemispheres, *Geophys. Res. Lett.*, *4*, 453-456, 1977b.
- Singh, H. B., and L. J. Salas, Measurement of selected light hydrocarbons over the Pacific Ocean: Latitudinal and seasonal variations, *Geophys. Res. Lett.*, *9*, 842-845, 1982.
- Singh, H. B., and L. J. Salas, Methodology for the analysis of peroxyacetyl nitrate (PAN) in the unpolluted troposphere, *Atmos. Environ.*, *17*, 1507-1516, 1983a.
- Singh, H. B., and L. J. Salas, Peroxyacetylnitrate in the free troposphere, *Nature*, *302*, 326-328, 1983b.
- Singh, H. B., L. J. Salas, H. Shigeishi, and A. Crawford, Urban-nonurban relationships of halocarbons,  $\text{SF}_6$ ,  $\text{N}_2\text{O}$  and other atmospheric trace constituents, *Atmos. Environ.*, *11*, 819-823, 1977.
- Singh, H. B., L. J. Salas, H. Shigeishi, and E. Scibner, Atmospheric halocarbons, hydrocarbons, and sulfur hexafluoride: Global distributions, sources, and sinks, *Science*, *203*, 899-903, 1979.

## REFERENCES

- Singh, H. B., L. J. Salas, and R. E. Stiles, Methyl halides in and over the eastern Pacific (40°N-32°S), *J. Geophys. Res.*, **88**, 3684-3690, 1983a.
- Singh, H. B., L. J. Salas, and R. E. Stiles, Selected man-made halogenated chemicals in the air and oceanic environment, *J. Geophys. Res.*, **88**, 3675-3683, 1983b.
- Singh, H. B., L. J. Salas, B. A. Ridley, J. Shetter, N. M. Donahue, F. C. Fehsenfeld, D. W. Fahey, D. D. Parrish, E. J. Williams, S. C. Liu, G. Hubler, P. C. Murphy, Relationship between peroxyacetyl nitrate (PAN) and nitrogen oxides in the clean troposphere, in press, 1985.
- Slemr, F., and W. Seiler, Field measurements of NO and NO<sub>2</sub> emissions from fertilized and unfertilized soils, *J. Atmos. Chem.*, **2**, 1-24, 1984.
- Smagorinsky, J. (Chairman), *Carbon Dioxide and Climate: A Second Assessment*, 92 pp., National Academy Press, Washington, DC, 1982.
- Smagorinsky, J., S. Manabe, and J. L. Holloway Jr., Numerical results from a nine-level general circulation model of the atmosphere, *Mon. Weather Rev.*, **93**, 727-788, 1965.
- Smith, A. K., An observational study of planetary wave propagation in the winter stratosphere, Ph.D. thesis, 71 pp., Washington Univ., Seattle, WA, 1982.
- Smith, A. K., Observations of wave-wave interactions in the stratosphere, *J. Atmos. Sci.*, **40**, 2484-2496, 1983.
- Smith, A. K., and L. V. Lyjak, An observational estimate of gravity wave drag from the momentum balance in the middle atmosphere, *J. Geophys. Res.*, **90**, 2233-2241, 1985.
- Smith, A. K., J. C. Gille, and L. V. Lyjak, Wave-wave interactions in the stratosphere: Observations during quiet and active wintertime periods, *J. Atmos. Sci.*, **41**, 363-373, 1984.
- Smith, C. J., R. D. DeLaure, and W. H. Patrick, Jr., Nitrous oxide emission from Gulf Coast wetlands, *Geochim. Cosmochim. Acta*, **47**, 1805-1814, 1983.
- Smith, M. A. H. (Ed.), Review of spectroscopic parameters for upper atmospheric measurements, *NASA Conference Publication 2396*, 28 pp., NASA, Langley Research Center, Hampton, VA, 1985.
- Smith, M. A. H., and C. P. Rinsland, Spectroscopic measurements of atmospheric HCN at northern and southern latitudes, *Geophys. Res. Lett.*, **12**, 5-8, 1985.
- Smith, M. A. H., C. P. Rinsland, D. Frieourch and K. Narahari Rao, Intensities and collision broadening parameters from infrared spectra, in *Molecular Spectroscopy in Modern Research*, Vol. 3, pp. 111-248, Academic Press, New York, 1985.
- Smith, P. L., H. E. Griesinger, J. H. Black, K. Yoshino, and D. E. Freeman, Interstellar O<sub>2</sub>. II. VUV oscillator strengths of Schumann-Runge lines and prospects for space telescope observations, *Astrophys. J.*, **277**, 569-575, 1984.
- Smith, R. M., A preview of the detection of mass return flow of air and water into the stratosphere using tritium as a tracer, *Tellus*, **20**, 76-81, 1968.
- Smith, W. L., H. M. Woolf, C. M. Hayden, D. Q. Wark, and L. M. McMillin, The TIROS-N operational vertical sounder, *Bull. Amer. Meteor. Soc.*, **60**, 1177-1187, 1979.
- Solomon, P. M., R. L. de Zafra, A. Parrish, and J. W. Barrett, Diurnal variation of stratospheric chlorine monoxide: A critical test of chlorine chemistry in the ozone layer, *Science*, **224**, 1210-1214, 1984.
- Solomon, S., and P. J. Crutzen, Analysis of the August 1972 solar proton event including chlorine chemistry, *J. Geophys. Res.*, **86**, 1140-1146, 1981.
- Solomon, S., and R. R. Garcia, On the distribution of nitrogen dioxide in the high-latitude stratosphere, *J. Geophys. Res.*, **88**, 5229-5239, 1983a.
- Solomon, S., and R. R. Garcia, Simulation of NO<sub>x</sub> partitioning along isobaric parcel trajectories, *J. Geophys. Res.*, **89**, 5497-5501, 1983b.
- Solomon, S., and R. R. Garcia, Transport of thermospheric NO to the upper stratosphere, *Planet. Space Sci.*, **32**, 399-409, 1984a.

## REFERENCES

- Solomon, S., and R. R. Garcia, On the distribution of long-lived tracers and chlorine species in the middle atmosphere, *J. Geophys. Res.*, **89**, 11633-11644, 1984b.
- Solomon, S., D. W. Rusch, J.-C. Gerard, G. C. Reid, and P. J. Crutzen, The effect of particle precipitation events on the neutral and ion chemistry of the middle atmosphere: II. Odd hydrogen, *Planet. Space Sci.*, **29**, 885-892, 1981.
- Solomon, S., P. J. Crutzen, and R. G. Roble, Photochemical coupling between the thermosphere and the lower atmosphere 1. Odd nitrogen from 50 to 120 km, *J. Geophys. Res.*, **87**, 7206-7220, 1982.
- Solomon, S., D. W. Rusch, R. J. Thomas, and R. S. Eckman, Comparison of mesospheric ozone abundances measured by the Solar Mesosphere Explorer and model calculations, *Geophys. Res. Lett.*, **10**, 249-252, 1983a.
- Solomon, S., G. C. Reid, D. W. Rusch, and R. J. Thomas, Mesospheric ozone depletion during the solar proton event of July 13, 1983, Part II. Comparison between theory and measurements, *Geophys. Res. Lett.*, **10**, 257-260, 1983b.
- Solomon, P. M., R. de Zafra, A. Parrish and J. W. Barrett, Diurnal variation of stratospheric chlorine oxide: A critical test of chlorine chemistry in the ozone layer, *Science*, **224**, 1210-1214, 1984.
- Solomon, S., J. M. Russell III, M. P. McCormick, D. W. Rusch, and J. M. Zawodny, Intercomparison of satellite datasets for NO<sub>2</sub> and odd nitrogen photo-chemistry, in press, 1985a.
- Solomon, S., R. R. Garcia, and F. Stordal, Transport processes and ozone perturbations, *J. Geophys. Res.*, **90**, 12981-12990, 1985b.
- Solomon, S., J. T. Kiehl, R. R. Garcia, and W. Grose, Tracer transport by the diabatic circulation deduced from satellite observations, *J. Atmos. Sci.*, in press, 1986.
- Somerville, R. C. J., and L. A. Remer, Cloud optical thickness feedbacks in the CO<sub>2</sub> climate problem, *J. Geophys. Res.*, **89**, 9668-9672, 1984.
- Spelman, M. J., and S. Manabe, Influence of oceanic heat transport upon the sensitivity of a model climate, *J. Geophys. Res.*, **89**, 571-586, 1984.
- Speth, P., and R. Madden, Space-time spectral analyses of Northern Hemisphere geopotential heights, *J. Atmos. Sci.*, **40**, 1086-1100, 1983.
- Spicer, C. W., M. W. Holdren, and C. W. Keigley, The ubiquity of peroxyacetyl nitrate in the continental boundary layer, *Atmos. Environ.*, **17**, 1055-1058, 1983.
- Sridharan, U. C., L. X. Qui, and F. Kaufman, Kinetics and product channels of the reactions of HO<sub>2</sub> with O and H atoms at 296K, *J. Phys. Chem.*, **86**, 4569-4574, 1982.
- Sridharan, U. C., L. X. Qui, and F. Kaufman, Rate constant of the OH + HO<sub>2</sub> reaction from 252 to 420K, *J. Phys. Chem.*, **88**, 1281-1282, 1984.
- St. John, D., W. H. Bailey, W. H. Fellner, J. M. Minor, and R. D. Sull, Time series analysis of stratospheric ozone, *Commun. Statist. Theory Methods*, **11**, 1293-1333, 1982.
- Staff, Upper Air Branch National Weather Service, Synoptic analyses, 5-, 2-, and 0.4-millibar surfaces for July 1974 through June 1976, *NASA Ref. Publ. 1023*, 330 pp., National Weather Service, Camp Springs, MD, 1978.
- Staffens, F. L., S. Kikkawa, and R. G. Phibbs, Meteorological rocket data processor and results from the solar eclipse of 7 March 1970, *J. Appl. Meteorol.*, **11**, 722-730, 1972.
- Staley, D. O., Evaluation of potential vorticity changes near the tropopause and the related vertical motions, vertical advection of vorticity, and transfer of radioactive debris from stratosphere to troposphere, *J. Meteorol.*, **17**, 591-620, 1960.
- Staley, D. O., On the mechanism of mass and radioactivity transport from stratosphere to troposphere, *J. Atmos. Sci.*, **19**, 450-467, 1962.
- Starr, W. L., R. A. Craig, M. Loewenstein, and M. E. McGhan, Measurements of NO, O<sub>3</sub>, and temperature at 19.8 km during the total solar eclipse of 26 February 1979, *Geophys. Res. Lett.*, **7**, 553-555, 1980.

## REFERENCES

- Stauffer, B., A. Neftel, H. Oeschger, and J. Schwander, CO<sub>2</sub> concentrations in air extracted from Greenland ice samples, in *Greenland Ice Core: Geophysical Geochemistry, and the Environment*, American Geophysical Union Monograph No. 33, edited by C. C. Langway, H. Oeschger, and W. Dansgaard, pp. 83-89, Washington, DC, 1985.
- Stedman, D. H., and J. O. Jackson, The photostationary state in photochemical smog, *Int. J. Chem. Kinetics Symposium*, 1, 493-501, 1975.
- Steed, J. M., A. J. Owens, C. D. Miller, D. L. Filkin, and J. P. Jesson, Two-dimensional model calculations of potential ozone perturbation by chlorofluorocarbons, *Nature*, 295, 308-311, 1982.
- Steele, L. P., P. J. Fraser, R. A. Rasmussen, M. A. K. Khalil, T. J. Conway, A. J. Crawford, R. H. Gammon, K. A. Masarie, and K. W. Thoning, The global distribution of methane in the troposphere, *J. Atmos. Chem.*, in press, 1985.
- Stelson, A. W., and J. H. Seinfeld, Relative humidity and temperature dependence of the ammonium nitrate dissociation constant, *Atmos. Environ.*, 16, 983-993, 1982.
- Stephens, G. L., and P. J. Webster, Sensitivity of radiative forcing to variable cloud and moisture, *J. Atmos. Sci.*, 36, 1450-1466, 1979.
- Stephens, G. L., S. Ackerman and E. A. Smith, A shortwave parameterization revised to improve cloud absorption, *J. Atmos. Sci.*, 41, 687-690, 1984.
- Stern, A. C., *Air Pollution, Vol. III*, Academic Press, New York, 1977.
- Stevens, C. M., and A. Engelkemeir, *J. Geophys. Res.*, in press, 1986.
- Stockwell, W. R., and J. G. Calvert, The mechanism of the HO-SO<sub>2</sub> reaction, *Atmos. Environ.*, 17, 2231-2235, 1983.
- Stolarski, R. S., Impact of large amounts of chlorine on stratospheric ozone, paper presented at the International Workshop on Current Issues in our Understanding of the Stratosphere and the Future of the Ozone Layer, BMFT, NASA, FAA, WMO, Feldafing, FRG, June 11-16, 1984.
- Stolarski, R. S., and R. J. Cicerone, Stratospheric chlorine: A possible sink for ozone, *Can. J. Chem.*, 52, 1610-1615, 1974.
- Stolarski, R. S., and A. R. Douglass, Parameterization of the photochemistry of stratospheric ozone including catalytic loss processes, *J. Geophys. Res.*, 90, 10709-10718, 1985.
- Stolarski, R. S., D. M. Butler, and R. D. Rundel, Uncertainty propagation in a stratospheric model. 2. Monte Carlo analysis of imprecisions due to reaction rates, *J. Geophys. Res.*, 83, 3074-3078, 1978.
- Stordal, F., I. S. A. Isaksen, and K. Horntveth, A diabatic circulation two-dimensional model with photochemistry: Simulations of ozone and ground released tracers, *J. Geophys. Res.*, 90, 5757-5776, 1985.
- Stout, J., E. B. Rogers, and E. Nunez, abst, 16th Conf. Hurricanes and Tropical Meteorol 14-17 May 1985, Houston, Texas., 1985.
- STRAC, Chlorofluorocarbons and their effects on stratospheric ozone, *Pollution Paper No 15*, HMSO, 1979.
- Stratospheric Analysis Group, *Meteor. Abh. Met. Inst. Berlin*, 1980.
- Strickland, A. C. (Ed.), *COSPAR International Reference Atmosphere*, Akademie-Verlag, Berlin, 1972.
- Strobel, D. F., Parameterization of the atmospheric heating from 15-120 km due to O<sub>2</sub> and O<sub>3</sub> absorption of solar radiation, *J. Geophys. Res.*, 83, 6225-6230, 1978a.
- Strobel, D. F., Photochemical radiative damping and instability in the stratosphere, II. Numerical results, *Geophys. Res. Lett.*, 5, 523-525, 1978b.
- Strobel, D. F., D. M. Hunten, and M. B. McElroy, Production and diffusion of nitric oxide, *J. Geophys. Res.*, 75, 4307-4321, 1970.
- Susskind, J., and J. E. Searl, Atmospheric absorption near 2400 cm<sup>-1</sup>, *J. Quant. Spectrosc. Radiat. Transfer*, 18, 581-589, 1977.
- Swanson, D., K. Brian, and H. S. Johnston, NO<sub>3</sub> quantum yield from N<sub>2</sub>O<sub>5</sub> photolysis, *J. Phys. Chem.*, 88, 3115-3115, 1984.

## REFERENCES

- Swider, W., and T. J. Keneshea, Decrease of ozone and atomic oxygen in the lower mesosphere during a PCA event, *Planet. Space Sci.*, *21*, 1969-1973, 1973.
- Swider, W., T. J. Keneshea, and C. I. Foley, An SPE-distributed D-region model, *Planet. Space Sci.*, *26*, 883-892, 1978.
- Syed, M. Q., and A. W. Harrison, Ground based observations of stratospheric nitrogen dioxide, *J. Canad. Phys.*, *58*, 788-802, 1980.
- Syed, M. Q., and A. W. Harrison, Seasonal trend of stratospheric NO<sub>2</sub> over Calgary, *Can. J. Phys.*, *59*, 1278-1279, 1981.
- Sze, N. D., Anthropogenic CO emissions: Implications for the atmospheric CO-OH-CH<sub>4</sub> cycle, *Science*, *195*, 673-675, 1977.
- Sze, N. D., paper presented at CMA Workshop on Stratospheric Chemistry, Gottingen, FRG, October, 1984.
- Sze, N. D., and M. K. Ko, CS<sub>2</sub> and COS in the stratospheric sulfur budget, *Nature*, *280*, 308-310, 1979.
- Sze, N. D., M. K. W. Ko, W. Swider, and E. Murad, Atmospheric sodium chemistry. 1. The altitude region 70-100 km, *Geophys. Res. Lett.*, *9*, 1187-1190, 1982.
- Sze, N. D., M. K. W. Ko, M. Livshits, W. C. Wang, P. B. Ryan, R. E. Specht, M. B. McElroy, and S. C. Wofsy, *Annual Report on the Atmospheric Chemistry, Radiation and Dynamics Program*, Atmospheric and Environmental Research, Inc., Cambridge, MA, 1983.
- Taine, J., and F. LePoutre, A photoacoustic study of the collisional deactivation of the first vibrational levels of CO<sub>2</sub> by N<sub>2</sub> and CO, *Chem. Phys. Lett.*, *65*, 554-558, 1979.
- Takahashi, M., A two-dimensional numerical model of the semi-annual zonal wind oscillation, in *Dynamics of the Middle Atmosphere*, edited by J. R. Holton and T. Matsuno, pp. 253-269, Terrapub, Tokyo, 1984.
- Tang, I. N., On the equilibrium partial pressures of nitric acid and ammonia in the atmosphere, *Atmos. Environ.*, *14*, 819-828, 1980.
- Telegades, K., The seasonal stratospheric distribution and inventory of excess carbon-14 from March 1955 to July 1969, *Rep. 243*, Health and Safety Lab., U.S. Atomic Energy Comm., Washington, DC, 1971.
- Tenenbaum, J., Integrated and spectral energetics studies of the GLAS general circulation model, *Mon. Weather Rev.*, *110*, 962-980, 1982.
- Terry, R. E., R. L. Tate, and J. M. Duxbury, Nitrous oxide emissions from drained, cultivated organic soils of S. Florida, *J. Air Poll. Control Assoc.*, *31*, 1173-1176, 1981.
- Thacker, D. L., C. J. Gibbins, P. R. Schwartz, and R. M. Bevilacqua, Ground-based microwave observations of mesospheric H<sub>2</sub>O in January, April, July, and September, 1980, *Geophys. Res. Lett.*, *8*, 1059-1062, 1981.
- Theon, J. S., W. Nordberg, C. B. Katchen, and J. J. Horvath, Some observations on the thermal behavior of the mesosphere, *J. Atmos. Sci.*, *24*, 428-438, 1967.
- Thomas, M. E., and R. J. Nordstrum, The N<sub>2</sub>-broadened water vapor absorption line shape and infrared continuum absorption, I. Theoretical development, *J. Quant. Spectrosc. Radiat. Transfer*, *28*, 81-101, 1982.
- Thomas, R. J., C. A. Barth, G. J. Rottman, D. W. Rusch, G. H. Mount, G. M. Lawrence, R. W. Sanders, G. E. Thomas, and L. E. Clemens, Ozone density distribution in the mesosphere (50-90 km) measured by the SME Limb Scanning Near Infrared Spectrometer, *Geophys. Res. Lett.*, *10*, 245-248, 1983a.
- Thomas, R. J., C. A. Barth, G. J. Rottman, D. W. Rusch, G. H. Mount, G. M. Lawrence, R. W. Sanders, G. E. Thomas, and L. E. Clemens, Mesospheric ozone depletion during the solar proton event of July 13, 1982, Part I-Measurement, *Geophys. Res. Lett.*, *10*, 253-255, 1983b.
- Thomas, R. J., C. A. Barth, D. W. Rusch, and R. W. Sanders, Solar Mesosphere Explorer Near Infrared Spectrometer: Measurements of 1.27  $\mu\text{m}$  radiances and the inference of mesospheric ozone, *J. Geophys. Res.*, *89*, 9569-9580, 1984a.

## REFERENCES

- Thomas, R. J., C. A. Barth, and S. Solomon, Seasonal variations of ozone in the upper mesosphere and gravity waves, *Geophys. Res. Lett.*, *11*, 673-676, 1984b.
- Thompson, A. M., and D. H. Lenschow, Mean profiles of trace reactive species in the unpolluted marine surface layer, *J. Geophys. Res.*, *89*, 4788-4796, 1984.
- Thompson, A. M., and O. C. Zafiriou, Air-sea fluxes of transient atmospheric species, *J. Geophys. Res.*, *88*, 6696-6708, 1983.
- Tolson, R. H., Spatial and temporal variations of monthly mean total columnar ozone derived from 7 years of BUUV data, *J. Geophys. Res.*, *86*, 7312-7330, 1981.
- Tomatsu, K., Spectral energetics of the troposphere and lower stratosphere, *Advances in Geophysics*, *21*, 189-205, 1979.
- Torabi, A., An investigation of the kinetics and excited state dynamics of the nitrate free radical, Ph.D. thesis, Georgia Institute of Technology, Atlanta, Georgia, 1985.
- Torres, A. L., Tropospheric nitric oxide measurements during GTE/CITE, *Eos Trans. AGU*, *65*, 835, 1984.
- Torres, A. L., and A. R. Bandy, Performance characteristics of the electrochemical concentration cell ozonesondes, *J. Geophys. Res.*, *83*, 5501-5504, 1978.
- Torres, A. L., P. J. Maroulis, A. B. Goldberg, and A. R. Bandy, Atmospheric OCS measurements on Project Gametag, *J. Geophys. Res.*, *85*, 7357-7360, 1980.
- Townsend, R. D., A diagnostic study of the zonally-averaged global circulation in isentropic coordinates. Ph.D. thesis, 221 pp., University of Wisconsin, Madison, 1980.
- Townsend, R. D., and D. R. Johnson, The mass and angular momentum balance of the zonally averaged general circulation, paper presented at Int. Conf. Prelim. FGGE Data Anal. Res., pp. 542-552, Bergen, 23-27 June 1980.
- Townsend, R. D., and D. R. Johnson, A diagnostic study of the isentropic zonally-averaged mass circulation during the first GARP global experiment, *J. Atmos. Sci.*, *42*, 1565-1579, 1985.
- Traub, W. A., "An upper limit for stratospheric hydrogen peroxide" and "Measurements of OH from 18 to 48 km", papers presented at the International Workshop on Current Issues in our Understanding of the Stratosphere and the Future of the Ozone Layer, BMFT, NASA, FAA, WMO, Feldafing, FRG, June 11-16, 1984.
- Traub, W. A., and K. V. Chance, Stratospheric HF and HCl observations, *Geophys. Res. Lett.*, *8*, 1075-1077, 1981.
- Traub, W. A., K. V. Chance, J. C. Brasunas, J. M. Vrtilik, and N. P. Carleton, Use of a Fourier Transform spectrometer on a balloon borne telescope and at the MMT, in *Proc. Soc. Photo-Opt. Instrum. Eng. Instrumentation in Astronomy IV*, *331*, 209-218, 1982.
- Tsao, C. J., and B. Curnutte, Line widths of pressure broadened spectral lines, *J. Quant. Spectrosc. Radiat. Transfer*, *2*, 41-91, 1962.
- Tsay, C. Y., Analysis of large scale wave disturbances simulated by an NCAR global circulation model, *J. Atmos. Sci.*, *31*, 330-339, 1974.
- Tuazon, E. C., R. Atkinson, C. N. Plum, A. M. Winer, and J. N. Pitts, The reaction of gas phase  $N_2O_5$  with water vapor, *Geophys. Res. Lett.*, *10*, 953-956, 1983.
- Tuazon, E. C., A. M. Winer, and J. N. Pitts, Jr., Trace pollutant concentrations in a multiday smog episode in the California South Coast air basin by long path length fourier transform infrared spectroscopy, *Environ. Sci. Technol.*, *15*, 1232-1237, 1981.
- Tuazon, E. C., R. Atkinson, H. MacLeod, H. W. Biermann, A. M. Winer, W. P. L. Carter, and J. N. Pitts, Jr., Yields of glyoxal and methylglyoxal from the  $NO_x$ -air photooxidations of toluene and m- and p- xylene, *Environ. Sci. Technol.*, *18*, 981-984, 1984.
- Tuck, A. F., Production of nitrogen oxides by lightning discharges, *Quart. J. Roy. Meteorol. Soc.*, *102*, 749-755, 1976.

## REFERENCES

- Tuck, A. K., A comparison of one- two- and three-dimensional model representations of stratospheric gases, *Phil. Trans. Roy. Soc. London*, A290, 477-494, 1979.
- Tucker, B. J., P. J. Maroulis, and A. R. Bandy, Free tropospheric measurements of CS<sub>2</sub> over a 45°N to 45°S latitude range, *Geophys. Res. Lett.*, 12, 9-11, 1983.
- Tucker, C. J., I. Y. Fung, C. D. Keeling, and R. H. Gammon, The relationship of global spectral vegetation indices to atmospheric CO<sub>2</sub> concentrations, *Nature*, in press, 1985.
- Tung, Ka Kit, On the two-dimensional transport of stratospheric trace gases in isentropic coordinates, *J. Atmos. Sci.*, 39, 2330-2355, 1982.
- Tung, Ka Kit, Modeling of tracer transport in the middle atmosphere, in *Dynamics of the Middle Atmosphere*, edited by J. R. Holton and T. Matsuno, pp. 417-444, Terrapub, Tokyo, 1984.
- Tung, Ka Kit, and R. S. Lindzen, A theory of stationary long waves. Part II: Resonant Rossby waves in the presence of realistic vertical shears, *Mon. Weather Rev.*, 107, 735-750, 1979.
- Turco, R. P., R. C. Whitten, O. B. Toon, J. B. Pollack, and P. Hamill, OCS stratospheric aerosols and climate, *Nature*, 283, 283-286, 1980.
- Turco, R. P., O. B. Toon, R. C. Whitten, R. G. Keesee, and P. Hamill, Importance of heterogeneous processes to tropospheric chemistry: Studies with a one-dimensional model, in *Heterogeneous Atmospheric Chemistry, Geophysical Monograph 26*, edited by David R. Schryer, pp. 231-240, American Geophysical Union, Washington, DC, 1982.
- Turner, N. C., S. Rich, and P. E. Waggoner, Removal of ozone by soil, *J. Environ. Qual.*, 2, 259-264, 1973.
- Turner, N. C., P. E. Waggoner, and S. Rich, Removal of ozone from the atmosphere by soil and vegetation, *Nature*, 250, 486-489, 1974.
- Twomey, S. A., M. Piegras and T. L. Wolfe, An assessment of the impact of pollution on global albedo, *Tellus*, 36B, 356-366, 1984.
- Tyndall, J., On radiation through the Earth's atmosphere, *Philos. Mag.*, 4, 200, 1863.
- Tyson, B. J., J. C. Arvesen, and D. O'Hara, Interhemispheric gradients of CF<sub>2</sub>Cl<sub>2</sub>, CFCI<sub>3</sub>, CCl<sub>4</sub>, and N<sub>2</sub>O, *Geophys. Res. Lett.*, 5, 535-538, 1978b.
- Uccellini, L. W., and D. R. Johnson, The coupling of upper and lower tropospheric jet streaks and implications for the development of severe convective storms, *Mon. Weather Rev.*, 107, 682-702, 1979.
- Uchino, O., M. Maeda, and M. Hirono, Applications of excimer lasers to laser-radar observations of the upper atmosphere, *IEEE J. Quant. Elec.*, QE-15, 1094-1107, 1979.
- U.S. Dept. of HEW, Public Health Service, *Air Quality Criteria for Photochemical Oxidants, NAPCA-PUB-AP-63*, 202 pp., National Air Pollution Control Administration, Arlington, VA, 1970.
- U.S. Standard Atmosphere Supplements*, Superintendent of Documents, 289 pp., U.S. Government Printing Office, Washington, DC, 1966.
- U.S. Standard Atmosphere, 1976*, U.S. Government Printing Office, Washington, DC, 1976.
- van Loon, H. K., K. Labitzke, and R. L. Jeene, Half-yearly wave in the stratosphere, *J. Geophys. Res.*, 77, 3846-3855, 1972.
- van Loon, H., C. S. Zerefos, and C. C. Repapis, Evidence of the southern oscillation in the stratosphere, *Publication No.3*, Academy of Athens, Research Center for Atmospheric Physics and Climatology, Athens, 1981.
- Varanasi, P., and F. K. Ko, Intensity and transmission measurements in the nu-3 fundamental of N<sub>2</sub>O at low temperatures, *J. Quant. Spectros. Radiat. Transfer*, 18, 465-470, 1977.
- Varanasi, P., L. P. Giver, and F. P. J. Valero, Intensity measurements in the V<sub>4</sub>-fundamental of <sup>13</sup>CH<sub>4</sub> at planetary atmospheric temperatures, *J. Quant. Spectros. Radiat. Transfer*, 30, 491-495, 1983.
- Vassy, A., Radiosonde speciale pour la mesure de la repartition verticale de l'ozone atmospherique, *J. Sci. Meteorol.*, 10, 63-75, 1958.
- Vaughan, G., and A. F. Tuck, Aircraft measurements near jet streams, in *Atmospheric Ozone*, edited by C. S. Zerefos and A. Ghazi, pp. 572-579, D. Reidel, Dordrecht, 1985.

## REFERENCES

- Vedder, J. F., B. J. Tyson, R. B. Brewer, C. A. Boitnott, and E. C. Y. Inn, Lower stratospheric measurements of variation with latitude of  $\text{CF}_2\text{Cl}_2$ ,  $\text{CFCl}_3$ ,  $\text{CCl}_4$ , and  $\text{N}_2\text{O}$  profiles in the Northern Hemisphere, *Geophys. Res. Lett.*, **5**, 33-36, 1978.
- Venne, D., The horizontal structure of traveling planetary-scale waves in the upper stratosphere, *J. Geophys. Res.*, 1984.
- Venne, D., and J. Stanford, An observational study of high-latitude stratospheric planetary waves in winter, *J. Atmos. Sci.*, **39**, 1026-1084, 1982.
- Veryard, R. G., and R. A. Ebdon, Fluctuations in tropical stratospheric winds, *Meteor. Mag.*, **90**, 125-143, 1961.
- Vienkorn-Rudolph, B., K. Bachmann, and B. Schwartz, Vertical profiles of hydrogen chloride in the troposphere, *J. Atmos. Chem.*, **2**, 47-63, 1984.
- Vigroux, E., Contribution a l'etude experimentale de l'absorption de l'ozone, *Ann. Phys.*, **8**, 709-762, 1953.
- Vincent, D. G., Mean meridional circulation in the Northern Hemisphere lower stratosphere during 1964 and 1965, *Quart. J. Roy. Meteorol. Soc.*, **94**, 333-349, 1968.
- Vincent, R. A., Gravity wave motions in the mesosphere, *J. Atmos. Terr. Phys.*, **46**, 119-128, 1984a.
- Vincent, R. A., MF/HF radar measurements of the dynamics of the mesopause region-A review, *J. Atmos. Terr. Phys.*, **46**, 961-974, 1984b.
- Vincent, R. A., Planetary and gravity waves in the mesosphere and lower thermosphere, in *Handbook for MAP, Vol. 16*, edited by K. Labitzke, J. J. Barnett, and B. Edwards, pp. 269-277, SCOSTEP Secretariat, Univ. of Illinois, Urbana, 1985.
- Vincent, R. A., and I. M. Reid, HF Doppler measurements of mesospheric gravity wave momentum fluxes, *J. Atmos. Sci.*, **40**, 1321-1333, 1983.
- Volz, A., U. Schmidt, J. Rudolph, D. H. Ehhalt, F. J. Johnen, and A. Khedim, Vertical profiles of trace gases at mid latitudes, *Jul-Report 1742*, Kernforschungsanlage Julich GmbH, D-5170 Julich, FRG, 1981.
- Vukovich, F. M., J. Fishman and E. V. Browell, The reservoir of ozone in the boundary layer of the eastern United States and its potential impact on the global tropospheric ozone budget, *J. Geophys. Res.*, **90**, 5687-5690, 1985.
- Vupputuri, R. K. R., The structure of the natural stratosphere and the impact of chlorofluoromethanes on the ozone layer investigated in a 2-D time dependent model, *Pure Appl. Geophys.*, **117**, 448-485, 1978/79.
- Vupputuri, R. K. R., Study the effect of El Chichon volcanic cloud on the stratospheric temperature structure and ozone distribution in a 2-D model, in *Atmospheric Ozone*, edited by C. S. Zerefos and A. Ghazi, pp. 59-60, D. Reidel, Dordrecht, 1985.
- Vyas, N., Numerical modelling of atmospheric processes, Ph.D. thesis, Oxford University, Oxford, 1984.
- Wale, M. J., and G. D. Peskett, Some aspects of the design and behavior of the Stratospheric and Mesospheric Sounder, *J. Geophys. Res.*, **89**, 5287-5293, 1984.
- Wallace, J. M., General circulation of the tropical lower stratosphere, *Rev. Geophys. Spa. Phys.*, **11**, 191-222, 1973.
- Wallace, J. M., The climatological mean stationary waves: Observational evidence, in *Large-scale Dynamical Processes in the Atmosphere*, edited by B. J. Hoskins and R. Pearce, pp. 27-53, Academic Press, New York, 1983.
- Wallace, J. M., and V. Kousky, Observational evidence of Kelvin waves in the tropical stratosphere, *J. Atmos. Sci.*, **25**, 900-907, 1968.
- Wallington, T. J., R. Atkinson, and A. M. Winer, Rate constants for the gas phase reaction of OH radicals with peroxyacetyl nitrate (PAN) at 273 and 297K, *Geophys. Res. Lett.*, **11**, 861-864, 1984.
- Wang, P.-H., M. P. McCormick, and W. P. Chu, A study on the planetary wave transport of ozone during the late February 1979 stratospheric warming using the SAGE ozone observation and meteorological information, *J. Atmos. Sci.*, **40**, 2419-2431, 1983.

## REFERENCES

- Wang, W.-C., and P. H. Stone, Effect of ice-albedo on global sensitivity in a one-dimensional radiative-convective climate model, *J. Atmos. Sci.*, *37*, 545-552, 1980
- Wang, W.-C., and N. D. Sze, Coupled effects of atmospheric N<sub>2</sub>O and O<sub>3</sub> on the Earth's climate, *Nature*, *268*, 589-590, 1980.
- Wang, W.-C., J. P. Pinto and Y. L. Yung, Climatic effects due to halogenated compounds in the Earth's atmosphere, *J. Atmos. Sci.*, *37*, 333-338, 1980.
- Wang, W.-C., Y. L. Yung, A. A. Lacis, T. Mo and J. E. Hansen, Greenhouse effects due to man-made perturbations of trace gases, *Science*, *194*, 685-690, 1976.
- Wang, W.-C., W. B. Rossow, M.-S. Yao and M. Wolfson, Climate sensitivity of a one-dimensional radiative-convective model with cloud feedback, *J. Atmos. Sci.*, *38*, 1167-1178, 1981.
- Wang, W.-C., D. J. Wuebbles, W. M. Washington, R. G. Isaacs and G. Molnar, Potential climatic effects of perturbations other than CO<sub>2</sub>, Chapter 6, in *State-of-the-art report*, edited by M. C. MacCracken and F. M. Luther, Dept. of Energy, Washington, DC, 1985
- Warmbt, W., Results of long term measurements of near surface ozone in the GDR, *Zeit. fuer Met.*, *29*, 24-31, 1979.
- Warneck, P., On the role of OH and HO<sub>2</sub> radicals in the troposphere, *Tellus*, *26*, 39-46, 1974.
- Washington, W. M., and G. A. Meehl, General circulation model experiments on the climatic effects due to a doubling and quadrupling of carbon dioxide concentration, *J. Geophys. Res.*, *88*, 6600-6610, 1983.
- Washington, W. M., and G. A. Meehl, Seasonal cycle experiment on the climate sensitivity due to a doubling of CO<sub>2</sub> with an atmospheric general circulation model coupled to a simple mixed-layer ocean model, *J. Geophys. Res.*, *89*, 9475-9503, 1984.
- Watanabe, K., M. Zelikoff, and E. C. Y. Inn, Absorption coefficients of several atmospheric gases, *Geophysical Research Paper No. 21*, Air Force Cambridge Research Lab., Bedford, MA, 1953.
- Waters, J. W., J. J. Gustincic, R. K. Kakar, H. K. Roscoe, P. N. Swanson, T. G. Phillips, T. de Graauw, A. R. Kerr, and R. J. Mattauch, Aircraft search for millimeter wavelength emission by stratospheric ClO, *J. Geophys. Res.*, *84*, 7034-7040, 1979.
- Waters, J. W., J. C. Hardy, R. F. Jarnot, and H. M. Pickett, Chlorine monoxide radical, ozone, and hydrogen peroxide: Stratospheric measurements by microwave limb sounding, *Science*, *214*, 61-64, 1981.
- Waters, J. W., J. C. Hardy, R. F. Jarnot, H. M. Pickett, and P. Zimmermann, A balloon-borne microwave limb sounder for stratospheric measurements, *J. Quant. Spectrosc. Radiat. Transfer*, *32*, 407-433, 1984.
- Watson, R. T., Rate constants of reactions of ClO<sub>x</sub> of atmospheric interest, *J. Phys. Chem. Ref. Data*, *6*, 871-918, 1977.
- Watson, R. T., Balloon intercomparison measurements of minor species, to be published, 1986.
- Watson, R. T., J. Rogers, L. Heidt, W. Pollock, K. Mauersberger, D. Kley, A. L. Schmeltekopf, D. L. Albritton, S. Oltmans, J. Mastenbrook, D. Murcray, W. F. J. Evans, C. Midwinter, N. Swann, and E. F. Danielsen, An intercomparison of stratospheric water vapor instruments, to be published, 1986.
- Wayne, R. P., *Chemistry of Atmospheres*, 361 pp., Clarendon Press, Oxford, 1985.
- WCP, Aerosols and their climatic effects, paper presented at World Climate Research Programme Report, WCP-55, Report of the experts meeting, Williamsburg, VA, 28-30 March 1983.
- Weaver, C., and R. Pearson, Ozone conservation and transport in cumulus clouds, *Eos Trans. AGU*, *65*, 836, 1984.
- Weaver, H., M. J. Mumma, J. L. Faris, T. Kostiuk, and J. J. Hillman, Infrared heterodyne spectroscopy of seven gases in the vicinity of chlorine monoxide lines, *Appl. Opt.*, *22*, 1562-1567, 1983.

## REFERENCES

- Webster, C. R., and R. T. Menzies, In situ measurements of stratospheric nitric oxide using a balloon-borne tunable diode laser spectrometer, *Appl. Opt.*, 23, 1140-1142, 1984.
- Webster, P. J., and G. L. Stephens, Tropical upper-tropospheric extended clouds: Inferences from Winter MONEX, *J. Atmos. Sci.*, 37, 1521-1541, 1980.
- Weeks, L. H., and L. G. Smith, A rocket measurement of ozone near sunrise, *Planet. Space Sci.*, 16, 1189-1195, 1968.
- Weeks, L. H., R. S. CuiKay, and J. R. Corbin, Ozone measurements in the mesosphere during the solar proton event of 2 November 1969, *J. Atmos. Sci.*, 29, 1138-1142, 1972.
- Wehrbein, W. M., and C. B. Leovy, An accurate radiative heating and cooling algorithm for use in a dynamical model of the middle atmosphere, *J. Atmos. Sci.*, 39, 1532-1544, 1982.
- Weiler, K. H., P. Fabian, G. Flentje, and W. A. Mathews, Stratospheric NO measurements: A new balloon-borne chemiluminescence instrument, *J. Geophys. Res.*, 85, 7445-7452, 1980.
- Weinreb, M. P., W. A. Morgan, I-Lok Chang, L. D. Johnson, P. A. Bridges, and A. C. Neuendorffer, High-altitude balloon test of satellite solar occultation instrument for monitoring stratospheric O<sub>3</sub>, H<sub>2</sub>O and HNO<sub>3</sub>, *J. Atmos. Oc. Tech.*, 1, 87-100, 1984.
- Weinstock, E. M., M. J. Phillips, and J. G. Anderson, In situ observations of ClO in the stratosphere: A review of recent results, *J. Geophys. Res.*, 86, 7273-7278, 1981.
- Weinstock, B., and H. Niki, Carbon monoxide balance in nature, *Science*, 176, 290-292, 1972.
- Weinstock, J., Nonlinear theory of gravity waves: Momentum deposition, generalized Rayleigh friction and diffusion, *J. Atmos. Sci.*, 39, 1698-1710, 1982.
- Weiss, R. F., The temporal and spatial distribution of tropospheric nitrous oxide, *J. Geophys. Res.*, 86, 7185-7195, 1981.
- Weiss, R. F., and H. Craig, Production of atmospheric nitrous oxide by combustion, *Geophys. Res. Lett.*, 3, 751-753, 1976.
- Wesely, M. L., Turbulent transport of ozone to surfaces common in the eastern half of the United States, in *Trace Atmospheric Constituents*, edited by S. E. Schwartz, pp. 345-370, Wiley, New York, 1983.
- Wesely, M. L., and B. B. Hicks, Some factors that affect the deposition rates of sulfur dioxide and similar gases on vegetation, *J. Air Poll. Control Assoc.*, 27, 1110-1116, 1977.
- Wesely, M. L., J. A. Eastman, D. R. Cook, and B. B. Hicks, Daytime variations of ozone eddy fluxes to maize, *Boundary-Layer Meteorol.*, 15, 361-363, 1978.
- Wesely, M. L., D. R. Cook, and R. M. Williams, Field measurement of small ozone fluxes to snow, bare wet soil, and lake water, *Boundary-Layer Meteorol.*, 20, 459-471, 1981.
- Wesely, M. L., J. A. Eastman, D. H. Stedman, and E. D. Yalvac, An eddy correlation measurement of NO<sub>2</sub> flux to vegetation and comparison to O<sub>3</sub> flux, *Atmos. Environ.*, 16, 815-820, 1982.
- Wetherald, R. T., and S. Manabe, The effects of changing the solar constant on the climate of a general circulation model, *J. Atmos. Sci.*, 32, 2044-2059, 1975.
- Whitten, G. Z., H. Hogo, and J. P. Killus, The carbon bond mechanism: A condensed kinetic mechanism for photochemical smog, *Environ. Sci. Technol.*, 14, 690-700, 1980.
- Whitten, R. C., W. J. Borucki, H. T. Woodward, L. A. Capone, C. A. Riegel, R. P. Turner, I. G. Poppoff, and K. Santhanam, Implications of smaller concentrations of stratospheric OH: A two-dimensional model study of ozone perturbations, *Atmos. Environ.*, 15, 1583-1589, 1981.
- Wigley, T. M. L., and M. E. Schlesinger, Analytical solution for the effect of increasing CO<sub>2</sub> on global mean temperature, *Nature*, 315, 649-652, 1985.
- Wilkniss, P. E., and R. E. Larson, Atmospheric radon measurements in the Arctic fronts, seasonal observations and transport of continental air to polar regions, *J. Atmos. Sci.*, 41, 2347-2358, 1984.
- Wilkniss, P. E., R. A. Lamontagne, R. E. Larson, J. W. Swinnerton, C. R. Dickson, and T. Thompson, Atmospheric trace gases in the Southern Hemisphere, *Nature*, 245, 45-47, 1973.

## REFERENCES

- Williams, A. P., Relaxation of the 2.7 $\gamma$  and 4.3 $\gamma$  bands of carbon dioxide, in *Mesospheric Models and Related Experiments*, edited by G. Fiocco, pp. 177-187, D. Reidel, Dordrecht, 1971.
- Williams, R. M., Uncertainties in the use of box models for estimating dry deposition velocity, *Atmos. Envir.*, 16, 2707-2708, 1982.
- Williams, W. J., J. J. Kusters, A. Goldman, and D. G. Murcray, Measurements of stratospheric halocarbon distributions using infrared techniques, *Geophys. Res. Lett.*, 3, 379-382, 1976.
- Wine, P. H., and A. R. Ravishankara, Kinetics of OH reactions with tropospheric sulfur compounds, in *2nd Symposium Composition of the Nonurban Troposphere*, pp. 258-260, May 25-28, 1982, Williamsburg, VA, AMS, Boston, MA, 1982.
- WMO, *The Stratosphere 1981. Theory and Measurements, WMO Global Ozone Research and Monitoring Project Report No. 11*, 516 pp., WMO, Geneva, 1982.
- WMO, Report of the WMO meeting of experts on potential climatic effects of ozone and other minor trace gases, *WMO Global Ozone Research and Monitoring Project, Report No. 14*, WMO, Geneva, 1983a.
- WMO, World Meteorological Organization project on research and monitoring of atmospheric CO<sub>2</sub>, *Report No. 10*, edited by R. J. Bojkov, 42 pp., Geneva, 1983b.
- WMO, Report of the WMO (CAS) Meeting of Experts on the CO<sub>2</sub> Concentrations from Pre-Industrial Times to I.G.Y. World Climate Programme, *WCP-53*, WMO/ICSU, 34 pp., Geneva, 1983c.
- Wofsy, S. C., Interactions of CH<sub>4</sub> and CO in the earth's atmosphere, *Ann. Rev. Earth Planet. Sci.*, 4, 441-469, 1976.
- Wofsy, S. C., J. C. McConnell, and M. B. McElroy, Atmospheric CH<sub>4</sub>, CO and CO<sub>2</sub>, *J. Geophys. Res.*, 77, 4477-4493, 1972.
- Wofsy, S. C., M. B. McElroy, and Y. L. Yung, The chemistry of atmospheric bromine, *Geophys. Res. Lett.*, 2, 215-218, 1975.
- Wolff, G. T., and P. J. Lioy, Development of an ozone river associated with synoptic scale episodes in the eastern United States, *Environ. Sci. Tech.*, 14, 1257-1261, 1980.
- Woodman, R. F., and A. Giullen, Radar observations of winds and turbulence in the stratosphere and mesosphere, *J. Atmos. Sci.*, 31, 493-505, 1974.
- Wu, M. F., M. A. Geller, J. G. Olson, and M. E. Gelman, Troposphere-Stratosphere (surface-55 km) monthly general circulation statistics for the Northern Hemisphere; 4 year averages, *NASA Techn. Memo. 86182*, NASA Goddard Space Flight Center, Greenbelt, MD, 1984.
- Wuebbles, D. J., Chlorocarbon emission scenarios: Potential impact on stratospheric ozone, *J. Geophys. Res.*, 88, 1433-1443, 1983a.
- Wuebbles, D. J., A theoretical analysis of the past variations in global atmospheric composition and temperature structure, *UCRL-53423*, Lawrence Livermore National Laboratory, Livermore, CA, 1983b.
- Wuebbles, D. J., and P. S. Connell, Interpreting the 1-D model-calculated nonlinearities from chlorocarbon perturbations, paper presented at International Workshop on Current Issues in our Understanding of the Stratosphere and the Future of the Ozone Layer, BMFT, NASA, FAA, WMO, Feldafing, FRG, June 11-16, 1984.
- Wuebbles, D. J., F. M. Luther, and J. E. Penner, Effect of coupled anthropogenic perturbations on stratospheric ozone, *J. Geophys. Res.*, 88, 1444-1456, 1983.
- Wuebbles, D. J., M. C. MacCracken, and F. M. Luther, A proposed reference set of scenarios for radiatively active atmospheric constituents, *Carbon Dioxide Research Division Report DOE/NBB-0066*, U.S. Department of Energy, Lawrence Livermore National Laboratory, Livermore, CA, 1984.
- Wyngaard, J. C., Toward convective boundary layer parameterization: A scalar transport module, *J. Atmos. Sci.*, 41, 1959-1969, 1984.
- Yamazaki, K. and C. R. Mechoso, Observations of the final warming in the stratosphere of the Southern Hemisphere during 1979, *J. Atmos. Sci.*, 42, 1198-1205, 1985.

## REFERENCES

- Yanai, M., J.-H. Chu, T. E. Stark, and T. Nitta, Response of deep and shallow tropical maritime cumuli to large-scale processes, *J. Atmos. Sci.*, **33**, 976-991, 1976.
- Yao, F., I. Wilson, and H. Johnston, Temperature dependent ultraviolet absorption spectrum for dinitrogen pentoxide, *J. Phys. Chem.*, **86**, 3611-3615, 1982.
- Yoshida, T., and M. Alexander, Nitrous oxide formations by nitrosomoses europsea and heterotrophic organisms, *Soil Sci. Soc. Am. Proc.*, **34**, 880-882, 1970.
- Yoshida, T., and M. Alexander, Hydroxylamine oxidation by nitrosomoses europea, *Soil Sci.*, **3**, 307-312, 1971.
- Yoshino, K., D. E. Freeman, J. R. Esmond, and W. H. Parkinson, High resolution absorption cross section measurements and band oscillator strengths of the (1,0) - (12-0) Schumann-Runge bands of O<sub>2</sub>, *Planet. Space Sci.*, **31**, 339-353, 1983.
- Yung, Y. L., M. B. McElroy, and S. C. Wofsy, Atmospheric halocarbons: A discussion with emphasis on chloroform, *Geophys. Res. Lett.*, **2**, 397-399, 1975.
- Yung, Y. L., J. P. Pinto, R. T. Watson, and S. P. Sander, Atmospheric bromine and ozone perturbations in the lower stratosphere, *J. Atmos. Sci.*, **37**, 339-353, 1980.
- Zafiriou, O. C., and M. McFarland, Nitric oxide from nitrite photolysis in the central equatorial Pacific, *J. Geophys. Res.*, **86**, 3173-3182, 1981.
- Zander, R., Presence de HF dans la stratosphere superieure, *C. R. Acad. Sc. Paris*, **281B**, 213-214, 1975.
- Zander, R., Recent observations of HF and HCl in the upper stratosphere, *Geophys. Res. Lett.*, **8**, 413-416, 1981a, Corrections, *Geophys. Res. Lett.*, **8**, 850, 1981.
- Zander, R., Evidence for variability in the total column of HCl over the Jungfraujoch Station, to be published, 1986.
- Zander, R., Trend in HF above the Jungfraujoch Station, to be published, 1986.
- Zander, R., H. Leclerq, and L. D. Kaplan, Concentration of carbon monoxide in the upper stratosphere, *Geophys. Res. Lett.*, **8**, 365-368, 1981.
- Zander, R., G. M. Stokes, and J. W. Brault, Simultaneous detection of FC-11, FC-12, and FC-22 through 8 to 13 micrometers IR solar observations from the ground, *Geophys. Res. Lett.*, **10**, 521-524, 1983.
- Zander, R., G. M. Stokes, and J. W. Brault, Spectroscopic detection of acetylene and ethane in the earth's atmosphere, through ground-based solar observations, *C. R. Acad. Sc. Paris*, **295**, 583-586, 1982.
- Zander, R., N. Louisnard, and M. Bangham, Stratospheric methane concentration profiles measured during the Balloon Intercomparison Campaigns, to be published, 1986.
- Zangvil, A. and M. Yanai, Upper tropospheric waves in the tropics. Part I: Dynamical analysis in the wavenumber frequency domain, *J. Atmos. Sci.*, **37**, 283-298, 1980.
- Zawodny, J. M., Short-term variability of nitrogen dioxide in the winter stratosphere., *J. Geophys. Res.*, in press, 1985a.
- Zawodny, J. M., Short term variability of nitrogen dioxide in the winter stratosphere., Ph.D. thesis, University of Colorado, Boulder, CO, 1985b.
- Zipf, E. C., and S. S. Prasad, A mesosphere source of nitrous oxide, *Nature*, **295**, 133-135, 1982.
- Zumbrunn, R., A. Neftel, and H. Oeschger, CO<sub>2</sub> measurements on 1-cm<sup>3</sup> ice samples with an IR laser spectrometer (IRLS) combined with a new dry extraction device, *Earth and Planetary Space Letters*, **60**, 318-324, 1982.